Fundamental Concepts of Inorganic Chemistry

Volume 1

Second Edition

Click Here t.me/thealchemylibrary

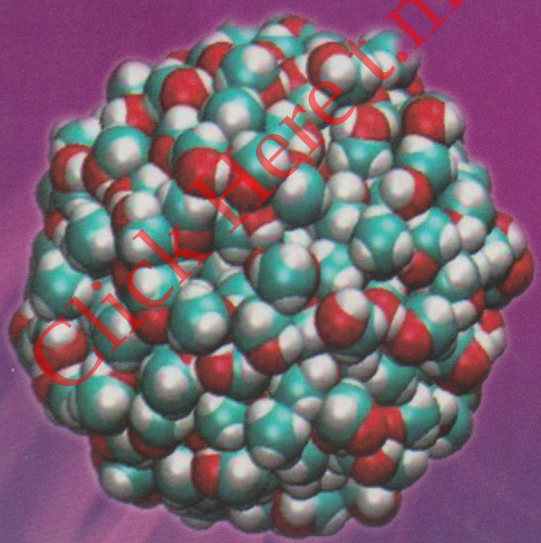

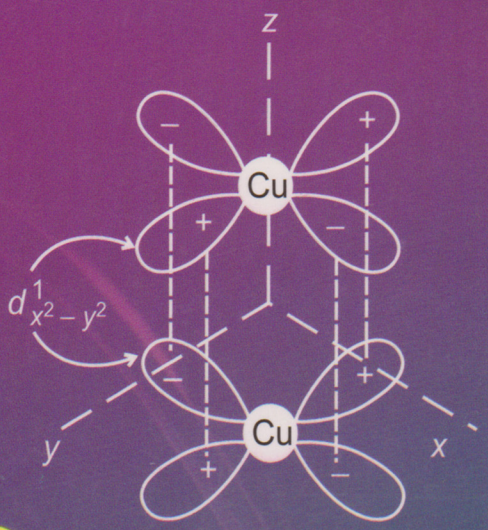

Asim K. Das

CBS Dedicated to Education
CBS Publishers & Distributors Pvt Ltd

Fundamental Concepts of Inorganic Chemistry

SECOND EDITION

Volume 1

Click Here t.me/thealchemylibrary

This Page is Intentionally Left Blank

Click Here t.me/thealchemylibrary

Fundamental Concepts of

Inorganic Chemistry

SECOND EDITION

Volume 1

Asim K. Das
MSc (Gold Medalist, CU), PhD (CU), DSc (Visva Bharati)
Professor of Chemistry
Visva Bharati University, Santiniketan 731235
West Bengal (India)

Assisted by

Mahua Das
MSc (CU), PhD (Visva Bharati)
Former Research Associate, Department of Chemistry
Visva Bharati University, Santiniketan 731235
West Bengal (India)

Click Here t.me/healchemylibrary

CBS

CBS Publishers & Distributors Pvt Ltd

New Delhi • Bengaluru • Chennai • Kochi • Kolkata • Mumbai
Hyderabad • Jharkhand • Nagpur • Patna • Pune • Uttarakhand

Disclaimer

Science and technology are constantly changing fields. New research and experience broaden the scope of information and knowledge. The authors have tried their best in giving information available to them while preparing the material for this book. Although, all efforts have been made to ensure optimum accuracy of the material, yet it is quite possible some errors might have been left uncorrected. The publisher, the printer and the authors will not be held responsible for any inadvertent errors, omissions or inaccuracies.

eISBN: 978-93-890-1750-2

Copyright © Authors and Publisher

Second eBook Edition: 2019

All rights reserved. No part of this eBook may be reproduced or transmitted in any form or by any means, electronic or mechanical, including photocopying, recording, or any information storage and retrieval system without permission, in writing, from the authors and the publisher.

Published by Satish Kumar Jain and produced by Varun Jain for
CBS Publishers & Distributors Pvt. Ltd.

Corporate Office: 204 FIE, Industrial Area, Patparganj, New Delhi-110092
Ph: +91-11-49344934; Fax: +91-11-49344935; Website: www.cbspd.com; www.eduport-global.com;
E-mail: eresources@cbspd.com; marketing@eduport-global.com

Head Office: CBS PLAZA, 4819/XI Prahlad Street, 24 Ansari Road, Daryaganj, New Delhi-110002, India.
Ph: +91-11-23289259, 23266861, 23266867; Fax: 011-23243014; Website: www.cbspd.com;
E-mail: publishing@cbspd.com; eduportglobal@gmail.com.

Branches

- **Bengaluru:** Seema House 2975, 17th Cross, K.R. Road, Banasankari 2nd Stage, Bengaluru - 560070, Karnataka Ph: +91-80-26771678/79; Fax: +91-80-26771680; E-mail: bangalore@cbspd.com
- **Chennai:** No.7, Subbaraya Street Shenoy Nagar Chennai - 600030, Tamil Nadu
  Ph: +91-44-26680620, 26681266; E-mail: chennai@cbspd.com
- **Kochi:** 36/14 Kalluvilakam, Lissie Hospital Road, Kochi - 682018, Kerala
  Ph: +91-484-4059061-65; Fax: +91-484-4059065; E-mail: kochi@cbspd.com
- **Mumbai:** 83-C, 1st floor, Dr. E. Moses Road, Worli, Mumbai - 400018, Maharashtra
  Ph: +91-22-24902340 - 41; Fax: +91-22-24902342; E-mail: mumbai@cbspd.com
- **Kolkata:** No. 6/B, Ground Floor, Rameswar Shaw Road, Kolkata - 700014
  Ph: +91-33-22891126 - 28; E-mail: kolkata@cbspd.com

Representatives

- **Hyderabad**
- **Pune**
- **Nagpur**
- **Manipal**
- **Vijayawada**
- **Patna**

Click Here t.me/thealchemylibrary

Dr. A.V. Saha, DSc
Head of the Department of Chemistry
Ramakrishna Mission Residential College
P.O. Narendrapur 743508, 24-Parganas (S)
West Bengal, India

Foreword

Present-day inorganic chemistry is no more a collection of unrelated facts. The scenario has undergone a drastic change over the last fifteen to twenty years with the application of kinetic, thermodynamic and structural studies to inorganic substances and with newer techniques providing newer information. Often the information gathered, has made theoreticians develop/modify valency theories and principles. In this situation every teacher and student realise the importance of a textbook that will help them develop the concepts and understanding of the subject. There are attempts by a few authors at achieving this goal but those seldom cover the whole curricula followed by most of the Indian Universities and Institutes. In many of these books the authors virtually neglect the evolutionary developments of the subject, creating undesirable lacunae in the readers' understanding. Here is an honest and sincere attempt at bridging these gaps and presenting a comprehensive textbook on concepts and understanding to the readers. The treatment of every topic is elaborate and is marked by remarkable clarity and the author has not compromised herewith the volume of his work. The book *Fundamental Concepts of Inorganic Chemistry* covers the inorganic chemistry curricula at the BSc (honours) and MSc preliminaries.

A large number of exercises and problems essential for modern teaching, have been incorporated meticulously at the end of each chapter to bridge the gaps, if any, in the understanding of the subject. Hope this earnest effort of Dr. Das, a teacher of distinction, will receive well-deserved acclaim from the students and teachers of this subject.

A.V. Saha

Click Here to me/trealchemylibrary

to

my teachers and well-wishers
who paved the way
to reach here

Click Here t.me/thealchemylibrary

श्रद्धावान् लभते ज्ञानम्

One who has shraddha acquires knowledge

Preface to the Second Edition

I do endeavour. He gives the strength and patience.

My beloved readers are requested first to accept my unconditional apology for this long time taken to shape the second edition of the book. Though the second edition incorporates some aspects of coordination chemistry, the readers desire the complete **Coordination Chemistry** which is expected to appear in the next volumes and the process is in progress.

I feel delighted to record the warm response which the first edition of the book has received from the students and teachers throughout the country. I have tried my best to incorporate all the suggestions received from the readers. The present edition has been thoroughly revised and substantially enlarged and, in fact, no single page has been left untouched. However, I have taken all the measures to retain the features for which the first edition has been so popular.

In this second edition of the book, scope of the book has been broadened by adding new topics and revisions of the earlier sections. The new topics are atomic units; NMR active nuclei and principles of NMR spectroscopy; nucleosynthesis of elements after big bang; nuclear waste management; Bose-Einstein condensate (BEC): fifth state of matter; bonding properties of *d*- and *f*-orbitals: comparison; application of Woodward–Hoffmann orbital symmetry rules; structure and properties of fluoroalkyl radicals and ions; structure and properties of zeolites and clay materials; aluminosilicates and surface acids; heteropoly and isopoly acid anions; hypervalency; molecular orbital diagrams of polyatomic molecules in terms of group orbitals (i.e. TASOs); 3c-4e versus 3c-2e bonding systems; geometry of the molecules in terms of Walsh diagrams; isolobal fragments; reaction-mechanism of the main group elements; different aspects of material science; PSPET- Wade's rule, Jemmi's rule; chemistry of boranes and carboranes; metal clusters and carbonyl clusters; Zintle ions; symmetry elements and point groups; fullerenes; intercalation compounds of graphite; band theory of solids – band splitting and band bending; electrical and magnetic properties of solids; piezoelectric solids; organic metals and organic semi-conductors; superconductivity; supramolecular chemistry; aqueous chemistry of amino acids; surface

Click Here t.me/thealchemylibrary

acids and solid acids; agostic interaction; ionic equilibria and related numerical problems; inorganic photochemistry; lithium battery; fuel cells; solar cells; EMF diagrams – Frost diagram, Pourbaix diagram; Tafel equation; stability field of water; chemistry of explosives; electroanalytical techniques– polarography, coulometry, ampereometry, LSV, CV, polarography; chemical clock reactions and oscillating chemical reactions.

In preparing the revised manuscript, I have freely consulted the books and reviews of different authors and I have borrowed their ideas whenever it has been required. I am extremely grateful and indebted to these authors. In fact, I have picked up the flowers from these gardens to prepare the garland to worship the goddess of learning.

The golden period of my student life at Ramakrishna Mission Residential College, Narendrapur, gives the foundation of my career. There I got a gifted teacher, Prof. AV Saha whose teaching in the subject is still remaining vibrant in my memory and his teaching is reflected at many places of this book.

The author is thankful to Prof. KL Sebastian, IPC, IISc, Bangalore; Prof. S Basu, Burdwan University; Prof. GN Mukherjee, Sir Rashbehari Ghose, Professor of Chemistry; Dr A Sen, Ramakrishna Mission Centenary College, Rahara, 24 Parganas; Dr MN Bishnu, City College, Kolkata; Prof. RN Mukherjee, IIT, Kanpur; Dr SP Banerjee, Retired Professor, Vivekananda Mahavidyalaya, Burdwan; Dr S Roy Chowdhury, Dinabandhu Andrews College, Garia, Kolkata; Prof. K Dey, Kalyani University; Prof. A Sarkar, Kalyani University; Dr. G Mukherjee, Kalna College, Burdwan; Dr N Koley, Retired Professor, Raghunathpur College, Purulia; Prof. B Pathak, Retired Professor, Presidency College, Kolkata; Dr B Saha, Burdwan University; Dr H Karak, St Paul's College, Kolkata, for their encouragement and suggestion.

I am thankful to all my colleagues for extending their moral support. I am specially thankful to my colleague Dr M Seikh for discussion on many topics and procuring some reference materials.

I am extremely grateful to Mr SK Jain, Managing Director, CBS Publishers and Distributors, New Delhi for his continued support. I am also thankful to Mr YN Arjuna, Senior Director (Publishing, Editorial and Publicity) and the staff involved in DTP for taking the troubles in processing the revised manuscript.

I am thankful to my PhD students, Dr M Islam and Sri R Bayen for their cooperation. I am indebted to my family members Dr (Mrs) Mahua Das (wife), Ankita Das (elder daughter) and Udita Das (younger daughter) for their moral support without which it would have been impossible to do this task.

Despite my best efforts, some mistakes and misconceptions might have crept in and for these inconveniences, I beg to be pardoned. Suggestions and criticisms are always welcome from the readers.

Santiniketan **Asim K. Das**

Click Here t.me/thealchemylibrary

Preface to the First Edition

—"No great work can be achieved by humbug. It is through love, a passion for truth; and tremendous energy, that all undertakings are accomplished."

—"I hold every man a traitor who, having been educated at their expense pay not the least heed to them."

Swami Vivekananda

Click Here t.me/healchemylibrary

As a student and also as a teacher, the author has experienced that for a systematic and comprehensive coverage of the present subject, one is forced to consult various books on different disciplines to collect the reading materials. Consequently, the students are specially constrained. Keeping this idea in mind, it has been attempted here to present a complete textbook on the subject. In a logical sequence, the book deals extensively with different aspects such as atomic structure (both classical and wave mechanical) and atomic spectra, fundamentals of quantum mechanics and wave mechanics, nuclear chemistry and radiation chemistry, different theories of valence forces and chemical forces including band and Bloch theory of solids, solid-state chemistry, acids and bases, nonaqueous solvents and redox potentials. It also covers the different aspects of materials science which is emerging with a great promise. Thus the present book covers the curricula followed by most of the Indian Universities and Institutes at the BSc and MSc levels. It also aims to help the students preparing for competitive examinations like NET, GATE, SLET, etc. Adequate stress on the basic theories and concepts has been given everywhere to rationalise the presentation. The ideas have been very often illustrated through solution of related numerical problems. Each chapter is ended with various types of questions and problems to afford an opportunity to the students for self-evaluation.

In writing a book of this nature, one accumulates indebtedness to the previous authors of different books. The books which have been consulted are listed separately and gratefully acknowledged.

The author expresses his deep sense of gratitude to Dr AV Saha, a gifted teacher, from whom the author had started to learn and understand the subject in his student life in Ramakrishna Mission Residential College, Narendrapur, for writing the foreword. The author's association for a fairly long period with the said Institute was highly fruitful in shaping the present ideas and the author must express his indebtedness to his teachers and the authorities of the Institute. The author is grateful to his wife, Dr M Das for various types of help, assistance and cooperation.

The author is specially grateful to Mr SK Jain, Managing Director of CBS Publishers and Distributors, New Delhi for his earnest interest in publishing the book. Thanks are also due to his colleagues and students.

In conclusion, the author's attempt will be amply rewarded, if it is found helpful to the students and teachers. In spite of all precautions, some errors might have crept in. Constructive criticism and valuable suggestions from the readers will be most welcome.

Asim K. Das

Click Here t.me/thealchemylibrary

Contents

Foreword *v*

Preface to the Second Edition *vii*

Preface to the First Edition *ix*

VOLUME 1

1. Classical and Vector Models of Atoms **1–110**

1.1 Cathode Rays and Electron **1**
Electric Discharge through Gases and Production of Cathode Rays; Properties of Cathode Rays; Determination of Charge to Mass Ratio (*e*/*m*) of an Electron by Thomson's Method; Determination of Charge of an Electron by Millikan's Oil-Drop Method

1.2 Anode Rays **8**
Production of Anode Rays; Properties of Anode Rays; Analysis of Positive Rays by Thomson's Parabola Method; Aston's Mass Spectrograph; Dempster's Mass Spectrometer; Bainbridge Mass Spectrometer

1.3 The Neutron as a Fundamental Particle **16**
The Discovery of Neutron; Properties of Neutron

1.4 Some Important Properties of the three Fundamental Particles **18**

1.5 The Hydrogen Spectrum **18**
Balmer Formula; Rydberg Formula; Ritz Combination Principle

1.6 Thomson's Plum-Pudding Model of Atom **20**

1.7 Scattering of α-Particles and Rutherford's Nuclear Model of Atom **21**

Click Here for more chemistry library

Rutherford's Nuclear Model of Atom; Rutherford's Theory of α-Particle Scattering; Nuclear Dimension from the α-Particle Scattering Experiment

1.8 Bohr's Atomic Model for the Hydrogen-like Systems **25**

Bohr's Atomic Model; Numerical Values of Radius and Energy in Bohr's Atom; Correction for the Finite Mass of the Nucleus; Bohr's Theory and the Spectral Lines in Hydrogen-like Systems; Ionisation and Resonance Potential for Hydrogen and Hydrogen-like Systems in the Light of Bohr's Theory; Bohr's Theory and Correspondence Principle; Moseley's Law in the Light of Bohr's Theory; Franck-Hertz Experiments (Nobel Prize in Physics, 1925) in the Light of Bohr's Atomic Model; Merits of the Bohr's Atomic Model; Drawbacks in the Bohr's Model

1.9 Fine Structure of Spectra and Sommerfeld's Atomic Model **45**

Sommerfeld's Atomic Model; Penetrating Power of the Orbits and Quantum Defect in Polyelectronic Systems in the Light of Sommerfeld's Theory; Achievements of the Sommerfeld's Theory; Drawbacks in the Sommerfeld's Model

1.10 Vector Model of the Atom **52**

Concept of Spatial Quantisation; Concept of the Spinning Electron; Quantum Numbers in the Vector Model; Four Quantum Number System and Pauli Exclusion Principle; Coupling Schemes and Atomic States in the Vector Model; $\vec{L}-\vec{S}$ and $\vec{j}-\vec{j}$ Coupling Schemes; Spatial Quantisation of the Resultant Vectors (i.e. $\vec{L}, \vec{S}, \vec{J}$) in Atoms or Ions; Determination of Microstates and Russel-Saunders Terms; A Simple Working Procedure to Determine the Term Symbols; Hund's Rules to Determine the Ground State Term; Derivation of the Ground State Terms in the Light of Hund's Rules; Spectral Selection Rules in the Vector Model; Intensity Rules for Spectral Transitions in the Vector Model; Fine or Multiplet Structure of the Spectral Lines in the Light of Vector Model; Nuclear Spin and Hyperfine Structure of the Spectral Lines; Orbital and Spin Magnetic Moments of an Electron; Stern-Gerlach Experiment—An Evidence in Favour of Space Quantisation and Spin Quantum Number; Explanation of the Magneto-Optic Phenomenon - the Zeeman Effect; Electronic Structure of the Atoms; Merits of the Vector Model

1.11 Electronic Configuration Scheme for Many Electron Systems **86**

Rules for Placing the Electrons in Different Energy Levels

Solved Numerical Problems **97**

Exercise-I **105**

2. Origin of the Quantum Theory **111–132**

2.1 Introduction **111**

2.2 Nature of Black-Body Radiations **111**

2.3 Different Laws and Theories of Black-Body Radiations **113**

The Stefan-Boltzmann Law; Wien's Law; Rayleigh-Jeans Law; Planck's Quantum Theory

Click Here t.me/thealchemylibrary

2.4 The Photoelectric Effect 118
Characteristics of Photoelectric Effect; Einstein's Theory of Photoelectric Effect; Work Function and Ionisation Potential

2.5 Compton Effect 121
Theoretical Background of Compton Effect; Compton Shifts at Different Cases; Characteristic Features of Compton Effect

2.6 Pair Formation 126

Solved Numerical Problems 127

Exercise-II 130

3. Fundamentals of Wave Mechanics 133–184

3.1 Introduction 133

3.2 Wave Particle Duality and de Broglie's Matter Wave 133
de Broglie Wavelength for Matter Waves; The de Broglie Wavelength for the Macroscopic and Microscopic Bodies; Difference between de Broglie Matter Wave and Electromagnetic Wave; The de Broglie Electron Wave; Relativistic Correction in the de Broglie Electron Wave; Verification of the de Broglie Electron Wave by Davisson and Germer's Experiment; Bohr's Quantum Restriction from the de Broglie Concept

3.3 The Heisenberg's Uncertainty Principle and its Implications 140
Uncertainty Principle; Illustration of the Uncertainty Principle in the Determination of the Position of a Particle by a Microscope: Compton Effect and the Uncertainty Principle; Applicability of the Uncertainty Principle to Large and Small Particles; Some Important Applications of the Uncertainty Principle

3.4 Schrödinger's Wave Equation 145
Representation of Schrödinger's Wave Equation; Physical Significance of Schrödinger's Equation and Hamiltonian Operator; Eigen Values and Eigen Functions; Physical Significance of the Wave Function (ψ); Normalised and Orthogonal Wave Functions

3.5 Some Applications of the Schrödinger's Wave Equation 150
Free Particle; Particle in a One-Dimensional Box; Particle in a Three-Dimensional Box; Importance of the Model - Particle in a Box; Some Applications of the Model - Particle in a Box; Quantum Mechanical Tunnelling Effect

3.6 Approximate Methods of Solving the Schrödinger's Wave Equation 165
Variation Method; The Linear Combination Method

Solved Numerical Problems 167

Exercise-III 177

Appendix 3A: Application of Variation Method in Hydrogen Atom 180

4. Wave Mechanical Model of Atom 185–235

4.1 Wave Mechanical Model for the Hydrogen-like Atoms or Ions 185
Wave Functions for the Hydrogen-like Systems; Wave Mechanical Genesis of the Quantum Numbers; Important Features of a Dirac Atom Developed from the.

Click here.t.me/thealchemylibrary

Relativistic Wave Mechanics; The Radial Wave Function and Radial Probability Distribution of Electron Cloud in Hydrogenic Systems; The Physical and Chemical Significance of the Nodal Points; Angular Wave Functions and Orbital Shapes; Electron Cloud Density Representation of the Orbitals in Hydrogen-like Systems; Symmetry of the Orbitals; Concept of Atomic Orbitals in Wave Mechanics in Relation to the Orbits in Classical Mechanics; Energy of the Electron in Hydrogen-like Systems; The Four Quantum Numbers; Pauli Exclusion Principle in the Light of Wave Mechanics

4.2 Wave Mechanical Model for Polyelectronic Systems 219

Self-Consistent Field (SCF) Method; Concept of Slater Orbitals; Concept of Shielding and Quantum Defect; Slater's Rules in Calculating the Shielding Constant (S) and Effective Nuclear Charge (Z*)

4.3 Bonding Properties of *d*- and *f*-Orbitals 225

Solved Problems 226

Exercise-IV 234

5. Atomic Nucleus and its Structure 236–308

5.1 The Atomic Nucleus 236

Composition of the Nucleus; Size of the Nucleus; Mirror Nuclei and Nuclear Radius; Nuclear Density; Shape of the Nucleus; Total Angular Momentum of the Nucleus : Magnetic Properties of the Nucleus and Nuclear Magnetic Resonance (NMR) Frequency and NMR Spectra of Some Representative Examples; Classification of the Nuclides; Nuclear Spin Isomerism in Diatomic Molecules : *Ortho*- and *Para*-Hydrogen : Intensity of the Rotational Lines in the Band Spectra of Diatomic Molecules

5.2 The Isotopes 253

Discovery and Characterisation of Nonradioactive Isotopes; Isotopic Shift in Optical Spectra; Characteristic Features of the Isotopes; Isotopic Composition of the Elements; Uses of Isotopes; Separation of Isotopes

5.3 Nuclear Stability 268

Even-Odd Nature of the Nucleons (Harkins' Rule); The Neutron to Proton Ratio and Stability of the Nuclides; The Neutron to Proton Ratio and Different Modes of Decay; Packing Fraction and Nuclear Stability; Mass Defect and Nuclear Binding Energy (NBE)

5.4 The Nuclear Forces 278

Nature of the Nuclear Forces; Exchange Force as the Nuclear Force; The Nuclear Potential and Nuclear Potential Barrier

5.5 Nuclear Models 282

Fermi Gas Model; The Liquid Drop Model; Nuclear Shell Model; The Optical Model

5.6 The Fundamental Particles 296

Solved Numerical Problems 299

Exercise–V 305

Click Here t.me/jhealchemylibrary

6. Radioactivity and Radiation Chemistry 309–382

6.1 Discovery of Natural Radioactivity 309

6.2 Types of Radioactive Emanations 310

6.3 Properties of Alpha, Beta and Gamma Radiations 311
Alpha (α)-rays; Beta (β)-Rays; Gamma (γ) Rays; Comparison among the Different Types of Radioactive Emanations

6.4 Detection and Measurement of Radioactivity 315

6.5 Units of Radioactivity 320

6.6 Different Modes of Radioactive Decay 322

6.7 The Fluorescence and Auger Effect 323

6.8 Disintegration Chain and Soddy-Fajan Group Displacement Law 324

6.9 The Decay Kinetics and Parent-Daughter Growth Relationships 325
Case I : The Daughter Nucleus is Stable; Case II : When the Daughter Element is Radioactive

6.10 Radioactive Equilibrium 332

6.11 Energetics of the Disintegration Processes 336

6.12 Some Important Aspects of Alpha Decay 338

6.13 Some Important Aspects of Beta Decay 340

6.14 Some Important Aspects of Gamma Emission 341

6.15 The Disintegration Series 342

6.16 Artificial or Induced Radioactivity 345
Discovery of Artificial Radioactivity; Production of Artificial Radioactivity

6.17 Applications of Radioactive Isotopes 347
Application of Radioisotopes in the Field of Chemistry; Application of Radioactivity in Biological Fields; Application of Radioactivity in Agriculture; Application of Radioactivity in the Medical Field; Application of Radioactivity in Industry; Application of Radioactivity in Age Determination

6.18 Some Important Aspects of Radiation Chemistry 363
Radiation Chemistry; Characteristics of Interaction of Medium Energy Charged Particles with Matter; Interactions of Neutrons with Matter; Interaction of Gamma–Radiation with Matter; Radiation Dosimetry; Radiolysis of Water

Solved Numerical Problems 371

Exercise–VI 379

7. Nuclear Reactions 383–447

7.1 Artificial Transmutations and Nuclear Reactions 383

7.2 Bethe's Notation of Nuclear Reactions 384

Click Here t.me/thealchemylibrary

7.3 Nuclear Reactions Versus Chemical Reactions 385

7.4 Classification of Nuclear Reactions 386

7.5 Conservation Laws in Nuclear Reactions 390
Conservation of Energy; Conservation of Linear Momentum; Conservation of Angular Momentum; Conservation of Neutrons and Protons

7.6 Threshold Energy of a Projectile for a Nuclear Reaction 392

7.7 Nuclear Reaction Cross-Section 392

7.8 Mechanisms of Nuclear Reactions 393
The Compound Nucleus Theory; Oppenheimer-Phillips Mechanism in Stripping Reactions; Direct Nuclear Reaction Mechanism

7.9 Charged Particle Accelerators 397
The Linear Accelerator; The Cyclotron

7.10 Filling in the Gaps in the Periodic Table: The Man-Made Elements 401

7.11 Transuranic and Translawrencium Elements: The Man-Made Elements 402

7.12 Nuclear Fission 406
Historical Background; Characteristic Features of Nuclear Fission; Bohr-Wheeler Theory of Nuclear Fission: Liquid Drop Model; Charge Distribution in Fission Products : Principle of Equal Charge Displacement

7.13 Fission Chain Reaction: A Source of Atomic Energy 415
Factors Controlling a Fission Chain Reaction; The Fertile and Fissile Nuclides as the Nuclear Fuels; Atom Bomb; Fermi's Four Factor Formula and Nuclear Reactor or Atomic Pile for the Controlled Nuclear Fission; Breeder Reactor; A Natural Fission Reactor : Okla Phenomenon; Nuclear Reactors in India; Recovery of Uranium and Plutonium from Spent Fuel

7.14 Nuclear Fusion: Thermonuclear Reaction 424
Characteristic Features of Nuclear Fusion; Hydrogen and Cobalt Bomb; Stellar Energy; Controlled Fusion Reactions : An Innocent and a Never-Ending Source of Energy; Cold Fusion

7.15 The Origin and Evolution of Elements : Nucleosynthesis of Elements 429
Nucleosynthesis of Elements from the Primordial Element Hydrogen in Stars; Cosmic Abundance of Elements

Solved Numerical Problems 435

Exercise–VII 444

8. Periodic Table and Periodic Trends of Different Properties of Elements 448–541

8.1 Historical Background of the Development of Periodic Classification 448
Law of Triads; Pattenkofer's Rule of Integral Multiple; Chancourtois Law of Telluric Screw; Newlands' Law of Octaves; Mendeleev's and Lothar Meyer's Periodic Laws

Click Here t.me/Inorganicchemylibrary

8.2 Mendeleev's Periodic Law and Periodic Table 451
Characteristics of Mendeleev's Short Periodic Table

8.3 Characteristics and Usefulness of the Mendeleev's Periodic Table 455
Systematic Classification of the Elements; Correction of Atomic Weights; Prediction of the Missing Elements

8.4 Defects in the Mendeleev's Periodic Table 456

8.5 Long Form of the Modern Periodic Table 458
Important Segments of the Long Form of the Modern Periodic Table; Advantages of the Long Form of Periodic Table; Defects of the Long Form Periodic Table

8.6 Extended Periodic Table: Superheavy Elements: Postactinides and Superactinides 462

8.7 Classification of the Elements Based on the Electronic Configuration and Chemical Affinities 464
Classification Based on the Position of the Differentiating Electron; Bohr's Classification Based on Electronic Configuration; Goldschmidt's Geochemical Classification of Elements Based on Chemical Affinity

8.8 Characteristics and Position of the Border Line Elements 467
Position of the *Zn*-Family; Positions of *Lu*, *Th* and *Lr*; Position of the Lighter Actinides; 4*f* Series (Lanthanides) vs. 5*f* Series (Actinides)

8.9 Lanthanide and Actinide Contractions (i.e. *f*-Contractions) 469
Nature of the *f*-Contraction; Explanation of *f*-Contraction; Effects of Lanthanide Contraction

8.10 Periodic Trends of Z^* and Size of the Atoms and Ions 473
Two Important Factors (n and Z^*) to Determine the Size of Atoms and Ions; Periodic Trends of Z^* (Effective Nuclear Charge); Variation of Size along the Periods; Variation of Size in a Group

8.11 Variation of Atomic Volumes in the Periodic Table 478
Atomic Volume : Definition and Limitation of the Parameter; Nature of Variation Trend of the Atomic Volume with the Atomic Number; Explanation of the Atomic Volume Curve

8.12 Variation of Ionization Energies in the Periodic Table (cf. Sec. 9.11 for Ionisation Energies of Molecules and Photoelectron Spectroscopy) 480
Periodic Variation of the Ionisation Energies; Factors Governing the Ionisation Energies and Explanations of the Periodic Trends; The Cases which Flout the General Periodic Trend; Ionisation Energy of Some Typical Molecular Species

8.13 Electron Affinity and its Variation Trend in the Periodic Table 486
Concept of Electron Affinity; Factors Governing the Electron Affinities; Variation of Electron Affinity in the Periodic Table

8.14 Concept of Electronegativity 491
Pauling's Electronegativity; Mulliken's Orbital Electronegativity; Jaffe-Hinze Electronegativities (Mulliken-Jaffe electronegativity); Allred-Rochow's Electronegativity;

Click Here t.me/thealchemylibrary

Sanderson's Electronegativity; Calculation of Charge Separation from Electronegativity: Concept of Electronegativity Equalization; Electronegativity Not an Inherent Property of the Elements; Examples Illustrating the Variation of Electronegativity Depending upon the Structural Characteristics; Group Electronegativity; Concepts of Absolute Electronegativity; Optical Electronegativity and Spectroscopic Electronegativity

8.15 Periodic Trends of Electronegativity 507

8.16 Applications of the Electronegativity Concept in Different Fields of Chemistry 507

8.17 Periodic Trends of Cohesive Energy (i.e. Melting and Boiling Points) 511

8.18 The Diagonal Relationship 511

Causes of the Diagonal Relationship; Comparison of the Physical Constants of the Three Diagonal Pairs; Similarities in the Pair, *Li* and *Mg*; Similarities in the Pair, *Be* and *Al*; Similarities in the Pair, *B* and *Si*

8.19 Basic Difference in Group Trends Between the Representative and Transition Elements 517

8.20 Secondary Periodicity : Anomalies among the Posttransition Elements and Postlanthanides 517

Secondary Periodicity and Consequences of Secondary Periodicities; Explanation of the Anomalies in Properties of the 4-th and 6-th Period Posttransition Elements; Relativistic Effects on Chemical Properties of the Fifth and Sixth Row Elements

8.21 Position of Hydrogen in the Periodic Table 524

8.22 Peculiarities of the First and Second Row Elements 525

Anomalous Properties of Fluorine : Superhalogen or Subhalogen?; Anomalous Properties of Lithium

8.23 Comparison of Transition (i.e. *d*-Block) and Inner Transition (i.e. *f*-Block) Metals 528

8.24 Variation of Oxidation States of *s*- and *p*-Block Elements 530

Solved Numerical Problems 532

Exercise-VIII 535

Appendices A-1–A-12

Appendix I: Units and Conversion Factors A-1

Appendix II: Some Physical and Chemical Constants A-4

Appendix III: Wavelength and Colours A-5

Appendix IV: Names, Symbols, Atomic Numbers and Atomic Weights of the Elements A-6

Appendix V: Some Useful Mathematical Relationships A-8

Appendix VI: Books Consulted A-11

Index I-1–I-20

Click Here for more chemistry library

VOLUME 2

9. Introduction to Chemical Bonding and Theories of Covalence: Valence Bond Theory (VBT) and Molecular Orbital Theory (MOT) 542–752

9.1 Historical Background 542
Development of the Concept of Valency; Lewis-Langmuir Concept; The Octet Rule; Sugden's View of Singlet Linkage ($2c$–$1e$) in Favour of Octet Rule; Sidgwick's Rule of Maximum Covalency; Hypervalence and Hypercarbon Compounds; The Main Types of Chemical Forces; Isosteric or Isoelectronic Species

9.2 The Theories of Covalent Bond : Born-Oppenheimer Approximation 550

9.3 The Valence Bond Theory (VBT) 551
The Valence Bond Theory for Hydrogen Molecule; The Major Conclusions Drawn from VBT; The Major Drawbacks in VBT

9.4 Molecular Orbital Theory (MOT) 557
The LCAO-MO Treatment of Diatomic Hydrogen Molecule Ion (H_2^+); The LCAO-MO Treatment of the Diatomic Hydrogen Molecule : A Two Electron-Two Centre (2e–2c) System; Comparison of VB and LCAO–MO Treatments on H_2; The Important Aspects of LCAO-MOT; Proof of Three Basic Conditions (EOS) in LCAO–MO Method

9.5 Symmetry and Overlap in Forming Molecular Orbitals in LCAO method 570

9.6 Sigma (σ)-, Pi (π)- and Delta (δ)-Molecular Orbitals, Phi (ϕ) and Mu (μ) Bonds 574

9.7 VBT versus LCAO-MOT 575

9.8 The United Atom Method in Molecular Orbital Theory 576

9.9 Simple Molecular Orbital Model for Homonuclear Diatomic Molecules 578
Simple Molecular Orbitals and Diagrams; Molecular Orbital Picture of Some Representative Homonuclear Diatomic Molecular Species; Limitations of the Simple Molecular Orbital Model; Simple Molecular Orbital Diagram for the Homonuclear Diatomic Molecules Involving $(n-1)d$ Orbitals

9.10 Modified Molecular Orbital Energy Diagram for the Homonuclear Diatomic Molecules (Specially for N_2 and Lighter Molecules) 589
Symmetry Interaction (Noncrossing Rule) among the Molecular Orbitals Obtained in the Simple Model; Molecular Orbital Energy Diagram by Considering the Participation of Hybrid (s-p interaction) Atomic Orbitals in Generating the Molecular Orbitals; Success of the Modified MO Energy Diagram : Reactivity of Some Molecular Species

9.11 Molecular Orbital Picture in Heteronuclear Diatomic Molecules: UV Photoelectron Spectroscopy and Photosensitivity in the Light of MOT 601
Molecules (i.e. XH) Containing a H-atom; Molecules (XY) in which both the Atoms (X, Y) Contain s- and p-Valence Orbitals; Ultraviolet Photoelectron Spectroscopy (UV-PES): Identification of the Nature of Molecular Orbital Energy Level; Colours and Photosensitivity of the Compounds in Terms of MOT

Click Here t.me/healchemylibrary

9.12 Molecular Orbital Treatment of Triatomic Molecules 620
Basic Concepts of Group Orbitals; Delocalised and Localised Molecular Orbitals; Molecular Orbital Treatment for H_3 and H_3^+ Molecular Species; Molecular Orbital Treatment for Linear Hydrides XH_2 Having Valence Electrons Four; Molecular Orbital Treatment for Bent Hydrides XH_2 Having Valence Electrons More Than Four; Illustration of Walsh Diagram for XH_2 Species; Molecular Orbital Energy Diagram of Some Representative Triatomic Hydrides in Terms of Hybridisation of the Central Atom; Triatomic Nonhydrides (XY_2)—Linear Species Having 16 Valence Electrons; Molecular Orbital Energy Diagram for Some Representative Linear Molecules like CO_2 and BeX_2 — Use of Hybridised Orbitals by the Central Atom; Molecular Orbital Picture of the Bent Molecule XY_2 (X and Y Second Period Elements); Molecular Orbital Energy Diagram for the Trigonal Planar Molecular Species XY_3; Molecular Orbital Energy Diagram of Some Representative Polyatomic Species; Characteristics of Three Centre Bonding

9.13 Hybridisation of Atomic Orbitals 669
Linear Combination of Atomic Orbitals in Hybridisation; Stereochemistry of the Hybrid Orbitals; Bonding Potentiality of the Hybrid Orbitals; Energetics of Hybridisation; Participation of d-Orbitals in Hybridisation in Nonmetals; Equivalence and Nonequivalence of the Hybrid Orbitals; Bent's Rule of Hybridisation

9.14 Summary of the Concept of Hybridisation 699

9.15 Conjugated Molecules and Delocalisation Energy 699

9.16 Resonance and Delocalisation 705
Concept of Resonance in VBT; Resonance Energy; Conditions for Effective Canonical Forms; Concepts of Formal Charge and Lewis-Langmuir Charge in Resonating Structures: Formal Charge and Oxidation Number; Resonance in the Light of Molecular Orbital Theory; Application of the Concept of Resonance in Some Inorganic Compounds

9.17 Limitations of the Concept of Resonance and Hybridisation 716

9.18 Multiple Bonds 717
Bond Length and Bond Multiplicity; p_π–p_π Bonding

9.19 Delta and Quadruple Bond 720

9.20 Odd Electron Covalent Bonds in Odd Electron Molecules 723

9.21 Electron Deficient Covalent Bonds and Electron Deficient Covalent Compounds 725

9.22 Molecular Orbital Theory in Explaining Higher Oxidation States of Nonmetals 734

9.23 Molecular Orbital Theory in Explaining the Bonding in Inert Gas Compounds: *3c–4e* Bonding Model 735

9.24 Isolobal Fragments 739

Exercise–IX 742

Appendix 9A: FMO Approach to Woodward-Hoffmann Orbital Symmetry Rule for Intramolecular Cyclisation and Concerted Intermolecular Cycloaddition Reactions 748

Click Here for more chemistry library

10. Covalent Compounds: Characteristics, Structure and Reactivity 753–976

10.1 Bond Energy 753

Bond Energy in the Diatomic Molecules; Thermodynamics of Bond Energy in the Diatomic Molecules; Average Bond Energy in Polyatomic Molecules; Thermochemistry in Computing Bond Energies; Bond Energies of Different Bonds; Intrinsic Bond Energy; Different Factors Governing the Bond Energy

10.2 Covalent Bond Lengths and Covalent Radii 764

Single Bond and Covalent Radii; Multiple Bond and Covalent Radii; Different Factors Governing the Bond Lengths

10.3 The Inert Pair Effect 770

Meaning and Illustration of the Inert Pair Effect; Interpretation of Inert Pair Effect in Terms of Bond Weakening Phenomena for the Heavier Congeners

10.4 Covalent-Ionic Resonance : Partial Ionic Character in Covalent Bonds 774

10.5 Dipole Moment and Molecular Polarity 777

Different Contributing Factors to the Molecular Polarity; Prediction of Geometry of the Molecules from Dipole Moment and Calculation of Dipole Moment; Dipolar Repulsive Interaction; Contribution of Hybrid Lone Pair Moments to the Molecular Polarity; Induced Dipole Moments; Application of the Concept of Dipole Moments

10.6 Covalency in Ionic Bonds : Deformation or Polarisation of Ions : Fajans' Rules 791

Polarisation and Covalency; Factors Governing the Degree of Polarisation; Fajan's Rules in Predicting the Melting and Boiling Points and Solubility of Some Compounds; Application of the Concept of Polarisation

10.7 Effects of π-Bonding (with Special Reference to the Involvement of *d*-Orbitals) on the Structural Properties and Reactivity 802

Comparison of Carbon and Silicon Compounds; Comparison of Nitrogen and Phosphorus Compounds; Comparison of Oxygen and Sulfur Compounds; Pi-Boding in Boron Compounds; Effect of $p_\pi \rightarrow d_\pi$ Bonding on the Properties of Different Oxyacids and Periodic Variation of Properties of Oxyacids; p_π–d_π Bonding Leading to Aromaticity in Inorganic Ring Compounds; Changes in Structure due to Electronegative Substituents; Synergistic Effect due to the π-Bonding and Stabilisation of Low Oxidation States of Metals in Complexes; π-Bonding in Soft-Soft Interactions; π-Bonding and *trans*-Influence, *trans*-Effect in Kinetics; π-Bonding and *cis*-Effect in Kinetics; π-Bonding and Isomerism in Coordination Compounds

10.8 Structure of Covalent Molecules: Molecular Topologies 824

Helferich's Rule; Concept of Hybridisation and Bent's Rule; Sidgwick-Powell Theory and Valence Shell Electron Pair Repulsion (VSEPR) Theory; Shape of the Molecules Having Stereochemically Active Lone Pairs Predicted from VSEPR Theory; Concept of Stereochemically Active and Inactive Lone Pairs; Structure of XeF_6 and Related Species; Limitations of VSEPR theory

10.9 Stereochemically Nonrigid Covalent Molecules : Fluxional Molecules 848

Atomic Inversion in Amines, Phosphines and Arsines; Berry Pseudorotation and Turnstile Rotation; Twisting Mechanism; Fluxional Molecule : Fluxionality and Time Scale of

Click Here for the Chemistry Library

Observation; ^{19}F-*NMR* Spectra and Fluxionality of PCl_2F_3 and ClF_3; Examples of Fluxional Molecules

10.10 Nucleophilic Substitution Reactions (e.g. Solvolysis) in Some Covalent Molecules of Nonmetals **861**

Thermodynamic and Kinetic Aspects of Chemical Reactions; Reaction Pathways of Nucleophilic Substitution Reaction; Energetics of *A* and *D* Processes; Some Representative Nucleophilic Substitution Reactions in Covalent Compounds of *p*-Block Elements; Some Representative Redox Reactions through Nucleophilic Substitution Reactions

10.11 Structure of Covalent and Molecular Crystalline Solids **884**

Diamond Cubic (*dc*) Structure; Graphite Structure; Properties of Graphite; Lamellar or Intercalation Compounds of Graphite; Reactivity of Graphite; Band Structure of Graphite; Comparison Between Graphite and Inorganic Graphite (i.e. Boron Nitride); Molecular Crystals; Buckministerfullerene; Carbon Clusters and Allotropic Forms of Carbon

10.12 Structure and Bonding in Higher Boranes and Carboranes **896**

Classification and Different Series of Boranes; Nomenclature of Boranes; Structure and Molecular Framework of Hydrides of Boron; Skeletal Electron Pair Counting and Wade's Rules : Polyhedral Skeletal Electron Pair Theory (PSEPT); Calculation of the Number of Electron Deficient Bonds; *stxy* Numbers and Topology of Boron Hydrides; Molecular Orbital Picture of Higher Boranes; Carboranes and their Structural Features; Calculation of Skeletal Electron Pairs (S) in Carboranes; Jemmis' Unifying Electron Counting Rule for Condensed Polyhedral Boranes

10.13 Synthesis and Reactivity of Boranes and Carboranes **917**

Synthesis of Boranes; Reactivity of Boranes; Synthesis and Reactivity of Carboranes

10.14 Molecular Symmetry and Point Groups **931**

Introduction; Symmetry Elements and Symmetry Operations; *n*-Fold Rotation Axis (i.e. *n*-Fold Proper Axis of Rotation) (C_n) and Rotation About a Symmetry Axis; Plane of Symmetry (i.e. Mirror Plane) and Reflection at the Plane of Symmetry; Inversion Centre (i.e. Centre of Symmetry) and Reflection Through the Inversion Centre; *n*-Fold Rotation-Reflection Axis and Rotation-Reflection (in either order); Identity Element (E or I); Point Groups and Identification of Point Groups; Special Point Groups with Multiple High-order Axes (more than one C_n, $n > 2$); Steps to Select a Point Group (excluding the special point groups with multiple high order axes); Symmetry Elements and Optical Activity; Symmetry Elements and Dipole Moment; Symmetry Number and Point Groups

Exercise–X **962**

Appendix 10A : Fluoroalkyl Radicals and Carbocations and Fluorocarbenes **972**

11. Structure, Bonding and Properties of Ionic Solids and Solid State Chemistry 977–1109

11.1 Characteristic Properties of Ionic Compounds **977**

11.2 Different Types of Ions and Electronic Configurations of the Ions Involved in Ionic Bonding **980**

Click Here t.me/thealchemylibrary

11.3 Electron Density (ED) Maps and Ionic Radii 982
Ionic Radii from X-Ray Electron Density Maps: Ionic Radii from Other Methods; Shannon's Crystal Radii; Comparison among Shannon's Crystal radii, Goldschmidt's Radii and Pauling's Radii

11.4 Factors Affecting the Ionic Radii 989

11.5 Energetics of Ionic Bond Formation: Born-Haber Cycle 994
Born-Haber Cycle in Ionic Bond Formation; Drawbacks in the Concept of Born-Haber Cycle; Factors Favouring the Formation of Ionic Bonds

11.6 Applications of Born-Haber Cycle 997

11.7 Theoretical Aspects of Crystal Forces: Lattice Energy of Ionic Crystals 1003
Born-Lande Equation of Lattice Energy; Verification of the Born-Lande Equation; Modification of the Born-Lande Equation; Kapustinskii Equation; Factors Affecting the Lattice Energy; Hardness of Ionic Compounds

11.8 Radius Ratio Rule and Preferred Structures of Ionic Compounds 1014
Limiting Radius Ratios for Some Common Geometries; Application of the Radius Ratio Rule; Limitations of the Radius Ratio Rule

11.9 Some Basic Crystal Geometries (i.e. Unit Cells) Involved in the Structure of Crystalline Solids 1024
Simple Cubic (*sc*) Unit Cell; Body Centred Cubic (*bcc*) Unit Cell; Face Centred Cubic, (*fcc*) Unit Cell; Diamond Cubic (*dc*) Unit Cell; Graphite Layer Lattice; Close Packing Models of Spheres; The Body Centred (*bcc*) Lattice in Terms of Close Packing of Spheres; Characteristic Features of *hcp*, *fcc* and *bcc* Structure

11.10 Structures of Ionic Crystals 1035
Structures of Ionic Crystals of AB Type; Structures of Ionic Crystals of AB_2 Type; Structures of Ionic Crystals of AB_3 Type; Structure of Ionic Crystals of A_2B_3 Type: Corundum (6:4 Coordination Crystals); Structure of Ionic Crystals Consisting of Polyatomic Ions; Comparison of the Basic Ionic Crystals

11.11 Structures of Mixed Metal Oxides 1042
The Spinel and Inverse Spinel Structure; The Ilmenite Structure ($FeTiO_3$); The Perovskite Structure ($CaTiO_3$); Mixed Oxides – Coloured Minerals and Gem Quality Crystals

11.12 Crystal Structure in Relation to Superconductivity and Ferroelectric Property 1047
$YBa_2Cu_3O_{7-x}$; $BaTiO_3$

11.13 Deviations from Simple Ionic Structures 1049
Layer Lattices (i.e. Two Dimensional Lattices); Chain Lattices (i.e. One Dimensional Lattices)

11.14 Structures of Silicates and Isopoly and Heteropoly Acids : Representative Examples of Complex Ionic Crystal 1051
Chemistry of Silicates and Cement; Isopoly and Heteropoly Acids

Click Here to me/thealchemylibrary

11.15 Crystal Defects in Ionic Solids 1063
Stoichiometric (i.e. Intrinsic) Defects; Nonstoichiometric (or Berthollide) (i.e. Extrinsic) Defects

11.16 Magnetic Materials : Magnetic Properties 1076
Terminology in Describing the Magnetic Properties and Different Units; Classification of Magnetic Substances; Cooperative Magnetism – Aniferromagnetism, Canted Magnetism; Ferrimagnetism and Ferromagnetism; Magnetic Properties of Metals; Temperature Dependence of Magnetic Susceptibility of Different Types of Magnetic Materials

11.17 Properties of Ferroelectric Materials and Piezoelectric Materials 1088
Ferroelectric Materials; Piezoelectricity and Piezoelectric Materials

11.18 Carbides 1091

11.19 Glasses and Glass Transition 1092

11.20 Structure of Liquids : General Aspects : Hole Theory of Liquids 1094

Solved Numerical Problems 1095

Exercise-XI 1102

Appendices A-1–A-12

Appendix I: Units and Conversion Factors A-1

Appendix II: Some Physical and Chemical Constants A-4

Appendix III: Wavelength and Colours A-5

Appendix IV: Names, Symbols, Atomic Numbers and Atomic Weights of the Elements A-6

Appendix V: Some Useful Mathematical Relationships A-8

Appendix VI: Books Consulted A-11

Index I-1–I-20

VOLUME 3

12. Bonding in Metals and Metal Clusters: Electrical Conductivities of Solids: Semiconductors and Superconductors 1110–1249

12.1 General Properties of Metals 1110

12.2 Crystal Structure of the Metals and the Effects of Lattice Structure on their Properties 1111

12.3 The Free Electron Theory of Metallic Bonding 1114
Drude-Lorentz Classical Free Electron Theory : Electron Sea Model; Sommerfeld's Quantum Mechanical Free Electron Theory and Fermi Dirac Distribution Function; Quantitative Aspects of Some Properties of Metals; Electrical Conductivity and Hall-Effect

Click Here to me/healchemylibrary

12.4 The Bloch Theory (i.e. Zone Theory) of Metallic Bonding 1131
Basic Concepts of Bloch Theory; Brillouin Zone, Forbidden Zone and Conductivity

12.5 Molecular Orbital Theory or Band Theory of Metallic Bonding 1136
Formation of Energy Bands and Brillouin Zones; Band Structure of Nontransition Metals; Band Structure of Transition Metals; Valence and Conduction Bands; Explanation of Electrical Conductivities of Solids in the Light of Band Theory; Optical Properties of Solids in the Light of Band Theory; Magnetic Properties Including the Temperature Independent Paramagnetis (TIP) (i.e. Pauli Paramagnetism) of the Metals in Terms of Band Theory; Ferromagnetism in Transition and Inner-transition Metals; Band Structure of Some Inorganic Solids and their Properties

12.6 Valence Bond Approach of Metallic Bonding 1154
Valence Bond Approach for the Short Period Metals; Valence Bond Approach for the Long Period Metals; Merits of the Valence Bond Approach; Demerits of the Valence Bond Theory

12.7 Solid Solutions : Alloys : Intermetallic Compounds 1156
Interstitial Alloys; Substitutional Alloys, Intermetallic Compounds and Hume-Rothery Rule

12.8 Metal-Metal Bonds in Metal Clusters 1161
Binuclear Compounds; Trinuclear Compounds; Octahedral Clusters; Chevrel Phase; Octahedral Metal Cluster; Carbonyl Clusters; Metal-only Clusters (Zintle Cluster Ions); Metal-Metal Bonds in Stacked Polymeric Structure; Conditions for Metal-Metal Bonding

12.9 Semiconductors and their Properties in the Light of Band Theory 1181
Characteristic Features of Intrinsic Semiconductor; Characteristic Features of Extrinsic or Doped Semiconductors; Temperature Dependence of Semiconductor Conductivity; Optical Properties of Solids; Uses of Semiconductors : Direct and Indirect Gap Semiconductors; Some Useful Semiconductor Materials and their Properties; Characteristics of *p–n* Junctions; Characteristic Features of *p-n-p* and *n-p-n* Junction Transistors; Some Applications of Semiconductor Devices

12.10 Semiconductivity and Metallic Conductivity of Metal Oxides : Hopping Mechanism of Conductivity 1209

12.11 Electrical Conductivity in One Dimensional Solids : Peierls Distortion 1214
Electrical Conductivity in KCP [Ptossium tetracyanoplatinate(II)] and Peierls Distortion; Electrical Conductivity in Polythiazyl $(SN)_x$ (i.e. $^{1}_{\infty}[SN]$ – a one dimensional metal); Electrical Conductivity in *trans*-Polyacetylene $(C_2H_2)_x$ or $(CH)_x$ – an Organic Semiconductor

12.12 Conducting Organic Substances : Organic Metals, Organic Semiconductors, Molecular Inorganic Superconductors 1218
Introduction; Some Representative Examples of Organic Salts as Conducting Substances: Organic Superconductors

12.13 Superconductivity 1222
Concept of Superconductivity; Characteristic Features of Superconducting Materials; BCS Theory of Superconductivity; Superconducting Materials; Structural Features of Some Copper-containing Superconducting Ceramic Materials (Warm Superconductors); Application of Superconductivity

Click Here to me/freedchemylibrary

12.14 **Electrical Conductivity of Solid Electrolytes** 1232
Solved Numerical Problems 1236
Exercise–XII 1241

13. Hydrogen Bonding and Other Weaker Chemical Forces Including Supramolecular Systems 1250–1342

13.1 **Hydrogen Bonding** 1250
Types of Hydrogen Bonding Depending on the Nature of Electron Clouds on Donor (D); Types of Hydrogen Bonding Depending on the Position of Donor (D); Participation of *C–H* Bonds in *H*–Bonding; Symmetrical and Unsymmetrical Hydrogen Bonding; Hydrogen Bond Energy and Bond Length; Effects of Intermolecular *H*-Bonding; Effects of Intramolecular *H*-Bonding; Detection of *H*-Bonding; Theories of Hydrogen Bonding; Agostic Interaction *vs*. Hydrogen Bonding Interaction; Comparison among *H*-bridge Bond, *H*-Bond and Agostic Interaction

13.2 **Hydrates and Clathrates or Cage Compounds** 1279
Hydrates; Clathrates or Cage Compounds; Configurational Entropy and Thermodynamic Aspects of Clathrate Compounds

13.3 **The Nature of Intermolecular Forces : van der Waals Forces : Lennard-Jones Potential: The 6-12 Potential** 1285
The Attractive Intermolecular Forces; Total Intermolecular Attractive Forces (van der Waals Forces); The Repulsive Intermolecular Forces; Lennard-Jones Potential

13.4 **Interaction Between Ionic and Covalent Compounds** 1295
Ion-Dipole Interaction; Ion-Induced Dipole Interaction; Metal-Ligand (neutral) Interaction in Terms of Ion-Dipole Interaction and Polarisation of the Metal Ions and Ligands; Hard-Hard Interaction (Electrostatic Interaction) and Soft-Soft Interaction (Mutual Polarisation)

13.5 **Noncovalent Interactions in Supramolecular Systems and Molecular Recognition** 1298
Interactions in Supramolecules; The Lock and Key Principle in Supramolecular Assemblies; Representative Examples of Supramolecular System; Double Helical Structure of DNA; Macrocyclic Systems (Synthetic Molecular Receptors for Cations); Molecular Recognition of Specific Metal Ions by Macrocyclic Systems; Crown Ethers as Receptors; Spherical Recognition of Metal Ions; Molecular Recognition of NH_4^+ and RNH_3^+ (Primary Alkyl Ammonium Cation) by [18]-Crown-6; Selective Perching or Nesting of NH_4^+ or RNH_3^+ on Crown-6; Cryptands; Synthetic Molecular Receptors for Different Types of Substrates – Cations, Anions, Neutral Molecules; Application of Macrocyclic Crown Ethers and Cryptands; Polyazamacrocycles and Polyazacryptands as Anion Receptors (Synthetic Receptors); Molecular Recognition by Macrocyclic Systems; Calixarenes as Receptors; Cyclodextrins (CDs) as Natural Receptors; Cyclophanes as Synthetic Receptors for Apolar Guests; *H*-Bond Directed Molecular Assembly; Metal Coordinated Self-assembly; Molecular Switch; Catenanes and Rotaxanes; Inverse Crown Ethers : Novel Anion Receptors

13.6 **Energetics of Dissolution** 1324
Thermodynamic Aspects and Conditions of Dissolution; Born Equation and Ion Solvation; Energetics of Solubilities of Ionic Salts in Polar Solvents; Solubilities of Ionic Salts in

Click Here to the/thealchemylibrary

Nonpolar Solvents; Solubilities of Nonpolar Solutes in Nonpolar Solvents; Solubilities of Nonpolar Solutes in Polar Solvents

13.7 Energetics of Phase Transitions – Melting, Boiling, Sublimation 1332
Phase Transition in Covalent Compounds; Ionic Compounds; Ionic-Covalent Compounds (i.e. Fajans Type Compounds); Ease of Phase Transition Depending on the Nature of Involved Chemical Forces

Exercise–XIII 1336

14. Acids and Bases and Ionic Equilibria in Aqueous Solutions 1343–1554

14.1 Definitions of Acids and Bases 1343

14.2 Arrhenius Theory of Acids and Bases 1343

14.3 Brönsted-Lowry Concept: The Proton Donor-Acceptor Concept: Protonic Concept : The Conjugate Acid-Base Theory 1344
Basic Concepts of Brönsted-Lowry Theory; Relative Strength of Acids and Bases : Differentiating and Levelling Solvents in the Light of Brönsted-Lowry Concept; Merits of the Brönsted-Lowry Concept; Limitations of the Brönsted-Lowry Concept; Cosolvating Agents and Acid-Base Strength; Application of Brönsted-Lowry Concept in Calculating pH of Aqueous Solutions : A Generalised Approach to Calculate the *pH* Values of Different Types of Aqueous Solutions; Acid-Base Behaviour of Amino Acids in Aqueous Solution: Isoelectric Point; The Chemistry of Proton in Water: Proton Transport Process

14.4 Mechanism of Buffer Action: Buffer Capacity 1370

14.5 Selection of Acid-Base Indicators in Acid-Base Titrations 1372

14.6 Hammett Acidity Function: Superacids 1382
Concept of Hammett Acidity Function (*H*); Concept of Superacids and Examples of Superacids; Application of Superacids

14.7 The Lewis Concept: The Electron Pair Donor-Acceptor System 1386
Basic Concepts and Characteristic Features of the Lewis Theory; Different Types of Lewis Acids; Classification of the Lewis Bases; Lewis Acid-Base Reactions and Redox Reactions; Some Typical Examples of Lewis Acids and Bases, Lewis Acid-Base Adducts; Covalent and Ionic Contributions in the Stabilities of the Adducts : Drago-Wayland Equation; Demerits of Lewis Acid-Base Theory; Solvent Properties in the Light of Lewis Acid-Base Concept; Change of Bond Length in Lewis Acid-Base Interaction

14.8 Strength of Brönsted (i.e. Protonic) Acids and the Governing Factors Involved and the Properties of Brönsted Acids and Bases 1414
Strength of Different Protonic Acids and Conjugate Acids of Some Bases; Born-Haber Cycle and Thermodynamic Parameters to Determine the Acid Strength: Acid Strength of Hydracids and Carboxylic Acids : Gas Phase Acidity; Factors Governing the Strength of Oxyacids; Hydrolysis and Aqua Acid Strength of Metal Ions in the Light of Brönsted-Lowry Concept; Basicity of the Anions; Periodic Variation of Acidic and Basic Character; Nucleophilicity and Basicity; Acid and Base Catalysis

Click Here t.me/neetchemylibrary

14.9 Some Important Factors Governing the Acid-Base Strength (both Brönsted and Lewis Acid-Base Systems) 1437
Inductive Effect : Entropic Effect, *d*-Orbital Participation; State of Hybridisation of the Central Atom; Steric Factors : *F*-Strain and *B*-Strain; Solvation Effects (cf. *H*-bonding); Resonance and π-Bonding and the Possibility of *d*-Orbital Participation in the Reacting Species; Effect of Resonance Stabilisation in the Product; Effect of *H*-Bonding on Acid Strength

14.10 Lux-Flood Concept 1466

14.11 Solvent System Definition 1468

14.12 Usanovich Concept 1472

14.13 A Generalised Concept of Acids and Bases 1472

14.14 Concept of Ultimate Acids and Bases 1472

14.15 Hard and Soft Acids and Bases (HSAB) 1473
Basic Concept and Principle of Hard and Soft Acids and Bases (HSAB) Theory; Basis of Classification of the Acids and Bases as Hard or Soft; Characteristics of Hard and Soft Species; Symbiosis in Hardening or Softening a Centre; Acid-Base Strength versus HSAB Principle; Application of HSAB Principle; Theoretical Background of HSAB Principle

14.16 Surface Acids and Solid Acids : Heterogenous Acid-Base Reactions 1492

14.17 Aqueous Solutions of Salts : Hydrolysis of Salts : Solubility Product of Sparingly Soluble Salts 1494
Hydrolysis of Salts; Solubility Product and Activity Product of Sparingly Soluble Salts; Application of the Principle of Solubility Product

Solved Numerical Problems 1510

Exercise–XIV 1541

15. Nonaqueous Solvents 1555–1576

15.1 Introduction 1555

15.2 Classification of Solvents 1555

15.3 Characteristics of Ionising Solvents 1556

15.4 Liquid Ammonia as a Solvent 1558

15.5 Liquid Hydrogen Fluoride as a Solvent 1564

15.6 Liquid Hydrogen Cyanide as a Solvent 1565

15.7 Acetic Acid (CH_3CO_2H) as a Solvent 1566

15.8 Sulfuric Acid as a Solvent 1567

15.9 Fluorosulfonic Acid (HSO_3F) as a Solvent and Superacids 1568

15.10 Liquid Sulfur Dioxide as a Solvent 1569

15.11 Bromine Trifluoride as a Solvent 1570

15.12 Oxyhalides as Solvents 1571

15.13. Molten Salts (i.e. Ionic Liquids) as Solvents 1572

Exercise–XV 1575

Click Here t.me/theaicentrylibrary

16. Redox System and Electrode Potential: Application of Electrode Potentials: Electroanalytical Techniques 1577–1783

16.1 Some Preliminary Aspects of Redox Reactions 1577

Ion Electron Method of Balancing Redox Reactions; Oxidation Number and Rules for Calculating Oxidation Number; Oxidative Addition and Reductive Elimination Reaction; Equivalent Weights of Oxidants and Reductants; Complementary and Noncomplementary Redox Reactions; Redox and Acid-Base Reactions; Disproportionation and Comproportionation Reactions

16.2 Electrode Potentials: Standard Potentials 1596

Electrical Double Layer and Genesis of Electrode Potential; Determination of Electrode Potential; Standard Electrode Potential : Nernst Equation: Stoichiometric Standard Potential and Formal Potential : Concept of *pE*; Sign Conventions of the Electrode Potentials; Standard Electrode Potentials of Metals and Electrochemical Series; Standard Reduction Potentials; Reversible Chemical Cells : Cells with and without Transference; Galvanic vs. Electrolytic Cell: Ohmic Potential and Observed Cell *emf*

16.3 Formal (Conditional) Potentials (cf. Conditional Stability Constant vs. Thermodynamic Stability Constant) 1607

16.4 Effects of Different Factors on Electrode Potential: Application of Such Effects in Analytical Chemistry 1610

Effects of *pH* on Electrode Potentials due to the Participation of H^+ or OH^- in Electrode Process (cf. Pourbaix diagrams); Effects of *pH* on Electrode Potentials due to the Formation of Sparingly Soluble Hydroxo-species (cf. Pourbaix diagrams); Effects of Precipitation (other than hydroxides) on Electrode Potentials; Effects of Complexation on Electrode Potentials; Chemistry of Aqua Regia and Dissolution of Noble Metals : Enhancement of Oxidisability of Metals through Complexation; Attack of Noble Metals by *HF* and by a Mixture of *HF* and HNO_3 : Enhancement of Oxidisability of Metals through Complexation; Dissolution of Antimony by a Mixture of Nitric Acid and Tartaric Acid : Enhancement of Oxidisability of Metals through Complexation

16.5 Periodic Trends of Electrode Potential 1640

Variation of Standard Oxidation Potential of the Metals; Variation of Oxidising Power of the Oxyanions in a Group

16.6 Function of Zimmermann-Reinhardt Solution (in Titrating *Fe*(II) by $KMnO_4$ in the Presence of Chloride) 1643

16.7 Instability of Some Species in Aqueous Solution 1644

16.8 EMF Diagrams 1647

Latimer Diagram; Frost Diagrams (Ebsworth Diagram); Pourbaix Diagram or Potential-*pH* (*E*–*pH*) Diagram

16.9 Equilibrium Constant from the Standard Electrode Potentials 1661

16.10 Disproportionation and Comproportionation Reactions 1663

16.11 Potential Profile in a Redox Titration 1672

16.12 Selection of a Redox Indicator 1677

16.13 Potentiometric Titrations 1680

Click Here : /medicinelibrary

16.14 Practical Applications: Electrochemical Cells and Batteries — Primary Cells, Secondary Cells, Fuel Cells : Corrosion 1686
Basic Requirements of an Electrochemical Cell to Act as a Power Source; Representative Examples of Primary and Secondary Cells; Some Representative Fuel Cells; Electrochemistry of Corrosion; Electrolytic Cell vs. Galvanic Cell : Electrolysis of Solutions and Electrodeposition; Decomposition Voltage of Electrolysis and Electrolytic Separations of Metals; Some Other Practical Applications of the Knowledge of Electrode Potential

16.15 Kinetic Factors in Electrode Process and Electron Transfer Reactions 1704
Importance of Kinetic Factors; Importance of Overpotential (in Electrode Process and Cell Potential): Tafel Equation; Redox Reactions Through Electron Transfer; Redox Reactions Through Atom Transfer

16.16 Photochemical Reactions: Photoredox Reaction and Photochemical Splitting of Water 1708
Some Representative Photochemical Reactions Illustrating the Characteristic Features; Photochemical Splitting of Water and Photochemistry of $Ru(bpy)_3^{2+}$; TiO_2, an Important Photocatalyst; Direct Photochemical Reduction of Dintrogen; Charge Transfer Band and Redox Stability

16.17 Ellingham Diagram: Reduction of Metal Oxides : Carbon - A Potential Reducing Agent 1719

16.18 Hydrometallurgy 1722

16.19 Electrode Potentials in Nonaqueous Systems 1723

16.20 Examples of Some Common Catalysed Redox Reactions 1724

16.21 Redox Activity in Relation to Explosive Action 1726

16.22 Chemistry of Some Important Electroanalytical Techniques 1727
Polarographic Method of Analysis; Cyclic Voltammetry (CV); Amperometric Titration; Coulometric Analysis

Solved Numerical Problems 1752

Exercise–XVI 1763

Numerical Problems 1770

Appendix 16A: Chemistry of Explosives 1773

Appendix 16B: Chemical Clock Reactions: Oscillating Reactions 1777

Appendices A-1–A-12

Appendix I: Units and Conversion Factors A-1

Appendix II: Some Physical and Chemical Constants A-4

Appendix III: Wavelength and Colours A-5

Appendix IV: Names, Symbols, Atomic Numbers and Atomic Weights of the Elements A-6

Appendix V: Some Useful Mathematical Relationships A-8

Appendix VI: Books Consulted A-11

Index I-1–I-18

Click Here to the/thealchemylibrary

1

Classical and Vector Models of Atoms

Click Here t.me/healchemylibrary

1.1 CATHODE RAYS AND ELECTRON

1.1.1 Electric Discharge through Gases and Production of Cathode Rays

Studies on the experiment of electrical discharge through different gases at a low pressure with a high potential gradient have gifted us a lot of fundamental information to the foundation of modern physics.

The cylindrical discharge tube made of glass consists of two metallic electrodes sealed to its two ends and a side tube is connected to a high vacuum pump and a pressure gauge. The cathode is connected to the negative terminal and the anode or anticathode is connected to the positive terminal of a source of high potential such as an induction coil to provide a potential gradient of the order of 350 volts/cm or more. When the pressure within the tube lies in the order of 1 mm of Hg, there will be a fine glow around the cathode followed by a dark space called ***Crookes dark space.*** Then there is an another glow called ***negative glow*** followed by the ***Faraday dark space***. The rest of the tube contains ***striations of positive glow*** up to the anode. When the pressure is brought to about 0.01 mm of *Hg*, in the presence of a high potential gradient, the Crookes dark space extends and the walls of the tube show glowing. It was established that the glowing was caused by some radiation coming from the cathode to impinge on the opposite walls. This radiation was termed as ***cathode rays.***

1.1.2 Properties of Cathode Rays

The nature of these rays was extensively investigated by J. Hittorf (1869), William Crookes (1870), J. Perrin (1895) and J.J. Thomson (1897). Some of the important properties are mentioned here.

i. The properties of the cathode rays are independent of the nature of the gas present in the discharge tube or the nature of cathode.
ii. They travel in straight lines perpendicular to the surface of the cathode.
iii. They possess momentum and kinetic energy by virtue of which they can cause a mechanical motion in small paddle wheels placed in their path of travelling.

iv. These are deflected by electric and magnetic fields. The mode of deflection indicates that *they consist of minute particles carrying negative charges*. These particles are named electrons.
v. They can produce ionisation in gases.
vi. They can produce fluorescence when incident on the glass walls of the discharge tube. Zinc sulphide also becomes fluorescent when placed in the path of the cathode rays.
vii. They can affect the photographic plates.
viii. They can produce *X-rays* on striking matter. Generally, they are allowed to impinge on a metallic target called *anticathode* and *X-rays* are emitted.

1.1.3 Determination of Charge to Mass Ratio (e/m) of an Electron by Thomson's Method

Apparatus : In Thomson's (1897) method, *e/m* is determined by subjecting a narrow beam of cathode rays produced in a discharge tube to the simultaneous action of electric and magnetic fields acting mutually at right angles. A schematic diagram of Thomson's discharge tube is shown in Fig. 1.1.3.1a. It consists of an evacuated discharge tube made of glass in which cathode rays are generated from the cathode (C) which is a small aluminium disc. The anode (A) is placed in a side tube. The cathode ray passes through two narrow brass slits (S_1 and S_2) which provide a narrow beam of rays which falls on the screen (BB') made of fluorescent materials like zinc sulphide or barium platinocyanide. The electrical field is applied through two plates (E_1 and E_2) fitted parallel to the path of the rays. A magnetic field is applied perpendicular to the electrical field by placing a strong electromagnet very close to the plates (E_1 and E_2) but outside the tube. The electric and magnetic fields are arranged to act in opposition to the cathode rays.

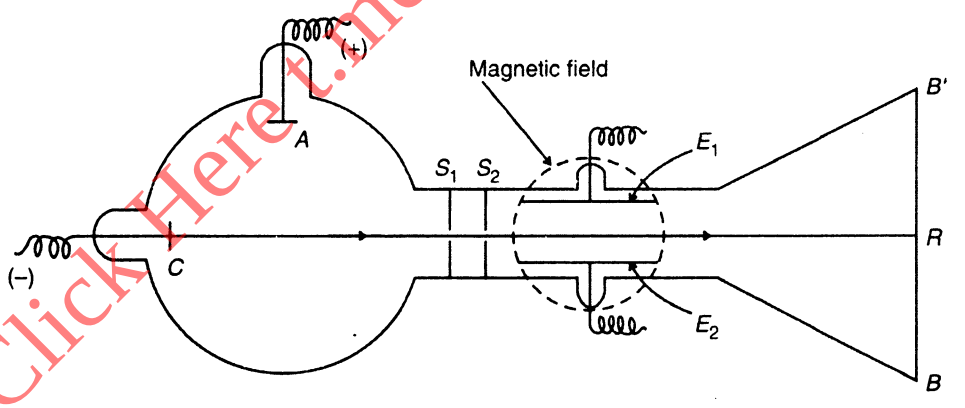

Fig. 1.1.3.1a. Thomson's experimental arrangement for the determination of *e/m* of cathode rays.

Working principle : To find the ratio, *e/m*, the deflection produced either by the magnetic field or electric field alone is to be measured. If the magnetic field is applied alone, the force on the particles leads the beam to travel in a circular path (Fig. 1.1.3.1b). On leaving the magnetic field, the beam will travel along the tangent to the circle at Q. In the case of the orbital (i.e. circular) motion of the particle in a circular path, the centrifugal force ($= mu^2/r$, u = velocity and r = radius of the path) is balanced by the centripetal magnetic force ($= Heu$, H = magnetic field strength). Thus,

$$\boxed{mu^2/r = Heu; \text{ or, } e/m = u/Hr} \qquad \ldots(1.1.3.1)$$

Click Here t.me/theallchemylibrary

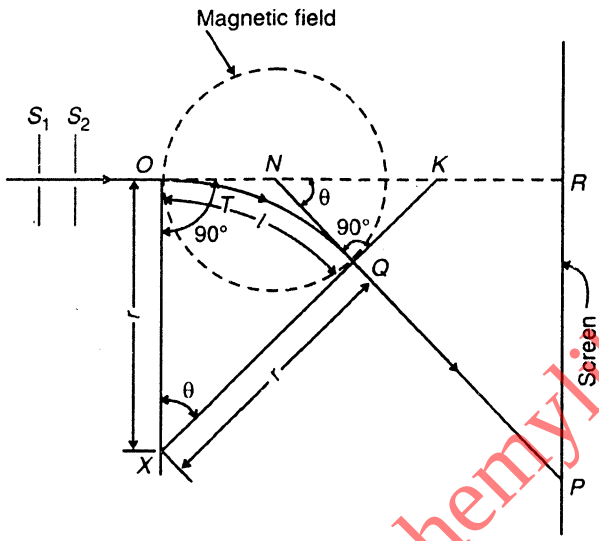

Fig. 1.1.3.1b. Motion of the cathode ray particles in a magnetic field in Thomson's experimental arrangement.

Knowing the values of u, r and H, the ratio e/m can be obtained.

Determination of u **:** Both the fields acting at the right angle are applied and they are adjusted in such a way that the beam remains undeflected and falls on the screen at R (Fig. 1.1.3.1a). Thus the downward magnetic force (= Heu) becomes equal to the upward electrical force (= Ee) acting on the electron. Thus, $Ee = Heu$; or, $u = E/H$ where E is the potential gradient between the plates E_1 and E_2 separated by d under the potential difference V. Hence,

$$u = \frac{V/d}{H} \text{ as, } E = V/d; \text{ or, } u = V/(dH) \qquad \ldots(1.1.3.2)$$

Determination of r **:** By considering Fig. 1.1.3.lb, r can be calculated when the deflection occurs due to the magnetic field alone. After passing through the slits (S_1 and S_2) the narrow beam enters into the magnetic field at O and leaves at Q. The circular path described by the electron due to the magnetic field is represented by OTQ having radius r (= $XO = XQ$). At Q, it runs in a straight line and falls on P. The deflection angle is shown by θ.

From Fig. 1.1.3.1b, $\theta = \angle QNR = \angle QXO$; and $\tan\theta = \frac{OK}{OX} = \frac{RP}{NR}$; (by considering the triangles, ΔOXK and ΔNRP) or, $\frac{OK}{r} = \frac{RP}{NR}$; or, $\frac{OTQ}{r} = \frac{RP}{NR}$; ($OK \approx OTQ$, length of the circular path travelled in the magnetic field)

$$\text{or, } l/r = RP/NR \qquad \ldots(1.1.3.3)$$

RP (vertical deflection) can be easily obtained from the screen. OTQ (= l), length of the magnetic field and NR (distance between the centre of the magnetic field and R) are constants for a particular apparatus and very often supplied by the makers of the apparatus.

Click Here t.me/thealchemylibrary

Equations 1.1.3.2 and 1.1.3.3 give the values of u and r respectively and by using these values, e/m is calculated from equation 1.1.3.1.

The following observations are found :

i. The value of e/m is independent on the nature of the gas in the tube and the materials of the cathodes. Thus the cathode ray particles (i.e. the electrons) are believed to be the fundamental particles. The average value of e/m is found 1.76×10^{11} coulombs/kg or $1.76\ 10^{7}$ emu/g or 5.2×10^{17} esu/g.

ii. The values of u are found to vary depending on the potential difference applied. It should vary between 1/5th to 1/10th of the velocity of light.

Drawbacks of the Thomson's method

i. The angle of deflection (θ) in the magnetic field measured by the vertical deflection (RP) on the screen is very small.

ii. All the electrons in the beam are not moving with identical velocities.

iii. When velocity of the electrons becomes comparable with that of light, the mass of the electron cannot be assumed to be constant.

According to the ***relativistic correction***, with the increase of the velocity due to the increased electrical field strength, the mass of the particle increases and e/m decreases. The change of mass is given by:

$$m = m_0/[1 - (u/c)^2]^{1/2}$$

where m_0 = rest mass of the electron, c = velocity of light. At lower velocities, the difference between m and m_0 is small but it increases with the increase of velocity. At $u = 1 \times 10^7$ m s^{-1} they differ by less than 0.05%, but at $u = 7 \times 10^7$ m s^{-1} they differ by about 3%; in fact, it was established by Kaufmann that e/m decreases with the increase of velocity and with the increase of potential gradient.

1.1.4 Determination of Charge of an Electron by Millikan's Oil-Drop Method

Apparatus : In 1909, R.A. Millikan developed his famous oil-drop experiment for the determination of charge of an electron. A schematic diagram of his experimental arrangement is shown in Fig. 1.1.4.1. It consists of a chamber maintained at a constant temperature. It is connected to a vacuum pump and a manometer. Out of the two metallic parallel plates (A and B), the upper one having a hole (C) is connected to a high voltage battery. The lower plate (B) is grounded. An atomiser (D) which sprays a nonvolatile oil into droplets is fitted in the vicinity to the hole. When an oil-droplet enters into the space between A and B through the hole (C), the hole can be closed to prevent the entry of further droplets. The residual air in the space between A and B can be ionised by using a beam of X-ray passing through the window (W_1). When the

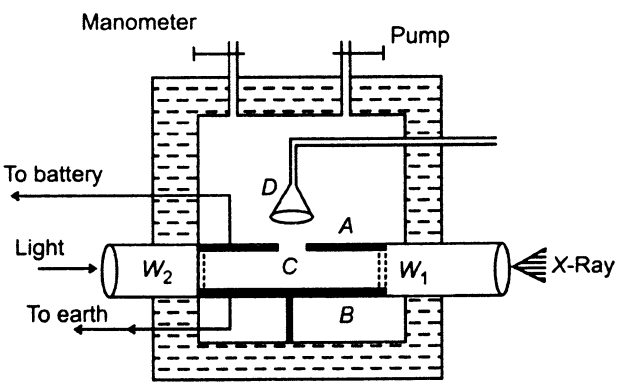

Fig. 1.1.4.1. Experimental arrangement of Millikan's oil drop method for the determination of charge (e) of an electron.

Click Here to me/thealchemylibrary

oil-droplet enters into the space, it gets charged in the ionised gaseous media and its movement due to the gravity and electrical field can be followed through a telescope fitted in the window (W_2) through which a powerful beam of light enters to illuminate the droplet. In the absence of the electrical field, the charged droplet moves down but by the application of a high electric potential of the order of 5000-10000 V, the droplet can be made move upward. On being short-circuited, again the droplet moves down due to the gravity.

Working principle : In the absence of the electrical field, the **downward velocity** (u_0) of the droplet is proportional to mg, i.e.

$$u_0 \propto mg \qquad \ldots(1.1.4.1)$$

where m = mass of the droplet, and g = acceleration due to gravity.

During the **upward velocity** (u_2), the electrical field strength (E) and gravity act mutually in opposition. Hence, u_2 is proportional to $(neE - mg)$, i.e.

$$u_2 \propto (neE - mg),\ neE > mg \qquad \ldots(1.1.4.2)$$

where e = charge of an electron, n (integers) denotes the number of electrons captured by the droplet. In fact in the presence of the electrical field, the droplet will be moving upwards, if, $neE > mg$ and it will move downwards, if, $mg > neE$. Here we shall consider the **condition for upward movement**, i.e. $neE > mg$.

If the separation between the plates is d and the potential difference applied to them is V, then, $E = V/d$. From Eqns. 1.1.4.1 and 1.1.4.2, we get;

$$\frac{u_0}{u_2} = \frac{mg}{neE - mg}\ ;\ \text{or,}\ \frac{t_2}{t_1} = \frac{mg}{neE - mg} = ;\ \text{or,}\ ne = \frac{mg}{E}\ (1 + t_1/t_2) \qquad \ldots(1.1.4.3)$$

where t_1 and t_2 are time taken by the droplet for the downward and upward movements between two fixed positions of cross-wires fitted in the telescope. If m is known, from Eqn. 1.1.4.3, ne can be calculated. n may have values 1, 2, 3, 4, ... ***This is why, the minimum value of ne gives the value of charge carried by an electron.***

Determination of m and r : If the oil droplet is considered to be a spherical one having radius r, its mass is given by: $m = (4/3)\pi r^3 \rho_0$ where ρ_0 gives the density of the oil.

Now **Stoke's law** can be applied for the falling droplet in a medium having viscosity coefficient η to calculate r. Here, the gravitational force (mg) acts in opposition to the buoyancy force (F_b) due to the displacement of equal volume of the medium having density ρ_m by the droplet.

Hence, the force of friction (F) is given by :

$$F = mg - F_b = (4/3)\pi r^3 g(\rho_o - \rho_m) \qquad \ldots(1.1.4.4)$$

According to Stoke's law,

$$F = 6\pi r \eta u_0 \qquad \ldots(1.1.4.5)$$

By considering Eqns. 1.1.4.4 and 1.1.4.5 (in the absence of the electrical field) we get :

$$u_0 = \frac{2r^2 g}{9\eta}(\rho_o - \rho_m) \qquad \ldots(1.1.4.6)$$

$$\text{and,}\ r = \left[\frac{9\eta u_o}{2g(\rho_o - \rho_m)}\right]^{1/2} \qquad \ldots(1.1.4.7)$$

Click Here t.me/thealchemylibrary

Now by considering the following two relations **(when *neE* > *mg*),**

$$(4/3)\pi r^3(\rho_o - \rho_m)g = 6\pi\eta r u_o \qquad \ldots(1.1.4.8)$$

and, $neE - (4/3)\pi r^3(\rho_o - \rho_m)g = 6\pi\eta r u_2$, u_2 = upward velocity $\qquad \ldots(1.1.4.9)$

We get Eqn. 1.1.4.10 by adding Eqn. 1.1.4.8. and Eqn. 1.1.4.9,

$$neE = 6\pi\eta r(u_2 + u_0) \qquad \ldots(1.1.4.10)$$

By using the value of r in the above equation, we get

$$ne = \frac{6\pi\eta^{3/2}}{E}\left[\frac{9u_o}{2g(\rho_o - \rho_m)}\right]^{1/2} \times (u_2 + u_o) \qquad \ldots(1.1.4.11)$$

Thus *ne* can be determined. *As n can have the minimum value one, the minimum value of ne gives the charge of an electron.*

For the small droplets of radius r comparable to the mean free path (λ) of the medium, Stoke's law should be modified and Eqn. 1.1.4.6 gets converted into:

$$u_o = \frac{2r^2 g}{9\eta}(\rho_o - \rho_m)\left(1 + A\frac{\lambda}{r}\right) \qquad \ldots(1.1.4.12)$$

where, A is a constant.

From Eqn. 1.1.4.12, r can be calculated and then m can be calculated as $m = (4/3)\pi r^3\rho_o$.
From Eqn. 1.1.4.3, we get :

$$ne = \frac{mg}{E}(1 + t_1/t_2) = \frac{4}{3}\frac{\pi r^3\rho_o g}{E}(1 + t_1/t_2) \qquad \ldots(1.1.4.13)$$

Taking the help of Eqn. 1.1.4.12, which gives the value of r, *ne* can be calculated from Eqn. 1.1.4.13.

Correction for variation in u_2 (when neE > mg) **:** Due to the attachment of different magnitude of charges (i.e. different number of electrons) at different times on the same drop under observation, its upward velocity u_2 changes very often during the observation.

Now, let us consider that its **upward velocity is u_2** when the attached charge is *ne*, and similarly for *n'e* charge, it is u_2'. Therefore:

$$\frac{u_o}{u_2} = \frac{mg}{ne \cdot E - mg}, \text{ (E stands for the potential gradient)}$$

$$\text{or, } ne = [(u_o + u_2)/u_o]\frac{mg}{E}; \text{ similarly for } u_2', \; n'e = [(u_o + u_2')/u_o]\frac{mg}{E}$$

$$\text{or, } (n - n')e = \frac{mg}{Eu_o}(u_2 - u_2')$$

where, $(n - n')$ can have values, ±1, ±2, ±3 and so on. Hence, the values of $(u_2 - u_2')$ obtained from a large number of observations must be some integral multiple (within the limits of experimental error) of a *minimum value.* This minimum value arises definitely due to the ±1 value of $(n - n')$. Thus, the charge (e) on the electron can be obtained from the following relation:

Click Here t.me/thealchemylibrary

$$\boxed{e = \frac{mg}{u_o E}(u_2 \sim u_2')_{\min}}$$

in which mg can be calculated as discussed earlier.

At the condition, mg > neE : Under the circumstances, even in the presence of the electrical field the droplet under consideration will move downwards with a slower speed (say, u_1) compared to u_0 (in the absence of the electrical field). Under this condition, we can consider the following relations:

$$(4/3)\pi r^3(\rho_o - \rho_m)g = 6\pi\eta r u_0, \text{ (cf. Eqn. 1.1.4.8)}$$

and,
$$(4/3)\pi r^3(\rho_o - \rho_m)g - neE = 6\pi\eta r u_1, \quad \ldots(1.1.4.14)$$

Subtracting Eqn. 1.1.4.14 from Eqn. 1.1.4.8 we get,

$$neE = 6\pi\eta r (u_0 - u_1) \quad \ldots(1.1.4.15)$$

We have:

$$r = \left[\frac{9\eta u_o}{2(\rho_o - \rho_m)g}\right]^{1/2}, \text{ (cf. Eqn. 1. 1.4.7; without considering the mean free path correction).}$$

Putting this value in Eqn. 1.1.4.15, we get :

$$ne = 6\pi \frac{\eta^{3/2}}{E}\left[\frac{9\eta u_o}{2(\rho_o - \rho_m)g}\right]^{1/2} \times (u_0 - u_1) \quad \ldots(1.1.4.16)$$

As in the case of u_2 (upward velocity in the presence of the electrical field), u_1 may vary for different sets of observation because of the same ground and in the same way, it can be shown that :

$$\boxed{e = \frac{mg}{u_0 E}(u_1 \sim u_1')_{\min.}}$$

where u_1 and u_1' are the downward velocities (in the presence of the electrical field) of the droplet at two different observations.

It was found from many sets of observation that the values of ne were the integral multiples (i.e. 1, 2, 3 ...) of the smallest value, 4.804×10^{-10} esu or 1.602×10^{-20} emu or 1.602×10^{-19} coulomb which is the charge carried by an electron.

Drawbacks of the Millikan's method

i. If the oil is not sufficiently nonvolatile, due to evaporation during the observation, the mass of the droplet will be changing.

ii. u_0 remains constant, if the same droplet is followed at each observation, but u_2 changes even for the same droplet. This occurs due to the attachment of different number of electrons to the droplet in different journies. This is why, the average value of t_1 remains more or less constant in different journies but t_2 varies significantly. To avoid this, application of a horizontal electrical field is preferred to the vertical one.

Mass of the electron : From the knowledge of e/m value (J.J. Thomson's experiment) and e value, mass of the electron can be calculated.

$$e/m = 1.759 \times 10^7 \text{ emu/g ; and } e = 1.602 \times 10^{-20} \text{ emu}$$

Click Here t.me/Realchemylibrary

It leads to $m = 9.108 \times 10^{-28}$ g or 9.108×10^{-31} kg.

It is very often called the *rest mass* (m_0).

Radius of the electron **:** Considering the electron to be a sphere of radius r, its electrostatic potential energy is given by e^2/r. According to the relativistic concept, its rest mass energy is given by m_0c^2. Now, rest mass energy = electrostatic potential energy, i.e.

$$m_0c^2 = e^2/r, \text{ (CGS system)}$$

$$\text{or, } r = \frac{e^2}{m_0c^2} = 2.82 \times 10^{-13} \text{ cm} = 2.82 \times 10^{-15} \text{ m.}$$

1.2. ANODE RAYS

1.2.1. Production of Anode Rays

In the discharge tube, by using a perforated cathode (Fig. 1.2.1.1) facing the anode, luminous rays were noticed behind the cathode by Goldstein (1886). The particles present in the rays were found to bear positive charges. These were called ***positive rays*** or ***canal rays*** as they passed through the canals or perforations in the cathode.

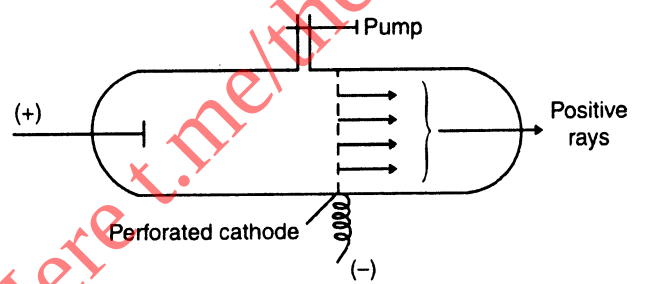

Fig. 1.2.1.1. Goldstein's discharge tube for the generation of positive rays.

1.2.2 Properties of Anode Rays

Some of the important properties are given as follows :

i. The anode rays start just behind the cathode and apparently the anode does not come into picture.
ii. The anode ray particles are positively charged and the masses are dependent on the nature of residual gas in the tube. To be more precise, the q/M (charge to mass ratio) values depend on the nature of gas.
iii. They travel in straight lines.
iv. Fluorescent materials respond to these rays.
v. The rays are deflected by both electric and magnetic fields and the direction of deflection is opposite to that of the cathode rays.
vi. The values of q/M for these rays are very low compared to that of the cathode rays and the values are dependent on the nature of the gas in the tube.

Click Here t.me/thealchemylibrary

vii. They can attack the photographic plate.

viii. Due to the much higher masses, the particles cannot move with a uniform velocity through the discharge tube while the lighter particles of the cathode rays travel with an almost uniform velocity.

ix. The maximum q/M value (about 1/1840 times that of an electron) is obtained when the residual gas is hydrogen. ***These particles are called protons.*** These are found as products in many nuclear reactions. These observations lead to the conclusion that these are also some other fundamental particles like the electrons in matter.

1.2.3. Analysis of Positive Rays by Thomson's Parabola Method

Apparatus : Fig. 1.2.3.1 represents a schematic sketch of Thomson's mass spectrograph. In the discharge tube, the cathode (C) is an aluminium rod pierced by an axial copper tube of very narrow diameter. The narrow tube acts as a slit to produce a very fine pencil of rays and it also separates the camera cell house from the discharge tube. The fluorescent screen (D) is placed in the camera cell house.

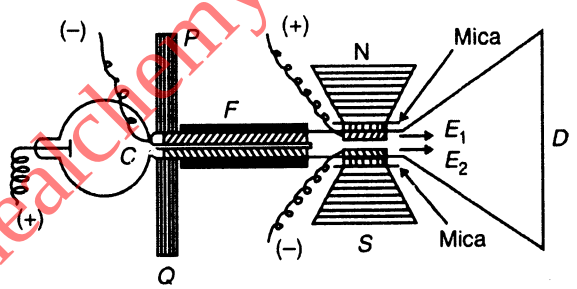

Fig. 1.2.3.1. Thomson's mass spectrograph.

The positive rays coming out of the copper tube pass through two parallel plates (E_1 and E_2) through which an electrical field can be applied. The pole pieces (N and S) of an electromagnet is placed just near the plates but separated by mica sheets. During the passing of rays through the copper tube, so that the rays cannot be affected by the electromagnet, it is surrounded by a soft iron tube (F). Similarly, the iron plate (PQ) protects the main discharge tube from the influence of the magnet.

Working principle : Here both the electrical and magnetic fields are mutually parallel and both the fields are perpendicular to the direction of motion of the positive ray particles and the corresponding deflections are at a right angle to each other. *Here it is worth noting that in the Thomson's cathode ray analysis, the fields were applied at right angles to each other.*

Due to the electrical field, the positive ray particles are deflected along the X-axis on the screen while the magnetic field leads the deflection along the Y-axis. If the electrical field strength is E then the force experienced by the positive ray particle (charge = q and mass = M) will be Eq, i.e. force = Eq. Hence, according to Newton's 2nd Law of motion, the acceleration (f) possessed by the particle along the X-axis is given by, $f = Eq/M$.

Let the length of the plates (E_1 and E_2) be l and the velocity of the particles in the horizontal plane be u, then the particles are accelerated in the electrical field for a time (t) given by, $t = l/u$. Hence, the displacement (x) in the plane of the paper, i.e. along the X-axis on the screen, is given by:

$$x \propto \frac{1}{2} ft^2 \text{ ; or, } x \propto \frac{1}{2} \frac{Eq}{M} (l/u)^2 \text{; or, } x = K_1 \frac{Eq}{Mu^2} \qquad \ldots(1.2.3.1)$$

The constant K_1 depends on the geometry of the spectrograph. It is mainly governed by l and the distance of the screen from the centre of the electrical field.

Click Here 1.me/thealchemylibrary

If the same positive ray particle is subjected to the magnetic field of intensity H, the acceleration attained is given by Hqu/M and the time of flight is given by l/u. Then the deflection perpendicular to the plane of the paper, i.e. along the Y-axis, is given by :

$$y \propto \frac{1}{2}\left(\frac{Hqu}{M}\right)(l/u)^2; \text{ or, } y = K_2\,\frac{Hq}{Mu} \qquad \ldots(1.2.3.2)$$

K_2 is a constant which depends on the geometry of the spectrograph.

Combining Eqn. 1.2.3.1 and 1.2.3.2, we get :

$$\frac{y^2}{x} = \left(\frac{K_2^2H^2q^2}{M^2u^2}\right)\left(\frac{Mu^2}{K_1Eq}\right) = \frac{K_2^2H^2}{K_1E} \times \frac{q}{M} \qquad \ldots(1.2.3.3)$$

$$\text{and } \frac{y}{x} = \frac{K_2Hu}{K_1E} \qquad \ldots(1.2.3.4)$$

Thus if the fields are kept constant for a particular mass spectrograph and if q/M is constant, then Eqn. 1.2.3.3 reduces to y^2/x = constant, **which is the equation of a parabola** whose latus rectum is given by $(K_2^2H^2q)/(K_1EM)$.

Let, O be the point of impact on the screen (D) of the undeflected particle in the absence of any field, and OM and OI are the deflection components of a particle by the magnetic and electrical field respectively. Hence the resultant impact point for the particle is R (Fig. 1.2.3.2). Now in the discharge tube, the different particles of the same q/M are produced at different positions between the anode and cathode and as a result, they will have different velocities. This is why, the different particles for their different velocities will produce different spots (Eqn. 1.2.3.4) on the parabolic arc TRP. Two such curves are shown in Fig. 1.2.3.2.

Thus all the particles irrespective of their velocities having the same value of q/M will lie on a particular parabola.

Another half of the parabola can be drawn on the screen by reversing the magnetic field half way during the experimental observation. Fig. 1.2.3.2 shows the two sets of such parabolas for two sets of particles having different q/M values.

Here it is noteworthy that many particles will lose their charges due to mutual collisions before experiencing the deflecting fields and these will remain undeflected to produce an intense blackening on the screen round the point O.

By measuring the latus rectum of the parabola produced on the screen, q/M can be obtained by knowing the values of K_2, K_1, E and H.

Analysis of the parabolic curves : Eqn. 1.2.3.3 indicates that the greater the value of q/M, the greater is the deflection suffered by the particle. The q/M value was found 10^4 emu/g for the most deflected particle and this value is identical with that of hydrogen

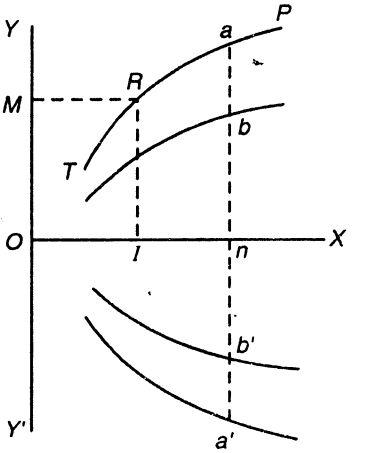

Fig. 1.2.3.2. Parabolic traces for positive rays in Thomson's mass spectrograph.

Click Here t.me/realCremylibrary

ion (H^+) obtained from electrolysis. This identity indicates that the curve arises due to H^+ (i.e. the hydrogen atom with a single positive charge).

Now let us consider a common line $abb'a'$ (Fig. 1.2.3.2) cutting the two parabolas for a certain value of x (say at n). Thus we have,

$$\frac{(aa')^2}{(bb')^2} = \frac{(2an)^2}{(2bn)^2} = \frac{(an)^2}{(bn)^2} = y_1^2 / y_2^2 \text{ , (say, } an = y_1 \text{ and } bn = y_2)$$

$$= \frac{q_1 M_2}{q_2 M_1} \text{ , (as, y} \propto q/M) \qquad \ldots(1.2.3.5)$$

(assuming K_2, K_1, E, H are the same for the two parabolas)

If it is assumed that the two parabolas arise due to the only difference of their masses and q is the same for them, then we have :

$$(an)^2 / (bn)^2 = M_2 / M_1$$

Thus, if the mass for one set of particles is known, then the mass for the other set of particles can be obtained.

Detection of isotopes from the analysis of the parabolas : It is evident from Eqn. 1.2.3.5 that if the charge is the same, the ratio of masses for the different sets of particles of a gas used in the discharge tube can be easily obtained. However, this prediction gets complicated if the different types of multiple ionisation take place. Here it is worth mentioning that the traces for singly ionised positive particles are always stronger than those for multiple ionised ones. Moreover, intensities of the traces for multiple charged particles reduce more sharply if the accelerating voltage between the cathode and anode is reduced. ***Thus for the same q values, the relative intensities of the traces give the measures of their relative abundances.***

When neon gas was taken as the residential gas in Thomson's experiment, two parabolic traces with their intensity 1:9 were found. The ratio did not change with the change of gas pressure in the tube and the accelerating potential. It indicates that the two sets of particles are having the same q. The atomic weight (more correctly, mass number) for the intense outer parabola corresponds to 20 while the fainter inner parabola corresponds to mass number 22. ***These two parabolic curves for neon were found inseparable from neon by any chemical treatment.*** Thus it was concluded that there are two sets of neon atoms differing only in mass but they are chemically indistinguishable. These were named as ***isotopes.*** From the isotopic abundances measured by the relative intensities, the atomic weight of normal neon was calculated to be $(20 \times 9 + 22 \times 1)/10 = 20.2$.

Similarly, the existence of isotopes in different elements was found.

Drawbacks in Thomson's method

i. Because of poor focussing of the ions on the photographic screen, the intensity of the parabolic traces is not good. It leads to an error in analysis.
ii. It is very much insensitive to separate atoms of higher atomic masses differing by only one or two units.

Click Here t.me/idealchemylibrary

1.2.4 Aston's Mass Spectrograph

Apparatus : F.W. Aston improved the Thomson's method by applying the electric and magnetic fields successively and perpendicularly to each other while in Thomson's method they were applied simultaneously and parallel to each other. Arrangements of Aston's mass spectrograph are shown in Fig. 1.2.4.1. The narrow beam of positive rays after passing through the slits (S_1, S_2) is deflected and dispersed in the electric field (E_1 and E_2) depending on the difference in their velocities. The dispersed beam is subjected to the magnetic field (M) which deflects the beam in opposite direction compared to the electric field. Thus the magnetic field produces a convergence in the dispersed beam consisting of particles of different velocities. The strength of the fields and their relative positions with respect to the photographic plate are adjusted in such a way that all the ions having the same q/M value but different velocities will be focussed on the photographic screen to produce a sharp and intense line.

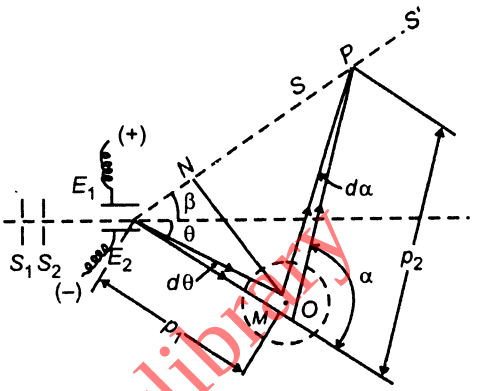

Fig. 1.2.4.1. Experimental arrangement of Aston's mass spectrograph.

Working principle : The required condition for focussing the ions having the same q/M value irrespective of their velocities can be obtained as follows :

The particle having mass M and positive charge q in passing the distance l with a velocity u in the electric field of intensity E will be laterally deflected in this field and it is given by,

$$x = \frac{1}{2}\frac{Eq}{M}(l/u)^2; \left(cf.\ s = ut + \frac{1}{2}ft^2\right) \qquad \ldots(1.2.4.1)$$

Hence the angular deviation is given by, $\theta = x / l$, (when θ is small):

$$\text{or, } \theta = \frac{1}{2}\frac{Eq}{M}\frac{l}{u^2} \qquad \ldots(1.2.4.2)$$

If the same ion travels l' with a velocity u in the magnetic field of intensity H, then the lateral deflection is given by,

$$x' = \frac{1}{2}\frac{Hqu}{M}(l'/u)^2 \qquad \ldots(1.2.4.3)$$

The angular deviation is given by,

$$\alpha = x' / l' = \frac{1}{2}\frac{Hq}{M}\frac{l'}{u} \qquad \ldots(1.2.4.4)$$

Thus, it is evident from Eqns. 1.2.4.2 and 1.2.4.4 that the angular deviation of the ions depends on their velocity if E and H are kept constant.

Differentiating Eqn. 1.2.4.2, we get :

$$d\theta = -\frac{Eq}{M}\frac{l}{u^3}du = -2\theta\frac{du}{u}; \text{ or, } \frac{d\theta}{\theta} = -2\frac{du}{u} \qquad \ldots(1.2.4.5)$$

Click Here to me/thealchemylibrary

Similarly, Eqn. 1.2.4.4. leads to :

$$d\alpha = -\frac{1}{2}\frac{Hq}{M}\frac{l'}{u^2}\,du = -\alpha\,\frac{du}{u};\ \text{or,}\ \frac{d\alpha}{\alpha} = -\frac{du}{u} \qquad \ldots(1.2.4.6)$$

Combining Eqs. 1.2.4.5 and 1.2.4.6, we have :

$$\frac{d\theta}{\theta} = 2\,\frac{d\alpha}{\alpha} \qquad \ldots(1.2.4.7)$$

or,

$$\frac{d\theta}{d\alpha} = \frac{2\theta}{\alpha} \qquad \ldots(1.2.4.8)$$

Let p_1 be the distance between the centres of the magnetic and electric field and p_2 be the distance between the centre of the magnetic field and the point of convergence on the screen. Thus the divergence created at the centre of magnetic field by the electric field is $p_1 d\theta$, similarly the width of convergent beam under the influence of the magnetic field is given by $p_2 d\alpha$. Now, if the magnetic field were absent, the beam would have travelled $(p_1 + p_2)$ distance in which p_2 suffers no deflection giving rise to total divergence $(p_1 + p_2)d\theta$. But the beam will converge by the magnetic field on the screen.

Hence, the convergence produced by the magnetic field is equal to the divergence produced by the electric field. Hence,

$$(p_1 + p_2)d\theta = p_2\,d\alpha;\ \text{or}\ \frac{d\theta}{d\alpha} = \frac{p_2}{(p_1 + p_2)}$$

or,

$$\frac{2\theta}{\alpha} = \frac{p_2}{(p_1 + p_2)},\ \text{(using Eqn. 1.2.4.8)}$$

or,

$$\frac{p_2}{p_1} = \frac{2\theta}{\alpha - 2\theta} \qquad \ldots(1.2.4.9)$$

This is the required condition for focussing.

If the photographic plate (SS') is inclined at an angle β to the incident beam, and ON is perpendicular to EP, then the consideration of the triangles ENO and OPN gives the following results.

$$ON = p_1 \sin(\theta + \beta) = p_2 \sin(\alpha - \beta - \theta);\ (\angle EOP = 180 - \alpha,\ \angle OPN = \alpha - (\beta + \theta),\ )$$

If the angles are small, $p_2(\alpha - \beta - \theta) = p_1(\theta + \beta)$;

$$\text{or,}\ \frac{p_2}{p_1} = \frac{\theta + \beta}{\alpha - \beta - \theta} \qquad \ldots(1.2.4.10)$$

Comparing this with Eqn. 1.2.4.9, we get, $\beta = \theta$.

Hence the photographic screen must be placed in such a direction that it makes the same angle with the incident beam as the deflection induced by the electric field.

The line traces compared to the arcs of the parabolic curves in Thomson's experiment produce more intensity giving rise to a great improvement over the Thomson's method.

Click Here t.me/thealchemylibrary

Different lines for different q/M values irrespective of their velocities are obtained. If the charge q remains the same, each line corresponds to a particular mass. By using the particles of known mass, the mass spectrograph can be calibrated with respect to which unknown masses can be determined if their charges are identical. In another way, by keeping the magnetic field constant, if the trace for an ion of mass M is located at some point for the electric field E, and the required electric field is E_1 to bring the trace for the ion of mass M_1 at the same point then we get the following results from Eqns. 1.2.4.2 and 1.2.4.4. Since the paths of the two types of ions are identical, we get from the electrical deflection :

$$\frac{E}{Mu^2} = \frac{E_1}{M_1 u_1^2}; \text{ or } \frac{E}{E_1} = \frac{M}{M_1}\left(\frac{u}{u_1}\right)^2$$

and from the magnetic deflection :

$$\frac{H}{Mu} = \frac{H_1}{M_1 u_1}; \text{ or, } \frac{H}{H_1} = \frac{M}{M_1}\left(\frac{u}{u_1}\right); \text{ or, } \frac{M}{M_1} = \left(\frac{H}{H_1}\right)^2 \left(\frac{E_1}{E}\right) = \frac{E_1}{E}; \text{ (if } H = H_1)$$

If the valus of E, E_1 and M are known, M_1 can be calculated.

1.2.5 Dempster's Mass Spectrometer

Apparatus : A.J. Dempster (1919) made some modifications in the mass spectrometer by introducing the direction of focussing. The arrangement is shown schematically in Fig. 1.2.5.1. Here the positive rays are generated by bombarding the electrically heated metal salt pasted end A of the cylinder with the emitted electrons from the filament (F). The narrow beam of the positive rays passes through the slits, S_1 and S_2. By using an electrical field, the positive ions are accelerated between S_1 and S_2. After coming out from S_2, they move in a circular path $S_2\ S_3\ S_4$ having radius r under the influence of a magnetic field of intensity H. After leaving the magnetic field, they run tangentially and fall on the metallic plate (Q). The particles having a certain q/M value can fall on the electrometer for a certain value of E (electrical field strength) and H (magnetic field strength).

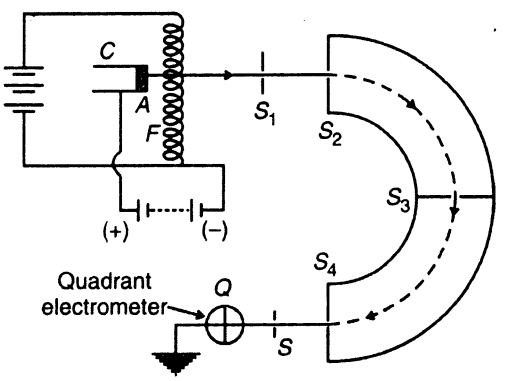

Fig. 1.2.5.1. Dempster's mass spectrograph.

Working principle : Here it is assumed that at S_1, the particles are with almost zero velocity. Hence, after acceleration by the electrical field (E) between S_1 and S_2, the particles having the same q/M value attain the same velocity (u) at S_2. After leaving S_2, they enter into the magnetic field (H) to travel along the circular path $S_2\ S_3\ S_4$.

Now, $$Eq = \frac{1}{2} Mu^2, \text{ (in the electric field);}$$

and, $$Hqu = \frac{Mu^2}{r}, \text{ (in the magnetic field).}$$

Click Here! me/chealchemylibrary

From these, we get, $q/M = 2\dfrac{E}{H^2 r^2}$ ...(1.2.5.1)

Eqn. 1.2.5.1 indicates that as r is fixed for a particular instrument, the particles having a particular value of q/M will be able to reach S_4 under only a set of fixed values of E and H. In practice, H is kept constant. Hence, all the particles having a particular q/M value will fall on the electrometer for a certain value of the electrical field strength E. The rate of charging of S is measured by current I. A plot of current I against the variable E is drawn (Fig. 1.2.5.2). The peaks correspond to different q/M values of the ions. Thus, by knowing E, the q/M values can be calculated from Eqn. 1.2.5.1 where, r and H are known. By using the particles of known q/M values, the instrument can also be calibrated with respect to which the unknown q/M values can be evaluated. For different isotopes of an element, in the plot of I vs. E, the heights of the peaks give the measure of their relative abundances (assuming q is the same for every set of particles). Such a plot for **magnesium** producing the **singly charged Mg-ions** (*i.e.* M/q = atomic mass) is given in Fig. 1.2.5.2, where the values of M have been calculated from their corresponding E values.

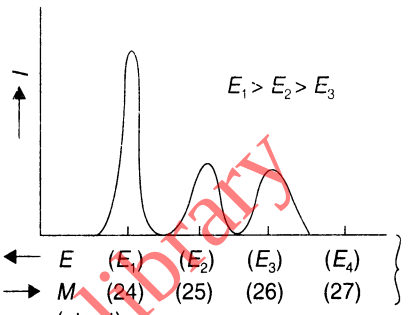

Fig. 1.2.5.2. Current strength (measured by electrometer) vs. electrical field strength (i.e. I vs. E) in Dempster's mass spectrometer to measure the relative abundance of the isotopes of an element (**illustrated for Mg** which produces the **singly charged Mg-ions** in the mass-spectrometer, *i.e.* Mg + e → Mg^+ + 2e). (see Vol. 7 for details).

Drawbacks of Dempster's mass spectrometer

The approximation that all the ions reaching S_1 are having zero velocities before acceleration by the electrical field may not occur in reality. Hence, the approximation considered here is not valid.

1.2.6 Bainbridge Mass Spectrometer

Apparatus: To remove the Dempster's drawbacks, Bainbridge used a velocity selector which separates the ions having different velocities. The design of Bainbridge's mass spectrograph is shown in Fig. 1.2.6.1. Its velocity selector consists of two parallel metallic plates (E_1 and E_2) between the two poles of a strong electromagnet of strength H_1. The beam of positive rays enters into the velocity selector after passing through the slits S_1 and S_2 and it comes out from the velocity selector through the slit S_3 and passes through the second magnetic field of H_2 strength and the particles travel in a circular path of radius r having a certain q/M value.

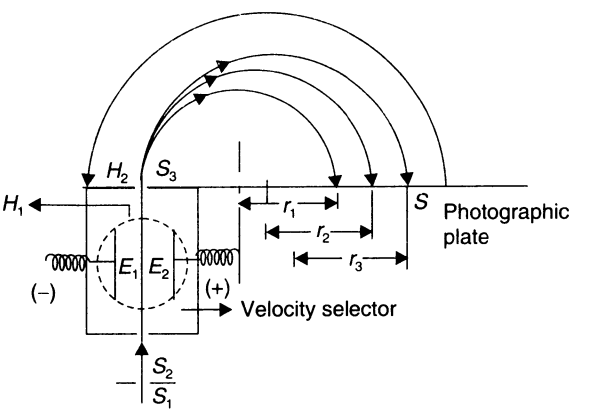

Fig. 1.2.6.1. Bainbridge mass spectrograph.

Working principle: In the velocity selector, the electrical field (E) and magnetic field (H_1) are applied in such away that the force experienced due to the fields by the particles having velocity u are equal and opposite.

Click Here 1.me/theachemylibrary

Hence, $$Eq = H_1qu; \text{ or } u = E/H_1 \quad \ldots (1.2.6.1)$$

Thus the particles having velocity u given by the above condition will be only able to reach the slit S_3. Under the condition, only the particles having velocity u experience the second magnetic field (H_2) which produces a dispersion in the beam depending on the value of q/M of the constituent ions. If r is the radius of the path of deflection suffered by the particles having charge q and mass M, then the following condition arises,

$$H_2qu = Mu^2/r; \text{ or, } q/M = \frac{u}{H_2r} = \frac{E}{H_1H_2r}, \text{ (using Eqn. 1.2.6.1)} \quad \ldots (1.2.6.2)$$

Thus, if q, H_1, H_2 and E are kept constant then the positions of the traces will be governed by the masses of the particles and the separation between the lines is directly proportional to their mass difference. Thus it has a linear mass scale. In Fig. 1.2.6.1, r_1, r_2 and r_3 denote the positions of the particles of charge q and masses M_1, M_2 and M_3 respectively when H_1, H_2 and E are remained constant. The relative abundances of the particles for different masses can be obtained from the relative intensities of the lines. By replacing the photographic plate (S), if a quadrant electrometer is placed, the relative intensities of current strength can be taken to measure their relative abundances.

1.3 THE NEUTRON AS A FUNDAMENTAL PARTICLE

1.3.1. The Discovery of Neutron

Analysis of the cathode rays and anode rays established that the lightest negatively charged and positively charged particles are electron (e) and proton respectively. Up to 1932, the protons and electrons were considered to be the major fundamental particles to constitute the matter, i.e. atoms. The mass of an electron is negligibly small compared to that of a proton. Hence the total mass of an atom was expected to be due to the protons existing within it. But it was noticed by Rutherford that the masses of all atoms could not be explained by considering only the mass producing particle proton. This is why, in a lecture in 1920, he predicted the existence of some kind of neutral particle having mass equal to that of a proton. In 1932, Chadwick, a student of Rutherford proved the prediction correct and this discovery earned him **Nobel Prize in Physics in 1935.** In his famous experiment, the light nuclei like *Li* or *Be* being bombarded by α-particles emitted the neutral particles. The particles were named ***neutrons*** because of their electrically neutral nature.

$$_4Be^9 + {}_2He^4 \longrightarrow {}_6C^{12} + {}_0n^1$$

Here it is worth mentioning that before Chadwick some nuclear physicists also noted this typical particle but they could not identify it. In 1930, Becker and co-workers observed a new radiation of high penetrating power coming out from the bombardment of α-particles on beryllium; the ray was found more penetrating than the hardest γ-ray known at that time. They also established the neutral state of the radiation from the studies of the effect of electrical field and their behaviour in *Wilson cloud chamber*. In 1931, Iren Curie and F.J. Curie also noted the same thing and they also observed the radiation to eject fast protons from the bombardment on paraffin. They were misguided by only considering the

Click Here t me/thealchemylibrary

new radiation as a special type of γ -rays. But Chadwick made the right conclusion : ***if this radiation is not of particle nature, it cannot eject the high energy protons from hydrocarbons, oxygen, nitrogen,*** etc. Ultimately he proved his conclusion which definitely got a striking hint from Rutherford's lecture (1920). Curies were unfortunate to miss the Rutherford's lecture which might have helped them to earn another Nobel Prize.

1.3.2 Properties of Neutron

i. Free neutrons at ordinary conditions decay ($t_{1/2}$ = 20 min) as follows,

$$\text{neutron } ({}_0n^1) \rightarrow \text{proton } ({}_{+1}p^1) + \text{electron } ({}_{-1}e^0) + \text{antineutrino } ({}_0\bar{\nu}^0) + 0.782 \text{ MeV}.$$

In this process, the lost mass (Δm) is converted into energy according to Einstein's law, $\Delta E = mc^2$. Here it is noteworthy that under a tremendously high pressure as in neutron stars, the neutron particles are stable.

Note : In ***neutron stars***, the matter is tremendously compressed and consequently the electrons and protons are fused into neutrons. The density of neutron stars is almost the density of nuclei i.e., million million tons per cc. The rotating neutron stars emit electromagnetic radiations at regular intervals and these radiations are called ***Pulsars.***

ii. They have a very high penetrating power.

iii. ***The neutrons are capable of knocking out the high speed protons from hydrogenous matter like hydrocarbons, water, etc.***

iv. The neutron beam has got the property of waves as for *X*-rays and γ-rays.

v. They can act as projectiles in different nuclear reactions. The neutrons having kinetic energy greater than 1.2 MeV (Sec. 7.12.3) are called ***fast neutrons*** while the neutrons of energy less than 1.0 eV are called ***slow neutrons***. Here it is worth noting that 1.2 MeV is the minimum energy required for the fission of U^{238}. The slow neutrons in thermal equilibrium with the medium are called ***thermal neutrons***. The most probable value for the kinetic energy of a thermal neutron is 0.026 eV ($= k_B T$) at 300 K. In the transmutation reactions, slow neutrons are more promising.

vi. Emission of β-rays from different radioactive elements is due to the conversion of neutrons into protons and electrons.

vii. Being neutral it cannot ionise the surroundings, but on collision, it produces charged particles such as protons which are capable of ionising the media. *This ionisation by the secondary charged particles may be utilised to detect them.*

viii. ***Magnetic properties of neutron*** : Though the neutrons are electrically neutral, they orient themselves like tiny magnets in a magnetic field. A neutron possesses a magnetic moment equivalent to that of a spinning electron. All these properties indicate its charge bearing properties though it is electrically overall neutral. **To explain this apparently contradictory behaviour, it is now believed that it consists of a positively charged core which is surrounded by a thin shell containing a negative charge, i.e. an electron.** This spinning electron is supposed to explain the magnetic properties of the neutron. The spin magnetic moment of a neutron is – 1.91 mN where μ_N stands for ***nuclear magneton*** (Sec. 5.1.6).

Click Here to the Chemistry Library

1.4 SOME IMPORTANT PROPERTIES OF THE THREE FUNDAMENTAL PARTICLES*

	Electron ($_{-1}e^0$)	*Proton* ($_{+1}p^1$)	*Neutron* ($_0n^1$)
Mass	9.108×10^{-28} g or, 9.108×10^{-31} kg or, 0.00054 amu	1.672×10^{-24} g or, 1.672×10^{-27} kg or, 1.00758 amu	Approximately same as in protons
Charge	-4.8×10^8 esu or, -1.602×10^{-19} C or, -1.602×10^{-20} emu	Same as in electron with opposite sign	Electrically neutral but it interacts with the magnetic field

(*Note* : Now it is believed that neutron and proton are constituted by the smaller particles called **quarks**. The force that interacts between the quarks is called **colour force** and the particle that is exchanged between the quarks is called **gluon.**)

1.5 THE HYDROGEN SPECTRUM

When an electric discharge is passed through hydrogen gas kept at a low pressure in a discharge tube, the radiation emitted being resolved shows the **existence of a number of lines of definite wavelengths in the ultraviolet, visible and infra-red regions. This is the emission spectrum of hydrogen atoms.** For any other elements taken in the gaseous condition within the discharge tube, the obtained emission spectrum is much more complicated.

1.5.1 Balmer Formula

By analysing the emission spectrum of hydrogen gas in the visible region, Balmer (1885) proposed that the wavelength of each line in the visible spectrum could be nicely expressed by the formula,

$$\lambda = K \frac{n^2}{n^2 - 4} \qquad \ldots(1.5.1.1)$$

where K is a constant for the whole series having the value 364.6 nm, and n is an integer like 3, 4, 5, 6... corresponding to H_α, H_β, H_γ, H_δ, ... lines in the series respectively. *This set of spectral lines mainly lying in the visible range is called the Balmer series according to the name of its discoverer.*

1.5.2 Rydberg Formula

Actually, the Balmer's equation indicated a stepping stone to Rydberg, the Swedish physicist to generalise the observation. He observed that besides the Balmer series in the simplest hydrogen spectrum, many other complicated elements bear different spectral lines in different series. The wave number $\bar{\nu}$ $(= 1/\lambda)$ for a spectral line in a particular series could be generally expressed as given by,

$$\bar{\nu} = \frac{1}{\lambda} = A - \frac{R}{(n+\alpha)^2} \qquad \ldots(1.5.2.1)$$

* Other fundamental particles will be discussed in Chapter 5 (see Table 5.6.1).

Click Here t.me/tnealchemylibrary

where R is called the ***Rydberg constant*** in tribute to its discoverer, A and α are constants for a particular series of an element. A and α depend on the nature of the elements and spectral series (i.e. a certain portion of the whole spectrum).

The Balmer's Eqn. 1.5.1.1 for the hydrogen spectrum can be reduced in the form of Rydberg's equation,

$$\bar{\nu} = \frac{1}{\lambda} = \frac{1}{K} - \frac{4}{Kn^2} = A - \frac{R}{(n+a)^2} \quad \ldots(1.5.2.2)$$

where, $A = \frac{1}{K}$ and, $R = \frac{4}{K}$ and $\alpha = 0$.

Thus, the Balmer's Eqn. 1.5.1.1 can be expressed in the form of Rydberg's formula as evident from the Eqn. 1.5.2.2.

It (i.e. Eqn. 1.5.1.1.) can be expressed also as,

$$\boxed{\bar{\nu} = \frac{4}{K}\frac{1}{2^2} - \frac{4}{K}\frac{1}{n^2} = R\left(\frac{1}{2^2} - \frac{1}{n^2}\right)} \quad \ldots(1.5.2.3)$$

Besides the hydrogen, many other elements also follow the Rydberg's formula where the Rydberg constant (R) gets multiplied by some other constants which are different for different elements.

1.5.3 Ritz Combination Principle

W. Ritz in 1908 introduced a more general relationship to express the wave number of different spectral lines of different spectral series for a particular atom or ion. It states that *the wave number of any spectral line may be represented as a combination of two terms, one of which is a constant for a particular series while the other varies regularly throughout the spectral series*. The general formula for a spectral line is given by,

$$\boxed{\bar{\nu} = \frac{R}{(m+\beta)^2} - \frac{R}{(n+\alpha)^2}} \quad \ldots(1.5.3.1)$$

where α, β are adjustment constants (see **quantum defect**, Sec. 1.9.2) which depend on the nature of the element; m is a fixed integer for a certain series and it is different for different series while n takes up different integral values corresponding to the different lines in a particular spectral series. Thus $R/(m+\beta)^2$ is constant for a particular series while the second term varies regularly for the same series.

As a matter of fact, in Rydberg's formula the first term A expresses actually $R/(m+\beta)^2$ in the Ritz combination principle.

For the hydrogen atoms, the adjustment constants alpha , beta are zero. Thus the expression for the Balmer series may be written as,

$$\bar{\nu} = R\left(\frac{1}{2^2} - \frac{1}{n^2}\right), n = 3, 4, 5 \quad \ldots(1.5.3.2)$$

which is identical with the one (see Eqn. 1.5.2.3) obtained from the Balmer's formula.

Similarly, other spectral series of the hydrogen atoms can be nicely explained by fixing some suitable integral values for m and n and the adjustment constants α and β to be zero. These are given in Table 1.5.3.1.

Click Here t.me/theacademylibrary

Table 1.5.3.1. Hydrogen Spectrum* and Ritz Combination Principle

Spectral series	*Spectral region*	*Values of m*	*Values of n*
Lyman Series	ultraviolet	1	2, 3, 4, . . .
Balmer Series	visible/ultraviolet	2	3. 4. 5 . . .
Paschen Series	near infra-red	3	4, 5, 6, ...
Brackett Series	far infra-red	4	5 6 7 . . . . .
Pfund Series	far infra-red	5	6 7 8 . . . . .

* $\alpha = \beta = 0$, $R = 109700\ cm^{-1}$

Many other elements also follow the general formula given by Ritz, but in these cases α, β are not necessarily zero, and the Rydberg constant gets multiplied by some other constants depending on the nature of the elements under consideration. Different spectral lines in the Balmer series for the hydrogen atom are shown in Fig. 1.5.3.1.

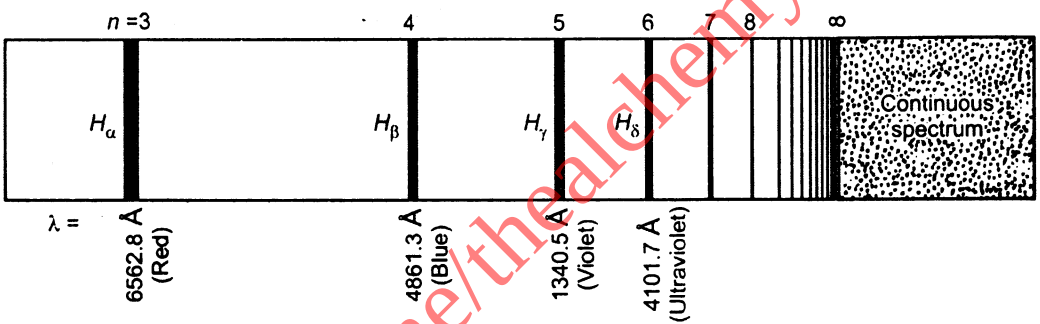

Fig. 1.5.3.1. Different spectral lines in Balmer series of hydrogen spectrum.

1.6. THOMSON'S PLUM-PUDDING MODEL OF ATOM

In the early days when there was no concept of atomic model, the emission spectrum of many elements, specially that of hydrogen was extensively studied with the mathematical formulations. But the fundamental question regarding the origin of spectral lines was in darkness. Actually, the discovery of the electron as a fundamental particle provided the first important insight into the atomic structure. The electrons were proved to bear negative charge. Hence to explain the electroneutrality, the existence of enough number of positively charged particles just to balance the negative charge was required to be considered. Based on this feature, J.J. Thomson in 1898 proposed that the *atoms are of unifrom spheres of positively charged matter in which the electrons are embedded in such a way that the electrostatic repulsion among the electrons and also within the positively charged matter is overcome due to the electrostatic attraction between the electrons and positively charged matter.* This plum-pudding model is shown in Fig. 1.6.1. This model at that time was applied to explain some observations as given below.

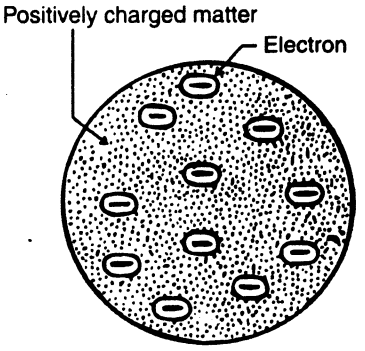

Fig. 1.6.1. Thomson's plum-pudding model of atom.

Click Here t.me/thealchemylibrary

i. ***Origin of emission spectrum*** : To explain the emission spectrum from the excited atoms, it was proposed that when the atoms are excited either by electric discharge or by heating, the normal situation is disturbed and the electrons start to vibrate around their equilibrium position emitting electromagnetic radiation corresponding to their vibrational frequencies. Thus the origin of the emission spectral lines was explained.

ii. ***Formation of ions*** : The gain of additional electrons in the matrix formed by the positive charge leads to the formation of anions and similarly, the loss of electrons convert the neutral atoms into the positive ions.

iii. ***Thermionic emission*** : If the element is highly heated then the vibrational energy of the electrons will be so increased that they can get no more bound by the electrostatic attractive force and they will come out.

iv. ***Kinetic theory of gas*** : The model provided an elastic hard model for the atoms which was required in the development of kinetic theory of gas.

Drawbacks of the Model

i. ***Contradiction to the classical theorem in electromagnetism*** : In the light of classical theory of electromagnetism, the stability in Thomson's model cannot be explained. According to Earnshaw's classical theorem, '*no system of charged particles of opposite nature can remain in a static equilibrium under the action of electrostatic forces alone*'. Thus no stability exists in the plum-pudding model where the negative charge particles are supposed to remain in an equilibrium with the positively charged matrix in a static condition.

ii. ***No explanation of atomic spectra in a quantitative way*** : Though the origin of the emission spectral lines was explained by considering the vibrating frequencies of the excited electrons, the calculated frequencies are different from those observed. Moreover, in the case of hydrogen atom (**one electron system**) only one spectral line was predicted, but in practice it leads to several series in which each series consists of several discrete spectral lines.

iii. ***No explanation of the observation of scattering of α-particles*** : In 1911, a definite experimental test was carried out by Geiger and Marsden under the suggestion of Ernest Rutherford to verify the validity of the model. This was the experiment of scattering of α-particles by a gold foil. No explanation of scattering for a very few α-particles by a large angle was provided by the Thomson's model, then the scientists were left without any alternative one but to reject the model and replace it by a new one which is the Rutherford's model.

Click Here t.me/thealchemylibrary

1.7 SCATTERING OF α-PARTICLES AND RUTHERFORD'S NUCLEAR MODEL OF ATOM

1.7.1. Rutherford's Nuclear Model of Atom

Lord Rutherford realised that the information regarding the internal structure of the matter could be revealed by bombarding the matter with the high speed α-particles. The α-particles are doubly ionised helium atoms, i.e. He^{2+}. Geiger and Marsden carried out the experiment under the suggestion of

Rutherford by bombarding a very thin foil (thickness of the order of 10^{-7} m) of gold (Z = 79) with a narrow beam of α-particles of high energy coming from radium, a radioactive material (Fig. 1.7.1.1). Behind the target foil, a fluorescent screen was placed to detect the fate of the α-particles after bombardment. It was found that ~ 99% of the incident particles passed the target gold foil being undeflected. Only a very small fraction got deflected by quite large angles and a very few of them were deflected by 90° or more.

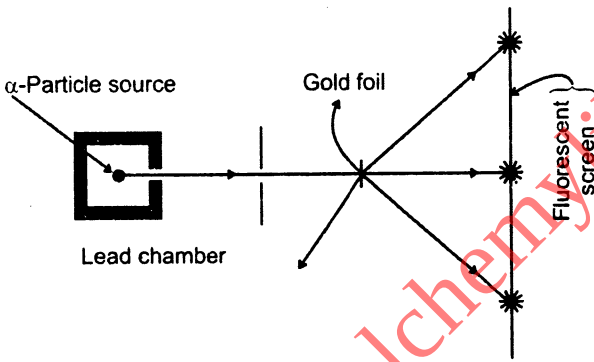

Fig. 1.7.1.1. Experimental design of α-particle scattering on gold foil.

Deflection by these large angles could not be explained from Thomson's atomic model in which positive charges were supposed to remain uniformly distributed throughout the volume of atomic dimension. The massive positive charge matter is responsible to deflect He^{2+}. Hence, if the model were correct we could have the observations as : (i) *the fate of all the incident α-particles would be the same* as the interacting positive charge matter is uniformly distributed throughout the space, (ii) the α-particles should experience only a very weak electrostatic repulsive barrier from the positive charge matter, as it is diluted due to its uniform distribution throughout the volume. **Such weak interactions can never produce deflection by large angles such as 90° or more.**

Thus the Thomson's atomic model could not survive in the experimental verification and Rutherford propose d his nuclear model in 1911 to explain the experimental observations. According to this model:

i. All the positive charges of an atom along with most of the atomic mass are concentrated within a very small central region of the atom. **The central region is called the *nucleus*.**

ii. The electrons which balance the positive charge are revolving around the nucleus in different circular orbits just like the planets around the sun. Due to the revolving nature, they acquire a **centrifugal force** ($= mu^2/r$, where m and u are the mass and velocity of the electron respectively, and r is the radius of the orbit) which balances the electrostatic attractive force towards the nucleus. Thus it saves them from falling in the nucleus and ensures the stability of the atom.

The proposed model explains the observations of α-particle scattering. When the α-particles collide with the nucleus or pass through the vicinity of the nucleus which occupies only a very small region in the whole atomic dimension are deflected by large angles. In this model, most of the space is vacant and transparent to the α-particles. *The negatively charged very light particles, i.e. the electrons, have nothing to do with the high energy massive α-particles*. They fail to attract the high energy massive α-particles

Click Here t.me/healchemylibrary

Drawbacks of the Rutherford's Model

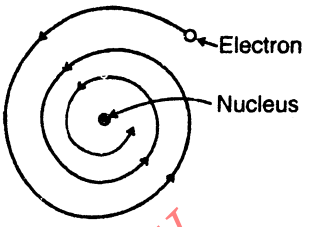

Fig. 1.7.1.2. Fate of the revolving electron in Rutherford's model.

i. ***Instability of the Rutherford's atom*** : Though it was attempted to explain the stability of the atoms by considering two strong foundation stones of the classical physics, i.e. Newton's law of motion and Coulomb's law of electrostatic force, it could not be supported by the electromagnetic theory, another big foundation stone of the classical physics. According to the demand of electromagnetic theory, ***a revolving electron under an acceleration will radiate its energy in the form of electromagnetic radiation.*** Thus by losing its energy, it will gradually spiral down (Fig. 1.7.1.2) into the nucleus and the atom will get destroyed. As a matter of fact, if it occurs so, it can be shown mathematically that the revolving electron will require about one hundred-millionth of a second to get plunged into the nucleus.

ii. ***No explanation of atomic line spectra*** : From the Rutherford's model, according to the electromagnetic theory, the energy radiated in the form of electromagnetic radiation from the revolving electron *should lead to a* ***continuous spectrum*** *covering all frequencies in a certain range*. But experimentally, *some well defined spectral lines corresponding to certain frequencies are noted instead of a continuous spectrum.*

1.7.2 Rutherford's Theory of α-Particle Scattering

In Fig. 1.7.2.1, let an α-particle of mass m_α and charge q be approaching with a velocity u along AO, when a nucleus of charge Ze is placed at D. Let the position of the α-particle at a particular instant at A be denoted by (r, ϕ) where r gives the distance between the particle and the nucleus. The repulsive force is given by:

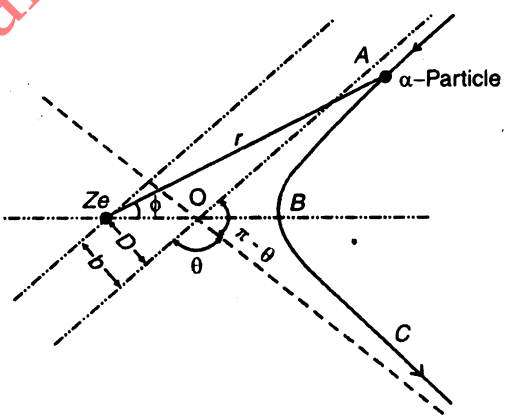

Fig. 1.7.2.1. Scattering of α-particles.

$$F = \frac{Zeq}{4\pi\varepsilon_0 r^2}, \text{ (SI unit)} \qquad \ldots(1.7.2.1)$$

$$F = \frac{Zeq}{r^2}, \text{ (CGS unit)} \qquad \ldots(1.7.2.2)$$

It can be mathematically proved that under the repulsive force, the *α-particle will move on a hyperbolic path along ABC with the nucleus at the focus D.*

If the perpendicular distance (i.e. shortest distance) between the nucleus (D) and the original line of approach (AO) of the α-particle is given by b, called ***impact parameter***, then we have :

$$\cot(\theta/2) = \frac{4\pi\varepsilon_0 m_\alpha u^2 b}{Zeq}, \text{ (SI unit)} \qquad \ldots(1.7.2.3)$$

$$= \frac{m_\alpha u^2 b}{Zeq}, \text{ (CGS)} \qquad \ldots(1.7.2.4)$$

The above equations indicate that the value of impact parameter (b) increases as θ decreases. In fact, when $b \to 0$, then $\theta \to 180°$, i.e. the particle moving in the direction of the nucleus will be deflected back in the same direction.

Click Here for the Chemistry Library

From Eqn. 1.7.2.3, it appears that, all the α-particles approaching a target nucleus with an impact parameter in the range zero to b, will be deflected by an angle $\geq \theta$. The circular area (πb^2) of radius b is called the *cross-section* for interaction. Any particle approaching towards the nucleus within this area will suffer deflection by θ or more (Fig. 1.7.2.2). If, the thickness of the foil target be t, and the number of nuclei be n per unit volume then the number of nuclei present in the cylinder of length t and cross-section πb^2 is $\pi b^2 nt$. As we are dealing with a very large number of α-particles, it is reasonably expected that the fraction (f) of the α-particles deflected by θ or more is given by :

$$f = \pi b^2 nt \quad \ldots(1.7.2.5)$$

Too thin foil – why?

Here it is worth mentioning that the foil must be sufficiently thin so that, (i) cross-sections of the adjacent nuclei do not overlap, (ii) an α-particle suffers its entire deflection from an encounter with a single nucleus, and (iii) it does not reduce the velocity of the α-particle which traverses it. Lastly it should be mentioned that in the treatment, it is assumed that the scattering nucleus remains at rest and this approximation is only reasonably valid for the heavier nucleus like that of gold.

Gold foil - why?

- **Condition of malleability :** In the α-particle scattering experiment, the foil was required to be very thin (ca. 10^{-7} m). The reasons behind the requirement of such a thin foil have been explained already. To make such a thin foil, *the material must be highly malleable*. The metals which possess the *fcc* structure are highly malleable because of the existence of large number of *slip systems* (cf. Sec. 12.2.1). **Gold having the *fcc* structure satisfies the condition of malleability.**
- **Condition of massive scattering nucleus :** During the interaction between the approaching α-particle and scattering nucleus, the scattering nucleus must be sufficiently massive so that the *scattering nucleus remains at rest*. ***Gold nucleus is sufficiently massive (nuclear mass : ca. 197 amu) to satisfy the condition.***
- **Condition of high positive charge of the scattering nucleus :** To deflect the α-particles (i.e. $^4He^{2+}$), by a large angle, the scattering nucleus should have **high positive charge** and this condition is satisfied for gold having $Z = 79$.

1.7.3 Nuclear Dimension from the α-Particle Scattering Experiment

It is known that the α-particle follows the trajectory (ABC) of a hyperbola (see Fig. 1.7.2.1) *due to the electrostatic repulsive force between the target nucleus and the positively charged α-particle*. The nucleus (D) is placed at the outer focus. Finally, the scattered α-particle follows the *asymptote OC*, after suffering a deflection by θ, the angle between the initial path *AO* which is the other asymptote of the hyperbolic trajectory (Fig. 1.7.2.1) and the final path *OC*.

The shortest distance between the nucleus (D) and the original path (AO) of the α-particle is called ***impact parameter*** (b) which has been already defined. *The physical significance of b is that all the α-particles lying in the cross-section of area πb^2 will suffer a deflection by θ or more* (see Fig. 1.7.2.2). The mathematical relation is already discussed in Sec. 1.7.2.

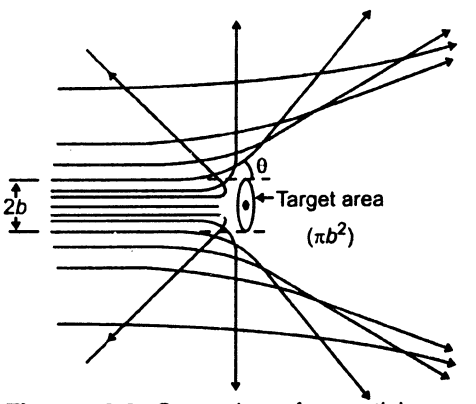

Fig. 1.7.2.2. Scattering of α-particles and impact parameter (b).

Click Here to Join Chemistry Library

When b becomes zero, θ becomes 180° (Fig. 1.7.2.2). Under this condition, *the kinetic energy of the α-particle is equal to the electrostatic repulsive energy at the closest distance r_0 between the α-particle and the target nucleus.*

Hence, $$\frac{1}{2}m_\alpha u^2 = \frac{Zeq}{4\pi\varepsilon_0} \times \frac{1}{r_0}; \quad or, \boxed{r_0 = \frac{Zeq}{4\pi\varepsilon_0\left(\frac{1}{2}\right)m_\alpha u^2}} \quad \ldots (1.7.3.1)$$

If the maximum kinetic energy $\left(=\frac{1}{2}m_\alpha u^2\right)$ is 7.7 MeV (7.7 MeV = 7.7×10^6 eV × 1.6×10^{-19} Joules/eV = 1.23×10^{-12} Joules ; $\varepsilon_0 = 8.854 \times 10^{-12}$; $q = 2e$ for α-particles), then by substituting these values we get, $r_0 = 3.8 \times 10^{-16}$ Z m. For the gold foil, Z = 79, and $r_0 = 3.8 \times 10^{-16} \times 79$ m = 3.0×10^{-14} m. ***Thus the radius of the nucleus of gold cannot be greater than 3.0×10^{-14} m,*** as r_0 gives the minimum possible distance between the α-particle (of 7.7 MeV) and the target nucleus. ***It indicates that the nucleus is about $1/10^4$ th of the dimension of the atom.***

1.8 BOHR'S ATOMIC MODEL FOR THE HYDROGEN-LIKE SYSTEMS

To remove the drawbacks in the Rutherford's model, combining some basic laws of classical physics and some principles of quantum theory (1900), Niels Bohr proposed in 1913 his famous atomic model which successfully explained the different properties of atom, such as : *stability of the atoms, spectral characteristics of the atoms, ionisation energies*, etc. Because of this contribution, he was awarded ***Nobel Prize in 1922***. It mainly deals with the hydrogen and hydrogen-like systems such as He^+, Li^{2+}, Be^{3+}, etc. where only one electron is present outside the nucleus.

1.8.1 Bohr's Atomic Model

Basic postulates of the model

i. The electrons are revolving in some specified circular orbits around the nucleus where the whole positive charge is concentrated. *These permitted orbits are restricted by the quantum condition that the angular momentum of the electron in the circular path about the nucleus must be an integral multiple of $h/2\pi$, where h is the Planck constant*, i.e. *angular momentum* = $\boldsymbol{mur = n(h/2\pi)}$, n = 1, 2, 3, 4, ... where m = mass of the electron; r = radius of the orbit; and u = tangential velocity of the revolving electron.

ii. When an electron is revolving in a permitted orbit, it will neither accept nor radiate any energy. This situation is called ***stationary state***. Here it is worth mentioning that this postulate ignores the demand of electromagnetic theory according to which for the revolving charged particle (e.g. electron), energy will be radiated in the form of electromagnetic radiation.

iii. When an electron jumps from an orbit of energy E_i to another orbit of energy E_f, a definite amount of energy in the form of radiation is emitted or absorbed depending upon whether the final state is at lower or higher energy compared to the initial one respectively. The frequency (ν) of radiation is given by : $h\nu = E_f \sim E_i$.

Click Here to the chemvi library

iv. For all other considerations, the model will obey the laws of classical physics, such as : for the revolving electron in a circular orbit in a stationary state, the electrostatic Coulombic force of attraction between the nucleus and electron is balanced by the centrifugal force (mu^2/r) due to angular motion of the electron as obtained from Newton's law of motion.

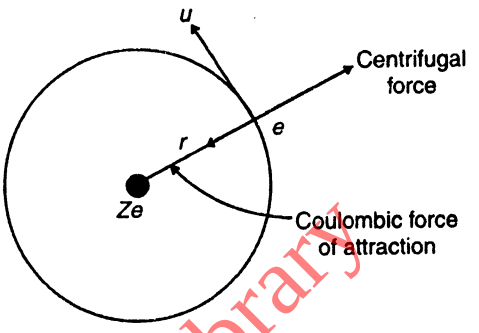

Fig. 1.8.1.1. Bohr's model for hydrogen-like systems.

(a) Expression for the radius of Bohr's orbit

Let an electron of charge e and mass m be revolving with the tangential velocity u in a circular orbit of radius r_n around the nucleus having charge Ze (Fig. 1.8.1.1). For hydrogen and different ***hydrogen-like systems***, such as He^+, Li^{2+}, Be^{3+}, ... the values of Z are 2, 3, 4 ..... respectively.

For the equilibrium condition, the electrostatic Coulombic force of attraction is balanced by the centrifugal force, as the gravitational force between the electron and the nucleus is negligible. The ***Coulombic force of attraction*** (F_e) *is given by,*

$$F_e = \frac{1}{4\pi\varepsilon_0}\left(\frac{Ze^2}{r_n^2}\right) \qquad \ldots(1.8.1.1)$$

where ε_0 is called absolute permitivity of the medium, i.e. vacuum in this case. Its value is 8.85×10^{-12} $C^2\ N^{-1}\ m^{-2}$.

The centrifugal force (F_c) ***is given by,***

$$F_c = mu^2 / r_n \qquad \ldots(1.8.1.2)$$

In equilibrium condition, $F_e = F_c$, i.e.

$$\frac{1}{4\pi\varepsilon_0} \times \frac{Ze^2}{r_n^2} = \frac{mu^2}{r_n}; \text{ or, } r_n = \frac{1}{4\pi\varepsilon_0}\left(\frac{Ze^2}{mu^2}\right), \text{ (SI unit)} \qquad \ldots(1.8.1.3)$$

According to the Bohr's quantum restriction,

$$mur_n = n(h/2\pi); \text{ or, } u = nh/(mr_n 2\pi) \qquad \ldots(1.8.1.4)$$

Substituting the value of u from Eqn. 1.8.1.4 in Eqn. 1.8.1.3 we get,

$$\boxed{r_n = \text{radius of the } n\text{-th Bohr's orbit} = \frac{n^2h^2\varepsilon_0}{\pi me^2Z} = \frac{(4\pi\varepsilon_0)n^2h^2}{4m\pi^2e^2Z} = r_1n^2, \text{ (S1 unit)}} \qquad \ldots(1.8.1.5)$$

In CGS system, $F_e = Ze^2 / r_n^2$ and $\frac{1}{4\pi\varepsilon_0} = 1$,

and,

$$\boxed{r_n = \frac{n^2h^2}{4\pi^2mZe^2}, \text{ (CGS unit)}} \qquad \ldots(1.8.1.6)$$

Click Here to me/thealchemylibrary

(b) Expression for energy of the revolving electron in Bohr's orbit

The total energy (E_n) of the electron is the sum of potential and kinetic energy where kinetic energy $= \frac{1}{2} mu^2$. The potential energy of the electron is given by the work done to bring the electron from infinity where potential energy is zero to r_n. Thus,

$$\text{potential energy} = \int_{\infty}^{r_n} F_e dr = \int_{\infty}^{r_n} \frac{1}{4\pi\varepsilon_0} \times \frac{Ze^2}{r^2} dr = -\frac{Ze^2}{4\pi\varepsilon_0 r_n}$$

The negative sign indicates that the work is done on the electron. Thus,

$$E_n = \frac{1}{2} mu^2 - \frac{Ze^2}{4\pi\varepsilon_0 r_n} = \frac{1}{2}\left(\frac{Ze^2}{4\pi\varepsilon_0 r_n}\right) - \frac{Ze^2}{4\pi\varepsilon_0 r_n}, \text{ (using Eqn. 1.8.1.3)}$$

$$= -\frac{Ze^2}{8\pi\varepsilon_0 r_n}$$

[*Note :* For hydrogen ($Z = 1$), $E_n = -\frac{e^2}{2r_n}$]

Now, substituting the value of r_n from Eqn. 1.8.1.5 we get :

$$\boxed{E_n = -\frac{me^4Z^2}{8\varepsilon_0^2 n^2 h^2} = \frac{E_1}{n^2}, \text{ in SI unit}} \quad \ldots(1.8.1.7)$$

$$\boxed{E_n = -\frac{2\pi^2 mZ^2 e^4}{n^2 h^2} = \frac{E_1}{n^2}, \text{ in CGS unit}} \quad \ldots(1.8.1.8)$$

(c) Frequency of radiation when an electron jumps from one level to another

Now, if an electron jumps from an outer n_i–th orbit to an inner n_f–th orbit, the frequency of the radiated energy is given by according to Bohr's postulate,

$$h\nu = E_{n_i} - E_{n_f} = \frac{Z^2 e^4 m}{8\varepsilon_0^2 h^2}\left(\frac{1}{n_f^2} - \frac{1}{n_i^2}\right)$$

$$\boxed{\text{or,} \quad \nu = \frac{Z^2 e^4 m}{8\varepsilon_0^2 h^3}\left(\frac{1}{n_f^2} - \frac{1}{n_i^2}\right)} \quad \ldots(1.8.1.9)$$

Hence, if it is expressed in terms of $\bar{\nu}$ ($= 1/\lambda$) called ***wave number***, it is given by,

$$\boxed{\bar{\nu} = \frac{1}{\lambda} = \frac{\nu}{c} = \frac{Z^2 e^4 m}{8\varepsilon_0^2 ch^3}\left(\frac{1}{n_f^2} - \frac{1}{n_i^2}\right) = RZ^2\left(\frac{1}{n_f^2} - \frac{1}{n_i^2}\right)} \quad \ldots(1.8.1.10)$$

Click Here t.me/thealchemylibrary

where c = velocity of light, R = **Rydberg constant** = $\frac{me^4}{8\varepsilon_0^2 ch^3}$.

It leads to : $\boxed{E_n = -\frac{RchZ^2}{n^2}}$

In CGS system, $\boxed{\bar{\nu} = \frac{2\pi^2 me^4 Z^2}{ch^3}\left(\frac{1}{n_f^2} - \frac{1}{n_i^2}\right) = RZ^2\left(\frac{1}{n_f^2} - \frac{1}{n_i^2}\right)}$ ...(1.8.1.11)

where, Rydberg constant, R is given by : $R = \frac{2\pi^2 me^4}{ch^3}$.

1.8.2 Numerical Values of Radius and Energy in Bohr's Atom

In hydrogen-like systems, the expression of radius (r_n) for the n–th orbit is given by,

$$\boxed{r_n = \frac{\varepsilon_0 n^2 h^2}{\pi me^2 Z}, \text{ (SI unit)}}$$

Substituting the values, $\varepsilon_0 = 8.85 \times 10^{-12}$ C^2 N^{-1} m^{-2}, $h = 6.625 \times 10^{-34}$ J s,

$m = 9.11 \times 10^{-31}$ kg, $e = 1.6 \times 10^{-19}$ C, we get :

$$r_n = \frac{n^2 \times 8.85 \times 10^{-12}\text{ C}^2\text{ N}^{-1}\text{ m}^{-2} \times (6.625 \times 10^{-34}\text{ J s})^2}{3.14 \times 9.11 \times 10^{-31}\text{ kg} \times (1.6 \times 10^{-19}\text{ C})^2 Z}$$

$$= \frac{n^2}{Z} \times 0.53 \times 10^{-10}\text{ m} = \frac{n^2}{Z} \times 53\text{ pm}$$

[$F = \frac{1}{4\pi\varepsilon_0} \times \frac{q_1 q_2}{r^2}$; thus the unit of ε_0 is C^2 N^{-1} m^{-2} ;

J = force × displacement = N × m = kg m^2 s^{-2}; N = kg m s^{-2}]

For hydrogen, $Z = 1$; thus the first Bohr's radius (r_1) is 53 pm.

$$\boxed{r_n = \frac{n^2}{Z} \times 0.53 \times 10^{-10}\text{ m} = \frac{n^2}{Z} \times 53\text{ pm}}$$

$$\boxed{\text{In CGS system, } r_n = \frac{n^2 h^2}{4\pi^2 mZe^2}}$$

It leads to : $r_n = \frac{n^2 \times (6.625 \times 10^{-27}\text{ erg s})^2}{4 \times (3.14)^2 \times 9.11 \times 10^{-28}\text{ g} \times (4.8 \times 10^{-10}\text{ esu})^2 Z}$

$$= \frac{n^2}{Z} \times 0.53 \times 10^{-8}\text{ cm}$$

[Coulombic force = $q_1 q_2 / r^2$; dyne = (esu)^2 / cm^2; erg = g cm^2 s^{-2}; esu = g$^{1/2}$ cm$^{3/2}$ s^{-1}]

Click Here to me/thealchemylibrary

• The size of **hydrogen-like systems** (e.g. He^+, Li^{2+}, Be^{3+}, Ne^{9+}, etc.) is given by r_1 which can be expressed in terms of $r_{1(H)}$ as follows :

$$r_{1(H)} = r(H) = 53 \text{ pm};$$

$$r(He^+) = \frac{53}{2} \text{ pm} = 26.5 \text{ pm}, (Z = 2 \text{ for } He^+);$$

$$r(Li^{2+}) = \frac{53}{3} \text{ pm} = 17.6 \text{ pm}, (Z = 3 \text{ for } Li^{2+});$$

$$r(Ne^{9+}) = \frac{53}{10} \text{ pm} = 5.3 \ (Z = 10 \text{ for } Ne^{9+}).$$

• For a *H*-like system, the **cross-sectional area** ($A = \pi r^2$) can be obtained from r_n values as follows:

$$A = \pi r^2 \propto n^4, (r \propto n^2)$$

Thus, $\frac{A(n=10)}{A(n=1)} = \frac{10^4}{1^4} = 10^4$, i.e. the cross-sectional area of a *H*-atom in the excited state (for $n = 10$) is 10^4 times higher than that of the ground state.

Expression of energy of an electron in a hydrogen-like system in the n–th orbit is given by :

$$\boxed{E_n = -\frac{Z^2 me^4}{8\varepsilon_0^2 n^2 h^2} = -\frac{RchZ^2}{n^2}, \text{ (SI unit)}}$$

$$E_n = -\frac{Z^2 \times 9.11 \times 10^{-31} \text{kg} \times (1.16 \times 10^{-19} \text{C})^4}{8 \times (8.85 \times 10^{-12} \text{C}^2 \text{ N}^{-1} \text{ m}^{-2})^2 \times (6.625 \times 10^{-34} \text{ J s})^2 n^2}$$

$$= -\frac{21.8 \times 10^{-19} Z^2}{n^2} \text{ J}$$

[unit of $\varepsilon_0 = C^2 N^{-1} m^{-2}$; $J = N\ m = kg\ m^2\ s^{-2}$]

Actually, $E_n = -\frac{21.8 \times 10^{-19} Z^2}{n^2}$ J/atom

$$= -\frac{21.8 \times 10^{-19} Z^2 \times 6.023 \times 10^{23}}{n^2} \text{ J/mole} = -\frac{1313.3 Z^2}{n^2} \text{ kJ/mole}$$

(*cf.* 1 mega joule = 1 MJ = 10^6 J)

For hydrogen atom, in the ground state $n = 1$ and $Z = 1$. Thus, $E_1 = -1313.3$ kJ/mole

Similarly in CGS system, $E_n = -\frac{21.8 \times 10^{-12} Z^2}{n^2}$ erg/atom

$$= -\frac{13.6 \times Z^2}{n^2} \text{ eV/atom}, (1 \text{ erg} = 6.25 \times 10^{11} \text{ eV})$$

Click Here to me/thealchemylibrary

$$1\ \text{eV} = (\text{charge of an electron}) \times 1\ \text{V} = 1.6 \times 10^{-19}\ \text{C} \times 1\ \text{V} = 1.6 \times 10^{-19}\ \text{J} = 1.6 \times 10^{-12}\ \text{erg}$$

$$1\ \text{eV/atom} \equiv \frac{1.6 \times 10^{-19} \times 6.02 \times 10^{23}}{4.2 \times 10^{3}}\ \text{kcal mol}^{-1} = 23.05\ \text{kcal mol}^{-1}$$

For hydrogen, $E_1 = -13.6$ eV/atom

In the same way, the value of **Rydberg constant (*R*)** can be calculated,

$$R = \frac{me^4}{8\varepsilon_0^2 ch^3}, \text{ in SI unit}$$

$$R = \frac{9.11 \times 10^{-31}\ \text{kg} \times (1.6 \times 10^{-19}\ \text{C})^4}{8 \times (8.85 \times 10^{-12}\ \text{C}^2\ \text{N}^{-1}\ \text{m}^{-2})^2 \times 3 \times 10^{8}\ \text{m s}^{-1} \times (6.625 \times 10^{-34}\ \text{J s})^3}$$

$$\approx 1.097 \times 10^{7}\ \text{m}^{-1}$$

$$\text{In CGS system, } R = \frac{2\pi^2 me^4}{ch^3} \approx 109700\ \text{cm}^{-1}$$

- Similarly, ν for transition from n_i to n_f can be calculated as follows :

$$\nu = \frac{me^4 Z^2}{8\varepsilon_0^2 h^3}\left|\left(\frac{1}{n_f^2} - \frac{1}{n_i^2}\right)\right| = RcZ^2\left|\left(\frac{1}{n_f^2} - \frac{1}{n_i^2}\right)\right|$$

By using the values of R and c, we get :

$$\nu = 3.29 \times 10^{15} Z^2 \left|\left(\frac{1}{n_f^2} - \frac{1}{n_i^2}\right)\right| = \text{cycles/sec.}$$

(Here, | | sign is considered, as the sign of corresponding ΔE depends on the sequence, $n_i > n_f$ or, $n_f > n_i$).

Different Atomic Parameters in Atomic Units (au)

The system of **atomic unit** (au) is defined as follows :

(i) **Mass :** Mass of an electron (m_e) = 9.1×10^{-31} kg = **1 *au of mass.***

(ii) **Length :** Radius of the 1st Bohr orbit of *H*-atom = 0.53×10^{-10} m = a_o = **1 *au of length.***

(iii) **Charge :** Charge (magnitude) of an electron = 1.6×10^{-19} C = **1 *au of charge.***

(iv) **Energy :** Twice the ionisation energy of *H*-atom = twice the magnitude of the energy of the electron in 1st Bohr orbit of H-atom = $2|E_H| = 2 \times 2.18 \times 10^{-18}$ J = 4.36×10^{-18} J = 27.12 eV = **1 Hartree = 1 *au of energy*** = $\frac{e^2}{r_1}$.

Rydberg is another unit of energy : **2 Rydberg = 1 Hartree.**

Click Here to me/thealchemylibrary

(v) **Angular momentum :** Angular momentum of the electron in the first Bohr orbit

$$= m_e u r_1 = 1\left(\frac{h}{2\pi}\right) = 1.05 \times 10^{-34} \text{ J s} = \mathbf{1}\ \textbf{\textit{au of angular momentum}}$$

(vi) $4\pi\varepsilon_0 = 1$ (in au), $\hbar = \dfrac{h}{2\pi} = m_e = |e| = 1$ (in au)

$$r_1 \text{ (i.e. } a_0) = \frac{(4\pi\varepsilon_0)\, h^2}{4\pi^2 m_e e^2} = 1 \text{ (in au)}$$

(vii) ***Speed*** **:** The speed of an electron in the 1st Bohr orbit of *H*-atom is the **atomic unit of speed.**

$$u_1 = \frac{h}{2\pi m_e r_1} = \frac{e^2 \times 2\pi}{h \times (4\pi\varepsilon_o)} = 1 \text{ au} = 2.188 \times 10^6 \text{ m s}^{-1}$$

i.e. speed of light (c) = 3×10^8 m s^{-1} $\approx$ 137 au

(viii) ***Time*** **:** The period of rotation of an electron in 1st Bohr orbit of *H*-atom is called the **atomic unit of time.**

$$t = \frac{2\pi r_1}{u_1} = \frac{(h/2\pi)^3}{m_e (e/\sqrt{4\pi\varepsilon_0})^4} = 1 \text{ au} = 2.42 \times 10^{-17} \text{ s}$$

Note **:** In actual definition m_e is replaced by the reduced mass μ of the system. The inclusion of reduced mass in the expressions has been explained in the next Section i.e. Sec. 1.8.3.

1.8.3 Correction for the Finite Mass of the Nucleus

In the above mathematical derivations, it was assumed that the mass of the nucleus (M) is so large compared with the mass of the electron (m) that the nucleus remained rest at the centre of the electronic orbit. *This is true if the mass of the nucleus is infinite, but in reality M is only finite.* In the case of hydrogen, the nucleus is about 2000 times heavier compared to the electron. **Because of this finite mass, nuclei are not at rest but they are revolving also.** Thus, both the nucleus and electron are rotating around their ***common centre of mass*** (Fig. 1.8.3.1) which is definitely very close to the nucleus. As the electron and nucleus are always on opposite sides of the centre of mass, their linear momenta are equal but opposite in direction.

Let, a_1 be the radius of the **electron orbit** and a_2 be the radius of **nuclear orbit** (Fig. 1.8.3.1) and a be the longest possible distance (i.e. electron and nucleus reside in the opposite sites of the centre of mass) between the centres of the electron and the nucleus.

Thus, $a = a_1 + a_2$ ... (1.8.3.1)

From the concept of linear momenta, $Ma_2 = ma_1$;

or, $$a_2 = \frac{m}{M} a_1 = \frac{m}{M}(a - a_2)$$

or, $$a_2\left(1 + \frac{m}{M}\right) = \frac{ma}{M}$$

or, $$a_2 = \frac{ma}{m + M} \quad \text{...(1.8.3.2)}$$

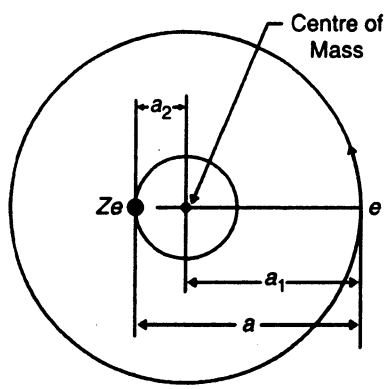

Fig. 1.8.3.1. Motion of the nucleus and electron about the common centre of mass in Bohr's model.

Click Here t.me/thealchemylibrary

Similarly, $$a_1 = \frac{Ma}{M+m} \qquad \ldots(1.8.3.3)$$

Now, let us calculate the kinetic energy (T) of the system which is the sum of kinetic energies of the nucleus and the electron having tangential velocities u_1 and u respectively.

$T = (½)\, Mu_1^2 + (½)\, mu^2 = (½)\, M\omega^2 a_2^2 + (½)\, m\omega^2 a_1^2$,

(ω = angular velocity of the system $= u_1/a_2 = u/a_1$)

$$T = (1/2)\left(\frac{Mm}{M+m}\right)\omega^2 a^2, \text{ (substituting the values of } a_1 \text{ and } a_2)$$

$$= (1/2)\,\mu\omega^2 a^2$$

where, μ is called the ***reduced mass*** given by,

$$\boxed{\mu = \frac{mM}{m+M} = \frac{m}{1+m/M}} \qquad \ldots(1.8.3.4)$$

Similarly, the total angular momentum of the system about the centre of mass is given by the sum of momenta due to the electron and nucleus. Thus,

angular momentum of the system $= ma_1^2\omega + Ma_2^2\omega$ $\qquad \ldots(1.8.3.5)$

$$= \mu a^2 \omega$$

Thus, from the above Eqns. 1.8.3.4 and 1.8.3.5, **it is evident that because of the finite mass of the nucleus, in all expressions given earlier, *m* must be replaced by μ.**

Thus, Eqn. 1.8.1.10 becomes,

$$\bar{\nu} = \frac{Z^2 e^4}{8\varepsilon_0^2 ch^3} m \frac{M}{M+m}\left(\frac{1}{n_f^2} - \frac{1}{n_i^2}\right) = RZ^2 \frac{M}{M+m}\left(\frac{1}{n_f^2} - \frac{1}{n_i^2}\right) \qquad \ldots(1.8.3.6)$$

The above relation indicates that the corrected value of R is given by,

$$\boxed{R_{(corr.)} = R\frac{1}{1+m/M};}$$

when $M = \infty$, $R_{(corr.)} = R$

Here it is evident that with the increase of the nuclear mass, M (i.e. mass number denoted by A), R_{corr} tends to R_∞. In fact, for the lighter element (i.e. smaller values of A), R_{corr} is only slightly less than R_∞. It is illustrated in Fig. 1.8.3.2.

Analysis of the corrected relation establishes the following facts which are also supported by the experiments.

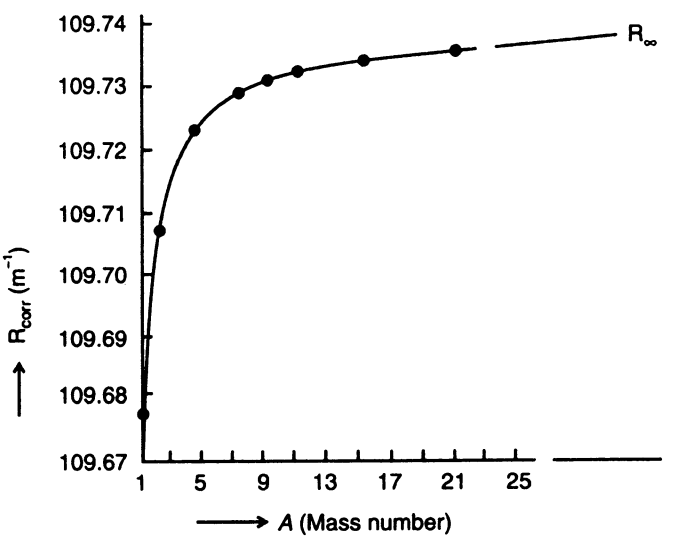

Fig. 1.8.3.2. Variation of R_{corr} (i.e. Rydberg constant) with atomic mass number.

Click Here to the/thealchemylibrary

(a) ***Determination of M_H/m ratio*** : We have,

$$R_{H(corr.)} = \frac{me^4}{8\varepsilon_0^2 ch^3} \times \frac{M_H}{M_H + m} = R \times \frac{1}{1 + m/M_H}$$

Similarly,

$$R_{He^+(corr.)} = \frac{me^4}{8\varepsilon_0^2 ch^3} \times \frac{M_{He}}{M_{He} + m} = R \times \frac{1}{1 + m/M_{He}} \quad \ldots(1.8.3.7)$$

$$\frac{R_{He^+(corr.)}}{R_{H(corr.)}} = \frac{1 + m/M_H}{1 + m/M_{He}} = \frac{1 + m/M_H}{1 + m/(3.97M_H)}$$

From the mass spectrograph experiments, $M_{He} = 3.97M_H$ is known; from the spectroscopic experiments, corrected values of R_H and R_{He^+} can be determined and by using these values, from Eqn. 1.8.3.7 the ratio M_H/m can be obtained. In this way, the ratio has been found about 1840 which is in good agreement with the values obtained from other methods.

(b) ***Discovery of isotopes*** : For a certain element, say, hydrogen, the masses of the nuclei are different for hydrogen and its isotope deuterium. Hence their Rydberg constants are also different as follows,

$$R_{H(corr.)} = R\frac{1}{1 + m/M_H} \text{ and } R_{D(corr.)} = R\frac{1}{1 + m/M_D}$$

Therefore, it is expected that the positions of their spectral lines will be different in a particular series. As a matter of fact, during the analysis of Balmer series of the hydrogen atoms, there were some weak lines with small separations along with the main intense lines. **These weak lines were argued to be due to the poorly abundant deuterium isotopes.** This prediction was later experimentally verified by analysing the spectrum of a sample of hydrogen which was chemically enriched with deuterium. Thus the weak lines due to the deuterium got intensified. In this way, deuterium was discovered spectroscopically (*cf.* Sec. 5.2.2).

***Illustration* [H_α (= 656.28 nm) and D_α lines in Balmer series]** : The separation ($\Delta\lambda$) between the lines can be calculated in terms of R_H and R_D where R_H and R_D stand for the corrected Rydberg constants of hydrogen and deuterium respectively.

$$\bar{\nu}_H = R_H\left(\frac{1}{2^2} - \frac{1}{3^2}\right) \text{ and } \bar{\nu}_D = R_D\left(\frac{1}{2^2} - \frac{1}{3^2}\right)$$

$$\frac{\bar{\nu}_H}{\bar{\nu}_D} = \frac{R_H}{R_D} = \frac{1 + m/2M_H}{1 + m/M_H}; (M_D = 2M_H)$$

$$1 - \frac{\bar{\nu}_H}{\bar{\nu}_D} = \frac{\bar{\nu}_D - \bar{\nu}_H}{\bar{\nu}_D} = \frac{1/\lambda_D - 1/\lambda_H}{1/\lambda_D} = \frac{\Delta\lambda}{\lambda_H}$$

$$\frac{\Delta\lambda}{\lambda_H} = 1 - \frac{1 + m/2M_H}{1 + m/M_H} \approx 27.23 \times 10^{-5}, \text{(using the values of } m \text{ and } M_H)$$

$\Delta\lambda$ = Separation between the lines of H and D

$= 27.23 \times 10^{-5} \times \lambda_H = 27.23 \times 10^{-5} \times 656.28$ nm = 0.18 nm.

Note : See Solved Problem 16 for illustration.

Click Here t.me/thealchemylibrary

1.8.4 Bohr's Theory and the Spectral Lines in Hydrogen-like Systems

Origin of the emission spectral lines at least in the case of hydrogen (H) and **hydrogen-like systems** (i.e., He^+, Li^{2+}, Be^{3+}, ... etc.) can be quantitatively explained in the light of Bohr's theory. If the electron falls to the first orbit ($n = 1$) from any higher orbit, the ***Lyman series*** is generated . According to Bohr's theory, the energy difference between the orbits in which the electron transition occurs is fixed and it leads to a certain frequency. For a particular system, the frequency of the spectral line depends on the values of n_f and n_i. Similarly, for ***Balmer, Paschen, Brackett and Pfund series*** the values of n_f are 2, 3, 4 and 5 respectively (Fig. 1.8.4.1).

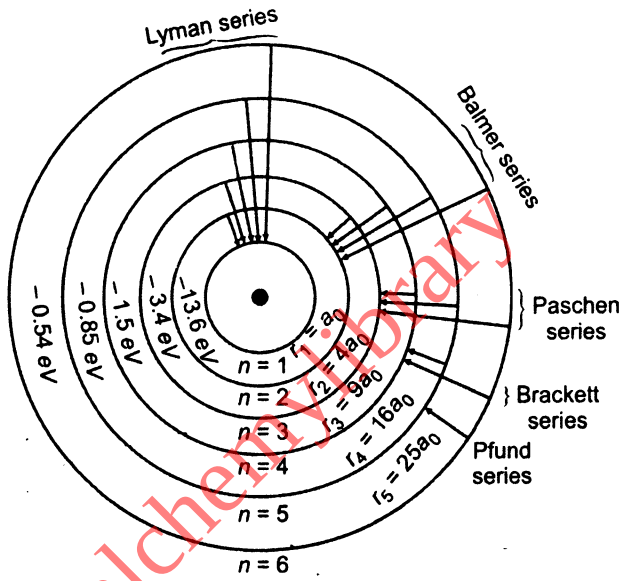

Fig. 1.8.4.1. Qualitative orbital diagram for hydrogen and hydrogen like systems and origin of different spectral lines.

The mathematical formulations for the frequencies (ν) and wave numbers ($\bar{\nu}$) for different spectral lines in different series are obtained from Bohr's theory as follows,

$$\nu = \frac{me^4Z^2}{8\varepsilon_0^2h^3}\left|\left(\frac{1}{n_f^2}-\frac{1}{n_i^2}\right)\right| = 3.3\times10^{15}\,Z^2\left|\left(\frac{1}{n_f^2}-\frac{1}{n_i^2}\right)\right| \text{ cycles/sec} \qquad \text{(cf. Eqn. 1.8.1.9)}$$

and $$\bar{\nu} = RZ^2\left|\left(\frac{1}{n_f^2}-\frac{1}{n_i^2}\right)\right| = 109.7\times10^5\,Z^2\left|\left(\frac{1}{n_f^2}-\frac{1}{n_i^2}\right)\right| \text{ m}^{-1} \qquad \text{(cf. Eqn. 1.8.1.10)}$$

(Values are obtained by using the standard values of m, ε_o, c and h in SI units).

For, **Lyman series**, $n_f = 1$, and $n_i = 2, 3, 4, 5$ .... [$n_i = 2$ (α–line), 3 (β–line) , 4 (γ–line), in the series]

Similarly for,

Balmer series, $n_f = 2$, and $n_i = 3, 4, 5, 6$ ....

Paschen series, $n_f = 3$, and $n_i = 4, 5, 6, 7$ ....

Brackett series, $n_f = 4$, and $n_i = 5, 6, 7$ ...

Pfund series, $n_f = 5$, and $n_i = 6, 7, 8$ ....

Here it is noteworthy that the more corrected values will be obtained *if the correction for the finite mass of the nucleus is taken into consideration.* However, a fairly good conformity between the calculated and experimental values of ν and $\bar{\nu}$ gives a sound basis of Bohr's model.

For a particular spectral line in hydrogen-like systems (e.g. He^+, Be^{2+}, Li^{3+}, etc.) we get :

Click Here t.me/thealchemylibrary

$$\frac{\bar{\nu}_{Be^{2+}}}{\bar{\nu}_H} = \frac{\lambda_H}{\lambda_{Be^{2+}}} = \frac{R_{Be^{2+}}}{R_H} \times 16, (Z = 1 \text{ for } H, Z = 4 \text{ for } Be^{2+})$$

$= 16$, (taking $R_{Be^{2+}} = R_H$ i.e. the nuclei are supposed to remain at rest).

Similarly, $\frac{\lambda_H}{\lambda_{Li^{3+}}} = 9, (Z = 3 \text{ for } Li^{3+})$

1.8.5 Ionisation and Resonance Potential for Hydrogen and Hydrogen-like Systems in the Light of Bohr's Theory

Resonance or excitation potential is the energy required to excite the electron in an isolated atom or ion (*hydrogen-like system, in the present consideration*) in gaseous condition from its ground state ($n = 1$) to its next higher orbit ($n = 2$) . Correctly, it is called *1st resonance or excitation potential.* Similarly, the transitions, $n = 1$ to $n = 3$ and $n = 1$ to $n = 4$ give the measures of *2nd and 3rd resonance potentials.* In the case of **ionisation potential,** it involves the excitation from $n = 1$ to $n = \infty$. *Here, it is worth mentioning that the parameters are of energy expression, but they contain the term potential. The term potential is introduced mistakenly, because to measure the excitation energy, it is very often imparted by applying a potential gradient.* From Bohr's theory, the following expressions (without considering the nuclear motion) come.

$$\text{1st Resonance Potential (RP)} = E_{n_2} - E_{n_1} = \frac{Z^2 me^4}{8\varepsilon_0^2 h^2}\left(\frac{1}{n_1^2} - \frac{1}{n_2^2}\right)$$

$$= \frac{Z^2 me^4}{8\varepsilon_0^2 h^2}\left(\frac{1}{1^2} - \frac{1}{2^2}\right)$$

and Ionisation Potential (IP) $= E_\infty - E_1$

$$= \frac{Z^2 me^4}{8\varepsilon_0^2 h^2}\left(\frac{1}{1^2} - \frac{1}{\infty^2}\right)$$

$$= \frac{Z^2 me^4}{8\varepsilon_0^2 h^2} = 21.8 \times 10^{-19} Z^2 \text{ Joules/atom}$$

It leads to : IP = 13.6 Z^2 eV/atom = 1313.3Z^2 kJ/mole, (see Sec.1.8.2).

For the hydrogen atom ($Z = 1$), the experimental values are in good conformity with the predicted values from Bohr's theory.

Ionisation energy for the polyelectronic system

Because of the ***shielding effect,*** the outermost electron experiences the effective nuclear charge Z^*e which is less than the actual charge Ze present in the nucleus. In such cases, the ionisation energy (IE) is given by :

$$\text{IE or IP} = \frac{13.6(Z^*)^2}{n^2} \text{ eV/atom}$$

Click Here t.me/thealchemylibrary

Z^* can be calculated by **Slater's rule** (cf. Sec. 4.2.4). Z^* can be also estimated from the experimental value of ionisation energy.

Illustration : Find Z^* experienced by the outermost electron in Li-atom if the 1st IP value of lithium is 5.4 eV.

Solution : The outermost electron is in 2*s* orbital in the present case. It leads to :

$$\frac{13.6(Z^*)^2}{n^2} = 5.4; \text{ or } (Z^*)^2 = \frac{2^2 \times 5.4}{13.6}$$

i.e. $Z^* = 1.26$

Thus the outermost electron experiences nuclear charge 1.26e instead of 3e in Li-atom. This is due to screening by the 1*s* electrons.

It may be noted that in terms of Slater's rule, Z^* becomes $3 - 2 \times 0.85 = 1.30$. This value is close to the value obtained from ionisation potential value of *Li*-atom.

1.8.6 Bohr's Theory and Correspondence Principle

In the microscopic world dealing with the fundamental particles, the principles of quantum physics are not very often governed by the classical physics, but in the macroscopic world which is in our sense, both of them lead to the identical conclusion. This is verified in many cases, such as : in the theory of relativity, theory of radiation and wave property of matter, etc. The same thing can also be proved in Bohr's theory.

Bohr's postulates appear to ignore the demand of classical physics for the revolving electron, but in 1923 Bohr established that **for *larger values of quantum number n, both the quantum theory and classical theory lead to the same result.* This is known as Bohr's correspondence principle.**

According to the classical electromagnetic theory, the revolving electron in a circular orbit radiates energy whose frequency is given by the frequency (f) of its revolution and its harmonics (i.e. integral multiple of the frequency of revolution).

Thus, $f = u/(2\pi r)$; (where u gives the linear velocity of the revolving electron).

In Bohr's theory, $\frac{mu^2}{r} = \frac{Ze^2}{4\pi\varepsilon_0 r^2}$; or, $u = e(Z/4\pi\varepsilon_0 rm)^{1/2}$

Hence, $f = \frac{u}{2\pi r} = \frac{e\sqrt{Z}}{\sqrt{(4\pi\varepsilon_0 mr)} \times 2\pi r} = \frac{e\sqrt{Z}}{2\pi\sqrt{4\pi\varepsilon_0 mr^3}}$

$$= \frac{e\sqrt{Z}}{2\pi\sqrt{(4\pi\varepsilon_0 m}}\left(\frac{\pi me^2 Z}{n^2h^2\varepsilon_0}\right)^{3/2}, \left(\text{putting } r = \frac{n^2h^2\varepsilon_0}{\pi me^2 Z}\right)$$

$$= \frac{e^4Z^2m}{4\varepsilon_0^2h^3}\left(\frac{1}{n^3}\right) = \frac{2RcZ^2}{n^3}, R = \frac{me^4}{8\varepsilon_0^2ch^3} \qquad \ldots(1.8.6.1)$$

Now let us consider the frequency (ν) of radiation for the transition from n_i to n_f where n stands for the very large values of principal quantum numbers.

$$\nu = \frac{mZ^2e^4}{8\varepsilon_0^2h^3}\left(\frac{1}{n_f^2} - \frac{1}{n_i^2}\right) = RcZ^2\left(\frac{1}{n_f^2} - \frac{1}{n_i^2}\right)$$

Click Here to me/headchemyjibrary

Now, let us consider the case fo $= n$ and $n_f = n - p$, where $p = 1, 2, 3, ...$,

Hence, $$\nu = \frac{Z^2me^4}{8\varepsilon_0^2h^3}\left[\frac{1}{(n-p)^2} - \frac{1}{n^2}\right] = \frac{Z^2me^4}{8\varepsilon_0^2h^3}\left(\frac{2pn-p^2}{n^2(n-p)^2}\right)$$

When, $n >>> p$, $2pn - p^2 \approx 2pn$; and $(n-p)^2 \approx n^2$

Thus, $$\boxed{\nu \approx \frac{Z^2me^4}{8\varepsilon_0^2h^3}\left(\frac{2p}{n^3}\right) = \frac{Z^2me^4}{4\varepsilon_0^2h^3}\left(\frac{p}{n^3}\right) = \frac{2RcZ^2p}{n^3}} \quad ...(1.8.6.2)$$

When $p = 1$, Eqns. 1.8.6.1 and 1.8.6.2 become identical and **the frequency of radiation is the frequency of revolution**. For $p = 2, 3, 4$ ..... harmonics of the fundamental frequency are obtained. **Thus, for the very high values of *n*, of the order of 10^4, both the results are identical, but for the smaller values of *n*, there appears a serious discrepancy.**

1.8.7 Moseley's Law in the Light of Bohr's Theory

Moseley's Experiment : In a discharge tube, when the anticathode is bombarded with high energy electrons, it generates two types of *X*-rays. **One type produces a continuous spectrum** whose frequency of the high energy end depends on the energy of the incident electron beam but the frequency of the **second type (line spectrum)** superimposed (Fig. 1.8.7.1) on the first type is independent of the energy of the incident electron beam but **it is a *characteristic property of the anticathode used***. For the generation of these characteristic *X*-rays, the energy of the incident electron beam should exceed a minimum value called *threshold value* which depends only on the nature of anticathode. **The characteristic *X*-ray spectra can be grouped in *K*-series, *L*-series, *M*-series,** etc. Each series consists of discrete spectral lines denoted by α, β, γ, ... etc.

The young physicist H.G.J. Moseley (1919) made a systematic study on the characteristic *X*-rays by using about 30 different elements as anticathodes. Crystals of potassium ferrocyanide were used to provide a diffraction grating and a photographic plate was used as a screen.

Moseley's Law : It was found (Fig. 1.8.7.2) that the square roots of the frequencies ($\tilde{\nu}$) of the characteristic *X*-ray lines (say, K_α lines or L_α lines or M_α lines, etc.) bear a linear relationship with $(Z - b)$ where Z stands for the atomic number (determined by Rutherford's experiment) of the anticathode used and b is a constant for a particular series. Mathematically, it is expressed as,

$$\boxed{\sqrt{\nu} = a(Z-b) = aZ - ab} \quad ...(1.8.7.1)$$

where a is the proportionality constant and it is different for different series, and b is the same for all the lines in a particular series; $b = 1$ and 7.4 for the K_α and L_α lines respectively. Actually b gives the measure of ***shielding constant*** and it can be calculated by ***Slater's rule*** which will be discussed at the appropriate place (Sec. 4.2.4). Generally K_α and L_α lines are followed, as these are the strongest lines in *K*- and *L*-group respectively.

Interestingly, when Z was replaced by the atomic weight, no such relationship was obtained. Thus it was concluded that the atomic number (Z) and not the atomic weight is the fundamental property of the elements.

Click Here: t.me/thearchemylibrary

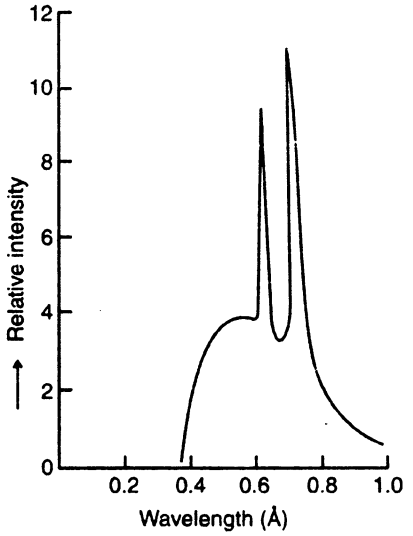

Fig. 1.8.7.1. Characteristic X-rays superimposed on the continuous X-ray spectrum (for molybdenum).

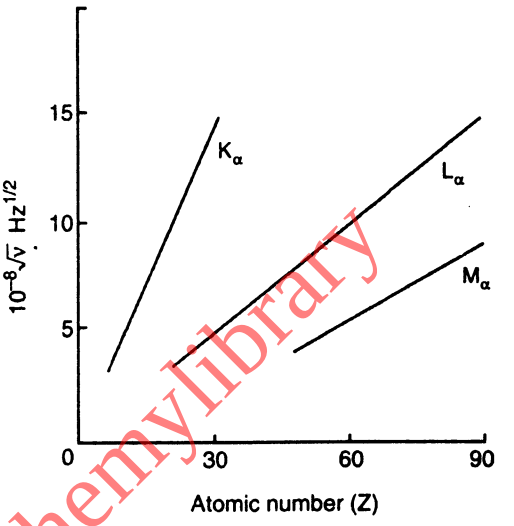

Fig. 1.8.7.2. Mosley's diagram for the characteristic X-ray.

Derivation of Moseley's Law from Bohr's Theory : Let us first consider the origin of characteristic *X*-rays. The high energy electron knocks out an electron from the nearest shell *K* (n = 1), thus the vacancy produced in the *K*-shell is filled in by an electron coming from the *L*-shell. Similarly, the vacancy produced in the *L*-shell is filled in by an *M*-shell electron and thus a ***cascade effect*** goes on. **These inner transitions lead to the production of the characteristic *X*-rays.** The vacancy in *K*-shell may also be filled in by an electron directly coming from n = 3, 4, etc. Thus if the final station of the journey is n_f = 1, it leads to the production of *K* series. Similarly for n_f = 2, it leads to *L* series, and so on. For example,

K_α (n_i = 2, n_f = 1), K_β (n_i = 3, n_f = 1), K_γ (n_i = 4, n_f = 1) are produced due to the transitions shown in the respective parentheses.

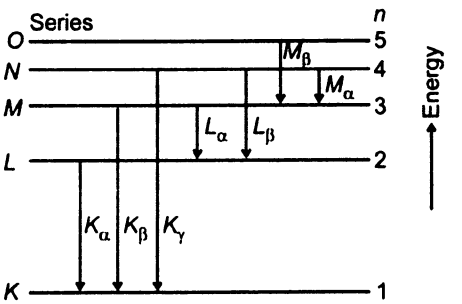

Fig. 1.8.7.3. Generation of characteristic X-rays.

According to the Bohr's theory (without the consideration of nuclear motion) the frequency of radiation for transition from n_i to n_f is given by,

$$\nu = \frac{me^4Z^2}{8\varepsilon_0^2h^3}\left(\frac{1}{n_f^2} - \frac{1}{n_i^2}\right)$$

in which the terms bear their usual significance.

Now it is worth mentioning that Bohr's theory is applicable only for the hydrogen-like systems in which only one electron is revolving. For the polyelectronic systems, it requires some modifications. In such systems, the electron involved in the transition will not definitely experience the whole positive charge *Ze* at the nucleus due to *the screening or shielding effect of the other electrons*. If the extent of

Click here to me/thealchemylibrary

shielding is measured by b then the effective nuclear charge experienced by the electron undergoing transition becomes $Z - b$. Hence the above equation can be rewritten as,

$$\boxed{\nu = \frac{me^4(Z-b)^2}{8\varepsilon_0^2 h^3}\left(\frac{1}{n_f^2} - \frac{1}{n_i^2}\right)}$$

For a given series (say, K_α or L_α), $\frac{me^4}{8\varepsilon_0^2 h^3}\left(\frac{1}{n_f^2} - \frac{1}{n_i^2}\right)$ is constant (for K_α : $n_f = 1$, $n_i = 2$; for L_α : $n_f = 2$ and $n_i = 3$) and if it is represented by a^2; then the equation becomes,

$\nu = a^2(Z-b)^2$; or, $\sqrt{\nu} = a(Z-b)$ which is the Moseley's observation.

Note :

- **For the K_α line ($b = 1$)**, we can write :

$$E_n = -\frac{13.6\,(Z-1)^2}{n^2}\text{ eV}$$

$$\Delta E = E_2 - E_1 = -13.6\,(Z-1)^2\left\{\frac{1}{2^2} - \frac{1}{1^2}\right\}$$

$$= 10.2\,(Z-1)^2\text{ eV}$$

$$\nu = \frac{\Delta E}{h} = \frac{10.2\,(Z-1)^2\text{ eV}}{4.14\times10^{-15}\text{ eV s}},\ (1\text{ erg} = 6.25\times10^{11}\text{ eV and } h = 4.14\times10^{-15}\text{ eV s})$$

i.e. $\sqrt{\nu} = 4.95\times10^7(Z-1)\text{ Hz}^{1/2} = a(Z-b)\text{ Hz}^{1/2}$

In indicates : $a = 4.95\times10^7\text{ Hz}^{1/2}$.

In the plot, $\sqrt{\nu}$ vs. Z, intercept = slope = $4.95\times10^7\text{ Hz}^{1/2}$ as $b = 1$

- **Moseley's equation can be expressed in terms of wavelength (λ) *of the characteristic X-rays by using the relation*, $c = \nu\lambda$,** i.e.

$$\sqrt{\frac{c}{\lambda}} = a\,(Z-b);\text{ or }\sqrt{\frac{1}{\lambda}} = \frac{a}{\sqrt{c}}(Z-b) = a'(Z-b),\left(\text{taking } a' = \frac{a}{\sqrt{c}}\right)$$

- ***Illustration*** : A cobalt ($Z = 27$) sample is bombarded with a beam of electrons. It produces the K_α line of $\lambda = 178.9$ pm for cobalt. It also shows a weak line ($\lambda = 143.5$ pm) of the K_α series due to an impurity. Identify the impurity.

Solution : For the K_α-lines we can write :

$$\sqrt{\frac{c}{\lambda_{Co}}} = a\,(Z_{Co} - 1) = a\,(27-1)$$

and $$\sqrt{\frac{c}{\lambda_X}} = a\,(Z_X - 1),\ (X \text{ denotes the impurity element}).$$

Click Here : me/thealchemylibrary

It leads to :

$$\sqrt{\frac{\lambda_{Co}}{\lambda_X}} = \frac{Z_X - 1}{27 - 1}; \text{ or } \sqrt{\frac{178.9}{143.5}} = \frac{Z_X - 1}{27 - 1}$$

or $$1.116 = \frac{Z_X - 1}{26}; \text{ or } Z_X = 30.0 \text{ (nearest integer)}$$

The atomic number of the impurity element is 30 i.e. the element is zinc (*Zn*).

Importance of Moseley's Law

i. ***Rectification of Mendeleev's periodic law*** : Moseley's experiment establishes the atomic number (*Z*) not the atomic weight as the fundamental property which governs the physical and chemical properties of the element. *Thus, atomic weight, the basis of Mendeleev's periodic law was replaced by the new basis, atomic number.* This modification removes the disputes in placing the elements *K* (*Z* = 19) and *Ar* (*Z* = 18); *Co* (*Z* = 27) and *Ni* (*Z* = 28); *Te* (*Z* = 52) ; and *I* (*Z* = 53) in the Periodic Table.

ii. ***Discovery of new elements*** : The proposed new elements can be easily identified by the analysis of their characteristic *X*-rays. The atomic number can be easily calculated from the experimentally determined characteristic *X*-ray frequency and if it is found new then the claim of the new element is established. In this way, technetium (*Z* = 43) , promethium (*Z* = 61), rhenium (*Z* = 75), etc. have been discovered and identified.

iii. ***Identification of lanthanides*** : The members of the lanthanide series are chemically so similar that they cannot be easily differentiated as different elements. In this case, Moseley's law has been helpful to identify and determine their atomic numbers.

1.8.8 Franck-Hertz Experiments (Nobel Prize in Physics, 1925) in the Light of Bohr's Atomic Model

Before we discuss the Franck-Hertz experiment, we should deal with some important terms such as, *critical potential* (*CP*), *resonance potential* (*RP*), *ionisation potential* (*IP*) and *inelastic collisions*.

Critical potential : It gives the measure of energy required to raise an electron from a lower level to a higher level. It is of two types : ***resonance potential*** (when the electron is raised to a higher level but not to infinity) and ***ionisation potential*** (when the electron is raised to infinity). According to Bohr's theory for the hydrogen-like systems,

$$CP = \frac{Z^2 me^4}{8\varepsilon_0^2 h^2}\left(\frac{1}{n_i^2} - \frac{1}{n_f^2}\right), n_f > n_i$$

when, $n_f = \infty$, $CP = IP$; and n_f = any finite value > n_i, $CP = RP$.

If $n_f = n_i + 1$, then it leads to 1st *RP* designated as $(RP)_1$; similarly, $n_f = (n_i + 2)$ leads to 2nd RP, i.e. $(RP)_2$, and so on.

For the hydrogen-like systems, $n_i = 1$. If the Bohr's equation is applied to any polyelectronic system then *Z* is replaced by $Z^* = Z - b$, where *b* gives the measure of screening effect, and n_i = the highest occupied level (*cf.* Sec. 1.8.5).

Click Here t.me/thalchemylibrary

Elastic and inelastic collision : When some high energy electrons bombard on the atoms of any element in a gaseous condition, and if the kinetic energy of the projectile electron is less than the *CP* of the element on which the bombardment occurs, only exchange of kinetic energy occurs between the projectile and the target atom suffering the collision. This type of collision is called ***elastic collision. In elastic collisions, electrons lose little energy when the collisions occur with the heavy atoms of the gas.*** This can be proved by applying the laws of conservation of energy and momentum. But when the kinetic energy of the incident projectile is sufficient to excite the atom to a higher level, the projectile suffers an ***inelastic collision*** by spending its energy to excite the energy state of the atom. Kinetic energy of the projectile electron beam can be monitored by placing it in a certain accelerating potential gradient (*V*). Hence the following conditions may be obtained.

$$\frac{1}{2}mu^2 = eV \geq CP, \text{ (inelastic collision)}; \quad \frac{1}{2}mu^2 = eV < CP, \text{ (elastic collision)}$$

Experiment : Franck and Hertz in 1914 carried out an experiment by bombarding the various elements taken in the vapour phase with the electrons of known energy. Fig. 1.8.8.1 shows the schematic representation of the experimental design. Here the electrons emitted from the heated filament (*F*) are accelerated towards the perforated grid (*G*) by a known potential (V_1), and a very small potential difference ($V_0 \approx 0.5$ V) called the ***retarding potential*** is maintained between the grid and plate (*P*) on which the electrons can fall to produce a current (*i*) . Within the tube, the ***pressure of the gas or vapour*** is adjusted so that the accelerated electrons may experience several collisions in the space between the filament and grid before to reach the grid. Thus the electron reaching the grid (*G*) having kinetic energy greater than eV_0 can only reach the plate *P* to produce a current. As the ***accelerating potential*** (V_1) increases, more and more electrons reach the plate to increase the current. It occurs so, if only the elastic collision (in which the electrons lose little energy) takes place with the gaseous atoms. If the accelerating potential just imparts the kinetic energy equal to 1st critical potential, i.e. 1st resonance potential, of the element under consideration, then the inelastic collision occurs.

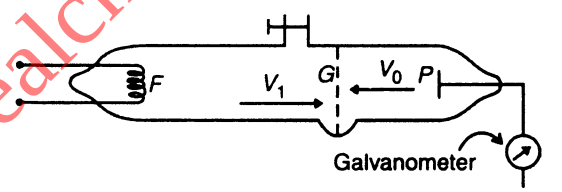

Fig. 1.8.8.1. Franck-Hertz experimental arrangement for determination of critical potentials of elements in gaseous phases.

Thus it follows as : when $V_1 > V_0$, but $eV_1 < (RP)_1$ where $(RP)_1$ stands for 1st resonance potential or 1st critical potential, the current increases with the increase of V_1. **In this range, only the elastic collision occurs.** But, at $eV_1 = (RP)_1$, the electrons will spend all the energy in the inelastic collision and will have no residual kinetic energy to reach the plate after overcoming the retarding potential V_0. At this point, the collector current drops abruptly. For hydrogen gas, it occurs at 10.2 V (cf. 10.2 eV is the ***first critical potential for hydrogen***). Similarly, for *Hg*-vapours, it occurs at 4.9 V.

If the accelerating potential (V_1) is further increased so that $eV_1 - (RP)_1 > eV_0$, then the current again starts to increase. Under this condition, the electrons after experiencing the ***first inelastic collisions*** will have the sufficient energy to reach the plate (*P*). If V_1 is gradually increased, then the current (*i*) is found to drop at higher values of V_1 which are approximately twice, three times, ... the value corresponding to the value of first drop. Thus for hydrogen gas, the drops occur at 1×10.2 V, 2×10.2

Click Here for more chemistry library

V, 3 × 10.2 V, ... and for *Hg*-vapour, these occur at 1 × 4.9 V, 2 × 4.9 V, 3 × 4.9 V, ... ***The first drop corresponds to the first critical potential.*** The first drop occurs when most of the accelerated electrons lose the energy ***in single inelastic collisions.*** The second, third, ... drops occur for the values of accelerating potentials (corresponding to twice, three times, ... the 1st critical potential) at which the electrons lose their energy in ***two, three, ... successive inelastic collisions of the same kind (i.e. first critical potential).*** These are illustrated in Fig. 1.8.8.2.

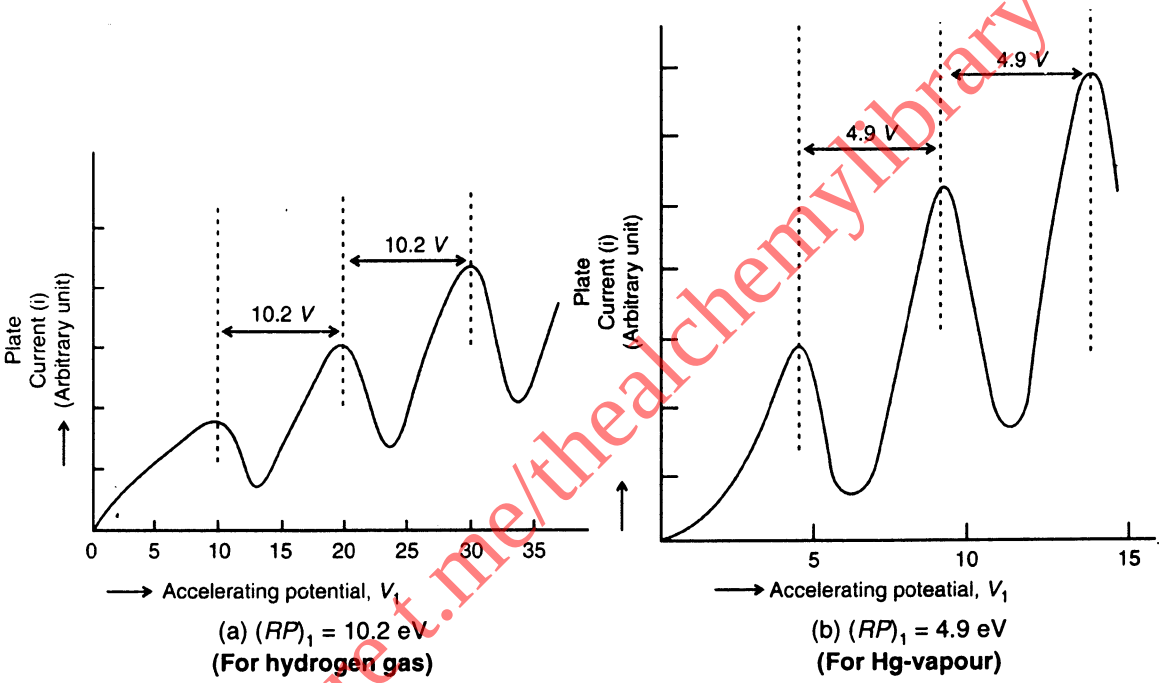

Fig. 1.8.8.2. Determination of 1st resonance potential by Franck-Hertz experiment under the condition, gas or vapour pressure in the tube is not very low. (a) Resonance potential curve for hydrogen. (b) Resonance potential curve for *Hg*-vapour.

Click Here t.me/thealchemylibrary

- ***If pressure of the gas or vapour in the tube is very low*** then the mean free path of the accelerated electrons will be large (i.e. chance of collisions with the atoms of the gas or vapour is less). In such a case, the accelerated electrons may experience the **first inelastic collisions** at different possible *RP* values, i.e. $eV_1 = (RP)_1, (RP)_2, (RP)_3$, ... The 2nd, third, ... inelastic collisions will occur at integral multiples of these *RP* values or of their sums. For *Hg*-vapour, the $(RP)_1$ and $(RP)_2$ values are 4.9 eV and 6.7 eV respectively and in the corresponding current-accelerating potential (i.e. i vs. V_1) curve, the breaks occur at multiples of these values (i.e. 4.9 V, 6.7 V) or of their sums. ***It indicates that Hg-atoms can take up energy in integral multiples of 4.9 eV and 6.7 eV.*** Thus analysis of i vs. V_1 curve obtained ***at low pressure of the gas or vapour*** can determine the different critical potentials.

The original Franck-Hertz experiment cannot distinguish between the *RP* and *IP* values (*IP* = 10.4 eV for mercury, IP = 13.6 eV for hydrogen). ***This is the limitation of the experiment.*** However, this difficulty has been overcome in the experiment designed by Davis and Goucher. This is not described here.

Illustration to support the Bohr's model and quantum theory :

(i) When ***hydrogen gas*** was taken **at a low pressure** in the discharge tube, in the plot of i vs. V_1, the minima occur at 10.2, 12.0, 12.7, 13.0 and 13.2 volts and at the integral multiples of these values or of their sums. The values 10.2 eV, 12.0 eV, ... are definitely the successive resonances or excitation potentials. From the Bohr's theory for hydrogen atoms,

$$CP = \frac{me^4}{8\varepsilon_0^2 h^2}(1 - 1/n_f^2) = Rch\,(1 - 1/n_f^2), \text{ (see Sec.1.8.5)}$$

$$= 1.097 \times 10^7 \text{ m}^{-1} \times 3 \times 10^8 \text{ m s}^{-1} \times 6.625 \times 10^{-34} \text{ J s}\,(1 - 1/n_f^2)$$

$$= \frac{1.097 \times 10^7 \times 3 \times 10^8 \times 6.625 \times 10^{-34} \text{ J}}{1.6 \times 10^{-19} \text{ J/eV}}(1 - 1/n_f^2)$$

$$= 13.6\,(1 - 1/n_f^2) \text{ eV}.$$

Now, for $n_f = 2$, $(CP)_1 = (RP)_1 = 10.21$ eV; $n_f = 3$, $(CP)_2 = (RP)_2 = 12.10$ eV; and, $n_f = \infty$, $IP = 13.6$ eV.

It indicates that critical potentials obtained from the Bohr's theory are in good agreement with the experimental ones.

Note : At the accelerating potential 13.6 eV, **ionisation of hydrogen will occur** and it will mask the resonance potential peaks. However, modified experimental techniques can differentiate the resonance and ionisation effects.

(ii) In the case of ***mercury vapour***, the 1st critical potential occurs at 4.9 V, and at that time, it shows an emission spectrum of a line of 2537 Å. The wavelength of the corresponding critical potential is found to be 2530 Å. Thus this is also in good agreement with the experimental value and it supports the basis of the quantum equation ($E = h\nu$) used in the development of the atomic model.

$$E = 4.9 \text{ eV} = 4.9 \times 1.6 \times 10^{-19} \text{ J} = h\nu = hc/\lambda$$

Thus,
$$\lambda = \frac{hc}{E} = \frac{6.625 \times 10^{-34} \text{ J s} \times 3 \times 10^8 \text{ m s}^{-1}}{4.9 \times 1.6 \times 10^{-19} \text{ J}}$$

$$= 2530 \times 10^{-10} \text{ m} = 2530 \text{ Å}$$

1.8.9 Merits of the Bohr's Atomic Model

It can nicely explain a number of facts such as :

i. ***Stability of the atoms*** : It explains the stability of the atoms while it is lacking in the Rutherford's model. The instability in the Rutherford's model is overcome by envoking the ***concept of stationary state.***

ii. ***Prediction of frequency of the spectral lines*** : The model not only explains the origin of the spectral lines in different series but also gives the mathematical formulations which nicely fit with the experimental observations at least made on the instruments of low resolving power.

iii. ***Rydberg constant (R)*** : Calculated value of R (considering the nuclear motion) nicely agrees with the experimental one.

Click Here to the chemyilibrary

iv. ***Critical potentials - resonance and ionisation potentials*** (cf. ***Frank-Hertz experiment***) **:** Bohr's formulation explains the critical potentials quantitatively for hydrogen-like systems and also for other systems under some approximations. For the *polyelectronic systems*, it requires the use of *effective nuclear charge Z*e* instead of the actual nuclear charge *Ze*. Measured ionisation potentials nicely fit with the predicted ones.

v. ***Explanation of Moseley's law*** **:** It offers a theoretical basis of Moseley's law.

vi. ***Isotopic shifts*** **:** By considering the nuclear motion, the *spectral shifts for the isotopes* of lighter elements such as hydrogen for which masses of the isotopes differ significantly (relatively) are experimentally verified (Section 1.8.3b).

vii. ***Mass ratio of proton and electron*** **(i.e. M_H/m) :** Corrected equation for the Rydberg constant ($R_{corr.}$) by considering the nuclear motion leads to the evaluation of the ratio M_H/m from the spectroscopic studies of He^+ and H. It has been discussed in the Section 1.8.3a. The ratio determined from other methods is in good agreement with this spectroscopic one.

viii. ***Bohr's correspondence principle*** **:** It indicates that for very higher values of n, the atom behaves also classically.

1.8.10 Drawbacks in the Bohr's Model

i. ***Involvement of both classical and quantum mechanics*** **:** Here, the principles of both quantum and classical mechanics have been taken into the consideration as and when required. Hence, theoretically the model cannot be supported.

ii. ***Fine spectra of the spectral lines*** **:** The model can explain the origin of the spectral lines along with their frequencies when they are observed with the instruments of low resolving power. But actually each single line is consisting of a number of fine lines which are closely packed. This has been observed (Fig. 1.8.10.1) by using the instruments of very high resolving power. These fine spectra cannot be explained by the Bohr's theory. For example, the H_α line in Balmer series arises due to the transition from $n = 3$ to $n = 2$, and it will lead to a change of a fixed amount of energy, $\Delta E = E_3 - E_2$ and as a result, only one line of a fixed frequency ($\nu = \Delta E/h$) will be obtained. But the spectral analysis indicates that for the above transition, different amounts of energy change (i.e. ΔE_1, ΔE_2, ΔE_3, ...) occur leading to different fine lines. But these are not expected from the Bohr's theory. *Here it is worth mentioning that the fine lines are not due to the isotopes.*

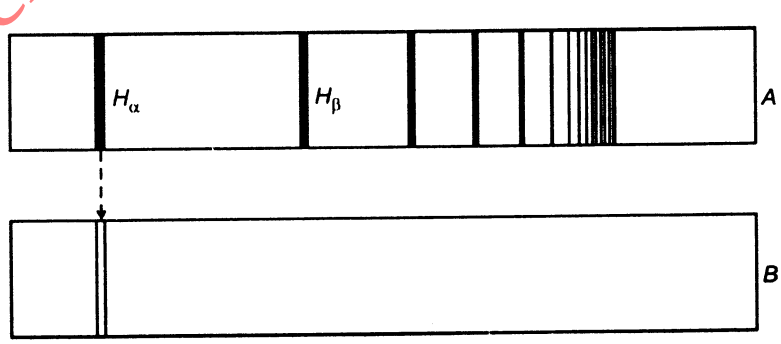

Fig. 1.8.10.1. Fine structure of H_α line in Balmer series. (A) under low resolution, (B) under high resolution, a doublet.

Click Here to meetthealchemylibrary

iii. ***Intensity of the spectral lines*** : Though the frequencies of the spectral lines (not the fine spectra) are predicted from the theory, the theory cannot predict anything regarding their relative intensities.

iv. ***Polyelectronic atoms*** : Though the theory is more or less good for the hydrogen and hydrogen-like systems, such as He^+, Li^{2+}, Be^{3+}, etc. which contain only one electron, for the systems of multielectrons, the theory as such is not at all promising.

v. ***Quantisation of angular momentum*** : The quantum restriction, $mur = n(h/2\pi)$ was taken arbitrarily without giving any sound explanation.

vi. ***Heisenberg's uncertainty principle*** : Consideration of a moving electron with a definite velocity in a circular orbit of a definite radius cannot be supported by Heisenberg's uncertainty principle according to which, it is impossible to determine both the velocity and the position of an electron *simultaneously with a certainty.*

vii. ***Zeeman Effect and Stark Effect*** : The single line in the spectrum is found to split into a number of closely spaced lines in the presence of an external magnetic field (Zeeman Effect, see Section 1.10.19) an electrical field (Stark Effect). Such splittings cannot find any support from the Bohr's theory.

1.9 FINE STRUCTURE OF SPECTRA AND SOMMERFELD'S ATOMIC MODEL

To explain the fine structure (see Fig. 1.8.10.1) observed under high resolutions of each individual spectral line, Bohr's theory was found inadequate and some modifications were required. Sommerfeld did this noble task. Fine structure indicates that an electron transition from one orbit (n_1) to another (n_2) leads to different amounts of energy change though they differ only slightly, otherwise more than one line cannot be generated. *This prediction immediately indicates that the number of the energy levels for a particular quantum number, n must be more than one and these sublevels are definitely closely spaced to one another.* This is why, the spectral lines appear as single lines without any fine structure of a certain width only, when viewed through the instruments of low resolving power. Being guided by this background, Sommerfeld made the required modifications as discussed below.

1.9.1 Sommerfeld's Atomic Model

According to Sommerfeld :

i. **Elliptic orbits :** In general, the electrons are revolving around the nucleus in some specified ***elliptic paths with different ecentricities*** (ε). It may be noted that Bohr's orbits are circular and the circular orbit is only a special case of Sommerfeld's elliptic orbits.

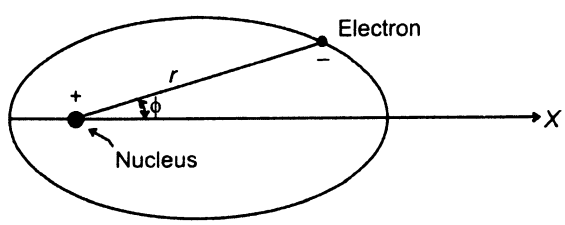

Fig. 1.9.1.1. Revolving electron in an elliptic orbit according to Sommerfeld's model.

ii. **Quantum restrictions :** If the position of a revolving electron around the nucleus at an instant is (r, ϕ) where r is the radius vector measured from the nucleus and ϕ is the angle between the radius vector and a fixed axis (say X-axis) (Fig. 1.9.1.1), then only certain elliptic orbits will be allowed which satisfy the conditions,

$$\oint p_\phi d\phi = kh; \text{ and, } \oint p_r dr = n_r h \qquad \ldots(1.9.1.1)$$

Click Here for more chemistry library

Here the integrals are taken over one complete cycle, p_ϕ and p_r are the **angular and radial momenta** of the electron respectively, h is the Planck constant, k and n_r are two positive integers called the ***azimuthal* and *radial quantum numbers*** respectively.

iii. ***Requirement of two quantum restrictions*** : $n = n_r + k$, where n is the principal quantum number as defined by Bohr. Here it is worth recalling that in Bohr's circular orbits, only one parameter, i.e. the vectorial angle ϕ, varies periodically as r remains constant, while in Sommerfeld's elliptic orbit both r and ϕ vary periodically. *This is why, in Bohr's theory only one quantum restriction was required while Sommerfeld's theory requires two quantum restrictions.*

A. Classical mechanical treatment without any relativistic correction (i.e. Sommerfeld's first modification)

From Fig. 1.9.1.1, it is evident that no force perpendicular to the radius vector is working, so there is no acceleration (a_ϕ) normal to it. Thus,

$$\frac{1}{r}\frac{d}{dt}r^2\frac{d\phi}{dt} = a_\phi = 0 \qquad \ldots(1.9.1.2)$$

The above equation leads to **Kepler's law of area** as follows,

$$r^2\frac{d\phi}{dt} = K = \text{constant} \qquad \ldots(1.9.1.3)$$

Hence the angular momentum (p_ϕ) is a constant as given by,

$$p_\phi = mr^2\frac{d\phi}{dt}, \ (m = \text{mass of the electron}) \qquad \ldots(1.9.1.4)$$

Thus from Sommerfeld's quantum restriction (Eqn. 1.9.1.1),

$$kh = p_\phi \oint d\phi = mr^2\frac{d\phi}{dt} \times 2\pi = p_\phi \times 2\pi$$

$$\text{or, } p_\phi = k(h/2\pi) \qquad \ldots(1.9.1.5)$$

This is in good agreement with the postulate of Bohr according to which the angular momentum of an electron in any stationary orbit is an integral multiple of $h/2\pi$.

The detailed mathematical analysis yields the following relations :

$$\frac{n_r + k}{k} = \frac{1}{\sqrt{1-\varepsilon^2}}; \text{ or, } 1-\varepsilon^2 = \frac{k^2}{n^2}, \ \varepsilon = \text{eccentricity of the elliptic orbit} \qquad \ldots(1.9.1.6)$$

$$E_n = -\frac{Z^2me^4}{8\varepsilon_0^2n^2h^2} = -\frac{RchZ^2}{n^2}, \ \varepsilon_o = \text{absolute permitivity} \qquad \ldots(1.9.1.7)$$

$$a_n \textbf{ (semi-major axis)} = \frac{n^2h^2\varepsilon_0}{\pi mZe^2} = \frac{n^2}{Z}a_o \qquad \ldots(1.9.1.8)$$

$$\left(\text{cf. } r_n = \frac{n^2}{Z}a_o, \text{ in terms of Bohr's theory}\right)$$

Click Here to Join/thearchemylibrary

$$b_n \text{ (semi-minor axis)} = \frac{nkh^2\varepsilon_0}{\pi mZe^2} = \frac{nk}{Z} a_o \qquad \ldots(1.9.1.9)$$

$$a_o = \frac{\varepsilon_o h^2}{\pi me^2} = 1\text{st Bohr radius of } H\text{-atom}$$

$$b_n / a_n = \sqrt{1-\varepsilon^2} = k/n \qquad \ldots(1.9.1.10)$$

Thus, the semi-major axis (a_n) is governed by the principal quantum number while the semi-minor axis is governed by both n and k.

Permitted values of k and n_r : Now let us determine the possible values of n_r and k. For a particular value of n, the possible values of k are : 0, 1, 2, ..., n while the corresponding values of n_r are n, $(n-1)$, $(n-2)$, ..., 0. *But when $k = 0$, b_n becomes zero and as a result, the ellipse gets converted into a straight line leading the moving electron to pass through the nucleus.* Hence for $k = 0$, the atom collapses. **So, $k = 0$ is not acceptable and the allowed values are as follows,**

$$k = 1, \quad 2, \quad 3, \quad \ldots, n$$
$$n_r = (n-1), (n-2), (n-3), \quad \ldots, 0$$

i. Shape of the orbits for a particular value of n

We have, $b_n/a_n = k / (k + n_r)$. Hence when $n_r = 0$; b_n and a_n become the same. **Thus the ellipse gets reduced into a Bohr's circular orbit.** Therefore, Bohr's circular orbit is only a special case in Sommerfeld's model. For a particular value of n it appears from Eqn. 1.9.1.10 that **as the value of k *increases the ellipticity of the orbit decreases and for the highest allowed value of k , it becomes a circular orbit; so, for the minimum values of k , it is the most elliptic one in nature*** (Fig. 1.9.1.2). Here for different k values, the corresponding orbits can be designated as follows,

Name of the orbit : *s*, *p*, *d*, *f*, ...
The value of k : 1, 2, 3, 4, ...

Here it is worth recalling that in *wave mechanics*, the azimuthal quantum number is designated by l; and l and k are related as follows,

$$l = k - 1$$

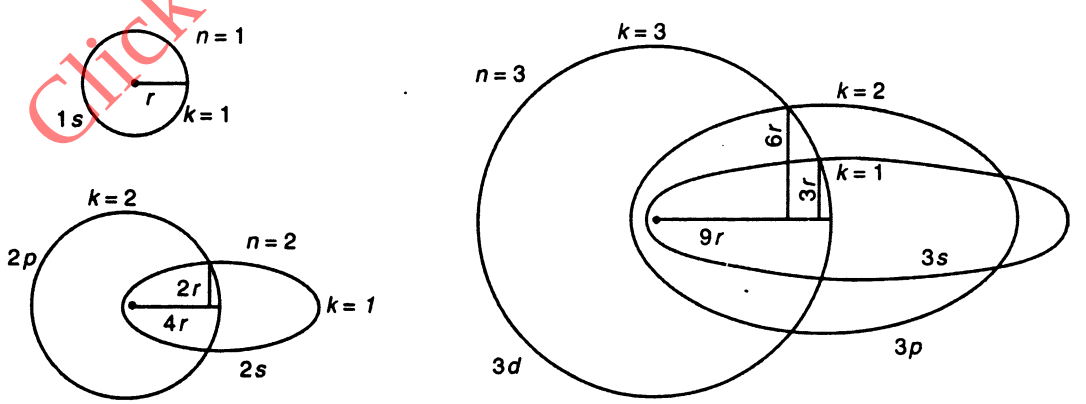

Fig. 1.9.1.2. Different Sommerfeld's orbits of H-atom. ($a_n = n^2 r_1$, $b_n = nkr_1$)

Click Here to Join Chemistry Library

ii. An attempt to explain the fine spectra in the light of Sommerfeld's first modification

Let us consider the probable ways of transition from, $n = 3$ to $n = 2$ to originate the H_α-line in Balmer series. For $n = 3$ and 2, the electron can have the following sets of quantum number,

	$n=3$			$n=2$	
k :	1	2	3	1	2
n_r :	2	1	0	1	0

Thus, here the transition ($n = 3$ to $n = 2$) may occur in a number of ways (Fig. 1.9.1.3). *Though mathematically, there are six possible transitions, all are not quantum mechanically allowed.*

In this model, we are having a number of ways in contrast to the only one way in Bohr's model to generate the line, but in all these cases the energy changes will be identical, ***because the energy is dependent only on n*** (Eqn. 1.9.1.7) ***as in Bohr's model.*** Eqn. 1.9.1.7 indicates that the energy of the revolving electron does not depend on n_r or k individually. Thus in spite of the existence of more the one possible way to produce the H_α-line in Balmer series, we get only one frequency for the radiations. Thus this *first modification* led by Sommerfeld cannot remove the drawback of the Bohr's model.

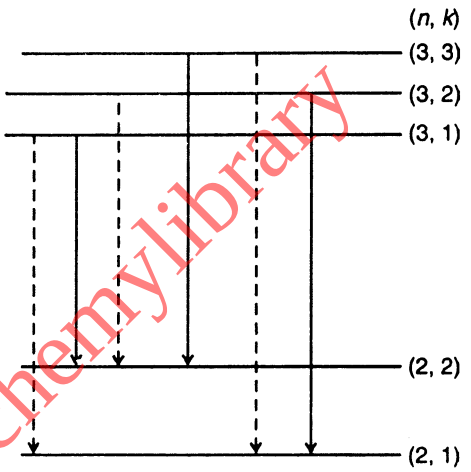

Fig. 1.9.1.3. Origin of fine structure of H_α line in Balmer series. (Quantum mechanically allowed transitions are shown by solid lines and forbidden transitions are shown by dotted lines.)

B. Sommerfeld's second modification, i.e. the relativistic correction, and explanation for the fine structure of the spectral lines

For the elliptic nature of the orbit, at different positions of the electron on the locus it will have different values of r, and consequently the electrostatic attractive force towards the nucleus varies from point to point. Thus the balancing force (i.e. the centrifugal force) which arises due to the angular motion also varies from point to point. The velocity of the electron becomes maximum when it is closest to the nucleus (i.e. ***perihelion position***) and the velocity is minimum when it is at the farthest (i.e. ***aphelion***) position from the nucleus. Due to this variation of velocity at different points, the electron suffers from a relativistic variation in the mass of the electron according to the following relation :

$$m = m_0 (1 - u^2 / c^2)^{-1/2}$$

where m and m_0 are the masses of the electron at the velocity u and zero respectively, c is the velocity of the light. As a result, there is a continual mass variation and it leads to generate a perturbation in the equilibrium force between the electron and the nucleus. Because of this fact,

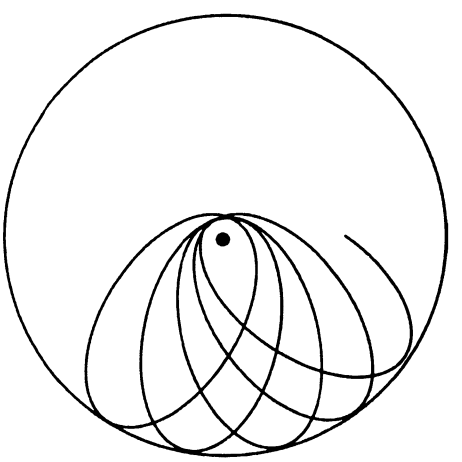

Fig. 1.9.1.4. A precessing Sommerfeld's electron orbit (rosette).

Click Here t me/healchemylibrary

the path of the electron is in fact a rosette (Fig. 1.9.1.4) *which is an ellipse whose major axis precesses slowly in the plane of the ellipse about an axis passing through one of its foci at which the nucleus is residing*. Considering this fact, the energy value (E_n) of an electron in the n-th principal quantum number is given by,

$$E_n = -\frac{me^4Z^2}{8\varepsilon_0^2h^2n^2}\left[1+\frac{\alpha^2Z^2}{n}\left(\frac{1}{k}-\frac{3}{4n}\right)\right]$$

or, $$\boxed{E_n = -\frac{RchZ^2}{n^2}-\frac{Rch\alpha^2Z^4}{n^3}\left(\frac{1}{k}-\frac{3}{4n}\right),\ R=\frac{me^4}{8\varepsilon_0^2h^3c}} \quad \ldots(1.9.1.11)$$

where α is called the ***fine structure constant*** and it has got no unit. It is a pure number and is given by, $\alpha = e^2 / (2\varepsilon_0 ch) = 1/137$ (dimension of $\alpha = \dfrac{C^2}{C^2\,N^{-1}\,m^{-2}\times m\,s^{-1}\times J\,s}$, thus it is a pure number). The second term of Eqn. 1.9.1.11 arises due to the relativistic correction.

The above expression shows that the total energy of the electron depends on both *k* and *n* for a particular value of *n*. There are *n* different (for *n* permitted values of *k*) energy levels for a particular value of *n*. Thus for the H_α line in Balmer series (i.e. $n = 3$ to $n = 2$) there should be six lines (Fig. 1.9.1.3). To make the theory in conformity with the experiment, it was required to restrict the number of lines. This is why, it was proposed to introduce the quantum restriction, i.e. **selection rule**, as: $\Delta k = \pm 1$, Δn = any value. This restriction when applied for the α-lines leads to only **three fine lines (i.e. triplet lines) for Balmer series** (Fig. 1.9.1.3) and **five fine lines (i.e. quintet) for Paschen series, and the α-line in Lyman series should show no fine structure (i.e. single line)**. Unfortunately, the number of components predicted from the theory does not agree with the experimental one. Vector model can explain the fine spectra (see Fig. 1.10.15.1).

1.9.2 Penetrating Power of the Orbits and Quantum Defect in Polyelectronic Systems in the Light of Sommerfeld's Theory

(a) Penetrating and Screening Power of the Orbits

From the studies of many physicochemical properties of different elements, it has been convincingly established that for a particular principal quantum number n, the attractive force towards the nucleus experienced by the electron is in the order : s-electron > p-electron > d-electron > f-electron. This order can be correlated with the ellipticity of the orbits under consideration as follows : ***more the ellipticity of the orbit, more the attractive force experienced by the electron of the orbit towards the nucleus.***

From Sommerfeld's theory, it is indicated that the s-orbits are maximum elliptic followed by the p-orbits and so on. It can be realised as follows : *as the ellipticity increases, the* ***penetrating power of the orbit*** *into the inner orbits increases* (Fig. 1.9.1.2) *and as a result, the electron in the more elliptic orbit spends more time in the vicinity of the nucleus by virtue of its more penetrating power*. Here it is worth mentioning that this penetrating power has been explained by considering the **radial distribution function (RDF)** in the light of wave mechanics which will be discussed in 4th Chapter (Secs. 4.1.4, 4.2.3).

In this connection, it is worthy to consider the ***screening or shielding power of the orbits***. Inner orbits will always try to prevent the outer orbits from facing the nuclear charge, but an outer orbit can

Click Here t.me/thealchemylibrary

overcome this screening barrier by virtue of its penetrating power measured by its ellipticity. If an electron penetrates into the inner electron clouds then it will definitely screen the other electrons. **Hence, it can be concluded :**

higher the penetrating power, higher the screening power towards the other electrons.

(b) Quantum Defect

The optical behaviour of the alkali metals is comparable to that of hydrogen and hydrogen-like systems. *The alkali metals contain only one valency electron in the outermost shell, and the electron is involved in the optical transition.* Here, it can be assumed that all the inner electrons have nothing to do with the outermost optical electron, and the outermost electron is experiencing only unit residual positive charge (i.e. $Z = 1$) at the nucleus. Hence, it is expected that the energy of this optical electron should be expressed as in the case of hydrogen-like systems, i.e. $E_n = -RchZ^2 / n^2$ where Z can be taken as one. But, from the spectral studies it is found as : $E_n = -RchZ^2/(n^*)^2$ where n^* is found to be nonintegral. This fact, i.e. **nonintegral principal quantum number**, definitely strikes at the very fundamental root of the Bohr-Sommerfeld theory. This fact is also observed in many other polyelectronic systems besides the alkali metals. The extent of departure of n^* from the integral values depends on the nature of the electron undergoing optical transition. The degree of departure follows the sequence :

$$s\text{-electron} > p\text{-electron} > d\text{-electron} > f\text{-electron}.$$

The deviation measured by δ from the actual integral principal quantum number is given by,

$$n^* = n - \delta \text{ and } \delta \text{ is called } \textbf{\textit{quantum defect}}.$$

This is maximum for the *s*-electrons. *This phenomenon can be nicely explained by considering the relative efficiency of the penetrating power of the orbits.* Due to this penetration, the electron experiences more positive charge at the nucleus, but this was not considered in the mathematical representation of the energy expression. This enhanced attractive force towards the nucleus can be rationalised mathematically either by considering the higher value of Z (i.e. $Z > 1$) for the outermost electron in the alkali metals or by the lower value of the principal quantum number n, as it is evident that the lower the value of n, the higher is the attractive force towards the nucleus. ***Thus it can be concluded :***

more the penetration, more the attractive force and hence more the quantum defect.

For the alkali metals, if the outermost electron spends 100% time outside the inner electrons then it would face $Z = 1$, but if it can penetrate the inner electrons, it will face $Z > 1$. This $Z > 1$ has been compensated by considering the lower values of n, i.e. n^*. *Thus the higher attractive force due to the interpenetration can be rationalised either by the quantum defect (δ) or by the higher positive charge which is actually experienced rather than the anticipated one without any consideration of interpenetration.*

Now it is worth concluding that the phenomenon of ***quantum defect*** is not an accident but a fundamental demand of Sommerfeld's elliptical orbits. Thus it offers an evidence in favour of the validity of Sommerfeld's model.

In this connection, the general formula known as **Ritz combination principle** (Sec. 1.5.3) is worth mentioning. According to Eqn. 1.5.3.1 of this principle, we get :

$$\bar{\nu} = \frac{R}{(m+\beta)^2} - \frac{R}{(n+\alpha)^2}$$

Click Here Link/thealchemylibrary

where, m and n are integers denoting the principal quantum numbers, and α and β are called ***adjustment constants***. *These constants α and β arise due to the quantum defect.* Thus the equation can be rewritten as,

$$\bar{\nu} = \frac{R}{(m-\delta_1)^2} - \frac{R}{(n-\delta_2)^2}$$

In the hydrogen-like systems where only one electron exists, no screening or shielding occurs and as a result, β and α (i.e. δ_1 and δ_2) become zero. But in the polyelectronic systems such as alkali metals, δ_1 and δ_2 are not zero and they are important in determining $\bar{\nu}$ of the spectral lines. Here it is worth noting that δ depends on the azimuthal quantum number and consequently on the principal quantum number. This is why for m and n it is given by different quantities δ_1 and δ_2 respectively.

(c) Quantum Defect and Ritz Combination Principle in the Spectral Series of Alkali Metals (see Fig. 1.10.15.2)

According to the Ritz combination principle, the wave numbers for different series (not considering the fine spectra) can be expressed as follows [see Section 1.10.15 (ii)]. Here the adjustment constants α and β are replaced by the quantum defects (δ) and Z by 1. Origin of different spectral series in alkali metals have been discussed in Sec. 1.10.15.

Principal series : $\bar{\nu}_P = \frac{R}{(3-\delta_S)^2} - \frac{R}{(n-\delta_P)^2}, n = 3, 4, 5, \ldots$

Sharp series : $\bar{\nu}_S = \frac{R}{(3-\delta_P)^2} - \frac{R}{(n-\delta_S)^2}, n = 4, 5, 6, \ldots$

Diffuse series : $\bar{\nu}_D = \frac{R}{(3-\delta_P)^2} - \frac{R}{(n-\delta_D)^2}, n = 3, 4, 5, \ldots$

Fundamental series : $\bar{\nu}_F = \frac{R}{(3-\delta_D)^2} - \frac{R}{(n-\delta_F)^2}, n = 4, 5, 6, \ldots$

The δ_S, δ_P, δ_D ..... designate the quantum defects in the corresponding term series. If the quantum defect is ignored, the wave number is determined by the term R/n^2 (assuming $Z = 1$) as expected from the Bohr's theory. Then the calculated principal quantum numbers designated as ***apparent principal quantum numbers*** (n^*) obtained from the experimental determination of wave numbers for the different series display a significant deviation from the nearest integral values. To overcome this, the *adjustment constants which are called here as quantum defects* are required. These quantum defects along with their apparent principal quantum numbers are given in Table 1.9.2.1. From the dependence of quantum

Table 1.9.2.1. Quantum defects for sodium atom

Term	*Apparent principal quantum number (n^*)*	*n*	*Quantum defect (δ)*	*l*
S	1.63	3	$\delta_S = 1.37$	0
P	2.12	3	$\delta_P = 0.88$	1
D	2.99	3	$\delta_D = 0.01$	2
F	4.00	4	$\delta_F = 0.00$	3

Click Here t.me/thealchemylibrary

defect (δ) on the azimuthal quantum number (l), it is found that, $\delta_S > \delta_P > \delta_D > \delta_F$. This sequence can be nicely explained by considering the penetrating efficiency of the orbits.

1.9.3 Achievements of the Sommerfeld' s Theory

In addition to the all merits (Section 1.8.9) in Bohr's theory, it has got the following additional successes:

i. ***Fine spectra*** : Sommerfeld's modification can explain the origin of fine lines by introducing two additional quantum numbers, k and n_r, though it fails to predict the exact number of the fine lines.

ii. ***Penetrating and screening power*** : Different orbits differing in ellipticity for different values of k even for a particular principal quantum number n, experience different amounts of positive charge at the nucleus because of their different penetrating powers. Thus the binding force for different electrons lies in the sequence, s-electron > p-electron > d-electron > f-electron. This prediction is verified in many properties such as ionisation potentials, electron affinity, etc.

iii. ***Quantum defect*** : It can also be rationalised by Sommerfeld's theory.

1.9.4 Drawbacks in the Sommerfeld's Model

i. ***Components of fine structure*** : It cannot predict the correct number of fine structure components.

ii. ***Relative intensity*** : It cannot say anything regarding the relative intensities of the fine structure components.

iii. ***Azimuthal quantum number*** : Sommerfeld's azimuthal quantum number (k) is different from the one (l) obtained in wave mechanics.

iv. ***Uncertainty principle*** : According to the uncertainty principle, simultaneous consideration of the exact position and velocity of the revolving electron cannot be supported.

v. ***Involvement of both classical and quantum mechanical physics*** : Involvement of these two physics as in the case of Bohr's theory cannot be theoretically supported.

vi. ***Polyelectronic systems*** : It mainly deals with the hydrogen-like systems, but for the other systems it does not work well.

1.10 VECTOR MODEL OF THE ATOM

It has been observed that Bohr-Sommerfeld model was only confined to hydrogen and hydrogen-like systems having only one electron and it appears incompetent to deal with the problems of complex systems having a large number of electrons. Though Sommerfeld's modification put forward a justification for the fine structure of hydrogen spectrum, it could not predict the relative intensity and the exact number of components. Besides these, no explanation of Zeeman effect, Paschen-Back effect and Stark effect discovered later on was available in Bohr-Sommerfeld model. Another drawback of the model was that it could not predict anything regarding the mode of electron distribution in polyelectronic systems. To overcome these drawbacks, the physicists were experiencing an urgency to have a new model which can successfully cope with these problems. The monumental efforts coming from Bohr, Sommerfeld, Uhlenbeck, Goudsmit, Pauli, Lande, Stern and Gerlach in this direction developed a new model known as ***vector model of the atom***. The foundation stone of this new model mainly lies on these pillars : (i) ***concept of spatial quantisation***, (ii) ***concept of the spinning electron***,

Click Here for more/healchemylibrary

(iii) ***Pauli exclusion principle.*** In this model, the properties arising from both orbital and spinning motion are considered as vector quantities *whose magnitudes and directions are quantised.* The model developed based on these considerations is called vector model of the atom in which the vector laws are obeyed.

1.10.1 Concept of Spatial Quantisation

In Bohr-Sommerfeld model, the magnitudes of moments were only quantised. Thus the corresponding orbits only in shape and size were quantised. But in the vector model, these are treated as vector quantities. Hence, both their direction and magnitude are quantised. Thus the orientations of the orbits in space are restricted only to certain directions as demanded by the quantum condition.

To quantise the orbits in space, we require **a certain reference direction** with respect to which the allowed directions will be defined. To have this required **reference direction,** we require the application of *an external field of force*. The orbits get oriented in space following the quantum restrictions with respect to the direction of the field.

Sommerfeld was the pioneer in developing this concept in connection with the interpretation of the Zeeman effect, i.e. splitting of the spectral lines in the presence of an external magnetic field.

1.10.2 Concept of the Spinning Electron

Sommerfeld's modification could not explain the exact number of fine structure components of the spectral lines of hydrogen atom. It indicated that besides the orbital momentum, there was something else. It was soon found that the common **yellow sodium *D* line** actually consists of two fine lines, 5889.96 Å (D_2) and 5895.93 Å (D_1). The components of this **doublet** (i.e. D_1 and D_2) differ by about 6 Å . Similarly, a closely spaced **triplet line** has been found for magnesium. For the heavier atoms, the splitting is very much prominent. *For example, in mercury the triplet is extended over about 1400 Å while the sodium D line splits by only about 6 Å.* Thus, the term, ***'fine structure'*** is appropriate for the lighter atoms but in the heavier atoms it becomes misnomer and it recoins the term, ***multiplet structure*** in preference to the term fine structure.

Besides these, the doublet sodium *D*-line experiences a complicated splitting pattern *in the presence of a moderately strong magnetic field* giving rise to four components in D_1 line and six components in D_2 line (Fig. 1.10.2.1). This phenomenon is called ***anomalous Zeeman effect*** to distinguish it from the ***normal triplet Zeeman effect.***

To explain these spectral observations, **Uhlenbeck and Goudsmit,** the two Dutch physicists proposed the **concept of the spinning electron** in 1925. In this concept, it is believed that in addition to the orbital motion, the electron is also spinning around its own axis. This spinning motion leads to the generation of an additional *mechanical angular momentum* along with an additional *magnetic moment.* These are also vector quantities and are quantised in both magnitude and direction by the quantum restrictions as in the case of orbital moments. Consideration of these new properties of the electron along with other properties led to a profound modification of the atomic model which is reflected in the vector model of the atom.

Thus, the total angular momentum of an atom is the vector sum of the contributions from both orbital motion and spinning motion of the electrons. Similarly, total magnetic moment arises from both spinning and orbital motion.

Click Here to me/thealchemylibrary

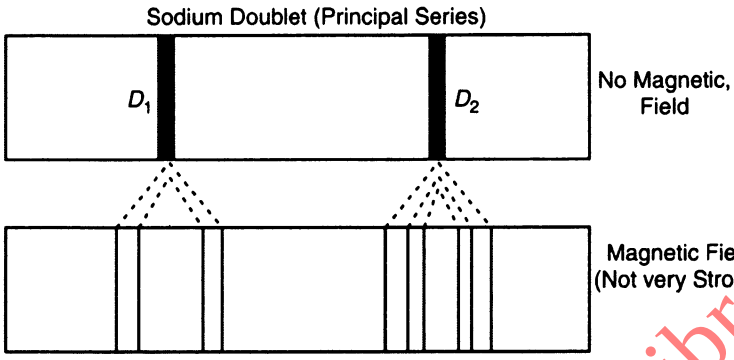

Fig. 1.10.2.1. Splitting of sodium D_1 and D_2 lines in the presence of a moderately strong magnetic field (anomalous Zeeman effect).

Experimental evidences in favour of the concept of space quantisation and spinning electron are obtained in the experiment of Stern and Gerlach (1921) which is discussed in Section 1.10.18.

1.10.3 Quantum Numbers in the Vector Model

i. ***Principal quantum number (n)*** **:** It is identical with the principal quantum number used in Bohr-Sommerfeld model. It takes up the integral values 1, 2, 3 ....

ii. ***Orbital quantum number (l)*** **:** It actually replaces the Sommerfeld's azimuthal quantum number k. For a particular value of n, it can have all the integral values in the range 0 to $(n-1)$. Thus l and k are related by $l = k - 1$. Conventionally, an electron having $l = 0$, is designated as an s-electron; similarly, for $l = 1$, p-electron; for $l = 2$, d-electron; and so on. The ***orbital angular momentum vector*** **($\vec{l}$ or, p_l)** is expressed in terms of the quantum number as : p_l or $\vec{l} = l(h/2\pi)$. Wave mechanically it is given by : $\vec{l} = \sqrt{l(l+1)}\,\dfrac{h}{2\pi}$.

iii. ***Spin quantum number (s)*** **:** The spinning idea was first introduced by Uhlenbeck and Goudsmit in 1925. The magnitude of s is ½ which is nonintegral and thus it apparently contradicts to the integral multiple rule of quantisation. But, experimentally this **nonintegral value** does not contradict. The ***spin angular momentum vector*** **($\vec{s}$ or p_s)** developed due to the spinning motion of the electron around its own axis is given by : p_s or $\vec{s} = s(h/2\pi)$. In wave mechanics it is modified as: $\vec{s} = \sqrt{s(s+1)}\,(h/2\pi)$.

iv. ***Total angular quantum number (j)*** **:** Both the spinning and orbital motion of the electron will contribute to the resultant angular momentum. This **resultant angular momentum vector** ($\vec{j}$ or p_j) requires the quantum number j. The vector $\vec{j}$ is given by, $\vec{j} = \vec{l} + \vec{s}$. The vector $\vec{j}$ can be expressed as : $\vec{j} = j\,(h/2\pi)$. In wave mechanics, it is : $\vec{j} = \sqrt{j\,(j+1)}\,(h/2\pi)$. Sometimes, j is called ***inner quantum number***. *Here it is worth mentioning that the vectors $\vec{l}$ and $\vec{s}$ of an electron can only combine in weak and ordinary fields, and this aspect will be discussed later.*

v. ***Quantum numbers involved in spatial quantisation*** **:** When the atoms are placed in an external magnetic field, the magnetic moments generated from the spinning and orbital motion of the electron, interact with the external field. Then with respect to the direction of the field, both the

Click Here t.me/thealchemylibrary

orbital and spin motion orient themselves in certain specified directions. These require **three more additional quantum numbers** as discussed below :

(a) Magnetic orbital quantum number (m_l)

It arises due to the spatial quantisation of the orbital angular momentum vector ($\vec{l}$) in the presence of an external magnetic field and it requires a quantum number m_l.

Orbital motion of an electron is equivalent to a current in a loop of wire. This orbital motion will produce a magnetic moment (μ_l) that will act normal to the plane of the orbit. The orbital angular momentum vector $\vec{l}$ is acting in the opposite direction of μ_l (cf. Sec. 1.10.17). An external field (H) will try to orient the $\vec{l}$ vector parallel to the field and the electronic orbit will be subjected to a torque ($= \mu_l H$). This will lead to the $\vec{l}$ vector to precess about the field (Fig. 1.10.3.1). This will also cause precession (called ***Larmor precession***, cf. Zeeman effect, Sec. 1.10.19) of the orbit. The precessional motion of the $\vec{l}$ vector describes the surface of a cone. **This phenomenon can be compared with the behaviour of a spinning top.** The angular momentum vector of the spinning top acting along the spin axis does not lie along the gravitational field but precesses around the direction of gravitational field.

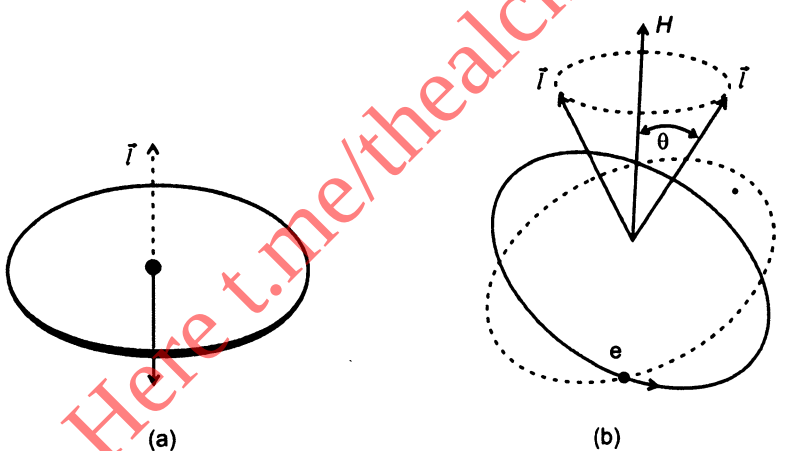

Fig. 1.10.3.1. (a) Representation of orbital angular momentum vector $\vec{l}$ and orbital magnetic moment (μ_l) acting in opposite directions; both μ_l and ($\vec{l}$) perpendicular to the orbital plane. (b) Illustration of *Larmor precession* of the $\vec{l}$ vector and the electronic orbit in presence of an external magnetic field (H).

The precessional motion of the electronic orbit creates new energy states in presence of the magnetic field. At a fixed field (H), energy of the new states depends on the angle (θ) between the $\vec{l}$ vector and external magnetic field.

Thus in presence of a magnetic field, the additional energy levels are introduced depending on the angle (θ) between the $\vec{l}$ vector and the field. If all possible values of θ are allowed, there would be an infinite number of new energy states. If it were so, the emission spectrum of an atom in presence of an external magnetic field would be a continuous one. But Zeeman effect shows only a few lines. This indicates only some allowed values of θ for which $\vec{l}\cos\theta$ (= projection of the $\vec{l}$ vector in the direction

Click Here t.me/thealchemylibrary

of the field) is an integer (denoted by m_l) i.e. $\vec{l}\cos\theta = m_l$. It indicates that the component of $\vec{l}$ vector along the field is given by the integral multiples of $h/2\pi$.

The term $m_l(h/2\pi)$ represents the magnitude of the projection of the vector $\vec{l}$ along the field direction. The quantum number m_l can take all the integral values ranging from $-l$ to $+l$ including zero. **Thus the orbital vector can take up $2l + 1$ possible orientations with respect to the direction of the field.** The vector $\vec{l}$ gets inclined at such angles (θ) with the direction of the external field that its projection, ($\vec{l}\cos\theta$) on the direction can be expressed by $m_l\,(h/2\pi)$. For, $l = 3$ (i.e. *f*-electrons), the vector $\vec{l}$ is given by $\sqrt{3(3+1)}\,(h/2\pi)$ and the permitted quantum numbers for spatial orientations are : $m_l = \pm 3, \pm 2, \pm 1, 0$. The magnitudes of the projections are respectively given by :

$$3(h/2\pi),\ 2(h/2\pi),\ 1(h/2\pi),\ 0(h/2\pi),\ -1(h/2\pi),\ -2(h/2\pi),\ \text{and}\ -3(h/2\pi),$$

For $l = 3$ the permitted orientations with respect to the applied field H are shown in Fig. 1.10.3.2. Each value of m_l corresponds to a possible value of θ indicating a spatial orientation of the electronic orbit in the external magnetic field.

(b) Magnetic spin quantum number (m_s)

Due to the spinning motion of the electron, it is associated with a magnetic moment which also interacts with the external field as the orbital magnetic moment does. Thus the spin angular momentum vector $\vec{s}$ interacts with the external magnetic field and precess around the field direction as in the case of the orbital vector $\vec{l}$. **The vector $\vec{s}$ can have $2s + 1$ allowed orientations with respect to the external field direction.** This spatial quantisation of $\vec{s}$ gives the m_s values from $-s$ to $+s$ without including zero; since s can have only nonintegral value 1/2 and it never takes zero. Thus the possible values of m_s are $\pm$ ½. The term $m_s(h/2\pi)$ represents the magnitudes of the projection of $\vec{s}$ vector along the field direction.

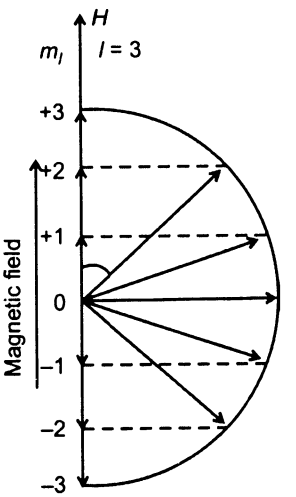

Fig. 1.10.3.2. The possible orientations of the orbital angular momentum vector ($\vec{l}$) for *f*-electron ($l = 3$) in the presence of a magnetic field i.e. possible m_l values for a particular value of l. The vectors (i.e. $\vec{l} = \sqrt{l(l+1)}\,h/2\pi = \sqrt{12}\,h/2\pi$, for $l = 3$) are in the unit of $h/2\pi$.

(c) Total magnetic angular momentum quantum number (m_j)

This arises due to the spatial quantisation of the total angular momentum vector $\vec{j}$ in the presence of an external magnetic field. The vector $\vec{j}$ gets oriented in such a way with respect to the direction of the field that its projection values along the direction differ by unity. The allowed corresponding m_j values cover the range $-j$ to $+j$. Thus the number of possible spatial orientations of $\vec{j}$ with respect to the direction of the field is given by $2j + 1$. The term $m_j\,(h/2\pi)$ gives the magnitudes of the projection of $\vec{j}$ along the field direction.

Note : In strong magnetic fields, the vectors $\vec{l}$ and $\vec{s}$ cannot combine vectorially and they precess about the field independently. Thus m_s and m_l exist only in strong fields where the coupling between $\vec{l}$ and $\vec{s}$ is broken down. On the other hand, $\vec{j}$ and m_j only exist in weak or ordinary fields. It may be

Click Here to the Chemy Library

noted that for the heavier elements, the nuclear charge is sufficiently high to force the coupling between the $\vec{l}$ and $\vec{s}$ vectors.

1.10.4 Four Quantum Number System and Pauli Exclusion Principle

Among the different quantum numbers associated with the electron, only four quantum numbers n, l, m_l and m_s or n, l, j and m_j are required to define an electron completely. The former set is used in the presence of a strong magnetic field when the coupling between $\vec{l}$ and $\vec{s}$ is broken down while the latter set is used in the rest of the cases. Here it is worth mentioning that for the heavier elements where the nuclear charge is sufficiently high to force the coupling between $\vec{l}$ and $\vec{s}$, the latter set is considered. For the lighter elements up to first transition series, the former set is used in practice. The values and designations given to these four quantum numbers are summarised as follows :

- **Ist set : n, l, m_l and m_s (in the presence of a strong magnetic fileld, and for lighter elements).**

Principal quantum number : $n = 1$ (i.e. K shell), 2 (i.e. L shell), 3 (i.e. M shell), 4 (i.e. N shell),...

Orbital quantum number or azimuthal quantum number : $l = 0$ (i.e. s-subshell), 1 (i.e. p-subshell), 2 (i.e. d-subshell), 3 (i.e. f-subshell), ... $(n - 1)$. It mainly determines the shape and size of the orbits.

Magnetic orbital quantum number : $m_l = l, (l - 1), (l - 2), 0 ..... (l - 1), -l$, i.e. for each value of l, m_l can have $2l + 1$ values.

Magnetic spin quantum number : m_s can have only two values, i.e. symbol $\pm \frac{1}{2}$, for a particular set of n, l and m_l.

- **2nd set : n, l, j, and m_j, (in the presence of weak and ordinary magnetic fields, and for too heavy elements).** The quantum numbers n and l bear the same significance as in the case of Ist set.

Total angular quantum number or inner quantum number : $j = l \pm s = l \pm ½$ where s (= ½) is the spin quantum number which arises due to the angular momentum for the spinning motion of the electron. When the vectors $\vec{l}$ and $\vec{s}$ are antiparallel, the negative sign arises and the positive sign appears for their parallel orientations.

Total magnetic angular momentum quantum number : $m_j = j, (j - 1), (j - 2), ..., 0, ..., -(j - 1), -j$. For each value of j, m_j can have $2j + 1$ values.

Pauli Exclusion Principle : It states that in an atom or ion there can be no two electrons having the four quantum numbers identical; for their individuality they must differ at least in one quantum number. This principle indicates that for the principal quantum number n, there can be maximum $2n^2$ electrons and it is evident from Table 1.10.4.1 (see also Sec. 1.11.1).

According to the principle, each sublevel (i.e. orbital) can accommodate maximum two electrons with *opposite spins*. **The *non-electrostatic* repulsive force between the electrons of the same spin is described as the *Pauli repulsive force* which operates sharply at very short range.** Because of this Pauli repulsive force, electrons having the same spin tend to occupy different orbitals or different regions of space. This Pauli repulsive force is the basis of the fundamental law known as *Pauli exclusion principle*.

1.10.5 Coupling Schemes and Atomic States in the Vector Model

To describe an electron, the individual quantised vectors and quantum numbers are sufficient, but to describe an atom as a whole we require the resultants of the quantised vectors of all the electrons

Click Here t.me/thealchemylibrary

Table 1.10.4.1. Total number of electrons in each shell in terms of defining four quantum numbers and Pauli exclusion principle.

Shell	n	l (0 to n–1)	m_l (+ l to –l)	$m_s = \pm ½$	Number of electrons in subshells, representation	Total number of electrons in each shell ($2n^2$)
K	1	0	0	+ ½, – ½	2, $1s^2$	$2 = 2 \times 1^2$
L	2	0	0	+ ½, – ½	2, $2s^2$	$2 + 6 = 8 = 2 \times 2^2$
	2	1	+ 1, 0, –1	+ ½, – ½	6, $2p^6$	
	3	0	0	+ ½, – ½	2, $3s^2$	2 + 6 + 10 = 18
M	3	1	+ 1, 0, –1	+ ½, – ½	6, $3p^6$	$= 2 \times 3^2$
	3	2	+ 2, + 1, 0, –1, –2	+ ½, – ½	10, $3d^{10}$	
	4	0	0	+ ½, – ½	2, $4s^2$	2 + 6 + 10 + 14
N	4	1	+ 1, 0, –1	+ ½, – ½	6, $4p^6$	$= 32 = 2 \times 4^2$
	4	2	+ 2, + 1, 0, –1, –2	+ ½, – ½	10, $4d^{10}$	
	4	3	+ 3, + 2, + 1, 0, –1, –2, –3	+ ½, – ½	14, $4f^{14}$	

present in the system. These resultant vectors are obtained by combining (vectorially) the vectors of the different electrons along with the consideration of space quantisation. Two methods for this vectorial combination of the individual components are highly useful and these are $\vec{L} - \vec{S}$ coupling and $\vec{j} - \vec{j}$ coupling.

Here it is noteworthy that the *small letters* such as *l, s, j* and *s, p, d, f,* etc. are used to *describe the electrons individually and to describe an atom as a whole, the capital letters* such as *L, S, J,* and *S, P, D, F,* etc. are used. If the resultant orbital quantum number (L) of the involved electrons becomes 0, 1, 2, 3, 4, 5, 6, 7, then the corresponding electronic states of the atom or ion as a whole are represented by *S, P, D, F, G, H, I, K* ... respectively (the term J for $L = 7$ is not included, as it has been already included as a quantum number). The resultant J values are shown at the lower right hand suffix (i.e. right subscript) of the corresponding term, and the resultant S is represented as $(2S + 1)$ at the upper left hand prefix (i.e. left superscript) of the term. It is illustrated by considering the following example.

Let, $L = 3$, $J = 4$ and $S = 1$. Hence, the term to express the atomic state becomes nothing ${}^{2S+1}F_4$, i.e. ${}^3F_4$.

Similarly, the term ${}^2D_{5/2}$ appears for, $L = 2$, $S = 1/2$ and $J = 5/2$.

The upper left superscript $(2S + 1)$ gives the ***spin multiplicity*** of the atomic state. For the multiplicity of 1 (i.e. $S = 0$), 2 (i.e. $S = 1/2$), 3 (i.e. $S = 1$), 4 (i.e. $S = 3/2$), 5 (i.e. $S = 2$), ... the states are designated by ***singlet, doublet, triplet, quartet, quintet,*** ... respectively.

1.10.6 $\vec{L} - \vec{S}$ Coupling Scheme

This scheme occurs frequently and this is why it is also known as ***normal coupling***. This coupling scheme is also known as ***Russell-Saunders Coupling***. In this scheme, orbital angular momentum vector, $\vec{l}$ for each of the electrons combines vectorially to produce the resultant orbital angular momentum vector, $\vec{L}$. Similarly, $\vec{s}$ for the different electrons combines to produce the resultant vector $\vec{S}$. Then

Click Here to me/thealchemylibrary

the resultant vectors $\vec{L}$ and $\vec{S}$ combine to give the resultant total angular momentum vector $\vec{J}$. Thus, it can be represented as,

$$\vec{J} = \vec{L} + \vec{S} = (\vec{l}_1 + \vec{l}_2 + \vec{l}_3 + ...) + (\vec{s}_1 + \vec{s}_2 + \vec{s}_3 + ...)$$

The resultant vectors, $\vec{L}, \vec{S}, \vec{J}$ can be expressed in terms of their corresponding resultant quantum numbers, i.e. L, S, J, as follows,

$$\vec{L} = \sqrt{L(L+1)}\,(h/2\pi), \vec{S} = \sqrt{S(S+1)}\,(h/2\pi) \text{ and } \vec{J} = J(J+1)\,(h/2\pi).$$

Here it is important to consider that the electrons in a closed shell contributes nothing to the resultant $\vec{L}$ and $\vec{S}$ (i.e. $\Sigma\vec{l}_i = 0$, $\Sigma\vec{s}_i = 0$). ***This is why, to define the atomic states, only the electrons in the valency shell which is not closed are to be considered.***

(a) Determination of $\vec{L}$ and L where $\vec{L} \approx L(h/2\pi)$

Only the electronic configuration of the valency shell is to be considered. Let us take some specific cases to illustrate the process :

(i) ***One electron system*** **($L = l$)** : (•) s^1-configuration (e.g. H, He^+, Li^{2+}, etc.); $l = 0$, i.e. $L = 0$ (S-state).

(•) p^1-configuration (e.g. B); $l = 1$, i.e. $L = 1$, (P-state).

(•) d^1- configuration (e.g. Ti^{3+}); $l = 2$, i.e. $L = 2$ (D-state).

(ii) ***Two electron system*** : (•) p^2-configuration ($l = 1$); $\vec{l}_1 = \vec{l}_2 \approx l(h/2\pi)$.

These two vectors can combine in the ways shown in Fig. 1.10.6.1 and the corresponding states are : S ($L = 0$), P ($L = 1$) and D ($L = 2$).

(•) d^2-configuration ($l = 2$); $\vec{l}_1 = \vec{l}_2 = 2(h/2\pi)$. Their vectorial combinations are shown in Fig. 1.10.6.2.

General rule for determination of L in vectorial combination of $\vec{l}_1$ and $\vec{l}_2$:

$$L = |(l_1 + l_2)|, |(l_1 + l_2) - 1|, |(l_1 + l_2) - 2|, ..., |(l_1 - l_2)|$$

(iii) ***Three electron system*** : p^3-configuration ($l = 1$) : $\vec{l}_1 = \vec{l}_2 = \vec{l}_3 \approx l(h/2\pi)$. In this case, $\vec{l}_3$ for the third electron can be vectorially added to the resultant $\vec{L}$ values obtained due to the interaction between $\vec{l}_1$ and $\vec{l}_2$. Thus $\vec{l}_3$ is to be combined with the states, i.e. $L = 2, 1, 0$, obtained for the p^2

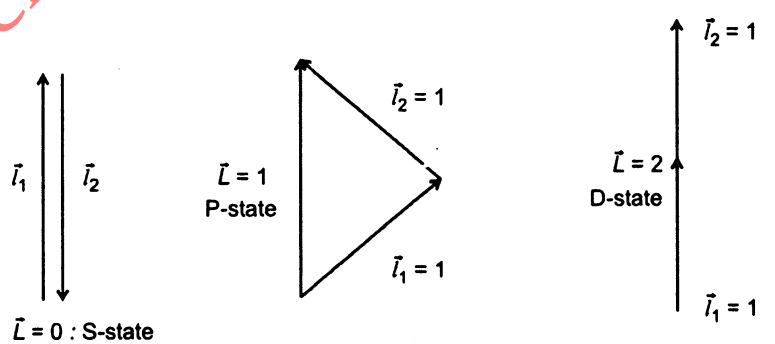

Fig. 1.10.6.1. Vectorial combination of $\vec{l}_1$ *and* $\vec{l}_2$ for p^2 configuration (i.e. $l_1 = l_2 = 1$). The vectors are in the unit of $h/2\pi$ where $\vec{l} \approx l(h/2\pi)$ and $l = 1$.

Click Here t.me/bhoalchemylibrary

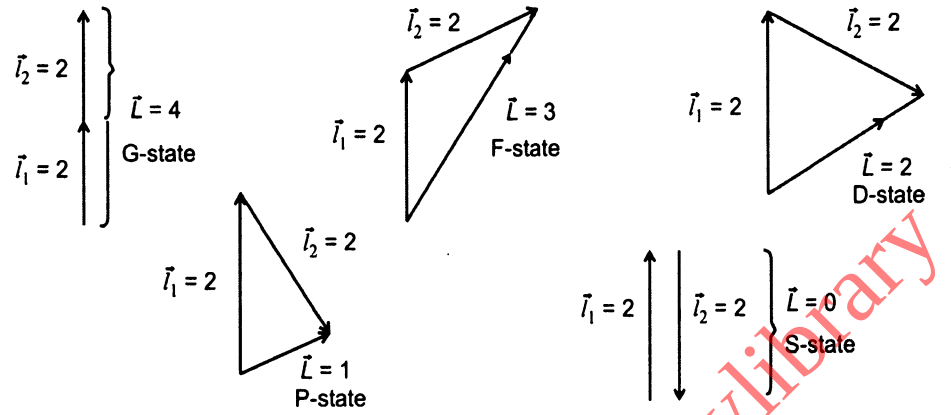

Fig. 1.10.6.2. Vectorial combination of $\vec{l}_1$ *and* $\vec{l}_2$ for d^2 configuration (i.e. $l_1 = l_2 = 2$). The vectors are in the unit of $h/2\pi$ where $\vec{l} \approx l(h/2\pi)$ and $l = 2$.

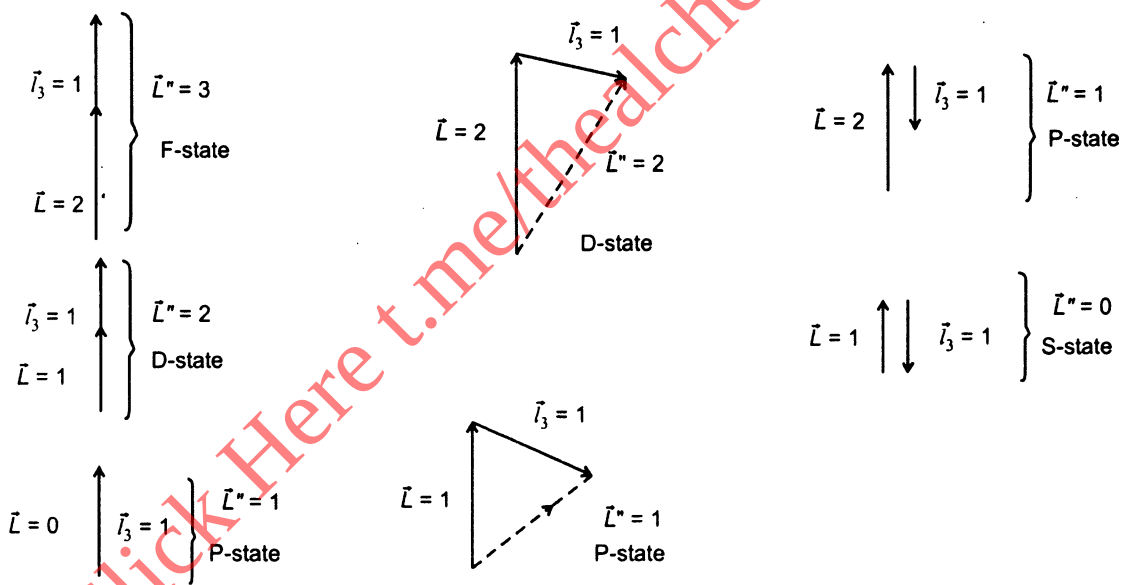

Fig. 1.10.6.3. Vectorial combination of $\vec{l}_1, \vec{l}_2$ and $\vec{l}_3$ for p^3-configuration (i.e. $l_1 = l_2 = l_3 = 1$). The vectors $\vec{l}_1 \approx l(h/2\pi)$ are represented in the unit of $h/2\pi$. $\vec{L}$ = resultant of $\vec{l}_1$ and $\vec{l}_2$, $\vec{L}''$ = resultant of $\vec{L}$ *and* $\vec{l}_3$.

configuration. It leads to one F state, two D states, three P states and one S state. The coupling is shown in Fig. 1.10.6.3 where the resultant vectors are denoted by $\vec{L}''$.

General rule for determination of L in vectorial combination of $\vec{l}$ ***in poly-electronic systems involving*** $\vec{l}_1, \vec{l}_2, \vec{l}_3, \vec{l}_4, ...$

- ***1st step*** : Vectorial combination between $\vec{l}_1$ and $\vec{l}_2$ leads to the resultant for which the quantum number L is given by :

$|(l_2 + l_2)|, |(l_1 + l_2) - 1|, |(l_1 + l_2) - 2|, ..., |(l_1 - l_2)|$, *i.e.* $L_1, L_2, L_3, ...$

Click Here t.me/thealchemylibrary

- ***2nd Step*** : Vectorial combination is to be considered due to the interaction of $\vec{l_3}$ on the states obtained in the Ist step. Hence the following resultant values are obtained.

  $\vec{L_1}$ and $\vec{l_3}$ which leads to $L = |(L_1 + l_3)|, |(L_1 + l_3) - 1|, |(L_1 + l_3) - 2|, ..., |(L_1 - l_3)|$

  $\vec{L_2}$ and $\vec{l_3}$ which leads to $L = |(L_2 + l_3)|, |(L_2 + l_3) - 1|, |(L_2 + l_3) - 2|, ..., |(L_2 - l_3)|$

  $\vec{L_3}$ and $\vec{l_3}$ which leads to $L = |(L_3 + l_3)|, |(L_3 + l_3) - 1|, (L_3 + l_3) - 2|, ..., |(L_3 - l_3)|$

  and so on.
- ***3rd step*** : Now the interactions of the fourth electron, i.e. $\vec{l_4}$, on the states produced in the 2nd step are to be considered and it goes on in the same way up to the n–th electron.

(b) Determination of $\vec{S}$ and S where $\vec{S} \approx S(h/2\pi)$

Here also the closed shells lead to $\vec{S} = 0$. Vectorial combination of $\vec{s_1}, \vec{s_2}, ...$ can be illustrated as follows.

i. ***One electron system*** : $\vec{s} = (½)\,(h/2\pi)$, i.e. $\vec{S} = (½)\,(h/2\pi)$ and $S = ½$.

ii. ***Two electron system*** **(e.g. p^2 or d^2-case):** Here, $\vec{s_1} = \vec{s_2} = (½)\,(h/2\pi)$ may couple in two ways (Fig. 1.10.6.4) to give $S = 0$ or 1. For $S = 0$, the two vectors are antiparallel i.e., the electrons are with opposite spins and for $S = 1$ they are parallel.

iii. ***Three electron system*** **(e.g. p^3 or d^3-case)** : It leads to $S = 1/2$ or $3/2$ (Fig. 1.10.6.4).

iv. ***Four electron system*** : It produces $S = 0$, 1 or 2 (Fig. 1.10.6.4). In general, if there are n-unpaired electrons with their parallel spins, S becomes $n/2$ (i.e. maximum possible value).

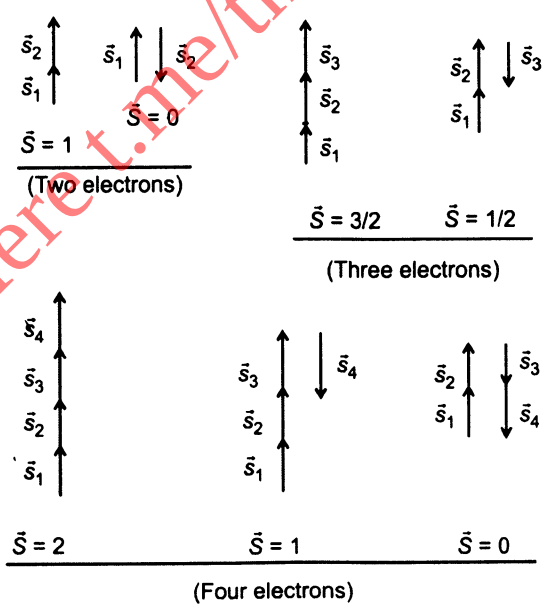

Fig. 1.10.6.4. Vectorial combinations of spin angular momentum vector $(\vec{s})$. The vectors are represented in the unit $h/2\pi$ where $\vec{s} \approx s(h/2\pi)$ *and* $s = 1/2$.

(c) Determination of $\vec{J}$ and J where $\vec{J} \approx J(h/2\pi)$

Vectorial combination of $\vec{S}$ and $\vec{L}$ leads to $\vec{J}$ (*i.e.* $\vec{J} \approx J(h/2\pi)$) which gives :

Click Here t.me/thealchemylibrary

$$J = |(L+S)|, |(L+S)-1|, |(L+S)-2|, ..., |(L-S)|$$

Vectorial addition of some cases, such as : $\vec{L}=0, \vec{S}=1$; $\vec{L}=1, \vec{S}=1$; $\vec{L}=2, \vec{S}=1$ are shown in Fig. 1.10.6.5.

It is evident that J can have integral or half integral values depending on the values of S. It has the integral values when both L and S are integers but it bears the half integral values when S is a half integer, as L always bears the integral values. ***The possible number of values of J*** **is** $(2S+1)$ ***when*** $|L| > |S|$ ***and it is*** $(2L+1)$ ***when*** $|S| > |L|$.

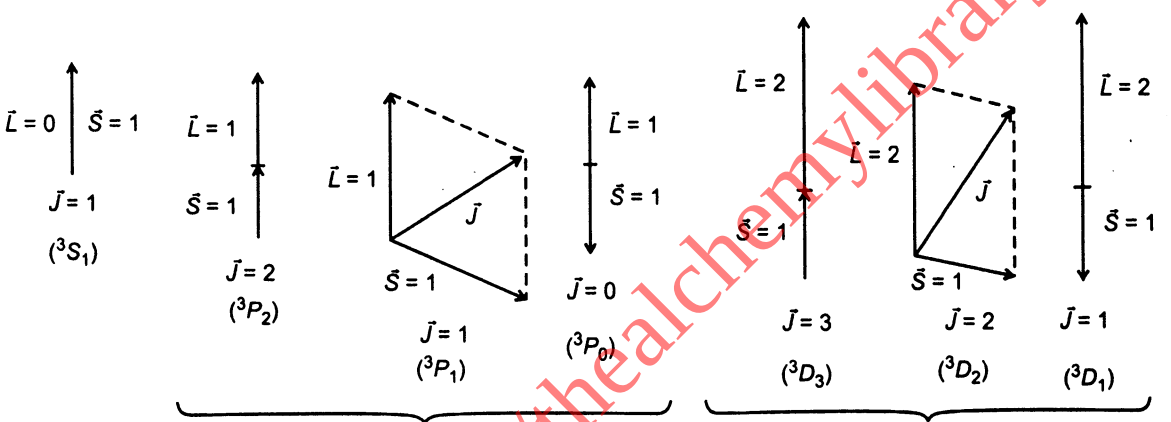

Fig. 1.10.6.5. Vectorial combinations of resultant $\vec{S}$ and $\vec{L}$ to give the resultant $\vec{J}$. The vectors are expressed in the unit of $h/2\pi$ where, $\vec{S} \approx S(h/2\pi), \vec{L} \approx L(h/2\pi), \vec{J} \approx J(h/2\pi)$.

(d) Application of *L-S* coupling in some cases

Here it is illustrated for two electron systems where the two electrons may be ***equivalent*** (i.e. same n and l value, e.g. s^2, p^2, d^2 etc. configurations) or ***nonequivalent*** (i.e. at least one of the quantum numbers between n and l will be different, e.g. s^1–p^1, p^1–p^1, d^1–d^1, etc.).

1. ***p^1–p^1, (nonequivalent differing in n values) and p^2 (equivalent) configuration*** : Here, $l = 1$ and it leads to :

   $\vec{l}_1 = \vec{l}_2 = l(h/2\pi)$. We can write :

   $L = |(l_1 + l_2)|, |(l_1 + l_2) - 1|, |(l_1 - l_2)| = 2, 1, 0$ and $S = 1, 0$.

   To determine the J values, the following interactions are to be considered.

   $(\vec{L}=2, \vec{S}=1); (\vec{L}=1, \vec{S}=1); (\vec{L}=0, \vec{S}=1); (\vec{L}=2, \vec{S}=0); (\vec{L}=1, \vec{S}=0)$; and $(\vec{L}=0, \vec{S}=0)$.

   Thus the corresponding J values become :

   $$J = (3, 2, 1); (2, 1, 0); (1); (2); (1); (0)$$

   Hence the corresponding spectroscopic terms are :

   $$(^3D_3, ^3D_2, ^3D_1); (^3P_2, ^3P_1, ^3P_0); (^3S_1); (^1D_2); (^1P_1); (^1S_0);$$

   These are all possible atomic states arising from p^1–p^1 or p^2 configurations. The p^1–p^1 configuration may be considered as an excited state of the p^2 configuration. **Thus it can be said that above**

Click Here t.me/thealchemylibrary

atomic states are *including both the ground and excited states for a p^2 configuration*, e.g. carbon system whose ground and excited state electronic configurations are given by $1s^22s^22p^2$ and $1s^22s^22p^13p^1$ respectively.

- For the **$2p^13p^1$ (i.e. p^1-p^1) electronic configuration** (where Pauli exclusion principle does not work), the possible values are :

  $L = 0$, 1 and 2; $S = 0$ and 1 for each value of L.

  It generates 6 terms (3 singlet and 3 triplet) :

$$\underbrace{{}^1S(J=0),\ {}^1P(J=1),\ {}^1D(J=2)}_{\textit{Singlet}};\ \underbrace{{}^3S(J=1),\ {}^3P(J=2,1,0),\ {}^3D(J=3,2,1)}_{\textit{Triplet}}$$

  These 6 terms produce 10 states (i.e. *fine structure components*) in terms of J. The first four terms (having a single value of J) do not split.

- If, the electronic configuration $1s^22s^22p^2$, i.e. **ground state (p^2)**, is considered then without violating the Pauli exclusion principle, only the following microstates are allowed from the above list.

$$\underbrace{{}^3P(J=2,1,0)}_{\textit{Triplet}};\ \underbrace{{}^1D(J=2),\ {}^1S(J=0)}_{\textit{Singlet}}$$

  The above mentioned 3 terms (one triplet and two singlets) produce 5 states in terms of J value (cf. for p^1–p^1 configuration, there are 10 states).

2. ***s^1–p^1 (nonequivalent) configuration*** : Here, $l_1 = 0$ and $l_2 = 1$. Thus the maximum possible value of L is 1, and also the minimum possible value of L is 1. The possible values of S are 1 and 0. It leads to the following terms :

$${}^3P\ (J = 2, 1, 0) \text{ and } {}^1P\ (J = 1), \text{ i.e. 4 states.}$$

3. ***d^1–d^1 (nonequivalent) configuration*** : Here, $l_1 = l_2 = 2$. Thus the possible values of L are 4, 3, 2, 1, 0 and S can have the values 0, 1 for each value of L. Thus, the following terms are generated:

$${}^3G(J = 5, 4, 3),\ {}^3F(J = 4, 3, 2),\ {}^3D(J = 3, 2, 1),\ {}^3P(J = 2, 1, 0),\ {}^3S(J = 1),\ {}^1G(J = 4),$$
$${}^1F(J = 3),\ {}^1D(J = 2),\ {}^1P(J = 1) \text{ and } {}^1S(J = 0), \text{ i.e. 18 states.}$$

   The last 6 terms do not split.

4. ***s^1–s^1 (nonequivalent) configuration*** : It generates the terms : ${}^1S\ (J = 0)$, ${}^3S\ (J = 1)$.
5. ***s^1–d^1 (nonequivalent) configuration*** : It generates the terms : ${}^1D\ (J = 2)$, ${}^3D\ (J = 3, 2, 1)$.
6. ***Three nonequivalent electrons* (e.g. s^1–p^1–d^1)** : The development of terms is shown in the following Scheme (cf. $s^1 - p^1$ leads to the terms ${}^3P$ and ${}^1P$) :

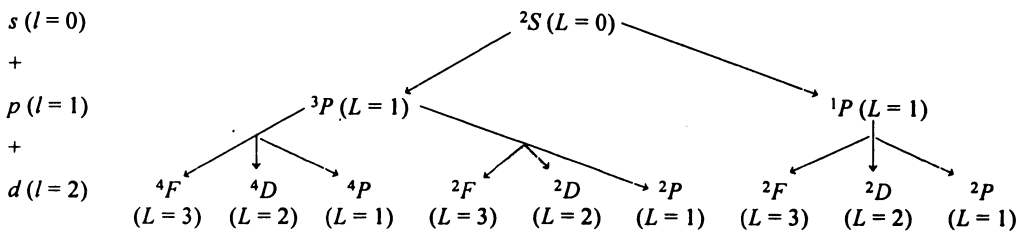

Click Here t.me/thealchemylibrary

Thus the terms are : ${}^4F, {}^2F, {}^2F; {}^4D, {}^2D, {}^2D; {}^4P, {}^2P, {}^2P$. In this way, the terms can be developed for nonequivalent multielectron systems. The states (i.e. fine structure components) can be determined in terms of the J value.

1.10.7 $\vec{J}-\vec{J}$ Coupling Scheme

In the systems where the nuclear charge is very high, the spin-orbit interaction for each electron is very high and their respective $\vec{l}$ and $\vec{s}$ vectors for the *individual electron* combine to generate $\vec{j}$ vectors. In these cases, no interaction among the spin vectors or the orbital vectors of the different electrons exist and as a result, the resultant vectors $\vec{L}$ and $\vec{S}$ become nonexistent. Thus, $\vec{J}$ can be represented in such cases as follows :

$$\vec{J} = \vec{J_1} + \vec{J_2} + \vec{J_3} + ... = (\vec{l_1} + \vec{s_1}) + (\vec{l_2} + \vec{s_2}) + (\vec{l_3} + \vec{s_3}) + ...$$

There are some systems where the nuclear charge is in the intermediate range where coupling scheme may be of an intermediate type of the *two limiting schemes*, and in such cases, the problem gets complicated. But it is a matter of fortune that the $\vec{L}-\vec{S}$ coupling scheme has been found effective in most of the cases.

Illustration of j–j coupling

(i) ***s^1–p^1 configuration*** : The first electron (i.e. s-electron having $l_1 = 0$, $s_1 = ½$) produces $j_1 = ½$. The second electron (i.e. p-electron having $l_2 = 1$, $s_2 = ½$) gives $j_2 = \frac{3}{2}, \frac{1}{2}$. Coupling of j_1 and j_2 produces $J = 2, 1$ and $1, 0$

i.e. $j_1 = \frac{1}{2}$ and $j_2 = \frac{3}{2}$ produce $J = 2, 1$

$j_1 = \frac{1}{2}$ and $j_2 = \frac{1}{2}$ produce $J = 1, 0$

Thus the total four states i.e. $(j_1, j_2)_J$ are :

$$\left(\frac{1}{2}, \frac{3}{2}\right)_2, \left(\frac{1}{2}, \frac{3}{2}\right)_1, \left(\frac{1}{2}, \frac{1}{2}\right)_1 \text{ and } \left(\frac{1}{2}, \frac{1}{2}\right)_0$$

The L–S coupling also produces 4 states.

(ii) ***p^1–p^1 configuration*** : We can write as follows :

$l_1 = 1$ and $s_1 = \frac{1}{2}$ produce $j_1 = \frac{1}{2}, \frac{3}{2}$

$l_2 = 1$ and $s_2 = \frac{1}{2}$ produce $j_2 = \frac{1}{2}, \frac{3}{2}$

Each j_1 can couple with each of the two j_2 values.

j_1	j_2	J	States, i.e. $(j_1, j_2)_J$	
3/2	3/2	3, 2, 1, 0	$(3/2, 3/2)_{3, 2, 1, 0}$	Total 10 states
3/2	1/2	2, 1	$(3/2, 1/2)_{2, 1}$	
1/2	3/2	2, 1	$(1/2, 3/2)_{2, 1}$	
1/2	1/2	1, 0	$(1/2, 1/2)_{1, 0}$	

It may be noted that L–S coupling also produces 10 states.

Click Here t.me/thealchemylibrary

1.10.8 Spatial Quantisation of the Resultant Vectors (i.e. $\vec{L}, \vec{S}, \vec{J}$) in Atoms or Ions

By considering the coupling schemes described above, only the magnitudes of the resultant vectors are available, but to describe the atom as a whole the resultant vectors must be quantised in direction. The number of permitted orientations of $\vec{L}, \vec{S}$ and $\vec{J}$ with respect to the direction of the external field are given by $(2L + 1)$, $(2S + 1)$ and $(2J + 1)$ respectively. They actually represent the corresponding resultant magnetic quantum numbers M_L, M_S and M_J respectively. The terms $M_L(h/2\pi)$, $M_S(h/2\pi)$ and $M_J(h/2\pi)$ represent the magnitudes of the projections of the vectors $\vec{L}, \vec{S}$ and $\vec{J}$ respectively in the direction of the field. The resultant quantum numbers are : $M_L = \Sigma m_l$ which can have all the integral values from $+L$ to $-L$ including zero; $M_S = \Sigma m_s$ which can have $(2S + 1)$ values from $+S$ to $-S$; and $M_J = \Sigma m_j$ which can have $(2J + 1)$ values from $+J$ to $-J$.

1.10.9 Determination of Microstates and Russel-Saunders Terms

To find out the microstates in the light of Russell-Saunders coupling, the following procedure (illustration for carbon, i.e. np^2, $l = 1$) is followed.

1. First we are to determine the maximum possible value of M_L $(= \Sigma m_l)$. Here it is 2, as m_l varies from $+l$ to $-l$. This M_L originates from $\vec{L} = 2$. Hence M_L can have values +2, +1, 0, –1 and –2.
2. Now we are to consider the maximum possible value of M_S $(= \Sigma m_s)$. Here it is 1 and it definitely originates from $\vec{S} = 1$. Hence M_S can have values +1, 0, –1.
3. Next we are to set up a chart of the possible microstates (i.e. combination of m_l and m_s) as shown in Table 1.10.9.1. Microstate $(1^+, 1^-)$ indicates that one of the two electrons bears $m_l = +1$ and $m_s = +\frac{1}{2}$ while the other bears $m_l = +1$ and $m_s = -\frac{1}{2}$, (in both cases, $n = 2$, $l = 1$ for carbon).
4. Now from Table 1.10.9.1, the microstates which are not in conformity with the Pauli exclusion principle are to be rejected. For example, the microstate $(1^+, 1^+)$ shows that both the electrons bear $m_l = +1$ and $m_s = +\frac{1}{2}$ in addition to the same values of n (= 2, for C-atom) and l (= 1 for the p-electrons). Hence it is not acceptable.
5. Now, Table 1.10.9.1 containing the allowed microstates is to be analysed for the term symbols. In the present case, i.e. np^2, M_L can have the maximum value 2, only when the two electrons are paired, i.e. $M_S = 0$. As M_L originates from $\vec{L} = 2$, it indicates the possible values of $M_L = +2, +1, 0, -1$ and -2. Each of these M_L values will have to bear $M_S = 0$. Thus the five microstates denoted by *** in the Table represent the term ^1D (as $L = 2$ and $S = 0$). Now, the next maximum possible value of M_L is 1 (i.e. $\vec{L} = 1$) for which the maximum possible value of M_S is 1 (i.e. $\vec{S} = 1$). Here the possible values of M_L are $+1, 0, -1$ and the possible values of M_S are given by $+1, 0, -1$. These M_L(i.e. + 1, 0, 1) and M_S (i.e. + 1, 0, – 1) values can combine in nine ways to produce nine microstates represented by ** in Table 1.10.9.1, and these are designated by the term ^3P (as $L = 1$, and $S = 1$). The last microstate $(0^+, 0^-)$ indicates $L = 0$ and $S = 0$. Hence its corresponding term is ^1S.

The total microstates under different term symbols are shown as follows (cf. Sec. 1.10.6d) :

Term symbol	Number of microstates = orbital multiplicity × spin multiplicity = $(2L + 1) \times (2S + 1)$
^1D	$(2 \times 2 + 1)(2 \times 0 + 1) = 5$
^3P	$(2 \times 1 + 1)(2 \times 1 + 1) = 9$
^1S	$(2 \times 0 + 1)(2 \times 0 + 1) = 1$

Click Here! .me/thealchemylibrary

Table 1.10.9.1. Microstates arising from a np^2 electronic configuration

$M_S \rightarrow$ / $M_L \downarrow$	+ 1	0	–1
+ 2	$(1^+, 1^+)$*	$(1^+, 1^-)$***	$(1^-, 1^-)$*
+ 1	$(0^+, 1^+)$**	$(0^+, 1^-)$**, $(0^-, 1^+)$***	$(0^-, 1^+)$**
0	$(0^+, 0^+)$* $(1^+, -1^+)$**	$(1^+, -1^-)$***, $(1^-, -1^+)$**, $(0^+, 0^-)$****	$(1^-, -1^-)$**, $(0^-, 0^-)$*
–1	$(0^+, -1^+)$**	$(0^+, -1^-)$**, $(0^-, -1^+)$***	$(0^-, -1^-)$**
–2	$(-1^+, -1^+)$*	$(-1^+, -1^-)$***	$(-1^-, -1^-)$*

* These are forbidden by Pauli exclusion principle. **States arise from ^3P. ***States arise from ^1D. ****State arises from ^1S.

6. The total number of microstates for x electrons (when it is half-filled or less than half-filled) in a certain orbit having orbital quantum number l is given by $^{2y}C_x$ where $y = 2l + 1$.

$$^{2y}C_x = \frac{(2y)(2y-1)(2y-2)....(2y-x+1)}{1\times2\times3\times4....\times x}; \quad \left(cf.\ ^nC_r = \frac{n!}{r!(n-r)!}\right)$$

Examples :

(a) *d^1–system* : $y = 2 \times 2 + 1$, $(l = 2)$; $x = 1$. Hence, the number of microstates = $^{10}C_1 = 10$.

(b) *p^3–system* : $y = 2 \times 1 + 1$, $(l = 1)$; $x = 3$. Hence the number of microstates = $^6C_3 = 20$.

(c) *d^5–system* : $y = 2 \times 2 + 1$, $(l = 2)$; $x = 5$. Hence, number of microstates = $^{10}C_5 = 252$.

1.10.10 A Simple Working Procedure to Determine the Term Symbols

Considering the Pauli exclusion principle, we can easily determine the allowed terms for a certain electronic configuration.

Examples :

(i) ***np^2 case*** : Here we can have $M_S = 0, \pm 1$. For $M_S = \pm 1$, both the electrons *must differ in m_l values* (Pauli exclusion principle), and for $M_S = 0$, *they must have opposite spins for which they may have the same or different m_l values*. Now, we have to consider the possible M_L values for a certain M_S value as shown in the following chart :

$M_S\ (= \sum m_s)$	S	$M_L\ (= \sum m_l)$, (+ L to – L)	L	***Term***	***No. of microstates*** $= (2L + 1)(2S + 1)$
± 1	1	1, 0, – 1	1	^3P	9
0	0	2, 1, 0, – 1, – 2	2	^1D	5
		0	0	^1S	1

Click Here t.me/theachemylibrary

(ii) ***nd² case*** : By following the same procedure the corresponding terms and microstates are determined as follows :

$M_S(=\sum m_s)$	S	$M_L(=\sum m_l)$, (+ L to − L)	L	*Term*	*No. of microstates* = (2L + 1) (2S + 1)
± 1	1	3, 2, 1, 0, − 1, − 2, − 3;	3	^3F	21
		1, 0, − 1	1	^3P	9
		4, 3, 2, 1, 0, − 1, − 2, − 3, − 4;	4	^1G	9
0	0	2, 1, 0, − 1, − 2	2	^1D	5
		0	0	^1S	1

Note :

- **For a particular *S*-value, the possible *L* values differ by 2-units.**
- ***np² case*** : For S = 1, M_L = + 1 is obtained in one way (+ 1, 0); M_L = 0 is obtained in one way (+ 1, − 1).
  For S = 0, M_L = + 2 is obtained in one way (+ 1, + 1); M_L = + 1 is obtained in one way (+ 1, 0); M_L = 0 is obtained in two ways (+ 1, − 1) and (0, 0).
- ***nd² case*** : For S = 1, M_L = + 3 is obtained in one way (+ 2, + 1); M_L = +2 is obtained in one way (+ 2, 0); M_L = + 1 is obtained in two ways (+ 2, − 1) and (+ 1, 0); M_L = 0 is obtained in two ways (+ 2, − 2) and (+ 1, − 1).
  For S = 0, M_L = + 4 is obtained in one way (+ 2, + 2); M_L = + 3 is obtained in one way (+ 2, + 1); M_L = + 2 is obtained in two ways (+ 2, 0) and (+ 1, + 1); M_L = + 1 is obtained in two ways (+ 1, 0) and (+ 2, − 1); M_L = 0 is obtained in three ways (0, 0), (+ 1, − 1) and (+ 2, − 2).

Terms arising from the various electronic configurations are shown in Table 1.10.10.1.

Table 1.10.10.1. Terms arising from various electronic configurations.

Configuration	*Terms (i.e. Russel-Saunders states)*
s^1	^2S *
s^2	^1S *
p^1, p^5	^2P *
p^2, p^4	^3P*, ^1D, ^1S
p^3	^4S*, ^2D, ^2P
p^6	^1S *
d^1, d^9	^2D*
d^2, d^8	^3F*, ^3P, ^1G, ^1D, ^1S
d^3, d^7	^4F*, ^4P, ^2H, ^2G, ^2D(2), ^2P, ^2F
d^4, d^6	^5D*, ^3H, ^3G, ^3F(2), ^3D, ^3P(2), ^1I, ^1G(2), ^1F, ^1D(2), ^1S(2)
d^5	^6S*, ^4G, ^4F, ^4D, ^4P, ^2I, ^2H, ^2G(2), ^2F(2), ^2D(3), ^2P, ^2S
d^{10}	^1S*

Note : ^2D(2) means, ^2D term appears twice, and so on for other representations; *makes the **ground state term.**

Click Here t.me/thealchemylibrary

1.10.11 Hund's Rules to Determine the Ground State Term

It has been already discussed that the inner closed shells and subshells produce $M_L = \sum m_l = 0$, i.e. $\vec{L}$ must be zero, and similarly $M_S = \sum m_s = 0$, i.e. $\vec{S}$ must be zero. **This is why, they contribute nothing to the vectors obtained from the unfilled shells (i.e. valency shells).** Thus, the term symbols or microstates only appear from the valency shell. To determine the ground state of an atom, Hund's rules are extremely important and these are formulated as follows:

1. ***Hund's first rule or the rule of spin multiplicity*** (effects of both **exchange energy:** E_{ex} and electrostatic repulsive **Coulombic energy** E_{coul}; see Sec. 1.11.1) : Ground state will be determined by the highest spin multiplicity (= $2S + 1$). In other words, it can be stated as : *if a number of degenerate* (i.e. *of the same energy*) *energy levels are available then the electrons will try to remain unpaired with parallel spins so long as possible.* It can be illustrated by taking as example, say C ($1s^2\ 2s^2\ 2p^2$), where for the accommodation of two *p*-electrons, there are three degenerate rooms. According to this rule, out of the different possible arrangements, only the arrangements **(I)** and **(V)** (Fig. 1.10.11.1) are allowed.

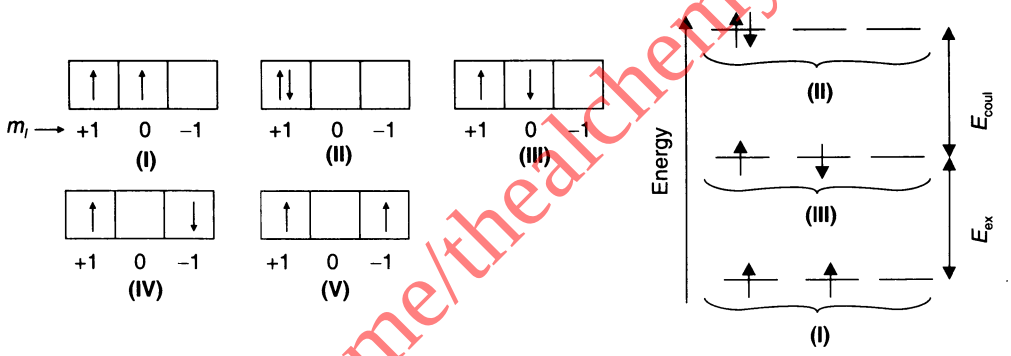

Fig. 1.10.11.1. Illustration of Hund's rule of spin multiplicity in the case of p^2 configuration (E_{coul} positive; E_{ex} negative). ($E_{ex} \propto {}^xC_2$, x = number of electrons with the same spin; see Sec. 1.11.1).

2. ***Hund's second rule of orbital multiplicity*:** After considering the maximum spin multiplicity, the ground state will be determined by the highest possible **orbital multiplicity** (= $2L + 1$), i.e. the highest possible value of L. For the higher L-values, interelectronic Coulombic repulsion (E_{coul}) is less. Here in practice, we have to determine the highest M_L ($\sum m_l$) value which will definitely correspond to the highest L value, as M_L ranges from $+L$ or $-L$. In Fig. 1.10.11.1, though the arrangements **(I)** (i.e. $\sum m_l = 1$) and **(V)** (i.e. $\sum m_l = 0$) are possible in the light of Hund's first rule, according to the second rule, only the arrangement **(I)** is allowed.
3. ***Hund's third rule or the rule of J*:** After considering the 1st and 2nd rule, out of the different possible J values, i.e. $|L + S|$ to $|L - S|$, for a half-filled or less than half-filled level, the ground state will have the lowest possible J value, whereas, for a more than half-filled level, the ground state will have the highest possible J value.

***Illustration of Hund's rules in the case of C*:** Hund's rules can be successfully applied to predict the order of energy of different states obtained from Russell–Saunders coupling. Here it will be applied for C having the electronic configuration $1s^2 2s^2 2p^2$. Here it is worth mentioning that the **Hund's rules cannot be used for the excited configuration** such as $1s^2 2s^2 2p^1 3p^1$ for C.

It has been already established (Secs 1.10.6 and 1.10.9) that C has one triplet term, i.e. ^3P, and two singlet terms, i.e. ^1D and ^1S. According to Hund's first rule, **the triplet state ^3P is the *ground state*.** In the light of the second rule, ^1D (i.e. $L = 2$) is stabler than ^1S (i.e. $L = 0$) though both of these have the

Click Here t.me/thealchemylibrary

same spin multiplicity. The triplet state ^3P can split into three states $^3P_2$, $^3P_1$ and $^3P_0$ depending upon the J values. According to the third rule, they are in the order of energy:

$$^3P_0 < {}^3P_1 < {}^3P_2, \text{ (for } \textbf{less than half-filled sublevel)}.$$

Considering the further splitting of the J values in the presence of a magnetic field into M_J values which can range from $+J$ to $-J$, the energy order of the fifteen microstates is shown in Fig. 1.10.11.2.

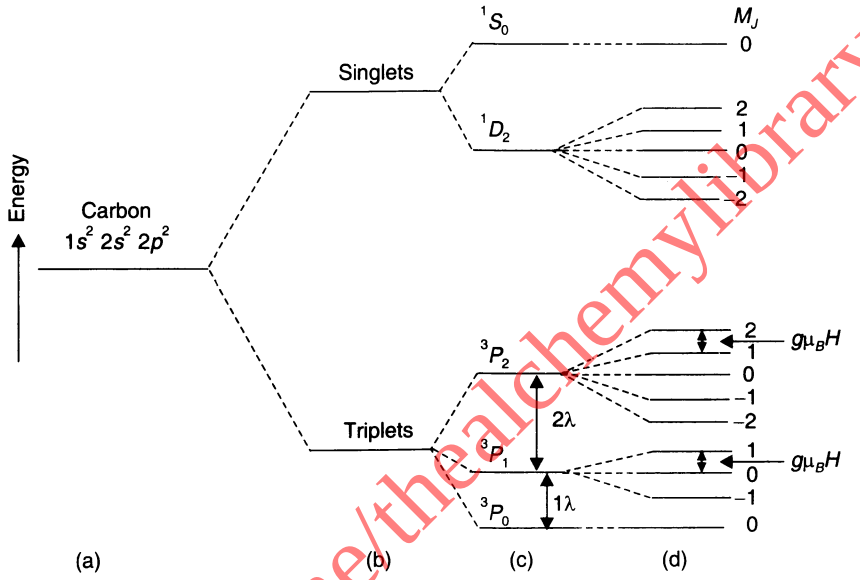

Fig. 1.10.11.2. Splitting of energy states developed from carbon (i.e. p^2 configuration). (a) electronic configuration; (b) spin-spin coupling; (c) orbit-orbit coupling followed by spin-orbit coupling; (d) splitting by a magnetic field (H). $E_J = \frac{1}{2}\lambda[J(J+1) - L(L+1) - S(S+1)]$

The energy separation between the successive states differing by only J values is governed by ***Lande Interval Rule.*** *It states that the energy separation between the successive levels having J values as J and J + 1 is proportional to the larger value of J,* i.e. $J + 1$. The energy difference between the successive J levels is actually given by the product of λ (***spin-orbit coupling constant***) and the larger one of the two J values, i.e.

$$\Delta E_{J,\,J+1} = (J + 1)\lambda$$

Thus the states $^3P_0$, $^3P_1$ and $^3P_2$ (Fig. 1.10.11.2) arising from np^2, have relative energy separations as 1 : 2. Similarly, the states $^4D_{1/2}$, $^4D_{3/2}$, $^4D_{5/2}$ and $^4D_{7/2}$ have the relative energy differences between the successive levels as 3:5:7.

In the presence of an external magnetic field, the energy levels are further split into $2J + 1$, equally spaced levels for the M_J values ranging from $+J$ to $-J$. Each level is separated from the nearest one by $g\mu_BH$, where g = Lande splitting factor, H = strength of the magnetic field, μ_B = Bohr magneton.

1.10.12 Derivation of the Ground State Terms in the Light of Hund's Rules

(i) ***ns*^{1} *and ns*^{2} *cases*** **:** Here, $l = 0$ and $m_l = 0$.

For *ns*^{1} : Spin multiplicity = 2, as $M_{S(\max)} = S_{(\max)} = 1/2$; $M_{L(\max)} = 0$, i.e. $L_{(\max)} = 0$; and $J = 1/2$. Thus, the state is given by $^2S_{1/2}$.

Click Here to the chemylibrary

For ns² : $M_{S(max)} = S_{(max)} = 0$, i.e. spin multiplicity = 1; $M_{L(max)} = 0$, i.e. $L_{(max)} = 0$ and $J = 0$. Hence the term is given by, $^1S_0$.

(ii) ***np² case*** : Here, $l = 1$ and $m_l = +1, 0, -1$. Here, $S_{(max)}$ arises when the two electrons remain unpaired with parallel spins, i.e. $M_{S(max)} = \Sigma m_s = 2 \times ½ = 1$; and the spin multiplicity, $2S + 1 = 3$. Maintaining the $S_{(max)}$ (= 1), M_L can be maximised as: $M_{L(max)} = \Sigma m_l = 1 + 0 = 1$. Hence, $L_{max} = 1$. The present case is less than half-filled. So, it will adopt $J_{(min)}$ which is $|L - S|$, i.e. 0. Thus, the term is $^3P_0$.

If the two electrons are placed in the room having $m_l = +1$, M_L can have the value 2, but S becomes 0 (according to Pauli exclusion principle) and it violates the Hund's first rule.

(iii) ***nd³ case*** : Here, $l = 2$ and $m_l = +2, +1, 0, -1, -2$. Here, $M_{S(max)} = 1/2 + 1/2 + 1/2 = 3/2$, i.e. $S_{(max)} = 3/2$; $M_{L(max)} = (+2 + 1 + 0) = 3$, i.e. $L_{(max)} = 3$. It is less than half-filled. Hence, $J_{(min)}$ will occur. The ground state term is $^4F_{3/2}$.

(iv) ***Spin-free* (i.e. *high spin*) *and spin-paired* (i.e. *low spin*) *condition*** : Let us illustrate the situation for nd^6 system. In the spin-free condition, it produces 4 unpaired electrons and the corresponding ground state is $^5D_4$ (i.e. $L_{max} = 2$) while for the spin-paired system, there is no unpaired electron and the corresponding ground state term is ^1I (i.e. $L_{max} = 6$ when the 6-electrons are placed in three orbitals characterised by $m_l = +2, +1, 0$).

Here it should be pointed out that for a particular electronic configuration, the *ground state term* generally corresponds to the most stable state generated from the spin-free configuration and Table 1.10.12.1 refers to this. *In terms of Hund's spin multiplicity rule, the spin-free state is more stable than the corresponding spin-paired state.*

Ground state terms for different electronic configurations are given in Table 1.10.12.1. Interestingly, it is observed that the p^n and p^{6-n} configurations have the same L and S values, and also the same thing occurs for d^n and d^{10-n} configuration. This is explained by ***the hole formalism or equivalence principle.***

Hole formalism rule : A partly filled level containing n electrons may be considered as a system consisting of $(N - n)$ positrons and N electrons where N gives the capacity of the level, e.g. p^3 (electron) $\equiv p^6$ (electron) + $p^{(6-3)}$ (positron) = p^6 (electron) + p^3 (positron); d^8 (electron) $\equiv d^{10}$ (electron) + $d^{(10-8)}$ (positron) = d^{10} (electron) + d^2 (positron). A filled level (e.g. d^{10}, p^6, etc.) does not contribute to $\vec{L}$ and $\vec{S}$ vectors (i.e. $L = 0$, $S = 0$). Thus we can write :

d^8 (electron) $\equiv d^2$ (positron); d^7 (electron) $\equiv d^3$ (positron); p^2 (electron) $\equiv p^4$ (positron), etc.

The magnitude of charge carried by each electron and positron is the same. ***This is why, the interelectronic repulsion is equivalent to interpositronic repulsion,*** i.e. d^2 (electron) $\equiv d^2$ (positron); d^n (electron) $\equiv d^n$ (positron); p^n (electron) $\equiv p^n$ (positron).

It may be noted that a half filled level (e.g. p^3, d^5) contributes nothing to $\vec{L}$ vector (i.e. $L = 0$). This is why p^{3+n} and p^n configurations generate the same term (i.e. same L) having different spin multiplicities. A similar situation arises for d^5 and d^{5+n} electronic configurations. These are illustrated in Table 1.10.12.1.

1.10.13 Spectral Selection Rules in the Vector Model

It has been already noticed that all the mathematically possible electron transitions among the allowed energy levels do not occur. There are some restrictions. To explain the finer structure of the hydrogen spectral lines in Sommerfeld's model, the quantum restriction, $\Delta k = \pm 1$ in electron transition was

Click Here to Head Chemyilibrary

Table 1.10.12.1. Ground State Terms arising from *p* and *d* electronic configurations

Electronic configuration	m_l value					$M_{L(max)}$ (i.e. $L_{(max)}$)	$M_{S(max)}$ (i.e. $S_{(max)}$)	Term symbol
	+2	+1	0	−1	−2			
p^1		↑				1	1/2	$^2P_{1/2}$
p^2		↑	↑			1	1	$^3P_0$
p^3		↑	↑	↑		0	3/2	$^4S_{3/2}$
p^4		↑↓	↑	↑		1	1	$^3P_2$
p^5		↑↓	↑↓	↑		1	1/2	$^2P_{3/2}$
p^6		↑↓	↑↓	↑↓		0	0	$^1S_0$
d^1	↑					2	1/2	$^2D_{3/2}$
d^2	↑	↑				3	1	$^3F_2$
d^3	↑	↑	↑			3	3/2	$^4F_{3/2}$
d^4	↑	↑	↑	↑		2	2	$^5D_0$
d^5	↑	↑	↑	↑	↑	0	5/2	$^6S_{5/2}$
d^6	↑↓	↑	↑	↑	↑	2	2	$^5D_4$
d^7	↑↓	↑↓	↑	↑	↑	3	3/2	$^4F_{9/2}$
d^8	↑↓	↑↓	↑↓	↑	↑	3	1	$^3F_4$
d^9	↑↓	↑↓	↑↓	↑↓	↑	2	1/2	$^2D_{5/2}$
d^{10}	↑↓	↑↓	↑↓	↑↓	↑↓	0	0	$^1S_0$

invoked, but it was found inadequate to predict the exact number of components. This is why, other restrictions involving the newly developed quantum numbers in the vector model were proposed. These restrictions are called *selection rules*. Initially though these were empirically formulated, now these are theoretically supported by the wave mechanics. For atoms, the resultant vectors introduce the quantum numbers S, L, J, M_L, M_S and M_J in terms of which the selection rules are formulated as follows.

i. ***The selection rule for L*** : $\Delta L = \pm 1$, i.e. only those transitions will occur for which the value of L changes by ± 1.

ii. ***The selection rule for S*** : $\Delta S = 0$, i.e. only the transitions can occur between the states which are having the same spin multiplicity.

iii. ***The selection rule of J*** : $\Delta J = \pm 1$ or 0, but $J = 0 \rightarrow J = 0$ is not allowed.

iv. ***The selection rule based on inter-dependence of L and J*** : The transitions leading to the change for L and J in the opposite directions (i.e., $\Delta L = -\Delta J$) are not allowed.

Forbidden transitions : Very often there are some transitions which violate the above selection rules, and these are called *forbidden transitions*. Actually some special mechanisms operate in reality to break down or relax the rules at least partially. In this connection, *vibronic coupling* is worth mentioning, by virtue of which some systems can partially relax the forbidden transitions governed by the selection rule of L. But the detailed discussions of these processes are presently remaining beyond our scope. Here it is important to know that the *forbidden transitions always show the weaker intensity.*

Click Here t.me/thealchemylibrary

1.10.14 Intensity Rules for Spectral Transitions in the Vector Model

Whether the transitions are allowed or not can be determined by the above mentioned selection rules, but to determine the relative intensity among the allowed transitions, there are some *intensity rules*. Initially, these were of only empirical basis, but now they are standing on a sound theoretical basis supported by wave mechanics. The intensity rules are formulated as follows :

i. The transitions which lead L and J to change in the same way (i.e. $\Delta L = \Delta J$) produce intense lines. The transitions leading to $\Delta L \neq \Delta J$ are weak.

ii. The transitions for which L decreases by unity (i.e. $L \rightarrow L - 1$, $\Delta L = -1$) are stronger compared to the transitions having $\Delta L = +1$.

iii. The transitions in which L and J change in the opposite directions (i.e. $\Delta L = -\Delta J$) are forbidden.

The intensity rules can be summarised as follows :

(a) $\Delta L = -1$, $\Delta J = -1$, (most intense lines);
(b) $\Delta L = -1$, $\Delta J = 0$, (less intense lines);
(c) $\Delta L = +1$, $\Delta J = +1$, (weak line);
(d) $\Delta L = +1$, $\Delta J = 0$, (very weak line);
(e) $\Delta L = +1$, $\Delta J = -1$, (forbidden transition);
(f) $\Delta L = -1$, $\Delta J = +1$, (forbidden transition).

1.10.15 Fine or Multiplet Structure of the Spectral Lines in the Light of Vector Model

By considering the number of optical electrons (i.e. the electrons which undergo transition), the atoms can be classified as *one-electron* or *multi-electron system*. Only the incomplete outermost shell is to be considered to determine the resultant quantum numbers, i.e. L, S and J. In ***one optical electron systems,*** $L = l$, $S = 1/2$ and $J = |L + S|$ to $|L - S|$, and the spin multiplicity ($= 2S + 1$) is 2. In the one optical electron system, hydrogen and different hydrogen-like systems (ns^1), e.g. He^+, Li^{2+}, Be^{3+} etc.; alkali metals, e.g. *Li*, *Na*, *K*, etc. and singly ionised alkaline earths, e.g. Be^+, Mg^+, Ca^+, etc. are the representative members. In all these cases, $L = l = 0$ (i.e. S state) and $J = ½$. Hence the ***ground state term*** *is* $^2S_{½}$.

(a) ***Fine structure of H_α-line*** **:** Let us consider the H_α-line in Balmer series where the transition occurs from $n = 3$ to $n = 2$. Now we ought to consider the energy levels arising from $n = 3$ and $n = 2$.

For $n = 3$, $l = 0, 1, 2$. Hence, L (one-electron system) = 0, 1, 2, and $S = 1/2$. Thus for $n = 3$, it splits into five energy states : $^2S_{1/2}$, $^2P_{1/2}$, $^2P_{3/2}$, $^2D_{3/2}$ and $^2D_{5/2}$.

Similarly, for $n = 2$, $l = 0, 1$. Hence, L (one electron system) = 0, 1; and $S = 1/2$. Thus, for $n = 2$, it splits into three energy states : $^2S_{1/2}$, $^2P_{1/2}$ and $^2P_{3/2}$.

According to the selection rules, only the following transitions are allowed :

(i) $^2D_{5/2}\ (n = 3) \rightarrow {}^2P_{3/2}\ (n = 2)$; $\Delta L = -1$, $\Delta J = -1$, $\Delta S = 0$
(ii) $^2D_{3/2}\ (n = 3) \rightarrow {}^2P_{3/2}\ (n = 2)$; $\Delta L = -1$, $\Delta J = 0$, $\Delta S = 0$
(iii) $^2D_{3/2}\ (n = 3) \rightarrow {}^2P_{1/2}\ (n = 2)$; $\Delta L = -1$, $\Delta J = -1$, $\Delta S = 0$
(iv) $^2P_{3/2}\ (n = 3) \rightarrow {}^2S_{1/2}\ (n = 2)$; $\Delta L = -1$, $\Delta J = -1$, $\Delta S = 0$
(v) $^2P_{1/2}\ (n = 3) \rightarrow {}^2S_{1/2}\ (n = 2)$; $\Delta L = -1$, $\Delta J = 0$, $\Delta S = 0$

Click Here t.me/thealchemylibrary

(vi) $^2S_{1/2}\,(n=3) \rightarrow {}^2P_{1/2}\,(n=2);\ \Delta L=+1,\ \Delta J=\ 0,\ \Delta S=0$

(vii) $^2S_{1/2}\,(n=3) \rightarrow {}^2P_{3/2}\,(n=2);\ \Delta L=+1,\ \Delta J=+1,\ \Delta S=0$

The states with the same values of n and J but different L values are called ***coincident states.*** Therefore, the two pairs of transitions : (iii) and (iv), i.e. $D_{3/2} \rightarrow P_{1/2}$ and $P_{3/2} \rightarrow S_{1/2}$; (v) and (vi), i.e. $P_{1/2} \rightarrow S_{1/2}$ and $S_{1/2} \rightarrow P_{1/2}$ will develop only two spectral lines instead of four lines. **Thus by considering the *coincident states, in spite of seven allowed transitions, only five lines are originated.*** These transitions are shown in Fig. 1.10.15.1 where coincident states are drawn close together.

According to the intensity rules, the two lines corresponding to the transitions (i) and the coincident pair (iii) and (iv) are the ***strongest ones*** as they have $\Delta L = -1$, $\Delta J = -1$. The two transitions (ii) and (v), where $\Delta L = -1$, $\Delta J = 0$, lead to two ***less intense lines.*** The (vii)-th transition is ***still weaker*** since it is having $\Delta L = +1$ and $\Delta J = +1$. The (vi)-th transition coincident with the (v)-th transition is the ***weakest one,*** as here $\Delta L = +1$ and $\Delta J = 0$, but it has got no separate existence as it is fused with the (v)-th transition.

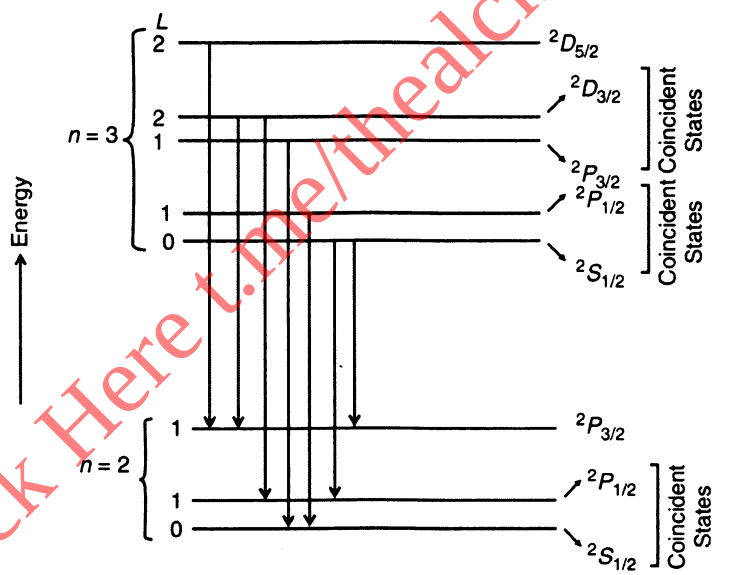

Fig. 1.10.15.1. Possible transitions leading to fine structure in H_α-line of Balmer series.

Though the H_α-line (Balmer series) produce fives components, very often it appears ***as a doublet due to the overlapping of the components as expected from Doppler effect.*** In 1936, R.C. Williams followed the transition under the condition of minimised *Doppler effect* and the five components as predicted theoretically were observed.

(b) ***Fine structure of spectral lines in alkali metals*** : Alkali metals bear ns^1 electron at the outermost shell, and rest of the electrons are in the inner closed shells which contribute nothing in determining the energy states of the atom as a whole. The outermost electron is the only ***one optical electron*** as in the case of hydrogen atom.

Click Here t.me/thealchemylibrary

Let us take the case of *Na* atom. Out of the eleven electrons of the atom, ten electrons are placed in the inner closed shells and the eleventh electron is $3s^1$ at the ground state. On excitation, it can go to $3p$ or $3d$ or $4s$ or $4p$ .... level. Hence in the analysis of emission spectrum, the electron can travel under quantum restrictions from the energy states corresponding to $3p^1$ or $3d^1$ or $4s^1$ .... to the energy states generated from $3s^1$. Now let us consider the possible energy states corresponding to the different possible electronic configurations.

Electronic configuration	*Energy states*
$3s^1$ (*Ground state*)	$^2S_{1/2}$ ($n = 3$)
$4s^1$	$^2S_{1/2}$ ($n = 4$)
$5s^1$	$^2S_{1/2}$ ($n = 5$)
$3p^1$	$^2P_{1/2}$ ($n = 3$), $^2P_{3/2}$ ($n = 3$)
$4p^1$	$^2P_{1/2}$ ($n = 4$), $^2P_{3/2}$ ($n = 4$)
$3d^1$	$^2D_{5/2}$ ($n = 3$), $^2D_{3/2}$ ($n = 3$)
$4d^1$	$^2D_{5/2}$ ($n = 4$), $^2D_{3/2}$ ($n = 4$)

According to the selection rules, $\Delta L = \pm 1$, $\Delta J = 0, \pm 1$ (except $J = 0 \rightarrow J = 0$) and $\Delta S = 0$, the following transitions in the emission spectrum of sodium are allowed :

$n\,^2P_{3/2,\,1/2} \rightarrow 3\,^2S_{1/2}$; $n = 3, 4, 5, ...$, **Principal (*P*) series.**

$n\,^2S_{1/2} \rightarrow 3\,^2P_{3/2,\,1/2}$; $n = 4, 5, 6, ...$, **Sharp (*S*) series.**

$n\,^2D_{5/2,\,3/2} \rightarrow 3\,^2P_{3/2,\,1/2}$; $n = 3, 4, 5, ...$, **Diffuse (*D*) series.**

$n\,^2F_{7/2,\,5/2} \rightarrow 3\,^2D_{5/2,\,3/2}$; $n = 4, 5, 6, ...$, **Fundamental (*F*) series.**

The energy level diagram for the emission spectral lines in different series are shown in Fig. 1.10.15.2.

Fine Structure of Sodium D-Line : The electron transition, $3p^1 \rightarrow 3s^1$ leads to the first doublet of the principal series. These transitions are given by :

$3\,^2P_{1/2} \rightarrow 3\,^2S_{1/2}$, ***Sodium D_1 line*** (5896 Å)

and $3\,^2P_{3/2} \rightarrow 3\,^2S_{1/2}$, ***Sodium D_2 line*** (5890 Å)

These are pictorially represented in Fig. 1.10.15.2. Thus it appears (Fig. 1.10.15.2) that *both the principal and sharp series are of doublets and the diffuse series contains the triplet lines.*

1.10.16 Nuclear Spin and Hyperfine Structure of the Spectral Lines

Initially the hyperfine structure was supposed to be due to the **isotope effect.** It has been already noticed that if the nuclear motion is taken into consideration in Bohr's model then for different isotopes, energy changes in spectral transitions are different (Sec. 1.8.3). *But the existence of the hyperfine structure in the case of heavy elements where the isotope effect is negligibly small and for the elements (e.g. bismuth) which do not have any stable isotope, indicated that there must be some other mechanism responsible for the hyperfine structure.* To explain this it was argued by W. Pauli (1927) that the *nuclear spinning motion produces an angular momentum given by* $\sqrt{I(I+1)}\,(h/2\pi)$ *where i is called nuclear angular spin quantum number* (see Sec. 5.16). This vector $\vec{I}$ interacts with $\vec{J}$ of the electronic system and produces

Click Here to me/theadchemylibrary

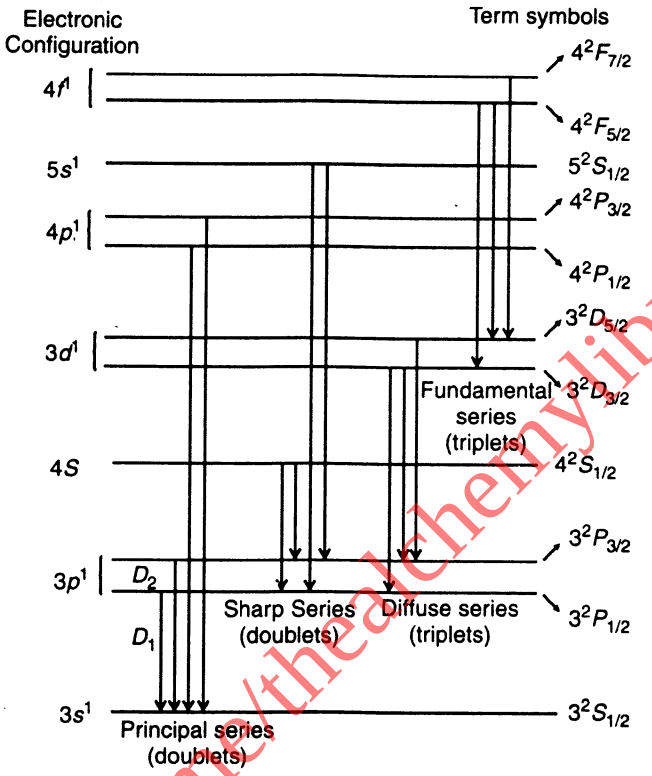

Fig. 1.10.15.2. Possible transitions giving rise to emission spectrum of sodium.

the *total angular momentum* $(\vec{F})$ *of the whole atom* where the vectorial model gives the values of $\vec{F}$. Corresponding quantum number F is given as follows :

$$F = |(J+I)|, |(J+I)-1|, |(J+I)-2|, ..., |(J-I)|$$

Consideration of these F values and the related selection rules involving F along with those for the outer electrons in the vector model can explain the hyperfine structures of the spectral lines, but its detailed discussion lies beyond the scope of this book. **It is evident that for $I = 0$, *there will be no hyperfine splitting.***

1.10.17 Orbital and Spin Magnetic Moments of an Electron in the Light of Orbital and Spinning Motion : Magnetic Moment of an Atom

(A) *Orbital magnetic moment* : If an electron of charge e revolves in an orbit then it produces a current i (in electromagnetic unit) given by :

$$i = -\frac{e}{cT} \qquad ...(1.10.17.1)$$

where, c and T are the velocity of light and time period of revolution of the electron respectively. This is in electromagnetic unit. It should be noted that 1 electromagnetic unit (emu) of current /1 electrostatic unit (esu) of current = c (velocity of light) i.e. $\frac{emu}{esu} = c.$ This current produces a magnetic field of moment μ_l given by :

$$\mu_l = iA \qquad ...(1.10.17.2)$$

Click Here t.me/theachemylibrary

where A is the area of the orbital plane. Thus the orbital magnetic moment μ_l is given by :

$$\mu_l = -\frac{eA}{cT} \qquad \ldots(1.10.17.3)$$

In SI units, $$\mu_l = -\frac{eA}{T}$$

To evaluate the area of the ellipse, let us consider a particular point (r, ϕ) where the elemental area, considering a triangle becomes $\frac{1}{2}(rrd\phi)$ (see Fig. 1.10.17.1).

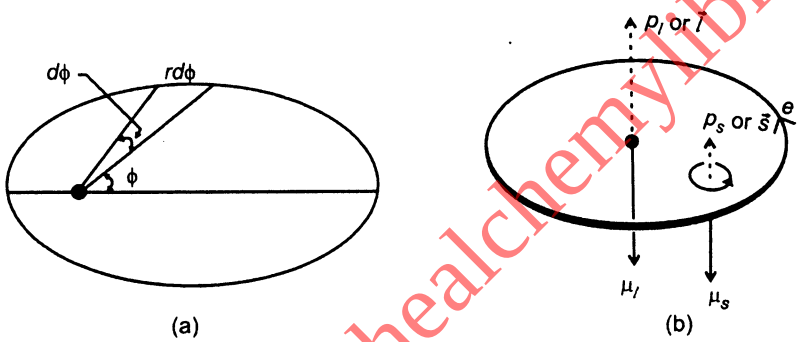

Fig. 1.10.17.1. (a) Sommerfeld's elliptic orbit. (b) Magnetic moments (μ_l and μ_s, denoted by solid lines) due to orbital and spin angular momenta vectors (ie. p_l or $\vec{l}$ and p_s or $\vec{s}$, denoted by dotted lines) are directed in the respective opposite directions (i.e. μ_l and p_l are in opposite directions; μ_s and p_s are in opposite directions).

Thus, $A = \int_0^{2\pi} \frac{1}{2}(r^2 d\phi)$, (where the elemental area of the triangle is $\frac{1}{2}r^2 d\phi$).

or $$A = \frac{1}{2}\int_0^{2\pi} r^2 d\phi \qquad \ldots(1.10.17.4)$$

The orbital angular momentum (p_l) is given by :

$$p_l = m_e r^2 \frac{d\phi}{dt} \qquad \ldots(1.10.17.5)$$

Considering Eqns. 1.10.17.4 and 1.10.17.5 we get :

$$A = \frac{1}{2}\int_0^T (p_l / m_e)\, dt = \frac{1}{2}(p_l / m_e)T \qquad \ldots(1.10.17.6)$$

Now, considering, $p_l = l(h/2\pi)$ (where l stands for the azimuthal quantum number), we get from Eqns. 1.10.17.3 and 1.10.17.6.

$$\mu_l = -p_l\left(\frac{e}{2m_e c}\right) = -l\left(\frac{eh}{4\pi m_e c}\right) \qquad \ldots(1.10.17.7)$$

If, $p_l = \sqrt{l(l+1)}\,(h/2\pi)$ is considered from wave mechanics, then μ_l becomes,

Click Here t.me/thealchemylibrary

$$\boxed{\mu_l = -\sqrt{l(l+1)}\left(\frac{eh}{4\pi m_e c}\right)} \qquad \ldots(1.10.17.8)$$

The *negative sign* in the above expressions indicates that the orbital magnetic moment (μ_l) is opposite in direction to the angular momentum vector (p_l).

Here, $eh/(4\pi m_e c)$ is a constant and is called ***Bohr magneton*** **(B.M.).** It has been regarded as the unit of magnetic moment and very often represented by the M_B or μ_B as :

$$\boxed{\mu_B \text{ or } M_B = eh/(4\pi m_e c) = 9.27 \times 10^{-21} \text{ ergs/gauss}}$$

The magnitude of ***Bohr magneton*** **(B.M.)** which is the basic unit of magnetic moment can be calculated as follows :

$$M_B \text{ or } \mu_B = \frac{eh}{4\pi m_e c}, \text{ (in Gaussian or CGS system)}$$

$$= \frac{(4.8\times10^{-10}\text{ esu})\times(6.62\times10^{-27}\text{ erg s})}{4\times3.14\times9.1\times10^{-28}\text{ g}\times3.10^{10}\text{ cm s}^{-1}}, \text{ (CGS units)}$$

$$= 9.27\times10^{-21}\text{ (esu) (erg) (g}^{-1}\text{) (cm}^{-1}\text{) (s}^2\text{)}$$

$$= 9.27\times10^{-21}\text{ erg G}^{-1}$$

$$\left[\text{esu} = \text{g}^{1/2}\text{ cm}^{3/2}\text{ s}^{-1}, \text{G (gauss)} = \text{g}^{1/2}\text{ cm}^{-1/2}\text{ s}^{-1}\right]$$

$$M_B \text{ or } \mu_B = \frac{eh}{4\pi m_e}, \text{ (in SI unit)}$$

$$= \frac{(1.6\times10^{-19}\text{ C})\,(6.62\times10^{-34}\text{ J s})}{4\times3.14\times9.1\times10^{-31}\text{ kg}}$$

$$= 9.27\times10^{-24}\text{ C J s kg}^{-1} = 9.27\times10^{-24}\text{ J T}^{-1}\text{ (or amp meter}^2\text{)}$$

$$[\text{T (tesla)} = \text{kg s}^{-1}\text{ C}^{-1}]$$

It may be noted that $1\text{G} = 10^{-4}$ T and 1 erg = 10^{-7} J and it leads to :

$$\mu_B = 9.27\times10^{-21}\text{ erg G}^{-1} = 9.27\times10^{-21}\times(10^{-7}\text{ J})\,(10^4\text{ T}^{-1})$$

$$= 9.27\times10^{-24}\text{ J T}^{-1}$$

$$\text{i.e.} \quad 1\text{ J T}^{-1} = 10^3\text{ erg G}^{-1}.$$

In terms of Bohr magneton (M.B.) we can write :

$$\boxed{\mu_l = \sqrt{l(l+1)}\,\mu_B = \sqrt{l(l+1)}\text{ B.M.,}}$$ (ignoring the negative sign of Eqn. 1.10.7.8)

(B) ***Spin magnetic moment*** **:** Because of the spinning behaviour of the electron around its own axis, it also possesses a magnetic field. *The relationship between the spin magnetic moment (μ_s) and spin angular momentum (p_s) cannot be derived theoretically in contrast to the case of orbital magnetic moment.* But from the experimental observations, it has been observed that it follows the following Eqn.,

Click Here t me/theadcrmylibrary

$$\mu_s = -\frac{2e}{2m_e c} p_s \qquad \ldots(1.10.17.9)$$

where p_s stands for the angular momentum due to spinning; p_s can be represented as :

$$p_s \approx s(h/2\pi), \qquad \ldots(1.10.17.10)$$

where s is the spin quantum number. The negative sign indicates that μ_s and p_s act in opposite directions.

Thus, $\mu_s = 2s \frac{eh}{2\pi m_e c} = 2s\ M_B$ or $2s\ \mu_B$, (ignoring the negative sign) ...(1.10.17.11)

In terms of wave mechanics, $\mu_s = 2\sqrt{s(s+1)}\ M_B = \sqrt{4s(s+1)}$ B.M. ...(1.10.17.12)

(c) ***Gyromagnetic ratio*** **(γ) :** *For the orbital motion of an electron*, it is defined as $\gamma_l = \frac{|\mu_l|}{|p_l|}$ (i.e. ratio of magnitudes of orbital magnetic moment and orbital angular momentum). It leads to :

$$|\mu_l| = \gamma_l |p_l|$$

$$\gamma_l = \frac{e}{2m_e c}, \text{ (by using the values of } \mu_l \text{ and } p_l \text{ in CGS units)}$$

$$= \frac{(4.8\times10^{-10}\text{ esu})}{2\times9.1\times10^{-28}\text{ g}\times3\times10^{10}\text{ cm s}^{-1}} = 8.8\times10^{6}\ \text{G}^{-1}\ \text{s}^{-1}\ \text{(CGS unit)}$$

Similarly $\gamma_l = \frac{e}{2m_e}$, (in SI unit)

$$= \frac{(1.6\times10^{-19}\text{C})}{2\times9.1\times10^{-31}\text{ kg}} = 8.8\times10^{10}\ \text{C kg}^{-1}$$

It can also be expressed as follows :

$$\gamma_l = \frac{\mu_B}{(h/2\pi)} = \frac{9.27\times10^{-21}\text{ erg G}^{-1}\times2\times3.14}{6.62\times10^{-27}\text{ erg s}} = 8.8\times10^{6}\ \text{G}^{-1}\ \text{s}^{-1}, \text{(CGS system)}$$

For the spinning motion of the electron, the gyromagnetic ratio (γ_s) is given by :

$$\gamma_s = \frac{|\mu_s|}{|p_s|} = \frac{e}{m_e c}, \text{ (in CGS system)}$$

Thus we can write : $\gamma_s / \gamma_l = 2$

Note **:** Nuclear spinning motion can produce also a magnetic moment. There is a parameter called ***nuclear magneton*** **or** ***Rabi magneton*** (μ_N) which is required to measure the *nuclear magnetic moment*. Rabi magneton is related to Bohr magneton. μ_N is given by :

$$\mu_N = \frac{eh}{4\pi m_p c}, \text{ (in Gaussian or CGS system)}$$

where m_p denotes the mass of a proton. Taking $m_p / m_e \approx 1836$, we got $\mu_B/\mu_N = 1836$. The characteristic features of nuclear magnetic moment have been discussed in Sec. 5.1.6.

Note : Magnetic moment due to the spinning motion of the nucleus is very small due to its relatively large mass. In fact, this magnetic moment is negligible in comparison with the contribution arising from the orbital and spinning motion of the electron.

Click Here t.me/thealchemylibrary

(d) ***Magnetic moment*** **(μ)** ***of an atom*** **(see Sec. 11.16) :** The Russel-Saunder term representing the system can generate the different J values ranging $|L+S|$ to $|L-S|$. For example, the term ^3F can generate the J-values 4, 3, 2. The corresponding states are $^3F_4$, $^3F_3$ and $^3F_2$. The ground state is decided by Hund's rule. The different energy states due to the different J-values constitute a ***multiplet*** in which each energy state is called a *component*. Thus, the states $^3F_4$, $^3F_3$ and $^3F_2$ constitute a multiplet for the term ^3F. The energy `gap between the successive components in a particulars multiplet is governed by ***Lande interval rule*** (cf. Fig. 1.10.11.2). In a multiplet, the *energy gap* (ΔE) between the successive J levels is called ***multiplet width.***

The population density in the components of a particular multiplet depend on the relative values of **multiplet width** (ΔE) and thermal energy (k_BT, k_B = Boltzmann constant, T = temperature in Kelvin scale). Under the condition, $\Delta E >> k_BT$, the lowest level is mainly populated (i.e. most of the species will populate the lowest energy level) and it contributes. On the other hand, under the condition, $\Delta E \approx k_BT$, the excited states (i.e. higher levels) are also sufficiently populated to contribute. The magnetic moment of a multielectron system depends on the relative magnitudes of ΔE and k_BT.

Case 1 : Multiplet width (ΔE) >> k_BT

In such cases, the $\vec{L}$ and $\vec{S}$ vectors interact strongly to produce the resultant $\vec{J}$ vectors. Thus, J becomes a good quantum number. Consequently, the quantum numbers L and S cannot dictate the magnetic moment. In such cases, the *total angular momentum* of an atom is given by $\sqrt{J(J+1)}\,(h/2\pi)$, and the total magnetic moment (μ_J) is given by :

$$\mu_J = -g\sqrt{J(J+1)}\,\frac{eh}{4\pi m_e c} = -g\sqrt{J(J+1)}\,\mu_B$$
$$= -g\sqrt{J(J+1)}\ \text{B.M.}$$

where the Lande g factor is defined as :

$$g = 1 + \frac{J(J+1) + S(S+1) - L(L+1)}{2J(J+1)}$$

The negative sign indicates that μ_J and total angular momentum vector act in opposite directions. Ignoring the negative sign, we can write :

$$\mu_J = g\sqrt{J(J+1)}\ \mu_B = g\sqrt{J(J+1)}\ \text{B.M.}$$

When there is no contribution of spin magnetic moment (i.e. $S = 0$, and consequently $L = J$ and $g = 1$), the *orbital magnetic moment only* (μ_L) is obtained from the above equation :

$$\mu_J = \mu_L = \sqrt{L(L+1)}\ \mu_B, \text{(ignoring the negative sign)}$$

When there is no contribution of orbital magnetic moment (i.e. $L = 0$ and consequently $J = S$ and $g = 2$), the *spin magnetic moment only* (μ_S) is obtained from the expression of μ_J.

$$\mu_J = \mu_S = 2\sqrt{S(S+1)}\ \mu_B = \sqrt{4S(S+1)}\,\mu_B = \sqrt{2S(2S+2)}\,\mu_B$$

If there are n-unpaired electrons, then the resultant spin quantum number S becomes $n \times (½)$ i.e. $n/2$. It leads to :

$$\mu_S = \sqrt{n(n+2)}\ \mu_B = \sqrt{n(n+2)}\ \text{B.M.}$$

Click Here t.me/thealchemylibrary

The quantity μ_S is very often denoted by $\mu_{\text{spin-only}}$, i.e. $\mu_{\text{spin-only}} = \sqrt{n(n+2)}$ B.M.

Case-II : Multiplet width (ΔE) << k_BT

The energy levels characterised by different J values in a particular multiplet are so closely positioned that the thermal energy makes all these levels almost equally populated. *In other words, the* $\vec{L}$ and $\vec{S}$ *vectors couple very poorly and they can maintain their individuality. Thus, under the condition, J is not a good quantum number*. The orbital motion and spin motion contribute to determine the overall magnetic property. In fact, the observed magnetic susceptibility is the sum of susceptibility due to orbital magnetic moment and spin magnetic moment. It leads to :

$$\mu_{L+S} = \sqrt{L(L+1) + 4S(S+1)}\ \mu_B$$

(***Note*** **:** The above expression is true for the *free atoms* or *ions*, but in complexes the orbital contribution is very often quenched).

Case-III : Multiplet width (ΔE) ≈ k_BT

Under his condition, all the J levels in a particular multiplet are not equally populated. Their extent of population density is governed by *Maxwell-Boltzmann distribution*. It leads to a complicated expression of total magnetic moment and susceptibility.

Note **:**

- $\mu_J = g\sqrt{J(J+1)}$ B.M. is mainly applicable for *trivalent lanthanides* (except to Sm^{3+} and Eu^{3+}) where $\vec{L}$ and $\vec{S}$ vectors strongly couple to make ΔE (multiplet width) $\gg k_BT$. For Sm^{3+} and Eu^{3+}, $\Delta E \approx k_BT$.
- $\mu_{\text{spin-only}} = \sqrt{4S(S+1)}$ B.M. $= \sqrt{n(n+2)}$ B.M. is mainly applicable for the first transition series metal complexes where the orbital contribution is very often quenched.

(E) ***Relationship between magnetic susceptibility and magnetic moment*** **:** It can be shown :

$$\chi_M = \frac{N\mu^2}{3k_BT} \quad i.e.\ \mu = \sqrt{\frac{3k_BT\chi_M}{N}}$$

where χ_M = molar susceptibility, i.e. susceptibility of one Avogadro number of molecules, μ is the effective magnetic moment of a single molecule, k_B is Boltzmann constant and T is the temperature in Kelvin scale.

$$\mu = \sqrt{\frac{3k_BT\chi_M}{N}} = \sqrt{\frac{3 \times (1.38 \times 10^{-16}\ \text{erg K}^{-1})\ (\text{T K})\ (\chi_M\ \text{cm}^3\ \text{mol}^{-1})}{6.023 \times 10^{23}\ \text{mol}^{-1}}}$$

$$= \sqrt{6.87 \times 10^{-40}\ \chi_M T\ \text{erg cm}^3}$$

$$= 2.63 \times 10^{-20} \sqrt{\chi_M T}\ \text{erg G}^{-1}$$

[erg = g cm^2 s^{-2}, G = g^{½} cm$^{-½}$ s^{-1}, i.e. erg cm^3 = erg^2 G^{-2}]

μ is generally expressed in B.M. (i.e. μ_B), 1 B.M. = 9.27 × 10^{-21} erg G^{-1}.

Click Here to me/heatchemylibrary

It leads to : $\mu = \frac{2.63 \times 10^{-20}}{9.27 \times 10^{-21}} \sqrt{\chi_M T}$ B.M.

$= 2.83 \sqrt{\chi_M T}$ B.M.

i.e. $$\boxed{\mu = \sqrt{\frac{3k_B T \chi_M}{N\mu_B^2}} = 2.83 \sqrt{\chi_M T} \text{ B.M., } (\chi_M \text{ in cm}^3 \text{ mol}^{-1})}$$

In SI unit, $\chi_M = \frac{N\mu^2\mu_0}{3k_B T}$

$k_B = 1.38 \times 10^{-23}$ J K^{-1},

$= 4\pi \times 10^{-7}$ J C^2 m^{-1} s^2, χ_M in m^3 mol^{-1},

μ_0 (permeability of vacuum)

Here, if μ is expressed in B.M. ($= 9.27 \times 10^{-24}$ J T^{-1}), then we get :

$$\mu = \sqrt{\frac{3k_B T \chi_M}{N\mu_0\mu_B^2}} = 797.6 \sqrt{\chi_M T} \text{ B.M., } (\chi_M \text{ in m}^3 \text{ mol}^{-1})$$

1.10.18 Stern-Gerlach Experiment—An Evidence in Favour of Space Quantisation and Spin Quantum Number

In this experiment, a beam of silver atoms produced from a heated wire was allowed to pass through an ***inhomogeneous magnetic field*** (Fig. 1.10.18.1). The inhomogeneous field was obtained by using the pole pieces of different shapes. The atoms behave like small magnets due to orbital and spinning motion of the unpaired electrons. If the applied magnetic field were homogeneous, the atomic magnets would rotate because of the couple experienced by deflection. But the inhomogeneous magnetic field leads the atomic magnets in the direction of the field but the degree of deflection suffered by the atoms depends on the field gradient dH/dx.

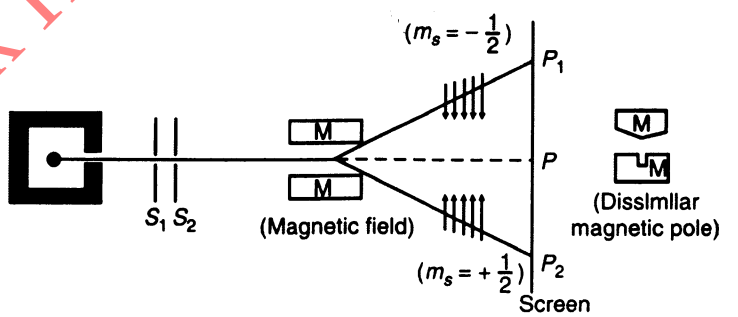

Fig. 1.10.18.1. Experimental arrangement of Stern-Gerlach experiment.

In practice, the narrow beam of silver atoms undergoes **bifurcation when the field is on.** The same thing also occurs for hydrogen, lithium, copper and gold atoms. Interestingly all these atoms have the electronic configuration ns^1 for the valency shell and the inner orbitals are fully closed (except hydrogen).

Click Here t.me/thealchemylibrary

Hence for the ground states of these atoms, $L = l = 0$; $S = s = ½$ and $J = ½$. Thus the magnetism associated with these atoms arises due to the spinning motion of the electron and it is given by, $\mu_S = 2\sqrt{S(S+1)}\, M_B$. These beams will split into components given by $(2J + 1)$, i.e. 2, as $J = 1/2$ which arises due to the spin value only, since $L = l = 0$.

The beams of zinc, cadmium and mercury do not suffer any deflection and splitting. Here, the outermost shell, i.e. the valency shell, has the configuration ns^2. Hence, $L = 0$, $S = 0$ and $J = 0$. This is why, they do not get deflected.

These experimental results support the following facts :

i. In the presence of a magnetic field, the splitting of the beams of the atoms in some certain directions indicates that ***the atoms can have only certain specified orientations in a magnetic field.*** Thus the concept of spatial quantisation gets verified.

ii. The **spinning concept** of the electron and $s = 1/2$ are now experimentally verified from the splitting behaviour of *Ag*, *Cu*, *Au*, *H* and *Li* atoms.

iii. The **zero value of the azimuthal quantum number ($l = 0$)** is now experimentally verified undoubtedly from the splitting behaviour of *Ag*, *Cu*, *Au*, *H* and *Li* atoms. If $l = 0$, then only the above experimental results can be explained. Here it is noteworthy that for Sommerfeld's model, the zero value of the azimuthal quantum number cannot be supported.

1.10.19 Explanation of the Magneto-Optic Phenomenon - the Zeeman Effect

It has been established that in the presence of a ***very strong magnetic field***, a spectral line **splits into triplet** and this magneto-optic phenomenon is called ***normal Zeeman effect*** while in the presence of an ***ordinary magnetic field***, the spectral line **splits in a complex manner** and this phenomenon is called ***anomalous Zeeman effect***. The *normal effect* generally occurs in the presence of an extraordinarily strong magnetic field while the *anomalous effect* is the most frequent phenomenon. ***Thus the normal one is a rare phenomenon.*** Actually the basis of this nomenclature lies in the fact that the *simple triplet splitting, i.e. normal effect, can be explained by the classical theory while the complex one cannot be explained by the classical theory.* **Thus it appears that the normal one is a strong field effect and the anomalous one is a weak field effect**. For the intermediate range of the magnetic field, the pattern of the splitting is different from the two limiting effects and this phenomenon is called *Paschen-Back effect* to tribute its discoverers, Paschen and Back (1913).

i. Debye's Explanation of the Normal Zeeman Effect in the Vector Model

Let us first consider the ***one optical electron system and ignore the spinning effect of the electron.*** Thus the mechanical angular momentum and magnetic moment will be contributed by its orbital motion only. The orbital angular momentum (p_l) and magnetic moment (μ_l) are given by:

$$p_l \approx l(h/2\pi)\ , \text{ and } \mu_l = -\, l(eh/\, 4\pi m_e c).$$

Both the vectors $\overrightarrow{p_l}$ *and* $\overrightarrow{\mu_l}$ act perpendicularly to the orbital plane (cf. Fig. 1.10.17.1b).

In the presence of a magnetic field of intensity H, the vector $\overrightarrow{p_l}$ will suffer a ***Larmor precession*** around the direction of the magnetic field. Due to this interaction, the energy level splits into $(2l + 1)$ levels due to ***spatial quantisation***. Actually the orbital magnetic moment quantum number (m_l) is given

Click Here t.me/thealchemylibrary

by $-l$ to $+l$ (including zero) to giv $l+1)$ levels. The Larmor precession will change the energy of the systems by ΔE which is given by

$$\Delta E = \frac{eh}{4\pi m_e c} Hm_l = \left(\frac{eH}{4\pi m_e c}\right) hm_l \qquad ...(1.10.19.1)$$

The factor, $eH/(4\pi m_e c)$ is called ***Larmor frequency*** (ν_L). Actually, the angular velocity of Larmor precession is given by $\frac{eH}{2m_e c}$. Thus, $\nu_L = \frac{angular\ velocity}{2\pi} = \frac{eH}{4\pi m_e c}$.

Thus, in terms of ν_L, ΔE can be expressed as follows,

$$\Delta E = h\nu_L m_l \qquad ...(1.10.19.2)$$

For a given value of l, m_l is restricted to $(2l + 1)$ integral values differing successively by unity. Hence, the energy difference between the successive sublevels for the different m_l values is given by $h\nu_L$, i.e. the levels are equidistant in terms of energy difference.

Now, let us consider the transition from l_1 to l_2. Let $E_{o(1)}$ and $E_{o(2)}$ be their energies respectively in the absence of the magnetic field, and E_1 and E_2 be their energies respectively in the presence of the magnetic field of intensity H. Hence these can be related as follows :

$$E_1 = E_{o(1)} + h\nu_L m_{l_1} \qquad ...(1.10.19.3)$$

and,

$$E_2 = E_{o(2)} + h\nu_L m_{l_2} \qquad ...(1.10.19.4)$$

Thus, under the magnetic field, the states will be split into $(2l_1 + 1)$ and $(2l_2 + 1)$ components for l_1 and l_2 respectively. Now a number of possible transitions may occur between these multiple states arising from l_1 and l_2. The frequency (ν_H) of transition in the presence of magnetic field is given by:

$$\nu_H = (E_2 - E_1)/h = \frac{E_{o(2)} - E_{o(1)}}{h} + (m_{l_2} - m_{l_1})\nu_L = \nu_o + \Delta m_l \nu_L \qquad ...(1.10.19.5)$$

where ν_o **represents the frequency of transition in the absence of any magnetic field.**

By considering the selection rule, $\Delta m_l = 0$ or ± 1, it is evident that ν_H may have values, ν_o, $(\nu_o + \nu_L)$ and $(\nu_o - \nu_L)$.Thus the given line will **split into three components** whose frequencies are :

$$\nu_o, \left(\nu_o + \frac{eH}{4\pi m_e c}\right) \text{and} \left(\nu_o - \frac{eH}{4\pi m_e c}\right).$$

The spectral transitions are shown in Fig. 1.10.19.1.

Note **:**

(a) Here only one optical electron system has been considered for which $L = l$, but for the polyelectronic systems the same result will be obtained by involving L and M_L in place of l and m_l respectively.

(b) Here, the spinning effect is ignored. Hence it is strictly followed by the singlet ($S = 0$) systems only.

(c) In the presence of a strong magnetic field where coupling between the orbital and spin vector is broken down (and *spin magnetic moment is ignorable*), then only the normal Zeeman effect is observed.

Click Here for the chemistry library

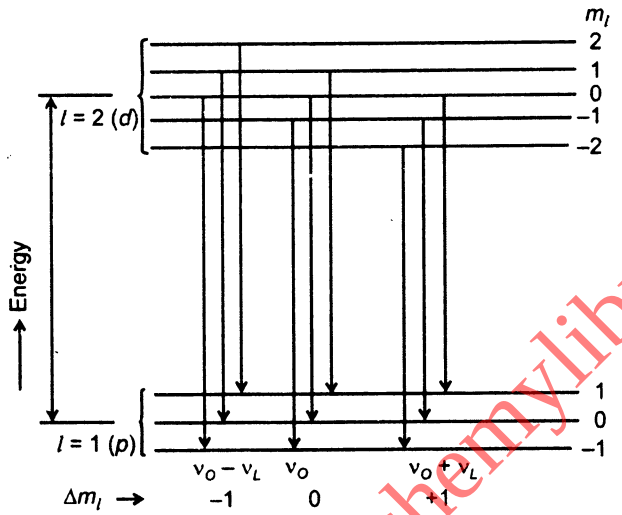

Fig. 1.10.19.1. Normal Zeeman effect for the transition from $l = 2$ to $l = 1$.

ii. Anomalous Zeeman Effect in the Light of Vector Model

If both the contributions from orbital and spinning motions are considered, then in terms of the resultant quantum numbers, L, S, J, the energy change (ΔE) of a state because of the precessional motion of $\vec{J}$ around the direction of the applied magnetic field of intensity H is given by :

$$\Delta E = h(eH/4\pi m_e c)gM_J = h\nu_L gM_J \qquad \ldots(1.10.19.6)$$

where g is given by :

$$g = 1 + \frac{J(J+1) + S(S+1) - L(L+1)}{2J(J+1)} \qquad \ldots(1.10.19.7)$$

and it is called ***Lande g factor.***

In the presence of a magnetic field, an energy state defined by L, S and J will undergo splitting depending on the M_J values which cover the range, $-J$ to $+J$. Transition between these multiplet magnetic sublevels developed from the original levels is governed by the selection rule, $\Delta M_J = 0$ or ± 1.

Now let us consider the sodium D_1 and D_2 line in the presence of a magnetic field.

$$\boldsymbol{D_2}\textbf{ line : } 3\,^2P_{3/2} \rightarrow 3\,^2S_{1/2};\ \boldsymbol{D_1}\textbf{ line : } 3\,^2P_{1/2} \rightarrow 3\,^2S_{1/2};$$

The splittings of the levels in the presence of the magnetic field are shown in Fig. 1.10.19.2. The 'g' factor can be calculated by using its expression. Let us consider the term $^2P_{3/2}$ where, $L = 1$, $S = ½$ and $J = 3/2$.

$$g = 1 + \frac{J(J+1) + S(S+1) - L(L+1)}{2J(J+1)}$$

$$= 1 + \frac{3/2 \times 5/2 + 1/2 \times 3/2 - 1 \times 2}{2 \times 3/2 \times 5/2} = 4/3$$

Hence here, gM_J can have the values as : 2, 2/3 , – 2/3 and –2.

Click Here t.me/thealchemylibrary

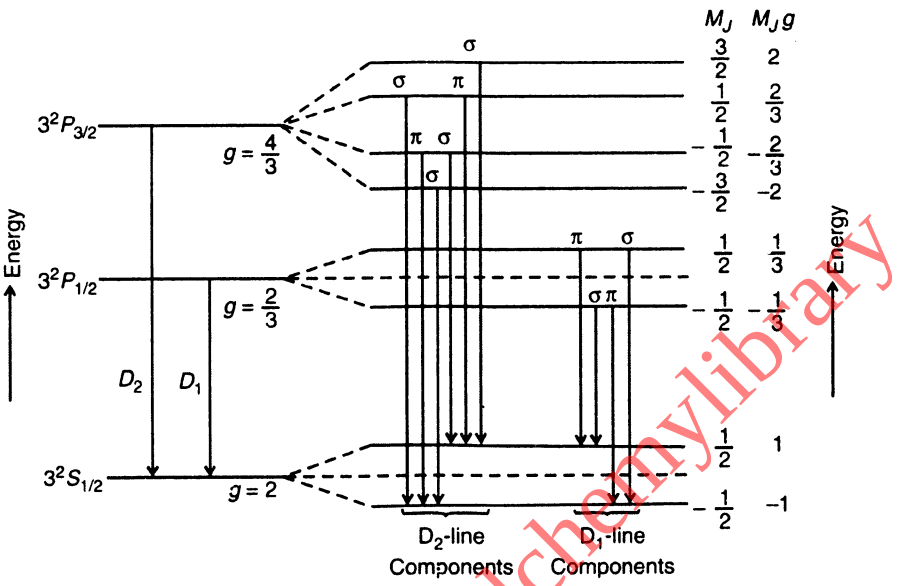

Fig. 1.10.19.2. Anomalous Zeeman effect for sodium D_1 and D_2 lines.

The values of L, S, J, g, M_J, and gM_J for each level involved in the origin of D_1 and D_2 line are shown in Fig. 1.10.19.2.

From Fig. 1.10.19.2, it is seen that the D_2 line splits into six components while the D_1 line produces four components. The components for $\Delta M_J = 0$ are called ***π-components*** while those for $\Delta M_J = \pm 1$ are called ***σ-components.***

Here, again it is noteworthy that ***under a tremendously high magnetic field, the orbital and spin magnetic moments are uncoupled and it is transformed into the normal Zeeman effect.***

(iii) Paschen-Back Effect and Stark Effect

The **Paschen-Back effect** (i.e. splitting of spectral lines in the presence of the magnetic field of intermediate strength) also gets a sound explanation in the vector model. The ***electro-optic phenomenon, Stark effect*** can also be nicely explained in the light of this model. But these are lying beyond our scope.

1.10.20 Electronic Structure of the Atoms

The distribution pattern of the electrons in the atoms heavier than hydrogen finds a sound basis in the vector model. In this regard, *Aufbau principle, Pauli exclusion principle and Hund's rule of spin multiplicity* along with the concept of space quantisation are of immense importance. These aspects will be described in a separate Section (Sec. 1.11).

1.10.21 Merits of the Vector Model

As a matter of fact, the concept of spinning electron along with the idea of spatial quantisation has created a revolution in the direction of proper understanding of the atomic structure with special reference to their spectral characteristics. The fine or multiplet structure of the spectral lines, magneto-optic

Click Here to me/thealchemylibrary

phenomena such as Zeeman effect - both normal and anomalous, Paschen-Back effect and electro-optic phenomenon - Stark effect can nicely be explained by using the model.

1.11 ELECTRONIC CONFIGURATION SCHEME FOR MANY ELECTRON SYSTEMS*

1.11.1 Rules for Placing the Electrons in Different Energy Levels

Both the vector model and wave mechanical model support the existence of 0 to $(n-1)$ azimuthal quantum numbers (l) for the principal quantum number n. In representing the electronic configuration of an atom, the principal quantum number (n) and the azimuthal quantum number (l) of the electrons are required. If x electrons possess the principal and azimuthal quantum number n and l respectively, they are expressed as nl^x. Thus if there are five p-electrons for $n = 3$, they are expressed as $3p^5$. To determine the mode of arrangements of the electrons in different levels and sublevels, the following principles are followed.

1. Pauli exclusion principle and the rule of maximum capacity of a shell and subshell

We have already discussed (Sec. 1.10.4) the *Pauli force* leading to the Pauli exclusion principle which states that in an atom no two electrons can have the four quantum numbers (i.e. n, l, m_l and m_s) identical and they must differ at least in one quantum number. This rule automatically leads to the conclusion (Sec. 1.10.4, Table 1.10.4.1) that for a particular value of n, it can have maximum $2n^2$ electrons. This maximum capacity rule is very often known as ***Bohr-Bury scheme***. It also concludes that a sublevel having azimuthal quantum number l can have maximum $2(2l + 1)$ electrons (Sec. 1.10.4, Table 1.10.4.1). Thus, for: s (i.e. $l = 0$), p (i.e. $l = 1$), d (i.e. $l = 2$) and f (i.e. $l = 3$) sublevels, the maximum number of electrons which can be accommodated are 2, 6, 10 and 14 respectively.

2. Aufbau principle

The German word *aufbau* means *building* or *construction*. The rule states that taking into consideration of the Pauli exclusion principle, the *orbitals of lowest energy will be occupied by the electrons first, then the orbitals of higher energy will start to accommodate the electrons (from the lower levels gradually)*.

- ***Relative positions of the energy levels***

Now to utilise the *aufbau* principle, it is required to know the relative sequence of the energy levels, i.e. orbitals coming from different principal quantum numbers. For a particular principal quantum number, the energies of the orbitals are in the sequence, $s < p < d < f$ .... This order can be explained by considering the **radial distribution probabilities** (Fig. 4.1.4.2) of the orbitals. It (Fig. 4.1.4.2) indicates

* In developing the model for many-electron systems, the basic conclusions drawn from the vector model are remaining unaltered and these have been theoretically supported by the wave mechanical model which will be discussed in the next chapter. Here it is noteworthy that some concepts are changed in the wave mechanics, such as, **probability concept introduces the orbitals instead of orbits.** Besides these, **Hartree's self-consistent field (SCF)** method to be discussed in the next chapter has contributed significantly to have an idea of the energies of different orbitals in many-electron systems. Thus the ideas obtained from Bohr-Sommerfeld model, vector model and wave mechanical model are fused together to have the present scheme discussed here.

Click Here t.me/theachemylibrary

that **for a particular value** ***of n, as the value of l decreases, the probability of existence of the corresponding electron at a closer distance towards the nucleus increases; as a result, for the lower values of l, the electrons get much more attraction towards the nucleus and consequently their energies decrease with the decrease of l. In Sommerfeld's model, the higher penetrating power of the orbits due to their higher ellipticity for the lower values of azimuthal quantum numbers can also explain the sequence of energy of s, p, d and f orbits for a particular value of n.***

The maximum capacity, i.e. $2n^2$, can also be shown mathematically as follows :

Let the maximum number of electrons which can be placed in a shell be denoted by N_{max}.

Hence, $N_{max} = \sum_{l=0}^{l=n-1} 2(2l+1)$

(where n is the principal quantum number and l is the corresponding azimuthal quantum number).

Thus, $N_{max} = 2 \times 1 + 2 \times 3 + 2 \times 5 + ... + 2\{2(n-1)+1\}$

$= 2[1 + 3 + 5 + ... + \{2(n-1)+1\}]$

$= 2\left[\frac{p(a+b)}{2}\right]$; ($a$ and b give the 1st and last terms of the series, p = number of terms in the series = n)

$= n[1 + 2(n-1) + 1] = 2n^2$

• ***(n + l) Rule*** **:** From the above discussion, it appears that both the wave mechanics and classical mechanics can predict easily the order of energy of the sublevels originated from a particular principal quantum number. But it becomes extremely difficult to predict the sequence of energy of different sublevels (i.e. orbitals) developed from different principal quantum numbers. In this connection, the empirical $(n + l)$ rule is of much practical importance at least for the lighter elements. It is also applicable for the orbitals of the same principal quantum number. It is formulated as :

(a) The energy of the orbitals increases with the increase of $(n + l)$ values. It is illustrated in the following cases :

Energy **:** $1s < 2s < 3s < 4s < 5s$; $4s < 3d < 4d < 4f$

$(n + l)$ **:** $1 < 2 < 3 < 4 < 5$; $4 < 5 < 6 < 7$

(b) For the same values of $(n + l)$ associated with a number of orbitals, the energy increases with the increase of n. It is illustrated as follows :

Energy **:** $3d < 4p < 5s$; $4f < 5d < 6p$

$(n + l)$ **:** $5 \quad 5 \quad 5$; $7 \quad 7 \quad 7$

n **:** $3 < 4 < 5$; $4 < 5 < 6$

Thus taking into the **consideration of the** $(n + l)$ **rule,** the following energy sequence can be formulated.

$1s < 2s < 2p < 3s < 3p < 4s < 3d < 4p < 5s < 4d < 5p < 6s < 4f < 5d < 6p < 7s < 5f < 6d < 7p < 8s$

This energy sequence can be represented by a mnemonic (assisting the memory) scheme as shown in Fig. 1.11.1.1. Here it is worth mentioning that the above energy sequence is strictly followed by the

Click Here to join/thealchemylibrary

lighter elements ($Z \leq 20$) only. But with some modifications on this, it is possible to have the ground state electronic configurations of the elements up to $Z = 103$ in which the transuranic elements start at $Z = 93$. **For the heavier elements, *with the increase of effective nuclear charge, the sequence gets modified. Generally, with the increase of effective nuclear charge, the energy of the orbitals falls but all do not change to the same extent*** **(cf. Fig. 1.11.1.2)**. After a certain limit, the energy of *d* or *f* orbitals falls more sharply compared to that of *s* or *p* orbitals and as a result, the energy sequence applicable for the lighter elements may get reversed for the heavier ones. It has been found that for $Z \geq 90$, the following order is maintained ***where the (n + l) rule is not followed.***

$1s < 2s < 2p < 3s < 3p < 3d < 4s < 4p < 4d < 4f < 5s < 5p < 5d < 5f < 6s < 6p < 6d < 7s < 7p < 8s$

Thus it appears that the relative positions of the different orbitals are strongly dependent on the atomic number *Z*. The relative variation trends of energy of different orbitals originated from different principal quantum numbers are shown in Fig. 1.11.1.2 and Table 1.11.1.1. Observation of Fig. 1.11.1.2 (cf. Fig. 9.10.2) strongly indicates the following points.

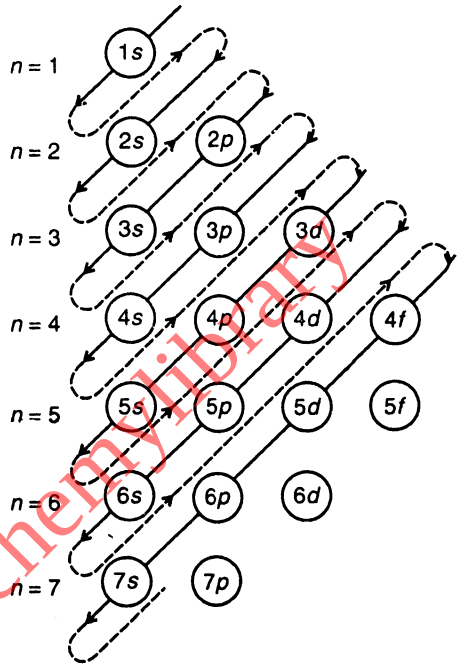

Fig. 1.11.1.1. This energy sequence (a mnemonic scheme) of different orbitals (i.e. illustration of $n + l$ rule).

(a) **For the heavier atoms, the energy sequence is mainly governed by the principal quantum number, i.e. the preference of filling the shells runs as follows :**

$K\,(n = 1) > L\,(n = 2) > M\,(n = 3) > N\,(n = 4)$ ....

Table 1.11.1.1. Orbital energies (eV) of different elements (*H* to *Ar*)
(1 eV = 96.5 kJ mol^{-1})

	H	*He*						
1*s*	– 13.6	– 24.6						
	Li	*Be*	*B*	*C*	*N*	*O*	*E*	*Ne*
1*s*	– 58	– 115	– 192	– 288	– 409	– 538	– 694	– 870
2*s*	– 5.4	– 9.3	– 12.9	– 16.5	– 20.2	– 28.5	– 38	– 48.6
2*p*			– 8.3	– 11.3	– 14.5	– 13.6	– 17.5	– 21.6
	Na	*Mg*	*Al*	*Si*	*P*	*S*	*Cl*	*Ar*
1*s*	– 1075	– 1308	– 1564	– 1844	– 2148	– 2476	– 2828	– 3206
2*s*	– 66	– 92	– 121	– 154	– 191	– 232	– 277	– 326
2*p*	– 34	– 54	– 77	– 103	– 134	– 168	– 207	– 249
3*s*	– 5.2	– 7.6	– 10.6	– 13.5	– 16.2	– 20.2	– 24.5	– 29.2
3*p*			– 6.0	– 8.2	– 10.5	– 10.4	– 13.0	– 15.8

Click Here t.me/thealchemylibrary

(b) For the heavier elements, the energies of all the sublevels (i.e. *s*, *p*, *d*, *f* .... orbitals) for a particular shell, i.e. principal quantum number, tend to be degenerate. **Thus it appears that *for the heavier elements the simple Bohr's model for the hydrogen-like systems appears correct in practice, in which the energy of the electron in an atom is considered to be governed only by n.***

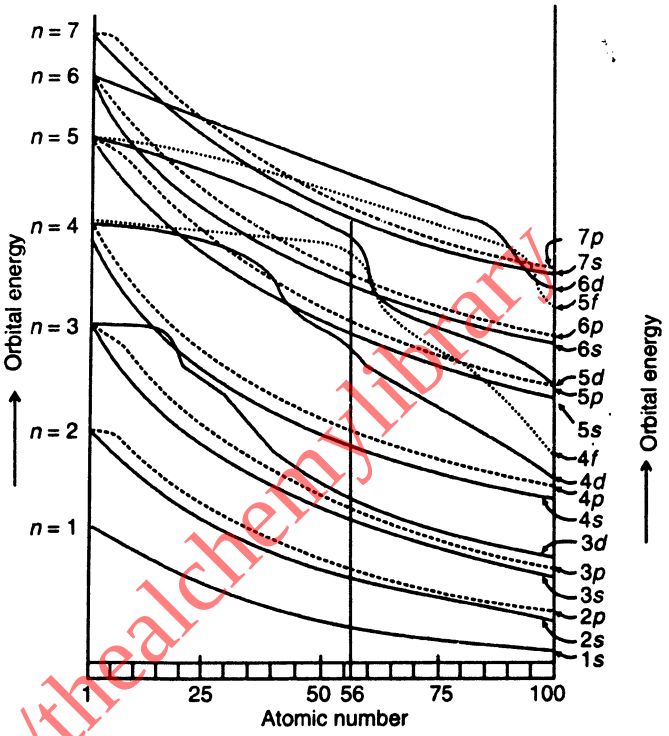

Fig. 1.11.1.2. Variation trends of energy sequence of the orbitals with the increase of atomic number.

Here it is worth mentioning that in the light of Bohr's theory for the hydrogen-like systems, all the sublevels (i.e., *s*, *p*, *d*, *f*, etc.) of a particular shell are degenerate while for the many electron systems, according to $(n + l)$ rule they lie in the sequence $f > d > p > s$ for a particular shell. ***This difference develops due to the shielding*** (by the inner electrons) experienced by the different sublevels under consideration in polyelectronic systems. In one-electron systems (i.e., hydrogenic systems), no question of shielding by the inner electrons arises and as a result, all the sublevels of a particular *n* become degenerate.

(c) **Upto atomic number (*Z*) 56,** the electronic configuration can be written by using the diagram shown in Fig. 1.11.1.1, but **discrepancy arises when the 4*f* level comes into consideration.** For the element *La* ($Z = 57$), the electronic configuration is $[Xe]4f^0\ 5d^16s^2$, i.e. a single 5*d* electron is added before the 4*f* level is occupied. The remaining 9 *d*-electrons of the 5*d* level are added after the 4*f*-subshell is completely filled with 14 electrons.

Approximately, upto $Z = 56$, the electronic configuration can be written by following the energy diagram given in Fig. 1.11.1.1 while for $Z > 56$, the electronic configurations can be predicted by using the energy diagram given in Fig. 1.11.1.2.

***Note* : Relativistic effects** on the energy of orbitals have been discussed in Sec. 8.20.3.

- ***Some exceptions to (n + l) rule***

(i) **Anomaly for the elements, $Z = 57$–58 :** *Ba* ($Z = 56$) is having the electronic configuration $[Xe]6s^2$ where $[Xe]$ represents the electronic configuration of *Xe* ($Z = 54$) having the arrangement 2, 8, 18, 18, 8. Now for *La* ($Z = 57$), the 57th electron should go in 4*f* and it should be represented

Click Here to me/thealchemylibrary

as: [*Xe*] $4f^1\ 6s^2$. But actually, it is having [*Xe*] $4f^0\ 5d^1\ 6s^2$. Here *4f and 5d are having the same* $(n + l)$ values, *so it should be* $4f < 5d$ *in energy according to the* $(n + l)$ *rule*. **Thus, here it is violated.** But it is interesting to note that for *Ce* ($Z = 58$), it is difficult to predict whether the configuration is [*Xe*] $4f^2\ 5d^0\ 6s^2$ or [*Xe*] $4f^1\ 5d^1\ 6s^2$, **as the energy difference between *4f* and *5d* in the range *Z* = 57-58 is very small (cf. Fig. 1.11.1.2), and no general rule can be formulated.**

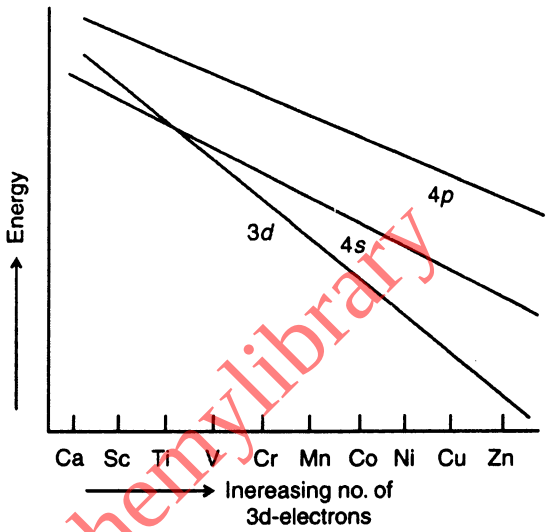

Fig. 1.11.1.3. Trend of energy change of the 3*d*, 4*s* and 4*p* orbitals for the first transition series (cf. Fig. 1.11.1.2).

(ii) **Anomaly in energy order of *5f* and *6d* orbitals in the range of *Z* = 90 :** For actinium, the same thing occurs as in the case of lanthanum. *Ra* ($Z = 88$) is having the configuration [*Rn*] $7s^2$ where *Rn* ($Z = 86$) is having the arrangement 2, 8, 18, 32, 18, 8. For *Ac* ($Z = 89$), the expected configuration is [*Rn*] $5f^1\ 6d^0\ 7s^2$ but it is actually [*Rn*] $5f^0\ 6d^1\ 7s^2$. **Here, again it is proposed that in this range, no significant energy difference exists between *5f* and *6d*.**

(iii) **$(n - 1)d$ level vs. *ns* level and $(n - 2)f$ level vs. $(n - 1)d$ level :** According to $(n + l)$ rule, for the transition series the $(n - 1)d$ level lies above the *ns* level, but when these, i.e. $(n - 1)d$ levels, are getting filled in, they tend to lie very close to *ns* level and for the heavier elements or ions where the effective nuclear charge (Z^*) is very high, even the reverse order may arise (Fig. 1.11.1.3). The same thing occurs for the $(n - 2)f$ and $(n - 1)d$ levels in the inner transition series.

Ionisation from the (n – 1)d orbital or ns orbital for the transition metals?

The **apparently contradictory observation** is noted in the mode of ***ionisation of the transition elements*** to form M^{2+} as follows (1st transition series, for example) :

$$M\,(1s^2\ 2s^2\ 2p^6\ 3s^2\ 3p^6\ 3d^x\ 4s^2) \xrightarrow{-2e} M^{2+}\,(1s^2\ 2s^2\ 2p^6\ 3s^2\ 3p^6\ 3d^x\ 4s^0)$$

This occurs for any transition element of the first series whether it is lighter or heavier. ***In general, ns^2 electrons are lost before the $(n - 1)d$ or $(n - 2)f$ electrons.*** **This is believable for the heavier ones where the $(n - 1)$ *d* levels lie below the *ns* level, but for the beginners of the series (e.g. *Sc*) where the *ns* level lies below the $(n - 1)d$ levels, it is surprising.** Moreover, the *ns* level gets filled in before the $(n - 1)d$ or $(n - 2)f$ levels as the *ns* orbital is having lower energy according to *aufbau* principle. Hence, when the electrons are to be lost, they are expected to come from the higher orbitals, i.e., $(n - 1)d$, $(n - 2)f$ levels. ***Thus, it apparently violates the aufbau principle.***

Click Here : new.chemylibrary

For the neutral atoms, the electronic configuration, $(n-1)d^x\ ns^2$ is having lower energy than the alternative configuration, $(n-1)d^{2+x}\ ns^0$, when all the possible electron-electron repulsions along with other energy terms are considered to estimate the overall energy of the system. On the other hand, for the ionised species M^{2+}, the electronic configuration, $(n-1)d^x\ ns^0$ is having lower energy than the configuration $(n-1)d^{x-2}\ ns^2$.

Here it is worth pointing out that the effective nuclear charge (Z^*) for M^{2+} is much greater than that of M; ***and as a result, in M^{2+}, the energy of the $(n-1)d$ level is so lowered compared to the ns level that the energy of the configuration, $(n-1)d^x\ ns^0$ is lower than that of the other possible configuration $(n-1)d^{x-2}\ ns^2$. Besides these, the less shielding in M^{2+} compared to that in M further favours the lowering of $(n-1)d$ level.*** In neutral M, having the electronic configuration $(n-1)d^x\ ns^2$, the ns^2 electrons shield the $(n-1)d^x$ electrons to increase the energy of the $(n-1)d$ orbitals. But in M^{2+}, no such shielding of $(n-1)d^x$ electrons occurs and it lowers the energy of the $(n-1)d$ level.

Besides the above factors, the overall energy of the $(n-1)d^x\ ns^0$ configuration is lower than that of the other possible configuration $(n-1)d^{x-2}\ ns^2$ **where the electron-electron repulsion is more.** The magnitude of electron-electron repulsion depends to some extent on the size of the orbital. In the larger d-orbitals, the said repulsion is less compared to that in the s-orbitals.

In conclusion, for M^{2+} the $(n-1)d^x\ ns^0$ configuration is stabler than the other possible configuration $(n-1)d^{x-2}\ ns^2$ because of the following factors :

- ***Enhanced effective nuclear charge*** in M^{2+} (compared to neutral M) lowers the energy of the $(n-1)d$ orbital more compared to that of the ns-orbital.
- ***Less shielding*** experienced by the $(n-1)d^x$ electrons in M^{2+} (compared to the case of neutral M) favours the lowering of energy of the $(n-1)d$ orbital (compared to the case of neutral M).
- ***Less electron-electron repulsion*** in the $(n-1)d^x\ ns^0$ configuration compared to that in $(n-1)d^{x-2}\ ns^2$ configuration favours the configuration $(n-1)d^x\ ns^0$ of M^{2+}.

Note : The ease of ionisation from the $4s$ level compared to the $3d$ level can also be realised **in terms of Z^* values** (that can be calculated by Slater's rule, Sec. 4.2.4) experienced by the $3d$ and $4s$ electrons. It is illustrated for chromium :

$$Cr : (1s)^2\ (2s,\ 2p)^8\ (3s,\ 3p)^8\ (3d)^5\ (4s)^1$$

$$\begin{cases} S\ (\text{for } 4s) = (2\times 1.0) + (8\times 1.0) + (8\times 0.85) + (5\times 0.85) = 21.05 \\ Z^*\ (\text{for } 4s) = 24 - 21.05 = 2.95 \end{cases}$$

$$\begin{cases} S\ (\text{for } 3d) = (2\times 1.0) + (8\times 1.0) + (8\times 1.0) + (4\times 0.35) = 19.4 \\ Z^*\ (\text{for } 3d) = 24 - 19.4 = 4.6 \end{cases}$$

Thus, in chromium, the $3d$ electron experiences more Z^* (i.e. more tightly bound) than the $4s$ electron. Consequently, during ionisation, the $4s$ electron is lost first.

(iv) **Half-filled and full-filled level :** The *aufbau* principle is again violated for the systems where half-filled or full-filled electronic configuration produces higher stability. This aspect has been discussed separately below.

Click Here t.me/dearchemylibrary

3. The rule of half-filled or completely filled orbitals

The half-filled or full-filled orbitals are much stabler compared to the nearest half-filled or full-filled orbitals respectively. This enhanced stability for the half-filled and full-filled orbitals can be nicely explained by considering the ***exchange energy*** (E_{ex}), ***a quantum mechanical phenomenon***, along with the Coulombic energy.

To understand the physical meaning of the exchange energy, we have to consider the following aspects. In the absence of any external field (electric or magnetic), the electrons in an atom with the parallel spins having the same n, l are *indistinguishable*. Thus the electrons can exchange their places. *More correctly the wave functions associated with the individual electrons are exchangeable*. Due to this exchange phenomenon among the indistinguishable electrons, the electrons of the system are getting a larger volume to travel. Now, according to the principle of the model, *particle in a box* (Sec. 3.5.5), the system is getting stabilised, when the electrons are now getting a larger dimension (a consequence of *extended delocalisation*) of the box in which they can travel. This extended delocalisation increases with the increases of the number of such indistinguishable electrons. Very often, the exchange energy is measured by the *number of sets* (N) *of two electrons* (which are indistinguishable, i.e. n, l are indentical) which can be arranged from the electrons with parallel spins. Thus, N is given by (for x number of electrons with parallel spins) :

$$N = {}^{x}C_2 = \frac{x!}{2!(x-2)!} = \frac{x(x-1)}{2}; \text{ and } E_{ex} \propto \frac{x(x-1)}{2}$$

$$E_{ex} = \frac{Kx(x-1)}{2}, K = \text{proportionality constant}$$

- **d^5 configuration and electronic configuration of chromium :** Now, let us consider the cases (Fig. 1.11.1.4), d^4 ($x = 4$), d^5 ($x = 5$) and d^6 ($x = 5$ and $x = 1$), (in d^6 system, the sixth electron is antiparallel with respect to the others). The exchange energies are :

$$E_{ex}(d^4) \propto {}^4C_2 < E_{ex}(d^5) \propto {}^5C_2 = E_{ex}(d^6) \propto ({}^5C_2 + {}^1C_2) = {}^5C_2$$

i.e. $E_{ex}(d^4) = 6K < E_{ex}(d^5) = E_{ex}(d^6) = 10K$; K = proportionality constant

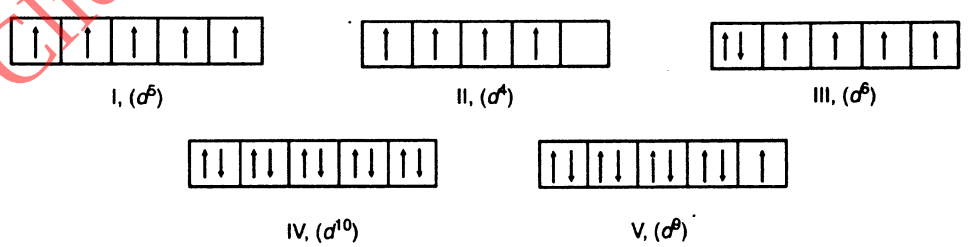

Fig. 1.11.1.4. Arrangements of electrons in d^4, d^5, d^6, d^9 and d^{10} systems.

Thus the exchange energy for the d^4 system is lower compared to those of the d^5 and d^6 systems. **Though the d^5 and d^6 systems are having the same exchange energy, in d^6, due to the pairing of**

Click Here t.me/thearchemylibrary

one electron, it suffers from the electron-electron Coulombic repulsive force. This is why the half-filled d^5-sytem is stabler compared to the other arrangements nearest to the half-filled one. Thus, for chromium, the ground state configuration is $3d^5\ 4s^1$ instead of $3d^4\ 4s^2$. **In moving the 4*s* electron to 3*d* level, the disfavour is overcome by the gain of exchange energy. Moreover, in the $3d^5 4s^1$ configuration, there is no Coulombic repulsion to pair the electrons, but in the $3d^4\ 4s^2$ configuration, there is a Coulombic repulsion to pair the electrons in the 4*s* level.**

• **d^{10} configuration and electronic configuration of copper :** Now, let us consider the cases (Fig. 1.11.1.4), d^9 ($x_{+1/2} = 5, x_{-1/2} = 4$), d^{10} ($x_{+1/2} = x_{-1/2} = 5$) where the lower right hand suffix of x indicates the magnetic spin quantum number of the group of the indistinguishable electrons, e.g. $x_{+1/2}$ indicates the electrons with $m_s = +\ 1/2$. The exchange energies are :

$$E_{ex}(d^9) \propto ({}^5C_2 + {}^4C_2 = 16) < E_{ex}(d^{10}) \propto ({}^5C_2 + {}^5C_2 = 20)$$

$$\text{i.e. } E_{ex}(d^9) = 16K < E_{ex}(d^{10}) = 20K$$

In d^{10} system, the exchange energy is higher than that of d^9 system, but it suffers from an additional electron-electron repulsion due to the pairing of the tenth electron. **The higher exchange energy probably (at least partially) overcomes the disfavour created due to the additional pairing in d^{10} system.**

Let us consider the electronic configuration of copper. For its $3d^{10}\ 4s^1$ electronic configuration, the exchange energy ($\propto 20$) is more than the alternative configuration $3d^9\ 4s^2$ for which the exchange energy is proportional to 16. In both the configurations, the number of paired electrons (= 5 pairs) is the same to make the Coulombic repulsion factor more or less the same. **However, in transferring one electron from the 4*s* level to the 3*d* level, there is a loss of *orbital energy* as the energy of 4*s* level is less than that of 3*d* level.** This loss of orbital energy is definitely less than the gain of exchange energy.

• **Anomalies :** However, some anomalies to the preference of half-filled and full-filled shells are known. These are:

Cr ($3d^5\ 4s^1$), *W* ($5d^4\ 6s^2$); *Ni* ($3d^8\ 4s^2$), *Pd* ($4d^{10}\ 5s^0$), *Pt* ($5d^9\ 6s^1$).

In such cases, where the half-filled or full-filled levels are not preferred, the ***loss of orbital energy*** due to the transfer of electrons from the *ns* level to the $(n-1)d$ level is probably more than the ***gain of exchange energy*** from the alternative configuration having the full-filled or half-filled level.

For the members of 5*d* series (e.g. *W, Pt* etc.), **the 6*s* orbital is contracted due to both *lanthanide contraction* and *relativistic contraction*.** Consequently, in such cases, transfer of 6*s* electron to the 5*d* level may lead to *loss of orbital energy* very high, and they tend to retain the electron in the 6*s* level. However, this simple consideration cannot explain fully the difference in electronic configurations of *Ni*, *Pd* and *Pt*. It indicates that many other factors are also involved.

• **Examples of this rule of half-filled or full-filled orbitals are given in Table 1.11.1.1.**

Click Here : me/thealchemylibrary

Table 1.11.1.1. Illustration of the enhanced stability for just half-filled and full-filled orbitals compared to the nearest ones.

Element	*Expected configuration*	*Actual configuration*
Cr ($Z = 24$)	$[Ar]\ 3d^4\ 4s^2$	$[Ar]\ 3d^5\ 4s^1$
Mo ($Z = 42$)	$[Kr]\ 4d^4\ 5s^2$	$[Kr]\ 4d^5\ 5s^1$
Gd ($Z = 64$)[a]	$[Xe]\ 4f^8\ 5d^0\ 6s^2$	$[Xe]\ 4f^7\ 5d^1\ 6s^2$
Cm ($Z = 96$)[a]	$[Rn]\ 5f^8\ 6d^0\ 7s^2$	$[Rn]\ 5f^7\ 6d^1\ 7s^2$
Cu ($Z = 29$)	$[Ar]\ 3d^9\ 4s^2$	$[Ar]\ 3d^{10}\ 4s^1$
Pd ($Z = 46$)	$[Kr]\ 4d^8\ 5s^2$	$[Kr]\ 4d^{10}\ 5s^0$
Ag ($Z = 47$)	$[Kr]\ 4d^9\ 5s^2$	$[Kr]\ 4d^{10}\ 5s^0$
Au ($Z = 79$)	$[Xe]\ 4f^{14}\ 5d^9\ 6s^2$	$[Xe]\ 4f^{14}\ 5d^{10}\ 6s^1$
Nb ($Z = 41$)*	$[Kr]\ 4d^3\ 5s^2$	$[Kr]\ 4d^4\ 5s^1$
Ru ($Z = 44$)*	$[Kr]\ 4d^6\ 5s^2$	$[Kr]\ 4d^7\ 5s^1$
Rh ($Z = 45$)*	$[Kr]\ 4d^7\ 5s^2$	$[Kr]\ 4d^8\ 5s^1$
Pt ($Z = 78$)*	$[Xe]\ 4f^{14}\ 5d^8\ 6s^2$	$[Xe]\ 4f^{14}\ 5d^9\ 6s^1$

* One of the two electrons from ns^2 moves to $(n-1)\,d$ level. For the transfer of one *ns* electron to the $(n-1)d$ level, there is a loss of *orbital energy* but it causes a gain of exchange energy from the $(n-1)d$ level. Moreover, the electron-electron repulsion in *ns* orbital is more than that in $(n-1)d$ orbital because of the larger size of *d*-orbitals.

(a) One electron from *nf* moves to $(n+1)d$ to make the *nf* half-filled.

For rest of the elements, electron shifting occurs between *ns* and $(n-1)d$ to make $(n-1)d$ half-filled or full-filled.

By considering the above mentioned three rules, i.e. Pauli exclusion principle, *aufbau* principle along with the idea of sequence of the energy levels and concept of extra stability for the half-filled and full-filled orbitals, the ground state electronic configurations of the elements $Z = 1$ to $Z = 103$ are given in Table 1.11.1.2.

(4) Electronic configuration and Hund's rule, i.e. the rule of maximum spin multiplicity

It has been already discussed in Section 1.10.11. Here again it is highlighted. It states that when the electrons enter into some degenerate sublevels (i.e. of the same energy, as they are having same *n* and *l*), the electrons will try to avoid pairing and try to remain unpaired so long as possible with parallel spins to generate the maximum spin multiplicity $\left(=2S+1, S=\sum s_i\right)$. It is believed that pairing or arrangements with antiparallel spins will reduce the ***exchange energy.*** Besides this, in pairing the electrons to overcome the electron-electron repulsion, ***pairing energy*** is also to be spent. ***Thus pairing leads to the loss of exchange energy and increase of repulsive energy while for the arrangements with unpaired antiparallel spins, only the exchange energy is lost but no repulsive energy is introduced.***

Click Here t.me/thealchemylibrary

Table 1.11.1.2. Ground state electronic configurations of the elements

Atomic number	Element	Electronic configuration	Atomic number	Element	Electronic configuration
1	*H*	$1s^1$	31	*Ga*	$[Ar]\ 3d^{10}\ 4s^2\ 4p^1$
2	*He*	$1s^2$	32	*Ge*	$[Ar]\ 3d^{10}\ 4s^2\ 4p^2$
3	*Li*	$[He]\ 2s^1$	33	*As*	$[Ar]\ 3d^{10}\ 4s^2\ 4p^3$
4	*Be*	$[He]\ 2s^2$	34	*Se*	$[Ar]\ 3d^{10}\ 4s^2\ 4p^4$
5	*B*	$[He]\ 2s^2\ 2p^1$	35	*Br*	$[Ar]\ 3d^{10}\ 4s^2\ 4p^5$
6	*C*	$[He]\ 2s^2\ 2p^2$	36	*Kr*	$[Ar]\ 3d^{10}\ 4s^2\ 4p^6$
7	*N*	$[He]\ 2s^2\ 2p^3$	37	*Rb*	$[Kr]\ 5s^1$
8	*O*	$[He]\ 2s^2\ 2p^4$	38	*Sr*	$[Kr]\ 5s^2$
9	*F*	$[He]\ 2s^2\ 2p^5$	39	*Y*	$[Kr]\ 4d^1\ 5s^2$
10	*Ne*	$[He]\ 2s^2\ 2p^6$	40	*Zr*	$[Kr]\ 4d^2\ 5s^2$
11	*Na*	$[Ne]\ 3s^1$	41	*Nb*	$[Kr]\ 4d^4\ 5s^1$
12	*Mg*	$[Ne]\ 3s^2$	42	*Mo*	$[Kr]\ 4d^5\ 5s^1$
13	*Al*	$[Ne]\ 3s^2\ 3p^1$	43	*Tc*	$[Kr]\ 4d^5\ 5s^2$
14	*Si*	$[Ne]\ 3s^2\ 3p^2$	44	*Ru*	$[Kr]\ 4d^7\ 5s^1$
15	*P*	$[Ne]\ 3s^2\ 3p^3$	45	*Rh*	$[Kr]\ 4d^8\ 5s^1$
16	*S*	$[Ne]\ 3s^2\ 3p^4$	46	*Pd*	$[Kr]\ 4d^{10}\ 5s^0$
17	*Cl*	$[Ne]\ 3s^2\ 3p^5$	47	*Ag*	$[Kr]\ 4d^{10}\ 5s^1$
18	*Ar*	$[Ne]\ 3s^2\ 3p^6$	48	*Cd*	$[Kr]\ 4d^{10}\ 5s^2$
19	*K*	$[Ar]\ 4s^1$	49	*In*	$[Kr]\ 4d^{10}\ 5s^2\ 5p^1$
20	*Ca*	$[Ar]\ 4s^2$	50	*Sn*	$[Kr]\ 4d^{10}\ 5s^2\ 5p^2$
21	*Sc*	$[Ar]\ 3d^1\ 4s^2$	51	*Sb*	$[Kr]\ 4d^{10}\ 5s^2\ 5p^3$
22	*Ti*	$[Ar]\ 3d^2\ 4s^2$	52	*Te*	$[Kr]\ 4d^{10}\ 5s^2\ 5p^4$
23	*V*	$[Ar]\ 3d^3\ 4s^2$	53	*I*	$[Kr]\ 4d^{10}\ 5s^2\ 5p^5$
24	*Cr*	$[Ar]\ 3d^5\ 4s^1$	54	*Xe*	$[Kr]\ 4d^{10}\ 5s^2\ 5p^6$
25	*Mn*	$[Ar]\ 3d^5\ 4s^2$	55	*Cs*	$[Xe]\ 6s^1$
26	*Fe*	$[Ar]\ 3d^6\ 4s^2$	56	*Ba*	$[Xe]\ 6s^2$
27	*Co*	$[Ar]\ 3d^7\ 4s^2$	57	*La*	$[Xe]\ 5d^1\ 6s^2$
28	*Ni*	$[Ar]\ 3d^8\ 4s^2$	58	*Ce*	$[Xe]\ 4f^2\ 6s^2$
29	*Cu*	$[Ar]\ 3d^{10}\ 4s^1$	59	*Pr*	$[Xe]\ 4f^3\ 6s^2$
30	*Zn*	$[Ar]\ 3d^{10}\ 4s^2$	60	*Nd*	$[Xe]\ 4f^4\ 6s^2$

(Contd.)

Click Here t.me/thealchemylibrary

Atomic number	Element	Electronic configuration	Atomic number	Element configuration	Electronic
61	*Pm*	$[Xe]\ 4f^5\ 6s^2$	83	*Bi*	$[Xe]\ 4f^{14}\ 5d^{10}\ 6s^2\ 6p^3$
62	*Sm*	$[Xe]\ 4f^6\ 6s^2$	84	*Po*	$[Xe]\ 4f^{14}\ 5d^{10}\ 6s^2\ 6p^4$
63	*Eu*	$[Xe]\ 4f^7\ 6s^2$	85	*At*	$[Xe]\ 4f^{14}\ 5d^{10}\ 6s^2\ 6p^5$
64	*Gd*	$[Xe]\ 4f^7\ 5d^1\ 6s^2$	86	*Rn*	$[Xe]\ 4f^{14}\ 5d^{10}\ 6s^2\ 6p^6$
65	*Tb*	$[Xe]\ 4f^9\ 6s^2$	87	*Fr*	$[Rn]\ 7s^1$
66	*Dy*	$[Xe]\ 4f^{10}\ 6s^2$	88	*Ra*	$[Rn]\ 7s^2$
67	*Ho*	$[Xe]\ 4f^{11}\ 6s^2$	89	*Ac*	$[Rn]\ 6d^1\ 7s^2$
68	*Er*	$[Xe]\ 4f^{12}\ 6s^2$	90	*Th*	$[Rn]\ 6d^2\ 7s^2$
69	*Tm*	$[Xe]\ 4f^{13}\ 6s^2$	91	*Pa*	$[Rn]\ 5f^2\ 6d^1\ 7s^2$
70	*Yb*	$[Xe]\ 4f^{14}\ 6s^2$	92	*U*	$[Rn]\ 5f^3\ 6d^1\ 7s^2$
71	*Lu*	$[Xe]\ 4f^{14}\ 5d^1\ 6s^2$	93	*Np*	$[Rn]\ 5f^4\ 6d^1\ 7s^2$
72	*Hf*	$[Xe]\ 4f^{14}\ 5d^2\ 6s^2$	94	*Pu*	$[Rn]\ 5f^6\ 7s^2$
73	*Ta*	$[Xe]\ 4f^{14}\ 5d^3\ 6s^2$	95	*Am*	$[Rn]\ 5f^7\ 7s^2$
74	*W*	$[Xe]\ 4f^{14}\ 5d^4\ 6s^2$	96	*Cm*	$[Rn]\ 5f^7\ 6d^1\ 7s^2$
75	*Re*	$[Xe]\ 4f^{14}\ 5d^5\ 6s^2$	97	*Bk*	$[Rn]\ 5f^8\ 6d^1\ 7s^2$
76	*Os*	$[Xe]\ 4f^{14}\ 5d^6\ 6s^2$	98	*Cf*	$[Rn]\ 5f^{10}\ 7s^2$
77	*Ir*	$[Xe]\ 4f^{14}\ 5d^9\ 6s^0$	99	*Es*	$[Rn]\ 5f^{11}\ 7s^2$
78	*Pt*	$[Xe]\ 4f^{14}\ 5d^9\ 6s^1$	100	*Fm*	$[Rn]\ 5f^{12}\ 7s^2$
79	*Au*	$[Xe]\ 4f^{14}\ 5d^{10}\ 6s^1$	101	*Md*	$[Rn]\ 5f^{13}\ 7s^2$
80	*Hg*	$[Xe]\ 4f^{14}\ 5d^{10}\ 6s^2$	102	*No*	$[Rn]\ 5f^{14}\ 7s^2$
81	*Tl*	$[Xe]\ 4f^{14}\ 5d^{10}\ 6s^2\ 6p^1$	103	*Lr*	$[Rn]\ 5f^{14}\ 6d^1\ 7s^2$
82	*Pb*	$[Xe]\ 4f^{14}\ 5d^{10}\ 6s^2\ 6p^2$			

Click Here t.me/thealchemylibrary

This is why, for a number of degenerate energy levels, **maximum spin multiplicity** (i.e. *maximum number of unpaired electrons with parallel spins*) is always favoured.

Examples **:** For nitrogen, the $3p$ electrons are to be placed in p_x, p_y and p_z. Here a number of possibilities considering the Pauli exclusion principle are shown in Fig. 1.11.1.4. In **II** and **III** arrangements, S is 1/2 while it is 3/2 in **I**. This is why, **I** is only acceptable. Here it is noteworthy that the **III** contains three unpaired electrons, but

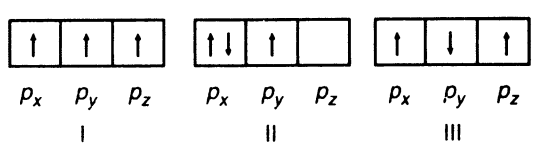

Fig. 1.11.1.5. Illustration of Hund's rule of spin multiplicity in p^3 *configuration.*

because of the antiparallel fashion, it is getting rejected. The arrangement is very often represented as, $p_x^1 p_y^1 p_z^1$.

That the unpaired antiparallel arrangement reduces the exchange energy is illustrated by considering the d^5 configuration.

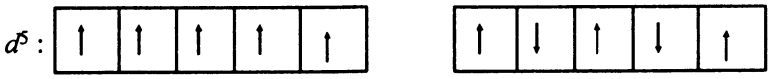

(I) (II)

Let us consider the above two possibilities. The exchange energies in the two cases are given by :

$$E_{es}\,\textbf{(I)} \propto {}^5C_2 = 10, \textbf{(case - I)}; \text{ and } E_{ex}\,\textbf{(II)} \propto ({}^3C_2 + {}^2C_2) = 3 + 1 = 4, \textbf{(case - II)}$$

Thus, E_{ex} **(I)** > E_{ex} **(II)** and the arrangement I is favoured.

Based on this principle, the electronic configurations of the following elements are shown :

C : $1s^2\,2s^2\,2p^1\,2p^1\,2p^0$; ***N*** : $1s^2\,2s^2\,2p^1\,2p^1\,2p^1$; ***O*** : $1s^2\,2s^2\,2p^2\,2p^1\,2p^1$; ***F*** : $1s^2\,2s^2\,2p^2\,2p^2\,2p^1$

(Here, the three *p*-orbitals, i.e. p_x, p_y and p_z, are energetically degenerate in the absence of any external field.)

SOLVED NUMERICAL PROBLEMS

***Problem* 1 :** In an oil drop experiment, the following data are obtained : speed of free fall of the oil drop in air (u_1) = 8.58×10^{-2} cm/s; electrical potential gradient (E) = 4000 V/cm; minimum difference, i.e. $(u_2 \sim u_2')_{min}$, in the speed of the drop in the upward direction at different times in the field = 6.78×10^{-3} cm/s; viscosity (η) of the air under experimental conditions = 1.824×10^{-4} g cm^{-1} s^{-1}; density (ρ) of the oil = 0.92 g cm^{-3}.

Calculate the charge on the electron taking, g = 980 cm s^{-2} (neglecting the buoyancy effect due to air).

***Solution* :** The electronic charge (e) is given by : $e = \dfrac{mg}{Eu_1}(u_2 \sim u_2')_{min}$, (see Sec. 1.1.4)

Now, $$mg = \frac{4}{3}\pi r^3 \rho g = \frac{4}{3}\pi\left(\frac{9\eta u_1}{2\rho g}\right)^{3/2}\rho g$$

Thus, $$e = \frac{4}{3}\pi\left(\frac{9\eta u_1}{2\rho g}\right)^{3/2} \times \rho g \frac{(u_2 \sim u_2')_{min}}{Eu_1}$$

$$= 18\pi\left[\frac{(1.824\times10^{-4})^3 \times 0.0858}{2\times0.92\times980}\right]^{1/2} \times \frac{6.78\times10^{-3}\times300}{4000},$$

$$\left(E = 4000 \text{ V/cm} = \frac{4000}{300}\frac{\text{statvolt}}{\text{cm}}\right)$$

$$= 4.88 \times 10^{-10} \text{ esu}$$

***Note* :** In CGS, potential is in statvolt unit. 1 statvolt = 300 volts.

Click Here t.me/trealchemylibrary

Problem 2 : A beam of 5 MeV alpha-particle is scattered on a gold foil of thickness 10^{-4} cm by an angle 45°. Find the impact parameter and the fraction of the incident particles scattered by 45° or more ($\rho = 1.93 \times 10^4$ kg m^{-3}, atomic weight of gold = 197, atomic number of gold = 79).

Solution : The impact parameter (b) is related with the angle (θ) of scattering as follows :

$$b = \frac{Zeq}{4\pi\varepsilon_0 m_\alpha u^2} \cot(\theta/2) = \frac{Zeq}{4\pi\varepsilon_0 \times 2\,(½)\, m_\alpha u^2} \cot(\theta/2), \text{ (cf. Eqn. 1.7.2.3)}$$

Here, $Z = 79$, $e = 1.6 \times 10^{-19}$ C, $q = 2e$, $\varepsilon_0 = 8.85 \times 10^{-12}$ C^2 N^{-1} m^{-2}

$(½)m_\alpha u^2 = 5$ MeV $= 5 \times 1.6 \times 10^{-3}$ J, (1 eV $= 1.6 \times 10^{-19}$ J)

Substituting these values in the above relation we get,

$$b = \frac{79 \times 1.6 \times 10^{-19}\ \text{C} \times 2 \times 1.6 \times 10^{-19}\ \text{C}}{8 \times 3.14 \times 8.85 \times 10^{-12}\ \text{C}^2\ \text{N}^{-1}\ \text{m}^{-2} \times 5 \times 1.6 \times 10^{-13}\ \text{J}} \cot(22.5^\circ)$$

$$= \frac{79 \times 1.6 \times 10^{-13}}{4 \times 3.14 \times 8.85 \times 5} \times 2.41\ \text{m} = 5.5 \times 10^{-14}\ \text{m}$$

Now the fraction (f) of the incident α-particles scattered by 45° or more is given in terms of the corresponding impact parameter (b) as follows :

$f = \pi b^2 nt$, (t = thickness of the foil = 10^{-6} m, n = number of atoms per unit volume)

Thus, $n = N_0\rho/A$, (N_0 = Avogadro's number, ρ = density of gold = 1.93×10^4 kg m^{-3} = 1.93×10^7 g m^{-3}, A = atomic wt. of gold = 197)

or, $$n = \frac{6.02 \times 10^{23} \times 1.93 \times 10^7}{197} = 5.90 \times 10^{28}\ \text{atoms/m}^3$$

Thus, $f = \pi b^2 nt = 3.14 \times (5.5 \times 10^{-14}\ \text{m})^2 \times 5.90 \times 10^{28}\ (\text{atoms m}^{-3}) \times 10^{-6}\ \text{m}$

$= 5.60 \times 10^{-4}$

i.e. only 0.056% of the incident particles get deflected by 45° or more.

Problem 3 : Calculate the radius of first Bohr's orbit, velocity, and the energy of the electron of He^+ in the ground state in both CGS and SI units.

Solution :

(i) In CGS system : $r_n = \frac{n^2h^2}{4\pi^2 mZe^2}$; for He^+, $Z = 2$

In the ground state, $n = 1$, thus,

$$r_1 = \frac{h^2}{4\pi^2 mZe^2} = \frac{(6.625 \times 10^{-27}\ \text{erg} \times \text{s})^2}{4 \times (3.14)^2 \times 9.1 \times 10^{-28}\ \text{g} \times 2 \times (4.8 \times 10^{-10}\ \text{esu})^2}$$

$$= 0.265 \times 10^{-8}\ \text{cm}, \left[\text{esu} = \text{g}^{1/2}\ \text{cm}^{3/2}\ \text{s}^{-1}\right]$$

Click Here t.me/thealchemylibrary

In SI system : $r_n = \dfrac{n^2h^2\varepsilon_0}{\pi me^2Z}$

i.e. $r_1 = \dfrac{(6.625\times10^{-34}\text{ J s})^2\times8.85\times10^{-12}\text{ C}^2\text{ N}^{-1}\text{ m}^{-2}}{3.14\times9.1\times10^{-31}\text{ kg}\times(1.6\times10^{-10}\text{ C})^2\times2} = 0.265\times10^{-10}\text{ m}$

(ii) From Bohr's quantum restriction, i.e. $mur_n = n(h/2\pi)$

or $u = \dfrac{nh}{2\pi mr_n}$

In the present case, $n = 1$

In CGS system, $u = \dfrac{6.625\times10^{-27}\text{ erg}\times\text{s}}{2\times3.14\times9.1\times10^{-28}\text{ g}\times0.265\times10^{-8}\text{ cm}} = 4.36\times10^{8}\text{ cm s}^{-1}$

In SI system : $u = \dfrac{6.625\times10^{-34}\text{ J s}}{2\times3.14\times9.1\times10^{-31}\text{ kg}\times0.265\times10^{-10}\text{ m}} = 4.36\times10^{6}\text{ m s}^{-1}$

(iii) In SI system : $E_n = -\dfrac{me^4Z^2}{8\varepsilon_0^2n^2h^2}$; for He^+, $Z = 2$

Thus, $E_1 = -\dfrac{9.1\times10^{-31}\text{ kg}\times(1.6\times10^{-19}\text{ C})^4\times(2)^2}{8\times(8.85\times10^{-12}\text{ C}^2\text{ N}^{-1}\text{ m}^{-2})^2\times(6.625\times10^{-34}\text{ J s})^2}$

$= -8.72\times10^{-18}\text{ J (per ion)}$

In CGS system : $E_n = -\dfrac{2\pi^2e^4mZ^2}{n^2h^2}$

or, $E_1 = -\dfrac{2\times(3.14)^2\times(4.8\times10^{-10}\text{ esu})^4\times9.1\times10^{-28}\text{ g}\times2^2}{(6.625\times10^{-27}\text{ erg}\times\text{s})^2}$

$= -8.72\times10^{-11}\text{ erg (per ion)}$

Very often, the electronic energy is expressed in electron volts (eV).

$1\text{ eV} = 1.602\times10^{-12}\text{ erg} = 1.602\times10^{-19}\text{ J}$

Thus, $E_1 = -54.4\text{ eV}$

Problem 4 : Calculate the third ionisation potential of *Li*.

Solution : The 3rd IP of *Li* leads to : $Li^{2+} \rightarrow Li^{3+} + e$. Here, Li^{2+} is a hydrogen-like system. Hence Bohr's theory can be applied.

Ionisation potential (IP) $= E_\infty - E_1 = \dfrac{Z^2e^4m}{8\varepsilon_0^2h^2}\left(\dfrac{1}{n_1^2} - \dfrac{1}{\infty}\right) = \dfrac{Z^2e^4m}{8\varepsilon_0^2h^2}\times1/1^2$

Click Here t.me/thealchemylibrary

By using the values of e, m, ε_o and h in SI unit we get :

$$\text{IP} = 21.8 \times 10^{-19}\, Z^2 \text{ Joules/ion} = 13.6\, Z^2 \text{ eV/ion, } (Z = 3 \text{ for } Li^{2+})$$

It is also very often expressed as :

$$\text{IP} = 21.8 \times 10^{-19} \times 6.023 \times 10^{23} \times 9 \text{ J/g ion} = 11817.1 \text{ kJ/g ion.}$$

Problem 5 : The wavelength of the first member (i.e. H_α) of Balmer series of hydrogen is 6563×10^{-10} m. Calculate the wavelength of its second member (i.e. H_β line).

Solution : H_α and H_β lines in Balmer series arise due to the transitions :

$n_i = 3 \longrightarrow n_f = 2$ (H_α line); and $n_i = 4 \longrightarrow n_f = 2$ (H_β line).

The expressions of the transitions are given by :

$$\left.\begin{aligned} \bar{\nu}_\alpha &= R\left(\frac{1}{2^2} - \frac{1}{3^2}\right) \text{m}^{-1}, \\ \text{and,}\quad \bar{\nu}_\beta &= R\left(\frac{1}{2^2} - \frac{1}{4^2}\right) \text{m}^{-1}, \end{aligned}\right\} \begin{aligned} &(Z = 1, \text{ and nuclear motion is not considered}) \\ &R = \text{Rydberg constant} = \frac{e^4 m}{8\varepsilon_0^2 ch^3} \end{aligned}$$

Thus, $\bar{\nu}_\alpha = \dfrac{5}{36} R \text{ m}^{-1}$, $\bar{\nu}_\beta = \dfrac{3}{16} R \text{ m}^{-1}$,

Hence, $\bar{\nu}_\alpha / \bar{\nu}_\beta = \dfrac{20}{27}$; or $\bar{\nu}_\beta = \left(\dfrac{27}{20}\right)\bar{\nu}_\alpha = \dfrac{27}{20} \times \dfrac{1}{6563 \times 10^{-10}} \text{ m}^{-1}$;

or, $1/\lambda_\beta = \dfrac{27}{20 \times 6563 \times 10^{-10}} \text{ m}^{-1}$; or, $\lambda_\beta = 4861 \times 10^{-10} \text{ m} = 486.1 \text{ nm}$

Here, λ_β stands for the wavelength of the H_β line in Balmer series.

Problem 6 : Calculate the wavelength of α and β lines in Lyman series of He^+, if the Rydberg constant is 109677 cm^{-1}.

Solution : The expression of wave number of the lines in Lyman series is given by,

$$\bar{\nu} = \frac{1}{\lambda} = RZ^2\left(\frac{1}{1^2} - \frac{1}{n^2}\right), \text{ (without considering nuclear motion)}$$

For α and β lines $n = 2$ and 3 respectively; and $Z = 2$ for He^+.

$$\frac{1}{\lambda_\alpha} = R(2)^2\left(\frac{1}{1} - \frac{1}{4}\right) = 109677 \times 4 \times \frac{3}{4} \text{ cm}^{-1};$$

or $\lambda_\alpha = 3.039 \times 10^{-6} \text{ cm} = 303.9 \times 10^{-8} \text{ cm}$

Similarly, $\dfrac{1}{\lambda_\beta} = 109677 \times 4 \times (1 - 1/9) = 109677 \times 4 \times (8/9) \text{ cm}^{-1}$;

or, $\lambda_\beta = 2.564 \times 10^{-6} \text{ cm} = 256.4 \times 10^{-8} \text{ cm}$

Click Here t.me/thealchemylibrary

Problem 7 : Compare the frequencies of the α-lines in Balmer series for hydrogen and Li^{2+}.

Solution : In hydrogen and hydrogen-like systems, the electron jumps from $n_i = 3$ to $n_f = 2$ to generate the α-line in Balmer series. The frequency (ν) of the corresponding radiation is given by:

$$\nu = \frac{me^4Z^2}{8\varepsilon_0^2h^3}\left(\frac{1}{2^2}-\frac{1}{3^2}\right) = \frac{me^4Z^2}{8\varepsilon_0^2h^3}\times\frac{5}{36};$$

$$\nu = \frac{9.1\times10^{-31}\text{ kg}\times(1.6\times10^{-19}\text{ C})^4\ Z^2}{8\times(8.85\times10^{-12}\text{ C}^2\text{ N}^{-1}\text{ m}^{-2})^2\times(6.625\times10^{-34}\text{ J s})^3}\times\frac{5}{36}$$

$$= 3.29\times10^{15}\ Z^2\times(5/36)\text{ Hz}$$

For H, $Z = 1$; and for He^+, $Z = 2$

Hence, $\nu_{(H)} = 3.29\times10^{15}\times1^2\times(5/36)\text{ Hz} = 4.56\times10^{14}\text{ Hz}$

and $\nu_{(He^+)} = 3.29\times10^{15}\times2^2\times(5/36)\text{ Hz} = 18.24\times10^{14}\text{ Hz}$

Problem 8 : Find out the energy of the electron at $n = 2$ in hydrogen atom according to Sommerfeld's model and compare with that of Bohr's model.

Solution : Energy of an electron in the n-th orbit is given by Sommerfeld's model as follows,

$$E_n = -\frac{me^4Z^2}{8\varepsilon_0^2h^2n^2} - \frac{me^4Z^2}{8\varepsilon_0^2h^2n^2}\times\frac{\alpha^2Z^2}{n}(1/k - 3/4n)$$

(where α is the fine structure constant = 1/137 and k = azimuthal quantum number = 1, 2, 3, ..., n)

By using the values of m, e, ε_0 and h, we get :

$$E_n = -\left\{\frac{13.6\ Z^2}{n^2} + 13.6\ Z^2\times\frac{\alpha^2Z^2}{n^3}(1/k - 3/4n)\right\}\text{eV}$$

In the present case $Z = 1$, and $n = 2$, and therefore, $k = 1, 2$. Fine structure constant = $\alpha = e^2/(2\varepsilon_0 ch)$ = 1/137 and it is a pure number.

Thus we ought to calculate the energy for two sets, i.e. $n = 2$, $k = 1$; and $n = 2$, $k = 2$.

$$E_{(n=2,\ k=1)} = \left\{\frac{-13.6}{4} - 13.6\times\frac{1}{(137)^2}\times\frac{1}{2^3}\left(1/1 - \frac{3}{4\times2}\right)\right\}\text{eV}$$

$$= (-3.4 - 9.05\times10^{-5}\times5/8)\text{ eV} = (-3.4 - 5.66\times10^{-5})\text{ eV}$$

and, $E_{(n=2,\ k=2)} = \{-3.4 - 9.05\times10^{-5}\ (1/2 - 3/8\}\text{ eV}$

$$= \{-3.4 - 1.13\times10^{-5}\}\text{ eV}$$

In Bohr's model, the energy is only dependent on the principal quantum number n.

Thus, $E_{(n=2)} = -\frac{me^4Z^2}{8\varepsilon_0^2n^2h^2} = -\frac{13.6}{4}Z^2\text{ eV} = -3.4\text{ eV}, (Z = 1)$

Click Here to the chemylibrary

Problem 9 : Apply sommerfeld's quantum restriction to determine the energy of a particle (a) moving in a one dimensional box, and (*b*) rotating in a plane about a fixed axis.

Solution :

(a) Let us consider: V (potential energy) = 0 (inside the box) and $V = \infty$ (outside the box), (cf. Fig. 3.5.2.1), mass of the particle = m; length of the box along the x-axis = a.
Since the potential energy within the box is constant (= 0), the momentum (p_x) is constant. The momentum (p_x) changes its sign on changing the direction of motion, i.e. p_x becomes $-p_x$ on changing the direction of the moving particle. Thus we can write :

$$\oint p_x dx = p_x \int_{x=o}^{x=a} dx + (-p_x) \int_{x=a}^{x=o} dx = ap_x - (-p_x)\, a = 2ap_x$$

According to Sommerfeld's quantum restriction,

$$\oint p_x dx = nh, \text{ i.e. } 2ap_x = nh$$

or, $$p_x = \frac{nh}{2a}$$

$$E = \frac{p_x^2}{2m} = \frac{n^2h^2}{8ma^2}, \text{ (cf. Eqn. 3.5.2.11).}$$

(b) When the particle rotates in a plane about a fixed axis, the azimuthal angle (ϕ) changes; and the angular momentum (p_ϕ) is given by :

$$p_\phi = I\left(\frac{d\phi}{dt}\right), I = \text{moment of inertia} = mr^2$$

According to Sommerfeld's quantum restriction :

$$kh = \oint p_\phi d\phi = p_\phi \oint d\phi = p_\phi \times 2\pi, (p_\phi = \text{constant})$$

i.e. $$p_\phi = \frac{kh}{2\pi}, \text{ and } E = \frac{p_\phi^2}{2I} = \frac{k^2h^2}{8\pi^2 I}$$

Problem 10 : Calculate the atomic number of an element which shows the K_α and L_α absorption edges at wavelength 0.138 nm and 1.3288 nm respectively. (Given : b = 1 for K_α and b = 7.4 for L_α-line).

Solution : Application of Bohr's theory in Moseley's experiment yields the following result.

$$\frac{1}{\lambda} = \frac{\nu}{c} = \frac{me^4 (Z-b)^2}{8\varepsilon_0^2 ch^3}\left(\frac{1}{n_f^2} - \frac{1}{n_i^2}\right) = R_H (Z-b)^2 \left(\frac{1}{n_f^2} - \frac{1}{n_i^2}\right), \text{ (cf. Sec. 1.8.7)}$$

For, K_α line, n_f = 1, n_i = 2; and for L_α line, n_f = 2 and n_i = 3).

K_α line : $$\frac{1}{\lambda_1} = R_H (Z-b)^2 \left(\frac{1}{1^2} - \frac{1}{2^2}\right) = R_H (Z-1)^2 \times \frac{3}{4}$$

Click Here t.me/thealchemylibrary

$$L_\alpha \text{ line : } \frac{1}{\lambda_2} = R_H\,(Z-b)^2\left(\frac{1}{2^2}-\frac{1}{3^2}\right) = R_H\,(Z-7.4)^2 \times \frac{5}{36}$$

Thus we have :

$$\frac{\lambda_2}{\lambda_1} = \left(\frac{36}{5}\right)\left\{\frac{(Z-1)^2}{(Z-7.4)^2}\right\}\left(\frac{3}{4}\right) = \left(\frac{27}{5}\right)\frac{(Z-1)^2}{(Z-7.4)^2}$$

or, $$\frac{(Z-1)^2}{(Z-7.4)^2} = \frac{5\lambda_2}{27\lambda_1} = \frac{5}{27}\left(\frac{1.3288}{0.138}\right) = 1.78$$

or, $$\frac{Z-1}{Z-7.4} = 1.335 \text{ or, } Z = 27.0$$

Atomic number of the sample = 27.0, i.e. the element is cobalt (Co).

Problem 11 : An α-particle ($u = 2 \times 10^9$ cm s^{-1}) approaches towards *Zn*-nucleus. From this experiment, estimate the approximate radius of *Zn*-nucleus.

Solution : At the closest distance between the approaching α-particle and *Zn*-nucleus, the kinetic energy of the α-particle will be balanced by the Coulombic potential energy of repulsion,

i.e. $$\frac{1}{2}mu^2 = \frac{(Ze)(q)}{r_{\min}},\ (Z = 30 \text{ for } Zn,\ q = 2e \text{ for } \alpha\text{-particle})$$

m = mass of an α-particle = $4 \times 1838 \times 9 \times 10^{-28}$ g

or, $$r_{\min} = \frac{2(Ze)\,q}{mu^2} = \frac{2 \times 30 \times 2 \times (4.8 \times 10^{-10} \text{ esu})^2}{4 \times 1838 \times 9 \times 10^{-28} \text{ g} \times (2 \times 10^9 \text{ cm s}^{-1})^2} \approx 9 \times 10^{-13} \text{ cm}$$

$$\left[(\text{esu})^2 = \text{dyne} \times \text{cm}^2 = \text{g} \times \text{cm} \times \text{s}^{-2} \times \text{cm}^2\right]$$

The radius of the target nucleus cannot be greater than $r_{\min}$. Thus the maximum possible value of radius of the nucleus is 9×10^{-13} cm.

Problem 12 : The first IP value of rubidium is 96.4 kcal mol^{-1}. Calculate the minimum frequency of light that can cause photoionisation of rubidium.

Solution : We have the condition : $Nh\nu_{\min} = 96.4$ kcal $= 96.4 \times 4.2 \times 10^{10}$ erg.

$$\nu_{\min} = \frac{96.4 \times 4.2 \times 10^{10} \text{ erg}}{6.02 \times 10^{23} \times 6.627 \times 10^{-27} \text{ erg s}} \approx 10^{15} \text{ cycle/s}$$

Problem 13 : The first IP value of a hydrogen atom is 21.8×10^{-19} J. Calculate the IP value when the electron resides at the 2*s* level.

Solution : $$\text{IP} = \frac{Z^2e^4m}{8\varepsilon_0^2h^2}\left\{\frac{1}{n^2}-\frac{1}{\infty}\right\} = \frac{Z^2e^4m}{8\varepsilon_0^2h^2} = 21.8 \times 10^{-19} \text{ J},\ (n = 1)$$

(for hydrogen, the electron resides at 1*s* level)

Click Here t.me/theolchemylibrary

$$\text{IP (for the electron at } 2s) = \frac{Z^2e^4m}{8\varepsilon_0^2h^2}\left\{\frac{1}{2^2}-\frac{1}{\infty}\right\} = \frac{21.8\times10^{-19}}{4}\text{ J} = 5.45\times10^{-19}\text{ J}$$

$(Z = 1 \text{ for } H)$; $(n = 2)$

Problem 14 **:** Calculate the velocity of the H-electron at the 2nd Bohr orbit. (Given : $a_0 = 0.53$ Å)

Solution **:** $mur_n = n\left(\frac{h}{2\pi}\right)$; $r_n = \frac{n^2h^2}{(4\pi^2me^2)} = n^2a_0$, (expressions in CGS units)

$$u = n\left(\frac{h}{2\pi}\right)\left(\frac{1}{mr_n}\right) = n\left(\frac{h}{2\pi}\right)\left(\frac{1}{mn^2a_0}\right) = \frac{6.623\times10^{-27}\text{ erg s}}{2\times3.14\times9.1\times10^{-28}\text{ g}\times2\times0.53\times10^{-8}\text{ cm}}$$

$$= 1.1\times10^8\text{ cm s}^{-1}$$

$(n = 2)$

i.e. velocity of the H-electron at $n = 2$ is 1.1×10^8 cm s^{-1}.

Problem 15 **:** The 1st IP values of helium and lithium are 24.5 eV and 5.4 eV respectively. Calculate the Z^* value and screening constant for the outermost electron in He and Li atom.

Solution **:** The electronic configurations of He and Li are :

$$1s^2\ (He) \text{ and } 1s^22s^1(Li)$$

The IP value in a polyelectronic system can be given as follows :

$$\text{IP} = \frac{13.6(Z^*)^2}{n^2}\text{ eV per atom}$$

For helium, $n = 1$ and $\text{IP} = 24.5 = \frac{13.6(Z^*)^2}{1^2}$

i.e. $Z^* = 1.34$

Thus the screening constant for $1s$ electron is $He = 2 - 1.34 = 0.66$. This screening is done by the other $1s$ electron.

For lithium, $n = 2$ and $\text{IP} = 5.4 = \frac{13.6(Z^*)^2}{2^2}$

i.e. $Z^* = 1.26$

Thus the screening done by the $1s^2$ electrons $= 3 - 1.26 = 1.74$

Note **:** From Slater's rule, for the He-atom, $Z^* = 2 - 0.30 = 1.70$ which is higher than the value obtained from the ionisation potential value. For Li-atom, it leads to : $Z^* = 3 - 2\times0.85 = 1.30$ which is close to the value obtained from the ionisation potential value.

Problem 16 **:** Compute the difference in wavelength for transition, $n = 1$ to n 2 in H and D. (Given: $m_H = 1.673\times10^{-27}$ kg, $m_D = 3.344\times10^{-27}$ kg, $R_H = 109679$ cm^{-1}).

Solution **:** For $\bar{\nu}(H) = R_H\left(\frac{1}{1^2}-\frac{1}{2^2}\right) = 109679\left(\frac{3}{4}\right)\text{cm}^{-1}$

$$= 82259\text{ cm}^{-1}$$

Click Here t.me/thealchemylibrary

$$\lambda(H) = \frac{1}{\bar{\nu}(H)} = \frac{1}{82259}\ \text{cm}$$

$$= 1.2157 \times 10^{-5}\ \text{cm}$$

$$= 1.2157 \times 10^{-7}\ \text{m} = 121.57\ \text{nm}$$

$$\frac{R(D)}{R(H)} = \frac{1 + \frac{m_e}{m_H}}{1 + \frac{m_e}{m_D}} = \left(1 + \frac{9.109 \times 10^{-31}\ \text{kg}}{1.673 \times 10^{-27}\ \text{kg}}\right)\left(1 + \frac{9.109 \times 10^{-31}\ \text{kg}}{3.344 \times 10^{-27}\ \text{kg}}\right)^{-1}$$

$$= \frac{1 + 5.444 \times 10^{-4}}{1 + 2.724 \times 10^{-4}} = 1.0003$$

$$R(D) = R(H) \times 1.0003 = 109679 \times 1.0003 = 109712$$

For D : $\bar{\nu}(D) = R_D\left(\frac{1}{1^2} - \frac{1}{2^2}\right) = 109712 \times \frac{3}{4}\ \text{cm}^{-1}$

$$= 82284\ \text{cm}^{-1}$$

$$\lambda(D) = \frac{1}{\bar{\nu}(D)} = \frac{1}{82284}\ \text{cm} = 1.2153 \times 10^{-5}\ \text{cm}$$

$$= 1.2153 \times 10^{-7}\ \text{m}$$

$$= 121.53\ \text{nm}$$

$$\lambda(H) - \lambda(D) = (121.57 - 121.53)\ \text{nm} = 0.04\ \text{nm}.$$

EXERCISE-I

A. General Questions

1. Discuss the working principle involved in the determination of *e/m* of an electron in Thomson's method. Mention the drawbacks of this method.
2. Develop the relation required to determine the charge of an electron in Millikan's oil drop experiment.
3. Discuss the Thomson's analysis of positive rays by parabola method to detect the isotopes.
4. Describe the basic principle of Aston's mass spectrograph.
5. Discuss the basic features of the Ritz combination principle. How does it accommodate the Balmer formula and Rydberg formula?
6. What are the major drawbacks in Thomson's plum-pudding model of the atoms ?
7. Discuss the theory behind the α-particle scattering on gold foil.
8. How did Rutherford develop his nuclear model of atom from the observations of α-particle scattering on gold foil? Discuss its major limitations.

Click Here t.me/healchemylibrary

9. How do we get the quantitative idea of nuclear dimension from the Rutherford's α-particle scattering experiment ?
10. By considering the basic postulates of Bohr's theory, develop the mathematical expressions for Rydberg constant (R) and wave number ($\bar{\nu}$) for the spectral transitions.
11. How does the concept of nuclear motion correct the Rydberg constant? What are the experimental evidences to support this correction ?
12. How do we support the Moseley's observations from the Bohr's theory? Mention the importance of Moseley's experiment.
13. Bohr's correspondence principle indicates that the principle of quantum physics in macroscopic world leads to the same result as expected from the classical physics. Justify the statement mathematically.
14. Discuss the features of critical potentials, elastic and inelastic collisions in connection with the Franck-Hertz experiment. How does the Bohr's theory explain the observations of Franck-Hertz experiment?
15. Give an expression of energy of an electron in Sommerfeld's elliptic orbit under the required quantum restrictions. How does the relativistic correction explain the origin of fine spectra? What is the fine structure constant (α)?
16. How does the Sommerfeld's azimuthal quantum number explain the shape, size and the relative penetrating power of the sublevels (i.e. orbits)? How does the model explain the phenomenon – *quantum defect*?
17. Discuss the different quantum numbers associated with an electron in the vector model. Define all the electrons in the lithium atom in terms of different quantum numbers.
18. Mention the basic principle of Russel-Saunders coupling scheme. Illustrate the principle for the p^2 and p^3 electronic configurations.
19. What are the possible Russell-Saunders terms for np^2, $np^1(n+1)p^1$, $(n-1)d^1np^1$ and nd^2 configurations?
20. Compute the possible values of J for : (i) $L = 2$, $S = 3/2$; (ii) $L = 3$, $S = 1$
21. Discuss the Hund's rule to determine the ground state term. Draw the energy diagrams of the different states developed from the d^2 and p^2-configurations. Illustrate the Lande interval rule in splitting the energy states arising from the p^2- and d^2-configurations.
22. (a) Deduce the ground state terms for the electronic configurations,
    d^2, d^7, d^9, d^3, d^8, f^4, f^{10}, f^5 and f^7.
    Show the validity of the hole-formalism rule from the above configurations.
    (b) Determine the ground state term symbols of the following ions:
    Ti^{3+}, Mn^{2+}, Ni^{2+}, Cu^{2+}, Pt^{2+}, Gd^{3+}.
23. What are the selection and intensity rules for the spectral transitions in the vector model?
24. Describe the fine structure of the spectral lines in hydrogen and alkali metals in the light of vector model.
25. Find out the magnetic moment of an electron due to its both orbital and spinning motion.
26. Discuss the Stern-Gerlach experiment and its importance to support the vector model.

Click Here t.me/thealchemylibrary

27. Define the Larmor frequency. How does this Larmor precession explain the normal Zeeman effect?
28. What is Lande *g* factor? How does this concept help us to explain the anomalous Zeeman effect (by taking the case of sodium D_1 and D_2 lines)?
29. Prove that for the principal quantum number *n*, the maximum capacity to accommodate the electrons is $2n^2$.
30. How do the Pauli exclusion principle, aufbau principle and Hund's rule of spin multiplicity develop the scheme for electronic configuration in polyelectronic systems? What do you mean by Pauli force?
31. Discuss the physical significance of exchange energy. How does it help to understand the enhanced stability in half-filled and full-filled orbitals?
32. Write notes on :

    (a) Cathode rays, (b) Anode or canal rays, (c) Neutron, (d) Ritz combination principle, (e) Limitations of Bohr's theory, (f) Sommerfeld's relativistic correction, (g) Zeeman effects, (h) Hyperfine structure of spectral lines, (i) Hund's rule, (j) *Aufbau* principle, (k) Rydberg constant and nuclear motion, (l) Lande interval rule, (m) Quantum defect and penetrating power of the orbits, (n) Sommerfeld's fine structure constant, (o) Selection and intensity rules in spectral transition, (p) Larmor precession and magnetic quantum numbers, (q) $(n + l)$ rule, (r) Exchange energy, (s) Atomic units of mass, length and energy, (t) Pauli force, (u) Bohr magneton, (v) Gyromagnetic ratio, (w) Magnetic moment of an atom, (x) Lande *g* factor, (y) μ_J, μ_{L+S}, $\mu_{spin\text{-}only}$, (xi) Multiplet width, (xii) Hole-formalism rule.

B. Justify the Following Statements

1. The electron is a fundamental particle of matter.
2. The value of *e/m* determined in Thomson's method depends on the electrical potential difference applied.
3. In Millikan's oil drop experiment, the upward velocity of an oil drop under an electrical potential varies in different observations. The minimum difference of the upward velocity obtained from different sets of observation gives the measure of an electronic charge.
4. Though the neutron is a neutral particle, it orients just like a tiny magnet in the external magnetic field.
5. Rydberg's formula for the spectral lines is also in agreement with the Ritz combination principle.
6. Thomson's plum-pudding model of atom cannot explain the scattering of α-particles by a large angle.
7. Rutherford's α-particle scattering formula is only applicable for the very thin foils of heavy elements.
8. Idea of nuclear dimension can be obtained from the α-particle scattering experiment.
9. The fundamental demand of Earnshaw's classical theorem is the cause of instability of Thomson's plum pudding model.
10. Though the fundamental demand of Earnshaw's classical theorem is satisfied in Rutherford's model, the demand of electromagnetic theory makes the system unstable.

Click Here to meet the Academy library

11. Continuous spectrum instead of the observed discontinuous line spectra is predicted from the Rutherford's model.
12. Ignoring the demand of classical electromagnetic theory and an introduction of the concept of stationary orbit provide the foundation of Bohr's model.
13. Spectral positions for different isotopes are not identical. The isotopic shift of the spectral lines provides the experimental support of nuclear motion in Bohr's model.
14. The finer spectra of the spectral lines cannot be explained from Bohr's theory.
15. Moseley's empirical law gets a sound theoretical basis from the Bohr's atomic model.
16. Observations of Franck-Hertz experiment are in conformity with the Bohr's model.
17. For the very high values of n (≈ 1000), Bohr's theory runs with the demand of classical physics.
18. Inelastic collisions occur in Franck-Hertz experiment only at certain potential gradients.
19. The magneto-optic phenomena (i.e. Zeeman effects) and electro-optic phenomenon (i.e. Stark effect) are not in agreement with the Bohr's theory.
20. In Sommerfeld's model, two quantum restrictions for the stationary orbits are required while in Bohr's model only one restriction is sufficient.
21. In Sommerfeld's model, the azimuthal quantum number can never take the zero value.
22. In Sommerfeld's model, the electronic orbit is in fact a rosette.
23. For a particular transition (say, $n = 3 \rightarrow n = 2$), different possible ways are available in Sommerfeld's model while in Bohr's model it gives only a single way.
24. Though Sommerfeld's first modification cannot explain the finer spectra, the second modification (i.e. relativistic correction) can explain the finer spectra, at least, semiquantitatively.
25. The number of components in the finer spectra does not run with the Sommerfeld's model.
26. Sommerfeld's azimuthal quantum number gives the measure of ellipticity of the orbits and consequently the penetrating power of the orbits.
27. The quantum defect can be nicely explained by considering the Sommerfeld's model.
28. The demand of uncertainty principle strikes apparently at the root of Bohr-Sommerfeld model.
29. Concept of spatial quantisation is required to explain the magneto-optic phenomena (i.e., Zeeman effects).
30. Concept of spinning electron is required to explain the doublet sodium D line.
31. Stern-Gerlach experiment not only supports the concept of spinning electron but also it supports its nonintegral value, $s = 1/2$.
32. The fine structure of the spectra for the lighter elements results into the multiplet structure for the heavier elements.
33. The H_α-line (Balmer series) consists of five fine lines while the sodium D line is doublet.
34. Due to the unavoidable Doppler effect, sometimes, the theoretically predicted number of components in fine structure of atomic spectra does not agree with the experimentally observed one.
35. Existence of hyperfine structure of atomic spectra supports the nuclear spin.

Click Here t.me/thealchemylibrary

36. The beam of *H* or *Ag* or *Au* atoms splits into two branches in Stern-Gerlach experiment while the beam of magnesium atoms does not split.
37. In Stern-Gerlach experiment, an inhomogeneous magnetic field rather than the homogeneous one is applied.
38. The anomalous Zeeman effect occurs frequently while the normal Zeeman effect is a rare phenomenon.
39. The normal Zeeman effect always produces three equidistant lines.
40. In anomalous Zeeman effect, the sodium D_2 line produces six components while the D_1 line gives four components.
41. Pauli exclusion principle gives the measure of maximum capacity of an orbit to accommodate the electrons.
42. Though the $(n + l)$ rule to determine the energy order of different sublevels is highly useful, it is not maintained in all cases.
43. The extra stability of the half-filled and full-filled orbitals arises mainly due to the exchange energy which is a quantum mechanical phenomenon.
44. For the heavy elements, all the orbitals of a particular shell tend to be energetically degenerate.
45. Though in hydrogen-like systems, the $3s$, $3p$ and $3d$ orbitals are having identical energies, in chlorine they are in the sequence, $3d > 3p > 3s$.
46. In the transition series, though the *ns* level is filled in before the $(n - 1)d$ levels, during ionisation the *ns* electrons are lost first.
47. The valence shell electronic configuration of *Cr* and *W* are different thought they are the congeners.
48. Stern-Gerlach experiment can support the values : $s = \frac{1}{2}$ and the lowest possible value of l as zero.

C. Numerical Problems

1. A 5 MeV alpha particle is scattered by an angle of 10° when it approaches a gold (Z = 79) nucleus. Calculate the impact parameter.
   (Ans. 2.6×10^{-13} m).
2. What fraction of a beam of 7.5 MeV alpha particles incident upon a gold (Z = 79) foil of 3×10^{-5} cm thick is scattered by 90° or more? (density of gold = 1.92×10^4 kg m^{-3}).
   (Ans. $f = 1.27 \times 10^{-5}$).
3. By what factor does the velocity of (u) an electron in hydrogen atom change when it is excited from the first to the third orbit?
   (Ans. $u_3/u_1 = 1/3$)
4. A spectral line in the Lyman series for hydrogen atom has wavelength 1216.5 Å. What transition is responsible for this radiation?
   (Ans. $n_i = 2 \rightarrow n_f = 1$)
5. The two excited states of hydrogen atom are having energy 12.0 eV. and 10.2 eV. Calculate the wavelength of the radiation produced by the transition between these two levels.
   (Ans. 6.9×10^{-7} m)

Click Here t.me/thealchemylibrary

6. Calculate the frequency and wave number of the radiation produced due to the transition of the electron from the third orbit to the second orbit in hydrogen atom.
   (Ans. $\nu = 4.5 \times 10^{14}$ Hz, $\bar{\nu} = 1.52 \times 10^{6}$ m^{-1})
7. Calculate the energy required to ionise a hydrogen atom when the electron is residing in the third orbit.
   (Ans. 1.50 eV).
8. Calculate the isotopic shift in terms of wavelength for the α lines of ^{1}H and ^{3}H in the Balmer series.
   (Ans. 2.37 Å).
9. Verify the Bohr's correspondence principle in hydrogen atoms for the transition, $n_i = 10001 \rightarrow n_f = 1000$.
10. Calculate the first and second resonance potentials for hydrogen atoms.
    (Ans. 10.21 eV, 12.10 eV)
11. In Franck-Hertz experiment, for the mercury vapour, the Ist critical potential occurs at 4.9 volts. Find out the wavelength of the corresponding radiation.
    (Ans. 2530 Å)
12. Find out the energy difference of the electron in the ground state of hydrogen in terms of Sommerfeld's model and Bohr's model. Given, fine structure constant (α) = 1/137 .
    (Ans. 2.9×10^{-23} J).
13. Calculate the wavelength of the H_β and H_γ lines in the Balmer series.
    (Ans. 4862 Å, 4341 Å).
14. Energy of an electron in the *n-th* Bohr orbit is expressed by A/n^2 where $A = 2.18 \times 10^{-18}$ J. Calculate the frequency and wave number of the radiation when the electron jumps from the 3rd orbit to the 2nd orbit.
    (Ans. 4.5×10^{14} Hz, $\bar{\nu} = 1.52 \times 10^{6}$ m^{-1}).
15. Calculate the values of the largest and the smallest wavelengths found in the Paschen series of hydrogen atoms.
    (Hints : for the smallest wavelength, the transition occurs from,
    $n = \infty \rightarrow n = 3$ while for the largest wavelength, $n = 4 \rightarrow n = 3$
16. Find out all the possible J values for (i) $L = 6$, $S = 3/2$; (ii) $L = 5$, $S = 5/2$.
17. Calculate the Russel-Saunders terms for the s^1-p^1, p^1-d^1, p^1-p^1, s^1-p^1-d^1, electronic configurations.
18. Show 1 M_B or 1 $\mu_B = 9.27 \times 10^{-21}$ erg G^{-1} or 9.27×10^{24} J T^{-1}.
19. Find the Gyromagnetic ratio (γ) for orbital motion and spinning motion of an electron.
    (Ans. $\gamma_l = 8.8 \times 10^{10}$ C kg^{-1}; $\gamma_s = 2\,\gamma_l$).
20. Define μ_N (nuclear magneton) and show $\mu_B = 1837\,\mu_N$.
21. Show : $\mu_{\text{spin only}} = \sqrt{n(n+2)}$ B.M.
22. Show : $\mu = 2.83\sqrt{\chi_M T}$ B.M.

Click Here t.me/thealchemylibrary

2

Origin of the Quantum Theory

2.1 INTRODUCTION

Newton's corpuscular theory of light (1675) was believed to be true for more than one hundred years, but to explain the phenomena of polarisation, diffraction, interference (i.e. Newtons' rings) along with the reflection and refraction of light, the wave theory appeared to be more useful at the beginning of the nineteenth century. As a matter of fact, no explanation in *corpuscular theory* was available to rationalise the interference. Though, Thomas Young was the pioneer in developing the wave theory, the name of Huygens is worth recalling in this connection. He proposed this concept much earlier but it could not survive at that time in vigour by the side of Newton's corpuscular theory. Here, Maxwell's contribution is also noteworthy. From the theoretical background, he established that light is an electromagnetic radiation and it consists of two transverse vibrations produced from the combination of electric and magnetic fields perpendicular to each other. The validity of this wave theory was supported from different observed phenomena almost throughout the nineteenth century.

But in the last two decades of the nineteenth century, a number of experimental observations were reported which did not have any explanation in the classical theory. These are the energy distribution in black body radiations, photoelectric effect, variation of heat capacity of solids with temperature, atomic spectral lines, etc. To explain these phenomena, Max Planck (1900) was the first one to introduce the concept of *Quantum Theory* based on the ***quantum nature of energy***, i.e. ***discrete energy packets.*** This new mechanics which contradicted the ***continuous nature of energy*** paved the new way in all directions of physics and chemistry.

Click Here to the Chemylibrary

2.2 NATURE OF BLACK-BODY RADIATIONS

A substance in a hot condition emits energy in the form of electromagnetic radiation which *depends on the temperature and nature of the substance*. It has been already discussed that the excited gases (in atomic state) produce **discrete line spectra.** On the other hand, the dense bodies such as solids produce

continuous spectra covering all the frequencies, at least in a certain range. Probably in solids, due to the closed packed situation of the atoms, their mutual interactions generate adjacent energy states which are almost indistinguishable separately and consequently, **a continuous energy band rather than the isolated discrete energy states is formed.** In isolated atoms, discrete energy states are produced.

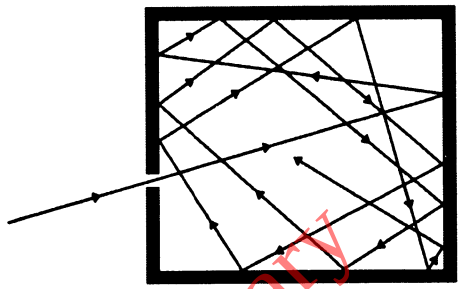

Fig. 2.2.1. An artificial black body.

For solids, at the low temperature, the emission spectrum mainly covers the low energy region, i.e. infrared region, but at the elevated temperature, the spectrum widens towards the high energy region. Here we can recall the behaviour of an iron rod. When it is being heated, it passes as : dull red → bright orange red → white hot. This distribution pattern of wavelength in the continuous spectrum is different at different temperatures for a particular solid substance; and it may also vary for different substances even at a particular temperature. ***But all black-bodies behave identically at a particular temperature. A black-body is a substance which absorbs completely all the radiations incident on it, regardless of frequency. Conversely, it emits radiations of all wavelengths possible.***

A black-body can be artificially fabricated in the laboratory by making a very small hole on the wall of an isothermal hollow body (Fig. 2.2.1). Any radiation penetrating through the hole will get trapped by repeated reflection back and forth until it is absorbed fully and thus it is heated to a higher temperature. The walls of the cavity thus constantly emit and absorb radiations. The radiation emerging through the hole of the cavity is called ***black-body radiation.*** In this black-body radiation, the distribution pattern of the wavelength is independent on the nature of the material, shape and size of the cavity. This is why, a black-body is an idealised radiator.

The spectral distribution pattern of the black-body radiation was extensively studied by Lummer and Pringsheim (1877-1900) at different temperatures. The energy E_λ corresponding to each range of wavelength λ was measured and E_λ was plotted against the wavelength (Fig. 2.2.2) where $T_1 > T_2 > T_3$. It is evident that as the temperature of the radiator increases, the peak of the curve shifts to the lower wavelength. Here $E_\lambda d\lambda$ gives the rate of emission of energy per unit area per unit time in the wavelength region λ and $\lambda + d\lambda$. Thus the total energy E per unit area and per unit time is given by the area covered by the curve. Thus it is given by :

$$E = \int_0^\infty E_\lambda d\lambda \qquad \ldots(2.2.1)$$

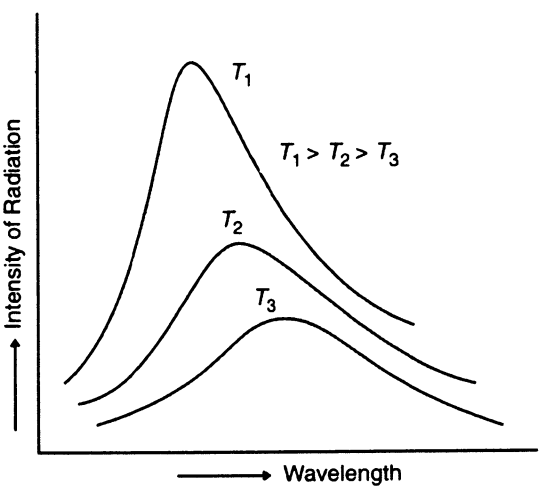

Fig. 2.2.2. Trends of variation of intensity of black-body radiation with the wavelength at different temperatures.

Click Here t.me/theallenmylibrary

2.3 DIFFERENT LAWS AND THEORIES OF BLACK-BODY RADIATIONS

2.3.1 The Stefan-Boltzmann Law

This law was experimentally formulated by Stefan in 1879 and it was theoretically established by Boltzmann in 1884 by considering the thermodynamic principles. The law states that *the intensity of the total radiation (i.e. the area covered by the curve) is proportional to the fourth power of its absolute temperature, i.e.*

$$\boxed{E \propto T^4; \text{ or, } E = \sigma T^4} \qquad \ldots(2.3.1.1)$$

where σ is called Stefan's constant. Its value is given by 5.67×10^{-5} erg s^{-1} cm^{-2} K^{-4} or 5.67×10^{-8} J m^{-2} s^{-1} K^{-4}.

2.3.2 Wien's Law

It states that the *wavelength of maximum intensity* (λ_{max}) *is inversely proportional to the absolute temperature T.* Thus,

$$\boxed{T \times \lambda_{max} = \text{constant} = 2.8 \times 10^{-3} \text{ m K}} \qquad \ldots(2.3.2.1)$$

Actually this appears as a special case of Wien's displacement law established from purely thermodynamic reasonings. It is given as,

$$E_\lambda d\lambda = A\lambda^{-5} \exp\left(-\frac{B}{\lambda T}\right) d\lambda \qquad \ldots(2.3.2.2)$$

where A and B are constants. This relation holds good in the lower range of the wavelength of the Lummer-Pringsheim curve but gets significantly deviated when applied to the range of longer wavelength.

2.3.3 Rayleigh-Jeans Law

The British scientists Rayleigh and Jeans developed a relation between E_λ and λ by considering the classical ***law of equipartition of energy*** to the oscillators of the black-body. It was assumed that the stationary waves of all frequencies are emitted from the black-body due to the different possible modes of vibration within the hollow cavity of the black-body. It can be shown from the classical physics that the number of modes of vibration (dn) per unit volume in the wavelength range λ and $\lambda + d\lambda$ is given by :

$$dn = (8\pi/\lambda^4)d\lambda \qquad \ldots(2.3.3.1)$$

Now, according to the principle of equipartition of energy, every mode of vibration possesses the average energy kT where k is **Boltzmann constant.** Thus the radiation energy density in that wavelength region is given by :

$$E_\lambda d\lambda = (dn)kT = 8\pi kT\lambda^{-4}d\lambda \qquad \ldots(2.3.3.2)$$

Hence,
$$E_\lambda = (8\pi kT)/\lambda^4 \qquad \ldots(2.3.3.3)$$

This is Rayleigh-Jeans law. The relation works well with the experimental observation in the longer wavelength region, but it fails for the shorter wavelength region. Moreover, the total energy (per second) carried by all the wavelengths given by $\int_0^\infty 8\pi kT\lambda^{-4}d\lambda$ becomes infinite at all temperatures,

Click here t.me/thealchemylibrary

except when $T = 0$. But this is an absurd result. In other words, as the frequency increases (i.e. the wavelength decreases) the energy density increases without showing any break or maximum and it tends to infinity at a finite temperature. This phenomenon is referred to as ***ultraviolet catastrophe*** which in fact offered nothing but a terrible jolt to the pillars of the classical physics.

2.3.4 Planck's Quantum Theory

It has been noted above that Wien's displacement law runs well with the experiment in the shorter wavelength region while the Rayleigh-Jeans law appears to be approximately correct in the limit of longer wavelength region but when extrapolated to the shorter wavelength region, it does not work. Moreover, it leads to the absurd phenomenon, ***ultraviolet catastrophe.*** In view of these facts, by considering some empirical conditions, Max Planck, a German physicist established in 1907 an intermediate expression from which the above two limiting laws could be reduced in the proper range of λ.

In developing the theory, Planck made a revolutionary proposition (discarding the classical concept) that an oscillator emits or takes up energy *not in a continuous manner* and proposed that the energy changes must occur *in discrete amounts in a discontinuous manner*. Thus the radiation can only be absorbed or emitted in quanta of energy $h\nu$, where h is a constant known as *Planck constant* and ν is the frequency of the radiation. The basic assumptions behind the theory are as follows:

i. The energy of an oscillator cannot have any amount of energy, i.e., **its energy cannot vary continuously.** Hence, it can have only certain definite amount of energies which can be expressed by the integral multiples of some minimum amount of energy ε, i.e. $E_n = n\varepsilon$ where n is an integer.

ii. The oscillator cannot have any arbitrary value of ν. It vibrates at only certain frequencies, so that it can radiate energy in quanta of magnitude $h\nu$ where h is a fundamental constant known as Planck constant to tribute its discoverer. Thus, this concept, i.e. $\varepsilon = h\nu$ and $E_n = n\varepsilon$, in fact introduces the concept of ***atomicity in the realm of energy.*** These assumptions lead to $E_n = n\varepsilon = nh\nu$. The Planck constant has the dimension of *energy* × *time* and it is given by 6.625×10^{-27} erg sec (in CGS system) or 6.625×10^{-34} joule sec (in SI system).

By considering the above basic postulates, the relation explaining the black-body radiation can be deduced as follows. Now let us consider the black-body radiator having oscillators with energies, $E_0 = 0(h\nu)$, $E_1 = 1(h\nu)$, $E_2 = 2(h\nu)$, $E_3 = 3(h\nu)$, ..., $E_s = s(h\nu)$... in the equilibrium state in the enclosure. Let there be n_0 oscillators with zero energy; similarly n_1, n_2, n_3,..... be the numbers of oscillators having energies E_1, E_2, E_3... respectively. According to the Boltzmann law, the number of oscillators at temperature T in each group is given by :

$$n_s = N_0 \exp(-sx), \ (s = 0, 1, 2, 3, ...) \qquad ...(2.3.4.1)$$

where N_0 is a constant, and $x = \varepsilon/kT = h\nu/kT$. Hence the total number of oscillators is given by :

$$N = \sum_i n_i = n_0 + n_1 + n_2 + n_3 + n_4 + ... + n_s + ... \qquad ...(2.3.4.2)$$

$$= N_0 + N_0 \exp(-x) + N_0 \exp(-2x) + N_0 \exp(-3x) + ... + N_0 \exp(-sx) + ...$$

$$= N_0 (1 + y + y^2 + ...); [y = \exp(-x) = \exp(-h\nu/kT), \text{say}]$$

$$= N_0 \left(\frac{1}{1-y}\right)$$

Click Here t.me/thealchemylibrary

[since, $(1-y)^{-1} = (1 + y + y^2 + ...)$

The total energy (E) of all the oscillators is given by : $E = \sum_i n_i E_i$

where, $E_i = i(h\nu)$

Thus, $E = 0 \times n_0 + n_1E_1 + n_2E_2 + ... + n_sE_s + ... = 0 + (h\nu)N_0 \exp(-h\nu/kT) +$

$2(h\nu)N_0 \exp(-2h\nu/kT) + ... + s(h\nu)N_0 \exp(-sh\nu/kT) + ...$

$= N_0(h\nu)(y + 2y^2 + 3y^3 + ... + sy^s + ...)$

$= N_0(h\nu)y(1 + 2y + 3y^2 + 4y^3 + ...)$

$= N_0(h\nu)y\,[1/(1-y)^2]$ ...(2.3.4.3)

The value of the series within the bracket is given by $1/(1-y)^2$. It is evaluated as follows :

$$(1 + 2y + 3y^2 + 4y^3 + ...) = \frac{d}{dy}(1 + y + y^2 + y^3 + ...) = \frac{d}{dy}\left(\frac{1}{1-y}\right) = 1/(1-y)^2$$

Thus the average energy ($\overline{E}$) per oscillator is given by :

$$\overline{E} = \left(\sum_i n_i E_i\right) / \sum_i n_i = E/N = h\nu\left(\frac{y}{1-y}\right), \text{ (by using Eqns. 2.3.4.2 and 2.3.4.3).}$$

$$\boxed{\overline{E} = h\nu\left[\frac{\exp(-h\nu/kT)}{1-\exp(-h\nu/kT)}\right] = \frac{h\nu}{\exp(h\nu/kT) - 1}} \quad ...(2.3.4.4)$$

obtained by dividing both denominator and numerator by $\exp(-h\nu/kT)$.

Note : When $h\nu < kT$ i.e. $h\nu/kT < 1$, $\exp(h\nu/kT) \approx 1 + h\nu/kT$. It leads to $\overline{E} \approx kT$ which is the classical value. ***Thus quantum theory reduces to classical theory when the temperature is very high or quatana are very small to satisfy the condition*** $h\nu/kT < 1$.

It is already discussed that the number of modes of vibration in the wavelength range λ and $\lambda + d\lambda$ per unit volume is given by : $dn = (8\pi/\lambda^4)d\lambda$. Hence, the energy density in the range λ and $\lambda + d\lambda$ is given by :

$$E_\lambda d\lambda = dn \times (\overline{E}) = (8\pi/\lambda^4)\left[\frac{h\nu}{\exp(h\nu/kT) - 1}\right] d\lambda$$

$$= \frac{8\pi hc}{\lambda^5}\left[\frac{1}{\exp(hc/\lambda kT) - 1}\right] d\lambda \quad ...(2.3.4.5)$$

$$\boxed{E_\lambda = (8\pi hc/\lambda^5) \times \left[\frac{1}{\exp(hc/\lambda kT) - 1}\right]} \quad ...(2.3.4.6)$$

The above Eqns. now satisfactorily hold good to explain the results of Lummer and Pringsheim (Fig. 2.3.4.1). From the Planck's relation, all the laws discussed earlier can be obtained by imposing the proper condition.

Click Here : me/thealchemylibrary

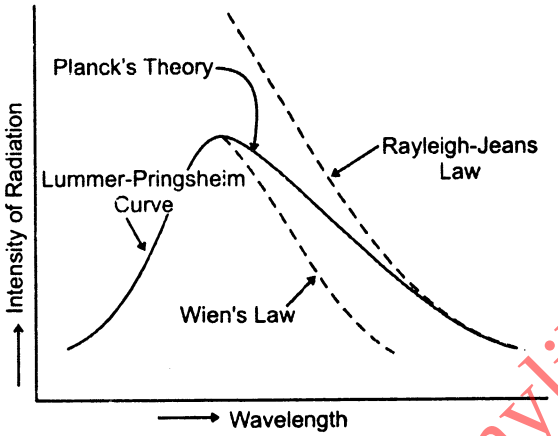

Fig. 2.3.4.1. Graphical representations of the laws : Wien's law, Rayleigh-Jeans' law and Planck's law along with the experimental one. Adapted from K.L. Kapoor, 'A Text Book of Physical Chemistry', Vol. 4, Macmillan India Ltd., 1992. Reproduced with permission.

Stefan-Boltzmann law from Planck's equation : The integration of the Planck's equation 2.3.4.5 over the whole wavelength region yields E as follows :

$$E = \int_0^\infty E_\lambda d\lambda = 8\pi ch \int_0^\infty \frac{1}{\exp(ch/\lambda kt) - 1} \times \frac{1}{\lambda^5} d\lambda$$

Let, $u = hc/\lambda kT$; i.e. $\lambda = (hc)/(ukT)$;

or, $$d\lambda = -\frac{hc}{u^2 kT} du$$

Substituting these values in the Planck's equation we get :

$$E_\lambda d\lambda = \frac{8\pi hc}{(hc/ukT)^5 [\exp(u) - 1]} \times \frac{-hc}{u^2 kT} du = E_u du, \text{ (say)} \qquad \ldots(2.3.4.7)$$

and, when $\lambda \to 0$, $u \to \infty$; and, when $\lambda \to \infty$, $u \to 0$

Thus, the involved integral gets reduced as follows :

$$E = \int_0^\infty E_\lambda d\lambda = \int_\infty^0 E_u du = 8\pi hc \int_\infty^0 \frac{1}{(hc/ukT)^5 [\exp(u) - 1]} \times \left(-\frac{hc}{u^2 kT}\right) du$$

$$= -\frac{8\pi (kT)^4}{(hc)^3} \int_\infty^0 \frac{u^3}{\exp(u) - 1} du = -\frac{8\pi (kT)^4}{(hc)^3} \left(-\frac{\pi^4}{15}\right), \text{ (using the standard integral value)}$$

$$= \frac{8\pi^5 k^4}{15(hc)^3} T^4 = PT^4, \text{ (P is a constant)} \qquad \ldots(2.3.4.8)$$

Click Here t.me/thealchemylibrary

On comparison this equation with that of Stefan-Boltzmann law (Eqn. 2.3.1.1), it indicates that $P = \sigma$, Stefan's constant where σ is given by :

$$\sigma = (8\pi^5 k^4)/[15\ (hc)^3]$$

Wien's equation from Planck's equation **:** In the lower range of wavelength, exp $(ch/\lambda kT)$ is much greater than unity, i.e. exp $(ch/\lambda kT) >> 1$.

Thus, the Planck's Eqn. 2.3.4.5 gets reduced into,

$$E_\lambda d\lambda = \frac{8\pi ch}{\lambda^5} \times \exp(-ch/\lambda kT) d\lambda = A\lambda^{-5} \exp(-B/\lambda T) d\lambda \quad \ldots(2.3.4.9)$$

where, $A = 8\pi ch$, $B = ch/k$.

Thus the above equation corresponds to **Wien's Eqn.** 2.3.2.2. Again differentiating the Planck's equation with respect to λ and equating the derivative to zero (for the condition of λ_{max}), we get, $\lambda_{max} T$ = constant, which is the **Wien's law** (cf. Eqn. 2.3.2.1). To get the above result, we are to start with the simpler form (Eqn. 2.3.4.9) of *Planck's equation applicable to the lower values of* λ *in which region Wien's law works*. Thus we have,

$$E_\lambda = \frac{8\pi hc}{\lambda^5} \exp(-hc/\lambda kT); \text{ or, } \frac{dE_\lambda}{d\lambda} = 8\pi hc \frac{d}{d\lambda}\left[\lambda^{-5} \exp(-hc/\lambda kT)\right];$$

For the condition of $\lambda = \lambda_{max}$, we have $\frac{dE_\lambda}{d\lambda} = 0$

But, $8\pi hc \neq 0$; it leads to : $\frac{d}{d\lambda}\left[\lambda^{-5} \exp(-hc/\lambda kT)\right] = 0;$

or, $$\left[-5\lambda^{-6} + \lambda^{-5}\left(\frac{hc}{\lambda^2 kT}\right)\right] \exp(-ch/\lambda kT) = 0$$

Again, $\exp(-hc/\lambda kT) \neq 0$; it leads to : $-5\lambda^{-6} + \lambda^{-7}(hc/kT) = 0;$

or, $\lambda T = hc/5k$ = constant; or $\lambda_{max} T$ = constant = 2.90×10^{-3} m K

Rayleigh-Jeans equation from Planck's equation **:** In the longer wavelength region, $(ch/\lambda kT)$ will have a small value and thus exp $(ch/\lambda kT)$ can be expressed as : exp $(ch/\lambda kT) \approx 1 + ch/\lambda kT$.

Thus, the Planck's equation gets reduced under this condition as follows :

$$E_\lambda d\lambda = \frac{8\pi ch}{\lambda^5} \times \frac{1}{1 + (ch/\lambda kT) - 1} d\lambda$$

$$= \frac{8\pi ch}{\lambda^5} \times \frac{\lambda kT}{ch} d\lambda = 8\pi kT\lambda^{-4} d\lambda$$

This is **Rayleigh-Jeans equation.** Thus the Planck's quantum theory nicely explains the main features of black body-radiation though the theory is standing on some arbitrarily chosen quantum restrictions. However, the theory is not getting confined only in black-body radiation but the concept

Click Here t.me/thealchemylibrary

can be extended to many other problems which do not find any explanation from classical mechanics. Among these the **photoelectric effect, heat capacity of the solids, Bohr-Sommerfeld atomic model and atomic spectra,** etc. are worthy to be mentioned. Its inclusion has been well illustrated in discussing the atomic models. The Planck constant, determined from many different sources is in good agreement within the limit of experimental error. It definitely provides a sound basis of the theory. As a matter of fact, it has opened a new direction in the modern outlook in both physics and chemistry.

2.4. THE PHOTOELECTRIC EFFECT

2.4.1 Characteristics of Photoelectric Effect

When a beam of ultraviolet light (in some cases, visible light) is incident on a metal plate preferably of alkali and alkaline earth metals, some electrons are emitted. An experimental design is shown in Fig. 2.4.1.1. When a beam of light is getting incident on the metal surface (P) in an evacuated tube, the emitted electrons from the metal plate are attracted to the positively charged plate (Q). Thus a current flows through the circuit and it can be detected by the Galvanometer (G). This photoelectricity follows the following characteristic features supported by the experimental facts.

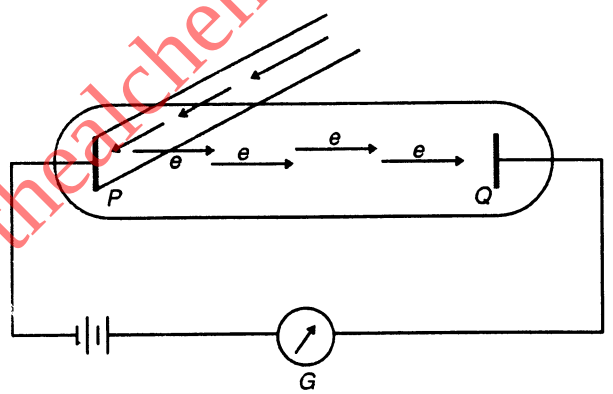

Fig. 2.4.1.1. Experimental device of photoelectric

(a) ***Dependence of photoelectric current on the intensity of incident light:*** *The total photoelectric current (i.e. the total number of electrons emitted from a given surface) is proportional to the intensity of the incident beam of a particular frequency.* Intensity of a beam of a particular frequency is measured by the number of photons getting incident per unit area of the surface per second. Thus it indicates: the more the number of incident photons of a particular frequency, the more is the number of emitted electrons and hence the more the current.

(b) ***Threshold frequency of the incident light to initiate the photoelectric effect:*** For a particular metal surface, the incident beam should have a minimum frequency below which there will be no emission of electrons. This minimum frequency required to start the phenomenon is called the ***threshold frequency*** of that particular metal. If the threshold frequency is not attained, whatever may be the intensity of the incident beam there will be no photoelectric current.

(c) ***Dependence of energy of the emitted electrons on the frequency of incident beam:*** The maximum velocity, or the maximum kinetic energy of the emitted electrons for a particular metal plate is completely independent of the intensity of the incident beam, **but the maximum energy of the electrons is linearly dependent on the frequency of the incident beam.** Thus the maximum energy of the electron is only dependent on the frequency of the incident beam and nature of the metal.

Click Here 1.me/thealchemylibrary

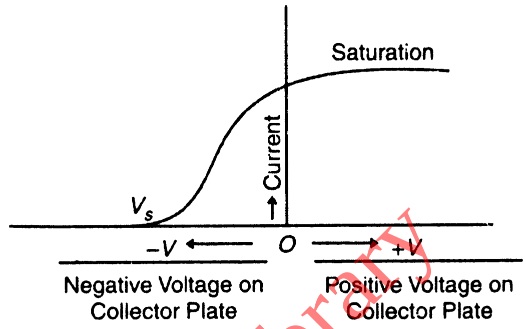

Fig. 2.4.1.2. Variation of photoelectric current with the change of potential on collector plate.

The above facts can be illustrated experimentally. In Fig. 2.4.1.1, if the plate (Q) is made negative with respect to P, then the emitted electrons will experience a *retarding potential* to reach the collector plate (Q). The electrons which will have only sufficient kinetic energy to overcome the retarding potential will only be able to reach the plate. *Thus, if the retarding potential is increased gradually for a particular incident beam of a certain frequency, then at a certain potential it will be found that no emitted electron will be able to reach the collector plate.* This minimum required retarding potential to stop the photo-electric current is called the ***stopping potential*** (V_s) (Fig. 2.4.1.2). Hence, under this condition,

$$\frac{1}{2} m u_{max}^2 = eV_s; \text{ or, } u_{max} = \sqrt{2eV_s/m} \qquad ..(2.4.1.1)$$

Here it is noteworthy that all the electrons emitted are not having the same velocity. The electrons emitted just from the surface will have the maximum energy while the electrons coming from the bulk will have the lower energy. **Thus the energy of the electrons may vary, but the maximum energy which can be associated with the emitted electrons is fixed for a certain frequency of the beam incident on a particular metal surface. Thus, the stopping potential is found to increase linearly with the increase of frequency of the beam while it is independent of the intensity of the beam.**

Now the potential of the collector plate is moved towards the positive direction with respect to the plate (P) and the current goes to increase. But after a certain positive value of the potential on Q, there will be no further increase of current (Fig. 2.4.1.2). This is called ***saturation current.*** It means that all the liberated electrons having energy, minimum (i.e. u_{min}) to maximum (i.e. u_{max}) have been able to reach the collector plate.

2.4.2 Einstein's Theory of Photoelectric Effect

The observation discussed in Sec. 2.4.1(a) is quite expected from the classical concepts but the other observations mentioned in Sec. 2.4.1 (b), (c) are quite unexpected from the classical concept of electromagnetic theory of radiation.

According to Einstein's theory, when a photon strikes an electron, **either the whole energy of the photon or no energy of the photon will be transferred to the electron.** Thus it follows the principle, ***all or none.*** If a photon gets incident on the metal surface and the energy transfer process occurs then a portion of the energy will be used to make the electron free from the binding forces of the metal and the residual energy will be utilised to impart the kinetic energy to the released or free electron.

If the target electron lies below the surface, it will require some additional amount of energy to reach the surface, but if the target electron originates on the surface, it will not require this additional energy. **Thus the energy of the incident photon will be utilised in three different successive steps:**

(i) bringing the target electron to the surface from the binding forces within the metal,
(ii) releasing the electron from the surface, and
(iii) imparting the kinetic energy to the released electron of zero velocity on the surface.

Click Here t.me/thealchemylibrary

This is why, for a particular type of photons of $h\nu$, the electron which originates on the surface will have the maximum kinetic energy because it does not require any additional energy as required by the bulk electron. Under such circumstances, the electron on the surface will require the minimum amount of energy (ω) to overcome the binding forces to get released. This minimum energy, ω represents the ***work function of the metal*** and it is expressed in terms of ***threshold frequency*** (ν_o) as: $\omega = h\nu_o$. It indicates that when the energy of the incident photon is less than ω or $h\nu_o$, there will be no emission of photoelectron.

In view of the above fact, for the incident photon of $h\nu$, according to the principle of conservation of energy, it can be written as follows :

$$\frac{1}{2}mu_{max}^2 + \omega = h\nu; \text{ or, } \frac{1}{2}mu_{max}^2 = h\nu - h\nu_o; \text{ or, } eV_s = h(\nu - \nu_o) \quad \ldots(2.4.2.1)$$

This is the Einstein's equation. The above equation can explain all the observations which did not get any support from the idea of classical electromagnetic theory. It implies the following conclusions:

- ***Concept of threshold frequency or work function*** **:** If the frequency of the incident photon is less than the threshold frequency ν_o (in terms of energy, $h\nu <$ work function, ω), there will be no photoelectric emission, regardless of the intensity (i.e. the number of photons getting incident on the metal surface per unit area per second).
- ***Relationship between stopping potential and frequency of the incident beam*** **:** The maximum kinetic energy and consequently the stopping voltage (V_s) are independent of the intensity of the incident photon but they bear a linear relationship with the frequency of the incident photon. This aspect is verified experimentally by Millikan. According to the Einstein's equation (Eqn. 2.4.2.1) we have :

$$V_s = h\nu/e - h\nu_o/e \quad \ldots(2.4.2.2)$$

Thus the plot of V_s against ν gives a straight line (Fig. 2.4.2.1) whose slope is given by (h/e) and the magnitude of the intercept is given by $\frac{h\nu_o}{e}$. From the slope, h can be obtained from the known value of charge of the electron. Millikan determined the value of Planck constant in this method and it was in good agreement with the result obtained from other sources. This verification definitely gives a sound support to the validity of the Einstein's equation.

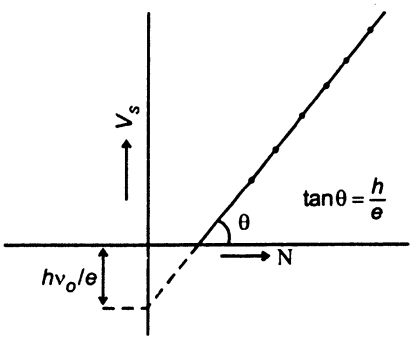

Fig. 2.4.2.1. Variation of stopping voltage for the emitted photoelectrons with the frequency of the incident radiation.

2.4.3 Work Function and Ionisation Potential

The electrons in a metal are having some potential energy. The potential energy of an electron for a particular metal depends on its position. The electrons at the outermost shell of the atoms residing at the surface are having the **minimum binding energy.** On the other hand, for the same type of electrons within the bulk, the binding energy is higher. This is why, the most loosely bound electrons (i.e. at the outermost shell) of the atoms at the surface require the minimum amount of energy to get released from the binding forces. This minimum required energy is called the ***work function*** **of the metal.** In the case of **ionisation potential,** it gives the required minimum amount of

Click Here t.me/thalcherylibrary

energy to release the most loosely bound electron from the metal atom in *isolated and gaseous condition*. Thus both the processes deal with the required minimum amount of energy to knock out the most loosely bound electron. But in the case of photoelectric effect, the metal atom is in the solid state at the exposed surface while in the case of ionisation potential, the metal atom is in gaseous and isolated condition. Table 2.4.3.1 gives a comparison between the ionisation potentials (first IP) and work functions of some metals. ***It is evident that the more the ionisation potential, the more is the work function. This is why, the alkali metals are very often used in photoelectric cells. The magnitude of work function is always lower compared to its corresponding ionisation potential. It indicates that for releasing an electron from an atom present in the aggregate form, it requires less energy compared to the process of releasing the electron present in an atom in isolated and gaseous condition.***

Table 2.4.3.1. Work function and ionisation potential of some metals.

Metal	*λ_0 (nm) (threshold)*	*Work function (in eV)*	*Ionisation (1st) potential (eV)*
Na	500	2.50	5.12
K	550	2.26	4.32
Cs	660	1.87	3.88
Cu	290	4.30	7.70
Ag	261	4.73	7.54
Zn	359	3.44	9.37
Fe	262	4.71	7.83
W	261	4.73	–
Pt	196.2	6.30	–

Click Here t.me/thealchemylibrary

2.5 COMPTON EFFECT

When light (specially, *X*-rays of sharply defined frequency) strikes on a material (specially of low atomic number in which the electrons are loosely bound to the parent atoms), it gets scattered and it suffers a change of frequency and wavelength. The wavelength of the scattered light is increased by a definite amount which depends on the angle of scattering but not on the wavelength of the incident beam. The scattered beam very often gets associated with the unchanged wavelength along with the new longer wavelength. This phenomenon is called ***Compton effect*** in the name of its discoverer, Arthur H. Compton (1923) of Chicago University.

Compton explained the phenomenon on the basis of quantum theory in which light is considered to be a flow of quanta of photons of energy, $h\nu$. ***According to the theory of relativity, mass and energy are equivalents.*** As the photons have energy, they can be considered as particles of definite momentum. Hence, the striking of light on a material can be considered as an elastic collision between the photon and the electron of the scatterer. **Thus, a photon of energy $h\nu$ on striking an electron will transfer some of its energy as kinetic energy to the electron; and consequently the photon will lose some energy. The scattered photon will have a longer wavelength, i.e. smaller frequency.** In terms of energy transfer, Compton effect does not obey the ***principle of all or none*** which is strictly maintained in photoelectric effect.

2.5.1 Theoretical Background of Compton Effect

A.H. Compton put forward a sound theoretical basis of the phenomenon by considering the fundamental aspects of ***quantum theory*** and the ***principle of relativity*** along with the principles of conservation of momentum and energy. In this consideration, an elastic collision between the particles, i.e. electron and photon, is considered. In this collision, the loss of energy by the photon is gained by the electron to increase its kinetic energy. If the incident photon is of frequency ν and it scatters with a lower frequency ν′ (Fig. 2.5.1.1) then, **loss of energy of the photon = gain of energy by the electron;**

or, $$\boxed{h(\nu - \nu') = T} \qquad \ldots(2.5.1.1)$$

Now, from the principle of relativity, we know :

$$m = m_o(1 - u^2/c^2)^{-1/2} \qquad \ldots(2.5.1.2)$$

where m and m_o stand for the mass of a moving particle at the velocity u and zero respectively; m_o is called the ***rest mass*** of the particle, and c is the velocity of light.

From the above relation for a moving particle we get :

$$m^2 = m_0^2/(1 - u^2/c^2);\ \text{or,}\ m^2(c^2 - u^2) = m_0^2c^2;\ \text{or,}\ m^2c^2 - p^2 = m_0^2c^2;$$

where $p = mu$ = momentum of the particle.

or, $p^2 = m^2c^4/c^2 - m_0^2c^2 = E^2/c^2 - m_0^2c^2$; ($E = mc^2$ = **total energy of a moving particle).**

or, $$\boxed{E = \sqrt{p^2c^2 + m_0^2c^4}} \qquad \ldots(2.5.1.3)$$

The above Eqn. 2.5.1.3 is applicable to any moving particle. In the case of photons which have no rest mass,

$$E = pc = mc^2, \text{ where } p = mc \text{ and } E = h\nu.$$

Hence, momentum of the photon = $p = E/c = h\nu/c$

Now let us consider the photon to collide with an electron at rest (for rigorous calculation, the motion of the electron is to be considered, but this motion is negligible compared with other velocities considered in the analysis) and the photon gets scattered at an angle θ while the electron will move at an angle ϕ with the direction of the incident photon (Fig. 2.5.1.1).

According to the **principle of conservation of energy,** the energy of the incident photon and the electron at rest before the collision will be the sum of energy of the scattered photon and the recoiling electron after the collision.

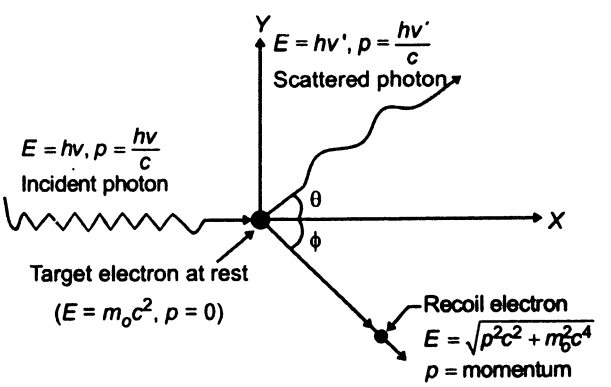

Fig. 2.5.1.1. Compton effect.

Click Here to me/thealchemylibrary

Thus, $h\nu + m_0c^2 = h\nu' + \sqrt{m_0^2c^4 + p^2c^2}$, **(Conservation of energy)**

(where m_0 = rest mass of the electron, $p = mu$ = momentum of the recoiling electron having mass m and velocity u)

or, $h(\nu - \nu') = \sqrt{m_0^2c^4 + p^2c^2} - m_0c^2 = E - m_0c^2$, (from Eqn. 2.5.1.3) ...(2.5.1.4)

or, $h(\nu - \nu') = E - m_0c^2 = T$, (from Eqn. 2.5.1.1) ...(2.5.1.5)

where, E = total energy of the recoiling electron $= \sqrt{m_0^2c^4 + p^2c^2}$

Resolving the momentum vectors in two perpendicular components and using the principle of **conservation of momentum** in the two directions, we get,

$h\nu/c + 0 = (h\nu'/c)\cos\theta + p\cos\phi$, ...(2.5.1.6)

(along the direction of the incident photon)

and, $0 = (h\nu'/c)\sin\theta - p\sin\phi$, ...(2.5.1.7)

(along the perpendicular direction to that of the incident photon)

From Eqns. 2.5.1.6 and 2.5.1.7, we get :

$$pc\cos\phi = h\nu - h\nu'\cos\theta \quad ...(2.5.1.8)$$

and, $$pc\sin\phi = h\nu'\sin\theta \quad ...(2.5.1.9)$$

To eliminate ϕ from the Eqns. 2.5.1.8 and 2.5.1.9, squaring each of these equations, they are added as follows,

$$p^2c^2(\cos^2\phi + \sin^2\phi) = (h\nu)^2 - 2(h\nu)(h\nu')\cos\theta + (h\nu')^2(\cos^2\theta + \sin^2\theta)$$

$$p^2c^2 = (h\nu)^2 - 2(h\nu')(h\nu)\cos\theta + (h\nu')^2 \quad ...(2.5.1.10)$$

Now, the total energy of the recoiling electron can be expressed as follows,

$E = m_0c^2 + T$, (from Eqns. 2.5.1.4 and 2.5.1.5); and $E = \sqrt{p^2c^2 + m_0^2c^4}$

Hence, $\sqrt{p^2c^2 + m_0^2c^4} = m_0c^2 + T$;

or, $p^2c^2 + m_0^2c^4 = m_0^2c^4 + T^2 + 2m_0c^2T$;

or, $p^2c^2 = T^2 + 2m_0c^2T$

$= (h\nu - h\nu')^2 + 2m_0c^2(h\nu - h\nu')$

$= (h\nu)^2 + (h\nu')^2 - 2(h\nu)(h\nu') + 2m_0c^2(h\nu - h\nu')$ ...(2.5.1.11)

Now, by considering Eqns. 2.5.1.10 and 2.5.1.11, we get :

$$2m_0c^2(h\nu - h\nu') = 2(h\nu)(h\nu')(1 - \cos\theta)$$

or, $$m_0c^2\left(\frac{c}{\lambda} - \frac{c}{\lambda'}\right) = h(c/\lambda)(c/\lambda')(1 - \cos\theta);$$

Click Here t.me/chealchemylibrary

or, $$m_0c\left(\frac{\lambda' - \lambda}{\lambda\lambda'}\right) = \frac{h}{\lambda\lambda'}(1 - \cos\theta);\ \text{or, } \lambda' - \lambda = \frac{h}{m_0c}(1 - \cos\theta);$$

or, $$\Delta\lambda = \frac{h}{m_0c}(1 - \cos\theta); \qquad \ldots(2.5.1.12)$$

or, $$\boxed{\Delta\lambda = 2\frac{h}{m_0c}\sin^2(\theta/2);} \qquad \ldots(2.5.1.13)$$

From the above equation, **it is evident that the change in wavelength ($\Delta\lambda$) very often called *Compton shift* is independent of the wavelength of the incident radiation and the nature of the scattering material, but it depends on the angle of scattering suffered by the photon.** The kinetic energy of the recoiling electron arises due to the gain of energy from the incident photon because it is assumed that the electron is remaining at rest before the collision. Thus the kinetic energy (T) of the recoiling electron is given by the following equation :

From Eqn. 2.5.1.1, $$T = h(\nu - \nu') = hc(\lambda' - \lambda)/\lambda\lambda' = \frac{hc \times \Delta\lambda}{\lambda(\lambda + \Delta\lambda)};\ (\lambda' - \lambda = \Delta\lambda)$$

or, $$T = \frac{h\nu \times \Delta\lambda}{\lambda + \Delta\lambda} = h\nu\,\frac{h(1 - \cos\theta)/m_0c}{\lambda + h(1 - \cos\theta)/m_0c},\ \text{(from Eqn. 2.5.1.12)}$$

or, $$T = h\nu\,\frac{[h(1 - \cos\theta)]/(m_0c\lambda)}{1 + [h(1 - \cos\theta)]/(m_0c\lambda)} = h\nu\,\frac{[h\nu(1 - \cos\theta)]/(m_0c^2)}{1 + [h\nu(1 - \cos\theta)]/(m_0c^2)} \qquad \ldots(2.5.1.14)$$

Fraction (f) of energy loss from the incident photon is given by :

$$f = \frac{h\nu - h\nu'}{h\nu} = \frac{c/\lambda - c/\lambda'}{c/\lambda}$$
$$= \frac{\lambda' - \lambda}{\lambda'} = \frac{\Delta\lambda}{\lambda + \Delta\lambda}$$

2.5.2 Compton Shifts at Different Cases

Case I : $\theta = 0^o$, i.e. the scattered light runs parallel to the direction of the incident radiation without suffering any deviation, i.e. $\Delta\lambda = 2(h/m_0c) \times 0 = 0$.

Hence, $\lambda = \lambda'$ and there is no shift in wavelength.

Case II : $\theta = 90^o$, i.e. the scattered light runs perpendicular to the direction of the incident radiation, i.e. $\Delta\lambda = 2(h/m_0c)\sin^2 45^o = (h/m_0c)$ = constant. This constant, (h/m_0c) is called ***Compton wavelength*** (λ_c) of the scattering particle, i.e. electron in this case. By using the standard values of h, m_0 and c, the value of Compton wavelength of electron becomes 0.024 Å; or 2.4×10^{-12} m.

Case III : $\theta = 180^o$, i.e. the scattered light comes back to the opposite direction of the incident light, i.e. $\Delta\lambda = 2(h/m_0c)\sin^2 90^o = 2(h/m_0c) = 2\lambda_c$.

θ can vary from 0° to 180°. Hence the wavelength of the scattered photon can vary from λ to $(\lambda + 2\lambda_c)$ where λ is the wavelength of the incident radiation. **Thus the maximum wavelength shift may occur by 0.048 Å. Such small changes are only noticeable for the *X*-rays whose wavelength**

Click Here t.me/holdchemistrylibrary

is of the order of 1 Å. In the case of visible light, the percentage of wavelength shift is negligibly small.

2.5.3 Characteristic Features of Compton Effect

(i) Co-existence of both modified (scattered by loosely bound electrons) and unmodified (scattered by tightly bound electrons) wavelengths

Fig. 2.5.3.1 shows the scattering of the *X*-ray obtained from molybdenum by graphite at different scattering angles. In each case, one peak corresponding to the original wavelength (called ***unmodified wavelength***) co-exists always with another one having a larger wavelength (called ***modified wavelength***) and the wavelength shift is in good agreement with the theoretical prediction from Eqn. 2.5.1.13.

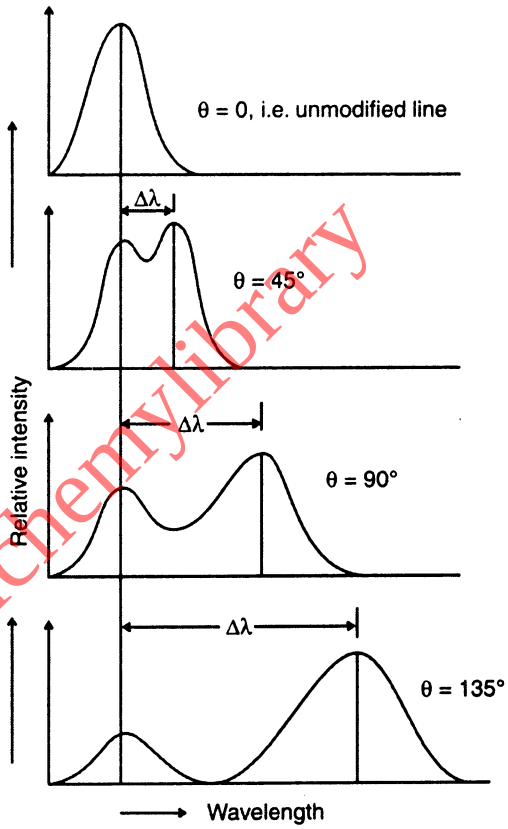

Fig. 2.5.3.1. Compton shift in scattering of the *X*-rays (obtained from molybdenum) by graphite at different scattering angles.

The existence of this unmodified wavelength can be easily explained. In developing Eqn. 2.5.1.13, it was assumed that **the scattering particle,** i.e. **an electron, is able to move freely. This assumption is reasonably valid only for the loosely bound electrons.** But all the electrons are not loosely bound even for the lighter atoms, and many of the electrons are tightly bound. ***This is why, when a photon strikes on a tightly bound electron, the entire atom as a whole recoils instead of the single electron.*** In such cases, m_0 actually represents the entire mass of the atom which is several thousand times greater than that of an electron. **Consequently, (h/m_0c) becomes negligibly small and Compton shift ($\Delta\lambda$) tends to be zero. In such cases, only the unmodified wavelength appears.** In fact, for the tightly bound electrons of carbon acting as the target, $\Delta\lambda$ becomes about 22,000 times smaller than the $\Delta\lambda$ for an electron (cf. a carbon atom is about 22,000 times heavier than an electron). Thus scattering of X-rays by the tightly bound electrons does not experience practically any wavelength change.

For the photons of high energy, most of the electrons as scattering particles appear more or less free and a large fraction of the incident photons suffer Compton shift. On the other hand, for the low energy photons such as the photons of visible light, all the electrons appear to be tightly bound and as a result, no Compton shift occurs. As matter of fact, for such radiations, photoelectric effect becomes important.

(ii) Compton shift is strikingly noticeable only for the X-ray – why?

It has been already mentioned that for the low energy photons (i.e. visible light), all the electrons of the scattering materials appear to be firmly bound and consequently, no Compton shift occurs. Besides this, if, at all, the Compton effect occurs, then the wavelength shift which may have the maximum value 0.048 Å becomes undetectable for the incident photons of longer wavelength. For the *X*-ray

Click Here! me/thealchemylibrary

photons, the energy is sufficiently high and consequently many electrons of the scattering material appear to be loosely bound to the incident beam. **Besides this, the wavelength of *X*-rays is sufficiently small, so that the Compton shift ($\Delta\lambda$) which may have the maximum value 0.048 Å is well noticeable.** For the very high energy photons, the Compton effect is expected to occur better but the new phenomenon, ***pair formation***, rather than the Compton effect becomes important. It has been experimentally observed that **for the radiations of energy less than 0.1 MeV, photoelectric effect is the predominant phenomenon; for the radiation of energy greater than 0.1 MeV but less than 1 MeV, Compton effect is important; and for the radiations having energy greater than 1 MeV, the pair formation becomes important.**

(iii) Broadening of peaks

Fig. 2.5.3.1 shows the broadening of both modified and unmodified peaks. This broadening can be accounted for the motion of the scattering electron which was supposed to be at rest in developing Eqn. 2.5.1.13.

(iv) Compton Shift independent of the wavelength of the incident photons

The equation, $\Delta\lambda = 2\,(h/m_0c)\sin^2(\theta/2)$ indicates that if Compton effect occurs, the shifting of wavelength is independent of the frequency or wavelength of the incident radiation and nature of the scattering material (*assuming the free stationary electron to be the scattering particle*). It only depends on the scattering angle θ. It has been already shown that depending on the scattering angle θ, the Compton shift can vary from 0 to $2(h/m_0c)$.

(v) Difference between the photoelectric effect and Compton effect

It has been already pointed out that for the low energy photons ($h\nu < 0.1$ MeV), the electrons in a matter mostly appear as firmly bound electrons and consequently the photoelectric effect rather than the Compton effect is important. Besides this, an important difference is : ***in photoelectric effect, the energy transfer follows the principle of all or none while in Compton effect, only a partial amount of energy transfer occurs.*** In photoelectric effect, there is a threshold frequency for a particular material, but in Compton effect no such threshold value is defined.

In photoelectric effect, incident photon loses its ***all energy*** in colliding with the both ***inner- and outer-shell electrons*** of the target atom. On the other hand, in Compton scattering, energy of the colliding photon is only ***partly*** lost in the encounter with the ***loosely bound electrons of outer shells.***

Compton scattering is only important for the loosely bound outer-shell electrons of lighter atoms (for which electron binding is less). ***In fact, for the heavier atoms, Compton scattering is of no significance.***

2.6 PAIR FORMATION

The radiations having energy more than 1 MeV strikes a matter and a pair of oppositely charged particles, i.e. positron and electron, are formed. In this process, the principles of conservation of energy and linear momentum are also maintained. These conservation principles are maintained only in the presence of the nuclei of the scattering material. **This is why, no pair formation occurs in**

Click Here t.me/thealchemylibrary

empty space. Roughly, the total energy including mass energy of the electron and positron equals to the photon energy, **as the kinetic energy carried by the scattering nucleus is negligibly small due to its relatively enormous mass.** But the momentum of the recoiling nucleus is sufficiently high and it cannot be ignored.

The positron and electron are bearing the same mass with opposite charge of equal amount. Hence, the total charge of the pair is zero which is the charge of the photon. In the process, the two particles of mass m_0 ($\approx 9.1 \times 10^{-31}$ kg) for each one are created from the energy of the photon. Hence, according to the principle of conservation of energy, **the energy of the photon must be at least $2m_0c^2$.** Its value is 2×0.511 MeV (= 1.022 MeV) which is called the ***threshold energy*** of the photon required for pair formation. Thus, for the photon having energy greater than the threshold energy, the additional energy, i.e. $(h\nu - 2m_0c^2)$, imparts the kinetic energy, equally to the particles. From the value of the threshold energy, it appears that for the pair formation, **it will require the photons of *gamma radiation*.** The gamma rays are found in nature from the emission of radioactive substances and also in cosmic rays. The process of pair formation can be pictorially represented in Fig. 2.6.1.

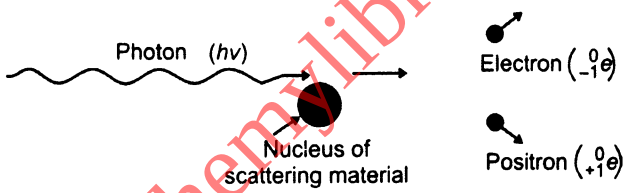

Fig. 2.6.1. The process of pair formation.

SOLVED NUMERICAL PROBLEMS

Problem 1 : A radiation of wavelength 150 nm falls on a metal surface whose work function is 5 eV. Find (i) the maximum velocity of the emitted electron, (ii) the kinetic energy of these electrons, and (iii) the stopping potential.

Solution : Work function (ω) = 5 eV = $5 \times 1.602 \times 10^{-19}$ J

If, ν_0 = threshold frequency, $\omega = h\nu_0$; or, $\nu_0 = \dfrac{5 \times 1.602 \times 10^{-19}}{6.625 \times 10^{-34}\ \text{J s}} = 1.21 \times 10^{15}\ \text{s}^{-1}$;

The frequency of the incident photon (ν) = $c/\lambda = \dfrac{3 \times 10^8\ \text{m s}^{-1}}{150 \times 10^{-9}\ \text{m}} = 2 \times 10^{15}\ \text{s}^{-1}$; (1 nm = 1×10^{-9} m)

Now, $\dfrac{1}{2} m u_{max}^2 = h(\nu - \nu_0)$; or, $u_{max}^2 = \dfrac{2h(\nu - \nu_0)}{m}$

or, $$u_{max} = \left[\frac{2 \times 6.625 \times 10^{-34}\ \text{J s} \times (2.0 - 1.21) \times 10^{15}\ \text{s}^{-1}}{9.11 \times 10^{-31}\ \text{kg}}\right]^{1/2} = 1.07 \times 10^6\ \text{m s}^{-1}$$

Hence, maximum kinetic energy = $\dfrac{1}{2} m u_{max}^2 = \dfrac{1}{2} \times 9.11 \times 10^{-31}\ \text{kg} \times (1.07 \times 10^6\ \text{m s}^{-1})^2$

$= 5.24 \times 10^{-19}\ \text{J} = 3.27\ \text{eV}$

Click Here to me/thealchemylibrary

Therefore, the stopping potential (V_s) can be obtained from the relation, $eV_s = \frac{1}{2} mu^2_{max} = 3.27$ eV.

Hence the stopping potential is 3.27 V.

Problem 2 : The work function of sodium is 2.4 eV. Find the threshold frequency and maximum wavelength of the light which will cause the emission of photoelectrons. Find out the stopping potential for the radiation of 2000 Å.

Solution : The work function (ω) = 2.4 eV = 2.4 × 1.6 × 10^{-19} J

and, $\omega = h\nu_0$, where ν_0 is the threshold frequency; or, $\nu_0 = \omega/h$

i.e. $$\nu_0 = \frac{2.4 \times 1.6 \times 10^{-19} \text{ J}}{6.625 \times 10^{-34} \text{ J s}} = 5.80 \times 10^{14} \text{ s}^{-1}.$$

Therefore, in terms of threshold wavelength (λ_0), $\lambda_{max} = \lambda_0 = \frac{c}{\nu_0}$

i.e. $$\lambda_{max} = \frac{3 \times 10^8 \text{ m s}^{-1}}{5.8 \times 10^{14} \text{ s}^{-1}} = 5.17 \times 10^{-7} \text{ m}$$

Thus the light to cause the emission of photoelectrons can have the maximum wavelength 517 nm or 5170 Å.

$$(K.E.)_{max} = h\nu - \omega = h(\nu - \nu_0) = hc(1/\lambda - 1/\lambda_0) = hc\left(\frac{\lambda_0 - \lambda}{\lambda\lambda_0}\right)$$

$$= 6.625 \times 10^{-34} \times 3 \times 10^8 \times \frac{(5.17 - 2.0) \times 10^{-7}}{5.17 \times 10^{-7} \times 2.0 \times 10^{-7}} \text{ J}$$

$$= 6.01 \times 10^{-19} \text{ J}$$

$$= 3.80 \text{ eV}, (1 \text{ eV} = 1.6 \times 10^{-19} \text{ J}; \lambda = 2000 \text{ Å} = 2 \times 10^{-7} \text{ m}).$$

Problem 3 : The threshold wavelength for the photoelectric emission of tungsten is 2,300 Å. Find the wavelength of light which will be required to release the electrons with the maximum kinetic energy 2 eV.

Solution : $(K.E.)_{max} = \frac{1}{2} mu^2_{max} = h(\nu - \nu_0)$, ($\nu_0$ = threshold frequency)

According to the given conditions, $(K.E.)_{max}$ = 2 eV = 2 × 1.6 × 10^{-19} J.

Thus, 2 × 1.6 × 10^{-19} J = 6.625 × 10^{-34} J s × $(\nu - \nu_0)$ s^{-1},

where, $$\nu_0 = c/\lambda_0 = \frac{3 \times 10^8 \text{ m s}^{-1}}{2300 \times 10^{-10} \text{ m}} = 1.30 \times 10^{15} \text{ Hz}$$

Hence, $$\nu - \nu_0 =] \frac{2 \times 1.6 \times 10^{-19} \text{ J}}{6.625 \times 10^{-34} \text{ J s}} = 0.483 \times 10^{15} \text{ s}^{-1}; \nu - \nu_0 = \frac{(K.E.)_{max}}{h}$$

or, $$\nu = (1.3 + 0.483) \times 10^{15} = 1.783 \times 10^{15} \text{ Hz}$$

Click Here t.me/thealchemylibrary

Thus the required wavelength (λ) is given by, $\lambda = c/\nu$;

i.e. $$\lambda = \frac{3\times10^{8}\ \text{m s}^{-1}}{1.783\times10^{15}\ \text{s}^{-1}} = 1.682\times10^{-7}\ \text{m} = 1682\ \text{Å}$$

Problem 4 : A monochromatic *X*-ray beam of wavelength 0.45 Å undergoes scattering by an angle 60°. Find the wavelength of the scattered beam.

Solution : We have, $\Delta\lambda = \lambda' - \lambda = 2(h/m_0c)\sin^2(\theta/2)$

Now putting the values of h, m_0, c and θ we get,

$$\Delta\lambda = \frac{2\times6.625\times10^{-34}\ \text{J s}}{9.1\times10^{-31}\ \text{kg}\times3.10^{8}\ \text{m s}^{-1}}\sin^2(30^\circ)$$

$$= 0.012\times10^{-10}\ \text{m} = 0.012\ \text{Å}$$

Hence, $\lambda' = \lambda + \Delta\lambda = 0.462\text{Å}$.

Problem 5 : Calculate the Compton wavelength of the proton.

Solution : When Compton shift occurs due to the collision between the incident photon and free stationary proton as a scattering particle, the rest mass of the proton is to be considered to calculate the Compton wavelength of the proton.

Thus, $\Delta\lambda = 2(h/m_0c)\sin^2(\theta/2)$; m_0 = rest mass of a proton in this case.

The Compton wavelength (λ_c) is obtained when, $\theta = 90$,

Hence, $$\lambda_c = 2(h/m_0c)\times\frac{1}{2} = h/m_0c = \frac{6.625\times10^{-27}\ \text{erg s}}{1.67\times10^{-24}\ \text{g}\times3\times10^{10}\ \text{cm s}^{-1}}$$

$$= 1.32\times10^{-13}\ \text{cm} = 1.32\times10^{-5}\ \text{Å}.$$

Problem 6 : Determine the average energy of all photons of frequency 10^{14} Hz at 1000 K.

Solution : $$\overline{E} = \frac{h\nu}{\exp(h\nu/kT)-1}$$, k = Boltzmann constant (cf. Eqn. 2.3.4.4)

$$\frac{h\nu}{kT} = \frac{6.62\times10^{-34}\ \text{J s}\times10^{14}\ \text{s}^{-1}}{1.38\times10^{-23}\ \text{J K}^{-1}\times1000\ \text{K}} = 4.8$$

and, $\exp(h\nu/kT) - 1 = \exp(4.8) - 1 = 120.22 - 1 = 119.22$

$$\overline{E} = \frac{6.62\times10^{-34}\ \text{J s}\times10^{14}\ \text{s}^{-1}}{119.22} = \frac{6.62\times10^{-20}\ \text{J}}{119.22} = 5.55\times10^{-22}\ \text{J}$$

(cf. energy of a single photon = $h\nu = 6.62\times10^{-20}$ J.

Problem 7 : Solar radiation shows the energy density maximum at 480 nm. Calculate the temperature of the surface of the sun. Consider the sun to act as a black body.

Solution : Wien's displacement law is :

Click Here t.me/theachemylibrary

$$T\lambda_{max} = \frac{hc}{5k} = \text{constant, } (k = \text{Boltzmann constant})$$

i.e.
$$T = \frac{hc}{5k\lambda_{max}} = \frac{6.62 \times 10^{-34}\ \text{J s} \times 3 \times 10^{8}\ \text{m s}^{-1}}{5 \times 1.38 \times 10^{-23}\ \text{J K}^{-1} \times 480 \times 10^{-9}\ \text{m}}$$

$$= 5996\ \text{K}$$

Temperature of the surface of the sun = 5996 K.

Problem 8 : A monochromatic X-ray beam of wavelength 22 pm experiences scattering from a graphite target at 85°. Find the Compton shift of the scattered rays and % of energy loss in the scattering.

Solution : Compton shift ($\Delta\lambda$) occurs due to the collision of the X-ray photon with the loosely bound electrons of the target. Compton shift is given by :

$$\lambda' - \lambda = \Delta\lambda = \frac{h}{m_o c}(1 - \cos\theta) = \frac{(6.62 \times 10^{-34}\ \text{J s})(1 - \cos 85^{\circ})}{(9.1 \times 10^{-31}\ \text{kg})(3 \times 10^{8}\ \text{m s}^{-1})}$$

$$\approx 2.2 \times 10^{-12}\ \text{m} = 2.2\ \text{pm}$$

Fraction (f) of energy loss in the encounter is given by :

$$f = \frac{h\nu - h\nu'}{h\nu} = \frac{c\left(\frac{1}{\lambda} - \frac{1}{\lambda'}\right)}{\frac{c}{\lambda}} = \frac{\lambda' - \lambda}{\lambda'} = \frac{\Delta\lambda}{\lambda + \Delta\lambda}$$

i.e. $$f = \frac{2.2\ \text{pm}}{(22 + 2.2)\ \text{pm}} \approx 0.09$$

Thus % of energy loss = 9.

EXERCISE-II

A. General Questions

1. What do we mean by a black-body? How is it designed in laboratory? Discuss the characteristic features of black-body radiation at different temperatures.
2. What is Stefan-Boltzmann law? Discuss the features along with their limitations of Wien's displacement law and Rayleigh-Jeans law in explaining the observations of black-body radiation.
3. Mention the basic assumptions of quantum theory proposed by Planck in explaining the black body radiation. Derive the Planck's equation to explain the observations of Lummer and Pringsheim in black-body radiation.
4. Arrive at (i) Stefan-Boltzmann law, (ii) Wien's displacement law, and (iii) Rayleigh-Jeans law from the Planck's equation of black-body radiation.

Click Here t.me/thealchemylibrary

5. Mention the characteristic observations of photoelectric effect. Point out the observations in this regard which are unexpected from the classical concept of electromagnetic wave nature of light.
6. Derive the Einstein's equation of photoelectricity? Explain all the observations in the light of Einstein's equation.
7. What is Compton effect? Derive the Compton's equation and explain the observations.
8. What are the differences between photoelectric effect and Compton effect?
9. Write notes on :
   (i) Ultraviolet catastrophe in Rayleigh-Jeans law
   (ii) Stopping potential in photoelectric effect
   (iii) Compton wavelength
   (iv) Pair formation
   (v) Lummer-Pringsheim curves.

B. Justify the Statements

1. Wien's displacement law agrees well with Lummer-Pringsheim curves only in the lower range of wavelength.
2. Rayleigh-Jeans law when applied in the lower range of wavelength, it leads to an unbelievable result.
3. Ionisation potential and work function of a metal are different in magnitude but they run in the same direction.
4. All the emitted photoelectrons even for a beam of perfectly monochromatic radiation are not of the same kinetic energy.
5. At some positive potential of the collector plate, the photoelectric current gets saturated.
6. Stopping potential in photoelectric effect is independent of intensity of the incident radiation.
7. Compton effect is not noticeable for the visible light and the radiations of far longer wavelength.
8. Compton effect generally occurs for the **scattering material of low atomic number.**
9. In the whole range of electromagnetic radiation, only a certain region of X-rays is ideal for noticing the Compton effect.
10. When Compton effect occurs, the modified line very often gets associated with the unmodified line.
11. Though there is no concept of threshold energy of the incident radiation to produce Compton effect, still consideration of energy of the incident radiation is extremely important to predict the occurrence of Compton effect.
12. Compton shift is independent of the wavelength of the incident radiation but dependent on the angle of scattering of the photon.
13. Compton shift has got a maximum limit.
14. Compton wavelength is dependent on the nature of the scattering of particle.
15. Gamma radiation only in contact with a matter produces positron and electron (i.e. pair formation) but in empty space they do not do so.

Click Here t.me/thealchemylibrary

C. Numerical Problems

1. For a certain metal, the threshold frequency is 1.4×10^{15} Hz. Find the maximum kinetic energy which can be possessed by the emitted photoelectrons when a light of 1.8×10^{15} Hz is incident on the metal plate. What is the value of the stopping potential ?
   (*Ans.* $E_{max} = 2.65 \times 10^{-14}$ J or 1.656 eV, Stopping potential = 1.656 volt).
2. Calculate the maximum kinetic energy of the photoelectrons emitted by a sodium surface when a monochromatic beam of light of wavelength 400 nm is incident on it. The work function of sodium is 2.20 eV. Calculate the value of the largest wavelength which can cause the emission of a photoelectron from a sodium surface.
   (*Ans.* $(K.E.)_{max} = 1.45 \times 10^{-19}$ J = 0.90 eV; λ_{max} = 564 nm).
3. Find the maximum velocity of the photoelectrons emitted from a metal surface (having threshold wavelength 6566 Å) when a beam of light of 3755 Å shines on it.
   (*Ans.* $u_{max} = 6.97 \times 10^5$ m s^{-1})
4. A beam of monochromatic X-rays is getting scattered by the free stationary electrons at 45°. If the wavelength of the scattered beam is 0.022 Å, find the wavelength of the incident beam.
   (*Ans.* 0.015 Å)
5. An X-ray beam of frequency 3×10^{19} Hz gets scattered through 90° by a free stationary electron. Find the frequency of the emerging beam.
   (*Ans.* 2.4×10^{19} Hz).

Click Here t.me/thealchemylibrary

3

Fundamentals of Wave Mechanics

Click Here to Join Chemyjibrary

3.1 INTRODUCTION

The quantum theory provided the convincing explanations of *black-body radiation* (1901), *photoelectric effect* (1905), *line spectra of atoms by Bohr's theory* (1913), *Compton effect* (1924) etc. On the other hand, the concept of electromagnetic wave nature of radiation provided a sound explanation of *interference, diffraction and polarisation*. ***Thus the dual character, i.e. wave nature and particle nature, of the radiation is experimentally established in different phenomena.***

Thus the concept of ***wave-particle dualism*** of radiation gave explanations of different phenomena of interaction of radiation with matter. The origin of the basic postulates (i.e. idea of quantum restriction for the stationary orbits) of Bohr-Sommerfeld model of atom which provided the explanation of line spectra appeared arbitrarily chosen. As a matter of fact, this **apparently inexplicable postulate,** (i.e. $mur = nh/2\pi$) became the great headache to the scientists. At that time, **Einstein's mass-energy equivalence ($E = mc^2$)** was found true in many cases. On this background, the French scientist, de Broglie proposed in 1924 that the wave-particle dualism is not only confined to the photons but also to other matter. This concept of ***matter wave*** when applied to the subatomic particles, yielded results in conformity with the observed ones. This new concept paved the way in the new direction called *wave mechanics* which have solved many problems in the microscopic world successfully.

3.2 WAVE PARTICLE DUALITY AND DE BROGLIE'S MATTER WAVES

3.2.1 de Broglie Wavelength for Matter Waves

In quantum theory, the energy (E) of a photon of frequency ν is given by :

$$E = h\nu \qquad ...(3.2.1.1)$$

According to Einstein's law of mass-energy equivalence, the photon must have a finite mass; and

its mass given by m is related with its energy E as follows : $E = mc^2$ (where c stands for the velocity of light). Comparing the above two equations, we get :

$$mc^2 = h\nu; \text{ or, } mc = h(\nu/c) = h/\lambda, (\nu = c/\lambda)$$

Thus, momentum of the photon ($mc = p$) is given by $p = h/\lambda$, (where λ is the wavelength of the photon).

In other words, the fundamental law of relativity gives the relation (cf. Eqn. 2.5.1.3), $E = \sqrt{p^2c^2 + m_0^2c^4}$. For photons, the rest mass (m_0) is zero. Hence,

$$\boxed{p = E/c = h/\lambda} \qquad \ldots(3.2.1.2)$$

The French scientist, de Broglie extended this idea *to all other particles travelling with a finite velocity*. The new idea helped the scientists to interpret a number of phenomena in the microscopic world and de Broglie was rightly rewarded **Nobel Prize in 1929.** Thus the wavelength of a particle of mass m moving with a velocity u is given by :

$$\boxed{\lambda = h/mu} \qquad \ldots(3.2.1.3)$$

This wave is called ***matter wave*** and the wavelength is called the ***de Broglie wavelength.*** More correctly, in the above Eqn. 3.2.1.3, m is given by, $m = m_0(1 - u^2/c^2)^{-1/2}$.

Note : In fact, Compton's observation (i.e. scattering photon by electrons) made a strong impression on de Broglie to propose the **converse hypothesis** that the particles like electrons, neutrons, protons will also show wave properties under certain conditions.

3.2.2 The de Broglie Wavelength for the Macroscopic and Microscopic Bodies*

(a) Wavelength of a moving subatomic particle

Let us consider the electron in a hydrogen atom to move with a velocity, $u = 2.3 \times 10^6$ m s^{-1}. Thus, the λ is given by :

$$\lambda = h/mu = \frac{6.625 \times 10^{-34} \text{ J s}}{9.1 \times 10^{-31} \text{ kg} \times 2.3 \times 10^6 \text{ m s}^{-1}}$$

$$= 0.316 \times 10^{-9} \text{ m}, (\text{J} = \text{kg m}^2 \text{ s}^{-2})$$

$$= 3.16 \times 10^{-8} \text{ cm} = 3.16 \text{ Å}$$

The value of this wavelength is comparable to that of X-rays and it is measurable as well as believable.

(b) Wavelength of a moving macroscopic particle

Let us take a marble ball of mass 1 g (i.e. 10^{-3} kg) to move with a velocity, $u = 2$ m s^{-1}. Thus, the corresponding λ is given by :

* A **microscopic particle** is defined as the one having the dimension of atomic and subatomic particles. Thus for the microscopic particles, the length is in the order of several angstroms at the most. On the other hand, a **macroscopic particle** can be observed with the naked eye or with an ordinary microscope having the resolving power of the order of 10^{-4} cm at the most.

Click Here to the Learchemy Library

$$\lambda = h/mu = \frac{6.625 \times 10^{-34} \text{ J s}}{10^{-3} \text{ kg} \times 2 \text{ m s}^{-1}} = 3.312 \times 10^{-31} \text{ m} = 3.312 \times 10^{-21} \text{ Å}$$

The value of this wavelength is exceedingly small and it is not measurable. Besides this, due to this exceedingly high frequency, the energy of the ball ($E = hc/\lambda$) becomes exceedingly high and here it is $\sim 6 \times 10^5$ J. **It indicates that when de-Broglie's hypothesis is applied to any macroscopic body, it is found to get associated with a tremendously high energy wave which is unbelievable in our sense. This is why, the de Broglie's wave equation has no significance for the macroscopic particles.**

3.2.3 Difference between de Broglie Matter Wave and Electromagnetic Wave

Though the nature of matter waves is quite different from that of electromagnetic waves, both of them follow the same mathematics, i.e. *they are mathematically identical.* Thus the waves from a vibrating string or from water ripples in a pond or sound waves and the matter waves follow the same mathematical equations. **The concept of matter waves works well in the world of subatomic particles but when applied to the macroscopic world, it leads to unconvincing conclusions.** To tell the fact, except the mathematics followed by the matter waves, the nature of matter waves lies really beyond our sense.

The **major differences** between the electromagnetic and matter waves are given below :

(i) The electromagnetic wave radiated from its source ultimately dissipates away in space, but the matter wave never gets separated from its source. *Thus though the electromagnetic waves can be absorbed or emitted, it does not occur so for the matter waves.*

(ii) *The electromagnetic wave consists of transverse vibrations produced from a combination of electric and magnetic fields perpendicular to each other, but it does not occur so for the matter waves.*

(iii) The velocity of the de Broglie matter wave depends on the nature of the particle under consideration *while the electromagnetic wave runs with the velocity of light.*

3.2.4 The de Broglie Electron Wave

It has been already seen that when the de Broglie's equation is applied to a moving electron, the calculated wavelength associated with the electron is quite reasonable. From Eqn. 3.2.1.3, it is evident that the higher the velocity, the smaller is the de Broglie wavelength. By subjecting a suitable potential gradient (V), the velocity (u) of the electron can be monitored as follows :

$$\text{kinetic energy} = \frac{1}{2} mu^2 = eV; \text{ or, } u = \sqrt{2Ve/m}; \text{ or, } mu = \sqrt{2emV}$$

By using Eqn. 3.2.1.3, we can have the corresponding wavelength, λ) as follows :

$$\lambda = h/mu = h/\sqrt{2emV} \approx h/\sqrt{2em_0V}, \text{ (taking, } m = m_0) \qquad \ldots(3.2.4.1)$$

By using the values of h, m_0, e and V (in volt) in SI system, we get :

$$\lambda = \frac{6.625 \times 10^{-34} \text{ J s}}{\sqrt{2 \times 9.11 \times 10^{-31} \text{ kg} \times 1.6 \times 10^{-19} \text{ C} \times V}} = \frac{12.27}{\sqrt{V}} \times 10^{-10} \text{ m} \qquad \ldots(3.2.4.2)$$

$$= \frac{12.27}{\sqrt{V}} \times 10^{-8} \text{ cm}$$

Click Here to the Chemistry Library

In CGS system, $\lambda = \dfrac{7.08 \times 10^{-9}}{\sqrt{V}}$ cm, ***where V is in statvolt*** (1 statvolt = 300 volts).

From the above equation, it is seen that when $V = 150$ volts, the electron beam produces wavelength ~ 1 Å. **Here it is worth noting that to have the *X*-rays of wavelength ~ 1 Å, it requires about 12,000 volts while for the electron wave of the same wavelength, only about 150 volts are required.** To have the wavelength of the order of 0.05 Å, ~ 50 kilovolts are required. Thus it is seen that by selecting a suitable potential difference the electron beam can be made to have a wavelength matching with that of *X*-rays. Such electron beams can be utilised in diffraction studies, as it is done by the *X*-rays.

3.2.5 Relativistic Correction in the de Broglie Electron Wave

When the potential difference is made significantly high (~ 50 kV) to have the electron beam of the wavelength of the order of 0.05 Å, the velocity of the electron is very high. Under the circumstances, the approximation $m \approx m_0$ is not valid and the consideration of relativistic correction becomes necessary. It is treated as follows :

The relativistic formula for the kinetic energy (T) is given by :

$$T = (m - m_0)c^2; \text{ or } eV = (m - m_0)c^2; \text{ or } m = m_0 + eV/c^2 = m_0\left(1 + \frac{eV}{m_0c^2}\right);$$

or,
$$\sqrt{m} = \sqrt{m_0}\left(1 + \frac{eV}{m_0c^2}\right)^{1/2}$$

Now, by substituting this for m in Eqn. 3.2.4.1, we get :

$$\boxed{\lambda = \frac{h}{\sqrt{2Vem_0}}\left(1 + \frac{eV}{m_0c^2}\right)^{-1/2} = \frac{12.27}{\sqrt{V}}\left(1 + \frac{eV}{m_0c^2}\right)^{-1/2} \text{ Å}} \quad \ldots(3.2.5.1)$$

Note : The expression of ***relativistic kinetic energy*** (T) is obtained as follows :
E (total energy) of a particle $= mc^2 = m_oc^2(1 - u^2/c^2)^{-1/2}$
m = moving mass of the particle having velocity u; m_o = rest mass of the particle
In terms of kinetic energy (T) we can write :

$$E = T + m_oc^2; \text{ or, } T = E - m_oc^2 = m_oc^2(1 - u^2/c^2)^{-1/2} - m_oc^2$$
$$= (m - m_o)\,c^2$$

If the rest mass energy (m_oc^2) is very small, then $E \approx T = mc^2 = pc$ (i.e. $m >> m_o$).
It may be noted that **classical kinetic energy** is given by $p^2/2m$ where p = momentum of the particle.

3.2.6 Verification of the de Broglie Electron Wave by Davisson and Germer's Experiment

It has been already shown that at the potential difference, ~ 150 volt, the electron beams are associated with the wavelength of the order of 1 Å which lies within the same order of magnitude of lattice

Click Here t.me/thealchemylibrary

spacings in the crystals. Hence, such electron beams are expected to produce a diffraction pattern when incident on the crystals. Actually, this idea was verified by Davisson and Germer by allowing the electron beam to impinge on a metallic nickel crystal.

In their experiment, a beam of electrons was directed towards the face of a nickel crystal, and the intensity of the scattered beam was measured at different variable conditions, such as : the energy of the electron beam (i.e. the wavelength of the beam), and the angle of scattering (θ). The experimental set-up is shown in Fig. 3.2.6.1 where *F* is a tungsten filament which on being heated produces a thermionic emission. From this thermionic emission, a narrow beam is allowed to pass through the electric field (*E*) of known potential difference which can be varied between 30-600 volts to accelerate the electrons as desired. This accelerated beam falls on the face of a **single nickel crystal** (*N*). The crystal (*N*) is mounted in such a way that it can be rotated about an axis parallel to the axis of the incident beam. The **face centered cubic single nickel crystal** is cut in such a way that it can have a smooth reflecting surface parallel to the plane (1, 1, 1) perpendicular to the body diagonal of its unit cell. The ionisation chamber (*C*) for detecting the scattered beam and the galvanometer (*G*) can be moved along a graduated circular scale. The angle of deflection can be measured from the position of the detector on the circular scale.

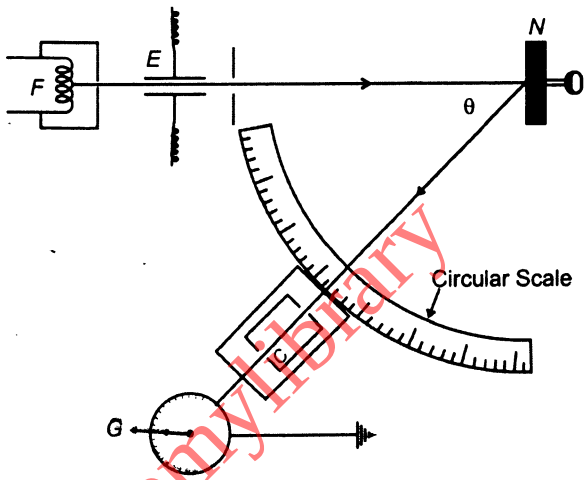

Fig. 3.2.6.1. Experimental set-up of Davisson and Germer's electron diffraction experiment.

From the measurement of intensity of the scattered beam received by the collector (*C*), it was found that **when *the electron beam gets incident perpendicularly to the surface of the crystal, at the colatitude or azimuth angle* (i.e., the angle between the incident beam and the beam entering the collector) *of* 50° *and at the potential* $V = 54$ *volt, the scattered beam shows the maximum intensity.*** From Eqn. 3.2.4.2 (without relativistic correction) the wavelength of the corresponding electron beam can be obtained as,

$$\lambda = \frac{12.27}{\sqrt{54}} \text{ Å} = 1.668 \text{ Å}$$

Observation : In fact, **polar graphs** (Fig. 3.2.6.2) were plotted measuring the intensity of the scattered electrons and the *angle of scattering* θ (called also *latitude* angle or *azimuth angle* or *colatitude angle*) for different accelerating voltage starting from 40 V to 68 V. In the plots, the radius vector gives the measure of the intensity of the scattered beam and the angle between the radius vector and the incident beam is the scattering angle θ. The graph remains smooth upto the voltage 44 V at which a ***spur* or *bump*** just appears for $\theta \approx 60°$. As the applied voltage increases, the length of the spur increases and it becomes maximum for the voltage = 54 V and $\theta = 50°$. With the further increase of the applied potential difference between the filament and plate, the *spur* or *bump* decreases and it disappears at 68 V and $\theta = 40°$.

Click Here to the Academy Library

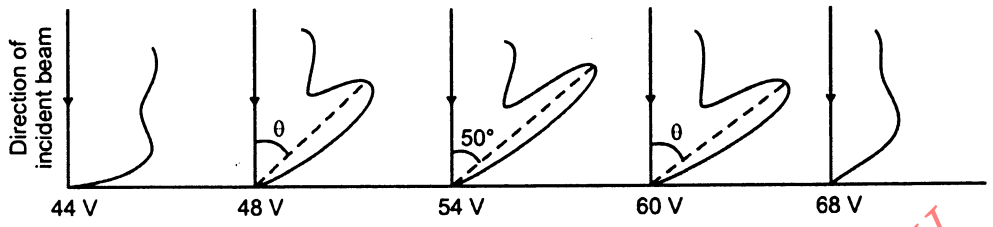

Fig. 3.2.6.2. Polar graphs showing the variation of intensity of scattered beam (which is proportional to the radius vector) and the scattering angle θ for different accelerating voltage 44 V to 68 V.

From the experimental condition, here we get a diffracted beam at a colatitude angle of 50°. Hence, the wavelength of the beam can be evaluated from the relation of a plane reflection grating known as ***grating equation*** **(i.e. *Bragg's equation*),** $n\lambda = d \sin\theta$, $n = 1, 2, 3.....$ referring to the order of diffraction.

In the present case, $n = 1$ (i.e. first order diffraction), d = **distance between the atoms on the surface of the crystal** = 2.15 Å obtained from crystallographic analysis and $\theta = 50°$, we get $\lambda = 1.65$ Å.

For the second order diffraction ($n = 2$), the corresponding values are : V = 181 volts, $\theta = 55°$. Thus we have from the grating equation, $2\lambda = 2.15 \sin 55°$; or, $\lambda = 0.88$ Å.

From de Broglie's equation, we get: $\lambda = \frac{12.27}{\sqrt{181}}$ Å = 0.91 Å. These values are also in good conformity.

Thomson repeated the same experiment by diffracting high energy electrons with a very thin gold foil. On considering the relativistic correction (cf. Eqn. 3.2.5.1), the results were also found in good agreement.

This good quantitative agreement between the results obtained from grating equation and de Broglie's wave equation provides an experimental verification of the de Broglie's concept.

Similarly, the wave properties of the neutron beam and different molecular beams are experimentally verified.

***Note* : *Expression of Bragg's Law in terms of glancing angle* (ϕ) or *scattering angle* (θ).**

Let us consider the Fig. 3.2.6.3.

According to **Bragg's law of diffraction maxima:**

$$\boxed{n\lambda = 2d' \sin\phi}$$

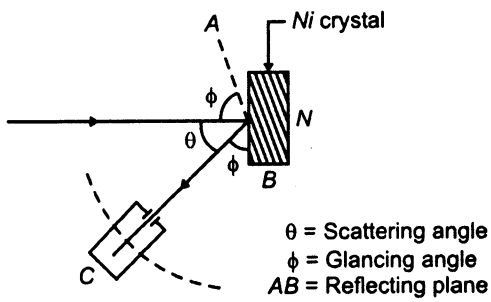

Fig. 3.2.6.3. Schematic representation of scattering angle (θ), glancing angle (ϕ) and reflecting plane.

where d' = interplanar distance between the successive reflecting plane = 0.91 Å (for the nickel crystal).

It is evident that :. $\phi + \theta + \phi = 180°$

i.e. $$\phi = \frac{1}{2}(180° - \theta)$$

In the present case, for first-order ($n = 1$) diffraction maxima, $\theta = 50°$, i.e. $2\phi = 180° - 50°$, or $\phi = 65°$. It leads to :

$$1 \times \lambda = 2 \times 0.91 \sin 65° = 1.65 \text{ Å}$$ **(close to the calculated value,** cf. Eqn. 3.2.4.2)

Click Here for more Chemistry Library

Now let us consider the Fig. 3.2.6.4, where d = distance between the *Ni*-atoms on the surface of the crystal = 2.15 Å.

$$d' = \text{interplanar distance between the reflecting planes} = d \sin(\theta/2)$$

Bragg's law :

$$n\lambda = 2d' \sin\phi = 2d \sin(\theta/2) \sin\phi = 2d \sin(\theta/2) \sin(90^\circ - \theta/2) = 2d \sin(\theta/2) \cos(\theta/2) = d \sin\theta = 2.15 \sin 50^\circ = 1.65 \text{ Å (for } n = 1)$$

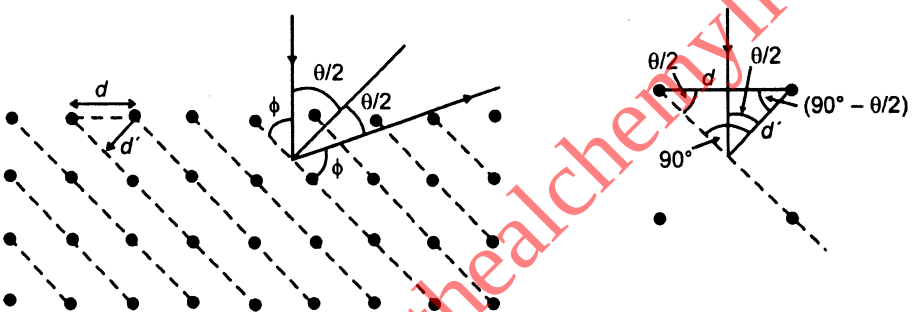

Fig. 3.2.6.4. Scattering of electron waves from the regularly spaced parallel planes in a crystal.

3.2.7 Bohr's Quantum Restriction from de Broglie Concept

According to Bohr's theory, the stationary orbits are defined by the relation, $mur = n(h/2\pi)$. Now in terms of wave-particle dualism, the revolving electron in a particular stationary orbit can be considered as a stationary wave, i.e. **the positions of its maxima (i.e. crests) and minima (i.e. troughs) do not change with time.** Such stationary waves can be obtained (Fig. 3.2.7.1), if the two ends of an electron wave meet in the same phase to produce a regular series of crests and troughs. To satisfy this condition, the circumference (= $2\pi r$) of the Bohr's circular orbit must be an integral multiple of the wavelength (λ), i.e.

$$2\pi r = n\lambda \qquad \ldots(3.2.7.1)$$

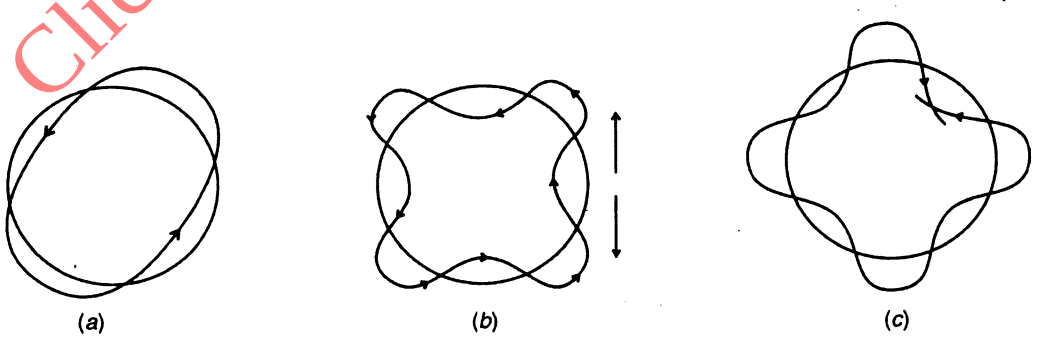

Fig. 3.2.7.1. Shapes of electron waves in a Bohr's electronic orbit (*a*, *b* : stationary waves; *c* : non-stationary wave).

Click Here t.me/thealchemylibrary

If the above condition is not maintained, the positions of crests and troughs will be changing with time and the electron wave will be out of phase giving rise to a destructive interference. Such electron waves are not stationary.

Now by considering the de Broglie's equation in the above condition (Eqn. 3.2.7.1), we have:

$$2\pi r = n(h/p);\ \text{or},\ 2\pi r = n(h/mu);\ \text{or},\ mur = n(h/2\pi)$$

which is the Bohr's quantum restriction to define a stationary orbit. Thus though the quantum restriction required to define a stationary orbit does not find any support in the classical theory, it gets a sound basis in the concept of wave-particle duality as proposed by de-Broglie.

3.3 THE HEISENBERG'S UNCERTAINTY PRINCIPLE AND ITS IMPLICATIONS

3.3.1 Uncertainty Principle

The **particle nature** of the electrons has been proved in the deflection by electrical or magnetic field. On the other hand, its **wave nature** has been experimentally verified in the diffraction studies by Davisson and Germer. In terms of wave-particle duality, the wavelength is given by, $\lambda = h/mu$. The relation shows that the **wave property (measured by λ)** and the **particle property (measured by momentum, *mu*)** are inversely proportional. Because of this dual behaviour of the subatomic microscopic particles (say, electron, neutron, etc.) which lie beyond the reach of our sense, it appears difficult to determine the exact position and momentum of such a particle at the same time. This problem was solved by Heisenberg by considering the theoretical aspects, and the corresponding principle is known as ***uncertainty principle. It states that it is impossible to determine the exact position and velocity (or momentum) of a subatomic particle simultaneously.***

The uncertainty principle is mathematically formulated as follows :

$$\boxed{\Delta x.\Delta p \approx (h/2\pi)} \qquad \ldots(3.3.1.1)$$

where Δx and Δp represent the uncertainties in determining the position and momentum of the particle respectively at the same time. It indicates that the product of the two uncertainties is approximately of the order of Planck's constant.*

The above Eqn. 3.3.1.1 indicates that the greater the accuracy in determining the position (i.e. Δx is small), the greater is the uncertainty in determining the momentum (i.e. Δp is high) and vice versa. **Thus a certainty in one quantity introduces an uncertainty in its conjugate quantity.** If one quantity is known free from error, the error in the other quantity becomes infinite. For example, if $\Delta x = 0$, then, $\Delta p \approx h/(2\pi\Delta x) = \infty$.

From Eqn. 3.3.1.1, the uncertainty in determining the velocity (Δu) can be obtained as follows:

$$\Delta p.\Delta x \approx h/(2\pi);\ \text{or},\ m\Delta u.\Delta x \approx (h/2\pi);\ \Delta u.\Delta x = h/(2\pi m) \qquad \ldots(3.3.1.2)$$

The uncertainty principle can also be applied for the **conjugate pair, energy and time.** It is obtained as follows. From the definition of frequency, the uncertainty in determining the frequency is given by :

* Different authors have considered different values of this constant. These are : h, $h/2\pi$, $h/4\pi$

Click Here t.me/thealchemylibrary

$\Delta\nu = 1/\Delta t$. The corresponding uncertainty in energy is related by $\Delta E = h\Delta\nu = h/\Delta t$; or, $\Delta E.\Delta t = h$. The more realistic treatment (cf. solved Problem 6) leads to:

$$\boxed{\Delta E.\Delta t \approx h/2\pi} \qquad \ldots(3.3.1.3)$$

Thus the relation is applicable to **any conjugate pair of variables** (e.g. momentum and position, energy and time, etc.). It can be concluded in a general way ***that the product of uncertainties of any two conjugate variables is always constant having the value h/2π approximately.***

3.3.2 Illustration of the Uncertainty Principle in the Determination of the Position of a Particle by a Microscope : Compton Effect and the Uncertainty Principle

To determine the position of a particle (say, an electron) with the help of a microscope, a beam of light is to interact with the particle through the microscope. The limit of accuracy of the determination of its position depends on the wavelength of the light used. To minimise this error, a light of shorter wavelength is preferred. But, the photon having a shorter wavelength will have a higher energy. These high energy photons during the collision with the electron particle will transfer their energy to the electron for recoiling according to Compton effect. Here it is worth mentioning that the electron can only be detected if the used photon collides with the electron and comes back. Thus during the collision between the photon and the electron, ***Compton effect is an unavoidable phenomenon*** specially when the light of shorter wavelength is used to minimise the error in determining the position. **Compton effect enhances the kinetic energy and consequently the momentum of the electron under observation,** thus both the measured quantities, i.e. momentum and position of the electron contain uncertainties. If the change in momentum of the electron under observation during the Compton effect is minimsed, the error in determining the position gets maximised.

The above phenomenon can be mathematically established by considering a model as discussed here. Let us consider an attempt to determine the position of an electron under a microscope (Fig. 3.3.2.1). Here, to locate the position of the electron, the incident photon on striking the electron must come back within the cone of angle 2α where α is the angular aperture of the microscope. The incident photon will undergo a Compton shift and the scattered photon with a lower frequency, i.e. higher wavelength, will enter into the microscope. The electron under observation will recoil with a higher momentum in the direction making an angle β with the x-axis, i.e. the direction of the incident photon.

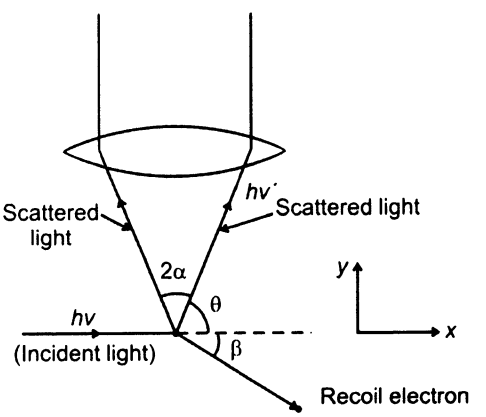

Fig. 3.3.2.1. Compton effect leading to the uncertainty principle.

From Fig. 3.3.2.1, according to the law of conservation of momentum along the x-axis, we get

$$\frac{h\nu}{c} = \frac{h\nu'}{c}\cos\theta + p\cos\beta;$$

$$\text{or, } p\cos\beta = \frac{h\nu}{c} - \frac{h\nu'}{c}\cos\theta \approx \frac{h\nu}{c}(1 - \cos\theta), \text{ (assuming } \nu \approx \nu')$$

Click Here 1.me/thealchemylibrary

Hence, $$p_x \approx \frac{h\nu}{c}(1 - \cos\theta) \quad \ldots(3.3.2.1)$$

where p_x stands for the component of momentum of the recoil electron along the x-axis.

From Fig. 3.3.2.1, it is evident that to observe the electron, θ can vary in the range $(90^o - \alpha)$ to $(90^o + \alpha)$. Hence, the momentum of the electron along the x-axis may have any value between the following two extremes.

$$p_{x(max)} = (h\nu/c)[1 - \cos(90 + \alpha)] = (h\nu/c)[1 + \sin\alpha], \text{ (putting, } \theta = 90^o + \alpha) \quad \ldots(3.3.2.2)$$

and, $$p_{x(min)} = (h\nu/c)[1 - \cos(90 - \alpha)] = (h\nu/c)[1 - \sin\alpha], \text{ (putting, } \theta = 90^o - \alpha) \quad \ldots(3.3.2.3)$$

Hence, the uncertainty in the value of p_x, i.e. the uncertainty in measuring the momentum along the x-axis, is given by :

$$\Delta p_x = p_{x(max)} - p_{x(min)} = 2(h\nu/c)\sin\alpha \quad \ldots(3.3.2.4)$$

Now the uncertainty in determining the location of a particle through a microscope depends upon its resolving power and it is given by :

$$\Delta x \approx \lambda/2(\sin\alpha) \quad \ldots(3.3.2.5)$$

Here Δx practically represents the minimum distance between the two points (in the field of view) that can be distinguished as separate points. In the present case, Δx gives the measure of uncertainty in the position x of the electron.

The above relation can be shown from the principle of classical optics. From Eqn. 3.3.2.4 and 3.3.2.5 we have :

$$\Delta p_x.\Delta x \approx \left(\frac{2h\nu\sin\alpha}{c}\right)\left(\frac{\lambda}{2\sin\alpha}\right) = h, \quad (\nu/c = 1/\lambda) \quad \ldots(3.3.2.6)$$

From rigorous calculations, it can be shown that

$$\Delta p_x.\Delta x \approx h/2\pi \quad \ldots(3.3.2.7)$$

The physical significance of Eqns. 3.3.2.4 to 3.3.2.7 can be pictured as discussed here. Eqn. 3.3.2.4 indicates that for a certain frequency of the photons, **the uncertainty in momentum is dependent on sin α, i.e. the angle of aperture of the instrument. Thus by making α small, Δp_x can be made minimised. But, from Eqn. 3.3.2.5, it is evident that for the smaller value of α, there will be a higher uncertainty in determining the position. On the other hand, according to Eqn. 3.3.2.4, the uncertainty in momentum can be made minimised for a certain aperture of the microscope by utilising the photons of low frequency (i.e. high wavelength), but according to Eqn. 3.3.2.5 the uncertainty in position gets increased.** Thus it is impossible to determine both the position and momentum precisely at the same time. The fundamental cause of this principle lies on the interaction between the particle and the measuring device. Here, **Compton effect is the fundamental cause of the uncertainty principle for the subatomic particles where the light of high frequency is to be used to determine their positions.**

Click Here t.me/thealchemylibrary

3.3.3. Applicability of the Uncertainty Principle to Large and Small Particles

i. In the case of large particles

Let us consider a ball of mass 2 g whose uncertainty in position is equal to 10^{-8} cm. Hence the corresponding uncertainty in its velocity would be :

$$\Delta u = \frac{h}{2\pi m \Delta x} = \frac{6.625 \times 10^{-34} \text{ J s}}{2 \times 3.14 \times 2 \times 10^{-3} \text{ kg} \times 10^{-10} \text{ m}} = 0.525 \times 10^{-21} \text{ m s}^{-1}$$

This uncertainty is definitely negligible to the usual velocity of the ball. Hence from the stand-point of practical consideration, both the velocity and position of the macroscopic particles can be determined precisely. Hence, in these cases, *the trajectories of these moving particles can be defined precisely.*

ii. In the case of small particles

Let us consider the fate of the electron in a hydrogen atom. The mass of an electron is 9.1×10^{-31} kg. Let us consider that the position of the electron from the nucleus can be determined with an uncertainty of 4 pm (i.e. 4×10^{-12} m). Thus it can be said (for instance) that the revolving electron may lie in the 1st Bohr orbit having r in the range 53 ± 4 pm. Hence the corresponding uncertainty in defining the velocity would be :

$$\Delta u = \frac{h}{2\pi m \Delta x} = \frac{6.625 \times 10^{-34} \text{ J s}}{2 \times 3.14 \times 9.1 \times 10^{-31} \text{ kg} \times 4 \times 10^{-12} \text{ m}} = 2.9 \times 10^{7} \text{ m s}^{-1}$$

Now we can compare this huge uncertainty with the expected velocity of the electron in the first Bohr's orbit. The expected velocity (u) of the electron from Bohr's theory is found to be 2.2×10^{6} m s^{-1}. **Thus it appears that Δu is much larger compared to the velocity of the electron.** Hence with such an uncertainty of velocity of the particle, the trajectory can never be defined. Thus, this principle strikes at the fundamental root of the Bohr's concept to have the existence of well defined orbits. ***Thus the Bohr's orbits become meaningless in the light of uncertainty principle.***

From the above examples, it appears that the uncertainty principle is of significance only for the microscopic particles like electrons, neutrons, etc. lying beyond the reach of our sense, but, for the macroscopic particles, it has got no significance.

3.3.4 Some Important Applications of the Uncertainty Principle

(a) An electron cannot exist in the nucleus but a proton or neutron can exist (cf. Solved Problem 14)

A typical nucleus is having radius less than 10^{-14} m. Hence, an electron to exist in the nucleus, its uncertainty in position cannot exceed the limit, 10^{-14} m, i.e. $\Delta x_{max} \approx 10^{-14}$ m. Hence, the corresponding uncertainty in its momentum is given by :

$$\Delta p_{min} = \frac{h}{2\pi \Delta x_{max}} = \frac{6.625 \times 10^{-34} \text{ J s}}{2 \times 3.14 \times 10^{-14} \text{ m}} = 1.1 \times 10^{-20} \text{ kg m s}^{-1}$$

This is actually the minimum possible uncertainty in determining its momentum. Thus to have any significant meaning of this happening, **the electron must have a momentum at least comparable**

Click Here : me/trealchemylibrary

with the value, i.e. 1.1×10^{-20} kg m s^{-1}. Now, if an electron possesses a momentum of the order of 10^{-20} kg m s^{-1}, its **classical kinetic energy** $\left(=\frac{p^2}{2m}\right)$ becomes much greater than the **rest mass energy** $(= m_0c^2)$. Under such conditions, we may find out the kinetic energy of the electron from the relativistic formula as follows:

relativistic kinetic energy of the electron $= pc = 1.1 \times 10^{-20}$ kg m $s^{-1} \times 3 \times 10^8$ m s^{-1}

$= 3.3 \times 10^{-12}$ J = 20.6 MeV, (1 eV = 1.6×10^{-19} J)

(cf. Eqn. 2.5.1.3, i.e. $E = \sqrt{m_0^2c^4 + p^2c^2} \approx \sqrt{p^2c^2}$ = K.E., when the rest mass energy is very small. In other words, relativistic kinetic energy $(T) = (m - m_o)c^2 \approx mc^2$ when $m >> m_o$, cf. Sec. 3.2.5).

Thus, it concludes that, if the electron is to be considered as a nuclear constituent, **it will have energy, at least, more than 20 MeV.** But experimentally it has been established that even for the most unstable atoms, an electron can never get associated with more than a fraction of this energy. Thus the consideration of electrons as nuclear constituents leads to an absurd result. **Based on this, *it can be firmly concluded that an electron cannot exist in a nucleus.***

Now, if the uncertainty principle is applied for the existence of protons within the nucleus, a strikingly different result is obtained. For a proton having momentum of the order of 1.1×10^{-20} kg m s^{-1}, the kinetic energy is much less than the rest mass energy, i.e. $T << m_0c^2$, (where m_0 stands for the rest mass of a proton). Under such conditions, **the kinetic energy of a proton can be calculated classically as follows:**

$$T = \frac{p^2}{2m} = \frac{(1.1 \times 10^{-20} \text{ kg m s}^{-1})^2}{2 \times 1.67 \times 10^{-27} \text{ kg}} = 3.6 \times 10^{-14} \text{ J} = 0.23 \text{ MeV}$$

The presence of such protons having kinetic energy of the order of 0.23 MeV in the nucleus is very much possible. Similarly, the existence of neutrons within the nucleus is also very much plausible.

Note : An electron cannot exist in a nucleus but a proton or neutron can exist there. This conclusion can also be supported from the result of the model, "***Particle in a Box***" (see Solved Problem 14).

(b) Probability concept of the electronic cloud

It has been shown that if a revolving electron is supposed to reside in the well defined trajectories, i.e. in the orbits of Bohr's model, then the uncertainty in its velocity becomes much greater than its expected velocity. Under this condition, an attempt to define a trajectory for the electron with its position and velocity, is of no significance. Thus, we can never locate the exact position around the nucleus for the revolving electron. Rather, we can define a probable region around the nucleus for the existence of the electron. **Thus, we have a *probability concept for the electronic cloud rather than a well defined trajectory for the electron.***

(c) Spectral band width and uncertainty principle

Let us consider the spectral transition from an excited state of an atom. The excited state radiates its excess energy by emitting photons of some characteristic frequency. Let us consider the average life period, Δt that passes between the time of excitation of the atom and the time when it emits energy. Hence, the larger the life time of the excited state, the larger is the Δt. Under the circumstances, the

Click Here t.me/tracienvylibrary

uncertainty of energy (ΔE) of the excited state is given by, $\Delta E.\Delta t = h/2\pi$; or, $\Delta E \approx h/(2\pi\Delta t)$. Hence, the uncertainty of frequency is given by, $\Delta\nu = \Delta E/h$; or, $\Delta\nu \approx 1/(2\pi\Delta t)$. Thus the frequency can have the uncertainty range, $\Delta\nu \approx 1/(2\pi\Delta t)$ and the corresponding transition has a band width $\Delta\nu$. This is called ***natural broadening*** **of the peak.** It indicates that the more the stability of the excited state, the more is the sharpness of the spectral peak. Thus a pure monochromatic transition (i.e. $\Delta\nu = 0$) is only expected when the life time of the excited state extends to infinity which is definitely impossible in practice. At high pressure (i.e, high concentration) and high temperature, due to the favourable mutual collisions, the life time (i.e. Δt) of an excited state decreases; and consequently the peak gets broadened. This is called ***collision broadening.*** **This is why, very often to have a sharp peak, spectral studies are to be carried out at low temperature and at low concentration.** This aspect has been specially realised in *nmr* and *esr* studies.

3.4 SCHRÖDINGER'S WAVE EQUATION

The above discussion evidently indicates that the **corpuscular nature of the electron** as considered by Bohr **violates the two fundamental laws,** viz, de Broglie's relation and the uncertainty principle, which successfully explain many properties of the electron. Besides this, it was required to have the **concept of probable distribution pattern of the electronic cloud rather than the well defined trajectory.** In this background, E. Schrodinger, an Austrian physicist introduced (1926) the mathematical concept of wave-particle dualism to the electron in an atom by considering the electron as a standing wave as in the case of a vibrating string fixed at both the ends. This new direction gave the development of wave mechanics to tackle the problems in both atomic and molecular physics.

Thus by considering the wave-like behaviour of the microscopic particles lying beyond the reach of our sense, Schrödinger gave a mathematical expression called, *Schrödinger's wave equation*. The equation can be applied to many cases, such as : **to the electrons to describe the atomic model; to the harmonic oscillators to define their energy levels; to the diatomic molecules to define their rotational and vibrational energy levels;** etc. The equation with *respect to space* can be written in the Cartesian coordinate system for the *stationary waves* (time independent) as follows :

$$\frac{\partial^2\psi}{\partial x^2} + \frac{\partial^2\psi}{\partial y^2} + \frac{\partial^2\psi}{\partial z^2} + \frac{8\pi^2 m}{h^2}(E - V)\psi = 0 \qquad \ldots(3.4.1)$$

Here, ψ (pronounced as *sigh*) is a mathematical function which is called ***wave function.*** ψ represents the amplitude of the matter wave associated with the particle at various points defined by *x, y, z* space coordinates with respect to a certain reference frame (e.g. in the case of an electron in an atom, *z, y, z* are defined with respect to the nucleus at 0, 0, 0), *m* stands for the mass of the particle, *h* is the Planck constant, *E* represents the total energy while *V* stands for the potential energy of the particle at the position *x, y, z*. The above second order differential equation is very often represented as :

$$\nabla^2\psi + \frac{8\pi^2 m}{h^2}(E - V)\,\psi = 0; \text{ where } \nabla^2 = \frac{\partial^2}{\partial x^2} + \frac{\partial^2}{\partial y^2} + \frac{\partial^2}{\partial z^2}$$

The term ∇^2 (pronounced as *del-square*) is called ***Laplacian Operator.***

3.4.1 Representation of Schrödinger's Wave Equation

Schrödinger's wave equation cannot be derived. In this regard, Newton's laws of motion in classical

Click Here to Join the Chemylibrary

mechanics are comparable. **In fact, both Newton's laws of motion and Schrödinger wave equation are the mathematical expressions of natural phenomena.** *The Schrödinger's wave equation, however, may be arrived by considering the fundamental equation representing a standing wave.* The equation for a **standing sine wave** of wavelength λ in a vibrating string fixed at the both ends is given by :

$$\boxed{\psi = A \sin (2\pi x/\lambda)} \qquad \ldots(3.4.1.1)$$

where ψ, called the wave function, represents the amplitude of the wave varying ***sinusoidally*** along the x-axis; A is a constant which gives the maximum amplitude.

On differentiating Eqn. 3.4.1.1 with respect to x, we get :

$$\frac{d\psi}{dx} = \left(A \cos \frac{2\pi x}{\lambda}\right)\left(\frac{2\pi}{\lambda}\right) = \frac{2\pi A}{\lambda} \cos \frac{2\pi x}{\lambda} \qquad \ldots(3.4.1.2)$$

On differentiating Eqn. 3.4.1.2 again with respect to x, we get,

$$\frac{d^2\psi}{dx^2} = \frac{2\pi A}{\lambda}\left(\frac{2\pi}{\lambda}\right)\left(-\sin \frac{2\pi x}{\lambda}\right) = -\frac{4\pi^2}{\lambda^2}\left(A \sin \frac{2\pi x}{\lambda}\right) = --\frac{4\pi^2}{\lambda^2}\psi;$$

or,
$$\frac{d^2\psi}{dx^2} + \frac{4\pi^2}{\lambda^2}\psi = 0 \qquad \ldots(3.4.1.3)$$

This is the ***classical wave equation*** **for the standing wave** as in the vibrating strings. The kinetic energy (T) of a moving particle of mass m and velocity u is given by :

$$T = \frac{1}{2}mu^2 = \frac{(mu)^2}{2m} = \frac{p^2}{2m}, (p = mu) \qquad \ldots(3.4.1.4)$$

Now from de Broglie's relation, $\lambda = h/p$, we get :

$$T = \frac{p^2}{2m} = \frac{h^2}{(2m\lambda^2)} \qquad \ldots(3.4.1.5)$$

Thus,
$$\frac{1}{\lambda^2} = \frac{2mT}{h^2} = \frac{2m}{h^2}(E - V) \qquad \ldots(3.4.1.6)$$

where, E = total energy = kinetic energy + potential energy = $T + V$. Now, using the value of $1/\lambda^2$ from Eqn. 3.4.1.6 in Eqn. 3.4.1.3, we get :

$$\frac{d^2\psi}{dx^2} + \frac{8\pi^2 m}{h^2}(E - V)\psi = 0 \qquad \ldots(3.4.1.7)$$

This is the Schrödinger's wave equation with respect to space* for a particle moving in one dimension, i.e. the matter wave is moving in the direction x. In three dimension, the equation becomes,

$$\frac{\partial^2\psi}{\partial x^2} + \frac{\partial^2\psi}{\partial y^2} + \frac{\partial^2\psi}{\partial z^2} + \frac{8\pi^2 m}{h^2}(E - V)\psi = 0 \qquad \ldots(3.4.1.8)$$

or,
$$\boxed{\nabla^2\psi + \frac{8\pi^2 m}{h^2}(E - V)\psi = 0} \qquad \ldots(3.4.1.9)$$

* For the Schrödinger's wave equation with respect to time, any standard textbook on modern physics can be consulted.

Click Here t.me/thealchemylibrary

The above Schrödinger's equation is also expressed in the following operator form,

$$\boxed{\left(-\frac{\hbar^2}{8\pi^2 m}\nabla^2 + V\right)\psi = E\psi;\ \text{or, } \hat{H}\psi = E\psi} \qquad \ldots(3.4.1.10)$$

where $\hat{H}$ is called the ***Hamiltonian Operator*** which is a function of various coordinates and potential energy V which is also a function of the coordinates.

3.4.2 Physical Significance of Schrödinger's Equation and Hamiltonian Operator

From the standpoint of the genesis of Schrödinger's wave equation, it is evident that the equation gets developed by incorporating the **nonclassical de Broglie's equation, $\lambda = h/(mu)$ into the classical wave equation.**

The Schrödinger's equation is given by :

$$E\psi = \frac{1}{2m}\left[-\hbar^2\frac{\partial^2\psi}{\partial x^2} - \hbar^2\frac{\partial^2\psi}{\partial y^2} - \hbar^2\frac{\partial^2\psi}{\partial z^2}\right] + V(x, y, z)\psi, \qquad \ldots(3.4.2.1)$$

or,
$$E\psi = \hat{K}\psi + \hat{V}\psi \qquad \ldots(3.4.2.2)$$

where $\hat{K}$ and $\hat{V}$ are operators; $\hat{K}$ and $\hat{V}$ stand for the kinetic and potential energy operators respectively; and $\hbar = h/2\pi$.

Now, let us try to have the significance of the operator $\hat{K}$. For this purpose, let us consider the expression for E in classical mechanics.

$$E = E_{kin} + E_{pot} \qquad \ldots(3.4.2.3)$$

$$= \frac{1}{2m}(p_x^2 + p_y^2 + p_z^2) + V(x, y, z) \qquad \ldots(3.4.2.4)$$

Comparing Eqns. 3.4.2.2 and 3.4.2.3, it reveals that corresponding to the classical E_{kin}, we have an operator $\hat{K}$ in wave mechanics. It is defined as :

$$\hat{K} = \frac{1}{2m}\left[-\hbar^2\frac{\partial^2}{\partial x^2} - \hbar^2\frac{\partial^2}{\partial y^2} - \hbar^2\frac{\partial^2}{\partial z^2}\right] = -\frac{\hbar^2}{2m}\nabla^2 \qquad \ldots(3.4.2.5)$$

Thus, it is evident that *corresponding to the classical momentum*, p_x there is an operator $\hat{p}_x$ in wave mechanics. Comparing Eqns. 3.4.2.4 and 3.4.2.5 we have :

$$(\hat{p}_x)^2 = -\hbar^2\frac{\partial^2}{\partial x^2} = i^2\hbar^2\frac{\partial^2}{\partial x^2} = \left(\pm i\hbar\frac{\partial}{\partial x}\right)^2, (i = \sqrt{-1})$$

Thus,
$$\hat{p}_x = -i\hbar\frac{\partial}{\partial x} \quad \text{and} \quad \hat{p}_x = i\hbar\frac{\partial}{\partial x}$$

Therefore, the operators corresponding to the momenta are :

$$\boxed{\hat{p}_x = -i\hbar\frac{\partial}{\partial x}, \hat{p}_y = -i\hbar\frac{\partial}{\partial y}, \hat{p}_z = -i\hbar\frac{\partial}{\partial z}}$$

Click Here t.me/thealchemylibrary

From the above discussions, it is evident that *corresponding to the classical kinetic energy E_{kin} there is an operator $\hat{K}$ in wave mechanics*. Thus the Hamiltonian operator $(\hat{H})$ is the sum of the operators for the kinetic energy and potential energy.

Thus, $$\hat{H} = \hat{K} + \hat{V} \text{ and } E\psi = (\hat{K} + \hat{V})\psi. \quad \ldots(3.4.2.6)$$

Comparing Eqns. 3.4.2.3 and 3.4.2.6, we see that the *Schrödinger's wave equation* (Eqn. 3.4.2.6) *is nothing but a wave mechanical analogue to the classical equation* (Eqn. 3.4.2.3) *of energy*.

3.4.3 Eigen Values and Eigen Functions

The Schrödinger's equation, being a second order differential equation may give rise to several solutions. All these solutions may not necessarily lead to any physical significance. **Acceptable solutions to the wave equation must satisfy the following conditions :**

(i) ψ must be **continuous** (cf. Fig. 3.4.3.1b).

(ii) ψ must be **finite** (cf. Fig. 3.4.3. la).

(iii) ψ must be **single valued**, i.e. at a particular point, there can never be more than one value for ψ (cf. Fig. 3.4.3. lc).

(iv) The first derivatives of ψ with respect to its variables $\left(\text{i.e. } \frac{\partial\psi}{\partial x}, \frac{\partial\psi}{\partial x} \text{ and } \frac{\partial\psi}{\partial x}\right)$ must be **continuous** with respect to x, y and z respectively. In other words, there must not exist any sudden change in ψ when its variables are changed (cf. Fig. 3.4.3.1d).

(v) The **probability of finding the particle** over the whole space must be unity. Mathematically it is represented by :

$$\int_{-\infty}^{+\infty} \psi^2 d\tau = 1, \ (d\tau \text{ gives the small volume element given by, } dx.\ dy.\ dz)$$

or, $$\int_{-\infty}^{+\infty} \psi^2 dx\, dy\, dz = 1$$

If, ψ is a complex function, then it would be $\int_{-\infty}^{+\infty} \psi\psi^* d\tau = 1$

where ψ^* is the conjugate wave function. Thus if, $\psi = a + ib$ then, $\psi^* = a - ib$ and consequently, $\psi\psi^*$ becomes real. **This is the *condition of normalisation of wave function.***

(vi) For the bound states, ψ as well as ψ^2 must vanish at infinity and in the case of a complex wave function $\psi\psi^*$ vanishes at infinity.

(vii) If ψ_1 and ψ_2 are two acceptable wave functions, they are orthogonal. **Condition of orthogonality** is :

$$\int_{-\infty}^{+\infty} \psi_1\psi_2 d\tau = 0$$

Some of the above conditions are pictorially represented in Fig. 3.4.3.1. The solutions, i.e. wave functions, which satisfy the above conditions are called **eigen functions** and the energies (E) corresponding to these eigen functions are called **eigen values.**

Click Here t.me/thealchemylibrary

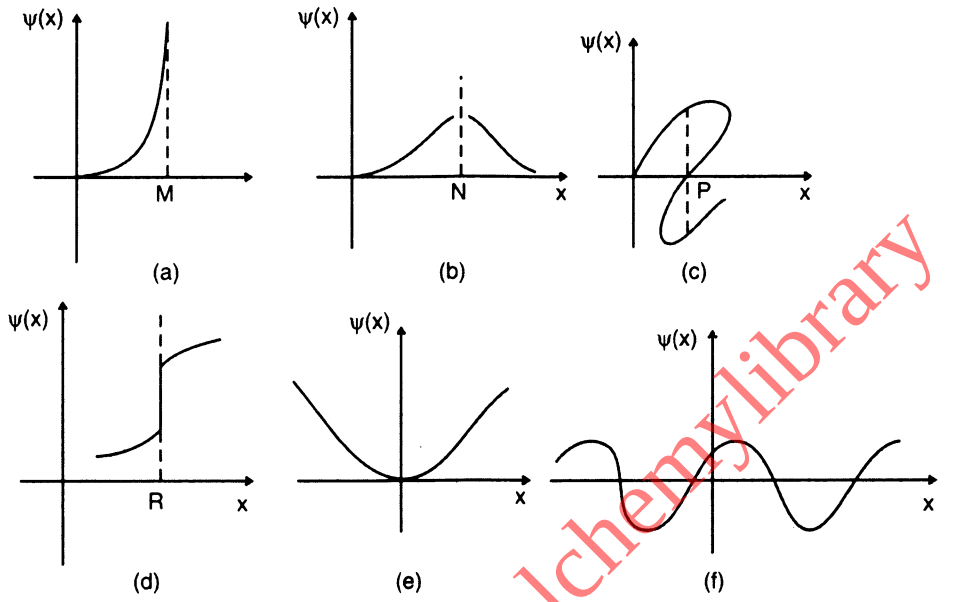

Fig. 3.4.3.1. Pictorial representation of the conditions of eigen wave functions. (a) not acceptable as it is infinite at *M*; (b) not acceptable as it is discontinuous at *N*; (c) not acceptable as it is multivalued at *P*; (d) not acceptable because though the function is continuous, the first derivative is not continuous (in other words, there is a sudden change at *R*); (e) not acceptable as $\int_{-\infty}^{+\infty} \psi^2 d\tau$ = infinite (in other words the function is not quadratically integrable). The present function x^2 leads to $\int_{-\infty}^{\infty} x^4 dx = \left|\frac{x^5}{5}\right|_{-\infty}^{\infty}$ $= \infty - (-\infty) = \infty$; (f) acceptable as the function and its first derivative are continuous, and other conditions are also satisfied.

3.4.4 Physical Significance of the Wave Function (ψ)

The eigen function (ψ) obtained from the Schrödinger's wave equation with respect to space has itself no physical significance while the ψ² (in general ψψ*) bears a meaningful significance. Here it is worth mentioning that the solution, i.e. ψ, may be a complex one and in such cases, ψ^2 contains the imaginary term which is of no practical significance. In such cases, ψψ* where **ψ* is the complex conjugate wave function,** (i.e. if, $\psi = a + ib$, then $\psi^* = a - ib$) is to be considered. Here, ψ^2 $(= a^2 + 2iab - b^2)$ is imaginary but ψψ* $(= a^2 + b^2)$ is a real quantity. If, ψ is a real one then $\psi = \psi^*$ and thus ψψ* becomes ψ^2. This is why, *in general we are to consider ψψ* for its interpretation.*

In classical mechanics, the **square of wave amplitude** (i.e. ψ) at any point associated with any electromagnetic radiation such as light waves, sound waves, etc. is interpreted as **a measure of *intensity effect*** at that point. By extrapolating this concept to the de Broglie's matter waves, **ψψ* or ψ^2 may be interpreted *as a measure of density of electronic charge* (when the wave equation is applied to the electron wave) or the particle at that particular point.** This interpretation was put forward by Schrödinger himself.

Another ***statistical interpretation*** of ψψ* or ψ^2 was given by Max Born in 1926. In this light, $\psi\psi^* d\tau$ or $\psi^2 d\tau$ is considered **as a measure of probability of finding the particle in the small volume**

Click Here t.me/thealchemylibrary

element, $d\tau$ (= $dx.dy.dz$) at a particular point defined by (x, y, z) in space. Thus, $\psi\psi^* d\tau$ or $\psi^2 d\tau$ is **proportional** to the probability of finding the particle in the volume $d\tau$. This latter interpretation is in good conformity with the demand of the Heisenberg's uncertainty principle. According to this principle, the position and momentum of a microscopic particle like an electron cannot be simultaneously measured exactly. Under such circumstances, the best thing what we can do is to predict the probability of existence of a microscopic particle in a certain region of space. The total probability over the whole space is unity (when the wave functions are normalised), i.e. $\int_{-\infty}^{+\infty} \psi\psi^* d\tau = 1$.

3.4.5 Normalised and Orthogonal Wave Functions

Here it is worth mentioning that, $\psi\psi^* d\tau$ or $\psi^2 d\tau$ is *proportional rather than equal* to the probability of finding the particle in the volume $d\tau$. If ψ is a solution to the wave equation, then $A\psi$ is also an acceptable solution to the same equation, where A is a constant. However, it is possible to evaluate a constant, N which is to be multiplied with ψ so that $(N\psi)(N\psi^*)d\tau$ gives the actual probability in the volume $d\tau$. This constant, N is called the *normalising constant*. It is evaluated as follows :

$$\int_{-\infty}^{+\infty} (N\psi)(N\psi^*)d\tau = 1; \quad \text{or, } N^2 \int_{-\infty}^{+\infty} \psi\psi^* d\tau = 1; \quad \text{or, } N^{-2} = \int_{-\infty}^{+\infty} \psi\psi^* d\tau$$

Hence, if ψ_1 and ψ_2 are two eigen functions and if they are **normalised,** then the following conditions are maintained,

$$\int_{-\infty}^{+\infty} \psi_1\psi_1^* d\tau = 1; \quad \text{and,} \quad \int_{-\infty}^{+\infty} \psi_2\psi_2^* d\tau = 1$$

and, if they are mutually **orthogonal,** then,

$$\int_{-\infty}^{+\infty} \psi_1\psi_2 d\tau = 0; \text{ or, } \int_{-\infty}^{+\infty} \psi_1^*\psi_2 d\tau = 0; \text{ or, } \int_{-\infty}^{+\infty} \psi_1\psi_2^* d\tau = 0$$

3.5 SOME APPLICATIONS OF THE SCHRÖDINGER'S WAVE EQUATION

3.5.1 Free Particle

Let us consider a particle (say, an electron) of mass m which is allowed to move freely without any restriction in a field. As there is no restriction in its movement, the potential energy may be assumed to be zero.

To find out the energy values (E) and wave functions (ψ) of the particle, we are to consider the Schrödinger's wave equation. Here the potential energy, $V = 0$. Thus, the Schrödinger's wave equation in one dimension becomes,

$$\frac{d^2\psi}{dx^2} + \frac{8\pi^2 m}{h^2}(E - V)\psi = 0; \text{ or, } \frac{d^2\psi}{dx^2} + \frac{8\pi^2 m}{h^2} E\psi = 0; \text{ (as, } V = 0) \qquad \ldots(3.5.1.1)$$

Click Here t.me/thealchemylibrary

The above equation has got the following solution,

$$\psi = A \sin (bx) + B \cos (bx) \qquad \ldots(3.5.1.2)$$

in which A, B and b are the arbitrarily chosen constant parameters for the present problem. Double differentiation of Eqn. 3.5.1.2 with respect to x, gives the result,

$$\frac{d^2\psi}{dx^2} = -b^2 [A \sin (bx) + B \cos (bx)] = -b^2\psi \qquad \ldots(3.5.1.3)$$

Now, comparing Eqns. 3.5.1.1 and 3.5.1.3, we get,

$$b^2 = \frac{8\pi^2 mE}{h^2} \qquad \ldots(3.5.1.4)$$

As there is no restriction in the movement of the particle in the field, the arbitrary constants A, B and b in the above Eqns. 3.5.1.2 and 3.5.1.4 can have any value. Thus, the wave function becomes,

$$\boxed{\psi = A \sin (\sqrt{8\pi^2 mE/h^2})\, x + B \cos (\sqrt{8\pi^2 mE/h^2})\, x} \qquad \ldots(3.5.1.5)$$

which is single valued, finite, and continuous with respect to x for any positive value of E. Thus the energy of the particle is given by :

$$\boxed{E = \frac{b^2h^2}{8\pi^2 m}} \qquad \ldots(3.5.1.6)$$

which is not quantised. Thus, a free particle moving in a field without any restriction has the continuous energy spectrum. On the other hand, a particle in a bound condition possesses the energy values which are quantised. Now, the occurrence of the discrete line spectra (even the band spectra for the molecules are consisting of some discrete lines) before ionisation of the atoms or molecules and the appearance of a continuum after ionisation can be rationalised. ***Before ionisation, the electron is bound in the atom or molecule with some restrictions and consequently the energy values are quantised, but after ionisation, the electron is free to move without any restriction and its energy values are not quantised.*** This is why, after ionisation, the atoms or molecules show the continuous spectrum.

3.5.2 Particle in a One Dimensional Box (cf. Sec. 12.3.2)

Let us consider a particle (say, an electron) of mass m which is subjected to move in a box in the x-direction from $x = 0$ to $x = a$. Thus the length of the box becomes a. The height of the walls at $x = 0$ and $x = a$ is infinite. Inside the box, the potential energy (V) of the particle is considered to be zero, so that it can move without any restriction within the box. But, at $x \leq 0$ and $x \geq a$, the potential energy is infinite. It means that the particle is fully confined within the box and it cannot escape from the box by crossing the walls of infinite height. The situation is shown in Fig. 3.5.2.1.

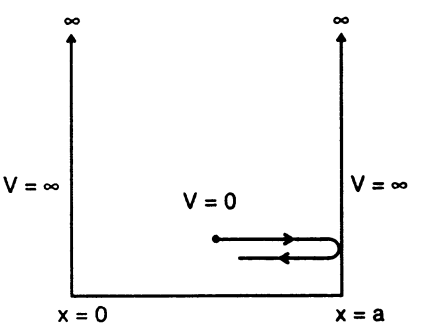

Fig. 3.5.2.1. Particle in a one dimensional rectangular box.

Click Here for more/thealchemylibrary

Now let us consider the Schrödinger's wave equation. Outside the box, it becomes,

$$\frac{d^2\psi}{dx^2} + \frac{8\pi^2 m}{h^2}(E - \infty)\,\psi = 0; (x \le 0, x \ge a) \qquad \ldots(3.5.2.1)$$

The equation is only satisfied if ψ is zero at all points outside the box and at the boundaries. In other words, there is no existence of the particle outside the box and at the boundaries.

Inside the box, the wave equation becomes,

$$\frac{d^2\psi}{dx^2} + \frac{8\pi^2 m}{h^2}(E - 0)\,\psi = 0; \text{ or, } \frac{d^2\psi}{dx^2} + \frac{8\pi^2 m}{h^2}E\psi = 0 \qquad \ldots(3.5.2.2)$$

The above equation has the following solution,

$$\psi = A \sin(bx) + B \cos(bx) \qquad \ldots(3.5.2.3)$$

where A, B and b are arbitrary constants.

On double differentiation, Eqn. 3.5.2.3 gives :

$$\frac{d^2\psi}{dx^2} = -b^2 [A \sin(bx) + B \cos(bx)] = -b^2\psi \qquad \ldots(3.5.2.4)$$

Comparing Eqns. 3.5.2.4 and 3.5.2.2, we get:

$$b^2 = (8\pi^2 mE)/h^2 \qquad \ldots(3.5.2.5)$$

Now let us apply the boundary conditions to find out the constants.

At, $x = 0$, $\psi = 0$, i.e.,

$$0 = A \sin(b \times 0) + B \cos(b \times 0) = A \sin(0) + B \cos(0); \text{ or, } B = 0$$

Thus, Eqn. 3.5.2.3 becomes,

$$\psi = A \sin(bx) \qquad \ldots(3.5.2.6)$$

At, $x = a$, $\psi = 0$, i.e., $0 = A \sin(ba) + 0 \times \cos(ba) = A \sin(ba)$, (as $B = 0$).

Here, A cannot be zero ($A \neq 0$). If $A = 0$, then it will lead to $\psi = 0$ for any value of x. It means that the particle does not exist in the box, and it is not acceptable. Hence, $\sin(ba) = 0 = \sin(n\pi)$, when $n = 0, 1, 2, 3,\ldots$

or,
$$ba = n\pi, \text{ or } b = n\pi/a \qquad \ldots(3.5.2.7)$$

Thus, the permitted wave functions are given by (using Eqns. 3.5.2.6 and 3.5.2.7) :

$$\psi = A \sin(n\pi x/a) \qquad \ldots(3.5.2.8)$$

where n is called the ***quantum number.*** Though the zero value of n is permitted, it leads to, $b = 0$ and $\psi = 0$ everywhere within the box. **Hence, $n = 0$ is not acceptable.** Thus, the quantum number (n) may have values, $n = 1, 2, 3....$ From Eqn. 3.5.2.5, we get :

$$\boxed{E = \frac{b^2h^2}{8\pi^2 m} = \frac{n^2h^2}{8ma^2}, \text{(using, } b = n\pi/a)} \qquad \ldots(3.5.2.9)$$

Click Here t me/thealchemylibrary

[*Note* :

- By considering the permitted values of wavelength $\left(\lambda = \frac{2a}{n}, \text{cf. Fig. 3.5.2.2}\right)$, from the relation $E = \frac{p^2}{2m}$ where the above mentioned results can be obtained (cf. Sec. 12.3.2).
- By using Sommerfeld's quantum restriction, the same result is also obtained (see solved Problem 9 in Chapter 1).]

Generally, the solutions for the eigen functions and eigen values are expressed for the quantum number n as follows,

$$\boxed{\psi_n = A \sin \frac{n\pi x}{a}} \qquad \ldots(3.5.2.10)$$

and

$$\boxed{E_n = \frac{n^2 h^2}{8ma^2} = n^2 E_1} \qquad \ldots(3.5.2.11)$$

It is evident that E_n value is independent of the coordinate of the particle.

If the potential energy within the box is not zero but constant and equal to V, then the energy of the particle for the quantum number n is given by :

$$E_n = \frac{n^2 h^2}{8ma^2} + V \qquad \ldots(3.5.2.12)$$

Here it is worth mentioning that compared to the free particle, the step leading to the introduction of the boundary conditions is responsible to the quantisation of the energy levels.

It is important to note that each eigen function (ψ) has one energy value but two momentum values :

$$E_n = \frac{p_x^2}{2m} + V = \frac{p_x^2}{2m}, (V = 0)$$

or,

$$\frac{p_x^2}{2m} = \frac{n^2 h^2}{8ma^2}; \text{ or } \boxed{p_x = \pm\sqrt{2mE_n} = \pm\frac{nh}{2a}}$$

- **Zero-point energy :** In the present case, where $V = 0$, the minimum energy which is purely a kinetic energy of the particle within the box is obtained for $n = 1$. **This is the lowest possible kinetic energy and it is called the *zero-point energy* which is given by :**

$$E_1 = E_{\text{zero-point}} = h^2/(8ma^2) \qquad \ldots(3.5.2.13a)$$

The existence of the zero-point energy which is nonzero indicates that even at 0 K, the particle is not at rest. Hence the position of the particle cannot be precisely determined even at 0 K. Hence, momentum of the particle cannot also be determined precisely. **Thus, *the existence of the zero-point energy is in conformity with the Heisenberg's uncertainty principle.*** Here it is noteworthy that in the classical mechanics, $E = 0$ is possible.

Click Here t.me/thealchemylibrary

• **Uncertainty principle :** By considering the uncertainty in position (Δx) and uncertainty in momentum (Δp_x) we get :

$\Delta x = a$ (because the particle may reside anywhere between o to a) and $\Delta p_x = +\left(\frac{nh}{2a}\right) - \left(-\frac{nh}{2a}\right) = \frac{nh}{a}$.

It leads to :

$$\boxed{\Delta p_x . \Delta x = nh = h \text{ (for } n = 1)} \quad \ldots(3.5.2.13b)$$

This result is in agreement with the uncertainty principle.

A. Normalisation and Orthogonality of the Eigen Functions of the Particle in a One Dimensional Box

From the condition of normalisation, the value of the constant A can be determined. Since, the probability of finding the particle within the box is unity, we can write:

$$\int_0^a \psi_n^2 \, dx = 1; \text{ or, } \int_0^a A^2 \sin^2\left(\frac{n\pi x}{a}\right) dx = 1$$

By using the relation, $\sin^2\theta = \frac{1}{2}(1 - \cos 2\theta)$, we get :

$$\frac{A^2}{2}\left[\int_0^a dx - \int_0^a \cos\left(\frac{2n\pi x}{a}\right) dx\right] = 1, \text{ or, } \frac{A^2}{2}(a - 0) = 1; \text{ or } A = \frac{\sqrt{2}}{\sqrt{a}}$$

Thus the normalised wave function of a particle in a one dimensional box is given by :

$$\boxed{\psi_n = \sqrt{2/a} \sin\frac{n\pi x}{a}} \quad \ldots(3.5.2.14)$$

Now to maintain the condition of orthogonality, the two normalised wave functions ψ_{n_1} and ψ_{n_2} for two different states of the particle within the box will be related as : $\int_0^a \psi_{n_1} \psi_{n_2} \, dx = 0$.

In the present case, it can be proved as follows that the above condition is attained.

$$\int_0^a \psi_{n_1} \psi_{n_2} \, dx = \frac{2}{a}\int_0^a \sin\left(\frac{n_1\pi x}{a}\right) \sin\left(\frac{n_2\pi x}{a}\right) dx$$

$$= \frac{1}{a}\int_0^a \left[\cos\left((n_1 - n_2)\frac{\pi x}{a}\right) - \cos\left((n_1 + n_2)\frac{\pi x}{a}\right)\right] dx$$

(cf. $\sin\alpha \sin\beta = \frac{1}{2}[\cos(\alpha - \beta) - \cos(\alpha + \beta)]$

$$= \frac{1}{2\pi}\left[\frac{a}{(n_1 - n_2)} \sin\left(\frac{(n_1 - n_2)\pi x}{a}\right) - \frac{a}{(n_1 + n_2)} \sin\left(\frac{(n_1 + n_2)\pi x}{a}\right)\right]_0^a = 0$$

Thus the eigen functions expressed in Eqn. 3.5.2.14 are normalised and orthogonal.

Click Here to me/thealchemylibrary

B. Characteristic Features of ψ_n, ψ_n^2 and E_n of the Particle within the One Dimensional Box

Fig. 3.5.2.2 shows the behaviour of ψ_n and ψ_n^2 and E_n with respect to x for different quantum numbers. The following points are noteworthy.

(i) **Internal nodal points :** For the ground state or lowest state wave function (i.e. $n = 1$), within the box there is no point except the boundaries for which the wave function is zero. On the other hand, for $n = 2, 3, 4,...$ there are one, two, three,... points respectively for which the corresponding wave function is zero. These points are called ***internal nodal points.*** At the nodal points, the probability of finding the particle is zero. **In general, for the quantum number *n*, there are $(n - 1)$ internal nodal points.** It is also evident from the wave equation as follows :

$$\psi_1 = \sqrt{\frac{2}{a}} \sin\left(\frac{\pi x}{a}\right), \text{(for } n = 1, \psi_1 = 0 \text{ only at } x = 0 \text{ and } a \text{ i.e. boundaries)}$$

Thus for ψ_1, there is ***no internal nodal point.***

$$\psi_2 = \sqrt{\frac{2}{a}} \sin\left(\frac{2\pi x}{a}\right) = 0 \text{ for } x = 0, \frac{1}{2}a \text{ and } a \text{ i.e. there is only } \textit{one internal nodal} \text{ point at } a/2.$$

$$\psi_3 = \sqrt{\frac{2}{a}} \sin\left(\frac{3\pi x}{a}\right) = 0 \text{ for } x = 0, \frac{a}{3}, \frac{2a}{3} \text{ and } a \text{ i.e. there are } \textit{two internal nodal points.}$$

It indicates that there are **$(n - 1)$ internal nodal points.**

(ii) **Probability of finding the particle as a function of *x* :** The probability of finding the particle depends on x. The probability of finding the particle at a particular point is given by $\psi_n^2\, dx$.

$$\psi_n^2\, dx = \left\{\sqrt{\frac{2}{a}} \sin\frac{n\pi x}{a}\right\}^2 dx = \frac{2}{a}\sin^2\left(\frac{n\pi}{a}x\right)dx$$

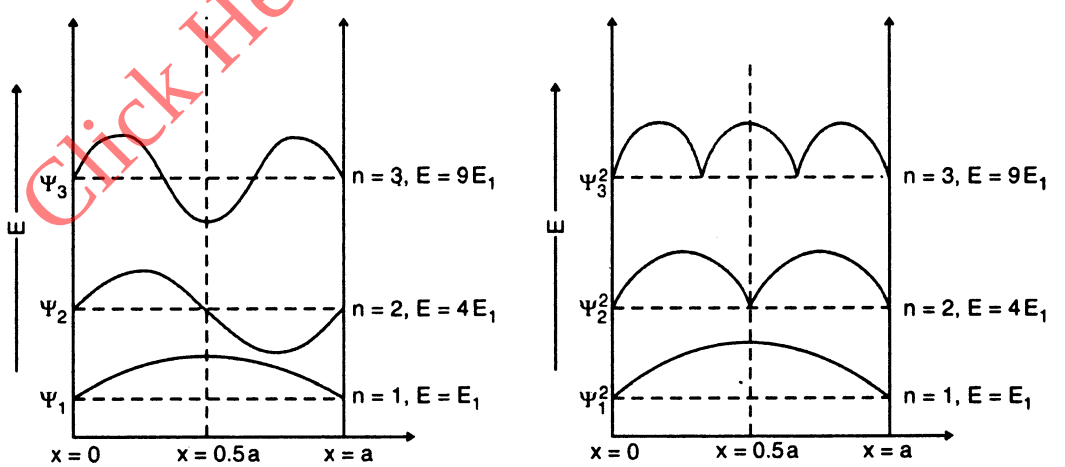

Fig. 3.5.2.2. The energy states, wave functions and probability densities of a particle in a one dimensional box.

Click Here t.me/thealchemylibrary

$$= \frac{2}{a}\sin^2\left(\frac{2\pi}{\lambda}x\right)dx, [a = n(\lambda/2), cf. \text{Eqn. } 3.5.2.15]$$

- For $n = 1$, $\psi_1 = 0$ only at the boundaries, i.e. for $x = 0$ and a, there is no nodal point between $x = 0$ to $x = a$. The maximum probability of finding the particle is at the centre of the box i.e. at $x = a/2$.
- For $n = 2$ (i.e. first excited state), ψ_2 vanishes at $x = a/2$ (i.e. *nodal point*). Thus ψ_2 vanishes at $x = 0$, $a/2$ and a. Thus the maximum probability of finding the particle exists at $x = a/4$ and $3a/4$. *It is interesting to note that though the particle has zero probability of its existence at the centre of the box, it has a finite probability of its existence at either side of the internal nodal point.* It indicates that the particle can travel from one side to another even without crossing the middle point of the box. It can be rationalised, if it is assumed that the particle is smeared as a wave over the entire space. *If the electron were considered as a particle, then it would not be possible.*

(iii) **Nature of wave function and energy depending on *n* :** *It is evident that with the increase of n, the number of nodes increases and the wavelength decreases and it corresponds to the increase of total energy which is the kinetic energy in nature in the present case.*

(iv) **Wavelength of the wave function :** The wave functions to be zero at the walls, **the length of the box must be an integral multiple of half-wavelength,**

i.e. $$\boxed{a = n(\lambda/2)} \qquad \ldots(3.5.2.15)$$

It can be easily proved as follows. Here the particle is having only kinetic energy, as the potential energy is assumed to be zero. Hence,

$$E_n = (1/2)mu^2 = p^2/(2m) = (h/\lambda)^2/(2m) = h^2/(2m\lambda^2) \qquad \ldots(3.5.2.16)$$

(cf. $\lambda = h/p$, de Broglie equation)

Again E_n is given by :

$$\boxed{E_n = \frac{n^2h^2}{8ma^2}} \qquad \ldots(3.5.2.17)$$

By comparing Eqns. 3.5.2.16 and 3.5.2.17 we get :

$$\frac{h^2}{2m\lambda^2} = \frac{n^2h^2}{8ma^2}; \text{ or, } \frac{1}{\lambda^2} = \frac{n^2}{4a^2}; \text{ or, } a = n(\lambda/2)$$

(v) **Even and odd functions :** Based on the symmetry of the functions with respect to the mid-point of the box, the wave functions can be classified as ***symmetric* or *even functions*** having a centre of symmetry and ***antisymmetric or odd functions*** having no centre of symmetry. From Fig. 3.5.2.2, it is evident that the ψ_1, ψ_3, ψ_5 ...are the symmetric functions while ψ_2, ψ_4, ψ_6, ...are the antisymmetric functions.

(vi) **Bohr's correspondence principle :** From the plot of ψ_n^2 against x, *it is evident that the probability distribution is not uniform and it is a function of x. This behaviour is markedly pronounced for the lower quantum numbers*. For the higher values of the quantum numbers, the probability distribution pattern becomes more and more uniform. **As a matter of fact, for the very large values of quantum numbers, the probability distribution becomes more or less identical at**

Click Here to me/heal chemy library

any value of x within the box. The same conclusion is drawn from the classical mechanics. It indicates that for the large values of n, both the quantum mechanics and classical mechanics lead to the same conclusion. This fact is in good agreement with the **Bohr's *correspondence principle.***

(vii) **Comparison with the behaviour of free particles and macroscopic particles :** The energy difference (ΔE) between the successive energy levels is given by :

$$\boxed{\Delta E = E_{n+1} - E_n = \frac{(n+1)^2 h^2}{8ma^2} - \frac{n^2 h^2}{8ma^2} = \frac{(2n+1)h^2}{8ma^2} = (2n+1)E_1} \quad \text{...(3.5.2.18)}$$

The energy difference decreases as the length of the box increases. **For the free particle moving in an unbound region without any restriction, the length (a) becomes very large (theoretically infinite)** *and as a result, the energy difference between the successive levels becomes almost zero.* In other words, it can be said that the energy levels for the free particles produce a continuous spectrum and the same result was obtained from the solution of the Schrödinger's equation when applied to the free particle.

For the macroscopic particles, the masses are sufficiently high and the box length is also quite large. For such systems, $\Delta E \to 0$ and it leads to a continuous spectrum of the energy levels. The same conclusion is also drawn from the classical mechanics when applied to the macroscopic particles. Thus, the results obtained for the macroscopic particles from the Schrödinger's equation are in good conformity with the ***correspondence principle.*** But when the model is applied for the microscopic particles like an electron for which the mass is very small and the length of the box is of the order of atomic or molecular dimension, it leads to quantised energy levels which are not expected from the classical mechanics.

(viii) **Uncertainty principle and zero-point energy :** The importance of ***zero-point energy*** in connection with the ***uncertainty principle*** has been discussed. It has been shown that the model can lead to $\Delta p_x \cdot \Delta x = h$ (i.e. uncertainty principle) (cf. Sec. 3.5.2.13b).

3.5.3 Particle in a Three Dimensional Box

Let us consider a particle of mass m moving in a three dimensional rectangular box having the sides a_x, a_y and a_z along the x, y and z axes respectively. Let us consider the potential energy within the box to be zero while at the boundaries and outside the box, it is infinite. Thus, the Schrödinger's equation within the box is then given by :

$$\frac{\partial^2 \psi}{\partial x^2} + \frac{\partial^2 \psi}{\partial y^2} + \frac{\partial^2 \psi}{\partial z^2} + \frac{8\pi^2 m}{h^2} E\psi = 0 \quad \text{...(3.5.3.1)}$$

Since the wave function (ψ) depends on the coordinates, it can be assumed that the wave function ψ is the product of three wave functions namely, ψ_x, ψ_y and ψ_z which are separately dependent on x, y and z respectively. Thus,

$$\psi = \psi_x \psi_y \psi_z \quad \text{...(3.5.3.2)}$$

Therefore,
$$\frac{\partial \psi}{\partial x} = \psi_y \psi_z \frac{d\psi_x}{dx}; \ (\psi_x \text{ depends only on } x);$$

or,
$$\frac{\partial^2 \psi}{\partial x^2} = \psi_y \psi_z \frac{d^2 \psi_x}{dx^2} \quad \text{...(3.5.3.3)}$$

Click Here t.me/thealchemylibrary

Similarly we can have :

$$\frac{\partial^2\psi}{\partial y^2} = \psi_x\psi_z\frac{d^2\psi_y}{dy^2} \qquad \ldots(3.5.3.4)$$

and

$$\frac{\partial^2\psi}{\partial z^2} = \psi_x\psi_z\frac{d^2\psi_z}{dz^2} \qquad \ldots(3.5.3.5)$$

Substituting the above relations given by Eqns. 3.5.3.3 – 3.5.3.5 in Eqn. 3.5.3.1 we get :

$$\psi_y\psi_z\frac{d^2\psi_x}{dx^2} + \psi_x\psi_z\frac{d^2\psi_y}{dy^2} + \psi_x\psi_y\frac{d^2\psi_z}{dz^2} + \frac{8\pi^2m}{h^2}E\,\psi_x\psi_y\psi_z = 0;$$

or,

$$\frac{h^2}{8\pi^2m}\left(\frac{1}{\psi_x}\frac{d^2\psi_x}{dx^2} + \frac{1}{\psi_y}\frac{d^2\psi_y}{dy^2} + \frac{1}{\psi_z}\frac{d^2\psi_z}{dz^2}\right) + E = 0 \qquad \ldots(3.5.3.6)$$

In this equation, the first term is a function of x only and independent of y and z; the second term is a function of y only and independent of x and z; similarly, the third term is a function of z only and independent of x and y. The fourth term is a constant. Now, if x is varied keeping y and z constant, the second and third terms will remain constant. Now, since the fourth term is a constant, the first term will also be a constant. Let it be E_x. Based on the similar arguments, the second and third terms must be constant separately, say E_y and E_z respectively. Thus Eqn. 3.5.3.6 can be split into three differential equations.

$$\frac{h^2}{8\pi^2m}\left(\frac{1}{\psi_x}\frac{d^2\psi_x}{dx^2}\right) + E_x = 0;$$

or,

$$\frac{d^2\psi_x}{dx^2} + \frac{8\pi^2mE_x}{h^2}\psi_x = 0 \qquad \ldots(3.5.3.7)$$

and,

$$\frac{d^2\psi_y}{dy^2} + \frac{8\pi^2mE_y}{h^2}\psi_y = 0 \qquad \ldots(3.5.3.8)$$

and,

$$\frac{d^2\psi_z}{dz^2} + \frac{8\pi^2mE_z}{h^2}\psi_z = 0 \qquad \ldots(3.5.3.9)$$

and also,

$$E = E_x + E_y + E_z \qquad \ldots(3.5.3.10)$$

Eqns. 3.5.3.7 – 3.5.3.10 can be solved in the same way as in the case of a one dimensional box. Thus, the normalised wave functions and the energies are given by,

$$\psi_x = \sqrt{2/a_x}\,\sin\left(\frac{n_x\pi x}{a_x}\right) \qquad \ldots(3.5.3.11)$$

$$E_x = \frac{n_x^2h^2}{8ma_x^2} \qquad \ldots(3.5.3.12)$$

$$\psi_y = \sqrt{2/a_y}\,\sin\left(\frac{n_y\pi y}{a_y}\right) \qquad \ldots(3.5.3.13)$$

Click Here to the chemylibrary

$$E_y = \frac{n_y^2 h^2}{8ma_y^2} \qquad \ldots(3.5.3.14)$$

$$\psi_z = \sqrt{2/a_z}\,\sin\left(\frac{n_z \pi z}{a_z}\right) \qquad \ldots(3.5.3.15)$$

$$E_z = \frac{n_z^2 h^2}{8ma_z^2} \qquad \ldots(3.5.3.16)$$

Therefore the eigen functions and eigen values of Eqn. 3.5.3.1 are given by :

$$\boxed{\psi = \psi_x \psi_y \psi_z = \sqrt{\frac{8}{a_x a_y a_z}}\,\sin\left(\frac{n_x \pi x}{a_x}\right)\sin\left(\frac{n_y \pi y}{a_y}\right)\sin\left(\frac{n_z \pi z}{a_z}\right)} \qquad \ldots(3.5.3.17)$$

and,

$$\boxed{E = E_x + E_y + E_z = \frac{h^2}{8m}\left(\frac{n_x^2}{a_x^2} + \frac{n_y^2}{a_y^2} + \frac{n_z^2}{a_z^2}\right)} \qquad \ldots(3.5.3.18)$$

If the box is a cubic one, $a_z = a_y = a_x = a$, then,

$$\boxed{E = \frac{h^2}{8ma^2}\left(n_x^2 + n_y^2 + n_z^2\right)} \qquad \ldots(3.5.3.19)$$

The occurrence of three quantum numbers (i.e. n_x, n_y, n_z) is a characteristic property of a three dimensional problem in wave mechanics. Here the **zero-point energy** (for, $n_x = n_y = n_x = 1$) is three times that of a one dimensional box.

A. Degeneracy of the Energy Levels

The existence of three quantum numbers in a three dimensional problem, introduces the existence of degenerate energy levels. The **lowest energy, i.e. the zero-point energy arises** for $n_x = n_y = n_z = 1$ and it is given by :

$E_1 = 3(h^2/8ma^2)$, (assuming, $a_x = a_y = a_x = a$)

$= 3E_0$, (where, $E_0 = h^2/8ma^2$)

The first excited state (E_2) arises when one quantum number becomes 2 and the other two are remaining unity each. Thus for E_2, there are three possibilities for the (n_x, n_y, n_z) set and these are (1, 1, 2), (1, 2, 1), (2, 1, 1). The energy of each possibility will be identical and it is given by $E_2 = 6E_0$. Similarly, the E_3 level will also be triply degenerate denoted by (1, 2, 2), (2, 1, 2) and (2, 2, 1) and each of which is having energy $9E_0$. For E_4, it is again triply degenerate given by (3, 1, 1), (1, 3, 1), (1, 1, 3) where $E_4 = 11E_0$ but E_5 given by $12E_0$ is nondegenerate and denoted by (2, 2, 2). The E_6 is sixfold degenerate. The existence of these degenerate levels is shown in Fig. 3.5.3.1.

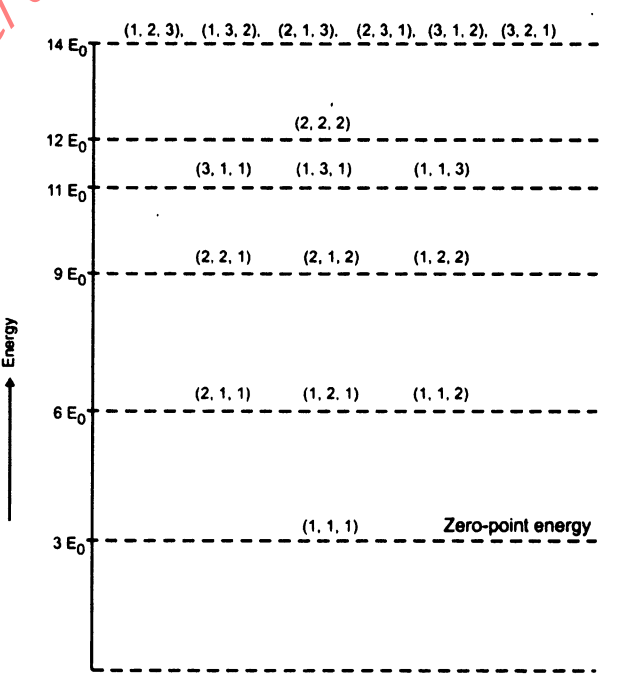

Fig. 3.5.3.1. The energy states (showing the occurrence of degenerate energy levels) of a particle in a three dimensional box.

Click Here to me/trealchemylibrary

B. Distortion of the Cubic Box and Fate of the Degeneracy

Now let us look into the fate of the degenerate energy levels due to distortion of the cubic symmetry. When the box is perfectly cubic, i.e. $a_x = a_y = a_z = a$, the energy of the state (2, 1, 1) is given by :

$$E_{(2,\,1,\,1)} = E_x + E_y + E_z = 4h^2/(8ma^2) + h^2/(8ma^2) + h^2/(8ma^2)$$

Now let us consider the distortion (say *elongation*) of the box along the x-axis by da. The new energy after distortion along the x-axis is $(E_x + dE_x)$.

Hence the new energy of the particle for the state (2, 1, 1) becomes,

$$E_{(2,1,1)} + dE_x = E_x + dE_x + E_y + E_z = 4h^2/(8ma^2) - \frac{h^2 da}{ma^3} +$$

$$h^2/(8ma^2) + h^2/(8ma^2) = 6h^2/(8ma^2) - \frac{h^2 da}{ma^3}$$

Thus the energy for the state (1, 2, 1) is given by,

$$E_{(1,2,1)} + dE_x = \left(\frac{h^2}{8ma^2} - \frac{h^2}{4ma^3}da\right) + \frac{4h^2}{8ma^2} + \frac{h^2}{8ma^2} = \frac{6h^2}{8ma^2} - \frac{h^2}{4ma^3}da$$

Similarly, $E_{(1,1,2)} + dE_x = \dfrac{6h^2}{8ma^2} - \dfrac{h^2}{4ma^3}da$

Thus, the distortion along the x-axis by da gives the energy states for E_2 as follows,

$\dfrac{6h^2}{8ma^2} - \dfrac{h^2}{ma^3}da$ for (2, 1, 1) state; $\dfrac{6h^2}{8ma^2} - \dfrac{h^2}{4ma^3}da$ for both (1, 2, 1) and (1, 1, 2) states.

Thus, it is seen that on distortion of the cube by da along the x-axis, the three-fold degenerate energy levels for E_2 are split into a nondegenerate level and two degenerate levels; and the energies of the new states are lowered compared to those of the undistorted ones.

It is a very common experience in chemistry that on a slight distortion, the electronic degeneracy of a system is removed and the energies of the new states are lowered down. Here the analogous phenomenon, *Jahn-Teller effect* can be mentioned. According to this theorem, *any nonlinear molecular system possessing degenerate electronic states will undergo a distortion giving rise to a system of lower symmetry of lower energy and the degeneracy will be removed.* Thus, such a nonlinear molecule undergoes a distortion from its most symmetric configuration to attain a configuration of lower symmetry and lower energy.

3.5.4 Importance of the Model - Particle in a Box

In dealing with the problem, *particle in a box*, the potential energy within the box is chosen either constant or zero. Such simple systems are really far away from the naturally occurring systems dealing with the problems of physics and chemistry. Hence apparently, it is quite natural to think that such simple systems can hardly throw any light on the real problems of chemical interest. Here it is worth

Click Here t.me/thealchemylibrary

mentioning that any real problem except the simplest hydrogen atom, in the light of wave mechanics is so complicated that the exact solution of the second order differential equation can hardly be obtained. But, in the simple problem like the particle in a box, we get the exact solutions which provide us with a proper insight in understanding and interpretation of the complex systems occurring in reality. The simple problem, on solution, yields some results which are very much quantum mechanically important. These are :

(i) concept of **quantisation of energy,**
(ii) existence of **quantum numbers,**
(iii) occurrence of three quantum numbers in three dimensional wave mechanical problems,
(iv) existence of **zero-point energy** in favour of ***Heisenberg's uncertainty principle,***
(v) good agreement with the ***correspondence principle,***
(vi) **removal of degeneracy** and attainment of the systems of lower symmetry and lower energy due to distortion,
(vii) lowering of energy of a system with the increase of the dimension of the box,
(viii) existence of ***nodal points*** within the box, etc.

3.5.5 Some Applications of the Model - Particle in a Box

(a) Stabilisation due to Conjugation, i.e. Delocalisation

It is well known that the systems having conjugated double bonds are stabler than the systems having isolated double bonds. Let us take two systems (Fig. 3.5.5.1) for example, in which the system **(I)** has conjugated double bonds and the system **(II)** has isolated double bonds. In the system **(I)**, due to the delocalisation of the π-electron cloud, the π-electrons can travel a longer length of the chain while such a delocalisation is not possible in the system **(II). These systems can be compared with the model, particle in a one dimensional box, where the particle is the π-electron and the length of the carbon chain through which the π-electron cloud can delocalise or travel gives the measure of the length of the box.** Now, we can consider the energy of the particle (i.e. electron) in this model (without considering the electron-electron repulsion) and it is given by, $E_n = n^2h^2/(8ma^2)$. From the above expression, it is evident that as the length of the box increases, the energy of the allowed levels decreases. In the conjugated systems, due to the delocalisation, the length through which the electron can move is much greater compared to the available length for electron movement in the nonconjugated systems where the π-electron cloud is localised between the adjacent carbon atoms. **This is why, the conjugated polyenes are stabler than the nonconjugated ones.**

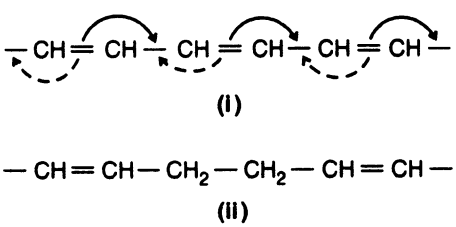

Fig. 3.5.5.1. Delocalisation in a conjugated polyene (I) compared to the system (II) having isolated double bonds.

This concept can be utilized to explain the stabilization due to the ***resonance and exchange phenomenon.***

Click Here to meethealchemylibrary

(b) Factors Influencing the Electron Transition Energy : Colour and Broadening of Peaks

The conjugated polyenes can be compared with the model, ***particle in a one dimensional box***, in which the length of the box is given by the length of the carbon - carbon chain through which the π-electron cloud can delocalise. The electrons can be placed in different allowed energy levels according to the *aufbau* principle along with the Pauli exclusion principle. The energy difference between the highest occupied level (n) and the lowest unoccupied level ($n + 1$) gives the measure of electron transition energy. This energy difference is obtained as follows :

$$\Delta E = E_{n+1} - E_n = \frac{(n+1)^2 h^2}{8ma^2} - \frac{n^2 h^2}{8ma^2} = (2n+1)\frac{h^2}{8ma^2} = (2n+1)E_1$$

Hence, the frequency (ν) and wave number ($\bar{\nu}$) of the transition are given by :

$$\nu = \Delta E / h = \frac{(2n+1)h}{8ma^2} \qquad \ldots(3.5.5.1)$$

and

$$\bar{\nu} = \Delta E /(hc) = \frac{(2n+1)h}{8ma^2 c} \qquad \ldots(3.5.5.2)$$

In the case of butadiene, there are four π-electrons which occupy the first two energy levels having $n = 1, 2$. Hence the electron transition occurs from, $n = 2 \rightarrow n = 3$. By taking the length of the molecule, $a = 5.78 \times 10^{-8}$ cm, the wave number can be given theoretically by using Eqn. 3.5.5.2.

$$\bar{\nu} = \frac{(2\times 2+1)\times 6.625\times 10^{-34}\ \text{J s}}{8\times 9.11\times 10^{-31}\ \text{kg} \times (5.78\times 10^{-10}\ \text{m})^2 \times 3\times 10^{8}\ \text{m s}^{-1}} = 4.53\times 10^{6}\ \text{m}^{-1}$$

The experimental value is $4.61 \times 10^6\ \text{m}^{-1}$. Thus, the calculated value agrees well with the experimental observation.

From the above relation given by Eqn. 3.5.5.1, it is evident that the colour due to the electron transition in the polyenes is sharply dependent on the length of conjugation (i.e. a). With the increase of conjugation in the linear polyenes, the frequency of transition moves to the lower region i.e. **red shift or bathochromic shift.** Thus the partial reduction, i.e. hydrogenation of the double bonds, in the conjugated systems leads to a decrease in the length of conjugation and as a result, **the colour shifts to red (i.e. the frequency of absorption moves to the higher direction) known as blue shift or hypsochromic shift.**

Let us take three conjugated polyenes: butadiene, vitamin A, and carotene (Fig. 3.5.5.2) to illustrate the above conclusion. The colours of these conjugated polyenes are as follows : ***Butadiene*** - colourless; ***Vitamin A*** - orange yellow; ***Carotene*** - ruby red. Comparing these polyenes with the model, particle in a one dimensional box, the trend of the colours of the compounds can be explained. According to this model, the minimum energy required for the electron transition occurs as follows:

butadiene : $n_i = 2 \rightarrow n_f = 3$ > **vitamin A :** $n_i = 5 \rightarrow n_f = 6$ > **carotene :** $n_i = 11 \rightarrow n_f = 12$

The lengths of the polyenes are in the sequence : carotene > vitamin A > butadiene.

Hence, according to Eqn. 3.5.5.1, the frequency of absorption lies in the reverse sequence, i.e.

$$\nu_{(\text{butadiene})} > \nu_{(\text{vitamin A})} > \nu_{(\text{carotene})}.$$

Click Here 1. The/headchemylibrary

As a matter of fact, for the butadiene, the absorption occurs in the ultraviolet region (λ = 217 nm) while for the other two polyenes, the absorption occurs in the visible range. **This is why, vitamin A and carotene are coloured while butadiene is colourless.** Actually, for butadiene, the absorption occurs at UV-region; for vitamin A, the absorption occurs at about 332 nm and for carotene it occurs at still higher wavelength.

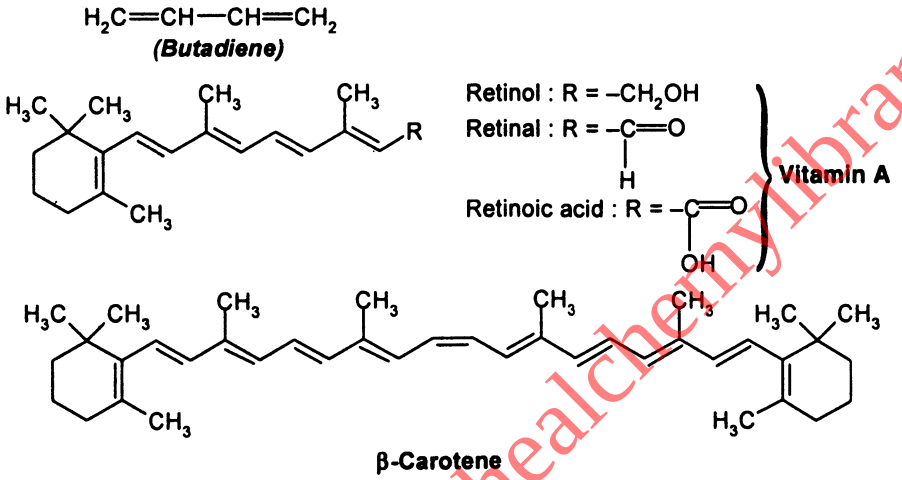

Fig. 3.5.5.2. Structures of butadiene, vitamin A and carotene showing the extent of conjugation.

Another important observation is that the large polyenes like vitamin A, carotene, etc. show **broad absorption peaks.** Actually, it follows the trend : ***the more the length of the polyene, the more is the broadening of peak.*** It is also expected from the model. **For the higher length of the polyene, the energy difference between the successive levels decreases and as a result, for a particular value of $\nu \pm \Delta\nu$ there are a number of possible ways of electron transition.** Thus, the **band width** of the three polyenes lies in the sequence:

carotene > vitamin A > butadiene.

(c) Explanation of Jahn-Teller Distortion

It has been noted that in the model, particle in a three dimensional cubic box, due to the occurrence of three quantum numbers, a number of degenerate energy levels appears. **But due to slight distortion in a particular direction, the degeneracy is removed and the system moves to adopt a new system which is having a lower symmetry and a lower energy.** In the nonlinear molecules, the same thing occurs in Jahn-Teller distortion. This aspect has been already discussed in Sec. 3.5.3 describing the fate of degenerate levels due to distortion. Thus, the well known Jahn-Teller distortion is nothing but a wave mechanical phenomenon.

(d) Zero-Point Energy and Uncertainty Principle

In solving the model, particle in a box, it has been pointed out that even at 0 K, **the system is having some kinetic energy. It indicates that even at that condition the particle is not at rest.** If it were in a rest condition, its position would be determined precisely without any uncertainty. If it were so, the uncertainty principle would not be applicable at 0 K. Thus, the existence of the zero-point energy gives

Click Here t.me/thealchemylibrary

a sound basis of the uncertainty principle. This aspect has been already discussed at the appropriate place (Sec. 3.5.2). It has been shown that by considering uncertainty in position ($\Delta x = a$) and uncertainty in momentum ($\Delta p_x = nh/a$), the relation $\Delta p_x \cdot \Delta x = nh$ satisfies the uncertainty principle.

(e) Correspondence Principle (cf. Sec. 3.5.2)

Wave mechanical model when applied to the macroscopic particles, it leads to the same results obtained from classical mechanics.

(f) Nonexistence of free electron in the nucleus

The model shows that if an electron lies within the nucleus, its kinetic energy becomes too high to be confined within the nucleus. But the massive particles like neutrons and protons can survive within the nucleus. (cf. Solved Problem 14 of this Chapter).

3.5.6 Quantum Mechanical Tunnelling Effect

Let us consider a particle in a one-dimensional box with the walls of finite thickness and height. **Classically, the particle cannot escape from the box, if its energy does not exceed the potential energy barrier (say V_o). But quantum mechanically, it can be shown that even when the total energy of the particle is less than V_o, there is a finite probability of finding the particle outside the box.** This quantum mechanical phenomenon is called ***tunnelling effect*** which allows the passage of the particle outside the box into the classically forbidden zone. The probability of transmission through tunnelling effect decreases exponentially with the increase of thickness of the barrier. It also depends on the height of the barrier and mass of the particle to be transmitted.

This tunnelling effect is important in chemistry for the particles like electron, hydrogen atom, etc. of *very small mass.* Some important cases are mentioned below :

(i) ***Redox reaction*** : In redox reactions, electrons can tunnel from one atom to another atom.

(ii) ***Emission of electron from metals*** : At low temperature and under high electric field strength, emission of electrons from the metals occurs through tunnelling effect.

(iii) ***Emission of alpha particle*** : In radioactive decay of atomic nuclei through the emission of α-particles, the tunnelling effect is important (*cf.* Sec. 6.12).

(iv) ***Transition state theory and tunnelling effect*** : In the ***transition state theory*** of reaction mechanism, there is a probability of the system to tunnel through the potential barrier i.e. activation barrier, rather than passing over the activation barrier. If this tunnelling effect contributes significantly then **a curvature in the *Arrhenius plot* or *Eyring plot*** of $\ln k$ against $1/T$ (where k = rate constant, T = temperature in Kelvin scale) is noticed. In fact, in formulating the Arrhenius and Eyring equations, only the rate process over the activation barrier has been considered, but the rate process through the tunnelling mechanism has not been considered.

This tunnelling mechanism is mainly important in the electron transfer process, and H-atom/H^+ ion/H^- ion transfer reactions. Some examples are given below :

(a) ***Inversion of NH_3 molecule*** : There is a potential barrier in the inversion of pyramidal NH_3 molecule. The height of this barrier is given by the potential energy (which is maximum) for planar configuration of the molecule. The tiny H-atoms can readily tunnel through this barrier to allow the inversion.

(b) ***Conformational change in CH_3CH_3*** : In this molecule, there is a potential barrier to its internal rotation. This barrier height is determined by the potential energy (which is maximum)

Click Here : me/theatchemylibrary

for the *eclipsed position of the atoms*. The tiny *H*-atoms can tunnel through the potential barrier from one *staggered* position to the other.

(c) ***Magnified kinetic isotope effect*: For deuterium** (which is heavier than the normal hydrogen), *the probability of tunnelling mechanism is less because of its heavier mass*. Thus, if the observed *kinetic isotope effect for deuterium is abnormally low, then it is reasonable to conclude that the reaction mechanism involves the tunnelling of H-atom.*

3.6 APPROXIMATE METHODS OF SOLVING THE SCHRÖDINGER'S WAVE EQUATION

The Schrödinger's wave equation is quite simple and solvable for the simple models like, particle in a box, but when it is applied to the atoms and molecules, the equation cannot be solved except for the hydrogen and hydrogen-like systems containing only one moving electron under the single nucleus. *In the polyelectronic systems, due to the inter-electronic interactions, various types of electron-nuclei (or nucleus in a single atom) interactions along with the consideration of nuclear motion, the problem is so complicated that it cannot be solved without any approximation.* The Schrödinger's equation cannot be solved exactly even for the hydrogen-like systems whose potential field is not spherically symmetrical in the presence of an electric or a magnetic field. To solve these complicated problems, only some approximate methods are developed. These are ***perturbation method, variation method, Born-Oppenheimer method*** (sometimes called fixed nucleus method), ***linear combination method,*** etc. The last one works well for the molecules in explaining the molecular orbitals. Here we shall discuss only the variation method and linear combination method.

3.6.1 Variation Method

The Schrödinger's wave equation can be written as,

$$\left(-\frac{h^2}{8\pi^2 m}\nabla^2 + V\right)\psi = E\psi; \text{ or, } \hat{H}\psi = E\psi \qquad \ldots(3.6.1.1)$$

where $\hat{H}$ is called the **Hamiltonian operator** which is a function of various coordinates and potential energy V which is also a function of the coordinates.

From Eqn. 3.6.1.1 we get :

$$\psi\hat{H}\psi = E\psi^2; \text{ or, } \int\psi\hat{H}\psi d\tau = \int E\psi^2 d\tau; \text{ or, } E = \frac{\int\psi\hat{H}\psi d\tau}{\int\psi^2 d\tau} \qquad \ldots(3.6.1.2)$$

If ψ is normalised, $E = \int\psi\hat{H}\psi d\tau$.

Note: In general, it is given by : $E = \dfrac{\int\psi^*\hat{H}\psi d\tau}{\int\psi\psi^* d\tau}$.

Now, if we make a guess of a **trial wave function** ψ_1 which is not the true wave function but an approximate one chosen intuitively based on the physical and chemical consideration, then from Eqn.

Click Here t.me/thealchemylibrary

3.6.1.2 we shall get the energy E_1 for ψ_1. **This E_1 is always greater than the true one, E_0 corresponding to the true wave function ψ_0.** If the approximation is a better one then the difference will be smaller. Now, if we guess another wave function ψ_2 which leads to E_2 and E_2 is again greater than E_0. If $E_2 < E_1$, we can say that ψ_2 is a better approximation. This is called ***variation principle.***

Generally, a trial wave function with different variable parameters c_1, c_2, c_3, ...is used so that the corresponding energy becomes a function of c_1, c_2, c_3, ... *Then the conditions are imposed on the variables in such a way that the energy value becomes minimum.* Application of this method has been illustrated at the **end of this Chapter** to calculate the energy of the electron in hydrogen atom.

3.6.2 The Linear Combination Method

Let the wave function be approximately expressed as :

$$\psi = c_1\psi_1 + c_2\psi_2 \qquad \ldots(3.6.2.1)$$

Therefore, the electronic energy of this wave function is given by :

$$E = \frac{\int \psi \hat{H} \psi d\tau}{\int \psi^2 d\tau} = \frac{\int (c_1\psi_1 + c_2\psi_2)\, \hat{H}\, (c_1\psi_1 + c_2\psi_2)\, d\tau}{\int (c_1\psi_1 + c_2\psi_2)^2 d\tau}$$

$$= \frac{c_1^2 \int \psi_1 \hat{H} \psi_1 d\tau + 2c_1c_2 \int \psi_1 \hat{H} \psi_2 d\tau + c_2^2 \int \psi_2 \hat{H} \psi_2 d\tau}{c_1^2 \int \psi_1^2 d\tau + 2c_1c_2 \int \psi_1\psi_2 d\tau + c_2^2 \int \psi_2^2 d\tau}$$

(as $\int \psi_1 \hat{H} \psi_2 d\tau = \int \psi_2 \hat{H} \psi_1 d\tau$)

or,
$$E = \frac{c_1^2 H_{11} + 2c_1c_2 H_{12} + c_2^2 H_{22}}{c_1^2 S_{11} + 2c_1c_2 S_{12} + c_2^2 S_{22}} \qquad \ldots(3.6.2.2)$$

where, $H_{ij} = \int \psi_i \hat{H} \psi_j d\tau$; and $S_{ij} = \int \psi_i \psi_j d\tau$;

and, $H_{ij} = H_{ji}$, $S_{ij} = S_{ji}$

H_{ii} is called ***Coulomb integral*** and H_{ij} is called ***resonance integral.*** If ψ_1 and ψ_2 are belonging to the different atoms, then the ***overlap integral*** S_{12} (i.e. S_{ij}) gives the measure of bond strength, and if they belong to the same atom, then **S_{ij} gives the measure of mutual interaction among the different orbitals to form the hybrid orbitals.** If ψ_i and ψ_j are normalised then $S_{ii} = S_{jj} = 1$. The above Eqn. 3.6.2.2 can be rearranged as follows :

$$c_1^2 H_{11} + 2c_1c_2 H_{12} + c_2^2 H_{22} = E\left(c_1^2 S_{11} + 2c_1c_2 S_{12} + c_2^2 S_{22}\right) \qquad \ldots(3.6.2.3)$$

Now, if the trial wave function is the closest one to the true wave function, then the energy E must be the lowest one. This condition can be attained if,

$$\frac{\partial E}{\partial c_1} = \frac{\partial E}{\partial c_2} = 0.$$

Click Here t.me/thealchemylibrary

Now, on differentiation with respect to c_1 keeping all other coefficients constants (H_{ij} and S_{ij} are always constants) Eqn. 3.6.2.3 gives,

$$2c_1H_{11} + 2c_2H_{12} = E(2c_1S_{11} + 2c_2S_{12}) + \frac{\partial E}{\partial c_1}\left(c_1^2S_{11} + 2c_1c_2S_{12} + c_2^2S_{22}\right) \quad \ldots (3.6.2.4)$$

Now, for the condition of minimum energy (i.e. $\partial E/\partial c_1 = 0$), we have :

$$2c_1(H_{11} - ES_{11}) + 2c_2(H_{12} - ES_{12}) = 0 \quad \ldots(3.6.2.5)$$

Similarly by considering the condition, $\partial E/\partial c_2 = 0$, we have :

$$2c_1(H_{12} - ES_{12}) + 2c_2(H_{22} - ES_{22}) = 0 \quad \ldots(3.6.2.6)$$

The above two equations give the following **set of secular equations,**

$$\left.\begin{aligned} c_1(H_{11} - ES_{11}) + c_2(H_{12} - ES_{12}) &= 0 \\ c_1(H_{12} - ES_{12}) + c_2(H_{22} - ES_{22}) &= 0 \end{aligned}\right\} \quad \ldots(3.6.2.7)$$

Now, if the above set of equations is to have any nontrivial solutions (i.e., $c_1 \neq 0$, $c_2 \neq 0$), the determinant of the coefficients c_1 and c_2 must vanish.

Therefore,

$$\begin{vmatrix} (H_{11} - ES_{11}) & (H_{12} - ES_{12}) \\ (H_{12} - ES_{12}) & (H_{22} - ES_{22}) \end{vmatrix} = 0 \quad \ldots(3.6.2.8)$$

By solving Eqns. 3.6.2.7 and 3.6.2.8, c_1/c_2 and E can be obtained. **As the secular determinant is of the second order, it gives the two roots of E, and the two corresponding wave functions.**

This approach gives the basis of **linear combination of atomic orbitals (LCAO)** to have the approximate energies corresponding to the wave functions representing the molecular orbitals.

This approach can also be applied for the general case,

$$\psi = \sum_i^n c_i\psi_i.$$

Application of this method has been illustrated in Sec. 9.4.1.

SOLVED NUMERICAL PROBLEMS

Problem 1 **:** Calculate the de Broglie wavelength associated with a stone having velocity 1 m s^{-1} and mass 100 g; and an electron having velocity 6×10^5 m s^{-1} and mass 9.1×10^{-31} kg. Which one of these is meaningful?

Solution **:**

For the stone piece : $\lambda = h/(mu) = \dfrac{6.625 \times 10^{-34}\ \text{J s}}{0.1\ \text{kg} \times 1\ \text{m s}^{-1}} = 66.25 \times 10^{-34}$ m, (J = kg m^2 s^{-2})

For the electron : $\lambda = h/(mu) = \dfrac{6.625 \times 10^{-34}\ \text{J s}}{9.1 \times 10^{-31}\ \text{kg} \times 6 \times 10^5\ \text{m s}^{-1}} = 1.21 \times 10^{-9}$ m.

Click Here to me/thealchemylibrary

It is evident that for the stone piece, the associated wavelength is exceedingly small, but the electron wavelength lies well within the measurable range.

Problem 2 : Calculate the wavelength of (a) an electron of energy 12 eV, (b) a photon of energy 12 eV, (c) a nitrogen nucleus of 150 MeV.

Solution : $\lambda = h/p$ and $E = p^2/2m$ i.e. $\lambda = \dfrac{h}{\sqrt{2mE}}$. In S.I. units, the values are given below (1 eV = 1.6×10^{-19} J) :

(a) $$\lambda = \frac{h}{\sqrt{2mE}} = \frac{6.62 \times 10^{-34}\ \text{J s}}{\sqrt{2 \times 9.1 \times 10^{-31}\ \text{kg} \times 12 \times 1.6 \times 10^{-19}\ \text{J}}} = \frac{6.62 \times 10^{-34}\ \text{m}}{18.7 \times 10^{-25}} = 3.54 \times 10^{-10}\ \text{m}$$

$$\frac{\text{J s}}{\sqrt{\text{kg J}}} = \frac{\text{kg m}^2\ \text{s}^{-2} \times \text{s}}{\sqrt{\text{kg}^2\ \text{m}^2\ \text{s}^{-2}}} = \text{m}$$

(b) $$E = h\nu = \frac{hc}{\lambda}, \text{ i.e. } \lambda = \frac{hc}{E} = \frac{6.62 \times 10^{-34}\ \text{J s} \times 3 \times 10^{8}\ \text{m s}^{-1}}{12 \times 1.6 \times 10^{-19}\ \text{J}}$$

$$= \frac{19.86 \times 10^{-7}\ \text{m}}{19.2} = 10.34 \times 10^{-8}\ \text{m}$$

(c) $$\lambda = \frac{h}{\sqrt{2mE}} = \frac{6.62 \times 10^{-34}\ \text{J s}}{\sqrt{2 \times 14 \times 1.66 \times 10^{-27}\ \text{kg} \times 150 \times 1.6 \times 10^{-19}\ \text{J}}}$$

$$= \frac{6.62 \times 10^{-34}\ \text{m}}{105.6 \times 10^{-20}} = 6.27 \times 10^{-16}\ \text{m}$$

(The mass of a nitrogen nucleus is $14\mu = 14 \times 1.66 \times 10^{-27}$ kg).

Problem 3 : An electron beam is accelerated from rest through a potential difference of 5000 V. Find out the de Broglie wavelength of the electron and its wave number. Calculate the spacing between the (1, 1, 1) planes of a metal crystal, if the electron beam shows a first order reflection at 2° 30′ (i.e. glancing angle) from the (1, 1, 1) plane (ignore the relativistic correction).

Solution : If, u is the velocity of the electron then,

$$(1/2)mu^2 = eV = 5000 \text{ electron-volt} = 5000 \times 1.6 \times 10^{-19}\ \text{J};$$

or, $$(mu)^2 = 2m \times 5000 \times 1.6 \times 10^{-19};$$

or, $$(mu) = \sqrt{2 \times 9.1 \times 10^{-31}\ \text{kg} \times 5000 \times 1.6 \times 10^{-19}\ \text{J}},\ \text{J} = \text{kg m}^2\ \text{s}^{-2}$$

$$= 3.82 \times 10^{-2}\ \text{kg m s}^{-1}$$

The de Broglie wavelength of the electron can be obtained as :

$$\lambda = h/(mu) = \frac{6.625 \times 10^{-34}\ \text{J s}}{3.82 \times 10^{-23}\ \text{kg m s}^{-1}} = 1.73 \times 10^{-11}\ \text{m}$$

Click Here t.me/theaChemyLibrary

Therefore, the wave number $(\bar{\nu})$ is obtained by, $\bar{\nu} = 1/\lambda = 5.76 \times 10^{10}\ m^{-1}$.

According to Bragg's equation, the spacing (d) between the parallel reflecting planes is given by $n\lambda = 2d \sin\theta$ (cf. Fig. 3.2.6.4);

or,
$$d = \frac{n\lambda}{2\sin\theta}$$

Here, $n = 1$, (for Ist order reflection).

Thus,
$$d = \lambda/(2\sin\theta) = \frac{\lambda}{2\sin(2^\circ\ 30')} = \frac{1.73 \times 10^{-11}\ m}{2 \times 0.0436}$$
$$= 19.83 \times 10^{-11}\ m = 1.983 \times 10^{-8}\ cm = 1.983\ Å$$

Problem 4 : Calculate the uncertainties in determining the position (Δx) of an electron and a dust particle, if the uncertainty in their velocity determination is 0.01%. Take velocity and mass of the dust particle as $10^{-5}\ m\ s^{-1}$ and 10^{-13} kg respectively; and for the electron, these are : $2.2 \times 10^6\ m\ s^{-1}$ and 9.1×10^{-31} kg respectively. Comment on the results. The dimensions of the dust particle and atom are of the order of 10^{-5} m and 10^{-10} m respectively.

Solution :

For the dust particle : Δu = uncertainty in velocity =

$$0.01\%\ \text{of}\ u = 0.01 \times 10^{-5} \times 10^{-2}\ m\ s^{-1} = 10^{-9}\ m\ s^{-1}.$$

Hence, the uncertainty in position, (Δx) is given by,

$$m\Delta u.\Delta x \approx h/2\pi;\ \text{or,}\ \Delta x = \frac{h}{2\pi m\Delta u} = \frac{6.625 \times 10^{-34}\ J\ s}{2 \times 3.14 \times 10^{-9}\ m\ s^{-1} \times 10^{-13}\ kg} = 1.05 \times 10^{-12}\ m$$

For the electron : $\Delta u = 0.01 \times 2.2 \times 10^6 \times 10^{-2} = 2.2 \times 10^2\ m\ s^{-1}$

and,
$$\Delta x = \frac{h}{2\pi m\Delta u} = \frac{6.625 \times 10^{-34}\ J\ s}{2 \times 3.14 \times 2.2 \times 10^2\ m\ s^{-1} \times 9.1 \times 10^{-31}\ kg} = 5.27 \times 10^{-7}\ m$$

Thus, for the dust particle, the uncertainty in determining the position is ~ 10^{-7} times compared to its dimension while for the electron (assuming its dimension is in the order of the dimension of an atom; actually the dimension of an electron is much smaller than that of an atom), the uncertainty in its position is ~ 10^3 times compared to its size. **Hence, for the dust particle, both the position and velocity can be precisely determined, but it cannot be done for the electron.**

Problem 5 : A car of mass 2.90×10^3 kg is moving with a velocity which can be measured with an accuracy $\pm$ 0.004 km hr^{-1} and its position can be determined with an accuracy of $\pm$ 0.02 km. Show that the uncertainty principle is not applicable here.

Solution : Uncertainty in velocity (Δu) is given by :

$$\Delta u = \frac{0.004 \times 10^3\ m}{3600\ s} = 1.11 \times 10^{-3}\ m\ s^{-1}$$

Therefore, the uncertainty in momentum is given by :

$$\Delta p = m\Delta u = 2.9 \times 10^3\ kg \times 1.11 \times 10^{-3}\ m\ s^{-1} = 3.22\ kg\ m\ s^{-1}$$

Click Here t.me/tnealchemylibrary

The uncertainty in position, $\Delta x = 0.02 \times 10^3$ m

Thus, $\Delta x.\Delta p = 0.02 \times 10^3 \text{ m} \times 3.22 \text{ kg m s}^{-1} = 64.4 \text{ J s}$, $\text{J} = \text{kg m}^2 \text{ s}^{-2}$

and, according to the uncertainty principle,

$$\Delta x.\Delta p \approx \frac{h}{2\pi} = \frac{6.625 \times 10^{-34} \text{ J s}}{2 \times 3.14} = 1.054 \times 10^{-34} \text{ J s}$$

Thus, in the case of the vehicle, $\Delta x \cdot \Delta p >>> \frac{h}{2\pi}$. **Thus, here the principle is not applicable.**

Problem 6 : By considering the relation, $\Delta p.\Delta x \approx h/2\pi$, establish the relation, $\Delta E.\Delta t \approx h/2\pi$, where ΔE and Δt represent the uncertainty in translational energy and time respectively.

Solution : For a moving free particle the translational energy is given by :

$$E = (1/2)mu^2 = p^2/2m$$

Therefore, $\Delta E = (p/m)\Delta p = (mu/m)\Delta p = u\Delta p = \left(\frac{\Delta x}{\Delta t}\right)\Delta p$; using the relation, $u = \frac{\Delta x}{\Delta t}$;

or, $\Delta E.\Delta t = \Delta x.\Delta p$

Now, if $\Delta x.\Delta p \approx h/2\pi$, then $\Delta E.\Delta t \approx h/2\pi$

Problem 7 : An electron is confined in a one-dimensional box of length 10 cm. What is the uncertainty in its velocity?

Solution : The possible maximum value of Δx is 10 cm, i.e. Δx = 10 cm = 0.1 m

$$\Delta p \times \Delta x = \frac{h}{2\pi}; \text{ or } \Delta p = \frac{h}{2\pi\Delta x} = \frac{6.625 \times 10^{-34} \text{ J s}}{2 \times 3.14 \times 0.1 \text{ m}}$$

$$= 10.54 \times 10^{-34} \text{ kg m s}^{-1}$$

$$\Delta u \text{ (uncertainty in velocity)} = \frac{\Delta p}{m}$$

$$= \frac{10.54 \times 10^{-34} \text{ kg m s}^{-1}}{9.1 \times 10^{-31} \text{ kg}}$$

$$= 1.16 \times 10^{-4} \text{ m s}^{-1}$$

Problem 8 : Find the uncertainty in location of a photon of wavelength 6000 Å assuming the uncertainty in wavelength to be 1 part per million (i.e. 1 ppm).

Solution : $p = \frac{h}{\lambda}$, i.e. $\Delta p = \frac{h\Delta\lambda}{\lambda^2}$

$\left[\text{cf. } p = \frac{h}{\lambda} \text{ and } p - \Delta p = \frac{h}{\lambda + \Delta\lambda}, (p \text{ and } \lambda \text{ are inversely related})\right.$

$\left.\text{On substraction, } \Delta p = \frac{h\Delta\lambda}{\lambda(\lambda + \Delta\lambda)} \approx \frac{h\Delta\lambda}{\lambda^2}\right]$

Click Here to me/thealchemylibrary

$$\Delta p \times \Delta x = \frac{h}{2\pi}; \Delta x \text{ (uncertainty in position)}$$

$$\text{i.e. } \Delta x = \frac{h}{2\pi\,\Delta p} = \frac{\lambda^2}{2\pi\Delta\lambda}, \left(\Delta\lambda = 1 \text{ ppm i.e., } \Delta\lambda = \frac{1}{10^6} \times 6000 = 6 \times 10^{-3} \text{ Å}\right)$$

$$= \frac{(6000)^2}{2 \times 3.14 \times 6 \times 10^{-3}} \text{ Å}$$

$$= 0.955 \times 10^9 \text{ Å} = 9.55 \text{ cm.}$$

Problem 9 : The average time gap between the excitation of an atom and consequent emission of a photon is 10^{-7} s. Find the uncertainty in frequency determination.

Solution : $\Delta t = 10^{-7}$ s; $\Delta E \times \Delta t = \frac{h}{2\pi}$

i.e. $$\Delta E = \frac{h}{2\pi\Delta t} = \frac{6.625 \times 10^{-34} \text{ J s}}{2 \times 3.14 \times 10^{-7} \text{ s}} = 1.05 \times 10^{-27} \text{ J}$$

$$\Delta\nu \text{ (uncertainty in frequency)} = \frac{\Delta E}{h} = \frac{1.05 \times 10^{-27}}{6.625 \times 10^{-34}} \text{ Hz}$$

$$= 1.59 \times 10^6 \text{ Hz}$$

Problem 10 : The position of an electron is determined at a particular instant with the uncertainty of $\pm$ 1 Å. Find the uncertainty of its position after 2 second.

Solution : $\Delta p = \frac{h}{2\pi\Delta x} = \frac{6.625 \times 10^{-34} \text{ J s}}{2 \times 3.14 \times 10^{-10} \text{ m}} = 1.05 \times 10^{-24} \text{ kg m s}^{-1}$, $\Delta x = 1 \text{ Å} = 10^{-8} \text{ cm} = 10^{-10} \text{ m}$

Δu = (uncertainty in velocity) = $\frac{\Delta p}{m} = \frac{1.05 \times 10^{-24} \text{ kg m s}^{-1}}{9.1 \times 10^{-31} \text{ kg}} = 1.15 \times 10^6 \text{ m s}^{-1}$

Δx (uncertainty in position) after t seconds = $t \times \Delta u$

i.e. $\Delta x = t \times \Delta u = 2 \text{ s} \times 1.15 \times 10^6 \text{ m s}^{-1} = 2.3 \times 10^3 \text{ km}$

Problem 11 : A ball of 1 g mass is moving with a speed of 5 cm s^{-1} in a one dimensional box of edge length 20 cm. Calculate the excitation energy, if the ball is to be excited to the next higher quantum level (assume the total energy as kinetic energy).

Solution : Kinetic energy of the ball = $(1/2)mu^2 = (1/2) \times 10^{-3} \text{ kg} \times (5 \times 10^{-2} \text{ m s}^{-1})^2$

$$= 12.5 \times 10^{-7} \text{ J} = E_n$$

The energy of a particle for the n-th level is given by :

$$E_n = \frac{n^2h^2}{8ma^2}, \ (a = \text{length of the box})$$

Click Here to me/thealchemylibrary

Therefore, $n^2 = \dfrac{E_n(8ma^2)}{h^2} = \dfrac{12.5\times10^{-7}\ \text{J}\times8\times10^{-3}\ \text{kg}\times(20\times10^{-2}\ \text{m})^2}{(6.625\times10^{-34}\ \text{J s})^2} = 9.11\times10^{56}$

or, $n \approx 3 \times 10^{28}$ (nearest integer)

Here, the ball is to be excited from, $n = 3 \times 10^{28}$ to $(n + 1)$, i.e. $(3 \times 10^{28} + 1)$

We have,

$$\Delta E = E_{n+1} - E_n = (2n+1)\frac{h^2}{8ma^2} = \frac{(2\times3\times10^{28}+1)\,(6.625\times10^{-34}\ \text{J s})^2}{8\times10^{-3}\ \text{kg}\times(20\times10^{-2}\ \text{m})^2} = 8.22\times10^{-35}\ \text{J}$$

Thus, the required excitation energy is very small. Hence, the energy of the ball can be expected to vary continuously as expected from the Newtonian mechanics.

Problem 12 : Vitamin A has five conjugated double bonds and it shows the first absorption peak at 332 nm. Find the length of the molecule.

Solution : The ten pi-electrons fill in the first five levels (n = 1 to 5) according to the model, particle in a one dimensional box.

Thus, the first transition involves, $n_i = 5 \rightarrow n_f = 6$

It leads to : $\Delta E = E_6 - E_5 = E_{n+1} - E_n = (2n+1)\dfrac{h^2}{8ma^2}$

(m = mass of an electron, a = length of the conjugated molecule, n = 5)

Hence, $\nu = \dfrac{(2n+1)h}{8ma^2}$; or, $\lambda = \dfrac{c}{\nu} = \dfrac{8ma^2c}{(2n+1)h}$

Here, $\lambda = 332\ \text{nm} = 332 \times 10^{-9}\ \text{m}$

Thus, $332\times10^{-9} = \dfrac{8\times9.1\times10^{-31}\times a^2\times3\times10^8}{(2\times5+1)\times6.625\times10^{-34}}$

It leads to : $a^2 = 110.7\times10^{-20}$; or, $a = 10.52\times10^{-10}\ \text{m} = 10.52\ \text{Å}$

Problem 13 : The ground state energy of an electron in a one dimensional box of length 100 pm is 4 eV. If the hydrogen electron is supposed to be confined in a cubic box of edge length 100 pm, then calculate the ground state energy of the electron present in the hydrogen atom.

Solution : The energy of a particle in a one dimensional box is given by,

$$E_n = \frac{n^2h^2}{8ma^2}, \text{ i.e. } E_1 = \frac{h^2}{8m\,(100\ \text{pm})^2} = 4\ \text{eV}$$

or, $\dfrac{h^2}{8m} = (100\ \text{pm})^2 \times (4\ \text{eV})$; ($h$, m in suitable units)

The energy of the particle in a three dimensional cubic box is given by :

$$E_{n_x, n_y, n_z} = \frac{h^2}{8ma^2}\left(n_x^2 + n_y^2 + n_z^2\right)$$

Click Here t.me/tlealchemylibrary

For the ground state, $n_x = n_y = n_z = 1$.

Therefore,

$$E_{1,1,1} = \frac{h^2}{8ma^2} \times 3 = \frac{(100 \text{ pm})^2 \times 4 \text{ eV} \times 3}{(100 \text{ pm})^2} = 12 \text{ eV}$$

Thus, under this condition, the ground state energy of the hydrogen electron is 12 eV.

Problem 14 : Consider an electron with an atom of size 2 Å and in a nucleus of dimension of the order of 10^{-14} m. Comment on the possibility of the existence of the electron in the nucleus.

Solution : Let us consider the electron ($m = 9.1 \times 10^{-31}$ kg) to lie within the box of an atom of dimension (a) 2×10^{-10} m. The minimum energy (E_1) is given by ($n = 1$) :

$$E_1 = \frac{h^2}{8ma^2} = \frac{(6.62 \times 10^{-34} \text{ J s})^2}{8 \times 9.1 \times 10^{-31} \text{ kg} \times 4 \times 10^{-20} \text{ m}^2}$$

$$= 1.5 \times 10^{-18} \text{ J} \approx 9.5 \text{ eV}$$

This E_1 value (which is considered to be kinetic energy) is quite reasonable when the electron drops from $n = 2$ to $n = 1$, the energy change is given by :

$$\Delta E = (2^2 - 1^2)\, E_1 = 4.5 \times 10^{-18} \text{ J} \approx 30 \text{ eV}$$

The corresponding wavelength of radiation is given by :

$$\lambda = \frac{ch}{\Delta E} = \frac{3 \times 10^8 \text{ m s}^{-1} \times 6.62 \times 10^{-34} \text{ J s}}{4.5 \times 10^{-18} \text{ J}} = 4.41 \times 10^{-8} \text{ m} = 441 \text{ Å}$$

This wavelength of radiation lies in the ultraviolet region and it is very often found in experimental observations.

Now let us consider the electron to exist in the nucleus of dimension (a) to 10^{-14} m. The energy is given by :

$$E_1 = \frac{h^2}{8ma^2} = \frac{(6.62 \times 10^{-34} \text{ J s})^2}{8 \times 9.1 \times 10^{-31} \text{ kg} \times (10^{-14} \text{ m})^2}$$

$$= 6 \times 10^{-10} \text{ J} \approx 3.75 \times 10^9 \text{ eV} = 3750 \text{ MeV}$$

Such a high energy value is unbelievable. The Coulombic energy which could bind the electron in the nucleus is :

$$E_{pot} = -\frac{e^2}{4\pi\varepsilon_0 r}, \text{(taking } Z = 1, r = a = 10^{-14} \text{ m)}$$

$$= -\frac{(1.6 \times 10^{-19} \text{ C})^2}{4 \times 3.14 \times (8.85 \times 10^{-12} \text{ J}^{-1} \text{ C}^2 \text{ m}^{-1}) \times (10^{-14} \text{ m})}$$

$$= -2.3 \times 10^{-14} \text{ J} \approx -0.14 \text{ MeV}$$

Click Here t.me/dreamchemylibrary

This Coulombic energy is negligible compared to the kinetic energy which would be associated with the electron if it is considered to exist in the nucleus. For the heavier particles like neutron, proton (cf. $m_p \approx m_n = 1836\, m_e$), the associated kinetic energy is not so fantastically high when they are supposed to exist in the nucleus.

Conclusion* : *An electron can exist within the dimension of an atom but not within the dimension of a nucleus. Here it may be mentioned that the uncertainty principle also leads to the same conclusion (cf. Sec. 3.3.4).

Problem 15 : Consider a dust particle (m = 0.1 g) enclosed in a one dimensional box of side 1 dm travels with a velocity of 10 cm s^{-1}. Comment on its energy.

Solution : $E_1 = \dfrac{h^2}{8ma^2} = \dfrac{(6.62\times10^{-34}\ \text{J s})^2}{8\times0.1\times10^{-3}\ \text{kg}\times0.1\times0.1\ \text{m}^2} \approx 5.5\times10^{-62}\ \text{J}$

Its kinetic energy = $E_n = \dfrac{1}{2}(0.1\times10^{-3}\ \text{kg})\,(0.1\ \text{m s}^{-1})^2 = 5\times10^{-7}\ \text{J}$

It leads to : $E_n = \dfrac{n^2h^2}{8ma^2} = n^2E_1^2$, i.e. $n^2 = E_n/E_1$

$$n^2 = \frac{E_n}{E_1} = \frac{5\times10^{-7}}{5.5\times10^{-62}} \approx 10^{55} \text{ i.e. } n \approx 3\times10^{27}$$

The energy difference between the $(n+1)$th and nth level is :

$$\Delta E = E_{n+1} - E_n = [(n+1)^2 - n^2]\frac{h^2}{8ma^2} = (2n+1)E_1 \approx 3.3\times10^{-34}\ \text{J}$$

This exceedingly small energy difference is beyond the measurement and perception. Thus the energy of the particle changes in a continuous fashion. It illustrates the ***Bohr's correspondence principle.***

Problem 16 : Calculate the length (a) of a one dimensional box for which the energy difference between the lowest energy levels of a molecule is comparable to its average kinetic energy at a particular temperature.

Solution : The average kinetic energy ($\bar{E}$) of a molecule (mass m) at a particular T (temperature in Kelvin scale) is given by :

$$\bar{E} = \frac{1}{2}k_BT,\ k_B = \text{Boltzmann constant}$$

According to the given condition :

$$\Delta E = E_{n+1} - E_n = (2n+1)\frac{h^2}{8ma^2} = \frac{1}{2}k_BT$$

i.e. $$a = \frac{h}{2}\left(\frac{2n+1}{mk_BT}\right)^{1/2} = \frac{h}{2}\left(\frac{3}{mk_BT}\right)^{1/2} \text{ (for } n = 1).$$

Click Here t.me/healchemylibrary

Problem 17 : Calculate the probability of existence of a particle in a one-dimensional box of length a in the region, $0 \le x \le \frac{a}{4}$ for the states $n = 1, 2$ and 3.

Solution : The wave function of the particle is given by :

$$\psi = \sqrt{\frac{2}{a}} \sin\left(\frac{n\pi x}{a}\right)$$

The required probability (P) is given by :

$$P = \frac{2}{a}\int_0^{a/4} \sin^2\left(\frac{n\pi x}{a}\right) dx = \frac{2}{a}\int_0^{a/4} \frac{1-\cos\left(\frac{2n\pi x}{a}\right)}{2} dx, (\cos 2\theta = 1 - 2\sin^2\theta)$$

i.e.
$$P = \frac{2}{a}\left[\int_0^{a/4} \frac{dx}{2} - \frac{1}{2}\int_0^{a/4} \cos\left(\frac{2\pi nx}{a}\right) dx\right]$$

$$= \frac{2}{a}\left[\frac{1}{2}\times\frac{a}{4} - \frac{a}{4n\pi}\left\{\sin\left(\frac{2n\pi x}{a}\right)\right\}_0^{a/4}\right]$$

$$= \frac{2}{a}\left[\frac{a}{8} - \frac{a}{4n\pi}\sin\left(\frac{n\pi}{2}\right)\right] = \frac{1}{4} - \frac{1}{2n\pi}\sin\left(\frac{n\pi}{2}\right)$$

For
$$n = 1, P = \frac{1}{4} - \frac{1}{2\pi} = 0.908$$

$$n = 2, P = \frac{1}{4} - \frac{0}{4\pi} = 0.25$$

$$n = 3, P = \frac{1}{4} - \left(-\frac{1}{6\pi}\right) = 0.303$$

Problem 18 : Calculate the probability of finding a particle in the vicinity of the centre of a one-dimensional box of length 1 cm, for the state $n = 1$.

Solution : The mid-point is at 0.5 cm from the edge. The wave function of the particle is given by:

$$\psi = \sqrt{\frac{2}{a}} \sin\left(\frac{n\pi x}{a}\right)$$

The probability of finding the particle at the vicinity of a particular point is given by :

$$P = \psi^2 dx = \frac{2}{a}\sin^2\left(\frac{\pi x}{a}\right) dx, (n = 1)$$

Click Here t.me/thealchemylibrary

In the present case, dx may be approximately taken as the interval 0.51 – 0.49 = 0.02 cm.

$$P = \frac{2}{a}\sin^2\left(\frac{\pi x}{a}\right)dx = \frac{2}{1\text{ cm}}\sin^2\left(\frac{\pi \times 0.5\text{ cm}}{1.0\text{ cm}}\right) \times 0.02\text{ cm}$$

$$= 2\sin^2\left(\frac{\pi}{2}\right) \times 0.02 = 0.04$$

Problem 19 : An electron is trapped in a cubic hole of edge length 1.0 nm in a crystal. Find the first excitation energy and corresponding frequency of the electron acting as a source of colour centre (i.e. *F*-centre).

Solution : The energy of an electron in a three dimensional cubic box is given by :

$$E_{n_x, n_y, n_z} = \frac{h^2}{8ma^2}\left(n_x^2 + n_y^2 + n_z^2\right)$$ where, m = mass of the electron and

a = edge length of the box.

Therefore the ground state energy of the electron is given by :

$$E_{1,1,1} = \frac{(6.625 \times 10^{-34}\text{ J s})^2}{8 \times 9.1 \times 10^{-31}\text{ kg} \times (1 \times 10^{-9}\text{ m})^2} \times 3 = 6.02 \times 10^{-20} \times 3\text{ J}$$

The energy of the first excited state which is triply degenerate is given by :

$$E_{1,1,2} = E_{1,2,1} = E_{2,1,1} = \frac{h^2}{8ma^2} \times (1^2 + 1^2 + 2^2) = 6.02 \times 10^{-20} \times 6\text{ J}$$

Therefore, the excitation energy is given by :

$$\Delta E = 6.02 \times 10^{-20}\ (6 - 3)\text{ J} = 18.06 \times 10^{-20}\text{ J}$$

and the corresponding frequency of radiation is obtained by :

$$\nu = \Delta E / h = 2.71 \times 10^{14}\text{ Hz}$$

Problem 20 : A cubic box of edge length 1 Å contains eleven electrons. Ignoring the electron-electron repulsion, calculate the first excitation energy, if the system obeys the principle of the model, particle in a box.

Solution : The energy is given by,

$$E_{n_x, n_y, n_z} = \frac{h^2}{8ma^2}\left(n_x^2 + n_y^2 + n_z^2\right)$$

$$= \frac{(6.625 \times 10^{-34}\text{ J s})^2}{8 \times 9.1 \times 10^{-31}\text{ kg} \times (10^{-10}\text{ m})^2}\left(n_x^2 + n_y^2 + n_z^2\right)$$

$$= 6.02 \times 10^{-18}\left(n_x^2 + n_y^2 + n_z^2\right)$$

Click Here t.me/tlcalchemylibrary

The energy levels are shown as follows :

n_x	n_y	n_z	E (J)	Distribution of electrons
1	1	1	$6.02 \times 10^{-18} \times 3$	↑ ↓
1	1	2	$6.02 \times 10^{-18} \times 6$	↑ ↓ ↑ ↓ ↑ ↓
1	2	1		
2	1	1		
1	2	2	$6.02 \times 10^{-18} \times 9$	↑ ↑ ↑
2	2	1		
2	1	2		
1	3	1	$6.02 \times 10^{-18} \times 11$	
1	1	3		
3	1	1		

The first excitation energy is given by :

$$\Delta E = E_{3,1,1} (= E_{1,3,1} = E_{1,1,3}) - E_{1,2,2} (= E_{2,1,2} = E_{2,2,1})$$

$$= 6.02 \times 10^{-18} \times (11 - 9) \text{ J} = 12.04 \times 10^{-18} \text{ J}$$

EXERCISE-III

A. General Questions

1. Derive an expression of the de Broglie wavelength associated with an electron accelerated through a potential difference V (taking the consideration of relativistic change in mass).
2. Discuss the Davisson and Germer's experiment to prove the wave nature of the electrons.
3. What is the uncertainty principle? Write down its significance in both macroscopic and microscopic world.
4. What do you mean by *wave-particle dualism*? What is de Broglie wavelength? How does the matter wave behave in microscopic and macroscopic particles? Discuss the similarities and dissimilarities between the matter wave and electromagnetic wave.
5. Quantitatively support the uncertainty principle in determining the position of a microscopic particle by using a microscope in the light of Compton effect.
6. Write down the different applications of uncertainty principle in naturally occurring phenomena.
7. Write down the Schrödinger's time independent equation with respect to space giving the meanings of all the terms involved. What is the Hamiltonian Operator $(\hat{H})$? What is the significance of $\hat{H}$? Define the eigen functions and eigen values.
8. Discuss the conditions for the acceptable solutions obtained from the 2nd order differential Schrödinger's wave equation.
9. Arrive at the Schrödinger's wave equation with respect to space by considering the laws of motion representing a standing wave.
10. Write down the physical significance of ψ and ψ^2.

Click Here to me/healchemylibrary

11. Give the Hamiltonian Operator for a particle in a box of one dimension. Deduce the normalised wave functions and the allowed energies for the system. Verify the condition of orthogonality in the system.
12. Discuss the characteristic features of ψ_n, ψ_n^2 and E_n of a particle in a one dimensional box.
13. Deduce the eigen functions and eigen values for a particle in a three dimensional box. Discuss the effect of distortion on degeneracy of the system considering the model, particle in a cubic box.
14. Discuss the variation principle and its application in linear combination of the orbitals.
15. Write notes on the followings :
    (i) Matter waves and electromagnetic radiation,
    (ii) Uncertainty principle,
    (iii) Uncertainty principle and spectral band width,
    (iv) Compton effect and uncertainty principle,
    (v) Jahn-Teller effect and distortion,
    (vi) Physical significance of ψ and ψ^2,
    (vii) Eigen functions and eigen values,
    (viii) Hamiltonian Operator,
    (ix) Variation principle,
    (x) Zero-point energy.

B. Justify the Statements

1. The matter wave associated with the large macroscopic particles is of no practical significance.
2. The revolving electron can never lie in some well defined orbits or trajectories.
3. The high energy electron or neutron beam shows the diffraction, a property of light.
4. The Bohr's postulate, $mur = n(h/2\pi)$ can find a strong support in the concept of wave- particle dualism.
5. The mathematics for both the matter wave and electromagnetic radiation are identical, but in nature, they are totally different.
6. The uncertainty principle is not applicable for the macroscopic particles.
7. The probability concept of the electronic cloud rather than the concept of well defined trajectories lies its origin in the uncertainty principle.
8. The free electron can never exist in the nucleus, if the uncertainty principle is true.
9. The Compton effect helps us to understand the uncertainty principle.
10. The spectral band width is also a demand of the uncertainty principle.
11. The normalised eigen functions for the particle in a box are automatically orthogonalised.
12. Vitamin *A* and carotene are coloured while butadiene is colourless.
13. Polyenes give the broad peaks while the atoms produce sharp lines.
14. For the eigen functions of a particle confined in a box, the quantum number cannot be zero though mathematically it is possible.
15. The existence of zero-point energy of a particle confined in a box provides a theoretical support in favour of the uncertainty principle.

Click Here t.me/thealchemylibrary

16. For the free particles, the energies vary almost continuously.
17. For the very large particles confined in a box, the conclusion drawn from Schrödinger's equation runs with that obtained from classical mechanics.
18. The correspondence principle can be supported from the model, particle in a box.
19. Stabilization due to resonance or delocalisation can be nicely explained from the model, particle in a box.
20. The model, particle in a box can be utilised to calculate the energy of spectral transitions in polyenes.
21. The existence of degenerate energy levels in three dimensional problems is due to the three quantum numbers required.
22. The stabilization due to Jahn-Teller distortion can be nicely explained from the model, particle in a three dimensional box.
23. The model, particle in a box is far away from the real problems occurring in nature, but it furnishes a lot of very useful information.
24. Nonexistence of free electrons but existence of neutrons and protons within the nucleus can be explained by considering the model, particle in a box.

C. Numerical Problems

1. Calculate the de Broglie wavelengths (nonrelativistic) in the following cases :
   (a) a neutron of kinetic energy 1 MeV,
   (b) a proton moving with a velocity of 1/20 th of the velocity of light,
   (c) an α-particle accelerated through a potential difference of 20,000 volts,
   (d) an electron accelerated by 500 volts. (Masses : proton = 1.67×10^{-27} kg ; α-particle = 6.64×10^{-27} kg; neutron = 1.67×10^{-27} kg; electron = 9.10×10^{-31} kg)

   Ans. (a) 2.64×10^{-14} m (b) 26.5×10^{-15} m (c) $7.2\ 10^{-14}$ m (d) 5.5×10^{-11} m.
2. Calculate the nonrelativistic de Broglie wavelength of (a) a 20 g particle moving with a speed of 120 cm s^{-1}, (b) a *Xe* atom (mass = 2.2×10^{-25} kg) moving with a velocity of 2.5×10^{2} m s^{-1}.

   Ans. (a) 2.76×10^{-32} m, (b) 1.20×10^{-11} m
3. The uncertainty in determining the velocity of an electron is 1 cm s^{-1}. Calculate the uncertainty in determining the position of the electron. (Mass of an electron = 9.1×10^{-31} kg)

   (Ans. 1.16 cm).
4. The position and velocity of a 1 kV electron are determined simultaneously. If the uncertainty in determining the position lies within 1 Å, calculate the percentage of nonrelativistic uncertainty in its momentum.

   (Ans. 6.2 %)
5. Calculate the uncertainty in the speed of an electron confined in a space of linear dimension of 10 Å

   (Ans. 1.16×10^{5} m/s).
6. A particle of mass *m* is confined to move back and forth in a one dimensional box extending from $-a$ to $+a$ and the origin lies at the centre of the box. Write down the Schrödinger's equation

Click Here t.me/thealchemylibrary

for the system at the boundaries, outside the box and inside the box; and derive the expression for the eigen functions and eigen values for the system under the following conditions of potential energy.

$V(x) = 0$ for $-a < x < +a$; $V(x) = \infty$ for $x \geq a, x \leq -a$.

7. Determine the first excitation energy for a xenon atom (mass = 2.2×10^{-25} kg) confined in a cubic box of edge length 1.0 cm.
(Ans. 7.48×10^{-39} J)
8. A conjugated system, hexatriene having the molecular length 7.3 Å shows an absorption peak at 2, 507 Å. Determine the electronic transition.
(Ans. $n_i = 3$ to $n_f = 4$).

APPENDIX 3A

APPLICATION OF VARIATION METHOD IN HYDROGEN ATOM

The principle of this method is illustrated in the following example.

Calculation of energy of the electron in hydrogen atom by variation method.

Process I (SI unit system) : Let us choose the **trial wave function** as follows :

$$\psi = \exp(-ar) \tag{3.6.1.3}$$

where a is an adjustable parameter.

The Hamiltonian operator (in SI system) for atomic hydrogen ($Z = 1$) is given by :

$$\hat{H} = -\frac{h^2}{8\pi^2\mu}\nabla^2 - \frac{e^2}{(4\pi\varepsilon_0)r} \tag{3.6.1.4}$$

where μ stands for the reduced mass of the system. The *Laplacian operator* ∇^2 in spherical coordinates is given by :

$$\nabla^2 = \frac{1}{r^2}\frac{\partial}{\partial r}\left(r^2\frac{\partial}{\partial r}\right) + \frac{1}{r^2\sin\theta}\frac{\partial}{\partial\theta}\left(\sin\theta\frac{\partial}{\partial\theta}\right) + \frac{1}{r^2\sin^2\theta}\frac{\partial^2}{\partial\phi^2} \tag{3.6.1.5}$$

(**Note :** See Sec. 4.1 for this expression).

The variational energy E is given by :

$$E = \frac{\int\psi^*\hat{H}\psi d\tau}{\int\psi^*\psi d\tau} = \frac{\langle\psi^*\hat{H}\psi\rangle}{\langle\psi^*|\psi\rangle} \tag{3.6.1.6}$$

The chosen trial wave function is independent of θ and ϕ. Thus ∇^2 is given by :

$$\nabla^2 = \frac{1}{r^2}\frac{\partial}{\partial r}\left(r^2\frac{\partial}{\partial r}\right) \tag{3.6.1.7}$$

$$\hat{H}\psi = -\frac{h^2}{8\pi^2\mu}\nabla^2\psi - \frac{e^2}{(4\pi\varepsilon_0)r}\psi \tag{3.6.1.8}$$

Click Here t.me/thearchemylibrary

$$\nabla^2\psi = \nabla^2 \exp(-ar) = \frac{1}{r^2}\frac{\partial}{\partial r}\left[r^2 \frac{\partial}{\partial r}\exp(-ar)\right]$$

$$= \frac{1}{r^2}\frac{\partial}{\partial r}\left[r^2(-a)\exp(-ar)\right] = -\frac{a}{r^2}\frac{\partial}{\partial r}\left[r^2\exp(-ar)\right]$$

$$= -\frac{a}{r^2}\left[r^2(-a)\exp(-ar) + 2r \times \exp(-ar)\right]$$

$$= \left(a^2 - \frac{2a}{r}\right)\exp(-ar) \qquad (3.6.1.9)$$

In the present case, $\psi = \psi^*$. Thus we can write :

$$\int \psi \hat{H} \psi d\tau = \int \exp(-ar)\left[-\frac{h^2}{8\pi^2\mu}\left(a^2 - \frac{2a}{r}\right)\exp(-ar) - \frac{e^2}{(4\pi\varepsilon_0)r}\exp(-ar)\right]d\tau$$

$$= \int\left[-\frac{h^2}{8\pi^2\mu}\left(a^2 - \frac{2a}{r}\right)\exp(-2ar) - \frac{e^2}{(4\pi\varepsilon_0)r}\exp(-2ar)\right]d\tau \qquad (3.6.1.10)$$

$$d\tau = r^2 dr \sin\theta\, d\theta\, d\phi \text{ where } \int_0^{\pi}\sin\theta\, d\theta \int_0^{2\pi} d\phi = 2 \times 2\pi = 4\pi$$

i.e.
$$\int_0^{\infty} d\tau = \int_0^{\infty} r^2 dr \int_0^{\pi}\sin\theta\, d\theta \int_0^{2\pi} d\phi = 4\pi \int_0^{\infty} r^2 dr \qquad (3.6.1.11)$$

$$\int_0^{\infty} \psi \hat{H} \psi d\tau = 4\pi \int_0^{\infty}\left[-\frac{h^2}{8\pi^2\mu}\left(a^2 - \frac{2a}{r}\right)\exp(-2ar) - \frac{e^2}{(4\pi\varepsilon_0)r}\exp(-2ar)\right] r^2 dr$$

$$= -\frac{h^2a^2}{2\pi\mu}\int_0^{\infty} r^2 \exp(-2ar)\, dr + \left(\frac{h^2 a}{\pi\mu} - \frac{4\pi e^2}{4\pi\varepsilon_0}\right)\int_0^{\infty} r\exp(-2ar)\, dr \qquad (3.6.1.12)$$

Let,
$$I_1 = \int_0^{\infty} r^2 \exp(-2ar)\, dr \qquad (3.6.1.13)$$

On integration by parts, i.e.

$$\int uv dx = u\int v dx - \int\left[\frac{du}{dx}\int v dx\right]dx$$

$$I_1 = \left[\frac{r^2\exp(-2ar)}{-2a}\right]_0^{\infty} + \frac{1}{a}\int_0^{\infty} r\exp(-2ar)\, dr$$

Click Here for more chemistry library

$$= \frac{1}{a}\int_0^\infty r\exp(-2ar)\,dr, \text{ (the first term vanishes for the limits)}$$

Let, $$I_2 = \int_0^\infty r\exp(-2ar)\,dr = \left[\frac{r\exp(-2ar)}{-2a}\right]_0^\infty + \frac{1}{2a}\int_0^\infty \exp(-2ar)\,dr$$

$$= 0 - \frac{1}{4a^2}\left[\exp(-2ar)\right]_0^\infty = -\frac{1}{4a^2}(0-1) = \frac{1}{4a^2}$$

$$I_1 = \frac{1}{a} \times I_2 = \frac{1}{4a^3}$$

It leads to :

$$\int_0^\infty \psi \hat{H} \psi d\tau = -\frac{h^2a^2}{2\pi\mu} \times \frac{1}{4a^3} + \left(\frac{h^2a}{\pi\mu} - \frac{4\pi e^2}{4\pi\varepsilon_0}\right)\frac{1}{4a^2}$$

$$= -\frac{h^2}{8\pi\mu a} + \frac{h^2}{4\pi\mu a} - \frac{\pi e^2}{4\pi\varepsilon_0} \times \frac{1}{a^2}$$

$$= \frac{h^2}{8\pi\mu a} - \frac{\pi e^2}{a^2(4\pi\varepsilon_0)} \qquad (3.6.1.14)$$

$$\int \psi\psi^* d\tau = \int r^2 \exp(-2ar)\,dr \int \sin\theta\, d\theta \int d\phi$$

$$\int_0^\infty r^2 \exp(-2ar)\,dr \int_0^\pi \sin\theta\, d\theta \int_0^{2\pi} d\phi = 4\pi \int_0^\infty r^2 \exp(-2ar)\,dr = 4\pi I_1 = 4\pi\left(\frac{1}{4a^3}\right) = \frac{\pi}{a^3} \qquad (3.6.1.15)$$

We have :

$$E = \frac{\int \psi^* \hat{H} \psi d\tau}{\int \psi^* \psi d\tau} = \frac{\dfrac{h^2}{8\pi\mu a} - \dfrac{\pi e^2}{(4\pi\varepsilon_0)\,a^2}}{\dfrac{\pi}{a^3}} = \frac{h^2a^2}{8\pi^2\mu} - \frac{e^2a}{4\pi\varepsilon_0} \qquad (3.6.1.16)$$

This *variational energy* incorporates the variable parameter a. For minimising it with respect to a, we have the following condition :

$$\frac{dE}{da} = 0$$

$$\frac{dE}{da} = \frac{h^2}{8\pi^2\mu}(2a) - \frac{e^2}{4\pi\varepsilon_0} = 0$$

Click Here to me/thealchemylibrary

or, $$\frac{h^2 a}{4\pi^2\mu} = \frac{e^2}{4\pi\varepsilon_0}; \text{ or } a = \frac{e^2(4\pi^2\mu)}{h^2(4\pi\varepsilon_0)} \qquad (3.6.1.17)$$

Hence, $$E_{min} = \frac{\hbar^2}{8\pi^2\mu}\left(\frac{e^2 \times 4\pi^2\mu}{h^2 \times 4\pi\varepsilon_0}\right)^2 - \frac{e^2}{4\pi\varepsilon_0}\left(\frac{e^2 \times 4\pi^2\mu}{h^2 \times 4\pi\varepsilon_0}\right)$$

$$= -\frac{2\pi^2\mu e^4}{h^2(4\pi\varepsilon_0)^2} = -\frac{\mu e^4}{8\varepsilon_0^2 h^2} \qquad (3.6.1.18)$$

It is important to note that this energy expression is identical with the one obtained from Bohr's theory (cf. Eqn. 1.8.1.7, where the ground state energy is obtained by putting $n = 1$, $Z = 1$, and m is to be substituted by reduced mass μ).

The same result is also obtained by direct solution of the wave equation, i.e. *R*-equation (cf. Eqn. 4.1.1.10) in the present case.

Note : The integrals may be evaluated from the standard values as follows :

$$\int_o^\infty x^n \exp(-mx)dx = \frac{n!}{m^{n+1}}$$

Process-II (a.u. system) : The above treatment may be simplified in terms of atomic unit (cf. *solved problem* 4 in Chapter 4) :

$$\hat{H}\psi = -\frac{1}{2}\frac{1}{r^2}\frac{\partial}{\partial r}\left[r^2\frac{\partial}{\partial r}\exp(-ar)\right] - \frac{1}{r}\exp(-ar)$$

$$= \left[-\frac{1}{2}\left(a^2 - \frac{2a}{r}\right) - \frac{1}{r}\right]\exp(-ar) \qquad (3.6.1.20)$$

$$E = \frac{\int \psi \hat{H}\psi d\tau}{\int \psi\psi d\tau}$$

$$= \frac{\int_0^\infty \exp(-ar)\left[-\frac{1}{2}\left(a^2 - \frac{2a}{r}\right) - \frac{1}{r}\right]\exp(-ar)\, r^2 dr \int_0^\pi \sin\theta\, d\theta \int_0^{2\pi} d\phi}{\int_0^\infty \exp(-2ar)\, r^2 dr \int_0^\pi \sin\theta\, d\theta \int_0^{2\phi} d\phi}$$

$$= \frac{-\frac{a^2}{2}\int_0^\infty r^2 \exp(-2ar)\, dr + a\int_0^\infty r\exp(-2ar)\, dr - \int_0^\infty r\exp(-2ar)\, dr}{\int_0^\infty r^2\exp(-2ar)\, dr}$$

Click Here t.me/thealchemylibrary

$$= \frac{-\frac{a^2}{2} \times \frac{2}{(2a)^3} + a \times \frac{1}{(2a)^2} - \frac{1}{(2a)^2}}{2/(2a)^3} = \left[\frac{a^2}{2} - a\right] \qquad (3.6.1.21)$$

$$\left(cf. \int_0^\infty x^n \exp(-mx)\, dx = \frac{n!}{m^{n+1}} \right)$$

To minimise E, we have :

$$\frac{dE}{da} = 0 = a - 1, \text{ i.e. } a = 1$$

It leads to : $$E_{min} = -\frac{1}{2} \text{ a.u.} = -13.6 \text{ eV} \qquad (3.6.1.22)$$

Atomic unit of energy = 1 Hartree = $2|E_H| = \frac{2\mu e^4}{8\varepsilon_0^2 h^2} = \frac{2 \times 2\pi^2 \mu e^4}{h^2 (4\pi\varepsilon_0)^2}$

$= 2 \times 13.6 \text{ eV} = 27.2 \text{ eV}$

Click Here t.me/thealchemylibrary

4

Wave Mechanical Model of Atom

Click Here t me/thealchemylibrary

4.1 WAVE MECHANICAL MODEL FOR THE HYDROGEN-LIKE ATOMS OR IONS

4.1.1 Wave Functions for the Hydrogen-like Systems

In the hydrogen atom and in different hydrogen-like systems such as He^{+}, Li^{2+}, Be^{3+} only one electron is revolving around a positively charged nucleus. If the nucleus contains $+Ze$ charge and the electron is at a distance r from the nucleus, then the electrostatic potential energy (V) is given by:

$$V = -\frac{Ze^2}{r}, \text{ (in CGS system); or, } V = -\frac{Ze^2}{4\pi\varepsilon_0 r}, \text{ (in SI system)}$$

Now, if the *nucleus is supposed to remain at rest,* then the Schrödinger wave equation for the hydrogen-like system is given (in CGS system) by :

$$\nabla^2\psi + \frac{8\pi^2 m}{h^2}\left(E + \frac{Ze^2}{r}\right)\psi = 0$$

in which the behaviour of the electron is described by the wave function, ψ and the corresponding energy by E. More correctly the **reduced mass,** μ replaces the mass (m) of the electron and it becomes,

$$\nabla^2\psi + \frac{8\pi^2 \mu}{h^2}\left(E + \frac{Ze^2}{r}\right)\psi = 0 \qquad (4.1.1.1)$$

where, $\mu = \dfrac{Mm}{M+m}$; if M (mass of the nucleus) >> m then $\mu \approx m$.

It becomes easier to solve the above equation, if it is expressed in terms of *spherical polar coordinates.* The relationship between the Cartesian coordinates x, y, z and the polar coordinates r, θ and φ for a

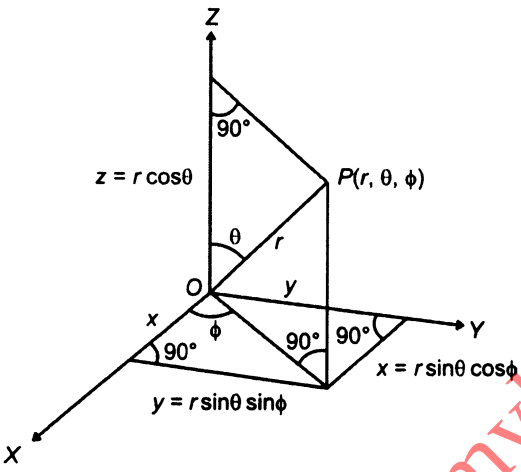

Fig. 4.1.1.1. Relationship between the Cartesian (x, y, z) and spherical coordinates (r, θ, ϕ).

particular point P is shown in Fig. 4.1.1.1. Here the point P can be the position of the electron, and the nucleus is remaining at rest at the origin O. Geometrically, the following relations are obtained,

$$\boxed{x = r\sin\theta\cos\phi,\ y = r\sin\theta\sin\phi,\ z = r\cos\theta, \text{ and } r^2 = x^2 + y^2 + z^2}$$

By using these relations, the wave equation is transformed into spherical coordinates as,

$$\frac{1}{r^2}\frac{\partial}{\partial r}\left(r^2\frac{\partial\psi}{\partial r}\right) + \frac{1}{r^2\sin\theta}\frac{\partial}{\partial\theta}\left(\sin\theta\frac{\partial\psi}{\partial\theta}\right) + \frac{1}{r^2\sin^2\theta}\frac{\partial^2\psi}{\partial\phi^2} + \frac{8\pi^2\mu}{h^2}\left(E + \frac{Ze^2}{r}\right)\psi = 0 \quad ...(4.1.1.2)$$

Note : In SI system, $\frac{Ze^2}{r}$ is replaced by $\frac{Ze^2}{(4\pi\varepsilon_0)r}$.

The wave function ψ is a function of the three variables r, θ and ϕ. **The wave function can be split into three parts, each of which is a function of a single variable.** Thus,

$$\psi(r, \theta, \phi) = R(r)\Theta\,\theta\,\Phi(\phi)$$

Substituting this relation in Eqn. 4.1.1.2 along with the mathematical manipulation we get,

$$\frac{\sin^2\theta}{R}\frac{d}{dr}\left(r^2\frac{dR}{dr}\right) + \frac{\sin\theta}{\Theta}\frac{d}{d\theta}\left(\sin\theta\frac{d\Theta}{d\theta}\right) + r^2\sin^2\theta\frac{8\pi^2\mu}{h^2}\left(E + \frac{Ze^2}{r}\right) = -\frac{1}{\Phi}\frac{d^2\Phi}{d\phi^2} \quad ...(4.1.1.3)$$

The left hand side of the above equation contains the variables r and θ and the right hand side contains only one variable ϕ. Thus, the sum of the two terms involved at the left hand side must always be equal to the term of the right hand side. **This can only happen if each side of the equation is equal to some constant.** Let the constant be m^2. Thus we get,

$$\textbf{Φ equation :}\ \boxed{\frac{1}{\Phi}\frac{d^2\Phi}{d\phi^2} + m^2 = 0} \quad ...(4.1.1.4)$$

Click Here t.me/thealchemylibrary

By using the above relationship in Eqn. 4.1.1.3 we get,

$$\frac{1}{R}\frac{d}{dr}\left(r^2\frac{dR}{dr}\right)+\frac{8\pi^2r^2\mu}{h^2}\left(E+\frac{Ze^2}{r}\right)+\frac{1}{\Theta\sin\theta}\frac{d}{d\theta}\left(\sin\theta\frac{d\Theta}{d\theta}\right)=\frac{m^2}{\sin^2\theta}$$

or,
$$\boxed{\frac{1}{R}\frac{d}{dr}\left(r^2\frac{dR}{dr}\right)+\frac{8\pi^2r^2\mu}{h^2}\left(E+\frac{Ze^2}{r}\right)=\frac{m^2}{\sin^2\theta}-\frac{1}{\Theta\sin\theta}\frac{d}{d\theta}\left(\sin\theta\frac{d\Theta}{d\theta}\right)} \quad ...(4.1.1.5)$$

Here, each side contains only one variable, hence they must be equal to some constant, say β. Thus, we get :

R-equation :
$$\boxed{\frac{1}{R}\frac{d}{dr}\left(r^2\frac{dR}{dr}\right)+\frac{8\pi^2r^2\mu}{h^2}\left(E+\frac{Ze^2}{r}\right)-\beta=0} \quad ...(4.1.1.6)$$

and **Θ-equation :**
$$\boxed{\frac{1}{\Theta\sin\theta}\frac{d}{d\theta}\left(\sin\theta\frac{d\Theta}{d\theta}\right)+\left(\beta-\frac{m^2}{\sin^2\theta}\right)=0} \quad ...(4.1.1.7)$$

Thus the original differential equation yields the following three simpler equations each containing one variable,

Φ-equation :
$$\boxed{\frac{1}{\Phi}\frac{d^2\Phi}{d\phi^2}=-m^2} \quad ...(4.1.1.8)$$

Θ-equation :
$$\boxed{\frac{1}{\sin\theta}\frac{d}{d\theta}\left(\sin\theta\frac{d\Theta}{d\theta}\right)+\left(\beta-\frac{m^2}{\sin^2\theta}\right)\Theta=0} \quad ...(4.1.1.9)$$

and **R-equation :**
$$\boxed{\frac{1}{R}\frac{d}{dr}\left(r^2\frac{dR}{dr}\right)+\frac{8\pi^2\mu}{h^2}\left(E+\frac{Ze^2}{r}\right)r^2=\beta} \quad ...(4.1.1.10)$$

where, $\beta = l\,(l+1)$

Eqns. 4.1.1.8 **(Φ equation)** and 4.1.1.9 **(Θ equation)** are called the ***angular equations*** as they express the angular part of the complete wave function. Eqn. 4.1.1.10 is called the ***radial equation*** **(*R* equation)** and it deals with radial part of the complete wave function.

The solutions are given as follows :

$$\Phi(\phi)=\frac{1}{\sqrt{2\pi}}\exp(im\phi);\ m=0,\pm1,\pm2,\pm3, \quad ...(4.1.1.11)$$

where $\frac{1}{\sqrt{2\pi}}$ *is the normalising constant.*

$$\Theta(\theta)=\frac{\sqrt{(2l+,1)\,(l-|m|)\,!}}{\sqrt{2(l+|m|)\,!}}P_l^{|m|}(\cos\theta) \quad ...(4.1.1.12)$$

Click Here to me/thealchemylibrary

where $(m = 0, \pm 1, \pm 2, \pm 3, ..., \pm l)$

and,
$$R(r) = -\left[\left(\frac{2Z}{na_0}\right)^3 \frac{(n-l-1)!}{2n[(n+l)!]^3}\right]^{1/2} \exp(-x/2)\, x^l L_{n+1}^{2l+1}(x) \qquad ...(4.1.1.13)$$

where,
$$x = \frac{2Zr}{na_0},\ a_0 = \frac{h^2}{4\pi^2 \mu e^2}$$

[*Note* : In atomic unit, a_0 is unity $\left(\text{i.e. } \mu = 1, e = 1 \text{ and } \frac{h}{2\pi} = 1\right)$. In SI unit, $a_0 = \frac{(4\pi\varepsilon_0)h^2}{4\pi^2 \mu e^2}$ and in atomic unit, $4\pi\varepsilon_0 = 1$. The R-equation can be expressed in atomic units (see solved Problem 4 of this Chapter).]

Here, $P_l^{|m|}(\cos\theta)$ is called ***Legendre Polynomial*** and $L_{n+l}^{2l+1}(x)$ is called ***Associated Laguerre Polynomial*** of degree $(n - l - 1)$. Some values of the **Associated Laguerre Polynomials** are given in Table 4.1.1.1.

The complete wave function for the hydrogen atom and hydrogen-like systems is given by :

$$\psi_{n,l,m}(r,\theta,\phi) = \frac{2Z^{3/2}}{n^2 a_0^{3/2}}\left(\frac{(n-l-1)!(2l+1)(l-|m|)!}{[(n+l)!]^3\, 4\pi(l+|m|)!}\right)^{1/2} \exp[-(x/2)]$$
$$x^l L_{n+l}^{2l+1}(x)\, P_l^{|m|}(\cos\theta) \exp(im\phi) \qquad ...(4.1.1.14)$$

where
$$x = \frac{2Zr}{na_0}$$

From the above relations the following quantum numbers automatically arise (Sec. 4.1.2).

(i) n is called the ***principal quantum number*** and it can have any integral value like, 1, 2, 3, ...

(ii) l is called the ***azimuthal quantum number*** and l can have values, 0, 1, 2, ..., $(n - 1)$.

(iii) m is called the ***magnetic quantum number.*** It can have any integral value from $-l$ to $+l$ including zero.

Table. 4.1.1.1. Some values of the Associated Laguerre Polynomials $\left(x = \frac{2Zr}{na_0}\right)$

$n = 1$,	$l = 0$,	$L_1^1(x) = -1$
$n = 2$,	$l = 0$,	$L_2^1(x) = -2!(2-x)$
	$l = 1$,	$L_3^3(x) = -3!$
$n = 3$,	$l = 0$,	$L_3^1(x) = -3!\left(3 - 3x + \frac{1}{2}x^2\right)$
	$l = 1$,	$L_4^3(x) = -4!(4-x)$
	$l = 2$,	$L_5^5(x) = -5!$

Click Here t.me/thealchemylibrary

From the above solution, it appears that the total wave function can be expressed as follows,

$$\psi_{total}(r, \theta, \phi) = \psi_{radial}(r) \times \psi_{angular}(\theta, \phi)$$

where, $\psi_{raidal} = R_{n,l}(r)$ and $\psi_{angular} = \Theta_{l,m}(\theta)\,\Phi_m(\phi) = A_{l,m}(\theta, \phi)$

Thus, $\psi_{total} = \psi_{n,l,m}(r, \theta, \phi) = R_{n,l}(r)\,\Theta_{l,m}(\theta)\,\Phi_m(\phi)$

Such a wave function describing an electron is called an ***orbital***. The allowed values of energy of the electron are obtained by solving the equations. It is generally expressed as:

$$E = -(2\pi^2\mu Z^2e^4)/(n^2h^2) \text{ in CGS system.}$$

Probability density : $\psi^2_{n,l,m}$ denotes the probability density for the electron per unit volume. Thus the probability of finding the electron in the volume element dV or $d\tau$ ($= r^2dr\sin\theta d\theta d\phi$) in the neighbourhood of the point (r, θ, ϕ) is given by :

$$\psi^2_{n,l,m}d\tau \text{ or } \psi_{n,l,m}\psi^*_{n,l,m}d\tau.$$

The total probability over the entire volume is unity, i.e. :

$$\int_0^\infty \int_0^\pi \int_0^{2\pi} \psi^2_{n,l,m} r^2 \sin\theta d\theta d\phi dr = 1 \text{ or, } \int_0^\infty \int_0^\pi \int_0^{2\pi} \psi_{n,l,m}\psi^*_{n,l,m} r^2 \sin\theta d\theta d\phi dr = 1$$

Conditions of normalisation of radial and angular parts of the wave functions are :

$$\int_0^\infty [R_{n,l}(r)]^2 r^2 dr = 1$$

$$\int_0^{2\pi} [\Phi_m(\phi)][\Phi^*_m(\phi)]d\phi = 1$$

$$\int_0^\pi [\Theta_{l,m}(\theta)]^2 \sin\theta d\theta = 1$$

4.1.2 Wave Mechanical Genesis of the Quantum Numbers

In classical mechanics, introduction of the different quantum numbers was mainly standing on the postulates required to make the models compatible and to explain the experimental findings. But, in the wave mechanical treatment of the atoms, the ***triplet set of the quantum numbers*** **(*n, l, m*)** develops automatically as a mathematical requirement of getting the well behaved solutions from the second order partial differential equations. Thus, in wave mechanics, the quantum restrictions are not arbitrarily imposed, rather these are the consequences of demanding the well behaved solutions. The genesis of the different quantum numbers in solving the wave equation is discussed below.

- **Genesis of the *magnetic quantum number* (*m*) (≡ m_l *in vector model*):** From the previous discussion, it is found that the solution of the differential equation (Φ equation), $\frac{1}{\Phi}\frac{d^2\Phi}{d\phi^2} = -m^2$, is :

Click Here t.me/thealchemylibrary

$$\Phi(\phi) = \frac{1}{\sqrt{2\pi}} \exp(im\phi),$$

Here $\frac{1}{\sqrt{2\pi}}$ appears as a *normalising constant* (N). The range of ϕ is 0 to 2π, i.e. :

$$\int_0^{2\pi} [\Phi(\phi)\Phi^*(\phi)]d\phi = N^2 \int_0^{2\pi} \exp(im\phi)\exp(-im\phi)d\phi = N^2(2\pi) = 1$$

$$\text{i.e. } N = \frac{1}{\sqrt{2\pi}}$$

Here $\Phi(\phi)$ is a part of the complete wave function ψ. Therefore, *the above solution to be acceptable must be single valued at a particular point in space*. This is a basic condition for the well behaved functions, i.e. eigen functions. From the relationship between the spherical coordinates (r, θ, ϕ) and Cartesian coordinates (Fig. 4.1.1.1), it is found that ϕ can vary from zero to 2π. Thus ϕ and ($\phi + 2\pi$) refer to the same meridian. **Hence, to maintain the condition for the single valued function, the following condition must be satisfied.**

$$\Phi(\phi) = \Phi(\phi + 2\pi); \text{ or } \frac{1}{\sqrt{2\pi}} \exp(im\phi) = \frac{1}{\sqrt{2\pi}} \exp[im(\phi + 2\pi)]$$

To satisfy the above condition, m must be given by : $m = 0, \pm 1, \pm 2, \ldots$ **Thus the values of *m* are restricted. Therefore, *m* is a quantum number. It is called the *magnetic quantum number*** (in vector model it is designated by m_l), as the energy of the electron in hydrogen-like systems in an external magnetic field depends on this quantum number.

- ***Genesis of the azimuthal quantum number (l)*** : We have the Θ equation :

$$\frac{1}{\sin\theta}\frac{d}{d\theta}\left(\sin\theta\frac{d\Theta}{d\theta}\right) + \left(\beta - \frac{m^2}{\sin\theta}\right)\Theta = 0$$

*By using the acceptable values of m in the above equation, the well behaved solutions for $\Theta(\theta)$ can only be obtained **under the restriction, $\beta = l(l+1)$, where l is related with m as follows :***

$$l = 0, 1, 2, 3, \ldots\ldots; \text{ and } m = 0, \pm 1, \pm 2, \ldots\ldots, \pm l$$

The actual mathematical procedure to have the restrictions is lying beyond the scope of this book. The above integer l is called the ***azimuthal quantum number* or *angular momentum quantum number***, as it is required to determine the angular momentum. The angular momentum is given by $\sqrt{l(l+1)}\,(h/2\pi)$.

From the above relations the allowed values of m and l are interrelated as follows :

$$m = -l, -(l-1), -(l-2), \ldots 0, \ldots, (l-1), l.$$

Thus, m can have any integral value in the range $-l$ to $+l$ including zero. For a particular value of l, m can have $(2l + 1)$ values.

- ***Genesis of the principal quantum number (n)*** : By using the value $\beta = l(l+1)$, when the R-equation $\frac{1}{R}\frac{d}{dr}\left(r^2\frac{dR}{dr}\right) + \frac{8\pi^2\mu}{h^2}\left(E + \frac{Ze^2}{r}\right)r^2 = \beta$ is solved, *it is found that for all positive*

Click Here to the chealchemylibrary

values of E, the function R(r) is well-behaved. The positive value of E indicates that the electron is not in the atom and the atom is ionised. Under this condition the electron can move freely for which there is no quantum restriction in having the energy which is purely kinetic energy (*cf.* the model, free particle, Sec. 3.5.1). As we are interested with the atom in which the electron is bound, consideration of the positive values of E is of no practical importance. *Therefore, to consider the electron within the atom, we must pay attention to the negative values of E.*

For the negative values of E, the function R(r) is only well defined when the values of E remain in the following restricted condition.

$$E_n = -\frac{2\pi^2 \mu Z^2 e^4}{n^2 h^2} \text{ when } n = 1, 2, 3\ldots \text{ and } l = 0, 1, 2, \ldots (n-1)$$

Thus, for a particular value of n, l can have values, 0, 1, 2, ... $(n-1)$. Here, again it is worth mentioning that the actual mathematical procedure to have the above restriction for n is very much complicated, and it lies beyond our present discussion. However, the integer, n is called ***the principal quantum number*** which is alone responsible to determine the energy of the electron in hydrogen-like systems.

From the above discussion, the **allowed values of quantum numbers** are given as follows :

$$n = 1, 2, 3, \ldots ; l = 0, 1, 2, \ldots (n-1) ; m = \pm l, \pm (l-1), \pm (l-2), \ldots, 0.$$

The **complete wave function** describing the electron *in terms of three quantum numbers n, l* and m can be shown as follows indicating the parts dependent on the respective quantum numbers,

$$\psi_{n,\,l,\,m}(r, \theta, \phi) = R_{n,\,l}(r)\, \Theta_{l,\,m}(\theta)\, \Phi_m(\phi).$$

- ***Spin quantum number in wave mechanics*** : *The above discussion shows the genesis of the three quantum numbers, n, l and m. In the above nonrelativistic wave equation, there is no existence of the* **spin quantum number.** Thus it appears very difficult to accommodate the concept of a spinning electron in wave mechanics. But, this concept introduced by Uhlenbeck and Goudsmit in the vector model is extremely important to explain a number of experimental facts which have been already discussed in Section 1.10.2. To solve the problem, Dirac (1928) introduced the *relativistic correction in the Schrödinger equation which on solution gave the wave mechanical genesis of the spin quantum number.* The value of the quantum number developed in the mathematical treatment in this relativistic model is identical with that of vector model.
- ***Complete wave function*** : In terms of these four quantum numbers, the complete wave function describing the electron should be expressed as follows :

$$\psi_{(n,\,l,\,m,\,s)} = \psi_{\text{orbital}} \times \psi_{\text{spin}} = \psi_{(n,\,l,\,m)} \times \psi_{\text{spin}}(s) = R_{n,\,l}(r)\, \Theta_{l,\,m}(\theta)\, \Phi_m(\phi) \times \psi_{\text{spin}}(s)$$

where, $\psi_{\text{spin}}(s)$ represents the *spin wave function* of the complete orbital describing an electron.

4.1.3 Important Features of a Dirac Atom Developed from the Relativistic Wave Mechanics

The important features of a Dirac atom are given below :

(a) **Spin quantum number :** The Dirac atom accommodates the fourth quantum number, i.e. the spin quantum number, along with the other three quantum numbers in its relativistic wave

Click Here to meetheal chemylibrary

mechanics. In nonrelativistic Schrödinger's wave equation, there is no existence of the spin quantum number.

(b) **Energy dependence on both *n* and *l* :** Though in the nonrelativistic model, the energy of the electron in hydrogen-like systems is independent of the azimuthal quantum number, in the Dirac's relativistic model, the energy of the electron in hydrogen-like systems is dependent on both the principal quantum number and the azimuthal quantum number. In this connection, the Sommerffeld's relativistic correction is comparable (Sec. 1.9.1.B).

(c) **Modified concept of nodes :** In the Dirac model, the true nodes (where the electron density is zero) which will be discussed later on do not exist. However, in this relativistic model, there are regions where the electron density is very small.

Though the Dirac model provides the more accurate treatment, the theoreticians prefer the nonrelativistic model because of its mathematical simplicity. The errors incorporated at the cost of its simplicity are definitely small.

4.1.4. The Radial Wave Function and Radial Probability Distribution of Electron Cloud in Hydrogenic Systems

The previous discussion shows that the radial wave function depends on only the two quantum numbers, principal quantum number (n) and azimuthal quantum number (l). It is very often expressed as : $\psi_{radial}(r) = R_{n,l}(r)$.

By using Eqn. 4.1.1.13, the expressions for normalised radial wave functions can be obtained. Some of them are given in Table 4.1.4.1

Table 4.1.4.1. Some representative normalised radial wave functions for hydrogen-like systems

n	l	Name of the orbital	Radial wave function = $R_{n,l}$
1	0	1*s*	$R_{1,0} = 2(Z/a_0)^{3/2} \exp(-u)$
2	0	2*s*	$R_{2,0} = \frac{1}{2\sqrt{2}}(Z/a_0)^{3/2}(2-u)\exp(-u/2)$
2	1	2*p*	$R_{2,1} = \frac{1}{2\sqrt{6}}(Z/a_0)^{3/2} u \exp(-u/2)$
3	0	3*s*	$R_{3,0} = \frac{2}{81\sqrt{3}}\left(\frac{Z}{a_0}\right)^{3/2}(27-18u+2u^2)\exp(-u/3)$
3	1	3*p*	$R_{3,1} = \frac{4}{81\sqrt{6}}\left(\frac{Z}{a_0}\right)^{3/2}(6u-u^2)\exp(-u/3)$
3	2	3*d*	$R_{3,2} = \frac{4}{81\sqrt{30}}\left(\frac{Z}{a_0}\right)^{3/2} u^2 \exp(-u/3)$

Z = nuclear charge, $a_0 = h^2/(4\pi^2\mu e^2) = 0\ 53$ Å, $u = Zr/a_0$

For the polyelectronic systems, the exact solutions of the wave equation are never obtained. In practice, neglecting the electron-electron repulsion, the hydrogen-like wave functions are taken for an approximate consideration in polyelectronic systems.

Click Here t.me/thealchemylibrary

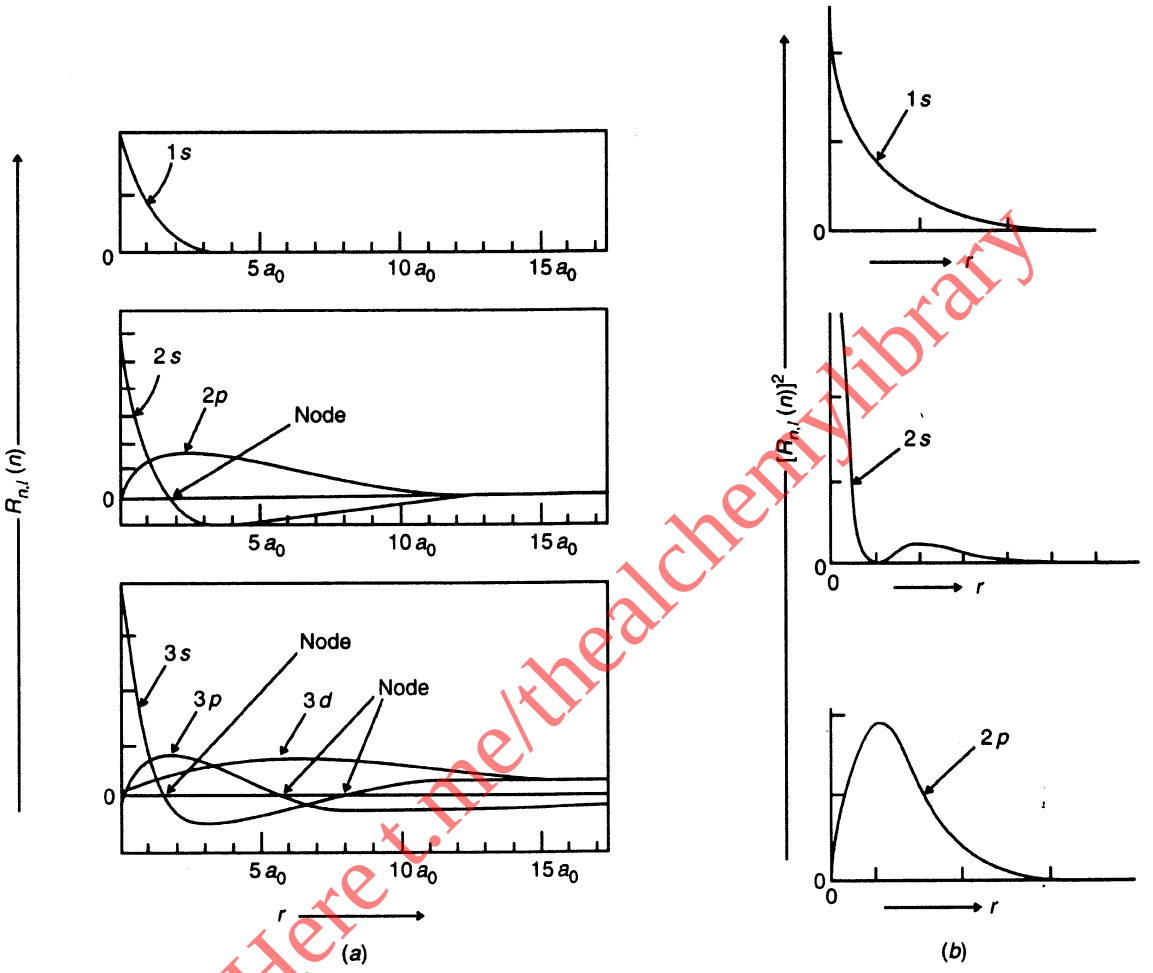

Fig. 4.1.4.1. (a) Variation of radial wave function with distance from the nucleus in hydrogen atoms. (b) Qualitative representation of radial probability density as a function of r for 1s, 2s and 2p orbital.

Characteristic Features of the Radial Wave Functions : From the graphical plots (Fig. 4.1.4.1) and expressions for the radial wave functions, the following points are evident.

(i) The expression always contains the **exponential decay term,** $\exp(-Zr/na_0)$ (comparable to that of first order kinetics as in the case of radioactive decay), and for the higher values of n the decay is slower. ***This is why, the most probable radius of the orbital increases with the increase of the principal quantum number (n).***

(ii) When $r \to \infty$ (practically for the larger value of r), $R \to 0$.

(iii) In each of the cases (e.g. 2s, 3s, 3p, etc.) for a certain finite value of r, the radial part $R_{n,l}$ of the orbital becomes zero. These values of r are different for different orbitals. These particular points are called ***radial nodal points.*** For example, for the 2s (i.e. $n = 2$, $l = 0$) orbital, at $r = (2a_0/Z)$, $R = 0$. At the nodal point, value of the radial wave function changes its sign from

Click Here t.me/thealchemylibrary

+ *ve* to – *ve*. It is evident that for the *s*-orbitals there are $(n-1)$ radial nodes while for the *p*- and *d*-orbitals these are $(n-2)$ and $(n-3)$ respectively.

Radial Distribution Function (RDF) : As usual, the square of the radial wave function gives the measure of probability of finding the electron at various points in space. Thus the probability of finding the electron in the small volume $d\tau$ enclosed between the concentric spheres of radius r and $r + dr$ measured from the nucleus supposed to exist at the centre of spheres is given by : $\psi^2_{radial} d\tau = R^2 d\tau$ where $d\tau = 4\pi r^2 dr$. This $d\tau$ can be obtained as follows, V = volume of a sphere of radius $r = (4/3)\pi r^3$. Therefore, $dV = 4\pi r^2 dr$. In our consideration, $d\tau = dV$. Therefore the *radial probability* of finding the electron in a shell of thickness dr at a distance r from the nucleus is given by,

$$\boxed{4\pi r^2 \psi^2_{radial} dr = 4\pi r^2 R^2 dr.}$$

Radial Probability Density and Radial Shell Probability Distribution Function (simply called Radial Distribution Function, RDF) : Now we are at the right position to clarify the significance of these two terms. The ***radial probability density*** $[P(r)]$ is given by the square of the radial wave function i.e.

$$P(r) = [R_{n,l}(r)]^2, \text{ (cf. Fig. 4.1.4.1b)}$$

$P(r)$ denotes the probability per unit volume.

For 1*s* orbital of *H*-atom,

$$R_{1s} = 2\left(\frac{1}{a_o}\right)^{3/2} \exp(-r/a_o)$$

$$P_{1s}(r) = [R_{1s}]^2 = \frac{4}{a_0^3} \exp(-2r/a_0)$$

The complete wave function of 1*s* orbital is :

$$\psi_{1s} = \frac{1}{(\pi a_0^3)^{1/2}} \exp(-r/a_0), \text{ (independent of } \theta \text{ and } \phi)$$

The probability is :

$$P_{1s}(\psi) = [\psi_{1s}]^2 = \frac{\exp(-2r/a_0)}{\pi a_0^3}$$

Thus though the magnitudes of **$P_{1s}(\psi)$ and $P_{1s}(r)$ are different** but they are of the same nature. In fact, for the *ns* orbitals, it happens so because the *ns* orbitals are independent of θ and ϕ angle. For the other orbitals like *p, d,* .... which are not spherically symmetrical, $P(\psi)$ depends on θ and ϕ. ***Thus, in general, $P(\psi)$ and $P(r)$ are two different parameters.*** **In such cases, we consider $P(r)$ *assuming the orbitals to be spherically symmetrical.***

If we plot (cf. Fig. 4.1.4.2-3), $P(r)$ vs. r for 1*s* orbital, it is evident that the *probability density* decreases exponentially. **It is maximum near the nucleus. But the total *probability* (i.e. *total amount of electron cloud*) *near the nucleus is very small as the volume near the nucleus is very small.***

Click Here to me/thealchemylibrary

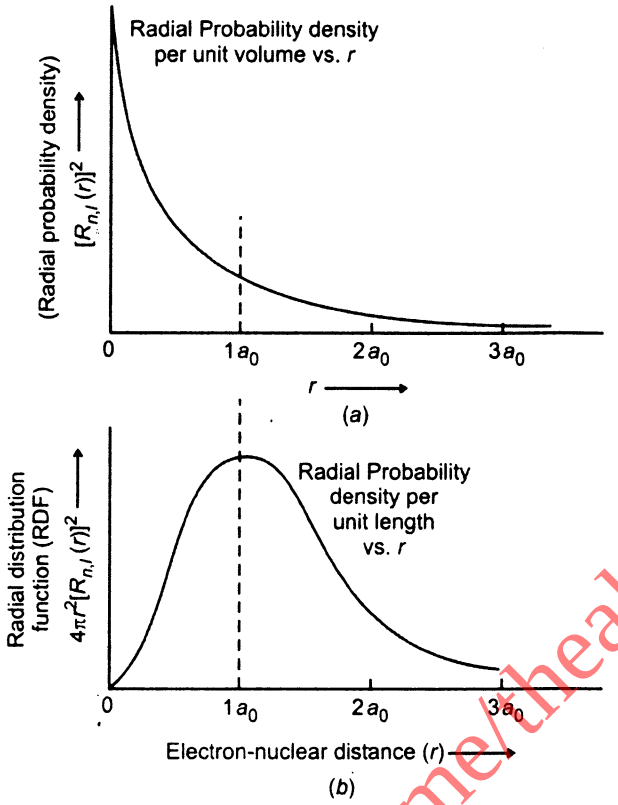

Fig. 4.1.4.2. Schematic representation of (a) radial probability $[P(r)]$ as a function of r and (b) radial distribution function (RDF) as a function r, for 1s electron of H-atom.
Note : RDF is nonsymmetrical around r_{max}. It makes $\bar{r} > r_{max}$ (cf. Solved Problem 7).

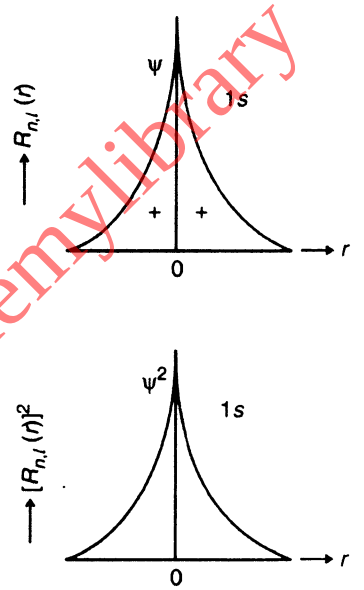

Fig. 4.1.4.3. Schematic representation of the wave function ψ and its probability density ψ^2 for the 1s electron of H-atom.

It is better to consider the **total probability of the existence of the electron cloud in the spherical shell bounded by the concentric spheres of radius r and $r + dr$** (measured from the nucleus). The volume of spherical shell is $4\pi r^2 dr$, and the probability of the existence of the electron cloud in the spherical shell is given by, $P(r)4\pi r^2 dr = D(r)dr$ where,

$$D(r) = 4\pi r^2 P(r)$$

Thus $D(r)dr$ gives the probability of finding the electron at a distance between r and $r + dr$ measured from the nucleus. Thus the distribution function $D(r)$ measures probability per unit radial distance. The function $D(r) = 4\pi r^2 R^2$ itself is not meaningful but the plot $4\pi r^2 R^2$ vs. r is informative.

This function $D(r)$ is called ***radial shell probability distribution*** or simply ***radial distribution function (RDF).***

For 1s-orbital it is :

$$D_{1s}(r) = 4\pi r^2 P_{1s}(r) = \frac{16\pi r^2}{a_0^3} \exp(-2r/a_0)$$

Click Here t.me/healchemylibrary

For the *s*-orbitals, the probability of electron density measured by $P(\psi)$ or $P(r)$ is maximum at the nucleus but **for all other orbitals this probability is zero at the nucleus** (*cf.* Figs. 4.1.4.1-3). However, for *s*-orbital also, the total probability given by $P(\psi)d\tau$ is zero for $r = 0$ because the volume element $d\tau$ goes to be zero at $r = 0$. **The RDF ($= 4\pi r^2R^2$) is always zero at $r = 0$ i.e. at the nucleus.**

- ***For the s-orbitals***, both the wave functions and probability density are independent of θ and ϕ. Consequently, electron density is spherically symmetrical around the nucleus. For the *s*-orbitals, *probability density per unit volume* is measured by $[\psi_{ns}]^2$ and *probability density per unit radial distance r* is measured by $4\pi r^2[\psi_{ns}]^2$.
- ***For the p or d orbitals*** (i.e. $l \neq 0$), the wave functions depend on θ and ϕ. In such cases, ψ^2 measuring the probability density depends on θ and ϕ. The same thing happens for $4\pi r^2\psi^2$. In such cases, the RDF i.e. $4\pi r^2R^2$ represents the probability of the electron in a spherical element at a distance *r* from the nucleus ***assuming the spherical symmetry of the orbital.*** However, these are not actually spherically symmetrical. **Thus the plot, $4\pi r^2R^2$ vs. *r* does not represent the real situation for the *p*, *d* orbitals for which $l \neq 0$.**
- ***For the s-orbitals***, if $4\pi r^2R^2$ is considered, then the values are only different from $4\pi r^2\psi_{ns}^2$ in terms of magnitude but not in terms of nature.

  For 1*s* orbital :

$$4\pi r^2[\psi_{1s}]^2 = \frac{4r^2}{a_0^3}\exp(-2r/a_0)$$

$$4\pi r^2[R_{n,l}]^2 = \frac{16\pi r^2}{a_0^3}\exp(-2r/a_0)$$

$$\text{i.e. } r^2[R_{n,l}]^2 = 4\pi r^2[\psi_{1s}]^2$$

  This $r^2[R_{n,l}]^2$ is also described as **radial probability density or RDF.**

  Because of the spherically symmetrical nature of the *s*-orbital, both the plots i.e. $4\pi r^2[\psi_{ns}]^2$ vs. *r* and $4\pi r^2R_{ns}^2$ vs. *r* are equally meaningful and they provide the same information.

Thus we can conclude :

- ***Radial probability density [P(r)] is the probability density per unit volume while radial distribution function (RDF) gives the idea of total probability of finding the electron in the spherical shell bounded by the spheres of radius r and r + dr. RDF measures the probability per unit length at the distance r.***

  Fig. 4.1.4.4 shows some representative plots of $4\pi r^2R^2$ vs. *r* and these plots are called *radial probability distribution curves* or *RDF curves* for the electrons.

- ***Characteristic Features of the Radial Distribution Function (RDF) Curves :***

  (i) ***RDF at r = 0 :*** $4\pi r^2R^2$ becomes zero at $r = 0$. It may be noted that for $r = 0$, $R^2 \neq 0$ for *s*-orbital, $R^2 = 0$ for other orbitals like *p*, *d*, etc. But RDF given by $4\pi r^2R^2$ is always zero for $r = 0$.

  (ii) ***Probability at r = ∞ :*** As $r \to \infty$, the probability tends to be zero. In a practical sense, at the larger values of *r*, the probability approaches to almost zero.

  (iii) ***Maximum probability regions (r_{max} values) :*** For the orbitals, as *r* increases from the nucleus, the probability increases and at a finite value of *r*, the probability becomes maximum then it

Click Here t.me/thealchemylibrary

falls down with the increases of r. Except the orbitals like $1s$, $2p$, $3d$, $4f$, ... i.e. **the orbitals appearing first time,** in all other cases, for more than one value of r, the maxima (of different magnitudes) appear. The r_{max} values for different orbitals are: $1s(a_o)$; $2s(0.77a_o, 5.23a_o)$; $2p(4a_o)$, etc. This nature is represented for different orbitals such as, $1s$ ($n = 1, l = 0$), $2p$ ($n = 2, l = 1$), $3d$ ($n = 3, l = 2$) in Fig. 4.1.4.4.

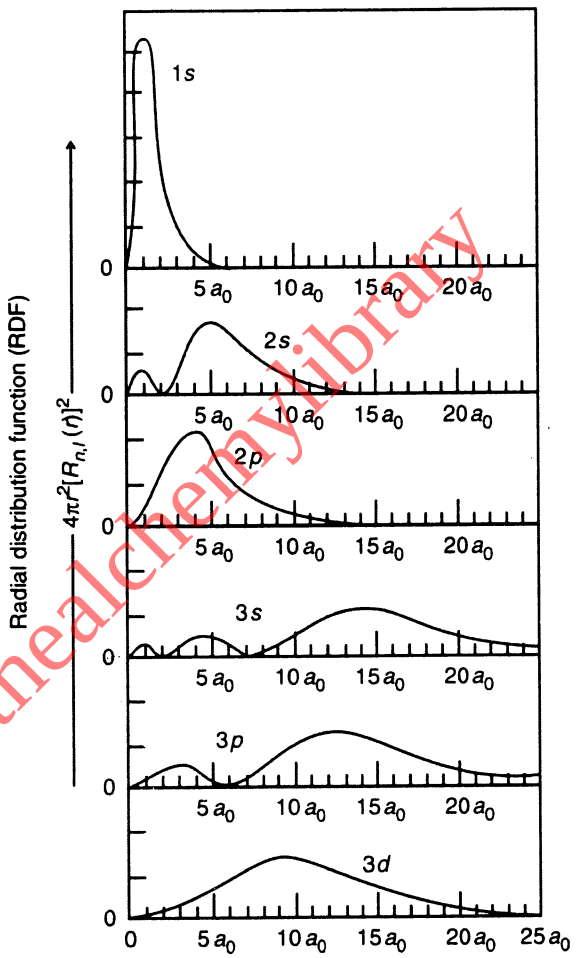

Fig. 4.1.4.4. Radial probability distribution curves i.e. RDF curves for different orbitals in hydrogen atoms.

(iv) ***Maximum probability region (r_{max}) for 1s orbital*** **:** For the probability distribution curve of $1s$ electron, it is evident that for hydrogen at $r = 0.529$ Å ($= a_0/Z$) (see solved Problem 1), the probability is maximum. Here it is worth remembering that in Bohr's model, the calculated value of the first Bohr's orbit (i.e. r_1) coincides with this value. But there is a striking difference between these concepts. In Bohr's model of hydrogen atom, the electron always resides at a well defined circular locus at a distance 0.529 Å from the nucleus. But in the wave mechanics, there is always a probability for any value of r (except $r = 0$, at nodal points, and ∞) in locating the electron in space around the nucleus but at the distance 0.529 Å, the probability for the $1s$ hydrogen electron is maximum (say, 95% < probability < 100%).

Note **:** See the solved problems 5 and 7 to understand the difference between r_{max} and $\bar{r}$ (average distance or expectation value).

(v) ***Radial nodes*** **:** For the orbitals like $2s$, $3s$, $3p$, etc. due to the existence of one or more radial nodes (Fig. 4.1.4.4), there are small maxima bearing electron density between the nucleus and the largest maximum. Thus the total number of maxima including the largest one for s, p, d, ... orbitals is given by n, $(n - 1)$, $(n - 2)$, $(n - 3)$,.. respectively where n is the principal quantum number. ***In general, there are $(n - l - 1)$ radial nodes (ignoring the nodal point at $r = 0$) in the radial distribution functions, and consequently there are $[(n - l - 1) + 1]$ maxima in the radial distribution function for the orbitals.***

For example, for the $2s$ electron (see Solved Problem 5), the ***first maximum*** (smaller one) appears at $r \approx a_0/Z = (0.529/Z)$ Å and the **largest one** arises at $r \approx (5a_0/Z)$ Å. Here it is

Click Here t.me/thealcremylibrary

noteworthy that the radial wave function is positive for $r < 2a_0/Z$ and negative for $r > 2a_0/Z$ (Fig. 4.1.4.1) ($Z = 1$ for hydrogen), but the probability is positive for everywhere as a consequence of squaring operation. At the nodal point ($r = 2a_0/Z$), the probability is zero. Thus, here the probability is zero for, $r = 0$, and 1.058 Å ($= 2a_0/Z$) and ∞. Similar distribution patterns also exist for the other orbitals.

(vi) ***r_{max} of the largest maximum probability region* and n :** The distance (measured from the nucleus) of the ***largest maximum probability region*** increases with the increase of its principal quantum number n. When there are intranodal maxima of relatively smaller magnitudes, the combined effect of all the maxima including the largest one determines the **average r_{max} i.e. $<r_{max}>$ which is smaller than the r_{max} of the largest one.** This $<r_{max}>$ determines the energy of the orbital. RDF curves indicate that $<r_{max}>$ increases with the increase of n. *This is why, energy of the orbitals increases with the increase of the principal quantum number.*

(vii) ***Intranodal maxima and penetrating power* :** For a comparison among the 3*s*, 3*p*, 3*d* orbitals (see also Sec. 4.2.3), it is evident that the **r_{max} for the largest maximum probability region** lies in the sequence: $r_{max}(3s) > r_{max}(3p) > r_{max}(3d)$ but, ***for the 3s and 3p orbitals, there are two and one additional intranodal maxima (smaller) at the lower distances towards the nucleus respectively.*** By considering these additional smaller peaks at the lower distances, it is found that the 3*s* orbital electron spends a larger fraction of its time closer to the nucleus compared to the 3*p* electron. The 3*d* electron spends relatively its least time close to the nucleus compared to the 3*s* and 3*p* electrons. By considering the combined effect of all the maxima of a particular orbital, we should consider the **average r_{max} value i.e. $<r_{max}>$.** It runs as (cf. Sec. 4.2.3 for calculation of $<r_{max}>$):

$$<r_{max}(3s)> \; < \; <r_{max}(3p)> \; < \; <r_{max}(3d)>$$

This is why, the 3s electrons are most tightly bound to the nucleus followed by the 3p and 3d electrons successively. Thus the energy sequence becomes, $3s < 3p < 3d$. This is why, for a given value of n, the ionisation energy runs in the sequence $ns > np > nd$.

In other words, we can say that the ***penetrating power*** of an orbital measured by the probability of locating the corresponding electron at the closer distance towards the nucleus lies in the sequence, $ns > np > nd$. Here it is worth mentioning that ***in Sommerfeld's model, the penetrating power of an orbit was explained in terms of its ellipticity, but in wave mechanics the concept of radial distribution function can nicely tackle the problem.***

In RDF curves, presence of the intranodal maxima at the lower distances towards the nucleus gives the measure of penetrating power of the orbital.

(viii) ***Relative bonding properties of d- (3d vs. 4d, 5d) and f- (4f vs. 5f) orbitals* :** The bonding properties of the *d*- and *f*-orbitals follow the sequence : $5d > 4d > 3d$; $5f > 4f$. This can be explained by considering their RDF curves (cf. Fig 4.3.1) and this aspect has been discussed in Sec. 4.3.

- ***Most probable distance* (r_{max}) vs. *average distance* ($\bar{r}$) (*corresponding to the same r_{max}*) *of electron from nucleus* :** r_{max} represents the distance at which probability of finding the electron is maximum. It can be obtained from the RDF. It can be evaluated from the following condition (see Solved Problem 1).

Click Here t.me/theadchemylibrary

$$\frac{d}{dr}[4\pi r^2 (R_{n,l})^2] = 0$$

The average distance $(\bar{r})$ is evaluated from the following condition (see Solved Problem 7).

$$\bar{r} = \int_0^{\infty}\int_0^{\pi}\int_0^{2\pi} \psi^* r \psi r^2 dr \sin\theta d\theta d\phi = \frac{n^2 a_0}{Z}\left[1 + \frac{1}{2}\left\{1 - \frac{l(l+1)}{n^2}\right\}\right] = \frac{a_0}{2Z}\left\{3n^2 - l(l+1)\right\}$$

$\bar{r}$ is described as **expectation value** of the distance of the electron from the nucleus. The electron is expected to be at this distance from the nucleus. Generally r_{max} is different from $\bar{r}$. For 1*s* orbital of *H*-atom : $r_{max} = a_0, \bar{r} = \frac{3}{2}a_0$ i.e. $\bar{r} > r_{max}$. For the 2*s* orbital, there are two values of r_{max} i.e. $r_{max} = 0.77a_0$ and $5.23a_0$. For the $r_{max} = 5.23a_0$, $\bar{r}$ becomes $6a_0$ (cf. Solved Problems 5 and 7). The reason behind this difference is that the radial wave function is not symmetrical when plotted as a function of *r* (cf. Figs. 4.1.4.1-2). This plot supports the large value of $\bar{r}$ compared to the corresponding r_{max}.

4.1.5 The Physical and Chemical Significance of the Nodal Points

Physical Significance

It has been already discussed that at the nodal points, there is no existence of the electron, but at both sides of the nodal point there is a finite probability of existence of the electron. Now, the question arises how the electron passes from one side of the node to the other, when the electron is absent at the node. If the electron is considered to be a particle then the question is fully valid, but if the electron is considered to be a standing wave then the problem does not arise, **as the standing wave can exist at both sides of a nodal point as evident in a vibrating string fixed at its two ends.** Thus at the nodal point, the sign (+ or –) of the wave function changes. Here it is worth mentioning that in Dirac's relativistic model, there are no nodes but there are some regions where the electron density is very small.

Chemical Significance

In the formation of a covalent bond, the extent of overlapping among the atomic orbitals is very much important. If the orbital region close to the nodal point in which the electron density is very small undergoes overlapping, then the formed covalent bond is weakened. *But fortunately, this factor does not get any serious consideration in determining the strength of a covalent bond, as mathematically it has been found that the nodal points lie so close to the nucleus that they can hardly affect the bonding.*

Actually, existence of the nodal points at the closer distances towards the nucleus is responsible to differentiate the relative energies of the different orbitals and their relative penetrating powers. For a particular principal quantum number *n*, for the larger number of nodal points at the closer distances, the electron is more tightly bound towards the nucleus. **For *ns*, *np* and *nd* orbitals the number of nodal points are given by $(n-1)$, $(n-2)$ and $(n-3)$ respectively and their energy sequence lies as : *ns* < *np* < *nd*.** Thus, it appears that this property, i.e. existence of the radial nodes, is very much important in understanding all the chemical and physical properties of the atoms and ions.

Click Here to meet healchemy library

4.1.6 Angular Wave Functions and Orbital Shapes

In the total wave function, $\psi_{n,\,l,\,m}(r, \theta, \phi)$, the angular part of the wave function is given by:

$$\psi_{\text{angular}}(\theta, \phi) = \Theta_{l,\,m}(\theta)\,\Phi_m(\phi) = A_{l,\,m}(\theta, \phi).$$

This composite wave function, a product of $\Theta_{l,\,m}(\theta)$ and $\Phi_m(\phi)$ belongs to a particular type of functions widely known as the ***spherical harmonics*** represented by $Y_{l,\,m}$ **which are not dependent on the principal quantum number.**

The angular dependence, i.e. the dependence of spherical harmonics, on θ and ϕ determines the shape of the orbitals. This is why, the shape of an orbital is independent of n which only determines the size of the orbital.

$\Phi_m(\phi)$ has got the general solution given by :

$$\boxed{\Phi_m(\phi) = (1/\sqrt{2\pi})\exp(im\phi)}$$

Note **:** The general solution of **the Φ equation** is given by :

$$\Phi_m(\phi) = A\exp(im\phi)$$

where A is the normalising constant. The function Φ shows the same value at $\phi = 0, 2\pi, 4\pi, \ldots$. The m-values are $0, \pm 1, \pm 2 \ldots$ The normalising constant is obtained as follows :

$$\int_0^{2\pi} \Phi_m \Phi_m^{*}\, d\phi = A^2 \int_0^{2\pi} \exp(im\phi - im\phi)\, d\phi = A^2(2\pi) = 1$$

It leads to $A = 1/\sqrt{2\pi}$. It is evident that the probability density ($\Phi\Phi^*$) does not depend on the angle ϕ. The Φ-part of the wave functions are given below:

$$\Phi_0 = \frac{1}{\sqrt{2\pi}},\ \Phi_{\pm 1} = \frac{1}{\sqrt{2\pi}}\exp(\pm i\phi),\ \Phi_{\pm 2} = \frac{1}{\sqrt{2\pi}}\exp(\pm 2i\phi)$$

Except for $m = 0$, in all cases, the solutions contain the imaginary exponents. In such cases, the linear combinations of the function (i.e. $\Phi_m \pm \Phi_{-m}$) are taken as the solutions without the imaginary components.

$$\boxed{\begin{aligned} \Phi(p_x) &= \frac{1}{\sqrt{2}}(\Phi_{+1} + \Phi_{-1}) = \frac{1}{2\sqrt{\pi}}[\exp(i\phi) + \exp(-i\phi)] = \frac{\cos\phi}{\sqrt{\pi}} \\ \Phi(p_y) &= \frac{1}{\sqrt{2}}(\Phi_{+1} - \Phi_{-1}) = \frac{1}{2\sqrt{\pi}}[\exp(i\phi) - \exp(-i\phi)] = \frac{i\sin\phi}{\sqrt{\pi}} \end{aligned}}$$

In the above expressions, $\frac{1}{\sqrt{2}}$ appears as the *normalising constant* for the linear combination of the function. To get the above results, **De Movier's formula**, $\exp(\pm im\phi) = \cos(m\phi) \pm i\sin(m\phi)$ has been taken into consideration. Thus it leads to:

$$\exp(i\phi) + \exp(-i\phi) = 2\cos\phi; \text{ and } \exp(i\phi) - \exp(-i\phi) = 2i\sin\phi$$

Click Here t.me/thearchemylibrary

Here, it is evident that the $\Phi(p_y)$ wave function obtained in this way still contains the i-term and to get the real wave function, it is to be divided by i. ***In fact, the properties of a wave function*** **(which is measured by $\Phi\Phi^*$)** ***does not change if it is simply multiplied or divided*** **by *i*.** This is why $\Phi(p_y)$ is expressed as follows :

$$\Phi(p_y) = \frac{1}{i\sqrt{2}}(\Phi_{+1} - \Phi_{-1}) = \frac{-i}{\sqrt{2}}(\Phi_{+1} - \Phi_{-1}) = \frac{\sin\phi}{\sqrt{\pi}}$$

For $m = 0$, the solution does not contain any imaginary term and the corresponding wave function of the p_z orbital is given by :

$$\Phi_0 = \Phi(p_z) = \frac{1}{\sqrt{2\pi}}$$

Some other required functions are :

$$\Phi(d_{x^2-y^2}) = \frac{1}{\sqrt{2}}(\Phi_{+2} + \Phi_{-2}) = \frac{\cos 2\phi}{\sqrt{\pi}}$$

$$\Phi(d_{xy}) = \frac{-i}{\sqrt{2}}(\Phi_{+2} - \Phi_{-2}) = \frac{\sin 2\phi}{\sqrt{\pi}}$$

By using Eqn. 4.1.1.12, the normalised wave functions, $\Theta_{l,m}$ for the hydrogen-like systems can be obtained as given in Table 4.1.6.1.

Table 4.1.6.1. The normalised functions, $\Theta_{l,m}$ for the hydrogen-like systems

l	m	$\Theta_{l,m}(\theta)$	
0	0	$\frac{1}{\sqrt{2}}$	(*s*-electron)
1	0	$(\sqrt{6}/2)\cos\theta$	(*p*-electron)
1	± 1	$(\sqrt{3}/2)\sin\theta$	
2	0	$(\sqrt{10}/4)(3\cos^2\theta - 1)$	(*d*-electron)
2	± 1	$(\sqrt{15}/2)\sin\theta\cos\theta$	
2	± 2	$(\sqrt{15}/4)\sin^2\theta$	

To have the idea regarding the angular wave function, it is better to consider the **spherical harmonics,** $Y_{l,m}$ rather than the individual components, i.e. $\Theta(\theta)$ and $\Phi(\phi)$. The spherical harmonics can be analysed in terms of the coordinates θ and ϕ or by transforming into the Cartesian coordinates x, y and z. As a matter of fact, the spherical harmonics can be better interpreted in the Cartesian coordinates, since we are more familiar with the Cartesian coordinates.

To carry out the transformation into the Cartesian coordinates, the following relationships are required.

Click Here t.me/thealchemylibrary

(i) $x = r \sin\theta \cos\phi$, $y = r \sin\theta \sin\phi$, $z = r \cos\theta$, and $r^2 = x^2 + y^2 + z^2$

(ii) $\sin 2\phi = 2\sin\phi \cos\phi = 2xy/r^2 \sin^2\theta$

i.e. $\sin^2\theta \sin 2\phi = (2/r^2)\, xy$ = constant × xy

(iii) $3\cos^2\theta - 1 = 3\cos^2\theta - (\sin^2\theta + \cos^2\theta) = 2\cos^2\theta - \sin^2\theta$

$\sin^2\theta \cos^2\phi = (x/r)^2$, $\sin^2\theta \sin^2\phi = (y/r)^2$

$\sin^2\theta = \sin^2\theta (\sin^2\phi + \cos^2\phi) = (1/r^2)(x^2 + y^2)$

i.e. $3\cos^2\theta - 1 = 2\cos^2\theta - \sin^2\theta = 2(z^2/r^2) - (1/r^2)(x^2 + y^2)$

$$= \frac{1}{r^2}(2z^2 - x^2 - y^2) = \frac{1}{r^2}\left\{(z^2 - x^2) + (z^2 - y^2)\right\}$$

$$= \text{constant} \times \left\{(z^2 - x^2) + (z^2 - y^2)\right\}$$

(iv) $\cos 2\phi = \cos^2\phi - \sin^2\phi$

i.e. $\sin^2\theta \cos 2\phi = \sin^2\theta \cos^2\phi - \sin^2\theta \sin^2\phi = \left(\frac{x}{r}\right)^2 - \left(\frac{y}{r}\right)^2$

$$= \frac{1}{r^2}(x^2 - y^2) = \text{constant} \times (x^2 - y^2)$$

• ***s-orbitals*** : For $l = 0$, $m = 0$, the normalised spherical harmonics $Y_{0,0}$ is independent of θ and ϕ. The corresponding orbital is called *s*-orbital. The corresponding $Y_{0,0}$ is given by, $Y_{0,0} = 1/2\sqrt{\pi}$.

Because of the independence of $Y_{0,0}$ on θ, ϕ, ***the s-orbital is spherically symmetrical.***

• ***p-orbitals*** : For, $l = 1$, there are three values of m, namely +1, 0, –1. The corresponding wave functions are expressed by,

$$Y_{1,0} = \psi(p_0) = \sqrt{(3/4\pi)} \cos\theta; \quad Y_{1,+1} = \psi(p_{+1}) = \sqrt{(3/8\pi)} \sin\theta \exp(i\phi);$$

and, $$Y_{1,-1} = \psi(p_{-1}) = \sqrt{(3/8\pi)} \sin\theta \exp(-i\phi).$$

These wave functions are called ***Schrödinger angular wave functions*** (Table 4.1.6.2). It is seen that for $m \neq 0$, the corresponding wave functions, i.e. $\psi(p_{+1})$ and $\psi(p_{-1})$, are imaginary. Because of the complex nature, it is very difficult to present these Schrödinger angular wave functions graphically. To remove this difficulty, the suitable linear combinations of these spherical harmonics are considered, as it is known that ***any linear combination of the wave functions is also an acceptable solution.*** Thus the analysis of the Shrödinger spherical harmonics or their linear combinations leads to the same conclusions. The linear combinations are taken in such a way that the resultant functions become real functions. Taking into the consideration of these linear combinations along with the $Y_{1,0}$, i.e. $\psi(p_0)$, we get the following orbitals for $l = 1$ and $m = 0, \pm 1$.

In order to combine the imaginary forms of the Schrödinger spherical harmonics to yield the real functions, we make use of the **de Moivre's theorem,** i.e. $\exp(\pm im\phi) = \cos(m\phi) \pm i \sin(m\phi)$.

Click Here t.me/thealchemylibrary

Table 4.1.6.2. The Schrödinger and normalised real spherical harmonics (i.e. angular wave functions) in terms of θ and ϕ

$Y_{l,m}$	Symbol	Schrödinger's	Symbol and combination	Real
$Y_{0,0}$	s	$1/\sqrt{4\pi}$	$s = s$	$1/\sqrt{4\pi}$
$Y_{1,0}$	p_0	$\sqrt{(3/4\pi)}\cos\theta$	$p_z = p_0$	$\sqrt{(3/4\pi)}\cos\theta$
$Y_{1,\pm1}$	$p_{\pm1}$	$\sqrt{(3/8\pi)}\sin\theta\exp(\pm i\phi)$	$p_x = \frac{1}{\sqrt{2}}(p_{+1} + p_{-1})$	$\sqrt{(3/4\pi)}\sin\theta\cos\phi$
			$p_y = -\frac{i}{\sqrt{2}}(p_{+1} - p_{-1})$	$\sqrt{(3/4\pi)}\sin\theta\sin\phi$
$Y_{2,0}$	d_0	$\sqrt{(5/16\pi)}(3\cos^2\theta - 1)$	$d_{z^2} = d_0$	$\sqrt{(5/16\pi)}(3\cos^2\theta - 1)$
$Y_{2,\pm1}$	$d_{\pm1}$	$\sqrt{(15/8\pi)}\sin\theta\cos\theta\exp(\pm i\phi)$	$d_{xz} = \frac{1}{\sqrt{2}}(d_{+1} + d_{-1})$	$\sqrt{(15/4\pi)}\sin\theta\cos\theta\cos\phi$
			$d_{yz} = -\frac{i}{\sqrt{2}}(d_{+1} - d_{-1})$	$\sqrt{(15/4\pi)}\sin\theta\cos\theta\sin\phi$
$Y_{2,\pm2}$	$d_{\pm2}$	$\sqrt{(15/32\pi)}\sin^2\theta\exp(\pm 2i\phi)$	$d_{x^2-y^2} = \frac{1}{\sqrt{2}}(d_{+2} + d_{-2})$	$\sqrt{(15/16\pi)}\sin^2\theta\cos 2\phi$
			$d_{xy} = -\frac{i}{\sqrt{2}}(d_{+2} - d_{-2})$	$\sqrt{(15/16\pi)}\sin^2\theta\sin 2\phi$

Thus, $\psi(p_x) = \frac{1}{\sqrt{2}}\left[Y_{1,+1} + Y_{1,-1}\right]$, $\left(\frac{1}{\sqrt{2}}\text{ is the normalising constant}\right)$*

$= \frac{1}{\sqrt{2}}\left[\psi(p_{+1}) + \psi(p_{-1})\right]$

$= \sqrt{(3/4\pi)}\sin\theta\cos\phi = \sqrt{(3/4\pi)}\,(x/r)$, (in Cartesian coordinates)

and $\psi(p_y) = -\frac{i}{\sqrt{2}}\left[\psi(p_{+1}) - \psi(p_{-1})\right] = \sqrt{(3/4\pi)}\sin\theta\sin\phi$

$= \sqrt{(3/4\pi)}\,(y/r)$, (in Cartesian coordinates)

and $\psi(p_z) = \psi(p_0) = \sqrt{(3/4\pi)}\cos\theta = \sqrt{(3/4\pi)}\,(z/r)$ (in Cartesian coordinates)

* Let, N be the normalising constant to the wave function ψ obtained from a linear combination of $\psi(p_{+1})$ and $\psi(p_{-1})$

Thus, $\psi = N\left[\psi(p_{+1}) + \psi(p_{-1})\right]$

Therefore, $\int\psi^2 d\tau = 1$; or, $N^2\int\left[\psi(p_{+1}) + \psi(p_{-1})\right]^2 d\tau = 1$

or, $N^2\int\left[\psi(p_{+1})\,\psi(p_{+1}) + 2\psi(p_{+1})\,\psi(p_{-1}) + \psi(p_{-1})\,\psi(p_{-1})\right]d\tau = 1$

or, $N^2(1 + 2\times 0 + 1) = 1$, here $\psi(p_{+1})$ and $\psi(p_{-1})$ are *orthogonal*

or, $N^2 = ½$

Click Here t.me/thealchemylibrary

Here it is worth mentioning that *there is no always one to one correspondence between the Schrödinger spherical harmonics* ($Y_{l,m}$) *and the real angular wave functions*. This one to one correspondence is only maintained for $m = 0$. **This is why, p_{+1} or p_{-1} cannot be considered to be equivalent to either p_x or p_y alone. Thus p_z is coming from p_0, and p_x and p_y are the combinations of p_{+1} and p_{-1}.**

Thus p_x and p_y are the *hybrid of wave functions* obtained through linear combination. Similarly, d_{xy}, d_{yz}, d_{zx} and $d_{x^2-y^2}$ are also hybrid wave functions.

The designation defined by x, y and z as in p_x, p_y and p_z respectively arises from the consideration of the maximum value of the corresponding real angular wave function in the given direction in the Cartesian coordinates (see Table 4.1.6.3). Thus for $\psi(p_x)$, it has the maximum value in the x-direction. The similar thing occurs for p_y and p_z orbitals.

• ***d-orbitals*** : For $l = 2$, and $m = \pm 2, \pm 1, 0$, there are five Schrödinger spherical harmonics: $Y_{2,+2} = \psi(d_{+2})$; $Y_{2,+1} = \psi(d_{+1})$, $Y_{2,0} = \psi(d_0)$; $Y_{2,-1} = \psi(d_{-1})$ and $Y_{2,-2} = \psi(d_{-2})$. Again as in the case of $l = 1$, $m = \pm 1, 0$, here the following linear combinations along with the $Y_{2,0}$ are taken for consideration to generate the five real angular d-wave functions (Table 4.1.6.2 and 4.1.6.3).

$$\psi(d_{z^2}) = \psi(d_0);\quad \psi(d_{xz}) = \frac{1}{\sqrt{2}}\left[\psi(d_{+1}) + \psi(d_{-1})\right]$$

$$\psi(d_{yz}) = -\frac{i}{\sqrt{2}}\left[\psi(d_{+1}) - \psi(d_{-1})\right];\quad \psi(d_{x^2-y^2}) = \frac{1}{\sqrt{2}}\left[\psi(d_{+2}) + \psi(d_{-2})\right]$$

$$\psi(d_{xy}) = -\frac{i}{\sqrt{2}}\left[\psi(d_{+2}) - \psi(d_{-2})\right]$$

Table 4.1.6.3. The real angular wave function i.e., spherical harmonics, in terms of Cartesian coordinates transformed from θ and ϕ

$Y_{l,m}$	Symbol and combination	Real spherical harmonics
$Y_{0,0}$	s	$1/\sqrt{4\pi}$
$Y_{1,0}$	$p_z = p_0$	$\sqrt{(3/4\pi)}\,(z/r)$
$Y_{1,\pm1}$	$p_x = \frac{1}{\sqrt{2}}(p_{+1} + p_{-1})$	$\sqrt{(3/4\pi)}\,(x/r)$
	$p_y = -\frac{i}{\sqrt{2}}(p_{+1} - p_{-1})$	$\sqrt{(3/4\pi)}\,(y/r)$
$Y_{2,0}$	$d_{z^2} = d_0$	$\sqrt{(5/16\pi)}\left[(z^2-x^2)/r^2 + (z^2-y^2)/r^2\right]$
$Y_{2,\pm1}$	$d_{xz} = \frac{1}{\sqrt{2}}(d_{+1} + d_{-1})$	$\sqrt{(15/4\pi)}\,(xz/r^2)$
	$d_{yz} = -\frac{i}{\sqrt{2}}(d_{+1} - d_{-1})$	$\sqrt{(15/4\pi)}\,(yz/r^2)$
$Y_{2,\pm2}$	$d_{x^2-y^2} = \frac{1}{\sqrt{2}}(d_{+2} + d_{-2})$	$\sqrt{(15/16\pi)}\left[(x^2-y^2)/r^2\right]$
	$d_{xy} = -\frac{i}{\sqrt{2}}(d_{+2} - d_{-2})$	$\sqrt{(15/16\pi)}\,(xy/r^2)$

Click Here 1.me/thealchemylibrary

The forms of the Shrödinger spherical harmonics along with those of real wave functions for *s*, *p* and *d* orbitals are given in Table 4.1.6.2 in terms of θ and ϕ.

For the purpose of visualizing the relationships, the real spherical harmonics are expressed in terms of the Cartesian coordinates as given in Table 4.1.6.3.

The real spherical harmonics i.e. angular wave functions, are pictorially represented in Fig. 4.1.6.1. *Here it must* be *remembered that these polar diagrams do not represent the total wave functions but only the angular parts of the total wave functions.* ***These polar diagrams are not presented as orbitals.***

The Characteristic Features of the Real Angular Wave Functions (cf. Fig. 4.1.6.1)

(i) ***Relation with the quantum numbers*** : The angular part of the wave function is dependent on the two quantum numbers *l* and *m* but independent of *n* and *this part determines the shape of the orbitals*. Thus the principal quantum number has nothing to do with the shape of the orbitals but it is important to determine the size of the orbitals as is evident from the radial part of the wave function.

(ii) ***Orbital shape*** : All *s*-orbitals ($l = 0$) are *spherically symmetrical*, as the corresponding spherical harmonics have no dependence on θ and ϕ. All other orbitals being dependent on θ and/or ϕ have got *directional properties*.

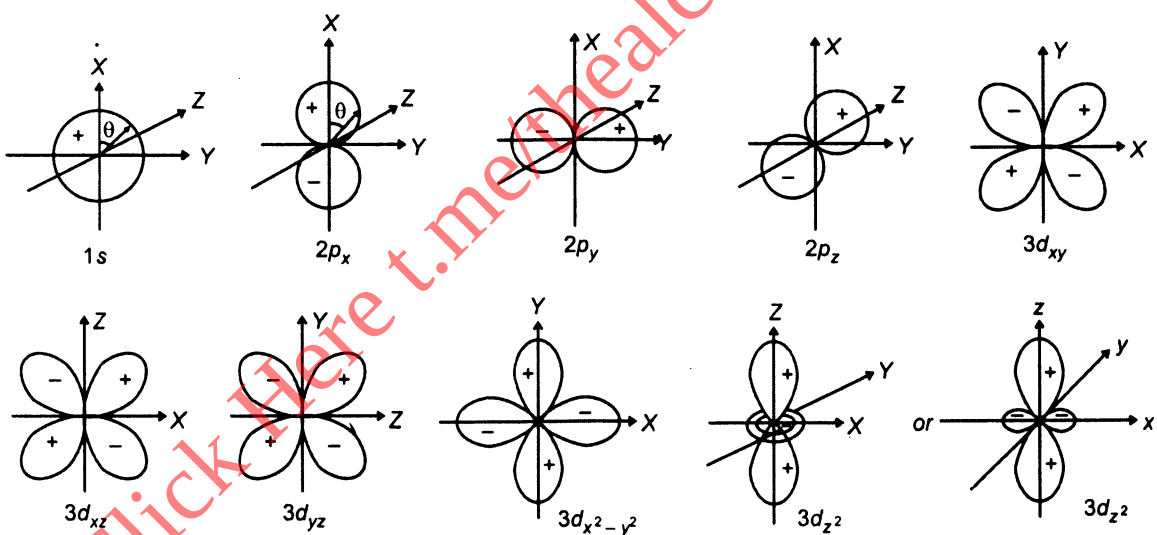

Fig. 4.1.6.1. The real angular wave functions (i.e. shapes) of different orbitals in hydrogen-like systems in Cartesian coordinates as polar diagrams.

Note : • ***These polar diagrams represent the boundary surfaces of the angular parts of the wave functions. They do not represent the total wave functions.***

• **For *s*-orbital (i.e. $Y_{0,0}$)** : amplitude in any direction = $\frac{1}{\sqrt{4\pi}}$, probability in any direction = $\frac{1}{4\pi}$. **For p_z-orbital (i.e. $Y_{1,0}$)** : amplitude along $z = \pm\sqrt{3/4\pi}$, probability along $z = 3/4\pi$; **For d_{z^2} orbital (i.e. $Y_{2,0}$)** : amplitude along $z = \sqrt{5/4\pi}$, amplitude in *xy* plane = $-\sqrt{\frac{5}{16\pi}}$, probability along $z = 5/4\pi$, probability in *xy* plane = $5/16\pi$. **For $d_{x^2-y^2}$ orbital** : amplitude along *x* and *y* axes = $\pm\sqrt{15/16\pi}$, probability along *x* and *y* axes = $15/16\pi$.

Click Here t.me/thealchemylibrary

(iii) ***Orbital designation*** : The designation of an orbital is determined by the expression of the corresponding *real spherical harmonic in terms of Cartesian coordinates* (Table 4.1.6.3). For the *p*-orbitals, the direction in which the real spherical harmonic is having the maximum value determines its designation. Similarly, for the three *d*-orbitals, i.e. d_{xy}, d_{yz} and d_{zx}, the plane containing the maximum value of the corresponding harmonic is considered to designate the orbital. ***Thus the directions or planes in which the major components of the real spherical harmonics exist are used to designate the orbitals.*** The designation for the five *d*-orbitals will be discussed in detail in the following point (vi).

(iv) ***Nodal surface and sign of wave functions*** : Except the *s*-orbitals, for any other orbital, in certain directions (i.e. coordinates) the angular wave function may have zero values. Such coordinates define the ***angular nodal surfaces***. For the p_x spherical harmonic, it becomes zero at $x = 0$, regardless of the values of y and z. Thus the yz-plane sets as a nodal plane in the angular part of the wave function. ***The wave function is positive in the +x direction while it is negative in the –x direction.*** Thus, the wave function changes its sign at $x = 0$. A similar observation is obtained for the p_y and p_z orbitals. In the absence of any external field, the three equivalent *p*-orbitals, i.e. p_x, p_y and p_z, are energetically degenerate.

The *d*-orbitals are relatively complicated. Except the d_{z^2} orbital, each of the other orbitals is having four lobes in which the opposing lobes are bearing the same sign. *Thus, in contrast to the p-orbitals having one nodal surface each, each d-orbital is having two nodal planes*. For example, the d_{xy} spherical harmonic has two nodal planes (i.e. xz- and yz-plane) on which the harmonic is always zero. ***The function is in the positive phase when both x and y are having the same sign, positive or negative while the function is in the negative phase for the opposite sign of x and y.***

(v) ***Energy of the orbitals*** : *In general, with the increase of the number of nodal surfaces in the real spherical harmonics, the energy of the orbitals increases*. Thus for a given value of n, the energy of the orbitals increases in the sequence, *s* (no nodal surface) < *p* (one nodal surface) < *d* (two nodal surfaces).

(vi) ***d-orbitals*** : The five *d*-orbitals developed from the real spherical harmonics are not equivalent. Each of the three *d*-orbitals namely, d_{xy}, d_{yz} and d_{zx} having four lobes lies symmetrically between corresponding axial directions. The d_{xy} orbital lies in the xy-plane between the x- and y-axes; similarly the d_{yz} and d_{zx} lie in the yz-and zx-plane respectively in the same manner. The $d_{x^2-y^2}$ is also four-lobed and it lies in the xy-plane with the lobes projected along the axial directions. Apparently, we should have two other four-lobed spherical harmonics namely, $d_{z^2-y^2}$ and $d_{z^2-x^2}$. But unfortunately they have no physical reality. However, it is convenient to think the d_{z^2} orbital as a linear combination of the two nonexistent orbitals, i.e. $d_{z^2-x^2}$ and $d_{z^2-y^2}$. This proposition is also mathematically established as is evident from the expression (Tables 4.1.6.2 and 4.1.6.3) of the d_{z^2} spherical harmonic given by,

$$\psi(d_{z^2}) = Y_{2,0} = \sqrt{(5/16\pi)}\left[(z^2 - x^2)/r^2 + (z^2 - y^2)/r^2\right]$$

$$= \sqrt{(5/16\pi)}\left(\frac{2z^2 - x^2 - y^2}{r^2}\right)$$

$$= \sqrt{(5/16\pi)}\left[3(z^2 - r^2/3)/r^2\right], r^2 = x^2 + y^2 + z^2$$

Click Here to join the chemistry library

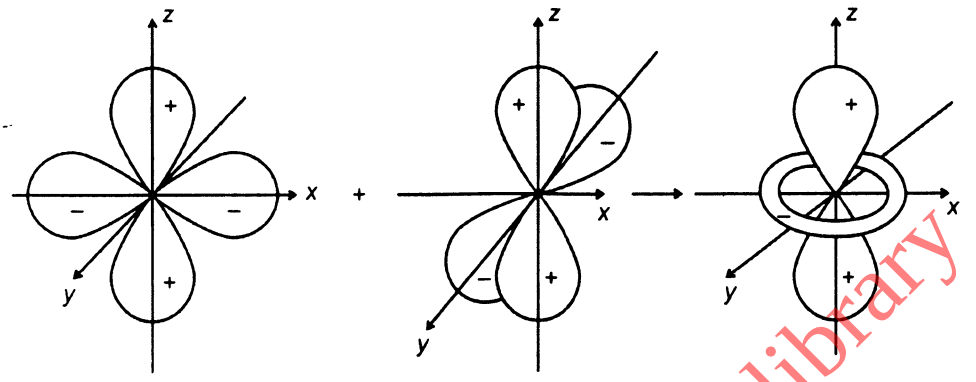

Fig. 4.1.6.2. Generation of d_{z^2} orbital through a linear combination of $d_{z^2-x^2}$ and $d_{z^2-y^2}$.

This is why, the d_{z^2} orbital should be designated as, $d_{3(z^2-r^2/3)}$ or, $d_{[(z-x^2)+(z^2-y^2)]}$ or $d_{2z^2-x^2-y^2}$ and the origin of the d_{z^2} orbital can be pictorially represented as in Fig. 4.1.6.2. Thus, both the properties of $d_{z^2-x^2}$ and $d_{z^2-y^2}$ are fused in the d_{z^2} orbital. **As both the precursor orbitals have high electron densities along the *z*-axis, the product orbital d_{z^2} is having a large amount of electron density along the *z*-axis.** The $d_{z^2-x^2}$ orbital has one component getting maximised along the *x*-axis and similarly, the $d_{z^2-y^2}$ orbital has one component getting maximised along the *y*-axis. This is why, the resultant orbital d_{z^2} has a component in the *xy*-plane. This component in the *xy*-plane is very often referred to as ***doughnut* or *belly band.***

Thus, the five real d-orbitals can be classified **into two groups.** One group containing $d_{x^2-x^2}$ and d_{z^2} ($\equiv d_{z^2-x^2} + d_{z^2-y^2}$) points along the axial directions, and another group consisting of d_{xy}, d_{yz} and d_{zx} orbitals points at 45° to the corresponding axial directions.

(vii) ***Angular probability function*** : To have the *probability functions* of the corresponding real spherical harmonics, we need simply the squaring of the harmonics. From the practical standpoint, there is no marked difference in the forms of a real harmonic and its probability function. Squaring the angular part of the wave function (i.e. $\psi_\theta^2\psi_\phi^2$) does not cause any remarkable change in the boundary surfaces of the angular wave functions i.e. ***boundary surfaces are similar for both the angular wave functions and angular probability functions.*** For the *p*-orbitals, the envelopes representing the angular probability functions become more elongated (cf. Figs. 4.1.4.1 and 4.1.6.3). However, for the spherically symmetrical *s*-orbital, there is no difference in the nature of boundary surfaces of the two plots (cf. Figs. 4.1.6.1 and 4.1.6.3). *In the probability function, the nodal surface remains unchanged and the probability function becomes always positive everywhere regardless of the positive or negative phase of the spherical harmonic.*

(viii) ***Spherical symmetry*** : It is interesting to note that as in the case of a single *s*-orbital which is spherically symmetrical, the summation of probability distribution contributed by a set of three *p*-orbitals or five *d*-orbitals or seven *f*-orbitals is also spherically symmetrical around the nucleus (see Solved Problem 3).

(ix) ***Symmetry of the orbitals (cf. Sec. 4.1.8)*** : The centrosymmetric orbitals (i.e. the same sign at the

Click Here to meet chemylibrary

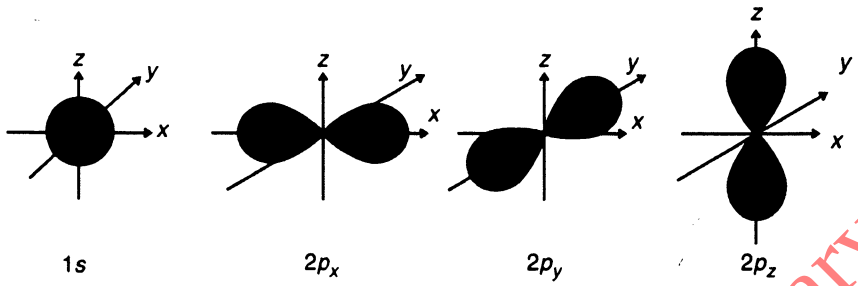

Fig. 4.1.6.3. Representation of the boundary surfaces of the angular probability functions of *s*- and *p*-orbitals in hydrogen-like systems.

Notes : Very often, *no distinction between the shape of angular probability functions and angular wave functions is strictly maintained.* ***The envelopes representing the probability function should not bear the sign of wave functions*** but sometimes these are given to bear the sign. *In fact, the envelopes of probability function as well as the wave functions are described as orbitals.*

same distance in opposite directions from the centre or nucleus) are called ***gerade*** (German word meaning *even*). The *s*- and *d*-orbitals belong to this group. The orbitals lacking in centre of symmetry i.e. opposite sign in opposite directions from the centre are called ***ungerade*** (German word meaning *uneven*). The *p*-orbitals belong to this group.

Complete real hydrogen-like wave function : These are given in Table 4.1.6.4

f-orbitals (ungerade)

There is no unique way to represent all the seven *f*-orbitals. The **general set** consists of :

$$f_{z^3}, f_{xz^2}, f_{yz^2}, f_{xyz}, f_{z(x^2-y^2)}, f_{x(x^2-3y^2)}, f_{y(3x^2-y^2)}$$

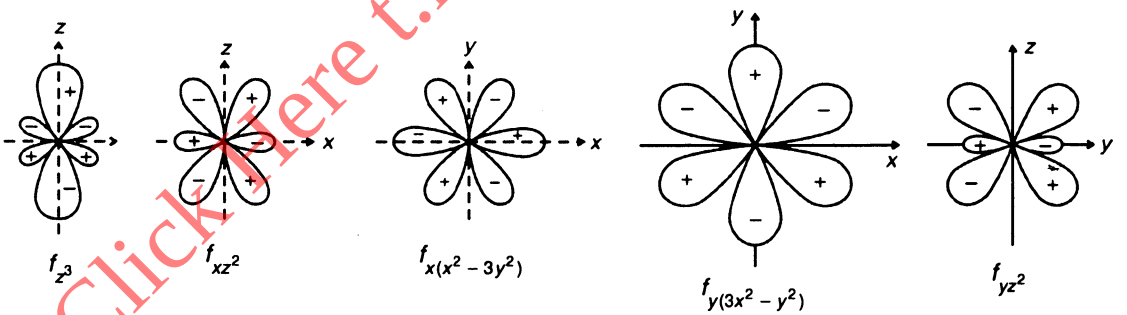

Fig. 4.1.6.4. Boundary surfaces (i.e. cross-sectional plots) of angular wave functions of some *f*-orbitals.

The **cubic set** consists of :

$$f_{z^3}, f_{x^3}, f_{y^3}, f_{xyz}, f_{z(x^2-y^2)}, f_{y(z^2-x^2)}, f_{x(z^2-y^2)}$$

In f_{z^3}, f_{x^3} and f_{y^3} orbitals, the main lobe is projected along the *z*–, *x*– and *y*-axes respectively. In f_{xyz}, the eight lobes are projected towards the corners of a cube when the nucleus resides at the centre. $f_{z(x^2-y^2)}$, $f_{y(z^2-x^2)}$ and $f_{x(z^2-y^2)}$ are similar to f_{xyz} but rotated 45° about the respective Cartesian axes. For the shape of the cubic set of *f*-orbitals, the readers may see the book, Inorganic Chemistry by D.F. Shriver et al.

Click here to chemistry library

Table 4.1.6.4. Complete real hydrogen-like wave functions, $\psi_{n,l,m}(r, \theta, \phi)$. Here $u = Zr/a_0$, $a_0 = \dfrac{h^2}{(4\pi^2 \mu e^2)} = 0.53\text{Å}$

$$\psi_{100} = \psi(1s) = \frac{1}{\sqrt{\pi}} (Z/a_0)^{3/2} \exp(-u)$$

$$\psi_{200} = \psi(2s) = \frac{1}{4\sqrt{2\pi}} (Z/a_0)^{3/2} (2-u) \exp(-u/2)$$

$$\psi_{210} = \psi(2p_z) = \frac{1}{4\sqrt{2\pi}} (Z/a_0)^{5/2} r \cos\theta \exp(-u/2)$$

$$\psi_{21\pm1} \begin{cases} \psi(2p_x) = \dfrac{1}{4\sqrt{2\pi}} (Z/a_0)^{5/2} r \sin\theta \cos\phi \exp(-u/2) \\ \psi(2p_y) = \dfrac{1}{4\sqrt{2\pi}} (Z/a_0)^{5/2} r \sin\theta \sin\phi \exp(-u/2) \end{cases}$$

$$\psi_{300} = \psi(3s) = \frac{1}{81\sqrt{3\pi}} (Z/a_0)^{3/2} (27 - 18u + 2u^2) \exp(-u/3)$$

$$\psi_{310} = \psi(3p_z) = \frac{\sqrt{2}}{81\sqrt{\pi}} (Z/a_0)^{5/2} (6-u) r \cos\theta \exp(-u/3)$$

$$\psi_{31\pm1} \begin{cases} \psi(3p_x) = \dfrac{\sqrt{2}}{81\sqrt{\pi}} (Z/a_0)^{5/2} (6-u) r \sin\theta \cos\phi \exp(-u/3) \\ \psi(3p_y) = \dfrac{\sqrt{2}}{81\sqrt{\pi}} (Z/a_0)^{5/2} (6-u) r \sin\theta \sin\phi \exp(-u/3) \end{cases}$$

$$\psi_{320} = \psi(3d_{z^2}) = \frac{1}{81\sqrt{6\pi}} (Z/a_0)^{7/2} r^2 (3\cos^2\theta - 1) \exp(-u/3)$$

$$\psi_{32\pm1} \begin{cases} \psi(3d_{xz}) = \dfrac{\sqrt{2}}{81\sqrt{\pi}} (Z/a_0)^{7/2} r^2 \sin\theta \cos\theta \cos\phi \exp(-u/3) \\ \psi(3d_{yz}) = \dfrac{\sqrt{2}}{81\sqrt{\pi}} (Z/a_0)^{7/2} r^2 \sin^2\theta \cos\theta \sin\phi \exp(-u/3) \end{cases}$$

$$\psi_{32\pm2} \begin{cases} \psi(3d_{x^2-y^2}) = \dfrac{1}{81\sqrt{2\pi}} (Z/a_0)^{7/2} r^2 \sin^2\theta \cos 2\phi \exp(-u/3) \\ \psi(3d_{xy}) = \dfrac{\sqrt{2}}{81\sqrt{\pi}} (Z/a_0)^{7/2} r^2 \sin^2\theta \sin 2\phi \exp(-u/3) \end{cases}$$

$E = -\dfrac{Z^2}{2n^2}$ a.u.

$n = 1, E_1 = -\dfrac{Z^2}{2}$ a.u.

$n = 2, E_2 = -\dfrac{Z^2}{8}$ a.u.

$n = 3, E_3 = -\dfrac{Z^2}{18}$ a.u.

$z = r\cos\theta$, $y = \sin\theta \sin\phi$, $x = r \sin\theta \cos\phi$. These wave functions can be expressed in a.u. taking $a_0 = 1$.

Click Here t.me/thealchemylibrary

4.1.7 Electron Cloud Density Representation of the Orbitals in Hydrogen-like Systems

It is established that the total wave function has got two parts, i.e. ***radial part and angular part.*** For this reason the complete wave function is given by :

$$\psi_{n,\,l,\,m}(r, \theta, \phi) = \psi_{\text{radial}}(r) \times \psi_{\text{angular}}(\theta, \phi) = R_{n,\,l}(r) \times A_{l,\,m}(\theta, \phi).$$

To determine the total probability of finding the electron, both the radial probability and angular probability are to be considered simultaneously. The corresponding probabilities are obtained by squaring the respective part of the complete wave function.

Let us consider the *s*-orbitals first. From the radial probability distribution, it is evident that with the increase of r from the nucleus the probability increases and it gets maximised at $r \approx a_0/Z = (0.529/Z)$ Å, then it falls down. **From the angular part of the wave function, the nature of probability distribution is spherically symmetrical.** By considering these two facts at the same time, the nature of electron cloud distribution can be represented as shown in Fig. 4.1.7.1. Thus for 1*s*, the probability is zero for $r = 0$ and ∞. On the other hand, for the 2*s* electron, again the probability density is spherically symmetrical around the nucleus but it is evident from the nature of radial wave function that at $r \approx 0$, $2a_0/Z$ and ∞ the probability is zero (cf. Fig. 4.1.4.4). The highest probability region lies at $r \approx 5a_0/Z$ and a smaller probability region lies between $r = 0$ to $r = 2a_0/Z$ and it gets maximised at $r \approx a_0/Z$. This is why, at $r = 2a_0/Z$ there is a node, actually a **spherical nodal surface.** Because of the same ground, for the charge

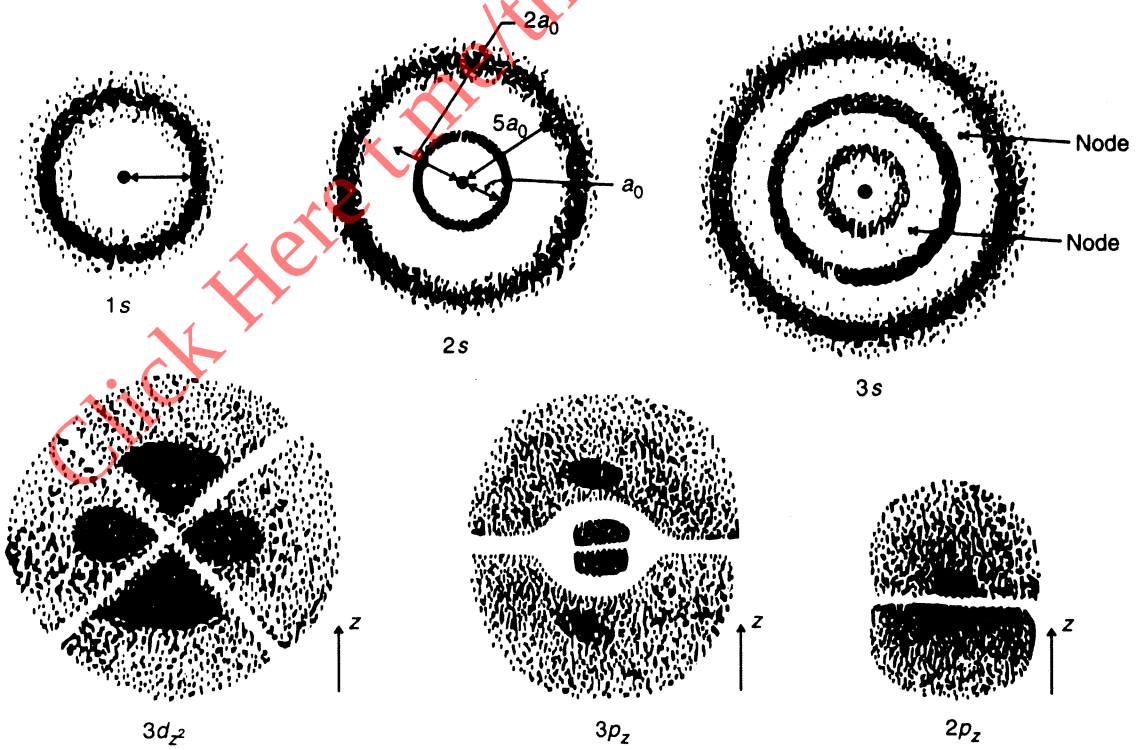

Fig. 4.1.7.1. Electron cloud distribution pictures in different orbitals of hydrogen atom.

Click Here to go to chemistry library

cloud representation of the 3*s* orbital, there are two nodes before the arrival of the highest probability region. These are pictorially presented in Fig. 4.1.7.1. Here it may be noted (cf. Solved Problem 5) for 2*s* orbital r_{max} lies actually at $0.77a_0/Z$ and $5.23a_0/Z$ distances.

Similarly, for the 2*p*-orbital, there is no node except at $r = 0$ and ∞; and the probability region gets maximised at $r = 4a_0/Z$. But, for the 3*p*-orbital before to attain the maximum probability region there is a node (cf. 2*s*-orbital). Now from the consideration of spherical harmonics, for $2p_x$ the nodal surface lies in the *yz*-plane and it lies at $r = 0$. Thus for the $3p_x$-orbital there are two nodal surfaces in the *yz*-plane at $r = 0$ and $6a_0/Z$. Similarly for the 3*d*-orbitals the two nodal planes exist at $r = 0$; and for the 4*d*-orbitals, in addition to this, there is another nodal zone before to attain the highest probability region.

In general there are $(n - l - 1)$ radial nodes (ignoring the nodal point at $r = 0$) in the radial distribution functions and there are l *nodal surfaces* (at $r = 0$) in the angular distribution functions of all the orbitals.

Thus by considering both the radial and angular probability functions, some representative pictorial representations of the orbitals are shown in Fig. 4.1.7.1.

Another important aspect is that the single *s*-orbital is spherically symmetrical. Similarly the probability summation of the set of three *p*-orbitals or the set of five *d*-orbitals or the set of seven *f*-orbitals is also spherically symmetrical.

Here, it must be remembered that the representation of the probability distribution function does not contain any negative sign, as it is positive everywhere except at the nodes and at infinity where it is zero. **But in the consideration of the corresponding wave function, signs (+ or –) describing the phase of the standing wave is extremely important from the standpoint of overlapping of the atomic orbitals.** Overlapping in the same phase strengthens the bond while overlapping in the opposite phase weakens the bond.

4.1.8 Symmetry of the Orbitals

On the basis of the centre of symmetry with respect to the signs of the wave functions, the orbitals can be classified as ***gerade* (*g*) and *ungerade* (*u*).** *These German words meaning even and uneven respectively are defined with respect to the existence of centre of inversion.* If on moving from a particular point through the centre to the opposite direction by an equal distance, an equivalent point with respect to the sign in the wave function is attained, then the orbital is considered to have the ***centre of inversion.*** The orbitals having the centres of inversion are said to be *gerade* and these are designated by *g*. On the other hand, the orbitals lacking in this symmetry element, i.e. centre of inversion, are referred to as *ungerade* and represented by *u*. In carrying out this symmetry operation, the nucleus of the atomic orbital is considered to be at the centre with respect to which the symmetry element is sought for.

Based on this consideration, the ***s*- and *d*-orbitals are called *gerade* while the *p*- and *f*-orbitals are called *ungerade*.** These are evident from the pictorial representations given in Fig. 4.1.6.1.

4.1.9 Concept of Atomic Orbitals in Wave Mechanics in Relation to the Orbits in Classical Mechanics

To describe the total behaviour of an electron in space, the complete wave function is to be considered. To determine the total probability distribution of the electron in space both the radial probability and

Click Here t.me/bhearchemylibrary

spherical harmonic probability are to be considered simultaneously. It has been established that at $r = 0, \infty$ and at the nodes, the probability is definitely zero; and everywhere except for these points, it is positive. **In reality, after a certain limit of *r*, it becomes almost zero but never equals to zero.** Thus, theoretically, though the probability of existence of the electron extends up to infinity, the consideration up to infinity is of no physical significance from the standpoint of practical distribution pattern. This is why an atomic orbital is defined as.:

The three dimensional region (which may not always be continuous because of the presence of nodes between the successive probable regions of existence of the electron) around the nucleus in an atom where there is a maximum probability (~ 90-95%) of finding the electron of a certain energy is called an atomic orbital.

It indicates that the atomic orbital defines a region around the nucleus in which the moving electron (*as a standing wave*) of a definite energy spends most of its time, say about 90-95%.

Orbit	*Orbital*
(a) In Bohr-Sommerfeld idea, an orbit is a ***well-defined two-dimensional locus*** for the revolving electron around the nucleus.	(a) An orbital represents a ***three dimensional region*** around the nucleus in which the moving electron *as a standing wave* of a definite energy spends most (90-95%) of its time.
(b) In the concept of an orbit, both the position and the momentum (i.e. velocity) of the electron are defined without any uncertainty. For example, in the ground state, the hydrogen electron revolves with a certain velocity always at the circular locus at 0.529 Å from the nucleus. ***Thus the Heisenberg's uncertainty principle is broken down.***	(b) An orbital never defines the exact position of the electron; only, it can at best define the most probable region of its existence. Thus, in the ground state, for the hydrogen electron, the most probable region (spherical shell) exists at 0.529 Å from the nucleus. **Thus the Heisenberg's uncertainty principle is not violated here.**
(c) The concept of an orbit gets originated from the consideration of ***particle nature of the electron.***	(c) The concept of an orbital gets developed by considering the ***electron as a standing wave.***
(d) In Sommerfeld's orbit, the **azimuthal quantum** number k cannot be zeo. It ranges from 1, 2, ... $(n-1)$, n for the principal quantum number n.	(d) In wave mechanics, the **azimuthal quantum number** l can be zero. It may have any integral value from 0 to $(n-1)$.
(e) In Bohr's model, all the orbits are ***circular*** in ***shape.*** In Sommerfeld's idea, the orbits are ***elliptic in nature*** in general. The degree of ellipticity is different for different orbits.	(e) The three dimensional orbitals have ***different shapes,*** e.g. *s*-orbital is spherically symmetrical, *p*-orbitals are dumb-bell shaped, the *d*-orbital in general is having four lobes.
(f) In classical orbits, the ***concept of nodes*** is not defined.	(f) In the concept of orbitals, there is an ***idea of nodes*** which arises due to the wave nature of the electron.
(g) Based on the symmetry elements with respect to the sign of the orbits, no question of gerade or ungerade to differentiate the orbits arises, ***as in the concept of orbits, there is no provision of the existence of sign.***	(g) Based on the sign of the wave function describing the orbitals, they can be classified **as *gerade (g) or ungerade (u).*** Consideration of this g or u symmetry is very important in determining the spectral transition. The concept of sign of the orbitals is also very important in the overlapping of the orbitals in covalent bond formation.

Click Here t.me/thealchemylibrary

4.1.10 Energy of the Electron in Hydrogen-like Systems

In wave mechanics, by solving the radial equation (Eqn. 4.1.1.10), the energy of the electron can be calculated. The variation method by considering a trial wave equation, also leads to the same result (see the end of Chapter 3). The energy of the electron is expressed as follows :

$$E_n = -\frac{2\pi^2 \mu Z^2 e^4}{n^2 h^2}, \text{(CGS system)}; \; E_n = -\frac{Z^2}{2n^2} \text{ a.u.}$$

The above relationship is identical with the one obtained in Bohr's model. The terms bear their usual significance. The above expression is true only in the ***nonrelativistic* wave mechanical model.** If the **relativistic correction** is considered as in the Dirac atom, then a small dependence of E_n on the azimuthal quantum number is observed. The same thing is also found to occur in Sommerfeld's relativistic atomic model. Here it is worth mentioning that in the nonrelativistic wave mechanical model for the **polyelectronic systems,** the energies of the different orbitals even for a particular principal quantum number largely depend on the azimuthal quantum numbers which determine the penetrating power of the orbitals under consideration.

4.1.11 The Four Quantum Numbers

We have already discussed the wave mechanical genesis of the three quantum numbers along with the fourth quantum number in the Dirac's relativistic model. Some characteristic properties of these quantum numbers have been discussed in this Chapter and in Chapter 1 (Sec. 1.10.3) in discussing the vector model. Here we are summarising and recapitulating all these properties discussed in different sections for convenience.

A. Principal Quantum Number (n)

Origin **:** In Bohr's model, it was introduced from the hypothesis, i.e. $mur = n(h/2\pi)$, while in the wave mechanics, it gets automatically originated in having the well-behaved radial wave functions, $R(r)$ from the solution of the Schrödinger wave equation.

It may have any nonzero positive integral value up to infinity, i.e. $n = 1, 2, 3, ..., \infty$

Information provided by the quantum number (n)

(i) **Energy of an electron :** In Bohr's model and in Schrödinger's nonrelativistic wave mechanical model, the energy of the electron in a hydrogen-like system is absolutely governed by the principal quantum number as follows :

$$\left.\begin{aligned} E_n &= -\frac{2\pi^2 m Z^2 e^4}{n^2 h^2}, \; (m = \text{mass of the electron}). \\ &= -\frac{2\pi^2 \mu Z^2 e^4}{n^2 h^2}, \; (\text{more correct representation, where } \mu = \text{reduced mass}). \end{aligned}\right\} \text{(in CGS system)}$$

$$\text{i.e.} \, |E| \propto \frac{1}{n^2}$$

Therefore, $E_1 < E_2 < E_3 < E_4 ...$, and $(E_\infty - E_1)$ gives the measure of *ionisation energy* for the hydrogen-like systems in ground state. Thus with the increase of n, the energy of the electron increases.

Click Here t.me/Unacademylibrary

The shells or energy levels are designated by the capital letters, *K, L, M,* ... according to the values of *n* as follows :

$$K\,(n = 1),\ L\,(n = 2),\ M\,(n = 3),\ N\,(n = 4),\ \ldots$$

(ii) **Radius of the orbit or orbital :** In Bohr's model, the position of the electron measured from the nucleus is governed by the quantum number, *n* as follows (in CGS system):

$$r_n = \frac{n^2h^2}{4\pi^2me^2Z};\ \text{or, } r_n \propto n^2$$

In the wave mechanical model, the most probable region for the existence of the electron cloud is governed by both *n* and azimuthal quantum number, *l* (cf. radial distribution function, Fig. 4.1.4.4). But it is worth mentioning that in the wave mechanical model also, the distance of the most probable region from the nucleus is majorly governed by the principal quantum number *and the effect of the azimuthal quantum number is comparatively small* (cf. Fig. 4.1.4.4). Thus the conclusion drawn either from the Bohr's model or from the wave mechanical model is roughly the same.

(iii) **Total capacity of a particular shell :** The principal quantum number determines the total number of electrons which can be accommodated in a particular shell. This maximum capacity is given by $2n^2$ as given below.

Shell :	*K*	*L*	*M*	*N*
Max. capacity :	2×1^2	2×2^2	2×3^2	2×4^2

This $2n^2$ relationship results from the consideration of Pauli exclusion principle (see Section 1.10.4).

B. Azimuthal Quantum Number (l)

Origin **:** In the Sommerfeld's atomic model (see Sec. 1.9.1), the azimuthal quantum number (*k*) gets originated from the hypothesis introduced in the concept of elliptical locus for the moving electron. But in the wave mechanical model, it comes to our picture to make the function, $\Theta(\theta)$ (a part of the spherical harmonic in the total wave function) acceptable.

The wave mechanical azimuthal quantum number (*l*) and the Sommerfeld's azimuthal quantum number (*k*) are related : $l = k - 1$. The quantum number *l* can have values, 0, 1, 2, ..., $(n - 1)$. It is also called the ***angular momentum quantum number*** as it gives the measure of angular momentum of the electron. It is also called ***orbital or subsidiary quantum number.***

Information provided by the quantum number (l)

(i) **Shape of the orbit or orbital :** In the Sommerfeld' model, the azimuthal quantum number determines the shape, i.e. the ellipticity of the orbit under consideration. In the wave mechanical model, the spherical harmonic i.e. the angular part of the complete wave function, determines the shape of the corresponding orbital. This spherical harmonic is dependent on both the azimuthal quantum number, *l* and the magnetic quantum number, *m* (previously, in the first Chapter in discussing the vector model it is represented by m_l). *Thus, in both the models, the azimuthal*

Click Here t.me/thealchemylibrary

quantum number determines the shape of the orbit or orbital. The *s*-orbital is spherically symmetrical, the *p*-orbitals are dumb-bell shaped and the *d*-orbitals are four lobed in general.

(ii) **Naming of the orbitals :** The types of the orbitals are designated by the values of the azimuthal quantum number as follows,

l :	0	1	2	3	4	5
Type of the orbital :	*s*	*p*	*d*	*f*	*g*	*h*

The names of the first four orbitals, i.e. *s*, *p*, *d* and *f* (the first letters of the spectroscopic terms, *sharp, principal, diffuse* and *fundamental* respectively), are coined from the spectroscopy. **The *corresponding spectral lines developed for the electron transition from the higher levels* i.e. *s*, *p*, *d* and *f*, are called sharp, principal, diffuse and fundamental respectively** (cf. Fig. 1.10.15.2). The names of the remaining orbitals follow alphabetically.

Thus, the number of orbitals for a particular shell is given as follows :

K-shell	*L*-shell	*M*-shell	*N*-shell
(n = 1)	(n = 2)	(n = 3)	(n = 4)
↓	↓	↓	↓
1*s*	2*s*, 2*p*	3*s*, 3*p*, 3*d*	4*s*, 4*p*, 4*d*, 4*f*

(iii) **Number of radial nodes and nodal surfaces :** In the radial wave function, the number of *radial nodes* (except the nodal point at $r = 0$) of the orbitals is given by $(n - l - 1)$. In the angular wave function, the number of *nodal surface* at $r = 0$ is given by l.

(iv) **Penetrating power of the orbit or orbital :** From the radial distribution probability in the wave mechanics, and from the ellipticity of the orbits in Sommerfeld's model, the penetrating power of the orbitals or orbits is given in the sequence, $s > p > d > f$ for a particular principal quantum number.

(v) **Orbital angular momentum and magnetic moment :** The orbital angular momentum p_l is quantised as follows,

$$\vec{l} = p_l = l\,(h/2\pi), \text{ (in classical mechanics)}$$
$$= \sqrt{l\,(l+1)}\,(h/2\pi), \text{ (in wave mechanics)}$$

The relationship between μ_l and p_l has been discussed in Chapter 1.

(vi) **Selection rule in spectral transition :** In spectral transition, the selection rule governed by l is given by, $\Delta l = \pm 1$. Δl value also controls the intensity rule (see Sec. 1.10.14).

(vii) **Energy of the orbit or orbital :** In both Dirac's relativistic wave mechanical model and Sommerfeld's relativistic classical model, the energy is found to depend slightly on l.

C. Magnetic Quantum Number, m (m_l in Vector Model)

Origin : To have the acceptable solutions of the function, $\Phi(\phi)$, a part of the spherical harmonic of the complete wave function, the magnetic quantum number m comes to the picture. In the vector model, it appeared to explain the Zeeman effect and Stark effect. In the vector model, we have designated this by m_l. In the vector model, the quantum number, m_l appears due to the quantised orientation of the orbital momentum vector with respect to the direction of the external magnetic field (cf. Fig. 1.10.3.1).

The magnetic quantum number, m can have values as : $m = \pm l, \pm (l - 1), \pm (l - 2)$. Therefore, for a particular value of l, it can have $(2l + 1)$ values.

Click Here t.me/thealchemylibrary

Information provided by the quantum number, m or m_l

(i) **Number of sub-energy levels or orbitals :** From the permitted values of m the following results appear.

	s-orbital ($l = 0$)	*p*-orbital ($l = 1$)	*d*-orbital ($l = 2$)	*f*-orbital ($l = 3$)
m :	0	$0, \pm 1$	$0, \pm 1, \pm 2$	$0, \pm 1, \pm 2, \pm 3$
	(one orbital)	*(a set of three orbitals)*	*(a set of five orbitals)*	*(a set of seven orbitals)*

(ii) **Origin and designation of different orbitals :** The wave functions developed from the permitted values of m are not always real (cf. Tables 4.1.6.1-3). The real wave functions such as : (p_x, p_y, p_z) or d_{xy}, d_{yz}, d_{zx}, $d_{x^2-y^2}$, d_{z^2} do not have one to one correspondence with the m values except when $m = 0$. For example, $m = 0$, ($l = 1$, $n = 2, 3...$) leads to p_z and $m = 0$, ($l = 2$, $n = 3, 4, ...$) leads to d_{z^2} while the orbitals like p_x, p_y, d_{xy}, d_{yz}, d_{zx}, $d_{x^2-y^2}$ are the linear combinations of the wave functions described by the nonzero values of m. For example, p_x and p_y are obtained from the linear combination of the wave functions developed from $m = \pm 1$, ($l = 1$, $n = 2, 3, 4...$). Similarly, $m = \pm 2$, ($l = 2$, $n = 3, 4, 5...$) produce $d_{x^2-y^2}$ and d_{xy} through the linear combinations. ***Thus the real wave functions of the orbitals are obtained through the linear combinations of the imaginary wave functions (i.e. spherical harmonics) produced from the nonzero values of m. The wave functions developed for m = 0 values are themselves real.***

(iii) **Shape of the orbitals :** The **spherical harmonic**, i.e. angular part of the complete wave function, is given by : $Y_{l,m} = \Theta_{l,m}(\theta) \times \Phi_m(\phi)$ which determines the shape of the orbitals. *Thus, l and m jointly determine the angular wave function, i.e. the shape of the orbitals.*

(iv) **Splitting of the orbitals in presence of an external field :** In the absence of any external magnetic field, the orbitals generated for a particular value of l due to the different m values (e.g. the three p-orbitals determined by $m = 0, \pm 1$ or the five d-orbitals determined by $m = 0, \pm 1, \pm 2$ or the seven f-orbitals determined by $m = 0, \pm 1, \pm 2, \pm 3$) are degenerate. But in the presence of any external magnetic or electric field, the degeneracy is removed. This splitting by an external magnetic field can explain the Zeeman effect (see Sec. 1.10.19) and similarly, the Stark effect is also explainable due to the splitting of the orbitals (having different m values for a particular value of l in the presence of an external electric field).

D. Spin Quantum Number (s)

Origin **:** In Dirac's relativistic wave mechanical model, the spin quantum number appears to make the solutions acceptable. But it has got no existence in the nonrelativistic Schrödinger's wave equation. In the vector model, the concept of a spinning electron was introduced by Uhlenbeck and Goudsmit. It is having the nonintegral value, 1/2. It actually measures the angular momentum of the electron due to its spinning motion. In a magnetic field, it has got only two quantised orientations giving rise to the **magnetic spin quantum number** (m_s) which is given by $\pm s$, i.e. $\pm 1/2$.

Information provided by the spin quantum numbers

(i) **Observation of Stern-Gerlach experiment :** It is extremely important to explain the observation in the experiment of Stern and Gerlach (see Sec. 1.10.18). Due to the two possible orientations

Click Here t.me/thealchemylibrary

of the spinning angular momentum vector in the presence of an external magnetic field, the beam of doublet $\left(S = \frac{1}{2}\right)$ atoms such as hydrogen, silver or copper etc. containing one unpaired electron undergoes bifurcation. The singlet systems ($S = 0$) containing paired electrons for which the resultant spin quantum number becomes zero, do not undergo any splitting in the presence of an external magnetic field. According to the Pauli exclusion principle, the two paired electrons are having the opposite spins.

(ii) **Spin angular moment and the magnetic moment :** The spin angular momentum (p_s) developed due to the spinning motion of the electron around its own axis is given by,

$$\vec{s} = p_s = s(h/2\pi), \text{ (in classical mechanics)}$$
$$= \sqrt{s(s+1)}\,(h/2\pi), \text{ (in wave mechanics)}$$

The relationship between μ_s and p_s has been discussed in Chapter 1.

(iii) **Spectral selection rule :** During the electron transition between the states, the selection rule, $\Delta S = 0$ (where S stands for the resultant spin quantum number) is maintained.

Other quantum numbers such as ***j* (inner quantum number), m_j (total magnetic quantum number)** developed through the coupling of the vectors have been discussed in Chapter 1 in Sec. 1.10.3.

4.1.12 Pauli Exclusion Principle in the Light of Wave Mechanics: Pauli Force

Let us consider a two-electron system in which the ***one-electron spatial wave functions*** are $\psi_1(1)$ and $\psi_2(2)$. By considering the exchange between the electrons, we can have two states :

$$\psi_{12} = \psi_1(1)\,\psi_2(2)$$

and

$$\psi_{21} = \psi_1(2)\,\psi_2(1)$$

The linear combination of the above two spatial wave functions leads to the results :

$$\psi_s = \frac{1}{\sqrt{2}}(\psi_{12} + \psi_{21}) = \frac{1}{\sqrt{2}}[\psi_1(1)\,\psi_2(2) + \psi_1(2)\,\psi_2(1)] \quad \ldots(4.1.12.1)$$

and,

$$\psi_a = \frac{1}{\sqrt{2}}(\psi_{12} - \psi_{21}) = \frac{1}{\sqrt{2}}[\psi_1(1)\,\psi_2(2) - \psi_1(2)\,\psi_2(1)] \quad \ldots(14.1.12.2)$$

where, the factor $1/\sqrt{2}$ appears as the required normalising constant.

The ψ_s is a ***symmetric* one,** as due to the interchange of the electrons, the wave function does not change its sign. On the other hand, ψ_a is an ***antisymmetric one*,** as the interchange of the electrons leads to : $\psi_a \rightarrow -\psi_a$.

To characterise the electrons completely, it is also required to consider the spin wave functions. Thus the **total wave function** is given by :

$$\psi_{total} = \psi_{orbital} \times \psi_{spin} \quad \ldots(14.1.12.3)$$

Regarding the spin wave functions, it is known that there are only two types of spins $\left(\pm\frac{1}{2}\right)$. Let, α and β be the corresponding spin wave functions. In the two-electron system, if the electrons are of

Click Here t.me/thealchemylibrary

opposite spin, then one is alpha and another one is beta. For the two-electron system, the following combined spin wave functions are consistent with the condition of indistinguishability.

$$\psi_{spin}(I) = \alpha(1)\,\alpha(2),\ M_s = +1 \qquad \ldots(4.1.12.4)$$

$$\psi_{spin}(II) = \beta(1)\,\beta(2),\ M_s = -1 \qquad \ldots(4.1.12.5)$$

$$\psi_{spin}(III) = \frac{1}{\sqrt{2}}[\alpha(1)\beta(2) + \alpha(2)\,\beta(1)],\ M_s = 0 \qquad \ldots(4.1.12.6)$$

$$\psi_{spin}(IV) = \frac{1}{\sqrt{2}}[\alpha(1)\,\beta(2) - \alpha(2)\,\beta(1)],\ M_s = 0 \qquad \ldots(4.1.12.7)$$

The first two functions correspond to the same spin for the both electrons while the last two functions correspond to the different spins of the electrons. The last two functions are the linear combinations of $\alpha(1)\,\beta(2)$ and $\alpha(2)\,\beta(1)$ which are equally probable. It is evident that the first three, i.e. $\psi_{spin}(I)$, $\psi_{spin}(II)$ and $\psi_{spin}(III)$, are ***symmetric*** while $\psi_{spin}(IV)$ is ***antisymmetric*** with respect to the exchange of electrons.

Now to get the total wave function (ψ_{total}), *the two spatial (i.e. orbital) wave functions*, ψ_s and ψ_a are to be combined with *the four spin wave functions*. This will lead to eight different combinations as in the *excited state of He-atom* ($1s^1 2s^1$, i.e. two different orbital wave functions for the electrons) :

$\psi_I = \psi_s \times \psi_{spin}(I)$,	symmetric × symmetric	**Symmetric**
$\psi_{II} = \psi_s \times \psi_{spin}(II)$,	symmetric × symmetric	
$\psi_{III} = \psi_s \times \psi_{spin}(III)$,	symmetric × symmetric	
$\psi_{IV} = \psi_s \times \psi_{spin}(IV)$,	symmetric × antisymmetric	**Antisymmetric**
$\psi_V = \psi_a \times \psi_{spin}(I)$,	antisymmetric × symmetric	
$\psi_{VI} = \psi_a \times \psi_{spin}(II)$,	antisymmetric × symmetric	
$\psi_{VII} = \psi_a \times \psi_{spin}(III)$,	antisymmetric × symmetric	
$\psi_{VIII} = \psi_a \times \psi_{spin}(IV)$,	antisymmetric × antisymmetric	**Symmetric**

It is experimentally established that the total wave function for a system of two-electron **must be antisymmetric** with respect to the simultaneous exchange of spatial coordinates and spins between the electrons. Hence, out of the eight possible wave functions, only four antisymmetric wave functions, i.e. ψ_{IV}, ψ_V, ψ_{VI} and ψ_{VII} are acceptable. **This is *Pauli exclusion principle which states that the total wave function* ($= \psi_{spin} \times \psi_{spatial}$) *of a two-electron system must be antisymmetric with respect to interchange of the positions of the two electrons.***

This *antisymmetric criterion is followed by all the particles which are having a half-integral spin.* Such particles are electrons, protons, neutrons, various nuclei with odd mass number, atoms and molecules having odd number of electrons, etc. The particles which follow the Pauli exclusion principle are called ***fermions*** (after E. Fermi) as they obey the *Fermi-Dirac Statistics*. *On the other hand, the particles having integral spins do not follow the Pauli antisymmetric criterion and they* ***follow the symmetric criterion.*** Such particles, e.g. photons; and atoms or molecules having an even number of electrons; nuclei with even mass number; etc. are called ***bosons*** (after S.N. Bose) as they follow the *Bose-Einstein statistics*. The properties of fermions and bosons have been discussed in Sec. 5.1.

Click Here t.me/thealchemylibrary

A More Familiar Form of Pauli Exclusion Principle

Pauli's antisymmetric criterion leads to the following conclusion which is more familiar to us. To illustrate the matter, let us take two electrons having the same spatial (i.e. orbital) wave functions, say $1s$ orbital as in *He atom* ($1s^2$). Thus the electrons are having the same values of n, l and m. Under these conditions, the allowed four antisymmetric total wave functions are given by :

$$\psi_{IV} = \frac{1}{\sqrt{2}}[\psi_{1s}(1)\,\psi_{1s}(2) + \psi_{1s}(2)\,\psi_{1s}(1)]\frac{1}{\sqrt{2}}[\alpha(1)\,\beta(2) - \alpha(2)\,\beta(1)]$$

$$\psi_{V} = \frac{1}{\sqrt{2}}[\psi_{1s}(1)\,\psi_{1s}(2) - \psi_{1s}(2)\,\psi_{1s}(1)] \times [\alpha(1)\,\alpha(2)]$$

$$\psi_{VI} = \frac{1}{\sqrt{2}}[\psi_{1s}(1)\,\psi_{1s}(2) - \psi_{1s}(2)\,\psi_{1s}(1)] \times [\beta(1)\,\beta(2)]$$

$$\psi_{VII} = \frac{1}{\sqrt{2}}[\psi_{1s}(1)\,\psi_{1s}(2) - \psi_{1s}(2)\,\psi_{1s}(1)] \times \frac{1}{\sqrt{2}}[\alpha(1)\,\beta(2) + \alpha(2)\,\beta(1)]$$

Here, ψ_V, ψ_{VI}, ψ_{VII} are zero. Thus only one, i.e. ψ_{IV}, in which the electrons are having different spins is acceptable. This leads to the statement, ***no two electrons in a given system can have all the four quantum numbers identical.*** Thus, if the electrons are having the same orbital wave functions (i.e. same n, l, m), they must have the opposite spins.

Note : In the ground state of *He* ($1s^2$), the electrons differ in spin quantum number ($m_s = \pm 1/2$) and other three quantum numbers n, l and m are the same. In the excited state of *He* ($1s^1 2s^1$), n is different for the electrons.

Pauli force: According to Pauli exclusion principle, two electrons of the same spin cannot occupy the same space, i.e. electrons of the same spin repel mutually and they tend to keep apart in space (cf. VSEPR). This **non-Coulombic repulsive force** among the same spins is called Pauli force.

4.2 WAVE MECHANICAL MODEL FOR POLYELECTRONIC SYSTEMS

The Schrödinger's wave equation can be exactly solved for the hydrogen-like systems containing only one electron. These aspects have been discussed in the previous section. When the wave equation is considered for an electron in a polyelectronic system, it is to accommodate all the possible inter-electron - electron repulsion terms in the expression for the potential energy of the said electron. The existence of these terms in the wave equation makes an exact solution impossible. Some approximate methods are to be used to have the satisfactory solutions to the problem. A method developed by Hartree and Fock, called *self-consistent field (SCF) method* is highly promising in this connection.

4.2.1 Self-Consistent Field (SCF) Method

Hartree's SCF method is actually based on a series of approximation which leads to a laborious computation task. The process is briefed here step-wise.

(i) Firstly, we have to assume a reasonable wave function for each of the electrons of the system except one, (say the ith one).

(ii) By considering the effect of the nucleus and the electrons whose wave functions have been reasonably chosen, on the ith electron, the potential energy of the ith electron is calculated. Thus,

Click Here to meet the academy library

the effect of all the electrons and the nucleus is considered on the ith electron to calculate the Hamiltonian operator $(\widehat{H}_i)$ for the ith electron.

(iii) Now, by using the relationship, $\widehat{H}_i\psi_i = E_i\psi_i$ where $\widehat{H}_i$ represents the Hamiltonian operator which has been calculated by using the approximately chosen one-electron wave functions for the $(n-1)$ electrons, the eigen function ψ_i for the ith electron is calculated. The corresponding energy E_i is also obtained. This ψ_i is not the actual wave function for the ith electron. It is the **first *improved wave function.***

(iv) Now we have to consider another electron, say, the jth electron, whose improved eigen function is determined as it is calculated for ψ_i. In obtaining ψ_j, the required $\widehat{H}_j$ is calculated by using the first improved eigen function (ψ_i) for the ith electron and the approximately chosen one-electron wave functions for the remaining $(n-2)$ electrons. Thus, by continuing the process, the first improved eigen functions for all the n-electrons are calculated. In this way, by completing this first cycle, we get **a complete set of first improved eigen functions.**

(v) By using the set of first improved eigen functions, we can calculate to have *a more improved set of wave functions in the second cycle*. Such cycles are repeated to have more and more improved sets of wave functions. **This process is continued until the set of improved wave functions exhibits no further change in two successive cycles. This set of improved wave functions thus obtained is said to be self-consistent.**

• **Comparison of the properties of orbitals of hydrogenlike systems and polyelectronic systems:** Thus the orbitals obtained for the polyelectronic systems do not radically differ in nature from the orbitals in hydrogen-like systems. The **striking differences** are mentioned as follows.

(i) **Energy dependence on *n* and *l* :** Because of the **inner electron-electron repulsion or shielding effect provided by the other electrons,** the energies of the different orbitals for a particular shell are not identical in contrast to the case of hydrogen-like systems. The sequence runs as follows : $f > d > p > s$. **Thus, *here the energy of an orbital is not only the function of n (in contrast to the case of hydrogen-like systems) but also a function of l.*** Here it is worth remembering that in Dirac's relativistic wave mechanical model for the hydrogen-like system, only a slight dependence of energy of the orbitals on l appears.

(ii) **Energy order of the orbitals :** There is no universal rule applicable for all the polyelectronic systems to describe the order of the energy levels. But the ***aufbau* principle** governed by the ***(n + l) rule*** is definitely promising in determining the electronic configuration of the polyelectronic atoms or ions. This aspect has already been discussed in Section 1.11.1.

(iii) **Energy dependence on *Z* :** In the polyelectronic systems, with the increase of Z, more correctly effective nuclear charge (Z^*), the orbitals are contracted, i.e. the energy of the orbitals decreases. This effect on all the orbitals for a particular shell is not identical. The orbitals having higher l values are much prone to the increase of effective nuclear charge. Thus, the decrease of energy for the d- and f-orbitals is much more prominent compared to the s- and p-orbitals. **The relative rate of decrease of energy of the orbitals with the increase of *Z* runs in the sequence, $f > d > p > s$. In fact, *after a certain value of Z, all the sublevels for a particular shell become energetically degenerate as in the case of hydrogen-like systems.*** This aspect has already been highlighted in Sec. 1.11.1 (cf. Fig. 1.11.1.2).

Click Here 1.me/healchemylibrary

4.2.2 Concept of Slater Orbitals

The concept of **orbital penetration and screening effect** is well documented but no quantitative treatment to deal with the matter has been attempted. In this connection, the contribution put forward by Slater is important to calculate the screening effect and its effect on the orbital wave function. According to this concept, the radial wave function is approximately obtained from Schrödinger's radial wave function for the hydrogen-like systems by assuming that only the highest order term is important. Thus the radial wave function of the Slater orbital is given by (distance in a_0 unit) :

$$R(r) = N_r\, r^{(n^* - 1)} \exp\,[-(Z^*/n^*)r]$$

where N_r is the normalising constant which is different for different orbitals depending on Z^* and n^*. Z^* is given by : $Z^* = Z$ – screening or shielding constant, and n^* is given by : $n^* = n$ – quantum defect. These Z^* and n^* are not necessarily integers like Z and n respectively.

The Z^* can be calculated by some **empirical rules** formulated by Slater himself. The n and n^* are related as follows.

n =	1,	2,	3,	4,	5,	6
n^* =	1,	2,	3,	3.7,	4.0,	4.2

The difference between n and n^* is called the ***quantum defect*** (see Sec. 1.9.2). It is evident that for the higher values of n, the quantum defect is maximum.

In the Slater radial wave function, there is no node except at r = 0 and ∞. Thus the 2*s* and 2*p* orbitals each have only one node at $r = 0$, but in Schrodinger's radial wave function, there is another radial node for the 2*s* orbital at $2a_0/Z$. **Thus, this approximation simplifies the problem *but such approximate wave functions can hardly explain the real nature of an electron's behaviour in the inner region towards the nucleus. But these wave functions at the larger distance from the nucleus (i.e. at the distance where covalent bond formations occurs) are fairly correct.*** Thus, the Slater orbitals are extremely important in explaining the bonding parameters in the atoms or molecules.

From the Slater wave function, the energy of an atom or ion is proportional to the sum of $(Z^*/n^*)^2$ for each electron in the polyelectronic system. From the radial distribution probability, the distance at which the maximum electron density prevails is governed by $(n^*)^2/Z^*$. This is very much comparable with that obtained from Bohr's model and Schrödinger wave mechanical model for the hydrogen-like systems.

This is why it can be concluded that the Slater orbitals are basically hydrogen-like orbitals in nature, but they differ in two aspects,

(i) **the nonexistence of the internal radial nodes, and**

(ii) **the use of Z^* and n^* instead of Z and n respectively.**

4.2.3 Concept of Shielding and Quantum Defect

Before we discuss the quantitative treatment to calculate the effect of shielding, we should have a qualitative picture of the phenomenon. This aspect has already been highlighted in Sommerfeld's model in terms of ellipticity of the concerned orbits (Sec. 1.9.1-2). This point has also been discussed in connection with the radial distribution probability curves of the orbitals (Sec. 4.1.4 and Fig. 4.1.4.4). For convenience, we once again recapitulate these aspects here.

Click Here 1.me/thealchemylibrary

In spite of limitations of the Bohr's atomic model, $<r_{max}>$, the expected distance (cf. Sec. 4.1.4) from the nucleus to the maximum in RDF can be roughly obtained from the Bohr's theory as follows :

$$<r_{max}> = a_0(n^*)^2/Z^*,\ a_0 = 53 \text{ pm}$$

The energy of an electron is a function of Z^2/n^2 (cf. Bohr's model and wave mechanical model for the one-electron systems). If it were true for the polyelectronic systems, then, for example, *Li* ($1s^2\ 2s^1$) would have the first ionisation energy 2.25 (= 9/4) times that of *H* ($1s^1$). But it is only 520 J mole^{-1} for lithium while it is 1312 J mole^{-1} for hydrogen. This lowered value for lithium arises mainly due to the following reasons.

In the case of lithium, the inner two electrons (i.e. $1s^2$) are screening the outermost $2s^1$ electron from facing the nuclear charge directly. It indicates that the outermost electron is not experiencing the full charge $Z = 3$. It is rather experiencing $Z^* = Z - S$ where S stands for the screening effect offered by the other electrons. **The magnitude of *S* depends on the efficiency with which the inner electrons can screen the outermost electron. It also depends on the penetrating power of the outermost electron into the inner electron clouds.**

Thus from the radial distribution function (RDF) curves (Fig. 4.1.4.4) the following points can be concluded.

(i) **Penetrating power of the orbitals for a particular value of *n* :** Because of the existence of one or more maxima for the *s*-orbitals at the closer distances towards the nucleus, the penetrating power of the *s*-orbital is maximum for a particular *n*. Thus, the *s*-electrons are least shielded or screened by the other electrons. Thus the **penetrating power** of the different orbitals lies in the sequence, $s\ (l = 0) > p\ (l = 1) > d\ (l = 2) > f\ (l = 2)$.

(ii) **Energy order of the orbitals for a particular value of *n* :** From the radial distribution function curves, it is evident that the **most probable radius** (i.e. the distance indicating the highest probable region of the electron) increases in the sequence, $ns > np > nd > nf$ for a fixed *n*. But the presence of radial nodes and intranodal maxima given by $(n - l - 1)$ increases in the sequence, $ns > np > nd > nf$. ***Thus, the concept of most probable radius and the existence of intranodal maxima are mutually opposing in measuring the nuclear charge experienced by the electron in the different orbitals for a particular principal quantum number.*** Quantitatively, it has been found that the second factor, i.e. the consideration of the **existence of intranodal maxima,** can overweigh the disfavour created by the larger most probable radius (cf. Sec. 4.1.4). By considering the combined effect of all the maxima including the largest one, it can be shown that $<r_{max}>$ runs in the sequence : $ns < np < nd < nf$. That is why, the penetrating power or Z^* experienced by the orbitals runs as : $ns > np > nd > nf$. In other words, the energy of the orbitals increases in the sequence : $nf > nd > np > ns$.

The concept of quantum defect giving n^* instead of n has already been discussed (Sec. 1.9.2).

4.2.4 Slater's Rules in Calculating the Shielding Constant (*S*) and *Z**

A set of empirical rules have been formulated by Slater to evaluate the shielding constant.

Rule 1 : The orbitals are grouped in the following manner and sequence, $(1s)\ (2s, 2p)\ (3s, 3p)\ (3d)\ (4s, 4p)\ (4d)\ (4f)\ (5s, 5p)\ \ldots$

Click Here to me/thealchemylibrary

Rule 2 : To calculate the shielding constant for the electron in the (*ns*, *np*) or (*nd*) or (*nf*) group, all the electrons in the higher groups lying right to the group contribute nothing.

Rule 3 : Each of the other electrons in a particular group screens 0.35 nuclear charge, except in the (1*s*) group where the screening is measured by 0.30 unit instead of 0.35 unit.

Rule 4 : For determining the screening constant for the (*nd*) or (*nf*) group electron, all the electrons in all preceding groups with $n' \leq n$ screens 1.00 unit nuclear charge each. For the (*ns*, *np*) group electron, all the electrons in the preceding groups with $n' = n - 1$ screen only 0.85 unit each and all other electrons residing in further preceding groups with $n' < n - 1$ screen 1.00 unit each.

The above rules can be systematically tabulated as follows to calculate the screening offered by the electrons.

Electron group with n for which shielding is to be estimated,	*Screening offered by each electron in*			
	All higher groups with $n' \geq n$	*Same group* $n' = n$	*Preceding groups with* $n' = n, n-1$	*Further preceding groups with* $n' < n-1$
(1*s*)	0, ($n' > n$)	0.30	–	–
(*ns*, *np*)	0, ($n' \geq n$)	0.35	0.85 ($n' = n-1$)	1.00
(*nd*) (*nf*)	0, ($n' > n$)	0.35	1.00 ($n' = n, n-1$)	1 00

Illustration of the Slater's Rules

(a) ***Shielding suffered by the valency electron in*** $_9F$ **and** $_9F^-$: For *F*, the grouping of the orbitals with the electrons is $(1s)^2\ (2s, 2p)^7$ while for F^- it is $(1s)^2\ (2s, 2p)^8$

Hence, *S* for $F = 6 \times 0.35 + 2 \times 0.85 = 3.80$; i.e. $Z^* = 9 - 3.80 = 5.20$

Similarly, for F^-, $S = 7 \times 0.35 + 2 \times 0.85 = 4.15$; i.e., $Z^* = 9 - 4.15 = 4.85$

(b) ***Shielding suffered by the valency and 3d electron for*** $_{34}Se$:

The orbital grouping for $_{34}Se$ is : $(1s)^2\ (2s, 2p)^8\ (3s, 3p)^8\ (3d)^{10}\ (4s, 4p)^6$

Hence, for the valency electron, $S = 5 \times 0.35 + 18 \times 0.85 + 10 \times 1 = 27.05$

Therefore, Z^* experienced by the valency electron is given by : $Z^* = 34 - 27.05 = 6.95$

Similarly for the 3*d* electron, $S = 9 \times 0.35 + 18 \times 1.00 = 21.15$

Hence, Z^* experienced by the 3*d* electron is given by : $Z^* = 34 - 21.15 = 12.85$

(c) ***Z^* for different types of electron in*** $_{21}Sc$: The orbital grouping for its electronic configuration is given by :

$(1s)^2\ (2s, 2p)^8\ (3s, 3p)^8\ (3d)^1\ (4s)^2$

$Z^*\ (1s) = 21 - 0.30 = 20.70$;

$Z^*\ (2s, 2p) = 21 - 7 \times 0.35 - 2 \times 0.85 = 16.85$

$Z^*\ (3s, 3p) = 21 - 7 \times 0.35 - 8 \times 0.85 - 2 \times 1 = 9.75$

$Z^*\ (3d) = 21 - 18 \times 1 = 3.0$;

$Z^*\ (4s) = 21 - 1 \times 0.35 - 9 \times 0.85 - 10 \times 1 = 3.0$

Click Here for more/thealchemylibrary

(d) ***Z^* for the valence electron in 2nd period elements*** : The general electronic configuration may be represented as : $(1s)^2\ (2s, 2p)^n$

$Z^*\ (2s, 2p) = (n + 2) - (n - 1) \times 0.35 - 2 \times 0.85 = 0.65n + 0.65$

(e) ***Z^* for the valence electron in d-block elements*** : Let us consider the general electronic configuration of an element in 3*d*-series :

$$(1s)^2\ (2s, 2p)^8\ (3s, 3p)^8\ (3d)^n\ (4s)^2$$

$$Z^*\ (4s) = (20 + n) - 1 \times 0.35 - (8 + n) \times 0.85 - 10 \times 1 = 2.85 + 0.15n$$

Note : • **For the *s*- and *p*-block elements, Z^* value for the valence *s*-electron increases more rapidly in moving left to right along the period by 0.65 unit per element.**

- **For the *d*-block elements, Z^* value for the valence *s*-electron increases relatively more slowly by 0.15 unit per element.**
- **If we apply the Slater's rule to calculate the Z^* value for the outermost *s*-orbital of the *f*-block elements, it becomes 2.85 irrespective of the number of $(n-2)f$ electrons, i.e. Z^* remains constant along the series. *It contradicts the observed f-contraction* (cf. Sec. 8.9.2).**

Limitations of the Slater's Rule

(i) **Overlooking the relative penetrating power of *s* and *p* orbitals :** In grouping the orbitals, *ns* and *np* have been equivalently treated and they have been placed in the same group. But from the knowledge of radial probability distribution curves (Fig. 4.1.4.4), it is evident that the *np*-electrons are much more screened than the *ns*-electrons because of the less penetrating power of the *np*-orbitals compared to that of the *ns*-orbital.

(ii) **Overlooking the relative penetrating power of the orbitals :** All the electrons residing in $(n - 2)$ shells and further preceding groups (for the calculation of screening experienced by the electron in *ns* – *np* group) screen with an equal efficiency which is independent of their penetrating power. This is also not properly justified.

(iii) **Overlooking the effect of intranodal maxima :** In conclusion, it is to be commented that the penetrating power majorly governed by the existence of intranodal maxima given by $(n - l - 1)$ is overlooked. It occurs so, as Slater considered the nonexistence of the radial nodes as an approximation in defining his orbitals.

(iv) **No explanation of *f*-contraction :** Z^* becomes 2.85 for the outermost *ns* orbital for the *f*-block elements irrespective of the number of $(n - 2)f$ electrons. It contradicts the *f-contraction.*

(v) **Unsatisfactory prediction for the heavier congeners of a particular periodic group :** For the heavier congeners of representative elements, Z^* remains constant in a particular group (e.g. Z^* = 2.85 for *Mg, Ca, Sr* and *Ba*; Z^* = 5.0 for *Ga, In, Tl*). This is unexpected. In fact, SCF method supports the slight increasing trend of Z^* for moving from top to bottom in a group. This aspect has been discussed in Sec. 8.10.

Thus, it can't explain the actual behaviour of the inner electron clouds. But in spite of the fact, the simplified treatment yields more or less satisfactory results for the valency electron lying most away from the nucleus. Better results are obtained by sacrificing the Slater's simplicity by using the rules formulated by E. Clementi and D.L. Raimondi which will not be discussed here.

Click Here to the chemylibrary

4.3 BONDING PROPERTIES OF *d*- (cf. 3*d* vs. 4*d*, 5*d*) AND *f*- (cf. 4*f* vs. 5*f*) ORBITALS (cf. Secs. 8.8, 8.20.3, 8.23)

• **3*d* orbitals vs. 4*d*, 5*d* orbitals :** From the radial probability distribution curves (cf. Figs. 4.1.4.4 and 4.3.1), it is evident that for the 3*d*-orbital, the maximum (i.e. r_{max}) lies within the maxima of 3*s*, 3*p*, 4*s* and 4*p* orbitals. ***Thus, the 3d-orbitals are deeply seated and they cannot generally participate in making covalent bonds*** (cf. Figs. 1.11.1.2–3, for energy comparison). $<r_{max}>$ of the 3*d* orbitals is smaller than those of the 4*s* and 4*p* orbitals (cf. Fig. 4.3.1).

$<r_{max}>$ and Energy: $3s < 3p < 3d < 4s < 4p$; $5d \approx 6s$, $6p$ (cf. Figs. 1.11.1.2–3)

In contrast, for the 4*d*- and 5*d*-series, the $\langle r_{max} \rangle$ of the *d*-orbitals becomes relatively closer to the $\langle r_{max} \rangle$ of the relevant valence *s*- and *p*-orbitals. Because of the **relativistic expansion** (caused by the better screening by the contracted inner *s* and *p*-orbitals), **$<r_{max}>$ of the $(n-1)d$ orbitals of the heavier congeners increases.** In fact, $<r_{max}>$ of the 5*d* and 6*s* orbitals become comparable. **Thus bonding ability of the 5*d* orbitals is increased.** In other words, relativistic expansion increases energy of the 5*d* orbitals (cf. Fig. 1.11.1.2) and the 5*d* electrons may be lost more easily to allow the attainment of higher oxidation states. This relativistic expansion effect runs as : $5d > 4d > 3d$. The effect of this phenomenon can be stated, in general, as follows. **The *d*-orbitals of the heavier congeners can participate better**

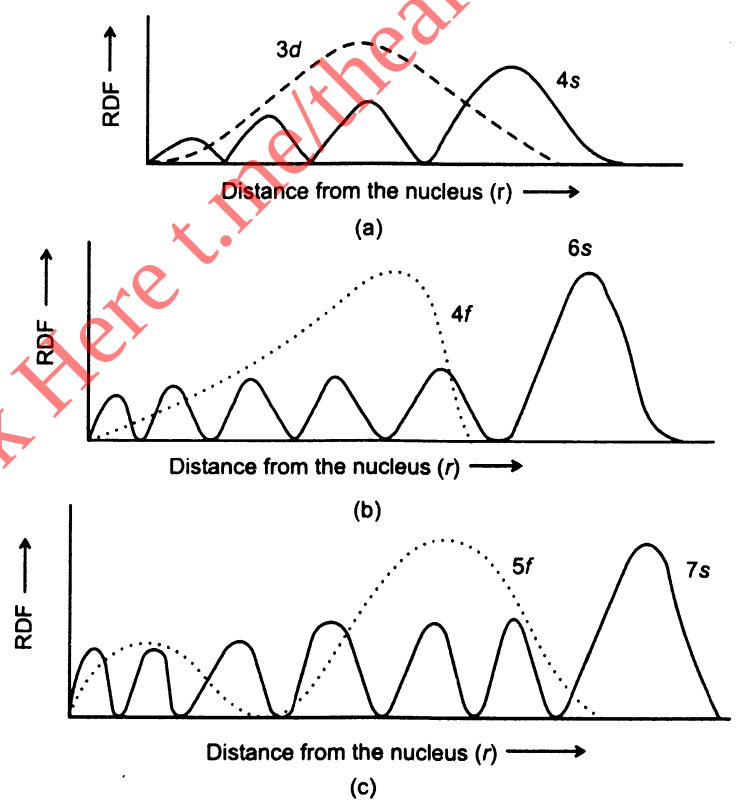

Fig. 4.3.1. Qualitative representation of RDF curves for (a) 3*d* vs 4*s*, (b) 4*f* vs 6*s* and (c) 5*f* vs 7*s*.
RDF = $4\pi r^2[R_{n,l}(r)]^2$

Click Here t.me/thealchemylibrary

in bonding activities. In fact, ***this makes the higher oxidation states more common in the heavier congeners of the d-block elements.***

• **4*f* orbitals vs. 5*f* orbitals :** *Similarly, the 4f-orbitals of the lanthanides are more deeply buried than the 5f orbitals of actinides* (cf. Fig. 4.3.1).

$\langle r_{max} \rangle$ and Energy: $4f < 6s, 6p$; $5f \approx 7s, 7p$, (cf. Figs. 4.3.1, 1.11.1.2)

Thus the 5f-orbitals can participate better in bonding activities and this also favours the attainment of their higher oxidation states.

• **Difference between the lighter and heavier congeners in a particular group :** Here it is important to mention that the ***relativistic expansion*** of the *d*- and *f*-orbitals for the heavier congeners also helps these orbitals to participate in bonding and in attainment of higher oxidating states. These aspects have been discussed in Sec. 8.20.3. Relativistic expansion follows the sequence $5d > 4d > 3d$; $5f > 4f$. It makes the $4f$ orbitals more deeply seated than the $5f$ orbitals (cf. Fig. 4.3.1); and $3d$ orbitals more deeply seated than the $4d$ and $5d$-orbitals.

• **Difference between the early and late members in a particular series :** Here it should be pointed out that *in a period* of the *d*- or *f*-block elements, the *d*- or *f*-orbitals are more diffused for the early members compared to those of the late members. **In other words, in a particular series, the $\langle r_{max} \rangle$ of the *d*- or *f*-orbitals of the early members is greater than that for the late members.** *This contraction in $\langle r_{max} \rangle$ along the series occurs due to gradual increase of Z^** and it is reflected in their energies (cf. Fig. 1.11.1.2). This contraction in $\langle r_{max} \rangle$ of the *d*- or *f*-orbitals along the series is responsible for the difference in bonding properties, spectral properties and other properties between the early members and late members of a particular series.

• **Crystal field effect on the *d*- and *f*-block elements :** The $\langle r_{max} \rangle$ of $(n-1)d$ orbitals lies (in general) close to that of *ns* orbital while for the *f*-block elements, the $\langle r_{max} \rangle$ of $(n-2)f$ orbitals is relatively smaller than that of *ns* orbital (cf. Fig. 4.3.1). Thus, in general, the $(n-1)d$ orbitals of the *d*-block elements are relatively better exposed towards the ligands compared to the $(n-2)f$ orbitals of the *f*-block elements. **This is why, crystal field effect, in general, is more important for the *d*-block elements.** For the *d*-block elements, the crystal field effect runs as : $5d > 4d > 3d$ while for the *f*-block elements, the crystal field effect runs as : $5f >> 4f$. These are reflected in their magnetic and spectral properties.

Click Here to Visit Chemistry Library

SOLVED PROBLEMS

Problem 1 : The radial wave function for a hydrogen-like system is given by :

$$R_{1,0}(r) = 2[(Z/a_0)^{3/2} \exp(-(Zr/a_0)).$$

Show that the most probable radius is given a_0/Z (given, the nodes exist at $r = 0, \infty$).

Solution : The radial distribution function (RDF) is given by :

$$4\pi r^2 [R_{1,0}(r)]^2 = 4\pi r^2 \times 4(Z/a_0)^3 \exp\{-(2Zr/a_0)\}$$

To find the distance at which the maximum probability region appears, the following condition is to be satisfied.

$$\frac{d}{dr}\left[4\pi r^2 \times 4(Z/a_0)^3 \exp\{-(2Zr/a_0)\}\right] = 0$$

On differentiating the radial distribution function with respect to r, we get:

$$\frac{d}{dr}\left[4\pi r^2 \times 4(Z/a_0)^3 \exp\{-(2Zr/a_0)\}\right]$$

$$= 8\pi r\left[4(Z/a_0)^3 \exp-\{(2Zr/a_0)\}\right] + 4\pi r^2\left[4(Z/a_0)^3\left(-\frac{2Z}{a_0}\right)\times \exp\{-(2Zr/a_0)\}\right]$$

$$= \left(8\pi r - \frac{8\pi r^2 Z}{a_0}\right)[R_{1,0}(r)]^2$$

$$= 8\pi r\left(1-\frac{Zr}{a_0}\right)[R_{1,0}(r)]^2$$

According to the conditions,

$$8\pi r\left(1-\frac{Zr}{a_0}\right)[R_{1,0}(r)]^2 = 0$$

Therefore, $$r = 0;\ \text{or},\ \left(1-\frac{Zr}{a_0}\right) = 0;\ \text{or}\ [R_{1,0}(r)]^2 = 0$$

We know that, $[R_{1,0}(r)]^2 = 0$ when $r = \infty$

It is known that at $r = 0$ and ∞, the nodes exist. Hence for the maximum electron density, the condition, $\left(1-\frac{Zr}{a_0}\right) = 0$ is applicable.

Thus, the maximum electron density appears at, $r = a_0/Z$ i.e. $r_{max} = a_0/Z$

Note : See the solved problem 5, where the radial wave function is expressed in atomic unit.

Problem 2 : The spherical harmonic ($Y_{l,m}$) is given by :

$Y_{2,\pm 2} = \left(\frac{15}{32\pi}\right)^{1/2} \sin^2\theta \exp(\pm 2i\phi)$. Show that, $d_{x^2-y^2}$ is a linear combination of the wave functions represented by d_{+2} and d_{-2}.

Solution : From the given spherical harmonic, the angular wave functions for d_{+2} and d_{-2} can be expressed as follows :

$$d_{+2} = \left(\frac{15}{32\pi}\right)^{1/2} \sin^2\theta(\cos 2\phi + i\sin 2\phi);\ d_{-2} = \left(\frac{15}{32\pi}\right)^{1/2} \sin^2\theta(\cos 2\phi - i\sin 2\phi)$$

Now, by adding the two wave functions, we get :

$$d_{+2} + d_{-2} = 2\left(\frac{15}{32\pi}\right)^{1/2}(\sin^2\theta\cos 2\phi) = 2\left(\frac{15}{32\pi}\right)^{1/2}\sin^2\theta(\cos^2\phi - \sin^2\phi)$$

Click Here t.me/thealchemylibrary

$$= 2\left(\frac{15}{32\pi}\right)^{1/2} (x^2 - y^2)/r^2 \text{ (as, } x = r \sin\theta \cos\phi, \text{ and } y = r \sin\theta \sin\phi)$$

From the above expression in terms of Cartesian coordinates, it is seen that the $d_{x^2-y^2}$ is a linear combination of d_{+2} and d_{-2}.

Problem 3 : The angular wave functions for p_x, p_y, and p_z are given as follows :

$\psi(p_z) = \sqrt{(3/4\pi)} \cos\theta$; $\psi(p_x) = \sqrt{(3/4\pi)} \sin\theta \cos\phi$; and, $\psi(p_y) = \sqrt{(3/4\pi)} \sin\theta \sin\phi$.

Show that the summation of electron distribution probability function of the three p-orbitals is spherically symmetrical.

Solution : The summation of electron distribution probability function is given by :

$$[\psi(p_x)]^2 + [\psi(p_y)]^2 + [\psi(p_z)]^2 = P \text{ (say)}$$

Thus,
$$P = \frac{3}{4\pi}\sin^2\theta\cos^2\phi + \frac{3}{4\pi}\sin^2\theta\sin^2\phi + \frac{3}{4\pi}\cos^2\theta$$

$$= \frac{3}{4\pi}\sin^2\theta\left(\cos^2\phi + \sin^2\phi\right) + \frac{3}{4\pi}\cos^2\theta = \frac{3}{4\pi}\left(\sin^2\theta + \cos^2\theta\right) = \frac{3}{4\pi}$$

Since the summation of the total probability function is independent of θ and ϕ, the summation is spherically symmetrical.

Problem 4 : Express the radial equation in terms of atomic units for the hydrogen like systems. Give the Hamiltonian operator in atomic units.

Solution : The radial equation is given by :

$$\frac{d}{dr}\left(r^2\frac{dR}{dr}\right) + \frac{8\pi^2\mu}{h^2}\left(E + \frac{Ze^2}{r}\right)Rr^2 = \beta R \text{ (see Eqn. 4.1.1.10)}$$

where $\beta = l(l+1), l = 0, 1, 2, 3$

In atomic units, $e = 1, \mu = 1, \frac{h}{2\pi} = \hbar = 1$. Thus we can write,

$$\frac{d}{dr}\left(r^2\frac{dR}{dr}\right) + 2r^2\left(E + \frac{Z}{r}\right)R - \beta R = 0$$

or,
$$\boxed{\frac{1}{r^2}\frac{d}{dr}\left(r^2\frac{dR}{dr}\right) + \left(2E + \frac{2Z}{r} - \frac{\beta}{r^2}\right)R = 0 \text{ (in a.u.)}}$$

The Hamiltonian operator (H_{op}) is given by :

$$H_{op} = -\frac{h^2}{8\pi^2\mu}\nabla^2 - \frac{e^2}{(4\pi\varepsilon_0)r}, \text{ (in SI unit)}$$

$$= -\frac{1}{2}\nabla^2 - \frac{1}{r}, \text{ (in a.u.)}$$

Click Here t.me/theachemylibrary

In a.u., $\mu = 1, \frac{h}{2\pi} = \hbar = 1, 4\pi\varepsilon_0 = 1, e = 1$

$$\nabla^2 = \frac{1}{r^2}\frac{\partial}{\partial r}\left(r^2\frac{\partial}{\partial r}\right) + \frac{1}{r^2\sin^2\theta}\frac{\partial}{\partial\theta}\left(\sin\theta\frac{\partial}{\partial\theta}\right) - + \frac{1}{r^2\sin^2\theta}\frac{\partial^2}{\partial\phi^2}$$

(see Eqns. 4.1.1.1 and 4.1.1.2)

$$= \frac{1}{r^2}\frac{\partial}{\partial r}\left(r^2\frac{\partial}{\partial r}\right),$$

(as for the *H*-like atom, the wave function at the ground state i.e. 1*s* orbital is independent of θ and ϕ).

It leads to

$$\boxed{H_{op} = -\frac{1}{2r^2}\frac{\partial}{\partial r}\left(r^2\frac{\partial}{\partial r}\right) - \frac{1}{r}, \text{(in a.u.)}}$$

Problem 5 : Find out the most probable distance of the electron from the nucleus in *H*-atom for the 1*s*, 2*s* and 2*p* orbitals (cf. Table 4.1.4.1 for the radial wave functions).

Solution : The radial probability distribution function $D(r)$ is given by :

$$D(r)\,dr = |R(r)|^2\,(4\pi r^2)\,dr, \textit{ i.e. } D(r) = 4\pi r^2\,|R(r)|^2$$

and at $r = r_{max}, \frac{dD(r)}{dr} = 0$

For H-atom, $Z = 1$.

(i) ***For 1s orbital,*** $R_{1s}(r) = 2\exp(-r)$, (in a.u.)

$|R_{1s}(r)|^2 = 4\exp(-2r)$, [i.e. $D(r) = 4\pi r^2 \times 4\exp(-2r)$]

$\frac{dD(r)}{dr} = 16\pi(2r - 2r^2)\exp(-2r) = 0$

$\exp(-2r)$ cannot be zero, i.e. $(2r - 2r^2) = 0$

i.e. $r = 1$ a.u. = 0.53Å.

(ii) ***For 2s orbital,*** $R_{2s}(r) = \frac{1}{2\sqrt{2}}(2 - r)\exp(-r/2)$, (in a.u.)

$$|R_{2s}(r)|^2 = \frac{1}{8}(4 - 4r + r^2)\exp(-r)$$

i.e. $D(r) = 4\pi r^2\,|R_{2s}(r)|^2 = \frac{4\pi}{8}(4r^2 - 4r^3 + r^4)\exp(-r)$

$$\frac{dD(r)}{dr} = \frac{4\pi}{8}(8r - 12r^2 + 4r^3)\exp(-r) + (-1)\times\frac{4\pi}{8}(4r^2 - 4r^3 + r^4)\exp(-r)$$

$$= \frac{4\pi}{8}(8r - 16r^2 + 8r^3 - r^4)\exp(-r)$$

Click Here t.me/thearchemylibrary

$$= \frac{4\pi r}{8}(8 - 16r + 8r^2 - r^3)\exp(-r) = 0$$

$\exp(-r)$ cannot be zero, i.e.

$$8 - 16r + 8r^2 - r^3 = 0; \text{ or } (2 - r)(4 - 6r + r^2) = 0$$

For, $2 - r = 0$, *i.e.* $r = 2$ a.u. $= 2a_0$, (this is a nodal point)

For, $r^2 - 6r + 4 = 0, r = \frac{6 \pm \sqrt{20}}{2} = 3 \pm \sqrt{5}$

i.e. $r = 5.23$ a.u. $= 5.23\ a_0$ or $r = 0.77$ a.u. $= 0.77\ a_0$

Thus two maxima appear at $r = 0.77$ a.u. and $r = 5.23$ a.u.

(iii) ***For 2p-orbital*** : $R_{2p}(r) = \frac{1}{2\sqrt{6}} r \exp(-r/2)$, (in a.u.)

$$D(r) = 4\pi r^2 \left|R_{2p}(r)\right|^2 = \frac{4\pi}{24} r^4 \exp(-r)$$

$$\frac{dD(r)}{dr} = \frac{4\pi}{24}\left\{4r^3 \exp(-r) + (-1) \times r^4 \exp(-r)\right\}$$

$$= \frac{4\pi}{24}(4r^3 - r^4)\exp(-r) = \frac{4\pi}{24} r^3 (4 - r)\exp(-r) = 0$$

$\exp(-r)$ cannot be zero, i.e. $4 - r = 0$, or $r = 4$ a.u. $= 4a_0$.

Problem 6 : Calculate the ratio of probability of finding the 1*s* electron of *H*-atom at $r = a_0$ and $r = 10a_0$.

Solution : ψ_{1s} (radial part) $= 2\left(\frac{1}{a_0}\right)^{3/2} \exp(-r/a_0)$; $D(r) = \text{RDF} = 4\pi r^2 \mid R(r)\mid^2$

At $r = a_0$, $D(r) = 4\pi r^2 \left|R_{1s}(r)\right|^2 = 4\pi (a_0)^2 \left(\frac{4}{a_0^3}\right) \exp\left(-\frac{2a_0}{a_0}\right) = \frac{16\pi}{a_0} \exp(-2)$

At $r = 10a_0$, $D(r) = 4\pi r^2 \left|R_{1s}(r)\right|^2 = 4\pi (10a_0)^2 \left(\frac{4}{a_0^3}\right) \exp\left(-\frac{20a_0}{a_0}\right) = \frac{1600\,\pi}{a_0} \exp(-20)$

The ratio of these probabilities is given by :

$$\frac{16\,\pi \exp(-2)}{1600\,\pi \exp(-20)} \approx 6.5 \times 10^5$$

Problem 7 : Calculate the average distance or expectation value $(\bar{r})$ of the electron for 1*s* and 2*s* orbitals in the *H*-like systems. Comment on $\bar{r}$ and r_{max}.

Solution : The average distance is given by :

$$(\bar{r}) \text{ or } \langle r \rangle = \int_0^{\infty} \int_0^{\pi} \int_0^{2\pi} \psi\, r\, \psi\, d\tau$$

Click Here to me/thealchemylibrary

In terms of radial part and angular part, the wave function can be expressed as :

$$\psi = R_{n,l}(r)\, Y_{l,m}(\theta, \phi)$$

The volume element $d\tau$ is given by :

$d\tau = r^2 dr \sin\theta\, d\theta\, d\phi$ where r can vary from 0 to ∞, θ can vary from 0 to π, and ϕ can vary from 0 to 2π.

It leads to :

$$\bar{r} = \int_0^{\infty} \left[R_{n,l}(r)\right]^2 r^3 dr \int_0^{\pi} \int_0^{2\pi} \left[Y_{l,m}(\theta, \phi)\right]^2 \sin\theta\, d\theta\, d\phi$$

The second part i.e. spherical harmonic is normalised to unity. Hence we can write :

$$\bar{r} = \int_0^{\infty} \left[R_{n,l}(r)\right]^2 r^3 dr$$

1s orbital : ψ_{1s} (radial part) = $2(Z)^{3/2} \exp(-Zr)$, (in a.u.)

$$\bar{r}_{1s} = \int_0^{\infty} \left[\psi_{1s}\right]^2 r^3 dr = 4Z^3 \int_0^{\infty} r^3 \exp(-2Zr)\, dr$$

$$= 4Z^3 \frac{3!}{(2Z)^4} = \frac{3}{2Z} \text{ a.u.} = \frac{3}{2Z} a_0$$

Note : $\int_0^{\infty} x^n \exp(-mx)\, dx = \frac{n!}{m^{n+1}}$

2s orbital : ψ_{2s} (radial part) = $\frac{1}{2\sqrt{2}} (Z)^{3/2} (2 - Zr) \exp(-Zr/2)$, (in a.u.)

$$\bar{r}_{2s} = \int_0^{\infty} \left[\psi_{2s}\right]^2 r^3 dr$$

$$= \frac{Z^3}{8} \int_0^{\infty} (2 - Zr)^2 \exp(-Zr)\, r^3 dr$$

$$= \frac{Z^3}{8} \int_0^{\infty} (4 - 4Zr + Z^2 r^2)\, r^3 \exp(-Zr)\, dr$$

$$= \frac{Z^3}{8} \left[\int_0^{\infty} (4r^3 \exp(-Zr)\, dr - \int_0^{\infty} 4Zr^4 \exp(-Zr)\, dr + \int_0^{\infty} Z^2 r^5 \exp(-Zr)\, dr\right]$$

$$= \frac{6}{Z} \text{ a.u., (using the standard integrals)}$$

$$= \frac{6}{Z} a_0.$$

Click Here t.me/tbeatchemylibrary

Note : • $\bar{r}$ and r_{max} are different. For 1*s* orbital of *H*-atom : $\bar{r} = \frac{3}{2}a_0 > r_{max} = a_0$. For 2*s* orbital of *H*-atom : $\bar{r} = 6a_0 > r_{max} = 5.23\, a_0$. This higher expectation values can be explained by considering the nonsymmetrical nature of radial wave function when plotted against *r* (cf. Fig. 4.1.4.2).

- $\bar{r}_{ns} = n^2 \left(\frac{3}{2Z}\right) a_0$
- $\bar{r}_{n,l} = \int_0^\infty \left[R_{n,l}(r)\right]^2 r^3 dr = \frac{1}{2Z} a_0 \left\{3n^2 - l(l+1)\right\}$
- $\overline{r^2} = \int_0^\infty \int_0^\pi \int_0^{2\pi} \psi r^2 \psi \, dr = \int_0^\infty \left[R_{n,l}(r)\right]^2 r^4 dr$

Problem 8 : Predict whether ionisation will occur from the 3*d* level or 4*s* level for a representative member of 3*d*-series.

Solution : Let us take chromium as the representative member of 3*d*-series.

$$Cr : (1s)^2\ (2s, 2p)^6\ (3s, 3p)^8\ (3d)^5\ (4s)^1$$

$$\begin{cases} S \text{ (for } 4s) = (2 \times 1.0) + (8 \times 1.0) + (8 \times 0.85) + (5 \times 0.85) = 21.05 \\ Z^* \text{ (for } 4s) = 24 - 21.05 = 2.95 \end{cases}$$

$$\begin{cases} S \text{ (for } 3d) = (2 \times 1.0) + (8 \times 1.0) + (8 \times 1.00) + (4 \times 0.35) = 19.4 \\ Z^* \text{ (for } 3d) = 24 - 19.4 = 4.6 \end{cases}$$

Thus, it is evident that the 3*d* electron experiences Z^* more (i.e. more tightly bound) compared to the 4*s* electron. Consequently, ionisation will occur first from the 4*s* level.

Problem 9 : Predict the sequence of ionic radii of the isoelectronic species is O^{2-}, F^-, Na^+, Mg^{2+} and Al^{3+} in terms of Z^*.

Solution : The electronic configuration of the isoelectronic species is $1s^2\ 2s^2\ 2p^6$ which can be grouped as $(1s)^2\ (2s, 2p)^8$.

$S = 2 \times 0.85 + 7 \times 0.35 = 4.15$

Species :	O^{2-}	F^-	Na^+	Mg^{2+}	Al^{3+}
Z^* (= $Z - S$) :	8 – 4.15 = 3.85	9 – 4.15 = 4.85	11 – 4.15 = 6.85	12 – 4.15 = 7.85	13 – 4.15 = 8.85

$\longrightarrow$

Z^* = increasing trend

r : decreasing trend

Problem 10 : By using the Slater's rules, calculate the first ionisation energy of lithium.

Solution : The first ionisation of *Li* can be represented as follows :

$$Li\ (1s^2\ 2s^1) \xrightarrow{-e} Li^+\ (1s^2)$$

Click Here t.me/thealchemylibrary

Therefore, the first ionisation energy (IE) is given by the difference in energy between Li^+ and Li.

Thus, $IE = E_{Li^+} - E_{Li}$

The energy of a polyelectronic system is given by the sum of the energy of each electron given by :

$$-\frac{me^4}{8\varepsilon_0^2 h^2}\left(\frac{Z^*}{n^*}\right)^2 = -13.6(Z^*/n^*)^2 \text{ eV}.$$

Thus, the energy of a system = $\sum -13.6(Z^*/n^*)^2$ eV

Therefore, $IE = E_{Li^+} - E_{Li} = -13.6\left[2(Z^*/n^*)^2_{(1s)}\right]_{Li^+}$

$$+13.6\left[2(Z^*/n^*)^2_{(1s)} + (Z^*/n^*)^2_{(2s,2p)}\right]_{Li} = \left[13.6\,(Z^*/n^*)^2_{(2s,2p)}\right]_{Li}$$

Here, $Z^*_{(2s,2p)Li} = Z - 2 \times 0.85 = 3 - 1.70 = 1.30$; and $n^* = n = 2$

Thus, $IE = 13.6\left(\frac{1.69}{4}\right) = 5.75$ eV

Problem 11 : Calculate the electron affinity of *F* and *Cl* by using the Slater's rule.

Solution : The electron affinity process for *F* and *Cl* can be simply represented as follows :

$$F\,(1s^2\,2s^2\,2p^5) \xrightarrow{+e} F^-\,(1s^2\,2s^2\,2p^6)$$

and,
$$Cl\,(1s^2\,2s^2\,2p^6\,3s^2\,3p^5) \xrightarrow{+e} Cl^-\,(1s^2\,2s^2\,2p^6\,3s^2\,3p^6)$$

Electron affinity {(*EA*)} is measured by, $(EA)_F = E_{F^-} - E_F$ = energy of F^- – energy of F

Similarly, $(EA)_{Cl^-} = E_{Cl^-} - E_{Cl}$

Now, by using the concept of Slater's rule,

$$(EA)_F = -13.6\left[2(Z^*/n^*)^2_{(1s)} + 8(Z^*/n^*)^2_{(2s,2p)}\right]_{F^-} + 13.6\left[2(Z^*/n^*)^2_{(1s)} + 7(Z^*/n^*)^2_{(2s,2p)}\right]_F$$

$$= -13.6\left[8(Z^*/n^*)^2_{(2s,2p)}\right]_{F^-} + 13.6 \times 7\left[(Z^*/n^*)^2_{(2s,2p)}\right]_F$$

Here, $Z^*_{(2s,2p)F^-} = 9 - 7 \times 0.35 - 2 \times 0.85 = 4.85$

and, $Z^*_{(2s,2p)F} = 9 - 6 \times 0.35 - 2 \times 0.85 = 5.20$

and $n^* = n = 2$

Therefore, $(EA)_F = -13.6\left[8 \times \frac{23.52}{4} - 7 \times \frac{27.04}{4}\right] = +3.80$ eV

Similarly, for chlorine it is given by :

$$(EA)_{Cl} = -13.6\left[\left|8(Z^*/n^*)^2_{(3s,3p)}\right|_{Cl^-} - \left|7(Z^*/n^*)^2_{(3s,3p)}\right|_{Cl}\right]$$

Click Here t.me/thealchemylibrary

where $Z^*_{(3s,3p)Cl^-} = 17 - (7 \times 0.35 + 8 \times 0.85 + 2) = 5.75$

and, $Z^*_{(3s,3p)Cl} = 17 - (6 \times 0.35 + 8 \times 0.85 + 2) = 6.10$

$$(EA)_{Cl} = -13.6\left[8 \times \left(\frac{5.75}{3}\right)^2 - 7 \times \left(\frac{6.10}{3}\right)^2\right] = -6.09 \text{ eV}, (n^* = n = 3)$$

EXERCISE-IV

A. General Questions

1. Write down the Hamiltonian operator for a hydrogen-like system in Cartesian coordinates. Transform the Shrödinger's wave equation for the hydrogen-like systems into spherical coordinates (r, θ, ϕ). Split the wave equation into radial and angular parts. Write down the solutions to the partial differential equations expressing the behaviour of the electron in hydrogen-like systems.
2. Discuss the wave mechanical genesis of the different quantum numbers. How does the wave mechanics deal with the spin quantum number?
3. What are the basic differences between the Schrödinger's nonrelativistic and Dirac's relativistic atom?
4. What do you mean by the radial distribution probability function? Discuss the characteristic features of radial distribution functions (RDFs) of different orbitals in hydrogen-like systems.
5. Discuss the chemical and physical significance of nodes in terms of Schrödinger's non- relativistic wave mechanical model.
6. What do you mean by spherical harmonics? Discuss the relations between the Schrodinger's spherical harmonics and the real angular wave functions representing the orbitals.
7. Show that there is no one to one correspondence between the set p_x, p_y, p_z and the set of orbitals defined by $m = 0, \pm 1$ except for $m = 0$.
8. Show that the d_{z^2} orbital is a linear of combination of the two orbitals $d_{z^2-y^2}$ and $d_{z^2-x^2}$. Classify the five d-orbitals in the light of angular distribution function. How do you get the real five d-orbitals from the spherical harmonics defined by $m = 0, \pm 1, \pm 2$?
9. Give the electron cloud distribution representation for the following orbitals, $1s$, $2s$, $2p_x$, $3p_x$, $3d_{z^2}$ and $3d_{xy}$.
10. Discuss the basic differences between the orbitals and orbits.
11. How does the polyelectronic system differs from the hydrogen-like system? The energy of the $3s$–, $3p$– and $3d$–orbitals in hydrogen-like systems is identical while they differ as $3d > 3p > 3s$ in a polyelectronic system - justify the observation.
12. How does the Slater orbital differ from the Schrödinger orbital? Discuss the Slater's rules to calculate Z^* and n^*. What are the limitations of the Slater's rule ?
13. Discuss the penetrating power of the different orbitals in the light of both wave mechanical and classical model.

Click Here to me/thealchemylibrary

14. What is the difference between ψ_r^2 and $4\pi r^2\psi_r^2$.
15. Represent the angular wave functions and their angular probability functions for $2s$, $2p$ orbitals.
16. Discuss the major drawbacks of Slater's orbitals and Slater's rule to calculate Z^*.
17. Distinguish between radial probability density and radial distribution function (RDF).
18. Discuss the relative bonding properties of (i) $3d$, $4d$ and $5d$ orbitals; (ii) $4f$ and $5f$ orbitals; (iii) $(n-1)d$ orbitals of d-block elements vs. $(n-2)f$ orbitals of f-block elements.

B. Justify the Statements

1. In wave mechanics, the existence of the quantum numbers is the consequence of having well-behaved functions while in classical mechanics, they appear as the consequence of the postulates chosen arbitrarily.
2. The existence of nodes is definitely problematic in the particle concept of an electron, but in wave mechanics it does not produce any problem.
3. The existence of intranodal maxima in the radial distribution functions can nicely explain the shielding or penetrating efficiency of the different orbitals.
4. Though the most probable radii i.e. r_{max} corresponding the largest maxima in hydrogen-like systems lie in the sequence, $ns > np > nd$, the energy sequence runs in the opposite direction.
5. The single s-orbital is spherically symmetrical, the p-orbitals are individually directional but the summation of the electron cloud distribution probability for the three p-orbitals leads to a spherical distribution of the electron cloud as in the case of a s-orbital.
6. p_z is a pure orbital, but p_x and p_y are really hybrid orbitals.
7. From the designation, the d_{z2} orbital should not have any electron cloud density in the xy-plane, but, in fact, it is having some electron cloud density in the xy-plane.
8. The Slater orbitals are not really good for the inner electrons.
9. In Schrödinger wave mechanics, the spin quantum number does not exist.
10. The d_{z2} orbital should be really designated by $d_{(z^2-r^2/3)}$.
11. The bonding properties of the d-orbitals of the d-block elements are in the sequence : $5d > 4d > 3d$.
12. The bonding properties of the f-orbitals of the f-block elements lie in the sequence : $5f > 4f$.
13. Crystal field effect is more important for the transition metals compared to the inner-transition metals.

C. Numerical Problems

1. Calculate the Z^* for the valence electron and the $3d$ electron for $_{30}Zn$. (Ans. 4.35; 8.85)
2. Calculate the first ionisation energy for fluorine by using the Slater's rule. (Ans. 15 eV).
3. Calculate the 2nd ionisation potential for carbon and compare with the experimental one, 24.4 eV.

Click Here 1.me/thealchemylibrary

5

Atomic Nucleus and its Structure

5.1 THE ATOMIC NUCLEUS

5.1.1 Composition of the Nucleus

The discovery of neutrons by Chadwick (1932) made a significant contribution in pacifying the stormy problem at that time regarding the composition of the nucleus. It has already been discussed (see Sec. 3.3.4a) that the existence of neutrons or protons within the nucleus does not break down the uncertainty principle, one of the strongest foundation stones in modern physics. Here, again it is worth recalling that the existence of free electrons within the nucleus contradicts (see Sec. 3.3.4a) the theoretical physics. Now it is believed that the protons and neutrons are the constituent particles of the nucleus. These nuclear constituent particles are in general called **nucleons** which follow the Fermi–Dirac statistics. The nucleus contains Z protons (Z denotes the atomic number) and N neutrons to give the mass number A ($= Z + N$). The atomic number defined by Z is the fundamental property of an element. For a particular value of Z, because of the different numbers of N, the isotopes appear. The *neutron–proton ratio and their oddness and evenness* are very much important in determining the stability of the nucleus.

The emission of β^--particles, i.e. electrons, from the nucleus does not contradict the **proton–neutron model of the nucleus.** It is now believed that the transformation of a neutron into a proton leads to the ejection of a β^--particle.

In this proton–neutron model, it is now believed that they are continuously changing one into another through the **exchange of a common property.** *Thus, within the nucleus, it is not appropriate to define a particle either as a proton or as a neutron.* They are really indistinguishable within the nucleus due to the exchange phenomenon. **This is why, within the nucleus,** ***the constituent particles are reasonably referred to as nucleons, and they can be characterised as protons or neutrons when they emerge from the nucleus.***

Click Here t.me/thealchemylibrary

Fermions and Fermi-Dirac Statistics; Bosons and Bose-Einstein Statistics; Bose-Einstein Condensate (BEC) – Fifth State of Matter

Maxwell-Boltzmann statistics is well documented to explain the properties (e.g. velocity distribution, energy distribution, etc.) of the assemblies (i.e. large number) of molecules of a gas. However, this classical mechanics is not applicable for the elementary particles like electrons, protons, neutrons, mesons, neutrinos, etc. and atomic nuclei. To deal with these particles, two quantum mechanical statistics, namely, **Fermi-Dirac statistics** and **Bose-Einstein statistics** are developed. The particles having half integral spins (e.g. electrons, protons, neutrons, positrons, etc.) which follow the Fermi-Dirac statistics are called ***fermions*** while the particles having the integral spins (e.g. photons, mesons, α-particles, etc.) which follow the Bose-Einstein statistics are called ***bosons***. The *fermions* follow the Pauli's exclusion principle while the *bosons* do not.

Fermions are characterised with **half-integer spin quantum numbers** (e.g. electron, $s = 1/2$). Bosons are characterised with **zero or integer** spin quantum numbers (e.g. photon, $s = 1$).

Fermions obey the Pauli exclusion principle and consequently only a single fermion particle can occupy a given quantum state. Bosons do not obey the Pauli exclusion principle and consequently, any number of bosons can pile up in a given quantum state. This assembly of bosons is called **Bose-Einstein condensate (BEC).** In 1995, a group of scientists became successful to obtain a such condensate of about 2000 *Rb*-87 atoms at a very low temperature (a ~ 10^{-7} K) at which the particles approximately possess zero speed. Thus the *Rb*-87 atoms were held **in a single quantum state of approximately zero energy.** This achievement has been described as the **Holy Grail of atomic physics** (Nobel Prize in 2001).

It may be noted that a group of Indian scientists (Sanjukta Roy, Saptarshi Chaudhury and C.S. Unnikrishnan) working at TIFR had been successful to achieve the Bose-Einstein Condensate (BEC) (DNA, 2007, Mumbai).

Fifth state of matter : BEC is described as the **fifth state of matter.** At very low temperature (close to 0 K i.e. – 276°C), at this state, a large number of boson particles will pile up at a single quantum state of approximately zero energy to produce a lump of matter described as a **superatom.**

The other four states of matter are : solid, liquid, gas and plasma (which is obtained at very high temperature at which atoms are completely dissociated into the constituent nuclei and electrons; plasma state is obtained in stars like sun).

Click Here t.me/thealchemylibrary

5.1.2 Size of the Nucleus

In this connection, we can recall the Rutherford's α–particle scattering experiment which provided the upper limit of the size of the large target nuclei. It was found (see Sec. 1.7.3) that the closest approach (r_{eq}) between the target nucleus and the α–particle is given by : $r_{eq} = 3.8 \times 10^{-16}\ Z$ meter where Z denotes the atomic number of the target nucleus. In this experiment, the deflection of the α–particles by the target nucleus was governed by Coulomb's law.

Similarly, scattering of other particles like fast electrons and neutrons may provide useful information regarding the size of the nucleus. Here it is worth pointing out that the electrons being charged particles may interact through the electrical force while the neutrons interact through the nuclear force which is

different from the Coulomb's force. *Thus the charged particle scattering due to Coulombic interaction (at least in part) provides the knowledge of radii of nuclear charge distribution while the neutron scattering due to nuclear force only provides information of radii of nuclear matter distribution.* Here it is important to mention that such scattering neutrons must have de Broglie wavelength smaller than the dimension of the target nucleus under observation. High energy charged particles (e.g. 40 MeV α–particles, 100–300 MeV protons) may also get scattered due to nuclear force.

From the above discussion, it is evident that a generalised single definition for the nuclear radii covering all the nuclear phenomena utilised to determine the size of the nucleus cannot be given. It depends on the nature of the probe taken into consideration. This variation lies within 10–20 per cent. Thus the nuclear radii can be compared with the different concepts of atomic radii. The nuclear radii can be classified as follows :

(i) ***Coulombic radii*** **:** Methods depending on the Coulombic interaction (at least in part) give the idea of Coulombic radii. Scattering of high energy electrons (several hundred MeV) is very much important in this connection.

(ii) ***Nuclear force or potential radii*** **:** Methods such as scattering of fast neutrons (≥ 20 MeV), high energy α–particles (40 MeV) and high energy protons (100–300 MeV) depending wholly on the nuclear force give the idea of nuclear force or potential radii.

It has been found that the nuclear force or potential radii are generally 10–20 per cent larger than the Coulombic radii.

From a number of experiments, it has been found that the volume of a nucleus is directly proportional to the mass number (A), i.e. the number of nucleons present in the nucleus.

Thus, $(4/3)\pi R^3 \propto A$, (R = the nuclear radius);

or, $$R^3 \propto \frac{3A}{4\pi}; \text{ or, } \boldsymbol{R = r_0 A^{1/3}}, r_0 = \text{some constant.}$$

The above relation is also obtained by considering another experimental observation, i.e. *the constancy of density* (rho) of the nuclear matter. It gives the relation,

$$\rho \propto \frac{A}{(4/3)\pi R^3} = \text{constant; or, } \boldsymbol{R = r_0 A^{1/3}}. \text{ The value of } r_0 \text{ is found as,}$$

$$\boxed{r_0 = 1.2 \times 10^{-15} \text{ m.}}$$

$$\text{i.e. } R = 1.2 \times 10^{-15} A^{1/3} \text{ m}$$

$$= 1.2\, A^{1/3} \text{ fm}$$

Note **:** Some authors use the relation, $\boxed{r_0 = 1.4 \times 10^{-15} \text{ m}}$

Now, it is evidently seen that the Å unit (1 Å = 10^{-8} cm = 10^{-10} m) is appropriate in dealing with the dimensions of atoms and molecules, but it is not an appropriate unit in measuring the nuclear dimension which is too small. Approximately, the atomic dimension measured by Å unit is about 10^5 times larger than the dimension of the nucleus. This is why, a new unit called ***fermi*** abbreviated as fm or F (1 fm = 10^{-13} cm = 10^{-15} m) has been chosen in the realm of nucleus.

Click Here to me/heal chemylibrary

By using the above relation, $R \approx 1.2 \times 10^{-15} A^{1/3}$ m = $1.2 \times A^{1/3}$ fm, the nuclear radii of different atoms can be calculated. Thus the radius of ${}^{238}_{92}U$ is found to be $R \approx 1.2\ (238)^{1/3}$ fm = 7.436 fm. Similarly, the radii for ${}^{12}_{6}C$, ${}^{107}_{47}Ag$ nuclei are found to be 2.7 fm and 5.7 fm respectively.

5.1.3 Mirror Nuclei and Nuclear Radius

It will be discussed later on that in a pair of mirror nuclei, the mass number remains identical, but the number of neutrons and protons differs by unity e.g. ${}^{A}_{Z}X_N$ and ${}^{A}_{N}Y_Z$ represent a pair of mirror nuclei. Thus the mirror nuclei are isobaric. Some sets are :

$${}^{3}_{1}H \text{ and } {}^{3}_{2}He,\ {}^{7}_{3}Li \text{ and } {}^{7}_{4}Be,\ {}^{11}_{5}B \text{ and } {}^{11}_{6}C.$$

In each set, one is unstable and it decays (β^- or positron emission) into the stable member of the set. The nuclear bending energy (*NBE*) of the nuclides can be measured or calculated. In a particular set, the added proton introduces some additional Coulombic repulsive energy. The nuclear force (which will be discussed later) depends on the number of nucleons irrespective of their charge. *In fact, after allowing the electronic repulsive force between the protons, the nuclear forces in the interactions,* $(n-n)$, $(n-p)$ and $(p-p)$ *are equal.* In a particular set of mirror nuclei, the number of nucleons in each nuclide is the same and consequently the binding energy between them differs only due to the *additional Coulombic repulsive energy* (ΔE_c) which can easily be calculated by the principle of classical electrostatics. **In a pair of mirror nuclei, one $(p-p)$ force is replaced by a $(n-n)$ force.** From the calculation, it is given by :

$$\Delta E_c \approx (6Ze^2)/(5R)$$

where Z = atomic number of the nuclide (of a particular mirror pair) without the additional proton, and R = radius of the spherical nucleus. According to the above argument, ΔE_c (= difference in nuclear binding energy (*NBE*) between the mirror nuclei) is a measurable quantity. From the above relation, for the cases A = 3 to 38, R has been calculated and it has been found as : $R = r_0 A^{1/3}$ where r_0 is a constant and it is $\approx 1.2 \times 10^{-15}$ m.

5.1.4 Nuclear Density

We have already mentioned that nuclear density is more or less constant and it is independent of the nature and size of the nuclei. Let us take the case of ${}^{12}_{6}C$ whose atomic mass is given by 12.0 u where u stands for **unified atomic mass unit** (≡ amu) and it is given by : 1 u = 1.66×10^{-27} kg. Now if the mass and binding energy of the six electrons present in ${}^{12}_{6}C$ are neglected, then the nuclear density (ρ) is given by:

$$\rho = \frac{m}{(4/3)\pi R^3} = \frac{12.0 \times 1.66 \times 10^{-27}\ \text{kg}}{(4/3)\pi \times (2.7 \times 10^{-15}\ \text{m})^3} \approx 2.0 \times 10^{17}\ \text{kg m}^{-3}$$

(Here, $R = 1.2\ A^{1/3} \times 10^{-15}$ m = 2.7×10^{-15} m)

The above figure indicates that the nuclear density is of the order of **billion tons per cubic inch. Thus, even, if *it were possible to isolate and collect* 1 *cm*³ *of nuclei, there would be no earthly container to withstand this enormous mass.*** In this connection, we can recall the stars like **neutron**

Click Here t.me/thealchemylibrary

stars, white dwarfs, etc. where due to the enormous gravitational collapse, the electron shells are collapsed and they have attained the density of the nuclear matter.

5.1.5 Shape of the Nucleus

In our previous consideration, the spherical nature of the nucleus has been considered. But the actual shape of the nucleus depends on the total angular quantum number or simply, **the *nuclear spin I*** and the ***electric quadrupole moment*** **(= *Q*)** of the nucleus under consideration. The parameter, *electric quadrupole moment* (Q) describes the interaction of the nucleus with the electric field gradient (e.g. $\partial E_x/\partial x$). Thus the term Q can be expressed as follows :

$$eQ = \int \rho(r)\,(3z^2 - r^2)\,dV$$

where e is the unit of electrostatic charge, $\rho(r)$ gives the electric charge density at a distance r from the centre of the nucleus with x, y, z as its coordinates whose origin also lies at the centre of the nucleus. Here the z-axis is chosen to obtain the quantity Q. *Q gives a measure of deviation of nuclear charge distribution from the spherical symmetry. If the charge is spherically and symmetrically distributed then it leads to*:

$$\int \rho(r)\,z^2 dV = \int \rho(r)\,y^2 dV = \int \rho(r)\,x^2 dV = \frac{1}{3}\int \rho(r)\,r^2 dV$$

In such cases **(i.e. *spherically symmetrical*) *eQ* = 0, i.e. *Q* = 0. *The positive value of Q indicates that the nucleus is elongated in the z-direction and the negative value indicates that the nucleus is contracted in the z-direction.***

It has been found that the systems having $I \geq 1$ and $eQ \neq 0$, are deviated from the spherical shape. On the other hand, the nuclei having, $I = 0, 1/2$ and $eQ = 0$, are perfectly spherical. In this parameter, e is the unit of electrostatic charge and Q gives the measure of deviation from sphericality of the nucleus. If eQ is positive, i.e. $eQ > 0$, then the nucleus becomes a ***prolate spheroid*** (i.e. egg shaped) while for $eQ < 0$, the nucleus becomes an ***oblate spheroid*** (i.e. discus or pumpkin shaped). These are shown in Fig. 5.1.5.1.

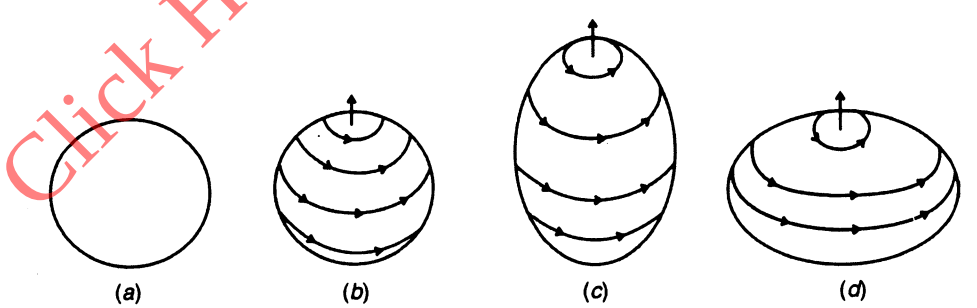

Fig. 5.1.5.1. Nuclear shapes and electric quadrupole moment (a) $I = 0$, $eQ = 0$, nonspinning spherical nucleus; (b) $I = 1/2$, $eQ = 0$, spherical spinning nucleus; (c) $I \geq 1$, $eQ > 0$, ellipsoidal (prolate) spinning nucleus; (d) $I \geq 1$, $eQ < 0$, ellipsoidal (oblate) spinning nucleus.

The *dimension of quadrupole moment* (Q) is cm^2 and it is very often expressed in the unit of 10^{-24} cm^2 (= 1 barn). The value for deuteron is 0.2×10^{-27} cm^2 = 0.2 mbarn (millibarn).

Click Here for more chemistry library

The ***nuclear ellipticity*** (ε) and ***quadrupole moment*** of an ellipsoidal nucleus having Ze charge with the *semimajor axis* (b) parallel to the z-axis (called *symmetry axis*) and *semiminor axis* (a) perpendicular to it is given by :

$$Q = \left(\frac{2}{5}\right) Z\,(b^2 - a^2) = \left(\frac{4}{5}\right) \varepsilon Z R^2$$

where $\varepsilon = 2(b-a)/(b+a)$ and $(b+a)/2 = R$ (the mean of radius of the nucleus).

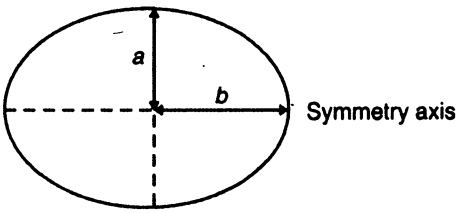

Fig. 5.1.5.2. Representation of semimajor axis (b) and semiminor axis (a) for an ellipsoidal nucleus; $b > a$ (prolate), $b < a$ (oblate).

^{176}Lu nucleus having the **largest positive value of Q** has become the ***most prolate ellipsoidal*** (ellipticity = 0.174 and $Q = 7b$) while ^{233}Pa nucleus has become the ***most oblate ellipsoidal*** (ellipticity = – 0.06 and $Q = -3b$) because of its most negative value of Q. **In general, most of the nuclei, ($I \geq 1$) have some degree of ellipticities.** For such nuclei, the difference between the semimajor and semiminor axes generally does not exceed by more than 20% and it is usually very much less than this maximum value. **On the other hand, the nuclei having even Z and even N (i.e. $I = 0$) are perfectly spherical.** Thus, from the standpoint of practical problems regarding the dimensions we can always consider the nuclei to be spherical.

5.1.6 Total Angular Momentum of the Nucleus : Magnetic Properties of the Nucleus and Nuclear Magnetic Resonance (NMR) Frequency and NMR Spectra of Some Representative Examples

• **Angular momentum vector of nucleus :** The total angular momentum of the nucleus arises from the orbital and spinning motion of the nucleons. But, very often, it is ***inappropriately*** described as the total momentum of spin and the corresponding quantum number is described as the ***nuclear spin quantum number*** (I). This nuclear spin (I) may be integral or half-integral. The method to calculate I has been discussed in Sec. 5.5.3. The total angular momentum of the nucleus is given by :

$$\vec{I} = \sqrt{I(I+1)}\,\frac{h}{2\pi} \qquad \text{...(5.1.6.1)}$$

The vector $\vec{I}$ arises through spin-orbit or jj-coupling of the nucleons. For electrons, $\vec{I}$ is replaced by $\vec{J}$. $\vec{I}$ can interact with $\vec{J}$ to generate the ***hyperfine quantum number F.*** This interaction can explain the *hyperfine splitting of spectral lines* (Sec. 1.10.16).

Due to ***space quantisation*** of the angular momentum vector $\vec{I}$, this cannot point in any arbitrary direction. This space quantisation requires a quantum number M_I. If z-axis is taken as the direction of an external magnetic field, the permitted values of the vector $\vec{I}$ along the direction of the field (i.e. z-axis) are given by the expression $M_I\left(\frac{h}{2\pi}\right)$ where the quantum number M_I can take the following values :

(i) ***For integral spin (I)*** : $M_I = I, (I-1), ..., 0, ..., -(I-1), -I$.

(ii) ***For half-integral spin (I)*** : $M_I = I, (I-1), ..., +1/2, ...-1/2, ..., -(I-1), -I$.

i.e. **M_I can vary from $+I$ to $-I$ at intervals of unity.**

Click Here t.me/thealchemylibrary

Thus there are $2I + 1$ components. These $2I + 1$ levels are degenerate, but the degeneracy is lifted in the presence of an external magnetic field and the direction of the field is taken as the reference direction.

The value of I depends on the composition of the nucleus as follows :

$I = 0$ **(for even *Z* and even *N*),** $I = \frac{1}{2}, \frac{3}{2}, \frac{5}{2}$, ... **(for odd *A*),** $I = 1, 2, 3$, ... **(for odd *Z* and odd *N*).**

• **Nuclear magnetic moment :** As in the case of electronic motion (Sec. 1.10.17), *the nuclear spin (I)* and *nuclear magnetic moment* (μ_I) are related as follows :

$$\mu_I = g_I \sqrt{I(I+1)} \left(\frac{eh}{4\pi m_p c} \right), \text{(in CGS unit)}$$

$$= g_I \sqrt{I(I+1)}\, \mu_N \qquad \ldots (5.1.6.2)$$

The parameter g_I is called the ***nuclear g-factor.*** The basic unit μ_N (called ***nuclear magneton* or *Rabi magneton,*** cf. Bohr Magneton μ_B for electron) is expressed for *hydrogen nucleus* (where $m_H \approx m_p$ = mass of a proton) as follows :

$$\mu_N = \frac{eh}{4\pi m_p c} = \frac{(4.8 \times 10^{-10} \text{ esu})\,(6.62 \times 10^{-27} \text{ erg s})}{4 \times 3.14 \times 1.67 \times 10^{-24} \text{ g} \times 3 \times 10^{10} \text{ cm s}^{-1}}$$

$$= 5.04 \times 10^{-24} \text{ erg G}^{-1}$$

$$(\text{esu} = \text{g}^{1/2}\,\text{cm}^{3/2}\,\text{s}^{-1},\ \text{G (gauss)} = \text{g}^{1/2}\,\text{cm}^{-1/2}\,\text{s}^{-1})$$

In S.I. unit :

$$\mu_N = \frac{eh}{4\pi m_p} = \frac{(1.602 \times 10^{-19} \text{ C})\,(6.62 \times 10^{-34} \text{ J s})}{4 \times 3.14 \times 1.67 \times 10^{-27} \text{ kg}}$$

$$= 5.04 \times 10^{-27} \text{ J T}^{-1}$$

$$(\text{T} = \text{kg s}^{-1}\,\text{C}^{-1} = \text{kg s}^{-2}\,\text{A}^{-1},\ \text{I T} = 10^4 \text{ G})$$

It indicates that $\mu_B / \mu_N \approx 1836$.

• ***Nuclear magnetic moment* (μ) *of nucleus and Schmidt limit* :** In the nucleus, a proton pairs with a proton and a neutron pairs with a neutron. Thus in a pair of proton, the individual magnetic moments are cancelled out. The paired *protons* and paired *neutrons* produce $I = 0$ and $\mu = 0$. These paired nucleons constitute the core of the nucleus. The single odd (i.e. unpaired) nucleons determine the resultant spin (I) and magnetic moment (μ) of the nucleus. The results are :

	Type of the nuclide	***I***	μ
(i)	Even *Z* and Even *N*	0	0
(ii)	Odd *A* (i.e. even *Z* + odd *N*, or odd *Z* + even *N*)	$\frac{1}{2}, \frac{3}{2}, \frac{5}{2}$,	$\neq 0$
(iii)	Odd *Z* + odd *N*	1, 2, 3, ...	$\neq 0$

Click Here t.me/tiwalchemylibrary

For the nuclides with odd A (i.e. only one nucleon remains unpaired), ***Schmidt limits*** are important to calculate the μ-value. These are :

For odd proton :
$$\begin{cases} \mu = (I + 2.293)\,\mu_N, \text{ where } I = j = l + s \\ \mu = \left(I - 2.293 \left[\dfrac{I}{1+I} \right] \right) \mu_N, \text{ where } I = j = l - s \end{cases}$$

For odd neutron :
$$\begin{cases} \mu = -1.913\,\mu_N, \text{ when } I = j = l + s \\ \mu = 1.913 \left[\dfrac{I}{1+I} \right] \mu_N, \text{ when } I = j = l - s \end{cases}$$

• ***NMR frequency for odd-A nucleus*** : The potential energy (E) of a nucleus in a magnetic field of strength H in z-direction is given by nuclear magnetic moment multiplied by magnetic field strength, i.e.:

$E = -H\mu_{I,z}$, $\mu_{I,z}$ denotes the z-component of the magnetic momentum vector.

$\mu_{I,z} = \mu_I \cos\theta = g_I \mu_N \sqrt{I(I+1)} \cos\theta$, μ_N = nuclear magneton

θ = angle between the magnetic momentum vector and the z-axis

Due to space quantisation, θ cannot have any arbitrary value. This condition of space quantisation for the component of angular momentum vector $(\vec{I})$ along the direction of the magnetic field leads to :

$$\sqrt{I(I+1)} \left(\frac{h}{2\pi} \right) \cos\theta = M_I \frac{h}{2\pi}, \textit{ i.e., } \sqrt{I(I+1)} \cos\theta = M_I$$

It leads to : $\mu_{I,z} = g_I \mu_N M_I$

and
$$\boxed{E = -M_I g_I H \mu_N}$$

The energy separation between the adjacent levels (where M_I differs by unity) is given by :

$$\Delta E = g_I H \mu_N \Delta M_I \text{ where } \Delta M_I = \pm 1$$

The corresponding radiation frequency is : $\nu = \dfrac{\Delta E}{h}$

For a proton $\left(M_I = +\frac{1}{2}, -\frac{1}{2} \right)$, $g_I = 5.585$, if $H = 1$ T, then the corresponding frequency is given by:

$$\nu = \frac{5.585 \times 5.04 \times 10^{-27} \text{ J T}^{-1} \times 1 \text{ T}}{6.62 \times 10^{-34} \text{ J s}}$$

$$= 4.26 \times 10^{7} \text{ Hz} = 42.6 \text{ MHz}$$

Click Here : me/thearchemylibrary

Thus a proton can be excited from lower energy level (M_I = + 1/2) to its higher energy level (M_I = – 1/2) in a magnetic field of 1 T by applying the energy in the form of electromagnetic radiation of frequency 4.26 × 10^7 Hz. **Generally, for NMR spectroscopy, the frequency lies in the radiofrequency region.**

Now let us consider the case of electron ($g = 2$, $\mu_B = 9.27 \times 10^{-24}$ J T^{-1}) in the presence of $H = 1$ T. It leads to :

$$\Delta E = g\mu_B H \Delta m_s = g\mu_B H, \ (\Delta m_s = \pm 1)$$

i.e.

$$\nu = \frac{\Delta E}{h} = \frac{2 \times 9.27 \times 10^{-24} \text{ J T}^{-1} \times 1 \text{ T}}{6.62 \times 10^{-34} \text{ J s}} = 2.8 \times 10^{10} \text{ Hz} = 28.0 \text{ GHz}$$

$\frac{\nu_{electron}}{\nu_{proton}} \approx 660$, i.e. the energy change for an electron is about 660 times larger than that for a proton.

Thus for *electron spin resonance (ESR)* spectra, it occurs at much higher frequency (in the range of microwave region). Because of this fact, the techniques for *NMR* and *ESR* spectroscopy differ widely.

NMR is observed for the *magnetic nuclei* (i.e. $I \neq 0$). However, **sensitivity** depends on many factors such as ***magnitude of nuclear magnetic moment, abundance of the magnetic nuclide* etc.** For example, the NMR signal is more easily observed for ^1H ($I = 1/2$, $g_I = 5.585$, natural abundance 99.98%) than for ^{13}C ($I = 1/2$, $g_I = 1.404$, natural abundance 1.1%). The important nuclides which are very often used in NMR spectroscopy are :

^1H, ^7Li, ^{11}B, ^{13}C, ^{14}N, ^{15}N, ^{17}O, ^{19}F, ^{23}Na, ^{27}Al, ^{29}Si, ^{31}P, ^{35}Cl, ^{59}Co, ^{117}Sn, ^{129}Xe, ^{195}Pt, ^{199}Hg, ^{203}Tl, etc.

The nuclei with $I = 1/2$ are most conveniently used. These are : ^{13}C, ^{19}F, ^{31}P, ^{29}Si, ^{117}Sn, ^{119}Sn, ^{195}Pt, etc. ***The nuclei with I > 1/2 produce the NMR spectra intrinsically weak.*** However, the elements such as ^{14}N ($I = 1$), $^{35,37}Cl$ ($I = 3/2$), ^{127}($I = 5/2$) are chemically abundant and they are very often used in NMR spectroscopy.

NMR spectra is very much important to follow the chemical environment of an NMR active centre.

- ***Intensity of NMR signal*** : The ratio of population density at two levels between which the transition occurs is given by :

$$\frac{n_2}{n_1} = \exp(-\Delta E / k_B T)$$

where n_2 = number of nuclei in the higher energy level (E_2), n_1 = number of nuclei in the lower energy level (E_1). k_B = Boltzmann constant, T = temperature in Kelvin scale, $\Delta E = E_2 \sim E_1$.

If $\Delta E \gg k_B T$, the lower energy level is more populated $\left(i.e.\ n_1 \gg n_2 \text{ or } \frac{n_2}{n_1} \ll 1\right)$; *if* $\Delta E \ll k_B T$, the population density at the upper level gradually increases, but still $n_1 > n_2$; $n_1 = n_2$ under the condition $\Delta E/k_B T = 0$ i.e. $T = \infty$, **this is an impossible condition.**

The *upward transition* (i.e. E_1-level to E_2-level) needs the absorption of radiation. At the same time, the excited nuclei come back to the lower level i.e. *downward transition* (E_2-level to E_1-level).

Click Here t.me/thealchemylibrary

Statistically, the rate of transition depends on the population density of the level from which the transition occurs. Generally, $n_1 \gg n_2$ i.e. *upward transitions are more than the downward transitions*. It makes a net absorption of the radiation. ***The intensity depends on the magnitude of net absorption.*** Thus, the intensity is high for the condition $n_1 >>> n_2$. In the case of *NMR* study, very often, the population density difference between the levels is small (i.e. n_1 is not too large compared to n_2). In such cases, the intensity of absorption is small. To increase the intensity, we should make $n_1 >>> n_2$ by ***lowering the temperature*** (i.e. k_BT becomes smaller) and ***by applying high magnetic field*** which makes ΔE larger. Thus under the high magnetic field at low temperature, $\Delta E/k_BT$ becomes high and $\frac{n_2}{n_1}\left[=\exp\left(-\Delta E/k_BT\right)\right]$ becomes very small. It increases the upward transition more to enhance the intensity of absorption.

• ***Illustrative examples of NMR spectra*** : It has been already mentioned that due to space quantisation of nuclear spin $(\vec{I})$, in presence of an external magnetic field, it produces different energy levels. In other words, the nucleus can have $2I + 1$ orientations where I gives the nuclear spin quantum number. It produces $2I + 1$ energy levels. The energy of an allowable state or level is given by :

$$E = -\mu_N g_N M_I H$$

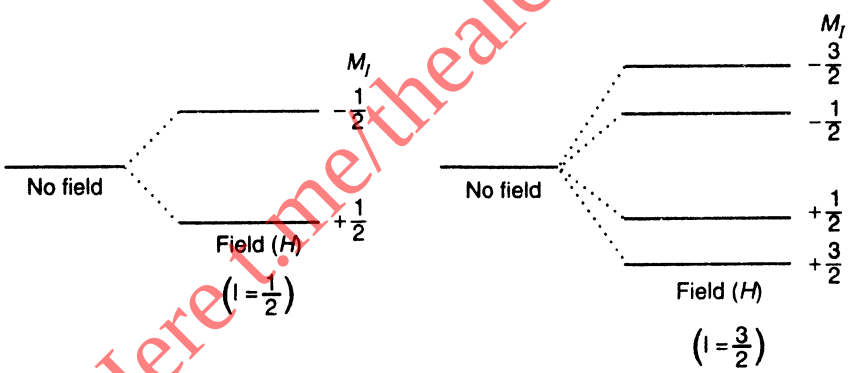

Fig. 5.1.6.1. The allowed energy levels in presence of a fixed magnetic field (H) for the nuclei $I = \frac{1}{2}$ and $= \frac{3}{2}$.

The selection rule for transition is $|\Delta M_I| = 1$. It leads to :

$$\Delta E = \mu_N g_N H \text{ and } \nu = \frac{\Delta E}{h} = \frac{\mu_N g_N H}{h} \quad (cf.\ \text{Fig. } 5.1.6.2)$$

In NMR spectroscopy, at a particular radiofrequency, the resonance absorption occurs for a fixed magnetic field strength (H). The energy of resonance depends on the *electronic environment* (i.e. chemical environment) around the NMR active nucleus. *The electrons shield the nucleus to face the magnetic field.* If the applied field is H_o, the nucleus experience H_N which is less than H_o,

$$H_N = H_o\,(1 - \sigma)$$

where σ (a dimensionless constant) is called the ***shielding constant*** which denotes the extent of shielding

Click Here t.me/thealchemylibrary

of the nucleus by the electrons. Thus σ *represents the chemical environment around the nucleus of study.* ***Generally, NMR spectra are recorded by using a constant oscillator frequency (usually 60 MHz) and varying the external magnetic field.*** For higher shielding constant, $H_{observed}$ (= H_N) is less than $H_{applied}$ (= H_o) and the resonance will occur at higher magnetic field.

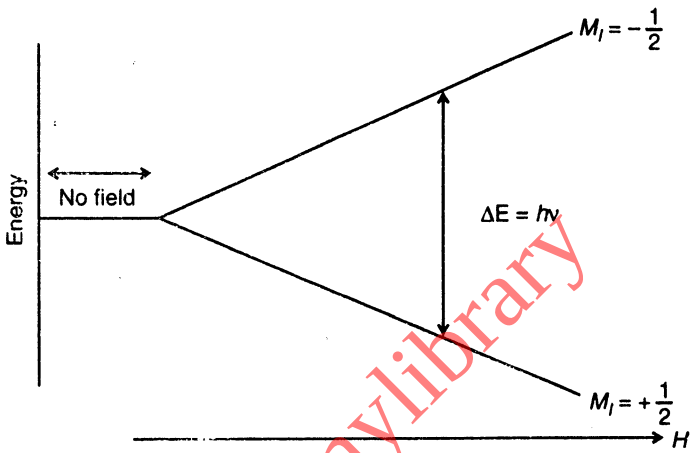

Fig. 5.1.6.2. Variation of ΔE (energy difference between the two energy levels) for a proton with the magnetic field strength (H).

• **CH_3–CH_2–OH:** Let us consider the NMR spectrum of H-nuclei of **ethanol (CH_3–CH_2–OH)** (Figs. 5.1.6.3-4). Here, the proton of *–OH* group is *least shielded* as it is attached to the highly electronegative *O*-atom (i.e. σ is minimum). ***This is why, for this proton the resonance absorption occurs at the lowest field.*** On the other hand, the protons of CH_3 group are most shielded and their signal arises at the highest field.

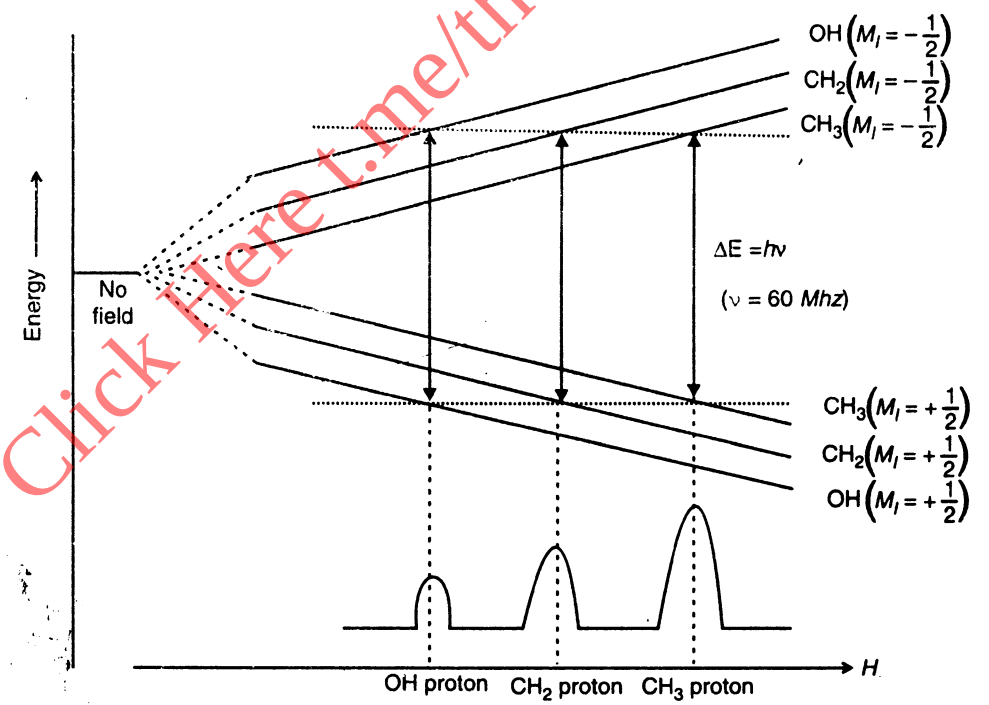

Fig. 5.1.6.3. Schematic representation of variation of potential energy levels of *OH*, CH_2 and CH_3 group protons of CH_3CH_2OH in the presence of a magnetic field (H). (Low resolution NMR spectrum of CH_3CH_2OH)

Click Here t.me/thealchemylibrary

$$\sigma_{CH_3} > \sigma_{CH_2} > \sigma_{OH}, H_o(1-\sigma_{CH_3}) < H_o(1-\sigma_{CH_2}) < H_o(1-\sigma_{OH})$$

$$i.e.(H_N)_{CH_3} < (H_N)_{CH_2} < (H_N)_{OH}$$

and $H_{appl} : CH_3 > CH_2 > OH$ for a particular ν

The intensities of the three peaks (measured by the area) are in the ratio 1 : 2 : 3 corresponding to the groups OH, CH_2 and CH_3 in which the number of protons are also in the same ratio.

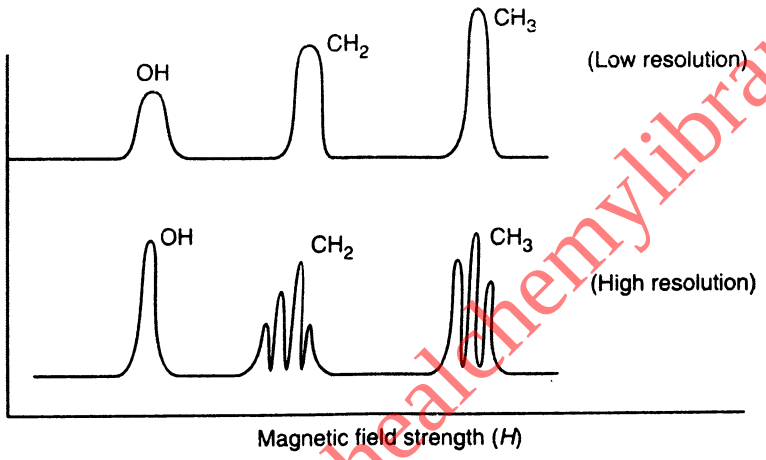

Fig. 5.1.6.4. NMR spectrum of CH_3CH_2OH.

The ***high resolution*** **of the NMR peaks** of ethanol indicates that the **peak due to OH group is a single line, the peak due to CH_2 group consists of four closely packed absorption lines, and the peak due to the CH_3 group is constituted by three lines.** This fine structure can be explained by considering the interaction between the neighbouring nuclei. This interaction called *spin-spin coupling* is measured by the *spin-spin coupling constant* J (in Hertz). It rapidly decreases with the distance through the chemical bond. The protons of CH_2 group are responsible for splitting the peak due to CH_3 group. The two protons of CH_2 groups can have the following three combinations giving three possible values of M_I :

$$\left(+\frac{1}{2},+\frac{1}{2}\right) \quad I_{total} = +1$$

(Parallel spin)
(1 spin state)

$$\left.\begin{matrix}\left(+\frac{1}{2},-\frac{1}{2}\right)\\ \left(-\frac{1}{2},+\frac{1}{2}\right)\end{matrix}\right\} I_{total} = 0$$

(Antiparallel spin)
(2 spin states)

$$\left(-\frac{1}{2},-\frac{1}{2}\right) \quad I_{total} = -1$$

(Parallel spins)
(1 spin states)

Due to spin-spin coupling, the protons of CH_3 group will experience different fields arising from the 3 different values of M_I of the CH_2 group protons. The CH_3 group protons will interact with the three possible states of the adjacent CH_2 group. ***Consequently, the peak will be a triplet one with the intensities 1:2:1 of the fine structure components.*** Similarly, the three protons of the CH_3 group can have four $\left(=2\times3\times\frac{1}{2}+1\right)$ possible combinations of spin to give 4 possible values of M_I. These are :

Click Here to the chemylibrary

(i) **1 spin state :** $+\frac{1}{2}, +\frac{1}{2}, +\frac{1}{2}$; i.e. $I_{total} = +\frac{3}{2}$

(ii) **3 spin states :** $+\frac{1}{2}, +\frac{1}{2}, -\frac{1}{2}; +\frac{1}{2}, -\frac{1}{2}, +\frac{1}{2}; -\frac{1}{2}, +\frac{1}{2}, +\frac{1}{2}$; i.e. $I_{total} = +\frac{1}{2}$

(iii) **3 spin states :** $+\frac{1}{2}, -\frac{1}{2}, -\frac{1}{2}; -\frac{1}{2}, +\frac{1}{2}, -\frac{1}{2}; -\frac{1}{2}, -\frac{1}{2}, +\frac{1}{2}$; i.e. $I_{total} = -\frac{1}{2}$

(iv) **1 spin state :** $-\frac{1}{2}, -\frac{1}{2}, -\frac{1}{2}$; i.e. $I_{total} = -\frac{3}{2}$

Consequently, the peak due to CH_2 group protons will be split into 4 components with intensities 1:3:3:1. The result is : ***a signal due to a nucleus of spin 1/2 will produce 2I + 1 lines when the nucleus interacts with a nucleus of spin I. If there are such n nuclei with spin I, to split a peak, then the number of lines is 2nI + 1.***

On the basis of above argument, the protons of CH_2 group should also split the signal due to the hydroxyl proton into three lines. However, experimentally it shows only a single line for the **OH** group. It is due to the fact that presence of a trace amount of protonic acid catalyses the ***proton exchange process*** among the *OH* groups of different C_2H_5OH molecules. This proton exchange process is very fast. ***The life time of a proton in OH group in a particular conformation is too short to experience spin-spin interaction with the CH_2 group protons.*** In an ultrapure sample having no trace of protonic acid to catalyse the said proton exchange process, the peak due to the *OH* group is really split into three lines as expected. The splitting by *OH* group leads to *8 lines from 4 lines* for the CH_2 group.

• ***ClF_3:*** In ***ClF_3*** (which is T-shaped, i.e. one equatorial fluorine and two axial fluorine), the signal due to the axial fluorine (^{19}F, I = 1/2) is split into a doublet by the single equatorial fluorine. On the other hand, the peak due to the equatorial fluorine is split into triplet by the two axial *F*-atoms. *Cl* ($I = 0$) does not split the ^{19}F signals. Thus the NMR spectrum of ClF_3 is in conformity with the structure predicted by VSEPR.

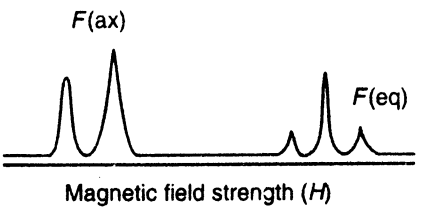

Fig. 5.1.6.5. NMR (^{19}F) spectrum of ClF_3.

Note : NMR spectra of different ***fluxional molecules*** like PCl_2F_3 have been discussed in Chapter 10.

• ***Concept of chemical shift*** : It is required to measure the field strength at which the resonance absorption occurs with respect to some reference. Let us consider that H_s and H_r are the applied fields for the protons of the sample and reference to undergo resonance. Then we can write :

$$H_N = H_s(1 - \sigma_s) \text{ and } H_N = H_r(1 - \sigma_r)$$

where H_N = the field experienced by the nucleus and it is constant for any proton. It leads to :

$$\frac{H_s}{H_r} = \frac{1-\sigma_r}{1-\sigma_s}; \text{ or } \frac{\sigma_s - \sigma_r}{1-\sigma_s} = \frac{H_s - H_r}{H_r}$$

The **shielding constant** σ_s is exceedingly small compared to 1. It leads to :

$$\delta \textbf{ (chemical shift)} = \sigma_s - \sigma_r = \frac{H_s - H_r}{H_r}$$

Click Here to meet chemistry library

Thus the **chemical shift** (δ) is the difference of the shielding constants of the sample and reference. To quantify this dimensionless parameter, it is often expressed in parts per million (ppm) as :

$$\delta = \frac{H_s - H_r}{H_r} \times 10^6 = \frac{(\nu_s - \nu_r) \times 10^6}{\nu_r}$$

For the *PMR (proton magnetic resonance)* spectrum of *H*-nuclei, ***tetramethylsilane*** (TMS, Me_4Si) is used as the reference. All the protons of TMS are equivalent and shielding constant is very high. They give a single intense peak at a very high field strength (for 60 MHz radiation, $H = 1.4092$ T). The δ-value for the reference compound (TMS) is generally set equal to zero and it increases downfield. ***The larger value of δ indicates a lower field resonance i.e. lower shielding constant (σ).***

$$\delta\text{-}scale\ (PMR): RCOOH^{*}(10\text{-}13) > ROH^{*}(2\text{-}5) > RNH_2^{*}(1\text{-}3) > RCH_3^{*}(0.6\text{-}1.2)$$

$$\sigma: \longrightarrow \text{increasing} \longrightarrow$$

In terms of **τ-scale (τ = 10 – δ)** where the TMS signal is assigned to a value of 10 (instead of zero), a lower value of τ indicates that the nucleus is shielded less.

TMS : δ-scale (0), τ-scale (10)

5.1.7 Classification of the Nuclides

(a) Classification on the Basis of Number of Nucleons

Depending on the number of neutrons (*N*) and protons (*Z*) present in the nuclei, they can be classified as follows.

(i) ***Isotopes*** : The nuclei which for a certain element only differ in the number of neutrons keeping the number of protons same are termed as isotopes of the element. In the isotopes, consequently, the mass number *A* (= *Z* + *N*) differs.

Examples : Isotopes of hydrogen (*Z* = 1) : ${}^{1}_{1}H_0, {}^{2}_{1}H_1, {}^{3}_{1}H_2$; Isotopes of chlorine (*Z* = 17): ${}^{35}_{17}Cl_{18}, {}^{36}_{17}Cl_{19}, {}^{36}_{17}Cl_{20}$; Isotopes of uranium (*Z* = 92) : ${}^{233}_{92}U_{141}, {}^{235}_{92}U_{143}, {}^{238}_{92}U_{146}$.

The isotopes are chemically indistinguishable because of their same atomic number, but their radioactive properties and other physical properties which depend on atomic mass are different.

(ii) ***Isobars*** : The nuclei of different neighbouring elements which differ in both *Z* and *N* but have the same mass number (*A*) are called isobars.

Examples : Isobars for *A* = 3 : ${}^{3}_{1}H_2, {}^{3}_{2}He_1$. Isobars for *A* = 14 : ${}^{14}_{6}C_8, {}^{14}_{7}N_7$. Isobars for *A* = 40 : ${}^{40}_{18}Ar_{22}, {}^{40}_{19}K_{21}, {}^{40}_{20}Ca_{20}$. The successive β-decay products are ***isobaric nuclides.*** The product and parent nuclides are also isobaric for β^+-decay and electron capture process. The isobars are chemically and physically different. The **mirror nuclei** are the pairs of isobars for which the proton and neutron numbers differing by unity are interchanged (having the relation $N - Z = 1$). We have already discussed (see Sec. 5.1.3) the importance of mirror nuclei in determining the radius of nuclei.

Examples of mirror nuclei : ${}^{3}_{1}H_2$ and ${}^{3}_{2}He_1$; ${}^{13}_{6}C_7$ and ${}^{13}_{7}N_6$; ${}^{15}_{7}N_8$ and ${}^{15}_{8}O_7$; ${}^{31}_{15}P_{16}$ and ${}^{31}_{16}S_{15}$.

(iii) ***Isotones*** : The nuclei of different elements which have the same number of neutrons and different number of protons are called isotones.

Examples : ${}^{3}_{1}H_2, {}^{4}_{2}He_2$; ${}^{14}_{6}C_8, {}^{15}_{7}N_8, {}^{16}_{8}O_8$.

Click Here t.me/thealchemylibrary

(iv) ***Nuclear Isomers*** (see. Sec. 6.14 and 6.16.2d) : The nuclei of a particular element having the same number of protons and neutrons but differing in energy states and consequently in radioactive properties are called *nuclear isomers or isobaric isotopes*. The quantum numbers which define the nuclear energy states are different in the isomers. It indicates that the isomers differ only in the mode of arrangement of the nucleons within the nuclei. The isomer having higher energy is called the ***metastable isomer*** and such isomers are represented by writing *m* after the mass number. The metastable isomer is generally radioactive with respect to γ–emission. Through γ–emission the metastable one comes to the ground state isomer which may also show a radioactive emanation. Such a γ–emission is very often referred to as ***isomeric transition (IT).***

In some cases, the parent isomer, i.e. the metastable isomer, is so short lived that no isomeric transition is observed, and in such cases no nuclear isomerism occurs. **For the observable isomeric transitions, half life period ($t_{1/2}$) of the metastable one should be at least greater than 10^{-7}s.** If $t_{1/2} < 10^{-7}$s, the transitions are virtually instantaneous. According to Weizsacker, the relative stability of the metastable isomer depends on the difference of spin states (i.e. ΔI) between the metastable and ground state. According to him, **to have the measurable isomeric transitions, it must satisfy the condition, $\Delta I \geq \pm 3$.** In such cases the transition is partially *forbidden* and as a result, the excited state has got an independent existence giving rise to a measurable isomeric transition. It has been observed that the increases of $|\Delta I|$ by one unit increases the half life period of the metastable state by a factor of the order of 10^6.

Examples of isomeric transition :

(i) $^{60m}_{2(+)}Co \xrightarrow[\Delta I = +3]{IT(\gamma),\ t_{1/2} = 10.4\ \text{min}} {}^{60}_{5(+)}Co \xrightarrow{\beta^-} {}^{60}Ni^* \xrightarrow{\gamma} {}^{60}Ni$

(ii) $^{80m}_{5(-)}Br \xrightarrow[\Delta I = +6]{IT(\gamma),\ t_{1/2} = 4.4\ \text{h}} {}^{80}_{1(+)}Br \xrightarrow{\beta^-} {}^{80}Kr^* \xrightarrow{\gamma} {}^{80}Kr$

(iii) $^{69m}_{9/2(+)}Zn \xrightarrow[\Delta I = -5]{IT(\gamma),\ t_{1/2} = 14\ \text{h}} {}^{69}_{1/2(-)}Zn$

^{69m}Zn and ^{80m}Br are synthesised in the following reactions, ^{68}Zn (d, p) ^{69m}Zn and ^{81m}Br $(n, 2n)$ ^{80m}Br respectively. Characteristics of isomeric transitions in ^{60m}Co and ^{80m}Br are discussed in Secs. 6.14 and 6.16.2d respectively.

(b) Classification on the Basis of Nuclear Stability

The nuclides can be classified based on their stability as *stable* and *unstable* nuclides. The stable nuclides are supposed to be permanent.* The corresponding nuclei will remain unchanged in all physico–chemical processes but they may change only in nuclear transmutation reactions carried out by the bombardment of external radiations or particles of high energy or by neutron capture. ^1_1H, ^2_1H, $^{16}_8O$, $^{18}_8O$, $^{19}_9F$, $^{23}_{11}Na$, $^{27}_{13}Al$, $^{31}_{15}P$, $^{35}_{17}Cl$, $^{37}_{17}Cl$, etc. are some representative examples of ***about 274 naturally occurring stable nuclei.*** Here the stability of ^1_1H can be critically commented. The Nobel Laureate scientist, A. Sakharov predicted the decay of protons. Recently (in 1981), a group of scientist of India and Japan reported (though not decisively) an imperceptibly slow decaying rate (one

* **Permanent nuclides** are supposed to remain unchanged about 10^{21} years. But in advanced technology, further slow decaying rates are reported.

Click Here t.me/thealchemylibrary

proton out of ~ 10^{30} per month) of protons in the depths of the Kolar gold mines to avoid the effect of cosmic rays and external radiations. If this result gets confirmed, even the materialistic universe will lose its eternality and it will decay away in its own course.

The unstable nuclides are very often radioactive and they pass through the disintegration process in such a way that they can attain the stable state. In this process, the ratio of neutron to proton and the configuration of the nucleons change. In discussing the radioactivity, these types of radioactive nuclides will be mentioned.

5.1.8 Nuclear Spin Isomerism in Diatomic Molecules : *Ortho-* and *Para-*Hydrogen : Intensity of the Rotational Lines in the Band Spectra of Diatomic Molecules

Nonzero value of nuclear spin (I) is the cause of existence of nuclear spin isomerism in diatomic molecules. **In such cases, the nuclear spins of the constituent atoms may be either parallel or antiparallel.** Parallel orientation of the nuclear spins gives the *ortho*-spin isomer (called *ortho*-form) while the antiparallel orientation of the spins gives the *para*-spin isomer (called *para*-form). Both the forms remain in a temperature dependent equilibrium. Nuclear spin isomerism has been established for H_2, D_2, T_2, $^{14}N_2$, $^{15}N_2$, $^{17}O_2$, $^{19}F_2$, HF etc. It is obvious that for the zero value of I of the constituent atoms, the case of nuclear spin isomerism does not arise.

Nuclear spin isomerism leading to *ortho-* and *para*-states arises for the diatomic molecules constituted by two identical nuclei with nonzero spin. In *ortho*-states, the nuclei have parallel spins while in *para*-states, the nuclear spins are antiparallel. The *ortho-* and *para*-states arise for the following cases where nuclear spins of the constituting atoms are given within the parentheses.

$^1H_2\left(\frac{1}{2}\right)$, $^2D_2(1)$, $^{14}N_2(1)$, $^{19}F_2\left(\frac{1}{2}\right)$, $^{35}Cl_2\left(\frac{5}{2}\right)$, *etc.* But $^{16}O^{18}O$, $^1H^{19}F$, etc. will not produce the condition for the existence of *ortho-* and *para*-states, i.e. ***ortho- and para-states cannot exist for the molecules having nonidentical nuclei.***

For hydrogen nucleus (^1H), the nuclear spin (I) is $\frac{1}{2}$. In *ortho*-H_2 (Fig. 5.1.8.1), the nuclear spins are parallel giving rise to the resultant nuclear spin 1 which is **three-fold degenerate** (= 2 × 1 + 1) i.e. a **triplet state**. In the *para*-H_2 (Fig. 5.1.8.1), the nuclear spins are antiparallel giving rise to the resultant nuclear spin 0 which is nondegenerate i.e. **singlet state** (= 2 × 0 + 1).

***Ortho*-H_2 (triplet) and *para*-H_2 (singlet) :** Because of the **forbidden triplet-singlet transition,** their mutual interconversion is a very slow process. Their mutual interconversion needs some suitable catalysts like *Pt*, *Pd*, Fe_2O_3, *NO*, NO_2, $Mn(aq)^{2+}$, $Fe(aq)^{2+}$, etc. The solid catalyst surface catalyses the process through the breaking of *H–H* bond followed by recombination of the dissociated atoms. The paramagnetic substances catalyse the process through magnetic perturbations.

For the triplet *ortho*-H_2, the resultant nuclear spin

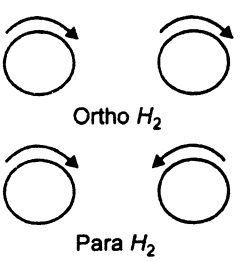

Fig. 5.1.8.1. Orientations of nuclear spins of the constituent atoms of H_2 giving rise to *ortho*-H_2 and *para*-H_2.

Click Here t.me/thealchemylibrary

may combine vectorially with the total angular momentum of the molecule in three possible ways while for the singlet *para*-H_2, it can occur only in one way. Thus statistically, the ratio of the molecules of *ortho*-H_2 (triplet state) : *para*-H_2 (singlet) should be 3:1 i.e. 75% *ortho*-H_2 and 25% *para*-H_2. **The singlet *para*-H_2 is of lower energy and at low temperature, *para*-H_2 is the predominant form.** With the increase of temperature, the equilibrium concentration of *ortho*-H_2 increases. At temperature close to 0 K, there is about 100% *para*-H_2 (i.e. *pure para*-H_2) and with the increase of temperature, % of *ortho*-H_2 increases and at the limiting condition, it gives the mixture containing 75% *ortho*-H_2 and 25% *para*-H_2. **Thus it is not possible to have a sample containing more than 75% *ortho*-H_2.**

Now let us consider D_2 and T_2. Nuclear spin : ^2D, $I = 1$; for ^3T, $I = \frac{1}{2}$. Thus ^1H and ^1T are **fermions** while ^2D is a **boson.** For D_2, the possible resultant nuclear spins are 2, 1, 0 and their statistical proportions (determined by spin multiplicities) are : 5:3:1. For deuterium system, **Bose-Einstein statistics** rather than **Fermi-Dirac statistics** (which is applicable for hydrogen and tritium system) is applicable. **Thus *ortho*-D_2 is the stable form at low temperature while *para*-H_2 and *para*-T_2 are the stable forms at low temperature.** For D_2, at temperature about 0 K, the *ortho*-form is about 100% (cf. for H_2 and T_2, the *para*-form is about 100% at ~ 0 K) and with the increase of temperature, the proportion of *para*-form gradually increases. At the limiting condition, a mixture of 6 *ortho*-D_2 : 3 *para*-D_2 is obtained. This ratio is predicted from their statistical weights determined by spin-multiplicities. Thus we cannot have a mixture containing more than 33.3% *para*-D_2. The distribution of *ortho*- and *para*-forms of T_2 is similar to that of hydrogen. These are shown and compared in Fig. 5.1.8.2.

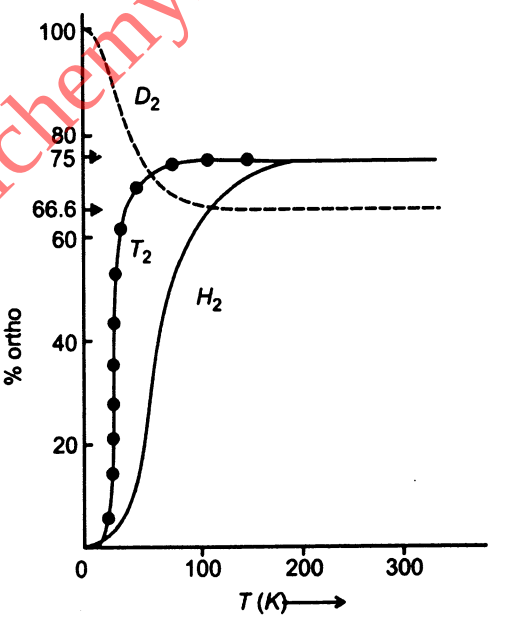

Fig. 5.1.8.2. Variation of the ratio, *ortho*- : *para*-forms for H_2, D_2 and T_2.

Nuclear spin isomers do not differ in chemical properties but their physical properties are affected. The physical properties of *ortho*-H_2 and *para*-H_2 are compared below.

	Ortho-H_2	*para*-H_2
B.P. (K)	20.45	20.29
M.P. (K)	14.05	13.80
Rotational specific heat (J mol^{-1} K^{-1})		
100 K	0.305	6.276
298 K	7.690	9.146
Thermal conductivity (Ratio)	1	1.5

Click Here t me/thealchemylibrary

It can be shown that **rotational energy levels** of the *ortho*-H_2 are different from those of *para*-H_2. It gives a difference in their electronic band spectra in terms of their hyperfine structure.

Nuclear spin and intensities of the rotational lines in band spectra : The electronic energy level of a molecule is subdivided into a number of vibrational energy levels which are further divided into rotational energy levels. These rotational energy levels are responsible for the **fine lines** in the band spectra of the molecules. **Multiplicity of a rotational energy level** is determined by the nuclear spins of the constituent nuclei and intensities of the rotational lines are determined by the multiplicity of the rotational energy levels. For a diatomic molecule constituted by the nuclei of different spins I_1 and I_2, **multiplicity of each rotational energy level is given by :**

$$(2I_1 + 1)\,(2I_2 + 1)$$

In such cases (e.g. $^{16}O^{18}O$), all the rotational lines are of equal intensity. If a diatomic molecule is constituted by two identical nuclei (e.g. $^1H_2$, $^2D_2$, $^{19}F_2$ etc.) of the same nuclear spin I, then the **multiplicities of the alternate rotational energy levels** are given by : $(I + 1)\,(2I + 1)$ and $I(2I + 1)$ respectively. In such cases **intensities of the alternate rotational lines will have the ratio :**

$$(I + 1) : I$$

For $^1H_2$, this ratio is found to be 3:1 which supports I for $^1H = \frac{1}{2}$. For $^2D_2$, the ratio is 2:1 which suggests I for $^2D = 1$.

For a diatomic molecule like $^{16}O_2$ ($I = 0$) where the nuclear spin is zero, alternate rotational energy levels will have the zero multiplicity. It will cause the ***missing of alternate rotational lines.***

For normal H_2, the more intense rotational lines correspond to odd rotational levels while the less intense lines correspond to the even rotational levels. The odd (i.e. odd J-value, rotational quantum number) and even (i.e. even J-value) levels are characterised by the *ortho*-H_2 and *para*-H_2 respectively. Thus the intensity ratio indicates the abundance ratio (3:1) of the *ortho*- and *para*-forms of H_2.

5.2 THE ISOTOPES

5.2.1 Discovery and Characterisation of Nonradioactive Isotopes

The discovery and characterisation of the isotopes of the lighter elements have already been discussed in connection with the mass spectrographs (cf. Sec. 1.2.4). By analysing the optical spectra, the **isotopic shift** helped the scientists to identify the isotopes of the lighter elements (e.g. hydrogen, carbon, nitrogen, oxygen, chlorine, etc.). This aspect will be discussed separately.

5.2.2 Isotopic Shift in Optical Spectra

The isotopic shift depends on the relative mass difference among the isotopes. This mass difference is well manifested only for the lighter elements. This is why, the isotopic shift is only measurable for the lighter elements. Here both the line spectra (i.e. atomic spectra) and band spectra (i.e. molecular spectra) will be discussed briefly.

Line Spectra

Let us consider the hydrogen–like systems where the corrected Rydberg constant (by considering the

Click Here : me/thealchemylibrary

nuclear motion) depends on the reduced mass of the system (cf. Sec. 1.8.3). The reduced mass (μ) is given by, $\mu = \dfrac{mM}{m+M}$ where m and M denote the masses of the electron and the nucleus respectively. Thus if two isotopes of mass M_1 and M_2 are taken for consideration, then the corresponding corrected Rydberg constants $R_{1(corr)}$ and $R_{2(corr)}$ will be related as follows,

$$\frac{R_{1(corr)}}{R_{2(corr)}} = \frac{M_1}{M_2} \times \frac{m+M_2}{m+M_1}$$

It is evident that if the ratio M_1/M_2 runs almost to unity then the relative difference in $R_{1(corr)}$ and $R_{2(corr)}$ becomes vanishingly small and consequently, the isotopic shift governed by the difference of Rydberg constants becomes undetectable. The most favourable situation arises for the isotopes ${}^{1}_{1}H$ and ${}^{2}_{1}H$. In fact, in analysing the Balmer series of hydrogen spectra, the existence of a weak (due to poor abundance) line due to deuterium indicated spectroscopically the existence of the isotope.

Band Spectra

(i) ***Microwave or Rotational Spectra*** : Here, the wave number separation ($\Delta\bar{\nu}$) between the successive lines for a particular diatomic molecule is given by :

$$\Delta\bar{\nu} = 2B/c = 2h/(8\pi^2 Ic),$$

where I = moment of inertia = μr^2, (μ = reduced mass, r = internuclear distance) and c = velocity of light. Therefore, $\Delta\bar{\nu} \propto 1/I$. Let us take, $H^{35}Cl$ and $H^{37}Cl$ molecules having moment of inertia I_1 and I_2 respectively. If the corresponding wave number separations are $\Delta\bar{\nu}_1$ and $\Delta\bar{\nu}_2$, then we get:

$$\Delta\bar{\nu}_1/\Delta\bar{\nu}_2 = I_2/I_1 = \mu_2/\mu_1 \text{ (assuming the same internuclear distance);}$$

or, $(\Delta\bar{\nu}_1/\Delta\bar{\nu}_2) - 1 = (\mu_2/\mu_1) - 1$; or, $\dfrac{\Delta\bar{\nu}_1 - \Delta\bar{\nu}_2}{\Delta\bar{\nu}_2} = \dfrac{\mu_2 - \mu_1}{\mu_1}$;

$(\Delta\bar{\nu}_1 - \Delta\bar{\nu}_2)$ is called the ***isotopic shift of wave number*** and it depends on the ratio μ_2/μ_1. In *HCl*, it has been found to be ~ 0.03 cm^{-1}.

(ii) ***Vibrational Spectra*** : In diatomic molecules, the ***equilibrium vibrational frequency*** ω is given by, $\omega \propto \sqrt{f/\mu}$, f = *force constant* and μ = reduced mass. In isotopic molecules, f and internuclear distance are supposed to be the same. Hence, for two isotopic molecules designated by subscripts 1 and 2, we have :

$$\frac{\omega_1 - \omega_2}{\omega_1} = \frac{(1/\mu_1)^{1/2} - (1/\mu_2)^{1/2}}{(1/\mu_1)^{1/2}} = 1 - (\mu_1/\mu_2)^{1/2}.$$

In terms of **frequency (ν) of transition** (assuming change of vibrational level, $\Delta v = 1$), we have:

$$\frac{\omega_1 - \omega_2}{\omega_1} = \frac{\nu_1 - \nu_2}{\nu_1} = 1 - \sqrt{\mu_1/\mu_2}$$

Actually in this range, we observe *rotational–vibrational spectra* (i.e. *ir*-spectra), and the centre of the band corresponds to ν. Thus $(\nu_1 - \nu_2)$ gives the separation of the centres of the corresponding

Click Here to me/heatchemylibrary

bands, and $(\nu_1 - \nu_2)$ is called the ***isotopic shift of frequency.*** It can also be expressed in terms of $\Delta\lambda$. In $H^{35}Cl$ and $H^{37}Cl$, $\Delta\lambda$ has been found to be ≈ 25 Å.

Let us consider the **IR-shift** in *A–H* and *A–D* (*D* stands for deuterium, an isotope of *H*). The vibrational frequencies are related as :

$$\frac{\nu_D}{\nu_H} = \sqrt{\frac{\mu_H}{\mu_D}} \approx \sqrt{\frac{m_H}{m_D}}$$

In fact, the reduced mass of the system is given by :

$$\frac{1}{\mu_H} = \frac{1}{m_A} + \frac{1}{m_H} \approx \frac{1}{m_H}, \quad \frac{1}{\mu_D} = \frac{1}{m_A} + \frac{1}{m_D} \approx \frac{1}{m_D}$$

The above condition is valid for $m_A >> m_H$ or m_D where m stands for atomic mass.

In $R_2As–H$, the *IR-band* for the *As–H* bond arises at 2080 cm^{-1}. For the corresponding *As–D* bond, the calculated stretching frequency is $2080\sqrt{\frac{1}{2}} \approx 1470$ cm^{-1}, and in fact the experimental value is 1475 cm^{-1}. **The *isotopic shift is prominant, if their reduced masses differ significantly.* In fact, for the *A–H* and *A–D* bonds, it is the most suitable case.**

Note **:** For a simple *harmonic oscillator* like a diatomic molecule, the energy of the *n*-th vibrational level is given by :

$$E_n = \left(n + \frac{1}{2}\right) h\omega, \; n = 0, 1, 2, \ldots. \text{ (called vibrational quantum number).}$$

$$\omega \text{ (oscillator frequency)} = \frac{1}{2\pi}\sqrt{\frac{f}{\mu}}$$

For $n = 0$, $\boldsymbol{E_0}$ **(*zero-point energy*)** $= \frac{1}{2} h\omega = \frac{1}{2} h \times \frac{1}{2\pi}\sqrt{\frac{f}{\mu}}$

For the transition, $n \longrightarrow n + 1$ (i.e. $\Delta n = 1$), we get :

$$\Delta E = E_{n+1} - E_n = \left(n + \frac{3}{2}\right) h\omega - \left(n + \frac{1}{2}\right) h\omega = h\omega$$

The corresponding *frequency of transition* is given by :

$$\nu = \frac{\Delta E}{h} = \frac{h\omega}{h} = \omega = \frac{1}{2\pi}\sqrt{\frac{f}{\mu}}; \quad \bar{\nu} = \frac{1}{\lambda} = \frac{1}{2\pi c}\sqrt{\frac{f}{\mu}}$$

Very often, $\boldsymbol{E_0}$ **(zero-point energy)** is denoted by $\frac{1}{2} h\nu_0$ (i.e. ω is replaced by ν). It leads to :

$$E = \left(n + \frac{1}{2}\right) h\nu_0$$

Click Here t.me/tiwaichemylibrary

Table 5.2.2.1. Vibrational wave numbers ($\bar{\nu}$) of some bonds illustrating the effect of *f* (force constant) and μ (reduced or effective mass)

Molecule	($\bar{\nu}$) (cm^{-1})	Bond/Group		($\bar{\nu}$) (cm^{-1})
		C – C		~ 1000
HCl	2885	C – N		~ 1000
Cl_2	557	C = N		~ 1500
Br_2	321	C ≡ N		~ 2000
CO	2143	O – H		~ 3600
NO	1876	CO (terminal)	metal carbonyls	~ 2000
		CO (bridging)		~ 1775
		O – O (peroxo)		~ 800
		O – O (superoxo)		~ 1150

(iii) ***Electronic spectra*** **:** Similar isotopic shifts also occur in the electronic spectra of a molecule, but the calculation is complicated. As a matter of fact, the isotopes of oxygen were discovered from the electronic spectra of oxygen. Intensity of the spectral lines depends on the abundance of the isotopic species.

5.2.3 Characteristic Features of the Isotopes

(i) ***Chemically indistinguishable*** **:** As the atomic number which is the fundamental property is identical, their chemical properties are also identical. Only physical properties such as rate of diffusion, density, etc. which depend on the atomic mass are different but this difference is not very much prominent for the heavy elements where the isotopic mass does not differ significantly. This is why, all the isotopes having the same atomic numbers are rightly placed at the same position in the Periodic Table. The Greek word isotopes mean the same place (*iso* = same, *topos* = place).

(ii) ***Isotopic effect and zero–point energy*** **:** The properties which are dependent on atomic mass are different for the isotopes. Because of this fact, the rate of reaction is different for the different isotopes and the thermodynamic parameters (e.g. equilibrium constants of exchange processes) differ for the different isotopes. The lighter species reacts faster and the process involving the heavier ones is less complete. These phenomena are very often referred to as ***isotopic effects.*** Again, the isotopic effect is well noticeable for the lighter elements only. By taking the advantage of the isotopic effect, the isotopes are separated in some processes.

The fundamental cause of this isotopic effect is due to the difference of zero–point energy among the different isotopic species. The zero–point energy is dependent on atomic mass.

(iii) ***Isotopic effect on bond energy*** **:** This aspect has been discussed in Sec. 10.12.

(iv) ***Kinetic isotope effect*** **:** It has been illustrated in Sec. 10.1.2 that the ***bonds involving the heavier isotopes are relatively stronger.*** **It is due to the higher zero-point energy of the species having heavier isotopes.** This effect is highly pronounced by the lighter elements like hydrogen. For the relatively heavier elements, this effect is less pronounced. The properties like bond energy, Lewis acidity, etc. are more or less the same for $^{10}BF_3$ and $^{11}BF_3$. But such properties are widely different for the species *A–H* and *A–D* where the isotopes are *H* and *D* ($m_D/m_H \approx 2$).

Click Here t.me/thealchemylibrary

If in a reaction, the rate determining step involves the rupture of *A–H* or *A–D* bond, then the rate will be significantly slower for the *A–D* bond whose bond energy is relatively higher. This effect is commonly described as ***primary isotope effect.*** This primary isotope effect is illustrated in the following reactions.

Chromic acid (H_2CrO_4) oxidation of secondary alcohol (e.g. $(CH_3)_2CHOH$ i.e. isopropanol) shows a remarkable primary kinetic isotope effect. The rate of oxidation of $(CH_3)CHOH$ is about 6-7 times faster than that of $(CH_3)_2CDOH$. It **indicates the rupture of *C–H* or *C–D* bond *at the rate determining step (rds).*** The proposed reaction mechanism is :

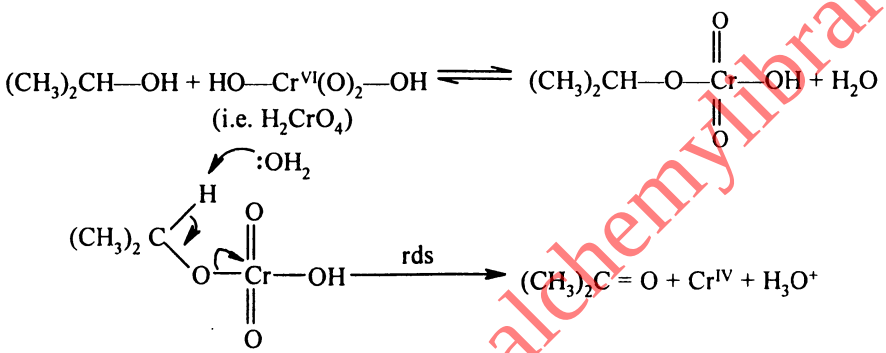

The Cr^{IV}-species reacts at the faster steps to produce the Cr^{III}-species. Here it may be noted that the rate of chromic acid oxidation of $(CH_3)_2CHOH$ and $(CD_3)_2CHOH$ does not differ significantly. The slight difference arises due to ***secondary isotope effect*** to be discussed later.

Now let us consider the ***secondary isotope effect.*** The rate of hydrolysis of the *Cr(III)–NCS* bond follows the sequence :

$$trans\text{-}[Cr(NCS)_4(NH_3)_2]^- < trans\text{-}[Cr(NCS)_4(ND_3)_2]^-$$

Here the rate enhancement for the ND_3-complex occur by a factor about 2. For such hydrolytic cleavages, the *N–H* or *N–D* bond does not rupture. ***It is known that the hydrogen bond N–D···O is stronger than the N–H···O hydrogen bond*** (see Sec. 10.1.2). This is why, the complex containing ND_3 is solvated better through *H*-bonding to facilitate the rate process.

The success of a **chemical exchange method** in separating the isotopes depends on the ***kinetic isotope effect.*** This aspect has been discussed in Sec. 5.2.6vi.

(v) ***Isotopic shift in optical spectra*** : It has already been discussed (see Sec. 5.2.2) that for the different isotopes (specially for the lighter elements), different spectral lines in both atomic and molecular spectra are noticed. The difference (in terms of wavelength) between the lines of isotopes gives the measure of isotopic shift. The intensity of the spectral lines depends on the abundance of the corresponding isotope.

(vi) ***Revival of Prout's hypothesis in the light of Aston's whole number rule*** : After the formulation of Dalton's atomic theory, Prout in 1815 proposed that the atoms of any element are formed by the condensation of hydrogen atoms (atomic weight = 1 was considered) and the atomic weights of the elements are the integral multiples (i.e. 2, 3, 4, ...) of that of hydrogen. But the discovery of fractional atomic weight, (e.g. 35.5 for chlorine) proved the hypothesis wrong.

But the Aston's work established a valid ground of Prout's hypothesis. According to Aston, the atomic weight of an element may be fractional due to the existence of isotopes. **Monoisotopic**

Click Here : me/healchemylibrary

elements always bear the integral atomic weights. All the isotopic masses are whole numbers as proposed by Prout considering the mass of a hydrogen atom to be unity. It indicates that the hydrogen atom is the fundamental unit in the construction of other atoms. The neutron and protons are now established as the nuclear constituents. The hydrogen nucleus contains only one proton. In terms of mass, the proton and neutron are almost identical. In all these propositions, the mass of the electrons in the atoms, and mass defect (which will be discussed later) in the construction of nucleus have been neglected.

(vii) ***Law of constant proportion is not universally valid*** **:** Due to the existence of the isotopes, the law of constant proportion in different samples of the isotopic compounds is not maintained. For example, percentage ratio of hydrogen and oxygen in water depends on the distribution pattern of ${}_1^1H$ and ${}_1^2H$ (i.e. *D*).

(viii) ***Atomic weight and isotopes*** **:** The atomic weight of an element depends on the number of isotopes and their relative abundances. Presently, the atomic weight is expressed in atomic mass unit (amu) in *C*–12 scale. Atomic mass unit is exactly 1/12–th of the mass of a *C*–12 atom. Thus,

$$1 \text{ amu} = \frac{12}{6.023 \times 10^{23}} \times \frac{1}{12} \text{ g} = 1.6603 \times 10^{-24} \text{ g}.$$

By considering the isotopes, the atomic weight of an element is defined by :

$$\text{atomic weight (in amu)} = \sum(x_i M_i)/\sum x_i, \text{ where } \sum x_i = 100.$$

Here, x_i denotes the percentage of abundance of the i–th isotope having mass M_i in amu and it is given by: $M_i = 1.007581Z + 1.00898N$, (neglecting the mass defect and the mass of the electrons) where, Z = number of protons and N = number of neutrons in the i–th isotope. 1.007581 amu = mass of a proton, and 1.00898 amu = mass of a neutron. Here, the mass of Z electrons and mass equivalent to nuclear binding energy have been ignored. For the sake of simplicity (except the very heavy nuclides where mass defect is high), M_i can be regarded as the mass number, i.e. $M_i = A_i = Z + N$, (A_i gives the mass number of the i–th isotope).

$$\text{Thus, atomic weight} = \sum(x_i A_i)/\sum x_i$$

Note : • The correct term is ***atomic mass*** not ***atomic weight.*** But conveniently, very often we use the term atomic weight.

- There are two scales – ***physical*** and ***chemical*** to express the atomic mass or atomic weight. These are discussed in Appendix-IV.
- **The parameter atomic mass is a ratio and it does not have *any unit.*** Thus atomic mass or weight does not give the actual mass of or weight of an atom of the element. This is why, the term ***Relative Atomic Mass*** **(RAM)** is a better choice.
- Sometimes, the term *molar mass* (g mol^{-1}) is used, e.g. molar mass of sodium is 22.9 g mol^{-1}.
- *Isotopic mass* of a nuclide is given in ***atomic mass unit*** **(amu) scale** which is given by:

$$1 \text{ amu} = 1\text{u} = \frac{1}{12} m\,(^{12}\text{C}) = 1.66057 \times 10^{-27} \text{ kg}$$

Click Here to me/thealchemylibrary

Atomic mass unit (amu) is also referred to as ***dalton***, i.e. 1 amu = 1 dalton = 1 Da.

'u' stands for ***unified*** **atomic mass unit scale,** i.e. 1u = 1 dalton (Da). Isotopic masses of ^{35}Cl and ^{37}Cl are 34.969 u and 36.966 u respectively.

Mass of a nitrogen atom is 14 amu or 14 u. It means that the mass of a nitrogen atom is $14 \times 1.66057 \times 10^{-27}$ kg.

- Presently, atomic mass (as well as molecular mass) is expressed in **amu** or **u** (u stands for *unified*) scale, e.g., atomic mass of aluminium is 27 amu or 27 u, molecular mass of water is 18 amu. For large biomolecules, the term Dalton (Da) is generally used, e.g. hemoglobin is a 64 kDa molecule meaning its molecular weight = 64,000.

(ix) ***Relative stability of the isotopes*** **:** The isotopic nuclides having even number of protons and neutrons are the most stable ones while the nuclides having both odd number of protons and neutrons are the least stable ones. The isotopes in which only either the neutrons or protons are odd (i.e. odd mass numbers) are intermediately stable. In this connection, the concept of ***packing fraction, nuclear binding energy, magic number, neutron–proton ratio*** are extremely important. These will be discussed later on separately.

5.2.4 Isotopic Composition of the Elements

It is now well established that out of the 93 nonradioactive elements (up to *Bi*) occurring in nature, there are only **21 elements** (viz., *Be, F, Na, Al, P, Sc, Mn, Co, As, Y, Nb, Rh, I, Cs, Pr, Tb, Ho, Tm, Ta, Au,* and *Bi*) **which are monoisotopic,** i.e. single species; and all other elements have two or more isotopes which may be stable or radioactive. In some cases, the number of isotopes is very high as shown in the following Table 5.2.4.1. ***$_{50}Sn$ shows the largest number of stable isotopes.***

Table 5.2.4.1. Number of stable isotopes for some elements.

Element	*Number of stable isotopes*	*Element*	*Number of stable isotopes*
$_{50}Sn$	(10)	$_{20}Ca$, $_{46}Pd$	(6)
$_{54}Xe$	(9)	$_{22}Ti$, $_{28}Ni$	(5)
$_{56}Ba$, $_{80}Hg$, $_{42}Mo$, $_{76}Os$	(7)	$_{16}S$, $_{24}Cr$	(4)

Naturally occurring isotopes (including radioisotopes) of some elements are shown in Table 5.2.4.2.

Table 5.2.4.2. Naturally occurring isotopes of some elements (*indicates radioisotopes).

Element (Atomic Number)	*Mass Number (Abundance, %)*	*Element (Atomic Number)*	*Mass Number (Abundance, %)*
H (1)	1 (99.98), 2 (0.015), 3*(0)	*Ca* (20)	40 (96.96), 42 (0.64), 43 (0.15), 44 (2.06), 46 (0.0033), 48 (0.19)
He (2)	3 (1.3×10^{-4}) 4 (99.99)	*Cr* (24)	50 (4.49), 52 (83.78), 53 (9.43), 54 (2.3)
Li (3)	6 (7.39), 7 (92.61)	*Fe* (26)	54 (5.81), 56 (91.64), 57 (2.21), 58 (0.34)
Be (4)	9 (100)	*Co* (27)	59 (100)

Click Here t.me/trealchemylibrary

Element (Atomic Number)	*Mass Number (Abundance, %)*	*Element (Atomic Number)*	*Mass Number (Abundance, %)*
B (5)	10 (18.80), 11 (81.20)	*Ni* (28)	58 (67.76), 60 (26.16), 61 (1.25), 62 (3.66), 64 (1.16)
C (6)	12 (98.90), 13 (1.10), 14* (10^{-10})	*Cu* (29)	63 (69.10), 65 (30.90)
N (7)	14 (99.62) 15 (0.38)	*Zn* (30)	64 (48.89), 66 (27.81), 67 (4.07), 68 (18.61), 70 (0.62)
O (8)	16 (99.76), 17 (0.04), 18 (0.20)	*As* (33)	75 (100)
F (9)	19 (100)	*Br* (35)	79 (50.5), 81 (49.5)
Ne (10)	20 (90.51), 21 (0.28), 22 (9.21)	*Ag* (47)	107 (51.35), 109 (48.65)
Na (11)	23 (100)	*Sn* (50)	112 (0.9), 114 (0.61), 115 (0.35), 116 (14.07), 117 (7.54), 118 (23.98), 119 (8.68), 120 (33.03), 122 (4.78), 124 (6.11)
Mg (12)	24 (78.60), 25 (10.11), 26 (11.29)		
Al (13)	27 (100)		
		I (53)	127 (100)
		Pt (78)	190* (0.012), 192 (0.78), 194 (32.80), 195 (33.70), 196 (25.40), 198 (7.23)
Si (14)	28 (92.28), 29 (4.67), 30 (3.05)	*Au* (79)	197 (100)
P (15)	31 (100)	*Hg* (80)	196 (0.15), 198 (10.10), 199 (17.0), 200 (23.30), 201 (13.20), 202 (29.60), 204 (6.70)
S (16)	32 (95.06), 33 (0.74), 34 (4.18), 36 (0.016)	*Pb* (82)	204 (1.50), 206 (23.60), 207 (22.60), 208 (52.30)
Cl (17)	35 (75.4), 37 (24.6)	*Bi* (83)	209 (100)
Ar (18)	36 (0.307), 38 (0.06), 40 (99.63)	*Th* (90)	232* (100)
K (19)	39 (93.30), 40* (0.011), 41 (6.70)	*U* (92)	234* (0.006), 235* (0.71), 238* (99.28)

5.2.5 Uses of Isotopes

This aspect will be discussed in the next Chapter (see Sec. 6.17).

5.2.6 Separation of Isotopes

Isotopes of different elements are of much importance from the viewpoint of their practical applications (see Sec. 6.17) in different disciplines, such as : in medicine, in research, in industry, in the production of nuclear energy, etc. That is why, their separation is of much practical importance. It has been already mentioned that the principle of different methods of separation depends on the difference in their physical (e.g. diffusion rate, etc.) and some physico–chemical (e.g., rate of reaction, equilibrium constant, etc.) properties which are governed by their atomic masses. That is why, the relative difference of the isotopic masses, measured by the **ratio of the isotopic masses** is extremely important in determining the efficiency of the processes. For the heavier elements, the ratio of the isotopic masses does not differ significantly from unity. This is why, their separation becomes a difficult task. For the lighter elements,

Click Here t.me/thealchemylibrary

the problem is relatively easier. In this connection, the separation of hydrogen isotopes where the mass ratio is two for deuterium and hydrogen is the most ideal situation.

Separation Factor **:** In separating two isotopes, the separation factor (s) for a particular method is to be considered, as it gives the measure of efficiency of a particular process. It is defined as the ratio of concentration of the two isotopes after processing compared to the ratio present before processing. Thus, if C_l and C_h are the concentrations of the light and heavy isotopes respectively before processing, and c_l and c_h are the corresponding concentration terms after processing in a particular method, then the separation factor to the lighter isotope (s_l) in that process for a single step is given by :

$$s_l = \frac{(c_l / c_h)}{(C_l / C_h)} = \frac{c_l C_h}{c_h C_l}$$

As the value of s_l increases compared to unity, the efficiency of the process increases. Generally at a single stage, s_l is slightly larger than unity. This is why, to get any effective separation, several successive stages are to be carried out. If n stages are carried out successively in a particular process, then the overall separation factor (S) to the lighter isotope for n stages is given by $S = (s_l)^n$. Thus, even for the s_l value very close to unity, if n is very large, then S may be significantly greater than unity giving rise to an appreciable extent of separation.

(i) Electromagnetic Method

The principle of this method is based on the working principle of Dempster's mass spectrograph (see Sec. 1.2.5). In this method, the element or its any suitable compound containing the isotopes is taken in a gaseous form which is made ionised by bombarding electrons emitted from an electrically heated filament. Then the ion beam is allowed to pass through the slits S_1 and S_2 between which a high electrical potential exists to accelerate the ions. After emerging from S_2, the ion beam is subjected to a magnetic field and it travels through a circular path under the influence of the magnetic field. The different isotopes get deflected to different extents depending on q/M (i.e. charge to mass ratio of the ions). The charges being identical, the degree of deflection depends on the isotopic masses. Here, we can recall the relation,

$$q/M = 2E/H^2r^2 \text{ (cf. Eqn. 1.2.5.1)}$$

From this relation, it is evident that if E (accelerating electrical potential) and H (intensity of the magnetic field) are kept constant, the heavier isotopes will travel the circular path of larger radius (i.e. $r \propto \sqrt{M}$). Thus by placing the receivers at appropriate positions, the different isotopes or their compounds can be collected (see Fig. 5.2.6.1).

Before to start the process, the entire set–up must be perfectly evacuated, otherwise the residual gas being ionised will contaminate the isotopes separated. *This method can yield isotopes of very*

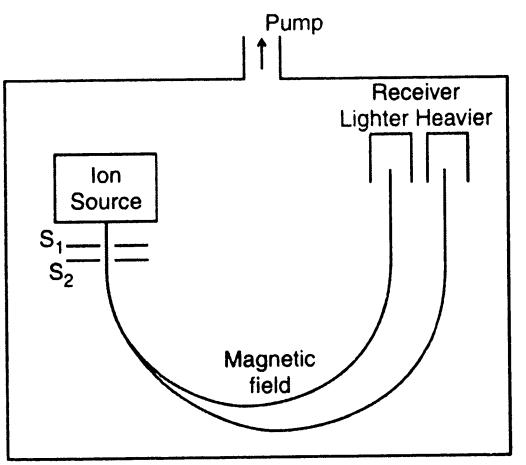

Fig. 5.2.6.1. Scheme for separation of isotopes by electromagnetic method.

Click Here to the/thealchemylibrary

high purity (~ 100%). But, this method is very much expensive. It is generally carried out for getting small quantities of isotopes of very high purity required for academic and research works.

(ii) Diffusion Method

The principle of this method lies on the Graham's law of diffusion for the gaseous compounds. According to this law, a gas diffuses through a porous barrier at a rate which is inversely proportional to the square root of its molecular weight. When a mixture of isotopes (or their suitable compounds) in a gaseous state is allowed to diffuse through a porous barrier, the diffused gas gets enriched in the lighter isotope because of its higher rate of diffusion. Here according to Graham's law, the separation factor for the lighter isotopes for a single stage is given by, $s_l = (M_h/M_l)^{1/2}$, where M_h and M_l are the molecular weights of the heavier and lighter species respectively. The above separation factor is realised from the kinetic energies of two ideal gases having molecular masses M_h and M_l.

$$\frac{1}{2}M_l u_l^2 = \frac{1}{2}M_h u_h^2 \text{ (at a fixed temperature)}$$

$$\text{i.e.} \quad \frac{u_l}{u_h} = \sqrt{M_h / M_l} = s_l$$

By using this principle, Aston made a partial separation of the neon isotopes. Normally, neon contains 90% ^{20}Ne and 10% ^{22}Ne. Here the separation factor s_l becomes $\sqrt{22/20} = 1.049$. Because of this small difference from unity, it requires several hundred operations to have an appreciable extent of separation. The efficiency of this method further falls for the heavier elements. However, the efficiency was remarkably improved by Hertz in Germany in 1932 by using the cascade principle through recycling (Fig. 5.2.6.2) in a series in a closed circuit. From Fig. 5.2.6.2, it is evident that the gas mixture travelling towards the left through the diffusion cells, D_1, D_2, D_3, D_4, ... containing the porous walls (W), gets gradually enriched in the lighter species, while the gas mixture moving towards the right becomes enriched in the heavier species. In this process, it was possible to have the gas mixture having 99% ^{20}Ne.

This method was successfully used during the 2nd World War time in separating ^{235}U from ^{238}U by using their hexa–fluoro compounds, i.e. $^{235}UF_6$, and $^{238}UF_6$ in which the former is present to an extent

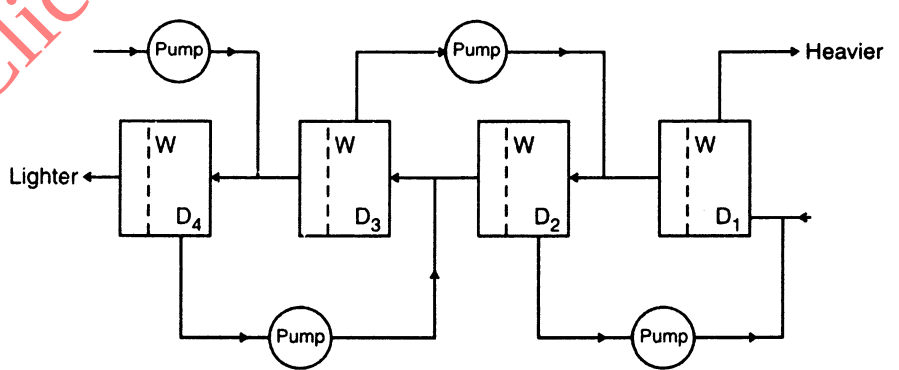

Fig. 5.2.6.2. Scheme for separation of isotopes by diffusion method.

Click Here 1.me/thealchemylibrary

of about 0.7% only. Here, for a single stage, the separation factor is $\sqrt{352/349}$, i.e. 1.0043. Thus after 200 stages of diffusion, % of $^{235}U_6$ increases from 0.7 to $0.7 \times (1.0043)^{200} = 1.68$. In practice, s is about 1.0014 instead of 1.0043. To isolate $^{235}UF_6$ which gives the nuclear fuel ^{235}U, several thousand diffusions are required. To get 100% separation, the enriched material obtained by this method is utilised in electromagnetic separation.

^{12}C and ^{13}C can be partially separated through the diffusion of methane.

To carry out the diffusion, *the dimension of the pores should be less than the one–tenth of the mean free path* (i.e. the average distance travelled by a molecule between successive collisions) of the gaseous molecules. Thus, the diameter of the pores becomes of the order of 10^{-6} cm. To have a such porous barrier, a thin sheet of *Ag–Zn* alloy is subjected to etching by dilute *HCl* which dissolves away some of the *Zn* atoms giving rise to a large number of submicroscopic holes in the sheet.

(iii) Thermal Diffusion Method

In 1938, Clausius and Dickel in Germany developed this technique in which an electrically heated (> 500°C) wire (platinum or nichrome) runs down along the axis of a long (~ 36 meter) vertical pipe. The walls of the pipe are kept cold by circulating water through a jacket and thus a temperature gradient between the wall and central zone develops. When a gas mixture containing the isotopes or their compounds is introduced into the pipe, the lighter species get concentrated in the hot central zone while the heavier ones get accumulated at the cold zone close to the walls due to the thermal diffusion. Very soon, a thermal convection current gets established. The heavier component goes downward along the cold wall while the lighter one runs upward along the hot wire. **Thus, the lighter one gets collected at the top region while the heavier one gets accumulated at the bottom** (see Fig. 5.2.6.3). This simple method gives a very rapid method for an effective separation of the isotopes. By utilising this method, $^{235}UF_6$ can be separated to an appreciable extent from $^{238}UF_6$. Then the enriched mixture can be subjected to the electromagnetic separation to have 100% $^{235}UF_6$. The separation factor is given by the following relation

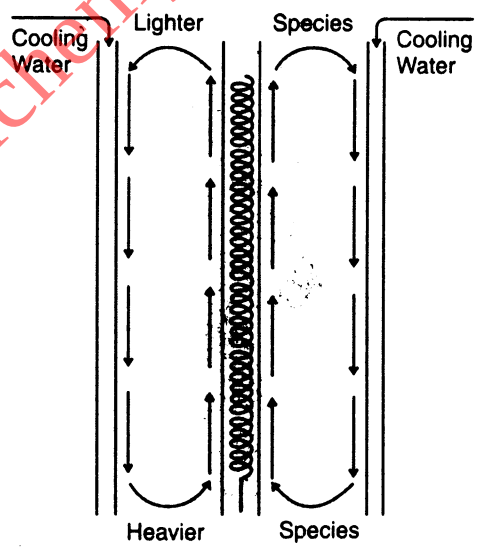

Fig. 5.2.6.3. Scheme for separation of isotopes by thermal diffusion method.

$$\ln s = A\left(\frac{M_h - M_l}{M_h + M_l}\right)\ln\left(\frac{T_2}{T_1}\right)$$

where M_h and M_l denote the molecular masses of heavier and lighter isotopic molecules respectively, T_2 and T_1 are the temperatures of the hot wire and wall respectively, A is a proportionality constant.

The efficiency of the process depends on the relative masses of the isotopic species and the temperature gradient. For the isotopic gaseous compounds, temperature of the central wire should be monitored in such a way that the species do not undergo any thermal decomposition.

Click Here to the Chemylibrary

The method is very much simple and rapid, but there is a large power consumption. This is why, this method is encouraging only for the enrichment of isotopes on a laboratory scale, but it is not economically viable for any large scale operation.

(iv) Fractional Distillation Method

The rate of evaporation of an isotopic element or its compound from a liquid mixture is inversely proportional to the square root of its molecular mass (cf. Graham's law of diffusion). This principle has been utilised in the present method. Thus, if evaporation is allowed to go on, then the lighter ones leave the surface more easily leaving the residual liquid enriched in the heavier components. The pressure should be very small, so that the lighter one evaporated may not return to the residual liquid surface. In developing this method, many workers such as, Keesom and Dijk (1931) in Holland, Urey and co-workers (1931) in USA, Bronsted and Hevesy (1920) in Denmark, etc. contributed significantly.

Thus when liquid oxygen is distilled at a very low pressure, the lighter isotope (^{16}O) comes off first and the residual liquid gets concentrated in the heavier one. Thus the first fraction containing the lighter one may be subjected to a fractional distillation at the second stage. Thus, by repeating the process, the isotopes can be separated to an appreciable extent.

By using the technique, the two isotopes of *Hg* have been successfully separated to an appreciable extent by carrying out the fractional distillation at 40–50°C at a very low pressure (~1–2 mm of *Hg*). The apparatus is shown in Fig. 5.2.6.4. In the two walled flask, the outer compartment of the flask containing *Hg* is kept at 40–50°C at a very low pressure while the inner compartment contains liquid air. On evaporation, the lighter fraction gets condensed on the liquid air cooled surface placed a little above the evaporating *Hg*. After some time, the residual mercury concentrated in the heavier isotope is taken out by opening the stopcock. On the other hand, the frozen mercury on the cold surface consists of a larger fraction of the lighter isotope. Thus by repeating the process, a separation to an appreciable extent is obtained.

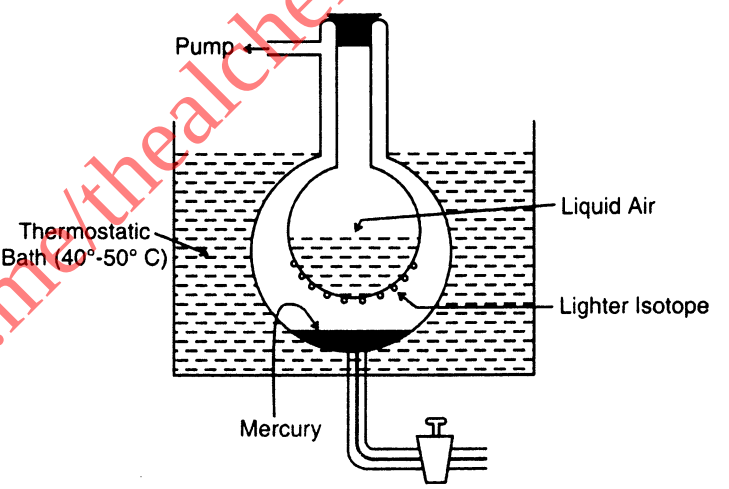

Fig. 5.2.6.4. Scheme for separation of mercury isotopes by fractional distillation method.

(v) Electrolytic Method

This method is specially applicable for isolating the heavy hydrogen in its compound, heavy water. It is found that when electrolysis of an aqueous *KOH* solution is carried out, the lighter isotope of hydrogen (^{1}H) is preferentially evolved ***because of its low overvoltage compared to that of the heavier one.*** Here, the separation factor depends on the relative difference of overvoltage. Thus, if the electrolysis is

Click Here t.me/thealchemyjourney

carried out for a long time, the residual electrolyte will be enriched in heavy water. By repeating the process in a recycling way, the concentration of deuterium from its initial value of 0.02% in ordinary water may be increased up to 99.9%. In practice, when the volume is reduced to 1/10–th, it is neutralised with CO_2 (otherwise, some of the deuterium will remain in the solution as KOD) and the enriched water is distilled off. The distillate is mixed with the unneutralised and undistilled electrolyte obtained from the previous stage to adjust the alkalinity and it is again subjected to electrolysis. In about 5–7 stages, relatively pure heavy water is obtained. The production of heavy water, ^2H_2O (i.e. D_2O) on a commercial scale is of enormous importance, as it is necessary for controlling the chain fission of uranium. In practice, the electrolytic procedure is usually carried out by electrolysis 0.5 N $NaOH$ or KOH solution with Ni–electrodes repeatedly.

Note : In India, heavy water (required mainly in nuclear reactors) is produced at Nangal (Punjab) by electrolytic method and distillation of liquid hydrogen.

(vi) Chemical Exchange Method

Though the different isotopic species are chemically indistinguishable, their rates of reaction are different*. The lighter one reacts faster (cf. Sec. 5.2.3). This fact is well noticeable for the lighter elements (e.g. C, N, O, S, etc.) where the relative mass difference among the isotopes is significant. This difference in reactivity has been exploited in enriching a particular isotope in a particular phase with the help of isotopic exchange reactions. In these reactions, an isotope in one compound exchanges with another isotope of the same element in another compound. **Because of the difference on the exchange rates of the isotopes, the equilibrium constant of the process is different from unity. The equilibrium constant gives the measure of the separation factor.**

Due to the difference in reactivity, when an isotopic species in a gaseous phase is in equilibrium with its another isotopic species in a liquid phase, the distribution function of the two isotopic species is different in two phases. In general, a suitable catalyst favours the attainment of the equilibrium.

Based on the above principle, $C^{16}O_2$ and $C^{18}O_2$ exchange with water at different rates giving the equilibrium constant (K) equal to 1.047 at 0°C.

$$\frac{1}{2}C^{16}O_2\,(g) + H_2{}^{18}O\,(l) \rightleftharpoons \frac{1}{2}C^{18}O_2\,(g) + H_2{}^{16}O\,(l);\ K = 1.047$$

Thus, in the above exchange process, the concentration of ^{18}O increases in the gaseous phase. **Here it is noteworthy that because of this equilibrium in nature, the atmospheric oxygen is relatively richer in ^{18}O content compared to that of water.**

Similarly, concentration of ^{15}N can be enhanced in the solution phase by passing ammonia gas through an aqueous solution of ammonium nitrate or sulphate falling downwards through a glass–bead–packing tower. Here the following exchange reaction occurs.

---

* **Reactivity of isotopes :** Here it is important to highlight the actual reason at the molecular level behind the difference in the reactivities of the isotopic species. **It is really due to the difference of zero-point energy** (cf. Sec. 5.2.2). If a **diatomic molecule** is supposed to vibrate harmonically, then its zero point energy (E_0) is given by, $E_0 = (1/2)h\omega$ where ω is the equilibrium vibrational frequency and it is given by $\omega = \frac{1}{2\pi}\sqrt{f/\mu}$, where f = force constant which is more or less constant for the isotopic molecules, and μ is the **reduced mass** and it is given by, $\mu = \frac{m_1 m_2}{m_2 + m_2}$, m_1 and m_2 are the atomic masses of the constituent atoms.

Click Here t.me/thedchemyjibrary

$$^{15}NH_3\ (g) + {}^{14}NH_4^+\ (\text{soln.}) \rightleftharpoons {}^{14}NH_3\ (g) + {}^{15}NH_4^+\ (\text{soln.});\ K = 1.033$$

Similarly, the following exchange reaction leads to an enrichment of ^{13}C in the gaseous phase containing *HCN*.

$$H^{12}CN\ (g) + {}^{13}CN^-\ (\text{soln.}) \rightleftharpoons H^{13}CN\ (g) + {}^{12}CN^-\ (\text{soln.});\ K = 1.026$$

As *HCN* is deadly poisonous, for a large scale operation, the chemical exchange reaction of CO_2 with an aqueous solution of $KHCO_3$ or NH_4HCO_3 is preferred.

$$^{13}CO_2\ (g) + H^{12}CO_3^-\ (\text{soln.}) \rightleftharpoons {}^{12}CO_2\ (g) + H^{13}CO_3^-\ (\text{soln.});\ K = 1.012$$

Some useful exchange reactions are shown below.

$$\frac{1}{2}S^{16}O_2\ (g) + H_2{}^{18}O\ (l) \rightleftharpoons \frac{1}{2}S^{18}O_2\ (g) + H_2{}^{16}O\ (l);\ K = 1.028$$

$$^{16}O_2\ (g) + 2H_2{}^{18}O\ (l) \rightleftharpoons {}^{18}O_2\ (g) + 2H_2{}^{16}O(l);\ K = 1.012$$

$$^{35}Cl_2\ (g) + 2H^{37}Cl\ (\text{soln.}) \rightleftharpoons {}^{37}Cl_2\ (g) + 2H^{35}Cl\ (\text{soln.})$$

$$^{34}SO_2\ (g) + H^{32}SO_3^-\ (\text{soln.}) \rightleftharpoons {}^{32}SO_2\ (g) + H^{34}SO_3^-\ (\text{soln.})$$

Most importantly, it has been attempted to produce heavy water by using the principle of the isotopic exchange reaction. The following exchange reaction is useful in enriching the deuterium in the steam:

$$^2H_2\ (g) + {}^1H_2O\ (\text{steam}) \rightleftharpoons {}^1H_2\ (g) + {}^2H_2O\ (\text{steam})$$

In practice, a mixture of hydrogen gas and steam is passed to flow upwards through a tower containing a catalyst bed, while liquid water runs downwards along the tower bed. Thus the steam enriched in ^2H gets condensed and carried downwards by the liquid water flowing downwards. Thus the emerging water from the bottom of the tower is essentially concentrated in ^2H_2O. By recycling the process in cascade, appreciably concentrated ^2H_2O (i.e., heavy water) may be obtained. This method is economically more viable compared to the electrolytic method to produce ^2H_2O, because here the power consumption is much less. Generally, the water enriched in ^2H_2O obtained in this method is finally subjected to the electrolytic method to have ~ 100% ^2H_2O.

(vii) Centrifugal Method

The gravitational force responsible to pull down a body is proportional to its mass. Thus if a mixture of two or more isotopes (or their suitable compounds) in a gaseous or liquid form is allowed to stand, the heavier one will get accumulated in the bottom region. In practice, the pseudo–gravitational force of a high magnitude is applied by a high speed rotating centrifuge. The extent of separation depends on the relative mass difference of the isotopic species. This technique was successfully utilised in separating the chlorine isotopes by using CCl_4 in 1939 by Beams and coworkers in USA.

(viii) Szilard–Chalmers' Process

Sometimes, by selecting some suitable nuclear reactions, the product isotopic nuclei can be easily separated from the parent isotopic nuclei because of their different chemical states. In this process, the (n, γ) type reactions are of interest. In this type of reactions, the product isotope differs by unity in mass number compared to the target isotopic nuclide.

Click Here t.me/thearchemylibrary

Let us take the reaction where, ^{127}I captures the slow neutron to produce $^{128}I^*$ which is in an excited state. The excited nuclide almost immediately emits the excitation energy in the form of γ–photons, i.e.

$$^{127}I + {}^{1}_{0}n \rightarrow {}^{128}I^* \text{ (excited)} \rightarrow {}^{128}I + \gamma.$$

According to the principle of conservation of momentum, during ejection of the γ–photon, the product recoil nuclide ^{128}I will acquire the momentum ($p = mu$) equal to that of the photon but in the opposite direction. Therefore,

momentum of the recoil nuclide = momentum of the γ–photon; or, $mu = E_\gamma/c$,

(E_γ = energy of the photon, u = velocity of the recoil nuclide and c = velocity of light).

Hence, the kinetic energy (E_r) of the recoil nuclide is given by :

$$E_r = p^2/2m = (mu)^2/2m = E_\gamma^2/(2mc^2)$$

Generally, E_γ is of the order of 1–5 MeV, and if mass number of the isotopic nuclide lies in the range 50–100, then the **recoil energy** (E_r) **becomes of the order of 5–250 eV** which is much greater than the chemical bond energy (~ 5 eV) holding the atom in a compound. **Hence during the ejection of the photon, the product nuclide gets automatically dissociated from the parent molecule.** Such atoms having energy excess of the thermal energy are called ***hot atoms.*** The dissociated isotopes being in a different chemical state with respect to the target isotopic nuclides which remain bound in the molecule, can be easily separated by selecting some suitable reactions. This is the basis of Szilard–Chalmers' reaction to separate the isotopes. Let us take the following example,

$$C_2H_5{}^{127}I + {}^{1}_{0}n \rightarrow C_2H_5{}^{128}I^* \rightarrow {}^{128}I + C_2H_5^*$$

Here, ethyliodide in the presence of water on being bombarded by the slow neutrons produces the radioisotope ^{128}I that readily passes into the aqueous phase (containing potassium iodide) while the nonactive isotope ^{127}I remains bound in the organic molecule. Thus the aqueous phase predominates in ^{128}I while the organic phase predominates in ^{127}I. By using suitable organic substances, the isotopes of *Cl*, *Br*, *I* can be generated and automatically separated in this process.

When an aqueous solution of $Na^{37}ClO_3$ is irradiated with a flux of slow neutrons, the (n, γ) reaction produces $^{38}Cl^-$ that remains as $^{38}Cl^-$ is aqueous solution. It can be precipitated as $Ag\,{}^{38}Cl^-$ by $AgNO_3$.

$$\underset{\text{(aqueous solution)}}{Na^{37}ClO_3} \xrightarrow{\text{Slow neutron}} \underset{\text{(aqueous solution)}}{{}^{38}Cl^-} \xrightarrow{AgNO_3} Ag^{38}Cl(s)$$

(ix) Separation by Internal Conversion

In some radioactive changes, the excitation energy which is supposed to be emitted as radiations is used up to expel an extranuclear electron from the radiating atom to convert it into an ion. This phenomenon is very often referred to as ***internal conversion of the γ–rays*** (see Sec. 6.6). The emitted electrons are different form the β–ray electrons. The emitted electrons from a particular shell due to the internal conversion are of almost the same energy. This is why they are referred to as ***line of electrons.*** On the other hand, the β–ray electrons produce ***a spectrum.***

During such internal conversions in the excited nuclides, the product *isomeric nuclides* remain in an ionised condition and as a result, the product isomers can be easily chemically separated as it is done

Click Here t me/thealchemylibrary

in Szilard–Chalmers' reaction. By taking this advantage, the isotopes produced in some suitable nuclear reactions get separated automatically. Let us consider the following example,

$$^{81}Br + {}^{1}_{0}n \rightarrow {}^{80}Br^{*}\ (\text{excited}) + 2\,{}^{1}_{0}n$$

$$^{80}Br^{*} \xrightarrow{\text{Isomeric Transition}} {}^{80}Br + \lambda$$

$$^{80}Br^{*} \xrightarrow{\text{Internal Conversion}} {}^{80}Br^{+} + e$$

Here, in the process $^{80}Br(n, 2n)\ ^{80}Br^{*}$, the excited isomer $^{80}Br^{*}$ can either go through an internal conversion or a simple isomeric transition. During the internal conversion, it forms $^{80}Br^{+}$ whose oxidation state is different and consequently, its chemical properties are different. Thus, separation of $^{80}Br^{+}$ becomes easier chemically. It is worth mentioning that due to ***Auger effect*** (see Sec. 6.7), $^{80}Br^{n+}$ (where n may be more than unity) with a high positive charge may result in practice.

(x) Cow and milk system to separate the daughter element from its parent radioactive nuclide

If the daughter element is in a radioactive equilibrium with its radioactive parent element, then removal of the daughter element by any physical or chemical method from the equilibrium mixture will generate the daughter element to restore the radioactive equilibrium. When the radioactive equilibrium is again established, the accumulated daughter element can be separated. Thus in this system, the parent radioactive element appears as the ***cow*** which can be ***milked*** at regular intervals (allowing the equilibriation) to collect the daughter element.

Let us consider the ***transient radioactive equilibrium*** between ^{99}Mo and ^{99m}Tc.

$$^{99}_{42}Mo \xrightarrow[t_{1/2} \approx 66\,h]{-\beta^-} {}^{99m}_{43}Tc \xrightarrow[t_{1/2} \approx 6\,h]{I.T.} {}^{99}_{43}Tc \xrightarrow[t_{1/2} = 2 \times 10^5\,y]{-\beta^-} {}^{99}_{44}Ru$$

Here, the $^{99m}_{43}Tc$ generator i.e. $^{99}_{42}Mo$ is the cow which can be milked at every 24th hour. ^{99m}Tc is separated as $^{99m}TcO_4^-$ (i.e. pertechnatate) through elution by 0.9% $NaCl$ solution. ^{99m}Tc is widely used in medical field as an ***imaging agent.***

$$^{226}Ra \xrightarrow[t_{1/2} = 1600\,y]{-\alpha} {}^{222}Rn$$

^{226}Ra and ^{222}Rn remain in a ***secular equilibrium.*** The daughter element radon is a gaseous substance and it can be separated from the parent element by simply heating. Thus, the **milking operation** is quite simple. The parent element radium (i.e. cow) can be milked at every 4th/5th day.

5.3 NUCLEAR STABILITY

Before we establish the factors responsible for giving the stability to the nuclides, we should discuss the characteristic features of the stable isotopes from the percentage of abundance of the different isotopes of different elements.

Click Here t.me/thealchemylibrary

5.3.1 Even–Odd Nature of the Nucleons (Harkins' Rule)

From the isotopic abundance (cf. Table 5.2.4.2) of different elements, the following points depending on the evenness or oddness of the nucleons appear to characterise the stable nuclides. These are known as **Harkins' Rule or Oddo-Harkins rule**

(a) **Harkins' rule : The nuclei having even number of neutrons and protons are the most stable and the most abundant ones as evident from Table 5.2.4.2.** This type of nuclides gives the composition of the earth's crust by ~ 85%. $^{16}_{8}O$, and $^{28}_{14}Si$ give the composition of the earth's crust by ~ 48% and ~ 26% respectively. The next abundant group consists of the elements with even number of neutrons and odd number of protons. These are (with % of abundance in the earth's crust) : $^{27}_{13}Al$ (8.5), $^{23}_{11}Na$ (2.8), $^{39}_{19}K$ (2.5), *etc.*

Table 5.3.1.1. Abundance distribution of stable nuclides *(illustrations of Harkins' rule).*

	Composition of nucleus			No. of stable nuclides	Abundance, % in the earth's crust	Examples
	Neutrons (N)	Protons (Z)	$A = Z + N$			
(i)	Even	Even	Even	~ 162	~ 85	$^{4}_{2}He$, $^{16}_{8}O$, $^{28}_{14}Si$, $^{40}_{20}Ca$, $^{56}_{26}Fe$, $^{208}_{82}Pb$
(ii)	Even	Odd	Odd	~ 52	~ 13	$^{27}_{13}Al$, $^{23}_{11}Na$, $^{39}_{19}K$
(iii)	Odd	Even	Odd	~ 50	~ 2	$^{17}_{8}O$, $^{25}_{12}Mg$
(iv)	Odd	Odd	Even	~ 4*	0	$^{2}_{1}H$, $^{6}_{3}Li$, $^{10}_{5}B$, $^{14}_{7}N$

* The 5–th one of this group is reported to be $^{180}_{73}Ta$.

Note : For **cosmic abundance** of the elements, please see the Fig. 7.15.2.1 and Sec. 7.15.2.

(b) **Equivalent character of nucleons :** From Table 5.3.1.1, it is evident that the second and third group each give almost equal number of stable nuclides which is about one–third of the first group. **It suggests that for odd A, the number of stable nuclides does not depend on whether N is odd or Z is odd.** *Thus, all the nucleons are behaving similarly in this respect irrespective of their charges.*

(c) **Pairing of nucleons only within a particular type :** From the frequency of distribution of the stable nuclides, **it appears that the nucleons of each kind tend to pair among themselves, but the nucleons of different kinds do not pair, i.e. a proton pairs with only another proton and not with a neutron, and the same thing also occurs for a neutron.**

(d) **($n + n$), ($p + p$), ($n + n$), ... rule leading to monoisotopic (Z = odd) and multiisotopic (Z = even) elements :** The tendency of a proton to pair with a proton or of a neutron with a neutron is evident from the distribution pattern of the stable isotopes for the lighter elements from oxygen to chlorine. *In this range, it is observed that the two neutrons and two protons are added successively to have the stable nuclides in the above range.* It suggests that the neucleons are added in the sequence, ($n + n$), ($p + p$), ($n + n$), ...
Violation of the above rule leads to an unstable nuclide. The rule is illustrated in Scheme 5.3.1.1.

Click Here to the/thealchemylibrary

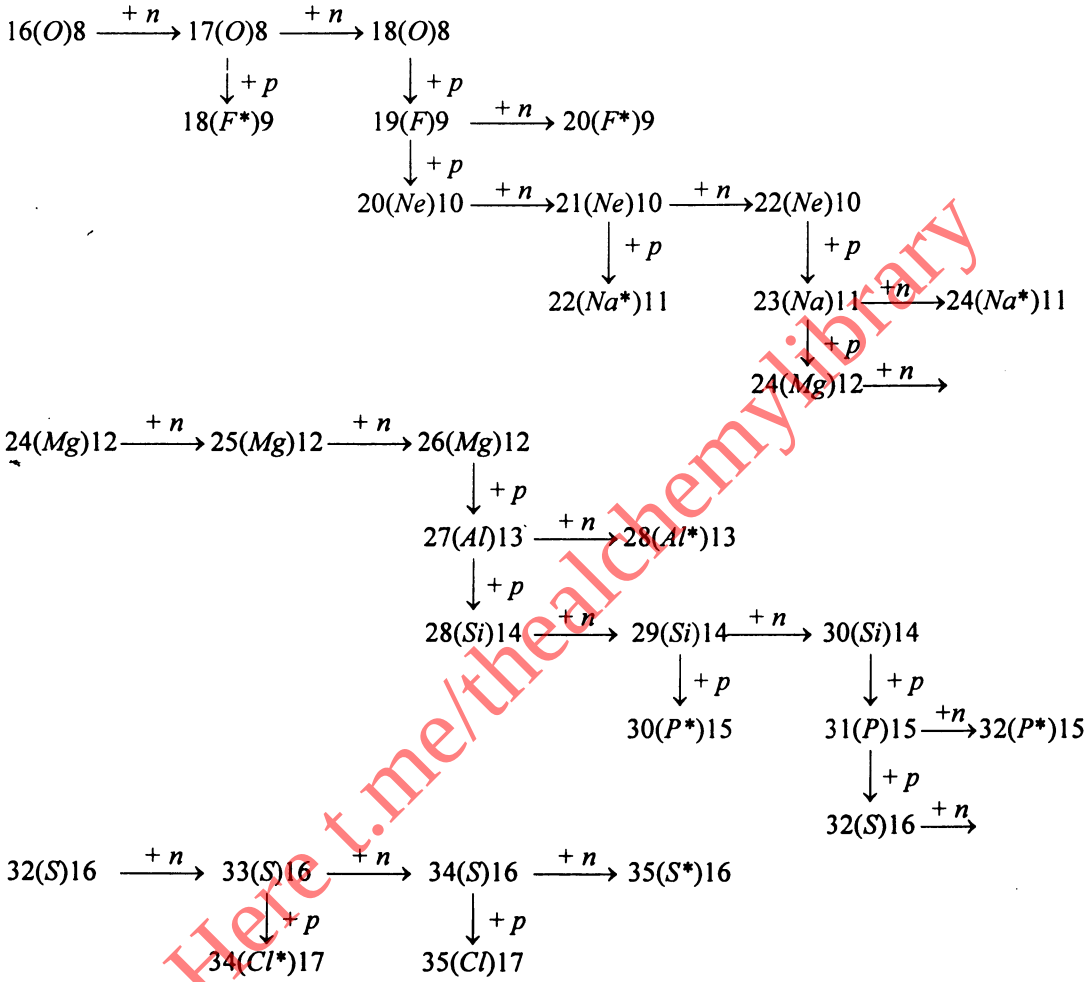

Scheme 5.3.1.1. Illustration of $(n + n)$, $(p + p)$, $(n + n)$, ... rule; deviation of the rule, e.g. $(n + p)$ or $(p + n)$ or $(n + n + n)$, leads to the unstable isotopes shown by *.

$A(X)Z$ denotes : mass number (element) atomic number.

From Scheme 5.3.1.1, it is evident that **for even Z, there are three isotopes having mass number A, $(A + 1)$ and $(A + 2)$. On the other hand, for odd Z, the elements are *monoisotopic*.**

Here it is worth mentioning that the above $n + n$, $p + p$, $n + n$, ... rule is supported by the fact that out of the **21 naturally occurring monoisotopic nuclides, there are 20 nuclides which are having odd Z.** Here $^{9}_{4}Be$ is the only exception. The **odd Z monoisotopic nuclides are:**

$^{19}_{9}F$, $^{23}_{11}Na$, $^{27}_{13}Al$, $^{31}_{15}P$, $^{45}_{21}Sc$, $^{55}_{25}Mn$, $^{59}_{27}Co$, $^{75}_{33}As$, $^{89}_{39}Y$, $^{93}_{41}Nb$, $^{103}_{45}Rh$, $^{127}_{53}I$, $^{133}_{55}Cs$, $^{141}_{59}Pr$, $^{159}_{65}Tb$, $^{165}_{67}Ho$, $^{169}_{69}Tm$, $^{181}_{73}Ta$, $^{197}_{79}Au$ and $^{209}_{83}Bi$.

(e) **Stability of α-particle nuclides and rule of Oddo :** Nuclides (e.g. ^{16}O, ^{20}Ne, ^{24}Mg, ^{28}Si, ^{32}S, ^{36}Ar, ^{40}Ca, etc.) having mass numbers as multiples of 4 (i.e. mass number of α-particle) are more

Click Here t.me/thealchemylibrary

abundant than their immediate neighbours. Such nuclides are described as ***α-particle nuclides*** (assuming the α-particles as the building units of such nuclides). **This illustrates the nuclear stability of 2-proton + 2-neutron combination.** This observation is described as the ***rule of Oddo.***

5.3.2. The Neutron to Proton Ratio and Stability of the Nuclides

The neutron to proton ratio (n/p) depending on Z, is important to predict the stability of the nuclides. For the elements of low atomic number (up to $Z = 20$), for the stable nuclei, the n/p ratio is unity. For the elements of higher atomic number, the n/p ratio increases gradually up to about 1.6. The variation of the n/p ratio with Z for the stable nuclides is shown in Fig. 5.3.2.1 known as ***Segre chart.*** In many cases, several stable isotopes exist for a particular value of Z. This is why, we get a stability zone which widens for the higher Z values. The nuclides lying outside the stability region are unstable. The actual cause of increase of n/p ratio for the higher Z values is not properly understood. Probably, this neutral particle minimises the increased proton–proton repulsion for the elements of higher atomic numbers. However, the best explanation of Segre chart is available by considering the **nuclear potential well in *Fermi gas model*** (cf. Sec. 5.5.1, Fig. 5.5.1.2). The fixed n/p ratio for a particular stable nuclide is explainable from the consideration of 1st order kinetics involved in the exchange process within the nucleons to attain the dynamic equilibrium (cf. Sec. 5.4.2A).

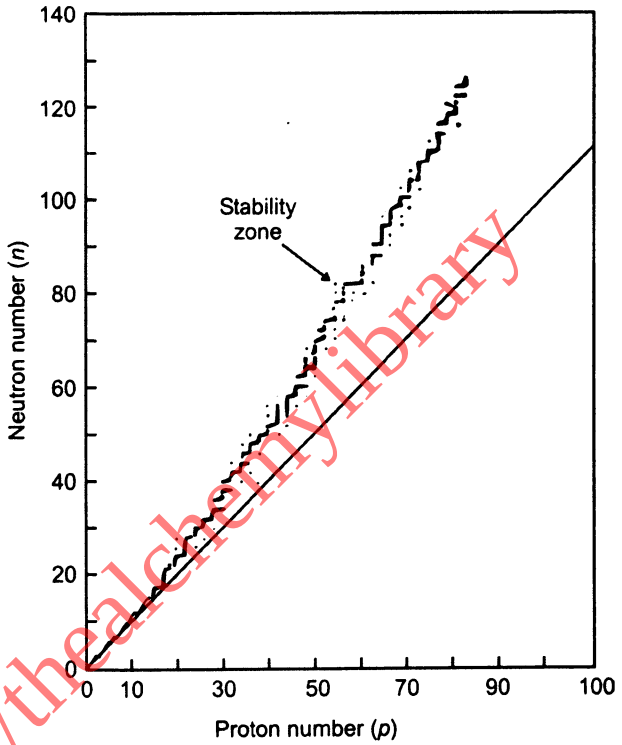

Fig. 5.3.2.1. Serge chart; neutron number (n) vs. proton number (p) (i.e. Z) for the stable nuclides.

Click Here to me/thealchemylibrary

5.3.3 The Neutron to Proton Ratio and Different Modes of Decay*

The nuclides lying below or above the stability region in Segre chart (cf. Fig. 5.3.2.1) will decay in such a way that the product nuclides can be placed in the stability region.

- **Case 1 (n/p ratio lying above the stability region) :** When the n/p ratio lies above the stability region, the unstable nuclide may decay in the following ways to decrease the n/p ratio.

(a) Beta Emission

Electrons in the β^--radiation get emitted due to the conversion of neutrons into protons as follows:

$$^{1}_{0}n \rightarrow {}^{1}_{+1}p + {}^{0}_{-1}e + {}^{0}_{0}\bar{\nu}$$

* Energetics and other characteristics of the processes are discussed in the next chapter (cf. Secs. 6.6 and 6.11).

The antineutrinos ($^{0}_{0}\bar{\nu}$) having zero mass and zero charge are considered theoretically to balance the spins, nuclear statistics, and energy (cf. Secs. 5.6 and 6.6). In this mode, the *n/p* ratio falls down. Examples are :

(i) $^{14}_{6}C\ (n/p = 1.33) \rightarrow {}^{14}_{7}N\ (n/p = 1.00) + {}^{0}_{-1}e + {}^{0}_{0}\bar{\nu}$

(ii) $^{141}_{56}Ba \xrightarrow[t_{1/2} = 18\ min]{\beta^-} {}^{141}_{57}La \xrightarrow[t_{1/2} = 3.7\ hrs.]{\beta^-} {}^{141}_{58}Ce \xrightarrow[t_{1/2} = 28\ days]{\beta^-} {}^{141}_{59}Pr$

$\frac{n}{p}$ = 1.51 1.47 1.43 1.39

In the second example, there is a series of β^- decays to produce the product nuclides progressively stabler as evident from the progressive increase of $t_{1/2}$ values along with the gradual decrease in the *n/p* ratio.

(b) Neutron Emission

Through the emission of neutrons, the *n/p* ratio can also be decreased. Though the neutron does not have any Coulombic potential barrier (cf. Fig. 5.4.3.1), due to its appreciably high nuclear binding energy (≈ 8 MeV) (cf. Fig. 5.5.1.1–2), the neutron emission takes place only in highly energetic nuclides. Examples are :

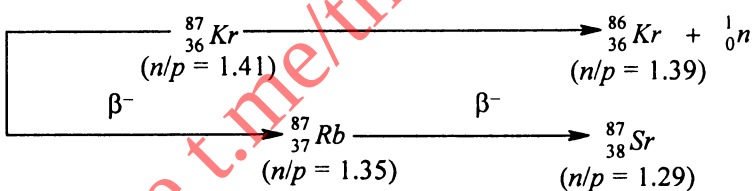

• **Case II (*n/p* ratio lying below the stability region) :** When the *n/p* ratio lies below the stability region, it may have different possible ways to decay to increase the *n/p* ratio.

(a) Positron Emission

Positrons are actually *positive electrons* and it leads to β^+-radiation due to the transformation of protons into neutrons as follows :

$$^{1}_{+1}p \rightarrow {}^{1}_{0}n + {}^{0}_{+1}e + {}^{0}_{0}\nu$$

Again the neutrino particle ($^{0}_{0}\nu$) having zero mass and zero charge is considered to balance the spin, energy and nuclear statistics as the antineutrinos are required in β^--decay (cf. Secs. 5.6 and 6.6). Positron emission from a nucleus is energy requiring (≥ 1.02 MeV) (cf. Sec. 6.11). Hence it occurs generally in relatively higher energetic nuclides. Examples are :

$$^{19}_{10}Ne\ (n/p = 0.9) \rightarrow {}^{19}_{9}F\ (n/p = 1.11) + {}^{0}_{+1}e + {}^{0}_{0}\nu;$$

$$^{11}_{6}C\ (n/p = 0.83) \rightarrow {}^{11}_{3}B\ (n/p = 1.2) + {}^{0}_{+1}e + {}^{0}_{0}\nu$$

Click Here t.me/theachemylibrary

(b) Orbital or K–Electron Capture

When sufficient energy ($\geq$ 1.02 MeV) for the positron emission is not available, the nucleus may capture an electron from the nearest shell, i.e. K–shell (less frequently L–shell), and consequently one proton gets converted into a neutron as follows: ${}^{1}_{+1}p + {}^{0}_{-1}e \rightarrow {}^{1}_{0}n + {}^{0}_{0}\nu$.

Due to the capture of an electron from the K–shell, a vacancy is created there. This vacancy is filled in by an electron jumping from the higher shells. Such transitions from the higher shells to the lower shells produce the ***characteristic X–rays.*** It may also initiate ***Auger effect*** (cf. Sec. 6.7). Examples are:

(i) ${}^{54}_{25}Mn\ (n/p = 1.16) + {}^{0}_{-1}e\ (K) \longrightarrow {}^{54}_{24}Cr\ (n/p = 1.25) + {}^{0}_{0}\nu$

(ii) ${}^{48}_{23}V \xrightarrow[(58\%)]{{}^{0}_{+1}e \text{ (positron decay)}} {}^{48}_{22}Ti + {}^{0}_{0}\nu$

K-capture (42%)

In the second example, the minimum energy (1.02 MeV) required for the positron emission is available; and in this case both the paths run parallel. *For the positron emission, the required energy is obtained due to the mass loss in the conversion,* parent nuclide $\rightarrow$ daughter nuclide (cf. Sec. 6.11).

(c) α–Emission

α–Particle emission also leads to the increase of the n/p ratio. It generally occurs for the heavy nuclides. One representative example is :

$${}^{238}_{92}U\ (n/p = 1.58) \rightarrow {}^{234}_{92}Th\ (n/p = 1.60) + {}^{4}_{2}He$$

(d) Proton Emission

Proton emission can also increase the n/p ratio, but in the proton emission, it will require an additional amount of energy (compared to the neutron emission) to cross the **Coulombic potential barrier** (cf. Fig. 5.4.3.1). Hence, this mode of decay occurs for the nuclides of very much high energy.

5.3.4 Packing Fraction and Nuclear Stability

With the development of mass spectrograph, it became possible to determine the atomic masses very precisely. Aston noticed that in most cases, there was a slight deviation from the nearest whole number (sum of the protons and neutrons) representing the mass number. The magnitude of this deviation from the nearest whole number (i.e. mass number) varies from nucleus to nucleus. This deviation was expressed in terms of packing fraction defined as follows :

$$\text{Packing fraction} = \frac{\text{nuclear mass} - \text{mass number}}{\text{mass number}} \times 10^4$$

The nuclear mass is equal to the atomic mass by ignoring the mass of the electrons, and the mass

Click Here t.me/thealchemylibrary

number is generally the nearest whole number to the atomic mass. The factor 10^4 is arbitrarily chosen to make the figure reasonable, otherwise the number becomes very small.

From the definition of packing fraction, it is found that it really expresses the loss or gain of mass per nucleon. For example, let us take the nuclide, ^{58}Ni whose mass is 57.942 amu. Here the packing fraction is given by,

$$\text{Packing fraction} = \frac{57.942 - 58}{58} \times 10^4 = -10.$$

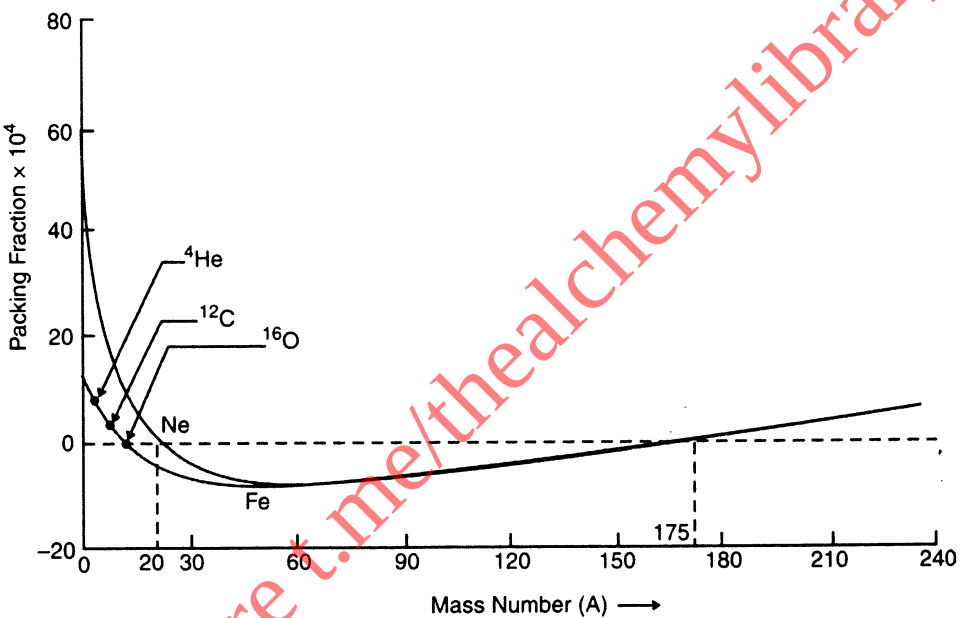

Fig. 5.3.4.1. Variation of packing fraction with mass number (A) (plotted in O-16 scale).

The variation of packing fraction for different mass numbers is shown in Fig. 5.3.4.1. It is observed from the figure that the packing fraction may be negative, positive and zero. ***Negative packing fraction means that there is a loss of mass which is converted into energy to bind the nucleons.*** **Thus the negative packing fraction stabilises the nuclides.**

In the same light, apparently the nuclides having positive and zero packing fractions should not be stable. **But some lighter nuclides having positive and zero packing fractions are known to be stable.** This apparent contradiction arises due to the consideration of mass number instead of the actual mass of the nucleons. ***The actual mass of the nucleons is always greater than the mass number.*** To clarify this point, let us take the helium nucleus whose mass is found experimentally to be 4.003 amu, but the actual mass of the constituent nucleus is : 2 × 1.0076 + 2 × 1.0089 = 4.033 amu. The actual masses of a proton and a neutron are 1.0076 and 1.0089 in amu respectively. Hence, here the actual mass loss is 0.03 units, and the packing fraction becomes :

$$\frac{4.003 - 4.033}{4} \times 10^4 = -75$$

Click Here t.me/thealchemylibrary

Similarly for all the stable lighter nuclides, there is an actual loss of mass to bind the nucleons and these are stable. Hence, to depict the true picture, the packing fraction should be defined as follows:

$$\text{Packing fraction} = 10^4 \times \frac{\text{nuclear mass} - \text{actual mass of the nucleons}}{\text{mass number}}$$

Then it will take care of loss of mass per nucleon in forming the nucleus.

Significance of the packing fraction parameter

In spite of the limitations of Aston's packing fraction, it gives some important information.

(i) **Prediction of stability region in terms of A :** If we ignore the portion of the curve for the lighter nuclides, it is seen that the curve gets a maximum negative value in the range of mass number 50 (i.e. transition elements, *Cr, Fe, Co, Ni*), and in fact such nuclides are the most stable ones and are highly abundant in nature. Again the curve becomes positive at about *Hg* ($A \approx 175$) indicating the instability of the heavier elements. This prediction also agrees with the observation. These conclusions are also supported by the consideration of nuclear binding energy (cf. Sec. 5.3.5).

(ii) **Prediction of fission and fusion :** Generally, **the nuclides having higher packing fractions** (i.e. more +ve values) **tend to move to the region where packing fraction is minimum** (i.e. most –ve values). ***This may be attained by the lighter elements through fusion and by the heavier ones through fission.*** This aspect is now verified. Presently we have a better parameter, ***nuclear binding energy,*** in indicating the stability of the nuclides. This will be discussed in the next section and it will be seen that the major conclusions drawn from the Aston's packing fraction remain unchanged.

(iii) **Interpretation of the rule of Oddo (i.e. Stability of α-particle nuclides) :** The bifurcation of the packing fraction curve for the lighter elements apparently shows a discrepancy, but it is very much meaningful. One branch contains ^4He, ^{12}C, ^{16}O while the other branch accommodates all the other lighter elements starting from ^1H to ^{20}Ne. It indicates that ^4He, ^{12}C and ^{16}O in which the mass numbers are the integral multiples of four (i.e. mass number of the α-particle) are relatively stabler (cf. ***rule of Oddo,*** Sec. 5.3.1). In fact, such nuclides are much more resistant to nuclear disintegration compared to the other neighbours. Here ^8Be is an exception. ***This is why, the α–particle is believed to act as an efficient subsidiary unit in constructing the lighter nuclides.*** This fact has also been established in the consideration of nuclear binding energy (cf. Fig. 5.3.5.1).

5.3.5 Mass Defect and Nuclear Binding Energy (NBE)

An atom ${}^A_Z X_N$ should have the mass given by the sum of the mass of the constituent particles, i.e. atomic mass = $(A - Z)m_n + Zm_p + Zm_e$, where m_n, m_p and m_e represent the mass of a neutron, a proton and an electron respectively. But, always the measured atomic mass (M) is less than the theoretically calculated value as given above. This loss of mass in the construction of the atom is called ***mass defect*** **(*D*)** defined as :

$$D = (A - Z)m_n + Zm_p + Zm_e - M = (A - Z)m_n + Zm_H - M$$

where, m_H = mass of a proton and an electron = mass of a hydrogen atom. The mass of an electron is negligibly small compared to that of the other constituent particles. Hence, the mass defect can be reasonably expressed as follows :

$$D = (A - Z)m_n + Zm_p - M.$$

Click Here for the Chemistry Library

This lost mass given by the mass defect is converted into energy according to Einstein's famous equation, $E = mc^2$ where E and m are the energy and mass converted into energy respectively. This energy is utilized in the construction of the nucleus. This gives :

$$1 \text{ amu or } 1 \text{ u} \equiv 1.66 \times 10^{-27} \text{ kg} \times (3 \times 10^8 \text{ m s}^{-1})^2 = 14.92 \times 10^{-11} \text{ J}$$

$$\approx 931 \text{ MeV}, (1 \text{ MeV} = 10^6 \text{ eV} = 1.6 \times 10^{-13} \text{ J})$$

Hence, for the mass defect, $D = \Delta m$ (expressed in amu), the nuclear binding energy (NBE) is given by: $NBE = \Delta m \times 931$ **MeV.** Very often, nuclear binding energy per nucleon, i.e. NBE/A denoted by $\overline{B}$ is considered for measuring the stability of a nucleus. Let us take some representative examples to clarify the concept.

(i) Heavy hydrogen or deuterium (^2_1H)

Atomic mass of ^2_1H = 2.0141 amu. Hence, mass defect (D) = Δm = (1.0076 + 1.0089 – 2.0141) amu = 2.4×10^{-3} amu. Hence, $NBE = 2.4 \times 10^{-3} \times 931$ MeV = 2.23 MeV. Therefore, $\overline{B} = NBE/2$ = 1.12 MeV per nucleon.

(ii) Iron ($^{56}_{26}Fe_{30}$)

Atomic mass of $^{56}_{26}Fe$ = 55.9350 amu. Hence, mass defect = Δm = (26 × 1.0076 + 30 × 1.0089 – 55.9350) amu = 0.5296 amu. Therefore, $\overline{B}$ = (0.5296 × 931)/56 = 8.80 MeV/nucleon.

The $\overline{B}$ gives a good indication for the stability of the concerned nuclides. **It is always positive whether the nucleus is stable or not. It indicates that during the construction of the nucleus, some mass is always annihilated to bind the nucleons within the nucleus.** The variation of $\overline{B}$ with the mass number is shown in Fig. 5.3.5.1 which is in fact, the reciprocal form of the packing fraction curve (cf. Fig. 5.3.4.1). The nuclear binding energy curve has got a theoretical basis in the liquid drop model (cf. Sec. 5.5.2).

Characteristic features of the nuclear binding energy curve

The following features are evident from Fig. 5.3.5.1.

(i) Light nuclides (A < 30)

The maxima for $\overline{B}$ vary periodically (cf. Fig. 5.3.5.1) for the values of A which are the integral multiples of four. These nuclides are : ^4_2He, $^{12}_6C$, $^{16}_8O$, $^{20}_{10}Ne$, $^{24}_{12}Mg$ and $^{28}_{14}Si$ which are very much stable. In this group, only ^8_4Be is an exceptional one and it actually disintegrates into two α-particles ($^8_4Be \rightarrow 2\ ^4_2He$). *Thus, the nuclides constructed by the alpha-particles as the blocking units are stabler compared to the neighbouring ones* (cf. ***rule of Oddo***, Sec. 5.3.1)..

(ii) Medium nuclides (A = 30–90)

There is a rise of $\overline{B}$ from 8.0 MeV (for A = 16) to ~ 8.30 MeV (for A = 28 – 32) and then it remains almost constant ($\overline{B}$ = 8.5 ± 0.2) up to $A \approx 90$. The region of transition metals, e.g. iron, cobalt, nickel,

Click Here t.me/thealchemylibrary

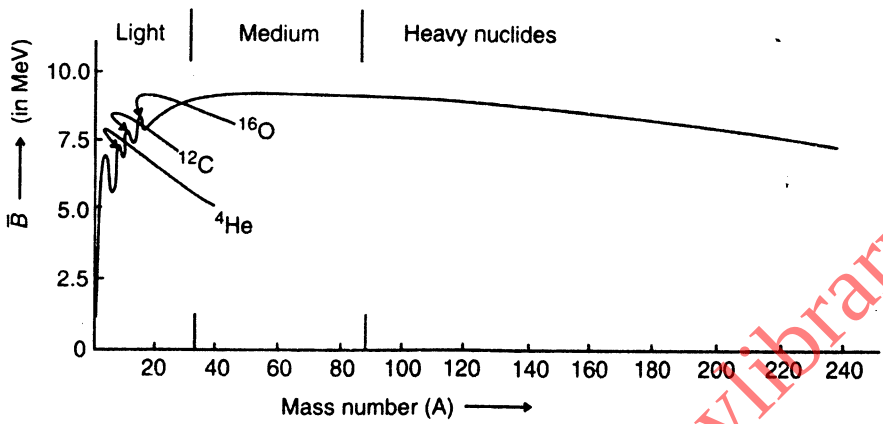

Fig. 5.3.5.1. Variation of nuclear binding energy per nucleon ($\bar{B}$) with mass number (A). Adapted from K.G. Krishnan, "Atomic and Nuclear Physics", Macmillan India Ltd., 1973. Reproduced with permission.

etc. at around A = 50–60 lies at the centre of the plateau. This range (A = 30–90) characterised by $\bar{B}$ = 8.5 ± 0.2 MeV per neucleon gives the largest zone of the most stability. **The value, $\bar{B}$ = 8.5 ± 0.2 is considered to be a diagnostic parameter in predicting the stability of the nuclides.** The nuclides having $\bar{B}$ < 8.5 ± 0.2 are considered to be relatively unstable.

(iii) Heavy nuclides (A > 90)

After zirconium, $\bar{B}$ falls down gradually from ~ 8.7 MeV to ~ 7.5 MeV at $A \approx 210$. Up to $A \approx 210$, the nuclides are stable but after this limit, the nuclides become very much unstable. ***In fact, $^{209}_{83}Bi$ is the heaviest nuclide known to be stable.***

It can be concluded that the stable nuclides ($A > 30$) possess $\bar{B}$ in the range 7.5–8.5 MeV. The nuclides ($A > 30$) having $\bar{B}$ less than 7.5 MeV are radioactive.

(iv) Nuclear fission and fusion

To obtain the maximum stability region characterised by $\bar{B}$ = 8.5 ± 0.2 MeV, the heavier nuclides undergo radioactive changes in such a way that the product nuclides may come to that stability region. **This is why, ^{82}Pb is the end product of all naturally occurring radioactive series. The stable isotopes of lead lie in the most stable region.** The heavier nuclides (e.g. $^{235}_{92}U$, $\bar{B} \approx 7.6$ MeV) undergo fission to produce the nuclides having $\bar{B} \approx 8.5$ MeV. In this process, a huge amount of energy will be released which is evident from Fig. 5.3.5.1. For example, per fission of ^{235}U atom, the energy release will be ≈ (8.5 – 7.6) × 235 MeV, i.e. 211.5 MeV. Similarly, if the lighter atoms (e.g. $^{1}_{1}H$) having low $\bar{B}$ values are fused to generate the elements having higher $\bar{B}$ values, then there will be also a release of a huge amount of energy. These aspects will be discussed separately.

It can be concluded that the nuclides will undergo changes in the directions which lead to $\bar{B}$ = 8.5 ± 0.2 MeV per nucleon.

Click Here to me/thearchemylibrary

5.4 THE NUCLEAR FORCES

5.4.1 Nature of the Nuclear Forces

In the nucleus of radius of the order of 10^{-15} m, an accumulation of a large number of positively charged protons leads to a **high repulsive potential energy.** If only this electrostatic potential were present, then the existence of no nucleus ($Z \geq 2$) would be possible. **It indicates that there are some attractive forces to counter–balance the repulsive force.** The well known attractive gravitational force is not surely operative here to solve the problem. It is of the order of $\sim 10^{-30}$ times of a proton–proton repulsion. Hence this force is too feeble to compensate the repulsive force. **Thus, the operative nuclear force is a special type of force which may prevail only within the nucleus.**

Before we speculate any theory behind the origin of the nuclear forces, we should know the characteristic nature of the forces. Then any theory proposed must comply with the following properties.

(i) ***Short range*** **:** Whatever may be the origin of the nuclear force, it operates only within the nuclear dimension. It abruptly vanishes to zero on just crossing the nuclear border. Outside the nuclear border, a simple Coulombic potential operates.

(ii) ***Charge independence*** **:** It has been observed that for the heavier stable nuclides, the proportion of neutrons compared to protons increases (cf. Fig. 5.3.2.1). Apparently, it can be inferred that in the heavier nuclides, to minimise the large number of proton–proton repulsions, it requires more neutrons which are electrically neutral. But it is not the whole story. *If it were true, nature could stabilise any heavy nuclide by introducing more and more neutrons.* But it is limited by the maximum value of the ratio $(n/p)_{max} = 1.6$.

It is believed that in the operative mechanism of the nuclear forces, protons and neutrons are indistinguishable. The charge has nothing to do with the nuclear force. **All the nucleons participate equally in the nuclear force. It indicates that all the possible interactions, viz,** *p–p*, *n–n*, *n–p*, **are equally probable and contributory after allowing for the electrostatic repulsive force between the protons.** It has been established in the mirror nuclei where replacement of a *p–p* force by a *n–n* force does not change the nuclear force except the *p–p* repulsive force (cf. Sec. 5.1.3). **Thus the nuclear force is charge independent.**

(iii) ***Saturation point*** **:** In Fig. 5.3.5.1, it has been observed that for the stable nuclides (A = 30–120) the $\overline{B}$ (= *NBE/A*, i.e. nuclear binding energy per nucleon) has got almost a constant and maximum value around 8.5 MeV/nucleon while the *n/p* ratio varies in the range from nuclide to nuclide. **It evidently indicates that the nuclear force has got a saturation limit characterised by, $\overline{B}$ = 8.5 MeV/nucleon.** This observation can roughly be compared with the phenomenon, saturation of valency.

(iv) ***Spin dependence*** **:** It has been observed that the nuclear potential developed from the inter-nucleon interactions depends somewhat on the spin state of the nucleons irrespective of their charge. This fact is well demonstrated through the existence of isomers which differ in energy due to the difference in spin orientation.

(v) ***Square well potential*** **:** The nuclear potential (V_r) developed within the dimension of the nucleus is very often referred to as square well potential which will be discussed later. It is characterised as : $V_r = 0$, $r \geq R$; $V_r = -V_0$, $r \leq R$, where R gives the radius of the nucleus. Usually, V_0 lies around 30 to 40 MeV. The negative sign denotes the attractive potential. **The depths of the**

Click Here to Join Chemistry Library

wells for neutrons and protons are appreciably different only for the heavier elements (cf. Fig. 5.5.1.2).

5.4.2 Exchange Force as the Nuclear Force

The model of exchange force among the nucleons can successfully explain all the characteristic features discussed in the previous section (cf. Sec. 5.4.1). The stabilisation due to the **exchange phenomena is a quantum mechanical consequence** as discussed in the model, particle in a box (cf. Sec. 3.5.5). **According to this theory, if an exchange interaction prevails through the sharing of some common property among the particles, then the overall energy of the system gets lowered down.** Sharing of electrons between the atoms through the covalent bond leads to the development of an exchange force giving rise to the stabilisation. Similarly, the stabilisation due to resonance or delocalisation arises due to the exchange phenomenon. Thus, the exchange phenomenon is well documented in the realm of chemical science. A similar situation may also arise among the nucleons through the exchange of some common property which may be charge, spin or position. These are discussed below.

(a) Heisenberg's Short Range Charge Exchange Force

Heisenberg first considered the charge as the common property for exchange between the neighbouring nucleons. He believed the electrons and positrons to be involved in the exchange phenomenon as follows: $n \rightleftharpoons p + electron$; $p \rightleftharpoons n + positron$ (to balance the spin, neutrinos are automatically involved). Unfortunately, Heisenberg's this concept was to be rejected, as calculations showed that such an interaction force is very much weaker compared to the actual nuclear force.

To overcome the Heisenberg's drawback, the Japanese physicist Hideki Yukawa (1935) proposed the **existence of mesons** which are now established as **π-mesons*** (or ***pions***). They may be charged (π^+ and π^-) or neutral (π^0). They are having masses lying between those of electrons and protons. Each of the π^+ and π^- mesons has the rest mass ~ $273m_e$ and a π^0 meson is having the rest mass ~ $264m_e$. They have no spin. According to Yukawa, the following inter-conversions are always going on very fast within the nucleus.

$$n \rightleftharpoons p + \pi^-,\ p \rightleftharpoons n + \pi^+;\ \text{and},\ p \rightleftharpoons p + \pi^0,\ n \rightleftharpoons n + \pi^0$$

Thus, the exchange of charged mesons explains the binding energy between the neighbouring neutrons and protons. Similarly the exchange of π^0 meson can explain the binding energy between the nucleons of each kind. The resultant attractive bindings are indicated by dotted lines as follows. ***All the interactions are supposed to be of the same strength after allowing for the Coulombic repulsive force between the protons.***

* The **meson particles** proposed by Yukawa were established by the British physicist C.W. Powel (1947) experimentally in cosmic rays. To create such a particle, it will require at least $m_\pi c^2$ (= 140 MeV) energy. This is why, it occurs only when high energy cosmic rays bombard the earth. Presently, they can be produced in laboratory by using high energy accelerators. The charged ***pions*** are having $t_{1/2} = 1.8 \times 10^{-8}$ s while the neutral pion is having $t_{1/2} = 7 \times 10^{-17}$s. Because of the very short life time of π^0 meson, it remained undiscovered up to 1950. Charged ***pions*** decay into μ-mesons (formerly called ***muons***), $\pi^\pm \rightarrow \mu^\pm$ + neutrinos/antineutrinos. The π^0 meson decays into a pair of γ rays, $\pi^0 \rightarrow \gamma_1 + \gamma_2$. The muons have rest mass $207m_e$. These do not interact with the nucleons. Another type of mesons called ***k*-mesons** or ***kaons*** are now established. It has rest mass $966m_e$ and $t_{1/2}$ very small.

Click Here to me/thealchemylibrary

$$+\pi^- \left(\begin{matrix}\rightarrow n \\ p \leftarrow\end{matrix}\right) - \pi^- ; \quad +\pi^+ \left(\begin{matrix}\rightarrow p \\ n \leftarrow\end{matrix}\right) - \pi^+ ; \quad +\pi^\circ \left(\begin{matrix}\rightarrow p \\ p \leftarrow\end{matrix}\right) - \pi^\circ ; \quad +\pi^\circ \left(\begin{matrix}\rightarrow n \\ n \leftarrow\end{matrix}\right) - \pi^\circ$$

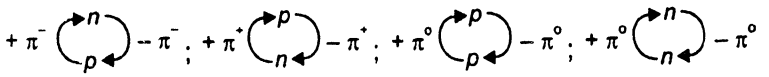

The above meson theory involving the inter-nucleon conversion can explain the requirement of a fixed n/p ratio for a particular number of p (cf. Fig. 5.3.2.1) for stability. *All the proposed inter-conversions are supposed to be governed by the principle of the first other kinetics.* Hence the rates of mutual conversion are dependent on their relative numbers. **All the conversion processes are in a dynamic equilibrium in a stable nucleus. If the number of any type of particle is arbitrarily increased, then the dynamic equilibrium will be lost and the nucleus becomes unstable. This is why, for a particular number of p, there should be a fixed n/p ratio.**

However, the **meson exchange theory** had to face a theoretical discrepancy. As the meson particles are having a finite mass, their exchange will lead to the changes of mass of the nucleons and also their energies. Thus a proton on capturing a π^- meson should increase its mass. But no such observation is noticed. Consequently, it leads to contradict the principle of conservation of mass and energy. The intelligent suggestion developed by Wick, from the Heisenberg's uncertainty principle offered a solution to this critical problem. According to him, **the exchange of a π-meson is only a virtual phenomenon.** The emitted π-meson is recaptured almost in no time (Δt), and it cannot go out of the nuclear dimension. In this situation, the life time Δt and energy change ΔE ($= m_\pi c^2$, m_π is the rest mass of the π-meson under consideration) are related through the **uncertainty principle** as follows :

$$\Delta E \times \Delta t \approx h/2\pi; \text{ or, } \Delta t \approx h/(2\pi m_\pi c^2) \approx 4.72 \times 10^{-24}\,\text{s}, (m_\pi = 273\, m_e)$$

The Δt is so small, that even if the π-meson runs with a velocity of light, it can travel only the distance, $r = c\Delta t = 1.4 \times 10^{-15}$ m = 1.4 fm. **Thus, the particle always lies within the nucleus, and its emission and recapturing go on almost incessantly. Consequently, the mass and energy of the nucleus always remain unchanged during the exchange of mesons.**

Another interesting point of the above calculation of r is that the nuclear exchange force operates only within the dimension of nuclear radius. **For the heavy nuclides, the nuclear size increases and as a result, the nuclear exchange force weakens but the electrostatic repulsive force operates. This is why, the heavy nuclides are unstable.**

- ***Mass of π-mesons and uncertainty principle*** : Let us consider a pion of mass m_π to run with a velocity u (close to c but actually less than c, velocity of light) from one nucleon to another nucleon. The emission of a pion will cause a temporary uncertainty in energy $\Delta E \approx m_\pi c^2$, (ignoring the kinetic energy of the pion).

Considering the nuclear force to operate within the range of 1.4 fm, Δt can be calculated as follows:

$$\Delta t \approx \frac{r}{u} \approx \frac{r}{c}, (r \approx 1.4 \text{ fm}, u \approx c = 3 \times 10^8 \text{ m s}^{-1})$$

Now we can write,

$$\Delta E \times \Delta t = \frac{h}{2\pi}; \text{ or, } m_\pi c^2 \left(\frac{r}{c}\right) = \frac{h}{2\pi}; \text{ or, } m_\pi = \frac{h}{2\pi r c}$$

$$m_\pi = \frac{6.625 \times 10^{-34} \text{ J s}}{2 \times 3.14 \times 1.4 \times 10^{-15} \text{ m} \times 3 \times 10^8 \text{ m s}^{-1}} = 2.5 \times 10^{-28} \text{ kg}$$

i.e. $$m_\pi = 250\, m_e$$

Thus the mass of a pion is 250 times higher than that of an electron.

Click Here t.me/thealchemylibrary

(b) Bartett's Spin Exchange Force

In this theory, only the spins between the neighbouring nucleons exchange keeping the position and charge unaltered.

(c) Majorana's Position Exchange Force

In this process, only positional coordinates (x, y, z) between the neighbouring nucleons are exchanged.

5.4.3 The Nuclear Potential and Nuclear Potential Barrier

The electrostatic force working outside the nucleus ($r \geq R$, R is the radius of the nucleus) indicates that there is a Coulomb barrier at the border line for the positively charged particles. **This electrostatic potential barrier opposes both the entry and escape of the charged particles.** On the other hand, for $r \leq R$, the nuclear exchange force becomes active and the situation is different.

Let us first concentrate ourselves on the ***electrostatic potential barrier.*** If a proton proceeds towards the nucleus having Z protons, then the developed electrostatic potential at r (where $r \geq R$) due to the nucleus is given by $Ze/(4\pi\varepsilon_0 r)$ and the corresponding Coulomb potential energy of the system containing the nucleus and the proceeding proton is given by $Ze^2/(4\pi\varepsilon_0 r)$. The variation of this Coulomb interaction with r ($r \geq R$) is shown in Fig. 5.4.3.1.

In fact, the **Coulomb barrier (E_{Coul})** for the penetration of a positively charged projectile (having $Z_1 e$ charge and radius R_1) into a nucleus (having $Z_2 e$ charge, and radius R_2) is given by :

$$E_{Coul} = \frac{Z_1 Z_2 e^2}{4\pi\varepsilon_0 (R_1 + R_2)}, \text{ in SI unit}$$

The radius is very often calculated by using the relation, $R = 1.44\ A^{1/3}$ fm (A denotes the mass number).

From the classical point of view, for the penetration of a proton into the nucleus, it must have sufficient energy to overcome the Coulomb potential barrier. Similarly, to escape a positively charged particle from the nucleus, it will also have to overcome the potential barrier. A neutron being neutral does not experience this electrostatic potential barrier either in penetration or in escaping away from the nucleus. Thus the potential barriers experienced by the neutrons and protons are different at $r > R$.

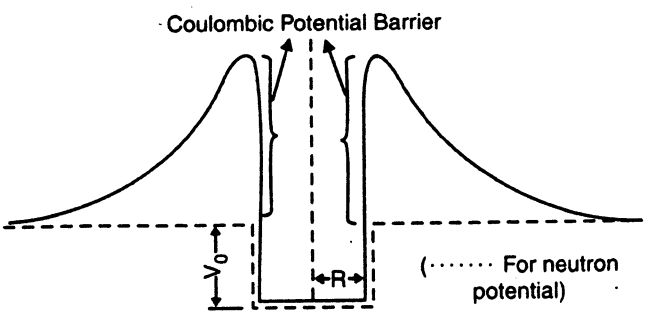

Fig. 5.4.3.1. Nuclear potential well and nuclear potential barrier.

Now, let us consider the *nuclear potential* (V_r) within the nucleus at $r \leq R$. We have already discussed that the exchange force operating within the nucleus is charge independent. Thus, the potential experienced by each of the particles, i.e. neutrons and protons, within the nucleus is identical. Different forms of potentials have been suggested but the ***model of square rectangular well potential*** is the simplest one. It is defined by:

Click Here t.me/thealchemylibrary

$V_r = 0, r \geq R$ and $V_r = -V_o, r \leq R$. The magnitude of V_o has been found of the order of 30-40 MeV. The variation of nuclear potential with r (at $r \geq R$ and $r \leq R$) is shown in Fig. 5.4.3.1. From the nature of variation, the name of the potential well is justified. Here, it is worth mentioning that the slight modifications to the perfectly square well potential concept are required to make the theory compatible with the observations. These are :

(i) The corners of the potential well are rounded so that the change $V_r = -V_0$ to $V_r = 0$ becomes more realistic (cf. Fig. 5.5.1.1).

(ii) Due to the electrostatic repulsive potential among the protons, the depth of potential for the neutrons is slightly greater compared to the depth for the protons. For the lighter elements ($Z \leq 20$), this difference is small, but for the heavier elements, the difference becomes gradually accountable (cf. Fig. 5.5.1.2). ***This is why for the stable lighter nuclides, n/p = 1 while the heavier nuclides, it is : n/p > 1.*** **This fact has been discussed in Sec. 5.5.1.**

(iii) Within the potential well, the energy levels are arranged for the nucleons. There is a Fermi-level up to which all the levels can be occupied in the ground state. **Hence to remove a nucleon, the energy required is given by the difference between the Fermi-level and the brink of the potential well.**

From the nuclear potential diagram (Fig. 5.4.3.1), it is evident that **a neutron of any energy can enter into the nucleus just like a *rolling ball on a smooth plane falling into a hole*. On the other hand, for a proton, in penetrating into the nucleus a *potential hill* is faced.** In the classical theory, its energy should be able to overcome the barrier to penetrate, but in quantum mechanics, the ***tunnel effect*** (cf. Sec. 3.5.6 and 6.12) allows the protons to penetrate the barrier even when the protons are not having the sufficient energy to cross the barrier classically.

Click Here t.me/thealchemylibrary

5.5 NUCLEAR MODELS

Construction of the nuclear models appeared as a challenging task to the scientists to rationalise the properties of the nuclides. Different models such as, Fermi gas model developed statistically, liquid drop model (Niels Bohr, 1936-48), nuclear shell model (G. Mayer, Haxel, Jensen and Suess, 1948-50), collective model (A. Bohr, son of Niels Bohr, and Mottelson, 1950-53), optical model (Feshback, Porter, Weisskopf and Saxon, 1940s) are important. The salient features of these models with special reference to the nuclear shell model will be discussed here.

5.5.1 Fermi Gas Model

The model was developed on statistical grounds. The basic principle is identical with that of Fermi gas model for conduction of electricity by the electrons in the materials. Here we shall point out the important features of this model.

(i) Concept of Energy Levels

The protons and neutrons move in an attractive potential within the nuclear dimensions. In the square well potential with the rounded corners, there are many energy levels in which the nucleons may reside. The energy levels for the protons are different from those for the neutrons.

***The nucleons follow the Pauli exclusion principle* and as a result, in each level maximum two nucleons of a particular kind with the opposite spins can reside.** The exclusion principle operates independently on each kind of nucleons because of their distinguishable energy levels.

The nucleons fill in gradually from the lower energy level to the higher level. The levels below which all the levels can be filled in at the ground state is called *Fermi level.* Fig. 5.5.1.1 shows the situation for the neutrons and a similar diagram holds good for the protons after incorporation of Coulombic potential (Fig. 5.4.3.1).

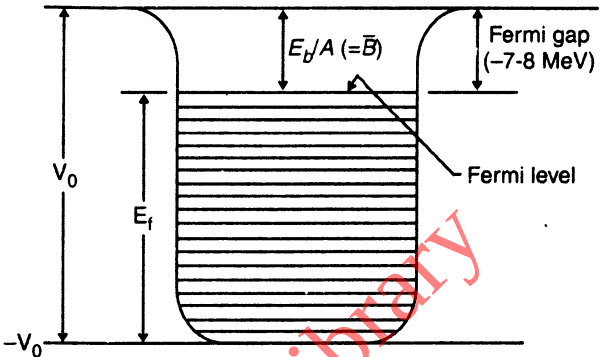

Fig. 5.5.1.1. Nuclear potential and nuclear potential barrier for neutrons.

(ii) Concept of Fermi Potential and Nuclear Potential

It gives a quantitative idea of the real potential for the ground state of a nucleus. The Fermi energy (E_f) for the neutrons is given by $E_f = (3^{2/3}\pi^{4/3}\hbar^2\rho^{2/3})/2M$, $\hbar = h/(2\pi)$ where M stands for the nucleon mass and ρ gives the nucleon density. By substitution of these values (considering the spherical nucleus) for the medium or heavy nuclides, the Fermi energy (E_f) becomes ~ 34 MeV. Actually E_f gives the height of the Fermi level. The excitation energy or binding energy ($= E_b / A = \bar{B}$), Fermi energy (E_f) and nuclear potential (V_0) are related (Fig. 5.5.1.1) as : $|V_0| = E_f + \bar{B} = 34 + 8 = 42$ MeV. **Thus, the binding energy gives the measure of energy required to withdraw a nucleon from the Fermi level to the mouth of the potential well.** It is given by $\bar{B}$ which has been found to be ~ 7-8 MeV for a large number of nuclides (cf. Fig. 5.3.5.1). More rigorous calculation shows $|V_0|$ = 50 MeV, which nicely agrees with the experimental observation. **Due to the *Coulombic repulsive potential* existent for the protons, the depth of the well is about 5 MeV less (cf. Fig. 5.5.1.2) compared to that of the neutrons for the medium of heavy nuclides.**

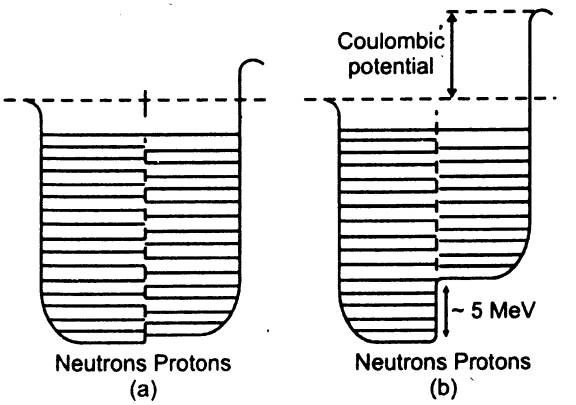

Fig. 5.5.1.2. Nuclear potential well for the neutrons and protons. (a) $n/p \approx 1.0$, (b) $n/p > 1.0$.

(iii) Tendency of Pairing among the Nucleons of Each Kind

As the interaction between the nucleons (irrespective of charge) is attractive, pairing of two protons or two neutrons which may reside in a particular level is always energetically favoured. **Thus is gives the explanation of the enhanced stability of the nuclei having even *Z* and even *N*,** (i.e. $(n + n)$, $(p + p)$, $(n + n)$... rule, cf. Sec. 5.3.1d) (Fig. 5.5.1.2).

Click Here t.me/theachemylibrary

(iv) Tendency of having N = Z for the Lighter Elements

From the Segre chart (cf. Fig. 5.3.2.1), it has been observed that for the lighter elements ($Z \leq 20$), the neutron to proton ratio is unity for the stable nuclides. From the Fermi gas model, we can have its explanation. We have already pointed out that for the lighter elements where Z is not sufficiently high, the Coulombic potential for the protons is not very much accountable compared to the nuclear exchange forces. **As a result, the depths of the potential well for the neutrons and protons are almost identical** (cf. Fig. 5.5.1.2a) **and thus the distribution pattern of the energy levels for both types of nucleons is more or less the same.** In such cases, the system gets stabilised for $Z = N$. This will lead to the highest energy levels (i.e. Fermi levels) occupied for the two kinds of nucleons to be comparable. **This is the condition for stable nuclides.** If, $N > Z$, the neutrons will have to occupy the higher energy levels and if, $N < Z$ then the protons will have to occupy the higher energy levels. Thus, for $N \neq Z$, the system gets relatively destabilised. This fact can also be established mathematically.

(v) Tendency of having N > Z for the Medium and Heavier Nuclides

Again from the Segre's chart (cf. Fig. 5.3.2.1), it is seen that for the medium and heavy nuclides the n/p ratio is greater than unity. In such cases, the Coulombic potential for the protons which opposes the nuclear forces cannot be ignored and as a result, **the potential well for the neutrons and protons become different as shown in Fig. 5.5.1.2b.** Actually the potential for the protons gets elevated ~ 5 MeV. **However, to stabilise the system, the highest energy levels (i.e. Fermi levels) occupied for the two kinds of nucleon must be comparable.** To attain this condition, the number of neutrons must be greater than that of protons.

5.5.2 The Liquid Drop Model

(a) Basic Postulates

The liquid drop model was developed by Niels Bohr and Gamow based on the following postulates compatible with a liquid drop.

(i) The protons and neutrons form an ideal homogeneous solution within the dimension of a nucleus.

(ii) The attractive forces among the nucleons are charge independent and very strong but their range is so small that each particle can only interact with its nearest neighbours only. **The attractive force is charge independent and all the interactions, i.e. *n–n*, *p–p*, *n–p*, are equivalent.**

(iii) The force being a **short range** one, saturates through the interactions only with the nearest nucleons.

(iv) Just like a liquid drop, the nucleus has got a surface tension force. The nucleons residing on the surface always experience a pull towards the centre of the nucleus because such nucleons cannot interact equally in all directions in contrast to the nucleons within the nucleus.

(iv) To explain the projectile capture nuclear reactions, it has been considered that the projectile gets captured in the target nucleus to form a ***compound nucleus.*** The excess energy of the captured projectile gets distributed throughout the drop. Thus the target nucleus gets excited. **The excited compound nucleus may de-excite in a number of ways :** (a) by radiation (cf. a liquid drop loses excess energy by radiating heat), (b) through the emission of one or more nucleons (cf. a liquid drop evaporates and here the nuclear binding energy is comparable with the heat of

Click Here t.me/thechemylibrary

vaporisation), (c) when the compound nucleus is highly excited, it may undergo splitting giving rise to two sizable fragments, i.e. nuclear fission may occur (cf. an excited liquid drop may split to form the smaller droplets).

(vi) Some small nuclides may fuse to form relatively heavier nuclides (cf. combination of a number of small droplets of mercury into a large one on a glass surface and such a fusion of droplets actually *decreases the surface area*).

(b) Calculation of Average Nuclear Binding Energy ($\overline{B}$) in the Liquid Drop Model

A number of energy factors are responsible for binding the nucleons within the nucleus. These are discussed below and developed mainly by Weizsacker.

(i) Volume energy (E_v)

It has been assumed that each nucleon can interact with its nearest neighbours only. If each nucleon-nucleon bond energy is U, then each nucleon gets a binding energy $(1/2)U$ from each bond. By considering the nucleons as incompressible spheres, within the nucleus each nucleon can interact with only 12 nearest nucleons. Thus from the 12 bonds, each nucleon gets $12 \times (1/2)U = 6U$ binding energy. Hence the total nuclear binding energy for a nucleus having mass number A is given by : $E_v = 6AU$. It is very often represented as :

$$E_v = a_v A, \text{ where } a_v = 14.1 \text{ MeV} \qquad ...(5.5.2.1)$$

E_v is called *volume energy*, as it depends on A which gives the measure of volume of a nucleus.

(ii) Surface energy (E_s)

The nucleons each residing on the surface cannot bind with 12 neighbours as discussed above. The number of such nucleons is directly proportional to the surface area. If the nucleus is having radius R, then its surface is given by :

$$4\pi R^2 = 4\pi r_0^2 A^{2/3}, (as, R = r_0 A^{1/3}; \text{ cf. Sec. 5.1.2}).$$

Therefore, the number of surface nucleons experiencing a less binding force compared to the nucleons within the bulk is directly proportional to $A^{2/3}$. Such nucleons definitely reduce the average nuclear binding energy ($\overline{B}$). Therefore, the surface energy (E_s) with the proper sign is given by :

$$E_s = -a_s A^{2/3}, (\text{where, } a_s = 13.0 \text{ MeV}) \qquad (5.5.2.2)$$

It is evident that for a large surface area, the average nuclear binding energy decreases. ***This is why, very large nuclei do not exist.*** A tendency to minimise the surface area for stabilisation is a very common phenomenon with the liquid drops.

(iii) Coulombic energy (E_c)

The proton-proton repulsion also reduces the nuclear binding energy. E_c is directly proportional to the number of pairs originated from the Z protons, and this number is given by $Z(Z-1)/2$. Again E_c is inversely proportional to the nuclear radius, $R = r_0 A^{1/3}$ (cf. Sec. 5.1.2). Therefore, E_c with the proper sign can be expressed as :

Click Here to me/tneachemylibrary

$$E_c = -a_c \frac{Z(Z-1)}{A^{1/3}}, \text{(where, } a_c = 0.60 \text{ MeV)} \qquad ...(5.5.2.3)$$

(iv) Asymmetry energy or neutron excess energy (E_a)

From the Segre chart (cf. Fig. 5.3.2.1), it is known that for the lighter elements, $N = Z$ while for the heavier elements, $N > Z$. Because of this excess neutron given by $(N - Z)$, an asymmetric distribution of the particles within the nucleus appears. In the Fermi gas model, in such cases, an asymmetric potential well gets developed (cf. Fig. 5.5.1.2). *Because of this asymmetric distribution of the nucleons, the asymmetry or neutron excess energy appears and it also reduces the nuclear binding energy.* It is given by:

$$E_a = -a_a(N-Z)^2A^{-1} = -a_a(A-2Z)^2A^{-1}, \qquad ...(5.5.2.4)$$

where $a_a = 19.0$ MeV

(v) Pairing energy (E_p)

We have already discussed that pairing between the nucleons of the same kind stabilises the system, i.e. such pairings increase the binding energy. Similarly, the unpairing leads to destabilise. Thus, if one type of the nucleons is paired, but other type is unpaired, then the net pairing energy contribution becomes zero. Here we should mention that the maximum number of unpaired nucleons in each kind is limited by unity. The pairing energy is given by $E_p = a_pA^{-3/4}$ (for even Z and even N); $= -a_pA^{-3/4}$ (for odd Z and odd N); $= 0$ (for odd A); where $a_p = 34.0$ MeV.

Therefore, the total nuclear binding energy (NBE) is given by :

$$NBE = E_v + E_s + E_c + E_a + E_p$$

$$= a_vA - a_sA^{2/3} - a_cZ(Z-1)A^{-1/3} - a_a(A-2Z)^2A^{-1} + (+1; \text{or, } 0; \text{or, } -1)a_pA^{-3/4} \qquad ...(5.5.2.5)$$

Hence, $$\overline{B} = NBE/A = a_v - a_sA^{-1/3} - a_cZ(Z-1)A^{-4/3} - a_a(N-Z)^2A^{-2} + (+1; \text{or, } 0; \text{or } -1)a_pA^{-7/4} \qquad ...(5.5.2.6)$$

The plot ($\overline{B}$ vs. A) obtained from Eqn. 5.5.2.6 is very much comparable with that one obtained experimentally (cf. Fig. 5.3.5.1). Thus it supports the validity of the liquid drop model.

Eqn. 5.5.2.5 can also be expressed in terms of mass by using the equation $E = mc^2$ (i.e. 1 amu = 931 MeV). The corresponding equation is called ***semi-empirical mass formula.*** The semi-emperical formula for the mass m_N of a nucleus is given by : $m_N = Zm_p + (A-Z)m_n - \frac{NBE}{931}$, (all the masses are expressed in amu units. NBE is obtained from Eqn. 5.5.2.5). Here it is important to mention that the constant (e.g. a_v, a_s, a_c, etc.) appearing in the semi-empirical formula are evaluated by considering the formula to explain all the observed facts. In fact, the measured nuclear masses are fitted into the equation by adjusting the constants using the least squares method.

• ***Application of the semi-empirical mass equation in β-decaying isobars*** : In the case of β-decaying series, the product nuclei are always isobaric with the parent nuclide (i.e. same A value throughout the series). In such cases, Eqn. 5.5.2.5 can be simplified as follows :

Click Here t.me/thealchemylibrary

$$NBE = D - a_c Z(Z-1)A^{-1/3} - a_a(A-2Z)^2 A^{-1}$$

$$\approx D - 0.6Z^2A^{-1/3} - 19(A^2 - 4AZ + 4Z^2)A^{-1}$$

[Taking $a_c = 0.6$ MeV, $a_a = 19$ MeV, $Z(Z-1) \approx Z^2$ when $Z \gg 1$]

$$= D' - 0.6Z^2A^{-1/3} + 76Z - 76Z^2A^{-1}$$

$$= D' - \frac{Z^2}{A}(0.6A^{2/3} + 76) + 76Z \quad \text{...(5.5.2.7)}$$

Here D and D' are constants and these depend on only A. Eqn. 5.5.2.7 indicates that the plot of NBE *versus* Z (at a particular value of A) is *parabolic* in nature. It further indicates that NBE is maximum for a particular value of Z (say Z_s). The condition is attained as follows :

$$\left[\frac{d(NBE)}{dZ}\right]_A = -\frac{2Z_s}{A}(0.6A^{2/3} + 76) + 76 = 0$$

i.e.
$$\boxed{Z_s = \frac{38A}{0.6A^{2/3} + 76}} \quad (5.5.2.8)$$

Thus for the isobaric series with $A = 180$, the stable nuclide is given by :

$$Z_s = \frac{38 \times 180}{0.6(180)^{2/3} + 76} \approx 72 \text{ (nearest integer)}$$

The corresponding stable nuclide is ${}^{180}_{72}Hf$.

• ***Application of the semi-empirical mass equation for a pair of mirror nuclei*** : In a pair of mirror nuclei (e.g. ${}^{A}_{Z}X_N$ and ${}^{A}_{N}Y_Z$) **the number of protons and neutrons are interchanged.** Thus in such a pair, $|N - Z| = 1$ is maintained. The examples are :

$${}^{3}_{1}H_2 \text{ and } {}^{3}_{2}He_1;\ {}^{7}_{3}Li_4 \text{ and } {}^{7}_{4}Be_3;\ {}^{31}_{15}P_{16} \text{ and } {}^{31}_{16}S_{15}$$

In a pair of mirror nuclei, one (p–p) force is replaced by a (n–n) force. The NBE for such a pair can be calculated as follows :

$$\left.\begin{aligned} B_1 = NBE(Z,N) &\approx D - a_c Z^2 A^{-1/3} - a_a(A-2Z)^2A^{-1} \\ B_2 = NBE(N,Z) &\approx D - a_c N^2 A^{-1/3} - a_a(A-2N)^2A^{-1} \end{aligned}\right\} \text{(taking } Z(Z-1) \approx Z^2\text{)}$$

where D terms are dependent on only A term. In the present case, the asymmetry energy terms containing the constant a_a are equal. Here :

$$A = Z + N \text{ and } |N - Z| = 1$$

$$(A-2Z)^2 = (Z + N - 2Z)^2 = (N-Z)^2 = 1$$

and,
$$(A-2N)^2 = (Z + N - 2N) = (N-Z)^2 = 1$$

i.e.
$$a_a(A-2Z)^2A^{-1} = a_a(A-2N)^2A^{-1}$$

Click Here t.me/thealchemylibrary

Thus, $\Delta B = B_1 - B_2 = a_c (N^2 - Z^2) A^{-1/3}$

$= a_c (N + Z) (N - Z) A^{-1/3}$

$= a_c A^{2/3}$, ($A = N + Z$ and $N - Z = 1$)

(c) Merits and Demerits of the Liquid Drop Model

The liquid drop model has got the following major achievements :

(i) The liquid drop model is very much important in understanding the mechanism of nuclear reactions. Specially, it is very much useful in explaining the nuclear fission and fusion reactions (which will be discussed later).

(ii) The semi-empirical mass equation obtained in the model is very much useful in understanding the nuclear binding energy per nucleon. The theoretically predicted curve runs well with that obtained practically.

In spite of the above facts, it cannot explain the following facts :

(i) The existence of magic numbers and closed shell structures for the stable nuclides.

(ii) It cannot say anything regarding the nuclear spin (I), parity and quadrupole moment which are very much important in understanding many important nuclear properties.

(iii) For the lighter nuclides where most of the nucleons reside on the surface, the semi-empirical mass equation does not work well.

(iv) The pairing effect and enhanced stabilisation for even Z and even N nuclides cannot be rationalised from the pairing energy (E_p) expression which contributes very little.

5.5.3 Nuclear Shell Model

Before we discuss the *Nuclear Shell Model*, we should discuss the *magic number* and its significance, as its discovery directed the course in the right direction to develop the model.

(a) Magic number and its significance

Existence of inert gas electronic configuration attained at $Z = 2$, 10, 18, 36, 54 and 86 is the cause of periodic classification of the elements. Similarly, the nuclear properties (e.g. stabilities, abundances, binding energy, etc.) are found to vary periodically in which the periods end with the number of protons or neutrons given by 2, 8, 20, 50, 82 or 126. These are called **magic numbers.** The numbers 114, 164 and 184 are also included in the series of magic numbers. Specially, the nuclides having these numbers of protons or neutrons or both (separately) are extraordinarily stable compared to their respective neighbouring nuclides. These members are very often called *magic numbers* and significance of the magic numbers is given below :

(i) Tendency of pairing among the nucleons of each kind

Existence of magic numbers indicates that the nucleons of each kind tend to pair (just like the electrons) among themselves. Thus, pairing among the neutrons or protons goes on for even number of nucleons in each group. This prediction is supported by the existence of $n + n$, $p + p$, $n + n$, ... rule (cf. Scheme 5.3.1.1).

Click Here t.me/thealchemylibrary

(ii) Nuclear stability

The highest stability measured by average nuclear binding energy (i.e. $\overline{B}$) is shown by the nuclides with **double magic numbers,** e.g. ${}^{4}_{2}He_2$, ${}^{16}_{8}O_8$, ${}^{40}_{20}Ca_{20}$, ${}^{208}_{82}Pb_{126}$. Similarly, the nuclides with one magic number either for the neutrons or protons are also stable compared to their neighbouring nuclides having no magic numbers. This is well illustrated by the **existence of the heaviest nonradioactive nuclide in nature** which is ${}^{209}_{83}Bi_{126}$ characterised by the magic number (126) of neutrons. Probably, **this is why $_{82}Pb$ with a magic number (82) of protons always exists as the end product of all the naturally occurring radioactive series.**

(iii) Stability island and superheavy elements

By considering the extra-stability at magic numbers, the elements having atomic numbers 114, 126, 164 should be stabler compared to their neighbours. Actually, transactinides are very much unstable. According to Seaborg, in the ***sea of instability***, there are some mountains at the very close vicinity of the elements having double magic numbers. The height of the mountains from the sea level gives the measure of stability of the island. After lead (Z = 82), the predicted *island of stability* occurs at the element ${}^{298}_{114}X_{184}$ (Z = 114, N = 184, both are magic numbers). The element is called ***'eka-lead'***. Thus the elements having atomic numbers 105-118 lying close to this island of stability are relatively stabler. In fact, some of these elements have been synthesised (cf. Sec. 7.11, synthesis of translawrencium elements) in reality to support the concept of ***island of stability***. The next island of stability occurs at the element having atomic number 164.

Seaborg's idea regarding the stability of the superheavy elements at the islands of stability may be realised in future with the further development in nuclear physics.

(iv) Abundance in nature

${}^{16}_{8}O_8$ with double magic numbers gives about 48% of the composition of the earth's crust. Other abundant nuclides in nature are also characterised by the magic numbers.

These are : ${}^{88}_{38}Sr_{50}$, ${}^{89}_{39}Y_{50}$, ${}^{90}_{40}Zr_{50}$, ${}^{118}_{50}Sn_{68}$, ${}^{138}_{56}Ba_{82}$, ${}^{139}_{57}La_{82}$, ${}^{208}_{82}Pb_{126}$, etc.

(v) Number of stable isotopes

Elements with the magic number of protons produce a large number of stable isotopes. For example (cf. Table 5.2.4.1), $_{20}Ca$, $_{50}Sn$, and $_{82}Pb$ produce 6, 10 and 4 stable isotopes respectively, but the elements with the atomic number, $Z + 1$ (Z = 20, 50, 82) are either monoisotopic or diisotopic (i.e. having two isotopes). A similar pattern also stands for isotones. For example, there are five naturally occurring isotones with N = 50.

(vi) Excitation energy

The first excitation energy of a nucleon in the nuclei having a magic number of nucleons of that particular type is very much high. **But the nuclides having nucleons just exceeding the magic number by unity show a remarkably low excitation energy for that type of nucleon.** This phenomena can be compared with the ionisation potentials of the inert gases and their immediate neighbours like alkali

Click Here t.me/tlearchemylibrary

metals. The above prediction is supported by the fact : $^{208}_{82}Pb_{126}$ (neutron separation energy, 7.40 MeV) and $^{209}_{82}Pb_{127}$ (neutron separation energy, 3.87 MeV). The neutron separation energy gives the energy required to remove the outermost neutron from the nuclear potential well.

(vii) Cross-section for neutron capture

Nuclides with a magic number of neutrons show a very small cross-section for neutron capture. This also reflects the higher stability due to the magic number. **But the nuclides running short by one neutron to attain the magic number show very large cross-sections for the neutron capture process.**

(vii) Tendency of α- and β-decay

The nuclides which can attain the nearest magic number through α- or β-decay are very much unstable while the nuclides already having the magic numbers are relatively stabler with respect to these radiations. Thus, the nuclides having already the magic numbers emit α-particles of low energy (i.e. $t_{1/2}$ high) and the nuclides to attain the magic numbers emit α-particles of high energy ($t_{1/2}$ small). These are illustrated in the following examples :

$$^{212}_{84}Po_{128} \xrightarrow[(t_{1/2} = 46\ s)]{\alpha\ (\text{long range})} {}^{208}_{82}Pb_{126},\ (E_\alpha = 8.8\ \text{MeV})$$

$$^{210}_{84}Po_{126} \xrightarrow[(t_{1/2} = 138.5\ \text{days})]{\alpha\ (\text{short range})} {}^{206}_{82}Pb_{124},\ (E_\alpha = 5.3\ \text{MeV})$$

Thus, from the concept of magic number, the **Geiger-Nuttall law** (see Sec. 6.12) can be qualitatively interpreted in some cases.

(b) Essential features in the construction of the nuclear shell model

Atoms with 2, 10, 18, 36, 54 and 86 electrons are having an extra chemical stability. Similarly, the nuclides with the magic number of neutrons or protons or both (separately) are known to exist with an additional stability. To explain the existence of magic numbers, the electronic shell structure was rightly translated in the language of nucleons within the nuclear potential well. The foundation of nuclear shell structure lies on the following considerations.

(i) Independent particle model

In constructing the shell structure of the electrons in an atom, the electrons are supposed to exist in the electrostatic field of the nucleus, while in the nucleus each nucleon is supposed to move independently of all other nucleons in an average force field produced by all other nucleons.

(ii) Concept of quantisation

If Schrödinger's wave equation is applied for a nucleon existing in a square well potential ($V_0 \approx -50$ V) with the rounded corners (to make the change, $V = V_0$ to $V = 0$, realistic), then it is found that the stationary states of the system can be characterised by the quantum numbers n, l, s. The corresponding magnetic quantum numbers bear the same significance as for the stationary states of the electrons in the atoms. Thus, the nucleons are characterised by some orbital functions dependent on the quantum numbers.

Click Here t.me/thealchemylibrary

(iii) Fermion nature of the nucleons

The statistical behaviour of the nucleons is governed by the ***Fermi-Dirac statistics*. Thus, they obey the Pauli exclusion principle.** No two nucleons of each kind (neutrons or protons) can have all the quantum numbers same in a nuclide. Thus, each orbital can be filled in with two nucleons of a particular kind with their opposite spins.

(iv) Separate shells for each kind of nucleons

The protons are having different orbitals and similarly the neutrons also do have different orbitals. In the orbitals of the protons, the neutrons cannot get accommodated, and also the reverse is true. Thus a proton always pairs with only another proton and similarly, a neutron only pairs with a neutron.

(v) Orbital representations and energy sequence

Generally, the orbitals for the nucleons are designated in the same way as in the case of electrons. For example, for l = 0, 1, 2, 3, 4, . . . the orbitals are designated as *s*, *p*, *d*, *f*, *g*, ... respectively. The principal quantum number is used as usual. For example, 4*f* means, $n = 4$ and $l = 3$.

However there is another convention to represent the orbitals. In this convention, the radial quantum number (ν) is introduced and it is related as, $\nu = n - l$. This radial quantum number takes the position of n in the former convention. Thus, for the nucleon having $n = 4$, $l = 3$, ν becomes 1 and it is designated as 1*f*.

For the sake of simplicity, in this book we shall use the first convention with which we are more familiar in connection with the orbitals of electrons.

If no spin-orbit coupling is considered, then the energy sequence becomes :

$1s < 2p < 3d < 2s < 4f < 3p < 5g < 4d < 3s < 6h < 5f < 4p < 7i < 6g < 5d < 4s$ ...

By using the notation involving radial quantum number ($\nu = n - l$) as the prefix, the orbital sequence becomes :

$$\underbrace{1s < 1p < 1d}_{(1,\,1,\,1)} \quad \underbrace{< 2s < 1f < 2p < 1g < 2d}_{(2,\,1,\,2,\,1,\,2)} \quad \underbrace{< 3s < 1h < 2f < 3p < 1i < 2g < 3d}_{(3,\,1,\,2,\,3,\,1,\,2,\,3)}$$

This sequence is helpful to memorise. But due to the inherent spin-orbit coupling, the sequence is changed. It will be discussed later.

(vi) Spin-orbit coupling and energy sequence of the nucleon orbitals

It is assumed that due to strong spin–orbit coupling for each individual nucleon, the total *angular quantum number j* (it bears the same significance as for the electrons) arises and it can have the two values, $l \pm 1/2$, as *s* can have only the value 1/2. But for $l = 0$, j can have only the positive value 1/2. **Thus, except the *s* orbital, all other orbitals are split into two sublevels characterised by $j = l \pm 1/2$.** The orbitals are designated (in terms of quantum number) as nl_j (e.g. $2p_{3/2}$, $2p_{1/2}$; $3d_{5/2}$, $3d_{3/2}$; etc.). Each orbital can accommodate maximum $(2j + 1)$ nucleons which will try to remain paired. *The sublevel having $j = l + 1/2$ has a lower energy compared to the one defined by $j = l - 1/2$.* The separation between the sublevels originated from a particular l rapidly increases with the increases of l. For the higher values of l, the energy of the $j = l - 1/2$ sublevel may be closer to that of the $j = l' + 1/2$

Click Here for more chemistry library

sublevel of the next higher l' compared to its own sublevel with $j = l + 1/2$ level. Consequently, the cross-overs may arise as shown in Fig. 5.5.3.1.

The order of filling of the nucleons is shown in Fig. 5.5.3.2.

(vii) Nuclear potential well

After invoking the idea of spin–orbit coupling, the potential well becomes an intermediate one between the square well potential and harmonic oscillator potential.

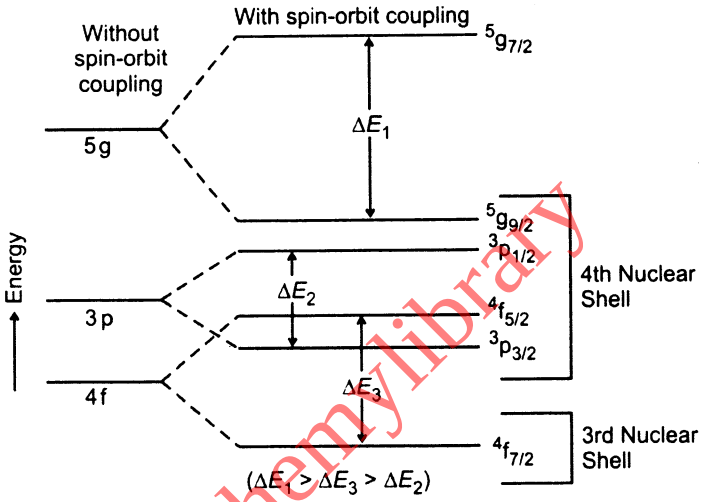

Fig. 5.5.3.1. Sequence of energy levels for the nucleons.

(vii) Nuclear configuration and nuclear spin

A particular level can accommodate maximum $2j + 1$ nucleons. The configurations for the neutrons and protons are represented separately. This is illustrated in the following examples (cf. Table 5.5.3.1). *In constructing this configuration, any rule analogous to the Hund's rule of spin multiplicity* (cf. electronic configuration) *is not maintained.* In ^7_3Li, two neutrons are placed in $2p_{3/2}$ sublevel which has a capacity to accommodate four neutrons. According to the Hund's rule, the two neutrons would remain unpaired, but these are paired as evident from the experimental nuclear spin. Closed shells are shown within the third bracket in the table.

Table 5.5.3.1. Nuclear configurations of some representative nuclides

Nuclides	*Protons*	*Neutrons*	*Nuclear spin (I) and parity*
$^6_3Li_3$	$\left[(1s_{1/2})^2\right](2p_{3/2})^1$	$\left[(1s_{1/2})^2\right](2p_{3/2})^1$	*1 +
$^7_3Li_4$	$\left[(1s_{1/2})^2\right](2p_{3/2})^1$	$\left[(1s_{1/2})^2\right](2p_{3/2})^2$	3/2 –
$^{16}_8O_8$	$\left[(1s_{1/2})^2\,(2p_{3/2})^4\,(2p_{1/2})^2\right]$	$\left[(1s_{1/2})^2\,(2p_{3/2})^4\,(2p_{1/2})^2\right]$	0
$^{17}_8O_9$	$\left[(1s_{1/2})^2\,(2p_{3/2})^4\,(2p_{1/2})^2\right]$	$\left[(1s_{1/2})^2\,(2p_{3/2})^4\,(2p_{1/2})^2\right](3d_{5/2})^1$	5/2 +
$^{27}_{13}Al_{14}$	$\left[(1s_{1/2})^2\,(2p_{3/2})^4\,(2p_{1/2})^2\right]$ $(3d_{5/2})^5$	$\left[(1s_{1/2})^2\,(2p_{3/2})^4\,(2p_{1/2})^2\right]$ $(3d_{5/2})^6$	5/2 +

* Experimental value

Note : In the nuclear potential well, interaction between the nucleons (irrespective of charge) is attractive. That is why, they always try to pair. In the case of electrons, due to mutual repulsion, they avoid pairing.

Click Here t.me/thealchemylibrary

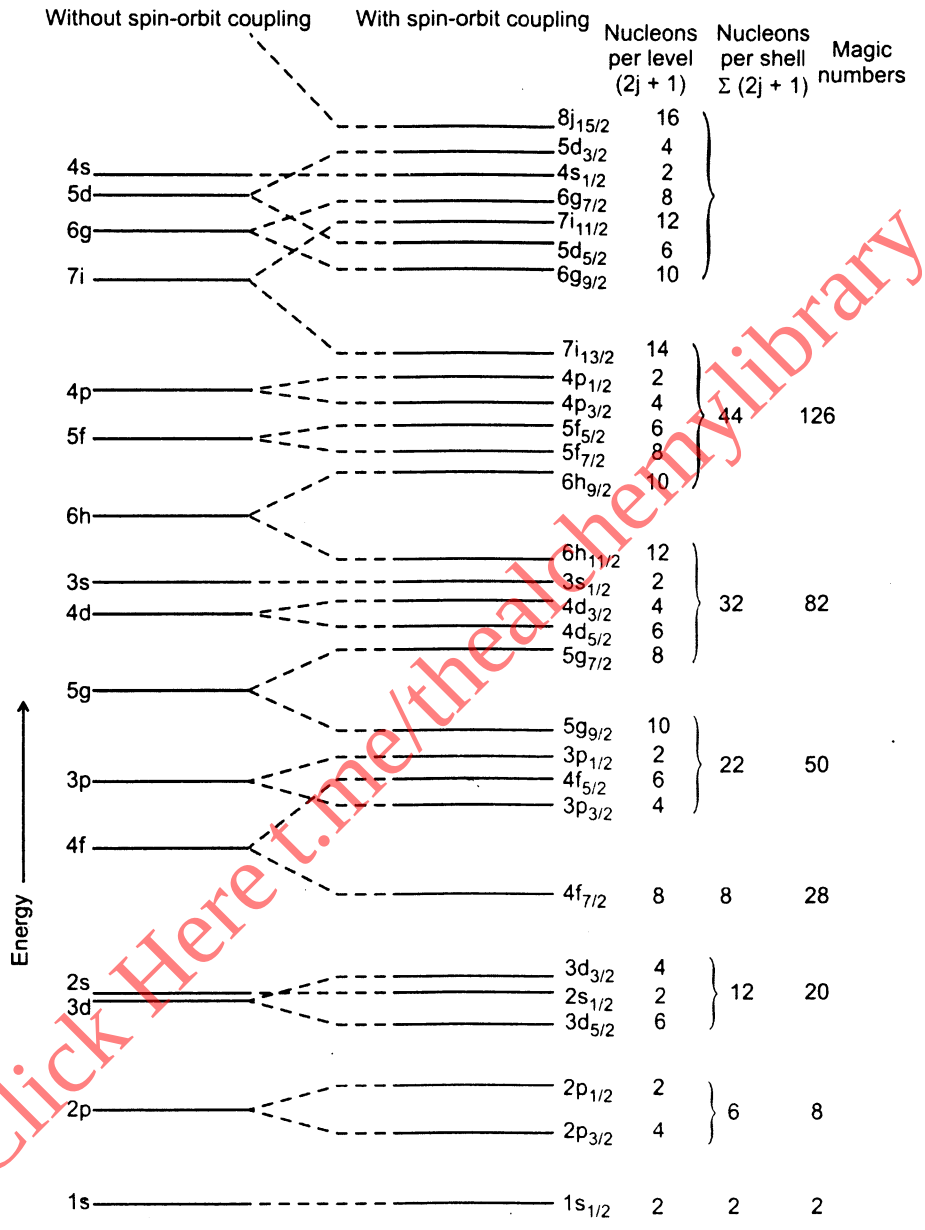

Click Here t.me/thealchemylibrary

Fig. 5.5.3.2. Sequence of filling of the energy levels by the nucleons of each kind according to shell model.

(ix) ***Determination of nuclear spin or total nuclear angular momentum quantum number (I) and parity of nuclides***

Based on the nuclear configuration, the nuclides can be classified into four groups.

(a) ***Closed shell nuclei with double magic numbers*** : The nuclides where both the protons and

neutrons are having magic numbers are extremely stable. In these cases, each kind of nucleons is paired separately and consequently $I = 0$. Examples :

$$^{4}_{2}He_{2},\ ^{16}_{8}O_{8},\ ^{40}_{20}Ca_{20},\ ^{208}_{82}Pb_{126}$$

(b) ***Nuclei having even number but not necessarily magic number of neutrons and protons*** **:** In such cases, each kind of nucleons pairs among themselves without maintaining any rule like Hund's rule giving rise to $I = 0$. Example : $^{6}_{2}He_{4}$

(c) ***Nuclei having odd A*** **:** In these cases, only one kind of nucleon is odd in number while the other kind is even in number. Thus only one nucleon (proton or neutron) remains unpaired, and j of that sublevel gives the value of I. Other kind of nucleon being paired contributes nothing in determining I.

Before we determine the *parity* of a nuclide, we should know the meaning of the term. A nucleon is of ***even*** **(+)** ***parity***, if its orbital is symmetric with respect to its sign, while a nucleon is of ***odd*** **(–)** ***parity***, if the corresponding orbital is not symmetric with respect to its sign. Thus in comparison with the symmetry of the electronic orbitals, '*g*' is equivalent to + parity while '*u*' is equivalent to – parity. Thus, the orbitals having $l = 0, 2, 4, 6, \ldots$ (i.e. *s*, *d*, *g*, etc.) denote + parity while the orbitals defined by odd l (e.g. *p*, *f*, *h*, ...) will have – parity.

In the present case, ***j* and parity of the unpaired nucleon will determine the nuclear spin and parity of the corresponding nuclide respectively.** Thus, in $^{41}_{20}Ca_{21}$, the unpaired, 21st neutron $(4f^{1}_{7/2})$ determines the nuclear spin and parity and it is 7/2 –. Examples :

$^{25}_{12}Mg_{13}$, (13-th neutron, $3d^{1}_{5/2}$), $I = 5/2$ +; $^{37}_{17}Cl_{20}$, (17-th proton, $3d^{1}_{3/2}$), $I = 3/2$ +; $^{59}_{27}Co_{32}$, (27-th proton, $4f^{1}_{7/2}$), $I = 7/2$ –.

(d) ***Nuclides having odd number of nucleons for each kind*** **:** In such cases, one proton and one neutron remain unpaired separately. In these cases, momenta of the unpaired nucleons interact to determine the spin and parity. Here it is worth mentioning that the nuclides of this group are only few. However, to determine I the ***Nordheim Rules*** are important. If $\vec{l}_p$ and $\vec{l}_n$ are the orbital angular momenta (l_p and l_n are the corresponding quantum numbers) for the unpaired proton and neutron respectively; and $\vec{j}_p$ and $\vec{j}_n$ (j_p and j_n are the corresponding quantum numbers) are their corresponding total angular momenta, then for $\vec{I}$, the corresponding quantum number I is given by :

$$I = \left| j_p - j_n \right| \qquad \text{when } (l_p + l_n + j_p + j_n) \text{ is even, and}$$

$$I = \left| j_p + j_n \right| \qquad \text{when } (l_p + l_n + j_p + j_n) \text{ is odd.}$$

The parity is even when l_p and l_n are both even or odd; and the parity is odd when l_p is even and l_n is odd or vice–versa. Examples are :

(i) $^{76}_{33}As_{43}$ (33rd proton, $4f^{1}_{5/2}$ and 43rd neutron, $5g^{1}_{9/2}$).

Here, $(l_p + l_n + j_p + j_n) = 3 + 4 + 5/2 + 9/2 = 14$ (even).

Hence, $I = 9/2 - 5/2 = 2$.

Here *f* is odd, but *g* is even. Hence the nuclear parity is odd. Thus the nuclear spin with parity of the above mentioned nuclide is given by $I = 2$ –.

Click Here t me/theachemylibrary

(ii) $^{6}_{3}Li_{3}$ (3rd proton, $2p^{1}_{3/2}$ and 3rd neutron, $2p^{1}_{3/2}$). Here, $(l_p + l_n + j_p + j_n) = (1 + 1 + 3/2 + 3/2) = 5$ (odd). Hence, $I = 3/2 + 3/2 = 3$, and parity is even, as both l_p and l_n are odd. But experimentally I is found 1 +.

Thus in general it is seen that the nuclear spin becomes :

$I = 1/2, 3/2, 5/2, 7/2...$ for odd A,

and $I = 1, 2, 3, 4...$ for odd Z and odd N.

Nuclear magnetic moments depend on I. These aspects have been discussed in Sec. 5.1.6.

Hybridisation of Nucleon Energy Levels : Spin of $^{19}_{9}F$

When two energy levels lie very closely, a nucleon from the lower filled level may move to the higher level. Mixing of such energy states may be considered as **hybridisation of nucleons.** It is illustrated for $^{19}_{9}F$ where the unpaired nucleon is the 9th proton. The proton configuration is : $[(1s_{1/2})^2 (2p_{3/2})^4 (2p_{1/2})^2](3d_{5/2})^1$ and it should have the nuclear spin and parity as $\frac{5}{2}(+)$. But experimentally it is found to be $\frac{1}{2}(-)$. It can be explained by considering the shifting of a proton from $2p_{1/2}$ level to $d_{5/2}$ level i.e. the unpaired proton resides in the $2p_{1/2}$ level.

(c) Merits of the Shell Model

Though the model does not shed any light for the excited states of the nucleus, it works well in the ground states. The merits are discussed below.

(i) ***Magic number and periodicity in the nuclides*** : In the atoms due to the filled shell of electrons at $Z = 2$, 10, 18, 36, 54 and 86, the periodicity in properties among the elements appears. Similarly due to the closed shell structure at the magic numbers, periodicities in different nuclear properties such as stabilities, binding energies, abundances, etc. arise. The shell model can nicely explain the existence of the magic numbers at 2, 8, 20, 28, 50, 82, 126.

(ii) ***Prediction of nuclear spin (I) and parity*** : We have already seen that it can nicely predict the nuclear spin and parity.

(iii) ***Nuclear quadrupole moment*** : The nuclear shell model can give an idea regarding this property which is very much important in determining the shapes of the nuclei and in understanding *NMR*, *NQR* (nuclear quadrupole resonance), etc.

5.5.4 The Optical Model

This model is useful in explaining some nuclear reactions. In explaining the Chadwick's discovery of neutron, the concept of compound nucleus formation is very much helpful. In the reaction, ^{9}Be captures the projectile α-particle to form the compound nucleus, ^{13}C which survives for an appreciable period before breaking down. Formation of such compound nuclei is possible due to the strong interactions between the target nuclei and the bombarding particles. But there are many reactions where such interactions are not sufficiently strong to allow the formation of a compound nucleus. For example, when the high energy neutrons (> 100 MeV) bombard on the target nuclei, they pass through the nuclei without showing any interaction with the nucleons existent in the target nuclei. *It is believed that the*

Click Here to the/thealchemylibrary

wavelength associated with these high energy neutrons is so small that they can easily pass through the target nuclei which behave like the semitransparent obstacles in the path of the neutron waves.

The square well potential model can only account for scattering. To explain these dual properties, i.e. **absorptive abilities** to form a compound nucleus for the low energy projectile particles, and the **transparent behaviour** to show an elastic scattering towards the high energy projectiles, the ***two term complex nuclear potential*** $U_{(r)}$, made up of a **real part** $V_{(r)}$ and an **imaginary part** $iW_{(r)}$ has been proposed as follows :

$$U_r = V_{(r)} + iW_{(r)}, i = \sqrt{-1}$$

The elastic scattering arises due to the real part $V(r)$ while the imaginary part $iW_{(r)}$ explains the absorptive properties leading to the nuclear reactions and compound nucleus formations. It is believed that the larger the value of W, the higher is the probability of projectile absorption and consequently the higher is the probability of compound nucleus formation. In other words, it can be said that the nucleus provides a homogeneous medium of complex refractive index whose imaginary part can explain the nonelastic interactions such as, absorption of projectiles, inelastic scattering, etc.

Thus, by comparing the nucleus with a transparent crystal, it is seen that the imaginary part of the potential introduces cloudiness to some extent in the nucleus which enables the inelastic interactions. This is why, the optical model is very often referred to as the ***cloudy crystal ball model.***

5.6 THE FUNDAMENTAL PARTICLES

The existence of electrons and nucleons (i.e. protons and neutrons) has been discussed so far. Besides these, a number of subatomic particles of different masses, life periods, charges and spins have also been discussed. Most of the other particles have been discovered in the interaction between matter and high energy projectiles. These are discussed below :

Antiparticles

P.A.M. Dirac predicted in 1928, from his relativistic wave mechanical model, the existence of the particle, ***antielectron*** which differs only in charge from the well–known particle, electron. Such a prediction at that time created a storm of criticism from several quarters, but it was set at rest in 1932 after the discovery of ***positron*** by Anderson. At that time, Anderson was involved in following the tracks developed in a strong magnetic field in the Wilson's cloud chamber due to the interaction of cosmic radiation with matter. Very infrequently, a pair of tracks due to a pair of oppositely charged particles was noticed. It was further confirmed that the pair of particles was originated on striking by the highly energetic cosmic radiation on matter. From other conditions, it was observed that the magnitudes of the charge and mass of the particles each were equal to those of an electron. This is why, the positive particle of the pair was named as positron. This discovery of the ***electron–positron pair*** (i.e. **pair formation**, cf. Sec. 2.6) proved the validity of Dirac's relativistic theory of quantum mechanics.

Later on, the existence of positron was found in many nuclear reactions as shown below.

$$^{10}_{5}B + {}^{4}_{2}He \rightarrow {}^{13}_{7}N + {}^{1}_{0}n,\ {}^{13}_{7}N \rightarrow {}^{13}_{6}C + {}^{0}_{+1}e;\ {}^{14}_{7}N + {}^{1}_{1}H \rightarrow {}^{15}_{8}O + \gamma,\ {}^{15}_{8}O \rightarrow {}^{15}_{7}N + {}^{0}_{+1}e$$

The positron and electron produce two γ–ray photons on annihilation (i.e. ${}^{0}_{+1}e + {}^{0}_{-1}e \rightarrow h\nu + h\nu'$).

Click Here to the chemistry library

In 1955, ***antiproton*** $(\bar{p})$ having a negative unit charge was discovered by Segre and his associates by bombarding a copper target with the protons accelerated to the energy of more than 6 billion electron volt.

In 1956, ***antineutron*** $(\bar{n})$ having opposite sign of spin compared to that of the neutron had been discovered by B. Cork and his associates. An antineutron along with a neutron is produced in a collision between a proton and an antiproton, $p + \bar{p} \rightarrow n + \bar{n}$.

Similarly, neutrino and antineutrino differ in the directions of spin.

Antinucleus : Antimatter : Antisubstance

Antinucleons (i.e. antiprotons, antineutrons) may constitute the antinucleus. Antinucleus and with suitable number of **antielectrons** (i.e. positrons) will constitute the **electrically neutral antimatter.** Thus **an antihydrogen atom** will consist of a antiproton and a positron (cf. a hydrogen atom consists of a proton and electron). Scientists have been successful in obtaining **antihydrogen, antideuteron** and **antihelium-3** for a few fleeting nanoseconds.

Antiatoms (i.e. antinucleus + adequate number of positrons) will produce antimatter i.e. anti-substance. Atoms (i.e. nucleus + adequate number of electrons) produce matter. Matter and antimatter cannot coexist. They will annihilate to release a huge amount of energy, i.e.

matter + antimatter ⟶ energy to cause the disaster

If in the universe, there is any region consisting of antimatter, the region must be separated by a long distance from the region containing matter. One may speculate the disaster, if an asteroid freed from a galaxy of antimatter collides our earth.

Click Here t.me/thedchemylibrary

Neutrino

The discovery of neutrino and antineutrino is very much important. In the β-decay, the energy of the β-particles (i.e. $\beta^{+/-}$) from a particular radioactive element is found to vary from zero to some definite upper limit. When the upper limit of energy of the emitted particle is considered, the energy lost by the nucleus equals to the kinetic energy of the β-particle. **Here, the recoil energy of the nucleus is negligibly small. Thus the *principle of conservation of energy*** is maintained only for the highest energy β-particle. But, for the β-particles of lower energy, the principle of conservation of energy is not maintained. **To explain this phenomenon, Fermi proposed the fundamental particle, neutrino or antineutrino which is emitted along with the β-particle, and the energy is distributed between the β-particle and neutrino or antineutrino.** When the β-particle stands at the maximum energy end of the spectrum, the neutrino or antineutrino possesses zero energy. In all other cases except the limiting points of the energy spectrum, the energy is distributed between the β-particles and these particles to maintain the principle of conservation of energy (cf. Secs. 6.11a, b and 6.13).

The neutrino or antineutrino has no rest mass and charge and these are just like the photons. But they possess both the energy and momentum as for the photons. **The neutrinos lacking in mass, charge and electromagnetic properties do not interact with matter.** This is why, though they are formed in many nuclear reactions, they escape away with some energies without showing any observable interaction with the surrounding matter. This is why, it was a very difficult task to detect the particles.

There was another theoretical reason to consider the existence of the particles from the stand-point

of ***conservation of spin angular momentum.*** β-emission may be considered due to the following transformations:

$$\beta^-\text{ (i.e. electron) emission : } {}^{1}_{0}n \rightarrow {}^{1}_{+1}p + {}^{0}_{-1}e + {}^{0\bar{}}_{0}\nu$$

$$\beta^+\text{ (i.e. positron) emission : } {}^{1}_{+1}p \rightarrow {}^{1}_{0}n + {}^{0}_{+1}e + {}^{0}_{0}\nu$$

where ${}^{0}_{0}\nu$ and ${}^{0\bar{}}_{0}\nu$ stand for the neutrino and antineutrino respectively. Each proton or each neutron is associated with the spin angular momentum 1/2 in the units of $h/2\pi$. **Hence to conserve the total angular momentum in the β-emission, a third particle with a spin 1/2 is to be considered.** If we ignore the formation of the third particle with a half integral spin, then the conversion of one particle of half-integral spin into two particles of half–integral spins (for each one) which can combine to form only integral spins violates the principle of conservation of spin angular momentum. This third particle is neutrino or antineutrino as proposed above.

In this connection, it is worth mentioning that to **remove the *nonconservation of statistics*,** consideration of a such third particle was also required. In β^- or β^+ decay, if such particles are not involved, the number of particles in the system increases by one. Thus an odd number of total particles becomes even after the β-decay or vice–versa. ***It leads to a change from Fermi–Dirac to Bose–Einstein statistics or vice–versa.*** It is not possible.

In 1956, C. Coen and F. Reins became successful in detecting the particle *neutrino*. When an intense beam of nuclear radiation was allowed to interact with a huge quantity of an organic liquid containing hydrogen, the simultaneous production of a neutron and a positron was believed due to the following reaction,

$${}^{0}_{0}\nu + {}^{1}_{1}H \rightarrow {}^{1}_{0}n + {}^{0}_{+1}e$$

Due to unbelievable power of the particle, i.e. ${}^{0}_{0}\nu$ (neutrino), to escape away, the possibility of the above reaction is very dim, but still a few did the reaction. **Thus, the elusive neutrino was ultimately caught and Fermi's dream got realised.**

Lastly, it should be mentioned that the neutrinos developed in the decay of $\pi^{\pm}$ mesons are different from those neutrinos obtained from β-emission.

Mesons

H. Yukawa predicted the existence of the meson particles to explain the nuclear exchange force. We have already discussed the π-mesons, μ-mesons and *K*-mesons in connection with the meson theory of nuclear forces. However, here we should remember that the neutrinos produced in the decay of $\pi^{\pm}$ mesons are different from those produced in $\beta^{\pm}$ emission.

$$\pi^+ \rightarrow \mu^+ + \nu_\mu, \text{ and } \pi^- \rightarrow \mu^- + \bar{\nu}_\mu.$$

This is why, the neutrions produced in β-emission are denoted by ν_e to differentiate from these neutrinos denoted by ν_μ.

Hyperons

There are some particles which are more massive than the protons and neutrons. These are called hyperons. They are classified into the three groups, **λ (lambda), Σ (sigma) and Ξ (xi)** particles. Some important fundamental particles are shown in Table 5.6.1 with their properties.

Click Here t.me/thealchemylibrary

Table 5.6.1. Fundamental Particles*

Class	Name	Symbol**	Spin momentum (in the unit of $h/2\pi$)	Rest Mass (in the unit of m_e)	Mean half life (in sec)
1. **Photon**	photon	γ	1	0	Stable
2. **Lepton**	e–neutrino	ν_e	1/2	0	Stable
	μ–neutrino	ν_μ	1/2	0	Stable
	electron	e^-	1/2	1	Stable
	μ–meson (i.e. muon)	$\mu^\pm$	1/2	207	2.2×10^{-6}
3. **Meson**	π-meson (i.e. pions)	$\pi^\pm$	0	273	1.8×10^{-8}
		π^0	0	264	7.0×10^{-17}
	K meson (i.e. Kaons)	K^+	0	966	8.0×10^{-9}
		K^0	0	974	$K_1^0 = 7.0 \times 10^{-11}$; $K_2^0 = 4.0 \times 10^{-8}$
	η-meson (eta)	η^0	0	1073	$\sim 10^{-18}$
4. **Baryon**	nucleons***	proton (p)	1/2	1836	Stable
		neutron (n)	1/2	1839	6.5×10^2
(Lambda)	Λ hyperon	Λ^0	1/2	2184	1.7×10^{-10}
(Sigma)	Σ hyperon	Σ^0	1/2	2333	$< 10^{-14}$
		Σ^+	1/2	2328	0.6×10^{-10}
		Σ^-	1/2	2342	1.1×10^{-10}
(Xi)	Ξ hyperon	Ξ^-	1/2	2585	1.2×10^{-10}
		Ξ^0	1/2	2571	2.0×10^{-10}
(Omega)	Ω hyperon	Ω^-	3/2	3276	$\sim 10^{-10}$

* Other particles like V–particles, Z–particles, etc. are not listed here.

** Except photon, π^0–meson, η^0–meson, all are having their antiparticles. **Generally antiparticles are denoted with bar,** (e.g. $\bar{\nu}$ stands for antineutrinos, $\bar{p}$ for antiprotons, etc.). Antiparticles are having the same mass and $t_{1/2}$ as for the particles; **antiparticles only differ either in the sign of charge or spin.**

*** The **quark particles** (Sec. 1.4) believed to constitute the nucleons are not included here.

Click Here : me/thealchemylibrary

SOLVED NUMERICAL PROBLEMS

Problem 1 : Calculate the nuclear density and atomic density in ${}_1^2H$.

Solution : In ${}_1^2H$, there is only one electron. The atomic size can be calculated by using Bohr's formula. Here $Z = 1$. Bohr's first orbit is given by :

$$r_1 = (\varepsilon_0 n^2 h^2)/(\pi m e^2 Z), \ (n = 1).$$

By using the standard values, we obtain, $r_1 = 0.529 \times 10^{-10}$ m. It gives the measure of size of the atom. Hence, atomic density $= \dfrac{\text{isotopic mass}}{\text{atomic volume}}$, where isotopic mass = mass of a proton + mass of a neutron + mass of an electron. If mass of the electron is ignored and mass of the proton and neutron are taken to be 1 amu (approximately) for each, then the isotopic mass becomes 2 amu ($= 2 \times 1.66 \times 10^{-27}$ kg). Therefore, atomic density $= \dfrac{2 \times 1.66 \times 10^{-27}}{(4/3)\pi(0.529 \times 10^{-10})^3} = 5.35 \times 10^3$ kg/m^3

The nuclear radius is given by :

$$R = 1.4 \times A^{1/3}\text{fm} = 1.4 \times 10^{-15} \times A^{1/3}\text{m}$$

Here, $A = 2$, and $R = 1.4 \times 10^{-15} \times 2^{1/3} = 1.76 \times 10^{-15}$ m

$$\text{Nuclear density} = \frac{\text{nuclear mass}}{\text{nuclear volume}} = \frac{2 \times 1.66 \times 10^{-27}\ \text{kg}}{(4/3)\pi(1.76 \times 10^{-15})^3\ \text{m}^3}$$

$$= 1.45 \times 10^{17}\ \text{kg/m}^3$$

Problem 2 : The electric quadrupole moment of $^{176}_{71}Lu$ is +7 barn. Find the ellipticity and ratio of the semimajor (b) and semiminor (a) axes of the nucleus.

Solution : By using the relation $R = 1.4 \times A^{1/3}$ fm, we get :

R (mean radius of the nucleus) of $^{176}Lu = 1.4 \times (176)^{1/3}$ fm

$= 7.84 \times 10^{-15}$ m

($1\ \text{fm} = 10^{-15}$ m)

$$R = \frac{b+a}{2}, \text{ i.e., } b + a = 2R = 2 \times 7.84 \times 10^{-15}\ \text{m}$$

$$= 15.68 \times 10^{-15}\ \text{m}$$

We have the relation :

$$Q = \frac{2}{5} Z (b^2 - a^2) = \frac{2}{5} \times 71 (b^2 - a^2)\ \text{m}^2$$

$$= 7 \times 10^{-28}\ \text{m}^2 \text{ (given)}$$

$$(1\ \text{barn} = 1 \times 10^{-28}\ \text{m}^2)$$

i.e $$\frac{2 \times 71}{5}(b^2 - a^2) = 7 \times 10^{-28}.$$

or, $$(b^2 - a^2) = \frac{7 \times 10^{-28} \times 5}{2 \times 71} = 2.46 \times 10^{-29}$$

or, $$(b + a)(b - a) = 2.46 \times 10^{-29}$$

or, $$(b - a) = \frac{2.46 \times 10^{-29}}{(b + a)} = \frac{2.46 \times 10^{-29}}{15.68 \times 10^{-15}} \approx 1.57 \times 10^{-15}\ \text{m}$$

The ellipticity (ε) is given by :

$$\varepsilon = \frac{2(b - a)}{(b + a)} = \frac{2 \times 1.57 \times 10^{-15}}{15.68 \times 10^{-15}} = 0.2$$

Solution of the equations : $b + a = 15.68 \times 10^{-15}$ m and $b - a = 1.57 \times 10^{-15}$ m gives

$b = 8.62 \times 10^{-15}$ m and $a = 7.06 \times 10^{-15}$ m and $b/a = 1.22$.

Click Here t.me/thealchemylibrary

Problem 3 : Calculate the nuclear binding energy per nucleon in $^{7}_{3}Li$, (given m_e = 0.000549 amu, m_p = 1.007277 amu, m_n = 1.008665 amu and atomic mass of $^{7}_{3}Li$ = 6.9814 amu)

Solution : Mass defect = $3m_e + 3m_p + 4m_n - 6.9814$

$= 0.00164 + 3.021831 + 4.034660 - 6.9814$

$= 7.058138 - 6.9814$

$= 0.076738$ amu.

This lost mass gets converted into the nuclear binding energy according to $E = mc^2$.

$$1 \text{ amu} = 1.66 \times 10^{-27} \text{ kg} \equiv (1.66 \times 10^{-27} \text{ kg})(3 \times 10^{8} \text{ m s}^{-1})^2 = 14.92 \times 10^{-11} \text{ J}$$

$$= 931 \text{ MeV}, (1 \text{ MeV} = 10^{6} \text{ eV} = 1.6 \times 10^{-13} \text{ J})$$

Thus, 0.076738 amu ≡ 931 × 0.076738 MeV = 71.44 MeV.

Therefore, nuclear binding energy per nucleon $(\overline{B})$ is given by :

$$\overline{B} = 71.44/7 = 10.20 \text{ MeV}.$$

Problem 4 : The nuclear binding energy per nucleon for $^{12}_{6}C$ is 7.683 MeV. The isotopic mass for $^{12}_{6}C$ is 12.00 amu. Find the mass defect and mass of six protons and six neutrons.

Solution : Total nuclear binding energy = 7.683 × 12 = 92.196 MeV.

It is known, 1 amu ≡ 931 MeV; or, 1 MeV ≡ 1/931 amu.

Thus, 92.196 MeV ≡ 92.196/931 = 0.0990 amu. Therefore, mass defect = 0.0990 amu.

We have : mass defect = mass of (six protons + six neutrons) – isotopic mass;

or, mass of the six protons and six neutrons = (12.00 + 0.099) amu = 12.099 amu.

Problem 5 : The Aston's packing fraction of $^{206}_{82}Pb$ is 2.22 amu. Determine the nuclear binding energy per nucleon in $^{206}_{82}Pb$ (given, M_H = 1.00814 amu, and mass of a neutron = 1.00866 amu).

Solution : Let us first establish a relationship between packing fraction (f) and mass defect per nucleon (= $\Delta m/A$).

Nuclear binding energy = mass defect (in amu) × 931 MeV.

Mass defect $(\Delta m) = Zm_p + Zm_e + (A - Z)m_n - M = ZM_H + (A - Z)m_n - M$;

(A = mass number, M = isotopic mass).

Aston's packing fraction is defined as : $f = \dfrac{M - A}{A} \times 10^{4}$; or, $M = A(f' + 1)$;

(assuming, $f' = 10^{-4} f$).

Hence, mass defect in terms of packing fraction is given by :

mass defect $(\Delta m) = ZM_H + (A - Z)m_n - A(f' + 1) = Z(M_H - m_n) + Am_n - A(f' + 1)$;

Hence, mass defect per nucleon is given by :

$$\frac{\Delta m}{A} = \frac{Z}{A}(M_H - m_n) + m_n - (f' + 1)$$

Click Here t.me/thealchemylibrary

In the present problem,

$$\frac{\Delta m}{A} = \frac{82}{206}(1.008140 - 1.00866) + 1.00866 - (2.22 \times 10^{-4} + 1)$$
$$= -2.0699 \times 10^{-4} - 2.22 \times 10^{-4} + 0.00866 = -4.2899 \times 10^{-4} + 0.00866$$
$$= 8.231 \times 10^{-3} \text{ amu/nucleon} \equiv 8.231 \times 10^{-3} \times 931 \text{ MeV/nucleon} = 7.66 \text{ MeV/nucleon}$$

Problem 6 : The average nuclear binding energy ($\overline{B}$) in $^{235}_{92}U$ and its fission products are 7.6 MeV and 8.5 MeV respectively. Calculate the energy liberated in the fission of 1 kg ^{235}U.

Solution : It is evident that in the fission product, the binding energy for a nucleon is greater than that in ^{235}U. The difference is (8.5 – 7.6) = 0.9 MeV per nucleon. It indicates that in the fission, 0.9 MeV energy is released per nucleon. Hence for the 235 nucleons, the released energy is given by 0.9 × 235 = 211.5 MeV (neglecting the neutrons emitted in the fission).

Thus, per fission, the liberated energy is 211.5 MeV. Therefore, per gm atom, i.e. 235 g of ^{235}U, the energy is given by : $6.02 \times 10^{23} \times 211.5$ MeV.

Therefore, 1 kg produces the energy (E) :

$$E = \frac{6.02 \times 10^{23} \times 211.5 \times 10^{3}}{235} \text{ MeV} = 5.42 \times 10^{26} \text{ MeV} = 8.67 \times 10^{13} \text{ J}.$$

($1 \text{ MeV} = 1.6 \times 10^{-13}$ J)

Problem 7 : The β-decaying nuclides form an isobaric series from $^{87}_{34}Se$ to $^{87}_{42}Mo$. Identify the most stable nuclide using the semi-empirical mass equation.

Solution : For the isobaric series, the modified equation is given by :

$$\text{NBE} = D' - \frac{Z^2}{A}(0.6A^{2/3} + 76) + 76Z, \text{ (cf. Eqn.5.5.2.7)}$$

where D' does not depend on Z and it is a function of A which is the same for the isobaric series.

For the most stable nuclide (having Z_s), NBE is maximum, i.e.

$$\frac{d(NBE)}{dZ} = 0 = -\frac{2Z_s}{A}(0.6A^{2/3} + 76) + 76 = 0$$

or,
$$Z_s = \frac{38A}{76 + 0.6A^{2/3}} = \frac{38 \times 87}{76 + 0.6 \times (87)^{2/3}}$$
$$= \frac{38 \times 87}{0.6 \times 19.63 + 76} = 37.7$$
$$\approx 38 \text{ (nearest integer)}$$

Thus the stable nuclide is $^{87}_{38}Sr$.

Problem 8 : Calculate the Coulomb barrier (E_B) for the approach of (i) a proton and (ii) an α-particle towards the nucleus $^{232}_{90}Th$.

Solution : Nuclear radius is given by : $R = 1.4\,A^{1/3}$ fm. The Coulomb potential barrier (E_B) is given by:

Click Here t.me/thealchemylibrary

$$E_B = \frac{Z_1 Z_2 e^2}{(R_1 + R_2)}, \text{(in CGS unit)}$$

$$E_B = \frac{Z_1 Z_2 e^2}{(4\pi\varepsilon_0)(R_1 + R_2)}, \text{(in SI unit)}$$

where $R = 1.4\, A^{1/3}$ fm $= 1.4\, A^{1/3} \times 10^{-15}$ m.

(a) For proton :

(In SI unit) : $E_B = \dfrac{90 \times 1 \times (1.6 \times 10^{-19}\text{C})^2}{1.4 \times 10^{-15}\left\{(232)^{1/3} + (1)^{1/3}\right\}\text{m} \times 4 \times 3.14 \times 8.85 \times 10^{-12}\,\text{J}^{-1}\,\text{C}^2\,\text{m}^{-1}}$

$$= \frac{90 \times 1 \times 1.6 \times 1.6 \times 10^{-38}}{1.4 \times 10^{-15} \times 7.14 \times 4 \times 3.14 \times 8.85 \times 10^{-12}}\,\text{J}$$

$$= 207 \times 10^{-14}\,\text{J} = \frac{207 \times 10^{-14}}{1.6 \times 10^{-13}}\,\text{MeV} \approx 13\,\text{MeV}$$

(1 MeV = 10^6 eV = 1.6×10^{-13} J = 1.6×10^{-6} erg)

(In CGS unit) : $E_B = \dfrac{90 \times 1 \times (4.8 \times 10^{-10}\ \text{esu})^2}{1.4 \times 10^{-13}\left\{(232)^{1/3} + (1)^{1/3}\right\}}$

$$= 207 \times 10^{-7}\ \text{erg} \approx 13\,\text{MeV}$$

(b) For α-particle (^4_2He):

(In CGS unit) : $E_B = \dfrac{90 \times 2 \times (4.8 \times 10^{-10}\ \text{esu})^2}{1.4\left\{(232)^{1/3} + 4^{1/3}\right\} \times 10^{-13}\ \text{cm}}$

$$= \frac{90 \times 2 \times 4.8 \times 4.8 \times 10^{-20}}{1.4 \times 10^{-13} \times 7.73}\ \text{erg}$$

$$= 383 \times 10^{-7}\ \text{erg} \approx 24\,\text{MeV}$$

(Coulombic force $\dfrac{q_1 q_2}{p^2}$; dyne $= \dfrac{(\text{esu})^2}{\text{cm}^2}$ or, dyne x cm = erg)

Problem 9 : Find out the binding energy of the last proton and last neutron in ^{12}C.

Solution : The last proton is added in the following reaction.

$$^{11}B + {}^1p \longrightarrow {}^{12}C,\ m\,(^{11}B) = 11.009305\ \text{amu},\ m\,(^1p) = 1.0078\ \text{amu}.$$

The mass loss in the reaction is given by :

$$\Delta m = [11.009305 + 1.0078 - 12]\ \text{amu} = 0.017105\ \text{amu}$$

Thus the proton binding energy is given by :

$$E = \Delta m \times 931 = 15.92\ \text{MeV}$$

Click Here to me/thealchemylibrary

The last neutron is added in the following reaction :

$$^{11}C + {}^{1}n \rightarrow {}^{12}C,\ m\ (^{11}C) = 11.001433 \text{ MeV}$$
$$m\ (^{1}n) = 1.0087 \text{ amu}$$

The corresponding binding energy (E) is given by :

$$E = \Delta m \times 931 \text{ MeV}$$
$$= (11.001433 + 1.0087 - 12) \times 931 \text{ MeV}$$
$$= 0.010133 \times 931 \text{ MeV} = 9.43 \text{ MeV}.$$

Problem 10 : Find out the neutron and proton separation energies for the nucleus $^{208}_{82}Pb$. Use the known values of isotopic masses required.

Solution : The neutron separation energy for the nucleus $^{A}_{Z}X_{N}$ is given by :

$$E_n = NBE\ (Z, N) - NBE\ (Z, N-1)$$

Similarly, the proton separation energy for the nucleus is given by :

$$E_p = NBE\ (Z, N) - NBE\ (Z-1, N)$$

The nuclear binding energy (NBE) may be obtained as :

$$NBE\ (Z, N) = \left[(A-Z)m_n + Zm_p - m(Z, N)\right] \times 931 \text{ MeV}$$
$$\approx \left[(A-Z)m_n + Zm_p + Zm_e - m(Z, N)\right] \times 931 \text{ MeV}$$
$$= \left[Zm_H + Nm_n - m(Z, N)\right] \times 931 \text{ MeV}$$

The standard values (in amu) are :

$$m_H = 1.007825,\ m_n = 1.008665,\ m(^{208}_{82}Pb) = 207.97666$$
$$m(^{207}_{82}Pb) = 206.9759,\ m(^{207}_{81}Tl) = 206.97739$$

Thus,

$$NBE\ (^{208}_{82}Pb) = [82 \times 1.007825 + 126 \times 1.008665 - 207.97666] \times 931 \text{ MeV}$$
$$= 1.75678 \times 931 \text{ MeV} = 1635.6 \text{ MeV}$$

Similarly,

$$NBE\ (^{207}_{82}Pb) = 1628.2 \text{ MeV},\ NBE\ (^{207}_{81}Tl) = 1627.6 \text{ MeV}$$

Thus,

$$E_n \text{ (neutron separation energy)} = NBE\ (^{208}_{82}Pb) - NBE\ (^{207}_{82}Pb)$$
$$= (1635.6 - 1628.2) = 7.4 \text{ MeV}$$

Click Here t.me/thealchemylibrary

$$E_p \text{ (proton separation energy)} = NBE\left({}^{208}_{82}Pb\right) - NBE\left({}^{207}_{81}Tl\right)$$
$$= (1635.6 - 1627.6)\ \text{MeV}$$
$$= 8.0\ \text{MeV}.$$

***Problem* 11 :** If the odd proton is in a *f*-orbit with its spin antiparallel to $\vec{l}$, then calculate its spin, parity and nuclear magnetic moment.

***Solution* :** For *f*-orbit, $l = 3$, $I\ (\equiv J) = l - s = 3 - 1/2 = 5/2$

Parity $= (-1)^l = (-1)^3 = -1$

Thus the spin and parity of the nuclide are given by : 5/2(–).

For the odd proton with $I = l - s$, the magnetic moment of the nuclide in nuclear magneton is given by (cf. *Schmidt Rule*) :

$$\mu = \left\{I - 2.293\left(\frac{I}{I+1}\right)\right\}\mu_N = \left\{2.5 - 2.293\left(\frac{2.5}{2.5+1}\right)\right\}\mu_N$$
$$= 0.86\ \mu_N.$$

***Problem 12* :** Calculate the NMR frequency of ${}^{31}P$ ($g_I = 2.26$, $H = 1\ T$) and ${}^{19}F$ ($g_I = 5.256$, $H = 1\ T$).

***Solution* :** $\Delta E = g_I \mu_N H$ and $\nu = \dfrac{\Delta E}{h} = \dfrac{g_I \mu_N H}{h}$

For ${}^{31}P$: $\nu = \dfrac{2.26 \times 5.05 \times 10^{-27}\ \text{J T}^{-1} \times 1\ \text{T}}{6.62 \times 10^{-34}\ \text{J s}}$, ($\mu_N$ = Nuclear magneton $= 5.05 \times 10^{-27}\ \text{J T}^{-1}$)

$= 17.24 \times 10^6\ \text{Hz} = 17.24\ \text{MHz}$

For ${}^{19}F$: $\nu = \dfrac{5.256 \times 5.05 \times 10^{-27}\ \text{J T}^{-1} \times 1\ \text{T}}{6.62 \times 10^{-34}\ \text{J s}} = 40\ \text{MHz}$

EXERCISE–V

A. General Questions

1. What are the different types of nuclear radii? How do you calculate the nuclear radius from the isobaric mirror nuclei?
2. Mention the factors responsible to determine the shape of a nucleus.
3. Classify the nuclides on the basis of number of nucleons. Mention the condition for observing the isomeric transitions (*IT*).
4. How do the isotopes influence on the line and band spectra? Mention the cases where the isotopes differ in properties.
5. What is the significance of odd–even rule in predicting the stability of the nuclides?

Click Here t.me/thearchemylibrary

6. Discuss the characteristic features of the neutron to proton ratio curve. How does the curve predict the modes of decay of the unstable nuclides?
7. Mention the major conclusions drawn from Aston's packing fraction curves. What are the limitations of the packing fraction curves?
8. What do you mean by mass defect and nuclear binding energy? Discuss the important features of the nuclear binding energy curves.
9. Discuss the characteristics of nuclear forces. What is the quantum mechanical significance of the exchange force?
10. How does the meson theory of exchange force explain the nuclear stability? Mention other types of exchange forces. How do you support the meson theory in terms of uncertainty principle?
11. Discuss the basic features of the nuclear potential well. How do the protons and neutrons behave in the potential well? What do you mean by nuclear potential barrier?
12. Discuss the basic assumptions in Bohr's liquid drop model of the nucleus. How does the model calculate the nuclear binding energy?
13. What are the magic numbers? Discuss the significance of the magic numbers.
14. Discuss the essential features of the nuclear shell model. How does the model explain the enhanced stability at the magic numbers? How do you determine the nuclear spin and parity?
15. Write down the nuclear configuration along with the nuclear spin and parity in the following cases:

$$^{17}_{8}O,\ ^{19}_{9}F,\ ^{31}_{15}P,\ ^{39}_{19}K,\ ^{64}_{27}Co,\ ^{60}_{39}Zn.$$

16. Write notes on: (i) Nuclear isomers, (ii) Quadrupole moment and nuclear shape, (iii) Segre chart, (iv) Isotope separation factor and its importance, (v) Isotope separation by chemical exchange method, (vi) Isotope effect and its significance, (vii) Szilard–Chalmer's reaction, (viii) Internal conversion and its application, (ix) Fermi level and nuclear binding energy, (x) Optical model of the nucleus, (xi) Antiparticles, (xii) Nuclear spin and parity, (xiii) Collective model of the nucleus, (xiv) Hot atom, (xv) Harkins' rule and nuclear stability, (xvi) Rule of Oddo and nuclear stability.

B. Justify the following Statements

1. Spectral study can predict the existence of isotopes.
2. The observed neutron-proton ratio ($n/p \geq 1$) for the stable nuclides can be explained nicely by considering the nuclear potential well.
3. The bifurcation of the packing fraction curve at the lighter elements furnishes a valuable information.
4. Fission of the heavier nuclides and fusion of the lighter nuclides are expected from the nuclear binding energy curve.
5. Nuclear binding energy curve is the reciprocal form of the packing fraction curve.
6. To remove a proton from a nucleus is much more energy requiring compared to the removal of a neutron.
7. The meson particles cannot escape away from the nucleus.

Click Here to the/thealchemylibrary

8. Though the depth of a nuclear potential well is ~ 50 MeV, the neutron removal energy from the well is only ~ 7.3 MeV.
9. For the lighter stable nuclides, $n/p \approx 1$, but for the heavier ones, $n/p > 1$.
10. There is no rule analogous to the Hund's rule of spin multiplicity in determining the nuclear configuration.
11. For the very fast neutrons, the nucleus is transparent while for the slow neutrons it shows some absorptive power.
12. Due to the surface energy (cf. liquid drop model), large and small nuclides become unstable.
13. Existence of neutrino was predicted theoretically much before its discovery.
14. Highest abundance of ${}^{16}_{8}O$; largest number of isotopes for ${}_{50}Sn$; ${}_{82}Pb$ as the end product of all naturally occurring radioactive series–all these can be explained by considering one common property.
15. Seaborg's stability island predicts the relatively stable superheavy element having atomic number 114.
16. Both internal conversion and β^--radiation lead to the emission of electrons, but in terms of energy spectrum of the emitted electrons, they are different.

C. Numerical Problems

1. Ordinary boron is an isotopic mixture of ${}^{10}_{5}B$ and ${}^{11}_{5}B$. Its composite atomic weight is 10.82. Find the % of composition of the mixture.
   (*Ans.* ${}^{19}B \rightarrow 10\%$, ${}^{11}B \rightarrow 81\%$).
2. Find the binding energy per nucleon in (i) ${}^{56}_{26}Fe$ whose atomic mass is 55.9571 amu, and (ii) ${}^{238}_{92}U$ whose atomic mass is 238.1252 amu (mass of a proton = 1.0081 amu, mass of a neutron = 1.0090).
   (*Ans.* (i) 8.70 MeV, (ii) 7.56 MeV).
3. Calculate the energy liberated in the reaction, $2\,{}^{1}_{2}H + 2\,{}^{1}_{0}n \rightarrow {}^{4}_{2}He$ (given, m_H = 1.0081 amu, m_n = 1.009 amu, and isotopic mass of ${}^{4}_{2}He$ = 4.004 amu).
   (*Ans.* 28.1 MeV).
4. Predict the mode of decay in the following nuclides in the light of n/p ratio.
   (i) ${}^{14}_{8}O$, (ii) ${}^{83}_{34}Se$, (iii) ${}^{66}_{29}Cu$, (iv) ${}^{228}_{88}Ra$, (v) ${}^{234}_{92}U$
5. How much energy is required in removing one neutron from ${}^{16}_{8}O$? (given : isotopic masses of ${}^{16}_{8}O$ and ${}^{15}_{8}O$ are 15.9949 amu and 15.0030 amu respectively, m_n = 1.009 amu).
   (*Ans.* 15.92 MeV).
6. From the concept of pion exchange nuclear force, calculate the approximate mass of a pion.
   (*Ans.* ~ 10^{-28} kg.)
   (Hints : $\Delta E \times \Delta t = h/2\pi$, $\Delta E \approx m_\pi c^2$,
   Nuclear dimension ($\approx 10^{-15}$ m $\approx c \times \Delta t$)
7. The electric quadrupole moment of ${}^{233}_{91}Pa$ is – 3 barn. Calculate the ellipticity and ratio of the semimajor axis (b) and semiminor axis (a).
   (*Ans.* $\varepsilon = -0.0555$, $b/a = 0.946$)

Click Here t.me/thealchemylibrary

8. Calculate the spin and pairity of $^{64}_{29}Cu$ and $^{86}_{37}Rb$ according to shell model.

   $\left(Ans.\ 1\,(+)\text{ for }^{64}_{29}Cu,\ 2\,(-)\text{ for }^{86}_{37}Rb\right)$

9. Find out the spin, parity and magnetic moment of $^{137}_{55}Cs$ and $^{83}_{36}Kr$ (assume no crossover).

   $\left(Ans.\ \frac{5}{2}(+),\ \mu = 4.8\,\mu_N\text{ for }^{137}_{55}Cs,\ \frac{9}{2}(+),\ \mu = -1.9\,\mu_N\text{ for }^{83}_{36}Kr\right)$

10. Calculate the difference of *NBE* in a pair of mirror nuclei by using the semiempirical mass equation.

    $(Ans.\ a_c A^{2/3})$

11. Find out the spin and parity of ^{19}F from nuclear shell model. Experimentally it is found $\frac{1}{2}(-)$. How do you explain this?

    $(Ans.\ \frac{5}{2}(+)$; experimental value can be explained by the concept of nucleon hybridisation; see text).

Click Here t.me/thealchemylibrary

6

Radioactivity and Radiation Chemistry

Click Here to me/thealchemylibrary

6.1 DISCOVERY OF NATURAL RADIOACTIVITY

Like many other great discoveries, the discovery of radioactivity by Henry Becquerel in 1896 was also quite accidental. At that time, Becquerel was engaged in studying the fluorescence in various compounds. It was noticed that a radiation coming from uranium salts even when coated with the thin layers of opaque materials was capable of attacking the photographic plates. Very soon it was established that the intensity of the radiation remained unchanged even in dark and was independent of the exposure to an external light. It also did not depend on the nature of uranium salts but on the presence of uranium content in the samples. Thus, the phenomenon was proved totally different from *fluorescence or phosphorescence*. This typical radiation emitted from uranium was named as ***Becquerel rays.*** Later, the term ***radioactivity*** was coined by a Polish student of Becquerel, Marie Sklodowska who became Madam Curie, the recipient of two Nobel prizes in Nuclear Science.

The Becquerel's discovery led the scientists to investigate for the possible radioactive elements occurring in nature. It was found that the radioactivity present in pitchblend, an ore of uranium was much greater than that shown by uranium itself. This observation led the Curie couple, Marie Curie and Pierre Curie to a search for the existence of new radioactive elements present in pitchblende. Finally the couple became successful to isolate two new radioelements, one ***polonium,*** named after Marie's native country and the other ***radium similar to barium.*** The most interesting aspect of this discovery is that the couple did the task almost without any financial assistance but with the firm belief and dedication. They had only a shed with a simple electroscope designed by Pierre himself for differentiating the active fraction from the rest. They had to take a prolonged painstaking toil to isolate the elements ***which were not more than a few milligrams in a tonne of the ore.*** By taking the help of ***carrier technique*****, polonium was separated as a sulphide along with bismuth sulphide and radium was crystallised (i.e. isomorphously coprecipitated, cf. carrier technique, Sec. 14.17.3) as radium chloride along with barium chloride.** Here it is worth mentioning that not the discovery of the radioelements but the way of searching stands as a milestone to all generations in the history of science.

Besides the Curies in France, many laboratories throughout the globe joined to explore the field. The works of Schmidt in Germany; Soddy, Rutherford and Ramsay in England were noteworthy.

The phenomenon of spontaneous emission of powerful penetrating radiations (which are not influenced by any external factors) from some heavy elements (not always heavy elements) is called ***natural radioactivity***, and such elements are called ***naturally occurring radioactive elements.***

6.2 TYPES OF RADIOACTIVE EMANATIONS

From the behaviour of the radioactive emanations in a magnetic or electric field, they are found to consist of three types of radiations. (i) **α–Rays,** *a soft radiation consisting of positively charged particles, easily absorbed by matter.* (ii) **β–Rays***, *a more penetrating radiation consisting of negatively charged particles.* (iii) **γ–Rays,** *a highly penetrating and electrically neutral radiation.*

Existence of the three types of radiation was experimentally verified. A small amount of a radioactive material was placed in a cavity of a lead block (see Fig. 6.2.1a) and a photographic plate was placed at a short distance above the block. The whole arrangement was kept in an airtight chamber. In the absence of any external magnetic field, the radiation attacks the plate at a particular point in a line with the channel which collimates the radiation into a narrow beam. *When a magnetic field is applied in a direction perpendicular to the plane of the figure, three darkened spots instead of a single spot are obtained.* Here, one point remains undeviated while the other two points get deflected in opposite directions depending on their nature of charge. The radiation which remains undeflected is uncharged and called γ-radiation. If the magnetic field is directed from top to the bottom (see Fig. 6.2.1a), the positively charged beam (i.e. α-rays) gets deflected to the left side according to Fleming's left hand rule. The radiation consisting of positively charged particles is called *α-rays*, while the radiation bearing the negatively charged particles is called *β-rays*. By using an electric field (see Fig. 6.2.1b) in place of a magnetic field, the α-rays are found to deflect towards the negatively charged plate and the neutral γ-radiation remains undeflected.

Click Here t.me/thealchemylibrary

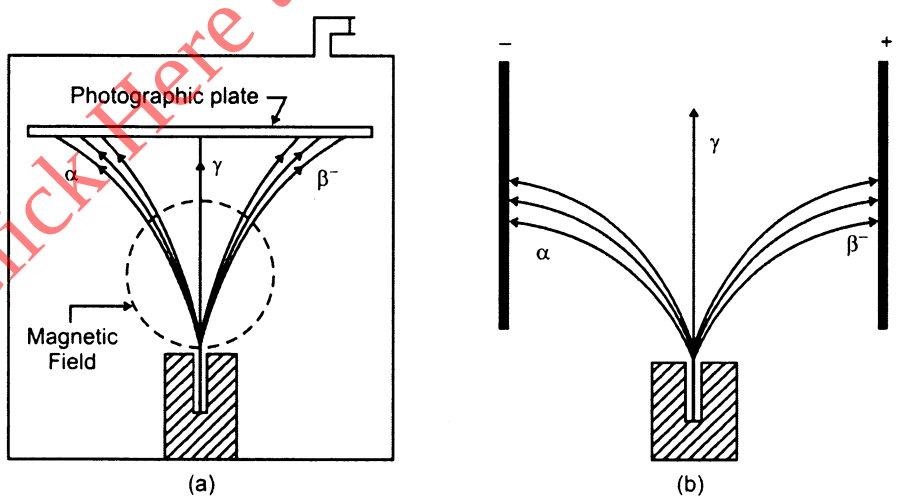

Fig. 6.2.1. Splitting of radioactive emanation in the presence of an external magnetic field (a); and electronic field (b).

* To differentiate from the **positron particles** which are represented by β^+, the negatively charged **beta particles** should be represented by β^-. But if no sign is given, then it indicates β^-.

6.3 PROPERTIES OF ALPHA, BETA AND GAMMA RADIATIONS

6.3.1 Alpha (α)-rays

(i) ***Nature*** : From the direction of deflection in an electric or a magnetic field, the particles are found to be positively charged. From the deflection, its q/M (i.e. charge to mass ratio) is found to be 5×10^7 C/kg. From the experiments of Rutherford and H. Geiger, its charge (q) is found 3.2×10^{-19} C which is almost double the charge carried by an electron. From these, its mass (6.64×10^{-27} kg) is found to be almost four times that of a hydrogen atom. Thus it appears that an α-particle is a doubly charged helium atom.

The indistinguishability between an α-particle and a doubly charged helium atom was further confirmed experimentally. In the experiment, a small quantity of purified radon gas known to give α–radiations was placed in a thin walled tube which is surrounded by an outer tube called *spectrum tube* having an arrangement for electric discharge (see Fig. 6.3.1.1). At the beginning of the experiment, the spectrum tube was made completely evacuated, then after two days, spectroscopic examination of the gas accumulated in the spectrum tube was carried out after passing an electric discharge. It indicated the existence of helium gas accumulated in the outer tube, i.e. spectrum tube. In a separate experiment, it was shown that when helium gas was kept in the inner tube instead of the α-particle radiating material, *helium gas could not penetrate the walls of the tube to appear in the spectrum tube, but the α–particles can pass the barrier*. Thus the existence of helium in the spectrum tube was due to the penetration of the α-particles coming from radon. Thus the identity of the particles was experimentally confirmed.

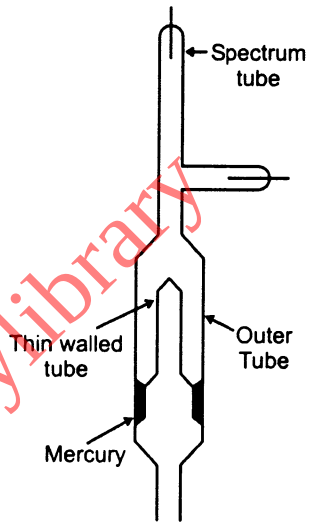

Fig. 6.3.1.1. Experimental verification of indistinguishability between α-particles and helium nucleus.

In many ores having heavy radioelements, trapped helium gas is found. In clevite (an ore of uranium) and monazite (an ore of thorium), very often helium gas is found trapped. It is due to the fact that the α-particles radiated from the elements accept electrons from the surroundings to form helium gas.

This helium gas gets mechanically trapped in the ores. **In the hot spring of Bakreswar in India, the presence of helium gas indicates the existence of α-active radioelements in its source.**

(ii) ***Velocity and range*** : The initial velocity of the α-particles emitted depends on the nature of the radioelements. It is found to vary in the range $(1.4 \text{ to } 2.2) \times 10^7$ m s^{-1}. For a particular source, all the particles are of almost the same velocity. The **range of the particles,** i.e. the distance through which they can travel before to lose their capacity to ionise the medium, depends on the nature of their source. The range of the particles can be easily measured and the knowledge of the range provides more information regarding the nucleus (see Sec. 6.12 (iii)).

(iii) ***Stopping power of a medium*** (see Secs. 6.12; 6.18.2c) : Though the α-particles can travel several centimetres in air, most of the particles can be stopped by using a thin sheet of aluminium and

Click Here to me/thealchemylibrary

even by a paper of ordinary thickness. The stopping power of matter depends on its atomic weight and density. Stopping power generally increases with the increase of atomic weight. *Actually, during the collision between the α-particles and the atoms of the absorber, the electrons from the atoms are knocked out and thus the energy of the α-particle is lost.*

(iv) ***Energy of the α-particles*** **:** The kinetic energy $\left(=\frac{1}{2}mu^2\right)$ of an α-particle again depends on the velocity (u) which varies from source to source. The α-particles obtained from different naturally occurring sources are found in the range of 4 to 10 MeV. However, the energy of the particles can be increased by using accelerators.

(v) ***Ionisation of air*** **:** An α-particle on its path collides with the molecules and atoms and knocks out the electrons to produce the ion–electron pairs. In this process, the energy of the α-particle is gradually lost and it falls down to a critical value below which no further ionisation is possible. In Wilson's cloud chamber, the tracks of the α-particles are observed due to their ionising power. **The α-tracks are shorter but straight.**

(vi) ***Fluorescence*** **:** The α-particles on being incident on *ZnS*, produce flashes. This phenomenon is utilised in the apparatus, *spinthariscope*, in which the α-particles strike on a screen coated with a *ZnS* layer. Each flash is mechanically observed through a lens and counted.

(vii) ***As projectiles in nuclear reactions*** **:** The α-particles are found very much effective as projectiles in carrying out many nuclear reactions.

(viii) ***Scattering of α-particles*** **:** The α-particles are scattered when they pass through a thin sheet of gold or silver (see Rutherford's experiment, Sec. 1.7).

(ix) ***Attacking the photographic plate*** **:** The particles can attack the photographic plates.

6.3.2 Beta (β)-Rays

(i) ***Nature*** **:** The β^--particles are nothing but high energy electrons. This is supported from its deflection pattern in an external magnetic or electric field. Here it is worth mentioning that the β^--particles are always associated with the antineutrinos, as the β^--particles and antineutrinos are simultaneously produced in the same reaction : ${}^1_0n \rightarrow {}^1_1p + {}^0_{-1}e + {}^0_0\bar{\nu}$.

(ii) ***Velocity*** **:** The initial velocities of the β^--particles are different for different sources. **Even for a particular source, all the β^--particles are not monoenergic, i.e. of the same energy** (*difference with the α-particles*). In fact, from a given source, the β^--particles show a distribution of energy from zero to a certain maximum value, E_{max}. **Actually, the energy is distributed** (see Sec. 6.11a, b) **between the antineutrino and the β^--particle ejected.**

The velocity of the β^--particles for a particular source may vary from zero to about that of light but surely less than that of light. Thus when the velocity (u) is very high, the kinetic energy is calculated by considering the relativistic corrections :

$$E_{\beta^-} = \frac{1}{2}mu^2; \text{ where } m = m_0\,(1 - u^2/c^2)^{-1/2}$$

In general, the velocities of the β^--particles are much higher than those of the α-particles.

(iii) ***Range*** **:** Though the β^--particles move with a high velocity, on account of their very small mass, on collision with the molecules or atoms of the absorber, they get easily deflected. **This is why,**

Click Here t.me/theachemylibrary

the β^--particles very often travel in a zigzag (*difference with the α-particles*) **while the α-particles travel in a more or less straight line** (see Fig. 6.3.2.1) **because of their high momentum.** This is why, it is very difficult to measure the exact length or range of the β^--particles.

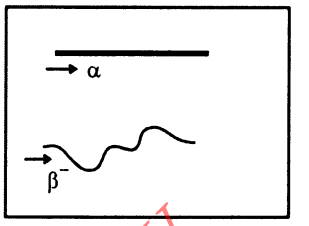

Fig. 6.3.2.1. Tracks of α- and β^--particles in Wilson's cloud chamber.

(iv) ***Penetrating power*** **:** The penetrating power of the β^--particles is greater than that of the α-particles. The highly energetic β^--particles can penetrate several mm thickness of an aluminium sheet (*difference with the α-particles*).

(v) ***Attacking the photographic plate*** **:** The β^--particles affect the photographic plates more strongly than the α-particles.

(vi) ***Interaction with matter*** **:** (a) *Absorption of β^--particles by matter*: The β^--particles may be simply absorbed by the absorbing material. (b) *Ionisation of the matter* : Like the α-particles, the β^--particles can also produce ion pairs on their tracks, but the ionising power is very much less compared to that of the α-particles (*difference*). (c) *Scattering the β^--particles* : Because of the low momentum, the β^--particles may be deflected and scattered by the absorbing material.

(vii) ***Fluorescence*** **:** The β^--rays can produce fluorescence on barium platinocyanide, calcium tungstate, willemite, etc.

(viii) ***Isobaric relationship*** **:** The product and parent nuclides are isobaric. This is also true for β^+ decay and *electron capture process*.

6.3.3 Gamma (gamma) Rays

(i) ***Nature*** **:** It is electrically neutral. It is an electromagnetic wave and similar to X–rays. It consists of photons and travels with the velocity of light. The wavelength lies in the range 10^{-4} to 10^{-1} nm. In comparison with the X–rays, it is worth mentioning that ***the origin of the X–rays is an extra-nuclear phenomenon while for the γ-rays it is an intra–nuclear phenomenon. The*** gamma–rays are emitted when the nucleus comes down from a higher energy state to some lower energy state. With the emission of α- or β^--particles, the product nuclei are very often in excited states, and in returning to the ground state, the γ-rays are emitted. Besides this, in isomeric transitions (*IT*), the γ-rays are also given out.

(ii) ***Interaction with matter*** (see Sec. 6.18) : This high energy electromagnetic radiation interacts with the electrons bound to the atoms of the interacting matter. *They lose a large fraction or total energy in a single encounter.* ***This is why, the term, range is not defined for the γ-rays.*** For the γ-rays of energy in the range 0.1 to 25 MeV, the following three interactions are important.

(a) ***Photoelectric effect*** **:** This process is important for the γ-photons of low energy. In this process, the total energy of the striking γ-photon is utilised in ejecting an orbital electron from an atom of the interacting matter. The kinetic energy of the ejected photoelectron is determined by the difference of the energy of the incident γ-photon and the binding energy (i.e. work function) of the electron to the atom. This phenomenon has been discussed in detail in Sec. 2.4. Thus the vacancy caused in the orbital may lead to X–ray generation or ***Auger effect*** (see Sec. 6.7).

(b) ***Compton effect*** **:** In this process, the striking γ-photon spends a fraction of its energy in a collision with an electron. The photon scatters with a higher wavelength in a new direction

Click Here to me/thealchemylibrary

while the electron recoils with a higher energy. This new photon with a lower energy may initiate a further photoelectric or *Compton effect*. For the Compton effect, the γ-rays of medium energy in the range 0.5 to 1.0 MeV are important. This interaction has been discussed in detail in Sec. 2.5.

(c) ***Positron-electron pair formation*** : For the γ-photons of energy greater than 1.0 MeV, this process becomes important. In the region of nucleus of the interacting matter, the energy of the γ-photon gets converted to produce the particles, positron and electron, and the residual energy of the photon imparts kinetic energy ($= E_{e^{+/-}}$) to the particles of the pair. The energy is conserved as :

$$E = h\nu = 2m_0c^2 + E_{e^-} + E_{e^+}$$

where, m_0 stands for the rest mass of the particle, i.e. electron or positron. The threshold energy 1.02 MeV is related as : 1.02 MeV = $2m_0c^2$. This phenomenon, pair formation has been discussed in detail in Sec. 2.6.

In contrast to the charged particles, i.e. α and β^--particles, which lose their energy in the interaction with matter through several steps, the γ-rays perform the task generally in a single step.

(iii) ***Diffraction*** : Like the X–rays, the γ-rays may be diffracted by the crystals.

(iv) ***Attacking the photographic plate and fluorescence*** : The γ-rays can affect the photographic plates more intensely than the α- and β^--rays. They can also produce fluorescence on suitable substances.

6.3.4 Comparison among the Different Radioactive Emanations

Some important properties of the three types of rays are tabulated here.

	Property	*α-ray*	*β⁻-ray*	*γ-ray*
1.	Nature	Positively charged particle	Negatively charged particle	Electromagnetic radiation like X–rays*** but of much shorter wavelength even compared to the hardest X–rays
2.	Mass*	6.64×10^{-27} kg (per particle)	9.10×10^{-31} kg (per particle)	Massless
3.	Charge** (in the unit of electronic charge)	+2	–1	Neutral
4.	Velocity	$(1.4–2.2) \times 10^7$ m s^{-1} (depends only on source)	0–99% of the velocity of light (depends on source; even for a particular source, the β^-–particles can cover a range)	Velocity of light
5.	Penetrating power (maximum)	0.002 cm thickness of an aluminium foil	0.02 cm thickness of an aluminium foil	5 cm thickness of a lead foil; $\gamma > \beta^- > \alpha$
6.	Ionising power in a gas	Very high	Less compared to the α-rays	Negligible; $\alpha >> \beta^- >> \gamma$

Click Here t.me/thearchemylibrary

7.	Attacking the photographic plate	+ ve	+ve	+ ve
8.	Momentum and cloud chamber tracks	Very high; this is why they are not deflected during collision and the tracks are straight	Not very high; they are deflected during collision and the tracks are zigzag	Zero, as massless; short and crooked tracks

* 1 Atomic mass unit = 1u or 1 amu = 1.66×10^{-27} kg.

** Multiple of elementary charge 1.609×10^{-19} C.

*** *X*- and γ-rays cover different portions of the electromagnetic spectrum. The origins of the two are also different. *X*–rays are produced due to some **extra–nuclear phenomenon** while the γ-rays are originated due to some **intra-nuclear phenomenon.**

6.4 DETECTION AND MEASUREMENT OF RADIOACTIVITY

The detection of nuclear reactions is a very difficult task. The dimension of the nuclear particles is too small to be imagined. As a matter of fact, if a typical nuclear particle is magnified about 10 billion times, then it only comes to the sense of our naked eyes. Regarding weight, six hundred million billion nuclear particles (i.e. neutrons and protons) weigh only about an ounce. How small they are! But, still we have so sensitive devices that with the help of which we can follow the motion of each particle and its interaction with the surrounding matter. Here we shall discuss some important devices with their operating principles.

Click Here t.me/thealchemylibrary

(a) The Electroscope

The basic units (see Fig. 6.4.1) are : (i) an ionisation chamber, and (ii) an electroscope box. Both the units are kept in a lead chamber. The electroscope box contains a thin gold leaf electroscope. The ionisation chamber contains two parallel plates (P_1 and P_2) between which the gas which is to be exposed to the radioactive emanation is kept at a low pressure. The upper plate P_1 is insulated and connected to the electroscope while the lower plate is earthed through the wall of the chamber. The radioactive material is kept on the plate P_2.

When the electroscope is charged, the gold leaf is pulled apart. When the nuclear radiation emanates, it ionises the surrounding air, and the ions pass into the electroscope chamber and consequently the gold leaf falls. The rate at which the leaf falls gives the measure of the intensity of the radiation.

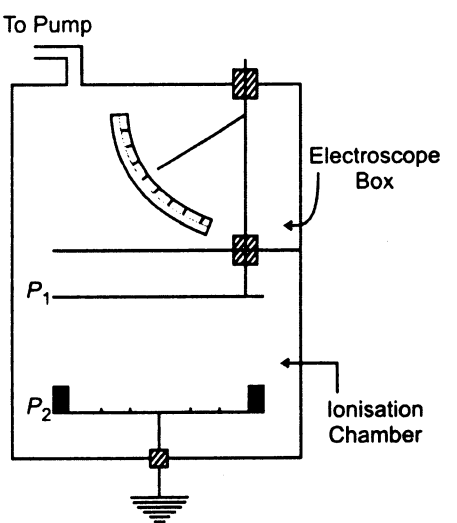

Fig. 6.4.1. Schematic representation of an electroscope.

(b) Parallel Plate Ionisation Chamber

In this method, two parallel metallic plates (P_1 and P_2) are fixed in a box (B) as shown in Fig. 6.4.2. Electrical potential can be applied between the plates by using the battery (E) as shown. If the nuclear radiation enters into the box through the window (W), then the air or gas kept in the

box gets ionised. The ions then move towards the respective electrodes and a small current produced can be recorded by the voltameter (V) placed in parallel with the resistance R. The small pulse can be amplified by using a vacuum tube amplifier. The intensity of current gives the measure of intensity of the radiation.

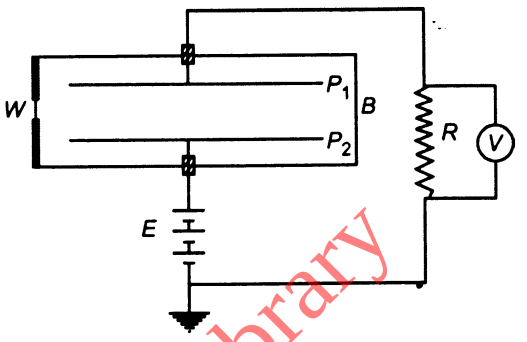

Fig. 6.4.2. Schematic representation of a parallel plate ionisation chamber.

(c) The Proportional Counter (i.e. the Cylindrical Plate Counter)

For the nuclear radiation of poor ionising power, the height of the electrical pulse produced is very small. The height of the pulse can be increased by increasing the electrical potential difference between the plates. When the electrical potential is very high, the ions produced at the ***primary process*** move towards the respective electrodes with a high kinetic energy. These high energy ions on collision with the surrounding gases are capable of producing new ion pairs. These are called ***secondary ions*** and the phenomenon is called ***gas multiplication*** measured by the ***gas multiplication factor***, m which indicates that each ion pair produced at the primary process leads to the generation of total m ion pairs. In the parallel plate system as in the simple ionisation chamber (see Fig. 6.4.2), to have an appreciable value of m, the inter–electrode potential difference is to be made too high which cannot be attained easily.

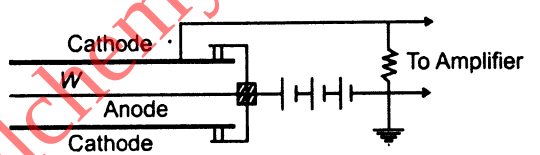

Fig. 6.4.3. Schematic representation of a proportional counter.

To remove the above difficulty, a *cylindrical electrode assembly* (see Fig. 6.4.3) has been utilised in both ***proportional and Geiger–Muller Counters.*** In this system, a tungsten wire (W) of radius r_1 (of the order of 10^{-3} cm) is fixed axially in a metallic cylinder of radius r_2 (of the order of 1 cm) with a polished inner surface. The axial wire is insulated from the cylinder. In this assembly, the field (E_r), at a distance r measured from the axis of the cylinder is given by :

$$E_r = \frac{V}{r \ln(r_2/r_1)} \qquad \ldots(6.4.1)$$

where V denotes the steady potential difference between the electrodes.

In the above cylindrical assembly, for the lower values of V, the value of m is unity but with the increase of V up to a certain limit, the value of m gradually increases. **For a given value of gas multiplication factor m, it is found that the pulse height (a measure of total number of ion pairs in the system) is directly proportional to the extent of ionisation produced at the primary process.** Thus from the pulse heights, the different types of radiations such as α-, β^-- and γ-rays differing significantly in ionising power can be differentiated. As a matter of fact, by using suitable electronic devices, the small pulses created by the weaker ionising radiations, i.e. β^-- and γ-rays, can be completely kept out from recording, so that only the stronger pulses created by the powerful ionising radiations

Click Here t.me/thealchemylibrary

like α-particles can be recorded. ***Here it is worth mentioning that this advantage is not available from the Geiger–Muller counter which will be discussed later.***

It is to be mentioned that the discharge causing the pulse due to the passage of the ionising particles should not be permanent and it must be automatically extinguished to get reset for recording the next event. This is attained by a suitable adjustment in the electric circuit along with a suitable composition of the gas mixture.

(d) The Geiger–Muller (G–M) Counter

The basic construction of the Geiger-Muller counter is the same as in the proportional counter. It possesses the cylindrical assembly of the electrodes as in the proportional counter (see Fig. 6.4.3), but **the applied potential is higher compared to that of the proportional counter. This higher voltage generates the characteristic feature that the amplitude of the output pulse due to the entry of an ionising radiation is independent of the number of ions produced in the primary process. Thus,** ***the G–M counter cannot differentiate the weak and strong ionising radiations but it can be done in the proportional counters.***

There are two types of G–M counters depending upon the penetrating power of the ionising radiations to be detected. Fig. 6.4.4 shows the basic construction of a G–M counter. The metallic cylinder acts as a cathode while the wire placed axially acts as an anode. The ionising radiation can penetrate into the cylinder through the window. If the radiation is of high penetrating power, the window is made of glass; and for the weak penetrating radiations, the window is made of very thin mica sheet or very thin glass.

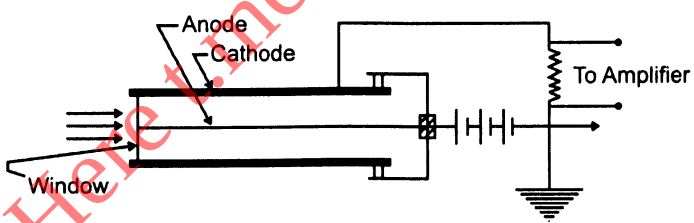

Fig. 6.4.4. Schematic representation of a Geiger-Muller (G-M) counter.

Here as in the proportional counter, the discharge causing the pulse due to the entry of the ionising radiation is not permanent and it automatically gets extinguished to get reset for recording the next event. When a pulse is being produced, at that time it cannot record any other event and this time is called ***dead time.*** The time required to get reset after recording a pulse is called ***recovery time.*** During the recovery time, it also cannot record anything. Thus, the dead time and recovery time which are of the order of 100 μs, restrict the counting rates to about 5000 pulses per second by a G–M counter.

To prevent the possibility of initiation of an electric discharge by the spurious electrons produced in the counter after a discharge, generally a small amount of polyatomic vapour* (e.g. ethanol, methane, etc.) is added with the noble gas kept in the counter. The disadvantage of the use of polyatomic vapour is that after some time all the molecules are dissociated and then the counter becomes useless. This

* Mechanism of the process is discussed in detail in *Atomic and Nuclear Physics* by K.G. Krishnan (Macmillan Co., India, 1982), p. 419.

Click Here t.me/thealchemylibrary

occurs after recording of about 10^9 pulses. But, if halogen vapour (e.g. bromine vapour) is used for the purpose, the dissociated molecules can again recombine to regenerate the molecules.

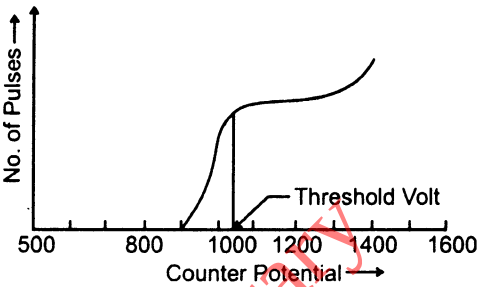

Fig. 6.4.5. Variation of intensity of output pulse with the change of counter potential (V) in a Geiger-Muller (G-M) counter. Adapted from K.G. Krishnan, "Atomic and Nuclear Physics", Macmillan India Ltd. (1973), reproduced with permission.

Basic Operating Principle of the Geiger–Muller Counter : Determination of the required potential difference for a particular G–M counter is very important. If the voltage is lower, the proper pulse is not generated. On the other hand, if it lies above the required range then the discharge becomes continuous. Thus to know the required range exactly is very much important. To achieve this, a radioactive source is kept near the counter and the voltage is gradually increased at steps (at each step only a few volts). The results are shown in Fig. 6.4.5. It is seen that up to about 900 volts, no impulse is recorded. It indicates that up to this limit there is **no secondary ionisation.** Then the multiplication factor, m increases with the increase of the applied voltage almost linearly. ***In this range, the counter can act as a proportional counter.*** After this, the *Geiger range* is achieved and in this range the number of output pulse becomes constant for all ionising radiations. This is why in this range, we get a plateau and the point at which the plateau starts is called ***Geiger threshold.*** If this threshold value is exceeded on the plateau, the number of output pulse remains the same but the size of the pulse amplitude increases. For a good G–M counter, the plateau should cover about 200 V, so that a small fluctuation from the applied potential in the Geiger range may not hamper the study.

In the cylindrical electrode assembly, we have already mentioned (see Eqn. 6.4.1) that the field at r from the axial wire is given by,

$$E_r = \frac{V}{r \ln (r_2/r_1)}$$

where V is the applied voltage, r_2 and r_1 are the radii of the cylinder and wire respectively. If the applied potential V lies in the Geiger range, then the secondary ion pairs (i.e. positive ion and electron) may be produced even at a distance away from the axial wire (i.e. anode). On the other hand, for the proportional counters in which V is lower than the Geiger range, the secondary ion pairs are mainly originated at the vicinity of the axial wire. This is why, in a G–M counter, the positive ions can have the chances to recapture the electrons giving rise to the ***emission of ultraviolet photons.*** In the proportional counter, as the ion pairs are at the vicinity of the anode wire, the electrons can easily reach the anode. This is why, the possibility of recapturing the electrons by the positive ions, before reaching of the electrons to the anode is very much low. ***Thus the probability of generation of ultraviolet photons in the proportional counter is negligibly small.*** But in the G–M counter, as the ion pairs are also produced away from the anode, the generation of the ultraviolet photons is favoured. These ultraviolet photons on collision with the gas molecules may again produce the ion pairs. **These ultraviolet photons and the accelerated ions (both primary and secondary) can spread the ionisation throughout the tube in less than a microsecond.**

Click Here to Join Chemistry Library

(e) The Wilson Cloud Chamber (Expansion type)

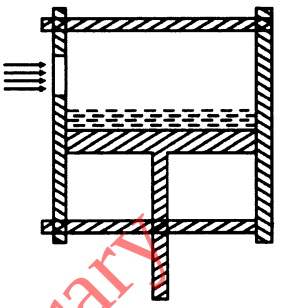
(Expansion Type)

Fig. 6.4.6. Schematic representation of Wilson cloud chamber (expan-sion type).

The cloud chamber method was developed by C.T.R. Wilson in 1896. In this method, **the tracks of the movement of the ionising particles are made visible through the photographic technique.** When the ionising radiation passes through the air supersaturated with water vapour, fogs are formed along the tracks. Actually the ionised particles favour the formation of fog acting as nuclei for the droplet formation.

Fig. 6.4.6 gives the schematic representation of the apparatus. In the chamber, there is a movable piston above which water is kept. The air above the piston is free from dust and it gets saturated with water vapour. On moving the piston downwards, **there is a sudden and adiabatic expansion of the air saturated with water vapour leading to a fall in temperature.** Thus the air gets supersaturated with the water vapour. On passing the ionising radiation through the chamber, water droplets are formed along the tracks and these can be visualised through the photographic technique.

The tracks of the droplets are photographed to analyse the behaviour of the particles. After recording a track, a small potential between the ceiling and the floor of the chamber is applied to remove away the residual ions, if any, left in the chamber. Then, it is again made ready for the next encounter.

Here it is worth mentioning that the ionising radiation should enter into the chamber immediately after (within ~ 0.5 s) the adiabatic expansion.

The advantage of this method is that it not only detects but also characterises the ionising particles. In a G-M counter, the particles cannot be characterised. The types of the tracks (see Fig. 6.3.2.1) followed by the different particles are different as evident from the photographs. Besides this, the cloud chamber being coupled with a magnetic field, yields a lot of information such as : mass, charge, energy, etc. of the particles.

Working Principle of the Cloud Chamber **:** Let us consider that the gas-vapour mixture over the liquid surface in the chamber has a volume V_0 and temperature T_0 with a saturation vapour pressure P_0. Considering the vapour to obey the ideal gas laws, we get,

$$P_0V_0 = n_0RT_0 \qquad \ldots(6.4.2)$$

where R is the gas constant and n_0 gives the number of moles of the gas–vapour mixture. Now let us carry out an adiabatic expansion from V_0 to V_1, and consequently the temperature falls to T_1. Now if the situation is considered just immediately after the expansion, when condensation has not yet started, we get :

$$P_1V_1 = n_0RT_1 \qquad \ldots (6.4.3)$$

where P_1 is the vapour pressure. The T_1 and T_0 are related from the adiabatic expansion as follows :

$$(T_0/T_1) = (V_1/V_0)^{\gamma-1} \qquad \ldots (6.4.4)$$

where γ gives the ratio of C_p and C_v for the gas-vapour mixture. If P be the saturation vapour pressure (obtained from standard tables at the temperature T_1) and P_1 is greater than P (i.e. $P_1 > P$) then the vapour is supersaturated at the temperature T_1. ***Under the supersaturation condition, the system cannot***

Click Here to the Library

remain in an equilibrium with the liquid and it undergoes condensation to attain $P_1 = P$. Now if the volume change due to such condensation is ignored and also the temperature change due to the withdrawal of latent heat during the condensation is ignored, we get,

$$PV_1 = nRT_1 \qquad \ldots (6.4.5)$$

where, n stands for the number of gas–vapour moles remained after condensation.

When the gas–vapour mixture is in supersaturation, the condensation preferably occurs on **condensation centres.** A droplet of radius r will form if the existing vapour pressure P_1 is greater than the equilibrium saturation vapour pressure P_r over the droplet of radius r. ***This saturation vapour pressure P_r is always lower for the charged droplets compared to the uncharged droplets. This is why, the charged particles are more efficient than the uncharged ones to carry out the condensations.*** In this regard, another parameter called *supersaturation ratio* σ $(= P_1/P)$ is very much important. It has been found that if, $\sigma > 4.1$, then the droplet enlarges whatever the initial radius may be. The σ value depends on the percentage of expansion as evident from the following relation.

$$\sigma = P_1/P = \frac{(n_0/V_1)}{(n/V_1)} = \frac{n_0}{n} = \frac{P_0V_0T_1}{PV_1T_0} = \frac{P_0}{P}\left(\frac{V_0}{V_1}\right)^{\gamma} \qquad \ldots (6.4.6)$$

(by using Eqns. 6.4.2, 6.4.4 and 6.4.5)

Lastly, it is important to mention that the ionising radiation must enter into the chamber within ~ 0.5 s after the adiabatic expansion, because in this period the supersaturation condition exists beyond which it tends to attain the equilibrium with a saturation pressure. To synchronise the processes, very often a counter is coupled with the cloud chamber.

(f) The Diffusion Cloud Chamber

In the expansion type cloud chamber, the recovery time for getting ready to record the next event is very much long and as a result, many important nuclear events of an experiment may remain unrecorded. To overcome this drawback, a diffusion type cloud chamber has been developed. The basic principle is the same, but the method of attaining the supersaturation is different. In this method, a steady temperature gradient between the ceiling and floor of a chamber is maintained by using a hot plate at the top and dry ice at the bottom surface (see Fig. 6.4.7). Two reservoirs (T, T) of a volatile liquid like methanol or ethanol are kept near the hot plate. In this chamber the vapour diffuses from top to bottom and at some region between the plates the required supersaturation ratio (σ) is attained. To make the region certain (tentatively), flat chambers of low height are preferred. As soon as the track is photographed, the residual ions, if any, are cleared up by a suitable sweep potential and the chamber again becomes ready for recording the next event.

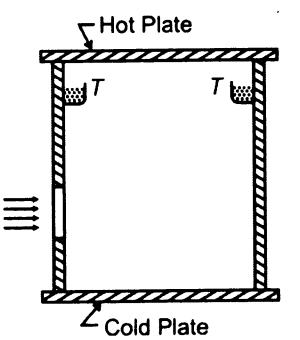

Fig. 6.4.7. Schematic representation of a diffusion cloud chamber.

6.5 UNITS OF RADIOACTIVITY

The activity of a radioactive substance is expressed in terms of ***curie*** **(Ci)** and its submultiples– *millicurie* (mCi) and *microcurie* (μCi). The curie is defined as the activity of a radioactive substance which gives

Click Here t.me/thechemlibrary

3.7×10^{10} ***disintegrations per second*** **(dps).** Here it is worth remembering that one gram radium produces 3.7×10^{10} disintegrations/second. 1.0 g ^{226}Ra contains $6.02 \times 10^{23}/226$ atoms having the disintegration constant, $k = 1.38 \times 10^{-11}$ s^{-1}. Thus, from $-dN / dt = kN$; we get :

$$1 \text{ Ci} = 1.38 \times 10^{-11} \times 6.02 \times 10^{23}/226 = 3.7 \times 10^{10} \text{ disintegrations/sec.}$$

Mathematically it is expressed as : $\left|\frac{-dN}{dt}\right| = 1$ curie $= 3.7 \times 10^{10}$ disintegrations per second (dps).

1 millicurie (mCi) $= 10^{-3}$ curie $= 3.7 \times 10^{7}$ disintegrations/sec and 1 microcurie (μCi) $= 10^{-6}$ curie $= 3.7 \times 10^{4}$ disintegrations/sec. **Rutherford (Rd)** is an another unit to express the radioactivity. It is defined as the activity of a radioactive substance which gives 10^6 disintegrations per second. Therefore, $\left|-\frac{dN}{dt}\right| = 1$ Rutherford (Rd) $= 10^6$ disintegrations/sec. 1 millirutherford (mRd) $= 10^{-3}$ Rd; 1 microrutherford (μRd) $= 10^{-6}$ Rd.

Becquerel **(Bq)** is the SI unit defined as the activity : one disintegration per second. Therefore, 1 Ci $= 3.7 \times 10^{10}$ Bq.

To clarify the concept quantitatively, we are to consider the law of disintegration (which will be discussed later) :

$$-\frac{dN}{dt} = kN, \; k = \text{disintegration constant.}$$

Now let us take the case of U^{238} whose k is 4.88×10^{-18} s^{-1}. 238 g of ^{238}U possess 6.02×10^{23} atoms. Let us take the mass of w g of ^{238}U to produce 3.7×10^{10} disintegrations per second (dps). The number of atoms in w g is given by : $N = w \times 6.02 \times 10^{23}/238$.

According to definition, $\left|-\frac{dN}{dt}\right| = 1 \text{ curie} = 3.7 \times 10^{10} \text{ dps} = kN$.

Thus, $3.7 \times 10^{10} = \frac{w \times 6.02 \times 10^{23}}{238} \times k = \frac{w \times 6.02 \times 10^{23} \times 4.88 \times 10^{-18}}{238}$;

or, $w = 30 \times 10^5 \text{ g} = 3 \times 10^3 \text{ kg}$.

Thus, 3×10^3 kg ^{238}U produce 1 curie activity. Similarly, it can be shown that 8.1×10^{-2} kg ^{238}U produce 1 rutherford activity.

Very often the activity is expressed per gram, e.g. *curies per gram*. Let us take the case of ^{238}U. Here the number of atoms present in 1 g is given by, $N = 6.02 \times 10^{23}/238$. Therefore, the activity per gram is given by :

$$\left|\frac{-dN}{dt}\right| = kN = 4.88 \times 10^{-18} \times \frac{6.02 \times 10^{23}}{238} = 1.2 \times 10^4 \text{ disintegrations per gram per second}$$

$$= \frac{1.2 \times 10^4}{3.7 \times 10^{10}} \text{ curies/g}$$

$$= 3.24 \times 10^{-7} \text{ curies/g}$$

Click Here to me/thealchemylibrary

6.6 DIFFERENT MODES OF RADIOACTIVE DECAY

The major modes of nuclear decay are given below.

(i) **α-*Decay*** : ${}_2^4He^{2+}$, i.e. α-particles, are ejected, i.e. ${}_Z^AX \rightarrow {}_{Z-2}^{A-4}Y^{2-} + \alpha$.

(ii) **β⁻-*Decay*** : In this process, electrons (i.e. β^-) are ejected, i.e.

$${}_Z^AX \rightarrow {}_{Z+1}^AY^+ + \beta^- + \bar{\nu}.$$

Actually, one neutron is converted into an electron along with an antineutrino.

$${}_0^1n \rightarrow {}_{+1}^1p + {}_{-1}^0e\ (i.e.\ \beta^-) + {}_0^0\bar{\nu}.$$

The energy is distributed between the β⁻ and antineutrino particles, and the energy of the β⁻ particle may vary from zero to a certain maximum value in a particular reaction (see Fig. 6.11.1). Some aspects of β^- decay have already been discussed in Secs. 5.3.3. and 5.6. The product and parent nuclides are ***isobars.*** This relation also holds good for the β^+-decay and *orbital electron capture process.*

(iii) **β⁺ (i.e. *Positron*) *Decay*** : In this process, one proton is converted into a neutron along– with the neutrino particle (ν).

$${}_{+1}^1p \rightarrow {}_0^1n + {}_{+1}^0e\ (i.e.\ \beta^+) + {}_0^0\nu, \text{ i.e. } {}_Z^XA \rightarrow {}_{Z-1}^AY^- + \beta^+ + \nu$$

As in the case of β^- decay, here the energy is distributed between β^+ and ν. The process has been discussed in Secs. 5.3.3. and 6.11.

(iv) ***Orbital Electron Capture*** : In this process, one electron from the nearest *K*-shell is captured by the nucleus to produce a neutron as follows :

$${}_{+1}^1p + {}_{-1}^0e \rightarrow {}_0^1n + {}_0^0\nu; \text{ i.e. } {}_Z^AX + {}_{-1}^0e \rightarrow {}_{Z-1}^AY + \nu$$

In this process, a vacancy in the electron shell is created. This vacancy can initiate other phenomena (i.e. *X*-ray production and Auger effect) which will be discussed later (sec. Sec. 6.7).

(v) **γ-*Emission*** : Very often the daughter nuclides produced remain in the excited states and the excess energy is emitted as γ-radiations in returning to the ground states. The isomeric transitions (see Sec. 5.1.7, 6.14, 6.16.2d) also lead to γ-emission.

$${}_Z^{Am}X \text{ (metastable nuclide)} \xrightarrow{\text{I.T.}} {}_Z^AX + \gamma$$

(vi) ***Internal Conversion*** : In some cases, the excess energy is not emitted as γ-radiations, but the energy is utilised in knocking out the electron from the orbitals. This process is referred to as *internal conversion* (see Sec. 5.2.6ix) of the γ-rays. If E_γ represents the energy of the γ-rays involved in the internal conversion and E_B is the binding energy of the electron to be knocked out, then the kinetic energy (E_K) of the ejected electron is given by : $E_K = E_\gamma - E_B$. Thus, if E_1 is the binding energy for the ${}^1S_{1/2}$ electron in the *K*-shell, the kinetic energy of the ejected electron is given by :

$$E_K = E_\gamma - E_1$$

Click Here to the/thearchenylibrary

Similarly, if for the electrons $^2S_{1/2}$, $^2P_{1/2}$ and $^2P_{3/2}$ in the L-shell, the binding energies are E_2, E_3 and E_4 respectively, then the kinetic energies for the corresponding electrons are given by:

$$E_{L(1)} = E_\gamma - E_2,\ E_{L(2)} = E_\gamma - E_3 \text{ and } E_{L(3)} = E_\gamma - E_4$$

Thus, it is evident that the *energy spectrum of the ejected electrons due to the internal conversion contains some discrete lines, while for the* β^-, *it covers a certain range (from zero) of the spectrum in a continuous way.*

Another difference between the processes is that in the β^--decay, antineutrino is ejected along with the β^--particle due to the conversion of a neutron into a proton in the nucleus (see Sec. 5.6) while in the internal conversion, the excitation energy of the nucleus only knocks out the orbital electron without any other particle like neutrino or antineutrino.

Note : **Both β^--decay and internal conversion lead to emission of electrons. But their origins are different. Their energy spectra are also different. β-decay leads to emission of antineutrino particles along with the electrons but internal conversion leads to emission of electrons only.**

6.7 THE FLUORESCENCE AND AUGER EFFECT

Though these two phenomena are not directly related with the nuclear phenomena, they appear as a consequence of some nuclear events, i.e. ***orbital capture*** and ***internal conversion***, leading to a vacancy in the electron orbitals, usually in the K or L shell. To fill in such energetically unstable vacancies, the electrons jump from the outer orbitals in cascade giving rise to the phenomena (i) the fluorescence or radiation emission, and (ii) the auger effect or electron emission.

Fluorescence or Radiation Emission : To fill in the vacancy in the inner orbital, an electron from a higher orbital jumps leading to the emission of energy given by, $h\nu = E_{B(\text{inner})} - E_{B(\text{outer})}$ where, $E_{B(\text{inner})}$ and $E_{B(\text{outer})}$ denote the *binding energies* of the inner and outer electrons respectively. The vacancy produced in the new orbital is filled in by an electron coming from the next higher orbital. This process goes on until the vacancy reaches the outermost orbital giving rise to +1 state of the atom. At each stage, the frequency of the radiation emitted is governed by the energy difference between the levels in which the electron transition occurs. Actually, this process leads to the **generation of *characteristic X–rays.*** This process is called ***fluorescence emission.***

The Auger or Electron Emission Effect : In this process, the energy released in jumping the outer electron to the inner vacancy, is utilised in ejecting the next outer electron as in the internal conversion process. If the innermost electron e_1 is lost initially by either the electron capture process or the internal conversion process, and the electron e_2 jumps to fill in the vacancy of e_1. In this downward transition of the electron e_2, the released energy may be used to knock out the electron e_3. Then the kinetic energy ($E_{K(3)}$) of the ejected electron e_3 (the second to be lost) in the process is given by :

$$E_{K(3)} = \left[E_{B(1)} - E_{B(2)}\right] - E_{B(3)} \qquad \ldots(6.7.1)$$

where $E_{B(i)}$ denotes the *binding energy* for the i–th electron. It is evident that the emission of e_3 with some kinetic energy is energetically possible, if $E_{B(1)} > E_{B(2)} + E_{B(3)}$. The loss of e_3 gives +2 state of the species. To fill in the vacancy of e_3, the next higher electron will jump leading to the emission of energy governed by the difference of energy between the states involved. This emitted energy may further

Click Here t.me/thealchemylibrary

knock out another electron if the energy condition permits. Thus the emission of electrons up to n–th electron (e_n) may go on in cascade so long as $E_{K(n)}$ (as given in Eqn. 6.7.1) is positive. The successive emission of the electrons in this process is called ***Auger effect.***

It is evident that in filling in the initial vacancy in the innermost shell, two resultant vacancies are generated which in turn may produce four vacancies at the next step (see Fig. 6.7.1) **and the process gradually goes on.** Thus in this process, very often high positively charged species are formed.

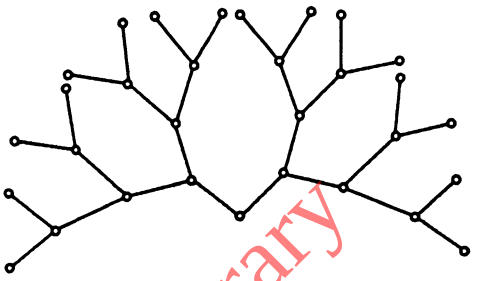

Fig. 6.7.1. Schematic representation of Auger effect.

6.8 DISINTEGRATION CHAIN AND SODDY–FAJAN GROUP DISPLACEMENT LAW

Naturally occurring radioactive substance– like uranium, actinium, etc. undergo a series of disintegration until a stable one is formed. A partial chain in a particular series is shown below. The daughter elements in the series, very often remain at excited states and return to ground states through γ-radiations.

$$^{226}_{88}Ra \xrightarrow{-\alpha} {}^{222}_{86}Rn \xrightarrow{-\alpha} {}^{218}_{84}Po \xrightarrow{-\alpha} {}^{214}_{82}Pb \xrightarrow{-\beta} {}^{214}_{83}Bi \longrightarrow$$

Thus a series consists of a number of radioactive elements whose modes of decay are also different. This is why, a naturally occurring radioactive substance produces an emanation which is a mixture of α, β and γ-rays.

To find a relation between the daughter and parent elements in the disintegration process, Soddy and Fajan (1931) established a simple rule, commonly known as ***Soddy–Fajan group displacement law or simply group displacement rule.*** The rule states as follows :

(i) On ejection of an α-particle from a radioactive element (i.e. parent element), the daughter element formed bears the mass number less by four units and atomic number less by two units compared to those of the parent element. Consequently, the daughter element will be placed two groups left (in the same period) to the parent element in the Mandeleev *Periodic Table*. This occurs due to the fact that the α-particle (which is nothing but $^{4}_{2}He^{2+}$) is having mass number and atomic number four and two units respectively.

Example :

$$^{215}_{84}Po \text{ (Gr. VIA i.e. 16)} \xrightarrow{-\alpha} {}^{211}_{82}Pb \text{ (Gr. IVA i.e. 14)}$$

The group numbers are 16 and 14 as per the IUPAC recommendation.

(ii) On ejection of a β^--particle from the parent element, the daughter element bears the same mass number but the atomic number gets increased by one unit. Therefore the daughter element will be placed to the next group (in the same period), just right to the parent element in the Periodic Table. **It indicates that the emission of an α-particle followed by the emission of two β^-–particles produces a daughter element which is an isotope of the starting parent element.**

Click Here t.me/thealchemylibrary

This observation can be explained by considering the genesis of a β^--particle from a neutron as:

neutron → proton + electron + antineutrino, i.e.

$$^{1}_{0}n \rightarrow {}^{1}_{+1}p + {}^{0}_{-1}e + {}^{0}_{0}\bar{\nu}$$

The electron produced in this way cannot exist in the nucleus and comes out as a β^--particle.

Examples : $^{211}_{82}Pb$ (IVA i.e. 14) $\xrightarrow{-\beta^-}$ $^{211}_{83}Bi$ (VA i.e. 15) $\xrightarrow{-\beta^-}$ $^{211}_{84}Po$ (VIA i.e. 16)

The effect of an alpha–decay followed by two beta —decays is shown below.

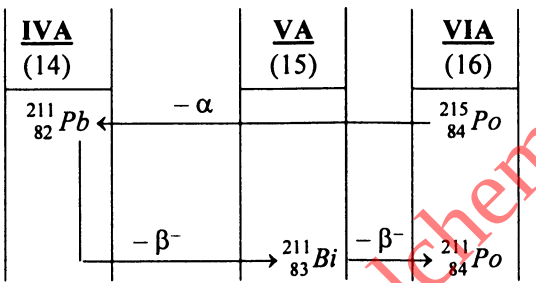

The group displacement law is illustrated in different radioactive series (see Tables 6.15.1–4)

6.9 THE DECAY KINETICS AND PARENT–DAUGHTER DECAY–GROWTH RELATIONSHIPS

6.9.1 Case I : The Daughter Nucleus is Stable

The rate of decay of a radioactive element at a particular instant is directly proportional to the number of disintegrating nuclides present at that instant. If N_1 is the number of disintegrating nuclides at a particular instant, then it follows the following relationship for the process,

$$\underset{(N_1)}{A} \xrightarrow{k_1} \underset{(N_2), \text{ at time } t}{B}$$

$-\frac{dN_1}{dt} \propto N_1$, (the negative sign indicates that the number N_1 decreases with time).

or,
$$-\frac{dN_1}{dt} = k_1 N_1, \qquad \ldots(6.9.1.1)$$

where k_1 is called the **disintegration constant of the parent nuclide.** This relationship is referred to as the **first order rate law.** The disintegration constant is a characteristic property of the parent nuclide and it is having the dimension, time^{-1}. From Eqn. 6.9.1.1 we get :

$$\frac{dN_1}{N_1} = -k_1 dt \qquad \ldots(6.9.1.2)$$

On integration, the above equation leads to :

$$\ln N_1 = -k_1 t + C \qquad \ldots(6.9.1.3)$$

Click Here to meet the Chemylibrary

where, C is the integration constant. To evaluate C, we have to consider the condition : when $t = 0$, $N_1 = N_{1(0)}$ and $N_2 = 0$

Using this condition in Eqn. 6.9.1.3, we get :

$$\ln N_{1(0)} = -k_1 \times 0 + C; \text{ or, } C = \ln N_{1(0)}$$

Putting the value of C in Eqn. 6.9.1.3, we get :

$$\ln N_1 - \ln N_{1(0)} = -k_1 t; \text{ or, } \ln \left[\frac{N_1}{N_{1(0)}}\right] = -k_1 t;$$

or, $$\boxed{2.303 \log \left[\frac{N_1}{N_{1(0)}}\right] = -k_1 t;} \quad \ldots (6.9.1.4a)$$

or, $$\boxed{N_1 = N_{1(0)} \exp(-k_1 t)} \quad \ldots (6.9.1.4b)$$

Alternatively, the above equation can be obtained by integrating Eqn. 6.9.1.2 between the limits $t = 0$ and $t = t$, i.e.

$$\int_{N_1 = N_{1(0)}}^{N_1 = N_1} \frac{dN_1}{N_1} = -k_1 \int_{t=0}^{t=t} dt; \text{ or, } \ln \left[\frac{N_{1(0)}}{N_1}\right] = k_1 t; \text{ or, } N_1 = N_{1(0)} \exp(-k_1 t)$$

or, $$\log \frac{N_1}{N_{1(0)}} = -\frac{k_1 t}{2.303}; \text{ or, } \log \frac{N_{1(0)} - N_2}{N_{1(0)}} = -\frac{k_1 t}{2.303}$$

or, $$\log [N_{1(0)} - N_2] = (-k_1/2.303)\, t + \log N_{1(0)} \quad \ldots (6.9.1.5)$$

where, N_2 *gives the number of the parent nuclides disintegrated in time* t, and it also gives the number of daughter nuclides produced in time t. For the growth rate of the daughter element, it follows the condition : $-\frac{dN_1}{dt} = \frac{dN_2}{dt} = k_1 N_1$.

At any time, it also maintains the conservation principle :

$$N_1 + N_2 = N_{1(0)}; \; (N_2 = 0 \text{ at } t = 0)$$

Therefore, $$N_2 = N_{1(0)} - N_1 = N_{1(0)} - N_{1(0)} \exp(-k_1 t)$$

$$\boxed{\text{or, } N_2 = N_{1(0)} [1 - \exp(-k_1 t)]} \quad \ldots (6.9.1.6)$$

The activity or the rate of disintegration of the parent nuclide at time t is defined as :

$$A_1 = \left|\frac{dN_1}{dt}\right| = k_1 N_1 = k_1 N_{1(0)} \exp(-k_1 t)$$

The activity per unit mass of a sample is referred to as **specific activity.**

The change of activity of the parent nuclide and the growth of the daughter element with time are shown in Fig. 6.9.1.1.

Click Here t.me/tlealchemylibrary

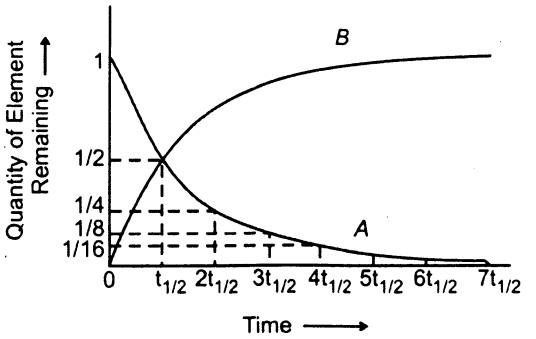

Fig. 6.9.1.1. Decay curve (A) of the parent radionuclide and growth curve (B) of the nonradioactive daughter nuclide.

(A) Some Interesting Features of the Radioactive Decay Kinetics

(i) Due to the exponential nature, i.e. $N_1 = N_{1(0)} \exp(-k_1 t)$, the process never gets completed.

(ii) The disintegration constant has the dimension, time^{-1}, i.e. sec^{-1} or s^{-1}.

(iii) Eqn. 6.9.1.5 indicates that a plot of log $[N_{1(0)} - N_2]$ vs. t is linear whose slope is given by $-(k_1/2.303)$ from which k_1 can be determined. This method is applicable only when N_2 is known. However from the plot of log A_t vs. t, k_1 can be determined (cf. Sec. 6.9.1B, Procedure II).

(iv) **The disintegration process is a *statistical one*.** Every nucleus in a sample has a certain probability to disintegrate, but there is no way to predict in advance to specify the nuclides which will decay in a particular time period.

(v) ***The Half Life Period*** **($t_{1/2}$):** As the time required to complete the process is infinite, another parameter, ***half life period*** is considered to compare the activity of different radioactive substances. It is defined as the time required for the activity of a radioactive sample (of a certain amount) to be reduced to half. From the definition at $t = t_{1/2}$, $N_1 = N_{1(0)}/2$.

Therefore, from Eqn. 6.9.1.4, we get :

$$\frac{N_{1(0)}}{2} = N_{1(0)} \exp(-k_1 t_{1/2}); \text{ or } 1/2 = \exp(-k_1 t_{1/2});$$

or, $$\ln(1/2) = -k_1 t_{1/2}; \text{ or, } \frac{2.303 \log(2)}{k_1} = t_{1/2};$$

or, $$\boxed{t_{1/2} = 0.693/k_1} \qquad \ldots(6.9.1.7)$$

Thus, it appears that the half life period of a radioactive element is ***independent of its initial concentration.*** Thus, in first $t_{1/2}$ period, the activity falls by 50%; in the second $t_{1/2}$ period, it falls by 75%; in the third $t_{1/2}$ period, it falls by 87.5%; in the fourth $t_{1/2}$ period, it is reduced by 93.5%, and so on (see Fig. 6.9.1.1). In every $t_{1/2}$ period, the activity falls by 50% irrespective of the concentration from which $t_{1/2}$ is being measured. For all practical purposes, it can be reasonably assumed that in about 6 to 8 half–lives, the disintegration process is more or less complete. After 6 half–lives, the activity becomes $(1/2)^6$, i.e. 1/64 of the initial activity. If A_o and A_n are activities at time zero and after n-half life period respectively, then

$$\boxed{A_n = A_o (0.5)^n}$$

Click Here time/treachemylibrary

(vi) ***Average Life Period*** **(t_{av}) :** It is related with $t_{1/2}$ as : $t_{1/2} = 0.693\ t_{av}$. These have been discussed separately (see Sec. 6.9.1C).

(vii) Sometimes, a radioactive nuclide may disintegrate in a number of ways. The kinetics of such parallel paths are discussed separately (see Sec. 6.9.1D).

Some important relations

If N_o = number of disintegrating atoms at $t = 0$; N_t = number of disintegrating atoms at time t; k = disintegration constant; $t_{1/2}$ = half-life period; t_{av} = average life period; then we can write:

$$t_{1/2} = \frac{0.693}{k}; t_{av} = \frac{1}{k};$$

$$N_t = N_o \exp(-kt); \quad \ln(N_t/N_o) = -kt,$$

$$2.303 \log(N_t/N_o) = -kt.$$

In terms of activity (A) :

$$A_t = A_o \exp(-kt); \quad \ln(A_t/A_o) = -kt$$

$$2.303 \log(A_t/A_o) = -kt$$

$$A_n = A_o(0.5)^n$$

A_n = activity after n-half periods

(B) Determination of Half Life ($t_{1/2}$) Period

It can be determined in a number of ways depending upon the situation as mentioned below :

Procedure–I **:** If the decay of a particular sample (see Fig. 6.9.1.1) is plotted against time, then $t_{1/2}$ can be obtained from its definition.

Procedure–II **:** From the standard relation, $N_t = N_0 \exp(-k_t)$, where N_t = number of disintegrating nuclides at t, we get activity at time t as follows :

$$A_t = \frac{dN_t}{dt} = kN_1 = kN_0 \exp(-kt);$$

or, $$\log A_t = \log(kN_0) - kt/2.303 = \log A_0 - kt/2.303$$

where, A_0 is constant for a particular sample.

Therefore, a plot of $\log A_t$ vs. t will produce a straight line whose slope is given by $-(k/2.303)$. Thus k is obtained. From the known value of k, $t_{1/2}$ can be calculated by the relation, $t_{1/2} = 0.693/k$.

If a radioactive sample contains two different radioelements X and Y and one is having much higher $t_{1/2}$ value compared to the other, e.g. $t_{1/2}(X) >> t_{1/2}(Y)$ then the following technique is adopted to find out their individual activities. From the assumed condition, at higher times the activity will be mainly due to the longer lived element, i.e. X. Thus the total activity at a particular time is related as follows :

A_t (total activity) = activity due to X + activity due to Y

$$= A_t(X) + A_t(Y)$$

or, $$A_t \approx A_t(X);$$ (at the higher value of t, at least after 5–6 half lives of Y).

Click Here t.me/thealchemylibrary

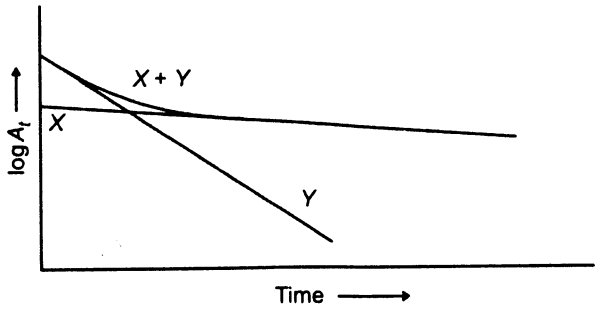

Fig. 6.9.1.2. Variation of activity (A_t) with time of a sample containing two different radioelements X and Y where $t_{1/2}$ (X) >> $T_{1/2}$ (Y). Adapted from K.G. Krishnan, "Atomic and Nuclear Physics", MacMillan India Ltd., 1973. Reproduced with permission.

Thus, from the plot of log A_t vs. t, by extrapolating the straight line portion of the curve (at higher values of t), up to $t = 0$, we get the line representing log A_t (X) vs. t. Thus from the straight line (see Fig. 6.9.1.2), the activity of X at any time can be obtained. Then from the total activity we get the activity of Y at any time by subtraction. Thus, A_t (X) and A_t (Y) can be individually determined at different values of t and from which the respective $t_{1/2}$ values can be obtained as usual.

Procedure–III : From the radioactive equilibrium (secular), i.e. $k_1N_1 = k_2N_2$, k_1 can be determined if other parameters are known.

Procedure IV : For the α-active radioelements, application of ***Geiger–Nuttall rule*** (see Sec. 6.12. iii) is very much helpful to determine the half life period.

(C) The Average Life Period

The disintegration process extends up to infinity. Thus, some nuclides of a radioactive sample may disintegrate almost immediately (i.e. $t = 0$) while some nuclides may survive up to infinity. The process is a statistical one. Hence, we cannot specify the nuclides which will disintegrate at $t = 0$ or at $t = \infty$ or at t = any specified intermediate value between these two extreme values. Thus actual life period of the nuclides may vary from zero to infinity. In this regard, the concept of average life period (t_{av}) is important. It is defined as the sum of the lives of all the nuclides divided by the total number of atoms to disintegrate.

Therefore,
$$t_{av} = \frac{t_1 dN_1 + t_2 dN_2 + t_3 dN_3 + \ldots}{dN_1 + dN_2 + dN_3 + \ldots} = \frac{\int_0^\infty t_i dN_i}{N_0} \qquad \ldots(6.9.1.8)$$

(Here, dN_i represents the number of nuclides having life period t_i).

Now, we have :
$$\frac{dN}{dt} = -kN; \text{ or, } dN = -kNdt ;$$

or,
$$dN = -kN_0 \exp(-kt)\, dt$$

Thus, $dN = kN_0 \exp(-kt)dt$. Here the negative sign is ignored, as it indicates merely the decreasing

Click Here t.me/thealchemylibrary

trend of dN nuclides with time. The number of such nuclides is itself a positive quantity. Therefore, by substituting the value of dN in the expression 6.9.1.8, we get :

$$t_{av} = \frac{\int_0^\infty tkN_0 \exp(-kt)\, dt}{N_0} = k \int_0^\infty t \exp(-kt)\, dt$$

Now, on integration by parts, i.e. $\int uv dx = u \int v dx - \int \left[\frac{du}{dx} \int v dx\right] dx$, we get :

$$t_{av} = k \left[\frac{t \exp(-kt)}{-k} - \int \frac{\exp(-kt)}{-k} dt\right]_0^\infty$$

or,
$$t_{av} = k \left[\frac{t \exp(-kt)}{-k} - \frac{\exp(-kt)}{k^2}\right]_0^\infty$$

$$= k\,[1/k^2] = 1/k \qquad \ldots (6.9.1.9)$$

Thus, t_{av} and $t_{1/2}$ are connected as follows :

$$\boxed{t_{av} = \frac{1}{k};\ t_{1/2} = 0.693/k = 0.693\ t_{av}} \qquad \ldots (6.9.1.10)$$

(D) Parallel Paths of Decay

In some cases, the radionuclides may disintegrate in more than one way, e.g.

$$C \xleftarrow{k_2} A \xrightarrow{k_1} B$$

In such cases, rate of formation of $B = k_1 N_t$ and rate of formation of $C = k_2 N_t$ where, N_t is the number of the parent radionuclides at time t. Therefore,

$$-\frac{dN_t}{dt} = k_1 N_t + k_2 N_t = (k_1 + k_2)\, N_t$$

It leads to :
$$N_t = N_0 \exp[-(k_1 + k_2)\, t\,];$$

or,
$$2.303 \log (N_0/N_t) = (k_1 + k_2)\, t = kt, \text{ (assuming, } k = k_1 + k_2) \qquad \ldots (6.9.1.11)$$

Another relationship holds good :

$$\frac{\text{Rate of formation of } B}{\text{Rate of formation of } C} = \frac{k_1 N_1}{k_2 N_1} = \frac{k_1}{k_2}$$

or,
$$\frac{k_1}{k_2} = \frac{\%\text{ of decay through } k_1 \text{ path}}{\%\text{ of decay through } k_2 \text{ path}} = \frac{\text{Amount of } B \text{ at a particular time}}{\text{Amount of } C \text{ at that particular time}}$$

Click Here t.me/thealchemylibrary

6.9.2 Case II : When the Daughter Element is Radioactive

In nature, generally a disintegration series is continued until a stable nuclide is obtained. Thus, the daughter elements undergo decay to produce new daughter elements in a series. For the sake of simplicity, let us first deal with the simplest possibility, i.e.

$$A \xrightarrow{k_1} B \xrightarrow{k_2} C \text{ (stable)},$$

where, A disintegrates into B which in turn disintegrates into C with the disintegration constants k_1 and k_2 for A and B respectively.

Let, N_1, N_2 and N_3 be the number of nuclides of A, B and C respectively at time t, while these numbers are $N_{1(0)}$, $N_{2(0)}$ and $N_{3(0)}$ at $t = 0$. Definitely, $N_{2(0)} = N_{3(0)} = 0$. The above process is governed by the **principle of kinetics of a *consecutive reaction*.** The rate of decay of A at t is given by :

$$-dN_1/dt = k_1N_1 \qquad \ldots (6.9.2.1)$$

The rate of accumulation of B is given by :

$$dN_2/dt = k_1N_1 - k_2N_2 \qquad \ldots (6.9.2.2)$$

Similarly, for C, $dN_3/dt = k_2N_2 - k_3N_3$, (when C is active), and so on.

From Eqn. 6.9.2.2 by using the relation, $N_1 = N_{1(0)} \exp(-k_1t)$, we get :

$$dN_2/dt = k_1N_{1(0)} \exp(-k_1t) - k_2N_2$$

or,
$$dN_2/dt + k_2N_2 = k_1N_{1(0)} \exp(-k_1t) \qquad \ldots (6.9.2.3)$$

Now, multiplying both sides by the integrating factor, $\exp(k_2t)$ we get :

$$\exp(k_2t)\frac{dN_2}{dt} + k_2N_2 \exp(k_2t) = k_1N_{1(0)} \exp[(k_2 - k_1)t]$$

or,
$$\frac{d}{dt}[N_2 \exp(k_2t)] = k_1N_{1(0)} \exp[(k_2 - k_1)t] \qquad (6.9.2.4)$$

On integration we get :

$$N_2 \exp(k_2t) = \frac{k_1}{(k_2 - k_1)} N_{1(0)} \exp[(k_2 - k_1)t] + C_1 \qquad \ldots (6.9.2.5)$$

where, C_1 is the constant of integration.

To evaluate C_1, we have to consider the condition, $N_2 = 0$ at $t = 0$.

At $t = 0$, from Eqn. 6.9.2.5 we get : $C_1 = -\dfrac{k_1}{k_2 - k_1} N_{1(0)}$

By substituting this value in Eqn. 6.9.2.5, we get :

$$N_2 \exp(k_2t) = \frac{k_1}{k_2 - k_1} N_{1(0)} [\{\exp(k_2 - k_1)t\} - 1], \exp(k_2 - k_1)t = \exp(k_2t) \exp(-k_1t)$$

or,
$$\boxed{N_2 = \frac{k_1N_{1(0)}}{(k_2 - k_1)}[\exp(-k_1t) - \exp(-k_2t)]} \qquad \ldots (6.9.2.6)$$

Click Here t me/thearchemylibrary

In terms of activity,

$$\boxed{A_2 = k_2 N_2 = \frac{k_2 A_{1(0)}}{(k_2 - k_1)} [\exp(-k_1 t) - \exp(-k_2 t)]} \quad \ldots(6.9.2.7)$$

where A_2 gives the activity of B at t and $A_{1(0)}$ gives the activity of A at $t = 0$.

In Fig. 6.9.2.1, decay and growth kinetics of the series are shown.

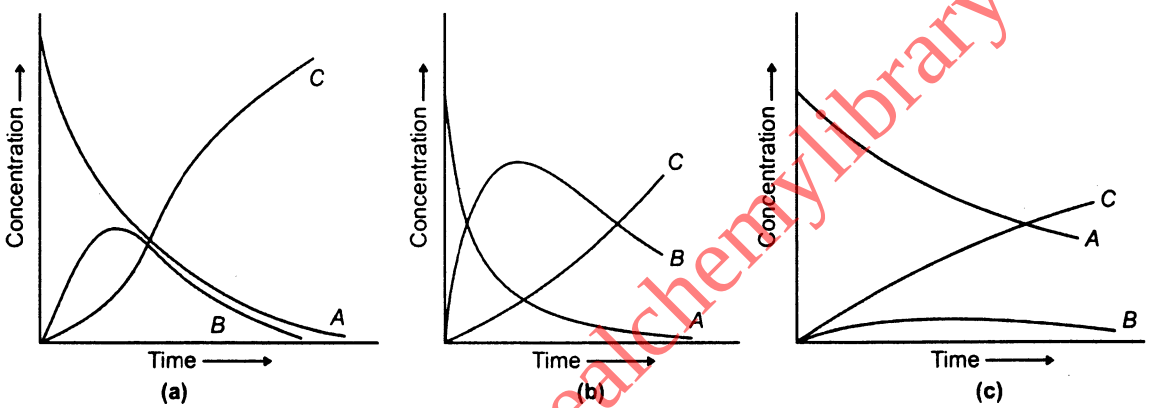

Fig. 6.9.2.1. (a) A typical variation trend of concentrations of A, B and C in a consecutive decay process. $A \xrightarrow{k_1} B \xrightarrow{k_2} C$. The actual variation trend depends on the relative values of k_1 and k_2. (b) A typical variation trend of concentration of A, B and C in the process, $A \xrightarrow{k_1} B \xrightarrow{k_2} C$ when $k_1 >> k_2$. (c) A typical variation trend of concentrations of A, B and C in the process, $A \xrightarrow{k_1} B \xrightarrow{k_2} C$ when $k_2 >> k_1$. Adapted from K.L. Kapoor, "A Text Book of Physical Chemistry", Vol. 4, Macmillan India ltd., 1992. Reproduced with permission.

Click Here to the chemylibrary

6.10 RADIOACTIVE EQUILIBRIUM

Now let us consider the Eqn. 6.9.2.6 in different cases,

$$N_2 = \frac{k_1}{k_2 - k_1} N_{1(0)} [\exp(-k_1 t) - \exp(-k_2 t)] \quad \ldots(\text{Eqn. } 6.9.2.6)$$

Case I : When the parent is long lived, i.e. $k_2 >>> k_1$. Under this condition, Eqn. 6.9.2.6 gets reduced into,

$$N_2 = N_{1(0)} (k_1/k_2) \exp(-k_1 t) \quad \ldots (6.10.1)$$

(as $\exp(-k_2 t)$ tends to almost zero).

Thus, $N_2 = (k_1/k_2) N_1$, (as $N_{1(0)} \exp(-k_1 t) = N_1$)

or, $$k_1 N_1 = k_2 N_2 \quad \ldots (6.10.2)$$

In a series, $$\boxed{N_1 k_1 = N_2 k_2 = N_3 k_3 = \ldots}$$

and in terms of activity, $$\boxed{A_1 = A_2 = A_3 = \ldots}$$

Eqn. 6.10.2 indicates that the rate of formation and the rate of disintegration of B are the same, i.e. $dN_2/dt = 0$ which means that at this condition, the concentration of B remains constant. In such cases, the daughter element is supposed to exist in a ***secular or permanent equilibrium with the parent nuclide.*** The examples are :

$$^{226}_{88}Ra \xrightarrow[t_{1/2} = 1600 \text{ yrs}]{k_1 = 1.3 \times 10^{-11} \text{ s}^{-1}} {}^{222}_{86}Rn \xrightarrow[t_{1/2} = 3.8 \text{ days}]{k_2 = 2.1 \times 10^{-6} \text{ s}^{-1}} {}^{218}_{84}Po \rightarrow \text{disintegration series}$$

$$^{238}_{92}U \xrightarrow[t_{1/2} = 4.5 \times 10^{9} \text{ yrs}]{k_1 = 4.9 \times 10^{-18} \text{ s}^{-1}} {}^{234}_{90}Th \xrightarrow[t_{1/2} = 24.5 \text{ days}]{k_2 = 3.3 \times 10^{-7} \text{ s}^{-1}} {}^{234}_{91}Pa \rightarrow \text{disintegration series}$$

Case II : *When both the parent and daughter nuclides are having more or less the comparable half lives*, i.e. k_1 and k_2 do not differ widely.

In such cases, at first, the daughter nuclide (B) reaches to a maximum concentration at $t = t_{max}$, then it decays at the rate of the longer lived one, between the parent and the daughter nuclides. The t_{max} is evaluated by using the following condition :

$$\frac{dN_2}{dt} = 0 = \frac{k_1}{k_2 - k_1} N_{1(0)} \left[-k_1 \exp(-k_1 t_{max}) + k_2 \exp(-k_2 t_{max}) \right]$$

Since, $$\frac{k_1}{k_2 - k_1} N_{1(0)} \neq 0, \; -k_1 \exp(-k_1 t_{max}) + k_2 \exp(-k_2 t_{max}) = 0$$

or, $$k_2/k_1 = \exp(k_2 t_{max})/\exp(k_1 t_{max}); \text{ or, } \ln(k_2/k_1) = (k_2 - k_1)\, t_{max}$$

or, $$\boxed{t_{max} = \frac{1}{(k_2 - k_1)} \ln(k_2/k_1)} \quad \ldots (6.10.3)$$

(a) ***For the condition $k_2 > k_1$*** (but k_1 is not negligible with respect to k_2), i.e. the parent is longer lived compared to the daughter. In such cases, **at higher values of t,** $\exp(-k_2 t)$ approaches zero faster than $\exp(-k_1 t)$. Thus, Eqn. 6.9.2.6 reduces to,

$$\boxed{N_2 = \frac{k_1}{(k_2 - k_1)} N_{1(0)} \exp(-k_1 t)} \quad \ldots (6.10.4)$$

or, $$\frac{N_2}{N_1} = \frac{k_1}{k_2 - k_1} = \text{constant; (as } N_1 = N_{1(0)} \exp(-k_1 t)) \quad \ldots (6.10.5)$$

Thus, both the parent and daughter nuclides will decay at higher times at the rate governed by k_1 (see Eqn. 6.10.4) and the ratio N_2/N_1 remains constant. **This type of equilibrium is referred to as transient equilibrium.** The examples are :

$$^{222}_{86}Rn \xrightarrow[t_{1/2} = 3.8 \text{ days}]{k_1 = 2.1 \times 10^{-6} \text{ s}^{-1}} {}^{218}_{84}Po \xrightarrow[t_{1/2} = 3.05 \text{ min}]{k_2 = 3.8 \times 10^{-3} \text{ s}^{-1}} {}^{214}_{82}Pb \rightarrow \text{disintegration series}$$

Click Here t.me/thealchemylibrary

$$^{234}_{90}Th \xrightarrow[t_{1/2} = 24.5 \text{ days}]{k_1 = 3.3 \times 10^{-7} \text{ s}^{-1}} {}^{234}_{91}Pa \xrightarrow[t_{1/2} = 1.18 \text{ min}]{k_2 = 9.8 \times 10^{-3} \text{ s}^{-1}} {}^{234}_{92}U \rightarrow \text{disintegration series}$$

Note : If $k_2 >>> k_1$ i.e. k_1 is negligible with respect to k_2, i.e. $k_2 - k_1 \approx k_2$, then Eqn. 6.10.5 leads to $k_1N_1 = k_2N_2$. ***Thus transient equilibrium is converted into secular equilibrium.***

(b) **For the condition, $k_1 > k_2$,** i.e. the daughter is longer–lived compared to the parent. In this case, ultimately Eqn. 6.9.2.6 reduces **at higher times to :**

$$N_2 = N_{1(0)} \frac{k_1}{k_1 - k_2} \exp(-k_2 t)$$

It indicates that at higher times, the concentration of the daughter decreases with its own rate. **After a certain time, the parent nuclide practically disappears and no equilibrium is attained.** The time at which the daughter activity is maximum is given by Eqn. 6.10.3. The change of activity in such cases is illustrated in Fig. 6.10.1.

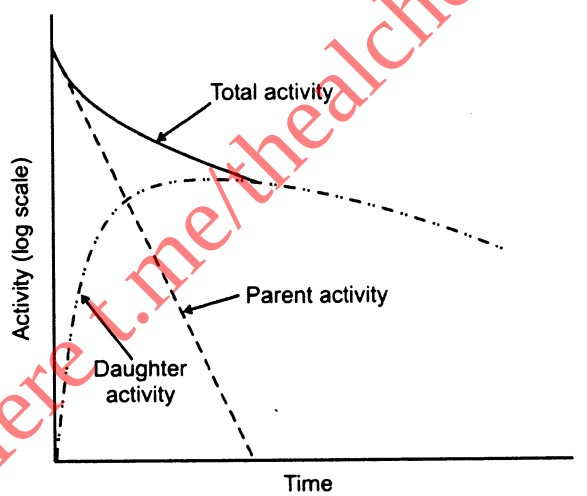

Fig. 6.10.1. Qualitative representation of decay curves where the parent nuclide decays faster than the daughter nuclide (i.e. $k_1 > k_2$) and ***no equilibrium.***

Examples :

$$^{218}_{84}Po \xrightarrow[t_{1/2} = 3.05 \text{ days}]{k_1 = 3.8 \times 10^{-3} \text{ s}^{-1}} {}^{214}_{82}Pb \xrightarrow[t_{1/2} = 26.8 \text{ min}]{k_2 = 4.3 \times 10^{-4} \text{ s}^{-1}} {}^{214}_{83}Bi \rightarrow \text{disintegration series}$$

$$^{210}_{83}Bi \xrightarrow[t_{1/2} = 5 \text{ days}]{k_1 = 1.6 \times 10^{-6} \text{ s}^{-1}} {}^{210}_{84}Po \xrightarrow[t_{1/2} = 138 \text{ days}]{k_2 = 5.8 \times 10^{-8} \text{ s}^{-1}} {}^{206}_{82}Pb \text{ (stable)}$$

These nuclides are present in $4n + 2$ series (Table 6.15.3).

Transient and Secular Radioactive Equilibrium : • *In a transient radioactive equilibrium* ($k_2 > k_1$), the relative amount of the daughter species, i.e. N_2/N_1, remains constant but the total activity due to the

Click Here t.me/thealchemylibrary

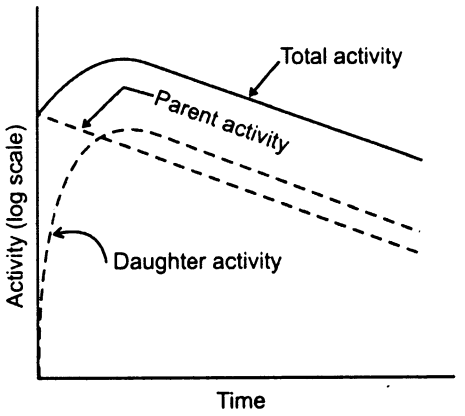

Fig. 6.10.2. Qualitative representation of transient equilibrium and nature of decay curves of the parent and daughter nuclide.

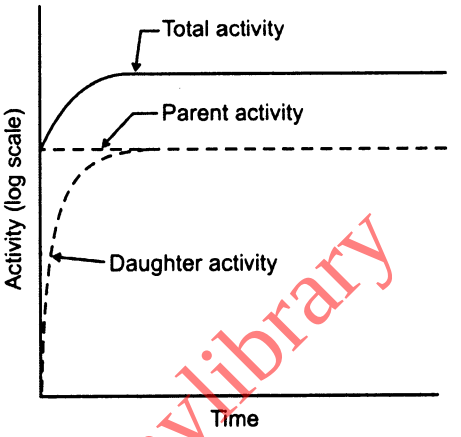

Fig. 6.10.3. Qualitative representation of secular equilibrium and nature of decay curves of the parent and daughter nuclide.

Click Here t.me/thearchenylibrary

both *parent* and daughter nuclides slowly decreases and it is controlled by the decay rate constant (k_1) of the parent nuclide. Eqn. 6.10.5 leads to the following relation :

$$\frac{N_2}{N_1} + 1 = \frac{k_1}{k_2 - k_1} + 1; \text{ or, } (N_2 + N_1)/N_1 = k_2/(k_2 - k_1)$$

or, $$(N_2 + N_1) = k_2 N_1/(k_2 - k_1) = [k_2 N_{1(0)} \exp(-k_1 t)]/(k_2 - k_1) \quad \ldots (6.10.6)$$

The total activity determined by $(N_2 + N_1)$ decreases exponentially governed by k_1 as given by Eqn. 6.10.6 (cf. Fig. 6.10.2).

- **In a secular equilibrium** ($k_2 >> k_1$), *the total activity as well as the relative amount of the daughter nuclide remains constant* (cf. Eqn. 6.10.2). In fact, the secular equilibrium is the limiting case of the transient equilibrium (when $k_2 >> k_1$, Eqn. 6.10.5 reduces to Eqn. 6.10.2) and both the daughter and parent species remain in **steady states.** At this equilibrium, though different amounts of the involved radioelements are present, all the elements disintegrate at the same rate (i.e. $k_1N_1 = k_2N_2 = k_3N_3 = ...$) (cf. Fig. 6.10.3).

- **Radioactive Equilibrium and Chemical Equilibrium :** In a radioactive disintegration series, under the condition of $k_2 > k_1$, the radionuclides will reach a *steady state* after a certain time (depending upon the relative magnitudes of k_1 and k_2). *This steady state condition is referred to as radioactive equilibrium and this steady state situation arises when the observation time is much greater than the average life period of the parent nuclide.* Depending upon the relative magnitudes of k_1 and k_2, the radioactive equilibrium may lead to *transient equilibrium* ($k_2 > k_1$, cf. Eqns. 6.10.5–6) and *permanent or secular equilibrium* ($k_2 >> k_1$, Eqn. 6.10.2) which is a limiting case of the transient equilibrium.

It indicates that the radioactive equilibrium which deals with the ***irreversible nuclear deacy processes in a radioactive disintegration series*** **is conceptually totally different from the chemical equilibrium which deals with the** ***reversible chemical reactions.*** A chemical equilibrium is attained when the rates of the forward and backward reactions are the same. External factors like temperature, pressure, etc. may influence the chemical equilibrium but a radioactive equilibrium is independent of such external

factors. A radioactive equilibrium deals with the nuclear reactions leading to the creation of isotopic species or new elements while a chemical equilibrium dealing with the chemical reactions does not produce any new element or isotopic species. The chemical reactions involve bond breaking and bond formation using the valency electrons. The differences between nuclear reactions and chemical reactions have been discussed in Sec. 7.3.

6.11 ENERGETICS OF THE DISINTEGRATION PROCESSES

If a nuclide ${}^{A}_{Z}X$ undergoes disintegration to produce ${}^{A-A'}_{Z-Z'}Y$ by emitting a particle ${}^{A'}_{Z'}P$, then the process can be represented as, ${}^{A}_{Z}X \rightarrow {}^{A-A'}_{Z-Z'}Y + {}^{A'}_{Z'}P + Q$; where Q is called *disintegration energy* determined by the difference in the masses of the initial and final species involved in the process. ***To make the disintegration process spontaneous, Q must be positive.*** This is why, the mass difference between the parent nuclide and the product bodies must be greater than zero to make the process energetically spontaneous, i.e. ***there must be a loss of mass.*** The Q is distributed among the disintegration products including the recoil daughter element as the kinetic energy. Now, let us consider the different cases.

(a) β^- decay : ${}^{A}_{Z}X \rightarrow {}^{A}_{Z+1}Y^{+} + {}^{0}_{-1}e + {}^{0}_{0}\bar{\nu} + Q$

${}^{0}_{0}\bar{\nu}$ stands for the antineutrino (massless, chargeless) **as the birth companion** (see Sec. 5.6) of the electron, ${}^{0}_{-1}e$. The product ${}^{A}_{Z+1}Y^{+}$ when produced will remain positively charged, because it has the atomic number $Z + 1$ while there are Z electrons in the orbitals. The mass loss, Δm is given by :

$$\Delta m = {}^{A}_{Z}m - \left[({}^{A}_{Z+1}m - m_e) + m_e\right] = {}^{A}_{Z}m - {}^{A}_{Z+1}m$$

where, ${}^{A}_{Z}m$ and ${}^{A}_{Z+1}m$ represent the masses of the corresponding neutral species, and m_e represents the mass of an electron. In expressing the mass of the product cation shown within braces ( ), the binding energy of the last electron in the atom is ignored. The error due to this assumption is very small, because the binding energies of the electrons are negligibly small compared to the other energies involved in the disintegration process.

Thus, $Q = 931\Delta m$ MeV, (when the masses are expressed in amu). Thus, the energy condition for the spontaneous β^- decay is given by :

$$\boxed{\Delta m = {}^{A}_{Z}m - {}^{A}_{Z+1}m \geq 0} \qquad \ldots (6.11.1)$$

The Q is distributed among the products, i.e.

$$Q = E_e + E_{\bar{\nu}} + E_r$$

where E_e, $E_{\bar{\nu}}$ and E_r denote the kinetic energies of the electron, the antineutrino and the recoil daughter nuclide respectively. **The energy of the recoil product is very small,** because it is measured by the ratio of the masses of the electron and the daughter nuclide. Hence, we can reasonably write,

$$Q = E_e + E_{\bar{\nu}}.$$

Thus, the whole energy gets distributed between the electron and the antineutrino in a continuous manner. Thus, the energy of the each particle (i.e. emitted antineutrino or electron) may

Click Here t.me/healchemylibrary

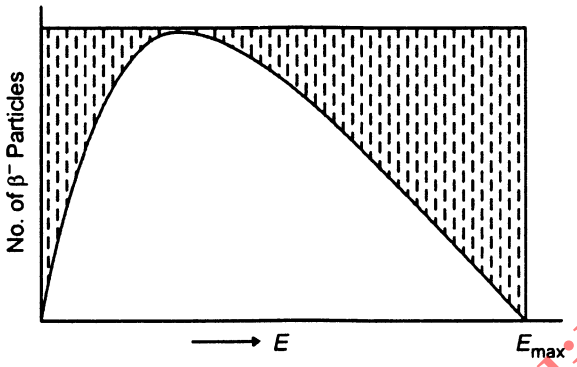

Fig. 6.11.1. Energy spectrum of β⁻-particles adapted from H.J. Arnikar, "Essentials of Nuclear Chemistry", Wiley Eastern Ltd., New Delhi, 1989. Reproduced with permission.

vary from zero to a maximum, $E_{max} = Q$. The distribution of energy is shown in Fig. 6.11.1. It indicates, $E_e = 0$ when $E_{\bar{\nu}} = Q$; and $E_e = Q$ when $E_{\bar{\nu}} = 0$.

(b) β⁺ decay : ${}^{A}_{Z}X \rightarrow {}^{A}_{Z-1}Y^{-} + {}^{0}_{+1}e + {}^{0}_{0}\nu + Q$

Here, ${}^{0}_{+1}e$ and ${}^{0}_{0}\nu$ stand for the positron and neutrino respectively. The product nuclide when produced remains mononegatively charged as the nucleus contains $Z - 1$ charges while there are Z electrons in the orbitals. The mass loss, Δm is given by:

$$\Delta m = {}^{A}_{Z}m - \left[({}^{A}_{Z-1}m + m_e) + m_e\right] = {}^{A}_{Z}m - {}^{A}_{Z-1}m - 2m_e$$

Symbols for m's and m_e bear the same significance as in β⁻ decay process. The mass of a positron is identical with that of an electron. Again, the process to be energetically allowed, the following condition (Eqn. 6.11.2) must be maintained. It indicates that the mass difference between the parent and daughter atoms must be at least $2m_e$ equivalent to 1.02 MeV :

$$\boxed{\Delta m = {}^{A}_{Z}m - {}^{A}_{Z-1}m - 2m_e \geq 0; \text{ or } ({}^{A}_{Z}m - {}^{A}_{Z-1}m) \geq 2m_e} \quad \ldots(6.11.2)$$

In this case, the energy, $Q = 931\Delta m$ MeV gets distributed between the positron and neutrino (i.e. $Q = E_e + E_\nu$) as their kinetic energies **in a continuous manner** (as in the case of β⁻ decay). **Here, the recoil energy of the daughter nuclide is ignored.**

(c) Electron Capture (EC)

In this process, an electron from the nearest shell, i.e. K-shell or at the furthest L-shell, is being captured by the nucleus. Electron capture from any further higher shell is more or less improbable. Even, the probability for L-capture is only 10% of that of K-capture. This process generates the same daughter nuclide as in the positron emission process. ***This process is energetically possible even when the mass difference (Δm) between the isobaric nuclides is less than $2m_e$.*** **The product species in this process is in the neutral state.**

$${}^{A}_{Z}X \xrightarrow[\text{or, } L\text{-capture}]{K\text{-capture}} {}^{A}_{Z-1}Y + {}^{0}_{0}\nu + Q$$

Click Here: me/thealchemylibrary

Here, the mass loss, Δm and energy condition are given by :

$$\boxed{\Delta m \approx {}^{A}_{Z}m - {}^{A}_{Z-1}m; \text{ and } Q = 931\,\Delta m \text{ MeV} \geq E_K \text{ or } E_L}$$

From the viewpoint of energy condition of the process, for K-capture, Q must be at least equal (i.e. $Q \geq E_K$) to the energy required (E_K) for removing an electron from the K-shell. Actually, E_K represents the binding energy of an electron in the K-shell. Similarly, for L-capture, the condition is: $Q \geq E_L$. The excess energy is mainly carried by the neutrino (recoil energy of the daughter nuclide is ignored). Therefore,

$$E_\nu = Q - E_K \text{ or } E_L.$$

(d) α-Decay : ${}^{A}_{Z}X \rightarrow {}^{A-4}_{Z+1}Y^{2-} + {}^{4}_{2}\alpha + Q$

Let, m_1, m_2 and m_α be the masses of the parent species, daughter species (neutral) and the α-particle respectively. Hence,

$$\Delta m = m_1 - [(m_2 + 2m_e) + m_\alpha] \approx m_1 - (m_2 + m_\alpha), \text{ (neglecting } m_e).$$

The daughter species formed bears two excess electrons in the orbitals. Thus, $Q = 931\Delta m$ MeV, Δm expressed in amu. For the energy condition to allow the process, $\Delta m \geq 0$. Now let us consider the aspects of energy distribution among the products. After ejection of the α-particle with a velocity, u_α, **the daughter nuclide will recoil with a velocity, *u* (say).** Now from the conservation of momentum, we have :

$$(m_2 + 2m_e)\, u = m_\alpha u_\alpha.$$

Here, $(m_2 + 2m_e)$ gives the mass of the product species which is dinegative. The binding energies of the electrons are ignored. Neglecting the masses of the two electrons, we can rationally write :

$$m_2 u = m_\alpha u_\alpha; \text{ or } u = (m_\alpha u_\alpha / m_2). \qquad \ldots(6.11.3)$$

For the process to run spontaneously, Q must be ≥ 0 and it is distributed between the product fragments. Therefore :

$$\boxed{Q = \frac{1}{2}m_2u^2 + \frac{1}{2}m_\alpha u_\alpha^2 = \frac{1}{2}m_2(m_\alpha u_\alpha / m_2)^2 + \frac{1}{2}m_\alpha u_\alpha^2 = \frac{1}{2}m_\alpha u_\alpha^2 (m_\alpha/m_2 + 1) = E_\alpha(m_\alpha/m_2 + 1)} \qquad \ldots(6.11.4)$$

where, E_α denotes the energy of the α-particle. Reasonably, m_α/m_2 can be taken as $4/(A-4)$, i.e. $m_\alpha/m_2 = 4/(A-4)$. Thus,

$$\boxed{Q = E_\alpha\left(\frac{A}{A-4}\right)} \qquad \ldots(6.11.5)$$

6.12 SOME IMPORTANT ASPECTS OF ALPHA DECAY

(i) ***Energetics of the α-Decay*** : It has been already discussed in the previous Section 6.11(d).

(ii) ***Range of the α-Particles*** : The alpha–particles can travel a few cm in air while it can get stopped by a 0.004 cm thick aluminium plate. Thus the range covered by the α-particles significantly depends on the nature of medium. The range is also dependent on the energy $E_\alpha\left(=Q\frac{A-4}{A}\right)$.

Click Here to me/thechemylibrary

The mean range (R) in air is related with the energy as, $R \propto (E_\alpha)^{3/2}$. The stopping power of a medium has been discussed in Sec. 6.18.2c. During the passage of the α-particles through a medium, the energy is lost in exciting and ionising the matter. When its energy falls below the ionisation energy of the matter, it takes up two electrons to form a neutral helium atom.

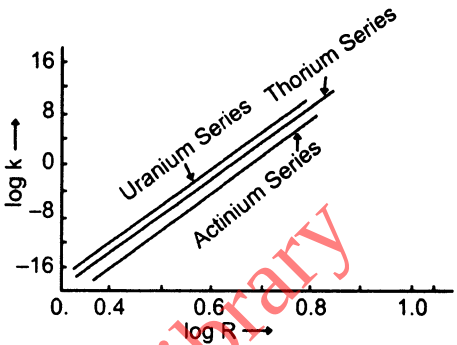

Fig. 6.12.1. Experimental verification of Geiger-Nuttall's law in the α-decay process. Adapted from K.G. Krishnan, "Atomic and Nuclear Physics", MacMillan India Ltd., 1973. Reproduced with permission.

(iii) ***Geiger-Nuttall's Law*** : An interesting relationship between the energy (E_α) of the α-particle emitted and the half–life period ($t_{1/2}$) of the source was observed. **With the increase of E_α of the particles emitted, the half life period of the sources falls abruptly.** It has been observed that for the increase of E_α by 2.25 times from 4 MeV to 9 MeV, the half life period falls from ~ 10^{17}s to ~ 10^{-7}s, i.e. by ~ 10^{24} times. From these observations, Geiger and Nuttall established an empirical rule named after them. The rule is expressed in terms of the decay constant ($k = 0.693/t_{1/2}$) as follows;

$$\log k = a \log E_\alpha + b \text{ (in terms of } E_\alpha)$$

$$= a' \log R + b' \left(\text{in terms of } R \propto E_\alpha^{3/2}\right)$$

$$= a'' \log u_\alpha + b'' \left(\text{in terms of } u_\alpha,\ E_\alpha = \frac{1}{2} m u_\alpha^2\right)$$

For a particular series, a and b (similarly other pairs, i.e. a', b'; a'', b'') are constant. **It is interestingly found that for the all naturally occurring radioactive series, a is the same but b differs. Thus, the lines are parallel** (see Fig. 6.12.1).

Though, at the time of formulation of the empirical rule, there was no theoretical explanation, in the light of wave mechanical theory of the α-particle decay, the rule gets a sound explanation. The rule is of much practical importance. By measuring the range of the α-particles, the $t_{1/2}$ and k for the very long lived or very short lived nuclides can be determined.

(iv) ***Theory of α-Decay***: Because of the Coulombic potential for the α-particle (see. Fig. 6.12.2), the height of the potential barrier is ~ 25 MeV. The Coulombic potential is governed by,

$$E_{Coul} = E_{pot}(x) = 2Ze^2/(4\pi\varepsilon_0 x),$$

where $E_{pot}(x)$ denotes the potential energy at the distance x from the centre of the nucleus having charge $+Ze$. For, x = nuclear radius (R), it gives the measure of the potential barrier. For most of the heavy nuclides emitting α-particles, the barrier height [$E_{pot} \approx 2Ze^2/(4\pi\varepsilon_0 R)$] is found ~ 25 MeV.

Click Here t.me/thealchemylibrary

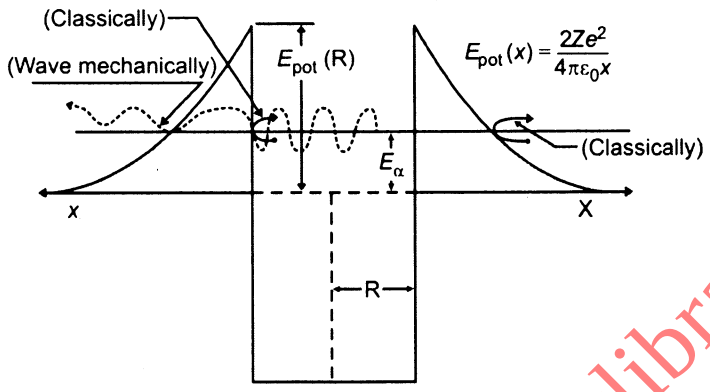

Fig. 6.12.2. Classical and wave mechanical (i.e. tunnel effect) models of α-decay.

Now let us consider the kinetic energy (E_α) associated with the α-particles emitted. It is given by Eqn. 6.11.5, i.e. $E_\alpha = Q\left(\frac{A-4}{A}\right)$ where $Q = 931\ \Delta m$ MeV. E_α has been found to lie in the range 4 to 9 MeV. For example, in the α-decay of $^{222}_{86}Rn$, $Q = 5.6$ MeV, and $E_\alpha = 5.49$ MeV.

From the idea of classical concept, for the escape of an α-particle, it must have at least the kinetic energy equal to the height of the barrier. Similarly, to penetrate into the nucleus, an α-particle should have at least the energy equal to the height of the barrier. Thus for penetration or emission of an α-particle, it must satisfy the condition, $E_\alpha \geq E_{pot}(R)$. But from our experience, it is found that the α-particles having much lower energy compared to the height of the barrier can perform task which *cannot be explained from the Classical Physics.* The wave mechanical concept can nicely explain the observation. The theory of α-particle decay based on the Schrödinger wave equation was independently established in 1928 by Gamow and by Condon and Gurney. In this consideration, the alpha–particle is supposed to be associated with a matter wave ($\lambda = h/m_\alpha u_\alpha$) and the wave gets incident on the potential barrier. **The incident wave partly gets reflected back and partly transmitted through the barrier.** Thus, the α–particle having energy, $E_\alpha < E_{pot}(R)$ can penetrate the barrier (see Fig. 6.12.2) provided the height and width of the barrier are not infinitely large. This phenomenon is called ***wave mechanical tunnel effect*** (cf. Sec. 3.5.6).

The wave mechanical treatment can also give the explanation of ***Geiger-Nuttall rule.*** Calculation shows that as the energy (E_α) of the α-particle to be emitted goes to increase, the probability of tunnelling of the particle through the barrier increases. **The higher probability of escaping of the α-particle from the nucleus leads to the higher decay constant of the nuclide.** Thus, for the α-particles with higher energies (consequently with a higher range), the corresponding parent nuclides are associated with the higher values of k and consequently the lower values of $t_{1/2}$.

6.13 SOME IMPORTANT ASPECTS OF BETA DECAY

(i) ***Energetics of the β-Decay*** : These have been discussed in Sec. 6.11a.

(ii) ***The Theory of β-Decay and Discovery of Neutrino*** : In the β^- and β^+ decay, antineutrino and neutrino are supposed to be present as their birth companions respectively.

Click Here to Free Chemistry Library

$$^{1}_{0}n \rightarrow {}^{1}_{+1}p + {}^{0}_{-1}e + {}^{0}_{0}\bar{\nu}; \quad {}^{1}_{+1}p \rightarrow {}^{1}_{0}n + {}^{0}_{+1}e + {}^{0}_{0}\nu$$

Similarly, for the *EC* process, the neutrino gets also involved, $^{1}_{+1}p + {}^{0}_{-1}e \rightarrow {}^{1}_{0}n + {}^{0}_{0}\nu$.

The existence of the antineutrinos and neutrinos were theoretically predicted to explain the following facts :

(a) **Conservation of energy** (see Secs. 6.11a; 6.11b; 5.6).

(b) **Conservation of angular momentum** (see Sec. 5.6).

(c) **Conservation of statistics** (see Sec. 5.6).

All these facts have been clearly discussed in Secs. 6.11 and 5.6.

The antineutrinos and neutrinos are chargeless, massless and they do not travel in the form of an electromagnetic wave. This is why, the cross–section of their interaction with matter is as low as 10^{-48} m^2. **This is why, it was a difficult task to catch hold of the particles to verify experimentally their existence.** However, the task was done in reality by Cowan and Reines in 1953 in an ingenious experiment. If the postulate, i.e. $^{1}_{+1}p \rightarrow {}^{1}_{0}n + {}^{0}_{+1}e + {}^{0}_{0}\nu$, is true, then the partial reverse process, i.e. $^{1}_{+1}p + {}^{0}_{0}\nu \rightarrow {}^{1}_{0}n + {}^{0}_{+1}e$, is supposed to occur to produce the neutrons. Based on this assumption, a flux of neutrinos obtained from a reactor containing a huge number of β^+ active nuclides was allowed to interact with a large amount of water giving protons to interact with the neutrinos. To identify the speculated product, i.e. neutron, cadmium chloride was used because cadmium is having a high *cross section* to interact with the neutron as : ^{113}Cd (n, γ) $^{114}Cd^{*} \rightarrow {}^{114}\text{Cd} + \gamma + \gamma + \gamma + \ldots$ The positron undergoes annihilation (reverse of pair formation) as : $^{0}_{+1}e + {}^{0}_{-1}e \rightarrow \gamma + \gamma$. In the experiment, thus both the positron and neutron were detected (see Sec. 5.6). It indicated indirectly the existence of the neutrinos.

(iii) ***Sargent's Curve* : *Relation between k and E_β* :** We have already mentioned that for a particular source, the energies of the emitted particles cover a spectral range (see. Fig. 6.11.1). The maximum energy $E_{\beta(max)}$ which can be associated with the β-particles lies at the highest energy end of the spectrum. Analogous to the Geiger-Nuttall's rule, it has been observed by Sargent that **with the increase of $E_{\beta(max)}$ the decay constant increases,** i.e. **the more the value of $E_{\beta(max)}$, the more is the value of decay constant.**

(iv) ***Isobaric relationship* :** The daughter and parent nuclides are isobaric in nature for both the types of β-decay and electron capture (EC) process.

Click Here to me/chealchemylibrary

6.14 SOME IMPORTANT ASPECTS OF GAMMA EMISSION

Very often the daughter nucleus formed remains in an excited state and its deexcitation may occur in the following ways.

We have already discussed the phenomena, ***Auger effect*** (see Sec. 6.7), ***X–ray emission*** (see Sec. 6.7) and ***internal conversion*** (see Secs. 5.2.6ix and 6.6vi).

Based on the $t_{1/2}$ period of the γ-transition, they are classified as ***instantaneous transitions*** ($t_{1/2} < 10^{-7}$s) and **isomeric transitions** (see Sec. 5.1.6iv; 6.16.2d) (*IT*) having $t_{1/2} > 10^{-7}$s. This time

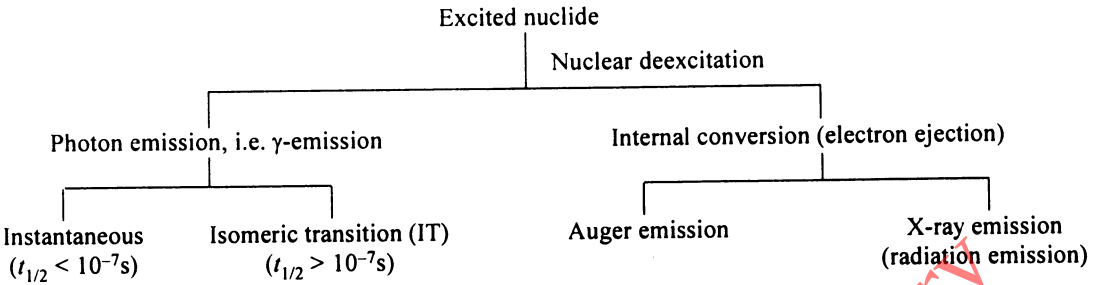

barrier is arbitrarily selected. In the case of γ-transitions, it is required to mention the spin (I) and parity (π) of the parent and daughter nuclides involved in the γ-transitions. In terms of change in energy (E), spin (I) and parity (π), we can consider the γ-transitions as follows.

(a) ***Change in energy*** : $\Delta E = E_i - E_f = h\nu$, ($i$ and f denote the initial and final states of the nuclide respectively).

(b) ***Change in spin*** : $\Delta I = I_i - I_f = \Delta I$ or L can have any integral value except zero in the range, $|I_i - I_f|$ to $|I_i + I_f|$.

(c) ***Change in parity*** : The parity change occurs in such a way that the parity of the entire system consisting of the photon, the parent nuclide and the daughter nuclide is conserved. Even and odd parity are counted by +1 and 0 (not by −1) respectively. If, $\pi_i + \pi_f + L$ = odd, then the transition is called *magnetic multipole (represented by ML) radiation*; and if, the sum is even, the radiation is called *electric multipole (represented by EL) radiation*. The transitions in the following systems are shown in the following scheme.

$\pi_i + \pi_f + L_{min}$	Transition	State
1 + 1 + 3 = 5 (odd) i.e. ***M3* type**	^{60m}Co	2 (+)
	IT ≀ γ_1 (10.5)	
	^{60}Co	5 (+)
	↓ $-\beta^-$	
1 + 1+ 2 = 4, (even) i.e. ***E2* type**	$^{60}Ni^*$	4 (+)
	≀ γ_2 (Instantaneous)	
1 + 1 + 2 = 4, (even) i.e. ***E2* type**	$^{60}Ni^*$	2 (+)
	≀ γ_3 (Instantaneous)	
	^{60}Ni	0 (+)

Click Here to meet the chemylibrary

6.15 THE DISINTEGRATION SERIES

There are three **naturally occurring radioactive series** represented by $4n + 0$, $4n + 2$ and $4n + 3$. There is **an artificially made series,** $4n + 1$. In the series, successive changes are carried out by α- and β-decays. An α-decay reduces the mass number by 4 units while the β-decay does not introduce any change in the mass number. This is why, all the elements involved in a particular series possess the mass numbers which can be expressed by $4n$, or $4n + 1$, or $4n + 2$, or $4n + 3$ where n is an integer. **The series are also *named after the name of the longest lived element* in a particular series.** This is why,

the $4n$, $4n + 1$, $4n + 2$ and $4n + 3$ series are called the *Thorium, Neptunium, Uranium* and *Actinium series* (exception) respectively. In the neptunium series (starting from ^{241}Pu) which has been prepared artificially, the longest lived element is ^{237}Np having $t_{1/2} = 2.2 \times 10^6$ years. It is expected that at the beginning of the earth, the series was naturally occurring but by this time it has decayed almost completely. This is why the $(4n + 1)$ series is missing in nature among the series $4n + x$, $x = 0$ to 3. The series are shown below. The half life periods for the respective members are also given.

Table 6.15.1. The Thorium Series ($4n$ series)

Element	A (X) Z*	Periodic Group**	Particle emitted	Half Life
Thorium	232 (Th)90		α	1.4×10^{10} years
Mesothorium–1	228 (Ra) 88		β	6.7 years
Mesothorium–2	228 (Ac) 89		β	6.12 hours
Radiothorium	228 (Th) 90		α	1.90 years
Thorium–X	224 (Ra) 88	IIA (2)	α	3.64 days
Thoron	220 (Rn) 86	VIIIA (18)	α	54.5 s
Thorium–A	216 (Po) 84	VIA (16)	α	0.16 s
Thorium–B	212 (Pb) 82	IVA (14)	β	10.6 hours
Thorium–C ↓ α, β	212 (Bi) 83	VA (15)	α, β	60.5 min
Thorium C′	212 (Po) 84	VIA (16)	α	3×10^{-7} s
Thorium–C″ ↓ β, α	208 (Tl) 81	IIIA (13)	β	3.1 min
Thorium–D	208 (Pb) 82	IVA 14)	Stable	Stable

* A (X) Z ≡ mass nuclear (symbol) atomic number. ** IUPAC group numbers are given within ( ).

Table 6.15.2. The Neptunium Series ($4n + 1$ series)

Element	A (X) Z	Periodic Group*	Particle emitted	Half life
Plutonium	241(Pu) 94		β	13.2 yrs.
Americium	241 (Am) 95		α	462 yrs.
Neptunium	237 (Np) 93		α	2.2×10^6 yrs.
Protoactinium	233 (Pa) 91		β	27 days
Uranium	233 (U) 92		α	1.62×10^5 yrs.
Thorium	229 (Th) 90		α	7340 yrs.
Radium	225 (Ra) 88	IIA (2)	β	14.8 days
Actinium	225 (Ac) 89	IIIB (3)	α	10 days
Francium	221 (Fr) 87	IA (1)	α	4.8 min
Astatine	217 (At) 85	VIIA (17)	α	0.018 s
Bismuth ↓ α, β	213 (Bi) 83	VA (15)	α, β	47 min
Polonium	213 (Po) 84	VIA (16)	α	4.2×10^{-6} s
Thalium ↓ β, α	209 (Tl) 81	IIIA (13)	β	2.2 min
Lead	209 (Pb) 82	IVA (14)	β	3.3 hour
Bismuth	209 (Bi) 83	VA (15)	Stable	Stable

* IUPAC group numbers are given within ( ).

Click Here t.me/thealchemylibrary

Table 6.15.3. The Uranium Series ($4n + 2$ series)

Element	A (X) Z	Periodic Group*	Particle emitted	Half life
Uranium–I	238 (U) 92		α	4.5×10^9 yrs.
Uranium–X_1	234 (Th) 90		β	24.5 days
Uranium–X_2	234 (Pa) 91		β	1.18 min
Uranium–II	234 (U) 92		α	2.7×10^5 yrs.
Ionium	230 (Th) 90		α	8.3×10^4 yrs.
Radium	226 (Ra) 88	IIA (2)	α	1590 yrs
Radon	222 (Rn) 86	VIIIA (18)	α	3.8 days
Radium–A	218 (Po) 84	VIA (16)	α	3.05 min
Radium–B	214 (Pb) 82	IVA (14)	β	26.8 min
Radium–C ┐	214 (Bi) 83	VA (15)	β, α	19.7 min
β ↓ ↓ α				
Radium–C′′	210 (Tl) 81	IIIA (13)	β	1.32 min
Radium–C′	214 (Po) 84	VIA (16)	α	1.5×10^{-4} s
α ↓ ↓ β				
Radium–D ←	210 (Pb) 82	IVA (14)	β	22 yrs.
Radium–E	210 (Bi) 83	VA (15)	β	5 days
Radium–F	210 (Po) 84	VIA (16)	α	140 days
Radium–G	206 (Pb) 82	IVA (14)	Stable	Stable

* IUPAC group numbers are given within ( ).

Table 6.15.4. The Actinium Series ($4n + 3$ series)

Element	A (X) Z	Periodic Group*	Particle emitted	Half life
Actinouranium	235 (U) 92		α	7.1×10^8 yrs.
Uranium–Y	231 (Th) 90		β	25.6 hours
Protoactinium	231 (Pa) 91		α	3.2×10^4 yrs.
Actinium	227 (Ac) 89		β	21.8 yrs.
Radioactinium	227 (Th) 90		α	18.9 days
Actinium–X	223 (Ra) 88	IIA (2)	α	11.2 days
Actinon	219 (Rn) 86	VIIIA (18)	α	3.92 s
Actinium–A	215 (Po) 84	VIA (16)	α	1.8×10^{-3} s
Actinium–B	211 (Pb) 82	IVA (14)	β	36 min
Actinium–C ┐	211 (Bi) 83	VA (15)	β, α	2.16 min
β ↓ ↓ α				
Actinium–C′′	207 (Tl) 81	IIIA (13)	β	4.76 min
Actinium–C′	211 (Po) 84	VIA (16)	α	0.56 s
α ↓ ↓ β				
Actinium–D ←	207 (Pb) 82	IVA (14)	Stable	Stable

* IUPAC group numbers are given within ( ).

Click Here t.me/healchemylibrary

6.16 ARTIFICIAL OR INDUCED RADIOACTIVITY

In some cases, the new elements formed in the nuclear transmutations are radioactive and they follow the laws of disintegration as in the case of naturally occurring radioelements. Since this radioactive property is produced by an artificial means, this phenomenon is called ***artificial or induced radioactivity.***

6.16.1 Discovery of Artificial Radioactivity

When Irene Curie and her husband Frederic Joliot Curie were studying the **nuclear transmutations** by bombarding α-particles on the elements like *B*, *Mg* and *Al*, they astonishingly noticed that **even after the removal of the α-particle source, the bombarded *Al* sheet continued to emit the positron particles** while the other ejectiles, i.e. proton and neutron, got stopped as soon as the α-particle source was taken away. **Chemical analysis showed the existence of *Si* and *P* in the bombarded *Al* foil.** The positron activity was found to fall exponentially ($t_{1/2} \approx 3$ min) as expected from the first order kinetics of radioactive decay. In practice, the α-particle bombarded *Al*–sheet was dissolved in hydrochloric acid and the hydrogen gas evolved was collected in a thin walled glass tube from which positron activity was observed.

To explain the observation, it was believed that during the impingement of the α-particle on the aluminium foil, two parallel paths of transmutation develop. In one path, protons come out as the ejectiles. In the second path, an isotope of phosphorus, **^{30}P is formed along with a neutron. ^{30}P being radioactive disintegrates into ^{30}Si and positron.** The phosphorus formed in this way produces $^{30}PH_3$ which gets collected along with H_2 in the acid treatment on the bombarded *Al* foil.

Phosphorus produced in the bombarded *Al*-sheet produces **aluminium phosphide (*AlP*) which produces phosphine during the treatment with acid.** The radioactive phosphorus thus produced was also isolated as phosphate. The bombarded *Al*-sheet was dissolved in aqua regia and then the solution was treated with sodium phosphate and zirconyl nitrate. **The precipitation of zirconyl phosphate carried down all the radiophosphate.** Thus the produced radioactive phosphorus was isolated as insoluble zirconyl phosphate through the ***carrier technique.***

The whole process can be expressed in the following nuclear reactions.

$$^{27}_{13}Al + {}^{4}_{2}He \rightarrow {}^{30}_{14}Si + {}^{1}_{1}H$$

$$^{27}_{13}Al + {}^{4}_{2}He \rightarrow {}^{30}_{15}P + {}^{1}_{0}n$$

$$^{30}_{15}P \xrightarrow{t_{1/2} = 3 \text{ min}} {}^{30}_{14}Si + {}^{0}_{+1}e + \text{neutrino}$$

Thus, the phenomenon, artificial radioactivity was discovered in 1934 by the wife–husband couple, I. Curie and F. Joliot Curie and they were awarded Nobel Prize in 1935.

For *Mg* and *B*, similar reactions occur.

Click Here to Join Chemistry Library

$$^{24}_{12}Mg + ^{4}_{2}He \longrightarrow ^{27}_{14}Si + ^{1}_{0}n$$

$$\xrightarrow[t_{1/2} = 5\text{ s}]{} ^{27}_{13}Al + ^{0}_{+1}e + \text{neutrino}$$

$$^{10}_{5}B + ^{4}_{2}He \longrightarrow ^{13}_{7}N + ^{1}_{0}n$$

$$\xrightarrow[t_{1/2} = 10\text{ min}]{} ^{13}_{6}C + ^{0}_{+1}e + \text{neutrino}$$

After the discovery of artificial radioactivity, this new field of research was opened to the nuclear scientists; and a large number of radioisotopes (artificially produced) for most of the elements were reported from different laboratories. In addition to the α-particles, many other projectiles such as protons, deutrons, neutrons and γ-rays were used in producing the radioisotopes.

6.16.2 Production of Artificial Radioactivity

(a) Artificial Radioactivity by Neutrons

Compared to the α-particles, the neutron beam has got some advantages as a projectile, because the neutron being neutral does not experience any Coulombic barrier. E. Fermi and his co-workers started the work by using the slow neutron. **In this process, mainly β⁻-active isotopes are produced and in a few cases, β⁺-active isotopes are generated. Some examples are given here.**

(i) $^{27}_{13}Al + ^{1}_{0}n \longrightarrow ^{24}_{11}Na + ^{4}_{2}He$; $^{24}_{11}Na \longrightarrow ^{24}_{12}Mg + ^{0}_{-1}e$,

(ii) $^{31}_{15}P + ^{1}_{0}n \longrightarrow ^{31}_{14}Si + ^{1}_{1}H$; $^{31}_{14}Si \longrightarrow ^{31}_{15}P + ^{0}_{-1}e$,

(iii) $^{127}_{53}I + ^{1}_{0}n \longrightarrow ^{128}_{53}I \longrightarrow ^{128}_{54}Xe + ^{0}_{-1}e$,

(iv) $^{39}_{19}K + ^{1}_{0}n \longrightarrow ^{38}_{19}K + 2\,^{1}_{0}n$; $^{38}_{19}K \longrightarrow ^{38}_{18}Ar + ^{0}_{+1}e$,

(neutrinos and antineutrinos are not shown).

In this connection, the (n, γ) reactions are very much important in synthesising isotopes (see Table 6.17.1) and neutron activation analysis (see. Sec. 6.17).

(b) Artificial Radioactivity by Deuterons

The transmutations of the types (d, p), $(d$, alpha) and (d, n) generally lead to the production of radioisotopes. Some examples are given here.

(i) $^{12}_{6}C + ^{2}_{1}H \longrightarrow \left(^{14}_{7}N\right) \longrightarrow ^{13}_{6}C + ^{1}_{1}H$

$$\longrightarrow ^{13}_{7}N + ^{1}_{0}n;\ ^{13}_{7}N \rightarrow ^{13}_{6}C + ^{0}_{+1}e$$

Here, $\left(^{14}_{7}N\right)$ represents the intermediate compound nucleus. The transmutation follows the two paths (d, p) and (d, n) but only the (d, n) path leads to artificial radioactivity.

(ii) $^{7}_{3}Li + ^{2}_{1}H \longrightarrow \left(^{9}_{4}Be\right) \longrightarrow 2\,^{4}_{2}He + ^{1}_{0}n$

$$\longrightarrow ^{8}_{3}Li + ^{1}_{1}H;\ ^{8}_{3}Li \longrightarrow ^{8}_{4}Be + ^{0}_{-1}e$$

Click Here t.me/thealchemylibrary

Here, the (*d*, *p*) path produces artificial radioactivity.

(iii) $^{26}_{12}Mg + {}^{2}_{1}H \longrightarrow {}^{24}_{11}Na + {}^{4}_{2}He$

$$\downarrow \longrightarrow {}^{24}_{12}Mg + {}^{0}_{-1}e$$

Here, the (*d*, α) path produces the induced radioactivity.

(c) Artificial Radioactivity by Protons

The transmutation reactions of the types (*p*, *n*) and (*p*, *gamma*) by the accelerated protons on the light nuclei lead to some radioactive elements. Some examples are given here.

(i) $^{11}_{5}B + {}^{1}_{1}H \longrightarrow {}^{11}_{6}C + {}^{1}_{0}n$; $^{11}_{6}C \longrightarrow {}^{11}_{5}B + {}^{0}_{+1}e$,

(ii) $^{12}_{6}C + {}^{1}_{1}H \longrightarrow {}^{13}_{7}N + \gamma$; $^{13}_{7}N \longrightarrow {}^{13}_{6}C + {}^{0}_{+1}e$

(d) Artificial Radioactivity by γ–Rays

Some typical examples are shown here.

(i) $^{81}_{35}Br + \gamma\,(i.e.\ h\nu) \longrightarrow {}^{80m}_{35}Br + {}^{1}_{0}n$

Here the produced **metastable isomer** $^{80m}_{35}Br$ suffers an **isomeric transition (*IT*)** followed by a β^--decay to form $^{80}_{36}Kr$, i.e.

$$^{80m}_{35}Br \xrightarrow[(t_{1/2} \approx 4.4\ \text{hrs})]{\text{IT}} {}^{80}_{35}Br \xrightarrow{\beta^-} {}^{80}_{36}Kr^{*} \xrightarrow[\text{(Instantaneous)}]{\gamma} {}^{80}_{36}Kr$$

(ii) $^{31}_{15}P + \gamma\,(i.e.\ h\nu) \longrightarrow {}^{30}_{15}P + {}^{1}_{0}n$

$$\downarrow \longrightarrow {}^{30}_{14}Si + {}^{0}_{+1}e$$

By using the accelerated high energy particles (e.g. *p*, *d*, α) and other heavy ions in **transmutation reactions or from fission fragments,** different radioisotopes covering the whole range have been prepared. Many of them are very much useful. Different modes of synthesis of some useful radioisotopes are given in Table 6.17.1.

6.17 APPLICATIONS OF RADIOACTIVE ISOTOPES

Many radioisotopes are very much useful in different disciplines such as research, medicine, analytical problems of chemistry, etc. Before we discuss the application of the radioisotopes, the methods of synthesis of some useful radioisotopes, and their properties are given in Table 6.17.1.

Technique of isotope labelling of a compound by the desired radioisotopes : Labelled compounds are widely used (cf. Sec. 6.17.1) to elucidate the reaction mechanism and structure. Isotope labelling technique is discussed below for some representative cases.

- ***^{14}C-labelling*** : ^{14}N (*n*, *p*) ^{14}C reaction can generate ^{14}C.

$$^{14}_{7}N + {}^{1}_{0}n \rightarrow {}^{14}_{6}C + {}^{1}_{1}H$$

Aluminium nitride (*AlN*) or berrylium nitride (Be_3N_2) is irradiated with a thermal neutron flux

Click Here t.me/thealchemylibrary

in a reactor. Thus the irradiated nitride in dissolved in dilute H_2SO_4 and then treated with H_2O_2. This releases $^{14}CO_2$ which can be absorbed in a suspension of $Ba(OH)_2$ to produce $Ba^{14}CO_3$ from which $^{14}CO_2$ can be extracted by the treatment with dilute acid. This $^{14}CO_2$ can be used in organic synthesis to prepare the desired tagged compound.

$$\text{Nitride salt} \xrightarrow{\text{neutron flux}} \text{Irradiated nitride} \xrightarrow[\text{(ii) } H_2O_2]{\text{(i) } H_2SO_4} {}^{14}CO_2 \xrightarrow{Ba(OH)_2} Ba^{14}CO_3 \xrightarrow{\text{Acid}} {}^{14}CO_2$$

Thus $Ba^{14}CO_3$ prepared is stored for the source of $^{14}CO_2$.

Table 6.17.1. Characteristics of some useful radioisotopes

Radioisotope	Mode of synthesis*	Mode of disintegration	Half life
^3H	$^{14}N\,(n, t)\,^{12}C$ / $^6Li\,(n, \alpha)^3H$	β^-	12.4 yr
^{14}C	$^{14}N\,(n, p)\,^{14}C$	β^-	5700 yr
^{22}Na	$^{24}Mg\,(d, \alpha)\,^{22}Na$	β^+, γ	2.6 yr
^{24}Na	(n, γ)	β^-, γ	14.9 hr
^{32}P	(n, γ)	β^-	14.3 d
^{35}S	(n, γ)	β^-	87.1 d
^{36}Cl	(n, γ)	β^-	3×10^5 yr
^{42}K	(n, γ)	β^-, γ	12.4 hr
^{45}Ca	(n, γ)	β^-	166 d
^{51}Cr	(n, γ)	int. conv.	26 d
^{56}Mn	(n, γ)	β^-, γ	2.6 hr
^{59}Fe	(n, γ)	β^-, γ	44.5 d
^{60}Co	(n, γ)	β^-, γ	5.3 yr
^{63}Ni	(n, γ)	β^-	100 yr
^{76}As	(n, γ)	β^-, γ	26.5 hr
^{82}Br	(n, γ)	β^-, γ	35.5 hr

* In (n, γ) reactions, the target nuclide is the corresponding stable isotope having mass number less than one.

- ***^{36}Cl- labelling*** : The (η, γ) reaction produces ^{36}Cl.

$$^{35}_{17}Cl + {}^{1}_{0}n \rightarrow {}^{36}_{17}Cl + \gamma$$

The produced ^{36}Cl is allowed to react with hydrogen to produce $H^{36}Cl$ which can be used to synthesise the desired compound.

- ***^{32}P-labelling*** : The (n, γ) reaction can produce ^{32}P. $^{32}S\,(n, p)\,^{32}P$ reaction can also produce ^{32}P.

$$^{31}_{15}P + {}^{1}_{0}n \rightarrow {}^{32}_{15}P + \gamma;\ {}^{32}_{16}S + {}^{1}_{0}n \rightarrow {}^{32}_{15}P + {}^{1}_{1}H$$

Thus the produced ^{32}P is converted into $H_3{}^{32}PO_4$ by the treatment of H_2O_2 in acidic condition.

$$^{32}S \xrightarrow{\text{neutron flux}} \text{Irradiated mass} \xrightarrow[(\text{at} \sim 600^\circ C)]{^{32}S \text{ (sublimed off)}} \text{Residue} \xrightarrow{H_2O_2,\ H^+} H_3{}^{32}PO_4 \xrightarrow{Ca(OH)_2} Ca_3(^{32}PO_4)_2$$

Click Here t.me/thealchemylibrary

Principle of Tracer Technique : To investigate many physico-chemical processes, the *tracer technique* is very much important. In this process, a very small amount of a substance (whose physico-chemical fate is to be established) containing a radioisotope is mixed with a relatively larger amount of the corresponding nonradioactive compound. In a large molecule only one suitable atom is labelled or tagged with its radioisotope. For example, in glycine, the nitrogen can be labelled as, $^*NH_2 - CH_2 - CO_2H$. The atom or position which will be labelled depends on the purpose of investigation. The labelled atom is represented by a star (*). If the thermodynamic and kinetic isotope effects (see Sec. 5.2.3ii) are ignored, then both the radioactive and nonradioactive molecules of the same compound will participate in the desired physico-chemical process in the same way. The extent of participation by the labelled or tagged species in the desired process depends on its concentration in the same way as in the case of nonlabelled molecules.

In fact, the thermodynamic (i.e. equilibrium constant) and kinetic (i.e. rate of reaction) isotope effects are very much significant for the lighter elements (e.g. hydrogen) only. This is why, the tracer technique is satisfactorily applied by tagging the relatively heavier elements where the relative mass difference among the isotopes is negligible.

Thus, in the absence of any isotope effect, if x mole of the labelled compound is mixed with y moles ($y >> x$) of the nonlabelled compound in a particular process, then the extents of participation by both the tagged and nontagged species after a certain period are related as : $\Delta x/\Delta y = x/y$. Here, even for the very small value of Δx (say, $10^{-10} - 10^{-12}$ M) it can be precisely estimated by measuring its activity. The knowledge of Δx determines Δy which may lie beyond the range of estimation by conventional methods.

For a successful tracer study, the following conditions are to be satisfied.

(i) Isotopic effect should be negligible.

(ii) Isotope exchange rate among the different molecules of different species should be very small.

(iii) The $t_{1/2}$ of the radioisotope to be used should be sufficiently long, so that during the operational period of the investigation it should not decay significantly. Generally for the biological experiments, the isotopes having $t_{1/2}$ relatively small are recommended so that after the experiment they cannot live in the biological system for a long time.

(iv) The amount of labelled species to be taken should be sufficient so that its fate can be studied by a measurable signal.

6.17.1 Application of Radioisotopes in the Field of Chemistry

(A) Determination of Structure

(i) ***Thiosulphate ion*** **:** The establishment of the structure of thiosulphate ion is the most classical example in this field. If the labelled sulphur (*S) is heated with a solution of nonradioactive sulphite ion, then the labelled thiosulphate ion is formed, i.e., $S^* + SO_3^{2-} \rightarrow {}^*SSO_3^{2-}$. The labelled thiosulphate ion on being decomposed by acidification produces elemental sulphur and sulphite; *and all the radioactivity is retained with the elemental sulphur and no trace of activity is found in the sulphite ion formed.* ***This observation clearly indicates that the two sulphur centres in thiosulphate are not equivalent.*** If they were equivalent, the activity would get distributed equally in both the fragments, i.e. sulphur and sulphite, each containing one sulphur atom. Thus the observation runs in conformity with the following structure of thiosulphite ion.

Click Here to the/thearchemylibrary

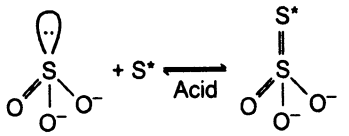

i.e. $SO_3^{2-} + S^* \longrightarrow {}^*SSO_3^{2-}$; ${}^*SSO_3^{2-} + 2H^+ \longrightarrow H_2SO_3 + S^*$

The labelled $Na_2S^*SO_3$ can also be prepared by the action of iodine on a mixture of Na_2SO_3 and Na_2S^*. It can be decomposed by heavy metal (preferring the *soft base sulfide*) salts like silver nitrate.

$$NaO - SO_2Na + I_2 + Na - {}^*SNa \rightarrow 2NaI + NaO - SO_2 - {}^*SNa \text{ (i.e. } Na_2{}^*SSO_3)$$

$$Na_2{}^*SSO_3 + 2AgNO_3 + H_2O \rightarrow Ag_2S^* + Na_2SO_4 + 2HNO_3$$

Formation silver sulfide is explained by considering the following structure of silver thiosulfate.

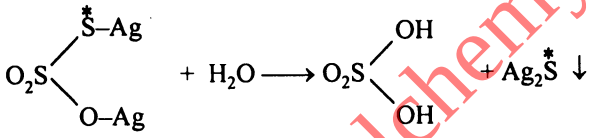

The above reactions support the following structure of thiosulfate.

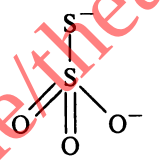

(i.e. existence of –*SH* group in the corresponding thiosulfuric acid which is unstable).

The corresponding parent acid, i.e. thiosulfuric acid ($H_2S_2O_3$) is extremely unstable in presence of water and it rapidly decomposes. *However, in absence of water, its decomposition can be prevented and it is quite stable.* In fact, in absence of water, it decomposes below 0°C as follows:

$$H_2S_2O_3 \longrightarrow H_2S + SO_3$$

This decomposition pattern is comparable to that of sulphuric acid.

$$H_2SO_4 \longrightarrow H_2O + SO_3 \ (> 300^\circ C)$$

The above similar reaction indicates the presence of –*SH* group in the corresponding thiosulfuric acid. Thus thiosulphuric acid $O_2S(OH)(SH)$ is structurally similar to sulfuric acid $O_2S(OH)_2$.

All these evidences indicate that thiosulfuric acid remains in an equilibrium mixture of two isomeric forms (i.e. *tautomers*).

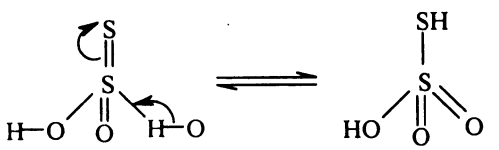

The position of the equilibrium depends on the experimental conditions. Thus the structure of thiosulfate ion should be shown as follows :

Click Here t.me/thealchemylibrary

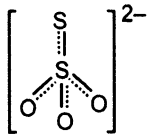

Note : **Prof. P. Ray** prepared the complexes containing both the tautomeric forms of thiosulfate. This is illustrated below by taking the isomeric complexes of *Co*(III).

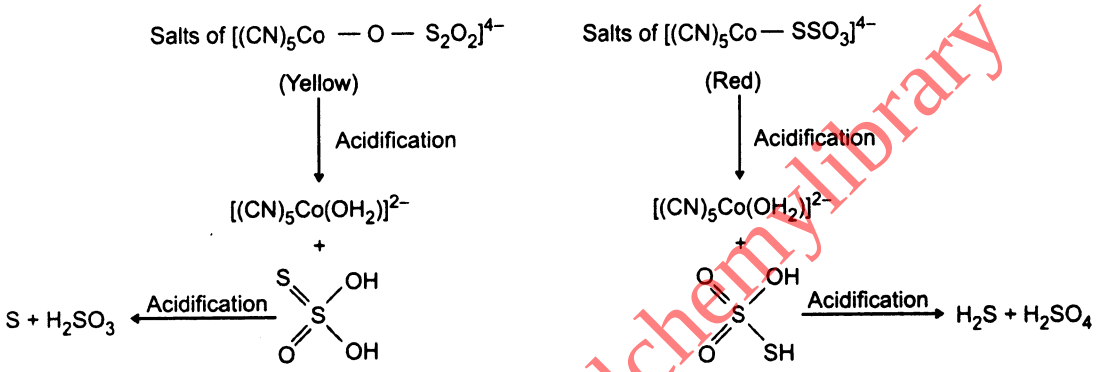

All these observations rule out the possibility of the symmetrical structure.

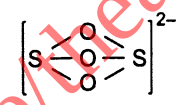

(ii) ***HgI_4^{2-} ion*** : All the iodines in the moiety, HgI_4^{2-} are equivalent. It can be proved in the following way.

Synthesis : $HgI_2 + 2NaI^* \rightarrow Na_2HgI_4^*$.

Decomposition : $Na_2HgI_4^* + 2AgNO_3 \rightarrow 2AgI^* + HgI_2^* + 2NaNO_3$.

Here, after decomposition of the labelled $Na_2HgI_4^*$, the radioactivity is distributed proportionately in both the fragments, though during synthesis there was no activity in HgI_2. It clearly indicates that all the iodines in HgI_4^{2-} are equivalent.

(iii) ***PCl_5*** : In ***PCl_5*** (trigonal bipyramidal structure), there are two types of chlorine, 2 axial *Cl* (relatively weakly bound) and 3 equatorial *Cl* (relatively strongly bound, i.e. shorter bond length). This is supported from the following sequence of reaction.

$$PCl_3 + {}^*Cl_2 \rightarrow P^*Cl_5 \xrightarrow{Hydrolysis} POCl_3 + 2H^*Cl$$

All the activity remains concentrated in the released *HCl*. It indicates that all the 5 *Cl*-atoms are not equivalent in PCl_5. The observation is in conformity with the following structure of PCl_5.

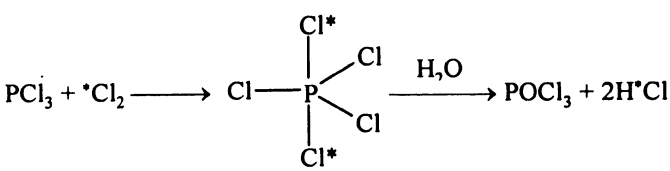

Click Here t.me/thealchemylibrary

(B) Establishment of Reaction Mechanism

(i) ***Esterification*** : In the reaction, $R\text{–}CO_2H + R'OH \rightarrow RCO_2R' + H_2O$, there are two possibilities:

Path I : 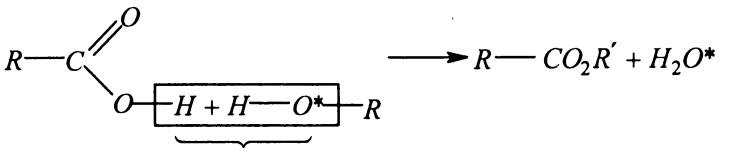

Path II : 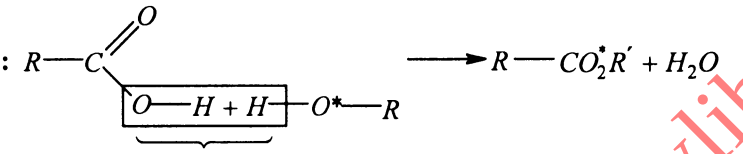

Now, if labelled $R'O^*H$ is used, the first path (i.e. $R'\text{–}OH$ bond rupture) leads to no accumulation of activity in the ester formed, while the second path (i.e. $R'O\text{–}H$ bond rupture) indicates the accumulation of total activity in the ester formed and no activity in the water formed. Thus, the actual path can be established.

(ii) ***Hydrolysis of ester*** : The reverse of the esterification process was carried out in H_2O^*, and it was found that in most of the cases, the activity was confined in the acid produced. This agrees with the following mechanism.

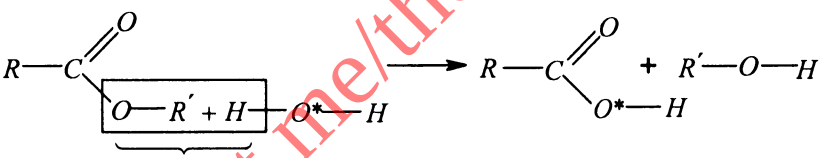

The other following possibility leads to no accumulation of activity in the acid formed.

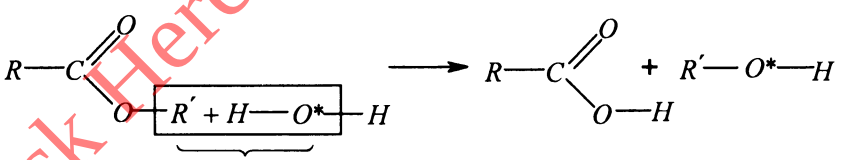

(iii) ***Decomposition of H_2O_2 by PbO_2*** : The reaction, $PbO_2 + H_2O_2 \rightarrow PbO + H_2O + O_2$, generates oxygen. It was a problem to establish the source of the oxygen liberated, as there are two sources for oxygen. It was previously believed that each of the reactants supplies one oxygen atom to form O_2. But, when the reaction was investigated with the labelled $H_2O_2^*$, it was found that the total activity was transmitted to O_2, and no activity was noticed in water. This fact supports the following mechanistic path.

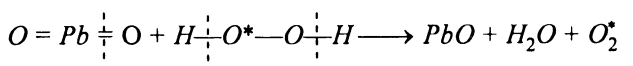

Similarly, by using PbO_2^* it can be shown that no activity exists in the oxygen liberated.

(v) ***Pseudo-substitution reactions at Co(III) centre*** : Generally, the ligand substitution process at *Co(III)* centre is kinetically very slow but there are some rapid pseudo-substitution reactions

Click Here t.me/thealchemylibrary

where actually *Co(III)*–ligand bond does not get ruptured and consequently these reactions are fairly fast. The mechanistic paths are established by using the isotopes. Such examples are :

$$[Co(NH_3)_5(CO_3)]^+ \xrightarrow{H^+,\ H_2O^*} [Co(NH_3)_5(OH_2)]^{3+} + CO_2$$

$$[Co(NH_3)_5(OH_2)]^{3+} \xrightarrow{HNO_2^* - NO_2^{*-}} [Co(NH_3)_5(ONO)]^{2+}$$

In the first reaction, in the presence of labelled H_2O^*, no labelled H_2O^* is found to get coordinated with the metal centre. Similarly, in the second reaction in presence of labelled NO_2^{*-} no labelled NO_2^{*-} is found to coordinate. These support that in both the reactions $Co(III) - O$ bond does not break. The proposed mechanisms are :

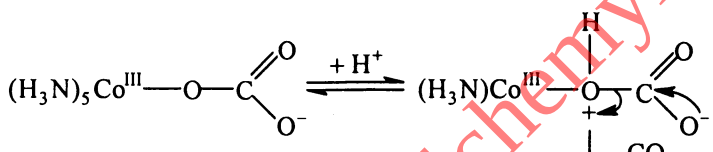

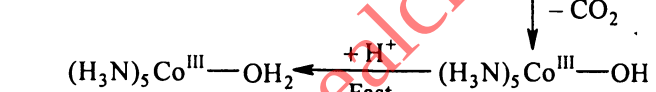

$$2HNO_2 \longrightarrow N_2O_3 + H_2O \quad \text{or} \quad NO_2^- + NO^+ + H_2O$$

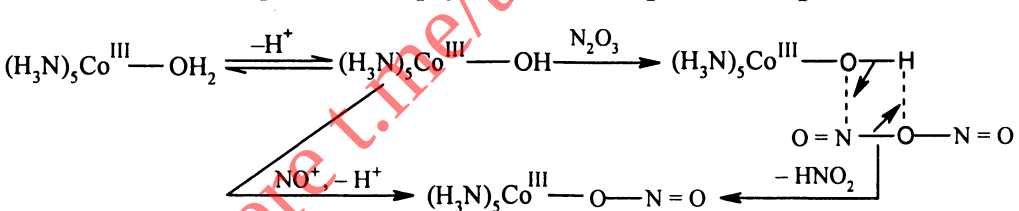

Thus if we start with the labelled complexes, i.e. $[Co(NH_3)_5(CO_3^*)]^+$ and $[Co(NH_3)_5\ (^*OH_2)]^{3+}$ we get the products with the labelled oxygen, i.e. $[Co(NH_3)_5(^*OH_2)]^{3+}$ and $[Co(NH_3)_5\ (^*ONO)]^{2+}$ in the respective reactions. In the ***O-nitrosation process*** the stable isomer $ONNO_2$ of N_2O_3 isomerises to $ONONO$ which is kinetically active.

(vi) ***Mechanism of electron transfer reaction*** **:** Let us consider the following reaction :

$$(H_3N)_5Co^{III} - Cl^*\Big]^{2+} + Cr(H_2O)_6^{2+} + 5H_2O \rightarrow Co(H_2O)_6^{2+} + 5NH_3 + (H_2O)_5Cr^{III} - Cl^*\Big]^{2+}$$

Here the tagged chloride is completely transferred in the product of Cr^{III}-complex. If the reaction is carried out in presence of free tagged chloride, **no tagged chloride is found in the Cr^{III}-complex,** i.e.:

$$(H_3N)_5Co^{III} - Cl\Big]^{2+} + Cr(H_2O)_6^{2+} + 5H_2O \xrightarrow{+\,Cl^{*-}} Co(H_2O)_6^{2+} + (H_2O)_5Cr^{III} - Cl\Big]^{2+} + 5NH_3$$

It indicates that during the electron transfer process (Cr^{II} to Co^{III}), Cl^- is transferred from *Co*-centre to *Cr*-centre. This is explained by considering the formation of a **binuclear complex** in which Cl^- acts as a **bridging ligand** and the electron transfer occurs within the binuclear complex at the rate determining step (i.e. ***inner sphere electron transfer***) :

Click Here t.me/bedchemylibrary

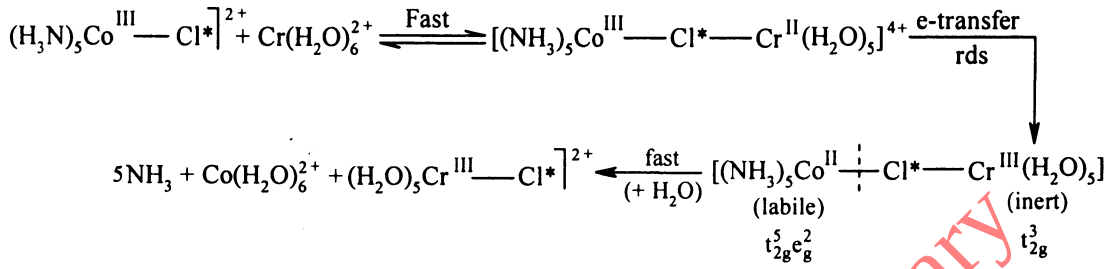

(C) Analytical Chemistry

Radioisotopes have got a wide spectrum of application in analytical chemistry in different directions such as radiochromatography, determination of solubility of a sparingly soluble solute, isotope dilution analysis, neutron absorptiometry, radiometric titrations, etc. Here we shall discuss some of these techniques.

(a) Determination of Solubility of a Sparingly Soluble Solute

(i) ***Solubility of $PbSO_4$ and other sparingly soluble salts*** : This method was first utilised by Hevesy and Paneth in 1913 to determine the solubility of $PbSO_4$. In this method, at first a known amount of $*Pb(NO_3)_2$ was mixed with a known quantity of ordinary $Pb(NO_3)_2$ to prepare a solution. A known volume of the solution was evaporated to dryness and the activity of the residue was determined. Then from a known volume of this solution, lead was precipitated out as lead sulphate. A known volume of the clear supernatant liquid was taken out and evaporated to dryness from which the activity of the residue (i.e. dissolved lead sulphate) obtained was determined in the same way as it was applied for the original solution before the precipitation of the salt. Thus, from the knowledge of the activity in the residue and the volume of the supernatant from which the residue was obtained, the solubility of lead sulphate could be determined.

Let, a_i be the activity for x g of lead obtained from the solution before precipitation, and a_f be the activity for the lead obtained from V_1 volume of the clear supernatant. Hence we can write :

$$a_i \propto x \text{ g lead, and } a_f \propto y \text{ g lead (say)}$$

Hence, $y = (xa_f/a_i)$ g lead in V_1 volume supernatant.

If V is the total volume of the supernatant, then the dissolved lead in V volume solution is given by,

$$w = (Vxa_f/V_1a_i) \text{ g lead.}$$

This principle can be applied to test the efficiency of a precipitation method in a quantitative analysis. This is very much promising in standardising the methods of quantitative separations of different rare earths through solvent extraction and ion exchange techniques.

(ii) ***Solubility of water in benzene and other hydrocarbons*** : It is a very difficult task in the conventional physical or chemical analysis. But by using water containing a known activity of ^3H_2O, it is very easy to determine the solubility of water in hydrocarbons in the same way as it is done in the case of $PbSO_4$.

Click Here to meet chemylibrary

(b) Isotopic Dilution Analysis

Principle : If y g of a species tagged with a radioisotope with the initial activity a_i (counts per gram per minute) are mixed with a sample containing x g (unknown) of the same species, then the activity gets uniformly distributed in the whole sample. After an intimate mixing, a small quantity of the species is isolated from the mixture and its specific activity a_f is determined. According to the ***principle of conservation of total activity***, we get as follows. In this process $t_{1/2}$ of the radioisotope should be sufficiently large, so that during the analysis time, specific activity does not change accountably.

$$(x + y)a_f = ya_i, \text{ or, } x = y\frac{(a_i - a_f)}{a_f}$$

This technique is very much useful in some problems of biochemistry where other conventional techniques are not at all useful.

(i) ***Determination of aureomycin in a large fermentation broth*** : In this process, a known amount (y g) of tagged aureomycin (^{14}C) is mixed with the sample. After separation of a small amount of pure aureomycin from the mixture, the specific activity (a_f) is determined. From the knowledge of a_i, the amount of aureomycin present in the sample can be determined. In the same way, the amount of glycine produced in the products of a protein hydrolysis can be determined.

(ii) ***Determination of total volume of blood in a living body*** : In this process, a suitable iron compound tagged with ^{59}Fe is injected into the body of a donor subject allowing sufficient time (several days) for incorporation of ^{59}Fe in the blood cells of the donor subject. Now, V_1 ml of the donor's blood with a specific activity a_i (counts per ml per min) are injected into the acceptor subject whose total blood content is to be determined. Then after proper circulation, a sample of blood from the acceptor is collected and its specific activity a_f is determined. Thus the total volume of blood of the acceptor subject is given by :

$$V_1 a_i = (V + V_1)\, a_f, \text{ or, } V = V_1\,(a_i - a_f)/a_f$$

It can also be done in another way which is a rapid method. About one ml of blood is withdrawn from the patient and then it is mixed with labelled $^*NaCl$. Then the specific activity (a_i) is determined and it is reinjected to the patient according to the principle of isotopic dilution principle. Within 25 minutes, after intravenous injection, the whole blood gets homogenized. Then the specific activity (a_f) in the blood is determined. From the knowledge of a_i, a_f and the amount of blood reinjected with a_i activity, the total volume of blood can be determined.

(c) Neutron Activation Analysis

Principle : The element which is to be estimated in a sample is subjected to (n, γ) transmutation reaction to produce the radioisotope of the element. Then by measuring the activity of the radioisotope produced and by comparing with the activity of a known amount of the element subjected to the same neutron flux for the same period, the unknown content of the element in the sample can be determined. This technique is highly promising for the elements having a ***large neutron capture cross–section.*** This technique is nondestructive because the sample remains unchanged after analysis, except for the nuclear transmutation of the atoms at the level of tracer concentration. The elements which respond to this technique are :

Na, P, Ca, Sc, Cr, Mn, Co, Cu, Zn, As, Se, Ag, Ir, Pt, Au, Sm, Tm, Eu, Gd, Dy, Ho, etc.

Click Here t.me/finalchemylibrary

For the both known and unknown sample, the same neutron flux must be used to irradiate for the same period under identical condition; and the activity must be measured for both the known and unknown samples after the same time lapse. Under this condition, the following relation holds good.

$$\frac{\text{weight of the element (say } X\text{) in the unknown sample}}{\text{weight of the element, } X \text{ in the standard sample}} = \frac{\text{activity at time } t \text{ time in the unknown sample}}{\text{activity at } t \text{ time in the standard sample}}$$

In some cases, a calibration curve by using the different amounts of the standard samples of X can be obtained, from which the unknown concentration of X can be estimated as usual.

If the sample contains a number of elements to respond to (n, γ) reactions, then the complication in analysis of a particular element is removed automatically because in most of the cases, disintegration characteristics (i.e. energy of the γ and/or β component, $t_{1/2}$ periods, etc) for the different radioisotopes of different elements significantly differ. Hence, to follow the activity of the radioisotopes of a particular element is not difficult.

If the element to be estimated is not monoisotopic, then the activity of a particular product from a particular isotope in the (n, γ) transmutation is determined, and its concentration is obtained. If the percentage of isotopic abundance which is determined from mass spectrographic study of a piece of sample of the element is known, then the total content of the element can be estimated.

Some examples of this method are mentioned below :

(i) ***Cr–content in a ruby laser*** : The involved nuclear transmutation is : $^{50}Cr\ (n, \gamma)^{51}Cr$, where the radioisotope ^{51}Cr shows $t_{1/2} = 26$ days. From a calibration curve obtained from different standard samples of ruby containing $Al_2O_3 + Cr_2O_3$ in different known proportions, the amount of Cr in a ruby laser is determined by measuring the activity of ^{51}Cr transmuted.

(ii) ***Mn content in tea leaves*** : The nuclear transmutation, $^{55}Mn\ (n, \gamma)^{56}Mn$ produces the isotope, ^{56}Mn having $t_{1/2}$ (β^-, γ active) 2.6 hr. From the activity measurement in calcined tea leaves and in a series of standard samples, the percentage of Mn-content can be estimated. It is found of the order of 0.12%.

(iii) ***As-content in hair, a diagnostic test of arsenic poisoning*** : In the (n, γ) reaction, the non-radioactive ^{75}As gets transmuted into its radioisotope ^{76}As having $t_{1/2} = 26.5$ hr with respect to β^-, γ activity. In arsenic poisoning, the arsenic preferably gets accumulated at the roots of hairs and then it propagates along the length of the hair as it grows. A strand of hair is collected from the suspected victim, and the arsenic content at different segments along the length of the hair is determined through the neutron activation analysis. The average As-content in the hair of a victim is much higher compared to that of a normal person. Generally, a normal hair shows the As content ~ 0.8 ppm which is more or less uniform along the length of the hair. But, in the case of the victims subjected to the slow poisoning by arsenic, the distribution pattern of As-*along the length of the hair follows a number of maxima and minima. From the knowledge of positions of the maxima and rate of growth of the hair, the dates of poisoning can be predicted.* It is interesting to mention that this technique has helped the historians to speculate the fact that the great emperor Napoleon Bonaparte died in 1821 due to a slow arsenic poisoning.

The principle of neutron activation analysis is of much importance in solving many archaeological problems.

Click Here for more chemistry library

(d) Radiometric Titrations

It is mainly applicable for the precipitation reactions. The basic principle states that as in all other titrations (where at the end point there is a sharp change of a particular property), here at the end point, the measurable property, i.e. activity either in the solution phase or in the solid phase (i.e. precipitate), changes abruptly to produce a point of inflection.

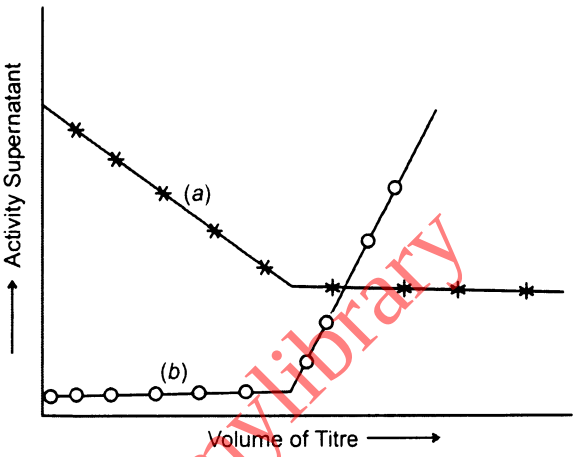

Fig. 6.17.1. Representative radiometric titration curves. (a) Decreasing activity attains sharply a minimum value at the end point. (b) Activity starts to increase rapidly at the end point.

(i) ***Titration of Ba^{2+}, Mg^{2+}, Pb^{2+}, UO_2^{2+} etc. by $Na_2HP^*O_4$:*** If the titration by using the labelled $Na_2HP^*O_4$ is carried out for the above mentioned metal ions, then with the progress of the titration, the metal ions are getting precipitated out. Before the end point, the supernatant does not contain any activity (ignoring the solubility of the precipitate) due to the labelled phosphate, but as soon as the end point is reached, there is a sharp increase of activity in the supernatant and it goes to increase gradually with the addition of titre (see Fig. 6.17.1b). During the measurement of activity in the supernatant, we should be careful, so that no precipitate remains as colloidally suspended. In practice, a G-M counter is fitted with the titration vessel in such a way that after each addition of phosphate, a certain fraction of the clear (i.e. free from any colliodally suspended precipitate) supernatant or filtrate can be sucked in the counter tube.

In the same way, Ag^+ can be titrated by using the labelled $NaCl^*$. If Ag^+ is labelled instead of $NaCl$, then the activity in the supernatant decreases gradually and at the end point it remains constant to a minimum (see Fig. 6.17.1 a).

(ii) ***Titration of Ca^{2+} by edta in the presence of a radioisotope as an indicator*** : In this case, the labelled indicator added remains insoluble but as the end point is over, the insoluble indicator gets soluble giving rise to a sharp increase of activity in the solution phase. In estimating Ca^{2+} by edta, $^*AgIO_3$ is used as an indicator. After the end point, due to the complexation, it forms a soluble, $^*Ag$-*edta* complex, giving a sharp hike in the activity in the solution phase. This is why it follows the titration curve as shown in Fig. 6.17.1b.

6.17.2 Application of Radioactivity in Biological Fields

(i) ***Establishment of the reaction mechanism of photosynthesis*** : There are two sources (i.e. CO_2 and H_2O) for liberation of molecular oxygen (i.e. O_2) in photosynthesis. The problem was solved by Ruben and co-workers (1941–1943) by using labelled H_2O^*. It was found that the total activity was confined in O_2, i.e.

$$6CO_2 + 12H_2O^* \rightarrow C_6H_{12}O_6 + 6H_2O + 6O_2^*.$$

It confirms that the entire oxygen liberated is originated from water not from CO_2. By using labelled CO_2^*, it has been observed that the activity is distributed between the glucose and

Click Here for more chemistry library

water formed in the reaction. It also supports the above mechanism. In this process, after some time, the labelled water (H_2O^*) formed may participate to liberate O_2^*. But this probability in the presence of a bulk amount of nonlabelled H_2O is very low. All these observations support the path proposed.

Similarly, by using labelled $^*CO_2$ with ^{14}C, it was possible to follow the exact sequence leading to the final product. In this way, Calvin and Benson established that phosphoglyceric acid is the first stable intermediate in the sequence.

(ii) ***Autoradiography*** **:** A living subject is first fed with some suitable radioelement and then its distribution pattern is followed through some photographic means. The β, γ radiations coming from the radioelement can produce images on a special photographic plate. Thus, the *DNA* bases tagged with tritium (^3H) can produce a lot of information such as : shape, location, mobility, etc. of the *DNA* molecules in the living cell through the analysis of the autoradiograph.

Similarly, by using a suitable radioisotope, the metabolic route of that particular element can be traced out from the analysis of the autoradiographs for different parts of the living body.

6.17.3 Application of Radioactivity in Agriculture

(i) ***Establishment of optimum amount and optimum time for using fertilizers*** **:** Let us take the case of intake of phosphorus by the plants. The plants take phosphorus from two sources, i.e. soil and phosphatic fertilizer. If the fertilizer tagged with radioactive phosphorus (^{32}P) is used then the amount of fertilizer taken by the plant can be obtained from the activity measurement in the plant. Thus from the knowledge of total phosphorus content (known from chemical analysis), the percentage of phosphorus taken from each source can be determined. The ratio for the two sources depends on the growth stage, pH of the soil, the chemical state of phosphorus present in both the soil and fertilizer, etc. This knowledge gives a quantitative idea of the requirement of an external phosphatic fertilizer to the plants.

For a particular type of plant, the phosphatic fertilizer intake is not uniform throughout the life period. It varies at different stages. The growth stages at which the phosphate intake is high can be determined by using a labelled fertilizer and counting the intake activity at different stages. This knowledge tells the farmers the optimum time for using the fertilizers. In most of the crops, it has been found that at the early stages, the intake of phosphatic fertilizer is about 60% while it is less than 30% at the later stages. **It evidently indicates that the phosphatic fertilizer should be used at the time of sowing.**

(ii) ***Control of plundering insects*** **:** In some cases, a large number of plundering insects fly over from a large distance to different zones. They plunder zones one after another very rapidly. To control these insects, it is important to know their migratory and breeding habits. For this purpose, a group of insects are dipped in a cobalt chloride solution tagged with ^{60}Co. The activity absorbed lies below the lethal dose but the activity retains measurable up to 6-8 months. By following the activity, their migratory tracks can be waved out. Besides this, it gives an indication of their hibernating shelter. Once, the hibernating shelter is located, they can be destroyed by spraying suitable insecticides.

For the some species of insects, if the radiophosphates are fed, it may transmit up to 2-3 generations. Such a transmission is immensely helpful in locating the colonies of the insects.

Click Here to meet the Chemistry Library

In some cases, if the male species are heavily irradiated with some suitable γ–doses, they become infertile giving rise to a control on multiplication.

6.17.4 Application of Radioactivity in the Medical Field

As a matter of fact, the radioisotopes have got a very large spectrum of application in solving the problems of health and diseases. Day by day, the scope of the field is getting extended. Here we shall only mention a few applications.

(i) ***Detection and location of brain tumor*** : The exact position of a tumor in the brain can be detected by using two radioisotopes, ^{131}I and ^{32}P successively. Firstly, **the labelled iodo-derivative of an organic dye, fluorescein (which gets preferably absorbed on a tumor)** is injected into the body of a patient. Then by placing a counter outside the skull, the position of the tumor can be located. The γ-ray from ^{131}I can pass out through the skull. Thus, once the location of the tumor is determined roughly, then ^{32}P is used as a tracer during surgery for determining the exact position and the area of the tumor. **Phosphates are concentrated preferably on the tumor site.** The β^- rays emitted from ^{32}P have a very short range. Hence, only when the counter is placed at the vicinity of its site of accumulation, it records the signals. By taking the advantage of this short range property of the β^--particle coming from ^{32}P, the exact position of the tumor is determined.

(ii) ***In the treatment of leukemia and polycythemia vera*** : In the treatment of leukemia characterised by overproduction of white blood cells, an intravenous injection of sodium phosphate tagged with ^{32}P is used. A similar treatment is also recommended for polycythemia vera in which the bone marrow produces an excessive amount of red blood cells. The phosphate is preferentially accumulated in the bone where the β^--rays emitted from ^{32}P destroy the malignancy.

(iii) ***Radiotherapy by ^{60}Co in the treatment of cancer*** : Radiation emitted from ^{60}Co is very much promising in destroying the malignancy in a cancerous growth.

(iv) ***Tumor diagnosis by the radioscintigraphic agents*** : There are some radiopharmaceuticals containing radionuclides having low energy γ-photons (so that the patients do not suffer from any radiation damage) and short half life periods (but sufficiently high to permit the preparation, administration and diagnostic application). **Such radiopharmaceuticals are preferably concentrated in the tumor zone.** The suitable radionuclides for this purpose are : ^{67}Ga, ^{99m}Tc, ^{97}Ru, etc. ^{67}Ga-citrate is the most promising one in this regard. Here it is worth mentioning that ^{67}Ga is also carcinostatic.

(v) ***Diagnosis and treatment of disorder in thyroids*** : Both the disorders in thyroids, i.e. *hyperthyroidism* (overactive) and *hypothyroidism* (underactive), can be diagnosed by administering NaI^* tagged with ^{131}I. The efficiency of absorbing iodine with time by the thyroids of the patient is compared with that of a normal person. In the case of hyperthyroidism, the therapeutic treatment is done either by ^{131}I or ^{126}I. The radiation emitted from the radioiodine can destroy the excess growth leading to hyperthyroidism.

(vi) ***Location of obstruction (e.g. thrombosis) in blood circulation*** : In this technique, sodium chloride tagged with ^{24}Na is injected into a vein of a forearm of the patient and the counter is placed at the foot. If the blood circulation is normal, very soon the counter begins to record the signal. But, if the circulation is impaired, it takes a larger time to reach the foot. Then by moving the counter to different parts of the body, the exact position of the circulatory impairment is detected.

Click Here t.me/thealchemylibrary

(vii) ***Determination of abnormalities in the pumping action of the heart*** : Sodium iodide tagged either by ^{24}Na or ^{131}I is administered into the blood stream, then a counter with an automatic pen recorder is placed on the heart. The entry and coming out of blood due to the rhythmic pumping action of the chambers of the heart are recorded by the counter and it can reflect the pumping action of the heart.

(viii) ***Estimation of total blood content in a patient*** : In some cases of the anaemic patients, it is required to estimate the total blood content of the patients. This is done by the principle of isotopic dilution technique as discussed earlier in Sec. 6.17.1C (b).

(ix) ***Radiation sterilisation of the surgical instruments*** : By using the γ-radiations at the optimum dose for a certain period, different surgical instruments, drugs and pharmaceuticals are being sterilised. It is now being attempted to sterilise the food stuff for preservation for a longer period.

(x) ***Radioimmunoassay (RIA)*** : It provides an important technique for assessing the concentration levels of many biologically important components in the body fluid, e.g. different types of antigens and antibodies, hormones, steroids, drugs, etc. The principle of the technique is illustrated for estimation of a particular antigen in a sample. For this purpose, a known amount of excess of the labelled antigen is added to the sample and it is incubated with a known amount of the corresponding antibody. Due to the specific interaction between the antigen and its antibody, the antigen–antibody complex gets precipitated out. The unbound excess antigen is separated by centrifuging in the presence of an immuno–adsorbent. Then the radioactivities of the supernatant containing the free antigen and the precipitate bound antigen are determined. The concentration of the antigen in the sample is obtained from a calibration curve, B/F vs. antigen concentration (where B and F denote the radioactivities of the precipitate and supernatant respectively).

The *RIA* technique is widely used for the estimation of insulin in diabetic patients and *HPL* (Human Placental Lactogen) of pregnant mothers. The knowledge of *HPL* concentration is informative to identify the normal and abnormal pregnancies.

6.17.5 Application of Radioactivity in Industry (see Sec. 7.11 for the application of man-made elements)

(i) ***Determination of friction and wear out of the pistons*** : For this purpose, very often the steel piston is made radioactive by exposing to (n, γ) transmutation reactions. Then the piston is fitted into the cylinder with a particular lubricating oil. After operation, the radioactivity lost from the surface of the piston gives the measure of wear out in friction. By varying the lubricating oils, the relative efficiency of the oils can be measured.

(ii) ***Thickness measurement in sheets and its automatic control*** : The thickness of metal-sheets, paper, plastic and rubber tyre fabrics may be measured and controlled by using a β-active isotope. Actually, in industry in the manufacture of such sheets, the sheet is allowed to pass between a β-source and a detector. If the uniformity in thickness of the sheet coming out is changed, then the strength of the signal recorded at the counter will be changed. Such changes will automatically reset the rolling machine for maintaining a uniform thickness of the sheet. Depending upon the thickness, the β-sources vary from ^{63}Ni (β, 67 keV) to ^{60}Co (β, 1.3 MeV). For the intermediate thickness, the sources of intermediate energy are used.

(iii) ***γ-Radiation in chemical synthesis*** : By taking the help of γ-photon induced reactions, some compounds such as C_2H_5Br (from C_2H_4 and HBr), gammexane (γ-isomer of $C_6H_6Cl_6$), etc. are

Click Here : me/neachemylibrary

being industrially manufactured. The radiation yield (G) analogous to the photochemical yield (ϕ) is very high.

$$C_2H_4 + HBr \xrightarrow{\gamma\,(^{60}Co)} C_2H_5Br, C_6H_6 + 3Cl_2 \xrightarrow{\gamma} C_6H_6Cl_6\ (\gamma - isomer, \sim 15\%)$$

(iv) ***Radioisotopes as a source of electricity*** **:** It has been being attempted to convert the energy radiated from the radioisotopes into electricity. In this regard ^{60}Co, ^{90}Sr are very much promising. However, it is only at the embryonic stage at present. **The *SNAP (strontium-ninety auxiliary power)* is being used in charging batteries in submarines, space crafts and in many other unmanned instruments.** In *SNAP, the heat generated from the radiation is utilised to produce thermojunctions of sufficient temperature gradient. By using suitable bimetallic couples at the junctions, electricity can be produced.*

(v) ***Radioisotopes in laundering industry*** **:** A good detergent after cleaning the garments should not be retained in the garments; because its retention will damage the clothes. To ascertain this property, generally the labelled detergents are used and after washing, the activity is measured on the clothes.

(vi) ***Finding of wealth in natural sources under the earth*** **:** A neutron probe, generally made of Po and Be, is sent along with the driller inside the earth. The α-particles from ^{210}Po emit neutrons by (α, n) reaction on Be. **Thus the composition, $^{210}Po + {}^{9}Be$ gives the source of neutron in the probe. The other neutron sources are : ($^{238}Pu + {}^{9}Be$), ($^{241}Am + {}^{9}Be$).** These manmade elements ^{238}Pu and ^{241}Am are α-emitters (Sec. 7.11). *The natural resources like water, petroleum, different metals, diamonds, etc. which respond to the (n, γ) reactions to produce the radioisotopes with the characteristic radiations can be detected* in this process. The emitted radiations on being analyzed can give information regarding the presence of the materials. In the same way, uranium and thorium can also be searched. In such cases, no artificial radioactivity is required through the (n, γ) process because these are naturally radioactive.

6.17.6 Application of Radioactivity in Age Determination

(i) ***Age of the minerals and rocks*** **:** Let us consider a rock containing ^{238}U having a half life period 4.5×10^9 yr. If we follow the uranium series (i.e. $4n + 2$ series), it is seen that ^{238}U which starts the series is having the highest half life period in the series. The nearest long lived element in the series is ^{234}U having a half life period 2.48×10^5 yr. Hence, it can reasonably be assumed that all the ^{238}U atoms disintegrated have been converted into the end stable product ^{206}Pb. Thus, if N^t_{U-238} and N^t_{Pb-206} represent the number of ^{238}U and ^{206}Pb atoms in a rock at the present time (t), then the number of ^{238}U atoms present at $t = 0$, i.e. at the time of creation of the rock, is given by :

$$N^o_{U-238} = N^t_{U-238} + N^t_{Pb-206}.$$

Hence, according to the relationship of radioactive decay, we get : $N^t_{U-238} = N^0_{U-238}\ \exp(-kt)$, where $k\ (= 0.693/t_{1/2})$ gives the decay constant of ^{238}U, and t denotes the age of the rock. Thus,

$$N^t_{U-238} = (N^t_{U-238} + N^t_{Pb-206})\ \exp(-kt);$$

or,

$$N^t_{Pb-206} = N^t_{U-238}\ \{\exp(kt) - 1\};$$

Click Here to me/thechemylibrary

or, $$1 = \left(1 + \frac{N^t_{Pb-206}}{N^t_{U-238}}\right) \exp(-kt)$$

Thus, if the ratio of atoms of ^{206}Pb and ^{238}U is known then the age can be calculated easily. By using a mass spectrometer, it can be done easily. In this principle, it has been assumed that at $t = 0$, there was no ^{206}Pb in the rock.

Now, if we consider the isotope ^{235}U ($t_{1/2} = 7.1 \times 10^8$ yr, highest in the actinium, i.e. $4n + 3$ series) of the actinium series and its end stable product ^{207}Pb, we get a similar relationship (under the assumption of nonexistence of ^{207}Pb at $t = 0$) :

$$N^t_{U-235} = \left(N^t_{U-235} + N^t_{Pb-207}\right) \exp(-k't)$$

where k' represents the decay constant of ^{235}U. Thus,

$$N^t_{Pb-207} = N^t_{U-235} \{\exp(k't) - 1\}$$

A simpler but accurate method of age determination is obtained by using the following relationships in $^{238}U - ^{206}Pb$, $^{235}U - ^{207}Pb$ series.

$$\frac{N^t_{Pb-206}}{N^t_{Pb-207}} = \frac{N^t_{U-238}[\exp(kt) - 1]}{N^t_{U-235}[\exp(k't) - 1]}$$

The atomic ratio of ^{206}Pb to ^{207}Pb and that of ^{238}U to ^{235}U can be determined in the sample by using a mass spectrometer.

All the above relations are true only when the sample did not contain any ^{206}Pb and ^{207}Pb at the time of formation of the rock. But there are some samples in which ^{204}Pb which is not the end product of any radioactive series exists. **The existence of ^{204}Pb in such samples indicates that at $t = 0$, the samples also contained a certain amount of ^{206}Pb and ^{207}Pb governed by the ratio of isotopic abundance of lead.** In such cases, the content of ^{204}Pb is determined from the mass spectrometer and then from the ratio of isotopic abundance (known from the distribution of the isotopes in a completely nonradioactive sample), the initial contents of ^{206}Pb and ^{207}Pb can be known. These are to be subtracted from the present contents of the respective isotopes.

The oldest mineral is found to have an age of the order of 4.5×10^9 years. Thus our earth must have at least this age.

(ii) ***Radiocarbon dating and age determination of archaeological objects*** : The neutrons present in the cosmic rays can carry out the nuclear transmutation, $^{14}N(n, p)\,^{14}C$ in atmosphere to generate the radioactive carbon ^{14}C having $t_{1/2} = 5700$ yr with respect to the following decay.

$$^{14}_{6}C \rightarrow {}^{14}_{7}N + {}^{0}_{-1}e + {}^{0}_{0}\bar{\nu}.$$

Thus, the produced ^{14}C actually exists as $^{14}CO_2$ in atmosphere. Formation and decay of ^{14}C in nature leads to an equilibrium mass ratio, $^{12}CO_2 : {}^{14}CO_2 = 1 : 10^{-12}$.

Plants take up carbon dioxide from atmosphere for photosynthesis to form carbohydrates. The ratios of ^{14}C to ^{12}C in the atmospheric carbon dioxide and in its reaction products (ignoring the isotopic effect in the kinetics of photosynthesis) are the same. **So long as the living plant is**

Click Here : me/medicinemylibrary

involved in the plant-animal-atmosphere carbon cycle, the same ratio of ^{14}C to ^{12}C in the whole cycle is maintained. But when it is fallen to death, it is kept away from the carbon cycle and no uptake of ^{14}C through photosynthesis is possible. Thus the accumulated ^{14}C in the plant during its living period decreases due to radioactive disintegration.

The fresh samples collected from various parts of the world show almost a constant value which is ~ 15.5 ± 0.3 disintegrations per gram of total carbon per minute. From the knowledge of specific activity of any archaeological object (i.e. wood, cloth, charcoal, etc.) containing carbon, the age (from the date of dying) of the sample can be calculated by using the relationship :

$$A_t = A_0 \exp(-kt)$$

where A_t, A_0 give the activity (specific) at $t = t$ and 0 (i.e. when the plant is fallen to death) respectively, and k denotes the decay constant of ^{14}C. Thus, the age (t) can be obtained. This method is very much useful to determine the age of the historic and archaeological substances. For developing this method, W.F. Libby was awarded Nobel prize in 1960. The $t_{1/2}$ for ^{14}C is not too high. This is why, the method works well for the objects having age up to 30,000 yrs (ca. up to five half life periods of ^{14}C). For further older substances, the activity is reduced to such an extent that it becomes difficult to measure the activity precisely. As a matter of fact, the petroleum products which were isolated from the carbon cycle about hundreds of millions of years ago show almost zero activity of ^{14}C.

(iii) ***Dating by tritium* (^3H) :** In atmosphere, in the interaction between the fast neutron flux present in the cosmic rays and ^{14}N in atmosphere, ^3H is being produced as follows:

$$^{14}_{7}N + {}^{1}_{0}n \rightarrow {}^{3}_{1}H + {}^{12}_{6}C$$

Ultimately, the produced tritium (T) gets oxidised into *tritiated water* (*HTO*). It decays as follows:

$$^{3}_{1}H \rightarrow {}^{3}_{2}He + {}^{0}_{-1}e + {}^{0}_{0}\bar{\nu}, (t_{1/2} \approx 12.4 \text{ yr})$$

From the formation and decay of ^3H, in ordinary water sources of large surface area open to atmosphere, the constant ratio, $^3H/^1H$ is maintained. If the water is withdrawn from the open source and stored in a closed system (isolated from open atmosphere), the β^--activity due to ^3H falls. Thus, by measuring the specific activity in any open source and in the closed or isolated source, the period for which the sample is withdrawn from the open source can be determined as in the process of radiocarbon dating.

As the $t_{1/2}$ (≈ 12.4 yr) is not much high, the procedure works well for the samples having age up to only 60 yrs (i.e. up to ~ 5 half lives). Another difficulty in the process is that as the energy of the β^--particle is very low ($E_{\beta^-} \approx 0.017$ MeV), it requires a special counting technique. Presently, due to the frequent thermonuclear explosions, the ratio $^3H/^1H$ in seas is varying from time to time. This is why, the dating by this process has become uncertain.

6.18 SOME IMPORTANT ASPECTS OF RADIATION CHEMISTRY

6.18.1 Radiation Chemistry

Photochemistry deals with the chemical transformations effected through the interaction of photons from visible and ultraviolet radiations covering the range 100–1000 nm having energy 1 eV to 24 eV

Click Here t.me/theachemylibrary

per mole. *In this range, excitation of the molecules, bond fission to produce the free radicals followed by the chain reaction are the major phenomena. Ionisations of the atoms or molecules are the rare phenomena.*

On the other hand, radiation consisting of *X*-rays, γ-rays or high energy charged particles like, α-particles, β-particles, protons, or neutral particles like neutrons or fission fragments may ionise innumerable molecules or atoms coming in the path of propagation of the radiation. The secondary products being sufficiently energetic can also carry out further ionisation and excitation. Besides this ionisation, innumerable molecules also get excited and dissociated to form radicals in this process. The energy of such radiations may be in the order of million electron volt per mole. **Such radiations leading to ionisation in the *primary process* are called *ionising radiations*. The transformations effected by such radiations are discussed in the discipline called *radiation chemistry*.**

In radiation chemistry, the ionising power of a radiation does not depend on its energy only but on the nature of the constituents in the radiation. ***The slow moving massive particles are more powerful ionising agents compared to the lighter particles.*** A proton having the same high energy as that of an electron is ~ 10^3 times more efficient in causing ionisation.

The highly energetic particles and γ-rays can also initiate the nuclear transmutation reactions.

In photochemistry, each quantum activates only one molecule at the primary step, but in the case of ionising radiations, the number of molecules getting ionised is extremely high. In comparison with the **photochemical yield** (ϕ)*, to measure the radiation effects in a quantitative way, the *G*-value is defined as follows :

$$G = \frac{\text{number of molecules reacting}}{\text{100 eV of energy introduced}}$$

The interactions of different types of particles and radiations with matter will be discussed separately. Here we shall restrict our attention for the radiation of medium energy covering the range, 100 eV–2 MeV. *For such radiations, the interactions are mainly concerned with the orbital electrons. For higher energy radiations (specially for the charged particles), nuclear reactions are mainly important.*

6.18.2 Characteristics of Interaction of Medium Energy Charged Particles with Matter

(a) ***Primary effects on matter*** : For the charged particles like He^{2+}, $\beta^{+/-}$, H^+, etc., the interactions with the orbital electrons of the interacting matter are important. In the primary process, the **three important phenomena** : excitation of electronic energy state, ionisation, and bond rupture of the molecules to generate free radicals are important. Here the important interactions involving H_2O are shown. **The primary processes are very often represented by the wavy arrows.**

(i) ***Excitation*** : $H_2O + e^- \rightsquigarrow H_2O^* + e^-$;

(ii) ***Ionisation*** : $H_2O + e^- \rightsquigarrow H_2O^{++} + 2e^-$;

(iii) ***Bond rupture (i.e. free radical generation)*** : $H_2O + e^- \rightsquigarrow \bullet H + \bullet OH + e^-$

If the electron (e^-) after carrying out any one event of the above processes bears sufficient energy to initiate any event of the above processes, then it can again carry out the events step by step. It

* ϕ is defined as, $\phi = \dfrac{\text{Number of molecules reacting}}{\text{Number of quanta or photons absorbed}}$

Click Here t.me/thoalchemylibrary

continues until its energy falls below the threshold value required to carry out an event of the primary processes. For other charged particles, the similar things happen. The ***primary radiolytic products*** (***prp***) may suffer different types of interactions to produce different types of final products.

(b) ***Radiation tracks and spurs*** : We have already discussed the principle of obtaining tracks through which the particles travel in Wilson's cloud chamber. We have mentioned that on the way of the charged particles, due to the primary events, electro-ion pairs, excited species and free radicals are formed. ***The primary products mainly exist as clusters called spurs.*** If the secondary electrons formed at the primary process have sufficient energy (~ 100 eV), they can also again carry out the events (i.e. ionisation, excitation, radical formation) to form **secondary spurs** on their tracks which get branched off from the primary tracks. **Such branches are called *δ-ray tracks.***

(c) ***Linear energy transfer*** (***LET***) : During the passage of the charged particles through the matter, they lose their energies in the primary events. The rate at which a charged particle will lose its energy is dependent on the nature of the matter, specially atomic mass and atomic number. On losing energy at the successive steps, it comes to a minimum value not sufficient to carry out any further ionisation. Thus the particle is said to be stopped. The main route to lose energy of the particle involves the collision with the orbital electrons of the matter.

Besides the collision with the orbital electrons, there is another route called, ***bremsstrahlung.*** When the moving charged particle appears close to the field of an atomic nucleus, it experiences an acceleration or retardation due to which it radiates electromagnetic radiation according to the classical electromagnetic theory (see Sommerfeld–Bohr atomic model). This radiation due to ***brake action*** lies in the *X*-ray region. This phenomenon is referred to as ***bremsstrahlung*** (a German word meaning literally **"*braking radiation*"**).

Thus, the net stopping power (*S*) of the medium depends on the two phenomena, i.e. *collision with the orbital electrons* and *bremsstrahlung*. The **stopping power (*S*)** is also called *linear energy transfer* (*LET*) of the substance and it is defined for the charged particles as :

$$S = LET = -\left(\frac{dE}{dx}\right)_{\text{coll}} - \left(\frac{dE}{dx}\right)_{\text{brem}}$$

where $$-\left(\frac{dE}{dx}\right)_{\text{coll}} \propto \frac{Mz^2}{E}, \text{ and } -\left(\frac{dE}{dx}\right)_{\text{brem}} \propto \frac{z^2 Z^2}{M^2}$$

where, z = charge of the moving particle (= 1 for $\beta^{+/-}$, = 2 for α), Z = nuclear charge of the stopping matter, M = mass of the moving charged particle and E = energy of the moving charged particle, and x = distance in the direction of propagation of the charged particle.

6.18.3 Interactions of Neutrons with Matter

In contrast to the charged particles, the neutrons being neutral do not experience any Coulombic potential barrier in penetrating the atomic nuclei of the stopping matter. Thus the neutrons perform different types of nuclear reactions depending on the energy of the neutrons, and mass number and atomic number of the target nuclei. These nuclear reactions are discussed in the next chapter.

Energy loss of the neutrons by elastic scattering : In elastic collisions with the atoms of stopping matter, the energy transfer occurs. Thus, the fast neutrons get slowed down. This aspect is very much important in processing the nuclear fissions (cf. **the role of moderators**).

Click Here t.me/thealchemylibrary

If the scattering atom is supposed to exist at rest before the collision with the neutron of energy E_0, then the *recoil energy* (E_r) transferred to the atom in a collision is given by :

$$E_r = E_0 \frac{4A\cos^2\theta}{(A+1)^2},$$

where A = atomic mass of the recoil atom, and θ = the angle between the direction of the impinging neutron and that of the recoil atom.

From the above expression, it is evident that if the elastic scattering is done by the lightest atom, i.e. hydrogen (A = 1), then the energy loss by the neutron becomes maximum. ***This is why, for slowing down the neutrons in nuclear reactors, light atoms are preferred. But hydrogen containing substances such as H_2O, paraffin, etc. are not recommended because of the large cross–section of the reaction, $H(n, \gamma)^2H$.*** But, heavy water (D_2O) and graphite are proved to be the best moderators for this purpose.

6.18.4 Interaction of Gamma–Radiation with Matter

In contrast to the charged particles, the γ-photons *lose their energy in a single encounter instead of successive encounters.* The gamma–photons may interact with matter in the following four modes.

(i) **Photoelectric effect** (see Sec. 2.4),
(ii) **Compton effect** (see Sec. 2.5),
(iii) **Pair formation** (see Sec. 2.6) and
(iv) **Nuclear reaction** (see next Chapter).

If the γ-photon possesses sufficient amount of energy to knock out the electron from the K or L shell, then **characteristic *X*–rays** (the **fluorescent radiation**) or **Auger emission** (see Sec. 6.7) may start.

We consider these three interactions, i.e. photoelectric effect, Compton effect and pair formation, mainly responsible for the absorption of energy of the γ-rays. Then it is evident that in contrast to the charged particles like α or β-particles which lose their energy through interaction with matter at multi-steps, **the *γ-photons lose their energy at a single step.*** This makes the absorption of energy of the γ-photons by the matter in an exponential manner. It indicates that there is always a certain probability for the γ-photon to pass through the barrier whatever its thickness may be (cf. first order kinetics for the decay of radioactive elements, Sec. 6.9.1). It follows the relationship,

$$I_x = I_0 \exp(-\mu);\ \mu = \mu_p + \mu_c + \mu_{pair};$$

where μ is the *absorption coefficient*, a linear sum of the absorption coefficients due to the photoelectric effect (μ_p), Compton effect (μ_c) and pair formation (μ_{pair}). I_0 and I_x denote the initial intensity and intensity at x distance respectively.

Theoretically, the γ-ray can pass through the infinite thickness. Analogous to the half life period, here we have, ***half value thickness*** ($x_{1/2}$) at which $I_x = \frac{1}{2}(I_0)$; $x_{1/2}$ is given by,

$$x_{1/2} = 0.693/\mu.$$

Click Here t.me/thealchemylibrary

6.18.5 Radiation Dosimetry

(a) ***Units of Dose*** : To deal with the radiation chemistry, the quantitative measurement of the radiation energy is very much important. Radiation energy is expressed in different units in different disciplines. There are also some methods to determine the amount of radiation energy absorbed.

Different units of radiation energy : The dose measured by the amount of radiation energy absorbed by a substance is expressed in the following units.

(i) ***The Rad (r)*** : It is defined as : 1 rad = absorption of 100 ergs per gram of a substance = 100 erg g^{-1} = 10^{-5} J g^{-1} = 6.24×10^{13} eV g^{-1}.

(ii) ***The Gray (Gy)*** : Gray is the SI unit of dose. It is defined as : 1 gray = absorption of one joule per kilogram of a substance = 1 J kg^{-1} = 100 rads.

(iii) ***The Rontgen (R)*** : It is defined based on the ionising power of the radiation. The unit, rontgen corresponds to the dose required to create an ionisation in 1 ml dry air at STP to such an extent to carry 1 esu of charge of either sign. This unit is generally used in physics. It is related as : 1R (air) ≈ 0.87 rad.

Rate of exposure to radiation may be expressed as *rontgen per hour* (i.e. Rh^{-1}) or millirontgen per hour (i.e. mR h^{-1}).

(iv) ***The RBE*** : Different types of radiations can produce different types of biological effects even for a particular amount of radiation energy absorbed by a living body. This is why, it requires the unit ***RBE*** (***Relative Biological Effectiveness***) for an ionising radiation. It is defined as follows :

$$\text{RBE} = \frac{\text{Absorbed dose (1 rad) of X-rays of 200 keV}}{\text{Absorbed dose in rads of the radiation (under consideration) that produces the same biological effect created by 1 rad of 200 keV X-ray}}$$

The RBE values for different types of radiations are :

RBE = 1 (for X-rays, γ-rays and β-rays)
= 2.5 (for thermal i.e. low energy neutrons)
= 10.0 (for α-particles, fast neutrons, protons, etc.)
= 10-20 (for accelerated ions of *O*, *N*, etc.).

RBE = 10 for fast neutrons indicates that 0.1 rad of a beam of fast neutron will cause the same biological damage as caused by 1 rad of 200 keV X-rays.

The product, RBE × rad = ***rem*** (***rontgen equipment man***) is generally used to express the tolerance limit. The corresponding SI unit is : ***Sievert*** (Sv) = 100 rem. The **prescribed *tolerance limit* (i.e. maximum permissible limit)** for occupational exposure is 5-6 rem per year. Here it may be noted that due to *background radiation* (i.e. cosmic rays, naturally occurring radioisotopes, man made activities, etc), a man generally experiences ca. 0.15 rem per year.

(b) ***Dosimetry*** : Dosimetry means the measurement of dose absorbed by a substance. The different physico-chemical changes dependent on the amount of doses (not on the rate of doses) absorbed can be utilised to measure the dose strength. In such cases, the extent of change is quantitatively dependent on the amount of dose received. Here, by using some known doses, the processes are

Click Here t.me/thealchemylibrary

first calibrated. **Such physico-chemical changes** are : **extent of ionisation in a particular gas, extent of blackening of photographic plates, intensity of coloration in some special type glasses,** etc. Similarly by taking the help of some radiation induced reactions (of known G values), the extent of conversion of such reactions is followed to measure the strength of a dose in comparison with some standard values or calibration curves. Such techniques are referred to as chemical dosimetry and the involved assembly is called a ***chemical dosimeter.*** This chemical dosimeter is analogous to the ***chemical actinometer**** used for the same purpose in photochemistry. Here we shall discuss the principle of two important chemical dosimeters.

(i) The Fricke Dosimeter

Principle : Here the radiation absorbed induces the oxidation of Fe^{2+} in aqueous (~ 10^{-3} M Mohr's salt) acidic (~ 0.4 M H_2SO_4) solution in the presence of dissolved air. The G value of the conversion is 15.5, i.e. $G = 15.5 = \dfrac{\text{No. of } Fe^{2+} \text{ ions converted into } Fe^{3+} \text{ ions}}{100 \text{ eV of the radiation absorbed}}$.

Thus, if a certain radiation of unknown strength is allowed to pass through a Fricke solution for a certain time, then the simple measurement (immediately after the radiation exposure) of Fe^{3+} concentration developed gives the amount of radiation energy absorbed from the known G value. From the knowledge of radiation exposure time, the radiation rate is known. This dosimeter works well up to 500 Gy.

Composition of Fricke Solution : [Mohr's salt, $FeSO_4 \cdot (NH_4)_2 SO_4 \cdot 6H_2O$] = 10^{-3} M; [H_2SO_4] = 0.4 M; [$NaCl$] (to prevent the oxidation of Fe^{2+} by other causes) = 6×10^{-3}%. The solution is made in distilled but aerated water.

Procedure : The freshly prepared Fricke solution is taken in the dosimeter cell of known volume and subjected to the radiation exposure whose dose strength is to be measured. After exposure for a definite period, the amount of Fe^{3+} produced is determined immediately after the radiation exposure. The concentration of Fe^{3+} produced is generally determined directly spectrophotometrically at 304 nm (ε = 2170 M^{-1} cm^{-1}) under the experimental condition. By developing the colour by ammonium thiocynate, Fe^{3+} can also be determined.

Radiolytic Reactions in Fricke Dosimeter Solution : The radiation induced oxidation of Fe^{2+} probably goes on through the following reaction paths initiated by the radiolytic products (e.g. $\bullet OH$, H_2O_2, $\bullet HO_2$, etc.) of water produced in the presence of oxygen (see Sec. 6.18.6).

$$Fe^{2+} + \bullet OH \rightarrow Fe^{3+} + OH^-; \; Fe^{2+} + H_2O_2 \rightarrow Fe^{3+} + \bullet OH + OH^-;$$

$$Fe^{2+} + \bullet HO_2 \rightarrow Fe^{3+} + HO_2^-; \; HO_2^- + H^+ \rightarrow H_2O_2.$$

The $\bullet HO_2$ needed in oxidation of Fe^{2+} is produced in the reaction, $\bullet H + O_2 \rightarrow \bullet HO_2$

---

* **Uranyl oxalate actinometer** is commonly used. On exposure of light the following reactions occur :

$$UO_2^{2+} + h\nu \rightarrow UO_2^{2+*}, \; UO_2^{2+*} + (CO_2H)_2 \rightarrow UO_2^{2+} + CO + CO_2 + H_2O$$

After the radiation exposure, undecomposed oxalic acid is determined. From the known values of ϕ, radiation intensity is determined.

Click Here t.me/thealchemylibrary

(ii) The Ceric Sulphate Dosimeter

Principle : Radiation induces the reduction of Ce^{4+} in a very dilute ceric sulphate solution (~ 1-10 mM) acidified strongly. In this radiation induced reaction, G value is 2.44. After the exposure of the radiation, fall in concentration of Ce^{4+} can be determined spectrophotometrically and it gives the amount of dose absorbed. It works well for higher radiation doses.

6.18.6 Radiolysis of Water

The knowledge of radiolysis of water is extremely important. Water is the major constituent of all living bodies. Hence, to understand the effect of radiation on the biological systems, the radiolysis of water is automatically involved. Water is also the major component of our total ecosystem. Similarly to know the effect of radiation in aqueous solution, the radiolysis of the solvent is involved (see Fricke dosimeter). Besides these, water is being used as the **primary and secondary coolants** in many nuclear reactors. Hence, the knowledge of radiolysis of water is extremely important from the standpoint of environmental pollution.

Besides the excitation of innumerable water molecules, a large number of ion–electron pairs along with the free radicals are formed. These can pass through a number of paths to produce different types of products such as : ionic products, hydrated electrons, free radicals, different molecular products, etc. The major radiolytic products are : H_2O^+, hydrated electron, $\bullet H$, $\bullet OH$, H_2, O_2, H_2O_2.

(a) ***Formation of ionic products in water radiolysis*** : The *wavy arrow* represents the ***primary processes*** while the *straight arrow* represents the ***secondary transformations.*** The starred species are in excited condition.

Primary process

$$H_2O + \gamma \rightsquigarrow H_2O^* \rightarrow H_2O^+ + e^-,$$

$$H_2O + e^- \rightsquigarrow H_2O^* + e^- \rightarrow H_2O^+ + 2e^-,$$

$$H_2O^* \rightarrow \bullet H + OH^+ + e^-;\ H_2O^* \rightarrow H^+ + \bullet OH + e^-,$$

Secondary process

$$H_2O + e^-; \rightarrow H_2O^+ + 2e^-;\ H_2O + e^-; \rightarrow O^+ + H_2 + 2e^-,$$

$$H_2O + H_2O^+ \rightarrow H_3O^+ + \bullet OH$$

In liquid phase, **among the positive ions, H_2O^+ is the most predominant one** and other reactions leading to H^+, OH^+, H_3O^+ are of importance only in vapour phase radiolysis of water. The ion pairs involve the cation (e.g. H_2O^+) and electron. *Formation of negative ions by capturing the electrons does not occur because of the instantaneous solvation of the electrons or recombination of the electrons with the positive ions.*

(b) ***Formation of free radicals and molecular products in water radiolysis*** : Free radicals are formed in the following primary processes.

$$H_2O + \gamma \rightsquigarrow H_2O^* \rightarrow \bullet H + \bullet OH;$$

$$H_2O + e^- \rightsquigarrow H_2O^* + e^- \rightarrow \bullet H + \bullet OH + e^-$$

Besides these, the positive ions formed can participate in the following ion–electron recombination reactions at the secondary steps to generate the free radicals.

$$H_2O^+ + e^- \rightarrow \bullet H + \bullet OH;\ H_3O^+ + e^- \rightarrow 2\bullet H + \bullet OH;$$

Click Here t.me/thealchemylibrary

$$H^+ + H_2O + e^- \longrightarrow 2\,{\bullet}H + {\bullet}OH;\ {\bullet}OH + H_2O \longrightarrow {\bullet}H + 2\,{\bullet}OH$$
$$H_2O^+ + H_2O + e^- \longrightarrow 2\,{\bullet}H + 2\,{\bullet}OH$$

We have already mentioned in connection with the radiolysis of Fricke solution that the dissolved oxygen forms perhydroxyl radical ${\bullet}HO_2$ in the reaction, ${\bullet}H + O_2 \rightarrow HO_2$. The free radicals formed may participate in chain reactions having both the steps, i.e. ***chain termination*** and ***chain propagation***, leading to different molecular products.

Let us first consider the radical–radical interactions in **chain termination steps** to produce the molecular products.

$${\bullet}H + {\bullet}OH \rightarrow H_2O;\ {\bullet}OH + {\bullet}OH \rightarrow H_2O_2;\ {\bullet}H + {\bullet}H \rightarrow H_2$$

In the presence of dissolved oxygen, the following reactions may occur.

$${\bullet}OH + {\bullet}HO_2 \rightarrow H_2O + O_2;\ {\bullet}H + {\bullet}HO_2 \rightarrow H_2O_2;\ 2\,{\bullet}HO_2 \rightarrow H_2O_2 + O_2$$

The composition of the radiolysis products largely depends on the energy and nature of the ionising radiation or particle. For the slow moving particles, H_2O_2 is predominantly formed while for the fast moving β^--particles the following routes are important :

$${\bullet}H + {\bullet}H \rightarrow H_2;\ \text{and,}\ {\bullet}H + {\bullet}OH \rightarrow H_2O$$

Chain propagations can be carried out by the following paths.

$$H_2O + {\bullet}OH \rightarrow H_2O_2 + {\bullet}H;\ H_2O + {\bullet}H \rightarrow {\bullet}OH + H_2;$$
$$H_2O_2 + {\bullet}H \rightarrow {\bullet}OH + H_2O;\ {\bullet}OH + H_2 \rightarrow {\bullet}H + H_2O;$$
$$HO{\bullet} + H_2O_2 \rightarrow H_2O + {\bullet}HO_2$$

(c) ***Hydrated electron*** : If the electron freed in the primary events are not of much high energy to carry out ionisation, excitation or bond rupture, then these can get solvated very quickly. This concept of solvated electron is well documented in chemistry. The ammoniated electrons obtained by dissolving alkali metals in liquid ammonia show blue coloration. In explaining the enormous reducing power of the nascent hydrogens, the concept of hydrated electron is put forward. Similarly, ***hydrated electron is considered as one of the major radiolytic products of water.***

$$H_2O + \gamma \rightsquigarrow H_2O^+ + e^-_{hyd};\ H_2O + e^- \rightsquigarrow H_2O^+ + 2\,e^-_{hyd}$$

In the radiolysis of water, besides the ${\bullet}H$ and ${\bullet}OH$ free radicals, the hydrated electron is also a major component of the ***primary radiolytic products*** (***prp***). Some important properties of the hydrated electrons are given here.

$$\lambda_{max} = 720\ \text{nm};\ E^0\,(e^-_{hyd} + H^+ \rightarrow H) = -2.77\ \text{V},\ 25^\circ\text{C};$$

Decay mode : $e^-_{hyd} \rightarrow {\bullet}H_{hyd} + OH^-_{hyd}$.

Because of the highly negative reduction potential of the hydrated electron, it can act as a powerful reducing agent.

Click here t.me/theachemylibrary

SOLVED NUMERICAL PROBLEMS

Problem 1 : ${}^{6}_{2}He$ is β^--active. Find the maximum energy which can be associated with the β^--particle.

(*Given* : Isotopic masses of ${}^{6}_{2}He$ and ${}^{6}_{3}Li$ are 6.01889 and 6.01512 in amu respectively).

Solution : The β^- disintegration process can be represented as follows :

$$ {}^{6}_{2}He \rightarrow {}^{6}_{3}Li^{+} + {}^{0}_{-1}e + {}^{0}_{0}\bar{\nu} $$

Here, the product species will remain as a cation at the moment of its production. Here the mass loss is given by :

$$ \Delta m = \text{mass of } {}^{6}_{2}He - \text{mass of } \left({}^{6}_{3}Li^{+} + \beta^- \text{ particle}\right) \approx \text{mass of } {}^{6}_{2}He - \text{mass of } {}^{6}_{3}Li $$

Neglecting the binding energy of the last electron in ${}^{6}_{3}Li$, the relevant electron binding step is:

$$ {}^{6}_{3}Li^{+} + \beta^- \rightarrow {}^{6}_{3}Li $$

Thus, Δm = (6.01889 – 6.01512) amu

= 0.00377 amu

$\equiv$ 0.00377 × 931 MeV = 3.50 MeV

Therefore, the maximum kinetic energy which can be associated with the β^--particle is 3.50 MeV. *At this condition, the antineutrino will not share any energy.*

Problem 2 : ${}^{13}_{7}N$ is found β^+-active. The β^+-particle is found to have the maximum energy 1.20 MeV. Find the isotopic mass of ${}^{13}_{7}N$. (Given, the masses of ${}^{13}_{6}C$ and an electron are 13.00335 and 0.00055 amu respectively).

Solution : The disintegration process is represented as follows :

$$ {}^{13}_{7}N \rightarrow {}^{13}_{6}C^{-} + \beta^+ + {}^{0}_{0}\nu $$

The carbon atom formed at that moment remains anionic. The mass loss in the process is given by:

$$ \Delta m = \text{mass of } {}^{13}_{7}N - \text{mass of } \left({}^{13}_{6}C^{-} + \beta^+\right) = \text{mass of } {}^{13}_{7}N - \text{mass of } \left({}^{13}_{6}C + m_e + m_e\right) $$

(considering, the mass of an electron = mass of a positron = m_e)

i.e. $$ \Delta m = \text{mass of } \left({}^{13}_{7}N - {}^{13}_{6}C\right) - 2m_e $$

According to the given condition :

$$ \Delta m \times 931 = 1.20 \text{ MeV; or } \Delta m = \frac{1.20}{931} \text{ amu} = 0.00129 \text{ amu} $$

Therefore, $0.00129 = \text{mass of } \left({}^{13}_{7}N - {}^{13}_{6}C\right) - 2m_e$

or, mass of ${}^{13}_{7}N = 0.00129 + 13.00335 + 2 \times 0.00055 = 13.00574$ amu

Click Here t.me/thealchemylibrary

Problem 3 : Calculate the kinetic energy of the α-particle and the recoil atom in disintegration of ^{244}Cm to ^{240}Pu. Given, the mass loss in the decay is 0.00633 amu.

Solution : We have the relation, $Q = E_\alpha \left(\frac{A}{A-4}\right)$ (cf. Eqns. 6.11.4-5)

where, $Q = 931 \times$ mass loss (where Q in *MeV*, mass loss in amu), E_α = kinetic energy of the α-particle, A = mass number of the parent nuclide.

Therefore, $E_\alpha = \frac{Q(A-4)}{A} = \frac{0.00633 \times 931 \times 240}{244} = 5.79$ MeV

Again, $Q = E_\alpha + E_{recoil}$ where E_{recoil} represents the kinetic energy of the recoil daughter species.

Thus, $E_{recoil} = (0.00633 \times 931 - 5.79)$ MeV $= 0.103$ MeV

Problem 4 : Predict the mode of decay of $^{7}_{4}Be$. (Given, the masses of $^{7}_{4}Be$, $^{7}_{3}Li$ and electron are 7.01693, 7.01600 and, 0.00055 amu respectively.)

Solution : In $^{7}_{4}Be$, the neutron to proton ratio is given by $n/p = 3/4 < 1$. Hence, from the knowledge of Segre's chart, it will decay in a way so that its n/p ratio goes to increase.

In such cases the following two processes appear important.

(i) $^{7}_{4}Be \rightarrow {}^{7}_{3}Li^{-} + \beta^{+} + {}^{0}_{0}\nu$;

(ii) $^{7}_{4}Be \xrightarrow[\text{or, } L\text{-capture}]{K\text{-capture}} {}^{7}_{3}Li$

From the energetics (see Sec. 6.11) of the processes the following conditions must be maintained. Energetically, we have the following conditions :

$$\text{mass of } (^{7}_{4}Be - {}^{7}_{3}Li) \times 931 \geq 2 \times 0.00055 \times 931, \textbf{ (for } \beta^{+} \textbf{ - decay)} \text{ and}$$

$\geq$ binding energy of K-electron or L-electron, **(for electron capture).**

Here, the mass difference between the parent $\left(^{7}_{4}Be\right)$ and daughter $\left(^{7}_{3}Li\right)$ species is given by,

$$7.01693 - 7.01600 = 0.00093 \text{ amu} < 2 \times 0.00055 \text{ amu}$$

Thus, here, the condition for β^{+} decay is not maintained. Hence, the process of decay passes through the orbital capture process.

Problem 5 : Calculate the mass of ^{234}U having $t_{1/2} = 2.5 \times 10^{5}$ yr to produce the activity of 1 curie and 1 rutherford..

Solution : The decay constant is given by :

$$k = 0.693/t_{1/2} = \frac{0.693}{2.5 \times 10^{5}} = 2.77 \times 10^{-6} \text{ yr}^{-1}$$

$$= \frac{2.77 \times 10^{-6}}{365 \times 24 \times 3600} \text{ s}^{-1} = 8.79 \times 10^{-14} \text{ s}^{-1}$$

Click Here t.me/thealchemylibrary

Let, w_1 gram be the mass of ^{234}U to produce 1 curie activity. The number of ^{234}U atoms present in w_1 is given by :

$$N = \frac{w_1 \times 6.02 \times 10^{23}}{234}$$

Therefore, $$\left| -\frac{dN}{dt} \right| = 1 \text{ curie} = 3.70 \times 10^{10} \text{ counts per second} = kN$$

or, $$3.7 \times 10^{10} = \frac{8.79 \times 10^{-14} \times w_1 \times 6.02 \times 10^{23}}{234}$$

or, $$w_1 = 163.6 \text{ g}$$

Similarly, if w_2 g is the required mass of ^{234}U to produce 1 rutherford activity, then :

$$\left| -\frac{dN}{dt} \right| = 1 \text{ rutherford} = 10^6 \text{ counts per second} = k \frac{w_2 \times 6.02 \times 10^{23}}{234}$$

or $$w_2 = \frac{10^6 \times 234}{8.79 \times 10^{-14} \times 6.02 \times 10^{23}} = 4.42 \times 10^{-3} \text{ g}$$

Problem 6 : The half life period of ^{60}Co is 5.3 years. Find the activity of a millicurie of the sample after six months.

Solution : We have the relation : $N_t = N_0 \exp(-kt)$; and $k = 0.693/t_{1/2}$

or, $$2.303 \log (N_t / N_0) = -kt;$$

or, $$2.303 \log (N_t / N_0) = -\frac{0.693 \times 0.5}{5.3}$$

or, $$\log (N_t / N_0) = -\frac{0.693 \times 0.5}{5.3 \times 2.303} = -0.0284; (t = 6 \text{ months} = 0.5 \text{ yr})$$

or, $$\frac{N_t}{N_0} = 0.936$$

According to the given condition, $N_0 \equiv 1$ millicurie. Hence, $N_t \equiv 0.936$ millicurie.

Problem 7 : A radioactive source, ^{147}Pm ($t_{1/2}$= 2.65 yr) is used for running an atomic battery from the energy of the emitted particles. Find the time when its activity (i.e. rate of beta emission) will be reduced to 20% of its initial value.

Solution : The decay constant is given by : $k = \frac{0.693}{t_{1/2}} = \frac{0.693}{2.65} = 0.261 \text{ yr}^{-1}$

The activity (i.e. rate of emission) is directly proportional to the number of disintegrating atoms at that time. Here the activity is reduced to 20% of initial value. Hence, N_t = 20% of N_0

or, $$N_t / N_0 = 20/100$$

Click Here t.me/thealchemylibrary

Therefore, from the relation, $N_t = N_0 \exp(-kt)$, we get :

$$2.303 \log (N_t/N_0) = -kt;$$

or, $$2.303 \log (1/5) = -0.261t;$$

or, $$t = 6.16 \text{ yr.}$$

Problem 8 : A radioactive sample shows activity 48 counts per minute, and after 5 min it reduces to 20 counts per min. Find the decay constant and half life period of the sample.

Solution : From the given condition, $\left|-\frac{dN}{dt}\right| = 48$ (at $t = 0$), $= 20$ (at $t = 5$ min)

From the relation, $-\frac{dN}{dt} = kN$, we have :

$48 = kN_0$, (at $t = 0$); and $20 = kN_t$, ($t = 5$ min);

or, $N_t/N_0 = 20/48$

By using the relation, $2.303 \log (N_t/N_0) = -kt$, we get :

$$2.303 \log (20/48) = -k \times 5;$$

or, $k = 0.175 \text{ min}^{-1}$ and, $t_{1/2} = 0.693/k = 3.96$ min

Problem 9 : A certain radioactive sample has a half life period of 40 days. How long will it require for 3/4 of the atoms to disintegrate? What fraction will remain unchanged after 3 half lives?

Solution : Let, t be the required time for the disintegration of 3/4 of the atoms present at $t = 0$

Thus, $N_t = N_0 (1 - 3/4) = N_0/4$; or, $N_t/N_0 = 1/4$

From the relation, $2.303 \log (N_t/N_0) = -kt$, wet get :

$$2.303 \log (1/4) = -\frac{0.693}{40} t; \text{ or, } t = 80 \text{ days}$$

$$3 \text{ half lives} = 3 \times 40 \text{ days}$$

$\therefore$ $$2.303 \log (N_t/N_0) = -k \times 120$$

or, $$\log (N_t/N_0) = -\frac{0.693 \times 120}{40 \times 2.303} = -0.903; \text{ or, } (N_t/N_0) = 0.125; \text{ or, } N_t = 12.5\% \text{ of } N_0$$

Thus, after three half lives, 87.5% will disintegrate away.

Problem 10 : On analysis, an ore of uranium shows the mass ratio for ^{238}U to $^{206}Pb = 6.08$. All ^{206}Pb atoms are supposed to appear from the disintegration of ^{238}U. Find the age of the ore. (Given, $t_{1/2}$ for $^{238}U = 4.5 \times 10^9$ yr, the next longest lived nuclide ^{234}U in the series shows $t_{1/2} = 2.5 \times 10^5$ yr).

Solution : As the $t_{1/2}$ for ^{238}U is much greater than that of any other nuclide in the series, at least by a factor of 10^4, it can be reasonably assumed that all ^{238}U atoms disintegrated are converted into the stable end product ^{206}Pb.

Click Here to the chemylibrary

Mass ratio of ^{238}U to ^{206}Pb is 6.08. Thus, if $^{238}U = 6.08\ y$ g, then $^{206}Pb = y$ g. We get :

$$6.08\ y \text{ g of } {}^{238}U \equiv \frac{6.08\ y \times 6.02 \times 10^{23}}{238} \text{ atoms of } {}^{238}U$$

and, $$y \text{ g } {}^{206}Pb \equiv (y \times 6.02 \times 10^{23})/206 \text{ atoms of } {}^{206}Pb.$$

One ^{238}U atom produces one atom of ^{206}Pb. Hence, $(y \times 6.02 \times 10^{23}/206)$ atoms of ^{206}Pb are produced from $(y \times 6.02 \times 10^{23})/206$ atoms of ^{238}U.

Therefore, the number (N_0) of ^{238}U atoms present at zero time (i.e. $t = 0$) is given by :

$$N_0 = (y \times 6.02 \times 10^{23})/206 + (6.08y \times 6.02 \times 10^{23})/238$$

and, $$N_t = \text{number of } {}^{238}U \text{ atoms at } t \text{ time} = (6.08y \times 6.02 \times 10^{23})/238$$

Thus,
$$\frac{N_0}{N_t} = \frac{y \times 6.02 \times 10^{23}\left(\frac{1}{206} + \frac{6.08}{238}\right)}{\frac{y \times 6.08 \times 6.02 \times 10^{23}}{238}} = 1.19$$

By using the relationship, $2.303 \log (N_0/N_t) = kt$, we get :

$$2.303 \log (1.19) = \frac{0.693}{4.5 \times 10^9} t; \text{ or, } t = 1.13 \times 10^9 \text{ yr}; (k = 0.693/t_{1/2})$$

Thus, the age of the ore is 1.13×10^9 years.

Problem 11 : An old piece of a wooden sample kept in a museum has a disintegration rate which is 30% of the disintegrations shown by an equal weight of a new piece of wood. Find the age of the wooden sample. (Given $t_{1/2}$ for $^{14}C = 5740$ yr).

Solution : The disintegration rate is directly proportional to the number of disintegrating atoms. Hence, if the activity, i.e. disintegration rate, falls to 30%, the number of disintegrating ^{14}C atoms also falls to 30%.

Therefore, $$N_t = 30\% \text{ of } N_0; \text{ or, } N_t/N_0 = 30/100$$

From the relation, $2.303 \log (N_t/N_0) = -kt$; and $k = 0.693/t_{1/2}$, we have :

$$2.303 \log (3/10) = -\frac{0.693}{5740} t; \text{ or, } t = 9974 \text{ yr.}$$

Thus, the age of the wooden sample is 9974 years.

Problem 12 : To assess the volume of blood in a patient by the *isotopic dilution method*, the following data are recorded. Initial activity in the labelled (with ^{32}P as phosphate) blood which was injected $= 12 \times 10^4$ counts per min per ml; volume of labelled blood injected = 1 ml; activity in the withdrawn blood after equilibriation = 30 counts per min per ml. Find the total volume of blood in the patient's body.

Solution : Volume of the labelled blood injected $= V_1 = 1.0$ ml

Initial activity $(A_1) = 12 \times 10^4$ counts per ml per min.

Click Here to me/thealchemylibrary

Final activity (A_2) = 30 counts per ml per min.

Let, V_2 be the volume of blood in the patient's body, then to maintain the total activity constant, we have :

$$V_1A_1 = (V_2 + V_1)A_2$$

or, $$\frac{1 \times 12 \times 10^4}{30} = V_1 + V_2; \text{ or, } 4 \times 10^3 = V_2 + 1; V_2 = 4 \text{ litre.}$$

Problem 13 : The half life period of ^{22}Na is 2.5 yr. It decays 90% through β^+ decay and the rest by electron capture. Find the decay constants and half lives in both the parallel modes of decay.

Solution :

$$^{22}Na \xrightarrow{k_1} \text{Positron decay product}$$

$$^{22}Na \xrightarrow{k_2} \text{Electron capture product}$$

Let, N_0 and N_t be the numbers of atoms of ^{22}Na at $t = 0$, and $t = t$ respectively. The rates of decay through positron decay and electron capture at $t = t$ are given by, k_1N_t and k_2N_t respectively.

Therefore, the total rate of decay of $^{22}Na = k_1N_t + k_2N_t = N_t(k_1 + k_2)$

or, $$-\frac{dN_t}{dt} = N_t(k_1 + k_2)$$

which leads to : $N_t = N_0 \exp[-(k_1 + k_2)t]$; or, $2.303 \log (N_0/N_t) = (k_1 + k_2)t$

From the given condition, $(k_1 + k_2) = 0.693/t_{1/2}$

or, $$(k_1 + k_2) = 0.693/2.5 = 0.277 \text{ yr}^{-1} \quad \ldots(i)$$

Now we have :

$$\frac{\text{Amount of decay through } \beta^+ \text{ emission}}{\text{Amount of decay through electron capture}} = \frac{\text{Rate of } \beta^+ \text{ emission}}{\text{Rate of electron capture}}$$

or, $$(90/10) = (k_1N_t)/(k_2N_t) = k_1/k_2; \text{ or, } k_1 = 9k_2 \quad \ldots(ii)$$

By solving Eqns. (i) and (ii) we get : $k_1 = 0.249 \text{ yr}^{-1}$, i.e. $t_{1/2} = \frac{0.693}{0.249} \text{ yr} = 2.78 \text{ yr}$

and, $$k_2 = 0.0277 \text{ yr}^{-1}, \; t_{1/2} = \frac{0.693}{0.277} \text{ yr} = 2.5 \text{ yr}$$

Therefore, the half lives in the k_2 and k_1 paths are 25.0 yr and 2.78 yr respectively.

Problem 14 : The disintegration process is :

$$^{140}Ba \xrightarrow[(t_{1/2} = 12 \text{ days})]{\beta^-, k_1} {}^{140}La \xrightarrow[(t_{1/2} = 12 \text{ hr})]{\beta^-, k_2} {}^{140}Ce \text{ (stable)}$$

(a) Find the activity of ^{140}La after 5 days, when the initial activity is 1000 counts per second in the pure ^{140}Ba sample,

(b) Find the time when ^{140}La shows the maximum activity,

(c) Find the time of equilibrium attainment.

Click Here t.me/thealchemylibrary

Solution : (a) If N_2 is the number of atoms of ^{140}La after 5 days and N_0 is the number of ^{140}Ba atoms present initially in the pure sample, then we get the standard relations :

$$N_2 = \frac{k_1 N_0}{k_2 - k_1}[\exp(-k_1 t) - \exp(-k_2 t)];$$

and $$k_1 = \frac{0.693}{12}\,\text{d}^{-1} = 0.057\,\text{d}^{-1};\quad k_2 = \frac{0.693}{0.5\,\text{d}} = 1.386\,\text{d}^{-1}$$

Thus, $$N_2 = \frac{k_1 N_0}{1.386 - 0.057}[\exp(-0.057 \times 5) - \exp(-1.386 \times 5)]$$

$$= \frac{k_1 N_0}{1.329}(0.75 - 9.8 \times 10^{-4}) \approx \frac{A_0}{1.329} \times 0.75 = 0.56 A_0$$

(initial activity = $A_0 = k_1 N_0$)

The activity due to ^{140}La is given by :

$$A_2 = k_2 N_2 = k_2 \times 0.56 A_0 = 1.386 \times 0.56 \times 1000,\ (A_0 = 10^3 \text{ counts per second})$$

$$= 776 \text{ counts per second.}$$

(b) The time when ^{140}La shows the maximum activity is given by :

$$t_{max} = \frac{\ln k_1 - \ln k_2}{k_1 - k_2} = \frac{2.303 \log (k_1/k_2)}{k_1 - k_2} = \frac{3.18}{1.329} = 2.4 \text{ days}$$

(c) At t_{max}, the rate of formation of ^{140}La is equal to the rate of its disintegration. Hence, at $t = t_{max}$ the ***transient equilibrium*** will be attained.

Problem 15 : In an ore, ^{238}U ($t_{1/2} = 4.5 \times 10^9$ yr) and ^{226}Ra ($t_{1/2} = 1.6 \times 10^3$ yr) are in equilibrium. Find the ratio of ^{238}U to ^{226}Ra.

Solution : k_1 = decay constant of $^{238}U = 0.693/t_{1/2} = 1.54 \times 10^{-10}\ \text{yr}^{-1}$

and k_2 = decay constant of $^{226}Ra = 0.693/t_{1/2} = 4.43 \times 10^{-4}\ \text{yr}^{-1}$.

As $k_2 >>> k_1$, the condition of ***permanent or secular equilibrium*** is attained. It leads to : $k_1 N_1 = k_2 N_2$, where, N_1 and N_2 denote the number of ^{238}U and ^{226}Ra atoms.

Thus : $1.54 \times 10^{-10} N_1 = 4.43 \times 10^{-4} N_2$; or, $N_1/N_2 = 2.87 \times 10^6$.

Problem 16 : The radioisotope $^{210}_{83}Bi$ is β^--active and the mean energy of the β^--particles is 0.34 MeV. The half life period of the isotope is 5 d. If a particular sample contains 0.4 mg of $^{210}_{83}Bi$, calculate the energy emission in watt.

Solution : The number of $^{210}_{83}Bi$ atoms in 0.4 mg is given by :

$$N = \frac{4 \times 10^{-4} \times 6.02 \times 10^{23}}{210} = 1.15 \times 10^{18} \text{ atoms}$$

The disintegration constant (k) = $\frac{0.693}{5\,\text{d}} = 0.1386\,\text{d}^{-1}$

Click Here t.me/healchemylibrary

$$\text{Activity} = kN = 1.15 \times 10^{18} \times 0.1386 \text{ disintegration per day}$$

$$= \frac{1.15 \times 10^{18} \times 0.1386}{24 \times 3600} \text{ dps} = 1.84 \times 10^{13} \text{ dps}$$

$$= 1.84 \times 10^{13} \times 0.34 \text{ MeV s}^{-1} = 6.25 \times 10^{12} \text{ MeV s}^{-1}$$

$$= 1.6 \times 10^{-13} \times 6.25 \times 10^{12} \text{ J s}^{-1}$$

$$= 1.0 \text{ J s}^{-1} = 1.0 \text{ watt}$$

$(1 \text{ MeV} = 1.6 \times 10^{-13} \text{ J}).$

Problem 17 : $Ba^{35}SO_4$ precipitate shows activity 40×10^3 counts per mg per min. 0.1 ml of its saturated solution dried under infrared lamp recorded 190 counts in 20 min. Find the solubility of $BaSO_4$ and its solubility product.

Solution : Initial activity $(A_i) = 40 \times 10^3$ counts per min per mg

$$\text{Final activity } (A_f) = \frac{190}{20} = 9.5 \text{ counts per min per 0.1 ml of the solution}$$

$$= 9.5 \times 10^4 \text{ counts per min per litre of the solution}$$

$$40 \times 10^3 \text{ counts per min} \equiv 1 \text{ mg } BaSO_4$$

$$\therefore \quad 9.5 \times 10^4 \text{ counts per min} \equiv \frac{1 \times 9.5 \times 10^4}{40 \times 10^3} \text{ mg } BaSO_4$$

$$= 2.375 \text{ mg } BaSO_4$$

i.e. $$\text{Solubility of } BaSO_4 = 2.375 \text{ mg L}^{-1}$$

$$= \frac{2.375}{1000 \times 233.3} \text{ mol L}^{-1}$$

$$\approx 1 \times 10^{-5} \text{ mol L}^{-1}$$

$$BaSO_4 \text{ (solid)} \rightleftharpoons Ba^{2+} + SO_4^{2-}$$

$$K_{SP} = \text{Solubility product} = [Ba^{2+}]\,[SO_4^{2-}] = S^2, \ (S = \text{molar solubility})$$

$$= (1 \times 10^{-5} \text{ mol L}^{-1})^2$$

$$= 10^{-10} \text{ mol}^2 \text{ L}^{-2}.$$

Problem 18 : 0.5 g of a ruby laser was irradiated by a neutron flux of 10^{12} neutrons $cm^{-2}\ s^{-1}$ for 24 hours and then the activity due to $^{51}_{24}Cr$ ($t_{1/2}$ = 27.7 d) was measured immediately thereafter. It was found 3.5×10^5 dps. Find the *Cr*-content in the ruby laser. (Given : σ for ^{50}Cr = 15.9 barn, natural abundance of ^{50}Cr = 4.45%).

Solution : If the sample contains *N* number of $^{50}_{24}Cr$ atoms, then the number of $^{51}_{24}Cr$ atoms produced in the said (n, γ) reaction for the exposure of neutron flux for 24 hour is given by :

$$x = N\phi\sigma t$$

where ϕ = neutron flux density (i.e. no. of neutrons colliding per second per cm^2 of the target) :

σ = reaction cross section; t = time in s

i.e. $$x = N \times 10^{12} \times 15.9 \times 10^{-24} \times 24 \times 3600, \ (1 \text{ barn} = 10^{-24} \text{ cm}^2)$$

Click Here t.me/thealchemylibrary

Activity due to ^{51}Cr is given by :

$$A = kx = \frac{0.693 \times x}{27.7 \times 24 \times 3600} \text{ dps, } (k = \text{disintegration constant for } ^{51}Cr)$$

i.e. $$3.5 \times 10^5 = \frac{0.693x}{27.7 \times 24 \times 3600}$$

or, $$x = \frac{3.5 \times 10^5 \times 27.7 \times 24 \times 3600}{0.693}$$

or, $$N \times 10^{-12} \times 15.9 \times 24 \times 3600 = \frac{3.5 \times 10^5 \times 27.7 \times 24 \times 3600}{0.693}$$

or, $$N = \frac{3.5 \times 10^5 \times 27.7}{15.9 \times 0.693 \times 10^{-12}} = 8.8 \times 10^{17} \text{ atoms}$$

$\therefore$ Mass of N number of ^{50}Cr atoms $= \frac{N \times 50}{6.02 \times 10^{23}}$ g

$$= \frac{8.8 \times 10^{17} \times 50}{6.02 \times 10^{23}} = 7.3 \times 10^{-5} \text{ g}$$

Natural abundance of $^{50}Cr = 4.45\%$

i.e. 4.45 g ^{50}Cr in a sample $\equiv$ 100 g Cr

$\therefore$ 7.3×10^{-5} g $^{50}Cr \equiv \frac{100 \times 7.3 \times 10^{-5}}{4.45}$ g Cr

$= 1.64 \times 10^{-3}$ g $= 1.68$ mg Cr

$\therefore$ 500 mg of the sample contains 1.64 mg Cr

i.e. Cr-content in the sample $= \frac{1.64 \times 100}{500} = 0.328\%$.

EXERCISE–VI

A. General Questions

1. What do you mean by natural radioactivity? How was it discovered? Discuss the characteristic properties of the radioactive emanation.
2. What are the advantages of the cylindrical electrode ionisation chamber compared to the parallel plate ionisation chamber? Discuss the working principle of a cylindrical electrode ionisation chamber. Why is it called a proportional counter?
3. Discuss the difference between a proportional counter and a G–M counter? Discuss their advantages and disadvantages.
4. What are the different types of disintegration? Discuss their modes of decay.

Click Here t.me/thealchemylibrary

5. Discuss the energetics of β^+, β^-, electron capture (EC) and α-decay. Mention the threshold mass difference (between the parent and product species) required for each process.
6. How does the wave mechanical concept explain the α-decay? Explain the foundation of the Geiger-Nuttall rule from this wave mechanical concept.
7. Discuss the decay and growth kinetics for a radioelement and its daughter element respectively when the daughter product is stable. Establish the relationship between $t_{1/2}$ and t_{av} from their definitions.
8. Discuss the kinetics of the disintegration series where the daughter product is radioactive.
9. What are the different types of radioactive equilibria? Derive the conditions for attaining these equilibria.
10. Mention the historical incident which led to discover the artificial radioactivity. Discuss the different routes to synthesise the artificial radioactivity.
11. What do you mean by the tracer technique? Discuss its application in the field of chemistry.
12. Give different types of application of different radioisotopes in the following fields : (i) Chemistry, (ii) Biology, (iii) Agriculture, (iv) Industry and (v) Medicine and therapy.
13. What is the difference between photochemistry and radiation chemistry? Define the G-value in radiation chemistry.
14. Discuss the different types of interactions between the charged particles of medium energy and matter.
15. Discuss the radiolysis of water along with its importance.
16. What do you mean by dosimetry? What are the units of dose? Discuss the basic principles of Fricke chemical dosimeter.
17. Write notes on : (i) Units of radioactivity, (ii) Wilson cloud chamber, (iii) Gieger–Nuttall rule, (iv) Sargent's curve, (v) Internal conversion, (vi) Auger effect, (vii) Interaction between γ-rays and matter, (viii) Linear energy transfer (LET), (ix) Tracks and δ-ray tracks, (x) Group displacement law, (xi) Isotopic dilution analysis, (xii) Neutron activation analysis, (xiii) Neutrino and its discovery, (xiv) Half–life period, (xv) Half value thickness for the γ-rays, (xvi) RBE and rem.

B. Justify the Statements

1. Radioactive emanation from the naturally occurring source is split into three parts in the presence of an external magnetic or electric field.
2. α-Tracks are straight while the β-tracks are zig–zag.
3. The mode of energy loss by the γ-rays in the interaction with matter is different compared to that by the charged particles.
4. For positron activity, the parent nuclide should be able to provide at least 1.02 MeV energy.
5. Quantum mechanical tunnel effect can explain the emission of α-particles having much lower energy compared to the height of the nuclear barrier.
6. Though the Geiger-Nuttall rule is an empirical one, it can be rationally justified.
7. A Geiger-Muller counter can be converted into a proportional counter.
8. The concepts of threshold Geiger and Geiger range are very important to operate a G-M counter.

Click Here t.me/thealchemylibrary

9. Wilson cloud chamber not only detects the radiation but also characterises the radiation. Such a characterisation is not possible in a G-M counter.
10. Auger effect and radiation emission (i.e. *X*-ray production) are not the nuclear phenomena.
11. α-Particles for a particular source are monoenergic, while the β^+ and β^- particles cover a spectral range continuously even for a particular source.
12. Though both the β^- radiation and internal conversion lead to the ejection of electrons, they are different.
13. *X*-rays and γ-rays not only differ in their position in the electromagnetic spectrum, but they also differ in their birth history.
14. Nuclear de-excitation can pass through a number of routes.
15. Aluminium foil on being bombarded by a neutron flux produces positrons which still continue even after the removal of the neutron source.
16. Labelling of hydrogen to follow its reaction pathway through the tracer technique is not much promising.
17. For slowing down the fast neutrons in the reactor, light atoms (e.g. D_2O, graphite) are used.
18. D_2O not H_2O is used in the nuclear reactor to thermalise the fast neutrons.
19. All elements do not respond to neutron activation analysis.
20. The term range is well defined for the α-particles while it is ill defined for the β^- particles and γ-radiations.
21. What do you mean by RBE and rem? Illustrate with examples.

C. Numerical Problems

1. Predict the unstable one along with the mode of its decay (from the consideration of energetics) in each of the following pairs.
   (i) ${}^{16}_{6}C$, ${}^{16}_{7}N$ (ii) ${}^{18}_{9}F$, ${}^{18}_{10}Ne$
   (Isotopic masses in amu are : ${}^{16}C = 16.01470$, ${}^{16}N = 16.00610$, ${}^{18}F = 18.00094$, ${}^{18}Ne = 18.00571$, and $m_e = 0.00055$)
   Ans. ${}^{16}C \rightarrow \beta^-$ active; ${}^{18}Ne \rightarrow$ both β^+ and *K*-capture.
2. Electron and its antiparticle annihilate on combination to form two γ-photons of equal energy. Find the energy of the γ-photon.
   Ans. 0.51 MeV for each photon.
3. The isotopic masses of ${}^{64}_{29}Cu$, ${}^{64}_{28}Ni$ and ${}^{64}_{30}Zn$ are 63.9499 u, 63.9481 u, and 63.9493 u respectively. Predict the mode of decay of ${}^{64}_{29}Cu$ and ${}^{64}_{28}Ni$ from the consideration of energetics.
   Ans. β^- emission by *Zn*; β^+ emission by *Ni*.
4. ${}^{231}_{90}Th$ undergoes β^- emission with a mass loss of 0.000226 u. Find the maximum energy of the β^- ray.
   Ans. 0.21 MeV.
5. ${}^{226}_{88}Ra$ emits α-particles. The atomic masses of ${}^{226}_{88}Ra$ and ${}^{222}_{86}Rn$ are 226.0254 u and 222.0175 u respectively. Calculate the kinetic energies of the α-particle and daughter recoil atom (Given: $m_\alpha = 4.0026$ u).
   Ans. $E_\alpha = 4.847$ MeV, $E_{recoil} = 0.087$ MeV.

Click Here t.me/thealchemylibrary

6. Calculate the number of disintegrations per gram of ^{226}Ra per second. ($t_{1/2}$ of ^{226}Ra = 1620 yr).
   Ans. 3.6×10^{10} s^{-1}.
7. ^{214}Pb decays with a half life of 26.8 minutes. Calculate the weights of the sample showing activity one curie and one rutherford. Calculate also the activity per gram.
   Ans. 1 curie ≡ 3.06×10^{-8} g, 1 Rd ≡ 8.3×10^{-13} g, specific activity = 3.28×10^{7} curies g^{-1}.
8. The half–life period of a radioactive sample is 4.8 min. If 1 mg of the sample is kept in a store, how much of the sample would remain unchanged after 10 min and four half lives?
   Ans. 0.236 mg after 10 min, 0.0625 mg after four half lives.
9. A radioactive sample has a half–life time 53,000 sec. Calculate the time when its activity will fall to 1/100th of its initial value.
   Ans. 3.54×10^{5} sec.
10. In the following series,

$$^{92}Sr \xrightarrow[t_{1/2} = 2.7 \text{ hr}]{} {}^{92}Y \xrightarrow[t_{1/2} = 3.6 \text{ hr}]{} \text{products (stable)}$$

    Find the time when ^{92}Y will show its maximum activity. When does it attain the equilibrium? Mention the type of the equilibrium.
    Ans. t_{max} = 4.49 hr; (in reality no equilibrium is attained)
11. In the following series,

$$^{90}Sr \xrightarrow[t_{1/2} = 28 \text{ yr}]{} {}^{90}Y \xrightarrow[t_{1/2} = 64 \text{ hr}]{} \text{products (stable)}$$

    what type of equilibrium do you expect? Calculate the amount of ^{90}Y remaining in equilibrium with 1 g of ^{90}Sr.
    Ans. Secular equilibrium, $^{90}Y = 2.6 \times 10^{-4}$ g.
12. On analysis of an uranium ore, it is found to contain 2.80 g ^{206}Pb and 16.7 g ^{238}U. The $t_{1/2}$ of ^{238}U is 4.5×10^{9} yr which is much higher (at least by a factor of 10^{4}) compared to that of any other member in the series. If all ^{206}Pb are supposed to be the decay product of ^{238}U, find the age of the ore.
    Ans. 1.13×10^{9} yr.
13. A piece of wood recovered in an excavation is found to have the activity 15% compared to that of a fresh sample. Find the dead time of the wood ($t_{1/2}$ of ^{14}C = 5578 yr).
    Ans. 15280 yr.
14. The ^{14}C to ^{12}C ratio in a piece of an old wood is 30% to that of the atmosphere. Calculate the age of the wood (given $t_{1/2}$ of ^{14}C = 5578 yr).
    Ans. 9696 yr.
15. Potassium content in sea water is given by 400 p.p.m. Natural potassium contains ^{40}K in the proportion of 120 p.p.m. Calculate the specific radioactivity of sea water. (Given, $t_{1/2}$ of ^{40}K = 1.2×10^{9} yr).
    Ans. 3.56×10^{-13} curie/g of sea water (assuring density of sea water as 1 g cm^{-3}).

Click Here t.me/thealchemylibrary

7

Nuclear Reactions

7.1 ARTIFICIAL TRANSMUTATIONS AND NUCLEAR REACTIONS

Artificial transmutation means conversion of an element into another element by some artificial means. Generally, by using some specific projectiles to bombard on some target nuclei, new nuclei are synthesised. In developing this branch of nuclear science, the following events carried out by different scientists are most noteworthy.

(a) **Rutherford's Experiment and Discovery of the Proton :** In 1919, it was observed by Rutherford that on passing of high speed α-particles from a radioactive source through nitrogen gas in a tube, it produces scintillations on a fluorescent screen kept at the end of the tube. When thick materials sufficient to stop the α-particles were placed between the screen and nitrogen gas, the scintillations were still existent. It vividly indicated that during the interaction between the α-particles and nitrogen gas, some long range fast moving particles capable of passing through the thick material were generated. From the behaviour of deflection of the newly generated radiation, it was confirmed that the particles in the radiation were hydrogen nuclei, i.e. protons. The observation was explained as:

$$^{14}_{7}N + ^{4}_{2}He \rightarrow ^{17}_{8}O + ^{1}_{1}H.$$

Thus in the reaction, nitrogen has been converted into oxygen. **This was the first evidence of nuclear transmutation, and it realised the dream of alchemists.**

This experimental observation was extended by Chadwick (1931), a student of Rutherford. It was found that with the exception of oxygen and carbon, all the elements from boron to potassium being bombarded by the fast α-particles produce proton.

$$^{10}_{5}B + ^{4}_{2}He \rightarrow ^{13}_{6}C + ^{1}_{1}H;\ ^{19}_{9}F + ^{4}_{2}He \rightarrow ^{22}_{10}Ne + ^{1}_{1}H;$$

$$^{32}_{16}S + ^{4}_{2}He \rightarrow ^{35}_{17}Cl + ^{1}_{1}H;\ ^{39}_{19}K + ^{4}_{2}He \rightarrow ^{42}_{20}Ca + ^{1}_{1}H$$

Click Here! me/bealchemylibrary

Limitations of α-particles as projectiles : The α-particles from a radioactive source spread away in all directions equally and as a result, the beam cannot be properly projected to the target nuclei. This significantly reduces the efficiency of the transmutation reactions. Besides this, the α-particles being positively charged face a ***Coulombic potential barrier*** in approaching the target nucleus. Under such circumstances, only the particles of very much high energy could do the task efficiently. To meet the purpose, particle accelerators have been developed (see Sec. 7.9).

(b) **Cockroft and Walton's Experiments :** In their experiment (1931), the high energy protons were produced in a hydrogen discharge tube having a very high potential difference and these were found better projectiles in preforming the artificial transmutation reactions. The accelerated beam was allowed to impinge on a thin foil of lithium oxide giving rise to the generation of alpha -particles. The reaction can be represented as :

$$_{1}^{1}H + {}_{3}^{7}Li \rightarrow 2\,{}_{2}^{4}He$$

(c) **Chadwick's Discovery of the Neutron :** In 1932, by bombarding beryllium with the α-particles, a new subatomic particle called neutron was discovered in the reaction :

$$_{4}^{9}Be + {}_{2}^{4}He \rightarrow {}_{6}^{12}C + {}_{0}^{1}n$$

The historical back-ground of this discovery has been highlighted in Sec. 1.3.1.

(d) **Curies' discovery (1934) of artificial radioactivity :** The following reaction has been already discussed (see Sec. 6.16.).

$$_{13}^{27}Al + {}_{2}^{4}He \rightarrow {}_{14}^{30}Si + {}_{1}^{1}H$$

$$_{13}^{27}Al + {}_{2}^{4}He \rightarrow {}_{15}^{30}P + {}_{0}^{1}n$$

$$_{15}^{30}P \xrightarrow{t_{1/2} = 3.2\ \text{min}} {}_{14}^{30}Si + {}_{+1}^{0}e + {}_{0}^{0}\nu$$

7.2 BETHE'S NOTATION OF NUCLEAR REACTIONS

Generally, a transmutation nuclear reaction is represented as follows :

$$_{Z_1}^{A_1}X + {}_{Z_2}^{A_2}P \rightarrow {}_{Z_3}^{A_3}Y + {}_{Z_4}^{A_4}E + Q$$

where the ***projectile*** $\left({}_{Z_2}^{A_2}P\right)$ bombards on the ***target nucleus*** $\left({}_{Z_1}^{A_1}X\right)$ to produce the product (new) nuclide $\left({}_{Z_3}^{A_3}Y\right)$ along with the particle $\left({}_{Z_4}^{A_4}E\right)$ to be *ejected*. The ejected particle is called ***ejectile***. In some cases, more than one particle may be ejected and in some cases, instead of particles only γ-photons are emitted. Q takes care of the energy change. Conservation of nuclear charge, i.e. $(Z_1 + Z_2) = (Z_3 + Z_4)$, is maintained. The Z-s are the characteristic properties for the particles and nuclides. Bethe made a shorter notation to represent the nuclear reaction as : ${}^{A_1}X(P, E)^{A_3}Y$, i.e. ***target nuclide (projectile, ejectile) product nuclide.***

Click Here t.me/thealchemylibrary

Examples :

$$^{10}_{5}B + ^{4}_{2}He \rightarrow ^{13}_{6}C + ^{1}_{1}H, \text{ i.e. } ^{10}B\,(\alpha, p)^{13}C;$$

$$^{12}_{6}C + ^{1}_{1}H \rightarrow ^{13}_{7}N + \gamma, \text{ i.e. } ^{12}C\,(p, \gamma)^{13}N;$$

$$^{63}_{29}Cu + ^{1}_{1}H \rightarrow ^{1}_{1}H + ^{1}_{0}n + 6\,^{4}_{2}He + ^{38}_{17}Cl \text{ i.e. } ^{63}Cu\,(p, p\,n\,6\alpha)^{38}Cl$$

7.3 NUCLEAR REACTIONS VERSUS CHEMICAL REACTIONS

The nuclear reactions differ from the chemical reactions in the following respects. We have already discussed the differences between **radioactive and chemical equilibrium** in Sec. 6.10.

(i) **Orbital electrons vs. nucleus :** Bond breaking and new bond formation are the basic steps of a chemical reaction*. *Thus, in a chemical reaction, the extra-nuclear electrons in different orbitals (mainly the outermost, i.e. valency, orbitals) are involved.* In such a process, no change in the nuclei of the reactant atoms occurs. Thus no new element or any isotope is produced here. *On the other hand, in a nuclear reaction, a nucleus suffers from a change giving rise to a new element or an isotope or a nuclear isomer.* Isotopes are produced in (n, γ) reactions. In **isomeric transitions (*IT*)**, the nuclear composition remains unchanged (i.e. no isotope or no new element is produced) but the energy state, i.e. nuclear configuration, changes. Thus, we can say that in a nuclear reaction, the composition and/or configuration of a nucleus are/is changed.

(ii) **Energy change :** In a chemical reaction, the energy change occurs due to the phenomena of bond breaking and bond formation while in a nuclear reaction, the energy change results from the conversion of lost mass into energy according to Einstein's $\Delta E = \Delta mc^2$ relation. This is why, the energy change in a nuclear reaction is about million times greater than that produced in a chemical reaction. For example, the energy produced in the radioactive decay of one gram of radium-226 is about 5×10^5 times larger than that involved in the conversion of one gram radium into radium chloride ($Ra + Cl_2 \rightarrow RaCl_2$).

(iii) **Conservation of mass :** In a chemical reaction, *conservation of mass* is maintained while it is apparently violated in a nuclear reaction. The lost mass actually is converted into energy. Thus, the consideration of ***mass-energy equivalence*** removes the apparent contradiction.

(iv) **Effect of chemical state :** The nuclear reaction is a purely nuclear phenomenon. Hence, it does not depend on the chemical state of the radioelement. Thus the radioactive property of radium-226 remains the same in its different chemical states such as elemental state and its different compounds like $RaCl_2$, $RaSO_4$, etc. On the other hand, a chemical reaction is highly dependent on the chemical state of a particular reactant. Thus Ra, $RaCl_2$ and $RaSO_4$ differ in their chemical properties.

(v) **Isotope effect :** Ignoring the thermodynamic and kinetic isotope effect, all the isotopes of a particular element behave identically in a chemical reaction because of their identical electronic configurations. On the other hand, the isotopes of a particular element may differ in their radioactive properties. For example, $^{12}_{6}C$ and $^{14}_{6}C$ show identical chemical properties but their

* There are some chemical reactions in which twisting, rotation or inversion (without any bond rupture) may lead to the configurational changes.

Click Here to Join Chemistry Library

radioactive properties are totally different. Though $^{12}_{6}C$ is very stable, $^{14}_{6}C$ disintegrates spontaneously into $^{14}_{7}N$ through the emission of a β^- particle, i.e.

$$^{14}_{6}C \rightarrow {}^{14}_{7}N + {}^{0}_{-1}e + {}^{0}_{0}\bar{\nu}.$$

(vi) **Effect of external factors :** The chemical reactions can be controlled by the external conditions such as temperature, pressure, catalyst, etc. but the nuclear reactions are not dependent on these external factors.

(vii) **Chemical equilibrium vs. radioactive equilibrium :** This aspect has been discussed in detail in Sec. 6.10.

7.4 CLASSIFICATION OF NUCLEAR REACTIONS

Based on the nature of the projectile and ejectile, the nuclear reactions can be classified as follows :

1. **Elastic Scattering,** e.g. $^{12}C\ (n, n)\ ^{12}C$.
2. **Inelastic Scattering,** e.g. $^{107}Ag\ (n, n)\ ^{107m}$Ag.
3. **Particle Projectile Capture,** e.g. $^{23}Na\ (n, \gamma)\ ^{24}Na$.
4. **Particle Projectile Capture and Particle Ejectile Emission Reactions,** (i.e. **Particle-Particle Reactions**).
5. **Photonuclear Reactions,** e.g. $^{2}H\ (\gamma, n)^1H$.
6. **Heavy ion Projectile Induced Reactions :** (i) Nucleon Transfer, (ii) Particle Ejectile
7. **Special Nuclear Reactions :** (i) Evaporation, e.g. $^{133}Cs\ (\alpha, 4n)\ ^{133}La$, (ii) Spallation, e.g. $^{63}Cu\ (\alpha, 14p\ 16n)\ ^{37}Cl$, (iii) Fission, (iv) Fusion, (v) Fragmentation, (vi) Stripping, e.g. $^{63}Cu\ (d, p)\ ^{64}Cu$.

1. Elastic Scattering Reactions

In this process, both the ejectile and projectile particles are the same and ***conservation of kinetic energy is maintained,*** i.e.

kinetic energy of the projectile (E_p) = gain of kinetic energy of the target nuclide (E_t) + kinetic energy of the ejectile (E_e)

If M and m are the masses of the target nuclide and projectile respectively, then the energy terms are related as follows,

$$E_t = \frac{4mM \sin^2 (\theta/2)}{(m+M)^2} E_p$$

where θ is the angle of scattering of the projectile by the target nuclide. Examples : $^{9}Be\ (n, n)\ ^{9}Be$, $^{12}C\ (n, n)\ ^{12}C$, etc.

2. Inelastic Scattering Reactions

In this process, the projectile and ejectile particles are the same but **the kinetic energy is not conserved.** A portion of the kinetic energy of the projectile is utilised to excite the target nuclide. Very often the excited nuclide deexcites either through instantaneous γ-radiation or isomeric transition (*IT*). Examples:

Click Here t.me/theachemylibrary

$$^{238}U\,(n, n)\,^{238}U^{*} \longrightarrow {}^{238}U + \gamma;$$
$$^{107}Ag\,(n, n)\,^{107m}Ag \xrightarrow{IT} {}^{107}Ag$$

3. Particle Projectile Capture (i.e. Radiative Capture) Reactions

In this process, the particle projectile is captured by the target nuclide followed by the emission of one or more γ-photons. The (n, γ) reactions tending to the synthesis (see Table 6.17.1) of different radioisotopes are well documented in this category. Many radioisotopes are prepared in this way. Examples :

(n, γ) reactions : $^{1}H\,(n, \gamma)^{2}H$; $^{23}Na\,(n, \gamma)\,^{24}Na$; $^{31}P\,(n, \gamma)\,^{32}P$.

(p, γ) reactions : $^{19}F\,(p, \gamma)\,^{20}Ne$; $^{27}Al\,(p, \gamma)\,^{28}Si$

4. Particle-Particle Reactions

Here, both the ejectile and projectile are particle in nature. Different particles can be used as projectiles. Except the neutron, all the other particles (e.g. *p*, *d*, α, etc.) being positively charged experience a **Coulombic potential barrier** and such particles are required to be accelerated by some devices. This category of reaction leads to a large number of reactions which can be subclassified as indicated in Table 7.4.1.

5. Photonuclear Reactions

In this process, γ-photons act as projectiles and the ejectile may be of different types of particles. Examples:

$$^{2}H\,(\gamma, n)\,^{1}H;\ ^{31}P\,(\gamma, n)\,^{30}P;\ ^{25}Mg\,(\gamma, p)\,^{24}Na;\ \text{etc.}$$

6. Heavy Ion Projectile Induced Reactions

By using the accelerators, heavy ions (heavier than the α-particles) can also be utilised as projectiles. Nuclei of *Li*, *C*, *N* or *O* have been utilised as projectiles. This class of reactions is of two types. **Most of the heavy ions exist in +6 state.**

(i) ***Nucleon transfer reactions*** : $^{14}_{7}N + {}^{10}_{5}B \rightarrow {}^{13}_{7}N + {}^{11}_{5}B,$

$$^{14}_{7}N + {}^{14}_{7}N \rightarrow \begin{cases} {}^{13}_{7}N + {}^{15}_{7}N \\ {}^{13}_{6}C + {}^{15}_{8}O; \end{cases} \qquad {}^{27}_{13}Al + {}^{14}_{7}N \rightarrow \begin{cases} {}^{25}_{13}Al + {}^{16}_{7}N \\ {}^{27}_{12}Mg + {}^{14}_{8}O \end{cases}$$

The mechanism of these reactions is comparable with that of the ***stripping reactions.***

(ii) ***Particle emission reactions*** : $^{51}_{23}V\left(^{16}_{8}O, 2n\right)^{65}_{31}Ga$; $^{93}_{41}Nb\left(^{12}_{6}C, 2n\right)^{103}_{47}Ag$.

This type of reactions is very much important in synthesising various transuranic elements.

7. Special Nuclear Reactions

Except the nuclear reactions induced by the highly energetic heavy ions, all other cases discussed above involve the change of *A* and/or *Z* of the target nuclide by a few units only. But there are some special types of reactions in which the target nuclide suffers a drastic change (compared to the other processes) in *A* and *Z*. These are discussed below :

Click Here to me/thealchemylibrary

Table 7.4.1. Common types of particle-particle nuclear reactions.

Projectile (Reaction)	*Example*	*Projectile (Reaction)*	*Example*
(i) **Alpha (α)**		(ii) **Triton (t)**	
(a) (α, p)	$^{14}N\,(\alpha, p)\,^{17}O$; $^{27}Al\,(\alpha, p)\,^{30}Si$	(a) (t, p)	$^{59}Co\,(t, p)\,^{61}Co$
	$^{10}B\,(\alpha, p)\,^{13}C$	(b) (t, d)	$^{6}Li\,(t, d)\,^{7}Li$
(b) (α, n)	$^{12}C\,(\alpha, n)\,^{15}O$; $^{9}Be\,(\alpha, n)\,^{12}C$	(c) (t, n)	$^{32}S\,(t, n)\,^{34}Cl$
	$^{7}Li\,(\alpha, n)\,^{10}B$		
(c) *(α, γ)	$^{7}Li\,(\alpha, \gamma)\,^{11}B$		
(iii) **Deuteron (d)**		(iv) **Proton (p)**	
(a) (d, α)	$^{6}Li\,(d, \alpha)\,^{4}He$; $^{16}O\,(d, \alpha)\,^{14}N$;	(a) (p, α)	$^{7}Li\,(p, \alpha)\,^{4}He$;
(b) (d, p)	$^{31}P\,(d, p)\,^{32}P$; $^{23}Na\,(d, p)\,^{24}Na$		$^{19}F\,(p, \alpha)\,^{16}O$;
(c) (d, n)	$^{12}C\,(d, n)\,^{13}N$; $^{6}Li\,(d, n)\,^{7}Be$;		$^{18}O\,(p, n)\,^{18}F$;
	$^{37}Cl\,(d, n)\,^{38}Ar$	(b) (p, n)	$^{23}Na\,(p, n)\,^{23}Mg$;
(d) (d, t)	$^{7}Li\,(d, t)\,^{6}Li$; $^{31}P\,(d, t)\,^{30}P$	(c) (p, d)	$^{9}Be\,(p, d)\,^{8}Be$;
			$^{7}Li\,(p, d)\,^{6}Li$
		*(d) (p, γ)	$^{27}Al\,(p, \gamma)\,^{28}Si$;
(v) **Neutron (n)**			$^{12}C\,(p, \gamma)\,^{13}N$
(a) (n, α)	$^{10}B\,(n, \alpha)\,^{7}Li$; $^{27}Al\,(n, \alpha)\,^{24}Na$		
(b) $(n, 2n)$	$^{12}C\,(n, 2n)\,^{11}C$; $^{238}U\,(n, 2n)\,^{237}U$	(vi) **Electron (e)**	
		(a) (e, ne)	$^{9}Be\,(e, ne)\,^{8}Be$
(c) (n, p)	$^{14}N\,(n, p)\,^{14}C$; $^{35}Cl\,(n, p)\,^{35}S$		
(d) (fission)	$^{235}U\,(n, xn)$ fission products		
*(e) (n, γ)	$^{27}Al\,(n, \gamma)\,^{28}Al$; $^{238}U\,(n, \gamma)\,^{239}U$		

* These are actually projectile-capture or radiative-capture reactions.

(i) ***Evaporation*** : In this process, a large number of nucleons generally neutrons are torn away in one lot. Example :

$$^{133}Cs\,(\alpha, 4n)\,^{133}La;\ ^{209}Bi\,(d, 12n)\,^{199}Po^{*}$$

Very often the excited product nuclide suffers a symmetric fission. As in the case of ^{209}Bi, the following fission is followed for ^{199}Po.

$$^{199}_{84}Po^{*} \xrightarrow[\text{fission}]{\text{symmetric}} {}^{99}_{42}Mo + {}^{100}_{42}Mo;\ {}^{99}_{42}Mo \xrightarrow{-2\beta^{-}} {}^{99}_{44}Ru$$

(ii) ***Spallation*** : It differs from the evaporation process in degree only. It is more violent than the evaporation process and as a result, the product nuclide differs largely by about 10-20 units from the target nuclide in both A and Z giving rise to the ejection of a large number (~ 10-20) of particles. Thus it differs from fission in which the target nuclide is split into two halves. Very often both the processes run parallel.

Click Here t.me/thearchemylibrary

It also differs from fission in other points as well. The threshold energy value of the projectile required for the spallation is ~ 110-170 MeV *which is much higher than that required for a direct fission.* Very often both the processes, i.e. spallation and direct nuclear fission, run simultaneously and complicate the analysis. For example.

$$\left.\begin{array}{l} {}^{63}_{29}Cu + {}^{1}_{1}H \rightarrow {}^{1}_{1}H + {}^{1}_{0}n + 6\,{}^{4}_{2}He + {}^{38}_{17}Cl \\ {}^{63}_{29}Cu + {}^{1}_{1}H \rightarrow {}^{1}_{1}H + 3\,{}^{1}_{0}n + 9\,{}^{4}_{2}He + {}^{24}_{11}Na \end{array}\right\} \textbf{spallation}$$

$$\left.\begin{array}{l} {}^{63}_{29}Cu + {}^{1}_{1}H \rightarrow {}^{64}_{30}Zn^{*} \rightarrow {}^{38}_{17}Cl + {}^{25}_{13}Al + {}^{1}_{0}n \\ {}^{63}_{29}Cu + {}^{1}_{1}H \rightarrow {}^{64}_{30}Zn^{*} \rightarrow {}^{24}_{11}Na + {}^{39}_{19}K + {}^{1}_{0}n \end{array}\right\} \textbf{fission}$$

This type of reaction (i.e. spallation reaction) induced by the very high energy projectiles was first observed by Seaborg and co-workers in 1947. The process is believed to proceed through direct knocking out of the nucleons by the striking projectile. The mechanism of the process has been discussed in Sec. 7.8.3. Examples :

$${}^{63}_{29}Cu + {}^{4}_{2}He\ (\sim 400\ \text{MeV}) \rightarrow {}^{37}_{17}Cl + 14\,{}^{1}_{1}H + 16\,{}^{1}_{0}n$$

$${}^{79}_{35}Br + {}^{1}_{1}H\ (\sim 200\ \text{MeV}) \rightarrow {}^{44}_{21}Sc + {}^{1}_{1}H + 7\,{}^{1}_{0}n + 7\,{}^{4}_{2}He$$

(iii) ***Fission*** **:** In this process, the target nuclide is torn into two comparable fragments. Example:

$${}^{235}_{92}U + {}^{1}_{0}n \rightarrow {}^{137}_{52}Te + {}^{97}_{40}Zr + 2\,{}^{1}_{0}n$$

Nuclear fissions can also be initiated by the high energy charged particles such as protons, deuterons, α-particles, etc. Similarly, the high energy γ-photons can also carry out the process. The reaction pathways along with the characteristic features of the fission process have been discussed in Sec. 7.12.

(iv) ***Fusion*** **:** At high temperature (~ $10^7 - 10^8$ K), the lighter nuclides may undergo combination or fusion to form the relatively heavier and stable nuclides. The reactions can only occur at a very high temperature and this is why these are very often referred to as **thermonuclear reactions.** Example:

$$4\,{}^{1}_{1}H \rightarrow {}^{4}_{2}He + 2\,{}^{0}_{+1}e;\quad 2\,{}^{2}_{1}H \rightarrow {}^{4}_{2}He$$

(v) ***Fragmentation*** **:** In this process, the target nuclide is torn into two unequal fragments, i.e. one half is heavier compared to the other half. It has got a similarity with the fission process.

(vi) ***Stripping*** **:** In this process, the projectile gets split in the joint field of the target nuclide and the projectile and then a fragment of the split projectile takes part in the nuclear reaction while the other fragment remains unchanged. For example, when a deuteron of relatively lower energy approaches the target nuclide, ^{63}Cu, **the projectile undergoes splitting to generate a neutron and a proton.** The neutron generated in this way participates in the reaction. **The neutron being**

Click Here t.me/thealchemylibrary

electrically neutral does not experience any Coulombic barrier to penetrate the target nuclide (cf. **Oppenheimer-Phillips mechanism,** Sec. 7.8.2).

$$^{63}_{29}Cu + d\ (\equiv n + p) \rightarrow {}^{64}_{29}Cu + p$$

The *nucleon transfer reactions* induced by the heavy ions as projectiles are also representative examples of this category.

7.5 CONSERVATION LAWS IN NUCLEAR REACTIONS

In a nuclear reaction, the following conservation laws are maintained.

7.5.1 Conservation of Energy

In a nuclear reaction, the total energy, i.e. the sum of the rest mass energies and kinetic energies of the reactants (i.e. target nuclide and projectile), must be conserved. In the reaction,

$$X + \text{projectile} \rightarrow Y + \text{ejectile},$$

we have:

$$(M_X + M_p)c^2 + E_p = (M_Y + M_e)c^2 + E_Y + E_e$$

where, M_X = mass of the target nuclide (X); M_p = mass of the projectile particle; M_Y = mass of the product nuclide (Y); M_e = mass of the ejectile particle; c = speed of light; E_p, E_Y and E_e = kinetic energies of the projectile, product nuclide and ejectile respectively.

Here, the target nuclide has been assumed to remain at rest. In terms of MeV (when the masses are expressed in amu), the above relation can be expressed as follows :

$$(M_X + M_p)931 + E_p = (M_Y + M_e)931 + E_Y + E_e;$$

or,
$$\boxed{[(M_X + M_p) - (M_Y + M_e)]931 = E_Y + E_e - E_p = Q;}$$

or, $\Delta m \times 931 = Q$ where, Δm is called the *mass loss* in the reaction. For the positive values of Δm, Q *becomes positive and the reaction is exoergic while for the negative values of* Q (i.e. *mass is to be created*), *it is endoergic*.

7.5.2 Conservation of Linear Momentum

The total linear momenta (p) in the reaction must be conserved. It follows that the trajectories of the incident projectile, ejectile and product nuclide (Y) must be coplanar (see Fig. 7.5.2.1).

Thus,

$$p_p = p_e \cos\theta + p_Y \cos\phi, \text{ (along the direction of the incident projectile)}$$

and, $\quad 0 = p_e \sin\theta - p_Y \sin\phi$, (along the perpendicular to the direction of the projectile).

In this regard, consideration of the formation of a compound nucleus in the nuclear reaction yields some important information. The mass of the compound nucleus is given by the sum of the masses of the projectile and target. Here, again from the principle of conservation of momentum, we have :

initial momentum of the projectile = momentum acquired by the compound nucleus;

Click Here t.me/healchemylibrary

i.e. $M_p u = (M_X + M_p)V$,

where u and V are the velocities of the incident projectile and the compound nucleus formed respectively. Thus we get the kinetic energy (E_C) of the compound nucleus as follows:

$$V = M_p u/(M_X + M_p);$$

or, $$E_C = (1/2)(M_X + M_p)V^2$$

$$= M_p E_p/(M_X + M_p),$$

where, $$E_p = (1/2)M_p u^2$$

Here, E_C and E_p denote the kinetic energies of the compound nucleus formed and the incident projectile respectively.

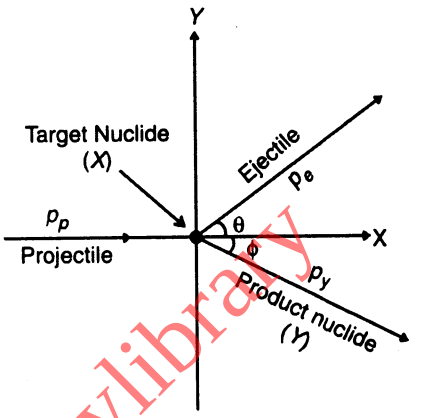

Fig. 7.5.2.1. Conservation of linear momentum in a nuclear reaction.

The energy measured by E_C is utilised in imparting the translational energy to the compound nucleus. Hence, the residual energy of the projectile given by ($E_p - E_C$) is available for carrying out the nuclear reaction. Thus we have :

the net available energy to effect the nuclear reaction $= E_p - E_C$

or,
$$\boxed{E_p - E_C = \frac{M_X}{(M_p + M_X)} E_p = \frac{1}{2}\mu u^2}$$

where μ is called the reduced mass of the system, i.e. $\mu = \dfrac{M_p M_X}{M_p + M_X}$

This portion of energy [$= M_X E_p/(M_p + M_X)$] ***available for carrying out the nuclear reaction is described as the kinetic energy of the projectile and target nuclide on the centre of mass system*** (*CMS*)*. Thus it is evident that total energy (E_p) of the projectile is not available for carrying out the nuclear reaction. The fraction, $M_X/(M_p + M_X)$ of E_p is only available to effect the nuclear reaction.

7.5.3 Conservation of Angular Momentum

The total angular momentum (i.e. a vectorial sum of the orbital angular momentum and spinning momentum) is conserved.

7.5.4 Conservation of Neutrons and Protons

Except the $\beta^{+/-}$ decay and electron capture processes, in all other nuclear reactions, the number of protons (i.e. nuclear charge) and neutrons are separately conserved.

Thus, $$\sum Z_{\text{reactants}} = \sum Z_{\text{products}}, \text{ and, } \sum N_{\text{reactants}} = \sum N_{\text{products}}$$

Therefore, $$\sum A_{\text{reactants}} = \sum A_{\text{products}}$$

For the $\beta^{+/-}$ decay and electron capture (*EC*) processes, the number of protons and neutrons are not conserved separately, but their summation, i.e. mass number (A), is conserved.

* In the **compound nucleus theory**, the excitation energy to effect the nuclear reaction is also obtained from the binding energy of the projectile particles in the compound nucleus (see Sec. 7.8. 1).

Click Here to meet the chemylibrary

7.6 THRESHOLD ENERGY OF A PROJECTILE FOR A NUCLEAR REACTION

For the exoergic process, the concept of threshold value of energy of a projectile is of no much importance, but for the endoergic process, it is very much important. This ***threshold value*** can be compared with the ***activation energy*** of a chemical reaction. Thus for both the endoergic and exoergic processes, the reactants must pass over the activation energy barrier.

We have already seen that the whole energy (E_p) of the incident projectile is not available for effecting a nuclear reaction, but a fraction given by $M_X/(M_p + M_X)$ is only available for carrying out a nuclear reaction. **For the *endoergic process*** (i.e. Q is negative) where mass is to be created, it must satisfy the following condition.

$$\boxed{M_X E_p/(M_X + M_p) \geq Q; \text{ or, } E_p \geq (1 + M_p/M_X)Q}$$

This minimum value of $E_p = (1 + M_p/M_X)Q$ for a particular reaction is called the ***threshold energy value of the projectile to effect the endoergic nuclear reaction.***

7.7 NUCLEAR REACTION CROSS-SECTION

The nuclear reaction cross-section (σ_i) gives a measure of the effective area around a target nucleus available for a projectile in a particular type (let it be i) of nuclear reaction. This concept has been already introduced in explaining the α-particle scattering phenomenon in Rutherford's experiment. This cross-section varies for different types of nuclear reactions.

Let us take a slab of a target material having area A and thickness t (very small). If there are n nuclei per unit volume, then the number of nuclei in the sample is given by ntA. Considering the reaction cross-section of a target nuclide in a particular type of reaction to be σ_i, we get the probability (p) of an incident projectile to interact with the target nuclide as follows.

$$p = \frac{\text{Aggregate cross-section of the nuclei}}{\text{Total geometric area of the slab}} = \frac{nAt\sigma_i}{A} = n\sigma_i t$$

The probability (p) can also be defined in another way :

$$p = \frac{\text{Number of interacting projectile particle}}{\text{Total number of incident projectiles on the target slab}} = \frac{N}{N_0}$$

By combining the above two relations, we get, $\sigma_i = N/(N_0 nt)$

There is another convenient way to define the nuclear reaction cross-section (σ_i) in terms of ***projectile flux density*** (ϕ_p expressing the number of projectiles striking the target per cm^2 per sec). Let us consider a thin target sheet to contain N_t nuclei per unit area and it to face a beam of projectiles passing perpendicularly to the target. If the projectile beam passes with the velocity u_p cm s^{-1} and the density of the projectile particles is n_p particles per cm^3, then the ***projectile flux density*** is given by: $\phi_p = u_p n_p$ projectiles cm^{-2} s^{-1}. Then the collision rate (i.e. number of collisions per cm^2 per sec) measuring the reaction rate is given by :

reaction rate = collision rate

Click Here t.me/thealchemylibrary

$$\text{reaction rate} \propto n_p u_p N_t$$

and

$$\text{reaction rate} = \sigma_i n_p u_p N_t = \sigma_i \phi_p N_t$$

or,

$$\sigma_i = \frac{\text{collisions cm}^{-2}\ \text{s}^{-1}}{\phi_p\ \text{projectiles cm}^{-2}\ \text{s}^{-1} \times N_t\ \text{target nuclei cm}^{-2}}$$

The nuclear cross-section (σ_i) is expressed in the units of **barn** (b) where, $1\text{b} = 10^{-28}\ \text{m}^2 = 10^{-24}\ \text{cm}^2 = 10^2\ \text{fm}^2$.

The nuclear reaction cross-section, σ_i for the target nuclide depends not only on the type of the reaction but also on the energy of the projectile particle. In the compound nucleus theory, it is believed that above the ground state, there are several higher energy states in the compound nucleus. If the energy of an incident projectile can just excite the compound nucleus to one of its excited level, then the projectile of that energy is very much effective in carrying out the nuclear reaction. This phenomenon is referred to as ***resonance capture.*** Because of the availability of more than one energy level, there are more than one energy value at which the resonance capture may occur in a particular reaction. For example, in the reaction on ^{238}U target by the neutron projectile, the resonance capture takes place for the energy values: 6, 20 and 38 eV of the incident neutron. **At the point of resonance capture or absorption, the reaction cross-section gets maximised compared to the neighbouring energy values.**

7.8 MECHANISMS OF NUCLEAR REACTIONS

No single mechanism can cover up all the nuclear reactions known to us. Different mechanistic pathways are established in different types of reactions. Out of these, *the compound nucleus theory, Oppenheimer-Phillips stripping reaction mechanism, direct nuclear reaction mechanism* are well known.

7.8.1 The Compound Nucleus Theory

Based on the basic postulates of the liquid drop model of the nucleus, Bohr (1916) proposed this theory in explaining this nuclear reaction pathways.

In this theory, it is proposed that a nuclear reaction occurs at ***two separate and independent stages.*** In the first stage, the projectile particle on striking the target nuclide fuses with the target one to form a new nucleus called ***compound nucleus*** (C^*) which remains in an excited state. In the second stage (which is independent of the first stage), the excited compound nucleus (C^*) undergoes deexcitation through the ejection of some nucleons or by γ-radiation or by both depending on the excitation energy of the compound nucleus. Thus, the whole process can be represented as follows:

Ist step : Compound nucleus formation

$$\underset{\text{(target nuclide)}}{{}^{A_1}_{Z_1}X} + \underset{\text{(projectile)}}{{}^{A_2}_{Z_2}P} \longrightarrow \underset{\text{(excited compound nucleus)}}{{}^{A_1+A_2}_{Z_1+Z_2}C^*}$$

2nd step : Deexcitation of the compound nucleus

$${}^{A_1+A_2}_{Z_1+Z_2}C^* \xrightarrow{\text{deexcitation}} \text{products (depending on the state of the excitation in } C^*)$$

Click Here to the/healChemyLibrary

(A) Characteristic Features of the Compound Nucleus (C*)

(i) ***Different routes leading to a particular compound nucleus*** : The same compound nucleus may be formed in a number of ways, but the nature of the reaction products does not depend on the route of generation of the compound nucleus. *It depends only on the state of excitation of the compound nucleus formed.* For example, the excited compound nucleus $^{28}_{13}Al^*$ may be formed in a number of ways, e.g.

$$^{24}_{11}Na + ^{4}_{2}He;\ ^{27}_{13}Al + ^{1}_{0}n;\ ^{27}_{12}Mg + ^{1}_{1}H;\ ^{26}_{12}Mg + ^{2}_{1}H, \textit{etc.}$$

(ii) ***Sources of excitation energy*** (E_{ex}) : The excitation energy (E_{ex}) in the compound nucleus is obtained from two sources, i.e. binding energy of the projectile neucleons and kinetic energy of the projectile in the centre of mass system (CMS) (see Sec. 7.5.2).

Thus, *excitation energy* (E_{ex}) in the compound nucleus is given by :

$$E_{ex} = \textbf{binding energies}^{1} \textbf{ of the projectile nucleons in the compound nucleus} + M_X E_P/(M_X + M_p) \textbf{ (i.e. kinetic energy of the projectile on } \textit{CMS}\textbf{).}$$

(iii) ***Random distribution of E_{ex} among the nucleons*** : The excitation energy is distributed randomly among the nucleons of the compound nucleus within the time period of 10^{-17} to 10^{-21} s called *natural nuclear time*.

(iv) ***Deexcitation*** : In the second step, the excited compound nucleus undergoes deexcitation in a relatively slower process in the time period of the order of 10^{-14} to 10^{-15} s. **Thus, the compound nucleus is relatively long lived.** This second step is an independent one. Consequently, the decay products may come out isotropically without showing any dependence on the direction of the approach of the incident projectile.

(v) ***Reaction product depending on the E_{ex}*** : The excitation energy is ***randomly not uniformly*** distributed among the nucleons. The nucleons sharing this excitation energy can escape away from the nucleus, ***if the shared energy per nucleon can satisfy the condition*** :

$$\textit{shared energy per nucleon} \geq 8 \text{ MeV} + \textit{Coulomb barrier energy.}$$

The ~ 8 MeV value denotes the separation energy between the *Fermi level* and the brink of the nuclear potential well without the Coulomb potential. *The Coulomb barrier exists only for the charged particles* (cf. Figs. 5.4.3.1, 5.5.1.1 and 5.5.1.2).

However, if the excitation energy shared (randomly) by the nucleons is not sufficient for expulsion of any nucleon then the deexcitation goes on through γ-emission.

(B) Verification of the Compound Nucleus Theory

In this theory, the two steps, i.e. formation of the compound nucleus and decay of the compound nucleus, are independent because of the relatively long life period of the compound nucleus. As a matter of fact, due to an appreciable time lag between the steps, the compound nucleus forgets its precursors or parentage. ***The second step is only dependent on the magnitude of the excitation energy.***

(a) **Reaction products independent of the route of compound nucleus formation :** In verification of the theory, the experiment carried out by the Indian physicist, **S.N. Ghosal** (1950) is noteworthy. In this experiment, the compound nucleus $^{64}_{30}Zn^*$ was generated in two routes, i.e. $^{60}_{28}Ni + ^{4}_{2}He$ and $^{63}_{29}Cu + ^{1}_{1}H$. *By adjusting the kinetic energy of the projectile on CMS, the*

[1] Given by 931 Δm MeV where Δm gives the loss of mass (in amu) in the formation of the compound nucleus.

Click Here : me/chemlibrary

excitation energy was made the same in both cases. ***The reaction products were found identical in the two cases.***

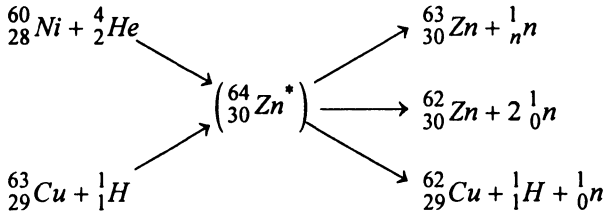

(b) **Reaction products depending on the state of excitation of the compound nucleus :** When $^{65}_{30}Zn^{*}$ is generated by a slow neutron, it passes through the reaction $^{64}Zn\,(n, \gamma)\,^{65}Zn$ while for the fast neutrons, particle emission occurs. ***Thus, depending on the excitation energy in the compound nucleus, the different decay products are formed.***

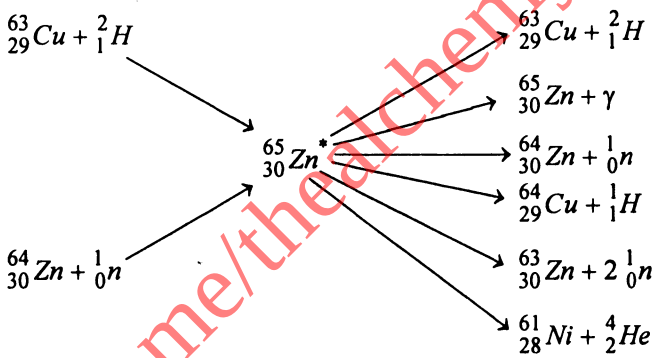

(c) **Reaction products depending on the state of excitation of the compound nucleus :** Similarly, for $^{28}_{23}Al^{*}$, the ***decay products depend on the extent of excitation.*** The different routes of formation of the compound nucleus along with the different modes of decay are shown below. The action of a slow neutron produces a low degree of excitation leading predominantly to γ-emission (i.e. *radiative capture reaction*). But the use of a high speed deuteron, or a fast neutron leads to the emission of one or more particles.

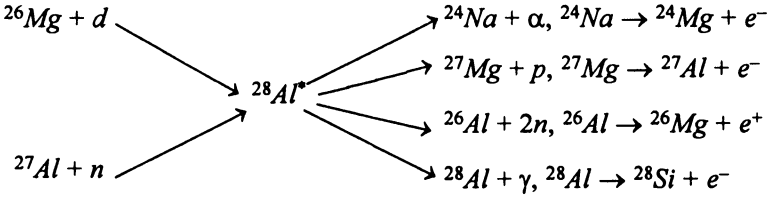

Here it is noteworthy that ^{24}Na (β^{-}-active), ^{27}Mg (β^{-}-active), ^{26}Al (β^{+}-active) and ^{28}Al (β^{-}-active) are radioisotopes.

(C) Limitations of the Compound Nucleus Theory

The theory works well for most of the reactions, but in stripping reactions, e.g. (d, p), (d, n), (t, p), etc., in ***buckshot type capture reactions*** initiated by the heavy ions, in high energy fragmentation reactions, in the reactions carried out by the ultra-high energy projectiles, the basic idea of the compound nucleus theory does not hold good.

Click Here t.me/thealchemylibrary

7.8.2 Oppenheimer-Phillips Mechanism in Stripping Reactions

In explaining the effectiveness of deuterons of relatively low energy as projectiles in the nuclear reactions, specially of the (*d*, *p*) type, the compound nucleus theory was proved to be inadequate. The deuterons being positively charged are expected to experience the Coulomb potential barrier in penetrating the target nucleus to form a compound nucleus. If it were so, the deuteron projectiles would be required to have significantly higher energy in carrying out the nuclear reactions. **But, in fact, the low energy (not sufficient to overcome the Coulomb potential barrier) deuterons are very much effective in performing the (*d*, *p*) reactions.**

To explain this surprising observation, Oppenheimer and Phillips proposed (hence, called the **Oppenheimer-Phillips mechanism** to honour the scientists) that the deuterons having a very low nuclear binding energy of *ca.* 1 MeV per nucleon (cf. $\overline{B}$ = 7-8 MeV for most of the other nuclei) undergo splitting in the joint Coulombic field of the target nuclide and the projectile to produce the constituents, i.e. ${}^{1}_{1}H$ and ${}^{1}_{0}n$. Thus, the released neutron being electrically neutral can enter easily (see Sec. 5.4.3) into the nuclear potential well of the target nuclide, and the proton generated outside the target nuclide is left out. **Thus, in all stripping reactions, the projectile particles undergo splitting outside the target nuclide in the joint Coulombic field.** Similar happenings may also occur in (*d*, *n*) reactions where the proton experiences a barrier but less than that by an unsplit deuteron. Examples:

(i) ${}^{31}_{15}P + {}^{2}_{1}H \rightarrow {}^{32}_{15}P + {}^{1}_{1}H$, i.e. (*d*, *p*);

(ii) ${}^{2}_{1}H + {}^{2}_{1}H \rightarrow {}^{3}_{1}H + {}^{1}_{1}H$, i.e. (*d*, *p*);

(iii) ${}^{81}_{35}Br + {}^{2}_{1}H \rightarrow {}^{82}_{35}Br + {}^{1}_{1}H$, i.e. (*d*, *p*);

(iv) ${}^{12}_{6}C + {}^{2}_{1}H \rightarrow {}^{13}_{7}N + {}^{1}_{0}n$, i.e. (*d*, *n*);

(v) ${}^{209}_{83}Bi + {}^{2}_{1}H \rightarrow {}^{210}_{84}Po + {}^{1}_{0}n$, i.e. (*d*, *n*);

The second reaction is of historical importance. ***It led to the discovery of tritium by Rutherford and co-workers* in 1934.**

The Oppenheimer-Phillips mechanism also operates in some ***triton induced reactions.*** Examples:

(i) ${}^{59}_{27}Co + {}^{3}_{1}H \rightarrow {}^{61}_{27}Co + {}^{1}_{1}H$ i.e. (*t*, *p*);

(ii) ${}^{6}_{3}Li + {}^{3}_{1}H \rightarrow {}^{7}_{3}Li + {}^{2}_{1}H$ i.e. (*t*, *d*);

(iii) ${}^{63}_{29}Cu + {}^{3}_{1}H \rightarrow {}^{64}_{29}Cu + {}^{2}_{1}H$ i.e. (*t*, *d*);

In the nucleon transfer reactions induced by the accelerated heavy ions, **it is believed that the heavy ion projectile undergoes splitting into its constituents in the joint Coulombic field,** and some of these constituents are captured by the target nucleus. ***This type of reaction is referred to as buckshot type capture reaction.*** Example :

The projectile, ${}^{14}N^{6+}$ on bombarding the target nuclide ${}^{27}Al$ is believed to split as follows :

$${}^{14}_{7}N^{6+} \xrightarrow[\text{Coulombic field}]{\text{Joint}} {}^{1}_{0}n + {}^{1}_{1}H + 3\,{}^{4}_{2}He$$

The split particles can carry out the transmutation reactions on ${}^{27}Al$ in different ways depending on the energy.

Click Here t.me/theachemylibrary

7.8.3 Direct Nuclear Reaction Mechanism

In the case of ultra-high energy projectiles, the projectiles can overcome all the barriers and can directly penetrate into the target nuclide. During the passage of the projectile through the target nuclide, it collides with the nucleons on its path. On the path of the penetrating projectile, some nucleons get sufficiently excited to get expelled from the nuclear potential well; some nucleons may be excited (excitation not sufficient for expulsion) and gradually they come to the ground state. After the expulsion of some nucleons, some vacancies are created. These lead to the *evaporation of some nucleons*. In this regard, it is worth mentioning that the expulsion of the nucleons during the collision with the penetrating projectile is ***not isotropic*** (cf. ***compound nucleus theory where it is isotropic***). Most of the nucleons ejected are in the direction of the incident projectile because the nucleons that lie on the path of the penetrating projectile are mainly excited. Depending upon the degree of expulsion and evaporation, the product nuclides can cover a long range of mass in a particular reaction. Example :

Spallation of ^{63}Cu by a high energy proton occurs as follows.

$$^{63}_{29}Cu \xrightarrow{+\ p\ \text{(very high energy)}} \text{Nuclides covering the mass range} \sim 60\text{-}20 + \text{ejectile particles to balance the charge and nucleons.}$$

7.9 CHARGED PARTICLE ACCELERATORS

To carry out the transmutations by using the charged particles as projectiles, some problems are faced. Due to the existence of the Coulombic potential barrier (see Sec. 5.4.3), the charged particles should have sufficient energy to cross the barrier (*classical concept*). The α-particles available from the naturally occurring sources may have maximum energy 9-10 MeV. By using such particles, a lot of information regarding the construction and structure of the nucleus were explored. **But, for the bombardment on the relatively heavier target nuclides, charged projectile particles of much higher energy are required.** Besides these, the α-particles obtained from any naturally occurring source have got no directional properties (i.e. isotropic distribution). **Using such isotropic radiations (which are equally probable in all directions) to the target placed in a particular direction, it yields very poor results.** To overcome these drawbacks, the scientists were experiencing the necessity of having the directed beams of high energy particles. The particle accelerators developed can meet this necessity.

The first device was developed in 1931 by Cockroft Walton by using a *voltage multiplier* to accelerate the protons. The voltage multiplier ultimately produced a potential difference of about 2 million volts leading to the generation of a 1-2 MeV proton beam. In 1931, Van de Graaff developed an electrostatic generator which could produce several million volts of potential difference to accelerate the particles.

Presently, *the accelerators which do not require any high potential difference are of much importance.* Some devices in this regard will be discussed here.

7.9.1 The Linear Accelerator

Apparatus : A series of co-axial hollow cylinders *A, B, C, D,...* increasing in length towards the target serves as the electrode system (see Fig. 7.9.1.1). The charged particle beam is allowed to pass through the cylinders to bombard the target. The electrode system and the target are kept in a vacuum chamber so that the accelerated particles may travel in a straight line without the possibility of collisions with the molecules in air. A high frequency of high voltage supply is applied to the electrode system in such a

Click Here : me/chealchemylibrary

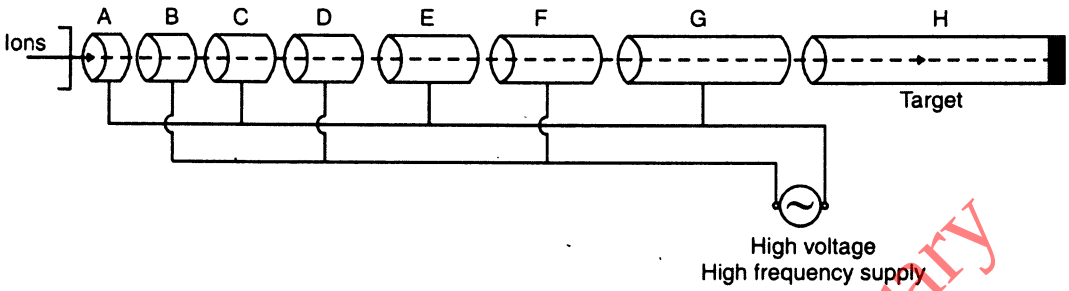

Fig. 7.9.1.1. Schematic design of a linear accelerator.

way that the alternate cylinders are connected to one terminal and other alternate cylinders are connected to another terminal. **If a positively charged particle reaches the gap between *A* and *B*, then it will get accelerated to the forward direction provided at that time the facing cylinder *B* is negative with respect to *A*.** Thus, the positively charged particle will be accelerated through the cylinders, if after reaching the gap it experiences a negative potential from the nearest facing cylinder and a positive potential from the cylinder from which it emerges. For this purpose, the length of the successive cylinders should be adjusted with respect to the frequency of the supply voltage. ***The required condition is that the time required by the particle to travel the length of a particular cylinder should be equal to the half of the time period of oscillation.***

Working principle : When the particle moves within a cylinder, it runs with a uniform velocity as it lies in a field free region. If a positively charged particle having a charge q travels with a velocity u_n in the n-th cylinder under the potential difference V (which is the peak voltage of the supply) then the particle acquires energy, $E = nqV$. In the preceding n gaps (including the gap facing the first cylinder) it has got n accelerations, each leading to an energy increase, qV. Thus,

$$E = nqV \qquad \text{...(7.9.1.1)}$$

and

$$E = (1/2)\,mu_n^2 = nqV \qquad \text{...(7.9.1.2)}$$

(m = mass of the particle)

Actually, nqV gives the measure of total energy acquired by traversing the distance l_n with the velocity u_n.

If l_n is the length of the n-th tube, then the time taken by the particle to travel the l_n distance is given by : $t = l_n/u_n$.

According to this condition :

t = half of the time period of oscillation = $\frac{1}{2}T = \frac{1}{2f}$, where f = frequency of the oscillator.

Therefore, we get :

$$l_n/u_n = \frac{1}{2f}; \text{ or, } l_n = \frac{u_n}{2f} = \frac{1}{2f}\frac{\sqrt{2nqV}}{\sqrt{m}}, \text{ (from Eqn. 7.9.1.2)}$$

or,

$$l_n = \frac{1}{f}\frac{\sqrt{qV}}{\sqrt{2m}}\sqrt{n} \qquad \text{... (7.9.1.3)}$$

Click Here t.me/thealchemylibrary

or, $l_n \propto \sqrt{n}$, (as all other terms involved for a particular system are constant).

Therefore, $l_1 : l_2 : l_3 : \ldots = \sqrt{1} : \sqrt{2} : \sqrt{3} :$

From the relationship, Eqn. 7.9.1.1, it is evident that the energy of the charged particle can be increased as desired by inserting the required number of cylinders. *But, in any way, the velocity of the accelerated particle cannot exceed that of light.* Specially for the lighter particles like electrons, they attain the velocity close to that of light after passing through several cylinders. At this saturation point, further acceleration will not increase the velocity but will increase the mass. This is evident from the following relation where m_o = rest mass of the particle, m = moving mass of the particle, c = velocity of light, u = velocity of the particle.

$$m = \frac{m_o}{\sqrt{(1 - u^2/c^2)}}$$

This is why, after saturation of the velocity, the cylinders are made of the same length.

7.9.2 The Cyclotron

It was developed by E.O. Lawrence, in the University of California, in 1933 and he was awarded Nobel Prize for this work.

Apparatus **:** It consists of two hollow semicircular D shaped boxes which are called **dees** (see Fig. 7.9.2.1). These are separated from each other by a narrow gap. The two dees are placed between the poles of an external powerful magnetic field perpendicular to the planes of dees. These are connected to the terminals of a high frequency alternating potential of high voltage in such a way that when one dee is positive, the other opposite dee is negative. The ion source is placed at the centre of the dees. For the α-particles, the radioactive sources are kept there. To have the heavy ions, the corresponding gas kept there is bombarded by the electrons emitted from an electrically heated filament. The whole device is enclosed in a vacuum chamber.

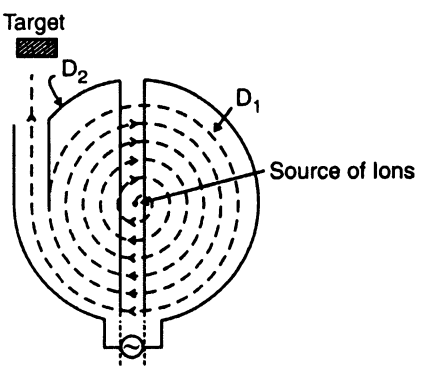

Fig. 7.9.2.1. Schematic design of a cyclotron.

Working principle **:** The particle at the centre with a positive charge q is attracted and accelerated to the negative pole of the electrode system. Because of the magnetic field of intensity H, acting perpendicular to the plane of the dees, the accelerated particle will travel in a circular path of radius r given by :

$$Hqu = (mu^2)/r \qquad \ldots(7.9.2.1)$$

where, m and u denote the mass and velocity of the particle respectively. After covering the semicircular path in a particular dee, the particle reaches the gap. **Now, if, by this time, the polarity is changed, i.e. the facing dee becomes negative, then it will be attracted to that dee.** Thus, if this condition is maintained throughout the journey of the particle, the particle gradually gains an increasing kinetic energy. To have this situation, the basic condition is that on leaving a particular dee, the particle will experience an attraction to the facing dee which has been negative due to the alternating potential by

Click Here t.me/thearchemylibrary

this time. Because of the gradual increased velocity, the path lengths of the successive semicircular trajectories are increased in such a way that ***in each case the time required to cover the path in a dee (i.e. semicircular path) becomes constant which is equal to half of the time period of oscillation.***

If ω is the angular velocity in a certain semicircular trajectory in a dee, then it is given by : $\omega = u/r = Hq/m$, (by using Eqn. 7.9.2.1). Thus, the time taken by the particle to cover that particular semicircular trajectory is given by :

$$t = \pi/\omega = \pi m/(Hq) \qquad \ldots(7.9.2.2)$$

Now, let us calculate the maximum possible kinetic energy (E_{max}) which can be attained by the particle. It is obtained as follows :

$$Hqu_{max} = mu_{max}^2/r_{max}; \text{ or, } u_{max} = Hqr_{max}/m$$

Hence,
$$E_{max} = \frac{1}{2} mu_{max}^2 = \frac{1}{2}(H^2q^2r_{max}^2/m) \qquad \ldots (7.9.2.3)$$

The magnetic field intensity H cannot be arbitrarily selected. It depends on the frequency of oscillation of the potential. We have already mentioned that the time taken by the particle to cover a semicircular path in a dee is equal to half of the time period of oscillation. Therefore, we have the condition as :

$$t = \text{half of the oscillation period} = \frac{1}{2}T = \frac{1}{2f}; (f = \text{ frequency} = 1/T).$$

Again, $t = \pi/\omega$. Considering these two relations, we get :

$$\pi/\omega = \frac{1}{2f}; \text{ or, } \pi m/(Hq) = \frac{1}{2f}; \text{(by using Eqn. 7.9.2.2);}$$

or,
$$H = 2f\pi m/q \qquad \ldots(7.9.2.4)$$

Ultimately, when the accelerated particle reaches the trajectory of r_{max}, it is bent out of the magnetic field by using a subsidiary electric field to direct the particle to the target.

Drawbacks in cyclotron : As the velocity increases, the mass of the particle increases, but the velocity of the particle can never exceed the velocity of light. Now let us see, how this change in mass affects the process. We have :

$$\omega = Hq/m = \frac{Hq}{m_0(1 - u^2/c^2)^{-1/2}} = \frac{Hq\,(1 - u^2/c^2)^{1/2}}{m_0}$$

Thus, with the increase of linear velocity, the angular velocity decreases. Consequently, to cover the semicircular path, the time taken (= π/ω) gradually increases, and when the particle reaches the gap, it may not necessarily face the negative pole due to its delayed reaching. As a matter of fact, it is too late for the particle to face the desired pole. **This is why, a cyclotron cannot be utilised to increase the kinetic energy very high unless the two operations are synchronised.** However it is suitable for the light particles like ${}_2^4He$, ${}_1^2H$, ${}_1^1H$.

To overcome this in-built drawback, a modified cyclotron known as ***synchrocyclotron*** has been developed in 1945. **In this machine, oscillator frequency is adjusted to compensate the time lag experienced by the particle in reaching the gap.**

Different types of particle accelerators such as *betatron, electron synchrotron, proton synchrotron, alternating gradient synchrotron*, etc. are available to serve the purpose.

Click Here t.me/thealchemylibrary

7.10 FILLING IN THE GAPS IN THE PERIODIC TABLE : THE MAN-MADE ELEMENTS

At the beginning of the thirtees of this century, there were four gaps in the periodic table corresponding to the elements $Z = 43, 61, 85$ and 87. Theoretically, it was predicted that these elements were unstable with respect to radioactive decay. This is why, these were not available in nature. Later, with the development of nuclear transmutation process, *all these elements were synthesised by bombarding the nearest elements with suitable projectiles.*

Z = 43 : Now it is established by the name ***technetium* (*Tc*).** In 1925, the element by name *masurium* was announced by Noddack et al from the *X*-ray emission spectra of different ores, but it was confirmed and isolated by Perrier and Segre in 1937 from a molybdenum deflector used for a long time in a cyclotron in Berkeley in USA. ***This is why, it was named technetium meaning artificial.*** It was produced by bombarding molybdenum ($Z = 42$) with the deuterons in the (d, n) reaction.

$$^{96}_{42}Mo + ^{2}_{1}H \rightarrow ^{97}_{43}Tc\ (t_{1/2} = 88\ \text{d}) + ^{1}_{0}n$$

Another isotope had been synthesised by Seaborg and Segre (1939) as follows :

$$^{98}_{42}Mo + ^{1}_{0}n \rightarrow ^{99}_{42}Mo \xrightarrow{-\beta^-} ^{93}_{43}Tc\ (t_{1/2} = 5 \times 10^5\ \text{yr})$$

Z = 61 : A group of scientists working at the University of Illinois (USA) announced the existence of the element by name *illinium* (to honour their working place) from the spectroscopic analysis of neodymium and samarium salts, but it could not be confirmed by other schools. In 1938-1942, a group of scientists working at Ohio State University (USA) on nuclear transmutation reactions at the targets of neodymium-samarium range by using the accelerated particles, noticed the radioisotope of the element (Z = 61) in the following type of reaction,

$$^{143}_{60}Nd + ^{4}_{2}He \rightarrow ^{146}_{61}X + ^{1}_{1}H$$

However, in 1947, Marinsky et al were able to isolate the element from the fission products of ^{235}U in a trace quantity. It was named ***promethium* (*Pm*)** after Prometheus who stole fire from heaven to the earth for the use of mankind in accordance with the Greek mythology.

A number of radioisotopes of *Pm* have been identified. It has also been synthesised through the neutron capture as follows:

$$^{144}_{60}Nd + ^{1}_{0}n \rightarrow ^{145}_{60}Nd \xrightarrow{-\beta^-} ^{145}_{61}Pm$$

Z = 85 : The element was first synthesised by Corson, Mackenzie and Segre in 1940 by bombarding bismuth with the high energy alpha particles. It was named **astatine** (Greek, unstable) and found alpha-active.

$$^{209}_{83}Bi + ^{4}_{2}He \rightarrow ^{211}_{85}At + 2\,^{1}_{0}n;\ ^{211}_{85}At \xrightarrow[(t_{1/2} = 7.5\ \text{h})]{} ^{207}_{83}Bi + ^{4}_{2}He$$

It may also pass through the electron capture process as follows :

$$^{211}_{85}At + ^{0}_{-1}e \rightarrow ^{211}_{84}Po \rightarrow ^{207}_{82}Pb + ^{4}_{2}He$$

Click Here to the Chemistry Library

Z = 87 : The element was confirmed by Perey (in 1939) in France as a minor decay product of ^{227}Ac. It was named ***francium*** **(*Fr*)** to honour her native country.

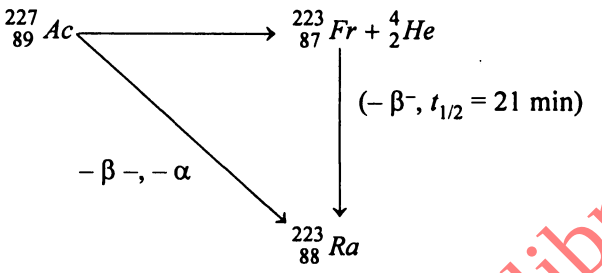

7.11 TRANSURANIC AND TRANSLAWRENCIUM ELEMENTS : THE MAN-MADE ELEMENTS

The elements having atomic numbers greater than that of uranium (Z = 92) are called **transuranic elements.** They and their daughters are generally radioactive. The routes of synthesis of these elements are shown below.

(a) Neptunium (Z = 93)

By bombarding slow neutrons on ^{238}U, ^{239}Np can be prepared (McMillian et al, 1940).

$$^{238}_{92}U + ^{1}_{0}n \xrightarrow[\text{capture}]{\text{resonance}} \left(^{239}_{92}U^{*}\right) \rightarrow ^{239}_{92}U + \gamma$$

$$^{239}_{92}U \xrightarrow[(t_{1/2} = 23.5\ \text{min})]{} ^{239}_{93}Np + ^{0}_{-1}e + ^{0}_{0}\bar{\nu}$$

By using fast neutrons, the most stable isotope can also be synthesised (Seaborg et al, 1942) as follows.

$$^{238}_{92}U + ^{1}_{0}n\ (\text{fast}) \rightarrow ^{237}_{92}U + 2\,^{1}_{0}n;\ ^{237}_{92}U \xrightarrow[(t_{1/2} = 6.5\ \text{d})]{} ^{237}_{93}Np + ^{0}_{-1}e + ^{0}_{0}\bar{\nu}$$

It can also be prepared (Seaborg et al, 1940) as follows :

$$^{238}_{92}U + ^{2}_{1}H \rightarrow ^{238}_{93}Np + 2\,^{1}_{0}n;\ ^{238}_{93}Np \xrightarrow[(t_{1/2} = 2.1\ \text{d})]{} ^{238}_{94}Pu + ^{0}_{-1}e + ^{0}_{0}\bar{\nu}$$

(b) Plutonium (Z = 94)

The spontaneous β^--emission from ^{239}Np leads to plutonium,

$$^{239}_{93}Np \xrightarrow{(t_{1/2} = 2.3\ \text{d})} ^{239}_{94}Pu + ^{0}_{-1}e + ^{0}_{0}\bar{\nu}$$

Similarly,

$$^{238}_{93}Np \xrightarrow{(t_{1/2} = 2.1\ \text{d})} ^{238}_{94}Pu + ^{0}_{-1}e + ^{0}_{0}\bar{\nu}$$

^{239}Pu ($t_{1/2}$ = 2.4 × 10^4 y) *undergoes fission with neutrons and it can be used to run the nuclear reactors and to make the atom bombs.*

Click Here t.me/thealchemylibrary

(c) Amerecium (Z = 95)

It was prepared by Seaborg et al (1944) as follows :

$$^{238}_{92}U + ^{4}_{2}He \rightarrow ^{242}_{94}Pu^{*} \rightarrow ^{241}_{94}Pu + ^{1}_{0}n;$$

$$^{241}_{94}Pu \xrightarrow{(t_{1/2} = 14\ y)} ^{241}_{95}Am + ^{0}_{-1}e + ^{0}_{0}\bar{\nu}$$

(d) Curium (Z = 96)

It was also synthesised by Seaborg et al (1944).

$$^{239}_{94}Pu + ^{4}_{2}He \rightarrow ^{242}_{96}Cm + ^{1}_{0}n$$

(e) Berkelium (Z = 97)

In 1949, it was prepared by Seaborg et al by using alpha -particles as projectiles.

$$^{241}_{95}Am + ^{4}_{2}He \rightarrow ^{243}_{97}Bk + 2\,^{1}_{0}n$$

(f) Californium (Z = 98)

The credit for its discovery goes to Seaborg et al (1950).

$$^{242}_{96}Cm + ^{4}_{2}He \rightarrow ^{244}_{98}Cf + 2\,^{1}_{0}n;\ ^{238}_{92}U + ^{12}_{6}C\ (i.e.\ C^{6+}) \rightarrow ^{244}_{98}Cf + 6\,^{1}_{0}n;$$

$$^{238}_{92}U + ^{12}_{6}C\ (i.e.\ C^{6+}) \rightarrow ^{246}_{98}Cf + 4\,^{1}_{0}n$$

Here it is interesting to note that **the isotope** $^{244}_{98}Cf$ ($t_{1/2}$ = 60 d) **undergoes a spontaneous fission with the liberation of an enormous amount of energy.** It is believed that the spontaneous fission of this isotope is responsible for the ***supernova explosions*** in some stars. The isotope is probably created by a series of neutron capture followed by β^{-}-decays.

(g) Einsteinium (Z = 99)

It was first prepared in 1953 from plutonium through a series of neutron capture and beta – emissions.

$$^{239}_{94}Pu + 14\,^{1}_{0}n \rightarrow ^{253}_{99}Es + 5\,^{0}_{-1}e + ^{0}_{0}\bar{\nu}$$

It can also be prepared by using the heavy ions as projectiles.

$$^{238}_{92}U + ^{14}_{7}N\ (\text{i.e. } N^{6+}) \rightarrow ^{247}_{99}Es + 5\,^{1}_{0}n$$

(h) Fermium (Z = 100)

It is prepared by using $^{16}_{8}O^{6+}$ as a projectile.

$$^{238}_{92}U + ^{16}_{8}O\ (\text{i.e. } O^{6+}) \rightarrow ^{250}_{100}Fm + 4\,^{1}_{0}n$$

Click Here t.me/thealchemylibrary

(i) Mendelevium (Z = 101)

It was prepared by Seaborg et al (1955) as follows :

$$^{253}_{99}Es + {}^{4}_{2}He \rightarrow {}^{256}_{101}Md + {}^{1}_{0}n;\ {}^{256}_{101}Md \rightarrow {}^{256}_{100}Fm + {}^{0}_{+1}e + {}^{0}_{0}\nu$$

(j) Nobelium (Z = 102)

It was produced by Seaborg et al in 1958 as follows :

$$^{246}_{96}Cm + {}^{12}_{6}C\ (i.e.\ C^{6+}) \rightarrow {}^{254}_{102}No + 4\ {}^{1}_{0}n$$

It was named to tribute the Swedish scientist Alfred Nobel.

(k) Lawrencium (Z = 103)

It was reported by a group of workers at Berkeley in 1961. It was named after E.O. Lawrence who first developed cyclotron.

$$^{246}_{98}Cf + {}^{11}_{5}B \rightarrow {}^{257}_{103}Lr \xrightarrow{(t_{1/2} = 8.6\ s)} {}^{253}_{101}Md + {}^{4}_{2}He$$

Note : Initially the element was represented by *Lw*. Now as per IUPAC recommendation, it is represented by *Lr*.

(l) Translawrencium elements (Z > 103) (cf. Sec 8.6)

The ***translawrencium elements*** ***(Z > 103)*** have been synthesised and characterised by using high energy heavy ions as projectiles. In these studies, besides the *Berkeley group*, other groups at *Dubna Laboratory* (Russia) and at *GSI* (Darmstadt, German) also contributed significantly. To prepare these heavy elements i.e. ***transactinides*** (Z = 104-112), two types of nuclear reactions – ***hot fusion*** **and** ***cold fusion*** have been used.

In hot fusion reactions, the projectiles are the *accelerated light nuclei* with Z = 5-10 (e.g. $_{5}B$, $_{6}C$, $_{7}N$, $_{8}O$, $_{10}Ne$, etc.) and the target nuclei are with Z = 92-98 (e.g. $_{92}U$, $_{94}Pu$, $_{95}Am$, $_{96}Cm$, $_{98}Cf$, etc.). The accelerated projectiles are allowed to bombard on such target nuclei to synthesise the elements with Z upto 106. **This hot fusion nuclear reaction was proved unsuccessful to synthesise the elements with Z > 106. For Z > 106, the desired compound nucleus produced through hot fusion was very much unstable. In fact,** ***the compound nuclei produced in such hot fusion reactions remain so excited that many nucleon particles randomly evaporate out from the compound nuclei to prevent the production of elements*** **with Z > 106.**

To remove the difficulty in hot fusion, an alternative route known as ***cold fusion*** was developed by the scientists working at Dubna. In cold fusion, the chosen *target nuclei* like $_{82}Pb$, $_{83}Bi$, possess very high *nuclear binding energy* (NBE) due to the *closed nuclear shell structure*; and the chosen projectiles are heavy ions of the nuclei like $_{24}Cr$, $_{26}Fe$, $_{28}Ni$ etc. characterised by the *near closed nuclear shell structure*. When the *target nuclei* (e.g. $_{82}Pb$, $_{83}Bi$ etc.) are bombarded with the moderately heavy ions of the nuclei like $_{24}Cr$, $_{26}Fe$, etc. as projectiles having energies just to overcome the Coulomb barrier to produce the compound nucleus, ***the compound nucleus produced possesses the low excitation energies.*** Such compound nuclei can survive from fission and they can generate new elements with $Z > 106$ through the emission of neutrons. The nuclear reactions leading to the synthesis of the elements up to $Z = 112$ are shown below.

$$^{242}Pu(^{22}Ne, 4n)^{260}Unq;\ ^{249}Cf(^{12}C, 4n)^{257}Unq;\ ^{249}Cf(^{15}N, 4n)^{260}Unp;$$

Click here t.me/idealchemylibrary

$^{243}Am(^{22}Ne, 4n)^{261}Unp$; $^{249}Cf(^{18}O, 4n)^{263}Unh$; $^{248}Cm(^{22}Ne, 4n)^{266}Unh$;

$^{208}Pb(^{58}Fe, 2n)^{264}Uno$; $^{209}Bi(^{55}Mn, n)^{263}Uno$; $^{209}Bi(^{58}Fe, n)^{266}Une$;

$^{208}Pb(^{62}Ni, n)^{269}Uun$; $^{209}Bi(^{64}Ni, n)^{272}Uuu$; $^{208}Pb(^{70}Zn, n)^{277}Uub$

The IUPAC (1977) names (see Sec. 8.6) of the elements for $Z = 104$, 105, 106, 107, 108, 109, 110, 111 and 112 are *Unq, Unp, Unh, Uns, Uno, Une, Uun, Uuu* and *Uub* respectively. Presently the elements for $Z = 104$, 105, 106, 107, 108 and 109 are known as *Rf* (rutherfordium), *Db* (dubnium), *Sg* (seaborgium), *Bh* (bohrium), *Hs* (hassium) and *Mt* (meitnerium). However, different names have been proposed for these elements from time to time (cf. Appendix IV).

It was predicted that in future some isotopes of the ***superheavy elements*** lying close to the ***island of stability*** may be reported. In 1968, Seaborg predicted the probable route to prepare the element (Z = 114).

$$^{238}_{92}U + {}^{238}_{92}U \rightarrow {}^{298}_{114}X + {}^{166}_{70}Yb + 12\,{}^{1}_{0}n$$

In fact, recently some elements with $Z > 112$ have been synthesised (cf. M.M. Greenwood, *J. Chem. Soc. Dalton Trans,* 2055, 2001). With the increase of atomic number in this range, the half life period drastically decreases (cf. $t_{1/2} = 65$ s for $Z = 104$ while $t_{1/2} = 1$ ms for $Z = 112$). The elements ***ekalead*** ($Z = 114$), ***ekapolonium*** ($Z = 116$) and ***ekaradon*** ($Z = 118$) have been synthesised. Among these, the element with $Z = 114$ is expected to be the most stable for the magic number of protons and in fact the isotope ^{298}[114] with double magic numbers (i.e. $Z = 114$ and $N = 184$) is relatively more stable (cf. **stability island,** Sec. 5.5.3). ***The common principle to synthesise such heavy elements is to use the heaviest possible magic number nuclei for both the target and projectile.***

The isotope ^{289}[114] has been prepared by bombarding PuO_2 (^{244}Pu, ca. 99%) with a current of projectile $^{48}Ca^{5+}$ for 32 days. The doubly magic number projectile ($Z = 20$, $N = 28$) is very much rare (cf. natural abundance, ca. 0.2%). In fact, for 5.2×10^{18} projectiles, only one isotope of ^{289}[114] is produced and it decays rapidly.

$$^{244}_{94}Pu + {}^{48}_{20}Ca \rightarrow {}^{289}[114] + 3\,{}^{1}_{0}n$$

$$t_{1/2}: \; {}^{289}[114] \xrightarrow[30.4\text{ s}]{-\alpha} {}^{285}[112] \xrightarrow[15.4\text{ min}]{-\alpha} {}^{281}[110] \xrightarrow[1.6\text{ min}]{-\alpha} {}^{277}[108] \xrightarrow[16.5\text{ min}]{\text{self-fission}} \text{Fission product}$$

By bombarding ^{242}Pu (ca. 97%) as PuO_2 with *ca.* 8×10^{18} projectiles of $^{48}_{20}Ca^{5+}$, one isotope of ^{287}[114] has been obtained.

$$^{242}_{94}Pu + {}^{48}_{20}Ca \rightarrow 3\,{}^{1}_{0}n + {}^{287}[114]$$

$$^{287}[114] \xrightarrow[t_{1/2} = 1.32\text{ s}]{-\alpha} {}^{283}[112]$$

By bombarding $^{208}_{82}Pb$ (with double magic numbers) with the projectile ^{86}Kr (heaviest stable isotope of *Kr*), the elements with $Z = 118$, 116 have been synthesised.

Click Here to the Research Library

$$^{208}_{82}Pb + ^{86}_{36}Kr \rightarrow ^{293}[118] + ^{1}_{0}n$$

$$^{293}[118] \xrightarrow{-\alpha} ^{289}[116] \xrightarrow{-\alpha} ^{285}[114]$$

Some Important Practical Applications of Man-Made Elements

- ***Nuclear fuels*** (i.e. fissile nuclides) : The fissile nuclides ^{233}U (prepared from ^{232}Th by slow neutrons) and ^{239}Pu (prepared from ^{238}U by using neutron projectiles) are widely used as nuclear fuels to run the nuclear reactors and also in making atom bombs.
- ***Neutron source*** : ^{238}Pu and ^{241}Am are α-emitters. These emitted α-particles can generate neutrons from ^{9}Be.

  $$^{9}_{4}Be + \alpha \rightarrow ^{12}_{6}C + n, \text{ i.e. } ^{9}_{4}Be\ (\alpha, n)\ ^{12}_{6}C$$

  Thus ($^{238}Pu + ^{9}Be$) or ($^{241}Am + ^{9}Be$) can be used as a source of neutron. ($^{241}Am + ^{9}Be$) *as a neutron source (ca. 10^7 neutrons per second per gram of ^{241}Am) is widely used to estimate how much oil is produced in a well in a given time.* The natural source petroleum responds to (n, γ) reaction to produce the radioisotopes having the characteristic radiation. This aspect has been discussed in Sec. 6.17.6.5.
- ***Power source*** : ^{238}Pu (α-emitter, $t_{1/2}$ = 87.7 y) is used as a thermal power source in heart pacemakers.

7.12 NUCLEAR FISSION

7.12.1 Historical Background

The discovery of neutron by Chadwick in 1932 set up **a new field of transmutation reaction by using the neutrons as projectiles.** In this line, the work from three groups of scientists : (i) **Enrico Fermi in Italy,** (ii) **F. Joliot Curie and Savitch in France,** and (iii) **Otto Hahn and Strassman in Germany,** paved the way (1934-1938) in discovering the nuclear fission.

In 1936, E. Fermi suggested that the compound nucleus ($^{236}U^*$) formed in the bombardment of slow neutrons on $^{235}_{92}U$ should undergo β^- decay because of a higher neutron to proton ratio in the compound nucleus. This suggestion was tested in laboratory and it showed β^--activity with four different half-lives. Considering four successive β^--decays in the daughter nuclei, there should be four transuranic elements having Z = 93, 94, 95 and 96. The group of J. Curie carried out chemical analysis on the uranium compounds bombarded by the slow neutrons. Astonishingly, they noticed a chemical species having properties close to those of Z = 56-57 far away from Z = 92 in the periodic table. **They noticed this surprising observation but did not confirm the observation. Thus the credit of the discovery of nuclear fission slipped away from their hands to the group of Otto Hahn who established barium (Z = 56) as one of the product in the $^{235}_{92}U + n$ reaction.** Thus the barium produced showed β^--activity. In the analysis, the production of krypton (Z = 36) was also proved. Thus, the product nuclides were found to be much lighter than the starting nuclide. This is why, it was suggested by **Meinter (a former associate of Hahn) and Firsch** that the uranium nucleus on being bombarded by a slow neutron splits into two lighter fragments of comparable size and the process was termed as ***nuclear fission.***

$$^{235}_{92}U + ^{1}_{0}n\ (\text{slow}) \rightarrow ^{236}_{92}U^* \rightarrow ^{141}_{56}Ba + ^{92}_{36}Kr + 3\ ^{1}_{0}n + \text{energy.}$$

Click Here to Join/thealchemylibrary

7.12.2 Characteristic Features of Nuclear Fission

(a) **Mass distribution in fission fragments :** The compound nucleus formed may undergo fission in a variety of ways. Some possibilities are given below :

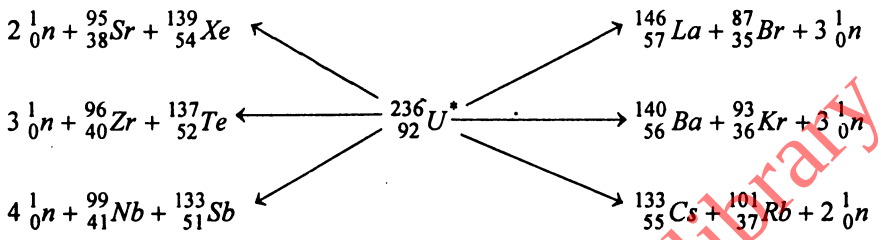

Thus, the compound nucleus ($^{236}U^{*}$) very often undergoes an **asymmetric fission** in about 30 routes. **The mass number of the lighter fission product lies in the range 85 to 104, while the heavier fragment covers the range, 130 to 149.** *The most probable fission path involves the fragments with mass numbers around* 95 *and* 139. The distribution of mass number can be represented in the ***fission yield curve*** (see Fig. 7.12.1.1) known as ***Bohr yield curve.***

The symmetric fission producing the fragments with mass number ~ 117 is a rare possibility and it is evident from Fig. 7.12.1.1. However, it has been proved that with the increase of energy of the projectile neutron effecting the fission, the probability of symmetric fission increases. It is experimentally verified in ^{239}Pu.

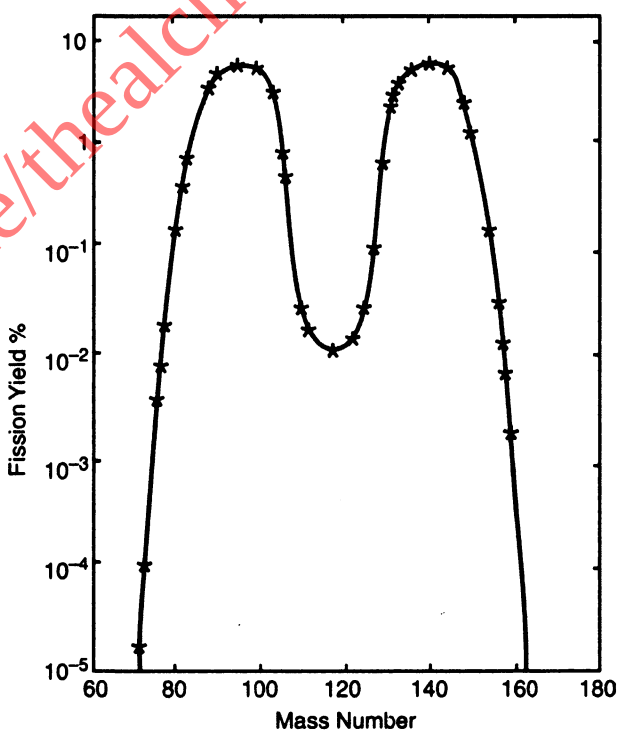

Fig. 7.12.1.1. Fission yield curve (known as Bohr yield curve) for ^{235}U.

(b) ***Energy distribution in fission fragments*** : The mass distribution pattern is intimately related with the energy distribution pattern among the fission products. If the com-pound nucleus undergoing fission is assumed to be at rest, and the energies shared by the emitted neutrons are neglected, then according to the law of conservation of momentum, it gives,

$$M_1u_1 = M_2u_2; \text{ or, } u_1/u_2 = M_2/M_1,$$

where M_1 and M_2 denote the masses of the two fragments, and u_1 and u_2 represent their corresponding velocities.

Click Here t.me/thealchemylibrary

Therefore, for kinetic energies we have :

$$E_1/E_2 = \frac{(1/2)\,M_1u_1^2}{(1/2)\,M_2u_2^2} = M_2/M_1; (\text{as } M_1u_1 = M_2u_2)$$

Thus, the masses and kinetic energies of the fragments are inversely related. The distribution of kinetic energy among the fission products can be measured by using an ionisation chamber.

(c) ***Emission of projectiles*** : The projectiles effecting the nuclear fission are again emitted (2-3 per fission) in the process. Thus, the ejectiles under a suitable condition can be reutilised as projectiles to make the process self-sustained.

Here it is worth mentioning that all the neutrons are not emitted at one instant. More than 99% are emitted almost instanteneously in a time of the order of 10^{-14} s. These neutrons are called ***prompt neutrons.*** The neutrons (~ 1%) which are emitted in late from the fission products are called ***delayed neutrons.***

Prompt neutrons are released within 10^{-14} s from the neutron-rich fragments of fission products. Thus the fission of ^{235}U by a thermal neutron can be represented as :

$$^{235}_{92}U + n \rightarrow (^{236}_{92}U^*) \rightarrow {}^{146}_{57}La + {}^{87}_{35}Br + 3n \,(\textbf{\textit{prompt neutrons}})$$

Here, ^{87}Br is a β^- emitter and it decays with a half life of 55.5 s to ^{87}Kr. ^{87}Kr is of sufficient energy to eject a neutron immediately to produce the stable nuclide ^{86}Kr, i.e.

$$^{87}Br \xrightarrow[\text{(slow)}]{-\beta^-} {}^{87}Kr^* \xrightarrow[\text{(fast)}]{} {}^{86}Kr + n \,(\textbf{\textit{delayed neutron}})$$

Here, the neutron emission rate is determined by the slow step ($t_{1/2}$ = 55.5 s). Such neutrons, emitted after a measureable time period of the fission are described as *delayed neutrons* which play an important role in controlling the nuclear fission in nuclear reactors. The delayed neutrons are of low energy while the prompt neutrons are of high energy.

(d) ***β^--Activity in the fission products*** : In the product fragments, the neutron to proton ratio lies far above their corresponding stability region as demanded from Segre's chart (see Fig. 5.3.2.1). **The starting nuclide (Z = 92) requires a relatively higher neutron to proton ratio for its stability and this high ratio on being transmitted to the fission products of much lower atomic number makes them unstable with respect to β^--activity.** The process goes on until the stable nuclei are formed. Thus in a particular fission reaction, **two different series of *isobaric nuclides*** with the mass numbers A_1 and A_2 (where the initial fragments are characterised with the mass numbers A_1 and A_2) are obtained. The β^--activities of some fission products are shown below.

$$^{141}_{56}Ba \xrightarrow{\beta} {}^{141}_{57}La \xrightarrow{\beta} {}^{141}_{58}Ce \xrightarrow{\beta} {}^{141}_{59}Pr;$$

$$^{92}_{36}Kr \xrightarrow{\beta} {}^{92}_{37}Rb \xrightarrow{\beta} {}^{92}_{38}Sr \xrightarrow{\beta} {}^{92}_{39}Y \xrightarrow{\beta} {}^{92}_{40}Zr;$$

$$^{140}_{54}Xe \xrightarrow{\beta} {}^{140}_{55}Cs \xrightarrow{\beta} {}^{140}_{56}Ba \xrightarrow{\beta} {}^{140}_{57}La \xrightarrow{\beta} {}^{140}_{58}Ce.$$

(e) ***Energy (Q) release in fission*** : The energy released per fission is ~ 200 MeV which is much greater than that released in any ordinary nuclear reaction. Due to the ejection of the projectiles,

Click Here to me/theachemylibrary

once the process is started, it can proceed in a chain reaction to release an enormous amount of energy in a moment. The calculation of energy release in the process can be done in two ways as discussed below.

(i) ***Mass defect method*** : For this purpose, let us consider one of the most probable fission reactions, i.e.

$$^{235}_{92}U + {}^{1}_{0}n \rightarrow {}^{98}_{42}Mo + {}^{136}_{54}Xe + 2\,{}^{1}_{0}n + 4\,{}^{0}_{-1}e + 4\,{}^{0}_{0}\bar{\nu}.$$

Here, mass loss $\Delta m \approx \left[m(^{235}U) + m(^{1}n)\right] - \left[m(^{98}Mo) + m(^{136}Xe) + 2m(^{1}n)\right]$

$= (235.044 + 1.0086) - (97.906 + 135.907 + 2 \times 1.0086)$

$= 236.0526 - 235.8302 = 0.2224$ amu

$\equiv 0.2224 \times 931$ MeV $= 207$ MeV

In calculating Δm, the mass of the emitted electrons has been neglected.

(ii) ***Nuclear binding energy (NBE) method*** : From the nuclear binding energy curves (see Fig. 5.3.5.1), it is evident that for the fissionable nuclides ($A \approx 235 - 240$), the binding energy per nucleon (i.e. $\overline{B}$) lies in the range ~ 7.5 MeV while the fission products stand on the curve where $\overline{B} \sim 8.5$ MeV. Thus in moving from the position of the fissionable nuclide to that of the fission products, ~ 1 (= 8.5 – 7.5) MeV energy is released per nucleon. Thus in each fission, ~ 235 × 1 = 235 MeV energy is released (neglecting the neutrons emitted as ejectiles).

7.12.3 Bohr-Wheeler Theory of Nuclear Fission : Liquid Drop Model

(a) ***The fission process*** : After the discovery of Otto Hahn and Strassman of nuclear fission, based on the liquid drop model of nucleus, Meinter and Frisch proposed a theoretical interpretation which was further developed by Bohr (in 1939) first qualitatively, and later quantitatively in collaboration with Wheeler.

The basic concept in the theoretical interpretation is represented in Fig. 7.12 3.1 in a series of steps. The compound nucleus formed at its birth-time is spherical. Depending upon the excitation energy, it passes through a number of events. The **excitation energy** (E_{ex}) is given by (see Secs. 7.5.2 and 7.6) :

E_{ex} = binding energy (E_B) of the additional neutron (i.e. projectile) in the compound nucleus + kinetic energy of the projectile on central mass system (CMS) $\approx E_B$
(for the slow or thermal neutrons having energy << 1.0 eV)

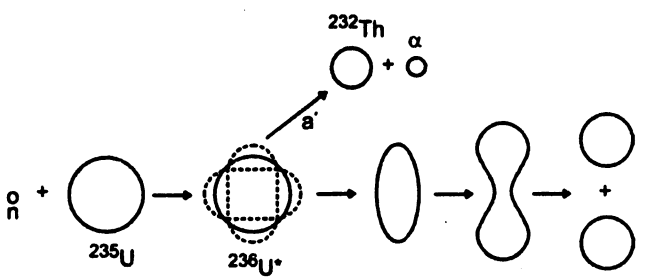

Fig. 7.12.3.1. Mechanistic steps of fission in the light of liquid drop model.

Click Here for the Chemylibrary

If the excitation energy is sufficient to distort the compound nucleus sufficiently then it passes through the chain.

$$\textbf{spherical} \xrightarrow{\text{distortion}} \textbf{ellipsoidal} \longrightarrow \textbf{dumb-bell shape} \longrightarrow \textbf{two fragments.}$$

If the excitation energy is not sufficiently high to carry out the fission then the compound nucleus may deexcite through the γ-radiation or evaporation of one or more nucleons and immediately it regains its spherical shape.

In the presence of the excess excitation energy, the strong oscillations set up within the nucleus lead to the nuclear fission. **Thus it depends on the excitation energy whether the compound nucleus will pass through the evaporation of some nucleons along with γ-radiation or nuclear fission.** To effect the nuclear fission, a threshold value of excitation energy is required.

It appears that for a liquid drop to be split into two smaller droplets, or for a nucleus to suffer a fission, there must be a ***critical extent of deformation*** **(corresponding to the threshold value of the excitation energy)** which can be attained only, if at least the threshold excitation energy is available.

Based on the principle of *liquid drop model*, the following expression for ***critical deformation energy*** of the compound nucleus was derived by Bohr and Wheeler :

$$E_{crit} \approx 0.89A^{2/3} - \frac{0.02\,Z\,(Z-1)}{A^{1/3}}, \text{(in MeV)}$$

The values 0.89 and 0.02 are also known as **Bohr-Wheeler constants** (for derivation of the relationship, the book, *Atomic and Nuclear Physics*, 2nd Edn. by K.G. Krishnan, Macmillan Ltd., New Delhi, may be consulted). Here, A and Z denote the mass number and atomic number of the compound nucleus formed through the capture of the projectile by the target nucleus during fission. Let us consider the possibility of fission of ^{235}U and ^{238}U by using the neutron projectile.

(i) $^{235}_{92}U + {}^{1}_{0}n \longrightarrow \left[{}^{236}_{92}U\right]^{*}$ **(Compound nucleus)**

$$E_{crit}\,(^{236}U) = 0.89 \times (236)^{2/3} - \frac{0.02 \times 92 \times 91}{(236)^{1/3}}$$

$$= 0.89 \times 38.19 - \frac{167.44}{6.18}$$

$$= 33.99 - 27.09 = 6.9 \approx 7 \text{ MeV}$$

(ii) $^{238}_{92}U + {}^{1}_{0}n \longrightarrow \left[{}^{239}_{92}U\right]^{*}$ **(Compound nucleus)**

$$E_{crit}\,(^{239}U) = 0.89 \times (239)^{2/3} - \frac{0.02 \times 92 \times 91}{(239)^{1/3}}$$

$$= 0.89 \times 38.5 - \frac{167.44}{6.2}$$

$$= 34.27 - 27.0 = 7.27 \text{ MeV} > E_{crit}\,(^{236}U)$$

Click Here i.me/thedchemistrylibrary

To make the fission energetically feasible by the ***thermal neutrons*** (energy < 1 eV) ***(for which the available kinetic energy from the projectile on CMS is negligible)*, the last neutron binding energy (E_B) in the compound nucleus must exceed the corresponding E_{crit} value (i.e. $E_B \geq E_{crit}$).** Calculation shows that for the last neutron binding energy in $^{236}U^*$ and $^{239}U^*$ are 6.4 MeV and 5.2 MeV respectively. Thus for the *thermal neutrons* (energy < 1 eV), E_B is very close to E_{crit} for the fission of ^{235}U while E_B is much less than E_{crit} for ^{238}U. In reality, thermal neutrons can cause fission in ^{235}U not in ^{238}U.

(b) ***Explanation of the asymmetric fission*** **:** The theory developed by Bohr et al apparently indicates the symmetric fission leading to the products of mass number ~ 117. But in practice, this symmetric mode of fission is one of the rarest possibilities. To explain this observation, ***shell closure effects*** **leading to the magic numbers to the two ends in the distorted compound nuclide (i.e. dumb-bell shape) are to be considered.**

Due to the excitation beyond the critical stage, the gradual deformation leads to the accumulation of the nucleons at the two ends of the dumb-bell shape in such a way (see Fig. 7.12.3.2) that ***one end collects the nucleons with double magic numbers (i.e. both types of the nucleons attain the magic numbers separately) with 50 protons and 82 neutrons, and the other end gains the magic number neutrons (i.e. 50) with 32-34 protons.*** Thus the two hard cores are formed before the fission by distributing the nucleons to impart the maximum possible stability. The preformed cores are almost spherical because of the closed shell structure and thus ***it requires the minimum deformation of the compound nuclide for fission.*** The residual nucleons (i.e. 12 neutrons, 8-10 protons) bridge the two hard cores. These bridging nucleons will be divided between the hard cores to yield the fission products. Some of the bridging neutrons may come out as ejectiles. **However, considering the expulsion of 2-3 neutrons and equal division of the residual bridging nucleons between the preformed cores, the mass numbers of the fission fragments become ~ 141 and ~ 93.** This prediction nicely conforms to the experimental observation. In fact, the bridging nucleons may be distributed in a number of ways leading to the different fission pairs.

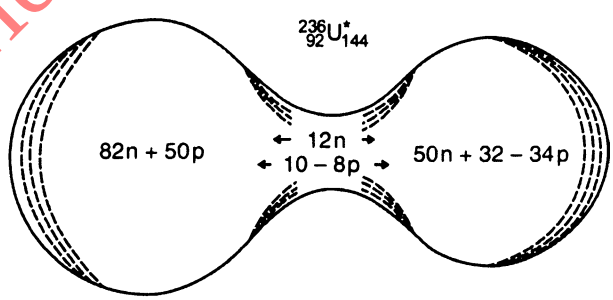

Fig. 7.12.3.2. Shell closure effects leading to the asymmetric fission. Adapted from H.J. Arnikar, "Essentials of Nuclear Chemistry, 2nd Edn., Wiley Eastern Ltd., 1989, Reproduced with permission.

Here, it may be mentioned that the **Coulombic potential** (E_{Coul}) for symmetric fission is also very high.

$$E_{Coul} = \frac{Z_1 Z_2 e^2}{(R_1 + R_2)(4\pi\varepsilon_0)}, \text{(SI unit)};$$

Click Here t.me/thealchemylibrary

$$Z_1 = Z_2 = \frac{1}{2}(Z);\ R_1 = R_2 = R = 1.4\left(\frac{A}{2}\right)^{1/3} \times 10^{-15}\ \text{m}$$

where Z and A denote the atomic number and mass number of the nuclide experiencing symmetric fission. For the **symmetric fission** of $^{236}_{92}U$, **calculated value of E_{Coul} becomes about 222 MeV** (see Solved Problem 14). For an **asymmetric fission** of $^{236}_{92}U$, the value of E_{Coul} becomes 211 MeV (see Solved Problem 16). ***Thus it is seen E_{Coul} value is relatively higher for the symmetric fission*** (cf. *Solved Problems 14 and 16*).

(c) ***Energetics of fission and conditions for fissionability*** : In a fission, the fission energy (E_f) is given by :

E_f = (mass loss) × 931 MeV, mass loss in amu units
= (mass of the reactants – mass of the products) × 931 MeV.
≈ (mass of the compound nucleus – mass of the products) × 931 MeV

It can also be calculated from the nuclear binding energy curve (see Fig. 5.3.5.1) or from the mass defect or from the semiempirical mass equation (see Eqn. 5.5.2.5, liquid drop model of nucleus).

There is an energy barrier (E_{Coul}) to prevent the fission. To understand the physical significance of E_{Coul}, we are to consider the nuclear potential well (see Figs. 5.4.3.1; 5.5.1.1; 5.5.1.2). The fission leads to fragments having charges Z_1 and Z_2, where $Z = Z_1 + Z_2$ gives the charge of the compound nuclide suffering the fission. From the nature of the ***Coulombic potential barrier***, it is realised (see Sec. 5.4.3) that if a positively charged particle (like α-particle) is to be expelled from the nucleus, then classically it must have the sufficient energy to overcome the barrier. Because of the same ground, in the nuclear fission where the positively charged fragments are getting separated, the ***Coulombic potential barrier*** [which is proportional to $Z_1Z_2/(R_1 + R_2)$] will also play the same role. **This is why, the charged fragments to be separated from each other will face a barrier (E_b) due to both the Coulombic interaction and nuclear force among the nucleons of the fissionable nuclide.** Very often, the Coulombic barrier (E_{Coul}) alone gives the approximate measure of E_b i.e. $E_b \approx E_{Coul}$.

Thus the following conditions arise.

(i) **$E_f > E_b$ gives the condition for spontaneous fission.** It arises for A ≥ 240. Mathematically, it has been shown that the spontaneous fission corresponding to zero half life period starts for, $Z^2/A \geq 45$. Thus for the element, $Z = 116$, $A = 300$, it is expected to undergo a **spontaneous fission** ($t_{1/2} \approx 10^{-20}$ s). The **heaviest nuclide,** $^{262}_{105}Ha$ ($Z^2/A = 42$) shows the half-life period 40 s.

(ii) **$E_f < E_b$ gives the condition of surviving from the spontaneous fission.** However, here it is worth mentioning that these conditions imposed work only in the classical theory. Considering the ***quantum mechanical tunnelling phenomenon***, the nuclides may undergo the **spontaneous fission** even for $E_f < E_b$. **But, for $E_b - E_f \approx$ 5–6 MeV, the spontaneous fissions through the tunnel effect lead to very long half lives with a small cross-section.** ^{233}U, ^{235}U, ^{239}Pu lie in the range, $E_b - E_f \approx$ 5–6 MeV.

Click Here Time/healchemylibrary

The **nonspontaneous fission** can be effected through the projectile under the critical condition,

$$E_{ex} \geq (E_b - E_f) = E^*$$

where, E_{ex} = excitation energy in the compound nucleus and $E_b - E_f = E^*$, i.e. ***activation energy*** of the process to generate the critical deformation in the compound nucleus.
We have already mentioned that E_{ex} is obtained as:

E_{ex} = projectile binding energy in the compound nucleus (E_B) + kinetic energy of the projectile on CMS $\approx E_B$ (for the slow neutrons having energy << 1 eV).

It has been observed that for the slow neutrons (< 1 eV), the condition, $E_{ex} \geq E^*$ for ^{233}U, ^{235}U and ^{239}Pu is attained. To attain the condition for the fission of ^{232}Th and ^{238}U, the fast neutrons (> 1.2 MeV) or highly energetic projectiles, e.g. α, *d*, are required.

The energetics of fissionability by the slow or thermal neutrons (0.026 eV) of some nuclides are given in Table 7.12.3.1.

Table 7.12.3.1. Energetics of fissionability of some nuclides by thermal neutrons

Nuclide	$E^* = E_b - E_f$ (MeV)	$E_{ex} \approx E_B$ (MeV)	$E_{ex} - E^*$ (MeV)	Fission cross-section (barn)
Natural uranium	–	–	–	3.92
$^{233}_{92}U$	4.6	6.5	1.9	530
$^{235}_{92}U$	5.4	6.4	1.0	580 (1.27)*
$^{238}_{92}U$	5.9	5.2	−0.70	~0
$^{232}_{90}Th$	6.5	5.1	−1.40	~0
$^{239}_{94}Pu$	4.0	6.4	2.4	750

* for fast neutrons (2 MeV).

Table 7.12.3.1 indicates that by using the slow neutrons, ^{233}U, ^{235}U and ^{239}Pu can be made to undergo fission with a large cross-section. **It is important to note that the nuclides having the odd number of neutrons show a relatively higher value of E_{ex} and reaction cross-section.** Probably, on pairing a neutron in the compound nucleus, a large amount of binding energy is released. ***For the nuclides already having the even number of neutrons, the process is not favoured.*** For example, the compound nuclei ^{236}U and ^{239}U created from ^{235}U and ^{238}U respectively through the neutron capture, release the binding energy (of the added neutron) 6.4 and 5.2 MeV respectively. For the ^{235}U nuclide, the released binding energy (E_B) exceeds the activation energy (E^*). **This is why, ^{235}U undergoes fission on the capture of a slow neutron even when the energy associated with the neutron is negligibly small.** Thus, both the slow and fast neutrons can effect the fission for ^{235}U. But the fission cross-section for the *thermal neutron* (*i.e.* slow neutron) is about 450 times compared to that for the *fast neutrons* (see Table 7.12.3.1). However, for ^{238}U to undergo fission, it will require at least (5.9 – 5.2), *i.e.* 0.7 MeV energy from the projectile on *CMS*. In fact, the **fast neutrons (as the projectiles) of energy greater than 1.2 MeV** can cause fission of ^{238}U and each fission yields, on an average, 2.55 fast neutrons of mean energy about 2 MeV. **But cross-section of such fast neutron mediated fission of ^{238}U is much smaller** than that of other non-fission reactions like inelastic collisions (causing thermalisation of fast neutrons), radiative and resonance capture of the fast neutrons. **Thus, the fast**

Click Here t.me/thealchemylibrary

neutrons are rapidly lost. Consequently, the number of available neutrons (≥1.2 MeV) becomes too small (*i.e.* **reproduction factor,** $K << 1$) to carry out the fission chain reaction of ^{238}U. **This is why, chain fission of natural uranium which is predominantly ^{238}U (ca. 99.5%) is not possible.**

(iii) **For the cases, $E_f << E_b$, (for $A < 225$),** the nuclides cannot undergo spontaneous fission, and by using thermal neutrons the nuclear fissions cannot be effected. **Fissions can be induced only by the highly energetic projectiles but with a low cross-section.**

7.12.4 Charge Distribution in Fission Products : Principle of Equal Charge Displacement

The initial or primary fission fragments are very often β-active and through the successive β-decay, *they produce* ***two series of isobaric nuclides.*** For a particular isobaric series (fixed A), the stable nuclide with atomic number Z_s having the maximum nuclear binding energy can be theoretically predicted from the *liquid drop model* (cf. Eqn. 5.5.2.8). It is given by:

$$Z_s = \frac{38A}{0.6A^{2/3} + 76}, \text{ (cf. Eqn. 5.5.2.8)}$$

Let us consider the following fission reaction:

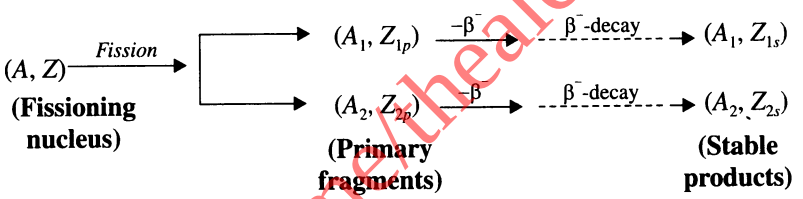

The initial or primary fragments are having the mass numbers A_1 and A_2 with atomic numbers Z_{1p} and Z_{2p} respectively. The ***stable chain enders*** are having the atomic numbers Z_{1s} and Z_{2s} respectively. These chain enders are produced through the successive β-decay. The primary product nuclides with atomic number Z_{1p} and Z_{2p} may not be always detected but they can be theoretically predicted by considering the ***principle of equal charge displacement*** which states that Z_{1p} and Z_{2p} will be equidistant from their respective ***stable chain enders*** respectively. Thus, we can write:

$$Z_{1s} - Z_{1p} = Z_{2s} - Z_{2p};\ Z_{1p} + Z_{2p} = Z, \text{ and } A_1 + A_2 = A$$

where, A and Z denote the mass number and atomic number of the fissioning nuclide.

The above relations lead to:

$$Z_{1p} = (Z + Z_{1s} - Z_{2s})/2 \text{ and } Z_{2p} = (Z + Z_{2s} - Z_{1s})/2$$

Let us illustrate the fission of $_{92}U$ by neutron projectile. The most probable fission fragments are with $A_1 = 144$ and $A_2 = 90$ with two ejectile neutrons. The **stable nuclides for the isobaric series** having $A = 144$ and 90 are characterised by $Z_s \approx 59$ (for $A = 144$) and 39 (for $A = 90$). These Z_s values can be theoretically calculated by considering the Eqn. 5.5.2.8. It leads to:

$$Z_{1p} = (92 + 59 - 39)/2 = 56 \text{ (i.e. } Ba);$$

$$Z_{2p} = (92 + 39 - 59)/2 = 36 \text{ (i.e. } Kr)$$

Click Here t.me/thealchemylibrary

7.13 FISSION CHAIN REACTION : A SOURCE OF ATOMIC ENERGY

7.13.1 Factors Controlling a Fission Chain Reaction

In the nuclear fission of ^{235}U, the secondary neutrons (i.e. ejectiles) can again participate in the process. The most probable mode of fission produces 2.5 (average) neutrons per fission. If the process goes on, the number of neutrons increases very rapidly almost in a geometrical progression during the process till the whole of the fissile material undergoes fission. **Thus, once the process is initiated, it can go on automatically *in a self-sustaining process as in a chain reaction.*** This possibility of having the enormous amount of energy released in a fission in a self-sustaining process draws the attention of the nuclear scientists to consider the nuclear fission as a source of atomic energy.

In practice, all the neutrons emitted are not generally available for carrying out the next fissions. This is why, some measures are to be taken to make the process a self-sustained one. In this connection, the parameter, ***multiplication factor or reproduction factor* (*K*)** is very much important. It is defined as follows :

$$K = \frac{\text{Number of neutrons in one generation}}{\text{Number of neutrons in the just preceding generation}}$$

Theoretically for ^{235}U, without considering any loss of neutrons in any manner, the value of reproduction factor becomes 2.5. It is very often represented as, $K_\infty = 2.5$. **But in reality, there are number of potential paths through which the neutrons can be lost.** These are :

(i) capture of neutrons by ^{238}U which are plentiful in natural uranium,

(ii) nonfission capture by ^{235}U as the compound nucleus ^{236}U may suffer from nucleon evaporation and other modes of deexcitation besides the fission, e.g.

$$^{236}_{92}U^* \rightarrow {}^{4}_{2}He + {}^{232}_{90}Th;\ {}^{235}_{92}U + n \rightarrow {}^{235}_{92}U + n, \text{(scattering)}$$

(iii) neutron capture by the impurities,

(iv) escape of neutrons through the surface.

These ways of neutron loss must be minimised so that K becomes at least unity for making the process self-sustained. ***Thus, the condition for a chain reaction is given by*** : $K \geq 1$.

Thus, if we start with the natural uranium, the loss of neutrons in the path (i) is so high that to satisfy the condition for fission chain reaction becomes only the rarest possibility. Even if we start with the pure ^{235}U, then the escapes of neutrons through the path (iv) and the path (ii) are still existing. Thus it will explode in a chain reaction only when the amount of ^{235}U exceeds ***some critical size*** where the neutron loss from the surface has been made optimum. **Critical size of a fissionable material** is defined as the minimum size of that material for which the number of neutrons produced in the fission balances the loss by the escape through the surface and nonfission capture in such a way that the fission becomes self-sustained. The corresponding mass is called *critical mass*. The conditions can be expressed in terms of

K* as : $K = 1$, *critical size*; $K > 1$, *supercritical size*; $K < 1$, *subcritical size.

The escape of neutrons occurs from the surface area. Thus, it is a ***surface effect.*** On the other hand, the production of neutrons occurs through the fission via neutron capture throughout the volume. Hence it is a ***volume effect.*** The non-fission capture (which cannot be controlled by imposing any external

Click Here : me/thealchemylibrary

condition) of neutron is also a ***volume effect.*** Thus to have $K \geq 1$, both the surface and volume must be optimised.

Considering the spherical shape of the fissile material, we get the conditions. Surface area of the spherical mass = $4\pi r^2$. Thus, escape rate of neutrons $\propto r^2$. Volume of the material = $(4/3)\,\pi r^3$. Hence, neutron production rate $\propto r^3$. Therefore,

$$\frac{\text{Escape rate of neutrons}}{\text{Production rate of neutrons}} = \frac{\text{Surface effect}}{\text{Volume effect}} \propto \frac{1}{r}$$

(Here, the nonfission capture of neutrons has been ignored).

From the above approximate relation, it is evident that to reduce the neutron loss, size of the material must be increased. For a particular value of size (i.e. r), the rates of loss and production are balanced to give $K = 1$. It gives the critical size (i.e. $r_{critical}$). Thus, by exceeding the critical size, the fission chain reaction may be set up as represented in Fig. 7.13.1.1.

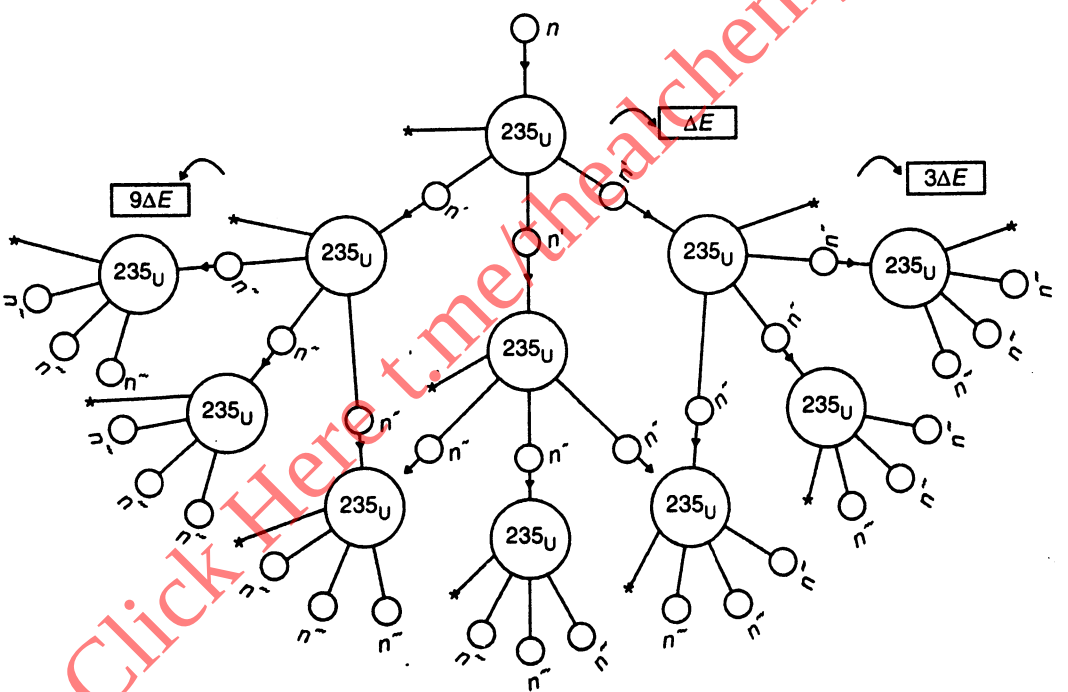

Fig. 7.13.1.1. Fission of ^{235}U by neutrons in a chain process (* denotes the fission products); at the n-th step, number of available neutrons is given by 3^n (considering the reproduction factor 3).

7.13.2 The Fertile and Fissile Nuclides as the Nuclear Fuels

In discussing the energetics and activation energy of nuclear fission, it has been found that the **three nuclides, ^{233}U, ^{235}U and ^{239}Pu** are the most promising ones. In this connection it is worth mentioning that for ^{238}U, K_∞ is 0.5. Thus, ^{238}U can never undergo the chain process of nuclear fission.

The fissile nuclides are very often artificially synthesised from the ***fertile*** **nuclides** (e.g. ^{232}Th, ^{238}U) which are not themselves fissionable but can produce the **fissile nuclides.**

Click Here t.me/thealchemylibrary

$^{238}_{92}U$: The naturally occurring uranium source contains only a negligible fraction of ^{235}U and the bulk fraction is ^{238}U. Hence, the sample must be enriched in ^{235}U content. The methods of enriching of ^{235}U have been discussed in Sec. 5.2.6.

$^{233}_{92}U$: It is again fissionable by the slow neutrons. This isotope is synthesised from ^{232}Th as follows.

$$^{232}_{90}Th + ^{1}_{0}n \xrightarrow{\text{resonance capture}} ^{233}_{90}Th^{*} \xrightarrow[(t_{1/2} = 23.5 \text{ min})]{\beta^-} ^{233}_{91}Pa \xrightarrow[(t_{1/2} = 27.5 \text{ d})]{\beta^-} ^{233}_{92}U$$

In our country, it has a potential source. The Western Coast is rich in $^{232}_{90}Th$ content.

$^{239}_{94}Pu$: It is synthesised from ^{238}U.

$$^{238}_{92}U + \underset{\text{(slow)}}{^{1}_{0}n} \xrightarrow{\text{resonance capture}} ^{239}_{92}U^{*} \xrightarrow[(t_{1/2} = 23.5 \text{ min})]{\beta^-} ^{239}_{93}Np \xrightarrow[(t_{1/2} = 2.3 \text{ d})]{\beta^-} ^{239}_{94}Pu$$

Though the naturally occurring ^{238}U is not a nuclear fuel, it can be utilised as a potent source of the nuclear fuel, ^{239}Pu. In our country, the first atom bomb experimented was made of ^{239}Pu. Thus ^{238}U and ^{232}Th are considered as the ***fertile nuclides.***

7.13.3 Atom Bomb

The working principle of an atom bomb depends on the conditions required for maintaining a self-sustained (i.e. chain reaction) nuclear fission. ^{235}U or ^{239}Pu are used as fuels. In the skeleton of an atom bomb, the fissile fuels are kept in two or several pieces, each of which is less than the ***critical mass.*** But on combination, they produce a ***supercritical size.*** Once the supercritical size is attained, the stray neutrons available from cosmic rays are sufficient to initiate the process leading to an uncontrollable explosion instantaneously. For this uncontrollable explosion, $K > 1$. In addition to the stray neutrons, a neutron source like $Ra + Be$ can also be placed to act as an initiator.

The explosive character of the bomb largely depends on the rapidity with which the ***subcritical masses*** **combine to produce a** ***supercritical mass.*** If it is carried out slowly, the explosion will not go on violently. The combining of the subcritical masses may be carried out in any one of the processes shown in Fig. 7.13.3.1. The two separated subcritical masses may be brought together by driving a very high speed trigger mechanism set up by an ordinary explosion (see Fig. 7.13.3.1a). The subcritical masses are kept separated by a spacer which can be removed away at the time of action through a trigger mechanism (see Fig. 7.13.3.1b). The subcritical masses may be kept on the periphery of a circle. The peripheral masses can be brought together at the centre of the circle through a high speed trigger at the time of explosion (see Fig. 7.13.3.1c).

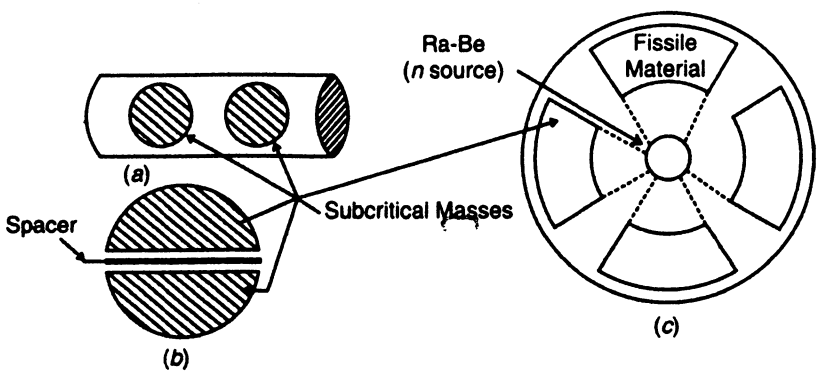

Fig. 7.13.3.1. Different ways to keep the subcritical masses of the fissile material in an atom bomb.

Click Here t.me/thealchemylibrary

The first atom bomb came to us in its most cruel form during the 2nd World War. The ***Little Boy*** was dropped on Hiroshima at 8.11 AM on August 6, 1945 from an altitude of 31,600 feet, and the second curse by name ***Fat Man*** came to Nagasaki at 11.02 AM on 9th August, 1945. The terrific explosive destruction occurred there is known to everyone. The ***Little Boy*** had two blocks of ^{235}U at the ends of a barrel which was operated through a trigger. The ***Fat Man*** had ^{239}Pu as its fuel. The total destructive powers of these bombs were equivalent to ~ 36 kilotonnes of TNT (trinitrotolune). The *Fat Man* was more destructive (~ 23 kilotonnes of TNT). The temperature was raised to ~ 10^7 °C and the atmospheric pressure was raised to several million times of normal pressure almost instantaneously. The explosions also produced a violent blast of visible, ultraviolet, X-ray and γ-radiation followed by a ***Black Rain*** full of radioactive ashes along with a number of radioactive elements which are still waiting to bear and propagate the memories of the saddest event.

7.13.4 Fermi's Four Factor Formula and Nuclear Reactor or Atomic Pile for the Controlled Nuclear Fission

In atom bomb, the reproduction factor is significantly higher than unity, i.e. $K > 1$. This is why, the process goes beyond our control leading to an explosion. But by choosing the external factors, the reproduction factor can be made just slightly higher than unity or equal to unity. In this connection ***Fermi's four factor formula*** which gives an idea how to optimise the situation is important. For nuclear reactors, the *delayed neutrons* (cf. Section 7.12.2c) play an important role.

(a) Fermi's four factor formula

This is very much important in connection with the steady rate for energy production in a nuclear reactor. This is illustrated for the fission of uranium.

(a) ***Fast neutron factor*** **(η) :** The slow neutron (i.e. thermal neutrons) first produces fast neutrons i.e. prompt neutrons (about 2.44 per fission of ^{235}U) in a fission. If the fission process is started with N *slow neutrons*, then it will generate ηN neutrons where η is called *fast neutron factor*. Thus η gives the average number of fast neutrons generated from each thermal neutron fission of ^{235}U and η is taken as 2.44.

(b) ***Fast fission factor*** **(ε) :** Out of the ηN fast neutrons, some cause fission in ^{238}U to generate fast neutrons. Consequently, the number of fast neutrons will be increased to $\eta N\varepsilon$ where ε is called ***fast fission factor.***

(***Note*** **:** η = 2.44 for ^{235}U; and η = 2.5 for natural uranium which contains about 0.72% ^{235}U. Only thermal neutrons can cause fission in ^{235}U but not in ^{238}U. However, the fast neutrons released from the fission of ^{235}U can cause fission in ^{238}U to release fast neutrons. This is why, apparently η becomes 2.5 for the natural uranium. Actually η (= 2.5) incorporates the factor ε which is about 1.03. It makes, 2.44 × 1.03 = 2.5).

(c) ***Fast neutron leakage factor*** **(l_f) :** Because of the finite size of the reactor, some fraction of the fast neutrons will be lost due to the leakage problem. So the number of fast neutrons remaining in the reactor after leakage is given by $\eta N\varepsilon\ (1 - l_f)$ when l_f denotes *the leakage factor*. The leakage factor can be minimised by increasing the size of the reactor.

(d) ***Resonance escape probability (p) and resonance capture loss*** **:** It is expected that the $\eta N\varepsilon(1 - l_f)$ fast neutrons will meet the moderator (e.g. graphite, heavy water, etc.) and *thermalisation* will occur through the successive collisions between the fast neutrons and the

Click Here t.me/bealchemylibrary

atoms of moderator. If there is no loss neutron during the thermalisation process, we should get the $\eta N\varepsilon\ (1 - l_f)$ slow neutrons. But during the thermalisation process, the neutrons with some specific energies described as ***resonance energies*** will be captured (called ***resonance capture***, cf. Sec. 7.7) by ^{238}U. For the target nuclide ^{238}U, the resonance capture of neutron occurs for the energy values 6, 20 and 38 eV of the incident neutron.

$$^{238}_{92}U + ^{1}_{0}n \xrightarrow[\text{capture}]{\text{resonance}} \left[^{239}_{92}U^{*}\right] \xrightarrow{\beta^-,\gamma} ^{239}_{93}Np \xrightarrow{\beta^-,\gamma} ^{239}_{94}Pu$$

The resonance capture produces the compound nucleus $^{239}U^*$ which experiences β-decays to produce the isobaric nuclides ^{239}Np and ^{239}Pu. If p is the ***resonance escape (i.e. avoidance) probability***, then the fraction of neutrons lost during the thermalisation process through resonance capture is given by $(1 - p)$. In other words, the number of neutrons which can escape (i.e. avoid) the resonance capture is $\eta N\varepsilon\ (1 - l_f)\ p$. Thus the number of slow neutrons produced after the thermalisation process is given by : $\eta N\varepsilon(1 - l_f)p$.

(e) ***Slow neutron leakage factor*** (l_s) : Some of the slow neutrons will be lost due to leakage from the reactor. Thus the total number of available slow neutrons obtained after leakage is given by :

$$\eta N\varepsilon\ (1 - l_f)\ p\ (1 - l_s)$$

Again l_s can be minimised by increasing the size of the reactor.

(f) ***Thermal utilisation factor*** (f) : Different impurities in the fuel, structural components of the reactor, different fission product with high neutron capture cross section will absorb a certain fraction of the slow neutrons. If the fraction of slow neutrons lost in this path is given by $(1 - f)$ then the total number of slow neutrons available for causing fission in ^{235}U is given by :

$$\eta N\varepsilon(1 - l_f)\ p\ (1 - l_s)\ f$$

In terms of ***multiplication factor*** (K), we can write :

N thermal neutrons produce $\eta N\varepsilon\ (1 - l_f)\ (1 - l_s)\ fp$ thermal neutrons in first generation or cycle i.e.

$$\boxed{KN = \eta N\varepsilon\ (1 - l_f)\ (1 - l_s)\ fp}$$

For a very large reactor, l_f and l_s may be taken as zero (i.e. no loss of neutron due to leakage) and it leads to :

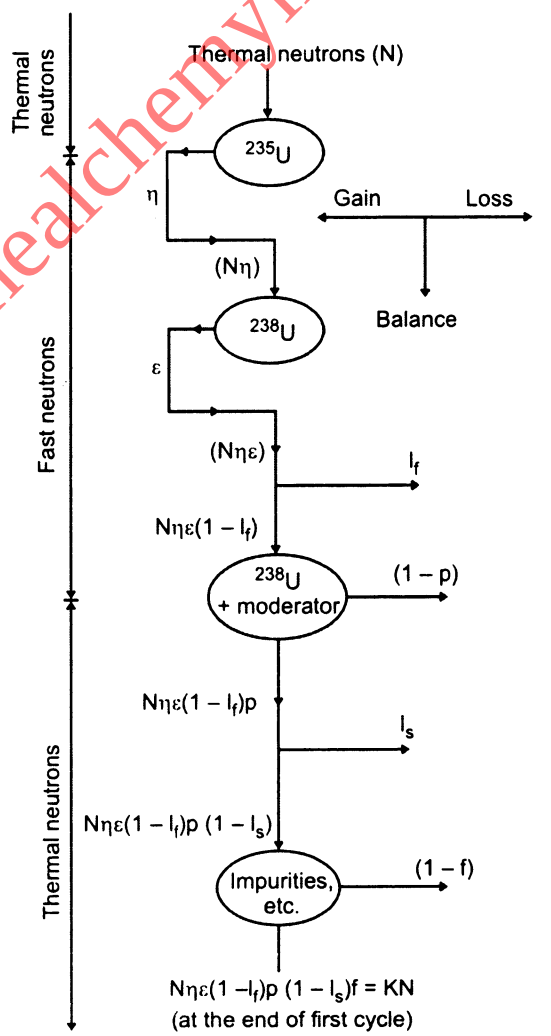

Fig. 7.13.4.1. Generation of thermal neutrons in a fission reactor and the multiplication factor.

Click Here t.me/thealchemylibrary

$$K_\infty N \approx \eta N \varepsilon f p, \text{ } (\infty \text{ stands for the large size reactor) i.e. } K_\infty = \eta \varepsilon f p$$

The above relation is described as **Fermi's *four factor formula.*** Depending on the value of K, the following situations may arise :

(i) ***K* ≈ 1 (*steady state*) :** The number of available slow neutrons in each generation or cycle remains the same. It makes the rate of energy output constant. In reality, for the *steady state* condition, K should be slightly greater than unity because in practice l_f and l_s can never be zero.

(ii) ***K* > 1 (*divergent state*) :** The energy output rate increases from cycle to cycle. Ultimately, it leads to an *explosion.*

(iii) ***K* < 1 (*convergent state*) :** It leads to stop the fission chain and the energy output rate gradually decreases and ultimately the reactor is quenched.

(b) Construction of a nuclear reactor

The construction of a reactor depends on the purpose for which it is being designed. It is being constructed for various purposes such as : conversion of atomic energy into electricity; atomic energy to run ships, submarines etc.; synthesis of different radioisotopes; research works; etc.

The principal units of a reactor are discussed below.

(i) ***The Reaction Core* :** Here the nuclear fission goes on. The nuclear fuels along with the nonfissionable material are arranged in such a way that K becomes unity.

(ii) ***The Moderator* :** It has been already discussed that the fission cross-section for the slow neutrons is about 450 times higher than that for the fast neutrons in the case of ^{235}U. Hence to carry out the nuclear fission effectively, the emitted ***prompt neutrons*** which are fast neutrons must be thermalised. For this purpose, moderators are required. To maximise the loss of kinetic energy of the neutrons through collisions, **the materials of low atomic mass** (see Sec. 6.18.3) **are preferred.** *But the material chosen must have a very low cross-section with respect to the neutron capture process.* For this purpose, graphite, beryllium oxide and heavy water (D_2O) are the most promising ones. The process of slowing down and thermalisation is represented in Fig. 7.13.4.2.

Here it may be noted that the deuterons (present in heavy water) are less likely to capture the neutrons than the protons (present in ordinary water). ***This is why, heavy water is used as a moderator but ordinary water is not used as a moderator.***

Depending on the nature and use of moderator, the reactors are classified as ***thermal reactors*** and ***fast reactors.*** Generally, the coolant used very often acts as the moderator. In thermal reactors, the use of a good moderator produces the sufficient thermal or slow neutrons from the fast neutrons. These thermal neutrons are highly efficient in causing the nuclear fission of ^{235}U (σ for the thermal neutrons ~ 580 barn). **Such neutrons as in PHWR (pressurised heavy water reactor) needs no enriched fuel. In fast reactors, the moderator is not efficient and it needs enriched fuel.** It happens so in BWR (boiling water reactor), PWR (pressurised water reactor) and LWGR (light water cooled graphite reactor) (to be discussed later). The loss of neutrons is reduced by using a neutron reflector.

(iii) ***The Controlling Device* :** To control the process, the necessary preventive measures must be taken so that the reproduction factor does not significantly exceed unity. For this purpose, some materials are used to absorb the thermalised neutrons efficiently. In this regard, *the*

Click Here t.me/thealchemylibrary

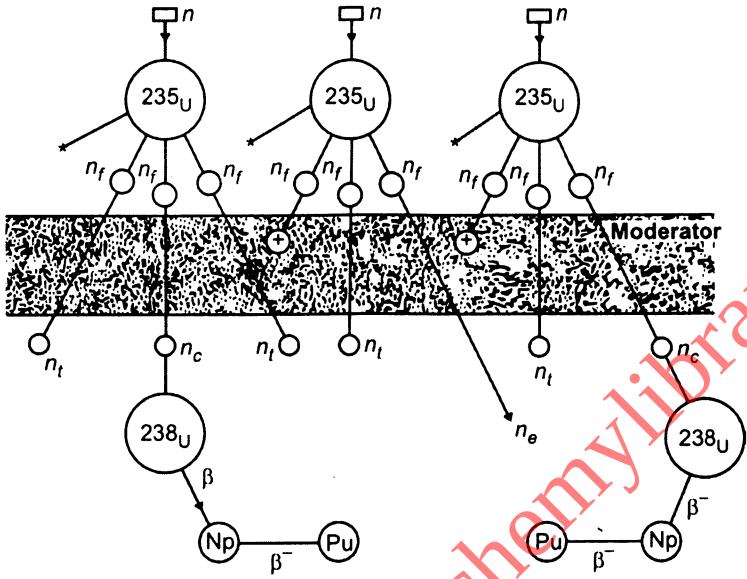

Fig. 7.13.4.2. Schematic representation of a moderator, * denotes the fission product, n = thermal (i.e. slow) neutron to start the process, n_f = fast neutron, n_t = thermalised neutrons available for fission at the next steps, n_c = neutrons captured by ^{238}U, n_e = escaping neutron, + indicates absorbed neutron by the moderator.

Click Here t.me/thealchemylibrary

nonfissile material such as boron or cadmium having a large neutron capture cross-section is selected. These are placed in the reactor in such a way that they can be moved up and down by an external mechanical device. When the energy release becomes violent (exceeding a certain limit), the rods are pushed down to absorb the thermal neutrons and thus the reactor dies down. To activate or build up the reactor, the rods are pulled out. In practice, an automatic device works on the controlling rods depending on the temperature raised in the reactor.

(iv) ***Cladding of nuclear fuel*** **:** Fuel materials (either in the form of rod or tablet) are packed (i.e. clothed) in *clad tubes*. The clad tubes are metal casing (*Al* or *Zr-Al* alloy) and the clad tubes prevent the release of fission products to the surrounding coolant. Thus, *cladding (≡ clothing) of nuclear fuel is quite important.*

(v) ***The Coolant*** **:** It is required to remove the heat generated in the fission to the site of utilisation. For this purpose, different fluids such as : *high boiling liquids* (e.g. liquid *Na* or *K*), *water*, *air blast*, etc. are used. Thus, the heat transferred from the reactor is utilised in generating power.

Water at *high pressure* (so that it cannot boil easily) is very often used as a coolant. In a ***pressurised water reactor*** **(PWR),** water is circulated at about 150 atm pressure to abstract the heat which is utilised in a *heat exchanger* to produce steam. Thus the steam produced is used to drive a turbine to generate electricity. In a ***boiling water reactor*** **(BWR),** water is circulated at about 70 atm pressure and it is *directly* allowed to boil to produce the steam. In a ***pressurised heavy water reactor*** **(PHWR),** heavy water is used both as a *moderator* and as a *coolant*. In a PHWR, *natural uranium can be used as a fuel* without any enrichment because heavy water is

a very good moderator. In fact, in a PHWR, along with the electricity, another nuclear fuel ^{239}Pu is obtained from the unused ^{238}U.

Light water cooled graphite reactors **(LWGR)** are also known. It is evident that in BWR, PWR and LWGR, light water (i.e. ordinary water) is used as the coolant and light water is not a good moderator. **Thus in such cases, the number of fission causing neutrons (i.e. thermal neutrons) is less and to run such reactors, we need the enriched fuel** (i.e. **% ^{235}U should be relatively high**). In PHWR, the heavy water used as a coolant is also a very good moderator and no such enriched fuel is required. Among the different reactors, PWR is the most popular one.

(vi) ***The Reactor Shield*** **:** From the reactor, high energy γ-rays, β^--rays, neutrons and heat waves come out. These are hazardous. To minimise the effect, a shielding over the reactor is essentially required. To the vicinity of the core, a thick iron covering is placed to cut down the radiations emerging from the reactor. **This first shield is referred to as *thermal shield.*** Outside the thermal shield, a concrete barrier is placed to absorb the radiations coming from the thermal shield. *This second shield is called the biological shield.*

A schematic representation of a power reactor is shown in Fig. 7.13.4.3. In a ^{235}U-run reactor, for initiating the process, the neutrons are generated by the action of alpha -particles from polonium on beryllium.

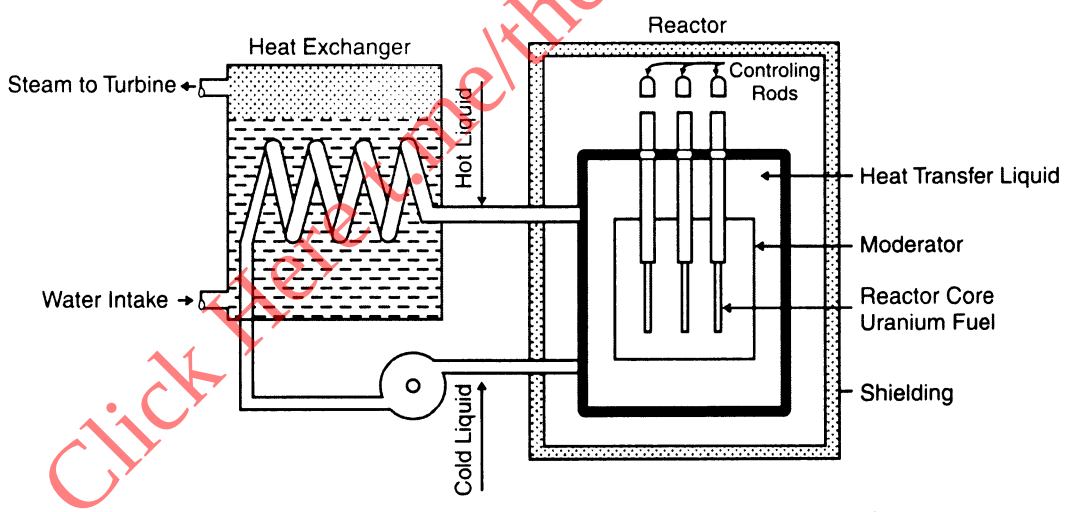

Fig. 7.13.4.3. Schematic representation of the different units of a nuclear reactor.

Click Here: me/theachemylibrary

7.13.5 Breeder Reactor

To enrich ^{235}U content from the naturally occurring source containing predominantly ^{238}U is a very laborious task. This is why, in a Breeder Reactor, ^{239}Pu produced from ^{238}U is utilised as a nuclear fuel. **^{239}Pu is a fissile nuclide *by both the slow and fast neutrons.***

$$^{238}_{92}U + {}^{1}_{0}n \xrightarrow{\text{resonance capture}} {}^{239}_{92}U^{*} \xrightarrow[(t_{1/2} = 23.5 \text{ min})]{\beta^-, \gamma} {}^{239}_{93}Np \xrightarrow[(t_{1/2} = 2.3 \text{ d})]{\beta^-, \gamma} {}^{239}_{94}Pu$$

In this process, first, a significant amount of ^{239}Pu is generated by using a flux of slow neutrons on natural uranium containing predominantly ^{238}U. The produced ^{239}Pu being chemically different from uranium can be separated easily. When a sufficient amount of ^{239}Pu is produced, it is used in the form of a rod as a nuclear fuel in the reactor known as ***fast breeder reactor.*** The ^{239}Pu rods are enclosed by the natural uranium. ***No moderator is used as the fission of ^{239}Pu goes on by both the fast and slow neutrons.*** The neutrons escaping from the core get absorbed by the surrounding uranium-238 to generate the fuel ^{239}Pu. **Thus, in one zone, the fuel is being consumed, while in the other zone, the same fuel is being generated. It is also possible to generate more fuels than that gets consumed.**

Similarly the mixture of uranium-233 and thorium-232 can also be used as a fuel in the breeder reactor.

$$^{232}_{90}Th + {}^{1}_{0}n \xrightarrow{\text{resonance capture}} {}^{233}_{90}Th \xrightarrow[(t_{1/2} = 23.5 \text{ min})]{\beta^-, \gamma} {}^{233}_{91}Pa \xrightarrow[(t_{1/2} = 27.5 \text{ d})]{\beta^-, \gamma} {}^{233}_{92}U$$

^{233}U is a fissionable nuclide. Thus, compared to the reactor run by ^{235}U, the breeder reactor in which a mixture of natural uranium and plutonium-239 (or, $^{233}U + {}^{232}Th$) is used gains some advantages. The main problem in the ^{235}U-run reactor is to get the fuel, but in the breeder reactor, no such problem appears. Because of this fact, this ***miracle machine***, i.e. the breeder reactor, has appeared with an enormous promise.

Uranium-plutonium mixed oxide ($UO_2 + {}^{239}PuO_2$) having about 25% PuO_2 is generally used as a fuel in fast breeder reactors.

7.13.6 A Natural Fission Reactor : Okla Phenomenon

It is now established that about two billion years ago when ^{235}U content in natural sources was relatively higher, nature had set up a fission reactor at ***Okla mine*** (in Western Africa). It is believed that rain water leached uranium salts present in Okla rocks into some pockets where ^{235}U was concentrated enough to initiate a fission chain reaction. Water accumulated there acted as a moderator. Probably it went on for about 60,000 to 150,000 years.

7.13.7 Nuclear Reactors in India

In India, there are establishments of a number of reactors. These are : Apsara (1956), Cirus (1960), Zerlina (1961), Tarapur (1969), Purnima I (1972), Kota (1973), Purnima II (1976), Kalpakkam I (1983), Kalpakkam II (1985), Dhruva (1985), Fast Breeder Reactor at Kalpakkam (1985), Narora-I (1990), Narora-II (1991), Kakrapar-I, II (1991-92). Kaiga-I and II (1995-96), Rajasthan III (1995-96), Kaiga-III-VI (1996-97), Tarapur-III and IV (1997-98), Rajasthan-V-VIII (1998-2000), Kudankulam-I and II (1998-99) and many other new projects.

Note : The topics like ***Nuclear Reactor Waste Management, Nuclear Reactor Accidents*** (e.g. *Chernobyl* in USSR in 1986, *Three Mile Island* in USA in 1979, etc.) have been discussed in the book, "Inorganic Chemistry : Biological and Environmental Aspects" by Asim K. Das, Books & Allied, Kolkata, 2004.

7.13.8 Recovery of Uranium and Plutonium from Spent Fuel

The spent fuel is cooled and kept in a safety place to allow the decay of all short-lived radioisotopes.

Click Here t.me/thealchemylibrary

However, to avoid the radiation hazard, all steps are remote controlled. By using HNO_3, *U* and *Pu* are dissolved out from the cladding material and they are separated by using *solvent extraction* and *anion exchange resin*. The steps are shown in Scheme 7.13.8.1.

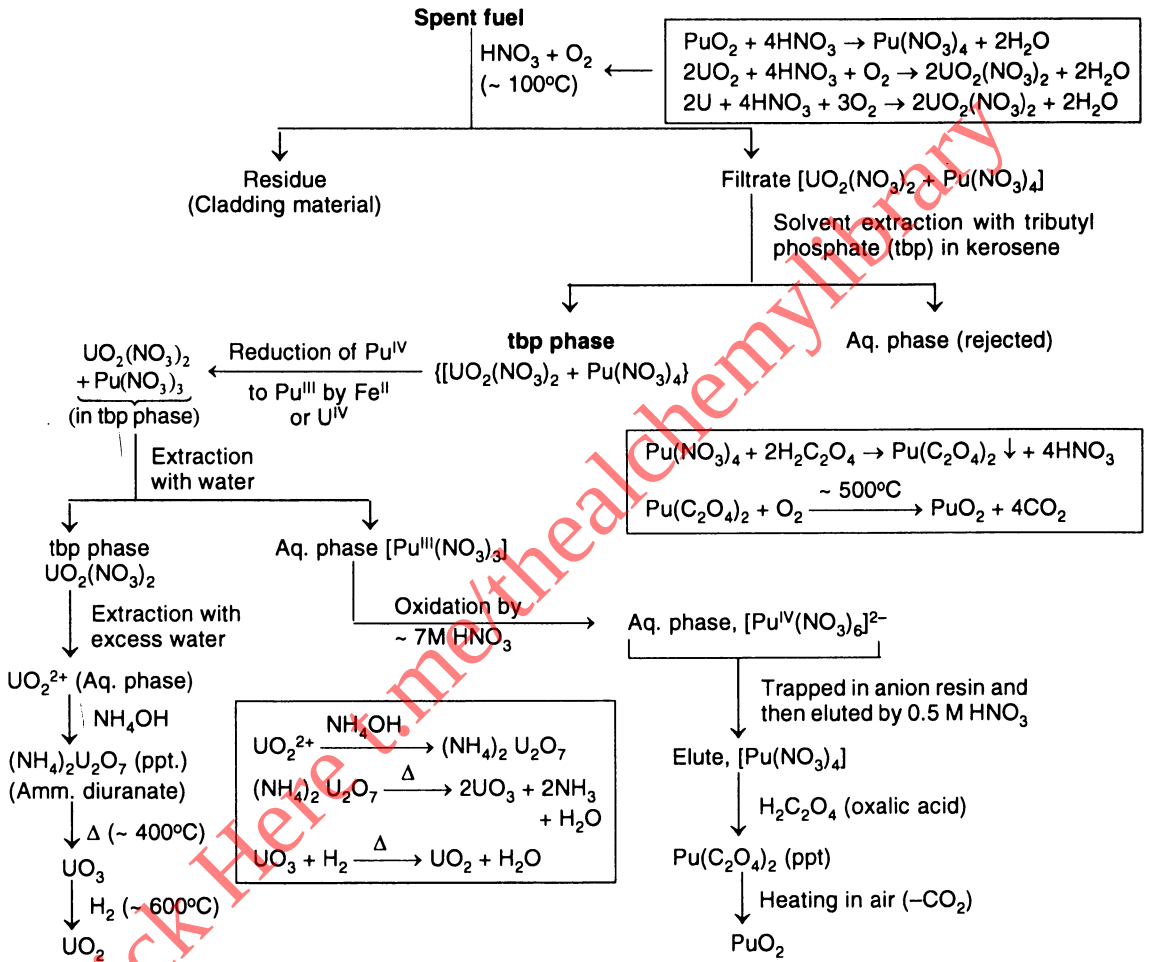

Scheme 7.13.8.1. Schematic representation of the steps for recovery of uranium and plutonium from the spent fuel.

Click Here to meet the chemyll library

7.14 NUCLEAR FUSION – THERMONUCLEAR REACTION

7.14.1 Characteristic Features of Nuclear Fusion

The nuclear binding energy curve (see Fig. 5.3.5.1) indicates that the stable nuclides are characterised by $\overline{B}$ = 8-8.5 MeV. **The heavier nuclides through fission move to stable region while the lighter elements move to this stable region through fusion.** Among the lighter elements, ^4_2He is probably the most striking one as it is having a comparatively higher $\overline{B}$ value (≈ 7 MeV). For example, for ^2_1H,

the $\overline{B}$ value is ~ 1 MeV. This is why, such lighter nuclides having very low nuclear binding energies will have a tendency to undergo fusion to reach the station, ${}^{4}_{2}He$. This driving force can be well understood from the calculation of mass defect in forming the respective nuclides.

${}^{2}_{1}H$ (i.e. deuteron) : Isotopic mass = 2.01419 amu; mass of the constituents (i.e. one proton and one neutron) = 2.01653 amu.

Hence, mass defect = (2.01653 – 2.01419) amu = 0.00234 amu
≡ 0.00234 × 931 MeV = 2.0 MeV; i.e. $\overline{B}$ = 1 MeV

${}^{4}_{2}He$ (i.e. helium) : Isotopic mass = 4.00298 amu. Mass of the constituent nucleons = 4.03328 amu.

Hence, mass defect = (4.03328 – 4.00298) amu = 0.0303 amu
≡ 0.0303 × 931 MeV = 28 MeV; i.e. $\overline{B}$ = 7 MeV.

To consider this process, i.e. fusion, only very light nuclides (e.g. ${}^{1}H$, ${}^{2}H$) are important. When the nuclides proceed to fuse with each other, they experience the ***Coulombic potential barrier*** (E_{Coul}) which is proportional to $Z_1Z_2/(R_1 + R_2)$. The height of the potential barrier depends on the product of the nuclear charges of the nuclides to be fused. Classically, to surmount the potential barrier, the required kinetic energy of the lighter nuclides can be attained at the temperature of the order of 10^7–10^8 °C which prevails only in the interior parts of the stars. For the relatively heavier nuclides, the potential barrier is still higher. Thus, it appears that to initiate the nuclear fusion, the temperature should be tremendously high (~ 10^7 °C) which can only be attained on earth through a nuclear fission.

This is why, the nuclear fusion reactions are referred to as the ***thermonuclear reactions.*** However, once the process is started, the energy liberated can sustain the process automatically. Thus, the process can be defined as :

the nuclear fusion is a process which occurs at a tremendously high temperature (of the order of ~ 10^7–10^8 °C) through the combination or fusion of two or more lighter nuclides (e.g. ${}^{1}H$, ${}^{2}H$) to produce a relatively heavier and stabler nuclide (e.g. ${}^{4}_{2}H$).

The temperature at which the hydrogen nuclides undergo fusion makes the hydrogen atoms completely ionised producing free electrons and positively charged nuclei. **This state of matter is referred to as plasma.** Examples :

$$\text{(i) } 4\,{}^{1}_{1}H \rightarrow {}^{4}_{2}He + 2\,{}^{0}_{+1}e + 27 \text{ MeV}; \quad \text{(ii) } 2\,{}^{2}_{1}H \rightarrow {}^{4}_{2}He + 24 \text{ MeV};$$

7.14.2 Hydrogen and Cobalt Bomb

In the thermonuclear bomb known as the *hydrogen bomb*, the basic reaction involves the fusion of hydrogen nuclei to form helium nuclei. The required temperature for this purpose is created by the explosion of a fission bomb placed at the centre. Thus in the hydrogen bomb, there is a small core of ${}^{235}U$ or ${}^{239}Pu$ bomb to function as a *detonator*. This is surrounded with a mixture of deuterium and tritium. Through the explosion of the fission bomb at the centre, the fusion process is started and continued with the liberation of a tremendous amount of energy. The destructive power of this thermonuclear bomb is frightening the whole mankind.

The probable reactions set in the hydrogen bomb are given below.

$${}^{3}_{1}H + {}^{2}_{1}H \rightarrow {}^{4}_{2}He + {}^{1}_{0}n + 17 \text{ MeV}; \quad {}^{3}_{1}H + {}^{1}_{1}H \rightarrow {}^{4}_{2}He + 20 \text{ MeV}; \quad {}^{3}_{1}H + {}^{3}_{1}H \rightarrow {}^{4}_{2}He + 2\,{}^{1}_{0}n + 11 \text{ MeV}$$

Click Here t me/thealchemylibrary

In the hydrogen bomb, there is no critical size in contrast to the atom bomb. This is why, hydrogen bomb of any size can be prepared.

The hydrogen bomb has been modified to the cobalt bomb which is more alarming to the mankind. In the ***cobalt bomb***, the hydrogen bomb is encapsulated within a thick sheath of cobalt. The flux of neutrons emitted from the fusion process produces the radioisotope ^{60}Co through the (n, γ) process. The intense radioactivity emanated from ^{60}Co is alarmingly lethal to the living kingdom, and the cobalt bomb covers a larger area of destruction compared to that by a hydrogen bomb.

7.14.3 Stellar Energy

Many stars and our sun have been emitting an enormous amount of energy continuously for millions and millions of years. Now it is believed that the thermonuclear reactions as in the hydrogen bomb are going on there. During the birth of the stars, due to the *enormous gravitational collapse*, the temperature developed in the interior parts of the stars was exceedingly high of the order of 10^7–10^8 °C. At this temperature, the matter remains in a ***plasma state*** and the fusion reaction, i.e. fusion of hydrogen nuclides to produce helium nuclides, is established. As a matter of fact, our sun contains about 35% hydrogen of its weight.

In 1938, Bethe and Weizsacker proposed independently different cyclic processes known as : (i) *carbon-nitrogen cycle*, (ii) *carbon-nitrogen-oxygen bicycle*, and (iii) *proton-proton cycle* to carry out the fusion process.

Carbon-nitrogen (CN) cycle : This is also called ***Bethe*** **cycle.** The cyclic process leading to the combination of four protons into a helium nucleus passes through the intermediary role of ^{12}C and ^{14}N nuclei. The process is shown below.

(i) $^{12}_{6}C + {}^{1}_{1}H \rightarrow {}^{13}_{7}N + Q_1$;

(ii) $^{13}_{7}N \xrightarrow[(t_{1/2} = 10.1\,\text{min})]{} {}^{13}_{6}C + {}^{0}_{+1}e + {}^{0}_{0}\nu + Q_2$;

(iii) $^{13}_{6}C + {}^{1}_{1}H \rightarrow {}^{14}_{7}N + Q_3$;

(iv) $^{14}_{7}N + {}^{1}_{1}H \rightarrow {}^{15}_{8}O + Q_4$;

(v) $^{15}_{8}O \xrightarrow[(t_{1/2} = 2.05\,\text{min})]{} {}^{15}_{7}N + {}^{0}_{+1}e + {}^{0}_{0}\nu + Q_5$;

(vi) $^{15}_{7}N + {}^{1}_{1}H \rightarrow {}^{12}_{6}C + {}^{4}_{2}He + Q_6$

i.e. (i) + (ii) + (iii) + (iv) + (v) + (vi) lead to :

$4\,{}^{1}_{1}H \rightarrow {}^{4}_{2}He + 2\,{}^{0}_{+1}e + 2\,{}^{0}_{0}\nu + \sum Q\,(= 28\ \text{MeV})$.

Thus, in the cycle, carbon and nitrogen nuclei act as catalysts. The whole cycle is represented schematically in Fig. 7.14.3.1. The cycle moves clockwise. The carbon-nitrogen cycle involves the participation of the relatively heavier nuclides like ^{12}C and ^{14}N. This is why, it is believed that the cycle predominantly operates in the **red giant stars** having a very high temperature ($\geq 10^8$ °C).

Click Here t.me/thearchemyjlibrary

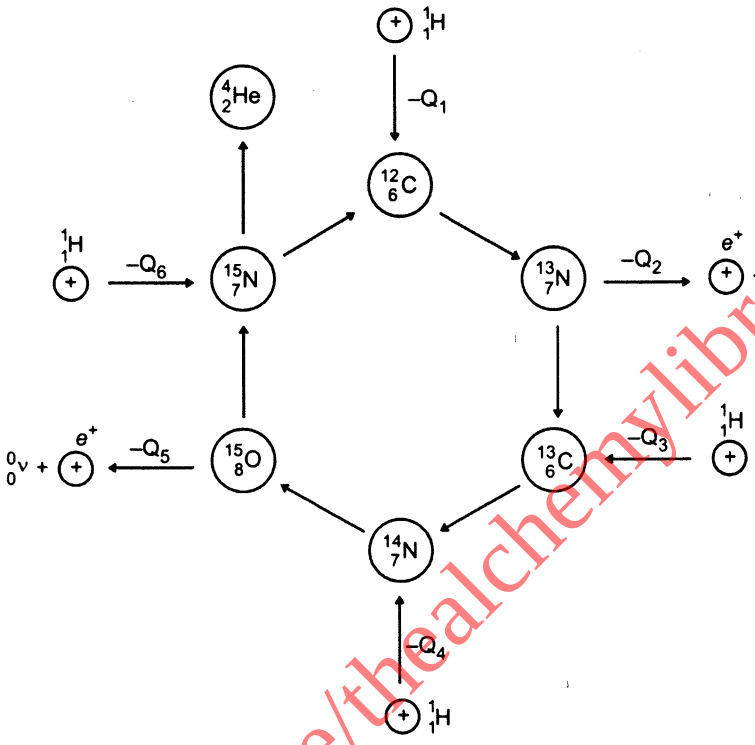

Fig. 7.14.3.1. Possible carbon-nitrogen cycle in stellar energy production.

Carbon-nitrogen-oxygen (CNO) bicycle : The reactions to maintain the *CNO* bicycle to produce helium from hydrogen are shown below :

(i) $^{15}_{7}N + {}^{1}_{1}H \rightarrow {}^{16}_{8}O + Q_1$

(ii) $^{16}_{8}O + {}^{1}_{1}H \rightarrow {}^{17}_{9}F + Q_2$

(iii) $^{17}_{9}F \rightarrow {}^{17}_{8}O + {}^{0}_{+1}e + {}^{0}_{0}\nu + Q_3$

(iv) $^{17}_{8}O + {}^{1}_{1}H \rightarrow {}^{14}_{7}N + {}^{4}_{2}He + Q_4$

Here, the starting nuclide $^{15}_{7}N$ originates from the *CN* cycle. It is important to point out that $^{14}_{7}N$ produced may be also utilised in the *CN* cycle. **This is why, the present cycle is described as a *bicycle*.** The *CNO* bicycle occurs less frequently than the *CN* cycle.

Proton-proton cycle : Here it is believed that a direct combination of two protons produces a deuteron which participates in the next reactions as follows.

(i) $^{1}_{1}H + {}^{1}_{1}H \rightarrow {}^{2}_{1}H + {}^{0}_{+1}e + {}^{0}_{0}\nu + Q_1$

(ii) $^{2}_{1}H + {}^{1}_{1}H \rightarrow {}^{3}_{2}He + Q_2$

(iii) $^{2}_{1}H + {}^{2}_{1}H \rightarrow {}^{3}_{2}He + {}^{1}_{0}n + Q_3$

Click Here t.me/thealchemylibrary

The chain may get transmitted in the following ways.

$$\text{(iv)}\quad {}^{3}_{2}He + {}^{1}_{1}H \rightarrow {}^{4}_{2}He + {}^{0}_{+1}e + {}^{0}_{0}\nu + Q_4$$

$$\text{(v)}\quad {}^{3}_{2}He + {}^{3}_{2}He \rightarrow {}^{4}_{2}He + 2\,{}^{1}_{1}H + Q_5$$

In the proton–proton cycle, the potential barrier experienced by the nuclides is less compared to that in the carbon-nitrogen cycle. **This is why, it is believed that this cycle is important for the stars like our sun where the temperature is relatively lower (of the order of 10^7 °C).**

7.14.4 Controlled Fusion Reactions : An Innocent and a Never-Ending Source of Energy

Compared to the nuclear fission, the nuclear fusion process as a source of energy is preferable in the following points.

Fuels **:** It uses hydrogen as a fuel. The oceans are the infinite sources of hydrogen. On the other hand, in the nuclear fission, the fuels are limited and it is also very difficult to have the fuels in the required form.

Here it is to be mentioned that though in the sun and stars, the normal hydrogen (which is abundant) undergo fusion to produce energy, the most feasible fusion reaction is the fusion of *deuterium* and *tritium*. In fact, fusion of the **heavier isotopes of hydrogen, deuterium (D) and tritium (T) is more practicable because of the *larger reaction cross section* and *lower threshold temperature.***

$${}^{2}_{1}H + {}^{3}_{1}H \rightarrow {}^{4}_{2}He + {}^{1}_{0}n + 17.6\ \text{MeV}$$

i.e. fusion of deuterium $\left({}^{2}_{1}D\right)$ and tritium $\left({}^{3}_{1}T\right)$.

Abundance of deuterium in water is very poor (ca. 1 part in 6500 parts). Another fuel is weakly radioactive tritium which practically does not exist in nature. It can be prepared in the fusion reactor in the following nuclear reaction.

$${}^{6}_{3}Li + {}^{1}_{0}n \rightarrow {}^{3}_{1}H + {}^{4}_{2}He$$

The projectile neutron is obtained from the fusion of deuterium and tritium. ***Thus, the fuels for the said fusion reaction are deuterium and lithium-6.*** ^{6}Li can breed the reactant fuel ^{3}H. This is why, the fusion reactor for the said fusion reaction is of ***breeder type.***

Radiation hazard **:** The nuclear fission gives the birth to a number of radioisotopes which in turn may create unmanageable problems. Actually, it creates a headache how to preserve the nuclear reactors when they will be exhausted. We have witnessed the *Chernobyl disaster* (1986) in USSR. In the fusion process, no alarming radioisotopes (except some ${}^{3}_{1}H$) are generated. Thus, the question of radiation hazard does not arise.

In spite of the above advantages, to execute the process in practice, there are some almost unsolvable (at least, presently) problems to the scientists. To set up the reaction, it requires a temperature of the order of 10^7 °C at which the matter exists in the ***plasma state.*** In the hydrogen bomb, the condition is attained by using an explosive nuclear fission. **In fact, it is a problem, how to get this temperature.**

Another problem is how to keep the plasma state. No container on our earth can tolerate this temperature. Besides these, the matter in its plasma state on colliding the surface of the container will

Click Here t.me/theachemylibrary

lose its energy and get thermalised. This thermalised matter cannot participate in the nuclear fusion process. Thus, if at all, any container is available, it cannot be used to preserve the plasma for the thermonuclear process.

However, to solve the above problems, it has been proposed that on passing a very strong electrical discharge (by using a very high potential) through the light gases kept at a low pressure, the plasma state can be attained. For keeping the plasma state, no earthly container is required, but this can be stored at the axial zone of a tube under a powerful magnetic field. In the plasma state, the free electrons and the positively charged nuclei are moving with a very high velocity. This is why, by using an external magnetic field, the plasma can be kept concentrated at the axial region of the magnetic field. This container is called ***magnetic bottle.*** But, unfortunately, the plasma state satisfying the conditions of a thermonuclear reaction cannot survive sufficiently long under this condition to execute the process. In this regard, ***Stellarater*** (in USA) and ***Tokomak*** (in USSR) have showed only a faint ray of light of hope. In Tokomak, a plasma of 5×10^6 °C having an ion density ~ 10^4 per unit volume has been created only for 0.02 s. But to execute the process, it requires higher temperatures, higher ion density and higher life period of the plasma.

7.14.5. Cold Fusion

In 1989, the scientists Pons and Fleischmann reported that during electrolysis of heavy water (D_2O) containing some *LiOD* with the use of *Pd*-electrodes, *the energy output was about 4 times larger than the electrical energy input.* The excess heat evolved was measured calorimetrically, but the results could not be reproduced in other laboratories.

The gain of excess energy was explained by Pons and Fleischmann by considering the concept of *cold fusion of D-atoms on the Pd-electrode surface where the partial pressure of deuterium was tremendously high.* The proposed cold fusion reactions are :

$$_1^2D + {}_1^2D \rightarrow {}_2^3He + {}_0^1n + 3.27 \text{ MeV}$$

$$_1^2D + {}_1^2D \rightarrow {}_1^3T + {}_0^1p + 4.02 \text{ MeV}$$

If all the *D*-atoms were supposed to undergo the said fusion reaction, the energy output to energy input ratio would be 10^5. The observed ratio is only 4 : 1. This low value was explained by considering the low efficiency of the process.

Now there are convincing evidences to discard the claim of cold fusion. The excess energy evolved (in the form of heat) was due to *Pd-deuterium interaction.* Moreover, the presence of tritium (^3T) in their experimental setup was due to the use of tritium contaminated *Pd*-electrode. In fact, the use of tritium free *Pd*-electrode did not show the presence of tritium in the experiment.

7.15 THE ORIGIN AND EVOLUTION OF ELEMENTS : NUCLEOSYNTHESIS OF ELEMENTS

Big-bang theory : It is believed that at the beginning, the universe was a **giant neutron star** (*ca.* 10^{17} neutrons cm^{-3}) with a temperature about 10^{10} K. It was of immense density under a tremendous pressure.

Click Here t.me/thealchemylibrary

About 10-20 billions of years ago, the universe started to expand abruptly and the free neutrons decayed. **The giant neutron star exploded, hence the name *big bang*.**

$$^{1}_{0}n\,(\text{free}) \rightarrow {}^{1}_{1}p + {}^{0}_{-1}e + {}^{0}_{0}\bar{\nu}$$

It produced the ***primordial mixture*** (called ***ylem***) ***of neutron, proton and electron.*** Combination of proton and electron produced the *element hydrogen*. **Then all other elements were produced from the *primordial element through nucleosynthesise in the steller interiors.*** Over the eons, the stars are ejecting the matter into interstellar space.

***Note* :**

- **Doppler effect** supports the fact that the universe is expanding. Light coming from the outermost galaxies possesses a longer wavelength than expected. It happens so because the galaxies are moving away from us. The gap created in space by the expanding universe is being continuously filled in by hydrogen.
- During **big bang,** sequential addition of neutrons and protons stopped at the point of $^{4}_{2}He$ formation

$$^{1}_{1}H + {}^{1}_{0}n \rightarrow {}^{2}_{1}H,\ {}^{2}_{1}H + {}^{1}_{1}H \rightarrow {}^{3}_{2}He,\ {}^{3}_{2}He + {}^{1}_{0}n \rightarrow {}^{4}_{2}He.$$

Formation of heavier nucleus than ^{4}He stopped because of the following reaction.

$$^{4}_{2}He + {}^{1}_{0}n \rightarrow {}^{5}_{2}He\ (t_{1/2} \approx 2 \times 10^{-21}\ \text{s})$$

i.e. $^{5}_{2}He$ **is tremendously unstable.**

7.15.1 Nucleosynthesis of Elements from the Primordial Element Hydrogen in Stars

(a) Burning of hydrogen

The continued gravitational collapse in the stars raised the temperature. Consequently, the kinetic energy of the primordial element increased sufficiently to overcome the ***fusion barrier.*** Then hydrogen burning started to generate the helium nuclides. The *H*-burning can occur through the ***carbon-nitrogen* (*CN*) *cycle, carbon-nitrogen-oxygen* (*CNO*) *bicycle* and *proton-proton cycle.*** These have been discussed in Sec. 7.14.3. The *H*-burning produces helium :

$$4\,{}^{1}_{1}H \rightarrow {}^{4}_{2}He + 2\,{}^{0}_{+1}e + 2{}^{0}_{0}\nu + \text{energy}$$

Thus at the cost of *H*-fuel, *He* is accumulated at the core of stars but *the process is slow*. Then the temperature gradually falls and the star becomes a **red giant.**

(b) Burning of helium

In the **red giant,** gravitational collapse raises the temperature ($\approx 10^{8}$ K) to allow the fusion involving the *He*-nuclei. Successive (α, γ) reactions produced the **poly-α-nuclides**, e.g. ^{8}B, ^{12}C, ^{20}Ne, ^{24}Mg, etc. The possible reactions are :

$$^{3}_{2}He + {}^{4}_{2}He \rightarrow {}^{7}_{4}Be + \gamma;\ {}^{7}_{4}Be + {}^{1}_{1}H \rightarrow {}^{8}_{5}B + \gamma;$$

$$^{7}_{4}Be + {}^{0}_{-1}e \rightarrow {}^{7}_{3}Li + \gamma;\ {}^{7}_{3}Li + {}^{1}_{1}H \rightarrow {}^{8}_{4}Be + \gamma;\ {}^{4}_{2}He + {}^{4}_{2}He \rightarrow {}^{8}_{4}Be + \gamma;$$

Click Here t.me/thealchemylibrary

$$^{8}_{4}Be + ^{4}_{2}He \rightarrow ^{12}_{6}C;\ ^{12}_{6}C + ^{4}_{2}He \rightarrow ^{16}_{8}O;$$

$$^{16}_{8}O + ^{4}_{2}He \rightarrow ^{20}_{10}Ne$$

Helium can be regenerated through the burning of hydrogen in the *CN* cycle.

Burning of *He*-fuel followed by the gravitational collapse produces the hotter star called ***white dwarf.***

(c) Burning of carbon and oxygen

Helium burning and gravitational collapse released the energy to raise the temperature $\geq 10^9$ K in *massive stars* (where the gravitational collapse is very much important). At this high temperature, the heavier nuclei like ^{12}C, ^{16}O generated in *He*–burning can undergo fusion to generate the still heavier nuclei.

Carbon burning reactions

$$^{12}_{6}C + ^{12}_{6}C \rightarrow ^{20}_{10}Ne + ^{4}_{2}He$$

$$\rightarrow ^{24}_{12}Mg + \gamma$$

$$\rightarrow ^{23}_{12}Mg + ^{1}_{0}n$$

$$\rightarrow ^{23}_{11}Na + ^{1}_{1}H$$

$$^{20}_{10}Ne + \gamma \rightarrow ^{16}_{8}O + ^{4}_{2}He$$

(i.e. *photodissociation of neon*)

$$^{20}_{10}Ne + ^{4}_{2}He \rightarrow ^{24}_{12}Mg + \gamma$$

Oxygen burning reactions

$$^{16}_{8}O + ^{16}_{8}O \rightarrow ^{28}_{14}Si + ^{4}_{2}He$$

$$\rightarrow ^{32}_{16}S$$

$$\rightarrow ^{31}_{16}S + ^{1}_{0}n$$

$$\rightarrow ^{31}_{15}P + ^{1}_{1}H$$

$$^{12}_{6}C + ^{16}_{8}O \rightarrow ^{28}_{14}Si + \gamma$$

(d) Burning of silicon

The ^{28}Si produced during carbon and oxygen burning can burn at temperature $\geq 3.4 \times 10^9$ K.

$$^{28}_{14}Si + ^{28}_{14}Si \rightarrow \underset{(unstable)}{^{56}_{28}Ni} \xrightarrow{-\beta^+} ^{56}_{27}Co \xrightarrow{-\beta^+} \underset{(stable)}{^{56}_{26}Fe}$$

The nuclear binding energy in ^{56}Fe is very high (ca. $\overline{B}$ = 8.8 MeV).

(e) α-capture process

In fact, *burning of heavier nuclides* ($Z > 16$) *through fusion is not energetically very much favourable because of very high activation energy*. Then the α-capture process produces the heavier nuclides. The α-particles are generated through the *photodissociation* of ^{20}Ne and ^{28}Si.

$$^{20}_{10}Ne + \gamma \rightarrow ^{16}_{8}O + ^{4}_{2}He,\ ^{28}_{14}Si + \gamma \rightarrow 7\ ^{4}_{2}He,$$

$$^{28}_{14}Si + \gamma \rightarrow ^{24}_{12}Mg + ^{4}_{2}He$$

The representative α-capture processes are :

$$^{28}_{14}Si + ^{4}_{2}He \rightarrow ^{32}_{16}S + \gamma;\ ^{32}_{16}S + ^{4}_{2}He \rightarrow ^{36}_{18}Ar + \gamma;$$

Click Here t.me/thealchemylibrary

$$^{36}_{18}Ar + {}^{4}_{2}He \rightarrow {}^{40}_{20}Ca\,;\; {}^{28}_{14}Si + 7\,{}^{4}_{2}He \rightarrow {}^{56}_{28}Ni$$

^{56}Ni being unstable undergoes disintegration (positron active)

$$\underset{\text{(unstable)}}{{}^{56}_{28}Ni} \xrightarrow{-\beta^+} {}^{56}_{27}Co \xrightarrow{-\beta^+} \underset{\text{(stable)}}{{}^{56}_{26}Fe}$$

Because of very high nuclear binding energy, ^{56}Fe is quite stable. ***This explains the high abundance of ^{56}Fe in nature.*** It is important to note that the heavy nuclide ^{56}Fe cannot be used as a nuclear fuel. ***Thus, the H-burning process ends up with the generation of stable nuclei of ^{56}Fe, i.e.***

$$\boxed{\textit{H}\text{-burning} \longrightarrow \textit{He}\text{-burning} \longrightarrow \textit{C, O,}\text{ and }\textit{Si}\text{-burning} \longrightarrow \alpha\text{-capture process} \longrightarrow {}^{56}_{26}Fe}$$

The nuclides ($Z \leq 26$) thus produced can participate in ***successive electron capture process and successive neutron ejection process to produce different nuclides.***

$$^{A}_{Z}X \xrightarrow{+e} {}^{A}_{Z-1}X \xrightarrow{+e} {}^{A}_{Z-2}B \xrightarrow{+e} \ldots\ldots (e\text{-capture})$$

$$^{A}_{Z}X \xrightarrow{-n} {}^{A-1}_{Z}X \xrightarrow{-n} {}^{A-2}_{Z}X \xrightarrow{-n} \ldots\ldots (n\text{-ejection})$$

(f) Synthesis of heavier elements (Z > 26)

The neutron capture (which does not experience any Coulombic barrier) *followed by the* β*-decay can produce the heavier elements*. The success of the process depends on the *cross-section of the neutron capture process*. The neutron is generated through the (α, n) reactions, e.g.

$$^{13}_{6}C + {}^{4}_{2}He \longrightarrow {}^{16}_{8}O + {}^{1}_{0}n$$

The successive neutron capture process (described as ***s-process***) occurs as follows :

$$^{A}_{Z}X + {}^{1}_{0}n \rightarrow {}^{A+1}_{Z}X + \gamma;\; {}^{A+1}_{Z}X + {}^{1}_{0}n \rightarrow {}^{A+2}_{Z}X + \gamma; \ldots\ldots$$

With this process, the n/p ratio gradually increases and they become β^--active to generate the elements of higher atomic number.

$$^{A+2}_{Z}X \rightarrow {}^{A+2}_{Z+1}Y + {}^{0}_{-1}e + {}^{0}_{0}\bar{\nu}$$

The element Y can again participate in neutron capture followed by β^--decay to produce the still higher elements.

There are two neutron capture processes : ***s-process*** (slow neutron capture process) and ***r-process*** (rapid neutron capture process).

In ***s-process***, the neutrons generated in (α, n) reactions, e.g. $^{13}_{6}C(\alpha, n)\,{}^{16}_{8}O$ are captured one by one by the ^{56}Fe nucleus. When the n/p ratio exceeds the stability zone, β-decay starts to correct the n/p ratio. It is illustrated below :

$$^{56}_{26}Fe \xrightarrow{+\,{}^{1}_{0}n} {}^{57}_{26}Fe \xrightarrow{+\,{}^{1}_{0}n} {}^{58}_{26}Fe \xrightarrow{+\,{}^{1}_{0}n} {}^{59}_{26}Fe \xrightarrow[(-\beta)]{\beta\text{-decay}} {}^{59}_{27}Co$$

Click Here to the chemylibrary

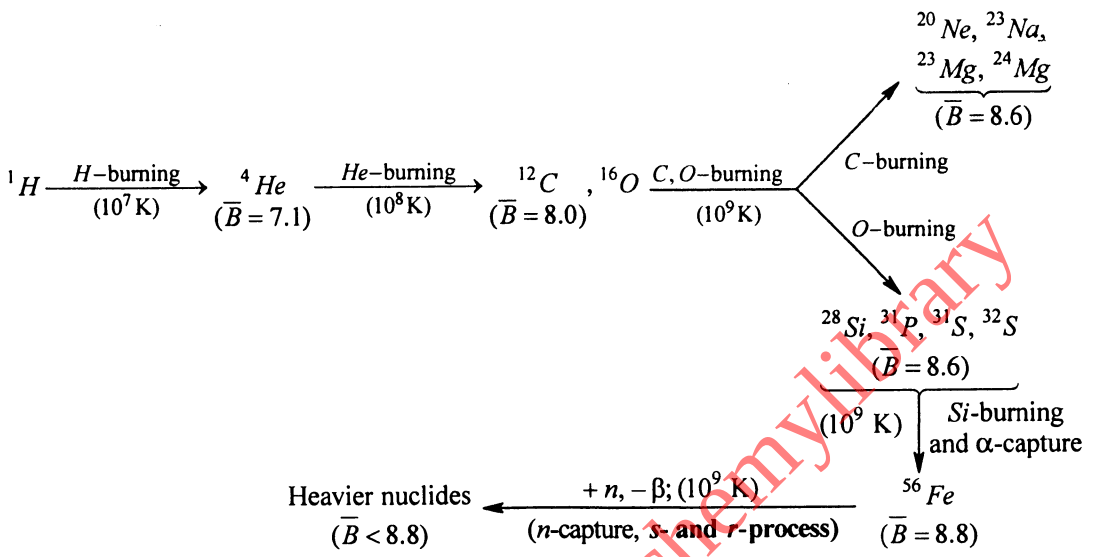

Scheme 7.15.1.1. Nucleosynthesis of elements ($\bar{B}$ stands for Nuclear Binding Energy, MeV per nucleon).

The *s*-process can generate the nuclei upto $^{209}_{83}Bi$.

In the *r-process*, many number of neutrons are captured very rapidly (within the time scale of 10^{-2} to 10 s). *The process is so rapid that the* β*-decay cannot occur within the time scale of neutron capture.* **The *r*-process can produce elements heavier than bismuth.** This process can occur when there is a large neutron flux at the time of ***supernova explosion.*** Thus the heavier nuclides generated are immediately dispersed into the universe. The process is illustrated below :

$$^{56}_{26}Fe \xrightarrow{+13\,^{1}_{0}n} {}^{69}_{26}Fe \xrightarrow[(-\beta)]{\beta\text{-decay}} {}^{69}_{27}Co$$

The *r*-process produces the **neutron rich nuclides.** The process can also produce the neutron rich lighter nuclides like ^{36}S, ^{46}Ca, ^{48}Ca, etc.

In a supernova, proton capture (called ***p-process***) can produce the **proton rich nuclides** like $^{74}_{34}Se$, $^{113}_{50}Sn$, $^{114}_{50}Sn$, etc.

7.15.2. Cosmic Abundance of Elements

Hydrogen and helium are regarded as the ***primordial nuclear fuels*** and heavier elements are produced from these nuclear fuels. Hydrogen and helium are the most abundant elements. Hydrogen alone accounts for 88.6% and helium for about 11.3% of all the atoms in the universe. ***Thus, these two primordial elements constitute about 99.9% of the total mass of the universe.***

Relative Cosmic Abundance is defined as the number of atoms of an element per 10^6 atoms of silicon which is the **second most abundant element in the earth crust.** Relative cosmic abundance (σ) of an element is generally expressed in logarithmic scale.

$$\sigma = \log \text{ (the number of atoms of an element per } 10^6 \text{ atoms of } Si)$$

Click Here to join chemylibrary

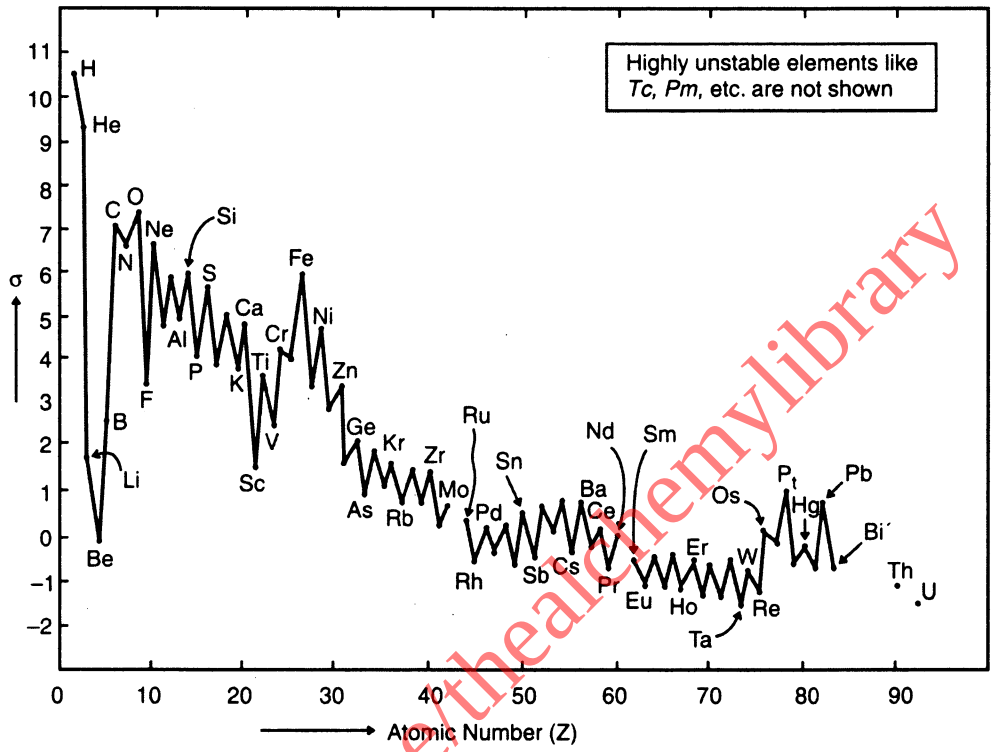

Fig. 7.15.2.1. Graphical representation of relative cosmic abundance of different elements.

Relative cosmic abundance curve (i.e. plot of σ vs. atomic number) (Fig. 7.15.2.1) indicates that the abundance of the elements decreases *rapidly and exponentially* upto atomic number, $Z \approx 42$ (*Mo*) after which the abundance remains reasonably constant. **The characteristic features of cosmic abundance of the elements are outlined below :**

(i) *H* is the most abundant element and *He* is the second most abundant element. *H* and *He* can account for the 99.9% of the atoms of universe. ***These are the most abundant elements.***

(ii) Cosmic abundance ***exponentially decreases*** **to about $Z = 42$** and then the elemental abundance of the elements ($Z > 42$) remains more or less constant.

(iii) Abundance of the elements follows the ***Oddo-Harkins rule*** i.e. elements with even *Z* are more abundant than their nearest neighbours having odd *Z*.

(iv) The following 11 elements ($Z < 29$) are relatively abundant (i.e. $\sigma \geq 0$).
${}_1H$, ${}_2He$, ${}_6C$, ${}_7N$, ${}_8O$, ${}_{10}Ne$, ${}_{12}Mg$, ${}_{14}Si$, ${}_{16}S$, ${}_{26}Fe$, ${}_{28}Ni$.

(v) Among the lighter elements, *Li*, *Be* and *B* are relatively less abundant though these are produced during *H* and *He* burning. These nuclides are also produced in small amounts in ***spallation reactions*** where high speed cosmic rays collide with *C*, *N* and *O* nuclides. The process generating the nuclides of *Be*, *B* and *Li* is called ***x*-process**. The process is named so because for many years, this process of generation of these less abundant light elements was not known. ***Probably, these nuclides are transmuted easily into other elements in nuclear reactions.*** **This explains their low abundance.**

Click Here to me/thealchemylibrary

(vi) The **α-particle nuclides** (i.e. mass numbers of these elements are the integral multiples of 4) like ^{16}O, ^{20}Ne, ^{24}Mg, ^{40}Ca, ^{48}Ti, are relatively more abundant compared to their neighbouring nuclides (cf. **Oddo's rule**).

(vii) The remarkably high abundance of ^{56}Fe arises due to its *very high nuclear binding energy* ($\overline{B} = 8.8$ MeV per nucleon). In fact, this nuclide resides at the topmost position of the nuclear binding energy curve (cf. Fig. 5.3.5.1). ^{56}Fe is the most stable nuclide produced through fusion.

(viii) The nuclides having ***small neutron capture cross-section*** are accumulated in larger amounts. The nuclides with ***magic numbers of neutrons*** (e.g. 2, 8, 20, 28, 50, 82 or 126) are relatively more abundant. Such nuclides have unusually low neutron absorption cross-sections.

(ix) Among the elements Z upto 20, the abundant nuclei e.g. $^{4}_{2}He$, $^{14}_{7}N$, $^{16}_{8}O$, $^{24}_{12}Mg$ and $^{40}_{20}Ca$ maintain the neutron : proton ratio 1 : 1. Among these, except $^{14}_{7}N$, all other elements have even number of neutrons and protons. The abundant lighter nuclei which do not maintain the neutron : proton ratio 1 : 1 are $^{19}_{9}F$, $^{23}_{11}Na$ and $^{27}_{13}Al$. But they have even number of neutrons and ***they possess very low neutron capture cross-section.***

(x) The elements like *Sc*, *Ti*, *V* and *Cr* lighter than *Fe* are more abundant than expectation. These are believed to be produced through *spallation reaction where the high speed cosmic rays collide with Fe*. In these spallation reaction, other lighter elements like *Li*, *Be* and *B* are also produced. But, *Li*, *Be*, *B* participate in nuclear transmutation reactions to produce the heavier nuclides.

(xi) The nuclides having ***magic number*** (e.g. 2, 8, 20, 50, 82 or 126) of neutrons or protons or both are relatively more abundant.

Click Here to me/thealchemylibrary

SOLVED NUMERICAL PROBLEMS

Problem 1 : When lithium is bombarded by a flux of 12 MeV deuterons, the ejectile neutrons are found to emerge at right angles to the direction of the incident projectile. Calculate (i) the energy available from the projectile to effect the nuclear reaction, (ii) the energy of the ejectile neutrons and recoil nuclide, (iii) angle of the recoil nuclide. (Atomic masses in amu are : $^{1}_{0}n = 1.00893$, $^{7}_{3}Li = 7.01784$, $^{2}_{1}H = 2.01472$, $^{8}_{4}Be = 8.00776$)

(Here the binding energy of the projectile in the compound nucleus has not been considered).

Solution : The nuclear transmutation is given by,

$$^{7}_{3}Li + ^{2}_{1}H \longrightarrow \left(^{9}_{4}Be^{*}\right) \longrightarrow ^{8}_{4}Be + ^{1}_{0}n$$

It can be pictorially represented as follows :

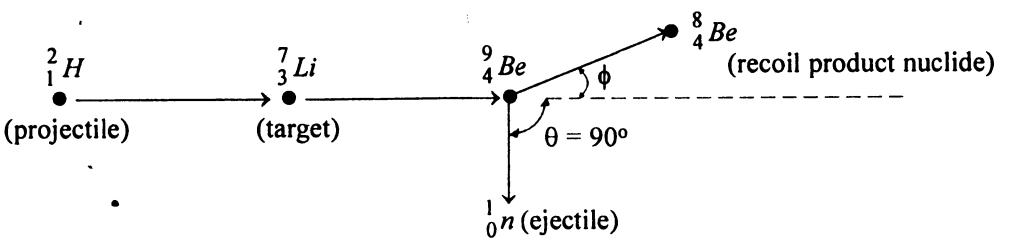

(i) The net available energy (E) to effect the nuclear reaction is given by :

$$E = E_p - E_C = M_X E_p / (M_p + M_X), \text{ (cf. Sec. 7.5.2)}$$

where, E_p = energy of the projectile; E_C = energy (translational) gained by the compound nucleus; M_p = mass of the projectile particle, M_X = rest mass of the target nuclide. Thus,

$$E = \frac{7.01784}{2.01472 + 7.01784} \times 12 = 9.33 \text{ MeV}$$

This E actually gives the kinetic energy on CMS.

(ii) From the principle of conservation of energy including the rest mass energy, we get :

$$(M_X + M_p)c^2 + E_p = (M_Y + M_e)c^2 + E_Y + E_e$$

where, M_X, M_p, M_Y and M_e represent the masses of the target nuclide, projectile particle, recoil nuclide and ejectile particle respectively.

Thus, $E_Y + E_e - E_p = (M_X + M_p - M_Y - M_e)c^2$

or, $E_Y + E_e - E_p \equiv (M_X + M_p - M_Y - M_e)\ 931 \text{ MeV}$

$= (7.01784 + 2.01472 - 8.00776 - 1.00898) \times 931 \text{ MeV}$

$= 0.01582 \times 931 \text{ MeV} \approx 14.8 \text{ MeV}$

or, $E_Y + E_e = 14.8 + E_p = 26.8 \text{ MeV}$

From the principle of conservation of momentum we get :

$p_p = p_e \cos\theta + p_Y \cos\phi$, (along the direction of projectile) ...(a)

and, $0 = p_e \sin\theta - p_Y \sin\phi$, (along the perpendicular direction to the approach of projectile) ... (b)

By using the relationship, $K.E. = p^2/2m$; we get :

$$p_p = \sqrt{2E_pM_p},\ p_e = \sqrt{2E_eM_e}, \text{ and } p_Y = \sqrt{2E_yM_Y}$$

In the present case, $\theta = 90^\circ$. Thus from (a) and (b) we get : $p_p = p_Y \cos\phi$, and $p_e = p_Y \sin\phi$. Squaring followed by the addition of these two relations, we get :

$$p_p^2 + p_e^2 = p_Y^2; \text{ or, } 2E_pM_p + 2E_eM_e = 2E_YM_Y$$

or, $E_pM_p + E_eM_e = E_YM_Y$; or, $E_e = E_Y(M_Y/M_e) - E_p(M_p/M_e)$

or, $E_e = (26.8 - E_e)(M_Y/M_e) - 12(M_p/M_e)$;

or, $E_e(1 + M_Y/M_e) = 26.8(M_Y/M_e) - 12(M_p/M_e)$;

or, $$E_e\left(1 + \frac{8.00776}{1.00893}\right) = 26.8\left(\frac{8.00776}{1.00893}\right) - 12\left(\frac{2.01472}{1.00893}\right)$$

or, $E_e = 21.15$ MeV. Hence, $E_Y = (26.8 - 21.15)$ MeV $= 5.65$ MeV

Click Here to me/theachemylibrary

Now from the relationship of momentum, we get :

$$p_e/p_p = (p_Y \sin\phi)/(p_Y \cos\phi) = \tan\phi$$

or, $$\tan\phi = \frac{\sqrt{2M_eE_e}}{\sqrt{2M_pE_p}} = \frac{\sqrt{2\times1.00893\times21.15}}{\sqrt{2\times2.01472\times12}} = 0.88$$

or, $$\phi = 41.4^\circ$$

Problem 2 : Find the excitation energy in the compound nucleus $^{236}U^*$ formed due to the capture of a slow neutron of 1 eV. If the activation energy of fission of ^{235}U is 5.4 MeV, predict the possibility of fission. (Atomic masses in amu are : $^{236}U = 236.0458$, $^1n = 1.0089$ and $^{235}U = 235.0439$).

Solution : The excitation energy in the compound nucleus is given by the summation of the nuclear binding energy released due to the capture of the particle and the kinetic energy of the projectile on *CMS*.

Nuclear binding energy released = mass loss (in amu) in the compound nucleus formation × 931 MeV.

The mass loss in the process, $^{235}_{92}U + ^1_0n \rightarrow \left(^{236}_{92}U^*\right)$ is given by :

$$\Delta m = m\left(^{235}_{92}U\right) + m\left(^1_0n\right) - m\left(^{236}_{92}U\right)$$

$$= 235.0439 + 1.0089 - 236.0458 = 7.0 \times 10^{-3} \text{ amu}$$

$$\equiv 7.0 \times 10^{-3} \times 931 \text{ MeV} = 6.51 \text{ MeV}$$

Kinetic energy on $CMS = \dfrac{m(^{235}U)}{m(^1n) + m(^{235}U)} E_p = 0.99$ eV

where, E_p = energy of the projectile = 1 eV.

Hence, total excitation energy = $(6.51 + 0.99 \times 10^{-6})$ MeV ≈ 6.51 MeV

As the excitation energy (E_{ex}) is greater than the activation energy ($E^{\neq}$), i.e. $E_{ex} > E^{\neq}$, the fission process will go on.

Problem 3 : ^{238}U releases 4.75 MeV as the nuclear binding energy on capturing a neutron to form the compound nucleus $^{239}U^*$. If activation energy for the fission of ^{238}U is 5.5 MeV. Calculate the energy of the neutron which can induce the fission.

Solution : To run the fission, the excitation energy (E_{ex}) must be greater than or equal to the activation energy ($E^{\neq}$), i.e. $E_{ex} \geq E^{\neq}$.

E_{ex} = nuclear binding energy released in the compound nucleus formation

+ kinetic energy of the projectile on $CMS = 4.75 + \dfrac{m(^{238}U)}{m(^1n) + m(^{238}U)} E_p$

$$= 4.75 + 0.99E_p.$$

where E_p (in MeV) = energy of the projectile neutron. Thus the critical excitation energy is related as follows :

Click Here t.me/thealchemylibrary

$$E^{\neq} = E_{ex} = 4.75 + 0.99\ E_p;\ \text{or, } 5.5 = 4.75 + 0.99E_p;$$

or, $$E_p = 0.75 \text{ MeV}$$

Thus to carry out the fission in ^{238}U by a neutron, the neutron should have at least 0.75 MeV energy.

Problem 4 : Calculate the Q value of the reaction, $^{6}_{3}Li(d, n)\ ^{7}_{4}Be$. (Atomic masses in amu are : $^{6}_{3}Li = 6.01697$, $^{7}_{4}Be = 7.01907$, $^{2}_{1}H = 2.01474$, $^{1}_{0}n = 1.00899$).

Solution : The nuclear reaction is : $^{6}_{3}Li + ^{2}_{1}H \rightarrow ^{7}_{4}Be + ^{1}_{0}n + Q$.

The mass loss in the reaction is given by :

$$\begin{aligned}\Delta m &= m(^6Li) + m(^2H) - m(^7Be) - m(^1n)\\ &= (6.01697 + 2.01474 - 7.01907 - 1.00899)\text{ amu}\\ &= 3.65 \times 10^{-3}\text{ amu} \equiv 3.65 \times 10^{-3} \times 931\text{ MeV} = 3.4\text{ MeV} = Q\end{aligned}$$

Problem 5 : Find the Q value of fission of ^{235}U by a slow neutron. Calculate the amount of energy liberated in the fission of 1 g uranium. If the heat of combustion of coal is 8.5×10^3 kcal/kg, then find out the equivalent amount of coal which can produce the same energy.

Solution : Q value for the fission of ^{235}U can be calculated by mass defect method or nuclear binding energy ($\overline{B}$) method (see Sec. 7.12.2e). Let Q be the 207.6 MeV for a representative fission reaction of ^{235}U.

It indicates that fission of an atom of ^{235}U produces 207.6 MeV.

$$1\text{ g } ^{235}U \equiv \frac{1 \times 6.02 \times 10^{23}}{235}\text{ atoms of } ^{235}U = 2.56 \times 10^{21}\text{ atoms of } ^{235}U.$$

Thus, 1 g ^{235}U produces energy through fission $= 207.6 \times 2.56 \times 10^{21}$ MeV

$$= 5.32 \times 10^{23} \times 1.6 \times 10^{-13}\text{ J}$$

$$= 8.50 \times 10^{10}\text{ J}$$

$$= 2.03 \times 10^{7}\text{ kcal.}$$

From the condition, 8.5×10^3 kcal $\equiv$ 1 kg coal.

$$\text{Hence, } 2.03 \times 10^7\text{ kcal} \equiv \frac{2.03 \times 10^7}{8.5 \times 10^3}\text{ kg coal} = 2.4 \times 10^3\text{ kg coal.}$$

Thus, 1 g $^{235}U \equiv 2.4 \times 10^3$ kg coal.

Very often, the energy released is expressed in terms of kilowatt-hour (kWh).

1 Watt = 1 joule per second, or 1 kilowatt = 10^3 Joules per second = 1 kJ/s

Hence, 1 kilowatt second = 1 kJ; or, 1 kilowatt hour = 60×60 kJ = 3600 kJ = 36×10^5 J

$$\text{Thus, } 8.5 \times 10^{10}\text{ J} = \frac{8.5 \times 10^{10}}{36 \times 10^5}\text{ kWh} = 2.36 \times 10^4\text{ kWh}$$

Click Here t.me/thedchemylibrary

Problem 6 : A submarine is driven by an atomic plant of ^{235}U. The submarine requires an average power 1000 kW for its journey. The efficiency of the engine is 25%. If the submarine is to run for 10 days, how much ^{235}U would be consumed in the journey. (Given, Q value of the fission = 200 MeV)

Solution : Average power required = 1000 kW = 10^6 watt

Hence, the energy consumed in the journey for 10 days = $10^6 \times 10 \times 24 \times 60 \times 60$ J

$= 10^6 \times 8.64 \times 10^5$ J

$= 8.64 \times 10^{11}$ J

Efficiency of the engine is 25%, i.e. 25 J are utilised for 100 J produced to run the submarine.

Thus, the required total energy to be generated = $8.64 \times 10^{11} \times (100/25)$ J = 34.56×10^{11} J

Fission of one ^{235}U atom produces 200 MeV or $200 \times 1.6 \times 10^{-13}$ J, i.e. 3.2×10^{-11} J.

Therefore, 3.2×10^{-11} J ≡ 1 atom of ^{235}U

or, 34.56×10^{11} J $\equiv \dfrac{34.56 \times 10^{11}}{3.2 \times 10^{-11}}$ atoms of ^{235}U

$= 10.8 \times 10^{22}$ atoms of $^{235}U \equiv \dfrac{10.8 \times 10^{22}}{6.02 \times 10^{23}}$ g atom of ^{235}U

$= 0.179$ g atom of $^{235}U = 0.179 \times 235$ g ^{235}U

$= 42.16$ g ^{235}U.

Thus, the submarine will consume 42.16 g ^{235}U.

Problem 7 : An atom bomb of 1 kg ^{235}U undergoes explosion. If only one neutron starts the initial fission with the reproduction factor 2.5, how much time would be required to complete the explosion ? Express the destructive power in terms of TNT.

(***Given*** : fission time of an ^{235}U atom = 10^{-8} s, Q = 200 MeV per ^{235}U atom, 1 kilotonne TNT = 4×10^{12} J).

Solution : 1 kg ^{235}U contains $\dfrac{6.02 \times 10^{23} \times 1000}{235} = 25.62 \times 10^{23}$ atoms.

Reproduction factor 2.5 means that each fission produces 2.5 neutron (on an average) available for running the fission process.

The fission propagates in a chain process. If it requires x steps to complete the fission of ^{235}U atoms present in 1 kg ^{235}U, then the total number of ^{235}U atoms suffering the fissions in x steps is given by $(2.5)^x$.

Therefore, $(2.5)^x = 25.62 \times 10^{23}$; or, $x \approx 61.0$.

To complete the 61 steps of the fission chain process, it will require 61×10^{-8} s = 6.1×10^{-7} s.

The energy released per fission = 200 MeV.

Hence, the fission of 25.62×10^{23} atoms ≡ $25.62 \times 10^{23} \times 200$ MeV

$= 51.24 \times 10^{25}$ MeV

$= 51.24 \times 10^{25} \times 1.6 \times 10^{-13}$ J

$= 82 \times 10^{12}$ J

Click Here to methodchemylibrary

$$\equiv \frac{82 \times 10^{12}}{4 \times 10^{12}} \text{ kilotonnes TNT}$$

$$= 20.5 \text{ kilotonnes TNT}$$

Problem 8 : In the artificial transmutation reaction, $^{14}N(\alpha, p)\,^{17}O$, the Q-value is –1.2 MeV. Calculate the threshold energy of the projectile.

Solution : The given transmutation reaction is *endo-ergic*. The threshold value of the energy of the projectile is given by (cf. Sec. 7.6) :

$$E_p = \left(1 + \frac{M_p}{M_X}\right) Q = \left(1 + \frac{4}{14}\right) 1.2 = 1.28 \times 1.2 = 1.54 \text{ MeV}$$

Problem 9 : It is found that 0.1189 weight fraction of a $^{10}_{5}B$-rod disappears in a year in the presence of continuous exposure of slow neutrons of flux 10^{16} m^{-2} s^{-1}. Calculate the cross-section (σ) of the neutron capture process.

Solution : The neutron capture reaction is :

$$^{10}_{5}B + ^{1}_{0}n \longrightarrow ^{7}_{3}Li + ^{4}_{2}He$$

Neutron flux density (ϕ) = Number of neutrons colliding per second per unit area of the target surface.

If N_o gives the number of target nuclei per unit area, then the collision rate is given by :

$$\text{Collision rate} \propto \phi N_o$$

Collision rate is the measure of reaction rate, i.e. reaction rate = $\sigma\phi N_o$.

The proportionality constant σ is described as the ***neutron capture cross-section.***

Number of ^{10}B atoms lost in time t = $\sigma\phi N_o t$

i.e. fraction lost due to transmutation $= \dfrac{\sigma \phi N_o t}{N_o}$

$$= \phi\sigma t$$

From the given condition :

$$10^{16} \text{ m}^{-2} \text{ s}^{-1} \times 60 \times 60 \times 24 \times 365 \text{ s} \times \sigma = 0.1189$$

or,
$$\sigma = \frac{0.1189}{10^{16} \times 3600 \times 24 \times 365} \text{ m}^2$$

$$= 3.77 \times 10^{-25} \text{ m}^2 = 3700 \text{ barn}$$

$$(1 \text{ barn} = 10^{-24} \text{ cm}^2 = 10^{-28} \text{ m}^2).$$

Problem 10 : A thin film of 4 mg of $^{59}_{27}Co$ (100%) was irradiated to the neutron flux (ϕ) 1.3×10^{14} cm^{-2} s^{-1} for 1 hour. Calculate the activity of ^{60}Co produced at the end of 1 hour. Given : Cross-section (σ) of the neutron capture by ^{59}Co = 19.6 barn; $t_{1/2}$ of ^{60}Co = 5.25 y).

Solution : The said (n, γ) transmutation reaction is :

Click Here t me/thealchemylibrary

$$^{59}_{27}Co + ^{1}_{0}n \longrightarrow ^{60}_{27}Co + \gamma$$

The number of ^{60}Co nuclides produced in 1 hour is given by :

$$N(^{60}Co) = N(^{59}Co)\,\phi\sigma\,t$$

$$4 \text{ mg } ^{59}Co \equiv \frac{4\times10^{-3}\times6.02\times10^{23}}{59} = 0.41\times10^{20} \text{ atoms of } ^{59}Co$$

i.e. $N(^{59}Co) = 0.41 \times 10^{20}$

$$N(^{60}Co) = 0.41 \times 10^{20} \times 1.3 \times 10^{14} \times 19.6 \times 10^{-24} \times 3600$$

$$= 3.76 \times 10^{14} \text{ atoms.}$$

The activity due to $N(^{60}Co)$ atoms of ^{60}Co is given by :

$$A = k \times 3.76\times10^{14}, \left(k = \text{decay constant} = \frac{0.693}{t_{1/2}}\right)$$

$$= \frac{0.693\times3.76\times10^{14}}{5.25\times365\times24\times3600} \text{ dps}$$

$$= 1.57 \times 10^{6} \text{ dps} = 1.57 \text{ MBq}$$

$$= \frac{1.57\times10^{6}}{3.7\times10^{10}} \text{ Ci} = 0.42\times10^{-4} \text{ Ci} = 0.042 \text{ m Ci}$$

(dps = disintegration per second, 1 Ci = 3.7×10^{10} dps, 1 Bq = 1 dps)

Problem 11 : Calculate the excitation energy (E_{ex}) of the compound nucleus in the reaction $^{20}Ne\ (d, \alpha)\ ^{18}F$ by using the deuterons of 8 MeV. Nuclide masses are to be taken from the standard tables.

Solution : The given nuclear reaction is :

$$^{20}_{10}Ne + ^{2}_{1}H \longrightarrow \left[^{22}_{11}Na^{*}\right] \longrightarrow ^{18}_{9}F + ^{4}_{2}He$$

i.e. the compound nucleus is $^{22}_{11}Na^{*}$.

The kinetic energy of the projectile on CMS is given by (cf. Sec. 7.5.2) :

$$\frac{E_p M_X}{(M_X + M_p)}$$

$$= \frac{8\times20}{(20+2)} \text{ MeV} = 7.27 \text{ MeV}$$

This energy is available to effect the nuclear reaction.

The binding energy of the deuteron in the compound nucleus

$$= [m(^{20}Ne) + m(^{2}H) - m(^{22}Na)] \times 931 \text{ MeV}$$

$$= [19.99244 + 2.01402 - 21.944] \times 931 \text{ MeV}$$

$$= 0.06246 \times 931 \text{ MeV} = 58.15 \text{ MeV}$$

(The masses in amu are obtained from the standard tables).

Click Here t.me/theachemylibrary

E_{ex} = Nuclear binding energy released in the compound nucleus formation + kinetic energy of the projectile on CMS = 58.15 + 7.27 = 65.42 MeV (see Sec. 7.8.1).

Problem 12 : ^{14}N has an excited state at 12.8 MeV. Calculate the required kinetic energy (KE) of the cyclotron accelerated α-particle in the reaction ^{10}B (α, n) ^{13}N for resonance capture.

Solution : The nuclear reaction is given below.

$$^{10}_{5}B + ^{4}_{2}He \longrightarrow \left[^{14}_{7}N^{*}\right] \longrightarrow ^{13}_{7}N + ^{1}_{0}n$$

Nuclear binding energy released during the compound nucleus formation is given by :

$$\left[m(^{10}B) + m(^{4}He) - m(^{14}N^{*})\right] \times 931 \text{ MeV}$$

$$= [10.012939 + 4.002604 - 14.003074] \times 931$$

$$= 0.012469 \times 931 \text{ MeV} = 11.6 \text{ MeV}$$

$$E_{ex} = 11.6 + \frac{E_p M_X}{M_X + M_p} = 11.6 + \frac{10E_p}{(10+4)}, \text{ (see Sec. 7.8.1)}$$

$$E_{ex} = 12.8 \text{ MeV (given)}$$

i.e. $$12.8 = 11.6 + \frac{10E_p}{14}; \text{ or } E_p = \frac{12.8 \times 14 - 11.6 \times 14}{10} = 1.68 \text{ MeV}$$

Thus the projectile α-particle should have the kinetic energy 1.68 MeV.

Problem 13 : In the fission of $^{235}_{92}U$, the stable end products are $^{94}_{40}Zr$ and $^{140}_{55}Ce$. Find the primary fission fragments.

Solution : According to the principle of equidistant charge displacement (cf. Sec. 7.12.4), the primary fission products characterised by the atomic number Z_{1p} and Z_{2p} are given by :

$$Z_{1p} = \frac{1}{2}(92 + 40 - 58) = 37 \text{ (i.e. } ^{94}_{37}Rb)$$

$$Z_{2p} = \frac{1}{2}(92 + 58 - 40) = 55 \text{ (i.e. } ^{140}_{55}Cs)$$

Problem 14 : Find out the fission barrier (E_b) for the symmetric fission of ^{236}U.

Solution : The symmetric fission of ^{236}U leads to :

$$\left[^{236}_{92}U^{*}\right] \longrightarrow ^{118}_{46}Pd + ^{118}_{46}Pd$$

The Coulombic barrier (E_{Coul}) may be approximately taken as the fission barrier (E_b) is given by :

$$E_b \approx E_{Coul} = \frac{Z_1 Z_2 e^2}{(R_1 + R_2)(4\pi\varepsilon_0)}, \text{ (in SI unit)}$$

Click Here to the/healchemylibrary

Here $Z_1 = Z_2 = \frac{Z}{2} = \frac{92}{2} = 46$, and $R_1 = R_2 = R$

Using the relationship, $R = r_0 A^{1/3} = 1.4A^{1/3}$ fm

$= 1.4 \times (118)^{1/3} \times 10^{-15}$ m

$= 1.4 \times 4.9 \times 10^{-15}$ m

It leads to :

$$E_b = \frac{(46)^2 \times (1.6 \times 10^{-19}\ \text{C})^2}{2 \times 1.4 \times (118)^{1/3} \times 10^{-15}\ \text{m} \times 4 \times 3.14 \times 8.85 \times 10^{-12}\ \text{J}^{-1}\ \text{C}^2\ \text{m}^{-1}}$$

$$= 3.55 \times 10^{-11}\ \text{J} = \frac{3.55 \times 10^{-11}}{1.6 \times 10^{-13}}\ \text{MeV}$$

$= 221.8$ MeV

(1 MeV = 1.6×10^{-13} J).

***Problem* 15 :** Find out the critical deformation energy (E_{crit}) for the fission of ^{239}Pu by using the thermal neutrons.

***Solution* :** For thermal neutrons (< 1 eV), the available kinetic energy on CMS is negligibly small.

In the present case, the compound nucleus is $^{240}_{94}Pu^*$. According to Bohr-Wheeler equation, E_{crit} is given by:

$$E_{crit} = 0.89 \times A^{2/3} - \frac{0.02 \times Z\,(Z-1)}{A^{1/3}}, \text{(in MeV)}$$

$$= 0.89 \times (240)^{2/3} - \frac{0.02 \times 94 \times 93}{(240)^{1/3}}$$

$$= 0.89 \times 38.6 - \frac{0.02 \times 94 \times 93}{6.21} = 34.35 - 28.15 = 6.2\ \text{MeV}$$

***Problem 16* :** Calculate the parameter E_b (fission barrier), E_f (fission energy), $E^{\neq}$ (activation energy of fission) of the following fission reaction.

$$^{235}_{92}U + {}^{1}_{0}n \longrightarrow \left[{}^{236}_{92}U^*\right] \longrightarrow {}^{95}_{39}Y + {}^{137}_{51}Sb + 4\,{}^{1}_{0}n + 2\,{}^{0}_{+1}e + 2\,{}^{0}_{0}\nu$$

Comment on the possibility of the above reaction.

***Solution* :** $E_f = \Delta m \times 931$ MeV, ignoring the mass of positron particles

$= [m\,(^{236}U) - m\,(^{95}Y) - m\,(^{137}Sb) - 4m\,(^{1}n)] \times 931$ MeV

$= [236.045733 - 94.912 - 136.91782 - 4 \times 1.0087] \times 931$ MeV

$= 0.1811 \times 931$ MeV $= 168.6$ MeV (per fission)

E_f may be calculated also as follows :

$E_f = [m\,(^{235}U) - m\,(^{95}Y) - m\,(^{137}Sb) - 3m\,(^{1}n)] \times 931$ MeV

$= [235.043933 - 94.912 - 136.91782 - 3 \times 1.0087] \times 931$ MeV

$= 0.188 \times 931$ MeV $= 175$ MeV

Click Here t.me/thealchemylibrary

Taking, $E_b \approx E_{Coul}$ = Coulombic barrier, and $R = 1.4\ A^{1/3} \times 10^{-15}$ m,

$$E_b = \frac{Z_1 Z_2 e^2}{(R_1 + R_2)\,4\pi\varepsilon_0} = \frac{39 \times 51 \times (1.6 \times 10^{-19}\ \text{C})^2}{1.4 \times 10^{-15} \times [(95)^{1/3} + (137)^{1/3}]\ \text{m} \times 4\pi \times 8.85 \times 10^{-12}\ \text{J}^{-1}\ \text{C}^2\ \text{m}^{-1}}$$

$$= \frac{39 \times 51 \times 10^{-11} \times 1.6 \times 1.6}{1.4 \times 9.72 \times 4 \times 3.14 \times 8.85}\ \text{J}$$

$$= 3.37 \times 10^{-11}\ \text{J} = \frac{3.37 \times 10^{-11}}{1.6 \times 10^{-13}}\ \text{MeV} = 210.6\ \text{MeV}$$

$\therefore$ $E^{\neq} = E_b - E_f = 210.6 - 168.6 = 42$ MeV, (Taking $E_f = 168.6$ MeV)

$E^{\neq} = E_b - E_f = 210.6 - 175.0 = 35.6$ MeV, (Taking $E_f = 175$ MeV)

E_{ex} = Projectile binding energy in the compound nucleus + available kinetic energy of the projectile on $CMS = E_1 + E_2$ (say).

For the thermal neutrons (energy less than 1 eV), the term E_2 is negligible compared to E_1 i.e. $E_{ex} \approx E_1$.

$$E_1 = [m\,(^{235}U) + m\,(^{1}n) - m\,(^{236}U)] \times 931\ \text{MeV}$$

$$= [235.043933 + 1.0087 - 236.045733] \times 931\ \text{MeV}$$

$$= 6.9 \times 10^{-3} \times 931\ \text{MeV} = 6.4\ \text{MeV}$$

Thus, $E_{ex} \approx E_1 = 6.4\ \text{MeV} << E^{\neq}$

i.e. the said fission reaction is not possible by using the thermal neutrons.

EXERCISE–VII

A. General Questions

1. Discuss the events which paved the way to realise the idea of the alchemists to synthesise the new elements artificially.
2. What are the differences between the nuclear and chemical reactions?
3. Discuss the conservation rules involved in a nuclear reaction.
4. Discuss the compound nucleus theory in explaining the nuclear reaction mechanism. How is it verified?
5. Discuss the Oppenheimer-Phillips Mechanism in Stripping Reactions.
6. Discuss the working principle of the linear accelerator and cyclotron in accelerating the projectile particles.
7. Discuss the theory of creation of the elements in the universe.
8. What are the characteristic features of the nuclear fission?
9. Discuss the mechanism of nuclear fission with special reference to the energetics of the process involved.
10. What are the basic conditions to be satisfied in making a fission process self-sustained?
11. Describe the chemistry of an atom bomb.

Click Here t.me/tlearchemylibrary

12. What are the fissile nuclides to be used in the nuclear reactors ? Describe the construction of a nuclear reactor.
13. A fusion reaction is called a thermonuclear reaction—why ? How does it work in a hydrogen bomb?
14. Discuss the prospects of the nuclear fusion as a source of energy with reference to the technical problems.
15. Discuss the routes leading to nucleosynthesis of ^{56}Fe in the universe. Explain the cosmic abundance of different elements.
16. Discuss the routes leading to nucleosynthesis of heavier elements than iron in the universe.
17. Write notes on : (i) Bethe's notation of nuclear reactions, (ii) Classification of the nuclear reaction, (iii) Spallation reaction, (iv) Cross-section of a nuclear reaction, (v) Resonance capture reactions, (vi) Compound nucleus, (vii) Stripping reactions, (viii) Buckshot type capture reactions, (ix) Direct nuclear reaction mechanism, (x) Synthesis of transuranic elements, (xi) Reproduction factor in a fission reaction, (xii) Fissile nuclides, (xiii) Breeder rector, (xiv) Stellar energy, (xv) Fermi's four factor formula, (xvi) Cold fusion, (xvii) Critical deformation in fission, (xviii) Cross-section of a nuclear reaction, (xix) Cosmic abundance of elements, (xx) *r*- and *s*-process in neutron capture, (xxi) *p*-process and *x*-process in the nucleosynthesis of elements.

B. Justify the Following Statements

1. Interaction of the α-particles with nitrogen produces a particle having a more penetrating power than that of the α-particles.
2. An aluminium plate being bombarded by the α-particles emits positron even after removal of the projectile beam.
3. Nuclear reaction is a purely nuclear phenomenon.
4. There is a basic difference between the spallation and fission reaction.
5. The stripping reactions cannot be explained by the compound nucleus theory.
6. Heavy ion particles as projectiles can induce two types of nuclear reactions.
7. The fusion reaction can only start at a very high temperature.
8. All the energy of a projectile is not available in effecting a nuclear reaction.
9. The concept of threshold energy of a projectile in effecting a nuclear reaction is very much important specially for the endoergic processes.
10. The concept of reaction cross-section is extremely important in measuring the efficiency of nuclear reactions.
11. The nature of product formation from a compound nucleus does not depend on the routes of its synthesis but on the degree of its excitation.
12. The successive two steps involved in the compound nucleus theory are mutually independent.
13. The deuteron projectiles face a high Coulombic potential barrier in striking the target nucleus, but still, the low energy deuterons are very much effective in carrying out some nuclear reactions.
14. The buckshot type capture and stripping reactions can be nicely explained by Oppenheimer-Phillips reaction mechanism.
15. Charged particles require to be accelerated in effecting the nuclear reactions.
16. There is a limit in accelerating the velocity of the particles in a particle accelerator.
17. The liquid drop model leads to the symmetric fission, but in practice, it leads to an asymmetric fission.

Click Here to me/thealchemylibrary

18. The slow neutrons are better projectiles compared to the fast neutrons in effecting the nuclear fission in ^{235}U.
19. The slow neutrons cannot effect the nuclear fission in ^{238}U, but the fast neutrons can do the task.
20. Only ^{235}U, ^{233}U and ^{239}Pu are the fissile nuclides with respect to the slow neutrons with a high cross- section area.
21. ^{238}U cannot act as a nuclear fuel but it can act as a potential source of a nuclear fuel.
22. ^{235}U is a nuclear fuel while ^{238}U is not a nuclear fuel and ^{238}U can never pass through a fission chain process.
23. No nuclide having mass number greater than 250 can survive from the spontaneous fission.
24. The energy yielding efficiency of a fusion reaction is much higher compared to that of a fission reaction.
25. Though the fusion reaction is a better source of energy compared to the fission process, it is almost impossible to execute the process in practice.
26. The cobalt bomb is more dangerous than the simple hydrogen bomb.
27. In an atom bomb, the subcritical masses of the fissile material are kept separated.
28. At the moment of action, a hydrogen bomb is more destructive than an atom bomb, but the after-effect of an atom bomb explosion is more dangerous.
29. The fission parameter Z^2/A is very much important to predict the stability of a nuclide with respect to its spontaneous fission reaction.
30. Practically, the Coulomb potential barrier E_{Coul} gives the measure of nuclear fission barrier (E_b).
31. The magnitude of E^* (activation energy in fission) depends on both fission barrier (E_b) and E_f (fission energy).
32. The critical deformation energy (E_{crit}) for fission of a compound nucleus can be obtained from the liquid drop model of nucleus.
33. The nuclear cross-section parameter is very important in predicting the efficiency of a nuclear reaction.
34. The basic condition for a fission reaction is : $E_{ex} \geq E^* = E_b - E_f$.
35. In terms of liquid drop model, the condition for a projectile (of low kinetic energy) promoted fission reaction is given by :
    E_B (= projectile binding energy in the compound nucleus) $\geq E_{crit}$.
36. The principle of *equal charge displacement* is important to predict the stable isobaric nuclides produced in a particular fission reaction.
37. Very often, a fission reaction leads to production of isobaric nuclides.
38. The stable nuclide in an isobaric series obtained through successive β-decay can be predicted by considering the semi-empirical mass equation.
39. All the elements of the universe are synthesised from hydrogen which was synthesised from neutron.
40. In the universe, iron is an abundant element.

. Numerical Problems

1. Find the Q value in the reaction $^{14}_{7}N\ (\alpha, p)\ ^{17}_{8}O$. The atomic masses of ^{14}N, ^{4}He, ^{17}O and ^{1}H are 14.00755, 4.00388, 17.00435 and 1.00815 respectively in amu.
   (*Ans.* ~ – 1.0 MeV)

Click Here t.me/thealchemylibrary

2. Calculate the Q value in the reaction, ${}^{30}_{14}Si\,(d, n)\,{}^{31}_{15}P$, given that,
   ${}^{30}_{14}Si + d \rightarrow {}^{31}_{14}Si + p + 4.37$ MeV; ${}^{31}_{14}Si \rightarrow {}^{31}_{15}P + {}^{0}_{-1}e + {}^{0}_{0}\bar{\nu} + 1.51$ MeV;
   $n \rightarrow p + {}^{0}_{-1}e + {}^{0}_{0}\bar{\nu} + 0.782$ MeV;
   (*Ans.* $Q = 5.10$ MeV)
3. Find the atomic mass of ${}^{7}_{3}Li$, if the Q value of the reaction ${}^{7}_{3}Li\,(p, \alpha)\,{}^{4}_{2}He$ is 17.3 MeV.
   (Given, the atomic masses in amu are : ${}^{4}He = 4.00388$ amu, ${}^{1}H = 1.00815$ amu).
   (*Ans.* 7.018 amu)
4. In the fission of ${}^{235}U$ by a thermal neutron, the fragments (along with two neutrons produced) are having nuclear binding energy 8.5 MeV per nucleon. If the fissile nuclide shows $\bar{B} = 7.8$ MeV, calculate the fission energy released.
   (*Ans.* 147.5 MeV per ${}^{235}U$ atom)
5. The fission fragments in the fission of ${}^{235}U$ are ${}^{98}_{42}Mo$ and ${}^{136}_{54}Xe$. Complete the reaction. Calculate the energy released per fission.
   (Given, the atomic masses are : ${}^{235}U = 235.044$ amu, ${}^{136}Xe = 135.907$ amu, ${}^{98}Mo = 97.906$ amu, ${}^{1}n = 1.0086$ amu).
   (*Ans.* : ${}^{235}_{92}U + {}^{1}_{0}n \rightarrow {}^{98}_{42}Mo + {}^{136}_{54}Xe + 4\,{}^{0}_{-1}e + 2\,{}^{1}_{0}n$; ~ 207 MeV per fission).
6. Calculate the energy released when 500 g deuterons are consumed as the nuclear fuel in the fusion reaction ${}^{2}_{1}H + {}^{2}_{1}H \rightarrow {}^{4}_{2}He$.
   (Given, the atomic masses are : ${}^{2}_{1}H = 2.0147$ amu, ${}^{4}_{2}He = 4.00388$ amu).
   (*Ans.* 2.88×10^{14} J)
7. Calculate the mass of ${}^{235}U$ required for fission to produce the same amount of energy obtained from 1000 tonnes of coal. The heat of combustion of coal = 8800 kcal / kg.
   (Given : 1 tonne $= 10^3$ kg, fission energy per fission = 180 MeV)
   (*Ans.* 499.6 g).
8. The Q-value for the ${}^{13}N\,(n, p)\,{}^{13}C$ reaction is 3.236 MeV. Calculate the threshold energy of the projectile for the reverse reaction denoted by ${}^{13}C\,(p, n)\,{}^{13}N$.
   (*Ans.* 3.48 MeV, Hints : cf. Sec. 7.6).
9. Calculate the magnitude of the Coulomb barrier for the penetration of an α-particle towards ${}^{66}_{30}Zn$. (Assume, $R = 1.4 \times A^{1/3}$ F).
   (*Ans.* 10.95 MeV).
10. Calculate the fission energy (E_f), fission barrier (E_b) and activation energy ($E^{\neq}$) for the symmetric fission of ${}^{114}_{50}Sn$., i.e. ${}^{114}_{50}Sn \rightarrow {}^{57}_{25}Mn + {}^{57}_{25}Mn$.
    (Given : $R = 1.4A^{1/3}$ F, $m\,({}^{114}Sn) = 113.903$ u, $m\,({}^{57}Mn) = 56.9383$ u).
    (*Ans.* $E_f = 24.6$ MeV, $E_b = 77.95$ MeV, $E^{\neq} = 53.4$ MeV).
11. Fission of ${}^{235}_{92}U$ leads to stable nuclides ${}^{94}_{40}Zr$ and ${}^{140}_{58}Ce$. Find the primary fission products.
    (*Ans.* ${}^{94}_{37}Rb$, and ${}^{140}_{55}Cs$)

Click Here t.me/thealchemylibrary

8

Periodic Table and Periodic Trends of Different Properties of Elements

8.1 HISTORICAL BACKGROUND OF THE DEVELOPMENT OF PERIODIC CLASSIFICATION

From the very old days, chemists had attempted to classify the elements into some groups based on their chemical and physical properties to systematise the study. At the early days, the chemists had always attempted to find such a relationship with the atomic weights of the elements. But, as the correct atomic weights of all the elements known at that time were not known before 1860, many early attempts such as one made by Gladstone in 1852 in this field failed. **Actually the laborious works of Cannizaro, Stass and others provided the correct atomic weights of almost all the elements in and around 1860.** Then within a few years, the periodic classification taking the atomic weights as the basis came out from the German chemist, Lothar Meyer (1868-70) and the Russian chemist, Mendeleev (1868-70). Such empirical classifications have now been supported theoretically with the advent of electronic structure of the elements. However, before the attainment of the Mendeleev's periodic law, some early attempts which provided the key routes to the thinking of Mendeleev and Lothar Meyer are worth mentioning. Some such important events are mentioned below just to record the progress of the historical development.

8.1.1 Law of Triads

Dobereiner's law of triads : J.W. Dobereiner (1829) pointed out that within a group of three elements

Table 8.1.1.1. Some representative triads of Dobereiner

Triad Elements	*Li*	*Na*	*K*	*Ca*	*Sr*	*Ba*	*S*	*Se*	*Te*	*Cl*	*Br*	*I*
Atomic weight	7	23	39	40	88	137	32	80	128	35.5	80	127
Mean value of the atomic weights of the 1st and 3rd members of the triad		23			88.5			80			81.25	

Click Here to the Chemylibrary

having similar chemical and physical properties, the atomic weight of the middle element is the mean of the other two. Some examples of such triads are given in Table 8.1.1.1. He also pointed out the triad - iron, cobalt and nickel in which the atomic weights of the elements are almost the same.

Though it was the first successful attempt to rationalise the problem, it could not be generalised or extended.

8.1.2 Pattenkofer's Rule of Integral Multiple

Pattenkofer's rule of integral multiple : Pattenkofer in 1850 pointed out that **the atomic weights of the chemically similar elements differ by an integral multiple of 8.** It is illustrated in the following cases.

Chemically similar elements	*Atomic weight*	*Difference in atomic weights between the successive members in a family*
Li	7	
Na	23	23–7 = 16 = 8 × 2
K	39	39–23 = 16 = 8 × 2
O	16	
S	32	32–16 = 16 = 8 × 2
Se	80	80–32 = 48 = 8 × 6
Te	128	128–80 = 48 = 8 × 6

8.1.3 Chancourtois Law of Telluric Screw

Law of telluric screw : The French geologist A.B. de Chancourtois in 1862 pointed out that **the elements differing by 16 units in atomic weights among the successive members form a family of similar elements.** Thus it has similarity with the Pattenkofer's rule of integral multiple. Actually, Chancourtois placed the elements in order of increasing atomic weights on the surface of a regular cylinder in the following manner. The surface of the cylinder was divided into sixteen equal vertical columns. Then a helix making an angle 45° to the axis of the cylinder was drawn. The atomic weights were plotted vertically along the spiral line (Fig. 8.1.3.1). Interestingly, in this arrange-ment, the chemically similar elements fall in a particular vertical column and the successive members in the group differ by 16 units in atomic weights. The periodic arrangement of the elements along the helix around the cylinder looks like a screw. This is why it is referred to as the ***law of telluric screw.***

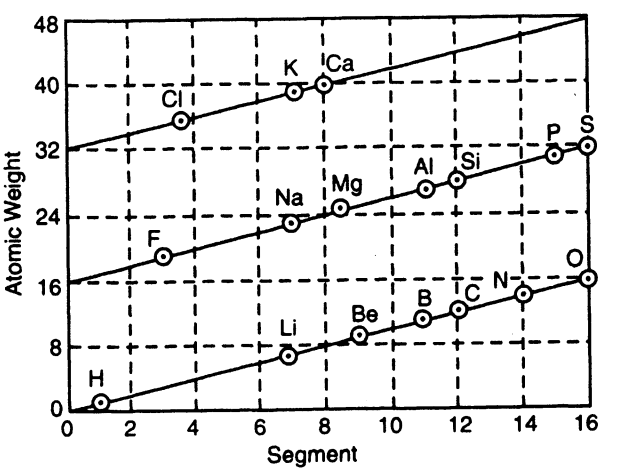

Fig. 8.1.3.1. The telluric screw of de Chancourtois.

8.1.4 Newlands' Law of Octaves

Law of Octaves : The English chemist J.A.R. Newlands reported (1864-66) that **if**

Click Here t.me/thearchemylibrary

the elements are arranged in order of increasing atomic weights, all the eighth elements have similar properties in most of the cases. As for examples, in the following series, in order of increasing atomic weight, the eighth elements differing in atomic weights by 7 units in each group, e.g. (*H*, *F*) or (*Li*, *Na*) or (*Be*, *Mg*), are similar in properties. This law of periodic recurrence of the properties is called ***Newlands' law of octaves*** because of its resemblance to the **musical scale** (*Sa Rae Ga Ma Pa Dha Ni Sa*).

Elements :	*H*	*Li*	*Be*	*B*	*C*	*N*	*O*	*F*	*Na*	*Mg*	*Al*
Atomic wt. :	1	2	3	4	5	6	7	8	9	10	11

The periodic classification of the elements according to the law of octaves is given in Table 8.1.4.1. Here it is worth mentioning that at that time, the inert gases were not known. The table consists of seven horizontal series (families) having analogous elements and eight vertical columns.

Table 8.1.4.1. Newlands' periodic classification of the elements

Group → / *Period* ↓	1	2	3	4	5	6	7	8
1	*H*	*F*	*Cl*	*Co, Ni*	*Br*	*Pd*	*I*	*Pt, Ir*
2	*Li*	*Na*	*K*	*Cu*	*Rb*	*Ag*	*Cs*	*Tl*
3	*Gl* (= *Be*)	*Mg*	*Ca*	*Zn*	*Sr*	*Cd*	*Ba, V*	*Pb*
4	*B*	*Al*	*Cr*	*Y*	*Ce, La*	*U*	*Ta*	*Th*
5	*C*	*Si*	*Ti*	*In*	*Zr*	*Sn*	*W*	*Hg*
6	*N*	*P*	*Mn*	*As*	*Di*, Mo*	*Sb*	*Nb*	*Bi*
7	*O*	*S*	*Fe*	*Se*	*Ro* (= *Rh*), *Ru*	*Te*	*Au*	*Os*

* *Di* stands for *didymium* which is actually a mixture of *Pr* and *Nd*. At that time, the mixture was obtained from the minerals and it was considered as the single element, didymium.

From the above table, it is evident that *though the octave rule works well for the lighter elements, it is deviated for the heavier elements.*

For the relatively heavier elements, marked inconsistencies existed in the above table because at that time the atomic weight data then available were incorrect and many elements which are now well known were unknown in Newlands' time.

8.1.5 Mendeleev's and Lothar Meyer's Periodic Laws

At the time of Newlands, many elements were not known and in some cases the actual atomic weights of the known elements, were not known. **Mendeleev pointed out that the properties of the elements are the periodic functions of their atomic weights.** Though this view at that time was strongly criticised, but the storm of criticism was pacified when he was awarded the highest honour, the Davy Medal by Royal Society, London in 1887. Lothar Meyer in Germany observed independently a similar relationship for different properties at the same time, but these were published in late. Thus the lion's share of the credit goes to Mendeleev. But, Lothar Meyer is still rightly remembered for his **atomic volume curve** which will be discussed later.

Click Here to me/thealchemylibrary

8.2 MENDELEEV'S PERIODIC LAW AND PERIODIC TABLE

The Mendeleev's periodic law states that the properties of the elements are the periodic functions of their atomic weights. In the modern periodic law, the atomic weight is replaced by the atomic number, because Moseley's work has clearly established that not the atomic weight but the atomic number is the fundamental property which governs the character of the elements under consideration.

In 1871, Mendeleev published the short periodic table. At that time, the inert gases were not discovered and only 63 elements were known. In his periodic table, Mendeleev specified some vacant sites for the undiscovered elements. He also predicted the properties of such elements in advance and in time the predictions were verified and found true. A long form of the periodic table was also proposed by Mendeleev.

8.2.1 Characteristics of Mendeleev's Short Periodic Table

The modern form of the short periodic table is shown in Table 8.2.1.1. The important features of the table are discussed here.

Table 8.2.1.1. Modern Version of Mendeleev's Short Periodic Table

Group → / Period ↓	0	I A	I B	II A	II B	III A	III B	IV A	IV B	V A	V B	VI A	VI B	VII A	VII B	VIII		
1	*He* 2	*H* 1																
2	*Ne* 10	*Li* 3		*Be* 4			*B* 5		*C* 6		*N* 7		*O* 8		*F* 9			
3	*Ar* 18	*Na* 11		*Mg* 12			*Al* 13		*Si* 14		*P* 15		*S* 16		*Cl* 17			
4		*K* 19		*Ca* 20		*Sc* 21		*Ti* 22		*V* 23		*Cr* 24		*Mn* 25		*Fe* 26	*Co* 27	*Ni* 28
	Kr 36		*Cu* 29		*Zn* 30		*Ga* 31		*Ge* 32		*As* 33		*Se* 34		*Br* 35			
5		*Rb* 37		*Sr* 38		*Y* 39		*Zr* 40		*Nb* 41		*Mo* 42		*Tc* 43		*Ru* 44	*Rh* 45	*Pd* 46
	Xe 54		*Ag* 47		*Cd* 48		*In* 49		*Sn* 50		*Sb* 51		*Te* 52		*I* 53			
6		*Cs* 55		*Ba* 56		*La** 57-71		*Hf* 72		*Ta* 73		*W* 74		*Re* 75		*Os* 76	*Ir* 77	*Pt* 78
	Rn 86		*Au* 79		*Hg* 80		*Tl* 81		*Pb* 82		*Bi* 83		*Po* 84		*At* 85			
7		*Fr* 87		*Ra* 88		*Ac*** 89-103												

The Rare Earths

* Lanthanide series (6th period)	*Ce* 58	*Pr* 59	*Nd* 60	*Pm* 61	*Sm* 62	*Eu* 63	*Gd* 64	*Tb* 65	*Dy* 66	*Ho* 67	*Er* 68	*Tm* 69	*Yb* 70	*Lu* 71
** Actinide series (7th period)	*Th* 90	*Pa* 91	*U* 92	*Np* 93	*Pu* 94	*Am* 95	*Cm* 96	*Bk* 97	*Cf* 98	*Es* 99	*Fm* 100	*Md* 101	*No* 102	*Lr* 103

Click Here t.me/theachemylibrary

Periods and Groups

The horizontal rows are called **periods** and the vertical columns are called **groups.** The elements are arranged in such a fashion that the elements of the same properties are placed in a group.

In the modern form of the table, there are **seven periods** and **nine groups** denoted by the letters (I to VIII and 0). The 0 (zero) group containing the inert gases was not initially recorded in the original Mendeleev's table. In terms **IUPAC recommendation,** the elements are classified into **18 groups (1 to 18)** where the inert gases are placed in Gr. 18.

Description of the Periods **:** (i) In the first period, there are only two elements, i.e. hydrogen and helium, and this is referred to as the ***very short period.*** (ii) The second (*Li* to *Ne*) and third (*Na* to *Ar*) periods contain eight elements each. These are called second and third ***short periods.*** (iii) The fourth and fifth periods consist of eighteen elements each. These are called ***long periods.*** (iv) The sixth and seventh periods consist of thirty two elements each. These are referred to as ***very long periods.*** The seventh period is still remaining incomplete. Most of the elements in this period are artificially prepared (see Sec. 7.11). Presently, the elements up to $Z = 112$ and $Z = 114$, 116 and 118 have been reported. Different names have been proposed (cf. Appendix IV) for these *translawrencium elements* ($Z > 103$).

Even and Odd Series **:** Each long period is divided into two series termed *even and odd* according to the serial number attached. In each of the long periods, the first seven elements (not considering the Gr-VIII elements) form the *even series* while the last seven (not considering the inert gas) elements form the *odd series*.

*Subgroups**

Except the 0 (zero) and VIII groups, all other groups are classified into *A* and *B* subgroups. *In the long periods, the elements of the even series are placed in A subgroup while the elements of the odd series are placed in the B subgroup.* Comparing with the properties of the heavier congeners in the long periods, the elements in the short periods are classified in the *A* and *B* subgroups. **In a particular group, the elements in a particular subgroup are chemically similar while except the valency, the similarity between the *A* and *B* subgroup elements in a particular group is lacking drastically.** For example in Gr I, the *A* subgroup ***alkali metals*** (i.e. *Li*, *Na*, *K*, *Rb*, *Cs*, *Fr*) differ drastically in properties from the *B* subgroup ***coinage metals*** (i.e. *Cu*, *Ag*, *Au*). This is revealed from the following comparison.

It is evident that the Gr *A* and Gr *B* elements in a particular group are very much dissimilar in properties. In general the Gr *B* elements are more electronegative (i.e. more nonmetallic) than the Gr *A* elements. **Thus, only in the short periods, all the elements in a particular group are chemically similar. Thus these elements are called typical or normal elements.**

Triad elements **:** In Gr VIII, there are three triads, each having three elements having very close atomic weights. *Each triad stands at the end of the even series of each long period.* The triads are *Fe, Co, Ni; Ru, Rh, Pd; Os, Ir, Pt.* The second and third triads are described as ***platinum metals*** after the name of the metal which has been most extensively studied. The atomic weights of the members in each triad are so close to one another that their placement in a single group is justified if the atomic weight is considered as the basis of the periodic arrangement. These triad elements were described as ***transitional*** or ***transition elements*** by Mendeleev.

* The designation of the subgroup by *A* and *B* appears quite arbitrary. Here the old designation is given. The modern books deal with a different convention which will be discussed later.

Click Here t.me/theachemylibrary

Table 8.2.1.2. Comparison of the properties of A and B subgroup elements of Gr-I.

Properties	*Group IA (Alkali metals)*	*Group IB (Coinage metals)*
(i) **Outermost electronic configuration**	ns^1	$(n-1)\,d^{10}ns^1$
(ii) **Valency**	1	*Cu*: 1, 2, (3*); *Ag* : 1, (2*, 3*); *Au* : 1, 3 (* denotes the unusual states)
(iii) **State of occurrence in nature**	They exist in compounds, and never exist in free state.	They exist both in chemical compounds and free state (e.g. *Ag, Au*).
(iv) **Electropositive character and reactivity**	They are highly electropositive in character and highly reactive.	They are less electropositive in character. The decreased activity makes them noble metals (e.g. *Ag, Au*).
(v) **Bond nature**	Ionic	Due to the higher polarising power they introduce more covalency in their bonds.
(vi) **Nature of oxide and hydroxide**	Highly alkaline	Slightly alkaline
(vii) **Complex compound**	No marked tendency is noticed to form coordination compounds (only some complexes with the *O*-donor are reported, no *LFSE*).	A marked tendency to form coordination complexes is noticed due to the ligand field stabilisation energy (*LFSE*) except for + 1 state.
(viii) **Colour of the compounds**	They generally form colourless compounds because of the absence of ligand field band (i.e. *d–d* transition) and charge transfer band (metal to ligand or ligand to metal.	They generally form coloured compounds due to the presence of the ligand field band (except in +1 state) and charge transfer band (ligand to metal due to the more polarising power of the metal ions).
(ix) **Hard-soft character of the cations**	Hard acids.	Soft and borderline acids.
(x) **Structure of metallic crystal**	They adopt the *bcc* (body centred cubic) structure and possess low cohesive energy giving rise to low melting points and density (packing efficiency ~ 68%)	They adopt the *fcc* (face centred cubic) structure and are highly malleable with a higher cohesive energy, higher melting point and higher density (packing efficiency 74%)

Group number and valency : The group number of an element gives its **highest possible valency** (called ***oxygen valency***) displayed in the binary compounds involving oxygen and the element; and the sum of the ***hydrogen valency*** (measured in the binary compounds of hydrogen) and ***oxygen valency*** is eight. This relationship is often referred to as ***Abegg's rule of contravalency.***

Inert gas elements : Each period ends with an inert gas and these are placed in the 0 (zero) group. Because of their chemical inertness, i.e. zero valency, they were placed under the ***Zero Group.*** But presently, some of the inert gas elements are found to form chemical compounds (see Sec. 9.23) with the highly electronegative elements like oxygen and fluorine.

Lanthanides (or lanthanoids) and actinides (or actinoids) (i.e. Rare earths) : In the sixth period, after *Ba*, the **fifteen elements** (*La* to *Lu*) are placed in a single room of Gr IIIA. The elements (*Ce* to *Lu*)

Click Here t.me/thalchemylibrary

are called *lanthanides*. Similarly, in the seventh period, the fifteen elements (*Ac* to *Lr*) are placed in a single room of Gr. IIIA. The elements (*Th* to *Lr*) are called ***actinides.*** Presently the IUPAC prefers the names ***lanthanoids*** and ***actinoids*** because the names ending with *-ide* mean negative ions. Similarly, the names ***lanthanons*** and ***actinons*** ending with *-on* which is preferred for the nonmetals are not encouraged. However, in this book, the widely used names, i.e. lanthanides and actinides, have been used. The placement of the lanthanides or actinides in a particular position is justified from the fact that the properties of the members in each family (i.e. lanthanides or actinides) are very much comparable though their atomic weight (more correctly atomic number) changes from one member to another. Lanthanides are widely used for making the ***pyrophoric alloy, mischmetal*** (*Ce* 50%, *La* 25%, *Nd* 18%, *Pr* 5% and other rare earths) used in lighter flints (alloyed with iron) and as an additive in steel to improve its malleability. Lanthanide complexes are also used as **NMR shift reagents** (cf. Sec. 8.23).

Transuranic elements **:** The seventh period remains yet incomplete and the elements after uranium are called ***transuranic elements.*** These are artificially prepared (see Sec. 7.11). The elements with $Z >$ 103 are called ***translawrencium elements*** (see Sec. 7.11 and Appendix IV).

Trivial names of different elements

(i) ***Alkali metals*** **:** *Li*, *Na*, *K*, *Rb*, *Cs*, *Fr* (in Gr. IA or 1). The hydroxides of the metals are strongly alkaline. This justifies the name.

(ii) ***Alkaline earth metals*** **:** *Ca*, *Sr*, *Ba*, *Ra* (in Gr. IIA or 2). The substances that remained unchanged by fire were called *earths* by the ancient chemists. The oxides i.e. lime, magnesia, strontia, baryta actually refer to the earths and these oxides (i.e. earths) are alkaline in reaction. **Thus, the term *alkaline earths* actually refers to the oxides of the metals.** It may be noted that *BeO* is amphoteric.

(iii) ***Chalcogens*** **:** *O*, *S*, *Se*, *Te*, *Po* (in Gr. IVA or 16). Greek word *chalcos* means *copper*. In nature, copper is usually found associated with sulfur and its congeners. This justifies the name.

(iv) ***Halogens*** **:** *F*, *Cl*, *Br*, *I*, *At* (in Gr. VIIA or 17). Greek word *halogen* means *salt-producer*. Elements of this group react with the metals to produce ionic halide salts. This justifies the name. In fact, the term halogen was first given to chlorine for its salt forming ability with the metals. The term was subsequently extended to all members of the group.

(v) ***Noble gases*** (inert or rare gases) : *He*, *Ne*, *Ar*, *Kr*, *Xe*, *Rn* (in Gr. VIIIA or 18). They are named so for their chemical inertness.

(vi) ***Lanthanum series*** **:** *La* to *Lu*. It is named so because the chemically similar elements appear after lanthanum.

(vii) ***Lanthanides* or *Lanthanoids or rare-earths*** **:** *Ce* to *Lu*. The word *earths* refer to the oxides and in fact, the elements were first discovered as their oxides. This is why, these were called rare earths (cf. alkaline earths). However, these are not rare and they occur widely in nature, usually together. **Thus the name is not appropriate.** In the ancient days, rare-earths included many *d*-block elements like *La, Sc, Y. Zr* and even actinides like *Th*.

(viii) ***Actinum series*** **:** *Ac* to *Lr*.

(ix) ***Actinides* or *Actinoids*** **:** *Th* to *Lr*. **Lawrencium** was originally represented by *Lw* but now as per IUPAC recommendation, it is represented by *Lr*.

(x) ***Coinage metals*** **:** *Cu*, *Ag*, *Au* (in Gr.IB or 11). These are known as *coinage metals* because of their former usage in making the coins used as primitive currency.

Click Here t.me/thealchemylibrary

(xi) ***Platinum metals*** : *Ru*, *Rh*, *Pd*, *Os*, *Ir*, *Pt* (in Gr. VIIIB or 8, 9 and 10). In this family, platinum is the oldest one and it is also the most abundant one in this family. Its chemistry is also most extensively studied among the members. This is why, the whole family is known by its name.

(xii) ***Noble metals*** : Platinum metals, *Au* (*Ag* and *Hg* are also included).

(xiii) ***Transuranium metals*** : Elements beyond *U*.

8.3 CHARACTERISTICS AND USEFULNESS OF THE MENDELEEV'S PERIODIC TABLE

8.3.1 Systematic Classification of the Elements

It is almost impossible to survey the chemistry of all the elements individually, but the periodic table indicates that the members in a particular subgroup in a group are having almost similar properties and the change in properties occurs among the same group members in a well defined order. This systematic classification has immensely helped the chemists to deal with the large number of elements into a few groups.

8.3.2 Correction of Atomic Weights

By placing the elements properly in the periodic table, Mendeleev became successful to determine the correct atomic weight in some cases.

(i) ***Atomic weight of Be*** : Because of the similarity in properties between *Be* and *Al*, *Be* was supposed to have the valency 3 like that of *Al*. From the equivalent weight (= 4.5) of *Be*, it was supposed to have the atomic weight = 3 × 4.5 (i.e. **atomic weight = valency × equivalent weight**) = 13.5. But in the group of *Al* (i.e., Gr III), there was no provision for an element having atomic weight 13.5. *Be* shows some similarities with the Gr II member *Mg*. Thus it was then considered as a bivalent one like *Mg*. It led to the atomic weight = 2 × 4.5 = 9 for *Be*, and there was an available site in the Gr II between *Li* and *B* for an element having atomic weight 9. In fact, in the later studies, the actual atomic weight determined was found to agree with the prediction.

(ii) ***Atomic weight of indium (In)*** : From the coexistence of *In* with the Gr II element *Zn* in nature, *In* was believed as a bivalent one. This led to its atomic weight = 2 × 38 = 76, where 38 stands for its equivalent weight. But in the Gr II, there was no vacant position to place an element having the atomic weight 76. Then considering it to be a trivalent one, its atomic weight was found to be 38 × 3 = 114, and it was placed in the Gr III between *Cd* (at. wt. 112, Gr II) and *Sn* (at. wt. 118, Gr IV). This predicted atomic weight has been confirmed from its specific heat (i.e. 0.055 cal/degree/gram) measurements (*cf.* **at. wt. × specific heat ≈ 6.4, Dulong and Petit's law**). Similarly, the atomic weights of many other elements were corrected.

8.3.3 Prediction of the Missing Elements

At the time of Mendeleev, only 63 elements were reported, but to place the elements in order of their increasing atomic weights based on the similarity in their properties, he had to keep some vacant rooms for the undiscovered elements. **Thus the vacancies indicated the *missing elements*.** He also predicted the properties of the undiscovered elements namely ***eka-boron, eka-aluminium*** which agreed well with scandium and gallium respectively discovered later during Mendeleev's life time. Similarly, in

Click Here : me/thealchemylibrary

Gr IV, he predicted ***eka-silicon*** which was subsequently confirmed as germanium. A comparison between the predicted properties of eka-silicon (*Es*) with the observed properties of germanium (*Ge*) is given in Table 8.3.3.1 as an illustration. Here it is worth noting that presently *Es* denotes the element einsteinium ($Z = 99$).

Mendeleev also predicted a missing element between *Mo* and *Ru* and it was confirmed in 1937 as ***technetium*** (*Tc*, $Z = 43$) with the development of nuclear chemistry. Other missing elements like ***promethium*** (*Pm*, $Z = 61$), ***astatine*** (*At*, $Z = 85$) have been artificially prepared (see Sec. 7.10).

Table 8.3.3.1. Predicted and observed properties of *Es* (*eka*-silicon) and *Ge*

Property	*Prediction for Es (1871, Mendeleev)*	*Observed for Ge (discovered by Winkler, 1886)*
Atomic weight	72	72.6
Specific gravity	5.50	5.40
Atomic volume	13.0 cc	13.2 cc
Colour	Dirty grey	Greyish white
Specific heat (cal/degree/g)	0.073	0.076
Oxide formation in heating in air	White powder, EsO_2	White powder, GeO_2
Properties of oxide	High melting point; sp. gr. 4.7; less basic than TiO_2 and SnO_2 but more basic than SiO_2. Mol. vol. 22 cc.	High melting point; sp. gr. 4.703; weakly basic. Mol. vol. 22.16 cc.
Preparation	Reduction of EsO_2 or K_2EsF_6 by *Na*.	Reduction of GeO_2 by *C* and K_2GeF_6 by *Na*.
Reaction with acids and bases	Slightly reactive with acids, but no remarkable reactivity with the base.	Not attacked by *HCl* but by aquaregia; attacked by *KOH* when only fused together.
Properties of chlorides	$EsCl_4$: b.p. 100°C; sp. gr. 1.9 (0°C)	$GeCl_4$: b.p. 86.5 C; sp. gr.1.887 (20°C)
Organometallic compound	$Es(C_2H_5)_4$: b.p. 160°C, sp. gr. 0.96	$Ge(C_2H_5)_4$: b.p. 160°C, sp.gr. < 1.0

8.4 DEFECTS IN THE MENDELEEV'S PERIODIC TABLE

(i) **Reverse atomic weight order in some cases :** Though the elements are placed in the order of their increasing atomic weights, in some cases the trend is reversed to allow the placement of the elements in proper groups in terms of properties. There are four such pairs :

I (127) and *Te* (128); *K* (39) and *Ar* (40); *Ni* (58) and *Co* (59); *Th* (232) and *Pa* (231).

However, the discrepancy in the atomic weight sequence results from the occurrence of isotopes. For example, in the pair *Ar* and *K*, both have three naturally occurring isotopes with different relative abundances shown below.

Element	*Atomic weight*	*Atomic number*	*Isotopic number*	*Natural abundance %*
Ar	40	18	36	0.34
			38	0.06
			40	99.6
K	39	19	39	93.1
			40	0.12
			41	6.78

Click Here t.me/thealchemylibrary

Here for *Ar*, the heaviest isotope is the most abundant one while for *K*, the lightest isotope is the most abundant one. This is why, the reverse sequence in their atomic weights is observed in the Mendeleev's periodic table.

(ii) **Triads in Gr-VIII :** Though the different elements are separately housed in different rooms, in Gr VIII, the three elements, i.e. *Fe, Co, Ni or Ru, Rh, Pd* or *Os, Ir, Pt*, are placed in each of the single rooms of the periods 4 to 6. The members in each triad (i.e. family) are not more similar compared to the other cases of adjacent elements in the periods. Thus, in terms of properties there is no speciality among the members of each triad, but still because of the absence of suitable vacant rooms, they are placed in the single rooms.

(iii) **Subgroup elements lacking in similarities :** Each group is subdivided into *A* and *B* subgroups, but in the long periods, similarity in the properties among the members of the two subgroups in a particular group is hardly found. For example, the alkali and coinage metals are widely different in properties which have been discussed earlier (Table 8.2.1.2).

(iv) **Positions of isotopes and isobars :** According to the Mendeleev's periodic law (i.e. placement in the order of atomic weight), the isotopes should have different positions while the isobars (atoms of the different elements but of the same mass numbers) should be placed in the same room. This is not justified.

(v) **Group valency :** Though the group number indicates the highest possible valency state (i.e. oxygen valency) of the elements, except *Ru* and *Os* of Gr VIII, no one in the group shows the valency 8.

(vi) **Missing link between the Gr-VIIB and Gr-IA elements :** The transition from the highly electronegative halogens (i.e. Gr VIIB) to the highly electropositive alkali metals (i.e. Gr IA) through the inert gases (i.e. Gr 0) can hardly be rationalised in terms of atomic weights.

(vii) **Relative stabilities of oxidation states :** The relative stabilities of the different oxidation states of an element cannot be interpreted from its group position and atomic weight.

(viii) **Peculiarity of the lightest congener in each group :** The first member (i.e. lightest congener) of each group is drastically different from the other members of the group (see Sec. 8.22).

(ix) **Diagonal relationship :** The existence of diagonal relationship (e.g. *Li* and *Mg*, *Be* and *Al*, *B* and *Si* pairs) for the short period elements can hardly be rationalised in terms of atomic weights.

(x) **Position of lanthanides and actinides :** The position of the lanthanides or actinides in a single room cannot be properly understood.

(xi) **Uncertainty in the prediction of the number of missing elements :** The successive members in the periods differ in atomic weights by different extents (i.e. 1 to 4 units). Hence, it is difficult to predict the number of missing elements present between the elements whose atomic weights are known. Because of the fact, it was difficult to predict the exact number of lanthanides and actinides from the knowledge of atomic weights.

(xii) **Position of hydrogen :** The position of hydrogen creates a confusion as it has similarities in properties with both the Gr-1A (i.e. alkali metals) and VIIB (i.e. halogens) elements (see Sec. 8.21).

(xiii) **Different capacities of the periods :** The different capacities (i.e. 2, 8, 8, 18, 18, 32, 32) of the different periods to house the elements cannot be rationalised from the Mendeleev's periodic law.

All these observations strongly hint that the choice of atomic weight as the basis of the periodic law

Click Here t.me/thealchemylibrary

is not correct and all these shortcomings are removed by considering the more fundamental property, i.e. atomic number, which governs the electronic configuration as the basis of the periodic law.

8.5 LONG FORM OF THE MODERN PERIODIC TABLE

By using the modern law in terms of atomic number, the defects in the Mendeleev's periodic table are largely overcome. Based on this idea, different workers have proposed different types of periodic tables to classify the elements. Out of these, the most widely used form is the ***long form of the periodic table.*** It is also referred to as ***Bohr's table*** (Table 8.5.1) as it follows the Bohr's classification of the elements based on the outermost electronic configuration governed by the ***aufbau*** **principle** of the elements. In

Table 8.5.1. Important Segments of the Long Form of the Modern Periodic Table

	← *s-block (ns)* →		← *d-block, (n-1)d* →										← *p-block (np), nonmetals* →					
Group→ Period ↓	**IA (1)**	**IIA (2)**	**IIIB (3)**	**IVB (4)**	**VB (5)**	**VIB (6)**	**VIIB (7)**	**VIIIB (8)**	**VIIIB (9)**	**VIIIB (10)**	**IB (11)**	**IIB (12)**	**IIIA (13)**	**IVA (14)**	**VA (15)**	**VIA (16)**	**VIIA (17)**	**VIIIA (18)**
1 (1*s*)	*H* 1		**Transition metals (d-block)**														*H* 1	*He* 2
2 (2*s*, 2*p*)	*Li* 3	*Be* 4											*B* 5	*C* 6	*N* 7	*O* 8	*F* 9	*Ne* 10
3 (3*s*, 3*p*)	*Na* 11	*Mg* 12											*Al* 13	*Si* 14	*P* 15	*S* 16	*Cl* 17	*Ar* 18
4 (4*s*, 3*d*, 4*p*)	*K* 19	*Ca* 20	*Sc* 21	*Ti* 22	*V* 23	*Cr* 24	*Mn* 25	*Fe* 26	*Co* 27	*Ni* 28	*Cu* 29	*Zn* 30	*Ga* 31	*Ge* 32	*As* 33	*Se* 34	*Br* 35	*Kr* 36
5 (5*s*, 4*d*, 5*p*)	*Rb* 37	*Sr* 38	*Y* 39	*Zr* 40	*Nb* 41	*Mo* 42	*Tc* 43	*Ru* 44	*Rh* 45	*Pd* 46	*Ag* 47	*Cd* 48	*In* 49	*Sn* 50	*Sb* 51	*Te* 52	*I* 53	*Xe* 54
6 (6*s*, 4*f*, 5*d*, 6*p*)	*Cs* 55	*Ba* 56	*La** 57	*Hf* 72	*Ta* 73	*W* 74	*Re* 75	*Os* 76	*Ir* 77	*Pt* 78	*Au* 79	*Hg* 80	*Tl* 81	*Pb* 82	*Bi* 83	*Po* 84	*At* 85	*Rn* 86
7 (7*s*, 5*f*, 6*d*, 7*p*)	*Fr* 87	*Ra* 88	*Ac*** 89	*Unq* 104 (*Rf*)	*Unp* 105 (*Db*)	*Unh* 106 (*Sg*)	*Uns* 107 (*Bh*)	*Uno* 108 (*Hs*)	*Une* 109 (*Mt*)	*Uun* 110	*Uuu* 111	*Uub* 112						
													← ***Posttransition metals*** →					

The Rate Earths, $(n-2)f$

f-block	****Lanthanide series (4f), Period : 6***	*Ce* 58	*Pr* 59	*Nd* 60	*Pm* 61	*Sm* 62	*Eu* 63	*Gd* 64	*Tb* 65	*Dy* 66	*Ho* 67	*Er* 68	*Tm* 69	*Yb* 70	*Lu* 71
	***** Actinide series (5f) Period : 7***	*Th* 90	*Pa* 91	*U* 92	*Np* 93	*Pu* 94	*Am* 95	*Cm* 96	*Bk* 97	*Cf* 98	*Es* 99	*Fm* 100	*Md* 101	*No* 102	*Lr* 103

In the present IUPAC system 1988, the groups are numberd from 1 to 18.

Click Here t.me/thealchemylibrary

fact, this periodic table is nothing but a graphical representation of the *aufbau* principle. **Actually, the long form of the periodic table can be obtained by extending the long periods through the splitting of the subgroups of the Mendeleev's short periodic table.** Hence, it is also referred to as the ***extended form of the periodic table.*** In Mendeleev's form, in numbering the groups, it over-emphasizes the slightest similarities between the *A* and *B* subgroup elements and there is a large number of elements in Group VIII. To avoid these, IUPAC have suggested (1988) to number the groups 1 to 18 (cf. Table 8.5.1).

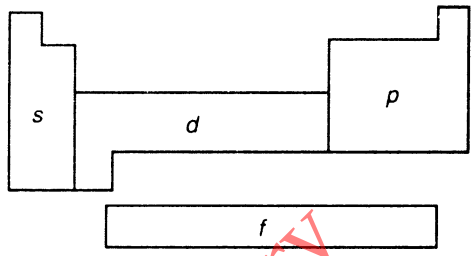

Fig. 8.5.1. Different segments (*s*–, *p*–, *d*–, *f*–block) of elements in the long form

(i) ***The left portion*** **(Gr. 1 and 2) :** It consists of Gr 1A or Gr 1 (i.e. *alkali metals*) and Gr IIA or Gr 2 (i.e. *alkaline earth metals*) which are characterised by the outermost electronic configurations ns^1 and ns^2 respectively. Based on the electronic configuration, hydrogen ($1s^1$) and helium ($1s^2$) are to be placed in this portion. The elements residing in this portion are also referred to as ***s-block elements*** because the differentiating electron goes to *ns*-level.

(ii) ***The middle portion*** **(Gr. 3-12),** *i.e.* ***B-block elements**** **:** This portion consists of the Gr 3 to 12 elements, i.e. Gr IIIB, IVB, VB, VIB, VIIB, VIII (i.e. VIIIB), IB and IIB elements. The electronic configuration of these elements can be generally represented as $(n-1)\,d^{1-10}ns^{1-2}$. **Generally, the differentiating electron goes to $(n-1)d$ sublevel.** This is why, this segment is very often referred to as ***d-block.*** These *d*-block elements are also described as *transition metals which are classically defined as the elements having incompletely filled* $(n-1)d$ *sublevel in their ground states at their elemental or stable ionic states*. Thus the *Zn*-family members should not be treated as the transition elements as neither in their elemental nor their most commonly occurring oxidation states, the *d* sublevels are partly filled in. But generally these are not excluded from the transition series. The arguments in favour of their inclusion will be discussed later (see Sec. 8.8 (i)). Thus the *d*-block or *B*-block elements are divided into four series.

(a) ***First transition series*** **(i.e. 3*d* series) :** ${}_{21}Sc$ to ${}_{30}Zn$ (10 elements).

(b) ***Second transition series*** **(i.e. 4*d* series) :** ${}_{39}Y$ to ${}_{48}Cd$ (10 elements).

(c) ***Third transition series*** **(i.e. 5*d* series) :** ${}_{57}La$ and ${}_{72}Hf$ to ${}_{80}Hg$ (10 elements).

(d) ***Fourth transition series*** **(i.e. 6*d* series) :** Most of the elements of this series are artificially synthesised (see Sec. 7.11). The elements in this series are : i.e. ${}^{89}Ac$, ${}^{104}Rf$ (rutherfordium), ${}^{105}Db$ (dubnium), ${}^{106}Sg$ (seaborgium), ${}^{107}Bh$ (bohrium), ${}^{108}Hs$ (hassium), ${}^{109}Mt$ (meitnerium). The other elements with $Z = 110, 111, 112$ have been synthesised and characterised (1994-96, at GSI, Darmstadt). For naming these translawrencium elements, the Appendix IV is referred.

(iii) ***Inner-transition series*** **(*i.e. lanthanide and actinide elements*) :** These two series belong to Gr IIIB (i.e. Gr 3), but because of their special type of electronic configuration they are placed away from the main body of the periodic table. For these series, generally the differentiating electrons go to the $(n-2)f$ sublevels. This is why, they are referred to as *f*-block elements.

* Presently the *d*-block elements are classified as *B*-group elements and the *p*-block elements are designated as *A*-group elements. Many books flow the opposite convention.

Click Here to the Chemistry Library

Lanthanides (i.e. 4*f* series): $_{58}Ce$ to $_{71}Lu$. **Actinides (i.e. 5*f* series) :** $_{90}Th$ to $_{103}Lr$.

(iv) ***The right portion* (Gr 13-18) :** It consists of Gr 13 to 18 i.e. Gr IIIA, IVA, VA, VIA, VIIA and Zero (i.e. Gr VIIIA). Except *He*, the differentiating electrons go to the *np* level. This is why, these are generally described as ***p-block elements.*** This segment can be further classified into different subsegments namely ***metalloids*** (e.g., *Ge, As, Se, Sb,* etc.), ***nonmetals and noble gases.*** There is no sharp line of demarcation to classify the metals and nonmetals, but the diagonal line (looking like a ***stair-step***) running from *B* to *At* (Table 8.5.1) is considered to divide the metals and nonmetals. The elements lying between the *d*-block elements and the stair-step diagonal line are metals and these are referred to as ***posttransition elements***. However, *Al* is not a posttransition element.

In the 7th period, some of the elements ($Z = 114, 116, 118$) in the *p*-block have been synthesised (see Sec. 7.11, ***translawrencium elements***).

8.5.2 Advantages of the Long Form of Periodic Table

(i) ***No reverse order for placement in terms of atomic number* :** By considering the more fundamental basis, i.e. atomic number, the problems of reverse order of atomic weights in placing the elements in the pairs, i.e. *I, Te; K, Ar; Ni, Co; Th, Pa*, are removed.

(ii) ***Interpretation of properties in terms of electronic configuration* :** The gradual change in properties along the periods and groups can be interpreted by considering the electronic configuration, i.e. atomic number.

(iii) ***No concept of subgroups and odd and even series* :** The *A* and *B* subgroup (the convention of designation by *A* and *B* is arbitrary, but presently the metals are placed in *B* subgroup and nonmetals in *A* subgroup) elements are placed separately. Hence the question of odd and even series does not arise.

(iv) ***Splitting of triad positions* :** Though the triads are placed in Gr VIII, i.e. VIIIB, in terms of electronic configurations, they are separately grouped having the general electronic configurations $(n-1)d^6ns^2$, $(n-1)d^7ns^2$ and $(n-1)d^8ns^2$ for the triad members respectively. According to IUPAC convention, Gr 8-10 constitute the triads.

(v) ***Positions of lanthanides and actinides* :** The fourteen lanthanides are not forced to be placed in a single room. In terms of electronic configurations of the $(n-2)f$ (i.e. $4f$) sublevel, the fourteen lanthanides have got fourteen rooms characterised by $4f^1$, $4f^2$,..... $4f^{14}$. The same thing appears for the actinides based on the electronic configurations of the $5f$ sublevel.

(vi) ***Interpretation of variable valence for the transition elements and fixed valency for the lanthanides* :** The common oxidation state +3 for the lanthanides arises due to the availability of three valency electrons in the outer levels. The differentiating electrons remain in the chemically inert $(n-2)f$ sublevel. In the same way, the common +2 oxidation state for the *d*-block elements arises due to the ns^2 electronic configuration. *For the transition series, the $(n-1)d$ sublevel in which the differentiating electrons are placed is not so inert. This is why, the variable valency for the transition series is a common phenomenon.*

(vii) ***Prediction of valences and stable oxidation states* :** In predicting the stable oxidation states, not the group number but the electronic configuration is a much better criterion.

Click Here t.me/thealchemylibrary

(viii) ***Splitting into s-, p-, d- and f-block elements in terms of the differentiating electron***: The splitting of the periodic table into *s*-, *p*-, *d*- and *f*-block elements provides a better understanding of the chemistry of the elements in each block.

(ix) ***Distribution of metals and nonmetals*** : The ***stair-step diagonal*** gives an idea of the distribution of the metals and nonmetals. The metals exist at the left side of the stair-step while the nonmetals are placed at the right side of the **stair-step.**

(x) ***Interpretation of the properties of s- and p-block elements*** : The chemical inertness of the noble gases having the electronic configurations ns^2np^6 can be understood from the concept of filled level. To show covalency, orbitals of the higher principal quantum number, i.e. $(n + 1)$, are to participate but it is not energetically favourable. Besides this, the filled level does not want to gain or lose any electron to disturb the filled level. The halogen family experiences a tendency to have the filled inert gas configuration ns^2np^6 from ns^2np^5 by gaining an additional electron. This is why, **the halogens show high electronegativity and electron affinity.** On the other hand, the alkali metals tend to attain the stable inert gas structure by losing the outermost ns^1 electron. **This is why, they are highly electropositive in character.** Thus the transition from the highly electronegative elements to the highly electropositive elements through the noble gases can be explained.

(xi) ***Interpretation of the capacity of periods to accommodate the elements*** : The maximum capacity of each period to accommodate the elements can be understood in terms of electronic configuration.

Period	*Orbitals involved*	*No. of involved orbitals*	*Capacity of the period (i.e. No. of elements)*
1st	1s	1	2 (= 2 × 1)
2nd	2s, 2p	1 + 3 = 4	8 (= 2 × 4)
3rd	3s, 3p	1 + 3 = 4	8 (= 2 × 4)
4th	3d, 4s, 4p	5 + 1 + 3 = 9	18 (= 2 × 9)
5th	4d, 5s, 5p	5 + 1 + 3 = 9	18 (= 2 × 9)
6th	4f, 5d, 6s, 6p	7 + 5 + 1 + 3 = 16	32 (= 2 × 16)
7th	5f, 6d, 7s, 7p	7 + 5 + 1 + 3 = 16	32 (= 2 × 16)

8.5.3 Defects of the Long Form Periodic Table

We have already mentioned that the long form of the periodic table stands on the ***aufbau* principle** of electronic configuration. This *aufbau* principle works well for the lighter elements while for the heavier elements it deviates significantly; and also for the half- and full-filled levels, the aufbau principle does not work. These aspects have been discussed in Sec. 1.11. **Thus the limitations of the aufbau principle are transmitted into the periodic table.** Some important defects are mentioned below.

(i) ***Dispute in the position of hydrogen*** : The problem regarding the position of hydrogen is not settled satisfactorily (see Sec. 8.21). In terms of electronic configuration ($1s^1$), it is to be placed in the alkali metal group. The formation of H^+ also supports its placement in the Gr IA i.e. Gr 1, but it can also form H^- like the halogens by taking an electron. Thus it shows a similarity with the halogens to get placed in Gr VIIA i.e. Gr 17. But in fact, hydrogen differs significantly from both the alkali metals and halogens.

Click Here t.me/thealchemylibrary

(ii) ***Dispute in the position of helium :*** Again the position of *He* is not settled. In terms of electronic configuration (i.e. $1s^2$), it should be placed in the alkaline earth metal group, i.e. Gr IIA i.e. Gr 2, but from the standpoint of the chemical inertness, it is placed in the family of inert gases (Gr VIIIA i.e. Gr 18) having the general electronic configuration ns^2np^6. Thus from the consideration of the properties, it is to be placed in the group of the inert gases while from the electronic configuration, it is to be placed in the Gr IIA i.e. Gr 2.

(iii) ***Detachment of f-block elements from the main periodic table*** : The inner-transition series (i.e. *f*-block elements) are thrown out from the main body of the periodic table. It indicates apparently that the members of these series do not obey the trends followed by the main body elements.

(iv) ***Position of isotopes of lighter elements*** : The isotopes have not got separate rooms. For the heavier elements, the properties of the isotopes of an element are more or less the same. But, for the isotopes of the lighter elements, the physical, kinetic and thermodynamic properties are drastically different. For example, the isotopes of hydrogen, i.e. hydrogen (*H*), deuterium (*D*) and tritium (*T*), are so different in properties that to place them in a single room is really surprising.

(v) ***Position not always determined by electronic configuration*** : In the *d*-block elements, the missing of the groups having electronic configurations, $(n-1)d^4ns^2$ and $(n-1)^9ns^2$ do not have any explanation apparently. *Cr* and *Mo* are having the configurations $(n-1)d^5\ ns^1$ (n = 4 for *Cr* and = 5 for *Mo*) while *W* is having the configuration $(n-1)d^4ns^2$ (n = 6), but still *W* is placed in the group of *Cr* and *Mo*. In fact, the electronic configurations for the members of 5*d* series (i.e. 5th period) differ from their respective congeners of the 3*d* and 4*d* series in many cases, but the periodic table does not care for it. This drawback is the reflection of the drawback present in the *aufbau* principle. A similar situation arises in the inner-transition series also. ***Thus it can be safely concluded that the heavier elements are placed in order of their increasing atomic numbers not in terms of electronic configuration.***

(vi) ***Border line elements*** : The border line elements (see Sec. 8.8) lying in the border range of two adjacent blocks, i.e. *s*- and *d*-block or *f*- and *d*-block or *d*- and *p*-block, are having some properties common to both the blocks. Hence, the separation by a sharp line of demarcation cannot be justified in such cases.

8.6 EXTENDED PERIODIC TABLE : SUPERHEAVY ELEMENTS : POSTACTINIDES AND SUPERACTINIDES

With the synthesis of $_{101}Md$, $_{102}No$ and $_{103}Lr$, the actinide series (i.e. 5*f* series) is completed. Among the ***transactinides*** (i.e. ***postactinides***) the elements up to $Z = 112$ have been synthesised to complete the 6*d* series. These are : $_{104}Rf$, $_{105}Db$, $_{106}Sg$, $_{107}Bh$, $_{108}Hs$, $_{109}Mt$ and the elements with $Z = 110$, 111 and 112 had been synthesised (1994-96, at GSI, Darmstadt). In fact, for these ***translawrencium*** **elements** different names have been proposed from time to time (cf. Appendix IV). Thus the 6*d* series is ended with $_{112}$*eka-Hg* i.e. $_{112}Uub$. After $_{112}$*eka-Hg*, the 7*p* orbitals will be filled in for the elements of atomic number 113 to 118. Thus the 7-th period will be ended with an inert gas element $_{118}$*eka-Rn*. The elements with $Z = 114$ i.e. $_{114}Uuq$, 116 i.e. $_{116}Uuh$ and 118 i.e. $_{118}Uuo$ have been synthesised (Sec. 7.11). Then the 8-th period starts with the elements of atomic numbers 119 ($8s^1$) and 120 ($8s^2$); and with the element

Click Here to the chemvlibrary

of atomic number 121 ($_{121}$*eka-Ac*) another transition series (i.e. 7*d* series) starts. Then the *eka*-actinides will start with the filling of the 6*f* orbitals as expected. At this position, the relative energy order among the orbitals is not known with a high degree of certainty. Normally, the expected sequence of energy of the orbitals is :

$$8s < 5g < 6f < 7d < 8p.$$

Hence it is expected that before the 6*f* series, the 5*g* series (having 18 elements) should exist. Theoretical calculation shows that at the very beginning of the series, 5*g*, 6*f* and 7*d* orbitals are very much comparable in energy but with the increase of atomic number, the 5*g* and 6*f* orbitals become energetically lower than the 7*d* orbitals. It is believed that the 5*g* and 6*f* sublevels are still almost degenerate energetically. **This is why, the existence of two separate inner series, $5g^{1-18}$ (i.e. 5*g* series) and $6f^{1-14}$ (i.e. 6*f* series) is called in question. Seaborg had proposed that the 5*g* and 6*f* series will be combined to give a *mixed inner series having 32 elements. This combined inner series has been described as superactinides*** which starts with the element of atomic number 122 and ends up with the element of atomic number 153. The superactinides are followed by the 7*d* series ending with $_{162}$*eka-eka-Hg*. Thus the 8-th period gets ended with the inert gas element of atomic number 168. Thus Seaborg has speculated the extended periodic table up to 168 elements. These are as follows.

6-th Period : $_{55}Cs$ to $_{86}Rn$; 5*d series* : $_{57}La$, $_{72}Hf$ to $_{80}Hg$

7-th Period : $_{87}Fr$ to $_{118}$*eka-Rn*; 6*d series* : $_{89}Ac$, $_{104}Rf$ to $_{112}$*eka-Hg*

8-th Period : $_{119}$*eka-Fr* to $_{168}$*eka-eka-Rn*; 7*d series* : $_{121}$*eka-Ac*, $_{154}$*eka-Rf* to $_{162}$*eka-eka-Hg*.

Lanthanides or lanthanoids (4f series) : $_{58}Ce$ to $_{71}Lu$;

Actinides or actinoids (5f series) : $_{90}Th$ to $_{103}Lr$.

Superactinides (a mixed inner series consisting of 5g and 6f series) : Atomic number 122-153.

Table 8.6.1. A part of the **extended periodic table** (upto the hyothetical element with $Z = 168$)

	s-block		*d-block* Transition Metals										*p-block*					
6th period : (6*s*, 4*f*, 5*d*, 6*p*)	Cs (55)	Ba (56)	La* (57)	Hf (72)	Ta (73)	W (74)	Re (75)	Os (76)	Ir (77)	Pt (78)	Au (79)	Hg (80)	Tl (81)	Pb (82)	Bi (83)	Po (84)	At (85)	Rn (86)
7th period : (7*s*, 5*f*, 6*d*, 7*p*)	Fr (87)	Ra (88)	Ac** (89)	Rf (104)	Ha (105)	(106)	(107)	(108)	(109)	(110)	(111)	(112)	(113)	(114)	(115)	(116)	(117)	(118)
8th period : (8*s*, 5*g*, 6*f*, 7*d*, 8*p*)	(119)	(120)	*** (121)	(154)	(155)	(156)	(157)	(158)	(159)	(160)	(161)	(162)	(163)	(164)	(165)	(166)	(167)	(168)

Inner-Transition Metals

6th period : Lanthanides* (4*f* series)	Ce (58)	Pr (59)	Nd (60)	Pm (61)	Sm (62)	Eu (63)	Gd (64)	Tb (65)	Dy (66)	Ho (67)	Er (68)	Tm (69)	Yb (70)	Lu (71)
7th period : Actinides (5*f*-series)**	Th (90)	Pa (91)	U (92)	Np (93)	Pu (94)	Am (95)	Cm (96)	Bk (97)	Cf (98)	Es (99)	Fm (100)	Md (101)	No (102)	Lr (103)
8th period : Superactinides* (5*g* + 6*f*)**	(122)	(123)	(124)	(125)									(152)	(153)

Click Here t.me/tnscchemistrylibrary

The **relativistic effects** (Sec. 8.20.3) are important for the heavy elements.

Now let us consider the possibilities of the existence of the ***translawrencium elements*** (see Sec. 7.11 for synthesis). Based on the expected extra stabilities of the elements having magic number atomic number, i.e. $Z = 50, 82, 126$, Seaborg predicted the ***stability islands*** (Sec. 5.5.3a) of the relatively more stable elements having atomic numbers close to the magic numbers. The concept of **magic number** includes the relatively more stable elements with $Z = 114$, 164 and 184. In fact, some of the elements (e.g. $Z = 112, 114, 116, 118$) close to the island of stability with $Z = 114$ have been synthesised (Sec. 7.11). The stability is increased if both the number of protons and neutrons are magic numbers. The suggested stable nuclides are $^{278}_{114}Uuq$, $^{298}_{114}Uuq$ and $^{310}_{126}Ubh$. **Whatever may be their stability, *they will be born in the experimental tube and they will die in the same tube.*** The life period may be only a tiny fraction of an instant. Hence, how difficult it is to characterise the elusive elements! It requires more sophistication in our analytical techniques.

Naming of Superheavy Elements (SHE) **:** The IUPAC (1977) has recommended a new method of naming the superheavy elements from the atomic number. The digits expressing the atomic number of an element are serially represented by using the following numerical roots.

0 (*nil*), 1 (*un*), 2 (*bi*), 3 (*tri*), 4 (*quad*), 5 (*pent*), 6 (*hex*), 7 (*sept*), 8 (*oct*), 9 (*enn*).

The successive roots are put together and the name is ended by ***ium.*** To avoid repetition of some letters, the following procedure is adopted.

bi+ium = bium, tri+ium = trium, enn+nil = ennil, etc.

The procedure of naming the elements based on atomic number is illustrated in some cases.

Atomic number	Numerical roots	Name	Symbol
101	un + nil + un	unnilunium	Unu
102	un + nil + bi	unnilbium	Unb
103	un + nil + tri	unniltrium	Unt
104	un + nil + quad	unnilquadium	Unq
105	un + nil + pent	unnilpentium	Unp
106	un + nil + hex	unnilhexium	Unh
107	un + nil + sept	unnilseptium	Uns
109	un + nil + enn	unnilennium	Une
111	un + un + un	ununium	Uuu
190	un + enn + nil	unennilium	Uen
200	bi + nil + nil	binilnilium	Bnn

Click Here t.me/thearchenyilibrary

8.7 CLASSIFICATION OF THE ELEMENTS BASED ON THE ELECTRONIC CONFIGURATION AND CHEMICAL AFFINITIES

8.7.1 Classification Based on the Position of the Differentiating Electron

It is done on the basis of the nature of the atomic orbital into which the additional or differentiating electron is accommodated. Thus we get *s*-, *p*-, *d*- and *f*-block elements.

(i) ***s-block elements*** **(Gr 1-2) :** The general electronic configuration is ns^{1-2}. The differentiating electron goes to be accommodated in the outermost *s* orbital (i.e. *ns* orbital). It consists of Gr IA i.e. Gr 1 elements (i.e. *H, Li, Na, K, Rb, Cs, Fr*) having ns^1 and Gr IIA i.e. Gr 2 elements (i.e. *Be,*

Mg, Ca, Sr, Ba, Ra) having ns^2 electronic configurations. Thus, these occupy the extreme left portion of the periodic table.

(ii) ***p-block elements* (Gr 13-18) :** The differentiating electron gets placed in the outermost *p* orbital, i.e. *np* orbital. The general electronic configuration of the outermost shell is represented by ns^2np^{1-6}. It consists of the groups, i.e.

Gr IIIA i.e. Gr 13 (elements : *B, Al, Ga, In, Tl*) : ns^2np^1;

Gr IVA i.e. Gr 14 (elements : *C, Si, Ge, Sn, Pb*) : ns^2np^2;

Gr VA i.e. Gr 15 (elements : *N, P, As, Sb, Bi*) : ns^2np^3;

Gr VIA i.e. Gr 16 (elements : *O, S, Se, Te, Po*) : ns^2np^4;

Gr VIIA i.e. Gr 17 (elements : *F, Cl, Br, I, At*) : ns^2np^5;

Group 0, i.e. VIIIA i.e. Gr 18 (elements : *Ne, Ar, Kr, Xe, Rn*) : ns^2np^6;

Here *He* (ns^2) is excluded from the *p*-block elements in terms of electronic configuration, but from the standpoint of its chemical behaviour, it is justified to place it in the zero group (i.e. Gr 18).

(iii) ***d-block elements* (Gr 3-12) :** These are referred to as the *transition elements*. The differentiating electron goes to be accommodated in the first penultimate shell. It goes to the $(n-1)d$ sublevel. The general electronic configuration is given by $(n-1)d^{1-10}ns^{1-2}$. This block consists of IIIB, IVB, VB, VIB, VIIB, VIIIB, IB and IIB. These are Gr 3-12 in IUPAC convention. It is better to classify the elements into the following *d* series including the Gr IB i.e. Gr 11 and Gr IIB i.e. Gr 12 elements.

***3d* series :** *Sc, Ti, V, Cr, Mn, Fe, Co, Ni, Cu, Zn.*

***4d* series :** *Y, Zr, Nb, Mo, Tc, Ru, Rh, Pd, Ag, Cd.*

***5d* series :** *La, Hf, Ta, W, Re, Os, Ir, Pt, Au, Hg.*

***6d* series :** ${}_{89}Ac$, ${}_{104}Rf$, ${}_{105}Db$, ${}_{106}Sg$, ${}_{107}Bh$, ${}_{108}Hs$, ${}_{109}Mt$, ${}_{110}Uun$, ${}_{111}Uuu$, and ${}_{112}Uub$ (i.e. ${}_{112}eka\text{-}Hg$).

(iv) ***f-block elements* :** These are also described as *inner-transition elements*. Here the differentiating electron is placed in the second penultimate shell and it goes to the $(n-2)f$ level. The general electronic configuration for these elements is given by, $(n-2)f^{1-14}\,(n-1)d^{0-1}ns^2$. It consists of two series : lanthanides (i.e. 4*f* series), ${}_{58}Ce$ to ${}_{71}Lu$ and actinides (i.e. 5*f* series), ${}_{90}Th$ to ${}_{103}Lr$.

***4f* series :** *Ce, Pr, Nd, Pm, Sm, Eu, Gd, Tb, Dy, Ho, Er, Tm, Yb, Lu.*

***5f* series :** *Th, Pa, U, Np, Pu, Am, Cm, Bk, Cf, Es, Fm, Md, No, Lr.*

***Note* :** It may be pointed out that **in the case of *Th*,** the electronic configuration is $[Rn]6d^27s^2$ i.e. $(n-1)d$ level possesses 2 electrons and $(n-2)f$ level i.e. 5*f* level remains vacant.

The 4*f* levels are more deeply seated than the 5*f* levels (cf. Secs. 4.3, 8.20.3, 8.23). Specially for the lighter members, the 5*f* orbitals may also participate in bonding purposes while the 4*f* orbitals are hardly affected by the ligands. **The +3 oxidation state is a characteristic feature of the 4*f* series and in special cases to attain the half-filled and full-filled level conditions, some special oxidation states such as Ce^{4+} ($4f^0$), Sm^{2+} ($4f^7$) and Yb^{2+} ($4f^{14}$) become important.**

The heavier actinides behave just like the lanthanides while the lighter actinides in which the 5f orbitals show some bonding interactions behave like the transition metals and they show the variable oxidation states.

Click Here t.me/tirathemylibrary

In fact, $(n-1)d$ orbital is not deeply seated and it can participate in bonding in different extents depending on the conditions and ***variable oxidation state is a characteristic property of the transition elements.***

The bonding properties of the $4f$ and $5f$ orbitals have been compared in Sec. 4.3. The **relativistic effects** to control their bonding properties are also quite important (cf. Sec. 8.20.3).

8.7.2 Bohr's Classification based on Electronic Configuration

It is done depending on the number of incomplete shells in the electronic configuration. In this light, the elements are divided into four groups.

(i) ***Inert gas elements*** **:** For these elements, the outermost s and p sublevels are full-filled having the electronic configuration ns^2np^6. Thus the zero group (i.e. Gr 18) elements are the members of this family. *He* $(1s^2)$ is also included here. Because of the ***full-filled shell structure,*** these are generally ***chemically inert*** with respect to other elements. But now, some compounds of *Xe* and *Kr* have been characterised. They generally remain as ***monoatomic species*** among which the weak London dispersion force operates.

(ii) ***Representative or normal elements*** **:** These are characterised by the ***incompletely filled outermost shell,*** i.e. the n-th shell is partly filled while all the other inner shells are completely filled. These actually consist of the s- and p-block elements which have been discussed earlier.

(iii) ***Transition elements*** **:** These are characterised by the incompletely filled $(n-1)d$ sublevels. Evidently for these elements, the ***two outermost shells are incompletely filled.*** The d-block elements already discussed are the members of this group.

(iv) ***Inner-transition elements*** **:** These elements are having $(n-2)f$ levels incompletely filled along with the partial filling of the $(n-1)d$ level and n-th shell. ***Thus three outermost shells remain partially vacant.*** *These are consisting of the f-block elements discussed earlier.*

8.7.3 Goldschmidt's Geochemical Classification of Elements Based on Chemical Affinity

Distribution of different elements in *crust, mantle* and *core* of the earth is governed by their *chemical affinities*. The elements are classified into four groups based on their relative affinities for *metallic, sulfidic, silicate* and *gaseous phases*. These are given below :

(a) ***Siderophiles*** **(i.e. *iron loving elements*) :** These elements (which are metals) tend to be associated with the *iron present in core in free state. These elements are characterised by the incompletely filled outermost shell.* The triads of Group VIIIB (i.e. Gr No. 8-10) are the examples of this group. The common examples are : *Fe, Co, Ni, Ru, Rh, Pd, Os, Ir, Pt, Au* etc.

(b) ***Chalcophiles*** **(i.e. sulfide loving elements) :** These elements (which are metals) tend to be associated with the sulfide minerals. Their ions are in general ***soft acids*** (cf. HSAB theory). The metal ions contain 18 *electrons* in the valency shell. The common examples are : *Cu, Zn, Cd, Hg, Pb, As, Sb* etc.

(c) ***Lithophiles*** **(i.e. stone loving elements) :** These are metals. These metal ions tend to be associated with the oxide ions. These ions are typically ***hard acids*** (cf. HSAB theory). The ions of lithophiles possess *eight electrons* in the outermost shell. The examples are : *alkali metals, alkaline earth metals* and *early members of transition series.*

(d) ***Atmophiles*** **(i.e. vapour loving elements) :** Such elements tend to remain as gaseous components in the atmosphere. The examples are : *N, O,* inert gases etc.

Click Here t.me/thealchemylibrary

△H[a]		**Atmophile:** △N														△He
Li	Be	**Lithophile:** Na, Ca, Ti									B	C	△N	△O[a]	F	△Ne
Na	Mg	**Chalcophile:** Zn									Al	Si	P	S	Cl	△Ar
		Siderophile: (Fe)														
K	Ca	Sc	Ti	V	Cr	Mn	Fe	Co	Ni	Cu	Zn	Ga	Ge	As	Se	Br	△Kr
Rb	Sr	Y	Zr	Nb	Mo		Ru	Rh	Pd	Ag	Cd	In	Sn	Sb	Te	I	△Xe
Cs	Ba	La-Lu	Hf	Ta	W	Re	Os	Ir	Pt	Au	Hg	Tl	Pb	Bi			

Fig. 8.7.3.1. Geoclassification of the elements. [a] denotes the character to a lesser extent; *H* and *O* are basically known as lithophiles.

Note : The chemical affinity of an element depends on the local environment. Chromium is lithophilic in crust but in oxygen deficient condition, it can exist as a chalcophile. ***Iron is siderophilic in the core but lithophilic in the crust.***

The relationship between the geochemical classification of the elements and their periodic position are shown in Fig. 8.7.3.1.

8.8 CHARACTERISTICS AND POSITION OF THE BORDER LINE ELEMENTS

8.8.1 Position of the Zn-Family

The transition metals are characterised by the presence of partially filled *d* orbitals either in their elemental states or most commonly occurring oxidation states. If we follow this rule strictly, the elements namely *Zn*, *Cd* and *Hg* should be excluded from the transition metal family. As a matter of fact, other characteristic properties of the typical transition metals such as formation of stable coordination compounds, characteristic colour due to the ligand field band (i.e. *d–d* transitions), paramagnetic behaviour (at least in weak field ligands), etc. are not shown by *Zn* and its congeners. But still, they show a more pronounced tendency to undergo complex formation compared to the other nontransition metals, i.e. representative elements. Because of the lack of crystal field stabilisation energy (CFSE) they form relatively weaker (thermodynamically) complexes as supported by the *Irving Williams natural stability order*. **Thus from the standpoint of the properties, *Zn*, *Cd* and *Hg* are not surely typical transition metals, but both the properties of the transition and representative elements are fused in the family having a predominant inclination towards the transition metals.** Thus it is worthy to consider these as the transition metals rather than as the representative elements.

8.8.2 Positions of *Lu*, *Th* and *Lr*

The electronic configurations of *Lu*, *Th* and *Lr* are given here.

$$_{71}Lu : [Xe]4f^{14}\ 5d^{1}\ 6s^{2};\ _{90}Th : [Rn]5f^{0}\ 6d^{2}\ 7s^{2};\ _{103}Lr : [Rn]5f^{14}\ 6d^{1}\ 7s^{2}.$$

Here it may be pointed out that for the lighter members (e.g. *Th*) of actinides, the 5*f* and 6*d* orbitals

Click Here to me/bhealchemylibrary

are very close in terms of energy. From the electronic configurations, *Lu*, *Th* and *Lr* should be better considered as transition metals rather than the inner-transition metals. But the nature of oxidation states, and other properties of these elements indicate that these are more close to the respective inner-transition series.

8.8.3 Position of the Lighter Actinides (i.e. $_{90}Th$, $_{91}Pa$, $_{92}U$, etc.) : 4*f* Series (Lanthanides) vs. 5*f* Series (Actinides) (cf. Secs. 4.3, 8.20.3, 8.23)

Compared to the lanthanides, the actinides, at least the lighter ones strikingly differ at this point. The ***bonding properties of 4f and 5f orbitals*** have been compared in Secs. 4.3, 8.20.3, 8.23. ***The relativistic expansion of the 5f orbitals is more pronounced than that of the 4f orbitals*** (cf. Fig. 4.3.1). The 4*f* orbitals in the lanthanides are more deeply seated in the inner shells and these are hardly affected by the ligand environment while for the lighter actinides, ***the 5f orbitals are more exposed to the ligand field like the d orbitals as in the case of the transition metals. Thus these 5f electrons offer variable oxidation states, a characteristic property of the transition metals.*** Besides these, because of the vibronic coupling (an effect of the ligands), the peaks due to *f–f* transitions in the lighter actinides are broadened and intensified as in the *d–d* transitions for the transition metals. On the other hand, for the lanthanides, the 4*f* orbitals are deeply seated and are not influenced by the ligand fields and the corresponding absorption spectra due to the *f–f* transitions are sharp looking like the line spectra.

Thus, if the properties such as variable oxidation states, nature of absorption spectra, etc. are considered then the lighter actinides are much closer to the transition metals than to the inner-transition metals. Because of such similarities, previously *Th*, *Pa* and *U* were believed as the members of 6*d* series and placed in the groups of *Ti*, *V* and *Cr* i.e. Gr IVB (4), VB (5) and VIB (6) respectively. As the atomic number among the actinides increases i.e. effective nuclear charge increases, the 5*f* levels go to behave like the 4*f* orbitals and **the heavier ones behave like the typical inner-transition metals.**

Seaborg's "Actinide Hypothesis" (1944)

(cf. G. Kauffman, *Chem. Eng. News.*, 68(47), 18-29, 1990)

At the early days, chemists were misguided by the peculiar properties of the early members of the so called actinides. In fact, *Th, Pa* and *U* were mistakenly placed in Gr IVB (4), VB (5) and VIB (6) respectively in *d*-block. In 1944, Seaborg pointed out this incorrect assignment and he proposed these elements to be the members of a new **inner transition series** analogous to the lanthanides. This new inner transition series was described as **actinides** in his famous **actinide hypothesis.** At that time, Seaborg was strongly criticised and warned not to publish his actinide hypothesis because it would destroy his scientific career. Sometime later he narrated the event humorously as, "*I didn't have any scientific reputation so I published it anyway*".

The actinide hypothesis saved the chemistry from a wrong direction. Here it is worth mentioning that Seaborg and his group had synthesised many elements of the second inner transition series i.e. actinides. This aspect has been discussed in Sec. 7.11.

Click Here t.me/thealchemylibrary

Note : The **electronic configuration of *Th*** is : $[Rn]5f^0 6d^2 7s^2$ i.e. there is no electron in the $5f$ orbital. Thus in terms of electronic configuration, it should be regarded as a *d*-block element. In fact, for the lighter members of actinide series, the energy difference between the $6d$ and $5f$ orbitals is not very much high.

8.9 LANTHANIDE AND ACTINIDE CONTRACTIONS (i.e. *f*-CONTRACTIONS)

The ***bonding properties of 4f and 5f orbitals*** have been compared and discussed in Secs. 4.3, 8.20.3, 8.23.

8.9.1 Nature of the *f*-Contraction

The *f*-contraction is extremely important to understand the properties of the heavier elements, specially the **postinner-transition elements.** This is why, it is specially dealt here. We shall pay our major attention to the lanthanide contraction from which the causes and effects of the actinide contraction can be guessed. Here it is important to mention the ***d-contraction*** (rarely referred to as ***scandide contraction***) in the transition series, but it is less significant. *Effect of scandide contraction* on the 4th period elements (*Ga* to *Kr*) has been discussed in Secs. 8.10.2, 8.20, 8.24.

If we consider the lanthanides (*Ce* to *Lu*) and actinides (*Th* to *Lr*), their atomic and ionic radii gradually decrease (Fig. 8.9.1.1) (in general) along the series with the increase of atomic number. This gradual shrinkage in size is, in general, described as ***f-contraction*** and ***lanthanide contraction*** in the lanthanides and ***actinide contraction*** in the actinides.

If we consider the atomic (i.e. metallic) radii (Fig. 8.9.1.1) for the lanthanides, two peaks appear at ${}_{63}Eu$ ($[Xe]4f^7\ 5d^0\ 6s^2$) and ${}_{70}Yb$ ($[Xe]4f^{14}\ 5d^0\ 6s^2$). At these two elements, to attain the extra stability through the half- (*Eu*) and full-filled (*Yb*) *f*-level, ***Eu and Yb each can provide only two electrons for metallic bonding while the other members each can provide three electrons for the bonding purposes.***

Because of this fact, *Eu* and *Yb* experience less cohesive energy giving rise to larger metal-metal

Table 8.9.1.1. Metallic*, covalent and ionic radii (in picometre, pm) of the lanthanides

Elements	r_1	r_2	r_3	*Elements*	r_1	r_2	r_3
${}_{57}La$	188	169	106	${}_{65}Tb$	178	159	92
${}_{58}Ce$	182	165	103	${}_{66}Dy$	177	159	91
${}_{59}Pr$	183	165	101	${}_{67}Ho$	177	158	89
${}_{60}Nd$	182	164	99	${}_{68}Er$	176	157	88
${}_{61}Pm$	–	–	98	${}_{69}Tm$	175	156	87
${}_{62}Sm$	180	166	96	${}_{70}Yb$	194	170	86
${}_{63}Eu$	204	185	95	${}_{71}Lu$	173	156	85
${}_{64}Gd$	180	161	94				

* Metallic radii for 12 coordination number;. r_1 = Metallic radii; r_2 = Covalent radii; r_3 = Ionic radii (Ln^{3+}).

Click Here for the Academylibrary

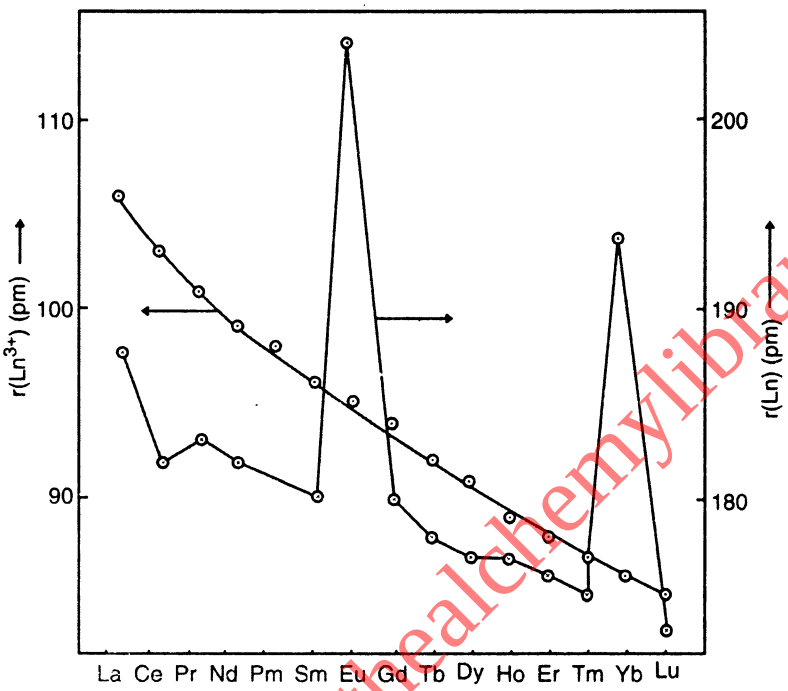

Fig. 8.9.1.1. Lanthanide contraction. $r(Ln^{3+})$ gives the ionic radii of Ln^{3+}; $r(Ln)$ gives metallic radii for C.N. = 12.

distance compared to the other members. Thus the two breaks in the smooth trend arise at *Eu* and *Yb*. Another interesting feature of the curve is that *the right hand segment of the curve from Gd is nothing but a duplication of the left hand segment*. The dividing point at *Gd* arises as it possesses the half-filled $4f$ shell ($[Xe]4f^7\ 5d^1\ 6s^2$).

8.9.2 Explanation of *f*-Contraction

In the *f*-series, the differentiating electron goes to the second penultimate shell in the $(n–2)f$ sublevel. The *f* levels are of very much low screening power because of their diffused shape. In fact, the penetrating power of the orbitals for a particular principal quantum number runs as : $s > p > d > f$ (see Secs. 1.9.2; 1.1.4). **Thus with the gradual addition of the *f* electrons, the effective nuclear charge (Z^*) experienced by the valence shell electrons gradually increases with the increase of atomic number along the series. This is why, there is a gradual shrinkage in the atomic and ionic radii along the series.** In the same way, the *d*-contraction due to the accommodation of the electrons in $(n-1)d$ levels in the transition series can be interpreted. But compared to the *f* levels, the *d* levels are more effective in screening. This is why, this effect is less pronounced. But still, the effect of *d*-contraction is reflected (Secs. 8.19 and 8.20) along the transition series and posttransition series. In fact, the small effect of *d*-contraction is also transmitted to the lanthanide contraction. ***Relativistic effects*** (Sec. 8.20.3) **on the 6*s* orbital of the lanthanides are also partly responsible for the lanthanide contraction.**

Here it should be mentioned that the relativistic effect causes the *contraction* of 6*s* orbital (for lanthanides) and 7*s* orbitals (for actinides) but the corresponding $(n–2)f$ orbitals are expanded (i.e.

Click Here to me/thealchemylibrary

relativistic expansion). The size is determined by the $<r_{max}>$ of the orbitals of the outermost shell not by the orbital of the (n–2) shell. Thus the observed f-contraction arises due to two factors :

(i) *poor shielding power of (n–2)f orbitals in which the differentiating electrons are gradually added*, (ii) *relativistic contraction of ns orbital.*

Note : If we apply the Slater's rule to calculate the Z^* experienced by the outermost s-orbital of the f-block elements, it leads to an interesting result, $Z^* = 2.85$ irrespective of the number of f-electrons. Thus n (outermost principal quantum number) and Z^* remain the same along the series. *Hence, the atomic size should remain unchanged along the series*. The experimental finding contradicts this prediction from the Slater's rule. ***This is a serious limitation of the Slater's rule.*** In reality, Z^* for ns orbital gradually increases along the series as the s-orbitals are good *penetrators* and the f-orbitals are *poor shielders*.

8.9.3 Effects of Lanthanide Contraction

(i) Unexpectedly low atomic and ionic radii of the postlanthanides

Generally, in a group, on moving from top to bottom, the size increases due to the increase of the outermost principal quantum number. It is evident for the s- and p-block elements. But in the d-block elements, the congeners of a particular group of the 4d and 5d series are almost comparable in their size. This is evident from the following Table 8.9.3.1. Thus the members of each pair of *Zr*, *Hf*; *Nb*, *Ta*; *Tc*, *Re*; *Ag*, *Au*; *Cd*, *Hg* become almost identical in size. It occurs so due to the transmission of the lanthanide contraction to the postlanthanides. ***Thus it can be concluded that if the lanthanides were not present, the members of the 5d series would be larger in size as usual.***

Table 8.9.3.1. Metallic radii * (pm) and covalent radii ** (pm) of the d-block elements.

Group→ Series ↓	IIIB (3)	IVB (4)	VB (5)	VIB (6)	VIIB (7)	VIIIB (8)	VIIIB (9)	VIIIB (10)	IB (11)	IIB (12)
3d	Sc 164 (144)	Ti 147 (132)	V 134 (122)	Cr 129 (117)	Mn 137 (117)	Fe 126 (117)	Co 125 (116)	Ni 125 (115)	Cu 128 (117)	Zn 137 (125)
4d	Y 182 (162)	Zr 160 (145)	Nb 147 (134)	Mo 140 (129)	Tc 135 -	Ru 134 (124)	Rh 134 (125)	Pd 137 (128)	Ag 144 (134)	Cd 152 (141)
5d	La 188 (169)	Hf 159 (144)	Ta 147 (134)	W 141 (130)	Re 137 (128)	Os 135 (126)	Ir 136 (126)	Pt 139 (129)	Au 144 (134)	Hg 155 (144)
	Ce-Lu 182-173 (165-156)									

*for 12 coordination numbers, ** given within the parentheses.

Click Here t.me/thealchemylibrary

(ii) Chemical similarity between the 4d and 5d congeners

Because of the ***lanthanide contraction*** and ***relativistic effects*** (Sec. 8.20.3), the *5d* members are almost similar in size with their respective congeners in the *4d* series. The chemical and physical properties are largely governed by the parameter, *charge to radius ratio*. This parameter becomes almost identical for the members in each of the pairs : *Zr, Hf; Nb, Ta*, etc. This is why, the members of each pair are chemically and physically very much comparable. As a matter of fact, *Zr* and *Hf* are so similar in their chemical behaviour that it is a very difficult task to separate them chemically. **Because of the same ground, *Zr* and *Hf occur naturally in the same source.*** The same thing also happens for the other pairs.

(iii) High density in the postlanthanides

The atomic numbers and hence the atomic weights of the postlanthanides are increased as usual but their sizes are not expectedly increased because of the lanthanide contraction. This is why, the densities of such metals are extremely high. As a matter of fact, the element having the highest density lies in this range. It is iridium of density 23.7×10^3 kg m^{-3}.

(iv) Introduction of nobility among the postlanthanides

The enhanced effective nuclear charge experienced by the valence shell electrons and consequently the decreased size among the postlanthanides make their ionisation energies high. This is why, these metals (e.g. *Pt, Ag, Au*, etc.) become noble.

(v) Abnormally high electron affinities among the postlanthanides

The enchanced Z^* and unusually small sizes in the postlanthanides, favour their electron affinities. This is why, very often their electron affinities are very much high. As a matter of fact, gold shows the highest electron affinity (~ 223 kJ mol^{-1}) among all the metals; and aurides (Au^-) are reported in the compounds like Cs^+Au^-.

(vi) Occurrence of Y with the lanthanides

As the size of Y^{3+} is very much comparable with those of the members of the lanthanide series, it is very much chemically similar with the lanthanides. This is why, *Y* often occurs in nature with the lanthanides.

(vii) Effect on the lanthanides

Because of the gradual shrinkage in size (i.e. gradual increase of the parameter, *charge/radius*) from *La*(III) to *Lu*(III), the following consequences appear.

(a) Covalency increases from *La*(III) to *Lu*(III).
(b) Propensity to hydrolyse increases from *La*(III) to *Lu*(III).
(c) Stability and tendency to form coordination compounds increase from *La*(III) to *Lu*(III).
(d) Acidity of the oxides increases from La_2O_3 to Lu_2O_3.
(e) Thermal stability of the oxy salts (e.g. carbonates, sulfates, etc.) decreases from *La*(III) to *Lu*(III).
(f) Ionisation potential and standard reduction electrode potential of the M^{3+}/M couple increase from *La* to *Lu*.
(g) Basicity decreases from *La* to *Lu* i.e. among the lanthanides, *La*(III) is the most basic while *Lu*(III) is the least basic.

Click Here for more/theallchemylibrary

Separation of lanthanides **: Here it is worth mentioning that *the span of variation of the chemical properties mentioned above among the lanthanides is very small.*** This is why, for their separation, the methods based on the fractional crystallisation of their salts and basicity difference of their compounds like hydroxides, oxides, carbonates, etc. are practised.

Separation by ion-exchange process **:** Because of the lanthanide contraction, the size of Ln^{3+} ions gradually decreases from Ce^{3+} to Lu^{3+} and their complexing power with the hard ligands like EDTA (ethylenediaminetetraacetic acid) gradually increases with the increase of atomic number among the lanthanides. The overall stability constant (K) of EDTA-complexes changes as : log $K \approx 15.3$ (for La^{3+}) to log $K \approx 19.2$ (for Lu^{3+}). When a mixture of Ln^{3+} ions is run through a cation exchange resin in H-form (i.e. R–H like Dowex-50), the Ln^{3+} ions are absorbed in the resin bed.

$$Ln^{3+}(aq) + 3\,R-H \rightleftharpoons \underset{\text{(Resin bound)}}{Ln(R)_3} + 3H^+\,(aq)$$

The span of binding constants with the resin for the Ln^{3+} ions is not sufficient to separate the Ln^{3+} ions. However, when the resin bed binding the Ln^{3+} ions is **eluted with the EDTA solution** (pH $\approx$ 8.0), the Ln^{3+} ion which forms the more stable complex with the EDTA solution under the specified condition (e.g. pH = 8.0, buffered solution), will be eluted first (i.e. removed first).

$$Ln(R)_3 + HEDTA^{3-} + 3NH_4^+ + xH_2O \rightleftharpoons [Ln(HEDTA)(H_2O)_x] + 3(R^-\ NH_4^+)$$

Thus, Lu^{3+} (forming the most stable complex) will be eluted first followed by Yb^{3+}, and so on.

8.10 PERIODIC TRENDS OF Z^* AND SIZE OF THE ATOMS AND IONS

8.10.1 Two Important Factors (n and Z^*) to Determine the Size of Atoms and Ions

To measure the sizes, different types of radii such as atomic radii, orbital radii, metallic radii, van der Waals radii, covalent radii, ionic radii, etc. are used. The characteristic features of these parameters have been discussed in detail in Sec. 10.2. Here we shall pay attention only to the trends of variation of the atomic and ionic radii in the periodic table. Before to discuss their periodic trends, we are to recapitulate the factors governing the parameters. **The *effective nuclear charge* (Z^* = Z – screening constant) experienced by the outermost electron and the value of the *outermost principal quantum number* (n) are important to determine the periodic trends of the sizes.** With the increase of the principal quantum number, the size increases while with the increase of Z^* (which is governed by the relative penetrating power of the orbitals) the size decreases. Here, it is worth mentioning that many other factors (see Sec. 8.11) as in the case of atomic volume come into consideration in the finer analysis of the trends of the radii.

Effect of n and Z^* on the size can be approximately realised by considering the Bhor model. The radius of an orbit measuring the size of an atom is given :

$$\boxed{\langle r_{max} \rangle \approx a_0 (n^*)^2 / Z^*}$$

where

a_0 = 53 pm (Bohr radius of H-atom),

n^* = effective principal quantum number for the valence shell electron,

Click Here t.me/thealchemylibrary

Z^* = effective nuclear charge experienced by the outermost electron and it can be obtained by using the Slater's rule. Though Bohr model is not accepted now, it can give a good approximate measure of $<r_{max}>$, the average distance from the nucleus to the maximum in the *radial probability distribution curve.*

It is illustrated for *Li.*

$$\langle r_{max} \rangle = 53 \times (2^2/1.30) = 163 \text{ pm}; n^* = 2, Z^* = 1.30$$

8.10.2 Periodic Trends of Z^* (Effective Nuclear Charge)

By considering the Slater's rule (cf. Sec. 4.24), it can be shown that Z^* for the valence electron changes along the period as follows :

***s-* and *p-block element* :** $Z^* = 0.65 + 0.65n$, (n = no. of valence electron)

***d-block element* :** $Z^* = 2.85 + 0.15n$, (n = no. of electrons in the $(n-1)d$ orbital).

Thus for the s- and p-block elements, Z^* experienced by the valence electron increase by + 0.65 unit along the series from one element to the next element, while for the d-block elements, the Z^* value increases more slowly (+ 0.15 unit per increase of atomic number by one unit).

This difference occurs due to the accumulation of differentiating electron in the $(n-1)$ shell for the *d*-block elements. On the other hand, for the *s*- and *p*-block elements, the differentiating electron is accumulated in the outermost shell. **Inner electrons shield better.** The $(n-1)d$ differentiating electrons can shield the outermost electron better than the differentiating electrons for the *s*- and *p*-block elements.

***Note* :** From the Slater's rule, Z^* becomes 2.85 for the *f*-block elements irrespective of the number of $(n-2)f$ electrons. **This is a failure of Slater's rule** to explain the lanthanide or actinide contraction (cf. Sec. 8.9.2).

For the *s*-block elements, *Z^* value remains unchanged in a group from the third period*, e.g. Z^* (= 2.85) remains the same for *Mg, Ca, Sr* and *Ba*. For the Gr-III(i.e. Gr 13) elements, the Z^* value rapidly increases from *Al* (3rd period element) to Ga (4th period element). This happens so due to the filling of $(n-1)d$ orbitals. From *Mg* to *Al*, Z^* value increases by 0.65 units as usual but from *Ca* to *Ga*, the Z^* value increases by 2.15 unit. This occurs due to the filling of ten electrons in $(n-1)d$ level between *Ca* and *Ga*. The same thing happens for, *Sr* to *In*, *Ba* to *Tl*. This explains, the relatively sharp hike in Z^* value for moving *Al* to *Ga. The Z^* (= 5.0) remains the same for In and Tl.*

Table 8.10.2.1. Variation of Z^* (calculated by Slater's rule) for the valence electron

	s-block ⟷		*p*-block ⟷					
	IA (1)	IIA (2)	IIIA (13)	IVA (14)	VA (15)	VIA (16)	VIIA (17)	VIIIA (18)
Period 2	Li 1.30	Be 1.95	B 2.60	C 3.25	N 3.90	O 4.55	F 5.20	Ne 5.85
Period 3	Na 2.20	Mg 2.85	Al 3.50	Si 4.15	P 4.80	S 5.45	Cl 6.10	Ar 6.75
Period 4	K 2.20	Ca 2.85	Ga 5.00	Ge 5.65	As 6.30	Se 6.95	Br 7.60	Kr 8.25

Click Here t.me/thealchemylibrary

Effect of scandide contraction (i.e. d-contraction) : The sharp increase of Z^* value for moving from *Al* to *Ga* by 1.5 unit and for moving from *Ca* to *Ga* by 2.15 unit can be explained by scandide contraction (to be discussed in Sec. 8.10.2). The new type orbital i.e. 3*d* first appears at *Sc* and the orbital accommodates 10 electrons between *Ca* and *Ga*.

$$Ca(Z^* = 2.85) \xrightarrow[\text{Contraction}]{\text{Scandide}} Ga(Z^* = 5.00)$$

8.10.3 Variation of Size along the Periods

As we move from left to right in a period, the outermost principal quantum number remains fixed. The **radial distribution function (RDF)** (cf. Sec. 4.1.2) of the electrons of the outermost shell determines the size of the species. From the Slater's rule (Sec. 4.2.4), it is noted that the *effective nuclear charge increases with the increase of atomic number in a period.* This is why, there is a gradual reduction in size along the period from left to right. This is more *pronounced for the s -and p -block elements* (see Table 8.10.3.1), i.e. representative elements. In fact, for the *s*- and *p*-block elements, Z^* (Slater's value) increases more sharply than for the *d*-block elements along the periods. For the *d*- and *f*-block elements, there is a gradual smooth decreases (see Tables 8.9.1.1 and 8.9.3.1) in size due to the *d*- and *f*-contraction respectively. For the *d*-block elements, Z^* (Slater's value) *slowly* increases from left to right. The variation of orbital radii in the periodic table is shown in Fig. 8.10.3.1. The orbital radius actually corresponds to the theoretically calculated distance (measured from the nucleus) in a free atom at which the radial

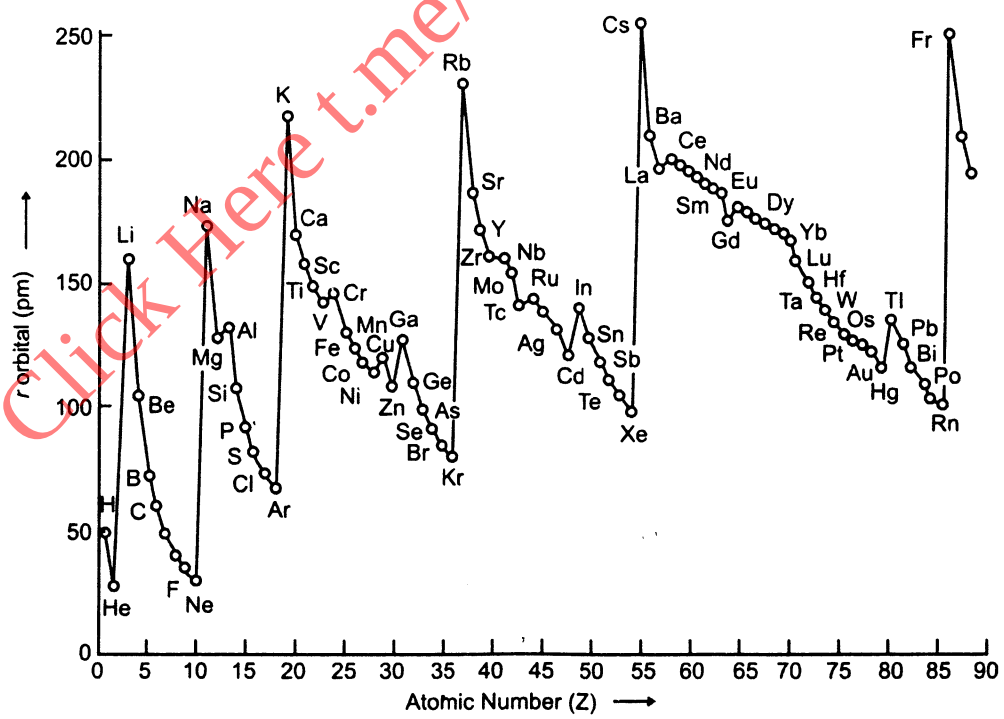

Fig. 8.10.3.1. Periodic trends of size (orbital radii) of the elements.

Click Here t.me/thealchemylibrary

distribution probability (see Sec. 4.1.2, radial distribution curve) of the outermost orbital electrons becomes maximum. As for $H(1s^1)$, it occurs at 53 pm. For *Li* it is 159 pm.

For the variation of ionic radii for a particular oxidation state, the same trend is noted (see Sec. 11.4). For the variation of size among the ***isosteric species***, Tables 11.4.1 and 11.4.2 are referred.

Table 8.10.3.1. Single bond covalent radii and atomic or metallic radii* (12 coordination number) (in pm) of the representative elements

IA (1)	IIA (2)	IIIA (13)	IVA (14)	VA (15)	VIA (16)	VIIA (17)	VIIIA** or, zero (18)
s-block		*p*-block					
H							*He*
30							120
Li	*Be*	*B*	*C*	*N*	*O*	*F*	*Ne*
123	89	80	77	74	74	72	160
(155)	(112)	(89)	(91)	(92)	–	–	–
Na	*Mg*	*Al*	*Si*	*P*	*S*	*Cl*	*Ar*
157	136	125	117	110	104	99	191
(190)	(160)	(143)	(132)	(128)	(127)	–	–
K	*Ca*	*Ga*	*Ge*	*As*	*Se*	*Br*	*Kr*
203	174	125	122	121	114	114	200
(235)	(197)	(153)	(137)	(139)	(140)	–	–
Rb	*Sr*	*In*	*Sn*	*Sb*	*Te*	*I*	*Xe*
216	191	150	140	141	137	133	220
(248)	(215)	(166)	(162)	(159)	(160)	–	–
Cs	*Ba*	*Tl*	*Pb*	*Bi*	*Po*	*At*	*Rn*
235	198	155	146	152	–	–	–
(267)	(222)	(171)	(175)	(170)	(176)	–	–

* Values are given within the parentheses

** The values correspond to the nonbonded radii, i.e., van der Waals radii;

Click Here t.me/thealchemylibrary

8.10.4 Variation of Size in a Group

For the ***representative elements***, in moving from top to bottom, the different types of radii like orbital radii, covalent radii, metallic radii and ionic radii (for a particular oxidation state) increase, but the relative rate of increase decreases with the heavier congeners (cf. Fig. 8.10.3.1 and Table 8.10.3.1). Thus the heavier congener species such as *Cs* and *Fr* or *Ba* and *Ra* become almost identical in size (Fig. 8.10.3.1). ***The general trend of increase of size for the heavier congeners arises due to the opening of new principal quantum number in moving from one element to the next in a group.*** It leads to decrease the electrostatic attraction between the outermost electrons and nucleus.

For the *lighter congeners*, Z^* does not remarkably change in moving down in a group, e.g. $Z^* = 1.3$ and 2.2 for *Li* and *Na* respectively; $Z^* = 3.9$ and 4.8 for *N* and *P* respectively. **This increasing trend of**

Z^* should contract the size but the effect principal quantum number which increases is more pronounced. The relative effect of Z^* and n (more correctly n^*) on the size can be realised from the following relationship.

$$\boxed{\langle r_{max} \rangle \propto (n^*)^2 ; \langle r_{max} \rangle \propto (Z^*)^{-1}}$$

It is evident that the **squared effect of n^* or n is more important.** Consequently, for the lighter congeners, the size increases in moving down in a group. But, for the heavier congeners (e.g. *Cs* and *Fr* or *Ba* and *Ra*) both the opposing factors, i.e. effect of Z^* and n, become comparable in controlling the radius. For such heavier congeners, Z^* gradually increases more remarkably, and n increases as usual. Here it may be noted that in terms of Slater's rule, Z^* remains constant for the heavier congeners, e.g. Z^* = 2.85 for *Mg*, *Ca*, *Sr* and *Ba*; Z^* = 5.0 for *Ga*, *In*, *Tl*. **This is a limitation of Slater's rule.** However, the gradual increase of Z^* for the *heavier congeners* is established in terms of SCF method. This occurs mainly due to the large number of low shielding *d* and *f* electrons in the inner shells. This effect is nicely illustrated among the postlanthanides.

Effect of scandide contraction : It is interesting to follow the increasing trend of size for the Gr IVA (i.e. Gr 14) elements (cf. Table 8.10.3.1). The increase of size of *Ge* in moving from *Si* is relatively less. This is due to *scandide contraction* (i.e. *d*-contraction). The new type orbital i.e. 3*d* appears at *Sc* and 10 electrons are gradually accumulated in the 3*d*-orbital between *Ca* and *Ga* which is just followed by *Ge*.

Effect of scandide contraction is also understood in terms of sharp increase of Z^* for moving from *Al* (Z^* = 3.5) to *Ga* (Z^* = 5.0). Because of these $3d^{10}$ electrons, Z^* increases in moving from *Ca* (Z^* = 2.85) to *Ga* (Z^* = 5.0) along the period (cf. Z^* differs by 0.65 unit between *Mg* and *Al*).

It may be noted that in moving from Ge to Sn, no such effect of d-contraction is noticed because both have experienced the effect of *d*-orbital filling equally. Similarly, effect of *scandide contraction* is well expressed in the size of *Al* and *Ga* of Gr IIIA (i.e. Gr 13). *In fact, this d-contraction effect is transmitted in the elements Ga to Kr of 4th period.*

Effect of lanthanide contraction : For the *d*-block elements, though there is a slight increase in size in moving down in a group from the 3*d* to 4*d* series, the congeners of the 4*d* and 5*d* series become almost identical in size (Table 8.9.3.1). This is an effect of ***lanthanide contraction. Relativistic effects*** (Sec. 8.20.3) on the 6*s* orbitals are also partly responsible for the similarity in size between the congeners of 4*d* and 5*d* series.

For a comparison between the representative and transition elements, let us consider and compare the metallic radii of the congeners in Gr V (15 and 5).

Gr VA (15) (*p*-block elements)			Gr VB (5) (*d*-block elements)		
Element	*Z*	r_0 (pm)	*Element*	Z	r_0 (pm)
As	33	139	*V*	23	134
Sb	51	159	*Nb*	41	147
Bi	83	170	*Ta*	73	147

Click Here t.me/thealchemylibrary

A similar comparison for the Pauling's tetravalent ionic radii in Gr IV (14 and 4) is given below.

Gr IVA (14) (*p*-block elements)			Gr IVB (4) (*d*-block elements)		
Species	Z	r_+ (pm)	Species	Z	r_+ (pm)
Ge^{4+}	32	53	Ti^{4+}	22	68
Sn^{4+}	50	71	Zr^{4+}	40	79
Pb^{4+}	82	84	Hf^{4+}	72	78

Note : • ***Effect of scandide contraction*** is expressed among the 4th period elements and ***effect of lanthanide contraction*** is expressed among the 6th period elements. However, effect of scandide contraction is relatively less.

• **Secondary periodicity** (Sec. 8.20.1) among the *p*-block elements originates due to scandide contraction and lanthanide contraction.

8.11 VARIATION OF ATOMIC VOLUMES IN THE PERIODIC TABLE

8.11.1 Atomic Volume : Definition and Limitation of the Parameter

Lothar Meyer is remembered for his famous atomic volume curve, i.e. periodic variation of the atomic volumes of the elements with the atomic weights. Presently the variation is plotted (cf. Fig. 8.11.2.1) against the atomic number.

Generally, the atomic volume is defined as the volume occupied by one gram atom of the element under consideration **in its solid state.** Thus,

$$\text{Atomic volume} = \frac{\text{Atomic weight}}{\text{Density}}$$

Before to discuss the variation trend of the parameter we should point out that ***the parameter is not a good parameter*** **for a comparison among the elements as it depends on various types of factors which are different for the different elements.** These factors are :

(i) ***Packing efficiency and crystal structure*** : It depends on the *packing efficiency* of the atoms in the solid state. Thus it is a function of crystal structure.

(ii) ***Magnitude of interatomic force*** : The inter-atomic separation in the solid state depends on the *magnitude of the inter-atomic forces* governed by electronic configuration, bond multiplicity, coordination number, polarisability, etc.

(iii) ***Allotropic forms*** : Different *allotropic forms* of a particular element possess different crystal structures having different packing efficiencies. Thus the atomic volume depends on the nature of the allotropic forms.

(iv) ***Temperature*** : The density depends on the *temperature*. Hence all the elements should be considered at a particular temperature at which they should remain as solids. Theoretically 0 K is the most desirable temperature for a comparison, but in practice it is not possible.

(v) ***Atomicity*** : The different elements exist in different states such as monoatomic, diatomic, triatomic, tetraatomic, etc. (e.g. *He*, *Ne*, H_2, Cl_2, O_2, O_3, P_4, As_4, S_8, etc.). These *different atomicities* influence the atomic volumes in different ways. Hence, if all the elements do not

Click Here t.me/thealchemylibrary

display the same degree of atomicity in their states, then the comparison among the different elements loses its importance.

Because of these various types of factors mentioned above, the interpretation of the variation trend of the parameter among the different elements gets complicated. But in spite of the fact, from the nature of the trend of periodic variation of the parameter, some important conclusions may be drawn.

8.11.2 Nature of Variation Trend of the Atomic Volume with the Atomic Number

It is shown in Fig. 8.11.2.1. The following characteristics of the curve are noteworthy.

(i) **Position of alkali metals :** The atomic volumes of the alkali metals are very high and they occupy the **peaks of the curve.**

(ii) **Positions of electropositive and electronegative elements :** With the increase of the atomic number in a period starting from the alkali metals (i.e., the peaks), the electropositive elements lie on the **descending limbs** while the electronegative elements lie on the **ascending limbs.**

(iii) **Position of transition metals :** For the transition metals, the atomic volumes remain almost unchanged along the period and they occupy the **flat region at the bottom** positions of the curve.

(iv) **Position of inner transition metals :** For the inner-transition series (i.e. *f*-series), the lanthanides and actinides occupy the **descending segments near the bottom** because of the lanthanide and actinide contractions (i.e. *f*-contractions) respectively.

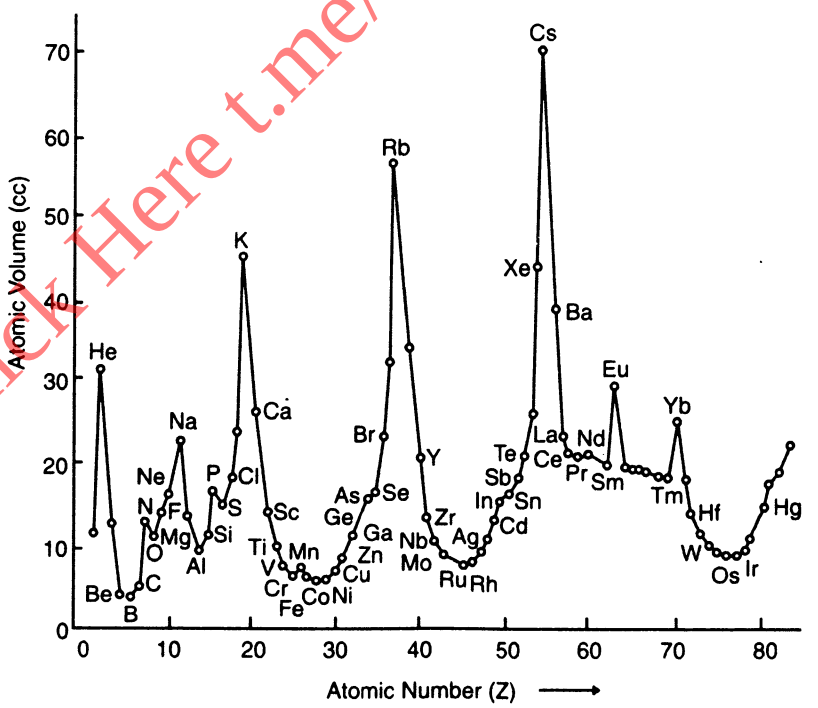

Fig. 8.11.2.1. Periodic trends of atomic volume of the elements.

Click Here t.me/thealchemylibrary

(v) **Position of the postlanthanides :** The observed decrease in the atomic volumes among the postlanthanides is more than the usual trend and it arises so due to the transmission of the lanthanide contraction. This is why, the elements having extremely high densities lie in this region and as a matter of fact, iridium having the highest density (23.7×10^3 kg m^{-3}) lies here.

8.11.3 Explanation of the Atomic Volume Curve

At the alkali metals, the new principal quantum numbers are initiated. Hence, their sizes are drastically increased compared to their respective preceding elements, i.e. inert gases. Now, starting from an alkali metal, the electrons are added one by one in the same principal quantum number with the increase of atomic number. At the beginning of the process, the newly added electrons experience more attractive forces towards the nucleus than the inter-electronic repulsions. But with the increase of the number of the added electrons, the inter-electronic repulsions outweigh the nuclear attraction and consequently the size increases. ***This is why, the electropositive elements having a very few electrons in the outermost new principal quantum number lie in the descending limbs while the electronegative elements having more electrons tending to fill in the outermost shell to attain the corresponding inert gas structures lie in the ascending segments of the curve.***

For the *d*-block elements, at the very beginning of the series, the *d*-contraction due to the placement of the incoming electrons in the $(n-1)d$ sublevel which is of low shielding power is prominent (cf. *the positions of Sc, Ti, V, Cr in the 3d series*). *But with the increase of the d-electron population in the* $(n-1)d$ *sublevel, the increase of electron-electron repulsion and the increase of effective nuclear charge having opposing effects become comparable. This is why, the heavier members of the transition series lie at the flat region at the bottom. On attaining the filled* $(n-1)d^{10}ns^2$ *configuration, there is a sudden increase in electron-electron repulsion which in turn is reflected in the slight increase of the atomic volume* (cf. *the positions of Cu :* $3d^{10}\ 4s^1$ and *Zn :* $3d^{10}\ 4s^2$).

For the lanthanides and postlanthanides, the *f*-contraction due to the accumulation of the added electrons in the $(n-2)f$ sublevel can explain their positions in the curve.

8.12 VARIATION OF IONIZATION ENERGIES IN THE PERIODIC TABLE (cf. Sec. 9.11 for Ionisation Energies of Molecules and Photoelectron Spectroscopy)

The term ionization energy is applicable for all the species like atoms, molecules, radicals and ions. Generally it is used for the atoms. It is defined as : ***the amount of energy required to knock out the most loosely bound electron in the outermost shell in an isolated atom in the gaseous phase to generate a singly charged cation is referred to as the first ionisation energy of the element.*** Similarly, the second, third, and higher ionisation energies can be defined. For *Al*, the involved processes are shown as follows:

$$Al_{(g)} \rightarrow Al^{+}_{(g)} + e,\ IE_1 = 578 \text{ kJ mol}^{-1};$$

$$Al^{+}_{(g)} \rightarrow Al^{2+}_{(g)} + e,\ IE_2 = 1816.7 \text{ kJ mol}^{-1};$$

$$Al^{2+}_{(g)} \rightarrow Al^{3+}_{(g)} + e,\ IE_3 = 2744.8 \text{ kJ mol}^{-1}$$

Click Here to Join Chemistry Library

The ionisation energies are expressed in eV per atom or kJ mol^{-1} (1 eV per atom = 96.48 kJ mol^{-1} = 23 kcal mol^{-1}). *The higher ionisation energies are always greater than the lower ionization energies.* It occurs so, because in removing an electron from a more positively charged species, more energy is always required. This is why, $IE_3 > IE_2 > IE_1$.

The ionisation energies for some molecules are given below.

$$CO_{(g)} \rightarrow CO^+_{(g)} + e,\ IE = 1352 \text{ kJ mol}^{-1};\ N_{2(g)} \rightarrow N^+_{2(g)} + e,\ IE = 1503 \text{ kJ mol}^{-1};$$

$$NO_{(g)} \rightarrow NO^+_{(g)} + e,\ IE = 894 \text{ kJ mol}^{-1};\ O_{2(g)} \rightarrow O^+_{2(g)} + e,\ IE = 1164 \text{ kJ mol}^{-1};$$

We have already mentioned (Sec 1.8.5) that the ionisation energies are very often ***mistakenly described as ionisation potentials*** because these parameters are experimentally determined by using the potential gradient. But we should remember that the potential is ***an intensive property*** measured by volt while the energy is an ***extensive property*** expressed by eV per atom or kJ per mole.

8.12.1 Periodic Variation of the Ionisation Energies

Fig. 8.12.1.1 and Table 8.12.1.1 show the variation trend of 1st ionisation energy of the elements with the increase of the atomic number. The following features of the curve are worth noting.

(i) ***Position of inert gases*** : The inert gases occupy the *peak positions.*

(ii) ***Position of alkali metals*** : The alkali metals reside at the *bottom positions* showing their lowest ionisation energies. From the peaks, there is a sharp fall for the respective alkali metals, then there is a gradual increase in the ionisation energy with the increase of the atomic number up to the climax having the position of the next inert gas.

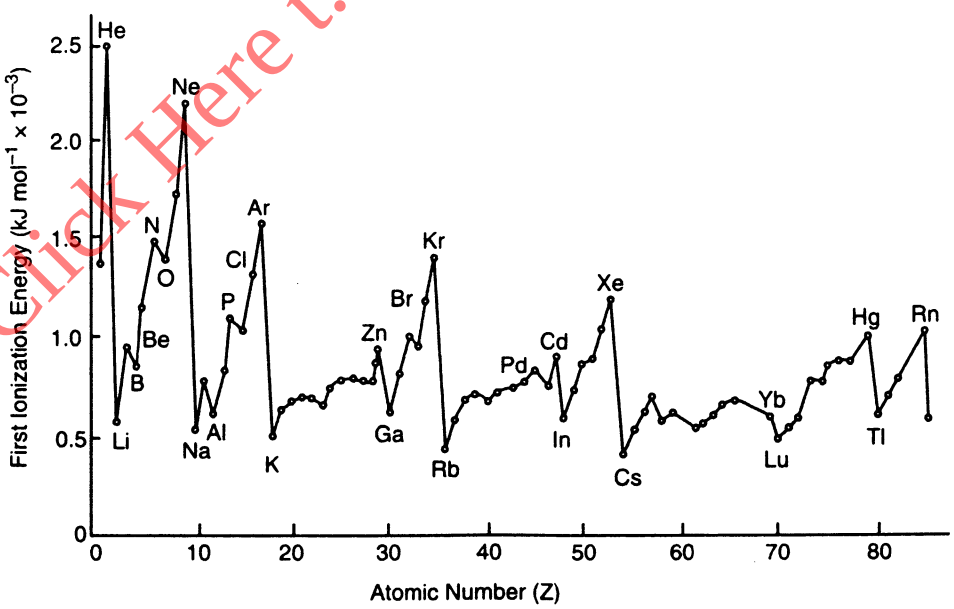

Fig. 8.12.1.1. Periodic trends of first ionisation energy of the elements.

Click Here t.me/thealchemylibrary

(iii) ***Position of transition metals*** : In the transition series, the variation is not so marked having a slight increasing tendency, but at the endings (i.e. *Zn*, *Cd*, *Hg*) there are sharp hikes.

(iv) ***Position of lanthanides*** : In the lanthanides, again the slight increasing trend is noted having a special hike at *Gd*.

Table 8.12.1.1. First ionisation energies of the elements (eV per atom)

H																	*He*
13.59																	24.58
Li	*Be*											*B*	*C*	*N*	*O*	*F*	*Ne*
5.39	9.32											8.30	11.26	14.53	13.61	17.42	21.56
Na	*Mg*											*Al*	*Si*	*P*	*S*	*Cl*	*Ar*
5.14	7.64											5.98	8.15	10.48	10.36	13.01	15.75
K	*Ca*	*Sc*	*Ti*	*V*	*Cr*	*Mn*	*Fe*	*Co*	*Ni*	*Cu*	*Zn*	*Ga*	*Ge*	*As*	*Se*	*Br*	*Kr*
4.34	6.11	6.54	6.82	6.74	6.76	7.43	7.90	7.86	7.63	7.72	9.39	6.00	7.88	9.81	9.75	11.84	14.00
Rb	*Sr*	*Y*	*Zr*	*Nb*	*Mo*	*Tc*	*Ru*	*Rh*	*Pd*	*Ag*	*Cd*	*In*	*Sn*	*Sb*	*Te*	*I*	*Xe*
4.18	5.69	6.38	6.84	6.88	7.10	7.28	7.36	7.46	8.33	7.57	8.99	5.78	7.34	8.64	9.01	10.45	12.13
Cs	*Ba*	*La*	*Hf*	*Ta*	*W*	*Re*	*Os*	*Ir*	*Pt*	*Au*	*Hg*	*Tl*	*Pb*	*Bi*	*Po*	*At*	*Rn*
3.89	5.21	5.61	6.65	7.88	7.98	7.87	8.7	9.0	9.0	9.22	10.43	6.10	7.41	7.29	8.43	9.2	10.75

(Conversion factor : 1 eV per atom = 96.48 kJ mol^{-1}).

Click Here to the chemistry library

8.12.2 Factors Governing the Ionisation Energies and Explanations of the Periodic Trends

The factors which affect the electrostatic attractive force experienced by the electrons at the outermost level govern the magnitude of the ionisation energy. Bohr's theory can explain the ionisation process quantitatively and it has been already discussed (Secs. 1.8.5 and 1.8.8). The important factors to determine the ionisation energy are :

(i) ***effective nuclear charge*** ($Z^* = Z$ – screening constant),

(ii) ***radius of the species*** (i.e. principal quantum number),

(iii) ***screening power of the inner electron clouds,***

(iv) ***penetrating power of the orbital from which the electron is to be knocked out*** (i.e., azimuthal quantum number of the electron to be knocked out),

(v) ***relative stabilities of the starting and end product species from the standpoint of half-filled and full-filled character of the orbitals involved.***

The above facts are illustrated in explaining the variation trend of the ionisation energy in the periodic table.

Variation trend in a group among the representative elements : In the representative elements, in moving from top to bottom in a group, the size increases due to the increase of the principal quantum number. On the other hand, the effective nuclear charge (Z^*) for the outermost electrons increases slightly but the effect of Z^* is relatively less important compared to the effect of n (cf. : $r \propto n^2$ i.e. ***squared effect***; $r \propto Z^{*-1}$). Because of the predominant effect of the increasing principal quantum number, r (measure of size) increases in moving down in a group. **This is why, the ionisation energy decreases in moving from top to bottom.**

For the heavier congeners, the effect of Z^* is relatively more important and consequently the size (i.e. r) do not increase so remarkably (compared to the lighter congeners). This is why, the decreasing trend of ionisation energy for the heavier congeners is not so pronounced (compared to the lighter congeners).

Variation trend in a period among the representative elements : In moving from left to right in a period, the effective nuclear charge per outermost electron increases while the corresponding principal quantum number remains the same. This is why, the size gradually decreases along the periods. Thus the electrostatic attraction towards the nucleus increases along the period and it reaches the climax at inert gases. **It explains the increasing trend of the ionisation energies along the period placing the alkali metals at the bottom and the inert gases at the peaks of the curve.**

Variation trend in the transition and inner-transition elements : Let us consider the comparison (see Table 8.12.2.1) of variations of the first ionisation energies in some groups of the *s*-, *p*- and- *d*-block elements.

Table 8.12.2.1. Comparison of variation trends of 1st ionisation energies in some *s*-, *p*- and *d*-block elements

s-block Gr IA(1)	*IE* (kJ mol^{-1})	*p-block* GI IVA(14)	*IE* (kJ mol^{-1})	*d-block* Gr IVB(4)	*IE* (kJ mol^{-1})	*d-block* Gr-VB(5)	*IE* (kJ mol^{-1})
Li	520	*C*	1086				
Na	496	*Si*	786				
K	419	*Ge*	760	*Ti*	658	*V*	650
Rb	403	*Sn*	708	*Zr*	674	*Nb*	664
Cs	375	*Pb*	715	*Hf*	760	*Ta*	761

It is evident that the trend of fall in ionization energies in a group towards the bottom in the representative elements is well noticed, but in the *d*-block elements the decreasing trend is not so noticeable, **rather in the heavier congeners *the reverse trend appears.*** It arises due to both the *d*- and *f*-contractions which produce high effective nuclear charges in the heavier congeners. It arises so from the relative efficiencies of the penetrating power of the orbitals which run in the sequence: $s > p > d > f$. Thus the 4*s* and 5*s* orbitals penetrate into the inner *d*-orbitals in the fourth and fifth periods respectively and the 6*s* orbital penetrates into the low screening 5*d* and 4*f* orbitals in the sixth period. The effect of the *d*- and *f*-contraction is also transmitted to the heavier posttransition *p*-block elements (cf. ionisation energies of *Sn* and *Pb*).

Thus, in general, for the *d*-block elements, the trend of variation of ionisation energies in a group is opposite to that observed in the representative elements. *It is not an exception, but rather, a rule for the d-block elements.*

Along the series, both the *d*- and or *f*-contractions and electron-electron repulsion operate. **This is why, for the d-block elements, only a slight increasing trend of ionisation energy in a period with the increase of atomic number is noticed.** But when an extra stability is attained through the half-filled (e.g. *Mn*, $3d^5\ 4s^2$) or full-filled (e.g. *Zn*, $3d^{10}\ 4s^2$) structure, a small hike exists.

Click Here t.me/theachemylibrary

8.12.3 The Cases which Flout the General Periodic Trend

(i) Effect of half-filled level

$$IE_1(N) = 1403 \text{ kJ mol}^{-1} > IE_1(O) = 1314 \text{ kJ mol}^{-1},$$
$$\text{but } IE_2(N) = 2856 \text{ kJ mol}^{-1} < IE_2(O) = 3388 \text{ kJ mol}^{-1}.$$

According to the general periodic trend, oxygen should have higher ionisation energies compared to those of nitrogen. This trend is maintained for the second ionisation energies but not for the first ionisation energies. It can be explained from the standpoint of electronic configuration.

$$N\,(1s^2 2s^2 2p^3) \xrightarrow{IE_1} N^+\,(1s^2 2s^2 2p^2);\ O\,(1s^2 2s^2 2p^4) \xrightarrow{IE_1} O^+\,(1s^2 2s^2 2p^3)$$

According to the concept of ***exchange energy*** (Sec. 1.11.1), **the half-filled level gains an extra stability compared to the system having electronic configurations nearest to the half-filled structure.** Thus from the standpoint of exchange energy, it is evident that for nitrogen the starting species is more stabilised compared to the product one while in the case of oxygen, the product species is more stabilised than the starting species. Thus in terms of electronic configuration, during the first ionisation, oxygen is favoured more than nitrogen. ***In fact, the contribution from the exchange energy can outweigh the opposing factor, i.e. increase of effective nuclear charge from nitrogen to oxygen.*** This is why, in this pair, the general periodic trend is violated.

Now let us consider the second ionisation processes.

$$N^+\,(1s^2 2s^2 2p^2) \xrightarrow{IE_2} N^{2+}\,(1s^2 2s^2 2p^1);\ O^+\,(1s^2 2s^2 2p^3) \xrightarrow{IE_2} O^{2+}\,(1s^2 2s^2 2p^2)$$

Now, for oxygen (i.e. O^+) there is a more loss of exchange energy. ***Thus the effects of both the increased Z^* and exchange energy disfavour the ionisation of O^+ more compared to N^+.***

In the same angle, the reverse trend in the pair of *P* and *S* can be explained.

$$P\,(1s^2 2s^2 2p^6 3s^2 3p^3) \xrightarrow{IE_1 = 1012 \text{ kJ mol}^{-1}} P^+\,(1s^2 2s^2 2p^6 3s^2 3p^2)$$
$$S\,(1s^2 2s^2 2p^6 3s^2 3p^4) \xrightarrow{IE_1 = 999 \text{ kJ mol}^{-1}} O^+\,(1s^2 2s^2 2p^6 3s^2 3p^3)$$
$$P^+\,(1s^2 2s^2 2p^6 3s^2 3p^2) \xrightarrow{IE_2 = 1903 \text{ kJ mol}^{-1}} P^{2+}\,(1s^2 2s^2 2p^6 3s^2 3p^1)$$
$$S^+\,(1s^2 2s^2 2p^6 3s^2 3p^3) \xrightarrow{IE_2 = 2251 \text{ kJ mol}^{-1}} S^{2+}\,(1s^2 2s^2 2p^6 3s^2 3p^2)$$

The above explanation works well for the lighter congeners but in the heavier congeners this is not followed. For example,

$$IE_1(Sb)\,(5s^2 5p^3) = 831.6 \text{ kJ mol}^{-1} < IE_1(Te)\,(5s^2 5p^4) = 869.3 \text{ kJ mol}^{-1};$$
$$IE_1(Bi)\,(6s^2 6p^3) = 703.3 \text{ kJ mol}^{-1} < IE_1(Po)\,(6s^2 6p^4) = 812 \text{ kJ mol}^{-1}$$

(ii) Effect of full-filled level and nature of orbital (i.e. azimuthal quantum number)

$$Be\,(1s^2 2s^2) \xrightarrow{IE_1 = 899 \text{ kJ mol}^{-1}} Be^+\,(1s^2 2s^1),\ B\,(1s^2 2s^2 2p^1) \xrightarrow{IE_1 = 801 \text{ kJ mol}^{-1}} B^+\,(1s^2 2s^2)$$

$$\text{but, } IE_2(B) = 2427 \text{ kJ mol}^{-1} > IE_2(Be) = 1757 \text{ kJ mol}^{-1}$$

Click Here to the Alchemy Library

It is known (Sec. 1.11.1) that the full-filled level gains an extra stability. The first ionisation breaks the full-filled level of *Be* while for *B*, the product (i.e. B^+) gains the full-filled level which favours the ionisation of *B* compared to *Be*. This factor can outweigh the opposing factor, i.e. the contribution from the increase of Z^* in reaching from *Be* to *B*. ***This is why, the first ionisation energy of Be is greater than that of B.***

In the case of the second ionisation process, the stability due to the full-filled level favours *Be* (Be^+, $1s^2\ 2s^1 \rightarrow Be^{2+}$, $1s^2$) but disfavours *B* (B^+, $1s^2\ 2s^2 \rightarrow B^{2+}$, $1s^2\ 2s^1$). Thus the disfavour due to both the full-filled level and effective nuclear charge (the general periodic trend) runs in the same direction to make $IE_2(B) > IE_2(Be)$.

In the same way we can explain the following trends in the pair of *Mg* and *Al*.

$$IE_1(Mg) = 738 \text{ kJ mol}^{-1} > IE_1(Al) = 578 \text{ kJ mol}^{-1};$$

$$IE_2(Mg) = 1450 \text{ kJ mol}^{-1} < IE_2(Al) = 1816 \text{ kJ mol}^{-1}.$$

In this regard, we are at the right position to consider the ***effect of penetrating power*** **(measured by *l*) of the orbital from which the electron is to be knocked out.** For a particular principal quantum number, the penetrating power of the orbitals into the inner electron clouds towards the nucleus is given in the sequence, $ns > np > nd > nf$. **Hence the energy required to knock out an electron from an orbital follows the sequence as :**

$$ns > np > nd > nf.$$

In the case of first ionisation process in the pairs (*Be*, *B*) and (*Mg*, *Al*), for *B* and *Al* the electron is knocked out from the 2*p* and 3*p* levels respectively while for *Be* and *Mg*, the involved orbitals are 2*s* and 3*s* respectively. *The s-electrons require more energy than the p -electrons to be knocked out and this factor also supports the trends*, $IE_1(Be) > IE_1(B)$ and $IE_1(Mg) > IE_1(Al)$.

- **For the inert gases,** during the first ionisation process, the starting neutral species are stabilised due to the full-filled structure, i.e. $ns^2\ np^6$ (and ns^2 for *He*). This factor along with the increased Z^* makes the ionisation process very much unfavourable at the inert gases.
- Now, let us consider the following sequence of first ionisation energy in kJ mol^{-1} (given within the parentheses).

$$_{29}Cu,\ 3d^{10}4s^1\ (745.5) <\ _{30}Zn,\ 3d^{10}4s^2\ (906.4) >\ _{31}Ga,\ 3d^{10}4s^24p^1\ (578.8)$$

For *Zn*, the ionisation process breaks down the full-filled $4s^2$ structure, while for *Cu* and *Ga* the products attain the full-filled level. Thus, the ionisation process for *Zn* is highly disfavoured. For *Ga*, the electron is removed from the *p*-level which further facilitates the process.

- In the same way, we can explain the following trends (1st ionisation energies are given within the parentheses in kJ mol^{-1}).

$$_{47}Ag(731) <\ _{48}Cd(867.7) >\ _{49}In(558.3);\ _{79}Au\ (890) <\ _{80}Hg\ (1007) >\ _{81}Tl(589);$$

$$_{70}Yb,\ 4f^{14}6s^2\ (603.4) >\ _{71}Lu,\ 4f^{14}\ 5d^16s^2\ (523.5)$$

Click Here t me/thearchemyjibrary

8.12.4 Ionisation Energy of Some Typical Molecular Species

It largely depends on the nature of *MO* from which the electron is to be lost. This aspect has been discussed in detail in Sec. 9.11.

Ionisation energy trends in binary hydrides : The observed order is :

$$CH_4 > NH_3 < H_2O < HF;\ SiH_4 > PH_3 < H_2S < HCl;$$

$$HF > HCl > HBr > HI;\ H_2O > H_2S > H_2Se;\ NF_3 > NH_3;\ PF_3 > PH_3$$

It is evident that with the increase of electronegativity of the central atom, the ionisation energy increases. It is also quite expected. **However, it is important to note that for CH_4 or SiH_4, the ionisation energy is quite high. It occurs so in these species because of the absence of non-bonding electron which can be lost easily.**

It is interesting to note that *IE* of NF_3 is higher than that of NH_3 by 268 kJ mol^{-1} while for going from PH_3 to PF_3, the ionisation energy increases by only 121 kJ mol^{-1}. This can be explained by considering the ***electron withdrawing inductive effect* and *electron pushing resonance effect of fluorine.*** The electron pushing resonance effect prevails only in PF_3 by using the vacant $3d$ orbitals of phosphorus and filled $2p$-orbitals of fluorine, i.e. $2p_\pi(F) \rightarrow 3d_\pi(P)$. Due to the electron withdrawing inductive effect of fluorine, substitution of hydrogen by fluorine should increase the ionisation energy. In **PF_3, the opposing π-back bonding lowers the *IE* value relatively.** No such π-back bonding is possible in NF_3 because of the absence of the vacant d-orbital on nitrogen.

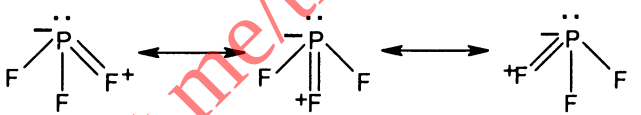

It may be mentioned that the ***proton affinity (PA)* values** also support the above fact. The *PA* of PF_3 is lower than that of PH_3 by only 106 kJ mol^{-1} while *PA* for NF_3 is lower than that of NH_3 by about 260 kJ mol^{-1}. This can be explained by considering the **excess electron density on phosphorus** in PF_3 due to back bonding ($F \rightarrow P$). In addition to this, the protonated species, PF_3H^+ is also resonance stabilised through the delocalisation of positive charge.

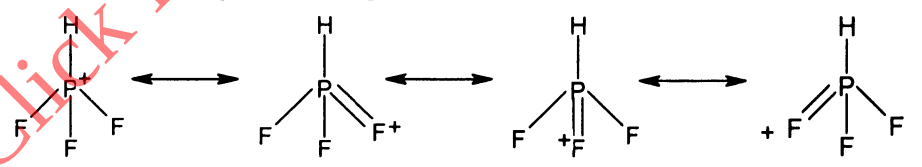

8.13 ELECTRON AFFINITY AND ITS VARIATION TREND IN THE PERIODIC TABLE

8.13.1 Concept of Electron Affinity

Electron affinity is defined as the amount of energy released when an electron is added to the valence shell of the isolated gaseous species (which may be an atom or an ion or a molecule). The positive value of the electron affinity indicates that the process, i.e. $X_{(g)} + e \rightarrow X^-_{(g)}$, is exothermic and the negative value indicates the process to be an endothermic one. ***Thus the convention accepted in defining***

Click Here t.me/thealchemylibrary

the electron affinity apparently contradicts the established convention in thermodynamics. It happens so because in the given definition the term, **'energy release'** has been coined but in all electron affinity processes, energy release may not occur and in some cases, energy absorption may occur.

Thus, $F_{(g)} + e \rightarrow F^-_{(g)}$, $\Delta H = -328$ kJ mol^{-1}, and $EA = 328$ kJ mol^{-1}

and $N_{(g)} + e \rightarrow N^-_{(g)}$, $\Delta H = 20.3$ kJ mol^{-1}, and $EA = -20.3$ kJ mol^{-1}

From the definition, it appears that the electron affinity is the reverse process of the ionisation process,

$$\text{i.e. } X^-_{(g)} \rightarrow X_{(g)} + e,\ IE(X^-) = \Delta H = EA(X).$$

In fact, the ionisation process (which accumulates positive charges) and electron affinity (which accmulates negative charges) are related in the same way in the relation involving the enthalpy change (ΔH) of the process and the amount of charge accumulation (q) on the species. By neglecting the higher terms, we get the following quadratic equation :

$$\boxed{\Delta H = \alpha q + \beta q^2} \qquad \ldots(8.13.1.1)$$

where, ΔH (thermodynamic convention) = ΣIE or ΣEA, and q is the charge on the species. ΔH relates with EA when q is –ve, and ΔH relates with IE when q is +ve. **The magnitude of β is large for the nonpolarisable and small species while it is small for the large and polarisable species.** For example,

$$\beta(F) > \beta(Cl) > \beta(Br).$$

This aspect will be discussed in Sec. 8.14.3. A representative plot is shown in Fig. 8.13.1.1.

As in the case of ionisation energies, the successive electron affinities, such as EA_1, EA_2, EA_3... can also be defined. EA_2 leads to the dinegative species while EA_3 produces the trinegative species. *It is always more difficult to place an additional electron to a species which is already bearing a negative charge compared to the process involving a neutral species.* ***This is why, higher electron affinities are always thermodynamically more unfavourable.*** In fact, EA_2 for all species are negative, i.e. the processes are endothermic.

From the plot of Eqn. 8.13.1.1, it is found that for all the active nonmetals, the acceptance of negative charge initially makes the process exothermic, but after the attainment of a certain value of q, it becomes saturated and ΔH becomes minimum (i.e. maximum exo-thermicity) at that point. After this ***critical value*** **of q,** the increased electron-

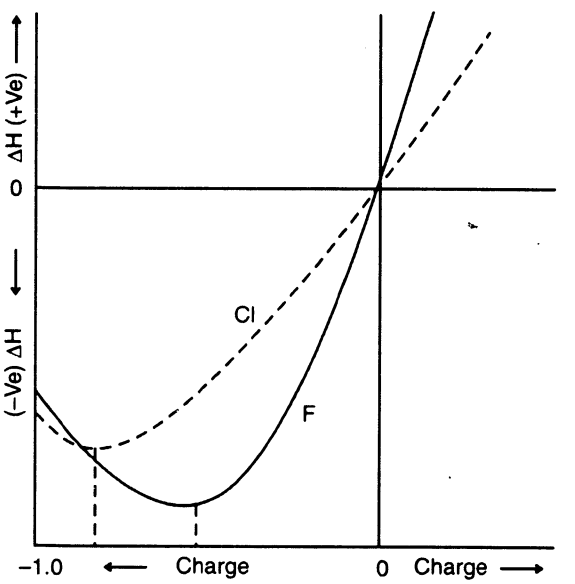

Fig. 8.13.1.1. Enthalpy change (not in scale) of a species in acquiring charge, positive or negative (graphical representation of Eqn. 8.13.1.1, $\Delta H = \alpha q + \beta q^2$).

Click Here to me/thechemylibrary

electron repulsion tends to make the process endothermic. This critical value of q is different for different species. For the formation of O^{2-}, S^{2-}, etc., the endothermicity outweighs the exothermicity.

$$O + e \rightarrow O^- \ (\Delta H = -141 \text{ kJ mol}^{-1}); \ O^- + e \rightarrow O^{2-} \ (\Delta H = +844 \text{ kJ mol}^{-1})$$

$$EA_1(O) = 141 \text{ kJ mol}^{-1}; \ EA_2(O) = -844 \text{ kJ mol}^{-1};$$

$$S + e \rightarrow S^- \ (\Delta H = -200 \text{ kJ mol}^{-1}); \ S^- + e \rightarrow S^{2-} \ (\Delta H = +590 \text{ kJ mol}^{-1})$$

$$EA_1(S) = 200 \text{ kJ mol}^{-1}; \ EA_2(S) = -590 \text{ kJ mol}^{-1};$$

The lower EA-s of the 2nd period nonmetals compared to those of the corresponding 3rd period congeners (e.g. F vs Cl; O vs. S) arise **due to the smaller critical values of q for the 2nd period elements, but the exothermicity for the lower values of q (below the respective critical values) is larger for the 2nd period elements** (cf. Fig. 8.13.1.1). This respect has been discussed in detail in Sec. 8.1.3.3.

8.13.2 Factors Governing the Electron Affinities

The factors which control the ionisation process come under consideration for the process measuring the electron affinity. **In general, the factors favouring the ionisation process disfavour the electron affinity process** (Fig. 8.13.2.1), **i.e. higher ionisation energy leads to higher electron affinity. But the species having half-filled or full-filled level possess high ionisation energies and low electron affinities.** The important factors are :

(i) ***Size of the species*** : If Z^* per electron at the periphery is more or less the same for different species (e.g. in a group of the representative elements), the electrostatic attraction towards the

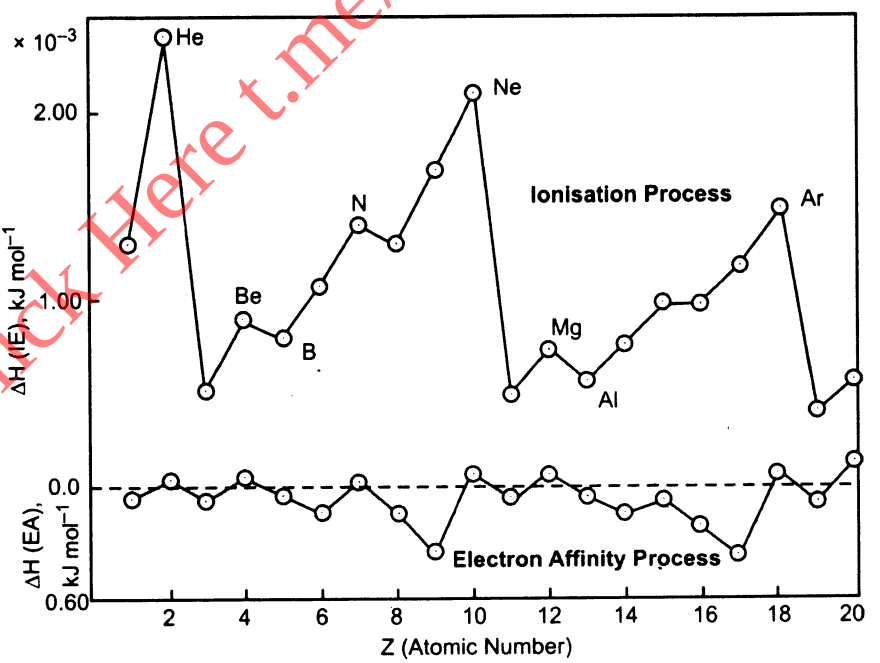

Fig. 8.13.2.1. Variation of enthalpy change (thermodynamic convention) in both the ionisation process and electron affinity process with the atomic number.

Click Here t.me/theacademylibrary

nucleus experienced by the electrons at the periphery is less for the larger species. In fact, for the representative elements, in a group the effect of slight increasing trend of Z^* is less important than the effect of increasing trend of n (principal quantum number) when we move from top to bottom (cf. $r \propto n^2$, i.e. **squared effect,** and $r \propto Z^{*-1}$). For such systems, the accommodation of an additional electron which is to be bound at the periphery by the attractive force of the nucleus is disfavoured more for the larger species. ***Thus in general, the smaller atoms in a group possess higher electron affinities.***

(ii) ***Effective nuclear charge*** **:** The species having higher Z^* at the periphery show higher electron affinities.

(iii) ***Nature of the orbital into which the new electron gets accommodation*** **:** The orbitals which can better penetrate into the inner electron clouds are more suitable to house the incoming electron. Thus the ease of accommodation of the incoming electron follows the sequence: $ns > np > nd > nf$.

(iv) ***Nature of the electronic configuration*** **:** If the species already bear an extra stability due to either the half-filled or full-filled level, then such species are very much reluctant in accepting the incoming electron. On the other hand, if the newly added electron creates the half-filled or full-filled level, the process is favoured.

This aspect disfavours the Gr IIA (2) elements (ns^2), Gr IIB (12) elements [$(n-1)d^{10}ns^2$], Gr VA (15) elements [ns^2np^3], noble gases [ns^2np^6] but favours the Gr VIIA (17) elements [ns^2np^5].

8.13.3 Variation of Electron Affinity in the Periodic Table

In a Period : The effective nuclear charge increases and the size decreases with the increase of atomic number in a period. This is why, the electron affinity, in general, increases in a period. In fact, **it reaches the climax for the Gr VIIA (17) (i.e. halogens) elements** (see Table 8.13.3.1).

Table 8.13.3.1. Electron affinities (kJ mol^{-1})

IA (1)	IIA (2)	IIIA (13)	IVA (14)	VA (15)	VIA (16)	VIIA (17)	Noble gas (18)
Li	*Be*	*B*	*C*	*N*	*O*	*F*	*Ne*
59.8	– 18	27	122	– 20.3	141	328	– 21
Na	*Mg*	*Al*	*Si*	*P*	*S*	*Cl*	*Ar*
53	– 21	44	134	72	200	349	0
		Ga	*Ge*	*As*	*Se*	*Br*	
		29	120	77	195	324	

Note : Electron affinity data differ from source to source. In fact, only in few cases, reliable values have been found.

Because of the special effect of the electronic configuration, the general trend is violated in some cases (e.g. *Be*, *N* in the 2nd period). These are :

(i) ***Gr IIA (2) metals*** **:** *Be, Mg, Ca*, etc. are having the ns^2 orbital structure. Hence, accommodation of the incoming electron brings the configuration ns^2np^1. This process is disfavoured in two ways : the addition of the new electron destroys the full-filled level structure and accommodation

Click Here to me/thealchemylibrary

of the new electron occurs in the *p* level which is less penetrating (i.e. of higher energy). Here it is worth noting that for the alkali metals, the accommodation occurs in the *ns* level giving rise to ns^2 configuration. Thus the process is favoured more in the Gr IA (1) elements compared to the Gr IIA (2) elements.

(ii) ***Transition series*** : In the transition series, the electron affinity values are given below in kJ mol^{-1}.

Sc	*Ti*	*V*	*Cr*	*Mn*	*Fe*	*Co*	*Ni*	*Cu*	*Zn*
0	20	50	64	0	24	70	111	118	0

The drop in *Mn* ($3d^5 4s^2$) arises as the starting species is stabilised due to its half-filled *d* level. The incoming electron breaks down this extra stability. The drop in *Zn* arises due to its full-filled structure ($3d^{10} 4s^2$).

(iii) ***Postlanthanides*** : Due to the lanthanide contraction, among the postlanthanides, the electron affinity is unusually high (Sec. 8.20).

In a Group : For the representative elements, in moving down in a group the size gradually increases due to the opening of new principal quantum number. In fact, the effect of slight increasing trend of Z^* is less important (relatively) compared to the effect of increasing principal quantum number (n) in moving down in a group (cf. $r \propto n^2$ i.e. **squared effect,** and $r \propto 1/Z^*$). **This is why, generally, the electron affinity falls down with the increase of atomic number.**

There are ***some exceptions***. These are :

(i) ***F < Cl, O < S, N < P, B < Al*** **:** Here it is interesting to note that the ***electronegativity sequence*** **is in the opposite order** and it is expected from the size sequence. To explain the observed sequence of electron affinity, we are to consider the other factors. Though the electrostatic attractive pull towards the nucleus favours the 2nd period elements more compared to the corresponding 3rd period elements, the added electron creates an unfavourable effect, i.e. ***electron-electron repulsion, which is more for the 2nd period elements because of their smaller sizes.*** This repulsive force is not so large in the 3rd period elements because of their larger size. ***In addition to this, possibility of the delocalisation of the increased electron density in the vacant 3d orbital reduces the repulsions for the 3rd period elements.*** This possibility to reduce the electron-electron repulsion through the participation of the *d* orbitals is significant for the heavier species, e.g. *S*, *Cl*, in the 3rd period. On the other hand, for the second period elements, this mechanism does not operate because of the absence of any suitable *d* orbital. ***Thus the reduced electron-electron repulsions in the 3rd period elements outweigh the favour due to the larger electrostatic attraction experienced in their corresponding second period elements.***

The above conclusion can be rationalised quantitatively in terms of Eqn. 8.13.1.1 (i.e. $\Delta H = \alpha q + \beta q^2$). For the smaller atoms, the critical value of q at which the electron acceptance gets saturated is smaller. **After the critical value of q, the process tends to become endothermic due to the increased electron-electron repulsion.** For the 2nd period elements, the initial exothermicity for the small values of q is larger compared to that of the 3rd period congeners (see Fig. 8.13.1.1). In fact, the slope of the curve for *F* is much steeper than that of *Cl* up to $q \approx -0.4$, but then it gets rapidly saturated at $q \approx -$ (0.5 to 0.6) for *F*, while for *Cl* the saturation is attained at $q \approx -0.9$. It has been found that the curve of *F* crosses that of *Cl* at

Click Here t me/thealchemylibrary

$q \approx -0.9$ (see Fig. 8.13.1.1). However, it is evident that ΔH depends on q (which may be fractional or integral). ***It indicates that up to $q \approx -0.9$, ΔH for F is more negative compared to that of Cl, but after this, the process becomes more endothermic for F compared to that of Cl.***

(ii) **Higher electron affinities of the heavier congeners of *d*-block elements :** For the *d*-block elements, in moving down in a group, because of the *d*- and *f*-contraction, the size does not increase smoothly while it increases smoothly in the case of the representative elements. Because of this fact, the general group trend is violated very often for the *d*-block elements. ***Because of the lanthanide contraction, the postlanthanides very often show the unusually high electron affinities*** (see Secondary Periodicity, Sec. 8.20). Let us consider the following elements (electron affinities are given in kJ mol^{-1}).

Co(70) < *Rh*(120) < *Ir*(160); *Ni*(111) < *Pd*(160) < *Pt*(205); *Cu*(118.3) < *Ag*(126) < *Au*(223)

It is striking to note that gold is having the highest electron affinity (223 kJ mol^{-1}) among the metals. It is a consequence of lanthanide contraction. As a matter of fact, ***ionic aurides*** (e.g. $Cs^+ Au^-$) are now well established (cf. Sec. 8.20.3).

8.14 CONCEPT OF ELECTRONEGATIVITY

Electronegativity is defined as the electron attracting power of an atom towards its nucleus when the atom is covalently bonded in a molecule. Thus the more electronegative element withdraws the bonding electron cloud more towards its own nucleus giving rise to an accumulation of negative charge on it.

From the definition, it is evident that the electronegativity of an element is ***not an inherent property of the element.*** It depends on its surrounding environment in the molecule in which the electronegativity of the element is being considered. Thus the electronegativity of *S* in the compounds, H_2S, SF_4 and SF_6 is not the same and it is different in different compounds. **Here it is worth mentioning that *the electronegativity of an element is not its inherent property but the electron affinity of an element is its inherent property.*** It is understandable from their definitions.

From the standpoint of measurement of electronegativity, there are different scales which will be discussed below.

8.14.1 Pauling's Electronegativity (χ_P)

It gets its origin in the concept of valence bond theory (VBT). In the formation of a covalent bond *A–B*, the ionic forms also contribute and the degree of contribution of the ionic forms depends on the electronegativity difference between *A* and *B*. The wave function of the *AB* molecule in the light of VBT is given by :

$$\Psi_{AB} = c_1\Psi_{A-B} + c_2\Psi_{A^+B^-} + c_3\Psi_{A^-B^+} \qquad ...(8.14.1.1)$$

If the electronegativities of *A* and *B* are almost identical, then $c_2 \approx c_3 << c_1$. But with the increase of electronegativity difference between *A* and *B*, the contribution of the ionic forms increases. If, $\chi(A) > \chi(B)$ then $c_3 > c_2$; and if, $\chi(B) > \chi(A)$ then $c_2 > c_3$.

Because of the *contribution of covalent-ionic resonance*, the actual bond energy (E_{A-B}) of *AB* is always greater than that of the corresponding hypothetical 100% covalent bond. This difference gives the measure of the contribution of ***covalent-ionic resonance energy.*** Thus, the covalent-ionic resonance energy (Δ) = actual bond energy – energy of the corresponding 100% covalent bond.

Click Here t.me/bdalchemylibrary

i.e. $$\Delta(A-B) = E_{A-B} - E_{A-B\,(cov)} \quad \ldots (8.14.1.2)$$

The energy of the corresponding 100% covalent bond can be theoretically calculated as the ***arithmatic mean*** as follows:

$$E_{A-B\,(cov)} = \frac{1}{2}(E_{A-A} + E_{B-B}) \quad \ldots(8.14.1.3)$$

where E_{A-A} and E_{B-B} denote the bond energies of A_2 and B_2 molecules respectively and these are measureable quantities. But by using the values of bond energy in this method, in some cases (e.g. *LiH*, *NaH*, *KH*, etc.), the resonance energy (Δ) becomes negative which is not acceptable. To overcome this shortcoming, $E_{A-B\,(cov)}$ has been defined as the **geometric mean** as follows :

$$E_{A-B\,(cov)} = \sqrt{(E_{A-A})(E_{B-B})} \quad \ldots(8.14.1.4)$$

Thus we get :

$$\Delta(A-B) = E_{A-B} - \sqrt{(E_{A-A})(E_{B-B})} \quad \ldots(8.14.1.5)$$

The resonance energy (Δ) arises due to the contribution of the ionic forms and it depends on the electronegativity difference of A and B. From this consideration, Pauling proposed the following relationships :

% of ionic character in $A-B$ bond $\propto \chi(A) \sim \chi(B) \propto \sqrt{\Delta(A-B)}$;

and $$\boxed{\chi(A) \sim \chi(B) = 0.102\sqrt{\Delta(A-B)}}$$ where Δ is expressed in kJ mol^{-1}. ...(8.14.1.6)

Units of covalent-ionic resonance energy (Δ)

Originally Pauling proposed that the electronegativity difference between the bonded atoms A and B is equal to $\sqrt{\Delta}$, when Δ is expressed in eV.

$$\chi(A) \sim \chi(B) = \sqrt{\Delta},\ \Delta \text{ in eV}$$

If Δ is expressed in kJ mol^{-1}, then by using the conversion factor, 1 eV per molecule = 96.5 kJ mol^{-1} we get :

$$\chi(A) \sim \chi(B) = \sqrt{\frac{\Delta}{96.5}} = 0.102\sqrt{\Delta}$$

Similarly, if Δ is expressed in kcal mol^{-1} (1 eV per molecule = 23.06 kcal mol^{-1}), we get :

$$\chi(A) \sim \chi(B) = \sqrt{\frac{\Delta}{23.06}} = 0.208\sqrt{\Delta}$$

To understand the basis of the relationship (Eqn. 8.14.1.6), we are to consider the following fact. In a number of systems, it has been found that ***Δ is not an additive property but $\sqrt{\Delta}$ is an additive property (at least approximately)***, i.e.

$$\Delta(A-B) + \Delta(B-C) \neq \Delta(A-C)$$

but, $$\sqrt{\Delta(A-B)} + \sqrt{\Delta(B-C)} \approx \sqrt{\Delta(A-C)}$$

The above observation strongly indicates that the % of ionic character is linearly related with $\sqrt{\Delta}$ not with Δ, i.e.

Click Here t.me/thealchemylibrary

$$\chi(A) \sim \chi(B) \propto \sqrt{\Delta(A-B)}$$

It leads to Eqn. 8.14.1.6 in which 0.102 appears as the proportionality constant in SI units.

In Eqn. 8.14.1.6, Δ is a measurable quantity. Hence, if the electronegativity of one element is known then the electronegativity of the other involved element can be calculated and by repeating the process the electronegativity of all other elements can be calculated. **Pauling assigned an arbitrary value 4.0 for fluorine and calculated the electronegativities of other elements.** The Pauling's values of electronegativities for different elements are given in Table 8.14.1.1

- ***Determination of electronegativity from thermochemical data*** : By using some approximations, ***the electronegativity difference can be obtained by using another experimental parameter*, i.e. *enthalpy of formation*.** The basis of this technique is illustrated in the case of AB molecule.

From Eqn. 8.14.1.6 we get :

$$\Delta(A-B) = 96.5[\chi(A) \sim \chi(B)]^2 \qquad ...(8.14.1.7)$$

By considering the $E_{A-B\,(cov)}$ as the arithmatic mean (see Eqn. 8.14.1.3) of E_{A-A} and E_{B-B}, we get from Eqn. 8.14.1.2 :

$$\Delta(A-B) = E_{A-B} - \frac{1}{2}[E_{A-A} + E_{B-B}] \qquad ... (8.14.1.8)$$

By combining Eqns. 8.14.1.7 and 8.14.1.8 we get :

$$96.5[\chi(A) \sim \chi(B)]^2 = E_{A-B} - \frac{1}{2}[E_{A-A} + E_{B-B}] \qquad ... (8.14.1.9)$$

The enthalpy of formation of AB in the reaction, $\frac{1}{2}A_2 + \frac{1}{2}B_2 = AB$, is given by :

$$-\Delta H(A-B) = E_{A-B} - \frac{1}{2}[E_{A-A} + E_{B-B}] \qquad ... (8.14.1.10)$$

Combining Eqns. 8.14.1.9 and 8.14.1.10 we get :

$$-\Delta H(A-B) = 96.5\,[\chi(A) \sim \chi(B)]^2$$

or,
$$\boxed{\chi(A) \sim \chi(B) = \frac{\sqrt{-\Delta H\,(A-B)}}{\sqrt{96.5}} = 0.102\sqrt{-\Delta H(A-B)}} \qquad ...(8.14.1.11)$$

If the idea is generalised for the compound, AB_n, then the enthalpy of formation of AB_n and the enthalpy of formation of $A-B$ bond are related as follows :

$$\frac{\Delta H(AB_n)}{n} = \Delta H(A-B) \qquad ...(8.14.1.12)$$

Thus we get :

$$-\Delta H(AB_n) = 96.5n[\chi(A) \sim \chi(B)]^2 \qquad ...(8.14.1.13)$$

or,
$$\boxed{\chi(A) \sim \chi(B) = \frac{\sqrt{-\Delta H(AB_n)}}{\sqrt{96.5n}} = \frac{0.102\sqrt{-\Delta H(AB_n)}}{\sqrt{n}}} \qquad ...(8.14.1.14)$$

Click Here t.me/thealchemylibrary

It should be remembered that Eqn. 8.14.1.14 is applicable only when the total number of covalent bonds in the formation reaction, $\frac{1}{2}A_2 + \frac{n}{2}B_2 \rightarrow AB_n$ does not change and the compound AB_n does not contain any multiple bond.

Table 8.14.1.1. Pauling electronegativities (χ_P) of different elements ($H = 2.1$)

Li	*Be*											*B*	*C*	*N*	*O*	*F*
1.0	1.5											2.0	2.5	3.0	3.5	4.0
Na	*Mg*											*Al*	*Si*	*P*	*S*	*Cl*
0.9	1.2											1.5	1.8	2.1	2.5	3.0
K	*Ca*	*Sc*	*Ti*	*V*	*Cr*	*Mn*	*Fe*	*Co*	*Ni*	*Cu*	*Zn*	*Ga*	*Ge*	*As*	*Se*	*Br*
0.8	1.0	1.3	1.5	1.6	1.6	1.5	1.8	1.8	1.8	1.9	1.6	1.6	1.8	2.0	2.4	2.8
Rb	*Sr*	*Y*	*Zr*	*Nb*	*Mo*	*Tc*	*Ru*	*Rh*	*Pd*	*Ag*	*Cd*	*In*	*Sn*	*Sb*	*Te*	*I*
0.8	1.0	1.2	1.4	1.6	1.8	1.9	2.2	2.9	2.2	1.9	1.7	1.7	1.8	1.9	2.1	2.5
Cs	*Ba*	*La-Lu*	*Hf*	*Ta*	*W*	*Re*	*Os*	*Ir*	*Pt*	*Au*	*Hg*	*Tl*	*Pb*	*Bi*	*Po*	*At*
0.7	0.9	1.1-1.2	1.3	1.5	1.7	1.9	2.2	2.2	2.2	2.4	1.9	1.8	1.8	1.9	2.0	2.2
Fr	*Ra*	*Ac*														
0.7	0.9	1.1														

Note : Electronegativity depends on oxidation states. The values given here refer to the most common oxidation states of the respective elements.

However, ***a correction in Eqn. 8.14.1.14 is required*** when the multiple bonds exist in A_2 and/or B_2 because in such cases all the bonds are not of the same energy. For example, $E_{(N \equiv N)} = 945$ kJ mol^{-1} > $3E_{(N-N)} = 3 \times 164$ kJ mol^{-1}. Thus, N_2 and O_2 are stabler than the hypothetical molecules having three and two independent single bonds respectively. These extra stabilities are to be taken into consideration. The extra stabilities per nitrogen and oxygen atoms are $226\left(=\frac{945-492}{2}\right)$ and $110\left(=\frac{496-276}{2}\right)$ kJ mol^{-1} respectively. By considering these factors, Eqn. 8.14.1.14 gets reduced as:

$$-\Delta H = 96.5\,\Sigma\,[\chi(A) \sim \chi(B)]^2 - 226n_N - 110n_O \qquad \text{...(18.14.1.15)}$$

i.e. $$\boxed{-\Delta H = 96.5n\,(\chi_A \sim \chi_B)^2 - 226n_N - 110n_O}$$

where n_N and n_O give the number of single bonded nitrogen and oxygen atoms present in the molecule and the summation is taken over all the bonds in the molecule. Eqn. 8.14.1.15 assumes that the compound does not contain any multiple bond. *Eqn. 8.14.1.15 indicates that the compounds containing the single bonded nitrogen will have a tendency to have the positive values of heat of formation, if the electronegativity difference between nitrogen and the other element to which nitrogen is singly bonded is zero or very small.* NCl_3 is an example of this group and in fact, it is an unstable compound. This instability originates due to the extraordinary strength of the triple bond $N \equiv N$. Similarly, the compounds like OF_2, Cl_2O having $\chi(A) \sim \chi(B)$ not so high are unstable. ***Thus to stabilise the compounds having single bonded nitrogen or oxygen, ionic resonance energy, i.e. difference in electronegativity, should be high.***

Click Here t.me/healchemylibrary

Let us illustrate the calculation of $\chi(A) \sim \chi(B)$ from the enthalpy of formation **in the case of BCl_3** having the enthalpy of formation – 400.5 kJ mol^{-1}. Here no nitrogen or oxygen is present. Hence their correction terms do not appear. From Eqn. 8.14.1.14 we get :

$$\chi(Cl) - \chi(B) = \frac{\sqrt{-\Delta H(BCl_3)}}{\sqrt{96.5 \times 3}} = \frac{\sqrt{400.5}}{\sqrt{96.5 \times 3}} = 1.18$$

Actually by using the enthalpy data, the electronegativities of the different elements are calculated assuming the arbitrary value $\chi(F) = 4.0$.

Pauling's electronegativities **(based on thermochemical data)** of different elements are given in Table 8.14.1.1.

Note **:** Pauling's original table of atom electronegativities was constructed mainly by using the **covalent-ionic resonance energy (Δ).** This original table had been revised by Allred (1961) by using extensive **thermochemical data.** Now these revised values are widely used.

8.14.2 Mulliken's Orbital Electronegativity (χ_M)

R.S. Mulliken (1934) proposed that the electronegativity is related with both the ionisation energy and electron affinity of the species under consideration. This original idea of Mulliken was further developed by Hinze and Jaffe in 1962-63. *The atoms having high ionisation energies possess generally high electron affinities and such species are highly electronegative.*

Mulliken proposed that the A–B bond will be purely covalent in nature if each of the species A^+B^- and A^-B^+ contributes to the same extent and this is attained when the electronegativities of A and B are the same. The energy of A^+B^- depends on the ionisation energy (IE) of A and electron affinity (EA) of B while the energy of A^-B^+ is determined by the ionisation energy of B and electron affinity of A. When both the forms contribute equally, we get the following condition, provided the Madelung energy in both the cases A^-B^+ and A^+B^- is identical.

$$IE_A - EA_B = IE_B - EA_A; \text{ or, } IE_A + EA_A = IE_B + EA_B.$$

Formation of A^+B^- is favoured when, $IE_A < IE_B$ and $EA_A < EA_B$; i.e. $IE_A + EA_A < IE_B + EA_B$. Similarly, A^-B^+ is favoured when, $IE_A + EA_A > IE_B + EA_B$.

Because of these facts, *Mulliken defined the electronegativity of an element in terms of the sum of its ionisation energy and electron affinity.*

If the electron affinity and ionisation energy are expressed in electron volts per atom, then χ_M is expressed as :

$$\boxed{\chi_M(A) = \frac{1}{2}(IE_A + EA_A); \text{ i.e. } \chi_M = \frac{1}{2}(IE + EA)} \quad \ldots(8.14.2.1)$$

The **Pauling's electronegativity (χ_P)** and **Mulliken's electronegativity (χ_M)** are related as follows:

$$\boxed{\chi_P = 0.168\,(IE + EA - 1.23) = 0.336(\chi_M - 0.615) = 0.336\,\chi_M - 0.2} \quad \ldots(8.14.2.2)$$

(when ***IE*** **and** ***EA*** **are given in eV/atom,** i.e. χ_M is expressed in **eV per atom).**

Thus, it is evident that χ_P and χ_M bear a linear relationship.

Click Here t.me/thealchemylibrary

Units of IE and EA

- $\chi_M = \frac{1}{2}(IE + EA)$, when IE and EA are expressed in eV per atom.

If IE and EA are expressed in kJ mol^{-1}, then

$$\boxed{\chi_M = \frac{1}{2 \times 96.5}(\text{IE} + \text{EA})}$$, 1 eV per molecule = 96.5 kJ mol^{-1}

Similarly, if IE and EA are expressed in kcal mol^{-1}, then,

$$\boxed{\chi_M = \frac{1}{2 \times 23.06}(IE + EA)}$$, 1 eV per molecule = 23.06 kcal mol^{-1}

- Some workers have proposed the following relationship between χ_P and χ_M.

$$\boxed{\chi_P = 1.35\sqrt{\chi_M} - 1.37}$$

- Here it should be pointed out that Pauling's original values of atom electronegativities have been revised by Allred (1961) by using the thermochemical data. These revised values of χ_P are related with the χ_M values through the linear relationships discussed.

Important features of Mulliken's electronegativity : Mulliken argued that the ionisation energy and electron affinity depend on the nature of the orbital involved. For a particular element, depending on the nature of the orbital, the electronegativity may vary. Hence to define the electronegativity, the valence state of the species must be taken into consideration. Thus to define the elctronegativity, we should consider the **valence state ionisation energy,** i.e. ***VSIE*** (IE_v), and the ***valence state electron affinity*** i.e. ***VSEA*** (EA_v). Thus, χ_M is given by,

$$\chi_M = \frac{1}{2}(IE_v + EA_v),$$

when the energies are expressed in eV per atom.

Using the *first* ionisation energy and electron affinity of an atom X (i.e. EA of X is IE of $X^-_{(g)}$), we get the ***absolute electronegativity*** (χ_{abs}) [= $(EA + IE)/2$] which is related with the ***absolute hardness*** (η_{abs}) [= $(IE - EA)/2$] of X (cf. Fig. 14.15.3.1).

$$\boxed{\chi \text{ or } \chi_{abs} = \frac{1}{2}(EA + IE),\ \eta \text{ or } \eta_{abs} = \frac{1}{2}(IE - EA)}$$

The valence state energy parameters can be calculated and it is illustrated for *Be* when it is *sp* hybridised.

$$Be\,(1s^2 2s^1 2p^1) \xrightarrow{IE_p} Be^+\,(1s^2 2s^1), \text{ and } Be\,(1s^2 2s^1 2p^1) \xrightarrow{IE_s} Be^+\,(1s^2 2p^1)$$

$$\text{i.e. } IE_{sp} = \frac{1}{2}(IE_p + IE_s).$$

Similarly, EA_{sp} can be evaluated.

Thus,
$$\chi_M(sp) = \frac{1}{2}(IE_{sp} + EA_{sp}).$$

Click Here t.me/idealchemylibrary

The electronegativity increases in the sequence $ns > np > nd$ and for the s–p hybridised orbitals, it is:

$$sp > sp^2 > sp^3.$$

Values (in eV per atom) of χ_M for some elements are given below.

$$\boldsymbol{H} = 7.2\,(s^1);\ Li = 3.1\,(s^1), 1.8\,(p^1);\ \boldsymbol{Be} = 4.8\,(di^2), 3.9\,(te^2);$$

$$\boldsymbol{B} = 6.4\,(tr^3);\ 6.0\,(te^3);\ \boldsymbol{C} = 10.4 \text{ and } 5.7\,(di^2\pi^2), 8.8 \text{ and } 5.6\,(tr^3\pi^1), 8.0\,(te^4);$$

$$\boldsymbol{N} = 15.7 \text{ and } 7.9\,(di^3\pi^2), 12.9 \text{ and } 8.0\,(tr^4\pi^1), 11.6\,(te^5);\ \boldsymbol{F} = 31.3\,(s^1), 12.2\,(p^1).$$

(Here, $di = sp$, $tr = sp^2$, $te = sp^3$)

Comparison between χ_P and χ_M : χ_P values calculated (by Eqn. 8.14.2.2) from χ_M values are given below for some elements to reveal the effect of % of s-character on electronegativity. **With the increase of s-character the electronegativity increases.**

	sp^3	sp^2	sp			s	p
C :	2.52	2.80	3.34	1.74;	F :	10.4	3.95
N :	3.74	4.18	5.14	2.52;	Cl :	6.3	3.00

Thus the accepted Pauling's value of 2.5 for carbon corresponds to its sp^3 state, while the value of 3.0 for nitrogen involves the valence state between sp^3 and p. For, $F(\chi_P = 4.00)$ and $Cl(\chi_P = 3.0)$, the p orbitals are considered.

Thus, *it appears that Mulliken's idea of orbital electronegativity is more justified than the Pauling's empirical treatment, but the* ***serious disadvantage*** *with the Mulliken's concept lies with the lack of the electron affinity data.* ***Sometimes, it is also difficult to determine the exact state of hybridisation or valence state.*** For example, in transition metals both sp^3 and sd^3 provide the same tetrahedral arrangement but the electronegativities of the two states widely differ. In such cases, the bond angle measurement cannot predict the state of hybridisation.

8.14.3 Jaffe-Hinze Electronegativities (known also as *Mulliken-Jaffe electronegativity*)

Jaffe and Hinze extended (1962-63) the idea of Mulliken and showed that the electronegativity of a *species depends not only on the nature of orbital*, i.e. *state of hybridisation, but also on the charge* (q) *of the species under consideration.* Here we are to recall the quadratic equation (Eqn. 8.13.1.1) involving the ionisation energy or electron affinity and charge, q, i.e.

$$\Delta H = \alpha q + \beta q^2$$

The slope of the curve, i.e. $\partial(\Delta H)/\partial q = \alpha + 2\beta q$, gives the measure of electronegativity.

Therefore,

$$\chi = \partial(\Delta H)/\partial q = \alpha + 2\beta q = a + bq \qquad \text{...(8.14.3.1)}$$

(putting $a = \alpha$ and $b = 2\beta$)

The relationship between the approach of Mulliken and Jaffe can be established by considering the suitable values of q. In the relationship, $\Delta H = \alpha q + \beta q^2$, for $q = +1$, the energy change gives the

Click Here to me/thealchemylibrary

ionisation energy (IE) while for $q = -1$, the energy change can be expressed in terms of electron affinity (EA).

$$IE = \Delta H = \alpha(+1) + \beta(+1)^2 \text{ and } -EA = \Delta H = \alpha(-1) + \beta(-1)^2$$

i.e. $$\boxed{IE + EA = 2\alpha; \text{ or } \alpha = \chi_M = \frac{1}{2}(IE + EA)}$$

and $$\boxed{2\beta = b = IE - EA}$$

Thus Eqn. 8.14.3.1 can be written as :

$$\chi = \chi_M + bq \qquad ...(8.14.3.2)$$

This is why, the electronegativity expressed in terms of Eqn. 8.14.3.2 is called **Mulliken-Jaffe electronegativity** (χ_{MJ}).

$$\chi_{MJ} = \chi_M + bq \qquad ...(8.14.3.3)$$

From Eqn. 8.14.3.1 it is evident that the electronegativity is a linear function of q, i.e. **with the increase of positive value of q on the species, the electronegativity increases, and with the increase of negative charge it decreases.** Thus the electronegativity of S in SF_4 is greater than that of S in SCl_4. Similarly the electronegativity of oxygen in $ClOH$ is greater than that of it in C_2H_5OH. *When $q = 0$, $\chi = a$, i.e. a $(= \alpha)$ gives the measure of electronegativity of the neutral species.*

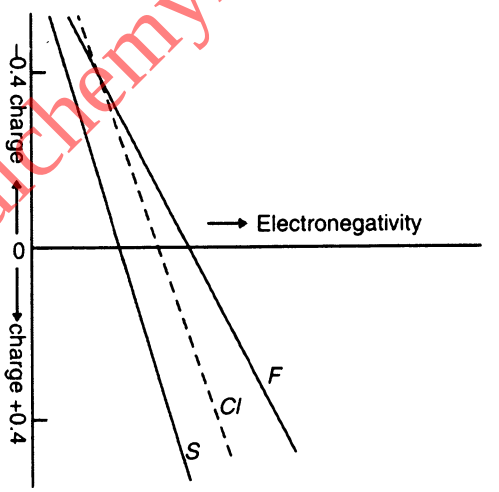

Fig. 8.14.3.1. Dependence of electronegativity on the amount of charge (q) on the species (i.e. $\chi = a + bq$).

The value of b which gives the measure of charge coefficient decreases with the increase of polarizability and size of the species. Thus for the species having large charge coefficients, the electronegativity changes more rapidly with the change of q (Fig. 8.14.3.1). Fluorine being smaller and less polarisable than chlorine bears the larger value of charge of coefficient (b). **This is why, the slope of the curve (Eqn. 8.14.3.1) for *F* is steeper compared to that of *Cl*.** It has been found that for the value of $q \approx -0.4$, the curve of F crosses the curve for Cl. Thus,

$$\boxed{\text{for } q \approx -0.4,\ \chi(F) \approx \chi(Cl);\ \text{when } q > -0.4,\ \chi(F) > \chi(Cl);\ \text{and, when } q < -0.4,\ \chi(F) < \chi(Cl).}$$

Thus it is evident that without mentioning the value of q (contribution of Jaffe and Hinze) and state of hybridisation (contribution of Mulliken), to give the electronegativity value is of no significance. However, the values given by Pauling, Allred and Rochow correspond to $q = 0$ (i.e. neutral state).

The charge coefficient *b* has got another physical significance. *It gives an inverse measure of charge capacity of an atom.* **The large polarisable species having small *b* values have a larger capacity to bear the charge while the small hard species (large *b*) have only a limited capacity to bear the charge.** *This is why for larger b values, the electronegativity rapidly changes with q.*

Click Here to meetheal chemylibrary

Lastly, it is worthy to conclude that the electronegativity obtained by using the *Mulliken-Jaffe-Hinze concept* (i.e. which takes care of both the valance state and charge on the species) is more theoretically justified compared to the values obtained by ***Pauling-Allred-Rochow concept*** (to be discussed later) which stands on some empirical considerations.

• ***Significance of b*** **:** In the case of partial charge (δ) separation, Eqn. 8.14.3.1 can be expressed as follows :

$$\chi = \frac{\partial(\Delta H)}{\partial \delta} = a + b\delta \qquad (8.14.3.4)$$

where $a = \chi_M = \alpha$ and $b = 2\beta$

It leads to :

$$\frac{\partial(\chi)}{\partial \delta} = b = IE - EA \qquad (8.14.3.5)$$

It indicates that the rate of change of electronegativity with the change of charge (δ) of the species is determined by *b*. ***This is why, for the larger values of b, the electronegativity changes rapidly with the change of q.*** Chemically, the charge coefficient parameter *b* gives the measure of the *increase of the charge capacity* or *polarisability*, i.e.

$$\boxed{b = \frac{1}{\text{Polarisability}}}$$

This is why, the small values of b indicate the higher polarisability and softness while the higher values of b indicate the nonpolarisability and hardness of the species. In fact, ***absolute hardness*** (η_{abs}) and *b* are related as (cf. Sec. 14.15.3) :

$$\boxed{\eta \text{ or } \eta_{abs} = \frac{1}{2}(IE - EA) = \frac{1}{2}b}$$

The *charge coefficient parameter* (*b*) is very much important in understanding different chemical properties like ***hardness*** (η), **inductive effect of *groups*** (Sec. 8.14.9), ***position of attack in nucleophilic substitution reactions*** (Sec. 8.14.8b). The values of *a* and *b* are given in Table 8.14.3.1 for some common elements.

Table 8.14.3.1. Values of *a* and *b* (cf. Eqn. 8.14.3.1)

Element	*Orbital involved*	*a (volts)*	*b (volts/electron)*
H	*s*	7.15	12.85
C	sp^3	8.15	11.40
	sp^2	8.90	11.50
	sp	10.40	11.70
N	*p*	7.40	13.10
	sp^3	10.70	13.15
	sp^2	11.80	13.20
	sp	14.00	13.30
O	*p*	9.65	15.30
	sp^3	14.00	15.55
	sp^2	15.50	15.60
F	*p*	12.20	17.60
Cl	*p*	10.90	11.30
Br	*p*	8.60	10.20
I	*p*	8.10	9.15

Click Here to me/freechemylibrary

8.14.4 Allred-Rochow's Electronegativity

Allred and Rochow (1958) attempted to explain the Pauling's experimental electronegativity (χ_P) scale theoretically. According to them, *electronegativity is a measure of electrostatic force experienced by the bonding electron* (i.e. valence electron) *towards the nucleus*. This electrostatic attractive force (F) depends on the Z^* (experienced by the valence electron) and covalent radius (r_{cov}).

$$F = \frac{e^2 Z^*}{r_{cov}^2}, \text{ (CGS system)}$$

They interpreted Pauling's electronegativity (χ_P) in terms of the attractive force or the parameter Z^*/r_{cov}^2. When the χ_P values (obtained from the thermochemical data) were plotted against Z^*/r_{cov}^2, an approximately straight line was obtained with a finite slope and an intercept. The observation (Fig. 8.14.4.1) can be expressed as follows :

$$\boxed{\chi_P \approx \frac{0.36Z^*}{r_{cov}^2} + 0.744} \qquad (8.14.4.1)$$

where r_{cov} is expressed in Å unit.

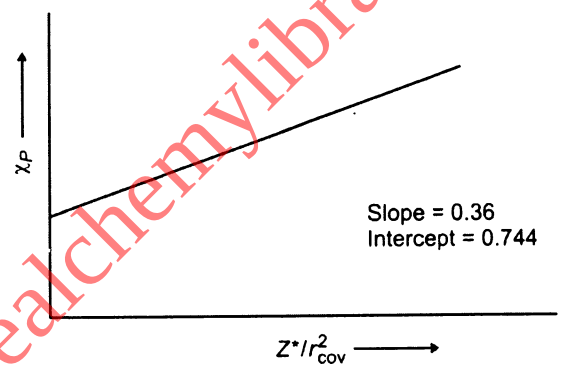

Fig. 8.14.4.1. Plot of χ_P against $\frac{Z^*}{r_{cov}^2}$ (r_{cov} in Å unit).

The **effective nuclear charge (Z^*)** can be calculated by using the ***Slater's rule.*** Thus the Pauling's electronegativity (χ_P) can be theoretically calculated by using the concept of Allred-Rochow. Thus, the calculated values do not differ significantly from the χ_P values obtained by using the thermochemical data (cf. Eqns. 8.14.1.11 and 8.14.1.15).

Electronegativity calculated by using Eqn. 8.14.4.1 is described as ***Allred-Rochow electronegativity*** (χ_{AR}) to honour the scientists, i.e.

$$\boxed{\chi_{AR} = \frac{0.36Z^*}{r_{cov}^2} + 0.744} \qquad (8.14.4.2)$$

Here Z^* is calculated by taking $(x + 1)$ valence electrons where x denotes the number of valence electrons in the isolated atom. In the **state of covalent combination,** $(x + 1)$ valence electrons are supposed to be present.

Note :
- It r_{cov} is expressed in pm, the factor 0.36 changes to 3600.
- **Calculation of Z^* :** To calculate the Z^* by Slater's rule, *all the valence electrons of an isolated atom are supposed to shield the incoming electron from the other combining atom.* Thus, if an isolated atom possesses x valence electrons, to count Z^* it is considered to possess $(x + 1)$ valence electrons *in the state of covalent combination.*

Click Here for the/thealchemylibrary

In other words, if Z^* of an isolated atom is calculated as usual, i.e. $(x - 1)$ electrons in the valence shell are supposed to shield the last electron when there are x valence electrons in the valence shell of the isolated atom, then Eqn. 8.14.4.2 is to be expressed as follows :

$$\chi_{AR} = \frac{0.36\,(Z^* - 0.35)}{r_{cov}^2} + 0.744 \qquad ...(8.14.4.3)$$

where Z^* = **effective nuclear charge of the *isolated atom*.** It is illustrated for bromine (*Br*) in a compound, say *HBr*.

Z* **for *Br*** is normally calculated as follows :

$$Z^*\,(Br) = 35 - 0.35 \times 6 - 0.85 \times 18 - 1.0 \times 10 = 7.6$$

But in *H–Br*, it is considered that there are 8 (= 7 + 1) electrons in the valence shell of *Br*. Then, the 7 electrons are supposed to shield the remaining electron. Thus, in the above calculation, the factor 0.35×6 is to be replaced by 0.35×7. This is why, to calculate the electronegativity by using the Z^* of neutral atom, the factor $(Z^* - 0.35)$ is to be incorporated (cf. Eqn. 8.14.4.3). However, this correction factor makes a little difference and this is why, sometimes, the **unmodified** Z^* (i.e. Z^* of neutral atom) is used to calculate the electronegativity.

The computation of the electronegativity by using the concept of Allred-Rochow with the help of Z^* which can be obtained by Slater's rule is much easier compared to the Pauling's techniques (see Sec. 8.14.1) based on the thermochemical data. The values obtained by Allred-Rochow method are comparable to those values given in Table 8.14.1.1. *However in the Allred-Rochow method, sometimes it becomes difficult to have the reliable values of covalent radius* (r_{cov}). *This is the limitation with the Allred-Rochow technique.*

The Allred-Rochow concept can explain the higher electronegativities of the post-transition (an effect of *d*-contraction) and postlanthanide (an effect of *f*-contraction) elements.

8.14.5 Sanderson's Electronegativity (S)

Sanderson (1954-55) defined electronegativity in terms of ***stability ratio* (*SR*)** which *gives the measure of compactness of the electron cloud around the nucleus*. It is expressed in terms of electron density (*ED*),

$$SR = (ED)/(ED_i) \qquad ...(8.14.5.1)$$

where *ED* gives the electron density (average) of the atom under consideration and ED_i gives the ideal electron density of the atom. This ED_i for a particular atomic number (Z) is obtained by interpolation of the curve obtained by plotting electron densities of the inert gases against their atomic numbers. Thus ED_i gives the electron density of the hypothetical atom which behaves like an inert gas at its own atomic number.

The electron density (*ED*) varies with the distance (r) measured from the nucleus. This is why, the average electron density is calculated. It is expressed as,

$$ED = \frac{No.\ of\ electrons\ (i.e.\ Z)}{\frac{4}{3}\pi r^3}$$

Click Here t.me/tlealchemylibrary

where r = covalent radius of the atom. It is evident that r depends on the attractive force experienced by the valence electron towards its nucleus. For the higher electronegative atom, the attractive force is higher (i.e. r is smaller) which in turn produces the larger electron density. This is why, the stability ratio actually gives the measure of electronegativity.

Thus, $$\chi_S = SR = (ED)/(ED_i) \quad ...(8.14.5.2)$$

From the definition of ED, we can express χ_S as follows :

$$\chi_S = r_i^3/r^3 \quad ...(8.14.5.3)$$

where r = covalent radius and r_i = radius of the atom obtained at its atomic number by interpolation of the plot of *radius of the inert gases versus the atomic number of the inert gases.*

8.14.6 Calculation of Charge Separation from Electronegativity : Concept of Electronegativity Equalization

Let us consider the A–B bond. The electronegativity difference will produce a separation of charge. If, $\chi(A) > \chi(B)$, then it will lead to $A^{q-} - B^{q+}$. According to Eqn. 8.14.3.1 (i.e. Jaffe-Hinze concept), we have, $\chi = a + bq$. **It appears that with the increase of negative charge on *A*, its electronegativity falls while the electronegativity of *B* increases with the accumulation of positive charge on *B*.** At equilibrium, the charge separation will occur to such an extent that the electronegativities of A and B become equal, i.e. $\chi(A^{q-}) = \chi(B^{q+})$. Therefore, by using Eqn. 8.14.3.1 we get:

$$\boxed{a_A - b_A q = a_B + b_B q \text{ or, } q = (a_A - a_B)/(b_A + b_B)} \quad ...(8.14.6.1)$$

This method was developed by Sanderson. Now let us apply the above equation to calculate q in HCl and HBr for which, $a_H = 7.15$, $b_H = 12.85$, $a_{Cl(p)} = 10.9$, $b_{Cl(p)} = 11.30$, $a_{Br(p)} = 8.60$, and $b_{Br(p)} = 10.20$. Here p denotes the p-orbital of the halogen. All the values of a and b are given in electron volt scale of Mulliken. For other elements, the values of a and b are available from the standard table (cf. Table 8.14.3.1.

Therefore, $$q_{HCl} = (10.9 - 7.15)/(11.30 + 12.85) = 0.15;$$

and $$q_{HBr} = (8.60 - 7.15)/(10.20 + 12.85) = 0.06$$

From the dipole measurement (see Sec. 10.4) we get, $q_{HCl} = 0.17$ and $q_{HBr} = 0.12$. The charge separation calculated by the Sanderson's approach is different compared to those obtained by other methods. The discrepancy with the Sanderson's approach originates because of the following facts. It was assumed that the total energy (see Eqns. 8.13.1.1 and 8.14.3.1) involved in the charge separation were ionisation energy and electron affinity. It would yield the correct results if the assumptions were correct. The ***exchange energy*** developed due to the overlap of the valency orbitals will reduce the charge separation, but the ***Madelung energy*** will favour the charge separation. These two factors were ignored in the Sanderson's approach. Here it is noteworthy that these two factors mutually oppose. Hence, their resultant contribution is not so high. ***This is why, the Sanderson's approach is only approximately correct.***

Click Here : my/dear chemylibrary

8.14.7 Electronegativity not an Inherent Property of the Elements

From the definition, **electron affinity* can be considered as an inherent property of the element** as it is defined for the atom in the isolated gaseous condition. But electronegativity of an atom is not an inherent property and it depends on the chemical environment in which it exists in a particular compound. The governing factors are :

(i) ***State of hybridisation*** : From the standpoint of penetrating power, the *s* orbitals are more electronegative than the *p* orbitals. Because of the same ground, for the hybrid orbitals the electronegativity sequence runs as : $sp > sp^2 > sp^3$. For *C*, the values in Pauling's scale are : $C(sp) = 3.34$, $C(sp^2) = 2.80$, $C(sp^3) = 2.52$. This aspect has been discussed in detail in Sec. 8.14.2.

(ii) ***Charge on the atom*** : From the relation, i.e. Eqn. 8.14.3.1, we have $\chi = a + bq$. Thus it is evident that with the increase of positive charge, the electronegativity increases while it decreases with the increase of negative charge. For the smaller nonpolarisable species having large charge coefficients (b), it changes rapidly with the change of q on the species (see Fig. 8.14.3.1). The electronegativity for the neutral species is given by a. This aspect has been discussed at a greater length in Sec. 8.14.3.

8.14.8 Examples Illustrating the Variation of Electronegativity Depending upon the Structural Characteristics

(a) Effect of hybridisation

(i) The acidity sequence (i.e., protonic character of the hydrogen bound to carbon) runs as:

$$H\text{–}C \equiv C\text{–}H > H\text{–}HC = CH\text{–}H > H\text{–}CH_2\text{–}CH_2\text{–}H.$$

The electronegativity of a hybrid orbital increases with the increase of *s*-character. Thus the electronegativity sequence, $C(sp) > C(sp^2) > C(sp)^3$ runs parallel to the acid strength sequence.

(ii) The base strength runs as, $\underset{(sp^3)}{R\text{–}\ddot{N}H_2} > \underset{(sp^2)}{C_5H_5N}$: (i.e. pyridine) $> \underset{(sp)}{R\text{–}C \equiv N}$:

The more electronegative nitrogen is more reluctant in donating its lone pair. This is why, the electronegativity sequence opposes the base strength sequence.

(b) Effect of charge accumulation (see Eqn. 8.14.3.1) and position of nucleophilic attack

The electron withdrawing (i.e. electronegative) substituents produce an electron deficiency (i.e. more positive charge) on the atom to which they are bound. Let us consider the following reactions,

$$H_3\overset{\delta+}{C} \rightarrow I^{\delta-} + OH \xrightarrow{\textbf{I process}} H_3C - OH + I^-$$

* In fact, electron affinity depends on the valence state, but in the isolated gaseous condition, only the ground state exists. Again from Eqn. 8.13.1.1, i.e. $\Delta H = \alpha q + \beta q^2$, it is evident that *EA* also depends on q which has been discussed in Sec. 8.13.1.

Click Here t.me/thealchemylibrary

$$\overset{\delta_3-\ \delta_2+}{F_3C} \longleftarrow \overset{\delta_1+}{I} + OH \xrightarrow{\textbf{I process}} F_3C-H+OI^-;\ (3\delta_3=\delta_2+\delta_1;\ \delta_1>\delta_2)$$

The nucleophilic attack (***Interchange Process***, I; see Sec. 10.10) occurs at the positive centre. Fluorines induce the positive charge at both *C* and *I*, but *I* is more polarisable than *C* because of the larger size of *I*. Thus the charge coefficient factor *b* is larger for *C*, i.e., *b* (*I*) < *b* (*C*). We have already mentioned (Sec. 8.14.3) that the *b* values give *an inverse measure of charge capacity*. This is why : δ_1 (+ 0.21) > δ_2 (+ 0.15) (calculated by Sanderson's approach). **Because of this fact, the nucleophilic attack occurs on *I*, not on *C* in CF_3I.** But in CH_3I, the nucleophilic attack occurs on *C* as expected from the nature of charge distribution.

In the same line of argument, the following reactions yielding different products can be explained.

$$Na^+[Mn(CO)_5]^- + CH_3I \rightarrow CH_3[Mn(CO)_5] + NaI$$

$$\begin{cases} Na^+[Mn(CO)_5]^- + CF_3I \rightarrow [Mn(CO)_5]I + CF_3Na \\ CF_3I + CF_3Na \rightarrow F_3C-CF_3 + NaI \end{cases}$$

The carbonylate anion can act as a base as well as a nucleophile. It makes a nucleophilic attack on '*C*' of CH_3I while it makes a nucleophilic attack on *I* in CF_3I.

8.14.9 Group Electronegativity

It has been already established that the electronegativity of an element is not its inherent property. It depends on the chemical environment, i.e. oxidation state, state of hybridisation, nature of the substituents, etc. The groups (e.g. CH_3, CF_3, NH_2, OH, etc.) may be considered as *single entities* whose electronegativities depend on the nature of the constituents, e.g. the electronegativities of the groups CH_3 and CF_3 are different. The group electronegativities (χ_G) can be theoretically calculated by using the atomic electronegativities of the constituent elements. The group electronegativity can be expressed in terms of *inherent group electronegativity* (a_G) and *charge coefficient parameter* (b_G) by considering the concept of Jaffe-Hinze electronegativity.

$$\chi_G = a_G + b_G\delta_G \text{ (cf. Eqn. 8.14.3.4)}$$

$$\approx \frac{\sum_{i=1}^{n} a_i}{n} + \frac{\sum_{i=1}^{n} b_i}{n^2}\delta_G \qquad (8.14.9.1)$$

where a_i and b_i denote the parameters of the constituent atoms. Thus, a_G is the *simply average value* of the inherent atomic electronegativities (a_i) while b_G is the average of charge coefficients (b_i) of the constituent atoms and *at the same time, inversely proportional to the number of constituent atoms where the proportionality constant is unity*. Thus, we can write :

$$a_G = \text{average of } a_i \text{ values and } b_G = \frac{1}{n} \text{ (average of } b_i \text{ values).}$$

The group electronegativities of some common groups are given in Table 8.14.9.1.

Click Here t me/thealchemylibrary

Table 8.14.9.1. Electronegativities of some common groups

Group	χ_G (in Pauling scale)	a_G (eV)	b_G (eV)
CH_3	2.30	7.42	4.65
CH_3CH_2	2.32	7.50	3.60
CF_3	3.32	10.50	5.32
CCl_3	3.20	10.10	4.32
NH_2	2.78	8.90	5.90
OH	3.42	10.80	8.85
CN	3.76	4.82	6.45
CO_2H	3.36	10.60	5.43
NO_2	4.32	13.50	6.95
C_6H_5	2.60	8.30	3.60

Note **:** a_G (in eV scale) represents the χ_M from which χ_G (in Pauling scale) can be calculated by the relations discussed in Sec. 8.14.2.

Significance of the charge coefficient parameter **(*b_G*)** ***and charge capacity*** **:** It is defined as $b_G = \frac{1}{n} \times \frac{\sum b_i}{n} = \frac{\sum b_i}{n^2}$. Thus it is evident that with the increase of n (i.e. the number of constituent atoms), the b_G value decreases, i.e. ***the larger groups are having the lower b_G values.*** The charge capacity (i.e. charge spreading capacity) is directly proportional to the number (n) of the constituent atoms of the group while charge coefficient is inversely proportional to n. These two parameters ***charge capacity*** and ***charge coefficient*** are inversely related.

Thus the charge capacity **and** ***polarisability*** **of a group increase with the increase of the number of constituent atoms.** In terms of charge capacity, the groups are referred to as ***superatoms*** which can absorb a large amount of charge (positive or negative). **The** ***inductive effect of a group largely depends on its capacity to accommodate the charge.*** This aspect has been illustrated to explain and compare the inductive effect of CH_3 and H.

Inductive effect of a group **:** To determine the inductive effect of a group, it is essential to consider both the *inherent electronegativity* (measured by a_G) and *charge coefficient parameter* (measured by b_G). *It is important to note that the groups are having much lower b-values compared to those of the constituent atoms* (cf. $b = 4.65$ for CH_3 while b for $H = 12.85$, and b for sp^3 $C = 11.40$). **Because of the lower values of b_G, the groups can better push or attract the electron cloud.**

Now let us compare the inductive effect of CH_3 and H. The electronegativity of CH_3 (= 2.30) is slightly higher that of hydrogen H (= 2.1), but the CH_3 group (and other alkyl groups) are better *electron pushing groups* than hydrogen. ***It is unexpected from the simple consideration of the inherent electronegativity.*** However, this can be explained by considering their b-values (cf. b_G of $CH_3 = 4.65$, b for $H = 12.85$). The b-values indicate that the charge capacity of CH_3 is much higher than that of hydrogen. ***The higher charge capacity of CH_3 arises due to the spread of positive charge as follows*** **:**

Click Here to me/thealchemylibrary

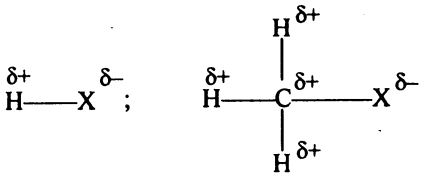

(X is more electronegative than both H and CH_3)

In H–X, the positive charge developed *through the electron pushing inductive effect* of H, is localised on H itself. On the other hand, in CH_3–X, the positive charge developed due to the *electron pushing inductive effect* of the CH_3 group is delocalised on four centres. This *charge delocalisation* (i.e. charge spreading) increases the charge capacity of the CH_3 group. ***This makes the CH_3 group a better electron pushing group compared to H.*** The electronegativity of CH_3 (= 2.30) and C_2H_5 (= 2.32) are more or less comparable, but C_2H_5 (b_G = 3.60) is a better pushing group than the CH_3 group (b_G = 4.65) because of the lower b_G value of C_2H_5 group. In other words, the charge capacity of C_2H_5 group is higher than that of the CH_3 group, i.e. the positive charge developed can spread on the larger number of atoms. **This is why, the larger alkyl groups are better electron pushing groups.**

8.14.10 Concepts of Absolute Electronegativity, Optical Electronegativity and Spectroscopic Electronegativity

(a) Absolute electronegativity

In terms of Mulliken's idea, the electronegativity is defined as $\chi = \frac{1}{2}(IE + EA)$. Thus the defined electronegativity is called ***absolute electronegativity*** (χ_{abs}) which can be correlated with ***absolute hardness*** (η_{abs}).

$$\text{i.e. } \chi_{abs} = \frac{1}{2}(IE + EA) \text{ and } \eta_{abs} = \frac{1}{2}(IE - EA) = \frac{1}{2}b, (cf. \text{Sec. } 14.3)$$

All these can be rationalised in terms of ***frontier molecular orbitals*** (FMO's) for the molecular system and ***frontier atomic orbitals*** (FAO's) for the atomic systems. This aspect has been discussed in detail in Sec. 14.15.3.

(b) Optical electronegativity

According to C.K. Jorgensen, the position of *charge transfer* (CT) bands of metal complexes can be considered to define the *optical electronegativity*. In a charge transfer band, electron moves towards the more electronegative moiety. Thus the ease of electron movement and direction of electron movement depend on the electronegativity difference between the concerned species, i.e. metal and ligand. In LMCT (i.e. ligand to metal charge transfer band), from the HOMO (predominant in the character of ligand orbital), the electron transfer occurs to LUMO (predominant in the character of metal orbital) and the wavenumber ($\bar{\nu}$) of the LMCT band is related with the optical electronegativities of the metal and ligand as follows :

$$\bar{\nu} = c\,(\chi_L \sim \chi_M)$$

Here c is a constant and the values of optical electronegativities become comparable with the values in Pauling scale for c = 30,000 cm^{-1}. Nonpolarisable hard ligands like H_2O, F^-, etc. show high values

Click Here t.me/thealchemylibrary

optical electronegativity while the polarisable soft ligands e.g. I^-, SH^-, etc show the low values of optical electronegativity.

In octahedral complexes for LMCT band, χ_L corresponds to the ligand π-orbital while χ_M corresponds to the t_{2g} metal orbital (≡ π* orbital in the terminology of MOT of the complex).

(b) Spectroscopic electronegativity

L.C. Allen (1989) had suggested that the electronegativity of a species may be defined ***in terms of the average one-electron energy*** of *s* and *p* electrons in *the valence shell* in the ground state of the free atom. The required energy terms can be obtained from the spectroscopic studies. The spectroscopic electronegativity (χ_S) is expressed as follows :

$$\chi_S = \frac{n_p E_p + n_s E_s}{n_p + n_s}$$

where E_p and E_s denote the energies of the electron in the *p* and *s* orbital respectively, n_p and n_s denote the number of *p* and *s* electron respectively. Though the spectroscopic electronegativity can explain the periodic properties of the elements, it cannot correlate the electronegativity with the hardness and softness, state of hybridisation, etc. of the elements. In fact, these factors control the electronegativity of the elements.

8.15 PERIODIC TRENDS OF ELECTRONEGATIVITY

The periodic trend of electronegativity is almost the same as in the case of electron affinity and ionisation energy.

In a Period : In moving from left to right in a period, the size gradually contracts and the effective nuclear charge increases. This is why, the electronegativity gradually increases with the increase of atomic number in a period up to the Gr VIIA (i.e. Gr 17) elements (i.e. halogens) at which it maximises.

In a Group : In the representative elements, in moving down in a group, the size increases while Z^* per electron at the periphery slightly increases (cf. relative effect of Z^* and *n*). This is why, the electronegativity generally falls in a group with the increase of atomic number.

For the *d*-block elements, in moving down from 3*d* to 4*d* series, the electronegativity falls slightly but in reaching the 5*d* series, the electronegativity increases due to the lanthanide contraction.

Among the posttransition elements (e.g. *Ga*, *Ge*, *As*, *In*, etc.), the enhanced electronegativity arises due to the effect of *d-contraction*. In fact, $\chi(Ga) > \chi(Al)$, $\chi(Ge) > \chi(Si)$, etc. This is due to ***scandide contraction*** (cf. Sec. 8.10). This will be discussed in detail in explaining the ***secondary periodicity*** (Sec. 8.20).

8.16 APPLICATIONS OF THE ELECTRONEGATIVITY CONCEPT IN DIFFERENT FIELDS OF CHEMISTRY

The concept of electronegativity is very much important in rationalising the different properties involving the structure and reactivity. These have been discussed in detail at the appropriate place (Sec. 10.10). Some important applications are summarised here.

Click Here t me/theadcremylibrary

(i) **Nature of bond and percentage of ionic character :** Ionic bonds are formed in the combination of electronegative and electropositive elements while the covalent bonds are formed among the elements having only smaller differences in their electronegativities. The percentage of ionic character in a bond can be quantitatively estimated from the knowledge of Pauling's equation (Eqn. 10.4.1) and the modified Hanny-Smyth's equation (Eqn. 10.4.2) which have been discussed at a greater length in Sec. 10.4.

(ii) **Electronegativity difference [$\chi(A) \sim \chi(B)$] and the heat of formation of a covalent compound:** We have already discussed the relationship (Eqn. 8.14.1.15) between the enthalpy of formation (ΔH) and the electronegativity difference, i.e.,

$$-\Delta H = 96.5\ \Sigma\ [\chi(A) \sim X(B)]^2 - 226 n_N - 110 n_O$$

The significance of all the terms in the above equation are given in Sec. 8.14.1. Thus it appears that if the electronegativity difference is negligible, the heat of formation does not favour the formation of the compound. *Specially, if the compound contains the single bonded nitrogen or oxygen, or any other element which is stabilised in the elemental state through the formation of multiple covalent bonds, then to stabilise the compound, the electronegativity difference should be significantly high.* Because of this fact, the compounds such as NCl_3 (~ 0.0), PH_3 (~ 0.0), AsH_3 (~ 0.0), etc. having very small electronegativity differences (shown within the parentheses) are only marginally stable. Here it is important to mention that in homonuclear diatomic molecules (e.g. H_2, O_2, N_2, etc.) though the electronegativity difference is zero, the stability is gained due to strong overlap between the identical orbitals.

(iii) **Shrinkage of bond length :** The electronegativity difference gives a shrinkage in bond length. It is given by Schomakar-Stevenson equation and Pauling's modified equation,

$$r_{A-B} = r_A + r_B - c\ [\chi(A) \sim \chi(B)]$$

which have been discussed in detail in Sec. 10.2.3 (vi).

(iv) **Hydrogen bonding :** The possibility and effectiveness of hydrogen bonding are largely influenced by the electronegativity difference. These are discussed in Chapter 13.

(v) **Possibility of *d* orbital participation in bonding in nonmetals:** The possibility of *d* orbital participation (Sec. 9.13.5) in the bonding of nonmetals in different compounds such as PCl_5, SF_6, XeF_4, etc. is strongly dependent on the magnitude of electronegativity difference of the combining elements. As a matter of fact, only the highly electronegative elements like *F*, *Cl*, *O* can create the favourable conditions for the participation of *d* orbitals of the central atom in bonding. These are discussed in detail in Sec. 9.13.5.

(vi) **Determination of bond angle and Bent's rule of isovalent hybridisation :** The concept of Bent's rule of isovalent hybridisation is extremely important in understanding the structural characteristics of many covalent compounds. The rule works mainly based on the concept of electronegativity difference. This aspect has been discussed in detail in Sec. 9.13.7.

(vii) **Acid-base strength :** The increased electronegativity of *A* in *A*—*H* gives the more protonic character to *H*. The increased electronegativity of *A* may result from the electron withdrawing inductive effect of the groups attached to *A*. Similarly, the increased electronegativity at the

Click Here to the Academy library

Lewis basic centre reduces its basicity. For the hydracids, besides the electronegativity difference, many other factors are involved to determine the acid strength. These are discussed in the chapter of acids and bases (Ch.14).

For the oxides, with the increase of electronegativity of the central element the acidity increases. It can explain the acidity sequence of the oxides,

$$Na_2O < MgO < Al_2O_3 < SiO_2 < P_4O_{10} < SO_3 < Cl_2O_7.$$

Because of the same ground, Fe_2O_3 is more acidic than FeO.

The acidic and basic characters of *AOH* depend upon the relative magnitudes of $\chi(O) - \chi(H)$ and $\chi(O) - \chi(A)$. If $\chi(O) - \chi(A) < \chi(O) - \chi(H)$, then the *O–H* bond will be more polar than the *A–O* bond and the ionisation occurs preferably as :

$$A\text{–}O\text{–}H + H_2O \rightleftharpoons AO^- + H_3O^+.$$

Thus, it shows the acidic character. The above condition arises only when *A* is highly electronegative and its electronegativity is comparable with that of oxygen. Thus, the electron withdrawing inductive effect of *A* in such cases favours the dissociation of hydrogen as a proton. Examples of this group are : *ClOH*, *IOH*, etc. But, if $\chi(O) - \chi(A) > \chi(O) - \chi(H)$, then the *A–O* bond is more polar than the *O–H* bond and it facilitates the dissociation in the following manner.

$$A\text{–}O\text{–}H + H_2O \rightleftharpoons [A\text{–}OH_2]^+ + OH^-$$

It explains the basic character of *A–OH*. Examples of this group are : *NaOH*, *CsOH*, $Mg(OH)_2$, etc.

(viii) **Paths of nucleophilic attack in nucleophilic substitution reactions :** In hydrolysis or solvolysis and many other nucleophilic substitution reactions, the nucleophile, *Nu* (e.g. OH^-, H_2O, etc.) will attack at the centre where the accumulation of positive charge is very high. In this connection, to proceed the reaction in an *associative path* (i.e. *A process* or S_N2 path), the centre should have the suitable vacant orbital to accommodate the nucleophile. These aspects have been largely discussed in Sec. 10.10.

Some interesting examples of nucleophilic substitution reactions have been discussed in Sec. 8.14.8b. These have been explained by considering the effect of ***charge coefficient parameter* (b) *which determines the charge capacity of a particular centre.***

(ix) **Calculation of charge separation by Sanderson's method :** By using the concept of electronegativity equalisation, in the Sanderson's approach, it is possible to calculate the magnitude of charge separation by using Eqn. 8.14.3.1, i.e. $\chi = a + bq$. It has been detailed in Sec. 8.14.6.

(x) **Colour of the compounds :** In the compounds (generally, the compounds of nontransition elements) where *d–d* transitions are not possible, the colour originates from the **charge transfer band** (generally, ligand → metal). The situation is favoured when the metal is highly polarising and the ligand is highly polarisable (i.e. low electronegativity and large size). *Thus with the increase of polarisability (i.e. decrease of electronegativity) of the ligand, the band suffers a red shift (i.e. absorption occurs at a lower frequency).* It is illustrated as follows :

***AgCl* : white, *AgBr* : pale yellow, *AgI* : yellow, Ag_2S : black.**

Click Here to me/thearchemylibrary

In terms of % of ionic character, it is empirically proposed that if the ionic character of the bond is less than ~ 20%, the compound becomes coloured. It is found that if the ionic character is less than 20% and if it decreases, the colour passes from yellow → orange → red → black. In the above cited compounds the ionic characters are given below.

$$AgCl\ (\sim 80\%),\ AgBr\ (\sim 24\%),\ AgI\ (\sim 15\%),\ Ag_2S\ (4\%).$$

Polarisability sequence : $S^{2-} > I^- > Br^- > Cl^-$

(**Note :** Colour of such covalent compounds can be explained in terms of positions of their HOMO and LUMO. This aspect has been discussed in Secs. 9.11.4, 10.6.4).

(xi) **Diagonal relationship :** The causes of *diagonal relationship* observed among the elements of the 2nd and 3rd periods can be rationalised in terms of electronegativity. This aspect will be discussed in Sec. 8.18.

(xii) **Distribution of metallic and nonmetallic properties among the elements :** The nonmetallic elements are characterised by their high electronegativities. This is why, in the periods, the nonmetallic character increases and it reaches the maxima at the Gr VIIA (17) elements while in a group, it decreases in moving down from top to bottom. This is well demonstrated in Gr IVA (14) and VA (15) elements. These are started with the nonmetals, i.e. *C* and *N*, but ended with the metals *Pb* and *Bi* respectively. Even in Gr VIIA (17), the cationic property of *I* is noted in some cases.

(xiii) **Nomenclature of the binary compounds :** In such cases, the binary compounds are generally considered as the derivatives of the more electronegative element which bears the anionic centre of the molecule. These are illustrated in the following examples.

(a) *ICl* is **iodine monochloride** not chlorine monoiodide as $\chi(Cl) = 3 > \chi(I) = 2.2$. This is why, it is written as *ICl* not as *ClI*.

(b) OF_2 is **oxygen difluoride** not fluorine monoxide as $\chi(F) = 4.0 > \chi(O) = 3.5$. Hence, it is represented as OF_2 not as F_2O. Here it is interesting to note that Cl_2O is chlorine monoxide not oxygen dichloride as $\chi(O) = 3.5 > \chi(Cl) = 3.0$.

Because of the above argument, ammonia should be regarded as the nitride of hydrogen not as the hydride of nitrogen; and it should be represented as H_3N instead of NH_3. But the conventional representation NH_3 is being retained.

(xiv) **Group electronegativity (cf. Table 8.14.9.1) and inductive effect :** To explain the inductive effect of different groups, both the *inherent electronegativity* (determined by a_G, cf. Jaffe-Hinze concept) and the ***charge coefficient parameter*** (b_G, cf. Jaffe-Hinze concept) are to be considered. *The lower values of b_G explains the higher charge accommodating capacity of a group*. The electronegativity of CH_3 and C_2H_5 group are more or less the same, but C_2H_5 is a better electron pushing group because of its lower b_G value. The electronegativity of CH_3 group is higher than that of *H* (hydrogen), but the CH_3 group is a better electron pushing group because of its lower b_G value. This aspect has been discussed in Sec. 8.14.9.

(xv) **Attainment of group valency :** For the more electronegative elements, the attainment of ***Group Valence*** is a difficult task for the low electronegative substituents like alkyl groups. For example, GeR_4 is more stable than GeR_2 while AsR_5 is less stable than AsR_3. Both *Ge* and *As* are the 4th

Click Here to me/thealchemylibrary

period elements. *Ge* is a Gr IVA (14) element while *As* is a Gr VA (15) element. The group valence 4 is attained in GeR_4 and it is stable. *As* is more electronegative than *Ge* and in the case of *As*, the group valence 5 cannot be stabilised by the low electronegative substituents like alkyl groups. This is why, AsR_5 is unstable. To stabilise the group valence of *As*, it needs the substituents (e.g. *F*) of higher electronegativity.

Note : This observation can be also explained in terms of ***d*-orbital participation in bonding, secondary periodicity** or **alternation effect** to be discussed later.

8.17 PERIODIC TRENDS OF COHESIVE ENERGY (i.e. MELTING AND BOILING POINTS)

The inert gases show the lowest melting points. For the representative elements, it reaches the maxima for the Gr IVA (14) elements in moving from left to right. The cohesive energy maximises at Gr IVA (14) and then it falls to the minima occupied by the inert gases. For the transition elements, it maximises at Gr VB (5) and VIB (6) elements. These are shown in Fig. 8.17.1.

The observation can be nicely explained from the consideration of the number of available bonding electrons (i.e. unpaired electrons). With the increase of the number of unpaired bonding electrons, the larger number of bonds may be formed to bring more cohesive energies. For the representative elements having *ns* and *np* as bonding orbitals, the maximum possibility (i.e. the four unpaired electrons are available for bonding probably through sp^3 hybridisation) is attained in Gr IVA (14). For the *d*-block elements, the unpaired *d*-electrons can also participate in bonding. These are attained in a maximum number in the region of Gr VB (5) and VIB (6) elements.

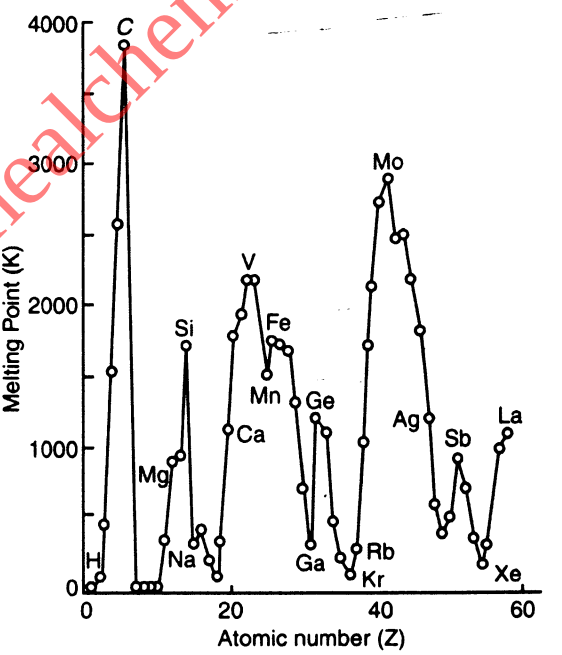

Fig. 8.17.1. Periodic variation of melting points among the elements.

8.18 THE DIAGONAL RELATIONSHIP

The diagonal relationship signifies the similarities in properties of the elements of the 2nd period with the respective diagonally opposite 3rd period elements between the successive groups in the periodic table. Such diagonally opposite pairs are : *Li* and *Mg*, *Be* and *Al*, *B* and *Si*. For other possible pairs the similarities are not so prominant. The diagonal pairs are shown below :

Click Here t.me/thealchemylibrary

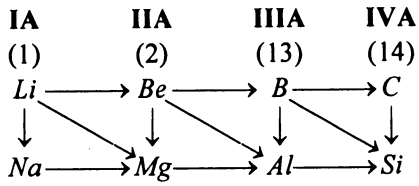

8.18.1 Causes of the Diagonal Relationship

Let us consider the pair *Be* and *Al*. To reach *Al* from *Be* there are **two routes :**

$$Be \rightarrow B \rightarrow Al \text{ and } Be \rightarrow Mg \rightarrow Al.$$

In moving $Be \rightarrow B$ (i.e. along the period), the size decreases but the effective nuclear charge and electronegativity increase, then in passing $B \rightarrow Al$ (i.e. in a group) the size increases and electronegativity decreases. In terms of polarising power, along the period it increases but it decreases in moving down the group. *Thus the polarising power, electronegativity and size remain more or less the same for the diagonal elements*, e.g. *Be* and *Al*. If we follow the route, $Be \rightarrow Mg \rightarrow Al$, we will come also to the same conclusion. Because of this fact, for the diagonal elements between the successive groups of these two short periods, the basic properties such as polarising power, radius, electronegativity, electron affinity, etc. which determine the chemical and physical properties of the elements remain more or less the same. *For the long period elements, because of the intervening d- and f-series, the diagonal relationship does not hold good.* It results so because the group trend of many properties in the transition elements is of opposite nature compared to that in the representative (specially in the short periods) elements; but the trends along the periods remain almost the same for both the representative and *d*-block elements.

8.18.2 Comparison of the Physical Constants of the Three Diagonal Pairs

These are given in Table 8.18.2.1

Table 8.18.2.1. Comparison of the physical constants of the diagonal pairs

Parameter ↓ / *Pairs* →	*Li*	*Mg*	*Be*	*Al*	*B*	*Si*
a) Covalent radius (pm)	123	136	89	125	80	117
b) Ionic radius (pm)	60	65	31	51	20	39
c) $10^2\ Z/r$	1.6	3.0	6.4	6.0	15	10.3
d) χ_P	1.0	1.2	1.5	1.5	2.0	1.8
e) E_0 (volts)	–3.0	–2.36	–1.85	–1.66	–	–
f) IE (first) (kJ mol^{-1})	520	737	899	577	801	786

(b) Ions of common oxidation states, i.e. Li^+, Mg^{2+}, Be^{2+}, Al^{3+}, B^{3+}, Si^{4+}.
(c) Ions of common oxidation states and radii in pm. *Z* denotes the ionic charge.
(d) Electronegativity in Pauling's scale.
(e) Reduction potentials for the process, e.g. $Li^+ + e \rightarrow Li$, $Be^{2+} + 2e \rightarrow Be$, $Al^{3+} + 3e \rightarrow Al$, etc.

The above comparison indicates that the electronegativities of the diagonal elements are very much comparable but the ionic potentials are not comparable except in the pair *Be* and *Al*. However, other

Click Here t.me/thealchemylibrary

properties recorded in the Secs. 8.18.3 - 8.18.5 have got similarities for the diagonal pairs compared to the other possible adjacent pairs (e.g. *Li* and *Na*; *Li* and *Be*; *B* and *Al*, etc.)

8.18.3 Similarities in the Pair, Li and Mg

(i) ***High polarising power*** : Compared to the other alkali metal ions (e.g. $r_{Na^+} = 95$ pm), Li^+ is very small in size ($r_{Li^+} = 60$ pm). Because of this fact, it is highly polarising and it has got more similarities (compared to other alkali metals) with Mg^{2+} ($r_{Mg^{2+}} = 65$ pm) though Mg^{2+} is more polarising than Li^+ (see Z/r_+ values). **It may be noted that Li^+ is more polarising compared to any other alkali metal ion.** This high polarising power is reflected in the following properties which are not shown by other alkali metal ions having low polarising powers.

(a) ***Hydration of salts*** : It has been discussed (Sec. 10.6.4) that the salts having powerful polarising cations get very often hydrated. However, this property can also be explained from the idea of inefficient packing of the lattices due to the small r_+/r_- values (Sec. 11.8.2 (iii)). Some of the hydrates of Li^+ and Mg^{2+} salts are given below.

$LiCl.2H_2O$; $LiClO_4.3H_2O$; $Li(NO_3).3H_2O$; $MgCl_2.6H_2O$; $Mg(ClO_4)_2.6H_2O$; $Mg(NO_3)_2.6H_2O$

Here it is worth noting that other alkali metals do not form stable hydrates.

(b) ***Thermal instability of the oxy-acid salts*** : It has been discussed that the thermal instability of the NO_3^-, $CO_3^=$, $SO_4^=$, BF_4^- salts arises (Sec. 10.6..4 (vii)) due to the polarising behaviour of the cation. This property can also be explained (Sec. 11.8.2 (ii)) by using the r_+/r_- concept. Some examples of *Li*- and *Mg*-salts are given below.

$$4Li(NO_3) \xrightarrow{\Delta} 2LI_2O + 4NO_2 + O_2; 2Mg(NO_3)_2 \xrightarrow{\Delta} 2MgO + 4NO_2 + O_2;$$

$$Li_2CO_3 \xrightarrow{\Delta} LI_2O + CO_2; MgCO_3 \xrightarrow{\Delta} MgO + CO_2$$

Other alkali metals give much stabler analogous salts.

(c) ***Covalence of the compounds*** : According to the *Fajans' rule*, *Li*-salts are more covalent than the other alkali metal salts. In this point, it has got more similarities with the *Mg*-salts than with other alkali metal salts. *This is why, the halides of Li and Mg are soluble in some oxygenated organic solvents.*

(d) ***Complexing power*** : Because of the high polarising power, Li^+ has got a tendency to form complexes. In this regard, Li^+ fits better with Mg^{2+} rather than with other alkali metal ions.

(e) ***Hydration energy*** : The hydration energy of Li^+ is much greater compared to that of any other alkali metal ion and in this regard, it is comparable with Mg^{2+}.

(ii) ***Action of H_2O*** : Both of them can decompose H_2O to liberate H_2.

$$2Li + 2H_2O = 2Li(OH) + H_2; Mg + 2H_2O = Mg(OH)_2 + H_2$$

(iii) ***Action of N_2*** : Both of them form nitrides when burnt in nitrogen. The nitrides are decomposed by H_2O to liberate NH_3.

$$6Li + N_2 = 2Li_3N; 3Mg + N_2 = Mg_3N_2; Li_3N + 3H_2O = 3Li(OH) + NH_3;$$

$$Mg_3N_2 + 6H_2O = 3Mg(OH)_2 + 2NH_3$$

Click Here t.me/thealchemylibrary

(iv) ***Action of Cl_2*** : Both of them form chlorides which form hydrates, i.e. $LiCl.2H_2O$ and $MgCl_2.6H_2O$.

$$2Li + Cl_2 = 2LiCl,\ Mg + Cl_2 = MgCl_2$$

(v) ***Action of O_2*** : On burning in oxygen, *Li* gives its normal oxide Li_2O, and *Mg* gives *MgO*. *Other alkali metals can form other types of oxides, such as superoxides* (O_2^-) *and peroxides* (O_2^{2-}) *but such oxides of lithium are unstable*. This instability can be explained by considering the low r_+/r_- value (Sec. 11.8.2). In this regard, *Li* fits better with *Mg* rather than with other alkali metals.

(vi) ***Carbide formation*** : In contrast to the other alkali metals, *Li* reacts with carbon to form an ionic carbide Li_2C_2 just like MgC_2.

(vii) ***Nature of hydroxides*** : Both the hydroxides of lithium and magnesium are less soluble in water and these are also less basic. On heating they form their oxides.

$$2Li(OH) \xrightarrow{\Delta} Li_2O + H_2O,\ Mg(OH)_2 \xrightarrow{\Delta} MgO + H_2O$$

(viii) ***Instability of the hydrosulfides*** : Both $LiSH$ and $Mg(SH)_2$ are unstable compared to their respective hydroxides. Both Li^+ and Mg^{2+} being *harder* prefer the *harder base* OH^- compared to the *softer one* SH^-.

(ix) ***Organometallic compounds*** : Like the Grignard reagent, *Li* also forms many organometallic compounds.

(x) ***Solubility*** : The halides of both *Li* and *Mg* are soluble in many organic solvents. It happens so because of the covalency in such salts. Li_2CO_3, Li_3PO_4, LiF, and the corresponding salts of *Mg* are insoluble in water.

As a matter of fact, *Li* is a typical alkali metal which differs significantly from its congeners in different properties discussed above but it shows a good deal of similarities with the Gr IIA (2) element, *Mg*.

8.18.4 Similarities in the Pair, *Be* and *Al*

(i) ***Occurrence and extraction*** : In nature they occur simultaneously in beryl, $3BeO, Al_2O_3.6SiO_2$. Both the metals are isolated by electrolysis of their fused salts in the presence of fluorides.

(ii) ***High polarising power*** : Because of the high polarising power of Be^{2+} and Al^{3+} as evidenced from the Z/r_+ value (see Table 8.18.2.1), they form *covalent compounds* having lower melting points and higher solubilities in organic solvents and they form hydrated salts. Because of the same ground, they yield high *hydration energies* in the formation of $Be(H_2O)_4^{2+}$ and $Al(H_2O)_6^{3+}$ species *and their carbonates are thermally unstable*. In these properties, Be^{2+} is more comparable with Al^{3+} rather than with other Gr IIA (2) cations.

(iii) ***Complexing power*** : In contrast to other Gr I (1) and Gr II (2) metals, Be^{2+} has got a strong propensity to form complexes. The complexes of Be^{2+} and Al^{3+} are comparable. The examples are: BeF_4^{2-} and AlF_6^{3-}, $Be(C_2O_4)_2^{2-}$ and $Al(C_2O_4)_3^{3-}$. *Be*(II) gives the tetrahedral complexes while *Al*(III) forms the octahedral complexes.

(iv) ***Action of HNO_3*** : Both *Be* and *Al* are rendered passive by HNO_3 due to the formation of their inert oxide coatings.

(v) ***Action of alkalies*** : *Be* forms beryllates while *Al* forms aluminates.

Click Here t.me/thealchemylibrary

$Be + 2NaOH = Na_2BeO_2 + H_2\uparrow$; $2Al + 2NaOH + 2H_2O = 2NaAlO_2 + 3H_2\uparrow$

(vi) ***Properties of the oxides and hydroxides*** : These are amphoteric for both the metals.

$$BeO + 2HCl = BeCl_2 + H_2O;\ Al_2O_3 + 6HCl = 2AlCl_3 + 3H_2O.$$

$$BeO + 2NaOH = Na_2BeO_2 + H_2O;\ Al_2O_3 + 2NaOH = 2NaAlO_2 + H_2O.$$

$Be(OH)_2$ and $Al(OH)_3$ behave similarly towards the acids and alkalis.

(vii) ***Properties of the halides*** : $BeCl_2$ actually forms the polymeric structure through the bridging by Cl. It can also attain the dimeric form $(BeCl_2)_2$ like the dimeric $(AlCl_3)_2$.

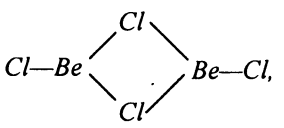

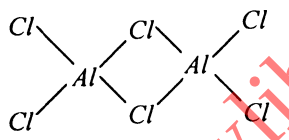

Both the halides are covalent and soluble in organic solvents. They are easily hydrolysed. They can also act as Lewis acids.

(viii) ***Properties of the hydrides*** : Both of them form polymerised hydrides through *hydrogen bridge bonds* ($3c - 2e$ bonds).

(ix) ***Properties of the carbides*** : Both Be_2C and Al_4C_3 yield CH_4 on hydrolysis.

$$Be_2C + 4H_2O = 2Be(OH)_2 + CH_4;\ Al_4C_3 + 12H_2O = 4Al(OH)_3 + 3CH_4$$

8.18.5 Similarities in the Pair, *B* and *Si*

(i) ***Occurrence and extraction*** : B exists as borates while Si exists as silicates. Both of them are isolated by reducing their respective oxides by Mg.

$$B_2O_3 + 3Mg = 3MgO + 2B,\ SiO_2 + 2Mg = 2MgO + Si$$

(ii) ***Physical texture*** : Both the nonmetals may have both the crystalline and amorphous allotropic forms.

(iii) ***Covalency*** : Because of the high ionic potentials, they form predominantly covalent compounds.

(iv) ***Action of alkalies*** : On fusion, B forms metaborates while Si forms metasilicates.

$$2B + 2NaOH + 2H_2O = 2NaBO_2 + 3H_2,\ Si + 2NaOH + H_2O = Na_2SiO_3 + 2H_2\uparrow.$$

(v) ***Properties of the oxides*** : On burning in the presence of O_2, both B and Si form stable oxides.

$$4B + 3O_2 = 2B_2O_3;\ Si + O_2 = SiO_2$$

They react with strong alkalies as follows.

$$B_2O_3 + 2NaOH = 2NaBO_2 + H_2O;\ SiO_2 + 2NaOH = Na_2SiO_3 + H_2O$$

They also react in the same way with HF.

$$BF_3 + HF = HBF_4,\ SiF_4 + 2HF = H_2SiF_6;$$

$$B_2O_3 + 6HF = 2BF_3 + 3H_2O,\ SiO_2 + 4HF = SiF_4 + 2H_2O$$

On heating with carbon in an electric furnace, they form carbides,

$$2B_2O_3 + 7C = B_4C + 6CO;\ SiO_2 + 3C = SiC + 2CO$$

Click Here t.me/thealchemylibrary

Both the carbides form the three-dimensional networks. They are inert to hydrolysis. They are very hard and used as abrasives.

On passing N_2 over the heated mixture of the oxide and carbon, the corresponding nitrides are formed.

$$B_2O_3 + N_2 + 3C = 2BN + 3CO;\ 3SiO_2 + 2N_2 + 6C = Si_3N_4 + 6CO$$

Both the nitrides can decompose steam to produce their corresponding oxyacids and NH_3.

$$BN + 3H_2O\ (\text{steam}) = H_3BO_3 + NH_3;\ Si_3N_4 + 12H_2O\ (\text{steam}) = 3H_4SiO_4 + 4NH_3$$

(vi) ***Properties of the halides*** **:** The chlorides are formed by passing Cl_2 over the heated mixture of the corresponding oxide and carbon.

$$B_2O_3 + 3Cl_2 + 3C = 2BCl_3 + 3CO;\ SiO_2 + 2Cl_2 + 2C = SiCl_4 + 2CO.$$

The corresponding fluorides are formed in the reaction between the respective oxides and HF.

$$B_2O_3 + 6HF = 2BF_3 + 3H_2O;\ SiO_2 + 4HF = SiF_4 + 2H_2O.$$

Both the chlorides, i.e. BCl_3 and $SiCl_4$, are liquid and are readily hydrolysed to form orthoboric acid and orthosilicic acid respectively.

$$BCl_3 + 3H_2O = H_3BO_3 + 3HCl;\ SiCl_4 + 4H_2O = H_4SiO_4 + 4HCl.$$

Both the fluorides are colourless gases and are hydrolysed in the same way.

$$BF_3 + 3H_2O = H_3BO_3 + 3HF,\ 3BF_3 + 3HF = 3HBF_4$$

i.e. $4BF_3 + 3H_2O = H_3BO_3$ (orthoboric acid) $+ 3HBF_4$ (fluoroboric acid)

$$SiF_4 + 4H_2O = H_4SiO_4 + 4HF,\ 2SiF_4 + 4HF = 2H_2SiF_6$$

i.e. $3SiF_4 + 4H_2O = H_4SiO_4$ (orthosilicic acid) $+ 2H_2SiF_6$ (fluorosilicic acid)

Both H_3BO_3 and H_4SiO_4 are weak acids. Both BX_3 and SiX_4 can act as Lewis acids.

$$BX_3 + L = BX_3L\ (\text{tertrahedral}),\ SiX_4 + 2L = SiX_4L_2\ (\text{octahedral})$$

Both the halides can be reduced by $LiAlH_4$ to produce their corresponding hydrides.

$$4BCl_3 + 3LiAlH_4 = 3LiCl + 3AlCl_3 + 2B_2H_6$$

$$SiCl_4 + LiAlH_4 = LiCl + AlCl_3 + SiH_4$$

(vii) ***Properties of the hydrides*** **:** The hydrides can be prepared by reducing their chlorides by $LiAlH_4$. They can also be prepared by using the magnesium boride and silicide respectively.

$$Mg_3B_2 + 6HCl = 3MgCl_2 + B_2H_6,\ Mg_2Si + 4HCl = 2MgCl_2 + SiH_4$$

Here, some higher hydrides are also formed. The hydrides have comparable properties. They can easily burn to form their oxides.

$$B_2H_6 + 3O_2 = B_2O_3 + 3H_2O;\ SiH_4 + 2O_2 = SiO_2 + 2H_2O$$

They hydrolyse in the same way.

$$B_2H_6 + 6H_2O = 2H_3BO_3 + 6H_2\uparrow;\ SiH_4 + 4H_2O = H_4SiO_4 + 4H_2\uparrow$$

(viii) ***Complexing power*** **:** Both B and Si have tendencies to form complexes. BF_4^-, SiF_6^{2-} are the halocomplexes.

Click Here t.me/thealchemylibrary

8.19 BASIC DIFFERENCE IN GROUP TRENDS BETWEEN THE REPRESENTATIVE AND TRANSITION ELEMENTS

The general and identical trends of variation of different properties *along the periods* hold good for both the representative and *d*-block elements. But the *group trends* of different properties such as effective nuclear charge, size, electronegativity, ionisation energy and electron affinity are very often remarkably different and opposite in nature between the representative and *d*-block elements. This difference mainly arises because of the ***d*- and *f*-contractions.** Sometimes, the immediate heavier posttransition elements violate the normal group trends which are followed by the common representative elements.

As a matter of fact, the general group trends are nicely maintained by the common representative elements like alkali metals, halogens, etc. except the 2nd period elements (*Li* to *F*) which show some anomalies. Thus, ***for the common representative elements, the gradual decrease of ionisation energies with the increase of atomic number in a group is a rule while for the transition series the opposite trend is not an exception but is a rule.***

Besides the *d*- and *f*-contraction, the ***relativistic effects*** (Sec. 8.20.3) leading to the expansion of *d*- and *f*-orbitals are responsible to explain the difference in group trends between the representative and transition elements. ***Relativistic expansion*** run in the same sequence : $5d > 4d > 3d$; $5f > 4f$. Their **bonding properties** run in the same sequence (Sec. 4.3). *Because of this relativistic expansion, the attainment of higher oxidation state becomes easier for the heavier congeners* (cf. Secs. 4.3, 8.20.3, 8.23).

8.20 SECONDARY PERIODICITY : ANOMALIES AMONG THE POSTTRANSITION ELEMENTS AND POSTLANTHANIDES (cf. Secs. 8.24, 10.3)

8.20.1 Secondary Periodicity and Consequences of Secondary Periodicities

The variation trends of different properties (e.g. ionisation energy, atomic or ionic radius, electron affinity, etc.) in a group (specially for the immediate posttransition elements, i.e. Gr IIIA (13), Gr IVA (14), VA (15) *do not occur in a smooth monotonous way, rather a number of inner small maxima and minima occur in the trends.* ***This nonmonotonous variation trend of different properties in a group is referred to as secondary periodicity*** as proposed by E.I. Biron and S.A. Shchukarev. This is shown in Fig. 8.20.1.1.

In the series, *C–Si–Ge–Sn–Pb*, the ionisation energies and electron affinities of *Ge* and *Pb* are higher than the normal expected values from extrapolation of the group trend. Similarly, their sizes are also decreased more from the smooth trend of variation.

The **sum of ionisation energies** (kJ mol^{-1}) for the ns^2 electrons of the Gr IV (14) elements are : *C* = 10820, *Si* = 7580, *Ge* = 7710, *Sn* = 6870, *Pb* = 7160. **It indicates the hikes at the 4-th (i.e. *Ge*) and 6-th (i.e. *Pb*) period elements.**

Again the **electronegativities** of the elements follow the same pattern : *C* = 2.60, *Si* = 1.91, *Ge* = 2.00, *Sn* = 1.94, *Pb* = 2.23 (values are calculated by using the bond energies and other experimental data by Allred and Rochow); (the Allred-Rochow electrostatic values are : *C* = 2.5, *Si* = 1.8, *Ge* = 2.0, *Sn* = 1.7, *Pb* = 1.6). Because of these facts, *Ge* shows more similarities with *C* rather than with its nearest congeners *Si* and *Sn*.

Click Here to the/thearchemylibrary

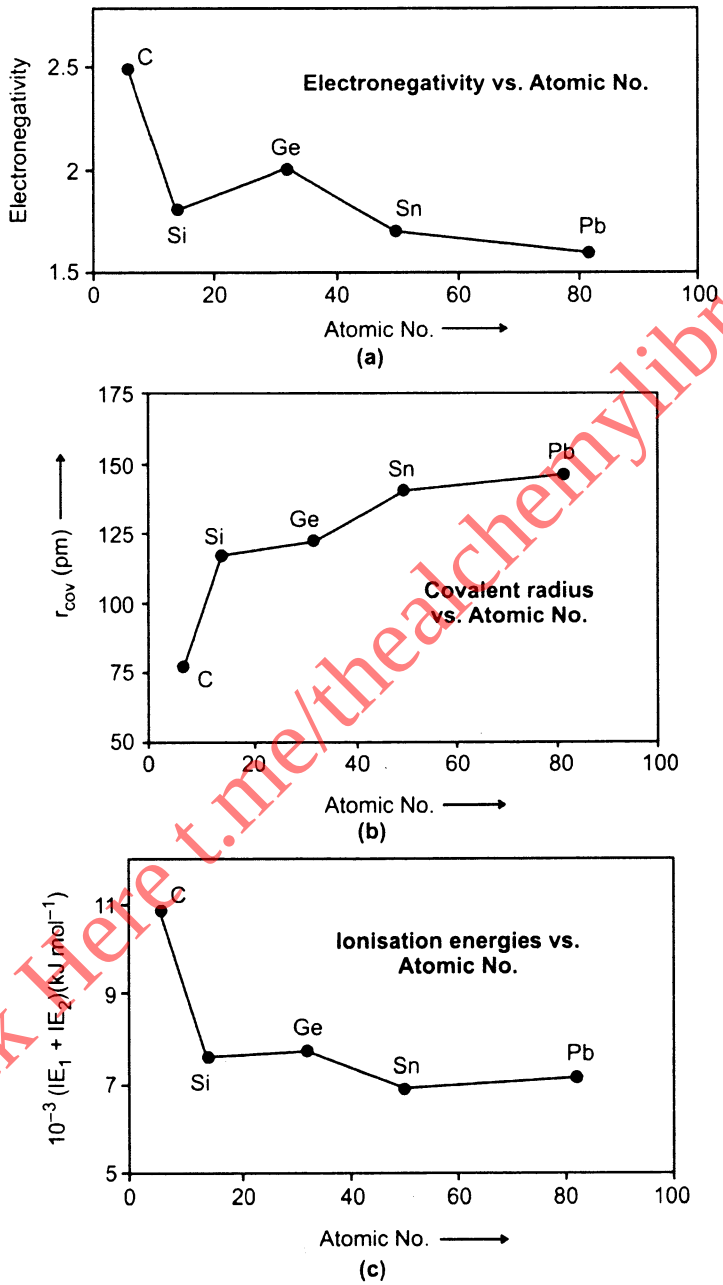

Fig. 8.20.1.1. Nonmonotonous variation trends of electronegativity, covalent radius and ionisation energy among the Gr IVA (14) elements (i.e. a representation of the secondary periodicity among the Gr IVA (14) elements).

These are explained by considering the penetration of the outer orbitals into the inner orbitals. In *Ge*, the 4*s* orbital penetrates into the $3d^{10}$ orbitals and in *Pb*, the 6*s* orbital penetrates into the $4f^{14}$ and $5d^{10}$ orbitals.

Click here t.me/thealchemylibrary

As a matter of fact, these anomalies due to the secondary periodicity are not only restricted to *Ge* and *Pb* but to all the posttransition elements in the **4-th (*Ga* to *Br*) and 6-th (*Tl* to *At*) periods. The relatively higher ionisation energies and electron affinities for these posttransition elements in the 4-th and 6-th periods are well documented.**

- **Relative instability of *As*(V) in Gr VA (15) :** The stabilities of the highest possible oxidation state (i.e., group number) in the 4-th period posttransition elements (e.g. *As*, *Se*, *Br*) are relatively less. For example, +5 oxidation states are more well known for *P* and *Sb* compared to *As*. Only AsF_5 is reported while PCl_5, PF_5, $SbCl_5$, SbF_5 are well documented.
- **Relative instability of *Se*(VI) in Gr VIA (16) :** Among the oxides (i.e. SO_3, SeO_3, TeO_3) of Gr VIA (16) elements, SeO_3 is the least stable one. Similarly among the fluorides (i.e. SF_6, SeF_6 and TeF_6), SeF_6 is the least stable one.
- **Relative instability of *Br*(VII) in Gr VIIA (17) :** In Gr VIIA (17), $HClO_4$ and HIO_4 are well known but $HBrO_4$ was unknown before 1968. It indicates that the attainment of the +7 oxidation state in *Br* is not so favoured compared to its nearest congeners. It is further evidenced by the more oxidising power of $HBrO_4$ compared to $HClO_4$ and HIO_4.
- **Relatively higher ionisation energies of *Ga* and *Tl* in Gr IIIA (13) elements :** In Gr IIIA (13), the sum of first three ionisation energies (kJ mol^{-1}) are : *B* = 6887, *Al* = 5044, *Ga* = 5521, *In* = 5084, *Tl* = 5439. The 4-th and 6-th period elements, *Ga* and *Tl* respectively show the hikes. The similar observations occur in the Gr IVA (14) elements.

All the above facts support that *for the posttransition elements in the 4-th and 6-th periods, the ionisation energies (consequently, electron affinities and electronegativities) are higher compared to their nearest heavier and lighter congeners.*

(***Note* : *Alternation effect*** (Secs. 8.24, 10.3) may be compared with **secondary periodicity.** See **Inert Pair Effect** and **Alternation effect**).

Origin of Secondary Periodicity (cf. Secs. 8.24, 10.3)

The 4th period *p*-block elements i.e. *Ga* to *Kr* experience the ***effect of scandide contraction*** (i.e. effect of $3d^{10}$ contraction) while the 6th period *p*-block elements i.e. *Tl* to *Rn* experience both the effects of ***lanthanide contraction*** (i.e. effect of $4f^{14}$ contraction) and ***relativistic effect*** leading to contraction of 6*s* orbital and expansion of 4*f* and 5*d* orbitals.

8.20.2 Explanation of the Anomalies in Properties of the 4-th and 6-th Period Posttransition Elements

The elements which just follow the **first filling of the low screening sublevels** (e.g. *d*, *f*) will display higher ionisation energies and reluctance in attaining the highest possible oxidation states. These are: 4th period posttransition elements (*Ga* to *Kr*, effect of $3d^{10}$-contraction i.e. ***scandide contraction***, Sec. 8.10.2), and 6-th period postlanthanides (i.e. *Hf* to *Rn*, effect of *f*-contraction of $4f^{14}$ i.e. ***lanthanide contraction***). In this line of argument, the elements e.g. *Na* and *Mg*, which follow the first filling of the *p* level (i.e. an effect of ***p-contraction*** as the *s* orbitals are more penetrating than the *p* orbitals) should form relatively less stable compounds (with positive oxidation states) compared to their nearest congeners. However, for *Na* and *Mg*, the 3*s* orbital is penetrating into the $2p^6$ electrons; while for the 4-th period posttransition elements, the 4*s* orbital is penetrating into the $3d^{10}$ electrons and for the postlanthanides

Click Here t.me/cheadchemylibrary

the 6*s* orbital is penetrating into the $4f^{14}$ and $5d^{10}$ electrons. This is why, the effects are well pronounced for the 4-th and 6-th period post-transition elements.

For the 6-th period posttransition elements (i.e. *Tl* to *Rn*), effects of both the *d*- and *f*-contractions ($5d^{10}$ and $4f^{14}$) are operating while for the 4-th period posttransition elements, effect of only *d*-contraction ($3d^{10}$) is operating. Relativistic effect is also a contributing factor for the 6th period elements (cf. Sec. 8.20.3).

8.20.3 Relativistic Effects* on Chemical Properties of the Fifth and Sixth Row Elements

When the velocity of the revolving electron is very high and comparable to that of light (c = 137 a.u.; a.u. stands for atomic unit, see Sec. 1.8.2 for definition of atomic units), the relativistic treatment based upon Dirac equation is required to explain the atomic properties.

In terms of Bohr treatment (applicable for hydrogen-like systems), the Bohr radius (r) and velocity u of the electron are given by :

$$r = \frac{n^2\hbar^2\,(4\pi\varepsilon_0)}{mZe^2} \text{ and } u = \frac{Ze^2}{n(4\pi\varepsilon_0)\hbar} = \frac{Z}{n} \text{ a.u.}$$

for, $n = 1$, $u = Z$ a.u.;

where $\hbar = h/2\pi$

Thus for the heavy elements, u of the *s* electrons approaches the speed of light. For mercury (Z = 80), under the conditions, $u = Z = 80$ a.u. for the 1*s* electrons and c = 137 a.u., the relativistic mass of the revolving electron is given by:

$$m = m_0\,(1 - u^2/c^2)^{-1/2} \approx 1.2m_0.$$

It will lead to 20% decrease of the orbital size. This ***orbital contraction*** is more pronounced for the *s* and *p* orbitals and for the *d*- and *f*-orbitals the effect is minimum. In fact, the degree of contraction depends on the penetrating power of the orbital under consideration. The *orbital contraction sequence runs* : $s > p > d > f$. This sequence also gives the penetrating power of the orbitals. In fact, compared to the *s*- and *p*-orbitals, the *d*- and *f*-orbitals are having fewer maxima near the nucleus in the radial distribution probability curve.

Relativistic contraction of s- and p-orbitals and relativistic expansion of d- and f-orbitals : In reality, the *s*- and *p*-orbitals are so contracted that they can effectively shield the low lying *d*- and *f*-orbitals. **Because of this enhanced shielding by the *relativistically contracted s*- and *p*-orbitals, the *d*- and *f*-orbitals become *relatively destabilised. It leads to a relativistic expansion of the d- and f-orbitals as a consequence of relativistic contraction of the s- and p-orbitals.***

The size of an atom is determined by the radius of the outermost *ns* and *np* valence orbitals not by the radius of the inner orbitals like $(n-1)d$ and $(n-2)f$ orbitals. ***Thus, though there is a relativistic expansion of the inner d- and f-orbitals, overall an atom contracts due to relativistic effect.***

The relativistic effect is mainly important for the heavier elements and it becomes accountable when Z (atomic number) reaches 60-70. ***Thus for the heavier elements like postlanthanides, postactinides, the effect of both f-contraction and relativistic effect are important.*** This combined effect prevents the increase of size in moving from the 4*d* series to 5*d* series in a particular group.

* Dr. Meckelvey, *J. Chem. Educ.* **60,** 112, 1983.

Click Here t.me/thealchemylibrary

The **important features of relativistic effects** are :

- *relativistic contraction of outer s- and p-orbitals*,
- *relativistic expansion of inner d- and f-orbitals*, sequence of relativistic expansion, $5d > 4d > 3d$; $5f > 4f$ (cf. Fig. 4.3.1),
- *overall relativistic contraction of atomic size,*
- *important only for the heavier atoms, most important for the 6th period elements like Hg and Au at the 6s-orbital.*

Relativistic effect to control the different properties of elements is illustrated in the following cases.

• **Inert pair effect :** The relativistic contraction of the *s* orbitals increases with the increase of atomic number and consequently, the stability of the *s* electrons increases towards the heavier elements. In the region of *Au* and *Hg*, the $6s^2$ electron pair is tightly bound. It is partly due to the relativistic effect. Consequently, $Hg(6s^2)$ is less reactive than $Zn(4s^2)$ or $Cd(5s^2)$. **The $6s^2$ electrons of *Hg* is so stable (i.e. inert) that it is rightly described as *noble or inert liquid*** (cf. inert gas). It also explains the increasing stability of +2 oxidation state in the direction :

$$Pb(6s^26p^2) > Sn(5s^25p^2) > Ge(4s^24p^2).$$

• ***Ionisation potentials (IP) of Zn, Cd, Hg; Ag and Au*** **:** These are given below :

Element,	IP (eV per atom)		
	1st	2nd	3rd
$Zn([Ar]3d^{10}4s^2)$	9.4	18.0	39.7
$Cd([Kr]4d^{10}5s^2)$	9.0	16.9	37.5
$Hg([Xe]4f^{14}5d^{10}6s^2)$	10.4	18.7	34.5

According to general group trend, the *IP* values should decrease in moving down in a group. The 3rd *IP* involving the *d* electrons decreases from Zn to *Cd* and drops even more sharply from *Cd* to *Hg*. The Ist and 2nd ionisation potentials involving the *s* electrons decrease from *Zn* to *Cd* and again increase from *Cd* to *Hg*. It is due to the more relativistic contraction of the *s* orbitals compared to the *d* and *f* orbitals. **In fact, *d*- and *f*-orbitals experience relativistic expansion.**

It also explains the sequence of *IP* values between $Au(5d^{10}6s^1)$ and $Ag(4d^{10}5s^1)$. The relativistic effect predicts that the *s* electrons are more tightly bound and the *d* electrons are more loosely bound. The first *IP* involving the *s* electrons runs as : $Au(9.22\ eV) > Ag(7.57\ eV)$ while the 2nd *IP* involving the *d* electron follows the **opposite sequence,** $Ag(21.5\ eV) > Au\ (20.5\ eV)$. The more tightly bound *ns* orbital in *Au* also explains the higher electron affinity (2.3 eV) of *Au* than that of either $Ag(1.2\ eV)$ or $Cu(1.22\ eV)$.

In addition to the effect of lanthanide contraction, the relativistic effects on the 6*s* orbital are also partly responsible for the similarity between the respective congeners (e.g. *Zr*, *Hf*; *Nb*, *Ta*; etc) of 4*d*- and 5*d* series.

• **Special properties of *Au* and *Hg* :** Their electronic configurations are :

$$Au : [Xe]4f^{14}5d^{10}6s^16p^0;\ Hg : [Xe]4f^{14}5d^{10}6s^26p^0$$

It has been already mentioned that the relativistic contraction becomes very high at 6*s*-orbitals of *Au* and *Hg* (in 6th period). This is why, **several interesting properties** like inertness of *Hg* and *Au*, high

Click Here t.me/thealchemylibrary

electronegativity and electron affinity of *Au* etc. arise at these two elements. *It may be mentioned that the lanthanide contraction is also partly responsible for these interesting properties.*

For *Au* and *Hg*, the 6*s*-orbital is contracted and stabilised to the maximum extent. Consequently, the energy difference between the 6*s*- and 6*p*-orbitals (which also experience the relativistic contraction, but its extent is much less than that for the 6*s*-orbital) becomes so high that the 6*p*-orbitals can hardly participate in bonding purposes. **In other words, for these elements, the 6*p*-orbitals can hardly be considered as the valence orbitals.** In fact, *Hg* with the electronic configuration $5d^{10}6s^2$ behaves **like a *noble liquid*** just like the noble gases in terms of *chemical reactivity*. *Au* tends to attain the electronic configuration of the *noble liquid* element (i.e. *Hg*) by accepting an electron. ***Thus, the relation between the halogen and its nearest inert gas is comparable to the relation between Au and Hg.*** The severe relativistic contraction of the 6*s* orbital favours the accommodation of electron in the 6*s* orbital. It accounts for the very high electron affinity (and consequently electronegativity) of *Au*.

$Au + e \longrightarrow Au^-$ ($5d^{10}6s^2$, stable electronic configuration of the noble liquid metal *Hg*)

The size of Au^- (called *auride*) is similar to that of Br^-. In fact, several compounds containing Au^- are now known. These are : *CsAu, RbAu*, etc.

• **Stability of the dimeric species, Au_2, Hg_2^{2+} :** Due to the relativistic contraction, the 6*s* orbitals of *Au* or Hg^+ are very much tightly bound and it explains the high dissociation energy of *Au – Au* (2.34 eV) compared to *Ag – Ag* (1.65 eV) or *Cu – Cu* (1.95 eV). Hg^+ is **isoelectronic** with *Au* and the relativistic effect can explain the remarkable stability of Hg_2^{2+} compared to that of Cd_2^{2+} or Zn_2^{2+}.

• **Aurophilicity :** *Au*(*I*) ($5d^{10}6s^0$) shows the coordination number 2. In many compounds, even after maintaining the coordination number 2, *Au*(*I*) shows the additional tendency to introduce the *Au*(*I*)–*Au*(*I*) interaction (ca. 32 kJ mol^{-1}, comparable to that of *H*-bonding). This tendency to form the *Au*(*I*)–*Au*(*I*) bond can lead to cyclisation or dimerisation. The *Au*(*I*)–*Au*(*I*) distance is shorter than that in the non-interacting pair.

Besides the *Au*(*I*)–*Au*(*I*) interaction, many other cations (called ***aurophilic cations***) may interact with the *Au*(*I*) centre. Such interactions are : *Au*(*I*)–*Ag*(*I*) (where *Ag*(*I*) is the lighter congener), *Au*(*I*)–*Hg*(*II*) (where *Hg*(*II*) is isoelectronic with *Au*(*I*)), *Au*(*I*)–*Tl*(*I*), *Au*(*I*)–*Pb*(*II*) (where *Tl*(*I*) and *Pb*(*II*) are isoelectronic with an inert pair $6s^2$). This tendency to interact with the *Au*(*I*) centre is called ***aurophilicity (cf. supramolecular interaction).*** It may be mentioned that the aurophilic cations like *Ag*(*I*), *Tl*(*I*), *Pb*(*II*), *Au*(*I*), *Hg*(*II*) etc. maintain their required coordination number and after maintaining the required coordination number they show the *aurophilicity* (i.e. ***aurophilicity not at the cost of inherent coordination number***). *Thus, aurophilicity introduces only a weak bonding interaction with the Au(I) centre.* Aurophilic interactions leading to cyclisation and dimerisation are shown in Fig. 8.20.3.1.

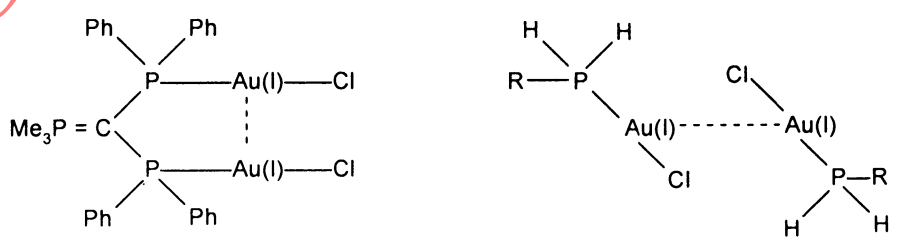

Fig. 8.20.3.1. (a) Intramolecular aurophilic interaction, (b) Intermolecular aurophilic interaction leading to dimerisation (cf. ***Supramolecular interaction***).

Click Here to me/thechemylibrary

The additional bonding ability of $Au(I)$ ($5d^{10}6s^0$) can be explained partly by considering the relativistic effect. ***The relativistic expansion of 5d-orbital facilitates the transfer of some electrons from the 5d-level to some orbitals which are contracted relativistically.*** **These transferred electrons probably participate in additional bonding.** It is important to note that the relativistic effect is also important for all other aurophilic cations.

In the interesting cation ***hedgehog cation*** $C(AuPR_3)_6^{2+}$ ($R = Ph$), the C-centre shows ***hypercoordination number*** 6 (i.e. C-centre interacts/binds with 6 Au centres through *three centre bonds*, i.e. *three Au–C–Au segments*). These Au–C–Au interactions are definitely weaker than the normal $2c$-$2e$ bonding interaction. The overall stability of the cation arises due to a larger number of $Au(I)$–$Au(I)$ **aurophilic interactions.** A similar interaction occurs in $N(AuPR_3)_5^{2+}$ where $R = Ph$. In this compound, nitrogen shows the hypercoordination number 5. Structures of **electron deficient carbon and nitrogen dications** are shown in Fig. 8.20.3.2.

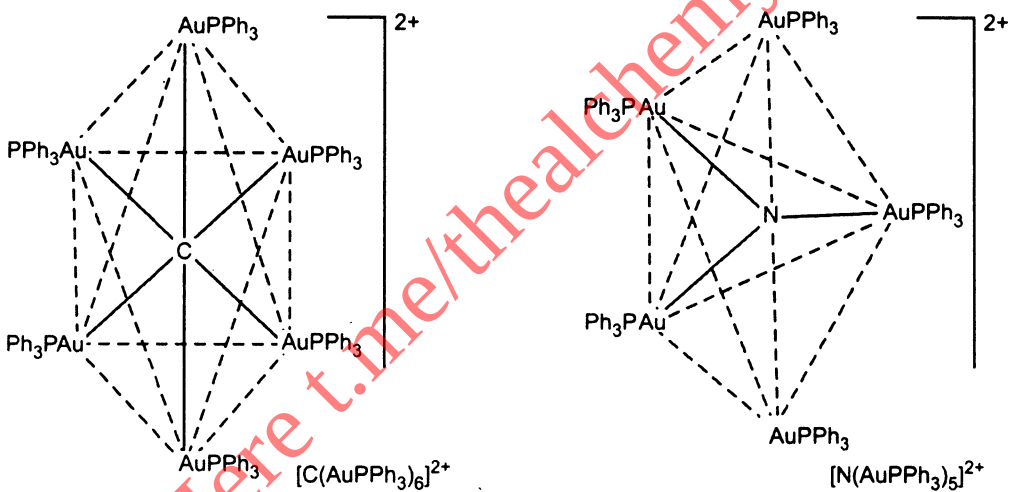

Fig. 8.20.3.2. Aurophilic interaction (shown by dotted lines) in $[C(AuPPh_3)_6]^{2+}$ (i.e. hedgehog cation and $[N(AuPPh_3)_5]^{2+}$.

Click Here t.me/thealchemylibrary

- **Stability of the higher oxidation states of the 5*d* series (cf. Sec. 4.3) :** Due to the relativistic effects on the $5d$ series, the contracted $6s$ orbital shields the d and f orbitals more effectively from the nuclear charge, and consequently the d and f electrons get loosely bound. ***This relativistic expansion of d-orbitals is important for the heavier congeners having 5d orbitals.*** Because of this fact, the $5d$ electrons can participate more fully for bonding purposes compared to the $4d$ electrons of the $4d$ series for which the relativistic effects are less. It explains the higher stabilities of the higher oxidation states of $5d$ series. Examples are :

$Pt(IV) > Pd(IV)$ and $Au(III) > Ag(III)$ (in terms of stability order).

- **Difference between the lanthanides and actinides (cf. Sec. 4.3) :** The inner $(n-2)f$ orbitals i.e. $4f$-orbitals of lanthanides and $5f$-orbitals of actinides are expected to have the poor bonding properties. But ***relativistic expansion*** of the f-orbitals can partially modify the bonding properties of the f-orbitals. The relativistic expansion of the $5f$-orbitals (of the actinides) is more important than that of the

4*f*-orbitals (of the lanthanides). In other words, because of the relativistic effect, the ***4f-orbitals of the lanthanides are more deeply seated than the 5f-orbitals*** (Fig. 4.3.1). Consequently the bonding properties of the 5*f*-orbitals are much better than those of the 4*f*-orbitals. This is why, the 5*f* orbitals, specially of the lighter members of the actinides, can participate in bonding and *the electrons from the 5f-orbitals are more easily ionised.* **For the heavier members of the series,** the 5*f*-orbitals are gradually contracted as usual due to the gradual increase of effective nuclear charge. This is why, the 5*f*-orbitals become less suitable for bonding in the heavier members of the actinide series.

The pronounced relativistic expansion of the 5*f*-orbitals of the early members of the actinides can explain their ***higher oxidation states*** (cf. oxidation states of uranium and neodymium, in fact *U* shows much higher oxidation states than *Nd*), ***relatively broader peak in electronic spectrum*** for the *f–f* transition (in actinides, the 5*f* orbitals being more exposed are influenced more by the ligand orbitals).

- **Spin-orbit coupling in heavier elements :** For the heavy elements, the *spin-orbit coupling* interaction becomes important. Consequently, in the *p*-block elements, the 6*p* orbitals split into the $6p_{3/2}$ and $6p_{1/2}$ levels in which each set of levels can accommodate $2j + 1$ electrons. Thus, the $6p_{3/2}$ levels can accommodate 4 electrons while the $6p_{1/2}$ levels can accommodate 2 electrons. **The $6p_{1/2}$ levels can penetrate better than the $6p_{3/2}$ levels. Consequently, relativistic contraction is better for the $6p_{1/2}$ levels. In some cases, the energy difference between the $6p_{1/2}$ and $6p_{3/2}$ levels become so high that the higher energy level $6p_{3/2}$ cannot participate in bonding purposes. This tendency is expected to be quite important in the *7th period elements* called *superheavy elements*.**

8.21 POSITION OF HYDROGEN IN THE PERIODIC TABLE

The position of hydrogen is not yet settled properly. It has got similarities to some extent with both the Gr IA (1) (i.e. alkali metals) and Gr VIIA (17) (i.e. halogens) elements.

Justification in placing hydrogen in Gr IA (1)

(i) Hydrogen has a similar outermost electronic configuration ($1s^1$).

(ii) It shows valency one like the alkali metals, but the alkali metals preferably show electrovalency while hydrogen predominantly shows covalency.

(iii) Hydrogen can display its electropositive character (i.e. $H \rightarrow H^+ + e$) like the alkali metals. On electrolysis of the fused alkali metal chlorides, the alkali metals are discharged on cathode. Similarly, the electrolysis of dilute *HCl* solution gives the release of hydrogen at the cathode.

(iv) Occlusion of hydrogen by palladium can be compared with the alloy formation by the metals.

The placement of hydrogen and helium in Gr IA (1) and inert gas group i.e. Gr VIIIA (18) respectively gives six vacant spaces between them in the first period. But it is surely impossible to get six elements between *H* and *He* which roughly differ by the three units in atomic weights and one unit in atomic number.

Justification in placing hydrogen in Gr VIIA (17)

(i) Hydrogen shows its monovalency which is a characteristic property of Gr VIIA (17).

(ii) Like the halogens, hydrogen can also behave like a nonmetal.

Click Here to the Treasure Library

(iii) Like the halogens, hydrogen forms its diatomic molecule.

(iv) In ordinary condition, like fluorine and chlorine, hydrogen is gaseous.

(v) In the hydrocarbons, hydrogens can be substituted by different halogens.

(vi) Like the halogens, hydrogen requires only one electron in reaching the nearest inert gas configuration (i.e. *He*).

(vii) Like the halogens, hydrogen can also form its anion (i.e. hydride, $H + e \rightarrow H^-$). But the size of H^- is too large and it is larger than any other the halide except I^-. Thus it does not properly fit in the trend of size of the Gr VIIA (17) anions.

(viii) Halogens form metallic halides and similarly hydrogen can form metallic hydrides with the highly electropositive metals (e.g. *LiH*, *NaH*, CaH_2, etc.). On electrolysis of the hydrides, hydrogen is evolved at the anode like the halogens as in the case of electrolysis of alkali metal halides.

(ix) With the nonmetals, hydrogen forms covalent bonds like the halogens.

(x) The placement of hydrogen at the top of Gr VIIA (17) leads to the difference by 18 units in atomic weights between the nearest congeners (i.e. *H* and *F*) and it is quite expected for the short period elements (e.g. the difference of atomic weights between *Cl* and *F* is 16). But its placement in Gr IA (1) gives the difference by 6 units in atomic weights between *H* and *Li*.

(xi) The placement of hydrogen in Gr VIIA (17) does not leave any vacancy between *H* and *He*.

(***Note*** : The half-filled electronic configuration of $H(1s^1)$ bears a formal analogy with $C\ (1s^2 2s^2 2p^2)$ which has also a half-filled outermost shell. The electronegativity of H ($\chi = 2.1$) is close to those of B ($\chi = 2.0$) and C ($\chi = 2.5$) rather than those of Li ($\chi = 1$) and F ($\chi = 4.0$). Based on these arguments, Sanderson (1964) suggested ***H* to be placed in a place just above between *B* and *C* in the periodic table**).

From the above discussion, hydrogen appears to be a ***naughty element*. To avoid this controversy, it is proposed that hydrogen should be given a separate room at the top of the periodic table.**

8.22 PECULIARITIES OF THE FIRST AND SECOND ROW ELEMENTS

We have already discussed the peculiarities of hydrogen, a first period element. The elements (*Li* to *F*) of the 2nd period are always remarkably different compared to their respective heavier congeners.

Lithium shows its anomalous behaviour (Secs. 8.18.2 and 8.18.3) compared to the other alkali metals and it shows similarities with the Gr IIA (2) element, *Mg*. Similarly, *Be* is more similar to the Gr IIIA (13) element, *Al* than to its own congeners (Secs. 8.18.2 and 8.18.4) in Gr IIA (2). Other diagonal pairs show the same trend.

In all these cases, **the anomalies of the 2nd period elements arise due to their special properties: (i) small size, (ii) nonavailability of the *d* orbitals which can control the chemistry of the relatively heavier nonmetals significantly, (iii) high polarising power of the cations (i.e. hard acids) and low polarisability of the anions (i.e. hard bases).**

8.22.1 Anomalous Properties of Fluorine : Superhalogen or Subhalogen?

Let us consider fluorine which is described as a ***superhalogen*** because of its peculiarities with respect to the other halogens. Some unique properties of fluorine are given below.

Click Here Lme/chealchemylibrary

(i) ***Very low bond energy*** : Because of the shorter *F–F* bond length (142 pm), the lone pair-lone pair repulsions lower the bond strength (155 kJ mol^{-1}). The bond energy of fluorine is lower than that of Cl_2 (240 kJ mol^{-1}) or Br_2 (190 kJ mol^{-1}) and it is only comparable to that of I_2 (149 kJ mol^{-1}).

(ii) ***High electronegativity and electron affinity*** : Though it is more electronegative than chlorine, its electron affinity is lower compared to that of *Cl* because of the increased electron-electron repulsion in the smaller species (i.e. F^-) (see Sec. 8.13.2).

(iii) ***High reduction potential*** : $\frac{1}{2}F_2/F^-$ couple shows the highest reduction potential (E_0 = 2.87 volts) because of the mainly low bond dissociation energy, high electron affinity and high hydration energy.

(iv) ***Instability of oxyacids*** : Its only known oxyacid is *HOF* while the other halogens form oxyacids having oxidation states + I to + VII. *HOF* is also unstable. Oxyacids of other halogens are stabilised through the d_π–p_π back bonding using the vacant *d*-orbitals of the halogen. This is not possible for fluorine.

(v) ***Strong bond formation in covalent compounds and high lattice energy in ionic compounds*** : *A–F* covalent bonds are generally stabler than any other corresponding *A–X* bond, because of the shortest *A–F* bond length. It arises also partly due to the possibility of *pi*-bonding (p_π–p_π bonding as in BF_3), and covalent-ionic resonance due to the highest possible electronegativity difference. Generally, such covalent fluorides are chemically more inert. In addition to the above factors, because of the low bond dissociation energy of F_2, the enthalpy of formation of such compounds is more negative. For example, $\Delta H_f\,(CCl_4)$ = – 115 kJ mol^{-1}, $\Delta H_f\,(CF_4)$ = – 917 kJ mol^{-1}. In the case of ionic salts, fluorides give more favourable lattice energies. For example, $U(NaF)$ = –539 kJ mol^{-1} and $U(NaCl)$ = –373 kJ mol^{-1}. High lattice energy of the fluorides arises from many factors like low bond dissociation energy, high electron affinity, low interionic separation.

(vi) ***Strong hydrogen bond formation*** : High electronegativity of *F* favours the formation of hydrogen bonding extensively (Chapter 13). HF_2^-, $H_2F_3^-$ exist but no such analogous species of the other halogens exist (see Sec. 13.1.9.2).

***Note : Fluorine—Superhalogen* or *Subhalogen*?** Apparently, fluorine forms more stable bonds both covalent and ionic, but a critical analysis shows the **bond weakening property of fluorine** in both covalent and ionic bonds. In fact, *this bond weakening property is measured from the extrapolated values* (cf. Fig. 8.22.1.1). In ionic compounds, the disfavour (i.e. bond weakening property) arises from the reduced electron affinity of fluorine (cf. chlorine shows the highest electron affinity). In fact, in ionic compounds of fluoride (e.g. M^+F^-), the extrapolated lattice energy is higher than the actual one by about 100 kJ mol^{-1}. It may be noted that from the normal trend of electron affinity, fluorine should have the electron affinity about 440 kJ mol^{-1} (extrapolated value) which is higher than the observed value by about 100 kJ mol^{-1}. **The bond weakening reasons present in *F–F* (difluorine) is also present in other covalent bonds like *C–F*, *H–F*, etc.** In fact, the extrapolated bond energies for such covalent bonds are much higher than those experimentally found.

Click Here t.me/thealchemylibrary

All these phenomena clearly indicate that the bonding potentiality of the ***real fluorine*** having the lone pair-lone pair repulsion is much less than that of the ***hypothetical fluorine*** in which the electron-electron repulsion remains absent. ***Based on these arguments, some authors have argued fluorine as the subhalogen not as the superhalogen.***

8.22.2 Anomalous Properties of Lithium

Now let us cite some *anomalous* (Secs. 8.18.2 and 8.18.3) *properties* of *Li* with respect to its congeners.

(i) **Low lattice energy :** Because of the low r_+/r_- value, for the larger anions (e.g. SO_4^{2-}, CO_3^{2-}, OH^-, SH^-, etc.), the nonefficient packing (Sec. 11.8.2) destabilises the compounds and this is evidenced from their low decomposition temperatures. The high polarising power of Li^+ can also explain this property (Sec. 10.6.4).

(ii) **High covalence, high complexing power etc. :** The high polarising power of Li^+ introduces some special properties like *increased covalency, tendency of hydration of its ionic salts, high hydration energy, better complexing power*. These aspects have been illustrated in Sec. 8.18.3.

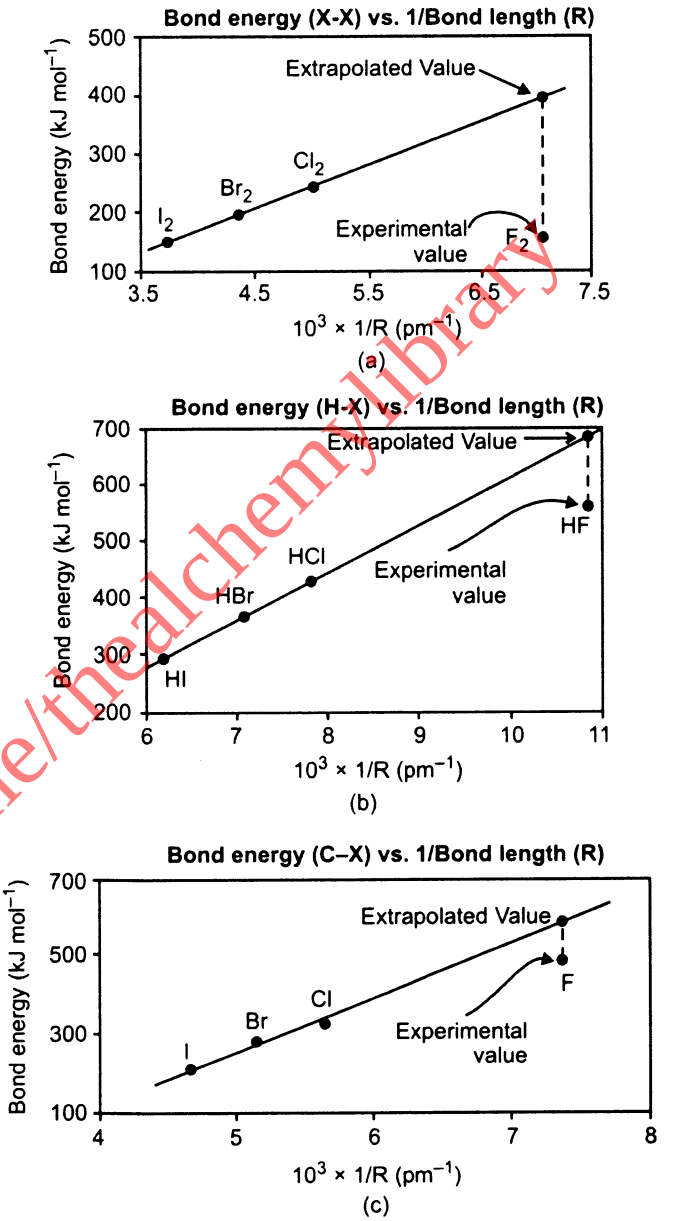

Fig. 8.22.1.1. Extrapolated bond energies for *F–F*, *H–F* and *C–F* bonds to illustrate the bond weakening property of fluorine.

(iii) **Flouting the radius ratio rule :** *Li*-salts very often violate the radius ratio rule (Sec. 11.8.3).

Other peculiar properties of *Li* have been discussed earlier (Sec. 8.18.3).

Click Here t.me/thealchemylibrary

8.23 COMPARISON BETWEEN TRANSITION (i.e. *d*-block) AND INNER TRANSITION (i.e. *f*-block) METALS

Here we shall consider the 3*d*-metals and 4*f*-metals for the sake of simplicity. It may be pointed out that the 3*d*-orbitals differ from the 4*d* and 5*d* orbitals of the heavier congeners in some aspects. Similarly, the lanthanides (i.e. 4*f*-series) differ from the actinides (i.e. 5*f*-series). The difference between the *d*- and *f*-block elements arises due to the ***difference in bonding properties of d- and f-orbitals.*** This aspect has been discussed in Secs. 4.3, 8.8 and 8.20.3.

The important points of difference are mentioned below. Here we shall mainly consider the 3*d* and 4*f* metals.

- ***Relative bonding properties of 3d and 4f orbitals*** : *The (n–2)f (i.e. 4f) orbitals are more deeply seated than the (n–1)d (i.e. 3d) orbitals*. Consequently, the 4*f*-orbitals cannot participate in metal-ligand interaction while the 3*d* orbitals can participate in metal-ligand interaction. This causes the following differences.
  - (a) ***LFSE*** : There is a *lack of LFSE* (ligand field stabilisation energy) in the complexes of lanthanides while LFSE contributes significantly in controlling the complexing power of the transition metal ions.
  - (b) ***Ionic interaction*** : In the complexes of lanthanides, *mainly ionic interaction* prevails and the lanthanide ions (Ln^{3+}) are typically *hard*. They mainly prefer the hard binding sites like *O*, *F*. Depending on the situation, varieties types of ligands can stabilise the transition metal complexes.
  - (c) ***Flexibility in geometry*** : Lack of LFSE makes the complexes of lanthanides *more flexible* in terms of geometry and coordination number. For the lanthanides, the common coordination numbers are 6, 7, 8, 9 while for the transition metal ions, the common coordination numbers are 4 and 6.
  - (d) ***Lability*** : Lack of LFSE makes the lanthanide complexes more labile.
  - (e) ***Nature of absorption spectra*** : The absorption spectra for *f–f* transition in lanthanides are quite sharp as the band width broadening cause through the metal-ligand covalent interaction remains absent in lanthanides (cf. Sec. 8.8). On the other hand, the spectra due to *d–d* transitions are relatively broader.
  - (f) ***Variable oxidation states*** : The transition metals show the variable oxidation states depending on the extent of $(n-1)d$ orbital participation in bonding. For the inner transition metals, the $(n-2)f$ orbitals (specially the 4*f* orbitals) are deeply seated (cf. Fig. 4.3.1) and they do not participate in bonding. In fact, for the lanthanides, +3 oxidation state is the most common oxidation state. However, the early member of the actinides can show the variable oxidation states to some extent because of the better bonding properties of 5*f* orbitals. However, the late members of the actinide series behave roughly like the lanthanides. These aspects have been discussed in Sec. 8.8.
- ***Relative complexing power*** : The ionic potentials (charge/radius ratio) of the trivalent lanthanides are relatively smaller compared to those of trivalent transition metal ions. It is due to the larger ionic radii of Ln^{3+} (cf. Cr^{3+} : 60 pm; Ln^{3+} : 85 to 106 pm). **Because of the lower ionic potentials and absence of LFSE, the complexing power of the lanthanides is relatively**

Click Here t.me/thealchemylibrary

smaller compared to that of the *d*-block metal ions. Because of the same ground, the actinides also form the relatively weaker complexes.

Note : Ln^{3+} ions fail to form alum type complexes because their poor complexing power cannot keep the coordinated water molecules firmly. But the trivalent main group metal ions like Al^{3+} can form alum. It is mainly due to the larger size of Ln^{3+} ions (cf. ionic radius : Al^{3+}, 52 pm; Ln^{3+}, 85-106 pm).

- ***Magnetic property of the complexes*** (cf. Sec. 1.10.17) : In 3*d*-series, very often, the orbital contribution is quenched by the crystal field and the observed magnetic moment corresponds to the spin only value. In lanthanides, the spin-orbit coupling interaction is high and the multiplet width is much greater than the thermal energy k_BT. In general, for the lanthanides, the magnetic moment is given by :

$$\mu_J = g\sqrt{J(J+1)}\ \text{BM}$$

For Sm^{3+} and Fu^{3+}, the multiplet width is comparable to k_BT and the expression of magnetic moment is quite complicated. For the heavier transition metal ions, the spin-orbit coupling interaction becomes quite strong and in such cases, the observed magnetic moment is different from the spin-only value.

- ***Reactivity*** : Lanthanides generally show the +3 oxidation state. In this respect, they are similar to *Cr* and *Co* which generally form stable complexes in +3 oxidation state. But in terms of reactivity, the free lanthanides are more reactive than the transition metal ions (cf. for the lanthanides, the sum of first three ionisation energies lies in the range 3500-4300 kJ mol^{-1} while these values for *Cr* and *Co* are 5200 kJ mol^{-1} and 5650 kJ mol^{-1} respectively). ***In fact, in terms of reactivity, the lanthanides are more similar to the alkali and alkaline earth metals.*** This enhanced reactivity of the lanthanides arises due to two factors : ***reduced ionisation energy*** and ***reduced atomisation energy.***

  For the *d*-block elements, the $(n-1)d$ orbital can better participate in metal-metal bonding, while for the *f*-block elements, the more deeply seated $(n-2)f$ orbitals can hardly participate in metal-metal bonding. ***Consequently, the metallic bonds in lanthanides are weaker.*** *This is why, the heat of atomisation for the lanthanides is much less while it is very high for the d-block elements.*

  Note :

  - ***Bonding properties of 4f (i.e. lanthanides) vs. 5f (i.e. actinides) orbitals (cf. Fig. 4.3.1)*** : The 5*f*-orbitals are more exposed than the 4*f*-orbitals because of more relativistic expansion of the 5*f*-orbitals. This is why, in the actinides, the ligand field effect (i.e. metal-ligand interaction) is more important to control the stability of their complexes; absorption peak pattern, magnetic moments of the complexes, etc. This is specially important for the lighter actinides (cf. Secs. 4.3; 8.8.3; 8.20.3) which roughly behave like the *d*-block metals.
  - ***Lanthanide complexes as NMR shift reagents:*** The β-diketonate [e.g. $F_3CCF_2C(O)CHC(O)CMe_3^-$ (***fod***), $Me_3CC(O)CHC(O)CMe_3^-$ (***dpm***)] complexes of the lanthanides find application as ***NMR shift reagents.*** The positions of PMR (proton magnetic resonance) signals are influenced by the paramagnetic complexes of the lanthanides. Sometimes (as in cholesterol), the PMR signals overlap and the interpretation becomes quite difficult. In presence of suitable NMR shift reagents, the PMR signals can be separated.

Click Here for more chemistry library

- ***Mischmetal*** : A mixture of finely divided particles of *Ce* and *La* and smaller amounts of other rare earths and iron is called *mischmetal*. This mixture is ***pyrophoric.*** By alloying with iron, its hardness can be enhanced. This alloy is used for producing flints in lighters. This is why it is named so.

8.24 VARIATION OF OXIDATION STATES OF *s*- AND *p*-BLOCK ELEMENTS

To understand this aspect, we are to consider the variation of valence shell electronic configurations and energy of the valence shell orbitals (Table 8.24.1, Figs. 8.24.1 and 8.24.2). The valence shell orbitals are *ns* and *np*.

Table 8.24.1. Energy difference (ΔE) between the *ns* and *np* orbitals of valence shell

$\Delta E = E_{np} - E_{ns}$ (in eV)

Group :	IA (1) ns^1	IIA (2) ns^2	IIIA (13) ns^2np^1	IVA (14) ns^2np^2	VA (15) ns^2np^3	VIA (16) ns^2np^4	VIIA (17) ns^2np^5	VIIIA (18) ns^2np^6
2nd period :	*Li*	*Be*	*B*	*C*	*N*	*O*	*F*	*Ne*
ΔE (eV) :	1.8	2.8	4.5	5.3	6.0	15.0	20.5	26.7
3rd period :	*Na*	*Mg*	*Al*	*Si*	*P*	*S*	*Cl*	*Ar*
ΔE (eV)	2.0	2.6	4.5	5.2	5.5	9.8	11.5	13.5
4th period :	*K*	*Ca*	*Ga*	*Ge*	*As*	*Se*	*Br*	*Kr*
ΔE (eV) :	–	–	6.0	6.7	6.8	10.5	12.1	13.3
5th period :			*In*	*Sn*	*Sb*	*Te*	*I*	*Xe*
ΔE (eV) :	–	–	5.3	5.8	6.5	8.8	10.0	–
6th period :			*Tl*	*Pb*	*Bi*	*Po*	*At*	*Rn*
ΔE (eV)			7.0	9.0	10.0	12.0	16.0	–
(approximate value)								

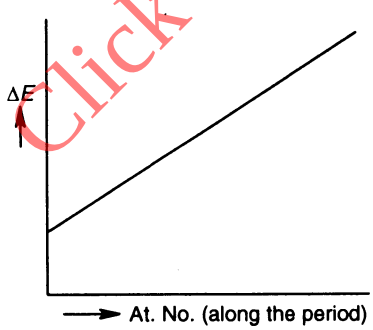

Fig. 8.24.1. Variation of ΔE along a period (qualitative representation) for the *p*-block elements.

$\Delta E = E_{np} - E_{ns}$

Note : The almost monotonic increasing trend of ΔE is simply represented by a straight line.

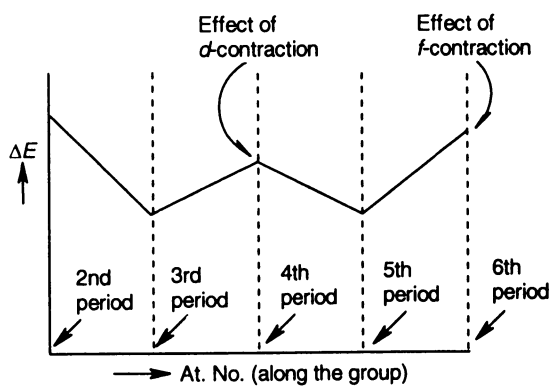

Fig. 8.24.2. Variation of ΔE in a group (qualitative representation) for the *p*-block elements.

$\Delta E = E_{np} - E_{ns}$

Click Here t.me/thealchemylibrary

• ***Variation of ΔE ($= E_{np} - E_{ns}$) and stability of higher oxidation states along a period for the p-block elements*** : It is evident that ΔE increases gradually almost in a monotonic fashion with the increase of the atomic number along a period. It indicates that for the late members of the series, energy of the *ns* electrons decreases (i.e. it gets more and more attracted towards the nucleus) and consequently its nonbonding property gradually increases. In other words, the probability of *ns* electrons to act as the valence electrons in chemical bond formation gradually decreases as we move from left to right along a period. ***This is why, for the beginners of a series, the ns orbital is more feasible for the bonding purposes while for the late members of the series, the more deeply seated ns orbitals are energetically less feasible for the bonding purposes.*** In fact, stability of the highest possible valence state (indicated by Group No.) gradually decreases in moving from left to right in a period of the *p*-block element. It is supported by the following stability sequence of the oxyanions.

$$\Delta E\ (= E_{np} - E_{ns})\ \underbrace{\textbf{Stability}: SiO_4^{4-} > PO_4^{3-} > SO_4^{2-} > ClO_4^-\ \text{(oxyanions of the 3rd period elements)}}_{\text{increasing sequence}}$$

It may be noted that for showing the highest possible valence state, both the ns and np orbitals are to participate in bonding. For the late members of the series, participation of the deeply seated *ns* orbital in bonding becomes energetically costly (cf. *bonding properties of 4f and 5f orbitals*).

Note : Highest valence state is generally attained in fluoro- and oxo-compounds, because F^- and O^{2-} can stabilise the higher positive oxidation states better. Moreover *A–F* and *A–O* bonds are strong because of their relatively shorter bond length and more covalent-ionic resonance. Here, *A* stands for a representative central element.

• ***Variation of ΔE ($= E_{np} - E_{ns}$) and stability of higher oxidation states in a group and secondary periodicity and alternation effect (cf. Sec. 10.3)*** : In a group, ΔE does not vary in a monotonic fashion with the increase of atomic number (cf. Fig. 8.24.2). It is evident that there is a hike in ΔE value for the 4th and 6th period elements. ***This is why, stability of the highest possible oxidation or valence state is relatively decreased for the 4th and 6th period elements.*** This is illustrated in the following examples:

	3rd period		**4th period**		**5th period**	
Stability sequence :	PCl_5	>	$AsCl_5$	<	$SbCl_5$	} Gr VA (15)
	SF_6	>	SeF_6	<	TeF_6	} Gr VIA (16)
	ClO_4^-	>	BrO_4^-	<	IO_4^-	} Gr VIIA (17)
$\Delta E(= E_{np} - E_{ns})$:	x	<	y	>	z	

This explains the secondary periodicity (cf. Sec. 8.20).

• ***Inert pair effect of the 6th period p-block elements*** : The energy difference between the 6*s*- and 6*p*-orbitals for the 6th period elements is very high (cf. Table 8.24.1 and Fig. 8.24.2). This is why, it becomes very difficult for the 6th period elements to display the highest possible oxidation state. **In other words, the $6s^2$ electron pair is so deeply seated** (i.e. highly stabilised) compared to the other valence orbitals (i.e. 6*p*-orbitals) that the $6s^2$ electrons do not participate in bonding and it remains as a nonbonding pair. This leads to ***inert $6s^2$ pair effect.*** This aspect has been illustrated in Sec. 10.3.

Click Here t.me/thealchemylibrary

Note : **In *d*-block elements,** the higher oxidation states are more easily attained for the heavier congeners because the *relativistic expansion of* $(n-1)d$ *orbitals* for the heavier congeners imparts the more bonding properties to the *d*-orbitals.

Inert pair effect, Alternation effect* (i.e. *Secondary periodicity*) *and opposing inert pair effect for the p-block elements (cf. Sec. 10.3)

- Inert pair effect is pronounced for the Gr. 13 and 14 elements.
- Secondary periodicity i.e. alternation effect is mainly pronounced for the Gr. 15 and 16 elements and to some extent for the Gr 17 elements.
- Gr. 17 and 18 elements oppose the inert pair effect i.e. stability of higher oxidation state increases for the heavier congeners.

These aspects are illustrated in Sec. 10.3.

• ***Odd-even rule for oxidation states*** : Elements of odd-numbered group show the odd oxidation states while the elements of even-numbered group show the even oxidation states. It is illustrated below:

Gr. VIIA **(17)** (ns^2np^5)

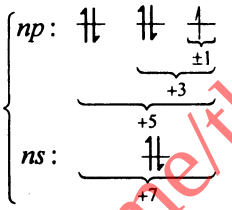

Possible oxidation states :
$\pm 1, +3, +5, +7$
(odd oxidation states)

Gr. VIA **(16)** (ns^2np^4)

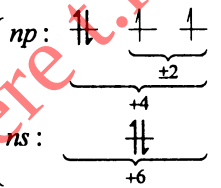

Possible oxidation states :
$\pm 2, +4, +6$
(even oxidation states)

SOLVED NUMERICAL PROBLEMS

Problem 1 : Calculate the electronegativity of *As* in AsF_3 and AsF_5. Given : $E_{As-As} = 146$ kJ mol^{-1}, $E_{F-F} = 155$ kJ mol^{-1}, $E_{As-F(AsF_5)} = 484$ kJ mol^{-1}, $E_{As-F(AsF_3)} = 406$ kJ mol^{-1}, $\chi_P(F) = 4.0$.

Solution : From the Pauling's concept of electronegativity,

$$\chi(A) \sim \chi(B) = 0.102\sqrt{\Delta(A-B)} = 0.102[E_{A-B} - \sqrt{E_{A-A} \times E_{B-B}}]^{1/2}$$

(all the bond energies are taken in SI units)

Therefore, $\chi(F) - \chi(As) = 0.102[484 - \sqrt{146 \times 155}]^{1/2}$, (*in* AsF_5)

$= 0.102 \times 18.26 = 1.86$

Click Here t.me/thealchemylibrary

Hence, $\chi_P(As) = 2.14$ (in AsF_5)

Similarly, $\chi(F) - \chi(As) = 0.102[406 - \sqrt{146 \times 155}]^{1/2}$, (*in* AsF_3)

$= 1.63$

Hence, $\chi_P(As) = 2.37$ (in AsF_3)

Note : One may use : $\chi_A \sim \chi_B = 0.102\,[E_{A-B} - \frac{1}{2}(E_{A-A} + E_{B-B})]$. The results differ slightly.

Problem 2 : Calculate the electronegativity of carbon from the following data :

$$\chi_P(H) = 2.1$$

$$C_{(s)} \rightarrow C_{(g)},\ \Delta H = 713.1 \text{ kJ mol}^{-1};\ H_{2(g)} \rightarrow 2H_{(g)},\ \Delta H = 436 \text{ kJ mol}^{-1}$$

$$C_{(s)} + 4H_{(g)} \rightarrow CH_{4(g)},\ \Delta H = -1659.6 \text{ kJ mol}^{-1}$$

Solution : By combining the following equations, we get the enthalpy of formation of CH_4.

$$C_{(s)} \rightarrow C_{(g)},\ +713.1 \text{ kJ mol}^{-1}$$

$$2H_{2(g)} \rightarrow 4H_{(g)},\ +872 \text{ kJ mol}^{-1}$$

$$\frac{C_{(g)} + 4H_{(g)} \rightarrow CH_{4(g)},\ -1659.6 \text{ kJ mol}^{-1}}{C_{(s)} + 2H_{2(g)} \rightarrow CH_{4(g)},\ -74.5 \text{ kJ mol}^{-1}}$$

From Eqn. 8.14.1.14, we get,

$$\chi(C) - \chi(H) = \sqrt{-\Delta H_f / (96.5 \times 4)} = 0.44,\ \Delta H_f = -74.5 \text{ kJ mol}^{-1})$$

or, $\chi_P(C) = 2.54$

Problem 3 : Calculate the enthalpy of formation of OF_2 and H_2O. Given, $\chi(H) = 2.20$; $\chi(F) = 4.0$, $\chi(O) = 3.45$

Solution : The enthalpy of formation (ΔH_f) of a compound is given by (see Eqn. 8.14.1.15) in SI units as follows:

$$-\Delta H_f = 96.5 \sum [\chi(A) \sim \chi(B)]^2 - 226 n_N - 110 n_O$$

where n_N and n_O give the number of single bonded nitrogen and oxygen atoms in the molecule respectively.

Therefore, for H_2O :

$$-\Delta H_f(H_2O) = 96.5 \times 2 \times (3.45 - 2.20)^2 - 226 \times 0 - 110 \times 1 = 191.6 \text{ kJ mol}^{-1}$$

i.e $\Delta H_f(H_2O) = -191.6 \text{ kJ mol}^{-1}$

For OF_2: $-\Delta H_f(OF_2) = 96.5 \times 2 \times (4.0 - 3.45)^2 - 226 \times 0 - 110 \times 1 = -51.6 \text{ kJ mol}^{-1}$

i.e. $\Delta H_f(OF_2) = 51.6 \text{ kJ mol}^{-1}$

Thus, formation of OF_2 is thermodynamically unfavourable.

Click Here to me/thearchemylibrary

Problem 4 : Calculate the electronegativity of chlorine in both Pauling's and Mulliken's scale. Given, $EA(Cl) = 4.0$ eV/atom and $IE(Cl) = 13.0$ eV/atom.

Solution : In Mulliken's scale, the electronegativity is given by :

$$\chi_M = \frac{1}{2}(IE + EA),\ IE \text{ and } EA \text{ given in eV/atom.}$$

Therefore, $$\chi_M(Cl) = \frac{1}{2}(4.0 + 13.0) = 8.5$$

Pauling's electronegativity (χ_P) and Mulliken's electronegativity are related as follows (cf. Eqn. 8.14.2.2) :

$$\chi_P = 0.336\chi_M - 0.2 = 0.336 \times 8.5 - 0.2 = 2.65$$

By using the following relationship, χ_P value may be also obtained.

$$\chi_P = 1.35\sqrt{\chi_M} - 1.37 = 1.35 \times \sqrt{8.5} - 1.37 = 2.56$$

Thus these two values of χ_P slightly differ.

Problem 5 : Calculate the electronegativity (χ_M and χ_P) of bromine from the following data :

$$IE = 272.3 \text{ kcal mol}^{-1},\ EA = 77.7 \text{ kcal mol}^{-1}$$

Solution : $\chi_M = \frac{1}{2}(IE + EA)$, IE and EA expressed in eV per atom.

Thus,

$$\chi_M = \frac{1}{2 \times 23.06}(IE + EA),\ IE \text{ and } EA \text{ expressed in kcal mol}^{-1};\ 1 \text{ eV per atom} = 23.06 \text{ kcal mol}^{-1}$$

$$= \frac{1}{2 \times 23.06}(272.3 + 77.7)$$

$$= 7.58$$

By using the following relationship, we get :

$$\chi_P = 0.336\ \chi_M - 0.2 = 2.34$$

By using the following relationship, we get :

$$\chi_P = 1.35\sqrt{\chi_M} - 1.37 = 2.34$$

Both the values are the same.

Problem 6 : Calculate the electronegativity of ^{33}As(III). Given, $r_{cov(As)} = 120$ pm.

Solution : We have the Allred-Rochow relation (cf. Eqn. 8.14.4.3).

$$\chi_{AR} = 0.36\ (Z^* - 0.35)/r_{cov}^2 + 0.744\ ,\ \chi_{cov} \text{ in Å unit and } Z^* \text{ for neutral } As \text{ atom}$$

where r_{cov} gives the magnitude of the covalent radius in angstrom unit. By using Slater's rule, we can calculate the screening constant for As, from the electronic configuration, $(1s)^2\ (2s,\ 2p)^8$, $(3s,\ 3p)^8$, $(3d)^{10}$, $(4s,\ 4p)^5$.

Click Here t.me/tlealchemylibrary

$$\sigma = 10 \times 1.00 + 18 \times 0.85 + 4 \times 0.35 = 26.70$$

Hence, $$Z^* = Z - \sigma = 33.0 - 26.70 = 6.30 \text{ and } (Z^* - 0.35) = 5.95$$

Therefore, $$\chi_{AR} = \frac{0.36 \times 5.95}{(1.20)^2} + 0.744 = 2.23, (120 \text{ pm} = 1.20 \text{ Å})$$

Note : For the correction factor 0.35, please see the reasoning behind the equation 8.14.4.3.

Problem 7 : Calculate the % of ionic character, charge separation and covalent-ionic resonance energy in *HI*. Given $a(H) = 7.17$, $b(H) = 12.85$, $a(I) = 8.10$, $b(I) = 9.17$ (where a and b are given in electron volt scale of Mulliken).

Solution : From the Jaffe-Hinze concept, we get, $\chi = a + b\delta$.

From the principle of electronegativity neutralisation (Sec. 8.14.6) in $H^{\delta+} - I^{\delta-}$, the charge separation will go to such an extent that,

$$\chi(H^{\delta+}) = \chi(I^{\delta-}); \text{ i.e. } a(H) + b(H)\delta = a(I) - b(I)\delta$$

or, $$\delta = \frac{a(I) - a(H)}{b(H) + b(I)} = \frac{8.10 - 7.17}{12.85 + 9.17} = 0.04$$

Hence the ionic character is 4%.

The magnitude of a actually gives the electronegativity in a particular (neutral) valence state as estimated by Mulliken, i.e.

$$\chi_M(H) = 7.17 \text{ and } \chi_M(I) = 8.10$$

Therefore, $$\chi_P(H) = 0.336\, \chi_M(H) - 0.2 = 2.21$$

and, $$\chi_P(I) = 0.336\, \chi_M(I) - 0.2 = 2.52$$

From the Pauling's concept of electronegativity, the covalent-ionic resonance energy (Δ) and electronegativity difference are related as follows,

$$\chi(A) \sim \chi(B) = 0.102\, \sqrt{\Delta}, \text{ (in SI unit)}$$

or, $$\Delta = 96.5[\chi(A) \sim \chi(B)]^2$$

Thus for *HI*, $$\Delta(HI) = 96.5(2.52 - 2.21)^2 = 9.3 \text{ kJ mol}^{-1}$$

Click Here t.me/thealchemylibrary

EXERCISE-VIII

A. General Questions

1. Give a brief account of the characteristic features of Mendeleev's short periodic table.
2. Discuss the merits and demerits of Mendeleev's periodic table.
3. Discuss the advantages of the long form of the periodic table with respect to Mendeleev's short form of the periodic table.

4. Give a brief account of the extended periodic table as proposed by Seaborg.
5. Classify the elements in terms of their electronic configuration.
6. Discuss the causes and effects of lanthanide contraction.
7. Discuss the periodic trends of size and atomic volume of the elements.
8. Discuss the different factors which control the ionisation energies. Discuss the nature of periodic trend of ionisation energy.
9. Define electron affinity. How does it vary in the periodic table?
10. Discuss the basis of determination of electronegativity in (i) Pauling's method, (ii) Mulliken's method, and (iii) Allred-Rochow's method. How are they get related ?
11. Discuss the applications of the concept of electronegativity in different fields of chemistry.
12. Discuss the chemistry of the diagonal relationship.
13. Discuss the similarities between the members in each of the pairs, *Li* and *Mg*, *Be* and *Al*, *B* and *Si*.
14. What do you mean by secondary periodicity? How do you explain the fact?
15. Write notes on : (i) Lother Meyer's atomic volume curve, (ii) Superactinides, (iii) Stability islands, (iv) Orbital electronegativity, (v) Secondary periodicity, (vi) Jaffe-Hinze electronegativity, (vii) Sanderson's stability ratio, (viii) Sanderson's electronegativity neutralisation principle, (ix) Diagonal relationship, (x) Relativistic contraction and expansion of orbitals, (xi) Aurophilicity and aurophilic cations, (xii) Subhalogen, (xiii) Superhalogen, (xiv) Group electronegativity, (xv) Inductive effect and charge coefficient parameter, (xvi) Electronegativity and hardness, (xvii) Scandide contraction, (xviii) Mischmetals, (xix) NMR shift reagents, (xx) Goldschmidt's geochemical classification of elements, (xxi) Separation of lanthanides, (xxii) Alternation effect, (xxiii) Seaborg's actinide hypothesis, (xxiv) Bonding properties of 3*d* vs. 5*d* orbitals, 3*d* vs. 4*f* orbitals, 4*f* vs. 5*f* orbitals.

B. Justify the Following Statements

1. Pattenkofer's Rule of integral multiple, Chancourtois law of telluric screw and Newlands' law of octaves are closely related in assigning the periodic trends.
2. In Mendeleev's periodic table, an attempt to find the similarities between the *A* and *B* subgroup elements in a particular group is an elusive task.
3. In Mendeleev's periodic table, all the elements always could not be placed in order of their increasing atomic weights.
4. Mendeleev's periodic law in terms of atomic weight was violated in some cases because of the differences in the pattern of the isotopic abundances of the concerned elements.
5. Without doing any experiment, Mendeleev was able to rectify the atomic weights in some doubtful cases.
6. The fates of the isobars and isotopes in the light of Mendeleev's periodic law are not acceptable.
7. Mendeleev's periodic law could not predict the exact number of lanthanides.
8. In the modern periodic table, the elements are placed in terms of their electronic configuration, but in the *d*-block elements, some elements having different types of electronic configuration are placed in the same group.

Click Here t.me/bhealchemylibrary

9. The positions of the isotopes, at least for the lighter elements are not yet satisfactorily solved.
10. The positions of *H* and *He* in the periodic table are the matters of discussion.
11. The first and second inner-transition series contain 14 elements each but the third inner- transition series in the extended periodic table consists of 32 elements.
12. The inclusion of the *Zn*-family in the transition metals; and *Lu*, *Th* and *Lr* in the inner-transition series raise some questions.
13. The lighter actinides were previously mistakenly considered as transition elements.
14. The 4*f* and 5*f* series (at least for the lighter members) elements differ significantly.
15. The metallic radii of ^{63}Eu and ^{70}Yb are much higher compared to the general trend of variation of metallic radii along the series.
16. The curve indicating the variation trend of metallic radii of the lanthanides can be divided into two segments, and one is nothing but the duplication of the other.
17. The members in each of the pairs, *Zr* and *Hf*, *Nb* and *Ta*, *Mo* and *W*,... are very much chemically similar.
18. *Zr* and *Hf* very often coexist in nature and their separation is a difficult task.
19. The separation of the lanthanides is a very difficult task.
20. Iridium shows the highest density. It is not at all surprising from its position in the periodic table.
21. Yttrium very often coexists with the lanthanides in nature.
22. The postlanthanides are not very much chemically active.
23. The electron affinity of *Au* is abnormally high and it may exist as aurides in some compounds.
24. Orbital radii and covalent radii are always different.
25. In Gr IA (1), the orbital radius remarkably increases in moving down among the lighter congeners but it becomes almost the same for the heavier congeners (e.g. *Cs* and *Fr*).
26. The trends of variation of size in a group are different for the transition and representative elements.
27. The atomic volume is not a good parameter for comparison among the different elements.
28. In the atomic volume curve, the alkali metals occupy the peaks, the electropositive metals occupy the descending limbs and the electronegative elements occupy the ascending limbs.
29. In the atomic volume curve, both the transition and inner-transition series occupy the bottom positions.
30. Generally, the atoms having high ionisation energies possess high electron affinities but it is violated in the elements of Gr IIA (2), Gr VA (15) and inert gases.
31. Higher ionisation energies are always higher than the lower ionisation energies.
32. The ionisation energies follow the sequence in the following cases as shown.
    (i) $IE_1(N) > IE_1(O)$, $IE_2(N) < IE_2(O)$;
    (ii) $IE_1(P) > IE_1(S)$, $IE_2(P) < IE_2(S)$;
    (iii) $IE_1(Be) > IE_1(B)$, $IE_2(Be) < IE_2(B)$;
    (iv) $IE_1(Mg) > IE_1(Al)$, $IE_2(Mg) < IE_2(Al)$;
    (v) $IE_1\ (_{29}Cu) < IE_1\ (_{30}Zn) > IE_1\ (_{31}Ga)$;
    (vi) $IE_1\ (_{79}Au) < IE_1\ (_{80}Hg) > IE_1\ (_{81}Tl)$;

Click Here t.me/thearchemylibrary

(vii) $IE_1\ (_{70}Yb) > IE_1\ (_{71}Lu)$;

(viii) $IE_1\ (_{63}Eu) < IE_1\ (_{64}Gd) > IE_1\ (_{65}Tb)$

33. The second electron affinity even for the nonmetals is always negative.
34. Both the ionisation and electron affinity processes for the Gr IIA (2), Gr VA (15) and Gr VIIIA (18) (i.e. zero group) elements are unfavourable.
35. The electron affinity and electronegativity sequences in a group for the 2nd and 3rd period elements are opposite in direction while both the trends run in the same direction for the heavier congeners in a group.
36. Fluorine is more electronegative than chlorine but the electron affinity of chlorine is more than that of fluorine.
37. In a group of the representative elements, electron affinity decreases with the increase of atomic number but it increases for the *d*-block elements in a group with the increase of atomic number.
38. Though the electron affinity of an element is its inherent property, the electronegativity is not an inherent property of an element.
39. Pauling's electronegativity can be determined from the enthalpy of formation of a compound.
40. Pauling's electronegativity can be determined from the bond energies.
41. To stabilise the compounds having single bonded nitrogen or oxygen, the elctronegativity difference between the combining atoms in the compounds should be high.
42. The concept of Mulliken's orbital electronegativity is more fundamental than the Pauling's electronegativity.
43. The electronegativity of an atom depends on its orbital involved and for the hybrid orbitals it follows the sequence : $sp > sp^2 > sp^3$.
44. The electronegativity of an species not only depends on the nature of the orbital but also on the charge of the species.
45. The concept of electronegativity equalisation can compute the extent of charge separation in a covalent bond.
46. The magnitude of charge separation calculated by the Sanderson's method is always different from the actual one and it only gives the approximate result.
47. The acidity sequence runs as : $C_2H_2 > C_2H_4 > C_2H_6$; $RN^+H_3 < C_5H_5N^+H < RCN^+H$
48. The nucleophillic substitution occurs as :

$CH_3I + {}^-OH \rightarrow CH_3 - OH + I^-$; but $CF_3 - I + {}^-OH \rightarrow CF_3H + OI^-$;

$CH_3I + Mn(CO)_5^- \rightarrow I^- + CH_3Mn(CO)_5$, but $2CF_3I + Mn(CO)_5^- \rightarrow I^- + C_2F_6 + Mn(CO)_5I$

49. *NaOH* is a base while *ClOH* is an acid.
50. *AgCl* is white while *AgI* is yellow.
51. OF_2 is a fluoride while Cl_2O is an oxide.
52. NH_3 should be regarded as a nitride of hydrogen.
53. The melting points of the Gr IVA (14), Gr VB (5) and Gr VIB (6) elements are very high.
54. The diagonal relationship is only applicable for the two short periods only.

Click Here t.me/thealchemylibrary

55. The second period elements are typical elements compared to their heavier congeners.
56. The trends of different properties along the periods vary in the same way for both the representative and transition elements but the group trends are remarkably opposite in many cases for the representative and transition elements.
57. The posttransition *p*-block elements in the 4-th and 6-th periods show much higher ionisation energies and electron affinities compared to the smooth trend of variation of these properties in the respective groups.
58. *Ge* is more similar to *C* than to its nearest neighbours *Sn* and *Pb*.
59. The electron affinity of *Pb* is much higher than the expectation from the group trend.
60. The secondary periodicities can be explained by considering the *d*- and *f*-contractions i.e. scandide and lanthanide contractions respectively.
61. Among the Gr VA (15) elements, *As* is much more reluctant than *Sb* and *P* to show the +5 oxidation state. Similarly, in Gr VIA (16), *Se* shows its more reluctance in attaining the +6 oxidation state compared to *S* and *Te*.
62. $HBrO_4$ is less stable than $HClO_4$ and HIO_4; and $HBrO_4$ is a better oxidising agent than $HClO_4$ and HIO_4.
63. Fluorine is referred to as a *superhalogen*. Similarly *Li* is also a *superalkali metal*.
64. Fluorides form stabler compounds (both ionic and covalent) compared to the other halides.
65. The reduction potential of $\frac{1}{2} F_2/F^-$ is remarkably high.
66. Inert pair effect for the heavier congeners in the posttransition *p*-block elements can be explained by relativistic effects.
67. *Hg*(*I*) exists as Hg_2^{2+}, but the analogous species of the lighter congeners, i.e., Cd_2^{2+}, Zn_2^{2+} are not known.
68. The first ionisation energy of *Au* is larger than that of *Ag*, but the reverse is true for the second ionisation energy.
69. In the presence of acid (i.e. H^+), hydrocarbons are stable but the silanes are decomposed to release molecular hydrogens.

    Hints : Electronegativity difference indicates the polarity as : $\overset{\delta+}{Si}—\overset{\delta-}{H}$ and $\overset{\delta-}{C}—\overset{\delta+}{H}$
70. The charge coefficient parameter (*b*) is quite important to explain different chemical phenomena.
71. Methyl group ($\chi_P = 2.3$) is more electronegative than hydrogen ($\chi_P = 2.1$) but methyl group is a better electron pushing group.
72. The electronegativity of CH_3 and C_2H_5 groups are more or less the same, but their inductive effects are different.
73. The charge coefficient parameter (*b*) of a group is much less than those of the constituent atoms.
74. In terms of charge capacity, the groups are *superatoms*.
75. Relativistic effect can cause the expansion of *d*- and *f*-orbitals.
76. Aurophilicity can be rationalised by considering relativistic effect.
77. Relativistic effect can explain the inertness of *Hg* and high electron affinity of gold.

Click Here t.me/trealchemylibrary

78. Relativistic effect is responsible for the observation : $4f$ orbitals are more deeply seated than the $5f$ orbitals.
79. In calculating χ_{AR}, Z^* of an atom should be replaced by $(Z^* - 0.35)$.
80. In Jaffe-Hinze electronegativity, $\chi = a + bq$, a can be expressed in terms of χ_M and b can be expressed in terms of absolute hardness (η).
81. Fluorine can be considered as a subhalogen as well as a superhalogen.
82. Ionisation energy of the binary hydrides follows the sequence :
    $CH_4 > NH_3 < H_2O < HF$; $SiH_4 > H_2S < HCl$, $HF > HCl > HBr > HI$
83. Ionisation energy of NF_3 is higher than that of NH_3 by 268 kJ mol^{-1} while ionisation energy of PF_3 is higher than that of PH_3 by only 121 kJ mol^{-1}.
84. Inherent group electronegativity (a_G) cannot alone determine the inductive effect of the group.
85. It is difficult to have anhydrous salts of lithium.
86. Many salts of lithium and magnesium are soluble in organic solvents.
87. Mercury can be described as a *noble liquid* (cf. *noble gas*).
88. In *hedgehog cation*, carbon shows hypecoordination number 6.
89. *Ag(I)*, *Tl(I)*, *Pb(II)*, etc. are considered as aurophilic cations.
90. Lanthanides are characterised by +3 oxidation state while transition metals and lighter actinides can show variable oxidation states.
91. For the superheavy elements (in the *p*-block), all the three *p*-orbitals are not equally available for bonding.
    (*Hints* : Spin-orbit coupling and relativistic effect).
92. For the *d*-block elements, heavier congeners stabilise the higher oxidation states better.
93. The nature of electronic spectra of lanthanide complexes differs from those of transition metal complexes.
94. Very often, the lanthanide complexes lack in LFSE.
95. Lanthanides, in general, are more reactive than transition metals.

C. Numerical Problems

1. From the following bond energies, calculate the covalent-ionic resonance energies for *F–O*, *F–Si*, and *Si–O* bonds. Show that, $\Delta(F\text{–}O) + \Delta(O\text{–}Si) \neq \Delta(F\text{–}Si)$ but, $\sqrt{\Delta(F-O)} + \sqrt{\Delta(O-Si)} \approx \sqrt{\Delta(F-Si)}$. Calculate the electronegativities of *O* and *Si* if $\chi_P(F) = 4.0$.
   Given, $E_{F\text{–}O} = 184.14$ kJ mol^{-1}, $E_{F\text{–}F} = 155$ kJ mol^{-1}, $E_{O\text{–}Si} = 372.46$ kJ mol^{-1},
   $E_{O\text{–}O} = 138.10$ kJ mol^{-1}, $E_{F\text{–}Si} = 535.60$ kJ mol^{-1}, $E_{Si\text{–}Si} = 179.95$ kJ mol^{-1}
   Ans. $\chi_P(O) = 3.53$; $\chi_P(Si) = 2.04$.
2. Calculate the electronegativity of hydrogen from the following data:
   $E_{H\text{–}H} = 458$ kJ mol^{-1}, $E_{F\text{–}F} = 155$ kJ mol^{-1}, $E_{H\text{–}F} = 565$ kJ mol^{-1}, $\chi_P(F) = 4.0$
   Ans. $\chi_P(H) = 2.24$

Click Here t.me/theachemylibrary

3. Calculate the heat of formation of NH_3, if the electronegativities of nitrogen and hydrogen are 3.0 and 2.0 in Pauling's scale.

   Ans. $\Delta H_f = -63.5$ kJ mol^{-1}.

4. Calculate the electronegativity of B if the enthalpy of formation of BCl_3 is -403 kJ mol^{-1} and $\chi_P(Cl) = 3.0$

   Ans. $\chi_P(B) = 1.82$.

5. Calculate the $\chi_P(Cl)$ and $\chi_M(Cl)$ from the following data :
   $EA(F) = 3.62$ eV/atom, $IP(F) = 17.4$ eV/atom.

   Ans. $\chi_P(F) = 3.32$, $\chi_M(F) = 10.51$.

6. Find out the electronegativity of ^{82}Pb having its covalent radius 158 pm.

   Ans. $\chi(Pb) = 1.55$.

7. Find out the magnitudes of charge accumulated on C, F and I in CF_3I. Given : $a(C) = 7.98$, $b(C) = 13.27$, $a(F) = 12.18$, $b(F) = 17.36$, $a(I) = 8.10$, $b(I) = 9.15$.
   (Values of a and b are given on electron volt scale of Mulliken).

   Ans. $\delta(I) = +0.21$, $\delta(C) = +0.15$ and $\delta(F) = -0.12$.

8. Find out the percentage of ionic character and covalent-ionic resonance energy in HF. Given: $a(H) = 7.17$, $b(H) = 12.85$, $a(F) = 12.18$, $b(F) = 17.36$ (the values of a and b are given in electron volt scale of Mulliken)

   Ans. $\delta(F) = -0.16$, $\delta(H) = +0.16$; % of ionic character = 16%, $\Delta(HF) = 276.4$ kJ mol^{-1}.

Click Here ← me/tlealchemylibrary

This Page is Intentionally Left Blank

Click Here t.me/thealchemylibrary

APPENDICES

APPENDIX-I

Units and Conversion Factors

Table 1. Basic physical quantities in SI units

Physical quantity	*Symbol for quantity*	*Name of unit*	*Symbol for unit*
Length	l	metre	m
Mass	m	kilogram	kg
Time	t	second	s
Electric current	I	ampere	A
Temperature	T	kelvin	K
Amount of substance	n	mole	mol
Luminous intensity	I_v	candela	cd

Click Here t.me/thealchemylibrary

Table 2. Derived physical quantities in SI units

Physical quantity	*Name of SI unit*	*Symbol and definition of SI unit*	*Named after*
Force, weight	newton (N)	$N = kg\ m\ s^{-2} = J\ m^{-1}$	Isaac Newton (1642–1727)
Work, energy, quantity of heat	joule (J)	$J = N\ m$	James Prescott Joule (1818–1889)
Power	watt (W)	$W = J\ s^{-1}$	James Watt (1737–1819)
Pressure	pascal (Pa)	$Pa = N\ m^{-2}$	B. Pascal (1623–1662)
Electrical charge	coulomb (C)	$C = A\ s$	Charles Auguste de Coulomb (1736–1806)
Electrical potential	volt (V)	$V = kg\ m^2\ s^{-3}\ A^{-1} = J\ A^{-1}\ s^{-1} = J\ C^{-1} = W\ A^{-1}$	Allesandro Volta (1745–1827)
Electric capacitance	farad (F)	$F = C\ V^{-1}$	Michael Faraday (1791–1867)
Electric resistance	ohm (Ω)	$\Omega = V\ A^{-1}$	Georg Simon Ohm (1787–1854)
Electric conductance	siemens (S)	$S = \Omega^{-1}$	W. von Siemens (1816–1892)
Magnetic flux	weber (Wb)	$Wb = V\ s$	W. Weber (1804–1891)
Magnetic flux density	tesla (T)	$T = Wb\ m^{-2}$	Nikola Tesla (1856–1943)
Inductance	henry (H)	$H = V\ s\ A^{-1}$	Joseph Henry (1799–1878)
Frequency	hertz (Hz)	$Hz = s^{-1}$	Heinrich Hertz (1857–1894)
Radioactivity	becquerel (Bq)	$Bq = s^{-1}$	A. Henri Becquerel (1852–1908)
Absorbed dose of radiation	gray (Gy)	$Gy = m^2\ s^{-2} = J\ kg^{-1}$	Louis H. Gray (1905–1965)
Area (A)	square metre	m^2	
Volume (V)	cubic metre	m^3	
Density (ρ)	kilogram per cubic metre	$kg\ m^{-3}$	
Velocity (u, v, w, c)	metre per second	$m\ s^{-1}$	
Acceleration	metre per square second	$m\ s^{-2}$	
*Concentration (c)	mole per cubic metre	$mol\ m^{-3}$	

*for concentration (c) in mol per litre, it is given by $mol\ dm^{-3}$

Table 3. SI prefixes

Fraction	*Prefix*	*Symbol*	*Multiple*	*Prefix*	*Symbol*
10^{-1}	deci	d	10	deka	da
10^{-2}	centi	c	10^2	hecto	h
10^{-3}	milli	m	10^3	kilo	k
10^{-6}	micro	μ	10^6	mega	M
10^{-9}	nano	n	10^9	giga	G
10^{-12}	pico	p	10^{12}	tera	T
10^{-15}	femto	f	10^{15}	peta	P

Click Here t.me/healchemylibrary

Table 4. CGS and SI units for some common physical quantities

Physical quantity	*CGS units*		*SI Units*	
	Name	*Symbol*	*Name*	*Symbol*
Length	centimetre	cm	metre	m
	Angstrom (10^{-8} cm)	Å		
Mass	gram	g	kilogram	kg
Time	second	sec	second	s
Temperature	celsius	°C	kelvin	K
	kelvin	°K		
Energy	calorie	cal	joule	J
	kilocalorie	kcal	kilojoule	kJ
	litre-atmosphere	lit-atm		
	ergs	erg		

* tonne (t) = 10^3 kg, lb = 453.59 g, Btu = 1.055×10^{10} erg = 252 cal

Table 5. Conversion of CGS units to SI units

Physical quantity	*Relation between the units*
Length	Angstrom (Å) = 10^{-10} m = 10^{-1} nm = 10^2 pm
	micron (μ) = 10^{-6} m
Volume	llitre (L) = dm^3
Force	dyne = 10^{-5} N
Energy*	erg = 10^{-7} J
	cal = 4.185 J
	eV = 1.602×10^{-19} J; eV/molecule = 96.484 kJ mol^{-1}
Pressure	atm = 1.013×10^6 dyne cm^{-2} = 101.33 kN m^{-2}
	atm = 760 torr
	mm Hg or torr = 133.32 N m^{-2}
	bar (10^6 dynes/cm^2) = 10^5 N m^{-2}
Viscosity	poise = 10^{-1} kg m^{-1} s^{-1}
Magnetic flux density	gauses = 10^{-4} T

* 1 cm^{-1} (wave number) = 2.86 cal mol^{-1}, reciprocal centimetre is known as **Kayser (K)** 1 kK (kilo Kayser) = 1000 cm^{-1}, 1 eV per molecule = 23.06 kcal mol^{-1}, 1 erg = 2.39×10^{-11} kcal. 1 eV = (charge of an electron) × 1 V = 1.6×10^{-19} C × V = 1.6×10^{-19} J,

$$1 \text{ eV/molecule} = \frac{1.6 \times 10^{-19} \times 6.02 \times 10^{23}}{1000} \text{ kJ/mole} = 96.488 \text{ kJ mol}^{-1}.$$

$$1 \text{ kK molecule}^{-1} = 10^3 \text{ cm}^{-1} \text{ molecule}^{-1}$$

$$= hc \times 10^3 \text{ cm}^{-1} \text{ molecule}^{-1} \left(cf.\ E = h\nu = \frac{hc}{\lambda} \right)$$

$$= 6.62 \times 10^{-34} \text{ J s} \times 2.99 \times 10^8 \text{ m s}^{-1} \times 10^5 \text{ m}^{-1} \text{ molecule}^{-1}$$

$$= 1.985 \times 10^{-20} \text{ J molecule} = 11.96 \text{ kJ mol}^{-1}$$

Table 6. Atomic Units (see text, Chapter 1, Sec. 1.8.2)

Click Here : me/theadchemylibrary

APPENDIX-II

Some Physical and Chemical Constants

Table 1. Values of some physical and chemical constants

Constant	*CGS and other units*	*SI-units*
Acceleration due to gravity (g)	980.665 cm sec^{-2}	9.80665 m s^{-2}
Avogadro's number (N_A)	6.02217×10^{23} molecules $mole^{-1}$	6.02217×10^{23} mol^{-1}
Bohr magneton (μ_B)	9.274×10^{-21} erg $gauss^{-1}$	9.274×10^{-24} J T^{-1}
Nuclear Magneton (μ_N)	5.04×10^{-24} erg G^{-1}	5.04×10^{-27} J T^{-1}
Bohr radius (a_o)	0.52918 Å	5.2918×10^{-11} m
Boltzmann constant (k_B or k)	1.3806×10^{-16} erg (degree K)$^{-1}$	1.3806×10^{-23} J K^{-1}
Debye	10^{-18} esu cm	3.3356×10^{-30} C m
Electronic charge (e)	4.80298×10^{-10} esu	1.60216×10^{-19} C
Electronic rest mass (m_e)	9.10953×10^{-28} g	9.10953×10^{-31} kg
Faraday (F)	96487 coulomb $equiv^{-1}$	9.6487×10^4 C mol^{-1}
Gas constant (R)	8.3144×10^7 erg (degree K)$^{-1}$ $mole^{-1}$ 8.31441 Joules (degree K)$^{-1}$ $mole^{-1}$ 82.053×10^{-3} litre-atm (degree K)$^{-1}$ $mole^{-1}$ 1.987 cal (degree K)$^{-1}$ $mole^{-1}$	8.3144 J K^{-1} mol^{-1} 8.3144 N m K^{-1} mol^{-1} 8.3144 Pa m^3 K^{-1} mol^{-1}
Permitivity of vacuum (ε_o)		8.854188×10^{-12} C V^{-1} m^{-1} ($C\ V^{-1}\ m^{-1} = C^2\ N^{-1}\ m^{-2}$)
Permeability of vacuum (μ_o)		$4\pi \times 10^{-7}$ H m^{-1}
Planck's constant (h)	6.62618×10^{-27} erg sec	6.62618×10^{-34} J s
Rest mass of proton (m_p)	1.672648×10^{-24} g	1.672648×10^{-27} kg
Rest mass of neutron (m_n)	1.674954×10^{-24} g	1.674954×10^{-27} kg
Atomic mass unit (u) (1 u = 10^{-3} kg mol^{-1}/N_A)	1.660565×10^{-24} g	1.660565×10^{-27} kg (≡ 931.48 MeV)
Vacuum speed of light (c)	2.99793×10^{10} cm sec^{-1}	2.99793×10^8 m s^{-1}
Standard atmospheric pressure	76 cm Hg 760 mm Hg (or torr) 1.1032×10^6 dyne cm^{-2}	101.325 kPa 1.01325 bar
Hartree energy (E_h)		4.3597×10^{-18} J
Zero of the Celsius scale	0°C	273.15 K

Click Here t.me/thealchemylibrary

APPENDIX - III
Wavelength and Colours

Table 1. Spectral Wavelength and Colours

Range of the wavelength absorbed (nm)	*Colour of the radiation absorbed*	*Complementary colour observed*
400–450	Violet	Green-yellow
450–470	Indigo	Yellow
470–490	Blue	Orange
490–500	Blue-green	Red
500–560	Green	Purple
560–575	Green-yellow	Violet
575–590	Yellow	Indigo
590–640	Orange	Blue
640–730	Red	Blue-green

Click Here t.me/thealchemylibrary

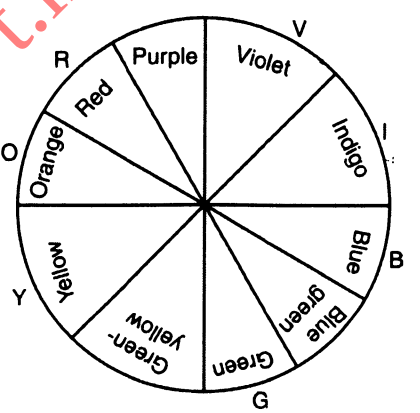

Artist's Wheel

APPENDIX-IV

Names, symbols, atomic numbers and atomic weights* of the elements

Element	*Symbol*	*Atomic number*	*Atomic weight*	*Element*	*Symbol*	*Atomic number*	*Atomic weight*
Actinium	*Ac*	89	227.03	Hafnium	*Hf*	72	178.49
Aluminium	*Al*	13	26.98	Helium	*He*	2	4.00
Americium	*Am*	95	(243)	Holmium	*Ho*	67	164.93
Antimony	*Sb*	51	121.75	Hydrogen	*H*	1	1.008
Argon	*Ar*	18	39.95	Indium	*In*	49	114.82
Arsenic	*As*	33	74.92	Iodine	*I*	53	126.90
Astatine	*At*	85	(210)	Iridium	*Ir*	77	192.2
Barium	*Ba*	56	137.34	Iron	*Fe*	26	55.85
Barkelium	*Bk*	97	(247)	Krypton	*Kr*	36	83.80
Beryllium	*Be*	4	9.01	Lanthanum	*La*	57	138.91
Bismuth	*Bi*	83	208.98	Lawrencium*	*Lr*	103	(260)
Boron	*B*	5	10.81	Lead	*Pb*	82	207.19
Bromine	*Br*	35	79.91	Lithium	*Li*	3	6.94
Cadmium	*Cd*	48	112.40	Lutetium	*Lu*	71	174.97
Calcium	*Ca*	20	40.08	Magnesium	*Mg*	12	24.31
Californium	*Cf*	98	(251)	Manganese	*Mn*	25	54.94
Carbon	*C*	6	12.01	Mendelevium	*Md*	101	(258)
Cerium	*Ce*	58	140.12	Mercury	*Hg*	80	200.59
Cesium	*Cs*	55	132.91	Molybdenum	*Mo*	42	95.94
Chlorine	*Cl*	17	35.45	Neodymium	*Nd*	60	144.24
Chromium	*Cr*	24	52.01	Neon	*Ne*	10	20.18
Cobalt	*Co*	27	58.93	Neptunium	*Np*	93	237.05
Copper	*Cu*	29	63.54	Nickel	*Ni*	28	58.71
Curium	*Cm*	96	(247)	Niobium	*Nb*	41	92.91
Dysprosium	*Dy*	66	162.50	Nitrogen	*N*	7	14.01
Einsteinium	*Es*	99	(252)	Nobelium	*No*	102	(259)
Erbium	*Er*	68	167.26	Osmium	*Os*	76	190.2
Europium	*Eu*	63	151.96	Oxygen	*O*	8	16.00
Fermium	*Fm*	100	(257)	Palladium	*Pd*	46	106.4
Fluorine	*F*	9	19.00	Phosphorus	*P*	15	30.97
Francium	*Fr*	87	(223)	Platinum	*Pt*	78	195.09
Gadolinium	*Gd*	64	157.25	Plutonium	*Pu*	94	(244)
Gallium	*Ga*	31	69.72	Polonium	*Po*	84	(209)
Germanium	*Ge*	32	72.59	Potassium	*K*	19	39.10
Gold	*Au*	79	196.97	Praeseodymium	*Pr*	59	140.91

(Contd.)

* Previously it was represented by *Lw*. Now as per IUPAC recommendation, it is represented by *Lr*.

Click Here t.me/theachemylibrary

Element	*Symbol*	*Atomic number*	*Atomic weight*	*Element*	*Symbol*	*Atomic number*	*Atomic weight*
Promethium	*Pm*	61	(145)	Technetium	*Tc*	43	(99)
Protactinium	*Pa*	91	231.04	Tellurium	*Te*	52	127.60
Radium	*Ra*	88	226.03	Terbium	*Tb*	65	158.92
Radon	*Rn*	86	(222)	Thallium	*Tl*	81	204.37
Rhenium	*Re*	75	186.2	Thorium	*Th*	90	232.04
Rhodium	*Rh*	45	102.91	Thulium	*Tm*	69	168.93
Rubidium	*Rb*	37	85.47	Tin	*Sn*	50	118.69
Ruthenium	*Ru*	44	101.07	Titanium	*Ti*	22	47.90
Samarium	*Sm*	62	150.35	Tungsten	*W*	74	183.85
Scandium	*Sc*	21	44.96	Uranium	*U*	92	238.03
Selenium	*Se*	34	78.96	Vanadium	*V*	23	50.94
Silicon	*Si*	14	28.09	Xenon	*Xe*	54	131.30
Silver	*Ag*	47	107.87	Ytterbium	*Yb*	70	173.04
Sodium	*Na*	11	22.99	Yttrium	*Y*	39	88.91
Strontium	*Sr*	38	87.62	Zinc	*Zn*	30	65.37
Sulfur	*S*	16	32.06	Zirconium	*Zr*	40	91.22
Tantalum	*Ta*	73	180.95				

* Values are based on the presently accepted ***physical scale*** of $^{12}C = 12.00000$ as the standard. The ratio of these atomic weights to those on older ***chemical scale*** assuming the value 16.00000 for the atomic weight of natural oxygen (composition : ^{16}O, 99.757%; ^{17}O, 0.039%; ^{18}O, 0.204%) is 1.000279. The values given within the parentheses are the mass numbers of the most commonly known isotopes.

The true atomic weight of natural oxygen is given by : $16 \times 0.99757 + 17 \times 0.00039 + 18 \times 0.00204 = 16.00447$.

$$\text{It gives : } \frac{\text{Physical atomic weight}}{\text{Chemical atomic weight}} = \frac{16.00447}{16.00000} = 1.000279$$

Presently the term ***atomic weight*** is replaced by ***atomic mass*** or ***relative atomic mass*** (RAM). These are expressed in terms of *amu* or *u* or *Da* (Dalton). These aspects have been discussed in Sec. 5.2.3.

** For the ***translawrencium*** elements with $Z > 103$, the currently used names (cf. Chemistry of the Elements by N.N. Greenwood and A. Earnshaw and IUPAC, 1997) are : $_{104}Rf$ (rutherfordium), $_{105}Db$ (dubnium), $_{106}Sg$ (seaborgium), $_{107}Bh$ (bohrium), $_{108}Hs$ (hassium), $_{109}Mt$ (meitnerium). However, other names to these elements have also been suggested from time to time. These are : $Z = 104$ (kurchatovium, *Ku*; dubnium, *Db*), $Z = 105$ (hahnium, *Ha*, neilsbohrium, *Ns*, joliotium, *Jl*), $Z = 106$ (rutherfordium, *Rf*), $Z = 107$ (neilsbohrium, *Ns*), $Z = 108$ (hahnium, *Hn*). The IUPAC (1977) recommendation, i.e. a ***hybrid Latin-Greek numerical method*** (cf. Sec. 8.6), is free from such confusions. The elements with $Z = 110, 111, 112, 114, 116, 118$ have been characterised.

Click Here 1.tre/thealchemylibrary

APPENDIX-V

Some Useful Mathematical Relationship

(A) Differentials

(u and v are the functions of x; a and m are constants).

(i) $\frac{dx}{dx} = 1$ (ii) $\frac{d}{dx}(au) = a\frac{du}{dx}$ (iii) $\frac{d}{dx}(u+v) = \frac{du}{dx} + \frac{dv}{dx}$

(iv) $\frac{d}{dx}x^m = m\,x^{m-1}$ (v) $\frac{d}{dx}\ln x = \frac{1}{x}$ (vi) $\frac{d\ln u}{dx} = \frac{1}{u}\frac{du}{dx}$

(vii) $\frac{d}{dx}(e^x) = e^x$ (viii) $\frac{d}{dx}(e^u) = e^u\frac{du}{dx}$ (ix) $\frac{d}{dx}(uv) = u\frac{dv}{dx} + v\frac{du}{dx}$

(x) $\frac{d}{dx}\left(\frac{u}{v}\right) = \frac{v\left(\frac{du}{dx}\right) - u\left(\frac{dv}{dx}\right)}{v^2}$ (xi) $\frac{d}{dx}(\sin x) = \cos x$ (xii) $\frac{d}{dx}(\cos x) = -\sin x$

(xiii) $\frac{d}{dx}(\tan x) = \sec^2 x$ (xiv) $\frac{d}{dx}(\sin u) = \cos u\frac{du}{dx}$ (xv) $\frac{d}{dx}(\cos u) = -\sin u\frac{du}{dx}$

(B) Integrals

(u and v are the functions of x; a and m are constants; for the indefinite integrals, there should be an addition of *arbitrary constant of integration*).

(i) $\int dx = x$ (ii) $\int au\,dx = a\int u\,dx$ (iii) $\int(u+v)dx = \int u\,dx + \int v\,dx$

(iv) $\int x^m\,dx = \frac{x^{m+1}}{m+1}, (m \neq -1)$ (v) $\int\frac{dx}{x} = \ln x$ (vi) $\int e^x dx = e^x$

(vii) $\int e^{ax}\,dx = \frac{1}{a}e^{ax}$ (viii) $\int \ln ax\,dx = x\ln ax - x$ (ix) $\int \sin x\,dx = -\cos x$

(x) $\int \cos x\,dx = \sin x$ (xi) $\int uv\,dx = u\int v\,dx - \int\left[\frac{du}{dx}\int v\,dx\right]dx$, (by parts)

(xii) $\int u\,dv = uv - \int v\,du$ (xiii) $\int_0^\infty x^n e^{-ax} = \frac{n!}{a^{n+1}}$, ($n$ positive integer)

(C) Trigonometric relationship

(i) $\sin(90^\circ - \theta) = \cos\theta$

(ii) $\cos(90^\circ - \theta) = \sin\theta$

(iii) $\exp(\pm im\theta) = \cos(m\theta) \pm i\sin(m\theta)$, (***Demovier's theorem***)

$$\cos(m\theta) = \frac{1}{2}[\exp(im\theta) + \exp(-im\theta)]$$

$$\sin(m\theta) = \frac{1}{2i}[\exp(im\theta) - \exp(-im\theta)]$$

Click Here t.me/thealchemylibrary

(iv) $\sin^2\theta + \cos^2\theta = 1$

(v) $\sin 2\theta = 2\sin\theta\cos\theta$

(vi) $\cos 2\theta = \cos^2\theta - \sin^2\theta = 2\cos^2\theta - 1 = 1 - 2\sin^2\theta$

(vii) $\sin(\alpha \pm \beta) = \sin\alpha\cos\beta \pm \cos\alpha\sin\beta$

(viii) $\cos(\alpha \pm \beta) = \cos\alpha\cos\beta \mp \sin\alpha\sin\beta$

(ix) $\sin\alpha \pm \sin\beta = 2\sin\frac{1}{2}(\alpha \pm \beta)\cos\frac{1}{2}(\alpha \mp \beta)$

(x) $\cos\alpha + \cos\beta = 2\cos\frac{1}{2}(\alpha + \beta)\cos\frac{1}{2}(\alpha - \beta)$

(xi) $\cos\alpha - \cos\beta = -2\sin\frac{1}{2}(\alpha + \beta)\sin\frac{1}{2}(\alpha - \beta)$

(xii) $\sin\alpha\sin\beta = \frac{1}{2}\cos(\alpha - \beta) - \frac{1}{2}\cos(\alpha + \beta)$

(xiii) $\cos\alpha\cos\beta = \frac{1}{2}\sin(\alpha - \beta) + \frac{1}{2}\cos(\alpha + \beta)$

(xiv) $\sin\alpha\cos\beta = \frac{1}{2}\sin(\alpha + \beta) + \frac{1}{2}\sin(\alpha - \beta)$

(D) Some Useful Expansions ($x^2 \leq 1$)

$(1 + x)^{-1} = 1 - x + x^2 - x^3 + \ldots\ldots$

$(1 - x)^{-1} = 1 + x + x^2 + x^3 + \ldots\ldots$

$(1 - x)^{-2} = 1 + 2x + 3x^2 + 4x^3 + \ldots\ldots$

$\ln(1 + x) = x - \frac{x^2}{2} + \frac{x^3}{3} - \frac{x^4}{4} + \ldots\ldots$

$\ln(1 - x) = -x - \frac{x^2}{2} - \frac{x^3}{3} - \frac{x^4}{4} \ldots\ldots$

$\exp(x)$ or $e^x = 1 + x + \frac{x^2}{2!} + \frac{x^3}{3!} + \frac{x^4}{4!} + \ldots\ldots$, (for all x)

$\exp(-x)$ or $e^{-x} = 1 - x + \frac{x^2}{2!} - \frac{x^3}{3!} + \ldots\ldots$

$\sin x = x - \frac{x^3}{3!} + \frac{x^5}{5!} - \frac{x^7}{7!} + \ldots\ldots$, (for all x)

$\cos x = 1 - \frac{x^2}{2!} + \frac{x^4}{4!} - \frac{x^6}{6!} + \ldots\ldots$, (for all x)

$\ln x! = x\ln x - x$ or $x! = \frac{x^x}{e^x}$ **(Stirling approximation,** 1730)

(for $x >$ *ca.* 10)

Click Here t.me/thealchemylibrary

(E) Progressions

(i) **Arithmatic progression :** $a, a + d, a + 2d, ...$

n-th term $(T_n) = a + (n - 1)d$;

Sum of first n terms $(S_n) = \frac{n}{2}(T_1 + T_n) = \frac{n}{2}\{2a + (n-1)d\}$

Sum of first n-natural numbers $= 1 + 2 + 3 + ... + n = \frac{n(1+n)}{2}$

(ii) **Geometric progression :** $a, ar, ar^2, ...$

n-th term $(T_n) = ar^{n-1}$; Sum of first n terms $(S_n) = \frac{a(1-r^n)}{(1-r)}$ when $r < 1$

$S_n = \frac{a(r^n - 1)}{(r-1)}$ when $r > 1$; sum to infinity $(S_\infty) = \frac{a}{1-r}$ when $|r| < 1$

(iii) **Useful results :**

$$\left.\begin{aligned} \sum_{x=1}^{n} x^2 &= \frac{n}{6}(n+1)(2n+1) \\ \sum_{x=1}^{n} x^3 &= \left[\frac{n}{2}(n+1)\right]^2 \end{aligned}\right\}$$ For first n natural numbers, 1, 2, 3, ..., n

(F) Permutations and combinations

$${}^nP_r = \frac{n!}{(n-r)!};\ {}^nP_n = \frac{n!}{0!} = \frac{n!}{1} = n!;\ {}^nC_r = \frac{n!}{r!(n-r)!};\ {}^nP_r = r!\,{}^nC_r;\ {}^nC_r = {}^nC_{n-r};\ {}^nC_n = {}^nC_0 = 1$$

$$n! = 1 \times 2 \times 3 \times ..... \times (n-2) \times (n-1) \times n;\ 0! = 1$$

(G) Logarithms

$\log(mn) = \log m + \log n$; $\log\left(\frac{m}{n}\right) = \log m - \log n$,

$\log(m^n) = n \log m$; $\log 1 = 0$; $\log_a a = 1$; $\ln(x) = 2.3 \log x$

Natural logarithm (base e); common logarithm (base 10).

(H) Mathematical Constants

$\pi = 3.14159265.....$, $e = 2.71828....$, $\ln x = 2.30258 \ldots \log_{10} x$

Click Here t.me/thealchemylibrary

APPENDIX-VI
Books Consulted

Akhmetov, N.	General and Inorganic Chemistry
Alexeyev, V.	Quantitative Analysis
Anantharaman, R.	Fundamentals of Quantum Chemistry
Arnikar, H.J. & Rajurkar, N.S.	Nuclear Chemistry through Problems
Arnikar, H.J.	Essentials of Nuclear Chemistry
Banerjea, D.	Inorganic Chemistry – Elements and Compounds
Banerjee, D.	Inorganic Chemistry (Principles)
Banerjea, D.	Fundamental Principles of Inorganic Chemistry
Beiser, A.	Concepts of Modern Physics
Castellan, G.W.	Physical Chemistry
Chanda, M.	Atomic Structure and Chemical Bonding
Chandra, A.K.	Introductory Quantum Chemistry
Charlot, G.	Qualitative Inorganic Analysis
Cotton, F.A. & Wilkinson, G.	Advanced Inorganic Chemistry
Cotton, F.A., Wilkinson, G., Murillo, C.A. and Bochmann, M.	Advanced Inorganic Chemistry
Cotton, F.A. & Wilkinson, G.	Basic Inorganic Chemistry
Das, Asim K.	Bioinorganic Chemistry
Das, Asim K.	Inorganic Chemistry : Biological & Environmental Aspects
Das, Asim K.	Environmental Chemistry with Green Chemistry
Day, M.C. & Selbin, J.	Theoretical Inorganic Chemistry
Day (Jr), R.A. & Underwood, A.L.	Quantitative Analysis
Dorain, P.B.	Symmetry in Inorganic Chemistry
Douglas, B.E. McDaniel, D.H. & Alexander, J.J.	Concepts and Models of Inorganic Chemistry
Dutta, P.K.	General & Inorganic Chemistry
Emeleus, H.J. & Anderson, J.S.	Modern Aspects of Inorganic Chemistry
Evans, R.C.	An Introduction to Crystal Chemistry
Glasstone, S.	Textbook of Physical Chemistry
Glasstone, S.	Sourcebook of Atomic Energy
Greenwood, N.N. & Earnshaw, A.	Chemistry of the Elements
Halliday, D., Resnick, R. & Walker, J.	Fundamentals of Physics
Huheey, J.E.	Inorganic Chemistry – Principles of Structure & Reactivity

Click Here t.me/thealchemylibrary

Huheey, J.E., Keiter, E.A., Keiter, R.L. and O.K. Mehdi	Inorganic Chemistry - Principles of Structure & Reactivity
Jolly, W.L.	Principles of Inorganic Chemistry
Kaplan, I.	Nuclear Physics
Kapoor, K.L.	A Textbook of Physical Chemistry (Vol. 1–4)
Kittel, C.	Introduction to Solid State Physics
Krisnan, K.G.	Atomic & Nuclear Physics
Laidler, K.J. & Meiser, J.H.	Physical Chemistry
Lee, J.D.	Concise Inorganic Chemistry
Mackay, K.M. & Mackay, R.A.	Introduction of Modern Inorganic Chemistry
Mahan, B.H.	University Chemistry
Mingos, D.M.P.	Essentials of Inorganic Chemistry
Moeller, T.	Inorganic Chemistry, A Modern Introduction
Mukherjee, G.N.	Semi-micro Qualitative Inorganic Analysis (University of Calcutta)
Orchin, M. & Jaffe H.H.	The Importance of Antibonding Orbitals
Potterfied, W.W.	Inorganic Chemistry : A Unified Approach
Purcell, K.F. & Kotz, J.C.	Inorganic Chemistry
Rajam, J.B.	Atomic Physics
Raghavan, V.	Materials Science & Engineering
Rakshit, P.C.	Physical Chemistry
Rao, C.N.R. (edited)	University General Chemistry
Shriver, D.F., Atkins, P.W. & Langford, C.H.	Inorganic Chemistry
Sarkar, R.	General & Inorganic Chemistry (Part I & II)
Sharpe, A.G.	Inorganic Chemistry
Smart, L. & Moore, E.	Solid State Chemistry – Introduction
Skoog, D.A., Holler, F.J. & Nieman, T.A.	Principles of Instrumental Analysis
Sodhi, G.S.	Fundamental Concepts of Environmental Chemistry
Vogel, A.I.	Inorganic Analysis - Quantitative and Qualitative
West, A.R.	Solid State Chemistry and its Applications
Wulfsberg, G.	Inorganic Chemistry

Click Here t.me/thealchemylibrary

Acknowledgement

The above listed references and sources have been freely consulted to borrow their views and ideas. The present authors are indebted to all these authors to an endless extent. The present author expresses his heartiest thanks and grateful acknowledgement to all of them.

Index

(T) indicates Table

α & A

α–Emission 273
α-Decay 322, 338*ff*, (Sec. 6.12)
α-Particle nuclides 271
α-Particle scattering 22, 23
Abegg's rule of contravalency 453, 543
Absolute electronegativity 496, 506, 1475, 1476
Absolute hardness 496, 1476
Acceptor number (A.N.) 1413
Acceptor-donor interaction 1392
Acetic Acid (CH_3CO_2H) as a solvent 1566
Acetylacetone 1268
Acid and base catalysis 1437
Acid dissociation constants 1415(T)
Acid storage cell 1688
Acid strength 1270, 1414*ff*
Acid strength of aqua metal ions 1430
Acid-base indicators 1372*ff*
Acid-base strength principle 1482
Acidity parameter 800, 1467
Acids and Bases 1343*ff*, (Ch. 14)
  definitions 1343
Actinides 453, 454, 468
  contraction 469*ff*
  hypothesis 468
  vs. lanthanides 468, (Sec. 8.8.3)
Actinium series 344
Actinoids 453, 454
Activated complex 863
Activation energy 413
Activation of alkane 1278
Activation parameters 864
Active methylene group 1458
Activity product 1496
Aerial oxidation of Fe(II) 1659
Agostic interaction 1253, 1278, (Sec. 13.1.10)
Alkali metals 452, 453, 454
Alkali storage cell 1688
Alkalides 1309, 1560
Alkaline earth dihalides (MX_2) 841
Alkaline earth metals 454
Alkenes 1405
Allotropes of carbon 893
Allotropes of crystalline carbon 887
Alloys 1156
Allred-Rochow's electronegativity 500
Alpha decay 338
Alternation effect 531, 532, 773, 1642
Ambidentate
  ligands 824, 1480, 1487
  solvent 1413
Amidine 1462
Amino acids 1361*ff*
Aminoboranes 812
Ammine complex formation 1507
Ammonia clock 848
Amperometric titration 1749, (Sec. 16.22.3)
Amphiboles 1053
Amphiprotic compounds 1345
Amphoteric behaviour 1561
Amphoteric behaviour of metal ions 1433
Amphoteric oxides 1346
Angular equations 187
Angular molecules 780
Angular orbital overlap 719
Angular probability function 207
Angular strength 679, 680*ff*, (Sec. 9.13.3)
Angular volume 1481
Angular wave functions 200, 203
Anion
  complexation 1447
  polarisation 794
  receptors 1312, 1322
  solvation 1260
  water 1260
Anode rays 8
  canal rays 8
  positive rays 8

Click Here t.me/realchemylibrary

Anodic protection 1693
Anomalous behaviour of ice 1266
Anomalous *pK*-value 1426
Anomalous properties of lithium 528
Anomalous Zeeman effect 84
Anomeric effect 975
Antiaromatic 1460, 1461
Antielectron 296
Antiferromagnetism 1079
Antifluorite structure 1038
Antimatter 297
Antineutrino, *see* antiparticles
Antineutron 297
Antinucleus 297
Antiparticles 296, 299
Antiproton 297
Antirutile structure 1039
Antisubstance 297
Antisymmetric or odd functions 156
Aphelion 48
Applications of radioactive isotopes 347*ff*
Aprotic solvents 1555
Aqua acid strength of metal ions 1429
Aqua acids 1429
Aqua regia 1629, 1638, (Sec. 16.4.5)
Arbusov reaction 808, 884
Arganic structure 687
Aromatic stability 1460
Aromaticity 815, 818
Arrhenius equation 861, 1068
Arrhenius plot 164
Arrhenius theory of acids and bases 1343
neutralisation 1343
Artificial radioactivity 345, 346, (Sec. 6.16)
Artificial transmutation 383*ff*, (Sec. 7.1)
Asbestos minerals 1053
Associated laguerre polynomials 188
Associative process 862
Aston's mass spectrograph 12
Aston's whole number rule 257
Asymmetric fission 411, 412
Ate complexes 1389
Atmophiles 466, 1486
Atom bomb 417
Atomic inversion 848
Atomic mass 258
Atomic mass unit (amu) 258
Atomic models (Ch. 1 and 4)
Atomic pile 418
Atomic states 57
Atomic units (au) 30
Atomic volume 478
Atomic volume curve 450
Atomic weight 258
Aufbau filling of a *d*-band 1147
Aufbau principle 86, 220
Auger effect 268, 273, 323
Auger emission 366
Aurophilic cation 522, 547
Aurophilic interactions 523
Aurophilicity 522
Autoionisation of solvents 1468
Autoprotolysis constant 1349
Autoradiography 358
Avalanche break-down 1201
Average life period 329
Average oxidation state 1581
Azeotropic behaviour 1259
Azeotropic mixtures 1260
Azide 1587
Azimuthal quantum number, *see* quantum number
Azulene 1461

β & B

β^- decay 336, 337, (Sec. 6.13)
β^+ (i.e. positron) decay 322, (Sec. 6.13)
β-alumina 1232
β-hydrogen elimination 1278
Back bonding 612
Back emf 1694, 1701
Back strain (*B*-strain) 1444, 1448, 1456
Bailer twist 851, 852
Bainbridge mass spectrometer 15
Balancing redox reactions 1577*ff*
Balmer formula 18
Balmer series 34
Band bending 1195, 1196
Band edge 1191
Band gap 1191
Band spectra 253, 254
Band splitting 1141, 1142, 1215
Band structure of diamond 1144
Band structure of
ionic compounds 1150
nontransition metals 1140
transition metals 1144
Band theory of
metallic bonding 1136*ff*
solids 1140*ff*
Banana bonds 719
Band width 144, 854, 1138
Barn 240, 393
Basic beryllium
carboxylates 545
nitrate 545
Basicity 1436
of anions 1434
of carbonyl compounds 1408
Bathochromic shift 162, 1273
Batteries 1686, (Sec. 16.14)
BCS theory of superconductivity 1227*ff*
Becquerel rays 309, 321
Bent's rule (Secs. 9.13.7, 10.8; Appendix 10A)
Bent bond concept 718, 807
Bent bonds 694–696, 697, 763, 819, 825, 835, 972
Benzoid form 1381
Berry pseudorotation 849*ff*, (Sec. 10.9.2)
Beta (β)-rays 312
Beta decay 340, (Sec. 6.13)
Beta emission 271, (Sec. 6.13)
Bethe cycle 426
Bethe-Slater curve 1153
Bethe's notation 384
Biacetyl 1269
Big-bang theory 429
Binuclear clusters 1162
Black rain 418
Black-body radiation 111*ff*, (Secs. 2.2, 2.3)
Bleaching powder 1584
Bloch theory 1131
Bloch walls 1083

Click Here t.me/chemvillibrary

Bloch wave function 1132
Bloomington shuffle 1166
Blue shift 1273, 1401
Body centred cubic (*bcc*) unit cell 1025
Bohr megneton (B.M.) 77
Bohr yield curve 407
Bohr-Bury scheme 86
Bohr-Wheeler constants 410
Bohr-Wheeler theory of nuclear fission 409
Bohr's atomic model 25, (Sec. 1.8)
Bohr's correspondence principle 36, 156, 157, 164, 174
Bohr's classification of elements 466
Bohr's orbit 26, 27
Bohr's quantum restriction 139
Bohr's periodic table 458
Boltzmann distribution function 1117
Bond dissociation energy 755
Bond (Ch. 10)
  energy 753*ff*, 758
  lengths 764*ff*
  multiplicity 717, 765
  order 568
  pair moment 778*ff*
  characteristics of carbonyl group 1175
3*c*–2*e* Bonding 667*ff*, 687*ff*, 726*ff*, 815, 1452, (Secs. 9.12.12, 9.21)
3*c*–4*e* Bonding 667*ff*, 687*ff*, 735*ff*, 1274*ff*, (Secs. 9.12.12, 9.23, 13.1.9)
3*c*–4*e* vs. 3*c*–2*e* Bonding 667*ff*, (Sec. 9.12.12)
4*c*–2*e* Bonding 732
2*c*–1*e* Bonding 973, (Appendix 10A)
2*c*–3*e* Bonding 973, (Appendix 10A)
Bonding in higher boranes 729*ff*, 896*ff*, (Secs. 9.21, 10.12)
Bonding in the noble gas compounds 735*ff*
Bonding potentiality 677, 679, 680*ff*
Bonding potentiality of the hybrid orbitals 681*ff*
  overlap integral 681*ff*
Bonding properties of
  3*d* and 4*f* orbitals 225, 528, (Sec. 4.3)
  4*f* and 5*f* orbitals 225, 468, 469, (Sec. 4.3)
Boranes 896*ff*, 917, (Secs. 10.12–13)
Borazanes 704
Borazine 703, 1584
Border line elements 462, 467*ff*
Border line species (HSAB) 1474
Born equation 1326*ff*
Born exponent 986, 1003, 1007
Born repulsion 1295
Born repulsive potential 1003
Born-Haber cycle 993*ff*, 997*ff*, 1325, 1414, 1416, 1640, (Secs. 11.5, 11.6)
  drawbacks 994
  proton affinity 997
Born-Lande equation 986, 1003*ff*, 1006, (Sec. 11.7)
Born-Mayer equation (Sec. 11.7.3)
Born-Oppenheimer approximation 550
Borosilicate glass 1093
Bose-Eeinstein condensate (BEC) 237
Bose-Einstein statistics 237, 252
Bosons 218, 237, 252, 1227
Brackett series 34
Bragg's equation 138
Bragg's law
  of diffraction 138
Bragg's method 983
Bragg's reflection 1132
Braking radiation 365
Brass 1636
Bravis lattices 1024
Bray-Liebhafsky (BL) reaction 1779
Break-down voltage 1201
Bredt's rule 1454
Breeder reactor 422, (Sec. 7.13.5)
Bremsstrahlung 365
Bridge cleavage 1392
Bridging alkyl groups 1392
Bridging bonds 726
Briggs-Rauscher (BR) oscillating reaction 1779, 1783
Brillouin zone 1133, 1134, 1136, 1138
Broadening of peaks 126, 162
Bromine trifluoride as a solvent 1570
Brönsted
  acidity 799, 1344*ff*
  equations 1437
  relationship 1436
Brönsted-Lowry theory 1344*ff*, (Sec. 14.3)
Brown ring complex 1590
Brucite sheet 1054
Buckminister fullerene 893*ff*
Buckshot type capture reactions 395
Bucky ball 893*ff*
Buffer action 1370, (Sec. 14.4)
Buffer capacity 1370, 1371
Buffer solutions 1356*ff*
Burning ice 1282, 1283
Butadiene 162, 701
Butanone 1270
BZ reaction 1780, 1782

C

^{14}C-dating 362
Cage compounds 1279*ff*
Calix[4]arene 1313
Calixarenes 1313*ff*
Calomel electrode 1596, 1597, 1629
Canal rays 8
Canonical forms 707
Canonical structures 911
Canted magnetism 1079, 1085
Capping principle 1178
Captodative effect 973
Captodative radical 974
Carbanion 1459
Carbenes
  properties 975, (Appendix 10A)
Carbides 1091
Carbido complexes 548
Carbocations 547, 1385
Carbon clusters 893

Click Here t.me/thealchemylibrary

Carbon-nitrogen cycle 426, 427
Carbon-nitrogen-oxygen (CNO) bicycle 427
Carbonium ion 1385
Carbonyl clusters 1171*ff*, (Sec. 12.8.5)
Carbonyl complexes 1171*ff*, 1406
Carbonyl hydrides 1408, 1589
Carborane-siloxane polymer 930
Carboranes 897*ff*, 917*ff*, (Secs. 10.12–13)
Carotene 162
Carrier mobilities 1194
Carrier technique 309, 345
Cascade effect
isotope separation 262
X-ray generation 38
Catalysed redox reactions 1724, (Sec. 16.20)
Catalytic converters 1059
Catenanes 1320
Catenation bond 1581
Cathode rays 1
Cathodic protection 1693, 1702
Cation polarisation 794
Cation receptors 1312
Cavity model 1550, 1559
Cells
with transference 1605
without transference 1605
Cement 1061
Centre of mass 31
Centrifugal method 266
Chadwick 16, 383
Chain lattices 891, 1050
Chain structure 1264
Chalcogens 454
Chalcophiles 466, 1486
Chancourtois law of telluric screw 449
Channel compounds 1283
Characteristic X–rays 37, 273, 323, 366
Charge capacity 499, 505
parameter 1420, 1421, 1438
coefficient parameter 505, 1419, 1420, 1438
Charge exchange force 279
Charge of an electron 4
Charge separation 502
Charge to mass ratio (e/m) of an electron 2
Charge transfer
band 617, 801, 1717
compound 1219, 1393
Chelate effect 1351
Chelation 1253
Chemical actinometer 368
Chemical clock reactions 1777, (Appendix 16B)
Chemical dosimeter 368
Chemical equilibrium 335
Chemical exchange method 265, 267
Chemical forces 548, 549
Chemical shift 248, 249
Chemical vapour deposition (CVD) 1193, 1194
Chemiluminescence 1709
Chevrel phases 1169, 1229
China clay 1056
Chloromethanes 781, 791
Chromium(II) acetate monohydrate 722, 1163
Chromophore 1273
Chronoamperometry 1744
Circular orbit 47
Cis-effect 823
Cladding 421
Classical kinetic energy 136, 144
Clathrate type complex 1058
Clathrate-hydrate 1283*ff*
Clathrates 1279*ff*, (Sec. 13.2)
Clay minerals 1054*ff*
Clock reactions 1777, (Appendix 16B)
Close packing models 1029*ff*
Cloud chamber 319
Cluster anions 1561, 1563
Cluster bonding 1169
Cluster bonding electrons 1170
Cluster valence electron (CVE) count 1171
Cobalt bomb 425, 426
Codeposition of copper and zinc 1636, 1698
Coercive field 1083
Cohesive energy 511, 1147
Cohesive forces 1111
Coinage metals 452, 453, 454
Coincident states 73
Cold fusion 429
Collector technique 979
Colour and hardness 1479
Colour centres 1072
Common ion effect 1496*ff*, 1507
Compensation method 1597, 1598
Competitive π-bonding 1481
Complementary redox reaction 1595
Components 85
123 Compound (superconductor) 1229
Compound nucleus 284, 393, 410
theory 393*ff*
Compound semiconductor 885, 1184, 1192, 1193
Compounds
hypercarbon 545
photosensitivity 617
Compressibility 1007
Comproportionation reaction 1596, 1651, 1663, (Sec. 16.10)
Compton effect 121, 141, 313, 366, (Sec. 2.5)
Compton shift 124*ff*
Compton wavelength 124
Condensation centres 320
Condition of orthogonality 148
Conditional or formal potential 1599, 1607, (*see* formal potential)
Conditional stability constant 1607
Conduction band (CB) 1148
Conductors 1135
Cone angle 1405
18*e*-Configuration 1406
Configurational entropy 1063, 1065, 1279, 1280, 1284
Consecutive reaction 331
Conservation laws in nuclear reactions 390*ff*
Conservation of angular momentum 391
Conservation of energy 390
Conservation of linear momentum 390
Conservation of momentum 123

Click Here! MethealChemyLibrary

Continuous spectra 112
Continuous X-ray spectrum 38
Contraction of *d*-orbitals 685
Controlled fusion reaction 428
Controlled nuclear fission 418
Coolant 421
Cooper pairs 1227
Cooperative magnetism 1079
  aniferromagnetism 1079
  canted magnetism 1079
  ferrimagnetism 1079
  ferromagnetism 1079
Coordination polymers 1282
Copper(II) acetate monohydrate 722, 1162*ff*
Coprecipitation 979, 1506
Corands 1301
Corona discharge 1208
Coronands 1301
Correspondence principle 36, 156, 157, 164, 174
Corrosion 1686, 1693
Corrosion of copper 1702
Corrosion of iron 1702
Corrundum 1040
Cosmic abundance 269
  of elements 433*ff*
Cosolvating agents 1350*ff*
Cottrell equation 1729, 1743, 1745
Coulomb barrier 281
Coulomb integral 166, 552, 554, 559, 563
Coulomb potential barrier 281
Coulombic energy (J) 552, 555
Coulombic interaction energy 552
Coulombic potential 411
Coulombic potential barrier 412
Coulometric analysis 1751
Coupling schemes 57
Covalent bond order 776
Covalent crystals 767
Covalent lattice energy 1291
  and symmetry 1292
Covalent radii 764
Covalent-ionic resonance 555, 705 763, 768, 774*ff*, (Sec. 10.4)
  energy 491, 495
Cow and milk system 268
Cradle shape 818
Craig-Paddock model 703, 815, 816
Cristobalite (SiO_2) structure 1039
Critical deformation 410
Critical magnetic field (H_c) 1224
Critical mass 417
Critical potential 40
Critical size 415
Critical temperature 1224
Crookes dark space 1
Cross-section (nuclear reaction) 392
Crown
  ethers 1301, 1308*ff*, (Secs. 13.5.6, 13.5.9)
  form 818
  shape 811
Crown-anthracene system 1318
Cryolite and anticryolite structure 1040
Cryptands 1301, 1306*ff*, (Secs. 13.5.6, 13.5.8-9)
Cryptate alkali metal cations 1180
Cryptates 1307*ff*
Cryptospherands 1302
Crystal defects 1063*ff*, 1209, (Sec. 11.15)
Crystal field effect 226
Crystal field stabilisation energy (CFSE) 1634
Crystal packing model 800
Crystal radii
  Shannon's 988
Crystal structure of the metals 1111
Cubic close packing 1032
Cubic perovskite structure 1047
Curie temperature 1082
Curie-Weiss law 1086
Curie's law 1986
Cyanuric acid (CA) 1317
Cyclic voltammetry (CV) 1741
Cycloaddition 749
Cyclodextrins 1283, 1314*ff*
Cycloheptatriene 1460
Cyclonite 1727
Cyclopentadiene 1269
Cyclophanes 1316
Cyclotriphosphazene 1284
Cyclotron 399
Cylindrical cryptand 1308

δ & D

δ-bonding 720*ff*, 1162
d-band formation 1212
d-block elements 465, 528
d-block vs. *f*-block elements 528*ff*
d-contraction 469, 475
d-orbital participation 686*ff*, 867, 1437*ff*, 1440, 1451*ff*, 1473, (Secs. 9.13.5, 10.7)
d-orbital resonance 1422
d-orbitals 204, 225, (Sec. 4.3)
d-orbital vs. *f*-orbital 225*ff*
DABCO 1439
Dalton 259
Dating by tritium 363
Dative bond moment 788
Davisson and Germer's experiment 136
DCD (Dewar, Chatt and Duncanson) model 1402
de Broglie 134*ff*, (Sec. 3.2)
  electron wave 135, 136
  matter wave 133, 135
  wavelength 134
de Moivre's
  theorem 200, 202
Debye (dipole moment) 774
Debye forces 1287
Debye–Huckel limiting law (DHLL) 1498
Decay kinetics 325
Decomposition potential 1694, 1699, 1701, 1731
Decomposition voltage 1698
Degeneracy of the energy levels 159
Degree of covalency 795*ff*
Delayed neutrons 408
Delayed reactions 1711
Delocalisation 161, 705
  energy 699*ff*, 702*ff*
Delocalised MOs 642
Delta bonding 720*ff*, 1162, (Secs. 9.6, 9.19, 12.8)
Delta molecular orbitals 575
Delta-bond 720,1162, (Secs. 9.6, 9.19, 12.8)
Deltahedra 900
Dempster's mass spectrometer 14

Click Here to me/thalchemylibrary

Density of energy states (DOS) 1117, 1139*ff*
Density of states (DOS) 1139, 1146
Depolarizers 1698
Designation of the MOs 597
Detection of *H*-bonding 1273
Detonation velocity 1776
Detonator 425, 1773, (Appendix 16A)
Dewar model 703, 815, 816
Di-molybdenum(II) complexes 721
Diagonal relationship 511*ff*
Diamagnetism 1086
Diamond cubic (*dc*)
  structure 884
  unit cell 1028
Diamond structure 1184, 1248
Diborane 726
Dicarbollide
  anion 929, 930
Dichoric 1180
Dielectric constant 1261, 1327, 1556
Dielectric saturation 1327
Diels-Alder reaction 749
Differentiating electron 464
Differentiating solvent 1347*ff*, (Sec. 14.3.2)
Diffuse (D) series 74
Diffusion cloud chamber 320
Diffusion current 1732
Diffusion method 262
Dihydrogen adduct 1407
Dihedral angle 790
Dihedral mirror planes 937
Dihydride complex 1407
Dihydrogen 1592
Dimeric chromium(II) acetate 722, 1163
Dimeric copper(II) acetate 722, 1162
Dimerisation 724
  of *NO* and NO_2 650
Dinitrogen adduct 1396, 1400
Dinitrogen complexes 1396*ff*, 1400
Diode 1194, 1202
Dioxygen 1592
Dioxygen adduct 1396*ff*
Dioxygenyl tetrafluoroborate 999
Diphenylamine 1679
Dipolar repulsion 780, 785, 1268, 1269
Dipole moment 777*ff*, 780, 960, 1401, 1556, (Sec. 10.5)
  of R_3NO and R_3PO 809
Dirac atom 191
Dirac model 192
Direct and indirect gap semiconductors 1190
Direct gap materials 1192
Discharge potential 1694
Disilenes 1405
Dismutation reaction
  see disproportionation reaction
Disintegration series 342*ff*, (Sec. 6.15)
Dispersion force 1288*ff*
Disproportionation reaction 1596, 1651, 1663, (Sec. 16.10)
Disproportionation of peroxide 884
Dissociation constants of some acids 1415
Dissolution 1258
Dissymetric 960
Distortion polarisability 1288
Dithionate 1586
Dithionite 1586
Dobereiner's law of triads 448
Donor number (D.N.) 1413
Donor-acceptor compound 1219
Dopant 1184
Doppler effect 73, 430
Dosimeter 367, 368
Double bond character in *P–O* linkage 809
Double helical structure of DNA 1265–66, 1301
Downhill migration 1195, 1197
Drago-Wayland equation 1411*ff*, 1491
Drift velocity 1121
Dropping mercury electrode 1728*ff*
Drude-Lorentz classical free electron theory 1114
DSD (diamond-square-diamond) 927
Dulong and Petit's law 455

E

Ebsworth diagram 1649
Eclipsed conformation 789
Edison cell 1688
Effective mass 1182
Effective nuclear charge 473, 474*ff*
Effects of different factors on electrode potential 1610*ff*
Eigen functions 148
Eigen values 148
Eighteen electron (18*e*) structure 981, 1406
Einstein's equation 120
Elastic collision 41
Elastic scattering 366, 386
Electric quadrupole moment 240
Electrical conductivities of solids 1148*ff*, (Sec. 12.5.5)
  conductors 1149
  insulators 1149
  semiconductors 1151
  semimetals 1149
Electrical conductivity 1120
Electrical double layer 1195
Electrides 1309, 1560, 1561
Electroanalytical techniques 1727*ff*
Electrochemical cells 1686
Electrochemical polarisation 1698
Electrochemical series 1602, 1603
Electrodeposition 1693
  of brass 1698
  of copper and zinc 1638, 1698
Electrolysis of solutions 1693
Electrolytic cell 1606, 1607, 1693
Electrolytic method 264
Electromagnetic method 261
Electromagnetic wave 135
Electron affinity 486*ff*, (Sec. 8.13), 997
Electron capture (EC) 337
Electron cloud density 210
Electron compounds 1158, 1160
Electron deficient bonds 905
Electron deficient compounds 544, 725, 1391
Electron deficient covalent bonds 725*ff*, (Sec. 9.21)

Click Here to the Chemylibrary

Electron deficient covalent compounds 725*ff*, (Sec. 9.21)
Electron deficient hypervalent compounds 691
Electron delocalisation effect 784
Electron density maps 982
Electron emission effect 323
Electron exchange phenomenon 552
Electron orbit 32
Electron sea model 1114
Electron transfer reaction 353
Electron waves 139
Electron-hole pair 1192
Electron-phonon interaction 1125
Electronegativity 491*ff*, (Sec. 8.14), 1431
  equalization 502
Electroneutrality 821
  principle 711
Electronic conduction 1076
Electronic spectra 256
Electronic wave function 550
Electroplating 1697
Electroscope 315
Elemental semiconductors 1193
Ellingham diagram 1719, (Sec. 16.17)
Ellipsoidal cavity 1312
Elliptic orbits 45, 76
EMF diagrams 1647, (Sec. 16.8)
Emission spectrum 18
Endoergic process 392
Endohedral complexes
  see fullerenes
Energetics of A and D processes 863
Energetics of dissolution 1324*ff*, (Sec. 13.6)
Energetics of fissionability 413*ff*
Energetics of hybridisation 682*ff*
Energetics of phase transitions 1332*ff*, (Sec. 13.7)
Energetics of solubilities 1328
Energetics of the disintegration processes 336
Energy bands 1136
Enthalpic disfavour 1301
Enthalpic favour 864, 1450
Entropic disfavour 1303, 1418, 1433, 1450, 1633, 1635
Entropic effect 1437, 1633, 1635
Entropic favour 864, 1258, 1285, 1298, 1390, 1419, 1438, 1777
Entropy of
  decomposition 1020
Entropy driven 733
  process 1285
  reactions 862
Eötvös-Ramsay-shields coefficients 1258
Equilibrium constant 1661
Equipartition of energy 1125
Equivalence and nonequivalence of the hybrid orbitals 693*ff*
Equivalent weights of oxidants and reductants 1595
Estimation of Fe(III) 1675
Ethyl acetoacetate 1269
Even (+) parity 294
Even and odd functions 156
Even and odd series 452
Exchange energy 92, 94, 555, 559, 706
Exchange force 279
Exchange integral 554, 564, 1152
Exchange interaction 1145, 1152
Excitation energy 409
Excitation potential 35
Exhaustion region 1189
Exoergic process 392
Expansion of octet 544
Explosive materials 1702, (Sec. 1621, Appendix 16A)
Extended periodic table 462
Extrinsic excitations 1192
Extrinsic or doped semiconductors 1184, 1189
Eyring equation 861
Eyring plot 164

F

f-block elements 465, 528
f-block vs. *d*-block elements 528*ff*
F-centre 1071
f-contraction 469*ff*
f-orbitals 208, 225, (Sec. 4.3)
f-orbitals vs. *d*-orbitals 225*ff*
Face centred cubic (*fcc*) unit cell 1026
Factors governing
  the acid-base strength 1414*ff*, (Sec. 14.8)
  the bond lengths 766*ff*
  the degree of polarisation 792*ff*
  the electrode potential 1610*ff*
  the molecular polarity 777*ff*
Fajans' rule 705, 791*ff*, 997, (Sec. 10.6)
Fajans' type compounds 1335
Faraday dark space 1
Fast breeder reactor 423
Fast neutrons 17
Fat man (atom bomb) 418
Feldspars 1056
Fermi 238
Fermi energy level 1182
Fermi gas model 271, 282
Fermi level 1117, 1188
Fermi potential 283
Fermi sphere 1160
Fermi temperature 1120
Fermi-Dirac distribution law 1183
Fermi-Dirac energy distribution 1117, 1118*ff*
Fermi-Dirac statistics 237, 252, 1117
Fermions 218, 237, 252, 291
Fermi's four factor formula 418
Ferrate ion 1658
Ferrimagnetism 1044, 1079, 1082
Ferrites 1044, 1082
Ferroelectric crystals 1262
Ferroelectric material 1047*ff*, 1088*ff*
Ferroin indicator 1678
Ferromagnetic materials 1085
Ferromagnetic property 1146
Ferromagnetism 1079, 1082, 1144, 1151*ff*
Fertile nuclides 416, 417
Fifth state of matter 237
Fine spectra 44, 48
Fine structure (spectra) 53, 73
Fine structure constant 49
Finite mass of the nucleus 31
Fire extinguishing species 974
Fissile nuclides 416
Fission 277, 389, 406
Fission chain reaction 415

Click Here t.me/thealchemylibrary

Fission yield curve 407
Fissionability 412
Fluorescence 323, 1318, 1708
  switch off 1318
  switch on 1318
Fluorescence emission 323
Fluorescent radiation 366
Fluorite (CaF_2) crystal 1038
Fluorite structure (AB_2) 1039
Fluoro compounds of xenon
  see xenon fluorides
Fluoroacetylacetone 1270
Fluoroalkyl radicals 972, (Appendix 10A)
Fluorocarbenes 972, 975, (Appendix 10A)
Fluorocarbons 1290
Fluoroethyl radicals 975, (Appendix 10A)
Fluoromethyl radicals 972, (Appendix 10A)
Fluorosulfonic acid 1568
Fluorosulfuric acid 1383, 1384
Fluxional behaviour 845*ff*, 1403, 1591
Fluxional molecules 248, 848*ff*, 852, 853, 857, (Sec. 10.9)
Fluxionality 848*ff*, 856
Football ligand 1307
Forbidden energy gap 1134, 1149
Forbidden transitions 71
Forbidden zone 1134
Forces 1285
  long-range 1285
  short-range 1285
Formal (conditional) potentials 1607, (Secs. 16.3, 16.4)
Formal charge 709*ff*, 713, 1578, 1579, (Secs. 9.16.4, 16.1.2)
Formal potential 1598, 1607, 1615, (Secs. 16.3, 16.4)
Forward biased junction 1196
Fractional distillation method 264
Framework bonding 1168
Franck-Hertz experiments 40
  critical potential 40
  ionisation potential 40
  resonance potential 40
Free electron theory 1115
Free electron theory of metallic bonding 1114*ff*, (Sec. 12.3)
Free particle 150
Frenkel defects 1064*ff*
Fricke dosimeter 368
Front strain (F-strain) 1444
Frontier atomic orbitals 506, 1475, 1476
Frontier molecular orbitals (FMOs) 506, 580, 1475*ff*, (Appendix 9A)
Frost diagrams 1649, (Sec. 16.8.2)
Fuel cells 1686, 1691, (Sec. 16.14.3)
Fuel gas 1711
Full-filled level 484
Fullerenes 894*ff*, (Sec. 10.11.5)
Fuller's earth 1056
Fulminates 710, 1727
Fulvene 1461
Fundamental (F) series 51, 74
Fundamental particles 16, 18, 296, 299, (Secs. 1.4, 5.6)
Furan 784
Fusion 277, 424

G

Galvanic cell 1606, 1693
Gamma (gamma) rays 313
Gamma emission 341, (Sec. 6.14)
Gas hydrate clathrate 1283*ff*
Gas hydrate structure 1280*ff*
Gas hydrates 1282, 1284
Gas multiplication factor 316
Gas phase acidity 1419*ff*, 1421
Gauche conformation 789
Geiger range 318
Geiger threshold 318
Geiger-Muller (G-M) counters 316, 317
Geiger-Nuttall rule 290, 329, 339, 340
Gem quality crystals 1046
Gemstones 1046
Geodesic dome 893
Giant neutron star 429
Gibbsite sheet 1054
Glass transition 1092
Glasses 1092
Goldschmidt's geochemical classification 466
Goldschmidt's radii 983, 988
Goldstein's discharge tube 8
Graphite 1144
  compounds 889*ff*
  layer lattice 1029
  like structure 803, 890
  structure 886*ff*, 1248
Gray (Gy) 367
Green photocatalyst 1214, 1717
Green solvents 1574
Grotthus mechanism 1266, 1369, 1557
Ground state terms 67–69
Group analysis 1484*ff*, 1499
Group displacement rule 324, (Sec. 6.8)
Group electronegativity 504, 1421
Group moment 779
Group orbitals (LGO) 620
Groups (periodic table) 452
Guanidine 1462
Guest-host
  chemistry 1298
  compounds 1284
  interaction 1058
Gunpowder 1726
Gutmann rule 1413
Gyromagnetic ratio 78

H

H-bonded ferroelectrics 1262
H-bonded structure of ice 1280
3*c*–4*e* *H*-bonding 1275
H-bridge bond 1277*ff*
Hagg's rule 1091
Half life ($t_{1/2}$) period 327, 328
Half value thickness 366
Half-filled and full-filled level 91
Half-filled level 484
Half-peak potential 1748
Half-wave potential 1734*ff*
Half-wavelength 156
Hall-coefficient 1131
Hall-effect 1130
Halocarbenes
  properties 975, (Appendix 10A)
Halogens 454
Halons 974
Hamiltonian operator 147, 166

Click Here t.me/thealchemylibrary

Hammett acidity function 1382*ff*, 1470
Hannay-Smyth equation 775
Hard and soft acids and bases (HSAB) 1473*ff*, (Sec. 14.15)
Hard-hard interaction 1488, 1489
Hard-soft interaction 1488, 1636
Hardness (HSAB) 1405*ff*, 1475
Hardness of ionic compounds 1013
Harkins' Rule 269
Harmonic oscilator 255
Hartree 30
Heat capacity 1125
Heaviest nuclide 412
Hedgehog cation 523, 547
Heisenberg's uncertainty principle 45, 140, 161, (Sec. 3.3)
Heitler-London wave functions 552
Helferich's rule 824
Helical structure 1318
Heme group 1396
Hemerythrin 1592
Hemispherands 1301*ff*
Hemocyanin 1592
Hemoglobin 1397, 1592
Henderson equation 1357
Heteronuclear Zintl ions 1178
Heteropoly acids 1061
Hexafluoroacetylacetone 1270
Hexagonal close packing 1029
High temperature superconductors 1228
Higher boranes 730
Highest occupied molecular orbital (HOMO) 580, 749–52, 973
Hole formalism rule 70
Hole theory of liquids 1094
Holes
  octahedral 1026, 1030
  tetrahedral 1026
HOMO-LUMO interaction 750, 1386, (Appendices 9A, 10A)
Homologous series 1289
  of alkanes 1293
Homonuclear diatomic molecules (MOT) 578*ff*
Homopolar bond 776
Homopolyatomic species 1178
Hopping conductivity 1074–75, 1210*ff*, 1212
Hopping semiconductivity 1045, 1074, 1210
Hopping semiconductors 1074, 1209*ff*
Hot atoms 267
HSAB principle 1473*ff*, 1482, (Sec. 14.15)
  atmophiles 1486
  chalcophiles 1486
  lithophiles 1486
  siderophiles 1486
Hückel molecular orbital method 699
Hückel's rule 817
Hume-Rothery rule 1157, 1158*ff*
Hund's rule 68, 69, 94, (Sec. 1.10.11)
Hybrid lone pair moments 777*ff*, 786*ff*, (Sec. 10.5.3)
Hybridisation 716, 825
Hybridisation energy 683, 760
Hybridisation of atomic orbitals 669*ff*
Hybridisation of nucleons 295
Hybridistion cost 683
Hydrated electron 370
Hydrates 1279*ff*, (Sec. 13.2)
Hydration energies 1330
Hydration spheres 1327
Hydride sponge 1447
Hydroboration 923
Hydrodynamic electrode 1729
Hydrogen (*ortho* and *para*) 251
Hydrogen bomb 425
Hydrogen bond 755, 1250*ff*, (Ch. 13)
Hydrogen bond energy 1254
Hydrogen bonding 1250*ff*, (Sec. 13.1)
Hydrogen bridge 1278, 1408, (Sec. 13.1.10)
Hydrogen electrode 1597
Hydrogen molecule (VBT and MOT) (Secs. 9.3, 9.4)
Hydrogen overvoltage 1699
Hydrogen spectrum 18, 20, (Sec. 1.5)
Hydrogen valency 453
Hydrogen-like systems 25, 26, 29, 213
Hydrogenic systems 192
Hydrolysis 1429
Hydrolysis constants of aqua metal ions 1431*ff*, 1433
Hydrolysis of alkyl phosphates 870
Hydrolysis of aryl phosphates 870
Hydrolysis of metal ions 1429
Hydrolysis of salts 1349, 1494*ff*, (Sec. 14.17)
Hydrometallurgy 1722
Hydron 1344
Hydronic concept 1344
Hydronium ion 1369
Hydrophilic interaction 1298
Hydrophobic effect 1299
Hydrophobic interaction 1290
Hydroxo acids 1429
Hydroxyl bond 1254
Hyper carbon 545*ff*
Hyperconjugation 736, 1452, 1466
Hyperfine quantum number 241
Hyperfine splitting 75
Hyperfine structure of the spectral lines 74
Hyperons 298
Hypervalence 545*ff*, 1391
Hypervalent electron deficient molecular species 547, 691
Hypophosphoric acid 1583
Hypophosphorous acid 707, 1425, 1583
Hypsochromic shift 1273
Hysteresis loop 1082, 1083, 1089

I

Ice (structure) 1254, 1280
Iceberg 1327
Ilkovic equation 1733
Ilmenite structure ($FeTiO_3$) 1045
Imaging agent 268
Imidazole 1462, 1463
Imidazoline 1462
Impact parameter 23
Impurity acceptor level 1186
Impurity donor level 1186
Impurity semiconductor 1184*ff*
Induced dipole moments 791
Induced radioactivity 345

Click Here! http://thealchemylibrary

Inductive effect 505, 779, 1418, 1437, 1438*ff*
Inductive effect of different groups 1420
Inelastic collision 41
Inelastic scattering reactions 386
Inert gas compounds 735*ff*, 972
Inert gas elements 466
Inert pair effect 521, 531, 532, 761, 763, 770*ff*, 980, 1143, (Sec. 10.3)
Infrared (IR) spectrum 1262
Inorganic benzene 1584 1584
Inorganic graphite 888, 893
Insulators 1135
Intensity of NMR signal 244
Intensity rules 72
Intercalated compound 1169, 1690
Intercalates of graphite 1222
Intercalation compounds 886*ff*, 888, 1169, 1171, 1213, 1690
Interchange or concerted process 504, 862
Interferring acid radicals 1499
Interhalogens 1401
Intermetallic compounds 1156, 1157
Intermolecular attractive forces 1293
Intermolecular forces 1286
Intermolecular *H*-bonding 1251
Internal conversion 267, 268, 322, 341
Internal *H*-bonding 1370
Internal nodal points 155
Interstitial alloys 1156
Intersystem crossing (ISC) 1708
Intramolecular *H*-Bonding 785, 1251, 1253, 1267, 1455
Intranodal maxima 198, 222
Intrinsic bond energy 753, 759
Intrinsic excitation 1192
Intrinsic homopolar dipole 777
Intrinsic semiconductor 1182, 1189
Inverse crown ethers 1322*ff*, (Sec. 13.5.19)
Inverse spinel structure 1042
Inversion energy barrier 848
Iodide clock reaction 1777
Iodometric titrations 1703
Ion electron method 1577*ff*
Ion solvation 1326*ff*, (Sec. 13.6.2)
Ion-exchange process 473
Ionic and covalent compounds 1295
interaction 1295
Ionic compounds (Ch. 11)
characteristic properties 977
disproportionation 1000
thermal stability 1019
Ionic conduction 1067, 1075
Ionic conductivity 1068
Ionic crystals of *AB* type 1035*ff*
Ionic crystals of AB_2 type 1038*ff*
Ionic crystals of AB_3 and A_2B_3 type 1040*ff*
Ionic equilibria 1343
Ionic liquids as solvents 1572*ff*, (Sec. 15.13)
Ionic mobility 1266, 1369
Ionic potential 792
Ionic radii 987, 989*ff*, (Sec. 11.4)
Pauling's 987
Ionic solution 1325
Ionisation energies 481*ff*, (Secs. 8.12, 9.11)
Ionisation potential 35, 40, 120, 481*ff*
Ionising solvents 1557
Ionophores 1307
IR-shift 255
see detection of *H*-bonding and carbonyls
IR-stretching frequency 1263
Irving-Williams stability order 1483
Island of stability 289, 405
Isobaric nuclides 249, 408, 414
Isobaric relationship 313, 341
Isobars 249
Isoelectric points 1361, 1364, 1366
Isoelectronic groups 549
Isoelectronic hydrides 1441
Isoelectronic species 549
Isoionic point 1366
Isolobal fragments, 739*ff*
Isolobal groups 913, 1166
Isomeric distribution 1267
Isomeric equilibria 791
Isomeric transition (IT) 250, 268, 341, 385
Isomerisation 824
Isomorphism
overgrowth 978
Isomorphous coprecipitations 1506
Isomorphous substitution 1046, 1052, 1057
Isopoly acids 1061, 1107
Isopoly anion 1061, 1107
Isosbestic point 1400
Isosteric anions 991
Isosteric cations 991
Isosteric or isoelectronic species 548, 985, 991
Isosters 715
Isostoichiometric species 549, 584
Isostructural 549
Isotones 249
Isotope effect 385
Isotope labelling 347
Isotopes 11, 33, 249, 253, 256, (Sec. 5.2)
discovery 33
separation 260*ff*, (Sec. 5.2.6)
uses 347*ff*, (Sec. 6.17)
Isotopic dilution analysis 355
Isotopic effect 256
Isotopic effect on bond energy 755
Isotopic shift 253, 257

J

Jablonski diagram 1711
Jaffe-Hinze electronegativities 497
Jahn-Teller destortion 160, 163, 980, 1215, 1634
Jemmis' *mno* rule 916, 1171
Jemmis' unifying electron counting rule 916
Joesphson junction 1232
Junction laser 1205
Junction potential 1605

K

Kaolin 1056
Kaolinite 1054, 1055

Click Here to the chemylibrary

Kaons (*see* Sec. 5.6)
Kapustinskii equation 1011
Katapinands 1310
Katapinate 1310
KCP 1180
Keesom forces 1286
Keggin structure 1062
Kepler's law of area 46
Keto-enol tautomerism 1268*ff*, 1459
Kieselguhr 1061
Kinetic factors 1704
Kinetic isotope effect 165, 256
Koopman's theorem 1476
Kossel's theory 543

L

L-S coupling 62
Lactams 1442
Lactones 1442
Lamellar compounds 888
Lande *g* factor 79, 84, 1079
Lande interval rule 69, 79
Lande splitting factor 1079
Lande's method 983
Landolt reaction 1778
Langevin paramagnetism 1086, 1151
Lanthanide contraction 469*ff*, 471, 477, 519, (Sec. 8.9)
Lanthanides 453, 454, 468
  vs. actinides 468, (Sec. 8.8.3)
Lanthanoids 453, 454
Lanthanum series 454
Lapis-Lazuli 1059
Laplacian operator 145
Lariat crown ethers 1303
Larmor frequency 83
Larmor precession 55
Laser 1040
Latimer diagram 1647, (Sec. 16.8.1)
Latimer equation 1327
Lattice energy 997, 1003*ff*, 1011*ff*
Lattice planes 1027
Lattice-electron scattering 1121
Law of equipartition of energy 113
Law of telluric screw 449
Law of triads 448
Layer lattices 1049
LCAO method 570*ff*
LCAO-MO treatment 558
Le Chatelier's principle 1497
Lead-acid battery 1688
Leclanche or dry cell 1687
Legendre polynomial 188
Lennard-Jones potential 1285, 1295, 1296, (Sec. 13.3.4)
Levelling solvents 1346, 1347*ff*, (Sec. 14.3.2)
Levitation effect 1223, 1231
Lewis acid and base property of the same substance 1410
Lewis concept 1386*ff*, (Sec. 14.7)
Lewis dot structure 1581
Lewis-Langmuir charge 709*ff*, 713, (Sec. 9.16.4)
Lewis-Langmuir concept 543
LFER 1436
Ligand group orbitals (LGOs) 620
Light emitting diode (LED) 1192, 1204
Light-emitting solids 1205
Line spectra 111, 253
Linear accelerator 397
Linear combination method 166
Linear combination of atomic orbitals (LCAO) 167, 557
Linear energy transfer (LET) 365
Linear free energy relationship (LFER) 1436
Linear sweep voltammetry (LSV) 1743
Linkage isomers 822, 824, 1480
Liquid ammonia as a solvent 1558*ff*, (Sec. 15.4)
Liquid crystals 1095
Liquid drop model 284, 409
Liquid hydrate 1280
Liquid hydrogen fluoride as a solvent 1563
Liquid hydrogen cyanide as a solvent 1564, 1565
Liquid *Na-S* battery 1234
Liquid sulfur dioxide as a solvent 1569
Lithium battery 1689
Lithium ion battery 1690
Lithium titanium disulfide battery 1213
Lithophiles 466, 1486
Little boy (atom bomb) 418
Localised MOs 647
Lock and key principle 1299
London dispersion forces 1284*ff*
London force 1284, 1288*ff*
Lone pair-lone pair repulsion 761, 763
Lone pair moments 777*ff*, 786*ff*, (Sec. 10.5.3)
Long form of the periodic table 458
Lorenz number 1114
Lothar Meyer's periodic laws 450
Lotka-Volterra model 1780
Lowest unoccupied molecular orbital (LUMO) 580, 750–52, 973
Luminescence 1709
Lummer-Pringsheim curve
  see black body radiation
Lux-Flood concept 1466*ff*
Lyate 1348, 1468
Lyman series 34
Lyonium 1348, 1468

μ & M

μ (mu)-bond 1402
Macrocyclic crown ethers 1308
Macrocyclic effect 1305
Macrocyclic systems 1301
Macroscopic and microscopic bodies 134
Macroscopic particle 134
Madelung
  constant 1005
  energy 1004, 1006
  interaction 776
Magic acid 1385, 1568
Magic number 288, 435
Magnetic bottle 429
Magnetic domains 1083
Magnetic materials 1076*ff*, (Sec. 11.16)
Magnetic moment 79, 80, 217
Magnetic properties 1076*ff*
Magnetic quantum number of the MOs 567
Magnetic susceptibility 80

Click Here to methodchemistry.com

Magnetisation 1084
Magnus' green salt 1180
Malathion 869
Malleability and ductility 1111, 1112
Man-made elements 401, 402, (Secs. 7.10, 7.11)
Manxine 1443
Markownikoff addition 923
Mass action law 1183, 1196
Mass defect 275, 409
Mass spectrograph 9, 12, 14
Mass spectrometer 15
Mass-energy equivalance 133, 385
Matter wave 133, 134
Mattheissen rule 1125
Max Born 149
Maximum suppressor on polarograms 1741
Maxwell-Boltzmann distribution law 1183
Measurement of cell EMF 1597
Mechanisms of nuclear reactions 393
Meissner effect 1223
Melamine (M) 1317
Melting and boiling points of salts 795*ff*
Melting and boiling points of alkanes 1289
Melting point of dicarboxylic acids 1292
Mendeleev's periodic law 451*ff*
Mendeleev's periodic table 455*ff*
Mendeleev's short periodic table 451
Mercaptan 1488
Mercuric halide (HgX_2) structure 1050
Mesogens 1095
Mesomeric effect 784
Meson exchange theory 280
Meson particles 279
Mesons 279, 298
Metal basicity 1408
Metal clusters 1161*ff*, (Sec. 12.8)
Metal disulfides 1050
Metal framework 1177, 1178
Metal-ammonia solution 1559*ff*
Metal-metal bonds 1161*ff*, 1166, 1180
Metal-olefin complexes 1402*ff*
Metal-only clusters 1178
Metallic conduction 1136
  in the monoxides 1211
Metallic conductivity 1209
Metallic lustre 1110, 1114
Metallic orbitals 1154, 1155
Metallophthalocyanins 1220
Metastable isomer 250, 347
Metathion 869
Methane hydrates 1283
Methyl orange 1382
Methyl red 1382
Methyl viologen 1714
Mica 1054
Micelles 1299, 1301
Microscopic particle 134
Microstates 65, 66
Migration current 1732
Miller indices (*hkl*) 1027, 1133
Millikan's oil-drop method 4
Mirror nuclei 239, 239, 287
Mischmetal 454, 530
Mixed fluorides (ABF_3) 1046
Mixed metal oxides 1042*ff*, (Sec. 11.11)
Mobil process 1059
Mobility of the defects 1068
Moderator 366, 420
Modes of radioactive decay 271, 322
Modifier 1093
Moh's scale 1013
Molar refractivity method 983
Molecular chameleon 1308
Molecular crystals 893
Molecular inorganic superconductor 1221
Molecular metals 1220
Molecular orbital picture of higher boranes 912, (Secs. 9.21, 10.12)
Molecular orbital theory (MOT) 557*ff*
  heteronuclear diatomic molecules 601*ff*
  homonuclear diatomic molecules 578*ff*
  polyatomic species 658*ff*
  triatomic molecules 620*ff*
  trigonal planar molecular species 654*ff*
Molecular polarity 777
Molecular recognition 1285, 1298, 1312, (Sec. 13.5.11)
  anion coordination 1312
  anion receptors 1312
  cation receptors 1312
  linar anion recognition 1312
  molecular chameleon 1313
  spherical recognition 1312
  tetrahedral recognition 1313
Molecular ribbon 1317
Molecular sieves 1057
Molecular solution 1325
Molecular superconductors 1221
Molecular switch 1318*ff*, (Sec. 13.5.17)
Molecular symmetry 931*ff*, (Sec. 10.14)
  symmetry operations 931*ff*
Molecular topologies 824*ff*, (Sec. 10.8)
Monoisotopic elements 257, 259, 269, 270
Montmorillonite 1055
Morpholine 1439
Moseley's law 37*ff*
Mu (μ) bonds 575
Mulliken-Jaffe electronegativity 497
Mulliken's electronegativity 495, 1476
Multiisotopic elements 269
Multiple bonds 717*ff*, 765
Multiplet structure 53, 72
Multiplet width 79
Multiplication factor 415, 419
Muons 279
Mutual polarisation 794, 821, 1297, 1432, 1488, 1558, (Secs. 10.6, 13.4.3)
Myoglobin 1397, 1592

N

n-type extrinsic semiconductors 1184
n-type superconductors 1231
Naked cluster ions 1178
Natural fission reactor 423

Click Here to Free Chemistry Library

Natural gas hydrate 1282, 1283
Naughty element 525
Neel temperature 1080
Negative hyperconjugation 975, 1466 (Appendix 10A)
Neptunium series 343
Nernst equation 1598
Neutrino 297
Neutron 16, 17
  fast neutrons 17
  neutron stars 17
  slow neutrons 17
  thermal neutrons 17
Neutron activation analysis 355
Neutron emission 272
Neutron stars 17
Neutron to proton ratio 271, (Secs. 5.3.2–3)
Newlands' law of octaves 449
Nickel arsenide (*NiAs*) structure 1037
Nickel storage cell 1688
Nickel-cadmium cell 1689
Niels Bohr 25
Nitrating mixture 1567
Nitroalkanes 1287
Nitroprusside 1590
Nitrosation of amines 883
Nitrous oxide 1587
NMR frequency 243
NMR shift reagents 529
NMR spectra 245, 856
NO (nitric oxide) as a ligand 1591
Noble gas compounds 736
Noble gas hydrates 1288
Noble gases 454
Noble gases as Lewis bases 1410
Noble liquid 522
Noble metals 1641
Nodal points 199
Nodal surface 206
Non-aufbau filling 1147
Nonaqueous solvents 1555*ff*, (Ch. 15)
Nonaufbau filling of a *d*-band 1147
Noncomplementary redox reaction 1595
Noncoordinating solvents 1574
Noncrossing rule 577, 589
Nonequivalent hybrid orbitals 670
Nonequivalent hybridisation 830
Non-Faradic current 1729, 1740
Nonstoichiometric compound 1048
Nonstoichiometric defects 1070, 1189
Nonstoichiometric oxides 1211
Nordheim rules 294
Normal Zeeman effect 82
Normalisation 154, 533, 560
Normalisation condition 676
Normalised and orthogonal wave functions 150*ff*
Normalising constants 150, 578
Nuclear binding energy (NBE) 275, 409
Nuclear binding energy curve 276
Nuclear configuration 292
Nuclear density 239, 299
Nuclear dimension 24
Nuclear ellipticity 241
Nuclear fission 277, 406*ff*, (Secs. 7.12, 7.13)
Nuclear forces 278
Nuclear fuels 406, 416
Nuclear fusion 277, 424*ff*, (Sec. 7.14)
Nuclear *g*-factor 242
Nuclear isomers 250
Nuclear magnetic moment 242
Nuclear magnetic resonance (NMR) 241
Nuclear magneton 17, 78, 242
Nuclear model of atom 21 (Sec. 1.7)
Nuclear models 282*ff*, (Sec. 5.5)
Nuclear orbit 32
Nuclear potential 281, 283
Nuclear potential barrier 281
Nuclear potential well 292
Nuclear quadrupole moment 295
Nuclear radius 239
Nuclear reactions 366, 386*ff*
  mechanism 393*ff*, (Sec. 7.8)
Nuclear reaction cross-section 392, (Sec. 7.7)
Nuclear reactor 418, 420*ff*
Nuclear reactor accidents 423
Nuclear shell model 288
Nuclear spin 74, 240, 292
Nuclear spin isomerism 251
Nuclear spin quantum number (*I*) 241
Nuclear stability 250, 268, 273, 289, (Sec. 5.3)
Nuclear wave function 550
Nucleus 236*ff*, (Sec. 5.1)
  density 239, 299
  shape 240
  size 237
  stability 250, 268*ff*, (Sec. 5.3)
Nucleons 236
Nucleophilic attack 503
Nucleophilic substitution reactions 861
Nucleophilicity 1409, 1436
Nucleophilicity vs. basicity 1436
Nucleosynthesis of elements 429, 430*ff*
Nuclides 249*ff*

O

Oblate ellipsoidal 241
Oblate spheroid 240
Octahedral and tetrahedral holes 1026
Octahedral metal cluster 1167, 1169
Octet rule 544
Odd (–) parity 294
Odd electron bond 568, 724, 725
Odd electron molecules 725
Odd-even rule for oxidation states 532
Oddo-Harkins rule 269, 434
Oddo's rule 435
Ohmic potential 1606, 1693
Ohm's law 1121, 1122
Okla mine 423
Okla phenomenon 423
One dimensional (1D) molecular metal 1215, 1216
One dimensional lattices 1050
One dimensional solids 1214
Onium salt 1389
Open circuit potential (OCP) 1686
Open-book configuration (H_2O_2) 789

Click Here t.me/thealchemylibrary

Oppenheimer-Phillips mechanism 390, 396
Optical activity 960
asymmetric 960
dissymetric 960
Optical electronegativity 506
Optical model 295
Optical properties of solids 1151, 1190
Orbital electron capture 322
Orbital electronegativity 495
Orbital energies 88, 93
Orbital magnetic moment 75
Orbital multiplicity 68
Orbital or K-electron capture 273
Orbital penetration 221
Orbital shapes 200, 205
Orbital symmetry rule 599
Orbitals 185*ff*, (Sec. 4.1)
Orbits vs. orbitals 211
Organic ionic liquids 1574
Organic metals 1220, 1394
Organic semiconductors 1217, 1218
Organic superconductors 1217, 1219, 1221, 1229, 1394
Organometallic compounds 857
Organometallic hydrides 1345
Organophosphorus insecticides 869
malathion 869
Ortbital symmetry rule 748
Ortho- and *para*-hydrogen 251
Orthogonality 154
Orthogonality condition 676
Oscillating reactions 1777, (Appendix 16B)
Overall stability constant 1389
Overlap integrals 553, 559, 568, 761
Overpotential 1695, 1705
Oxidation number 713, 1578, 1593
Oxidation states 530, 1579
Oxidative addition 882, 1389, 1407, 1594
Oxidative halogenation 1002
Oxidisability of metals 1639, 1640
Oxidising oxyanions 1707
Oxo acids 1429
Oxyacids 1423
Oxyacids for phosphorous 1426
Oxyanions 1642, 1708
Oxygen balance 1775
Oxygen carrier 1396
Oxygen overvoltage 1699
Oxygen scavanger 1324
Oxygen valency 453
Oxyhalides as solvents 1571
Ozone 1587

π & P

p–n Junctions (Diodes) 1194
π-acid ligands 1388, 1394, 1402
p-block elements 465
π-bonding 802*ff*, (Sec. 10.7)
p-contraction 519
p-n-p and *n-p-n* junction transistors 1202
p-n junction 1195
p-process 433
p-type extrinsic semiconductors 1187
p-type semiconductors 1074, 1075
p-type superconductors 1231
P. Ray 351, 851–52
Packing fraction 273–275
Pair formation 126, 296, 314, 366
Parabolic curves 10
Parallel paths of decay 330
Parallel plate ionisation chamber 315
Paraquat 1316
Parathion 869
Parity 292, 342
Parity of nuclides 293
Partial ionic character 774
Participation of *d*-orbitals 684, 867
Particle accelerators 397*ff*, (Sec. 7.9)
Particle in a box 144, 160, 161, 1116, (Sec. 3.5)
Particle in a one dimensional box 151, (Sec. 3.5.2)
Paschen series 34
Paschen-Back effect 85
Passivity 1693
Pattenkofer's rule of integral multiple 449
Pauli exclusion principle 53, 57, 86, 217, 219, 555
Pauli force 217, 219, 970
Pauli magnetism 1086
Pauli paramagnetism 1086, 1129, 1151
Pauli repulsive force 970
Pauling equation and % ionic character 775
Pauling relationship (bond length) 770
Pauling-Allred-Rochow concept 499
Pauling-Pearson paradox 1488, 1489
Pauling's crystal radii 985
Pauling's electronegativity 491, 1432
Pauling's electroneutrality principle 711
Pauling's empirical rule (acid strength) 1424
Pauling's ionic radii 987
Pauling's univalent radii 984
pE 1598, 1599
Pearson's equation 1490
Peierls distortion 1180, 1214, 1221
theorem 1215
Pendant arm 1303
Penetrating power 198, 222, 485
Penetrating power of the orbit 49
Per cent ionic character 774
Perching complexes 1306
Perdisulfate 1587
Perihelion position 48
Periodic table 451*ff*
Periods 452
Permitivity 1556
Perovskite structure ($CaTiO_3$) 1040, 1045, 1047, 1229
Peter equation 770
Pfund series 34
pH scale 1353, 1469, 1562
pH values (calculation) 1353*ff*, (Sec. 14.3.6)
Phase diagram of *Cu-Zn* system 1159
Phase transfer catalyst (PTC) 1309
Phase transition 1333
Phenolphthalein 1381
Phi (ϕ) bonds 575
Phonons 1124, 1227

Click Here to the chemylibrary

Phosphazenes 815*ff*, 818
Phosphazene bases 1465
Phosphazene molecule 703
Phosphinic acid 707, 1425, 1583
Phosphonic acid 707, 808, 1425
Phosphorescence 1708
Phosphors 1205
Photocatalyst 1213, 1715, (Sec. 16.16.3)
Photochemical reactions 1708, (Sec. 16.16)
Photochemical redox decomposition 1769
Photochemical reduction of dintrogen 1717
Photochemical splitting of water 1711
Photochemical yield 364
Photoconductivity 1072, 1206
Photocopying process 1208
Photodiode 1206–1207
Photodissociation 431
Photoelectric effect 118, 313, 366, 1114, (Sec. 2.4)
Photographic processes 619
Photography 1718
Photoinduced electron transfer (PET) 1318
Photonuclear reactions 387
Photosensitivity 617, 619
Photovoltaic effect 1207
Pi-acid ligands 819
Piezoelectric materials 1056, 1088, 1090*ff*
Piezoelectric property 1056
Pions 279
Piperazine 1439
Piperidine 1439
Planck's equation 116
Planck's quantum theory 114
Plasma state 426, 428
Plastic deformation 1125
Plasticisers 1094
Platinum metals 452, 455
Plum-pudding model of atom 20
Point defects 1064
Point groups 931*ff*, 946, (Sec. 10.14)
  identification 946
Polar diagrams 205
Polar graphs 137–138
Polarisability 499, 1290, 1291, 1420
Polarisation 836, 1698
Polarisation and covalency 791*ff*
Polarisation of central atom 841
Polarisation of ions 791*ff*
Polarographic method of analysis 1728, (Sec. 16.22.1)
Polaron 1222
Poly acids 1061
Polyacetylene 1217
Polyatomic species 658
Polyazacryptands 1310
Polyazamacrocycles 1310
Polyborates 812
Polyhedral frameworks of ice 1280
Polyhedral skeletal electron pair theory (PSEPT) 903*ff*, 1171, (Secs. 10.12.4, 10.12.7, 12.8.5–6)
Polymeric structure 796
Polymerisation of oxyanions 812
Polymetallic ring 1324
Polymorphs 1037
Polynuclear metal carbonyls 859
Polyphosphazene skeleton 817
Polyphosphoric acid 1426*ff*
Polythiazyl $(SN)_x$ 1216
Polythionates 1586
Polytopal isomerism 857
Polytopal rearrangement 853
Porterfield equation 770
Position of hydrogen 524
Positive rays 8
Positron emission 272
Post-precipitation 1506
Postactinides 462*ff*
Postlanthanides 471
Potassium tetracyanoplatinate (KCP) 1180, 1214
Potential energy curve 754, 1254
Potential-pH (E–pH) diagram 1655
Potentiometric titrations 1680, (Sec. 16.13)
Pourbiax diagram 1646, 1655, (Sec. 16.8.3)
  of iron 1656*ff*
  of manganese 1660
Powerful oxidising agents 1604
Powerful reducing agent 1605
Primary cells 1686, 1687, (Sec. 16.14.2)
Primary isotope effect 257
Primary oxides 1643
Primary process 316
Primary radiolytic products (prp) 365, 370
Primordial element 430
Principal (P) series 74
Principle of conservation of energy 122
Principle of electroneutrality 821
Principle of relativity 122
Probability density 189
Prolate ellipsoidal 241
Prolate spheroid 240
Prompt neutrons 408, 420
Prompt reactions 1709, 1711
Propellants 1773
Prophyllite 1054
Proportional counter 316
Protolysis 876, 877
Proton affinity 486, 998, 1348, 1419
Proton emission 273
Proton in water 1369
Proton magnetic resonance (PMR) 249
Proton reservoir 1370
Proton reservoir concept 1371
Proton sponge 1370, 1445–1447
Proton transfer equilibrium 1353
Proton transport process 1369
Proton-proton cycle 427
Protonic concept (acid-base) 1344*ff*
Prototropic tautomerism 707*ff*, 1268*ff*, 1427
Prout's hypothesis 257
Prussian blue 1581
PSEPT 903*ff*, 1175, (Secs. 10.12.4, 10.12.7, 12.8.5–6)
Pseudo noble gas configuration 981
Pseudo-noble gas type cations 794, 981
Puckered ring 818
Pulsars 17
Purple benzene 1310
Push-pull mechanism 876*ff*

Click Here to the Chemistry Library

Pyramidalisation 972, (Appendix 10A)
Pyridine 1463
Pyrite 1050
Pyrophyllite 1055
Pyroxene 1053
Pyrrole 784, 1463

Q

Quadruple bonding 720*ff*, 1164, (Secs. 9.6, 9.19, 12.8)
Quadruple interaction 766, 1163
Quadrupole moment 240, 241
Quantum defect 19, 50, 221
Quantum numbers 54, 188, 213, (Secs. 1.10.3, 4.1.2, 4.1.11)
Quantum restrictions 45
Quantum theory 43, 111, (Ch. 2)
Quantum yield 1771
Quark particles 18, 299
Quenching agent 1713, 1715
Quinonoid form 1381
Quintuple (5 bonds) bonds 720
Quinuclidine 1439, 1444

R

r-process 432
Rabi magneton 78, 242
Racemisation 809, 849, 866, 876, 884
Rad (R) 367
Radial distribution function (RDF) 194, 196, 225, 475, (Sec. 4.1.4)
Radial equation 187
Radial nodal points 193
Radial nodes 197, 211
Radial probability density 193, 194
Radial probability distribution 192
Radial wave function 192, 193
Radiation chemistry 363*ff*, (Sec. 6.18)
Radiation dosimetry 367*ff*
Radiation emission 323
Radiation hazard 428
Radiative capture 387
Radical stabilisation energy (RSE) 972, (Appendix 10A)
Radioactive decay 322, (Sec. 6.6)
Radioactive decay kinetics 327, (Sec. 6.9)
Radioactive emanations 310, 314
Radioactive equilibrium 332, 335, (Sec. 6.10)
Radioactive isotopes (applications) 347*ff*, (Sec. 6.17)
Radioactivity 309*ff*, (Ch. 6)
Radioactivity in age determination 361
Radioactivity in agriculture 358
Radioactivity in industry 360
Radioactivity in the medical field 359
Radiocarbon dating 362
Radioimmunoassay (RIA) 360
Radiolysis of water 369*ff*
Radiopharmaceuticals 359
Radioscintigraphic agents 359
Radius ratio rule 1014*ff*, (Sec. 11.8)
Randles-Sevcik equation 1748
Raoult's law 1259
Rare earths 453
Raschig synthesis of hydrazine 881
Ray-Dutt twist 851, 852
Rayleigh-Jeans Law 113
RBE (relative biological effectiveness) 367
RDF 192, 196*ff*, (Sec. 4.1.4)
RDF curves 197, 225
RDX (cyclonite) 1727
Reaction quotient 1600
Reactor shield 422
Real angular wave functions 205
Receptors (molecular recognition) 1298, 1302*ff*
Recoil energy 267
Recoil nuclide 267
Recovery factor 1533
Rectifier 1201, 1204
Rectifier equation 1198
Red giant stars 426, 430
Red shift 162, 1274
Redox indicator 1677, (Sec. 16.12)
Redox stability field of water 1655
Redox stability of water 1645
Redox titration 1672, (Sec. 16.11)
Reduced mass 32, 185, 265
Reductive dehalogenation 1002
Reductive elimination 808, 1003, 1594
Reference electrode 1597
Refractory metals 1181
Relative atomic mass (RAM) 258
Relative cosmic abundance 433
Relativistic contraction 136, 520
Relativistic correction 4, 48, 213
Relativistic effects 464, 470, 517, 520*ff*, 980
Relativistic expansion 225, 226, 517, 520
Relativistic kinetic energy 136, 144
Relativistic wave mechanics 191
Relaxation energy 753, 756, 759, 761
REM (Rontgen equivalent man) 367
Representative elements 466, 476
Reproduction factor (*K*) 415
Repulsive intermolecular forces 1294
Resonance 705, 713, 714, 716, 1451, 1457
Resonance and exchange phenomenon 161
Resonance caputre 393
Resonance effect (R) 779
Resonance energy 705, 706*ff*
Resonance integral 166, 559, 564, 568
Resonance potential (RP) 35, 40
Resonating structure 911
Retrobonding 612, 820
Reverse biased junction 1197
Rhenium trioxide (ReO_3) structure 1040
Rhombic twist 851
Ring compounds 815
Ring whizzer system 858
Ritz combination principle 19, 50
Rocket fuel 1775
Rocking chair model 1690
Rontgen (R) 367
Room-temperature ionic liquid (RTIL) 1573*ff*
Rosette 48
Rotational energy level 253
Rotational lines 253
Rotational spectra 254

Click Here to the Freechemybrary

Rotaxanes 1320
Ruby 1040
Ruby red colour 1046
18*e* Rule 1175
Rule of duplet 544
Rule of eight 543
Rule of maximum spin multiplicity 94
Rule of Oddo 270, 271, 275
Russel-Saunders states 67
Russel-Saunders terms 65
Russell-Saunders coupling 58
Rutherford (Rd) 21, 321
Rutherford's model 23
Rutile (TiO_2) structure 1039
Rydberg 30
Rydberg constant (R) 19, 28, 30
Rydberg formula 18

S

s-block elements 464
s-process 432
Sacrifical anodes 1693
Salt effect 1497
Salting in 1498
Salting out 1499
Salting-out term 1499
Sanderson's electronegativity 501
Sargent's curve 341
Scandide contraction 469, 475, 477, 519
Schmidt limit 242, 243
Schomaker-Stevenson equation 768*ff*, 770
Schottky defects 1064*ff*
Schrödinger angular wave functions 202
Schrödinger's wave equation 145, 147, 150, (Secs. 3.4, 3.5)
Schwesinger phosphazenes 1464
Scrambling of the bridging and terminal carbonyls 859
Screening effect 221
Screening power of the orbits 49
Sea of instability 289
Secondary cells 1686, 1687, (Sec. 16.14.2)
Secondary isotope effect 257
Secondary periodicity 517*ff*, 532, 773, 1642
Secular determinant 559
Secular equations 167, 559
Secular equilibrium 268, 334, 335
Secular or permanent equilibrium 333
Segre chart 271
Selection rules 70
Self-association 1275
Self-consistent field (SCF) 220
Semi-empirical mass equation 286
Semiconductor conductivity 1189, 1209
Semiconductor materials 1193
Semiconductors 1135, 1181*ff*, (Sec. 12.9)
Semimetals 1136
Semitopological representation 909
Separation factor 261
Separation of Cu^{2+} and Cd^{2+} 1501
Separation of isotopes 260
Separation of lanthanides 473
Serpentine 1054
Shannon's crystal radii 988
Shape of the nucleus 240
Sharp (S) series 74
Sheet structure 1264
Shell closure effects 411
Shielding 221
Shielding constant 37, 222, 245, 248
Shielding effect 35
Shielding power of the orbits 49
Short range repulsive force 992
Siderophiles 466, 1486
Sidgwick-Powell theory 825
Sidgwick's rule of maximum covalency 545
Siemens 1123
Silanol groups 1060
Silenes 803, 1405
Silica gel 1060, 1494
Silica surface 1493
Silicates 1051*ff*, (Sec. 11.14)
Silicones 802, 1108, 1051
Siloxane bonds 1060
Simple cubic (*sc*) unit cell 1025
Simultaneous deposition of copper and zinc 1636
Singlet linkage bond 544
Singly occupied molecular orbital (SOMO) 580, 749, 973
Size of the nucleus 237
Skeletal electron pairs 900, 914
Skeletal pairs 900
Slater orbitals 221
Slater's rules 36, 37, 222, 471, 474, 500, 984, (Sec. 4.2.4)
Slip direction 1112
Slip forces 1112
Slip plane 1113
Slip system 1113
Slow neutrons 17
Smith acidity functions 1467, 1537
Soccerball cryptand 1307, 1308
Soda glass 1093
Soda lime glass 1056
Sodalite cage 1057
Soddy–Fajan group displacement 324*ff*, (Sec. 6.8)
Sodide 1309, 1560
Sodium D-line 53, 74
Sodium nitropruside 1590
Sodium-sulfur battery 1234
Soft-soft adduct 794
Soft-soft interaction 794, 821, 1488, 1626, 1636
Softness parameter 1477
Solar cell 1207
Solid acids 1492*ff*
Solid electrolyte 1213, 1232*ff*, (Sec. 12.14)
Solid gas hydrates 1284
Solid surface acids 1493
Solubility 797
Solubility product 1494*ff*, 1496, 1499
Solvation effects 1449*ff*
Solvay process 1265
Solvent cavity 1559
Solvent extraction 1272
Solvent system definition 1468*ff*, (Sec. 14.11)
Solvolysis 861
Solvolysis reactions 1562

Click Here to Free Chemistry Library

Sommerfeld's atomic model 45, (Sec. 1.9)
Sommerfeld's free electron model 1115, 1120*ff*
Sommerfeld's orbits 47
Sommerfeld's quantum mechanical free electron theory 1115*ff*
SOMO 580, 749, 973
Space charge region 1195
Space quantisation 81, 241
Spallation 388, 389
Spallation reactions 434
Spatial quantisation 53, 65
Specific heat capacity 1126
Specific heat of metals 1127
Spectral lines 34
Spectral selection rule 217
Spectral series of alkali metals 51
Spectral transitions 72
Spectroscopic electronegativity 507
Spent fuel 423
Sphalerite 885, 1036
Spherand 1301, (Sec. 13.5.6)
Spherical coordinates 186
Spherical harmonics 200, 201, 204
Spherical nodal surface 210
Spherical recognition 1304, 1305, 1307
Spherical recognition of metal ions 1301
Spin 342
Spin angular moment 217
Spin exchange force 281
Spin magnetic moment 77
Spin multiplicity 58, 68
Spin quantum number 191
Spin-orbit coupling 291, 524
Spin-orbit coupling constant 69
Spin-spin coupling 247
Spin-spin coupling constant 247
Spinel and inverse spinel structure 1042*ff*
Spinning electron 53
Spontaneous fission 413
Spurs 365
Squids 1232
Stabilisation of low oxidation states 819
Stabilisation of unusual oxidation states 1486
Stability constants 1389*ff*, 1629, 1738
Stability field of water 1645, 1646, 1655, 1660
Stability island 289, 464
Stability of the isotopes 259
Stability ratio 501
Stacking fault 1034
Stacking interaction 1298, 1316
Staggered form 789
Standard electrode potential 1598
Standard hydrogen electrode 1596
Standard reduction potentials 1603 (T)
Standing sine wave 139, 146
Standing wave 139, 146
Stark effect 45, 85
Stationary electrode 1729
Stationary orbit 140
Stationary state 25
Statistical concept 1428
Stefan-Boltzmann law 113, 116
Stellar energy 426
Stellarater 429
Stepwise stability constants 1389
Stereochemical nonrigidity 845
Stereochemically active and inactive lone pairs 689, 842, 844
Stereochemically active lone pairs 842
Stereochemically inactive lone pair 689
Stereochemically nonrigid molecules 845, 853
Stereochemistry 767
Stereoselective reactions 925
Steric factors 1444*ff*
  B-strain 1444
  F-strain 1444
Stern-Gerlach experiment 81
Stirling's approximation 1066
Stoichiometric (i.e. intrinsic) defects 1064
Stoichiometric standard potential 1598
Stoke's law 5
Stopping potential 119
Storage cell 1688
Strength of acids and bases 1414*ff*, (Sec. 14.8)
Strength of hydracids 1414*ff*
Strength of organic carboxylic acids 1417*ff*
Strength of oxyacids 1423*ff*
Stripping 389
Stripping reactions 387*ff*
Structure breaking 1328
Structure making 1328
Structure of ionic crystals 1035*ff*, (Sec. 11.10)
Structure of liquids 1094
stxy numbers 907*ff*
Subatomic particle 134
Subcritical size 415
Subgroups 452
Subhalogen 525*ff*, 527
Substitutional alloys 1157
Subvalent compounds 545
Sugden's view 544
Sulfation of battery 1688
Sulfuric acid as a solvent 1567
Superacids 1382*ff*, 1384, 1564, 1568*ff*, (Secs. 14.6, 15.9)
Superactinides 462*ff*
Superatoms 505
Superbases 1446, 1464
Superconducting electrons 1226
Superconducting gap 1225
Superconducting materials 1228
Superconductivity 1047, 1222*ff*, (Sec. 12.13)
Superconductors 1048*ff*, 1228*ff*
Supercritical mass 417
Supercritical size 415, 417
Superexchange mechanism 1080, 1162
Superhalogen 525, 526
Superheavy elements (SHE) 289, 405, 462*ff*, 464, 524
Superlattice 1157
Supernova explosion 403, 433
Supramolecular interaction 522, 1285, 1298*ff*, (Sec. 13.5)
Supramolecular polymer 1317

Click Here to the chemylibrary

Supramolecular systems 1298*ff*, (Sec. 13.5)
Surface acids 1492*ff*, (Sec. 14.16)
Symbiosis 1479*ff*
Symbiotic effect 1475
Symbiotic theory 1282, 1480
Symmetric fission 412
Symmetric or even functions 156
Symmetrical and unsymmetrical hydrogen bonding 1253
Symmetrical molecules 780
Symmetry allowed reaction 751
Symmetry elements 931*ff*, (Sec. 10.14)
Symmetry elements in the cubic system 1025
Symmetry elements in the MOs 571
Symmetry forbidden reactions 751
Symmetry interaction 589, 594
Symmetry number 961
Symmetry of the orbitals 207, 211
Symmetry operations 931
Symmetry-adapted linear combinations (SALCs) 620
Symmetry-adapted orbitals 620
Synchrocyclotron 400
Synergistic action 819*ff*, (Sec. 10.7.8)
Synergistic polarisation 794
Synthetic natural gas (SNG) 1722
Szilard–Chalmers' process 266

T

Tafel equation 1647, 1705, 1706
Talc 1054
TASO 620*ff*
Tautomeric forms 1268*ff*, 1459, 1585
Tautomerism 707*ff*, 808, 868, 1268*ff*, 1427, 1585
TCNQ 1219
Technetium (*Tc*) 401
Temperature Independent Paramagnetism (TIP) 1086, 1129, 1151
  Langevin paramagnetism 1151
  Pauli paramagnetism 1151
Term symbols 66
Terminal atom symmetry orbitals (TASOs) 620*ff*
Tetracyanoethylene (*tcne*) 1392
Tetrahedral (T_d) hole 1026
Tetrahedral recognition 1308, 1313
Tetramethylsilane 249
Tetrasulphur tetraimide 818
Tetrathiazyl tetrafluoride 818
Tetrathionate 1586
Thermal conduction 1128
Thermal diffusion method 263
Thermal stability of the carbonates, sulfates 800
Thermal stability of the hydrides 763
Thermionic emission 1110, 1114
Thermistor 1190, 1206
Thermochemical radii Yatsimirskii's 988
Thermochemistry 757
Thermonuclear reactions 389, 424
Thiazyl trifluoride 819, 1584
Thiosulfate 349-50, 1585
Thixotropic properties 1056
Thomson's mass spectrograph 9
Thomson's method 2
Thomson's parabola method 9
Thorium series 343
Three centre bonding 667*ff*, (Sec. 9.12.12)
Threshold frequency 118, 120
TIP 1086, 1129, 1151
TMTSF 1219
Tokomak 429
Tolman cone angle 1405*ff*
Topology of boron hydrides 907
Tracer technique 349
Trans-effect 821
Trans-influence 821
Transactinides 404, 462
Transient radioactive equilibrium 268, 333, 334
Transistors 1202–1204
Transition elements 452
Transition state 863
Transition state theory 164
Translawrencium elements 402, 404, 452, 454, 462, 464
Transmission coefficient 861
Transmutations 383*ff*
Transuranic elements 402, 454
Triad elements 452
Triads of Dobereiner 448
Trial wave function 166
Triatomic molecules (MOT) 620*ff*
Tridymite (SiO_2) structure 1039
Triflic acid 1383, 1385
Trigonal twist 851
Triiodide 1587
Trinuclear clusters 1166
Triplet and singlet oxygen molecules 583
Trisilylamine 1456
Trithionate 1586
Tropone 1461
TTF 1219
Tungsten bronze 1213
Tunnelling effect 164, 282, 340, 413, 861
Tunnelling of Copper pairs 1232
Turnstile rotation 849, 850
Twisting mechanism 851*ff*, (Sec. 10.9.3)
  Ray-Dutt twist 851
  Rhombic twist 851
Two dimensional lattices 1049
Two fluid model 1225

U

Uhlenbeck and Goudsmit 53
Ultimate acids and bases 1472
Ultramarines 1059
Ultraviolet catastrophe 114
Ultraviolet photoelectron spectroscopy (UV-PES) 614*ff*
Uncertainty principle 140, 141, 143, 144, 154, 157, 163, 280, 854, (Sec. 3.3)
Unified atomic mass unit scale 259
Unit cell 1024
United atom method 557, 576
Units of radioactivity 320
Unsaturated hydrocarbon 719
Uphill migration 1195, 1197
Uranium series 344
Urea crystal 1283
Usanovich concept 1472
Uses of isotopes 260, 347*ff*, (Sec. 6.17)
UV photoelectron spectroscopy 601*ff*, 615*ff*
UVPES 601*ff*, 615*ff*, 617

Click Here t.me/thealchemylibrary

V

Valence bond approach of metallic bonding 1154, (Sec. 12.6)
Valence bond theory (VBT) 551*ff*
Valence shell electron pair repulsion (VSEPR) theory 825*ff*, 970, (Sec. 10.8 3)
Valency 542*ff*
secondary or residual or auxiliary valency 542
Valinomycin 1310
van der Waals forces 1285*ff*, 1293, (Sec. 13.3)
van der Waals radii 765
Variation method 166, 559, (Appendix 3A)
Vaska's complex 1397*ff*, 1404, 1407, 1591, 1592, 1594
Vector model of the atom 52, (Sec. 1.10)
Pauli exclusion principle 52
Verkade base 1464
Vermiculite 1055
Vibrational spectra 254
Vibrational wave numbers 256
Vinyl chloride 784
Viscosity 1259
Vitamin A 162, 163
VSEPR theory 683, 694, 825*ff*, 970, (Sec. 10.8.3)

W

Wade-Mingos Lahure rules *see* Wade's rule
Wade's rule 900, 903*ff*, (Secs. 10.12.4, 10.12.7, 12.8.5–6)
Walsh diagram 631*ff*
Walsh's rules 629*ff*, 630, 842
Warm superconductors 1229
Water gas reaction 1722
Water gas shift reaction, WGSR 1722
Water of constitution 1261
Water of crystallisation 1261
Watson-Crick base pairing 1265
Wave function 145, 149
orbital 185*ff*, (Sec. 4.1)
Wave mechanical model 185*ff*
Wave mechanics 133, (Ch. 3)
Wave number 27, 115
Wave-particle dualism 133*ff*, 177
Weiss constant 1086
Weiss indices 1027
Weston cadmium cell 1598
White dwarf 431
Wiedemann-Franz law and Lorenz number 1127
Wiedemann-Franz's law 1110, 1114
Wien's equation 117
Wien's Law 113, 117
Wilson cloud chamber 319
Wittig reaction 600, 752, 810
Woodward-Hoffmann orbital symmetry rule 748*ff*, (Appendix 9A)
Work function 120
Wurtzite 1037
Wurtzite structure 885

X

x-process 434
X-ray (generation) 37, 273, 323, 366
X-ray photoelectron spectroscopy (XPS) 617
Xenon fluorides 735*ff*, 844*ff*, 972, 1410, 1467
Xenon hexafluoride (XeF_6) 844*ff*
Xerox 1208

Y

Yatsimirskii's thermochemical radii 987
Ylids 810

Z

Zeeman effect 45, 53, 82
Zeise's salt 1394, 1402*ff*
Zener break-down 1202
Zener diode 1201, 1204
Zeolites 1057*ff*, 1493
Zero-point energy 153, 147, 159, 161, 163, 255, 256, 265, 854
Zimmermann-Reinhardt (Z-R) solution 1643, (Sec. 16.6)
Zinc blende 885, 1036
Zintle anions 1561, 1563
Zintle cluster ions 904, 1178*ff*
Zintle phase 1161
Zone theory of metallic bonding 1131*ff*
ZSM-5 1059
Zwitterionic forms 1360, 1365

Click Here to the chemylibrary

Fundamental Concepts of
Inorganic Chemistry

This is the completely revised, enlarged and updated edition of the textbook in three volumes, aimed at the honors and postgraduate students. In a logical sequence, the book deals extensively with different aspects such as atomic structure (both classical and wave mechanical) and atomic spectra, fundamentals of quantum mechanics and wave mechanics, nuclear chemistry and radiation chemistry, different theories of valence forces and chemical forces, band and Bloch theory of solids, solid state chemistry, supramolecular chemistry, acids and bases, nonaqueous solvents and redox potentials. It also covers the different aspects of materials science which is emerging with a great promise.

The important additions in the second edition include

• Hypervalency • Molecular orbital diagrams of polyatomic molecules in terms of group orbitals (i.e. TASOs) • 3c-4e *vs.* 3c-2e bonding systems • Geometry of the molecules in terms of Walsh diagrams • Isolobal fragments • Reaction-mechanism of the main group elements • Different aspects of material science • PSPET- Wade's rule, Jemmi's rule • Chemistry of boranes and carboranes • Metal clusters and carbonyl clusters • Zintle ions • Symmetry elements and point groups • Fullerenes • Intercalation compounds of graphite • Band theory of solids – band splitting and band bending • Electrical and magnetic properties of solids • Piezoelectric solids • Organic metals and organic semiconductors • Superconductivity • Agostic interaction • Supramolecular chemistry • Aqueous chemistry of amino acids • Surface acids and solid acids • Ionic equilibria and related numerical problems • Inorganic photochemistry • Lithium battery • Fuel cells , Solar cells • EMF diagrams – Frost diagram, Pourbaix diagram • Tafel equation • Stability field of water • Chemistry of explosives • Electroanalytical techniques – polarography, coulometry, ampereometry, LSV, CV, polarography • Chemical clock reactions and oscillating chemical reactions.

Asim K. Das MSc (Gold Medalist, CU), PhD (CU), DSc (Visva Bharati)

is now Professor of Chemistry, Visva Bharati, Santiniketan. He has over 20 years of teaching experience at both the undergraduate and postgraduate levels. He passed both the BSc (Hons in Chemistry) examination in 1981 and MSc (specialization in Inorganic Chemistry) in 1983, standing first class first from the University of Calcutta. He received his PhD from the same University in 1988 under the supervision of Prof. D. Banerjea, the then Sir Rashbehari Ghose Professor of Chemistry. He received his DSc degree from Visva Bharati in 2002.

Dr Das has published 80 research papers in the field of thermodynamic and kinetic aspects of metal complexes in reputed national and international journals. He has also written: *A Textbook on Medicinal Aspects of Bioinorganic Chemistry* (1991), *Inorganic Chemistry: Biological and Environmental Aspects* (2004), *Bioinorganic Chemistry* (2007), *Environmental Chemistry with Green Chemistry* (2010).

Click Here t.me/thealchemylibrary

Dedicated to Education

CBS

CBS Publishers & Distributors Pvt Ltd

4819/XI, Prahlad Street, 24 Ansari Road, Daryaganj, New Delhi 110 002, India

E-mail: delhi@cbspd.com, cbspubs@airtelmail.in; Website: www.cbspd.com

New Delhi | Bengaluru | Chennai | Kochi | Kolkata | Mumbai

Hyderabad | Jharkhand | Nagpur | Patna | Pune | Uttarakhand